Radical Adventures in Photochemistry

Terry McCallum

A thesis submitted to the

Faculty of Graduate and Postdoctoral Studies

In partial fulfillment of the requirements for the

PhD degree in Chemistry

Department of Chemistry and Biomolecular Sciences

Faculty of Science

University of Ottawa

Abstract

A field in bloom: photoredox catalysis has allowed chemists access to highly reactive intermediates via the photo-mediated excitation of transition metal complexes and organic dyes for the mild generation of free radicals. These complexes and dyes are designed based on Nature's blueprints of light-harvesting biomolecules that transform solar energy (photons) into chemical energy during photosynthesis. Light-mediated chemical activation is regarded as one of the most sustainable forms of chemical activation being that the energy provided by the sun is considered renewable and largely underutilized and presents an attractive avenue for research and development of new transformations that are mild, efficient, and waste-limiting in organic synthesis.

Radical chemistry and photochemistry are united in their inherent ability to undergo single (or photoinduced) electron transfers by one-electron reaction modes. Combining these unique fields, photoredox catalysis has emerged as a mild and efficient alternative to classic alkyl radical generation using hazardous initiators and organostannanes. Photoredox catalysis has been dominated by ruthenium- and iridium-based polypyridyl complexes. These complexes are limited by their inherent redox potentials, restricting their reactivity towards relatively activated bonds. Nonactivated bromoalkanes and arenes are considered challenging substrates to engage using redox chemistry and typically only accessible in the realm of organostannane chemistry. Described herein are the efforts towards the discovery of free radical based organic transformations derived from nonactivated bromoalkanes and arenes mediated by photochemical excitation of polynuclear gold(I) complexes as photoredox catalysts. This work represents some of the first uses of a photoredox

catalyst in the reduction of substrates having such high reduction potentials and offers a practical and useful alternative to classic radical reactions mediated by initiators (peroxides, persulfates, and azo compounds) and toxic organostannanes (Bu_3SnH). Using gold based photoredox catalysts, the research conducted has provided many methodological advancements for the mild and efficient formation of carbon–carbon bonds using nonactivated bromoalkanes and a large collection of radical acceptors.

Establishing the use of these photoexcited polynuclear gold(I) complexes in the context of classic radical reactions in organic synthesis was important for their validation as useful photocatalysts. First, the Ueno-Stork cyclization of nonactivated bromoalkanes was used to demonstrate the powerful reducing capabilities of the excited-state gold(I) complexes. Next, a photo-mediated variant of the Appel reaction was described, where the transformation of an alcohol to a bromoalkane was achieved using carbontetrabromide and *N,N*-dimethylformamide through the intermediacy of a Vilsmeier-Haack reagent. In combination with the hydrodebromination chemistry developed with photoexcited polynuclear gold(I) complexes, a photo-mediated one-pot formal deoxygenation reaction of alcohols was described; a useful alternative to the organostannane mediated Barton-McCombie deoxygenation reaction. Finally, in the field of medicinal chemistry, the functionalization of heteroarenes is of high interest for the discovery of drug candidates and bioactive molecules. In this respect, one of the most useful reactions for the functionalization of heteroarenes by alkyl radicals is the Minisci reaction using silver salts, carboxylic acids, and persulfates. Detailed are the efforts for the development of a photo-mediated redox-neutral improvement of the Minisci reaction,

needing only gold(I) photocatalyst and nonactivated bromoalkane in the presence of heteroarenes.

Overall, the work described in this thesis represents the push for mild and efficient alternatives to the relatively harsh conditions and/or toxic reagents and byproducts associated with classic radical chemistry. These studies demonstrate the ability to control highly reactive alkyl radical intermediates with the goal of their broader application in synthetic organic chemistry. The use of photoexcited polynuclear gold(I) complexes as potent reductants compared to ruthenium- and iridium-based polypyridyl complexes is illustrated through the genesis of highly reactive alkyl radicals from nonactivated bromoalkanes.

Acknowledgments

I am unduly thankful to have had the opportunity to pursue my doctoral studies in the Barriault Lab. During this time, I have had the chance to work with excellent students in a challenging research environment. The hard-working students of our group that continually strive for excellence have helped me grow into the curious chemist that I have become. We have one of the most collegial lab climates that facilitates refining of project development through open discussion amongst each other. I am grateful to have interacted with many of the faculty in the University of Ottawa's diverse Department of Chemistry and Biomolecular Sciences and appreciative of the expert insight gained from the fruitful discussions over the past few years. I've also had the unique experience of travelling around the globe to attend leading-edge conferences that has allowed for networking, personal growth, and nourishment of the curious mind; an opportunity I would not have had otherwise.

First and foremost, I must thank Louis for the opportunity to work in his lab. He has been an incredible supervisor and mentor, has supported me in all my endeavours, and his passion for organic synthesis is inspiring. He has motivated me to grow academically through providing the freedom to explore a variety of new topics to the research group, all with the hopes of discovering something new and useful to organic chemists. He has also shown me the inner workings of academia that have cultivated my ambition for continued scientific pursuit.

I need to thank Professors Scaiano, Pratt, Gagosz, and Beauchemin for providing their expert insight on a variety of research-based inquiries I've had over my studies. Being pointed in the right direction goes a long way for finding solutions to complex research-oriented questions. I thank Michel Grenier for advice on

photochemical reactor design and LED development. Dr. Guillaume Revol was my in-lab supervisor at the beginning of my studies and initiated my love for radical chemistry, photochemistry, and designing meaningful experiments using practical methodology, and for this I am thankful. With this concept in mind, I'd also like to thank the past and present leaders in the field that have deciphered the fundamentals and continue to push the boundaries of radical and photochemistry; without these intrepid explorers, our work would be without foundation.

Thanks to the many motivated past and current group members that I've been grateful to work with over these years. Dr. Mathieu Morin was instrumental in discussing and working on many of the projects presented herein, held enlightening conversations about the world at large, and above all, is a great friend. Dr. Christopher McTiernan and Dr. Spencer Pitre were extremely motivated students that I have had the opportunity to collaborate with and my research would not have been the same otherwise. Phillipe McGee has been another student that I've had many productive conversations about synthesis and experiment design and a great friend to travel with. Dr. Alex Cannillo was a great chemist and friend to work with, live with, and explore the finer points of Ottawa with. Many undergraduate students that went on to pursue graduate studies of their own are to be thanked for their commitment to research and friendship, including Ekaterina Slavko, Sherif Kaldas, Huy Tran, Lea Thai-Savard, Andre Costisella, Prajesh Joshi, Sam Rohe, Montse Zidan, Rowan Swann, and Avery Morris. I also need to especially thank Dr. Frank Magnan, Dr. Spencer Pitre, and Thomas Charlton for their unwavering friendship and support throughout my graduate studies. The past and present CGSA members that have created events that foster a

collegial environment amongst the hard-working graduate students of the department are appreciated. Dr. Sharon Curtis of the Mass Spectrometry group and Dr. Bulat Gabadullin at the X-ray facility are thanked for their efforts in compound structure elucidation.

Finally, my family has been my most important support system throughout the best and worst times of my life. I've been met with enduring love and support to seek the things in life that make me happy. Through this path I have met my best friend and wife, McKinsey, and our canine companion, Nymeria. You are the wind in my sails and calm the waters when they storm. True happiness is found in the time spent with those you love. We are a great team and I have to say that you are pretty funny and know a lot about hip-hop.

Thank you!

Contribution Statement

Organic chemistry projects require great efforts in the laboratory to acquire adequate data for comprehensive exploration of reaction scope generality and concise mechanistic understanding. Considering these requirements, organic chemistry labs are highly collaborative settings, where multiple students working towards a goal is commonplace, and in suitable conditions, working with multiple laboratories yields the highest quality results.

All the projects described in this thesis were conducted under the guidance and supervision of Professor Louis Barriault. The multidisciplinary nature of the described studies has benefitted from collaboration with Professor Tito Scaiano and his laboratory. I am both grateful and appreciative to work with a supervisor that is willing to work with others and has given me the freedom to pursue diverse topics during my doctoral studies. While the work discussed in this thesis is largely my own, it is necessary to delineate the contributions made by other students in this work. All starting material synthesis, product isolation, and corresponding characterization described in the experimental and characterization sections pertain to my work, unless otherwise noted. Compounds that appear in each chapter that do not appear in the experimental section were likely synthesized by students under my guidance and have/will appear in other theses. The following is an in-depth explanation of the contributions to the papers and projects described in this thesis.

In chapter 2, the use of binuclear Au(I) bisphosphine complexes for the photo-mediated reductive hydrodebromination reactions of bromoalkanes and arenes was conceived by Professor Louis Barriault. The synthesis and initial characterization of the binuclear Au(I) bisphosphine complexes was carried out by Dr. Guillaume Revol.

Experimental design was developed by all authors affiliated with this work. My contributions entailed the synthesis of the starting materials, product isolation, and corresponding characterization. In section **2.5 – Further Information**, the photo-physical and electrochemical characterization of a variety of multinuclear Au(I) phosphine and carbene complexes are described. These complexes were synthesized by Dr. Mathieu Morin, where the complete description of their characteristics was carried out by Dr. Christopher McTiernan in a collaboration that I initiated with Professor Tito Scaiano. While this work was not carried out by myself, it is necessary to the full mechanistic understanding concerning these complexes. In this mechanistic work, my contribution extended to the discovery that these complexes were participating in dimerization reactions of bromoalkanes, and ultimately, their expansion to a project that focused on evaluation of the dimerization reaction scope and the development of mechanistic reactions. The extension of this chemistry to iodoarenes was carried out by Huy Tran under my guidance during his undergraduate studies.

In chapter 3, the photo-mediated bromination of alcohols using CBr_4 in DMF to generate Vilsmeier-Haack reagents was discovered during my conception of a photoredox mediated one-pot formal deoxygenation of alcohols as a continuation of my studies into hydrodebromination chemistry with Au(I) complexes. The scope of the bromination reaction was explored by Ekaterina Slavko under my supervision during her undergraduate studies. My contributions also included the development of the one-pot deoxygenation methodology along with product isolation and subsequent characterization.

In chapter 4, my continued work into substrate tolerance in the photo-mediated generation of Vilsmeier-Haack reagents using CBr_4 in DMF led to the observation that symmetric anhydrides were formed when starting from carboxylic acids and that amides were generated when amines were also present. My contributions included the synthesis of all materials and their subsequent characterization along with advice from my supervisor for scope application and development.

In chapter 5, the powerful reducing capabilities of photoexcited binuclear Au(I) bisphosphine complexes and their use for alkyl radical genesis from bromoalkanes was applied to the Minisci reaction, as proposed by Professor Barriault. My role consisted of the development of the reaction conditions, synthesis of the starting materials, isolation of the products, subsequent characterization, and designing corresponding mechanistic studies.

In chapter 6, the development of photo-mediated alkylation reactions of heteroarenes with alcohols and ethers evolved from my work in chapter 5. My initial role was in the discovery that photoexcited protonated heteroarenes could generate methylated heteroarene products in the presence of methanol. Much work was done by Dr. Mathieu Morin in the optimization of this reaction. Mechanistic studies were carried out by Dr. Spencer Pitre (summarized in the Results and Discussion as well as the Experimental sections of chapter 6) through a collaboration with the laboratory of Professor Tito Scaiano, gaining integral data towards understanding of the underlying mechanism of the transformation. My contribution then extended to the final development of the reaction conditions using HCl as the acid to protonate the heteroarenes, investigation of the reaction scope, discovery of *i*PrOH as a reductant

to heterocycles, product isolation, subsequent characterization, deuterium isotope labelling studies, and synthesis of the 2,4-diphenylquinoline catalyst. Dr. Pitre also carried out the catalytic reactions and their corresponding isolation. Development of a mechanistic proposal was arrived at by input from all authors over numerous fruitful discussions.

To conclude, fascinating chemistry has been developed during the past five years in many different topics during my doctoral studies. The chemistry appears simple in its refined form, however, has been difficult at times to comprehend and was only possible through advice from Professor Barriault, collaboration with Professor Scaiano, Dr. McTiernan, and Dr. Pitre, and the many students I have had the opportunity to work with and train in the Barriault Lab. Chapter 7 is evidence of their commitment to continued efforts in this program as eluded to by the new reactivity being developed under my guidance.

Table of Contents

List of Figures

List of Schemes

List of Tables

Abbreviations

Ac	acetyl
AIBN	azobisisobutyronitrile
ATRA	atom transfer radical addition
BDE	bond dissociation enthalpy
Bn	benzyl
Boc	*tert*-butyloxycarbonyl
bpy	2,2'-bipyridine
brsm	based on recovered starting material
Cbz	carboxybenzyl
CFL	compact fluorescent lightbulb
Collidine	2,4,6-trimethylpyridine
DABCO	1,4-diazabicyclo[2.2.2]octane
DBU	1,8-diazabicyclo[5.4.0]undec-7-ene
DMA	*N,N*-dimethylacetamide
DMAP	4-dimethylaminopyridine
DMF	*N,N*-dimethylformamide
DMS	Dimethylsulfide
dmpm	1,1-bis(dimethylphosphino)methane
dppm	1,1-bis(diphenylphosphino)methane
dtbbpy	4,4'-di-*tert*-butyl-2,2'-bipyridine
EDG	electron donating group
Eq.	equation

equiv	equivalents
Et	ethyl
EWG	electron withdrawing group
HRMS	high-resolution mass spectrometry
IC	internal conversion
*i*Pr	isopropyl
*i*Pr$_2$NEt	*N*,*N*-diisopropylethylamine
IR	infrared
ISC	intersystem crossing
KIE	kinetic isotope effect
LED	light emitting diode
Me	methyl
MeCN	acetonitrile
MLCT	metal-to-ligand charge transfer
PCET	proton-coupled electron transfer
PET	photoinduced electron transfer
Ph	phenyl
ppm	parts per million
ppy	2-phenylpyridine
PTOC	pyridine-2-thione-*N*-oxycarbonyl
PTSA	*p*-toluenesulfonic acid
rt	room temperature
R$_3$N:	tertiary amine base

SCE	saturated calomel electrode
SSCE	sodium-saturated calomel electrode
SET	single electron transfer
TBS	*tert*-butyldimethylsilyl
TEA	triethylamine
Tf	triflyl, trifluorosulfonyl
TFA	trifluoroacetic acid
THF	tetrahydrofuran
TLC	thin layer chromatography
TMS	trimethylsilane
Ts	tosyl, toluenesulfonyl
UVA	ultraviolet A
vs	*versus*

1. A Logic to Redox-Neutral C–C Construction with Alkyl Radicals Using Photoredox Catalysis

1.1 Photochemistry and Radical Chemistry

The year is 1912 and the International Congress of Applied Chemistry is meeting in New York. Ciamician, an experimental organic photochemist, delivers a talk on the prospects of photochemistry powering the worlds energy needs that resonates through the organic chemistry community:[1c]

> "On the arid lands there will spring up industrial colonies without smoke and without smokestacks; forests of glass tubes will extend over the plains and glass buildings will rise everywhere; inside of these will take place the photochemical processes that hitherto have been the guarded secret of the plants, but that will have been mastered by human industry which will know how to make them bear even more abundant fruit than nature, for nature is not in a hurry and mankind is."

In this time, not so different than today, fossil fuel dominated civilization as the preferred form of energy, where Ciamician posited that greater interest in solar energy (at the very least, in the organic chemistry community) could offer a viable alternative to man's energy and technological needs. His vision of the future has merit in the organic chemistry community, however, man remains infatuated with the black luster of fossil fuel; perhaps one of the greatest societal issues of our time.[2]

Though the fundamentals of photochemistry were being described, experimental organic chemistry was beginning to take shape.[3] One of the first photo-mediated organic transformations, Ciamician and Silber reported the photoreductive coupling of benzophenone **1.1**, resulting in the formation diol **1.2** (**Scheme 1.1**, Eq. (1)).[1] Ciamician

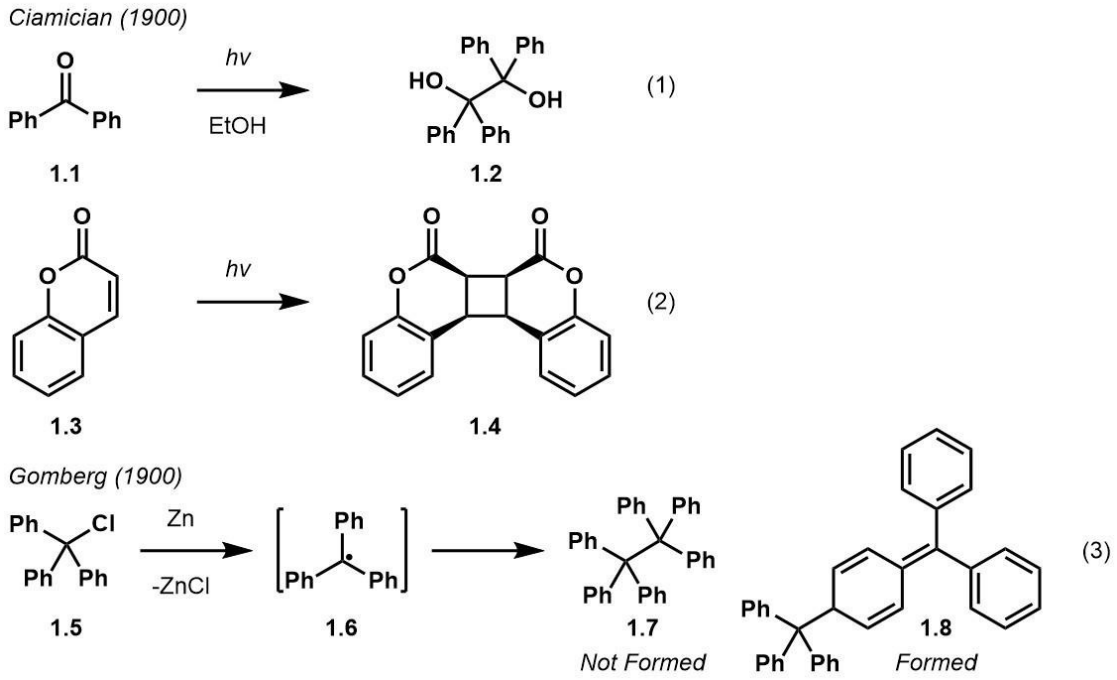

Scheme 1.1 The beginning of photochemical and radical transformations in experimental organic chemistry.

was also involved in the discovery the [2 + 2] photocycloaddition of coumarin **1.3** (**Scheme 1.1**, Eq. (2)).[1b] Remarkable is the proposal of the cyclobutane ring **1.4** while being cautious not to assign incorrect stereochemistry as the tools for this type of structural elucidation were limited at the time.[1e] These topics are still areas of vigorous interest as developments in photochemical transformations using benzophenone as well as methodology for functionalized cyclobutane synthesis are actively researched today.

Widely regarded as the first observation of an organic radical, Gomberg reported the formation of the triphenylmethyl radical **1.6** from the reaction of triphenylmethyl chloride **1.5** and Zn and its corresponding reactivity (**Scheme 1.1**, Eq. (3)).[4] The proposed structure of the product was hexaphenylethane **1.7**, a desired synthetic target in his research program. Realizing the great potential in this finding, he expressed his wishes to reserve this field, however, the wide interest generated in radical chemistry could not be contained to one man. It took over 50 years to elucidate the actual structure of the

transformation, where the quinoid dimer **1.8** was determined through study of the functionalization of the *p*-positions of the triphenylmethyl chloride.[4e]

Flashforward nearly a century, the properties governing the reactivity and selectivity of alkyl radicals are being established with the leading method of radical generation; the use of initiators and organostannanes.[5] While the "tin method" is extraordinarily efficient for the generation of alkyl radicals, its toxicity and requirement for potentially hazardous initiators (explosive azo-compounds such as AIBN, pyrophoric Et_3B with O_2, or peroxides/persulfates) warrant alternative means of radical initiation to escape the "tyranny of tin".[6]

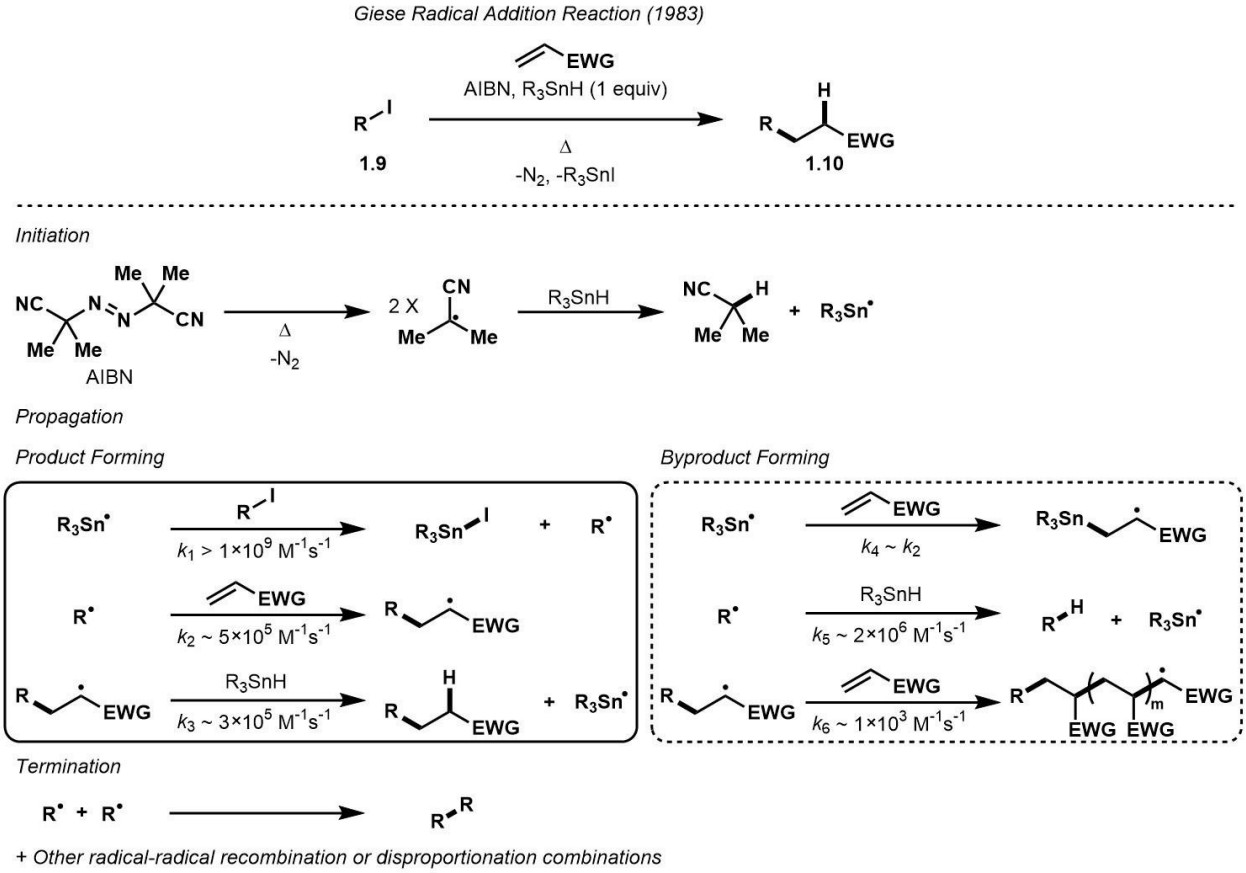

Figure 1.1 The Giese reaction and its considerations with organostannanes.

There is no better reaction to describe the potential pitfalls of the tin method than the Giese reaction, that is, the addition of an alkyl radical to an activated alkene (**Figure 1.1**).[7] The Giese reaction bears striking similarities to the 1,4-addition of a nucleophile to a Michael acceptor; a relatively nucleophilic alkyl radical formed from the electrophilic iodoalkane **1.9** is electronically favoured towards addition to an electrophilic alkene (EWG substituted) over a nucleophilic alkene (EDG substituted) and upon reduction from a hydrogen donor source, furnishes product **1.10**. In the seminal publication, steric interactions were also found to play an important role in the selectivity of alkyl radical addition to alkenes. The rates for each step of this reaction are given in **Figure 1.1**: After initiation (decomposition of AIBN and liberation of the tributyltin radical), the tributyltin radical reacts efficiently with iodoalkane **1.9** ($k_1 > 1\times10^9$ $M^{-1}s^{-1}$), the relatively nucleophilic alkyl radical may then add to the activated alkene ($k_2 \sim 5\times10^5$ $M^{-1}s^{-1}$), and the resulting relatively electrophilic radical can undergo a HAT reaction with the hydrogen atom donor ($k_3 \sim 3\times10^5$ $M^{-1}s^{-1}$, tributyltin hydride), giving the final product **1.10** and regenerating the tributyltin radical. The steps described are product forming, however, they are also in competition with potential by-product forming steps, where the tributyltin radical may also add to the activated alkene at a rate comparable to the alkyl radical ($k_4 \sim k_2$), the alkyl radical can undergo HAT with the hydrogen atom donor at a rate faster than alkene addition ($k_5 \sim 2\times10^6$ $M^{-1}s^{-1}$, tributyltin hydride) leading to reduced alkane by-products, and finally, the electrophilic radical proceeding an alkyl radical addition onto the activated alkene may also add to another activated alkene ($k_6 \sim 1\times10^3$ $M^{-1}s^{-1}$) leading to polymerized by-products. To manage these potential product and by-product forming reactions, concentration of reagents is key and several factors must be considered: 1) [alkene] must be low enough to favour the formation of the alkyl radical (k_1) over addition

of a tributyltin radical (k_4); 2) [alkene] > [Bu_3SnH] to favour addition of the alkyl radical over reduction (k_2 over k_5); and 3) $k_3 > k_6$ to favour reduction of the final product over polymerization reactions. The complex system usually requires an excess of activated alkene (~ 10 equiv) relative to the iodoalkane and the addition of the tributyltin hydride via syringe pump, underscoring the need for further methodological developments in this useful reaction. Could photochemical processes offer experimental organic chemists a solution to these limitations?

1.2 Redox-Neutral C–C Construction with Alkyl Radicals Using Photoredox Catalysis

Inspired by Ciamician's vision of the future, organic (photo)chemists have made great progress in the uses and understanding regarding photochemical processes. For over a century, chemists have found inspiration in the sophistication of light-harvesting biomolecules, owing the development of photo-excitable complexes to furthering our knowledge of the well-kept "secrets of the plants".[8] Excited-state transition-metal based complexes and organic dyes are able to access high energy intermediates under mild conditions (room temperature, visible light) that trigger single electron transfer (SET) processes (reductive or oxidative) that led to highly reactive and synthetically useful organic intermediates; a field known as photoredox catalysis.[9] This fundamental process allows for the photochemical conversion of solar energy into kinetic energy.

To appreciate the photochemical properties of such complexes and dyes, we must first consider the fundamentals of what makes a complex ideal for photochemistry.[10] A Jablonski diagram serves well for such a task (**Figure 1.2**, **A**). The first law of photochemistry states that a given molecule must absorb a photon to become excited

(usually denoted by *) to induce any chemical changes. Upon excitation of a given ground-state compound (S_0), an electron may be promoted from the highest occupied molecular orbital (HOMO) to a higher vibrational level in the singlet-state (S_n) of the lowest unoccupied molecular orbital (LUMO), which eventually falls to the most stable vibrational level (S_1, Kasha's rule).[10b] During this process, energy can be lost in the form of emitting a photon known as fluorescence (F) or to other vibrational modes known as internal conversion (IC). Alternatively, intersystem crossing (ISC) may occur, leading to the triplet-state excited molecule (T_1). From the triplet state, a molecule may also emit a photon through a process known as phosphorescence (P, a longer process producing a lower energy photon than fluorescence because a "forbidden" spin-flip is required for an electron to return to the ground state), or IC. In general, it is assumed that the electron moves at rates much faster than molecular reorganization and photochemical phenomena occur in the same molecular structure as the ground-state (Franck-Condon principle and Born-Oppenheimer approximation).[10b]

It is through these excited states that the SET chemistry between an excited-state complex (or dye) and a substrate is observed that is inherent to photoredox catalysts. Other photochemical processes can occur; oxygen sensitization, Forster resonance energy transfer (FRET), Dexter energy transfer, triplet-triplet annihilation. In general, luminescent complexes and dyes that have longer excited-state lifetimes serve as better catalysts for SET events. Upon excitation by mild sources of light, SET events are triggered through oxidative or reductive quenching of the excited-state photocatalyst. Interestingly, excited-state complexes are always better electron donors and acceptors than their parent ground-state complexes. Another important aspect to consider is that excited-state complexes (R*) are necessarily more oxidizing and reducing compared to

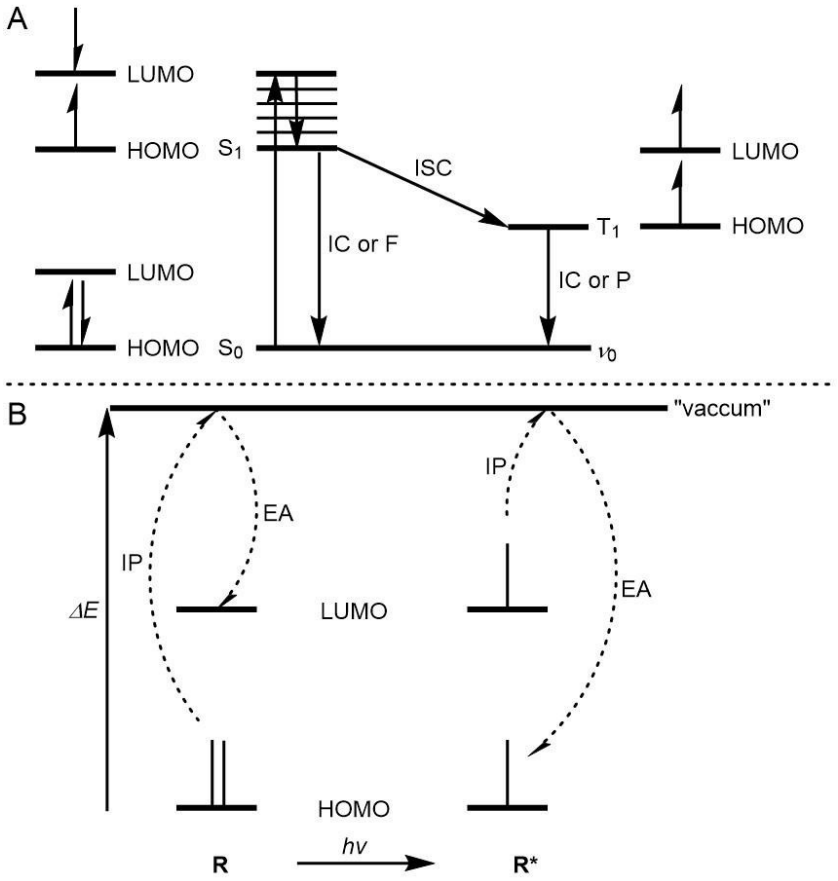

Figure 1.2 Principles of photochemical excitation.

their ground-state (R, **Figure 1.2**, **B**). For reduction of the complex (oxidation of a donor), the electron affinity (EA) is more favourable. For oxidation of R* (reduction of an acceptor), the ionization potential (IP) required to donate an electron is decreased.

Considering this information, the properties essential to the development of mild, efficient, and waste-limiting methodology using photoredox catalysis are summarized: 1) the photocatalyst is excited in the solar spectrum (UV-Vis); 2) the starting materials and products of the process do not undergo background excitation/decomposition; 3) the photocatalyst has a long lived excited-state to facilitate interaction with substrate; and 4) ideally planning a redox-neutral catalytic system to limit the need of extraneous reagents such as oxidants/reductants/additives.

1.2.1 Catalyst, Substrate, and Reaction Design

Over the past decade, an explosion in research effort towards advancements in photo-mediated methodology has provided a better understanding of catalyst and substrate selection with respect to designing desirable organic transformations. In general, photoredox transformations proceed via SET mechanisms but can be mediated by energy transfer pathways as well. A photocatalyst (**PC**) is selected based on its inherent excited-state (**PC***) ability to undergo oxidative or reductive quenching pathways (**Figure 1.3**). In the oxidative quenching cycle, **PC*** acts as a reductant towards an acceptor substrate (**A**) by injecting an electron resulting in the formation of $\mathbf{PC^{1+}}$ (now an oxidant) and an organic radical derived from **A**. $\mathbf{PC^{1+}}$ can then accept an electron by oxidizing a donor substrate (**D**), which may be an additive or an intermediate generated

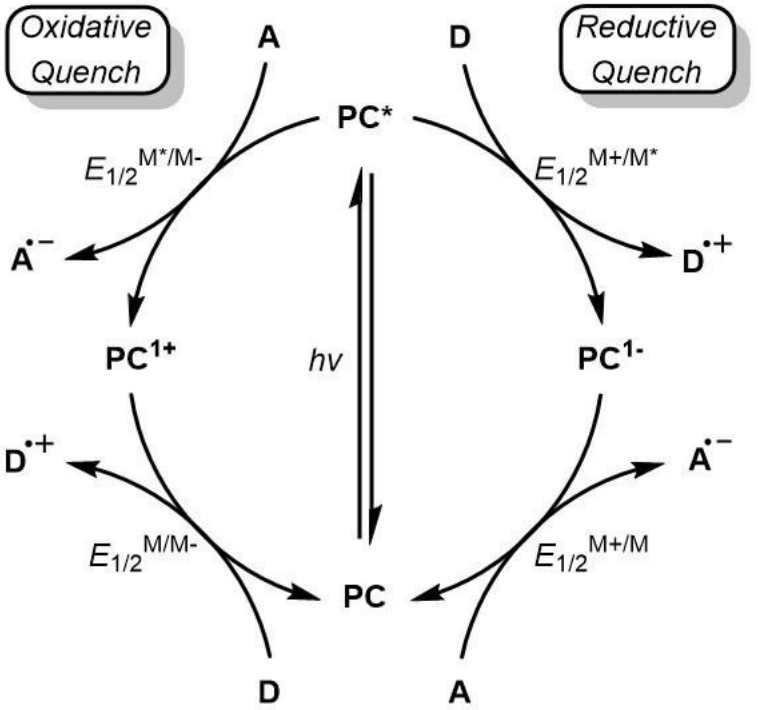

Figure 1.3 Oxidative and reductive quenching pathways.

during the reaction, regenerating ground-state **PC**. In the reductive quenching cycle, **PC*** acts as an oxidant towards **D** by removing an electron resulting in the formation of $\mathbf{PC^{1-}}$

(now a reductant) and an organic radical derived from **D**. $\mathbf{PC^{1-}}$ can then donate an electron by reducing **A**, which may be an additive or an intermediate generated during the reaction, regenerating ground-state **PC**. Reactions using stoichiometric additives are considered net-oxidative or reductive whereas transformations that employ reaction intermediates for catalyst turnover are considered net redox-neutral.

When selecting a photocatalyst, several factors are considered: 1) the wavelength of light required for excitation; 2) the excited-state lifetime, usually ns for singlet-state, $\mathbf{^1[PC]^*}$, and μs for triplet-state, $\mathbf{^3[PC]^*}$; and 3) the redox potentials associated with oxidative and reductive quenching pathways. The properties of some common photoredox catalysts are given below (**Table 1.1**).[11] Ru- and Ir-based polypyridyl complexes are some of the most prolific to date. These complexes undergo SET processes through an outer-sphere metal-to-ligand charge transfer (MLCT) mechanism. The ability to modulate the electronic properties of these complexes through structural modification to the polypyridyl ligands makes these complexes quite appealing. Homoleptic complexes such as $Ir(ppy)_3$ (ppy = (C^N) or LX) stabilize the HOMO and LUMO of the excited-state complex on the phenyl and pyridine portions of each ligand, respectively. Conversely, heteroleptic complexes such as $[Ir(ppy)_2(dtbbpy)]PF_6$ (bpy = (N^N) or LL) result in spatial separation of the HOMO and LUMO of the excited-state complex, where the HOMO is stabilized by the phenyl portion of the (C^N) ligands and the LUMO is stabilized by the pyridine portions of the (N^N) ligand. The spatial separation of the HOMO and LUMO in the excited-state complex enable the photophysical properties of heteroleptic complexes (i.e. $[Ir(C^N)_2(N^N)]^+$) to be more easily tuned by ligand modification than homoleptic complexes. Operating through a MLCT mechanism, the excited-state complexes can be thought of as an electron being transferred from the metal

centre to a polypyridyl ligand. Incorporation of EWGs on the (C^N) ligand and EDGs on the (N^N) ligand stabilize the MLCT resulting in longer excited-state lifetimes and more oxidizing excited states ($E_{1/2}^{(M^*/M^-)}$). The opposite is observed when opposing electronics are incorporated upon the respective ligands. Homoleptic $Ir(C^N)_3$ complexes tend to have more reducing excited states that are less sensitive to substituent effects.

Table 1.1 Properties of common photocatalysts.

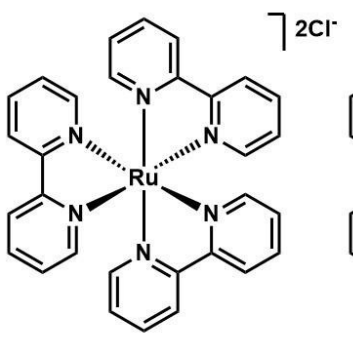

$[Ru(bpy)_3]Cl_2$

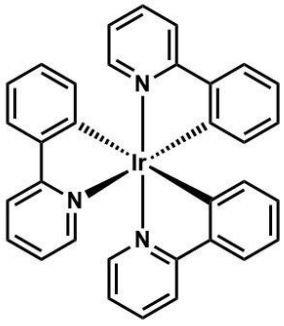

$Ir(ppy)_3$

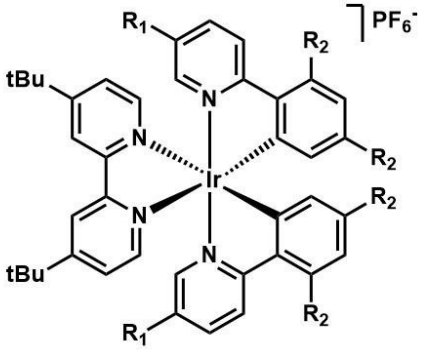

R_1 = H, R_2 = H
$[Ir(ppy)_2(dtbbpy)]PF_6$
R_1 = CF_3, R_2 = F
$[Ir(dF(CF_3)ppy)_2(dtbbpy)]PF_6$

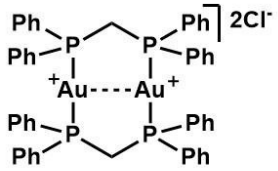

$[Au_2(\mu\text{-dppm})_2]Cl_2$

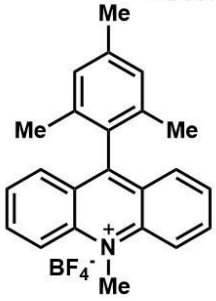

$[Mes\text{-}Acr\text{-}Me]BF_4$

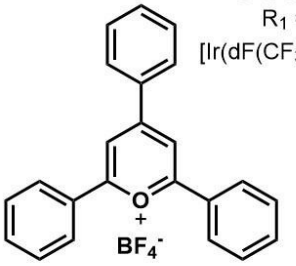

$[TPP]BF_4$

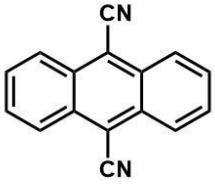

DCA

Entry	Complex	λ_{ex} (nm)	λ_{em} (nm)	τ_0 (ns)	*Oxidative*[a] $E_{1/2}$ (M^+/M^*)	*Oxidative*[a] $E_{1/2}$ (M^+/M)	*Reductive*[a] $E_{1/2}$ (M^*/M^-)	*Reductive*[a] $E_{1/2}$ (M/M^-)
1	$^3[Ru(bpy)_3]Cl_2$	452	615	1100	−0.81	+1.29	+0.77	−1.31
2	$^3Ir(ppy)_3$	375	494	1900	−1.73	+0.77	+0.31	−2.19
3	$^3[Ir(ppy)_2(dtbbpy)]PF_6$	410	581	557	−0.96	+1.21	+0.66	−1.51
4	$^3[Ir(dF(CF_3)ppy)_2(dtbbpy)]PF_6$	380	470	2300	−0.89	+1.69	+1.21	−1.37
5	$^3[Au_2(\mu\text{-dppm})_2]Cl_2$	365	560	850	−1.53	+0.70	+0.60	−1.63
6	$^1[Mes\text{-}Acr\text{-}Me]BF_4$	425	500	6	---	---	+2.18	−0.49
7	$^1[TPP]BF_4$	415	465	4	---	---	+2.55	−0.32
8	^1DCA	422	460	15	---	---	+1.99	−0.91

[a]Potentials in V vs SCE measured in MeCN at 298 K, unless otherwise stated.

Also shown is a binuclear Au(I) bisphosphine complex that operates via an inner-sphere exciplex mechanism (*vide infra*) that has similar photophysical properties to $Ir(ppy)_3$. A few common organic dyes that are proposed to operate from the singlet-state are included, where the electron-deficient (or EWG substituted) structures prove to be potent oxidants in their excited states. Depending on the desired cost/outcome of a proposed transformation, a suitable photocatalyst may be selected from this information.

Next, the selection of a suitable substrate for excited-state quenching can be made based on one's preference for ease of synthesis, ability to undergo quenching with a photocatalyst, and by-product formation. The properties of the most commonly used nonactivated alkyl radical precursors are given below (**Table 1.2**).[12] Substrates most frequently compatible with the reductive quenching cycle of a photocatalyst have redox potentials that are oxidizable by the excited-state photocatalyst ($E_{1/2}^{(M^*/M^-)} > E_{1/2}^{(Q^+/Q)}$) which include carboxylates, oxalates (derived from alcohols), trifluoroborates (boronic acids/esters), silicates, tertiary amines, and substituted Hantzsch esters. On the other hand, substrates that are most commonly utilized with the oxidative quenching cycle of a photocatalyst have redox potentials that are reducible by the excited-state photocatalyst ($E_{1/2}^{(M^+/M^*)} > E_{1/2}^{(Q/Q^-)}$) which include haloalkanes, *N*-hydroxyphthalimide esters (derived from carboxylic acids), cyclopropylketones, and triphenylpyridinium salts (derived from amines). When considering these precursors, substrate availability, shelf-life, and cost indicate that carboxylates and haloalkanes are some of the most useful compounds for alkyl radical generation via a photoredox catalysis strategy.

Table 1.2 Properties of common alkyl radical precursors.

Compatible with Reductive Quench

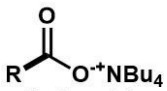
Carboxylate & Oxalate


Trifluoroborate & Boronic acid

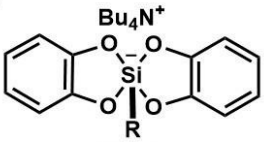
Silicate

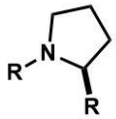
Tertiary amine
R = H, SiR_3

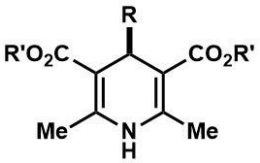
Hantzsch ester

Compatibile with Oxidative Quench


X = I, Br, Cl
Haloalkane

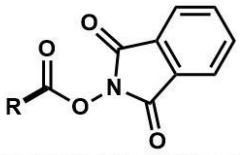
N-Hydroxyphthalimide ester

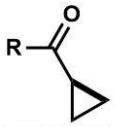
Cyclopropylketone

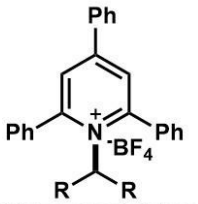
Triphenylpyridinium

Entry	Alkyl Precursor	$E_{1/2}^{(Q+/Q)}$	$E_{1/2}^{(Q/Q-)}$	By-products
1	Carboxylate	+1.2	---	CO_2
2	Oxalate	+1.3	---	2 X CO_2
3	Trifluoroborate	+1.5	---	BF_3
4	Boronic acid/ester	>+2.5	---	$B(OR)_3$
5	Silicate	+0.9	---	Bis(catechol)Si
6	Tertiary amine	+0.8	---	HX or R_3SiX
7	Hantzsch ester	+1.1	---	Hantzsch pyridine
8	Iodoalkane	---	−1.2	HI
9	Bromoalkane	---	−2.0 to −2.5	HBr
10	Chloroalkane	---	>−2.8	HCl
11	*N*-Hydroxyphthalimide ester	---	−1.3	HNPhth, CO_2
12	Cyclopropylketone	---	−1.3	---
13	Triphenylpyridinium	---	−0.9	Triphenylpyridine

*Potentials in V vs SCE; see references for details.

Taken in combination, a redox diagram may be constructed to illustrate catalyst and substrate compatibility when considering reaction design (**Figure 1.4**). The usefulness of excited-state organic dyes in the reductive quenching boron-containing substrates becomes apparent given their potent oxidizing capabilities along with the use of $[Ir(dF(CF_3)ppy)_2(dtbbpy)]PF_6$ with a variety of other alkyl radical precursors. $Ir(ppy)_3$ becomes a likely photocatalyst choice for alkyl radical precursors accessible through oxidative quenching pathways. Apparent here is the need for photocatalysts that can efficiently engage bromoalkane substrates as they are ubiquitous in organic synthesis.

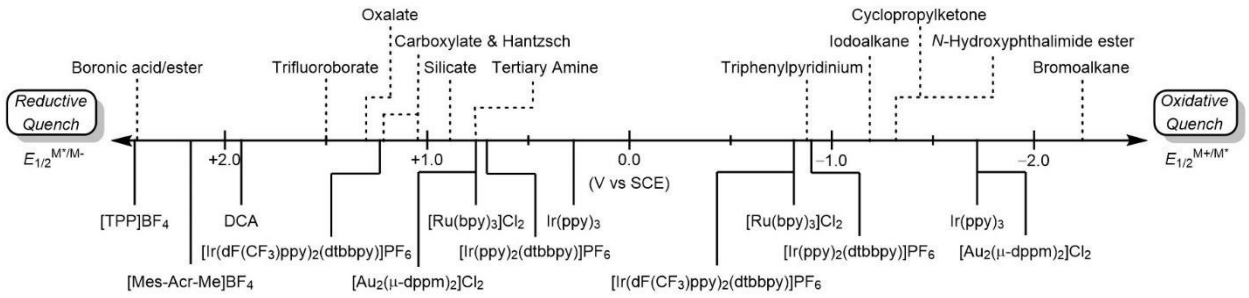

Figure 1.4 Redox diagram for comparing common photocatalysts and substrates.

Binuclear Au(I) complexes serve well for this task despite their inherent excited-state redox potential being much lower than that required to undergo reductive quenching with bromoalkanes and will be discussed in further detail in section **1.2.4** of this chapter. Evaluation of the differences in redox potentials between excited-state photocatalysts and substrates provides the thermodynamic feasibility of a SET process, however, measuring the quenching rates using Stern-Volmer analysis or laser-flash photolysis techniques gives the kinetic feasibility of a SET process; an accurate measure of the ability for reaction to occur.

Once an efficient system is chosen for the generation of alkyl radicals, the fates of these intermediates must be considered (**Scheme 1.2**). The most common uses for radical intermediates in organic synthesis are found in their applications toward reduction reactions, atom transfer radical addition (ATRA), addition reactions (alkenes, alkynes, (hetero)arenes, etc.), and polymerization chemistry. For designing a reaction that is net redox-neutral, an efficient system requires the further reaction of a radical intermediate with an intermediate of the photocatalyst (i.e. reduced or oxidized) generated after initial radical generation via excited-state quenching – also known as a closed cycle. Of course, this requires that the reaction does not propagate via chain reaction between an intermediate radical and another equivalent of starting material, however, in some cases

this is desirable, and the underlying mechanism can be probed using actinometry and rotating-sector methods of reaction analysis. Intermediates arising from addition reactions, especially to alkenes and heteroarenes, are ideal for redox-neutral transformations and are applicable in a wide variety of organic transformations that are of high interest to the synthesis community.

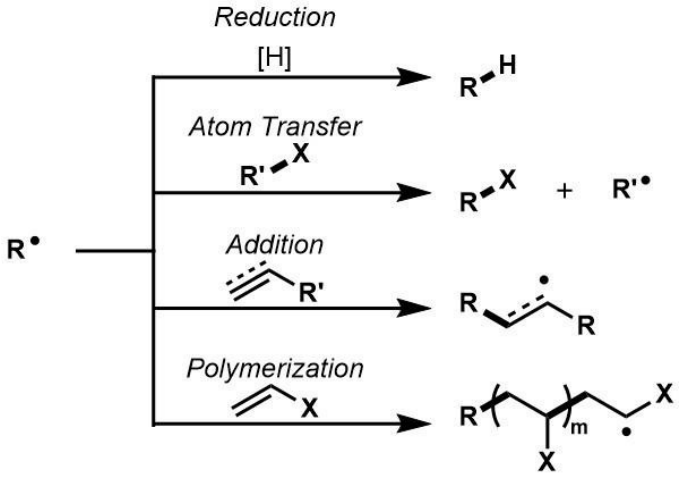

Scheme 1.2 Fates of radical intermediates in organic transformations.

Revisiting the Giese reaction, a mainstay reaction for the development of new methodology with alkyl radicals, the benefits of designing a redox-neutral strategy become evident. In the years following Giese's initial report of the addition of alkyl radicals to electron-deficient alkenes, Okada and coworkers identified the ability of *N*-hydroxyphthalimide esters (**1.11**) to produce alkyl radicals under photochemical conditions.[13a] In 1991, Okada and coworkers developed the net-reductive photoredox Giese reaction using substrate **1.11** and $[Ru(bpy)_3]Cl_2$ in an oxidative quenching manifold (**Figure 1.5**, Eq. (1)).[13b] The use of 1-benzyl-1,4-dihydronicotinamide (BNAH) as stoichiometric reductant was essential for the success of this transformation. As important of a discovery in the development of alternatives to the tin method as this may be, one can surmise that this reaction could benefit from optimization with the goal of limiting by-

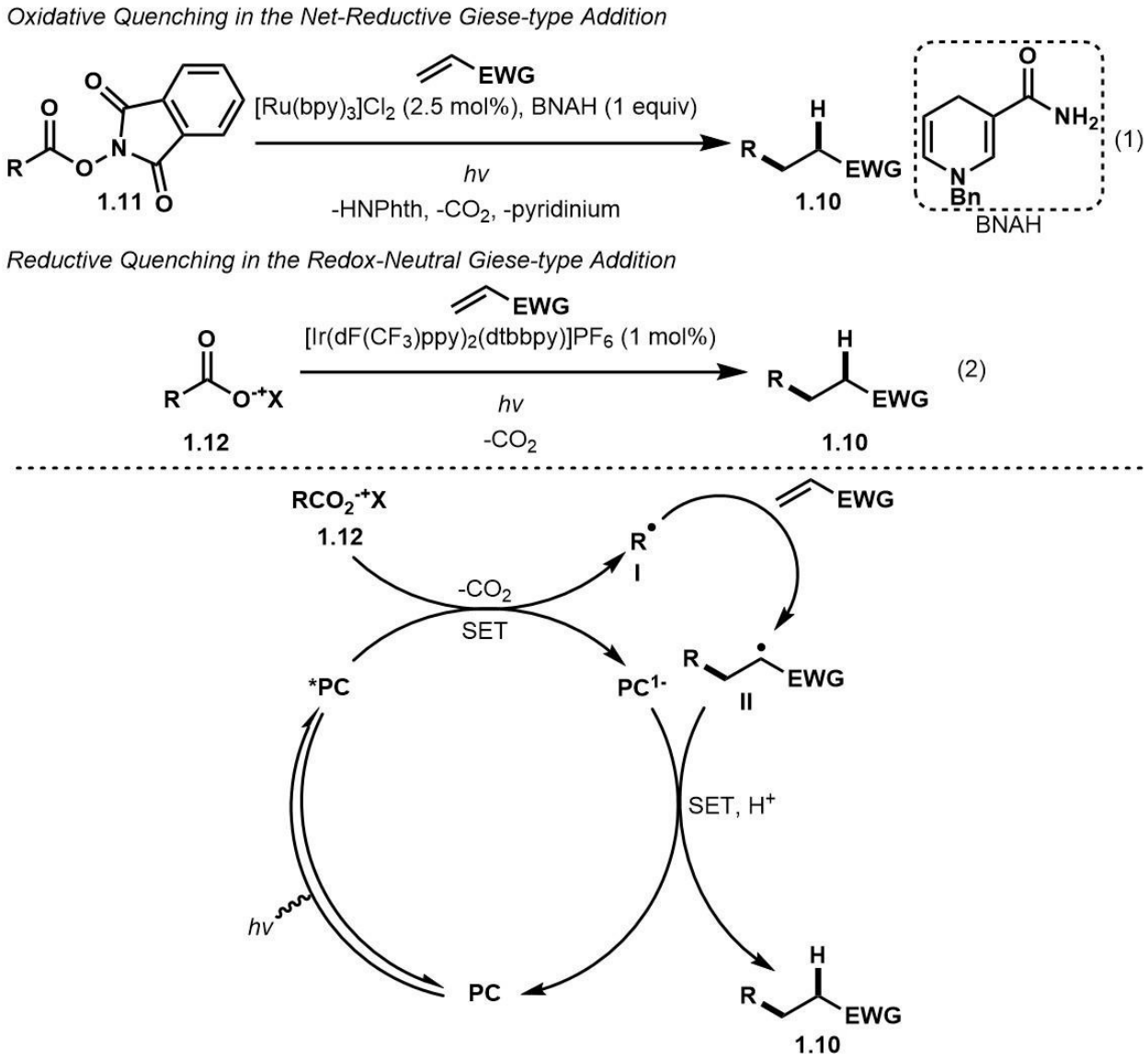

Figure 1.5 Photo-mediated Giese reaction.

products. In 2014, MacMillan and coworkers did just that with their report on the redox-neutral photoredox Giese reaction using carboxylates in a reductive quenching strategy with $[Ir(dF(CF_3)ppy)_2(dtbbpy)]PF_6$ as photocatalyst (**Figure 1.5**, Eq. (2)).[14] In this process, an alkyl radical (**I**) is generated via reductive quenching of the excited-state $\mathbf{Ir^{III}}$ complex with the carboxylate **1.12**, giving $\mathbf{Ir^{II}}$ (a reductant) and releasing CO_2 as the sole by-product. The alkyl radical can then add to the electron-deficient alkene, giving the

relatively electrophilic radical intermediate **II** that is prone to reduction, in this case, by the $\mathbf{Ir^{II}}$ complex, providing the final product **1.10** and regenerating the ground-state catalyst.

Using this approach, a variety of photo-mediated addition reactions have been developed that utilize alkyl radicals (**Scheme 1.3**). Apart from the Giese reaction, (hetero)arylation, allylation, and alkenyl-/alkynylation reactions have been established.[15] The generation of radical intermediates after addition of an alkyl radical to an acceptor unite each of these transformations as they pertain to radical precursors ($R–X_{ox}$) that underwent oxidation via reductive quenching processes with an excited-state catalyst.

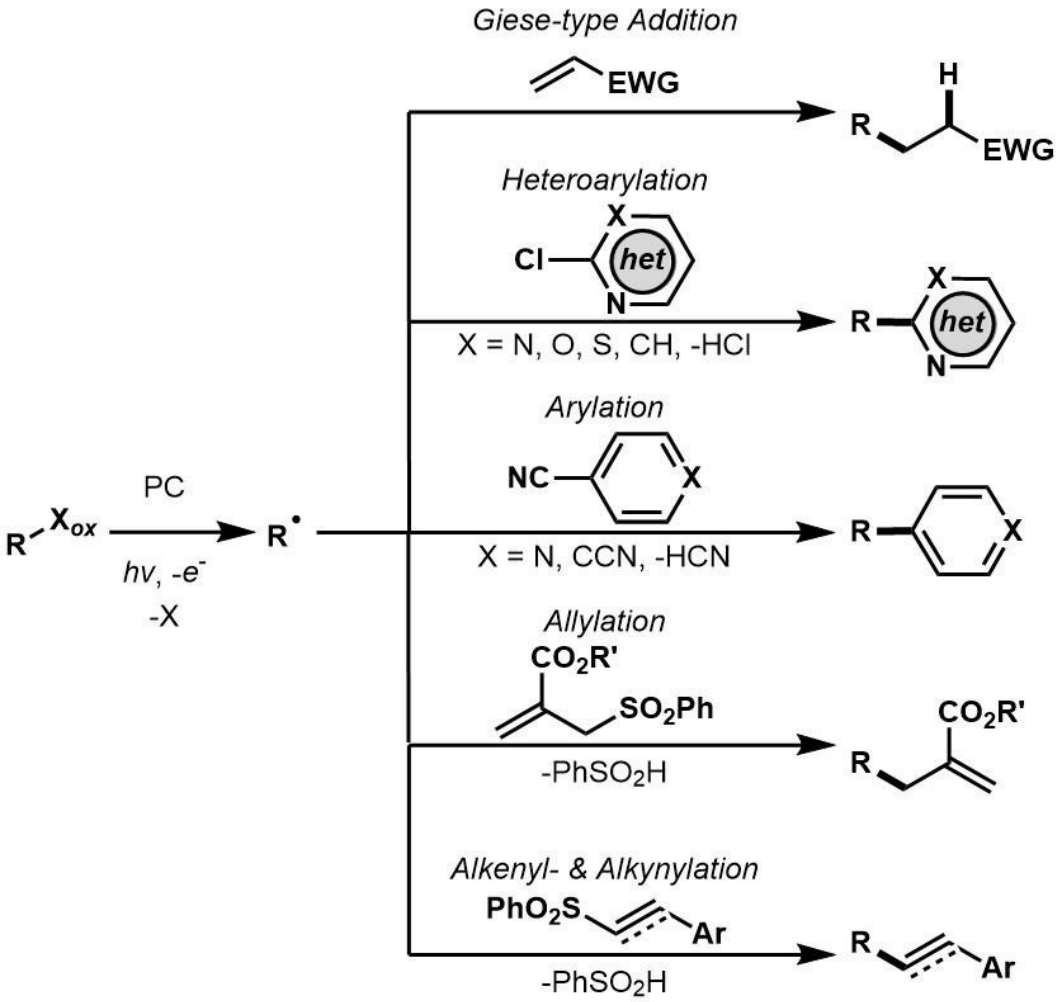

Scheme 1.3 Net redox-neutral organic transformations arising from reductive quenching processes.

The Minisci reaction is another important transformation in radical chemistry and organic synthesis, that is, the addition of an alkyl radical to a protonated heteroarene base, resulting in the rapid functionalization of medicinally relevant structures. The original work in this transformation was made in the early 1970's by Minisci and coworkers where alkyl radicals were generated from carboxylic acids (**1.12**) using $AgNO_3$ and persulfates (**Figure 1.6**, Eq. (1)).[16] Upon addition of these alkyl radicals to a protonated heteroarene base (**1.13**), the desired product (**1.14**) is obtained through further oxidation processes. Relatively nucleophilic alkyl radicals are electronically well aligned to addition to protonated heteroarenes as these radical acceptors are more so electrophilic upon protonation. Under these somewhat harsh conditions, by-product formation (such as **1.15**) along with reduced yields were observed in many cases. Much work has been done with respect to this transformation, however, a recent photoredox mediated methodology was reported by Glorius and coworkers in 2017 that bears resemblance to Minisci's original report.[17] In this report, photoredox catalyst $[Ir(dF(CF_3)ppy)_2(dtbbpy)]PF_6$ was used in place of the silver catalyst in the original report to generate alkyl radicals from carboxylic acids via a reductive quenching mechanism (**Figure 1.6**, Eq. (2)). The report also utilized persulfates for further oxidation processes required to provide the desired product. Although this methodology is mild, an excess of carboxylic acid along with stoichiometric oxidants are required for obtaining desired product successfully. A photo-mediated redox-neutral variation of the Minisci reaction where the photoredox catalyst undergoes oxidative quenching with radical precursors would provide a mild and efficient coupling strategy that circumvents the need for excess reagents/oxidants.

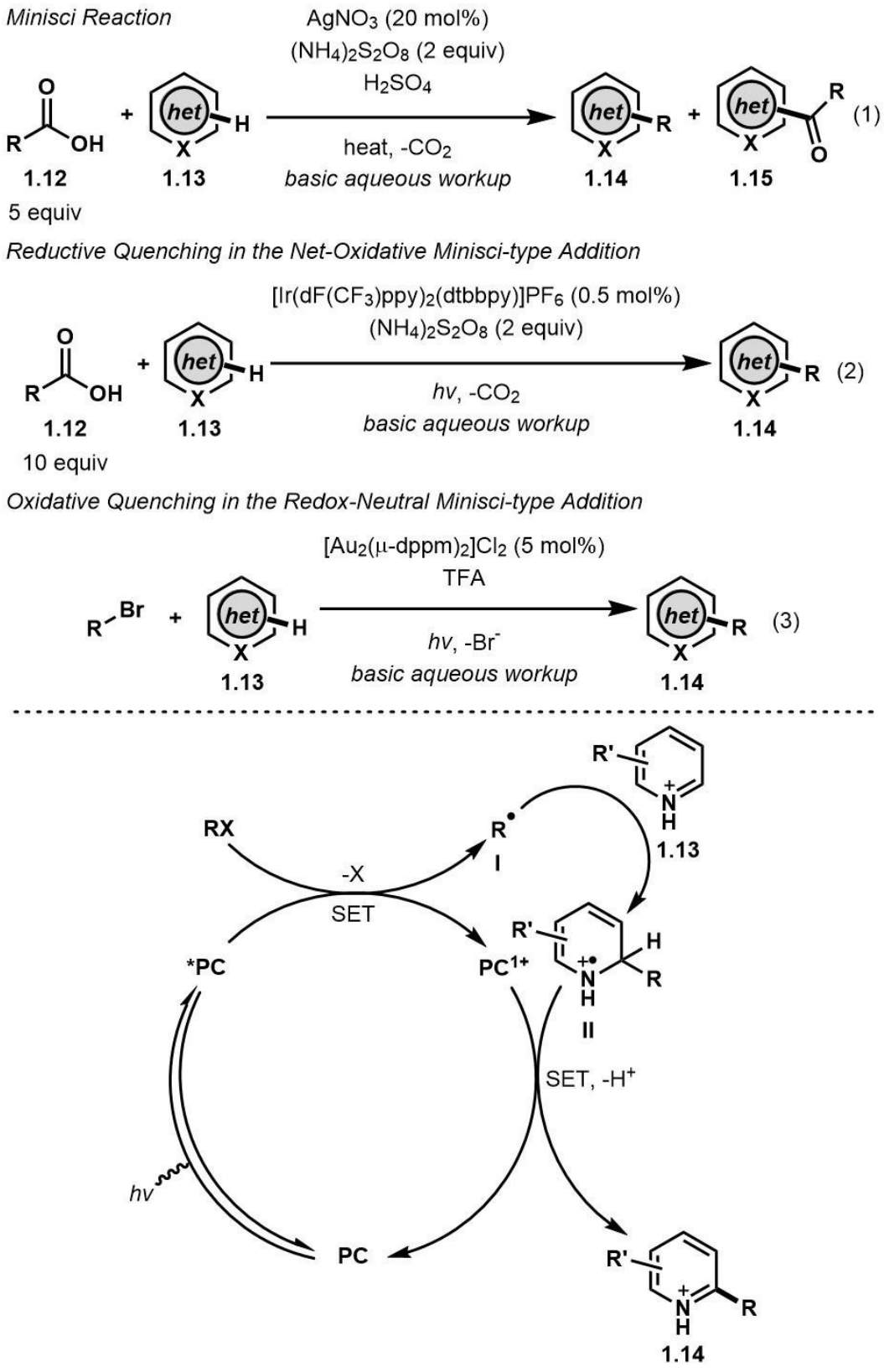

Figure 1.6 Photo-mediated Minisci reaction.

In 2016, Barriault achieved this advancement using a binuclear Au(I) bisphosphine photocatalyst, $[Au_2(\mu\text{-dppm})_2]Cl_2$, with bromoalkanes (**Figure 1.6**, Eq. (3)).[18a] Since this time, a number of redox-neutral variations of this reaction have been reported that utilize substrates such as iodoalkanes, *N*-hydroxyphthalimides esters, and triphenylpyridinium salts.[18b-g] In these systems, ***PC** undergoes oxidative quenching with an acceptor substrate (**RX**), generating **PC^{1+}** (an oxidant) and an alkyl radical (**I**) which may then add to a protonated heteroarene (**1.13**), generating radical intermediate **II**. The intermediate is prone to oxidation, in this case, by **PC^{1+}**, providing the desired product **1.14** and regenerating **PC**.

Taking advantage of this tactic, many photo-mediated organic transformations have become common starting points for evaluating the potential for a combination of

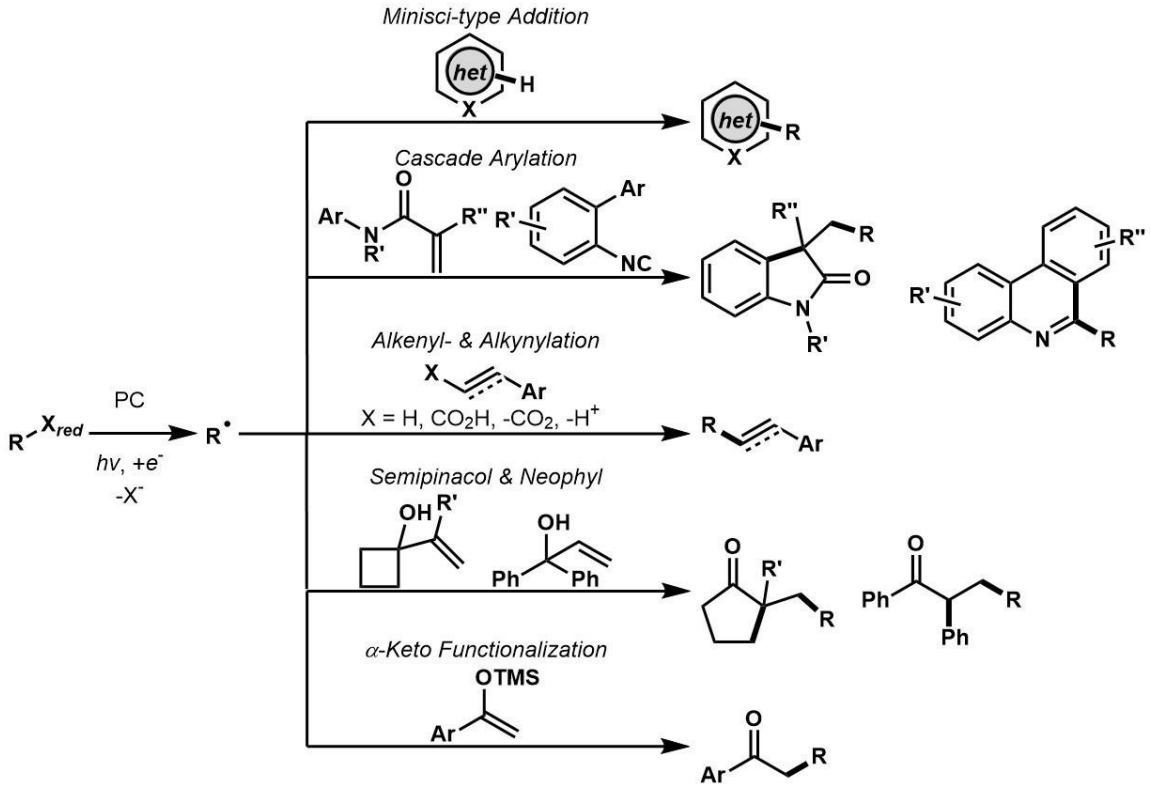

Scheme 1.4 Net redox-neutral organic transformations arising from oxidative quenching processes.

photoredox catalyst and substrate (**Scheme 1.4**). In addition to the Minisci reaction, cascade arylation, alkenyl-/alkynylation, semipinacol/neophyl rearrangements, and α-keto functionalization reactions have been identified.[19] The production of radical intermediates from addition of an alkyl radical to an acceptor from radical precursors ($R–X_{red}$) that underwent reduction via oxidation quenching processes with an excited-state catalyst are common to each of these reactions.

It should be noted that many of the reactions highlighted in **Schemes 1.3** and **1.4** have become benchmark comparisons in the field of photoredox catalysis, especially Giese, Minisci, and reduction reactions. Strategies include substituting either the photocatalyst or radical precursor in redox-neutral systems, approaching every combination one can think of. Further, many other reports detail net-oxidative or net-reductive versions of each photocatalyst/radical precursor system, that require stoichiometric oxidants, reductants, or additives to achieve the desired transformation. To mention each would become exhaustive and equally mundane as the point remains; the potential of photoredox catalysis in synthetic organic chemistry is of great interest to the synthetic community (these reviews serve the point well).[11, 20] In fact, research interest in this field is so high that numerous top peer-reviewed journals have dedicated special issues to the cause.[21]

1.2.2 Sensitization

Differing from SET mediated reactions, transformations that are initiated by sensitization or energy transfers are also of interest in organic synthesis that are often achieved without the need for additives. The triplet-triplet energy transfer (TTeT) is a process that is controlled by a photosensitizer (**PS**) with a high energy triplet excited-state that can transfer its energy to an acceptor substrate. The photosensitized isomerization

of *E*-alkenes (**1.15**) to *Z*-alkenes (**1.16**), proceeds via energy transfer from the ***PS** to the alkene, leading to a diradical intermediate that eventually funnels towards the favoured product depending on the substituents (**Scheme 1.5**, Eq. (1)).[22] Shown is a diagram depicting the triplet excited-state photosensitizer (**^{3}[PS]***) undergoing energy transfer with the substrate (**Sub (S_0)**), leading to ground-state **PS** and a triplet-sensitized substrate (**^{3}[Sub]**).[10b] There has been much work in the field of [2 + 2] photocycloadditions leading to complex structural cyclobutane motifs, however, a few recent examples of enantioselective intramolecular reactions between an enone and an alkene are mentioned. In the first example, an article detailing the use of chiral thioxanthone catalysts developed by Bach and coworkers was used to effect this transformation with 4-substituted 2-quinolones (**1.17**, **Scheme 1.5**, Eq. (2)).[23] The chiral thioxanthone catalyst gives extraordinary enantioselectivity first by engaging the substrate through H-bonding and π-π interactions. The proximity to the thioxanthone moiety facilitates energy transfer to the substrate and provides facial selectivity towards the [2 + 2] photocycloaddition for the formation of **1.18**. The authors also note that the reaction is sluggish in the absence of the chiral thioxanthone catalyst, indicating that the catalyst is required for initial absorption of the photon and that the H-bonding interaction may sufficiently lower the energy of the enone, further facilitating the energy transfer process between the catalyst and substrate. In the second example, a chiral Ir-based polypyridyl complex (Λ-Ir) was synthesized by the Yoon group and its ability to preform a similar reaction was evaluated in 2017 (**Scheme 1.5**, Eq. (3)).[24] This complex also participates in H-bonding and π-π

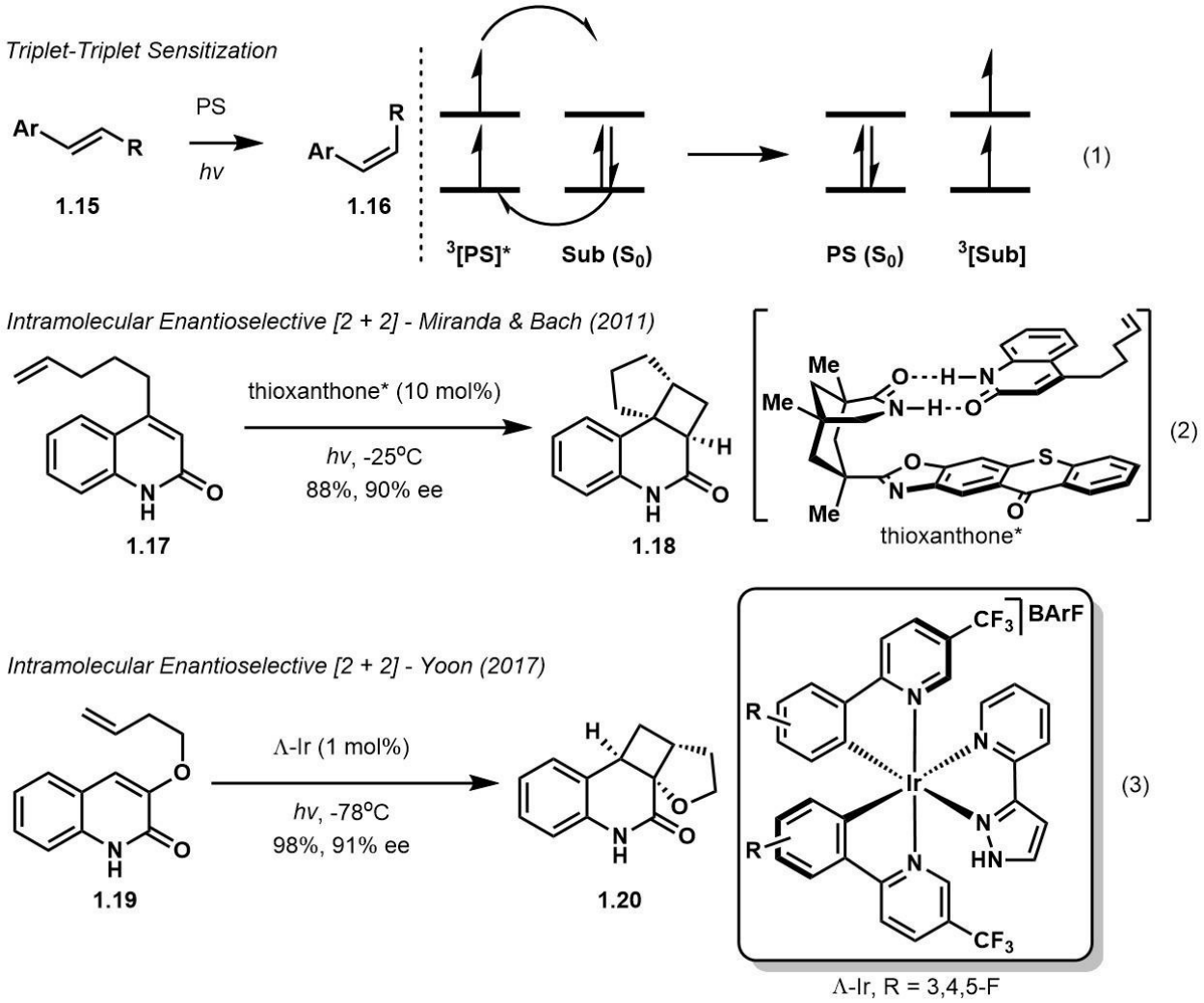

Scheme 1.5 Photosensitization reactions and [2 + 2] photocyclization.

interactions with substrate **1.19**, facilitating the energy transfer process by the substrate's proximity to the photosensitizer, where the polypyridyl ligands transpose their chiral information during the cycloaddition and give cyclobutane product **1.20** in high yield and enantiomeric excess (ee). Experiments blocking the H-bonding ability of the pyrazole group on one of the ligands of Λ-Ir were conducted and loss of stereoinduction was observed, demonstrating the role of the ligand in the transformation.

1.2.3 Hydrogen Atom Transfer (HAT)

Hydrogen atom transfer (HAT) reactions when viewed in the context of a redox-neutral scope represent the most waste-limiting transformations as there are little by-products formed. In the past decade, a tungsten-based complex, $[W_{10}O_{32}](NBu_4)_4$ (TBADT), has been shown to be extraordinarily efficient at undergoing HAT reactions with alkanes in its excited-state.[25] Shown below is the photo-mediated direct β-functionalization of ketones (**1.21**) using TBADT and an electron-deficient alkene in a Giese-type radical addition (**Scheme 1.6**, Eq. (1)). In a simplified model, proposed is an oxygen-based radical intermediate upon excitation of **TBADT** where this relatively electrophilic heteroatom-based radical has an affinity for HAT processes (S_H2) with relatively nucleophilic C–H bonds. Interesting, HAT at the α-position cyclopentanone would lead to a relatively electrophilic alkyl radical; a polarity mismatch. Considering HAT at the β-position of **1.21** would lead to a polarity-matched relatively nucleophilic alkyl radical, the authors offer this explanation to describe the observed selectivity in this reaction. These complexes undergo the reaction with a variety of alkanes, largely at the position with the most nucleophilic C–H bond, each with BDEs lower than 96 kcal/mol.[26] Upon generation of the relatively nucleophilic alkyl radical (**I**), this intermediate is also electronically well suited to add upon an electron-deficient alkene, giving relatively

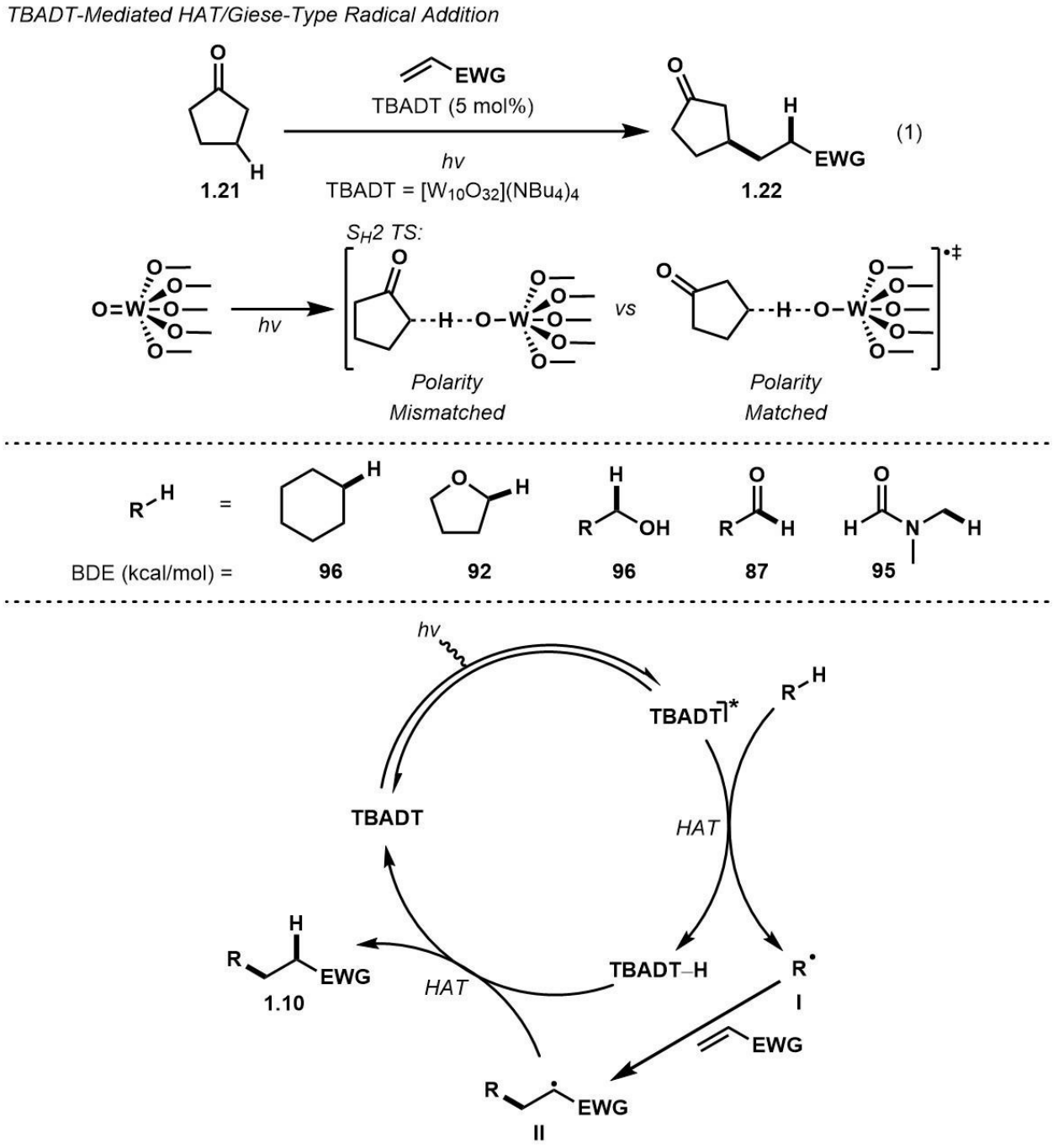

Scheme 1.6 Excited-state TBADT mediated HAT/Giese-type radical addition.

electrophilic radical intermediate **II**. Proposed is a HAT process between radical intermediate **II** and the intermediate **TBADT–H**, giving the final product **1.10** (**1.22** when using **1.21**) and regenerating the ground-state **TBADT**. Potential chain-propagating reactions must also be considered between radical intermediate **II** and the equivalent of

Table 1.3 Substrates used for intramolecular [1,5] HAT/coupling reactions.

Intramolecular [1,5] HAT/Coupling Strategy

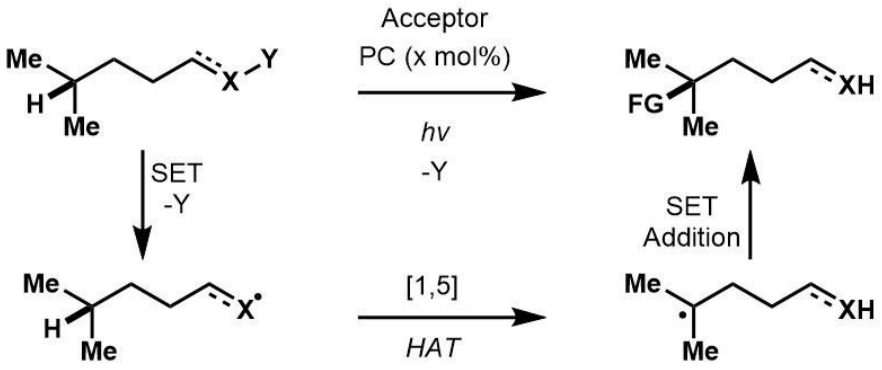

Entry	Precursor	$E_{1/2}^{(Q+/Q)}$	$E_{1/2}^{(Q/Q-)}$	By-products
1[a]	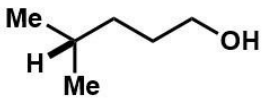	~+1.9	---	---
2	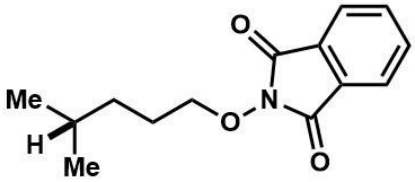	---	−1.3	HNPhth
3[b]	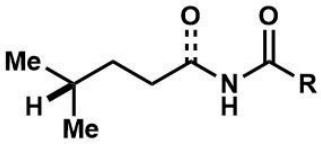	+1.0	---	---
4	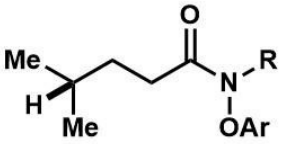	---	−0.2 to −1.0	HOAr
5	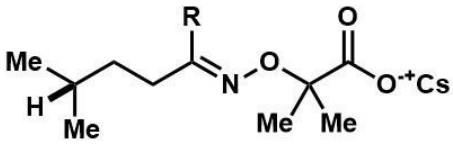	+1.7	---	CO_2, $(CH_3)_2CO$
6	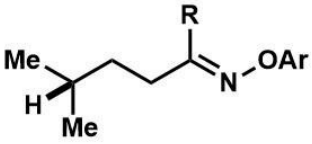	---	−1.0	HOAr

*Potentials in V vs SCE; see references for details. [a]$CeCl_3$ as photoactivating complex. [b]In the presence of base.

Table 1.4 Substrates used for fragmentation/coupling reactions.

Fragmentation Strategy

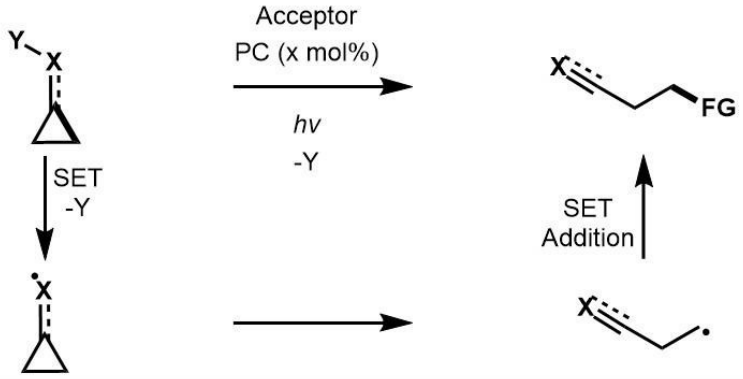

Entry	Precursor	$E_{1/2}^{(Q+/Q)}$	$E_{1/2}^{(Q/Q-)}$	By-products
1		+1.4	---	---
2	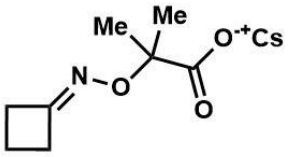	+1.7	---	CO_2, $(CH_3)_2CO$
3	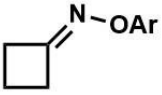	---	−1.0	HOAr

*Potentials in V vs SCE; see references for details.

alkane coupling partner as they could also be considered electronically aligned to undergo HAT processes.

When considering SET processes, a variety of substrates can be harnessed to make electrophilic heteroatom-based radicals that are capable of undergoing HAT reactions, especially intramolecular [1,5] processes (summarized in **Table 1.3**).[27] A variety of substrates are therefore compatible with the reactions mediated by an excited-state photoredox catalyst through reductive and oxidative quenching processes described in section **1.2.1**. These electrophilic heteroatom-based radicals include alkoxy, amidyl, imidyl intermediates where reactions have enjoyed success in one of the synthetic

chemist's favourite radical reactions; the Giese reaction (intermolecular *vide infra*). On a side note, recent work has seen the ability to induce fragmentation reactions providing alkyl radicals that may participate in addition reactions utilizing some similar functional groups (**Table 1.4**).[28] After reductive or oxidative quenching from an excited-state photoredox catalyst, alkoxyl and imidyl radicals functionalized with cyclic alkanes may release strain through fragmentation, resulting in longer chain radicals bearing ketone and nitrile functionality that can undergo further addition/coupling reactions.

1.2.4 Inner-Sphere C–X Bond Activation with $[Au_2(\mu\text{-dppm})_2]X_2$

Nonactivated bromoalkanes are synthetically useful bench-stable precursors to alkyl radicals. Given their prevalence in most synthetic laboratories, methodology in photoredox catalysis would be highly valuable. The stability of these compounds also translates into their relatively large redox potential (>-2.0 V *vs* SCE) and thus few photoredox catalysts are capable of oxidative quenching ($E_{1/2}^{(M+/M^*)}$), *vide supra* (**Figure 1.4**). As eluded to previously, binuclear Au(I) bisphosphine complexes such as $[Au_2(\mu\text{-dppm})_2]Cl_2$, were found to be powerful reductants in their excited-states, capable of engaging nonactivated bromoalkanes via an oxidative quenching pathway. In 1989, the discovery of these complexes was made by investigators curious as to the affect of Au–Au interactions to the photophysical and photoredox properties of such complexes.[29a–c] In the years since, much effort has been placed in understanding the nature of the aurophilic interactions inherent to these binuclear structures. In 2015, an elegant study by Che and coworkers was reported that highlighted the extent of aurophilic interaction present in the ground-state *vs* excited-state of binuclear Au(I) bisphosphine complexes.[29d] Utilizing an ultrafast time-resolved spectroscopic study, it was shown that these complexes bear little

aurophilic interaction in the ground-state, however, upon excitation ($[Au_2]^*$), an electron is promoted from an anti-bonding $5d_z^2$ orbital into a $6s/6p_z$ ($_z$ as defined by the plane made between the Au atoms) bonding orbital (^{1}5dσ*6pσ), forming a Au–Au bond and undergoing ISC to ^{3}5dσ*6pσ at rapid timescales (~0.15 ps) (**Figure 1.7**, **A**). The complex was found to live for ~510 ps (in DCM) with a tendency to increase coordination number at the Au(I) centre by inner-sphere oxidative quenching (exciplex formation) with a C–X bond of the solvent, forming an intermediate [$ClAu^I$–$Au^{II}Cl_2$] complex. The described phenomenon allows the excited-state complex to engage in redox chemistry with alkyl radical precursors (such as bromoalkanes/arenes) that have much higher redox potentials than the excited-state complex ($E_{1/2}^{M+/M^*}$ = –1.6 V *vs* SCE).

In 2016, Barriault and Scaiano used circular dichroism spectroscopy to show that the binuclear Au(I) complex in the presence of a chiral bromoalkane induced a differential absorption profile, supporting the inner-sphere interaction between the excited-state complex and bromoalkane.[11b] A series of UV–Vis spectra were taken of $[Au_2(\mu\text{-dppm})_2]Cl_2$ and $[Au_2(\mu\text{-dppm})_2](NTf_2)_2$ with varying concentrations of bromobutane present (Job plot) to investigate ground-state pre-association of the binuclear Au(I) complex and bromoalkane, however, changes to the complex's absorption profile were not observed, indicating that the inner-sphere interaction occurs in the excited-state (exciplex). The inner-sphere exciplex pathway is distinct from the outer-sphere MLCT mechanism that is operative with Ru- and Ir-based polypyridyl complexes. In a redox-neutral catalytic system, the excited-state Au(I) complex **II** undergoes oxidative quenching with a bromoalkane via the described inner-sphere exciplex (**III**). After quenching, an alkyl

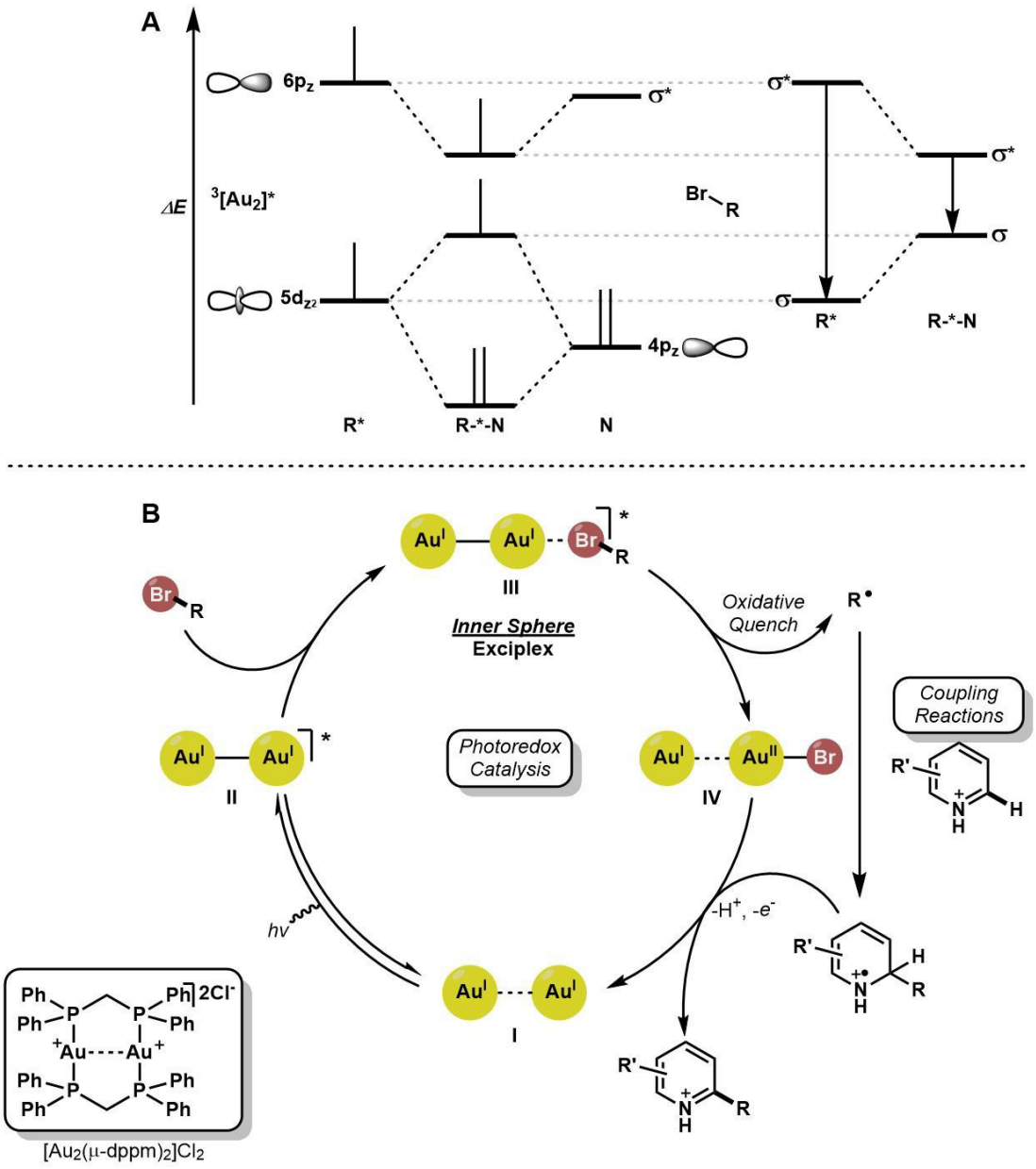

Figure 1.7 Photoredox catalysis with binuclear Au(I) bisphosphine complexes.

radical is born that may participate in addition/coupling reactions such as the Minisci reaction along with Au-based intermediate **IV** (an oxidant). The intermediate arising from the addition reaction can then be oxidized by intermediate **IV**, giving the desired product and regenerating the ground-state photocatalyst.

With these tactics for synthesis using photoredox catalysis in hand, the synthetic organic chemist can apply these concepts to dual photoredox strategies and challenging

enantioselective transformations; a notoriously difficult topic in radical chemistry arising from the sp^2 nature of alkyl radicals.

1.3 Strategies in Dual Photoredox Catalysis and Enantioselective Transformations

As with most radical-mediated organic transformations, enantioselective radical reactions are rooted in the use radical initiators and organostannane chain carriers. The tin method traditionally uses radical initiators such as AIBN that require heat for initial decomposition and initiation of radical chains. Enantioselective transformations often require cooled conditions, -78°C for instance, to achieve high enantioselectivity; a challenging task for the tin method. In 1995, Porter and coworkers identified that the tin method could be used in combination with a Et_3B/O_2 initiation protocol to surmount the current limitation.[30a-c] Now able to initiate radicals derived from iodoalkanes at cool temperatures, a chiral Lewis acid chelation strategy was developed for an enantioselective transformation combining the Giese and Keck (an allylation reaction that producing tributyltin radicals that is advantageous over using tributyltin hydride in intermolecular transformations) reactions using $Zn(OTf)_2$ and a chiral BOX ligand (**Scheme 1.7**, Eq. (1)). Upon chelation of the metal/ligand to the oxazolidinone-bearing **1.23**, an alkyl radical undergoes addition to this activated intermediate, resulting in an electrophilic radical (Eq. (1)). The preference of relatively nucleophilic alkyl radicals to undergo addition reactions on electron-deficient alkenes (**1.23**) over electron-rich alkenes (**1.24**) allowed for the chemoselectivity observed in this reaction. The electrophilic alkyl radical is subject to the chiral environment created by the metal/ligand bound to the auxiliary group (proposed as a tetrahedral Zn-intermediate based on the observed

enantioselectivity) and is electronically matched to undergo addition to electron-rich alkene **1.24**, giving the enantioenriched product **1.25** and a chain propagating tributyltin radical. Notably, the reaction does not proceed efficiently in the absence of the chelating metal/ligand, indicating that this interaction sufficiently lowers the barrier of reaction.

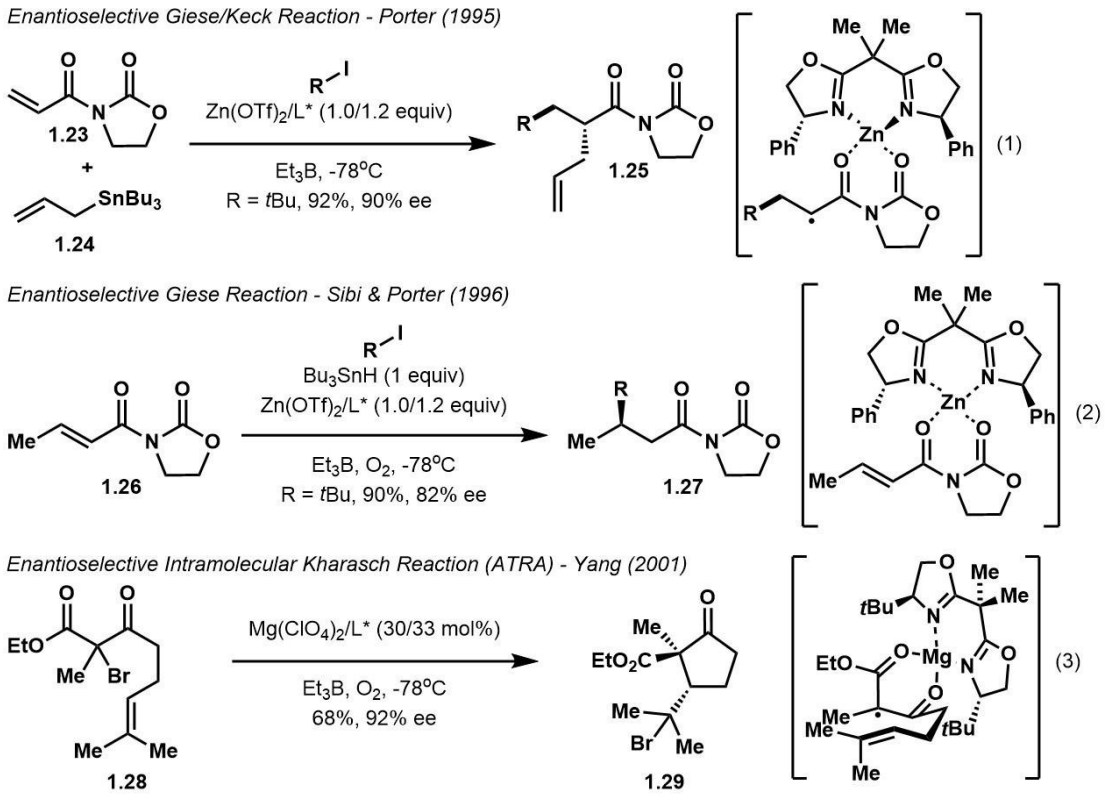

Scheme 1.7 Enantioselective radical reactions mediated by the tin method.

Work by Sibi and Porter demonstrated that this system was also applicable to the Giese reaction using prochiral **1.26** functionalized with an oxazolidinone auxiliary using tributyltin hydride, leading to enantioenriched product **1.27** (**Scheme 1.7**, Eq. (2)).[30d] The observed enantioselectivity was proposed to derive from a square planar Zn-intermediate in this case (a tetrahedral intermediate was also considered but would require the enone portion of **1.26** to have a *s-trans* configuration believed to be higher in energy due to steric interactions over the *s-cis* configuration shown in Eq. (2)). Perceptively realizing that the reaction of **1.26** was facilitated by the activating chelation of the metal/ligand to the

auxiliary, Sibi later developed an efficient catalytic system similar to Eq. (2) to achieve an enantioselective catalytic Giese reaction mediated by chiral Lewis acids.[30e]

In 2001, Yang and coworkers realized that α-bromoesters such as **1.28** were efficient radical bromo-transfer reagents capable of Kharasch-type ATRA reactions without the need for organostannanes (**Scheme 1.7**, Eq. (3)).[30f, g] Using a similar system with a Mg-based Lewis acid and chiral BOX ligand combination, enantioenriched **1.29** was obtained by a proposed square planar Mg-intermediate. A variety of organic transformations not mentioned herein have been possible with these advancements in enantioselective radical reactions.[30h]

Combining the concepts developed in photoredox catalysis with enantioselective radical transformations, organic chemists were keen to identify methodology that would allow for mild and efficient enantioselective photo-mediated organic transformations.[31] The following is a highlight of impactful redox-neutral dual catalytic strategies and enantioselective transformations using photoredox catalysis.

1.3.1 Dual Photoredox Catalysis with Chiral Lewis Acids

In 2015, Yoon and coworkers reported the enantioselective dual photoredox chiral Lewis acid catalyzed Giese reaction; a staple in radical chemistry (**Scheme 1.8**, Eq. (1)).[32a] Employing the reductive quenching pathway of $*[Ru(bpy)_3]Cl_2$ with trialkylamine **1.30**, the resulting α-amino radical underwent addition to electron-deficient alkene **1.31**. The enantioselectivity observed in this reaction was mediated by a catalytic Sc-based Lewis acid ligated with a chiral PYBOX ligand on the auxiliary portion of **1.31**. The authors noted a significant rate acceleration for radical addition to the Lewis acid activated alkenes, allowing the transformation to proceed efficiently at room temperature with low catalytic loadings of Lewis acid/ligand. After addition, the resulting electrophilic radical is

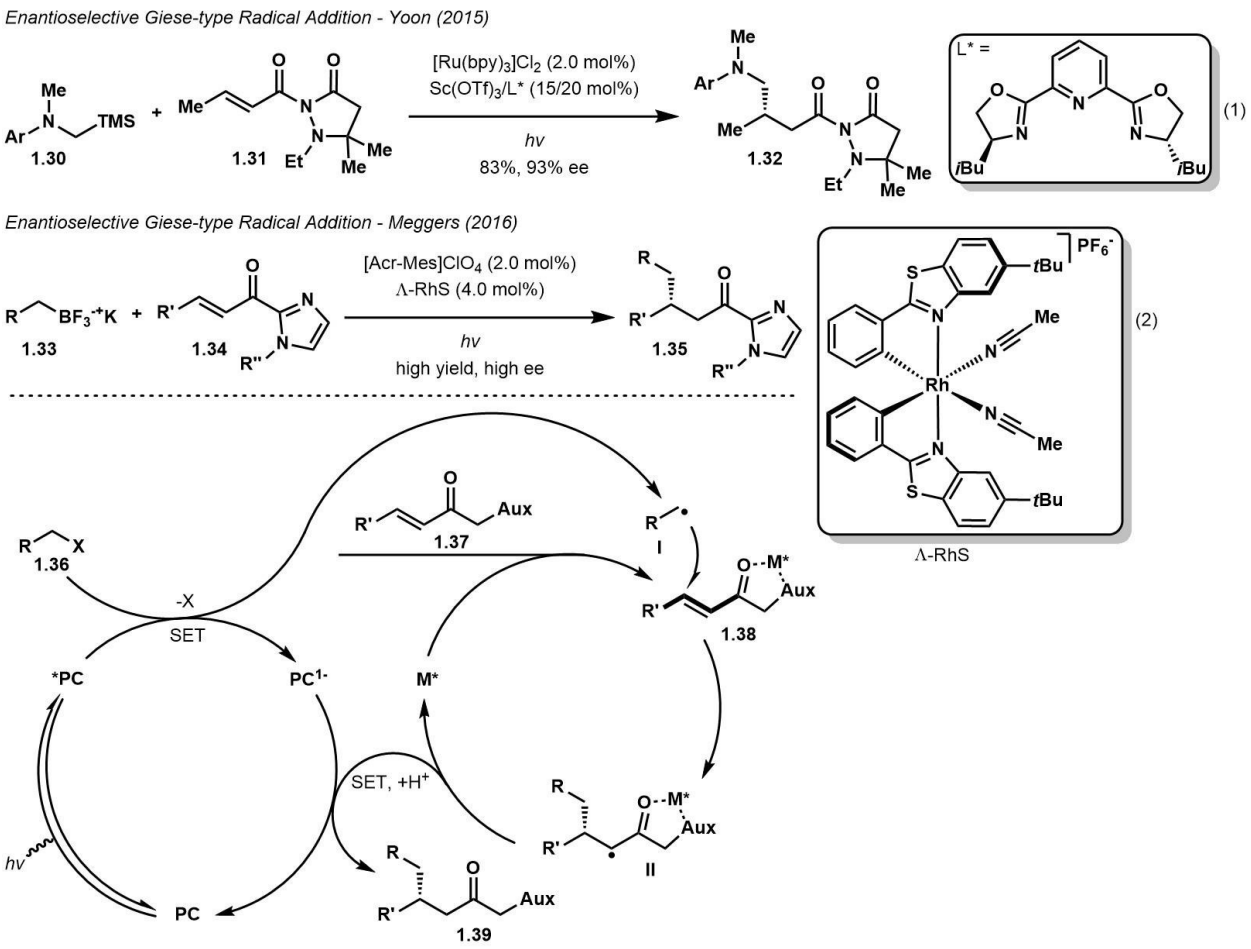

Scheme 1.8 Enantioselective photo-mediated Giese reaction.

reduced by the intermediate Ru-complex (**PC^{1-}**), giving product **1.32** and regenerating the photoredox catalyst.

In the following year, Meggers and coworkers reported a similar transformation using an organic based dye, [Mes-Acr-Me]ClO_4, as photoredox catalyst to undergo reductive quenching with trifluoroborates (**1.33**, **Scheme 1.8**, Eq. (2)).[32b] The radical generated from this process added efficiently to the auxiliary functionalized electron-deficient alkene **1.34** which was chelated by an interesting Rh-complex (Λ-RhS). The result was a highly efficient system giving excellent yields and high ee for products related to **1.35**. In general, redox-neutral dual photoredox and chiral Lewis acid catalyzed

transformations such as the enantioselective Giese reaction proceed via a reductive quenching pathway between ***PC** and radical precursor **1.36**, giving an alkyl radical (**I**) and **PC^{1-}** (a reductant). Upon chelation of an activated alkene (**1.37**) to a chiral Lewis acid/ligand, alkyl radical **I** can add enantioselectively to **1.38**, leading to electrophilic radical intermediate **II**, where upon reduction by **PC^{1-}** leads enantioenriched products such as **1.39** and regenerates the photoredox catalyst.

1.3.2 Chiral Thiyl Radical Catalysis

In 2014, Maruoka and coworkers described an enantioselective variation of a photoinitiated thiyl radical-mediated cascade cyclization manifold using a chiral thiol catalyst (**Scheme 1.9**, Eq. (1)).[33] The chiral thiol catalyst, a marvel of construction, consisted of a highly decorated thiophenol, providing significant steric interactions to bound intermediates. After photoinitiation using benzoyl peroxide (BPO), the chiral thiyl radical can add to the cyclopropane functionalized alkene **1.40**, giving electrophilic radical intermediate **I**, now electronically compatible for addition to electron-rich alkene **1.41**, giving intermediate **II**. The steric environment provided by the chiral thiol allows for the diastereo- and enantioselective *5-exo-trig* cyclization and subsequent fragmentation giving product **1.42** in excellent yields while regenerating the chiral thiyl radical catalyst.

1.3.3 Dual Photoredox Catalysis with Organocatalysis

In 2008, MacMillan reported the seminal contribution to dual photoredox organocatalyzed transformations, substantiating the concept of SOMO activation, that is, the one-electron chemistry derived from redox processes with enamines (**Scheme 1.10**, Eq. (1)).[34a, b] In this transformation, *$[Ru(bpy)_3]Cl_2$ undergoes oxidative quenching with radical precursor **1.44**, giving oxidized Ru^{III} intermediate (**PC^{+}**, an oxidant) and an alkyl radical **I**. The radical then proceeds to add to chiral enamine **II** (derived from the

condensation of MacMillan's catalyst **1.45** and aldehyde **1.43**), giving enantioenriched intermediate **III**. The intermediate is then oxidized by **PC⁺**, thus regenerating the photoredox catalyst and upon hydrolysis, gives product **1.46** and regeneration of **1.45**. It should be noted that Melchiorre and coworkers have shown that this transformation may

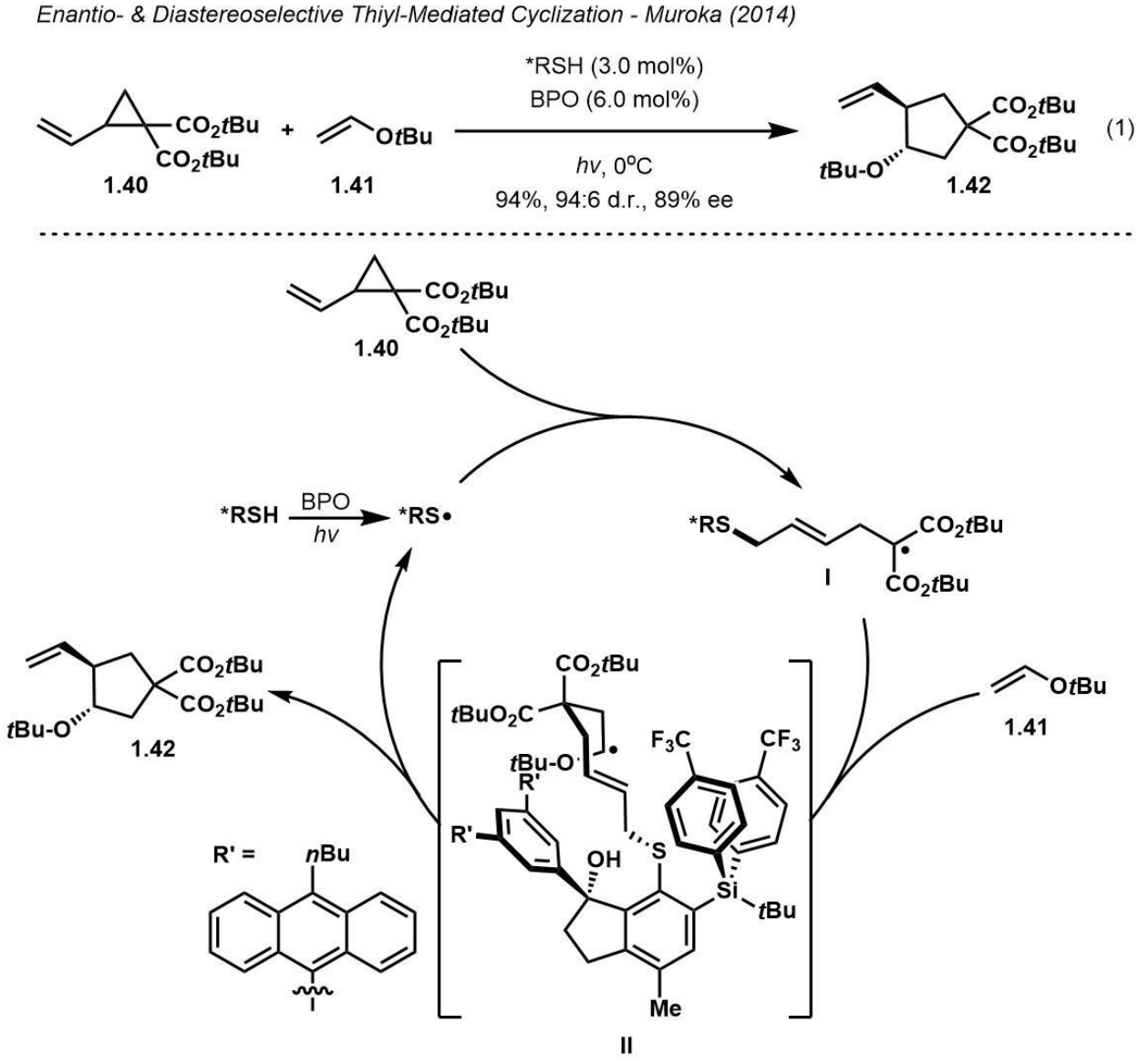

Scheme 1.9 Photo-initiated chiral thiyl radical catalysis.

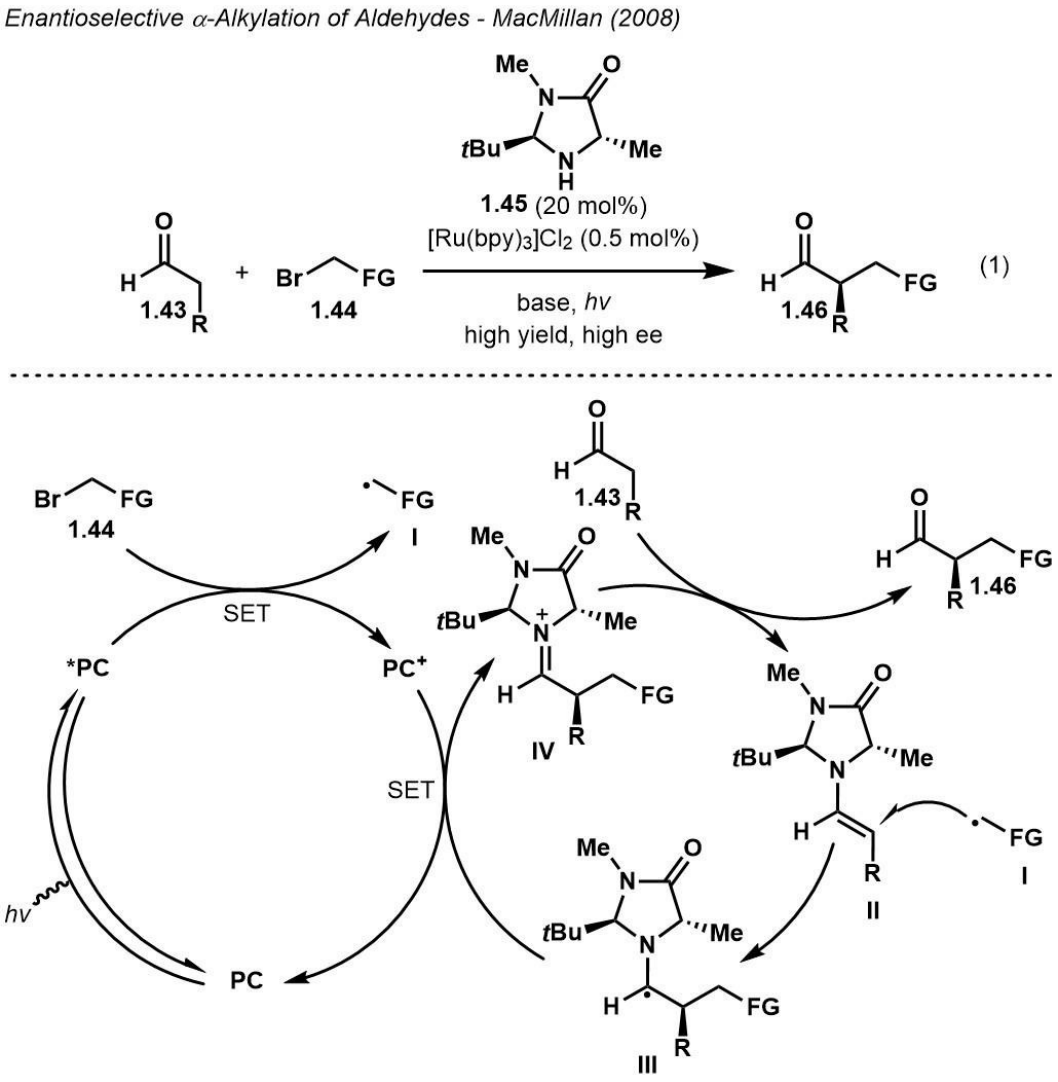

Scheme 1.10 Enantioselective dual photoredox and organocatalysis.

be mediated by light without need of photoredox catalyst via an excited donor-acceptor (EDA) complex when **1.44** is sufficiently activated.[34c]

In 2016, Fagnoni and Melchiorre disseminated the enantioselective dual photoredox organocatalyzed Giese reaction, demonstrating the prospects of combining photocatalysis with LUMO-lowering strategies (iminium catalysis, **Scheme 11**, Eq. (1)).[34d] In this study, the HAT properties of ***TBADT** were used to generate alkyl radicals from tertiary C–H bonds (**1.48**). The ensuing radical was then added to the activated chiral

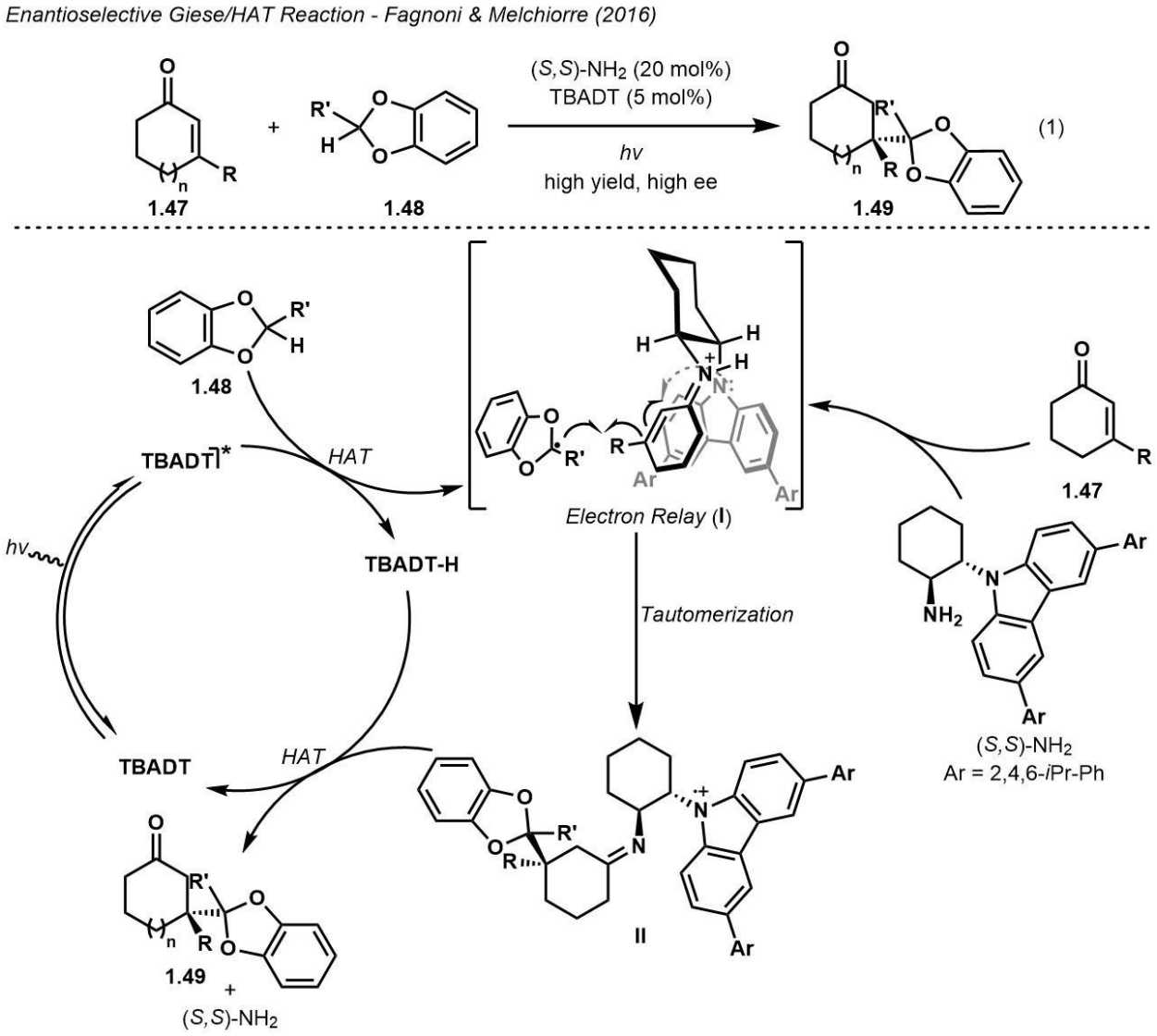

Scheme 1.11 Enantioselective dual photoredox and organocatalyzed HAT Giese reaction.

iminium complex derived from the condensation of diamine organocatalyst (*S,S*)-NH_2 and cyclic enone **1.47**. The authors propose that the inclusion of a pendent carbazole functionality in the diamine catalyst is essential for the proximity induced (as judged by X-ray crystallographic analysis) electron relay (**I**) SET pathway between the intermediate electrophilic intermediate radical and carbazole, leading to intermediate **II** after tautomerization. The authors suggest that subsequent HAT processes arise between

intermediate **II** and **TBADT–H**, regenerating the photocatalyst and upon hydrolysis, giving enantioenriched product **1.49** and the organocatalyst.

1.3.4 Dual/Triple Photoredox with Transition Metal/HAT Catalysis

In 2014, the groups of Molander and Doyle/MacMillan published the dual photoredox and Ni-catalyzed cross-coupling of alkyl trifluoroborates or carboxylates with haloarenes; a discovery garnering comparable interest to the Suzuki-Miyaura cross-coupling (**Scheme 1.12**, Eq. (1)).[35a, b] This discovery provided organic chemists with an alternative strategy for alkyl-aryl cross-coupling reactions that has often been limiting in substrate scope and difficult to control with respect to by-product formation (i.e. β-hydride elimination reactions when using Pd-catalysis). In this reaction, excited-state Ir-based complex (***PC**) undergoes reductive quenching with **1.51**, generating an alkyl radical and **PC^{1-}** (a reductant). Upon oxidative insertion of the Ni^{0}-catalyst **I** with haloarene **1.50** (**FG–X**), forming FG–Ni^{II}–X intermediate **II**, the alkyl radical may add to intermediate **II**, giving alkyl-substituted FG–Ni^{III}–X intermediate **III**. Reductive elimination from intermediate **III** gives the cross-coupled desired product **1.52** and Ni^{I}–X intermediate **IV**. Reduction of intermediate **IV** from **PC^{1-}** regenerates both the active Ni^{0}-catalyst **I** and the ground-state photoredox catalyst **PC**. An array of transformations has been successful in cross-coupling 1°, 2°, and 3° alkyl radicals with alkyl, alkenyl, and aryl coupling partners.[35c] The authors were successful in developing enantioselective variations by incorporating chiral ligands into the cross-coupling strategy (**Scheme 1.12**, Eq. (2)).[35d, e]

In this time, a variety of strategies have been devised for the photo-mediated dual and triple catalyzed coupling reactions involving HAT processes mediated by organocatalysts (**Scheme 1.13**).[36] Vital to the HAT processes with a variety of alkanes

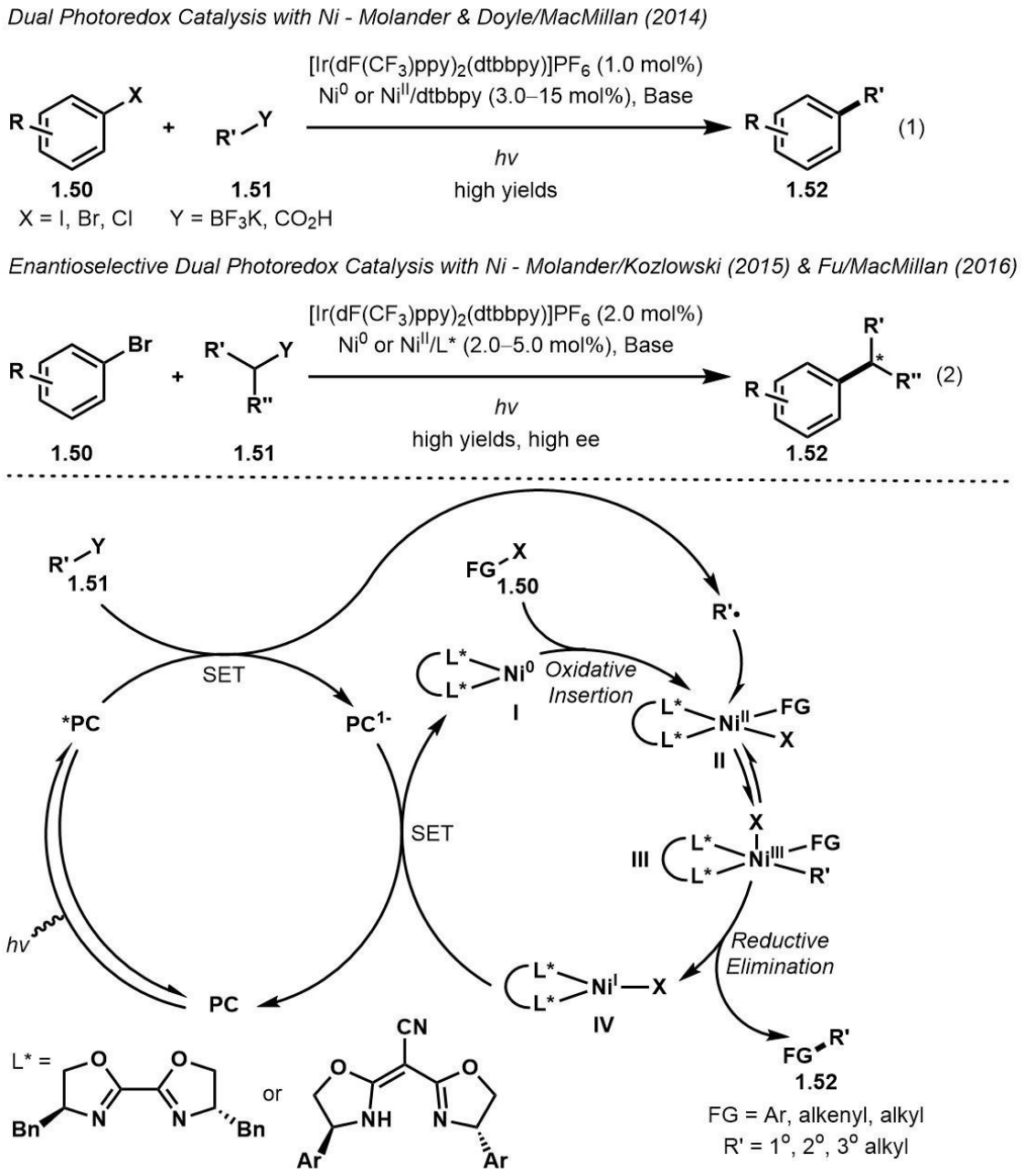

Scheme 1.12 Enantioselective dual photoredox and Ni catalysis.

(BDE < 96 kcal/mol, **R–H** in mechanism below) is the reductive quenching of organic based reagents (**X**$^{-}$ below) such as quinuclidines, amides, thiols, and phosphates (**A**) with the excited state of a photoredox catalyst, ***PC**, resulting in **PC**$^{1-}$ and catalytic intermediate electrophilic heteroatom-based organic radicals (**B**, BDEs range 87–103 kcal/mol for **C**) capable of HAT reactions with **R–H**. Upon HAT, **X–H** (**C**) is formed along with a relatively

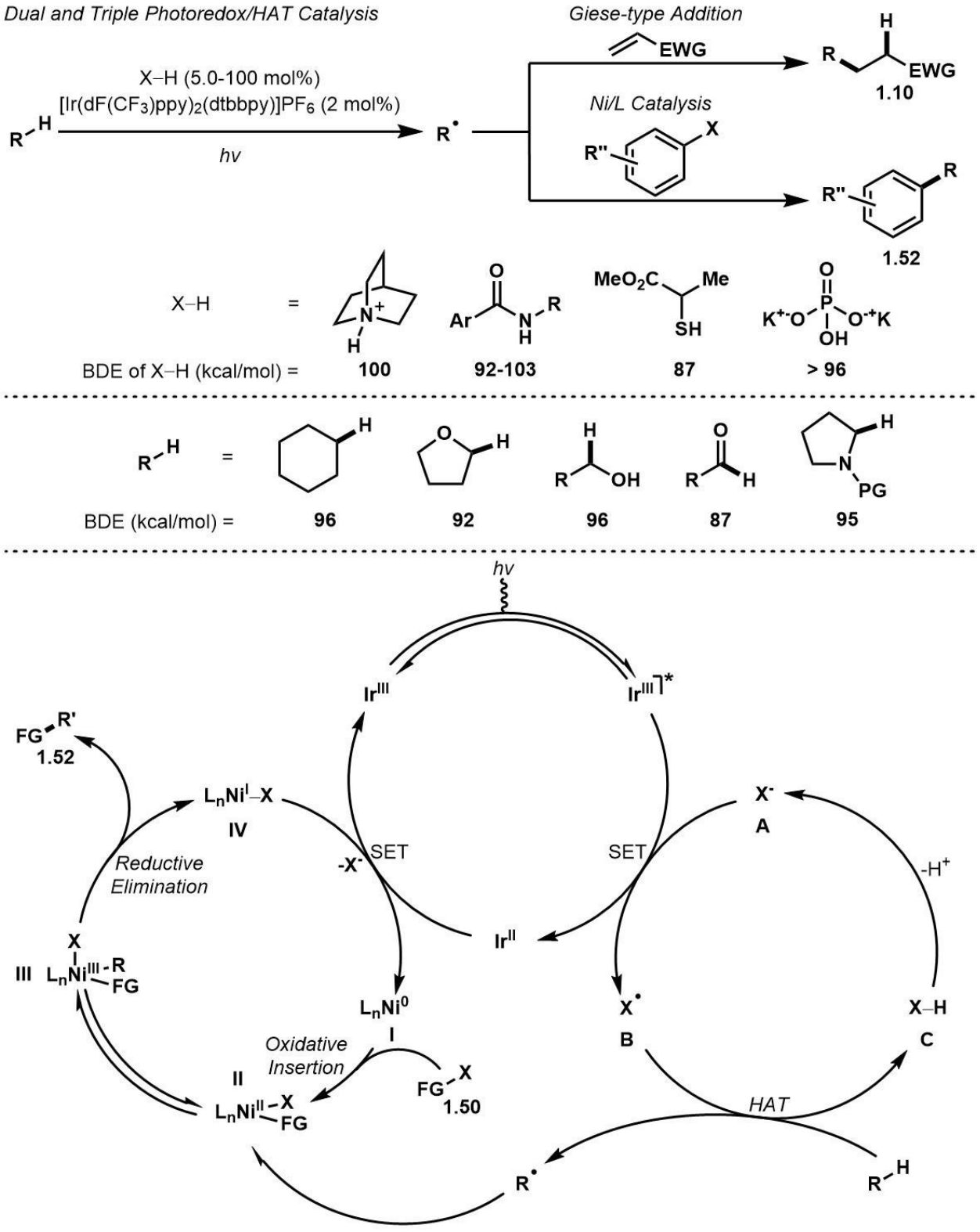

Scheme 1.13 Dual and triple photoredox, HAT, and transition metal catalysis.

nucleophilic alkyl radical capable of participating in transformations such as the Giese reaction (dual catalysis) and Ni-catalyzed cross-coupling (triple catalysis).

Since the publication of the triple photoredox organo-mediated HAT/Ni-catalyzed cross-coupling reaction, Molander and Doyle have described methodology to achieve the similarly cross-coupled products (**1.52**) without the use of the organocatalyst (**Scheme 1.14**, Eq. (1)).[37] In the proposed mechanism, the Ar–Ni^{II}–X intermediate **II** undergoes

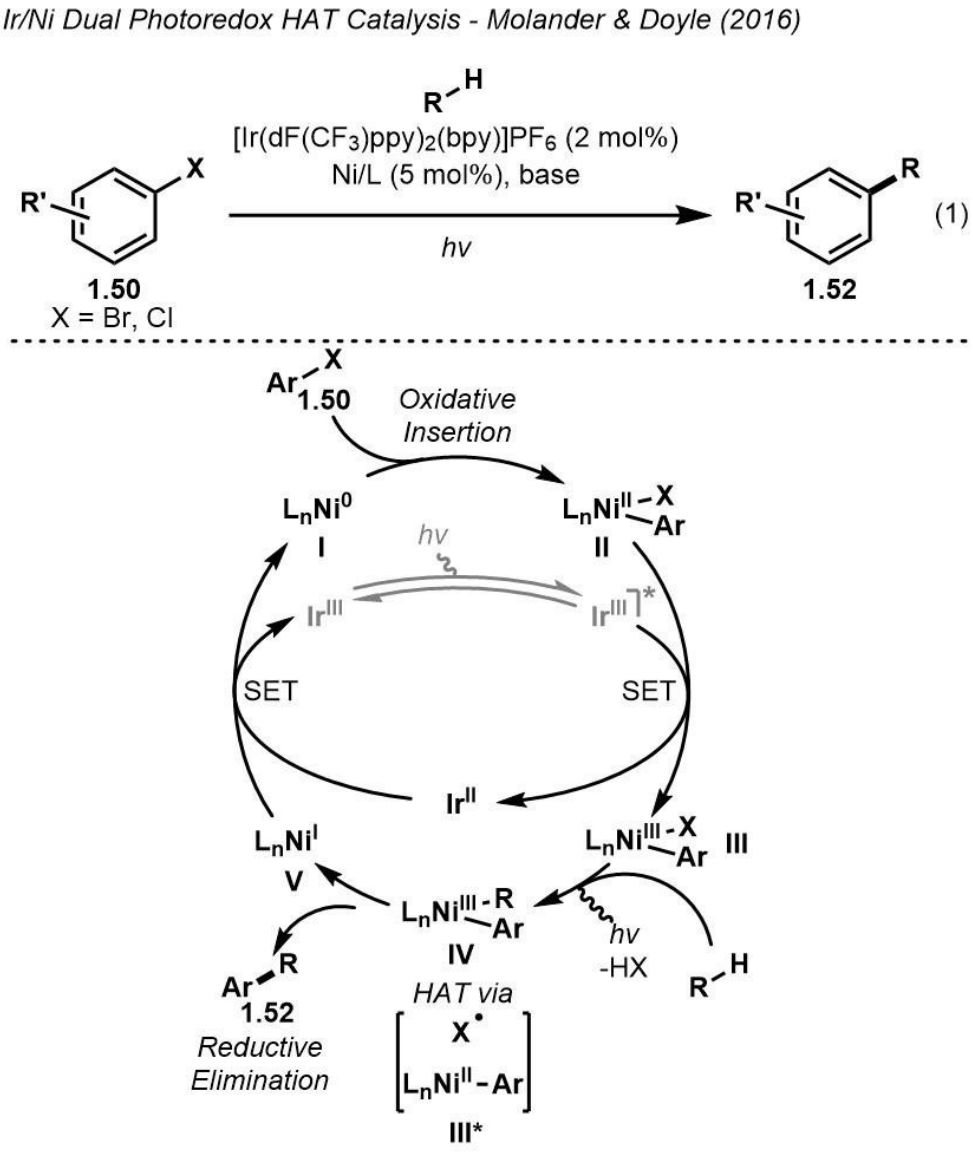

Scheme 1.14 Alternative dual photoredox/HAT strategy.

reductive quenching with ***PC**, giving Ar–Ni^{III}–X intermediate **III** and $\mathbf{PC^{1-}}$. Upon absorption of a photon, intermediate ***III** participates in a HAT reaction with an alkane and the alkyl radical formed may add upon the Ar–Ni^{II} intermediate, leading to alkyl-functionalized Ar–Ni^{III} intermediate **IV**. Reductive elimination of IV gives the desired product **1.52** and Ni^{I}-intermediate **V**, where reduction by $\mathbf{PC^{1-}}$ leads to regeneration of Ni^{0}-intermediate **I** and **PC**. Clearly the photochemical properties of transition-metal complexes/intermediates in cross-coupling reactions are of high interest to the organic community and with further scrutiny, curious advancements can be expected in the future.

Dual photoredox/HAT catalytic Minisci Addition with Alcohols - MacMillan (2015)

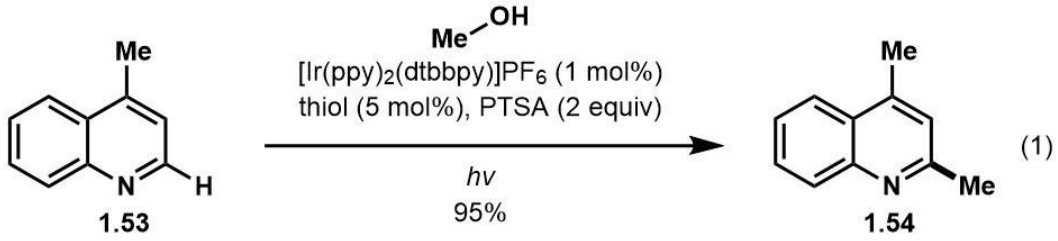

Scheme 1.15 Dual photoredox/HAT catalysis in the Minisci reaction with alcohols.

In 2015, MacMillan also reported the dual photoredox organo-mediated HAT catalyzed Minisci reaction using alcohols as the alkyl radical precursor and is worth mentioning herein (**Scheme 1.15**, Eq. (1)).[38a] Proposed is the generation of a thiyl radical that mediates this transformation via HAT with the alcohol (although other heteroatom centred radicals may be formed that derive from PTSA that could participate in this HAT event). When considering a potential HAT reaction between thiyl radical and an alcohol, intriguing is the difference in BDE between the resulting thiol (87 kcal/mol) and the α-alkoxyl C–H bond of the alcohol substrate (96 kcal/mol). Based on this analysis, one would not expect reaction to occur, however, if considering Roberts' concept of polarity-reversal catalysis (PRC) in HAT reactions, the opposite expectation is true.[38b] Intrinsic to

PRC is the notion of favourable HAT reactions occurring readily between polarity-matched substrates, for example, an electrophilic thiyl radical participating in HAT reactions with a nucleophilic (or hydridic) α-alkoxyl C–H bond. The resulting nucleophilic α-alkoxyl radical is then electronically poised to add upon the electrophilic protonated heteroarene **1.53**, where a variety of reduction processes may occur (not depicted herein) to give alkyl-functionalized **1.54** and regenerate the ground-state $\mathbf{Ir^{III}}$ catalyst. The transformation represents a facile and by-product limiting methodology for the direct alkylation of heteroarenes using commercially available alcohols.

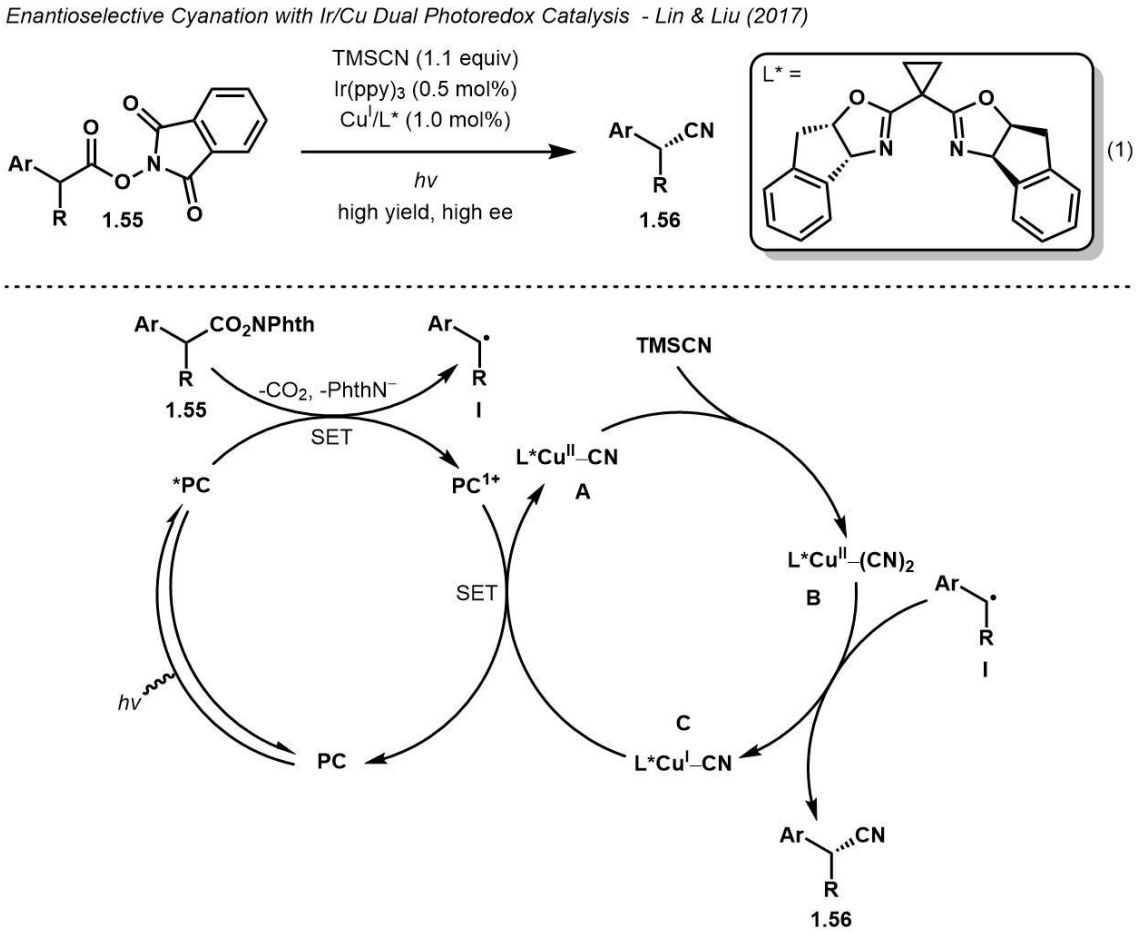

Scheme 1.16 Dual photoredox and copper catalysis.

Many of the dual photoredox catalysis reaction models have been controlled by the reductive quenching pathway, however, Lin and Liu have recently published an

enantioselective dual photoredox Cu-catalyzed cyanation reaction that operates via an oxidative quenching pathway with *N*-hydroxyphthalimide esters **1.55** (**Scheme 1.16**, Eq. (1)).[39] This reaction features a chiral BOX ligated Cu^{II}-$(CN)_2$ complex **B** as the active species that undergoes enantioselective reaction with alkyl radical **I** that was formed through the quenching process, giving **1.56** and Cu^{I}-CN complex **C**. From here, complex **C** is oxidized by $\mathbf{PC^{1+}}$, leading to the Cu^{II}-CN (**A**) precursor to complex **C** (after reaction with TMSCN) and regeneration of the photocatalyst.

1.3.5 Dual Photoredox Catalysis with Chiral Phosphoric Acids

In 2013, Knowles and coworkers reported the enantioselective cyclization of ketone bearing hydrazone **1.57** (**Scheme 1.17**, Eq. (1)).[40] Although this transformation was net-reductive using Hantzsch ester (HEH), it set precedence for the use of chiral phosphoric acids in photoredox catalysis. Through a reduction of the aryl ketone, the resulting radical intermediate **I** underwent enantioselective intramolecular cyclization via complexation with the chiral phosphoric acid catalyst, giving product **1.58** in great yield.

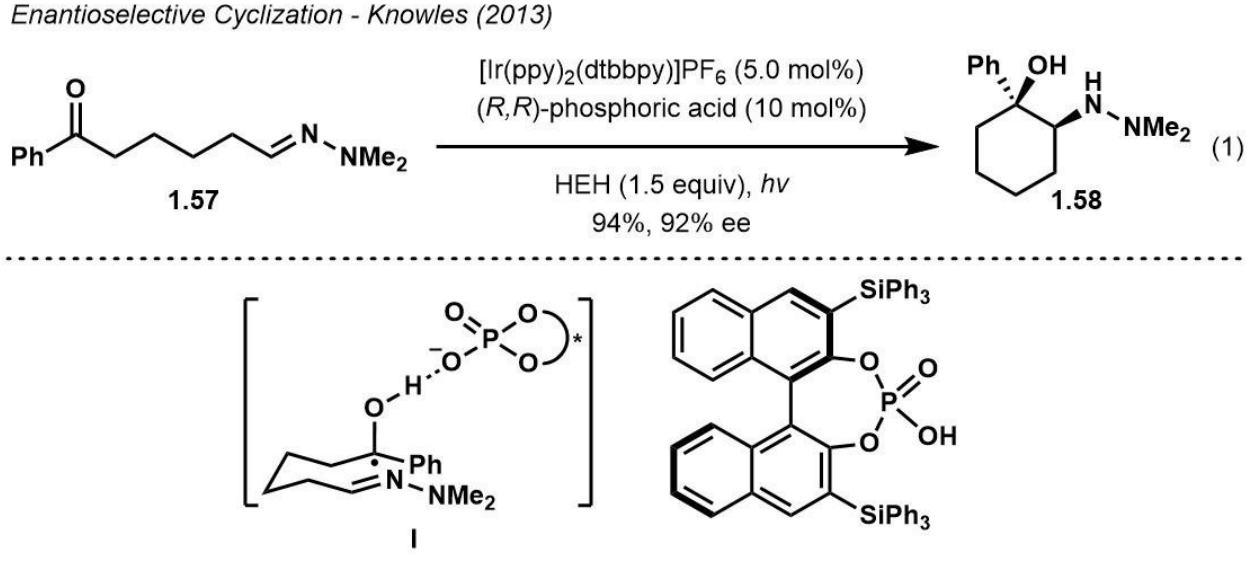

Scheme 1.17 Dual photoredox and chiral phosphoric acid catalysis.

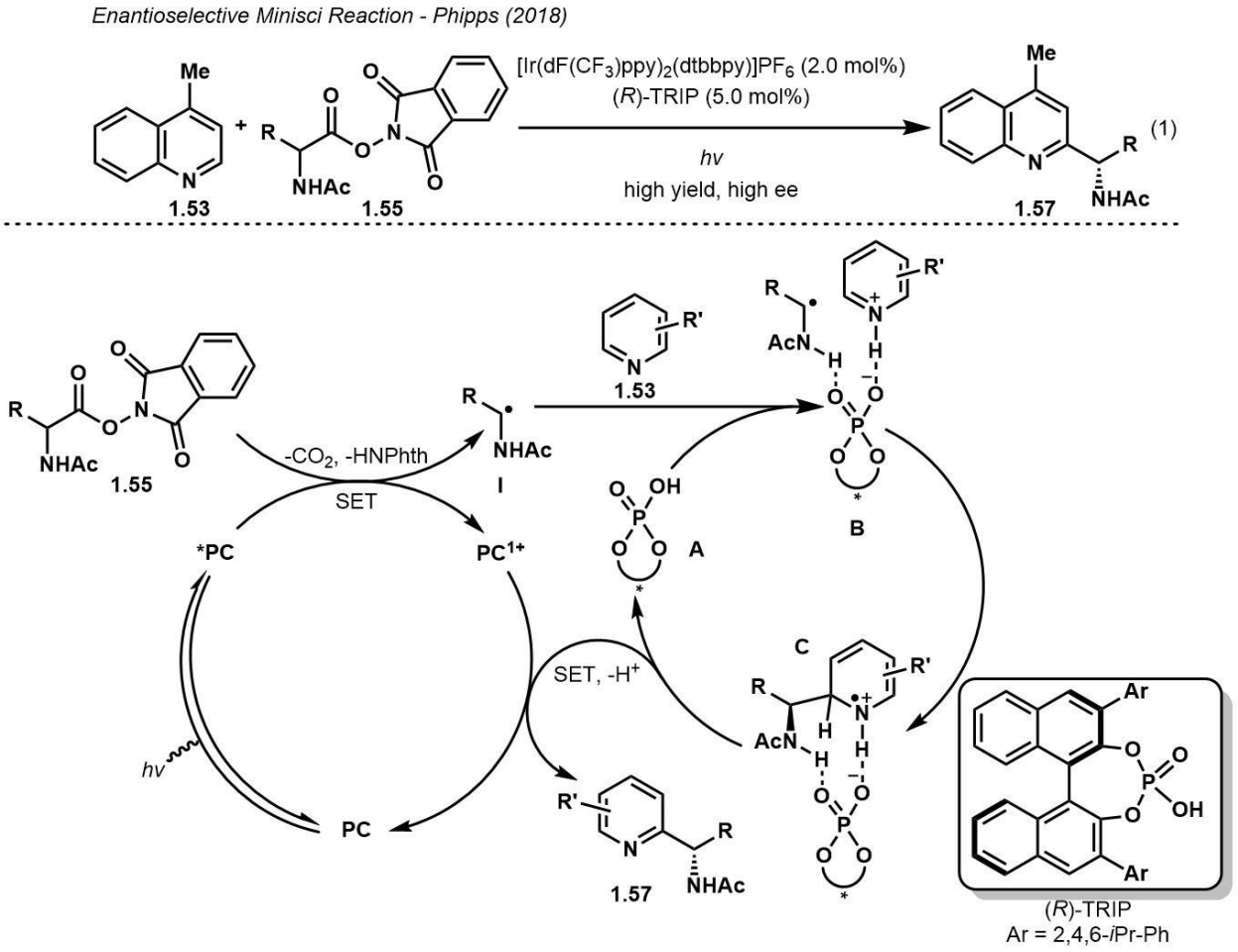

Scheme 1.18 Enantioselective dual photoredox and phosphoric acid catalyzed Minisci reaction.

In 2018, Phipps and coworkers disclosed the enantioselective dual photoredox phosphoric acid catalyzed Minisci reaction; a first of its kind. Building on redox-neutral photoredox Minisci reactions with *N*-hydroxyphthalimide esters **1.55**, the excited-state Ir^{III}-complex ***PC** proceeds via oxidative quenching with **1.55**, leading to **PC^{1+}** and NHAc functionalized alkyl radical **I**. The chiral phosphoric acid catalyst **A** ((*R*)-TRIP) binds to heteroarene **1.53**, activating the heteroarene towards addition of **I**. The chiral phosphoric acid guides the addition of **I** to **1.53** (**B**), leading to **C**, where oxidation by **PC^{1+}** gives the enantioenriched desired product **1.57**, and regeneration of **PC** and **A**. Selection of an aprotic solvent favours organization of the starting materials and intermediates that

facilitate the high enantioselectivity observed. Further mechanistic studies will likely yield more information on the nature of this complex coupling interaction and to which processes owe the observed enantioselectivity.

1.4 Outlook

The applications of photoredox catalysis in the context of radical based organic transformations are growing rapidly. The understanding of concepts associated with these photoexcited complexes and their corresponding reactivity have enabled the discovery of new reactions and innovation of classic reactions. By designing redox-neutral photocatalytic cycles, organic chemists can effectively choose photoredox catalyst and alkyl radical precursor combinations to effect high yielding methodology that is mild and waste-limiting. The chapter sought to provide the reader with a background understanding of the many ways of generating nonactivated alkyl radicals and using them in a conscientious redox-neutral manner that also extends to the elegant examples that are multi-catalytic and enantioselective. In the future, the field will be led by transformations using the most cost-effective readily available precursors that form the least by-products to achieve complex targeted-oriented synthesis, ideally under enantioselective conditions. Alkanes would be a good place to start. Of course, there are many examples that include activated alkyl or aryl radicals and their applications in dual catalytic/enantioselective transformations, but for the purposes of this thesis, they could not be included; I make no apologies for that. Although this thesis does not include examples of enantioselective transformations with triple catalysis, the topics and concepts described above have guided the formulation of our research into the unknown.

1.5 References

[1] a) Ciamician, G.; Silber, P. *Ber. Dtsch. Chem. Ges*. **1900**, *33*, 2911–2913; b) Stobbe, H. *Liebigs Ann. Chem*. **1908**, *359*, 1–48; c) Ciamician, G. *Science* **1912**, *36*, 385–394; d) Albini, A.; Dichiarante, V. *Photochem. Photobiol. Sci*. **2009**, *8*, 248–254; e) Papeo, G.; Pulici, M. *Molecules* **2013**, 18, 10870–10900.

[2] Obama, B. *Science* **2017**, DOI: 10.1126/science.aam6284.

[3] *Advances in Photochemistry*; Neckers, D. C., Wolman, D. H., Von Bunau, G., Eds.; Wiley-Interscience: New York, 1997.

[4] a) Gomberg, M. *J. Am. Chem. Soc*. **1900**, *22*, 757–771; b) Gomberg, M. *J. Am. Chem. Soc*. **1901**, *23*, 496–502; c) Gomberg, M. *J. Am. Chem. Soc*. **1903**, *25*, 1274–1277; d) Gomberg, M. *J. Chem. Educ*. **1932**, *9*, 439–451; e) Lankamp, H.; Natua, W. Th.; MacLean, C. *Tetrahedron Lett*. **1968**, *9*, 249–254.

[5] a) Curran, D. P. in *Comprehensive Organic Synthesis*; Trost, B. M., Fleming, I., Semmelhack, M. F., Eds.; Pergamon: Oxford, 1991; Vol. 4, 715–779; b) *Radicals in Organic Synthesis*; Renaud, P., Sibi, M. P., Eds.; Wiley-VCH: Weinheim, 2001; c) Togo, H. *Advanced Free Radical Reactions for Organic Synthesis*; Elsevier, 2004; d) *Topics in Current Chemistry, Radicals in Synthesis I and II*; Gansuer, A., Ed.; Springer: Berlin, 2006; Vols. 263 and 264; e) *Encyclopedia of Radicals in Chemistry, Biology and Materials*; Chatgilialoglu, C., Studer, A., Eds.; Wiley: Chichester, 2012; Vols. 1 and 2.

[6] a) Chatgilialoglu, C. *Chem. Rev*. **1995**, *95*, 1229–1251; b) Baguley, P. A.; Walton, J. C. *Angew. Chem. Int. Ed*. **1998**, *37*, 3072–3082; c) Ollivier, C.; Renaud, P. *Chem. Rev*. **2001**, *101*, 3415–3434; d) Studer, A.; Amrein, S. *Synthesis* **2002**, 835–849; e) Gilbert, B. C.; Parsons, A. F. *J. Chem. Soc., Perkin Trans. 2* **2002**, 367–387; f) Murphy, J. A.; Khan,

T. A.; Zhou, S. Z.; Thomson, D. W.; Mahesh, M. *Angew. Chem. Int. Ed*. **2005**, *44*, 1356–1360; g) Quiclet-Sire, B.; Zard, S. Z. *Pure Appl. Chem*. **2011**, *83*, 519–551; h) Ekomié, A.; Lefèvre, G.; Fensterbank, L.; Lacôte, E.; Malacria, M.; Ollivier, C.; Jutand, A. *Angew. Chem. Int. Ed*. **2012**, *51*, 6942–6946.

[7] a) Giese, B. *Angew. Chem. Int. Ed. Engl*. **1983**, *22*, 753–764; b) Giese, B.; Gonzalez-Gomez, J. A.; Witzel, T. *Angew. Chem. Int. Ed. Engl*. **1984**, *23*, 69–70; c) Walling, C. *Tetrahedron* **1985**, *41*, 3887–3900.

[8] a) Albini, A.; Fagnoni, M. *Green Chem*. **2004**, *6*, 1–6; b) Balzani, V.; Credi, A.; Venturi, M. *ChemSusChem* **2008**, *1*, 26–58.

[9] Harriman, A. *Nature* **1978**, *276*, 15–16.

[10] a) Photochemistry and Photophysics of Metal Complexes; Roundhill, D. M., Fackler Jr., J. P., Eds.; Springer: New York, 1994; b) *Principles of Molecular Photochemistry: An Introduction*; Turro, N. J., Scaiano, J. C., Ramamurthy, V., Eds.; University Science Books: Sausalito, 2009.

[11] a) Prier, C. K.; Rankic, D. A.; MacMillan, D. W. C. *Chem. Rev*. **2013**, *113*, 5322–5363; b) McTiernan, C.; Morin, M.; McCallum, T.; Scaiano, T.; Barriault, L. *Catal. Sci. Technol*. **2016**, *6*, 201–207; c) Romero, N. A.; Nicewicz, D. A. *Chem. Rev*. **2016**, *116*, 10075–10166.

[12] *For redox potentials of common substrates*: *For carboxylates*: a) Galicia, M.; Gonzalez, F. J. *J. Electrochem. Soc*. **2002**, *149*, D46–D50; *For oxalates*: b) Nawrat, C. C.; Jamison, C. R.; Slutskyy, Y.; MacMillan, D. W. C.; Overman, L. E. *J. Am. Chem. Soc*. **2015**, *137*, 11270–11273; *For boronic acids/esters and trifluoroborates*: c) Matsui, J. K.; Primer, D. N.; Molander, G. A. *Chem. Sci*. **2017**, *8*, 3512–3522; *For silicates*: d) Corcé,

V.; Chamoreau, L.-M.; Derat, E.; Goddard, J.-P.; Ollivier, C.; Fensterbank, L. *Angew. Chem. Int. Ed*. **2015**, *54*, 11414–11418; *For amines*: e) Roth, H. G.; Romero, N. A.; Nicewicz, D. A. *Synlett*, 2016, *27*, 714–723; *For Hantzsch esters*: f) Gutiérrez-Bonet, A.; Remeur, C.; Matsui, J. K.; Molander, G. A. *J. Am. Chem. Soc*. **2017**, *139*, 12251–12258; *For haloalkanes*: g) Fry, A. J.; Krieger, R. L. *J. Org. Chem*. **1976**, *41*, 54–57; h) Rondinini, S.; Mussini, P. R.; Muttini, P.; Sello, G. *Electrochim. Acta* **2001**, *46*, 3245–3258; *For N-hydroxyphthalimide esters*: i) Murarka, S. *Adv. Synth. Catal*. **2018**, *360*, 1735–1753; *For cyclopropylketones*: j) Mandell, L.; Johnston, J. C.; Day Jr., R. A. *J. Org. Chem*. **1978**, *43*, 1616–1618; *For triphenylpyridinium salts*: k) Grimshaw, J.; Moore, S.; Trocha-Grimshaw, J. *Acta. Chem. Scand. B* **1983**, *37*, 485–489.

[13] a) Okada, K.; Okamoto, K.; Oda, M. *J. Am. Chem. Soc*. **1988**, *110*, 8736–8738; b) Okada, K.; Okamoto, K.; Morita, N.; Okubo, K.; Oda, M. *J. Am. Chem. Soc*. **1991**, *113*, 9401–9402.

[14] Chu, L.; Ohta, C.; Zuo, Z.; MacMillan, D. W. C. *J. Am. Chem. Soc*. **2014**, *136*, 10886–10889.

[15] For redox-neutral Giese reactions: a) Miyake, Y.; Nakajima, K.; Nishibayashi, Y. *J. Am. Chem. Soc*. **2012**, *134*, 3338–3341; b) Choi, G. J.; Knowles, R. R. *J. Am. Chem Soc*. **2015**, *137*, 9226–9229; ref 12b; c) Chinzei, T.; Miyazawa, K.; Yasu, Y.; Koike, T.; Akita, M. *RSC Adv*. **2015**, *5*, 21297–21300; d) Ramirez, N. P.; Gonzalez-Gomez, J. C. *Eur. J. Org. Chem*. **2017**, *2017*, 2154–2163; e) Lima, F.; Sharma, U. K.; Grunenberg, L.; Saha, D.; Johannsen, S.; Sedelmeier, J.; Van der Eycken, E. V.; Ley, S. V. *Angew. Chem. Int. Ed*. **2017**, *56*, 15136–15140; *For heteroarene substitutions*: f) McNally, A.; Prier, C. K.; MacMillan, D. W. C. Science, **2011**, *334*, 1114–1117; g) Singh, A.; Arora, A.; Weaver, J.

D. *Org. Lett*. **2013**, *15*, 5390−5393; h) Prier, C. K.; MacMillan, D. W. C. *Chem. Sci*. **2014**, *5*, 4173−4178; i) Zuo, Z.; MacMillan, D. W. C. *J. Am. Chem. Soc*. **2014**, *136*, 5257−5260; *For allylation/vinylation*: ref 12c and j) Noble, A.; MacMillan, D. W. C. *J. Am. Chem. Soc*. **2014**, *136*, 11602−11605; *For reviews featuring decarboxylation chemistry*: k) Liu, P.; Zhang, G.; Sun, P. *Org. Biomol. Chem*. **2016**, *14*, 10763−10777; l) Patra, T.; Maiti, D.; *Chem. Eur. J*. **2017**, *23*, 7382−7401; m) Li, Y.; Ge, L.; Muhammad, M. T.; Bao, H. *Synthesis* **2017**, *49*, 5263−5284.

[16] Minisci, F.; Bernardi, R.; Bertini, F.; Galli, R.; Perchinummo, M. *Tetrahedron* **1971**, *27*, 3575–3579.

[17] Garza-Sanchez, R. A.; Tlahuext-Aca, A.; Tavakoli, G.; Glorius, F. *ACS Catal*. **2017**, *7*, 4057−4061.

[18] a) McCallum, T.; Barriault, L. *Chem. Sci*. **2016**, *7*, 4754−4758; b) Jin, Y.; Jiang, M.; Wang, H.; Fu, H. *Sci. Rep*. **2016**, *6*, 20068; c) Cheng, W.-M.; Shang, R.; Fu, Y. *ACS Catal*. **2017**, *7*, 907; d) Cheng, W.-M.; Shang, R.; Fu, M.-C.; Fu, Y. *Chem. Eur. J*. **2017**, *23*, 2537−2541; e) Klauck, F. J. R.; James, M. J.; Glorius, F. *Angew. Chem. Int. Ed*. **2017**, *56*, 12336−12339; f) Nuhant, P.; Oderinde, M. S.; Genovino, J.; Juneau, A.; Gagné, Y.;́ Allais, C.; Chinigo, G. M.; Choi, C.; Sach, N. W.; Bernier, L.; Fobian, Y. M.; Bundesmann, M. W.; Khunte, B.; Frenette, M.; Fadeyi, O. O. *Angew. Chem. Int. Ed*. **2017**, *56*, 15309−15313; for alkylperoxyesters: g) DiRocco, D. A.; Dykstra, K.; Krska, S.; Vachal, P.; Conway, D. V.; Tudge, M. *Angew. Chem. Int. Ed*. **2014**, *53*, 4802−4806.

[19] *For heteroarene/cascade synthesis review*: a) Boubertakh, O.; Goddard, J.-P. *Eur. J. Org. Chem*. **2017**, *2017*, 2072−2084; *For vinyl-/alkynylation*: see corresponding reviews in ref 15; *For semipinacol/neophyl*: b) Zidan, M.; McCallum, T.; Thai-Savard, L.; Barriault,

L. *Org. Chem. Front*. **2017**, *4*, 2092–2096; c) Weng, W.-Z.; Zhang, B. *Chem. Eur. J*. **2018**, *In Press*; *For α-keto functionalization*: d) Kong, W.; Yu, C.; An, H.; Song, Q. *Org. Lett*. **2018**, *20*, 349−352.

[20] *Some recent reviews in photoredox catalysis*: a) Yoon, T. P.; Ischay, M. A.; Du, J. *Nat. Chem*. **2010**, *2*, 527–532; b) Narayanam, J. M. R.; Stephenson, C. R. J. *Chem. Soc. Rev*. **2011**, *40*, 102–113; c) Teplý, F. *Collect. Czech. Chem. Commun*. **2011**, *76*, 859–917; d) Shi, L.; Xia, W. *Chem. Soc. Rev*. **2012**, *41*, 7687–7697; e) Xuan, J.; Xiao, W.-J. *Angew. Chem. Int. Ed*. **2012**, *51*, 6828–6838; f) Curran, D. P. *Nat. Chem*. **2012**, *4*, 958; g) Schultz, D. M.; Yoon, T. P. *Science* **2014**, *343*, 985–1239176–8; h) Studer, A.; Curran, D. P. *Nat. Chem*. **2014**, *6*, 765−773; i) Pitre, S. P.; McTiernan, C. D.; Scaiano, J. C. *ACS Omega* **2016**, *1*, 66–76; j) Studer, A.; Curran, D. P. *Angew. Chem. Int. Ed*. **2016**, *55*, 58−102; k) Ravelli D.; Protti, S.; Fagnoni, M. *Chem. Rev*. **2016**, *116*, 9850–9913; l) Xie, J.; Jin, H.; Hashmi, A. S. K. *Chem. Soc. Rev*. **2017**, *46*, 5193−5203; and refs 21e and g.

[21] a) Stephenson, C. R. J.; Studer, A.; Curran, D. P. *Beilstein J. Org. Chem*. **2013**, *9*, 2778−2780; b) Griesbeck, A. G. *Beilstein J. Org. Chem*. **2014**, *10*, 1097−1098; c) Yoon, T. P.; Stephenson, C. R. J. *Adv. Synth. Catal*. **2014**, *356*, 2739; d) Shenvi, R. A. *Synlett* **2016**, *27*, 678−679; e) Stephenson, C. R. J.; Yoon, T. P. *Acc. Chem. Res*. **2016**, *49*, 2059−2060; f) Kozlowski, M.; Yoon, T. P. *J. Org. Chem*. **2016**, *81*, 6895−6897; g) Beeler, A. B. *Chem. Rev*. **2016**, *116*, 9629−9630; h) Zard, S. Z. *Org. Lett*. **2017**, *19*, 1257−1269; i) Kueckmann, T. *Asian J. Org. Chem*. **2017**, *6*, 349; j) Konig, B. *Eur. J. Org. Chem*. **2017**, *2017*, 1979−1981.

[22] *Recent examples*: a) Singh, K.; Staig, S.; Weaver, J. D. *J. Am. Chem. Soc*. **2014**, *136*, 5275–5278; b) Metternich, J. B.; Gilmour, R. *J. Am. Chem. Soc*. **2015**, *137*, 11254–11257.

[23] Muller, C.; Maturi, M. M.; Bauer, A.; Cuquerella, M. C.; Miranda, M. A.; Bach, T. *J. Am. Chem. Soc*. **2011**, *133*, 16689–16697.

[24] Skubi, K. L.; Kidd, J. B.; Jung, H.; Guzei, I. A.; Baik, M.-H.; Yoon, T. P. *J. Am. Chem. Soc*. **2017**, *139*, 17186–17192.

[25] a) Okada, M.; Fukuyama, T.; Yamada, K.; Ryu, I.; Ravelli, D.; Fagnoni, M. *Chem. Sci*. **2014**, *5*, 2893–2898; b) Ravelli, D.; Fagnoni, M.; Fukuyama, T.; Nishikawa, T.; Ruy, I. *ACS Catal*. **2018**, *8*, 701–713; *For review*: c) Capaldo, L.; Ravelli, D. *Eur. J. Org. Chem*. **2017**, *2017*, 2056–2071.

[26] Blanksby, S. J.; Ellison, G. B. *Acc. Chem. Res*. **2003**, *36*, 255–263.

[27] *For redox-potentials and corresponding coupling reactions*: *For alcohols*: a) Mayeda, E. A.; Miller, L. L.; Wolf, J. F. *J. Am. Chem. Soc*. **1972**, *94*, 6812–6816; b) Hu, A.; Guo, J.-J.; Pan, H.; Tang, H.; Gao, Z.; Zuo, Z. *J. Am. Chem. Soc*. **2018**, *140*, 1612–1616; *For N-hydroxyphthalimide esters*: c) Zhang, J.; Li, Y.; Zhang, F.; Hu, C.; Chen, Y. *Angew. Chem. Int. Ed*. **2016**, *55*, 1872–1875; d) Zhang, J.; Li, Y.; Xu, R.; Chen, Y. *Angew. Chem. Int. Ed*. **2017**, *56*, 12619–12623; *For amides*: ref 15b; e) Choi, G. J.; Zhu, Q.; Miller, D. C.; Gu, C. J.; Knowles, R. R. *Nature* **2016**, *539*, 268–271; f) Chu, J. C. K.; Rovis, T. *Nature*, **2016**, *539*, 272–275; g) Gentry, E. C.; Knowles, R. R. *Acc. Chem. Res*. **2016**, *49*, 1546–1556; h) Yuan, W.; Zhou, Z.; Gong, L.; Meggers, E. *Chem. Commun*. **2017**, *53*, 8964–8967; i) Chen, D.-F.; Chu, J. C. K.; Rovis, T. *J. Am. Chem. Soc*. **2017**, *139*, 14897–14900; *For O-aryl amides/oximes*: j) Davies, J.; Svejstrup, T. D.; Reina, D. F.;

Sheikh, N. S.; Leonori, D. *J. Am. Chem. Soc*. **2016**, *138*, 8092−8095; *For α-aminooxy acids*: k) Jiang, H.; Studer, A. *Angew. Chem. Int. Ed*. **2017**, *56*, 12273−12276; l) Davies, J.; Sheikh, N. S.; Leonori, D. *Angew. Chem. Int. Ed*. **2017**, *56*, 13361−13365; m) Dauncey, E. M.; Morcillo, S. P.; Douglas, J. J.; Sheik, N. S.; Leonori, D. *Angew. Chem. Int. Ed*. **2018**, *57*, 744−748; n) Jiang, H.; Studer, A. *Angew. Chem. Int. Ed*. **2018**, *57*, 1692−1696.

[28] *For cycloalkanol fragmentation and cyclopropylketones yielding similar products*: a) Jia, K.; Zhang, F.; Huang, H.; Chen, Y. *J. Am. Chem. Soc*. **2016**, *138*, 1514−1517; b) Amador, A. G.; Sherbrook, E. M.; Yoon, T. P. *J. Am. Chem. Soc*. **2016**, *138*, 4722−4725; c) Yayla, H. G.; Wang, H.; Tarantino, K. T.; Orbe, H. S.; Knowles, R. R. *J. Am Chem. Soc*. **2016**, *138*, 10794−10797; d) Guo, J.-J.; Hu, A.; Chen, Y.; Sun, J.; Tang, H.; Zuo, Z. *Angew. Chem. Int. Ed*. **2016**, *55*, 15319−15322; e) Wozniak, L.; Magagnano, G.; Melchiorre, P. *Angew. Chem. Int. Ed*. **2018**, *57*, 1068−1072; f) Huang, X.; Lin, J.; Shen, T.; Harms, K.; Marchini, M.; Ceroni, P.; Meggers, E. *Angew. Chem. Int. Ed*. **2018**, *57*, 5454−5458; *For α-aminooxy acid fragmentation*: ref 27m; *For O-aryl oxime fragmentation*: g) Li, L.; Chen, H.; Mei, M.; Zhou, L. *Chem. Commun*. **2017**, *53*, 11544−11547; h) Yu, X.-Y.; Chen, J.-R.; Wang, P.-Z.; Yang, M.-N.; Liang, D.; Xiao, W.-J. *Angew. Chem. Int. Ed*. **2018**, *57*, 738−743.

[29] a) Che, C.-M, Kwong, H.-L, Yam, V. W.-W, Choc, K. C. *J. Chem. Soc., Chem. Commun*. **1989**, 885–886; b) King, C.; Wang, J.-C.; Khan, M. N. I.; Fackler, Jr., J. P. *Inorg. Chem*. **1989**, *28*, 2145–2149; c) Kwong, H.-L.; Yam, V. W.-W.; Li, D. D.; Che, C.-M. *J. Chem. Soc., Dalton Trans*. **1992**, 3325–3329; d) Ma, C.; Chan, C. T.-L.; To, W.-P.; Kwok, W.-M.; Che, C.-M. *Chem. Eur. J*. **2015**, *21*, 13888–13893; e) McCallum, T.; Rohe, S.; Barriault, L. *Synlett* **2017**, *28*, 289−305.

[30] a) Nozaki, K.; Oshima, K.; Utimoto, K. *J. Am. Chem. Soc*. **1987**, *109*, 2547–2549; b) Porter, N. A.; Giese, B.; Curran, D. P. *Acc. Chem. Res*. **1991**, *24*, 296–304; c) Wu, J. H.; Radinov, R.; Porter, N. A. *J. Am. Chem. Soc*. **1995**, *117*, 11029–11030; d) Sibi, M. P.; Ji, J.; Wu, J. H.; Gurtler, S.; Porter, N. A. *J. Am. Chem. Soc*. **1996**, *118*, 9200–9201; e) Sibi, M. P.; Ji, J. *J. Org. Chem*. **1997**, *62*, 3800–3801. f) Yang, D.; Gu, S.; Yan, Y.-L.; Zhu, N.-Y.; Cheung, K.-K. *J. Am. Chem. Soc*. **2001**, *123*, 8612–8613; g) Kharasch, M. S.; Skell, P. S.; Fisher, P. *J. Am. Chem. Soc*. **1948**, *70*, 1055–1059; h) Sibi, M. P.; Manyem, S.; Zimmerman, J. *Chem. Rev*. **2003**, *103*, 3263–3295.

[31] a) Brimioulle, R.; Lenhart, D.; Maturi, M. M.; Bach, T. *Angew. Chem. Int. Ed*. **2015**, *54*, 3872–3890; b) Skubi, K. L.; Blum, T. R.; Yoon, T. P. *Chem. Rev*. **2016**, *116*, 10035–10074; c) Miyabe, H.; Kawashima, A.; Yoshioka, E.; Kohtani, S. *Chem. Eur. J*. **2017**, *23*, 6225–6236; d) Miyabe, H. *Eur. J. Org. Chem*. **2017**, *2017*, 3302–3320; e) Zou, Y.-Q.; Hormann, F. M.; Bach, T. *Chem. Soc. Rev*. **2018**, *47*, 278–290; f) Garrido-Castro, A. F.; Maestro, M. C.; Aleman, J. *Tetrahedron Lett*. **2018**, *59*, 1286–1294.

[32] a) Espelt, L. R.; McPherson, I. S.; Wiensch, E. M.; Yoon, T. P. *J. Am. Chem. Soc*. **2015**, *137*, 2452–2455; b) Huo, H.; Harms, K.; Meggers, E. *J. Am. Chem. Soc*. **2016**, *138*, 6936–6939.

[33] a) Feldma, K. S.; Romanelli, A. L.; Ruckle Jr., R. E.; Miller, R. F. *J. Am. Chem. Soc*. **1988**, *110*, 3300–3302; b) Miura, K.; Fugami, K.; Oshima, K.; Utimoto, K. *Tetrahedron Lett*. **1988**, *29*, 5135–5138; c) Hashimoto, T.; Kawamata, Y.; Maruoka, K. *Nat. Chem*. **2014**, *6*, 702–705.

[34] a) Nicewicz, D. A.; MacMillan, D. W. C. *Science* **2008**, *322*, 77–80; b) Shih, H.-W.; Vander Wal, M. N.; Grange, R. L.; MacMillan, D. W. C. *J. Am. Chem. Soc*. **2010**, *132*, 13600–13603; c) Arceo, E.; Jurberg, I. D.; Alvarez-Fernandez, A.; Melchiorre, P. *Nat. Chem*. **2013**, *5*, 750–756; d) Murphy, J. J.; Bastida, D.; Paria, S.; Fagnoni, M.; Melchiorre, P. *Nature* **2016**, *352*, 218–222.

[35] a) Tellis, J. C.; Primer, D. N.; Molander, G. A. *Science* **2014**, *345*, 433–436; b) Zuo, Z.; Ahneman, D. T.; Chu, L.; Terrett, J. A.; Doyle, A. G.; MacMillan, D. W. C. *Science* **2014**, *345*, 437–440; c) Twilton, J.; Le, C.; Zhang, P.; Shaw, M. H.; Evans, R. W.; MacMillan, D. W. C. *Nat. Rev. Chem*. **2017**, *1*, 0052; d) Gutierrez, O.; Tellis, J. C.; Primer, D. N.; Molander, G. A.; Kozlowski, M. C. *J. Am. Chem. Soc*. **2015**, *137*, 4896–4899; e) Zuo, Z.; Cong, H.; Li, W.; Choi, J.; Fu, G. C.; MacMillan, D. W. C. *J. Am. Chem. Soc*. **2016**, *138*, 1832–1835.

[36] a) Cuthbertson, J. D.; MacMillan, D. W. C. *Nature* **2015**, *519*, 74–77; b) Jeffrey, J. L.; Terrett, J. A.; MacMillan, D. W. C. *Science* **2015**, *349*, 1532–1536; c) Shaw, M. H.; Shurtleff, V.; W.; Terrett, J. A.; Cuthbertson, J. D.; MacMillan, D. W. C. *Science* **2016**, *352*, 1304–1308; *For amide*: ref 27e; d) Margrey, K. A.; Czaplyski, W. L.; Nicewicz, D. A.; Alexanian, E. J. *J. Am. Chem. Soc*. **2018**, *140*, 4213–4217; e) Tanaka, H.; Sakai, K.; Kawamura, A.; Oisaki, K.; Kanai, M. *Chem. Commun*. **2018**, *54*, 3215–3218; f) Twilton, J.; Christensen, M.; DiRocco, D. A.; Ruck, R. T.; Davies, I. W.; Macmillan, D. W. C. *Angew. Chem. Int. Ed*. **2018**, *57*, 5369–5373.

[37] a) Heitz, D. R.; Tellis, J. C.; Molander, G. A. *J. Am. Chem. Soc*. **2016**, *138*, 12715–12718; b) Shields, B. J.; Doyle, A. G. *J. Am. Chem. Soc*. **2016**, *138*, 12719–12722.

[38] a) Jin, J.; MacMillan, D. W. C. *Nature* **2015**, 525, 87–90; b) Roberts, B. P. *Chem. Soc. Rev*. **1999**, *28*, 25–35.

[39] Wang, D.; Zhu, N.; Chen, P.; Lin, Z.; Liu, G. *J. Am. Chem. Soc*. **2017**, *139*, 15632–15635.

[40] a) Rono, L. J.; Yayla, H. G.; Wang, D. Y.; Armstrong, M. F.; Knowles, R. R. *J. Am. Chem. Soc*. **2013**, *135*, 17735–17738.

[41] Proctor, R. S. J.; Davis, H. J.; Phipps, R. J. *Science* **2018**, *360*, 419–422.

2. Gold Photoredox Reactions of Nonactivated C–Br Bonds

Revol, G.; McCallum, T.; Morin, M.; Gagosz, F.; Barriault, L. Photoredox Transformations with Dimeric Gold Complexes. *Angew. Chem. Int. Ed.* **2013**, *52*, 13342–13345.

2.1 Abstract

Nonactivated bromoalkanes and arenes have long been used in radical chemistry due to their wide availability and usefulness as functional groups. Classic methodology for alkyl radical generation from bromoalkanes/arenes has been largely limited to hazardous methodology requiring the use of organostannane hydrides, initiators, and additives. Recently, photoredox catalysis methodology has enabled the generation of alkyl/aryl radicals from activated organohalides with use of Ru- and Ir-based polypyridyl complexes and organic dyes. This major advancement in mild and highly efficient radical generation has been facilitated by the synthetic organic chemistry community's great interest in the development of methodology for the formation of C–C, C–N, and C–O bonds. Nonactivated bromoalkanes/arenes have been largely inaccessible to activation by Ru- and Ir-based polypyridyl complexes as they are limited by their redox potentials that are not sufficiently reducing for reaction with these substrates. Described herein is the use of binuclear Au(I) bisphosphine complexes that become powerful reductants upon excitation with UVA light, capable of alkyl/aryl radical generation from nonactivated bromoalkanes and arenes. These substrates underwent a light-enabled reductive radical cyclization in the presence of $[Au_2(\mu\text{-dppm})_2]Cl_2$ as the photocatalyst. Sunlight can be used as the energy source for this simple and efficient radical reaction, which circumvents the use of potentially hazardous and toxic chemical reagents and provides an alternative to reactions mediated by organostannane hydrides.

2.2 Introduction

The conversion of solar energy into chemical energy in photosynthesis has enthralled scientists for decades. Sunlight could be used as an inexpensive, green, and sustainable source of energy to induce chemical reactions.[1, 2] However, many organic compounds do not absorb sunlight or visible light, and the application of photochemistry in synthesis is therefore restricted. In response to this limitation, several light absorbing photocatalysts have been developed in an effort to mimic the light-harvesting abilities of bio-complexes found in natural processes such as photosynthesis.[3] Ru- and Ir-based polypyridyl complexes are among the most used one-electron photoredox catalysts for research in energy storage, water splitting, and photovoltaic devices.[4, 5] Increased attention is being placed on visible light mediated photoredox processes for the development of efficient and waste-minimizing processes of general applicability that should decrease our dependence on toxic chemical products.[6]

During the last decade, Ru- and Ir-based polypyridyl complexes have proven their potential in absorbing light and transforming it into electronic energy that can be used in organic synthesis to generate new C–C, C–N, and C–O bonds through SET processes (**Scheme 2.1**, Eq (1)).[6f] In general, photoredox transformations can operate through two distinctive pathways, the oxidative quenching cycle or the reductive quenching cycle (**Scheme 2.1**; paths **A** and **B**). In the former, the photoexcited metal complex transfers an electron to an acceptor such as a haloalkane or arene (R–X). The radical intermediate is converted into a product, whereas the oxidized $\mathbf{PC^{1+}}$ returns to its original oxidation state by accepting an electron from a donor – in this case, R_3N:. In the latter pathway, the excited metal complex acts as an oxidant and accepts an electron from a donor source such as R_3N: to generate $\mathbf{PC^{1-}}$ that may function as a reducing agent towards haloalkanes

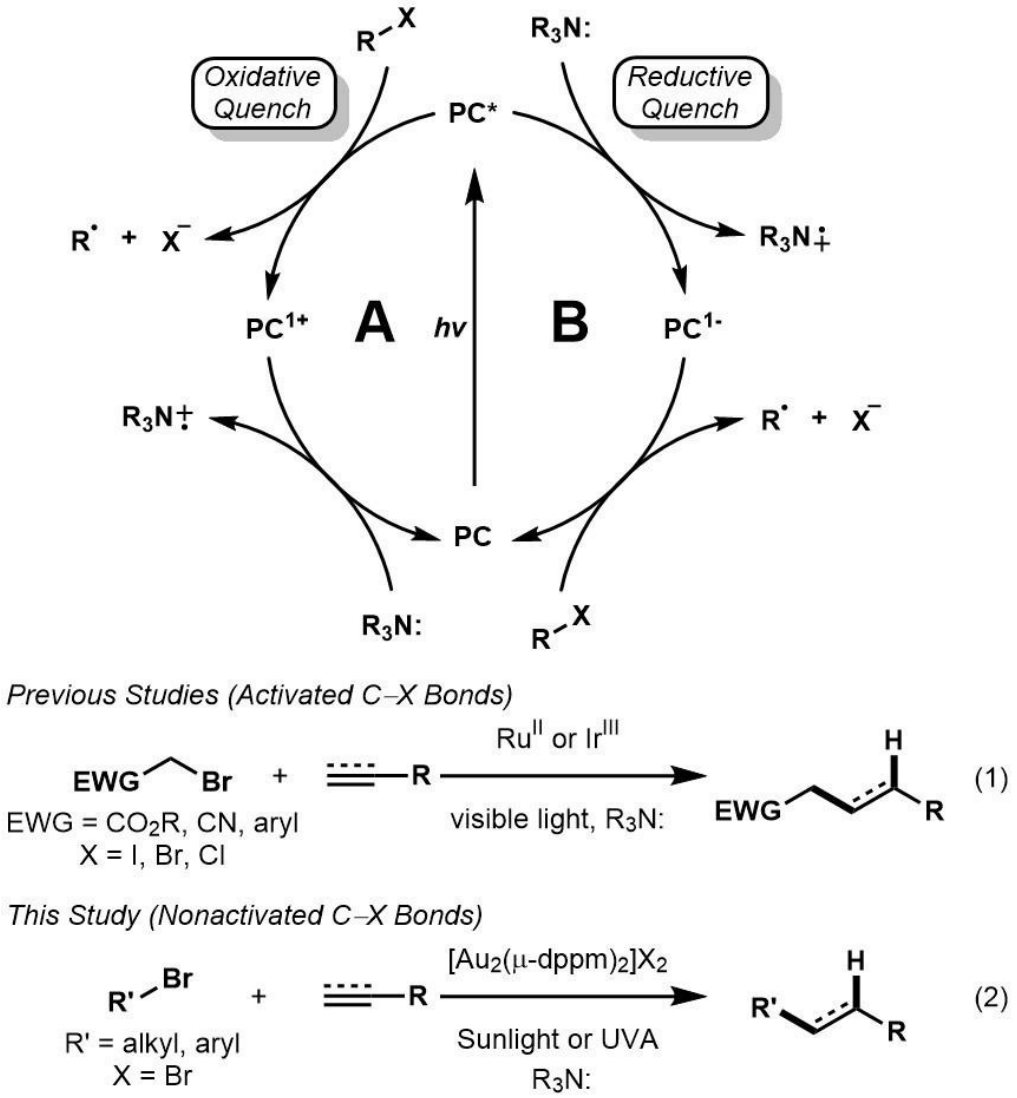

Scheme 2.1 General mechanism for metal-catalyzed photoredox reactions.

and arenes. The newly formed alkyl radical may then participate in coupling and reduction reactions (**Scheme 2.1**, Eq. (2)).

The reduction of C–X bonds to produce alkyl radical intermediates is one of the most useful processes for accessing new reactivity in radical coupling reactions and has broad scope for application in chemical synthesis.[7] Typically, methods to generate alkyl, vinyl, and aryl radicals from C–X bonds require the use of potentially hazardous and/or toxic chemical reagents/initiators such as organostannanes, AIBN, trialkylboranes, and

peroxides.[8] The use of photoexcited Ru- and Ir-based polypyridyl complexes is an attractive alternative for efficient synthetic transformations involving the cleavage of C–X bonds, however the reduction potential inherent to these complexes limits the range of possible radical intermediates to those derived from highly activated C–X bonds (polyhalomethanes, bromomalonates, electron-deficient benzyl halides, and iodo-alkanes/arenes).[9–12] Although important advances in photocatalysis have been made in the last decade, one might concede that efficient methods for the photocatalyzed reductive scission of nonactivated C–X bonds have yet to be described.

In this context, the design of a photocatalytic system of broader applicability must fulfill specific criteria. Aside from an appropriate redox-potential window, the catalyst must possess a long-lived excited state to undergo productive quenching with nonactivated C–X bonds or R_3N:. Furthermore, photoexcitation of the catalyst should occur within a readily accessible wavelength range and thus require no special equipment. Based on the rich photochemistry of binuclear gold complexes, we report a conceptually novel photocatalytic system for the efficient generation of carbon–centered radical intermediates from nonactivated bromoalkanes ($E_{1/2}^{red}$ = –1.90 to –2.50 V *vs* SCE) and bromoarenes ($E_{1/2}^{red}$ = –2.05 to –2.57 V *vs* SCE) under remarkably mild conditions.[13]

2.3 Results and Discussion

On the basis of studies by Che and co-workers, we considered the use of cationic $[Au_2(\mu\text{-dppm})_2]^{2+}$ (**1**) species as potential photocatalysts.[14] These binuclear gold species absorb light in the UV region (λ_{max} = 295 nm, up to 365 nm) to produce a high-energy and long-lived excited-state (Φ_{em} = 0.23) with a strong reduction potential ($E_{1/2}^{(M+/M^*)}$ = –1.6 to –1.7 V *vs* SSCE).[15] To demonstrate the applicability of binuclear gold complexes in

synthesis, we selected the radical cyclization of bromoalkene **2.2** as the benchmark reaction (**Table 2.1**). A survey of binuclear gold catalysts in conjunction with trialkylamine bases as sacrificial electron and hydrogen donors revealed that the radical cyclization of alkyl bromide **2.2** to give **2.3** proceeded in excellent yield in the presence of *i*Pr$_2$NEt in MeCN with sunlight as the light source (entry 2). Although the counterion had little effect on the conversion of the radical cyclization, we found the gold complex **2.1e** to be the most robust and photostable binuclear gold complex (entries 3–6).[16] UVA light (315–400 nm) proved to be a good surrogate for sunlight (entry 7). Rigorous control experiments showed complete recovery of the starting material (0% conversion) when the reaction was carried out in the absence of gold catalyst **2.1e** or light (entries 8 and 9). Similarly, no cyclization product **2.3** was observed when the visible light photocatalysts [Ru(bpy)$_3$]Cl$_2$ (**2.4**), [Ir(ppy)$_2$(dtbbpy)]PF$_6$ (**2.5**), and Ir(ppy)$_3$ (**2.6**) were used under standard conditions (with a 23W CFL or white LEDs; entries 10–12).[11, 12] These results confirmed that no background reactions took place in the absence of sunlight (UVA) or the gold(I) binuclear complex and photoexcited **2.4**–**2.6** cannot reduce nonactivated alkyl C–Br bonds by MLCT.

The scope of the reaction with respect to the bromoalkane or bromoarene substrate was explored (**Tables 2.2** and **2.3**). The radical cyclization of bromoalkanes **2.7**–**2.10** with *i*Pr$_2$NEt (2 equiv; procedure A) in MeCN gave the corresponding cyclic products **2.14**–**2.17** in yields ranging from 58–93% (**Table 2.2**, entries 1–7). Irradiation with sunlight rather than UVA light led to a slight improvement in the reaction yield (entries 2, 4, and 6). Complete conversion of **2.11** into the corresponding pyrrolidine **2.18** required a prolonged irradiation time of 36 h (entry 8). To decrease the reaction time, we examined various hydrogen donors. It was found that the addition of formic acid in the presence of

Table 2.1 Optimization of the photoredox reaction.

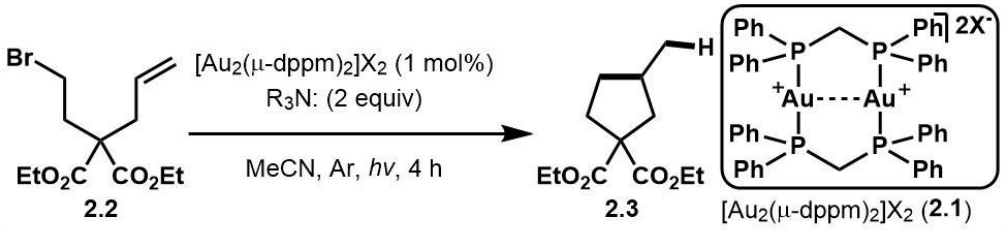

Entry	X =	R_3N:	Light source	Yield [%]
1	**2.1a** OTf	Et_3N	sunlight	20
2	**2.1a** OTf	iPr_2NEt	sunlight	94
3	**2.1b** NTf_2	iPr_2NEt	sunlight	72
4	**2.1c** BF_4	iPr_2NEt	sunlight	70
5	**2.1d** SbF_6	iPr_2NEt	sunlight	90
6	**2.1e** Cl	iPr_2NEt	sunlight	86
7	**2.1e** Cl	iPr_2NEt	UVA (315-400 nm)	74
8[a]	---	iPr_2NEt	sunlight/UVA	s.m.
9[b]	**2.1e** Cl	iPr_2NEt	---	s.m.
10[c]	**2.4**	iPr_2NEt	23 W CFL/LEDs	s.m
11[c]	**2.5**	iPr_2NEt	23 W CFL/LEDs	s.m
12[c]	**2.6**	iPr_2NEt	23 W CFL/LEDs	< 5

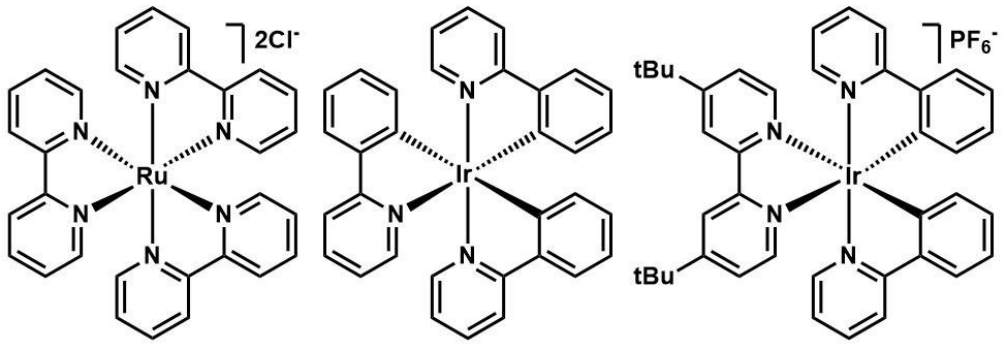

$[Ru(bpy)_3]Cl_2$ (**2.4**) $Ir(ppy)_3$ (**2.5**) $[Ir(ppy)_2(dtbbpy)]PF_6$ (**2.6**)

[a]The reaction mixture was irradiated for 18 h. [b]The reaction mixture was heated at 60°C for 24 h.
[c]The reaction mixture was irradiated for 36 h.

*i*Pr2NEt greatly enhanced the rate of the reaction.[17] Indeed, the conversion of **2.11** was completed after 1 h to produce **2.18** in 66% yield (entry 9). As expected, the cyclization of bromides **2.12** and **2.13** gave the desired pyrrolidines **2.19** and **2.20** in 86% and 63% yields, respectively (entries 10 and 11).

Table 2.2 Photoredox cyclization of bromoalkanes.

Entry	Substrate	Product	Procedure[a] (type of light)	Yield [%] (ratio)[b]
1	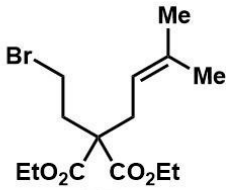 **2.7**	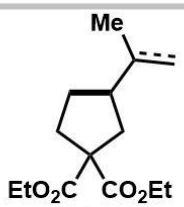 **2.14 a,b**	A (UVA)	81 (73:27)
2			A (sunlight)	92 (65:35)
3	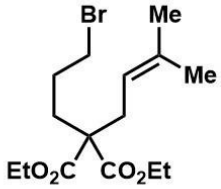 **2.8**	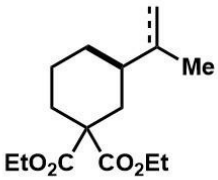 **2.15 a,b**	A (UVA)	58 (84:16)
4			A (sunlight)	81 (86:14)
5	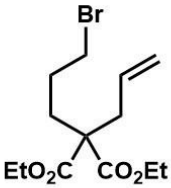 **2.9**	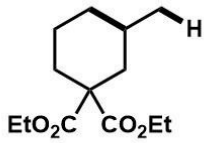 **2.16**	A (UVA)	58
6			A (sunlight)	60
7	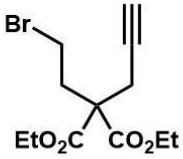 **2.10**	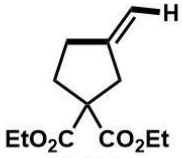 **2.17**	A (UVA)	93
8	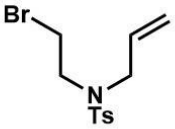 **2.11**	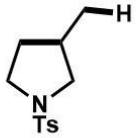 **2.18**	A (UVA)	63
9			B (UVA)	66
10	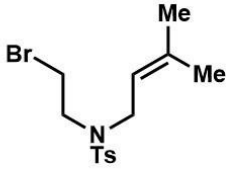 **2.12**	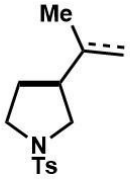 **2.19 a,b**	B (UVA)	86 (50:50)
11	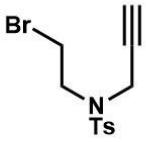 **2.13**	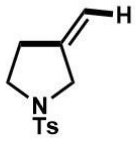 **2.20**	B (UVA)	63

[a]Procedure A: **2.1e** (2.5 mol%), *i*Pr_2NEt (2 equiv), MeCN, Ar degas, 2–8 h irradiation; procedure B: **2.1e** (2.5 mol%), *i*Pr_2NEt (5 equiv), formic acid (2 equiv), MeCN, Ar degas, 1–4 h irradiation. [b]Ratio of the isopropyl- to isopropenyl-substituted product.

Having confirmed the applicability of the binuclear gold complexes in photoredox processes with bromoalkanes, we examined the reductive cleavage of bromoarenes (**Table 2.3**). The reductive radical cyclization of **2.21** afforded the cyclized product **2.25** in 75% yield (entry 1). The cyclization of sulfonamide *N*-Ac and *N*-Ts protected substrates **2.22a**,**b** proceeded to the formation of indolines **2.26** and **2.27** in 90% and 77% yields, respectively (entries 2 and 3). The reductive dehalogenation of bromoarenes **2.23** and **2.24** afforded products **2.28** and **2.29** in nearly quantitative yields. Like the bromoalkane series, control experiments confirmed that the reduction of bromoarenes did not operate in the absence of the binuclear gold complex or without irradiation. A comparative study using catalysts **2.5** or **2.6** under visible light irradiation did not yield any products from substrates **2.2**, **2.11**, or **2.22a** (See section **2.7**, **Table 2.8**).[20a,b] In such cases, the redox potentials of the iridium complex (*[Ir^{III}] or [Ir^{II}]) are not sufficiently reducing to engage reactivity with the substrate. Recent work by the Stephenson group has shown that addition of $(TMS)_3SiH$, a known reagent capable of radical reaction with nonactivated bromoalkanes/arenes, can be used in conjunction with photoredox conditions using Ir-based polypyridyl complexes for the activation of otherwise unreactive substrates.[20c]

Labeling experiments with d_2-formic acid (2 equiv), **2.11**, and *i*Pr_2NEt (2 equiv) indicated that formic acid and *i*Pr_2NEt may act as a hydrogen-atom source (**2.18**:**d-2.18** (4:1), **Scheme 2.2**, **A**).[18] Although superior reactivity was observed for reactions with formic acid, insufficient data was available to permit a detailed mechanistic discussion.[19] However, it is possible that highly reducing carbon dioxide radical anions are formed from the HAT reaction of alkyl radicals and formate under the described conditions (oxidative or reductive quenching pathways, **Scheme 2.2**, **B**). The highly reactive intermediate may

Table 2.3 Photoredox cyclization and dehalogenation of bromoarenes.

Entry	Substrate	Product	Yield [%]
1	 **2.21**	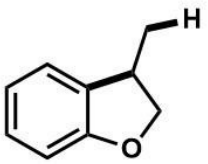 **2.25**	75[a]
2	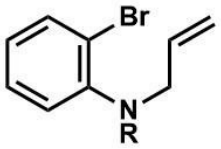 **2.22a** R = Ac	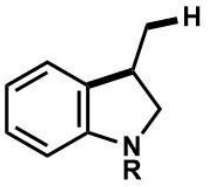 **2.26** R = Ac	90
3	**2.22b** R = Ts	**2.27** R = Ts	77
4	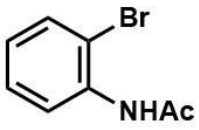 **2.23**	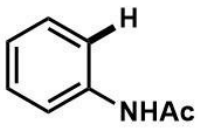 **2.28**	95
5	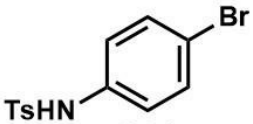 **2.24**	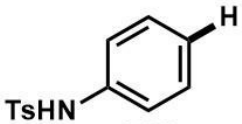 **2.29**	94

[a]Procedure: **2.1e** (5.0 mol%), *i*Pr_2NEt (5 equiv), formic acid (2 equiv), MeCN, Ar degas, 8–16 h irradiation using UVA. [a]contained ~10% of **2.21** and dehalogenated material.

reduce Au intermediates in the catalytic cycle or act as a chain-carrier by reduction of bromoalkane/arenes, where carbon dioxide is formed in each scenario (**Scheme 2.2**, **C**).

We sought to further validate the Au-catalyzed photoinduced C–C bond forming reaction by including intermolecular processes (**Scheme 2.3**). Notably, bromoarene **2.30** was converted into dihydrophenanthrene **2.31** in the presence of formic acid (procedure B) in 44% yield. To gain more insight into the reaction mechanism, we exposed **2.30** to UVA irradiation for 16 h in the presence of *i*Pr_2NEt and obtained the bibenzyl product **2.32** in 33% yield. Irradiation of compound **2.32** according to procedure B produced

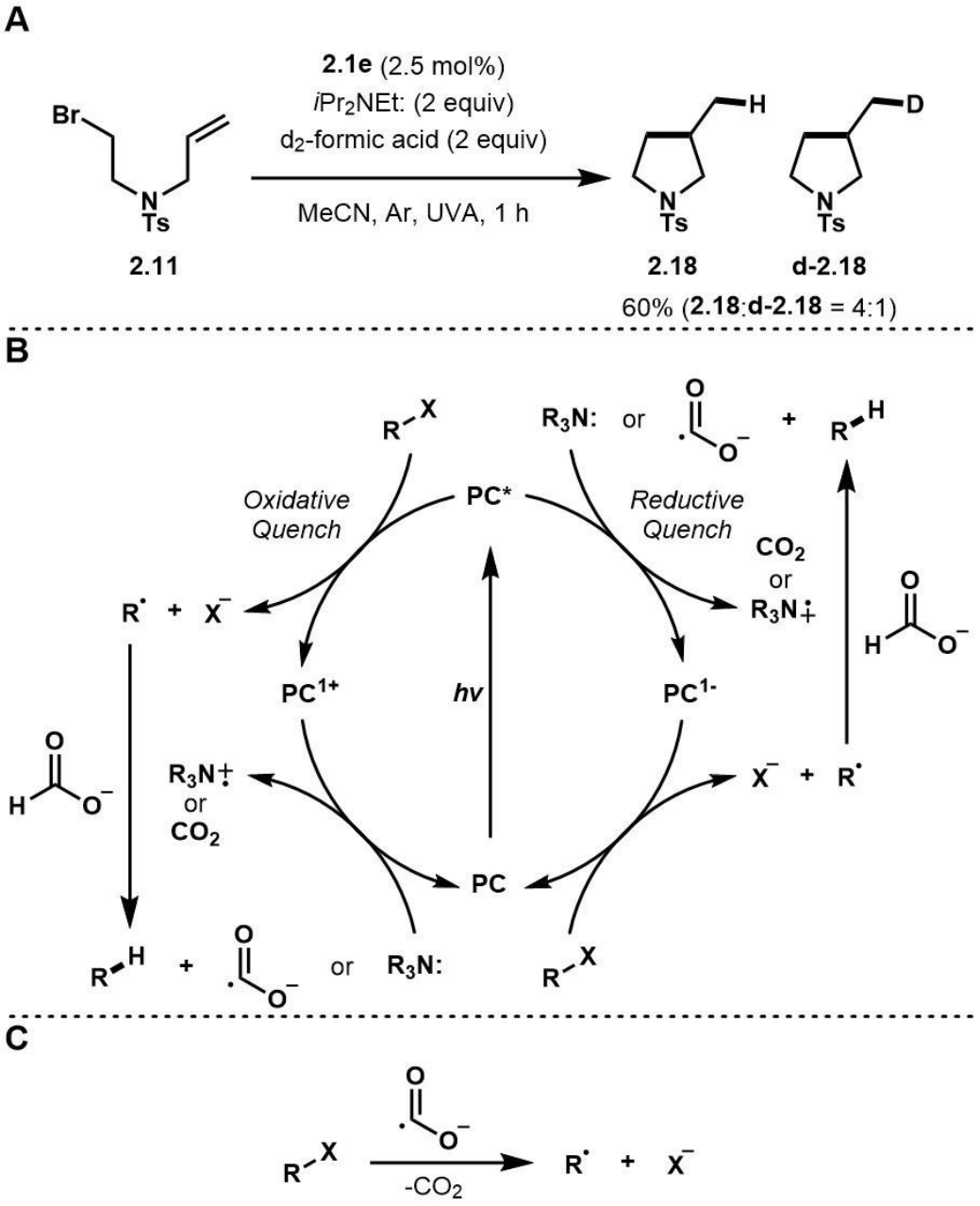

Scheme 2.2 Deuterium labelling experiment.

dihydrophenanthrene **2.31** in 64% yield along with the dehalogenation product **2.33** in 9% yield. These results suggest that the transformation most likely proceeds by an initial recombination of benzyl radicals.[20] The ring closure leading to compound **2.31** could then be explained by the subsequent generation of an aryl radical, which would attack the other aromatic ring in a formal *ipso*-substitution of the bromine atom.

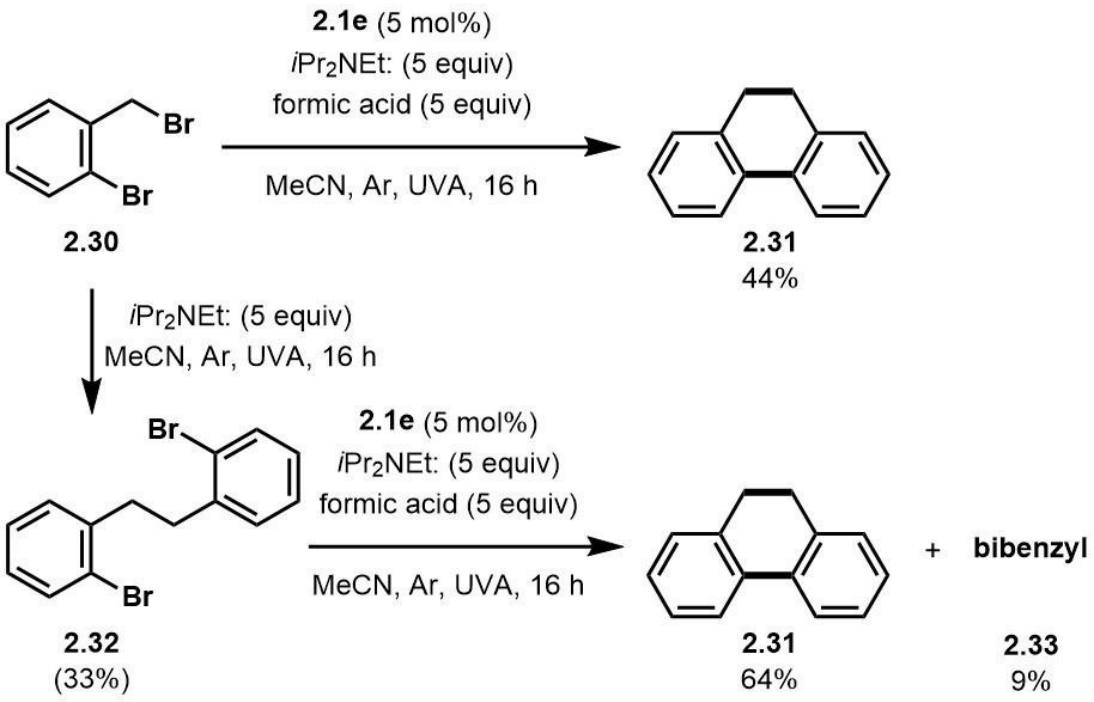

Scheme 2.3 Intermolecular radical addition/cyclization reaction.

2.4 Conclusions

In summary, we have described a light-enabled reductive radical reaction of nonactivated bromoalkanes and bromoarenes in the presence of a binuclear gold complex as the photocatalyst. It was demonstrated that the applicability of this photoredox process is not limited to intramolecular processes, but that intermolecular transformations are also possible. Although no clear mechanism has been established with respect to the use of formic acid, our results clearly demonstrate the uniqueness of this photoredox process and its high synthetic potential. We are currently exploring the application of this method in the context of synthesis and working toward a full understanding of the reaction mechanism.

2.5 Further Information

1) McTiernan, C. D.; Morin, M.; McCallum, T.; Scaiano, J. C.; Barriault, L. Polynuclear gold(I) complexes in photoredox catalysis: understanding their reactivity through characterization and kinetic analysis. *Catal. Sci. Technol*. **2016**, *6*, 201–207.

2) Tran, H.; McCallum, T.; Morin, M.; Barriault, L. Homocoupling of Iodoarenes and Bromoalkanes Using Photoredox Gold Catalysis: A Light Enabled Au(III) Reductive Elimination. *Org. Lett*. **2016**, *18*, 4308–4311.

Owing to the uncertainty in the mechanism of this transformation, further studies to clarify the behaviour of the excited-state complex **2.1e** were conducted. As the endeavour began, an elegant study by Che and coworkers highlighted the nature of the ground-state *vs* excited-state binuclear Au(I) complex with respect to bonding of the Au atoms.[21] Using an ultrafast time-resolved spectroscopic study, it was shown that the complex bears little aurophilic interaction in the ground-state. Upon excitation ($[Au_2]^*$), an electron is promoted from an anti-bonding $5d_z^2$ orbital into a $6s/6p_z$ bonding orbital (^{1}5dσ*6pσ), forming a metal–metal bond, undergoing ISC to ^{3}5dσ*6pσ at rapid timescales (~0.15 ps). The complex was found to have a lifetime of ~510 ps (in DCM) with a tendency to increase coordination number at the Au(I) centre by inner-sphere oxidative quenching (exciplex) with a C–X bond of the solvent. The described phenomenon allows the complex to engage in redox chemistry with substituents like bromoalkanes/arenes that have much higher redox potentials than the excited-state complex **2.1e** ($E_{1/2}^{M+/M^*}$ = –1.63 V *vs* SCE).

During mechanistic studies conducted in collaboration with the Scaiano group, distinct quenching pathways were discerned by photophysical and electrochemical description of some binuclear Au(I) complexes.[22] Using laser flash photolysis techniques,

excited-state quenching rates of phosphine bridged binuclear Au(I) complexes with trialkylamines (DIPEA) and bromoalkanes (*n*BuBr) were evaluated (**Scheme 2.4**, **B**). The data indicated that **2.1e** underwent reductive quenching with trialkylamines (k_q^{DIPEA} = 2.7×10^7 $M^{-1}s^{-1}$) at a rate faster than nonactivated bromoalkanes (k_q^{nBuBr} = 2.9×10^6 $M^{-1}s^{-1}$). Given these rates and the excess of trialkylamine base used, the reductive quenching mechanism of excited-state **2.1e**, where the corresponding Au^{I}–Au^{0} complex undergoes SET with bromoalkanes/arenes, providing alkyl/aryl radicals and regeneration of the ground-state catalyst is proposed (**Scheme 2.4**, **A**). Interestingly, modification of the ligand with relatively electron-donating Me substituents (complex **I**; dmpm ligand), produced a more reducing complex that underwent oxidative quenching at faster rates with bromoalkanes than reductive quenching with trialkylamines (**Scheme 2.4**, **B**). Alternatively, relatively electron-withdrawing aryl ligand (complex **II**; Ar = C_6H_3(3,5-diCF_3)) produced a more oxidizing complex that underwent reductive quenching at faster rates with trialkylamines than oxidative quenching with bromoalkanes. Trinuclear Au(I) complex **III** was found to quench with DIPEA at rates nearly three orders of magnitude greater than *n*BuBr. When replacing the phosphines with relatively donating carbene ligands, complex **IV** was found to quench with bromoalkanes at faster rates than trialkylamines. Taken along with data from complex **I**, these results indicate that relatively donating complexes undergo quenching preferentially with bromoalkanes. In general, complexes with withdrawing ligands had longer excited-state lifetimes, more oxidizing E_{pa} redox potentials, quench preferentially with trialkylamines from the excited state (reductive quench) and may have smaller [Au^{I}–Au^{I}] ground-state distances; the opposite is found for Au(I) complexes with donating ligands. Electron-deficient ligands that remove electron

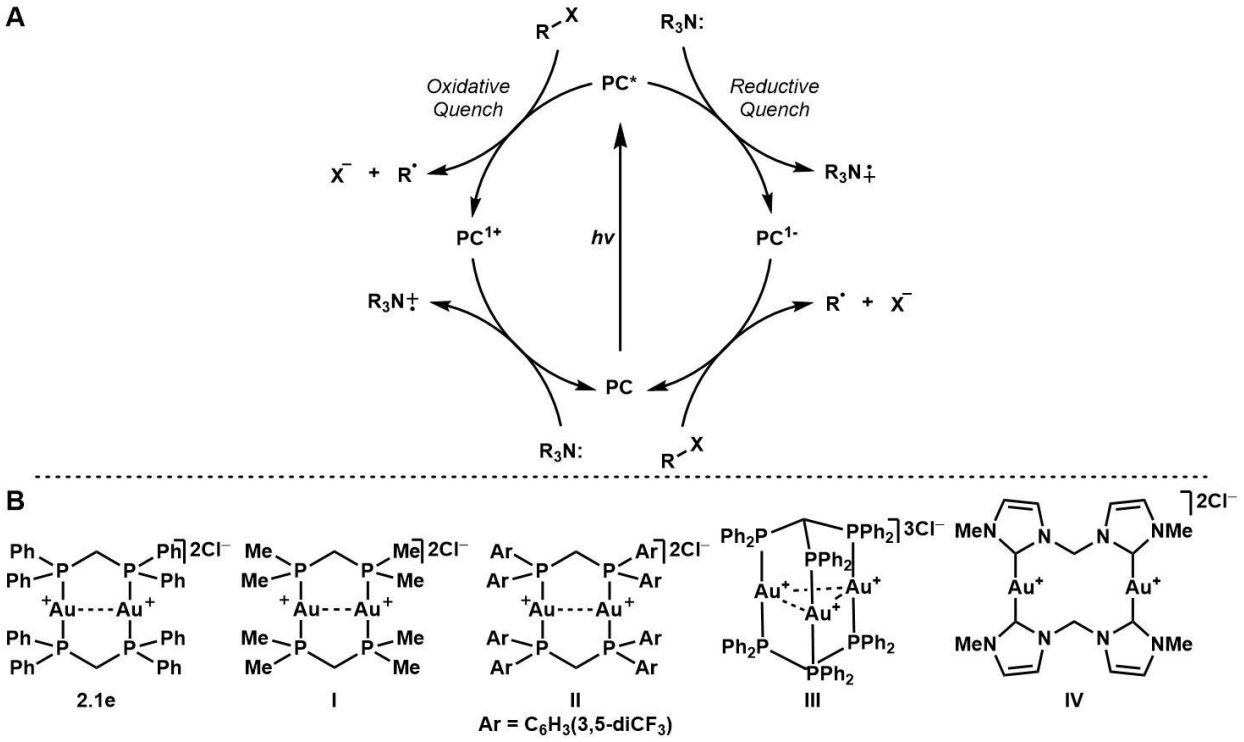

Complex	λ_{ex}[a] (nm)	ε_{ex}[a] (M^{-1} cm^{-1})	λ_{em}[a] (nm)	Φ_{em}[b]	$^3\tau_0$[c] (ns)	$^*E_T$[d] (kJ mol^{-1})	E_{pa}[e] (V *vs.* SCE)	E_{pc}[e] (V *vs.* SCE)	k_q^{DIPEA} (M^{-1} s^{-1})[f]	k_q^{nBuBr} (M^{-1} s^{-1})[f]	Au - - - Au (Å)	^{3}Au-Au (Å)
2.1e	355	73163	560	0.137	850	215	+0.70	−1.63	2.7×10^7	2.9×10^6	2.962(1)[g]	2.677[k]
I	308	3813	525	0.028	400	228	+0.49	−1.77	2.1×10^7	1.1×10^9	3.010[h]	---
II	355	6539	590	0.006	10000	203	+1.41	−1.65	1.1×10^9	4.8×10^5	---	---
III	355	3780	545	0.028	1500	220	+1.09	−1.54	1.6×10^9	4.5×10^6	2.9220(8)[i]	---
IV	308	491	510	0.017	20	235	+0.34	---	1.6×10^8	1.2×10^9	3.525(6)[j]	---

[a]Measured in MeCN at 298 K. [b]Photoluminescence quantum yield relative to $[Ru(bpy)_3]Cl_2$ as standard (ϕ_{MeCN} = 0.095). [c]Triplet lifetime measured in MeCN degassed with nitrogen after 10 mJ laser pulse at λ_{ex}. [d]Triplet-state energy determined from low-temperature (77 K) phosphorescence spectra. [e]Cyclic voltammetry conditions: scan rate = 100 mV s^{-1}, 0.5–2.0 mM Au(I) complex in MeCN degassed with argon with 100 mM Bu_4NClO_4 supporting electrolyte, Pt wire working electrode, Pt wire counter electrode, Ag wire pseudo-reference electrode, Fc/Fc^+ redox couple internal reference (0.41 V vs. SCE), oxidation and reduction potential reported as peak anodic (E_{pa}) and peak cathodic (E_{pc}) potentials due to irreversible nature. [f]Determined from slope of corresponding kinetic quenching plot (k_{decay} vs. [Q]) see ref. 22 for each. [g]ref. 23. [h]ref. 24. [i]ref. 25a. [j]ref. 25b. [k]ref. 25c.

Scheme 2.4 Proposed mechanism and characterization data. Reductive quenching of excited binuclear Au(I) complexes with trialkylamines for the dehalogenation of bromoalkanes (**A**) accompanied by photophysical and electrochemical data (**B**).

density from the Au(I) centres may result in more pronounced aurophilic interactions, leading to absorption maxima shifted towards the visible spectrum. The stabilizing effect (lowering HOMO-LUMO gap) may be observed with the lower energy emission of complex **II** (590 nm) and is an excellent starting point for further structural elaboration in polynuclear Au(I) complexes. The photophysical and electrochemical data for these complexes are summarized in **Scheme 2.4**, **B**.

The origin of the hydrogen atom transfer step in the final products of the described hydrodebromination/cyclization reactions was another aspect that warranted mechanistic insight. The deuterium labelling experiments (**Scheme 2.2**, **A**, and ref. 18) evaluated if d_2-formic acid or d_3-MeCN led to deuterium incorporation (**d**-**2.18**) in the transformation of **2.11** to **2.18**. The observation of small amounts of **d**-**2.18** indicated that formic acid and the solvent had the ability to undergo HAT reactions under the optimized conditions. At the time, deuterium labelled trialkylamine (d_{15}-Et_3N:) was not available and the extent to which the it participated in the HAT reactions could not be evaluated.

An alternative approach to evaluate the extent of the participation of amines in the HAT reaction was the observation of the reduced-to-oxidized ratio (**a**:**b**) of products in the hydrodebromination/cyclization reaction of **2.7** and **2.12** (**Table 2.4**). It was reasoned that amine bases that have faster rates of HAT reaction with alkyl radicals or have reducing reaction intermediates should produce larger ratios in favour of the reduced products **2.14a**, **2.14'a**, or **2.19a**. For example, Hantzsch ester contains a dienyl moiety like cyclohexadiene (CHD) that favours HAT. On the other hand, strained amine bases that cannot undergo further decomposition of the radical cation after reductive quenching with the excited-state binuclear Au(I) complex (i.e. DABCO) should produce larger ratios in favour of the oxidized products **2.14b**, **2.14'b**, or **2.19b**. With the reaction conditions utilizing amine base (2 equiv), **1e** (2.5 mol%), in MeCN (0.067 M) with UVA irradiation for 36 h, *i*Pr_2NEt gave a product distribution of 65:35 (**2.14a**:**b**, entry 1). Addition of CHD, a known HAT reagent, gave only reduced product **2.14'a** with 88% yield in the presence of *i*Pr_2NEt (entries 2 and 3). The comparable Hantzsch ester yielded a ratio of 95:5 (**2.14a**:**b**) in 75% yield (entry 4). Interestingly, DABCO reversed the reaction selectivity to a ratio of 20:80 (**2.14a**:**b**) in 66% yield (entry 5). The oxidized product **b** likely arises from oxidation

processes via interaction with various catalyst intermediates or through disproportionation processes when HAT reaction rates are less competitive. Using substrate **2.12**, a similar trend is observed in comparable yields, where *i*Pr$_2$NEt, Hantzsch ester, and DABCO gave ratios of 67:33, 95:5, and 25:75 (**2.19a**:**b**), respectively (entries 6, 8, and 9). The addition of formic acid to reactions utilizing *i*Pr$_2$NEt and DABCO had little effect upon the product distribution of **2.19** (entries 7 and 10). Poor conversion was observed when using HMPA or DBU as the amine additive (entries 11 and 12). Notably, the biologically relevant reductant NADH (similar to Hantzsch ester), gave a ratio of 36:64 (**2.19a**:**b**) in 65% yield (entry 13). The ability of amines to participate in HAT reactions is demonstrated.

Table 2.4 Variation of amine base and effect on product distribution.

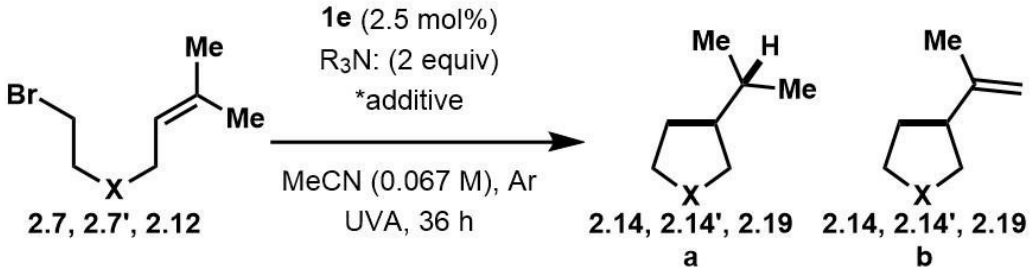

Entry	X =	R_3N:	additive [equiv]	a:b	Conv. [%][a]	Yield [%]
1	**2.7** $C(CO_2Et)_2$	*i*Pr$_2$NEt	---	**2.14** 65:35	>95	20
2[b]	**2.7'** $C(CO_2Me)_2$	*i*Pr$_2$NEt	CHD, 5.0	**2.14'** 100:0	>95	88
3[b]	**2.7'** $C(CO_2Me)_2$	---	CHD, 5.0	**2.14'** 100:0	58	18
4	**2.7** $C(CO_2Et)_2$	Hantzsch Ester	---	**2.14** 95:5	85	75
5	**2.7** $C(CO_2Et)_2$	DABCO	---	**2.14** 20:80	>95	66
6	**2.12** NTs	*i*Pr$_2$NEt	---	**2.19** 67:33	75	---
7	**2.12** NTs	*i*Pr$_2$NEt	formic acid, 5.0	**2.19** 50:50	>95	86
8	**2.12** NTs	Hantzsch Ester	---	**2.19** 95:5	20	---
9	**2.12** NTs	DABCO	---	**2.19** 25:75	>95	65
10	**2.12** NTs	DABCO	formic acid, 5.0	**2.19** 25:75	55	---
11	**2.12** NTs	HMPA	---	**2.19** 50:50	20	---
12	**2.12** NTs	DBU	---	**2.19** 75:25	10	---
13[c]	**2.12** NTs	NADH	---	**2.19** 36:64	>95	65

[a]Conversion was assigned by comparison of product to remaining starting material, as judged by ^{1}H NMR. [b]12 h irradiation with UVA LED using 5 mol% catalyst. [c]3:1 MeCN:H_2O used as solvent, 5 mol% catalyst.

During mechanistic studies of the hydrodebromination/cyclization reaction, a peculiar byproduct was observed when applying the similar reaction conditions (**Table 2.2**) with substrate **2.2** under UVA LED irradiation instead of UVA lightbulbs or sunlight. The formation of dimerized product **2.3a** was observed (40:60, **2.3**:**2.3a**, **Table 2.5**, entry 1). Using TEA (1 equiv) in MeCN:MeOH (1:1) gave an improved ratio of 24:75 (**2.3**:**2.3a**, entry 2). As previously demonstrated, HAT reactions from the amine base or the solvent led to reduced product **2.3**, where it was reasoned that using deuterated solvents and amine base should minimize products arising from reduction reactions (HAT) and maximize dimerized product **2.3a**. Using substrate **2.2'**, this strategy proved to give the highest ratios of dimer **2.3a'** in the best yield (9:89, **2.3'**:**2.3a'**, 53% yield, entries 3–5). To demonstrate the ability of HAT reactions to occur under these conditions, CHD (3 equiv)

Table 2.5 Optimization of a photoredox mediated dimerization reaction.

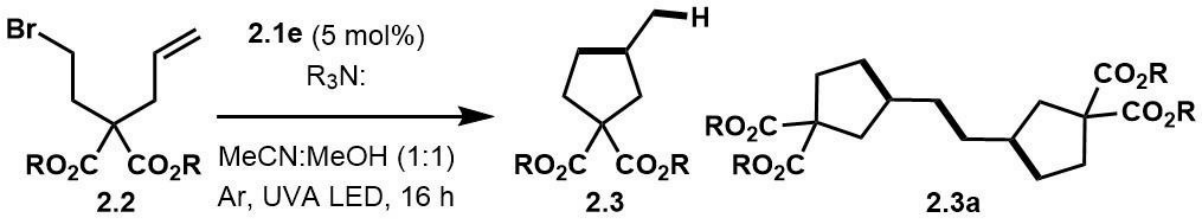

Entry	[M], R =	R_3N: [equiv]	Additive [equiv]	Yield 2.3:2.3a [%]
1	0.2, **2.2** Et	*i*Pr_2NEt 5.0	---	40:60[a]
2	0.5, **2.2'** Me	Et_3N 1.0	---	24:75
3	0.5, **2.2'** Me	d_{15}-Et_3N 1.0	---	20:72
4	0.5, **2.2'** Me	Et_3N 1.0	---	7:66[b]
5	0.5, **2.2'** Me	d_{15}-Et_3N 1.0	---	9:89(53)[b,c]
6	0.5, **2.2'** Me	Et_3N 1.0	CHD, 3.0	95(68):0
7	0.5, **2.2'** Me	Et_3N 1.0	TEMPO, 2.0	SM
8	0.5, **2.2'** Me	---	---	---
9	0.5, **2.2'** Me	Et_3N 1.0	---	SM[d]
10	0.5, **2.2'** Me	Et_3N 1.0	---	SM[e]

Yields determined by ^{1}H NMR analysis using mesitylene as an internal standard (isolated). [a]The reaction time was 0.1 h. [b]Deuterated solvents were used. [c]**d-2.3** was the byproduct. [d]In absence of photocatalyst. [e]In absence of irradiation.

was used as an additive and led to compound **2.3** as the sole product in 68% yield (entry 6). The use of TEMPO as a radical trapping reagent resulted in recovery of the starting material and may be due to TEMPO quenching the excited-state photocatalyst rather than the trialkylamine (entry 7). Interruption of the product forming pathways results in no trapping of alkyl radical intermediates with TEMPO. Finally, various control experiments demonstrated the need for trialkylamine, photocatalyst, and irradiation for product formation (entries 8–10).

Table 2.6 Scope of dimerization reaction.

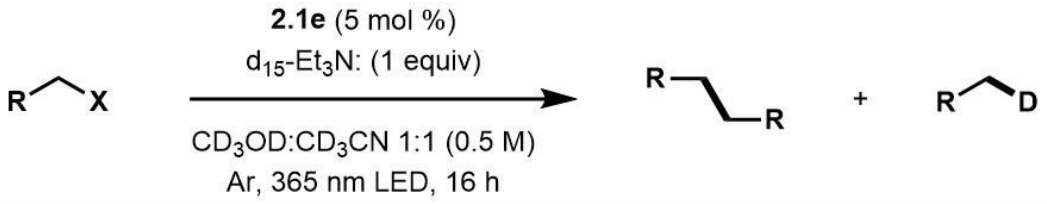

Entry	Substrate	Product	Yield [%]
1	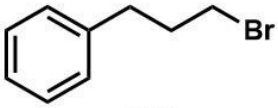 **2.34**	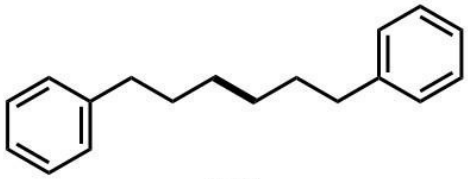 **2.38**	50
2	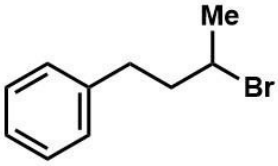 **2.35**	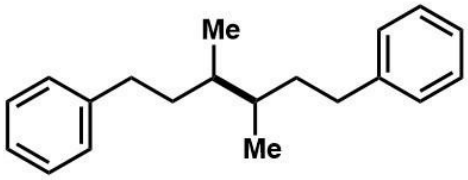 **2.39**	51
3	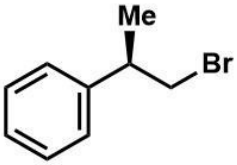 **2.36**	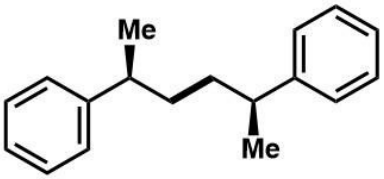 **2.40**	51
4	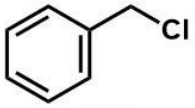 **2.37**	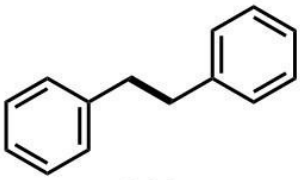 **2.33**	77

A small scope was examined to evaluate the broader applicability of this transformation with simple bromoalkanes (**Table 2.6**). Substrates **2.34**–**2.37** participated in the dimerization reaction in moderate yields ranging from 50–77% (entries 1–4). Notably, enantiopure **2.36** participated in the dimerization reaction without loss of stereochemical information, leading to **2.40** in 51% yield. An identical reaction using racemic **2.36** resulted in a statistical mixture of diastereomers (See section **2.7**). Benzyl chloride **2.37** resulted in the most efficient coupling (77%) owing to the increased stability of benzyl radicals. The by-products were the corresponding reduced alkanes (**d-2.33**, **d-2.38**–**2.40**) likely arising from deuterium atom transfer, albeit under conditions intended to minimize by-product forming pathways.

Further expansion of the reaction scope to iodoarenes was investigated (**Table 2.7**). Under similar conditions to the bromoalkane dimerization with addition of K_2HPO_4 (1 equiv), compound **2.41** afforded biaryl **2.61** in 91% yield. Iodoarenes **2.42** and **2.43** (*m*- and *o*-substituted methyl benzoates) gave products **2.62** and **2.63** in 66% and 14% yield, respectively, demonstrating that steric effects can be detrimental to the transformation. Electron-poor iodoarenes **2.44**–**2.53** gave biaryl products **2.64**–**2.73** ranging 31–63% yields. Interestingly, iodoarene **2.54** gave acetanilide **2.74** in 85% yield which likely arises from HAT processes. Electron-neutral alkyl functionalized iodoarenes **2.55**–**2.57** gave biaryl products **2.75**–**2.77** in moderate yield (34–53%). Electron-rich **2.58** gave biaryl **2.78** in 29% yield indicating that iodoarenes functionalized with electron donating groups are not well tolerated in this reaction. Finally, phenylalanine and estrone surrogates **2.59** and **2.60** were found to undergo the dimerization reaction, giving **2.79** and **2.80** in 66% and

28% yields, respectively, demonstrating the application of this methodology in more complex chemical environments.

Table 2.7 Scope of the dimerization reaction with iodoarenes.

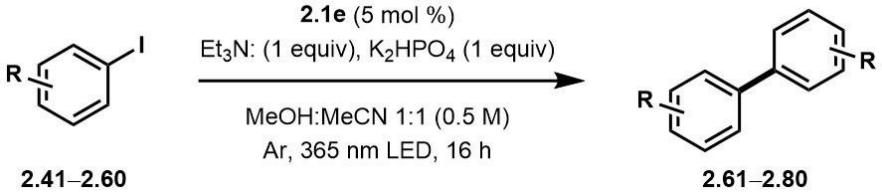

2.41–2.60 **2.61–2.80**

Entry	Substrate	Yield [%]	Entry	Substrate	Yield [%]	Entry	Substrate	Yield [%]
1	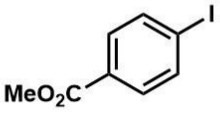 **2.41**	91	8	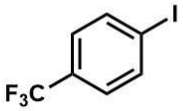 **2.48**	61	15	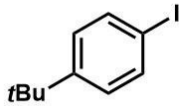 **2.55**	53
2	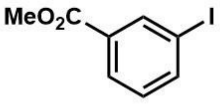 **2.42**	66	9	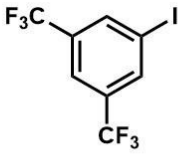 **2.49**	35	16	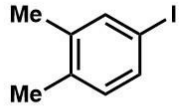 **2.56**	47
3	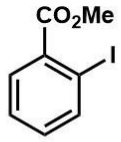 **2.43**	14	10	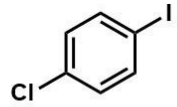 **2.50**	52	17	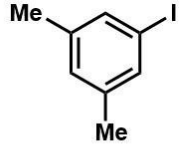 **2.57**	34
4	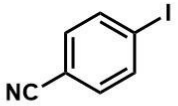 **2.44**	60	11	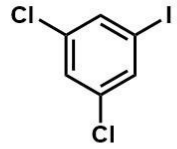 **2.51**	52	18	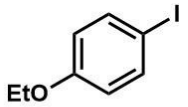 **2.58**	29
5	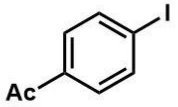 **2.45**	63	12	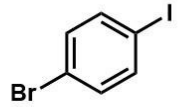 **2.52**	31	19	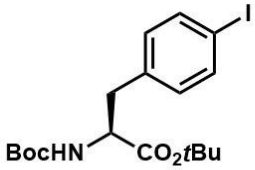 **2.59**	66
6	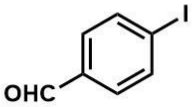 **2.46**	59	13	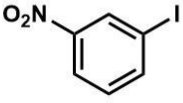 **2.53**	39			
7	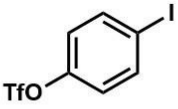 **2.47**	57	14	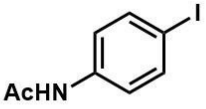 **2.54**	85[a]	20	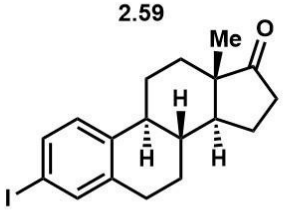 **2.60**	28

[a]The reduced product acetanilide was isolated rather than dimer product.

The proposed mechanism for this transformation is summarized in **Figure 2.1.** As demonstrated with laser flash photolysis experiments, the increased quenching rate of the excited-state binuclear Au(I) complex with trialkylamines over bromoalkanes indicates a reductive quenching pathway is operative. Upon reaction of intermediate **II** with a bromoalkane, the ground-state catalyst is regenerated along with a free alkyl radical (as indicated by the reduced alkane products in the presence of CHD) and is also supported by the lack of reactivity observed in the absence of trialkylamine base. Under the optimal conditions, it seems plausible that the rate of radical generation may be greater than the rate of alkyl radical reduction by solvent/reagents. When the concentration of alkyl radical is sufficiently high, they may add to an Au-centre, generating Au(II) intermediate **III**. The intermediate may be susceptible to another radical addition, resulting in difunctionalized Au(III) intermediate **IV** which upon reductive elimination, may lead to dimerized products. The current study cannot rule out radical-radical coupling reactions that may lead to the dimerized products. Also, it cannot be ruled out that the alkyl radicals may be associated with the metal-centre, resulting in a relatively more stable radical-bound-to-gold intermediate. A more in-depth kinetic analysis of this reaction would be necessary to the further understanding of this process, where absolute rates of HAT between two carbon atoms, although slow, could be determined as well as respective kinetic isotope effects and rates of alkyl radical addition to metal centres.

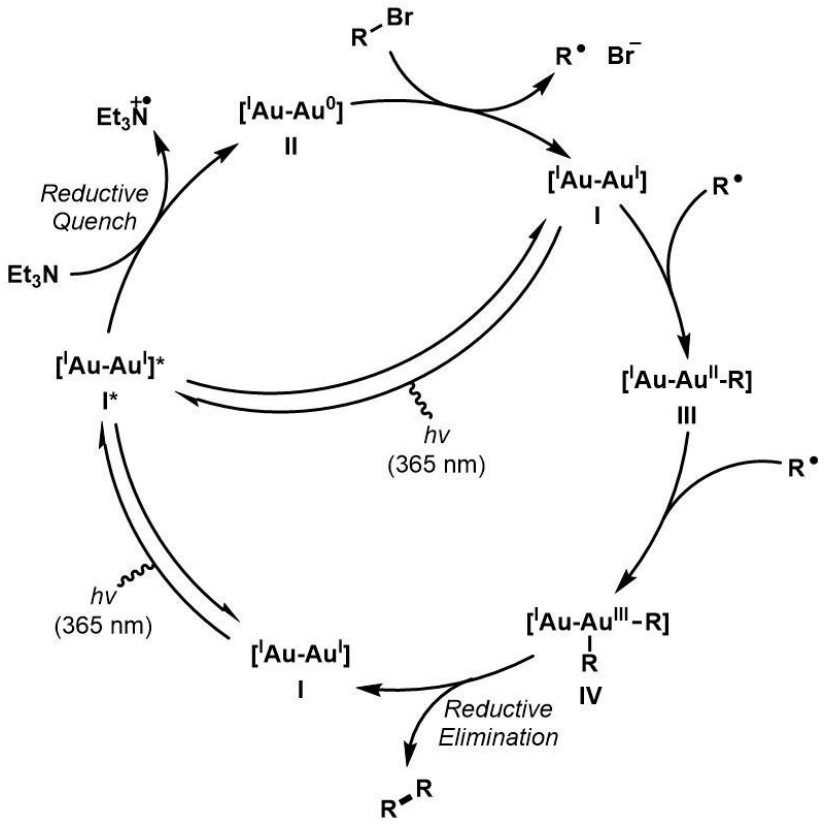

Figure 2.1 Proposed mechanism for the formation of dimer products.

2.6 Conclusions Pertaining to Further Information

During subsequent mechanistic studies, it was found the **2.1e** proceeds through a reductive quenching pathway when performing hydrodebromination reactions of bromoalkanes in the presence of trialkylamines. A study of the structure of various ligands demonstrated that relatively withdrawing ligands lend to more oxidizing excited-state Au(I) complexes that undergo preferential quenching with trialkylamines and relatively donating ligands produce excited-state Au(I) complexes that preferentially quench with bromoalkanes. In hydrodebromination reactions involving radical cyclization leading to tertiary alkyl radicals, the trialkylamine base was found to influence the ratio of products arising from reduction of the radical *versus* oxidative processes leading to alkenyl-containing products. Specifically, amine bases such as Hantzsch ester led to reduced

products likely due to structural similarity to cyclohexadiene and thus having hydrogen atom donor characteristics. On the other hand, DABCO led to the highest ratio of oxidized products likely due to the inability to donate a hydrogen atom based on its structure. Switching to UVA LEDs from a UVA photoreactor led to dimerized products arising from two alkyl radicals coupling. From these studies, an Au(I)/Au(III) photoredox cycle is proposed, where reductive elimination may be the key bond forming process, although radical-radical processes cannot be ruled out. The dimerization reaction was also tolerant of iodoarenes, leading to the formation of biaryl compounds in good yields.

2.7 Experimental Procedures

General Procedure 1 (GP1) – *Preparation of Binuclear Au(I) Complexes*

Commercially available [AuDMS]Cl (0.34–2.58 mmol, 1.0 equiv) stored in a glovebox was transferred to a flame-dried round bottomed flask and solvated in dry DCM (0.2 M) under argon, at ambient temperature. To this solution was added dppm (1.0 equiv) and allowed to stir for 1 h. After this time, the solvent was mostly evaporated, and complexes were precipitated with ether. The white powder was isolated and washed by filtration using ether, yields for **2.1e** ranging from 40–85% yield. Complexes **2.1a–d** were obtained from $[Au_2(\mu\text{-dppm})_2][Cl]_2$ (**2.1e**) by solvation of the complex (0.2 mmol, 1.0 equiv) in DCM (2 mL, 0.1 M) and adding AgX (0.4 mmol, 2.0 equiv) to the solution (X = OTf (**a**), NTf_2 (**b**), BF_4 (**c**), and SbF_6 (**d**)). After 1 h of stirring, the solutions were filtered over a silica pad using ether or EtOAc and the filtrate was concentrated *in vacuo*, affording the complexes in 44–76% yield, as white powders that were characterized with proton, carbon, and phosphorus NMR (400, 101, and 121 MHz, respectively; ^{31}P NMR was standardized using 85% phosphoric acid as external reference), HRMS, and IR.

General Procedure 2 (GP2) – *Preparation of Starting Materials*

To a flame-dried round bottomed flask was added NaH (1.01 equiv, 60% in mineral oil), suspended in dry THF(0.1–1.0 M), and cooled to 0°C in an ice bath. Diethyl malonate or corresponding phenol (1.00 equiv) were then added dropwise to the solution, allowed to stir for 30 minutes, and in this time the solutions became transparent. Corresponding bromoalkanes and substituted allyl bromides (0.90–3.00 equiv) were then added and the mixtures were allowed to stir overnight at ambient temperature. After completion as judged by TLC, the resulting reaction mixtures were then quenched with saturated ammonium chloride. The aqueous solution was extracted with DCM, dried with magnesium sulfate, and concentrated *in vacuo*. Crude products were further purified by column chromatography (2–20% EtOAc:Hex), concentrated *in vacuo*, and characterized by proton and carbon NMR (400 and 101 MHz, respectively), HRMS, and IR. Allylated malonates were further purified by Kugelrohr distillation during each alkylation between 50–70°C, affording pure allyl bromoalkyl diethyl malonates.

Allyl, Dimethylallyl, or propargyl functionalized tosylamines (1.00 equiv) were solvated in DCM (0.2 M), to which triethylamine (3.00 equiv) and 4-(dimethylamino)pyridine (0.05 equiv) were added and cooled to 0°C using an ice bath. The solution was allowed to stir for 15 minutes upon which tosyl chloride was added (1.10 equiv) portion wise. Reactions were allowed to stir overnight, when judged by TLC as complete, were quenched using ammonium chloride. Mixtures were washed with DCM, where the organic fractions were combined and concentrated *in vacuo*. Crude products were then isolated by column chromatography (25% EtOAc:Hex). The resulting *N*-tosyl-*N*-allyl or *N*-tosyl-*N*-propargyl amines were then submitted to Hassner's conditions to yield the corresponding *N*-tosyl-*N*-allyl-*N*-alkyl bromides and *N*-tosyl-*N*-propargyl-*N*-alkyl bromide.[26]

General Procedure 3 (GP3) – *Cyclization/Reduction of C–Br Bonds*

To an 8 mL Pyrex screw-top reaction vessel was added $[Au_2(\mu\text{-dppm})_2][X]_2$ (1–5 mol%), halogenated substrate (0.2 mmol, 1.0 equiv), MeCN (3 mL, 0.067 M), trialkylamine base (0.4–1.0 mmol, 2.0–5.0 equiv; procedure A), formic acid additive if necessary (0.4 mmol, 2.0 equiv; procedure B), and degassed under argon by sparging. The reaction mixtures were then placed under sunlight or in a UVA photoreactor for 2−24 h and in this time, became dark yellow, red, or brown solutions. The mixtures were then concentrated and purified by flash chromatography (1−25% EtOAc:Hex), where relevant fractions were combined, and concentrated *in vacuo*. Products were characterized with proton and carbon NMR (400 and 101 MHz, respectively), HRMS, and IR.

General Procedure 4 (GP4) – *Dimerization Reactions of Bromoalkanes*

To an 8 mL Pyrex screw-top reaction vessel was added $[Au_2(\mu\text{-dppm})_2]Cl_2$ (5 mol%), halogenated substrate (1.0 equiv), d_3-MeCN:D_3COD (1:1, 0.5 M), d_{15}-Et_3N (1.0 equiv), and degassed under argon by sparging. The reaction mixtures were then placed under UVA LED irradiation for 16 h. The mixtures were then concentrated and purified by flash chromatography (1−25% EtOAc:Hex), where relevant fractions were combined, and concentrated. Products were characterized by proton and carbon NMR (400 and 101 MHz, respectively), HRMS, and IR.

Comparative Studies Using Ir-Based Photoredox Catalysts

Table 2.8 Comparative studies with Ir-based photoredox catalysts.

Entry	Substrate	Product	Procedure[a]	Conv. [%][b]
1	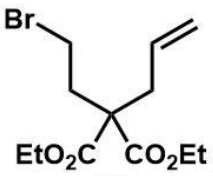 **2.2**	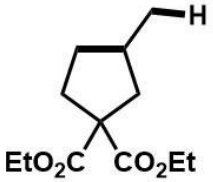 **2.3**	A	6
2			B	17
3			B (no **6**)	0
4	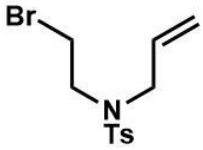 **2.11**	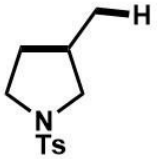 **2.18**	A	0
5			B	<5
6	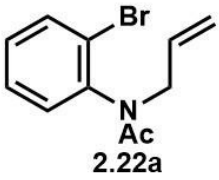 **2.22a**	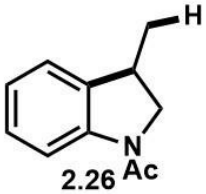 **2.26**	A	0
7			B	0
8			B (no **2.6**)	0

[a]Procedure A: **2.5** (2.5 mol%), nBu$_3$N: (10 equiv), formic acid (10 equiv), MeCN, Ar degas; procedure B: **2.6** (3.0 mol%), iPr$_2$NEt (10 equiv), MeCN, Ar degas; reactions were irradiated for 20–32 h using Blue LED strips and a 100W lightbulb. [b]Product conversion assigned by ratio of starting material to product as judged by ^{1}H NMR.

2.8 Characterization Data

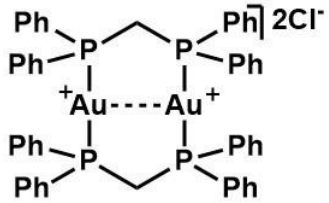

[Au$_2$(μ-dppm)$_2$]Cl$_2$ (2.1e)

Characterized according to GP1.

IR (neat, cm^{-1}): 3356(br), 3050(s), 3013(m), 2922(m), 2850(m), 1567(m), 1435(s), 1370(m), 1101(s), 742(s), 689(s); **^{1}H NMR** (400 MHz, $CDCl_3$): δ = 7.90 (m, 16H), 7.42–7.33 (m, 24H), 4.76–4.74 (m, 4H) ppm; **^{13}C NMR** (101 MHz, $CDCl_3$): δ = 133.9 (16×CH), 131.9 (8×CH), 129.2 (16×CH), 128.2 (8×C), 29.8 (2×CH_2) ppm; **^{31}P NMR** (121 MHz, $CDCl_3$): δ = 33.3 (4×P) ppm; **HRMS** (ESI): m/z calc'd for $C_{50}H_{44}Au_2P_4Cl$ [M^+-Cl] 1197.1413, found 1197.1451.

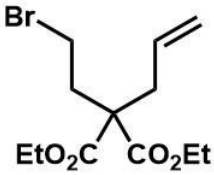

Diethyl (2-bromoethyl)(2-propenyl)malonate (2.2)

Synthesized according to GP2 and characterized by NMR comparison.[27]

^{1}H NMR (400 MHz, $CDCl_3$): δ = 5.73–5.58 (m, 1H), 5.21–5.11 (m, 2H), 4.21 (qd, *J* = 7.2, 0.7 Hz, 4H), 3.37 (t, *J* = 8.2 Hz, 2H), 2.67 (d, *J* = 7.3 Hz, 2H), 2.45 (t, *J* = 8.3 Hz, 2H), 1.27 (t, *J* = 7.1 Hz, 6H) ppm; **^{13}C NMR** (101 MHz, $CDCl_3$): δ = 170.2 (2×C), 131.8 (CH), 119.7 (CH_2), 61.6 (2×CH_2), 57.5 (C), 37.7 (CH_2), 36.2 (CH_2), 27.1 (CH_2), 14.0 (2×CH_3) ppm.

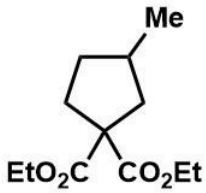

3-methyl-cyclopentane-1,1-dicarboxylic acid diethyl ester (2.3)

Synthesized according to GP3.

IR (neat, cm^{-1}): 2955(m), 1724(s), 1447(m), 1366(s), 1254(s); **^{1}H NMR** (400 MHz, $CDCl_3$): δ = 4.17 (q, *J* = 7.1 Hz, 4H), 2.44 (dd, *J* = 13.2, 7.1 Hz, 1H), 2.36–2.26 (m, 1H), 2.19–2.08 (m, 1H), 2.08–1.98 (m, 1H), 1.90–1.78 (m, 1 H), 1.66 (dd, *J* = 13.4, 10.0 Hz, 2H), 1.24 (t, *J* = 7.1 Hz, 6H), 1.01 (d, *J* = 6.7 Hz, 3H) ppm; **^{13}C NMR** (101 MHz, $CDCl_3$): δ = 172.8 (2×C), 61.2 (2×CH_2), 60.3 (C), 42.5 (CH_2), 34.4 (CH), 34.1 (CH_2), 34.0 (CH_2), 19.6 (CH_3), 14.0 (2×CH_3) ppm; **HRMS** (EI): m/z calc'd for $C_{12}H_{20}O_4$ [M^+] 228.1362, found 228.1320.

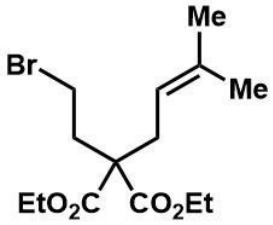

Diethyl (2-bromoethyl)(2-prenyl)malonate (2.7)

Synthesized according to GP2.

IR (neat, cm^{-1}): 2995(m), 2927(m), 2359(m), 1728(s), 1445(m), 1367(s), 1180(s); **^{1}H NMR** (400 MHz, $CDCl_3$): δ = 4.95 (tquin, *J* = 7.4, 1.4 Hz, 1H), 4.20 (q, *J* = 7.2 Hz, 4H), 3.38–3.30 (m, 2H), 2.62 (d, *J* = 7.5 Hz, 2H), 2.47–2.39 (m, 2H), 1.70 (d, *J* = 1.0 Hz, 3H), 1.63 (s, 3H), 1.26 (t, *J* = 7.2 Hz, 6H) ppm; **^{13}C NMR** (101 MHz, $CDCl_3$): δ = 170.6 (2×C), 136.2 (C), 117.1 (CH), 61.5 (2×CH_2), 57.7 (C), 36.2 (CH_2), 31.9 (CH_2), 27.4 (CH_2), 26.0 (CH_3), 17.9 (CH_3), 14.0 (2×CH_3) ppm; **HRMS** (EI): m/z calc'd for $C_{14}H_{23}O_4Br$ [M^+] 334.0780, found 334.0737.

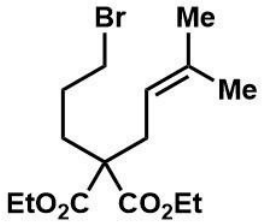

Diethyl (2-bromopropyl)(2-prenyl)malonate (2.8)

Synthesized according to GP2.

IR (neat, cm^{-1}): 2978(m), 2920(m), 1724(s), 1447(m), 1366(s), 1235(s); **^{1}H NMR** (400 MHz, $CDCl_3$): δ = 4.96 (tquin, *J* = 7.4, 1.5 Hz, 1H), 4.18 (qd, *J* = 7.3, 2.1 Hz, 4H), 3.38 (t, *J* = 6.6 Hz, 2H), 2.61 (d, *J* = 7.4 Hz, 2H), 2.04–1.93 (m, 2H), 1.83–1.72 (m, 2H), 1.70 (d, *J* = 1.1 Hz, 3H), 1.62 (d, *J* = 0.7 Hz, 3H), 1.25 (t, *J* = 7.2 Hz, 6H) ppm; **^{13}C NMR** (101 MHz, $CDCl_3$): δ = 171.3 (2×C), 135.7 (C), 117.4 (CH), 61.2 (2×CH_2), 57.1 (C), 33.3 (CH_2), 31.3 (CH_2), 31.0 (CH_2), 27.7 (CH_2), 26.0 (CH_3), 18.0 (CH_3), 14.1 (2×CH_3) ppm; **HRMS** (EI): m/z calc'd for $C_{15}H_{25}O_4Br$ [M^+] 348.0936, found 348.0954.

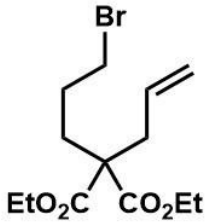

Diethyl (2-bromopropyl)(2-propenyl)malonate (2.9)

Synthesized according to GP2.

IR (neat, cm^{-1}): 2978(m), 1724(s), 1447(m), 1366(s), 1230(s); **^{1}H NMR** (400 MHz, $CDCl_3$): δ = 5.65 (ddt, *J* = 17.1, 9.9, 7.5 Hz, 1H), 5.17–5.06 (m, 2H), 4.20 (q, *J* = 7.1 Hz, 4H), 3.39 (t, *J* = 6.5 Hz, 2H), 2.65 (d, *J* = 7.4 Hz, 2H), 2.06–1.95 (m, 2H), 1.85–1.74 (m, 2H), 1.26 (t, *J* = 7.1 Hz, 6H) ppm; **^{13}C NMR** (101 MHz, $CDCl_3$): δ = 170.9 (2×C), 132.1 (CH), 119.2 (CH_2), 61.4 (2×CH_2), 56.8 (C), 37.1 (CH_2), 33.2 (CH_2), 31.0 (CH_2), 27.5 (CH_2), 14.1 (2×CH_3) ppm; **HRMS** (EI): m/z calc'd for $C_{13}H_{21}O_4Br$ [M^+] 320.0623, found 320.0599.

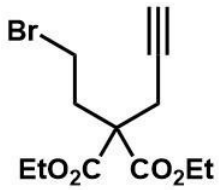

Diethyl (2-bromoethyl)(2-propynyl)malonate (2.10)

Synthesized according to GP2.

IR (neat, cm^{-1}): 3290(s), 2982(m), 2357(m), 1724(s), 1447(m), 1369(s), 1196(s); **^{1}H NMR** (400 MHz, $CDCl_3$): δ = 4.23 (qd, *J* = 7.1, 3.1 Hz, 4H), 3.45–3.35 (m, 2H), 2.85 (d, *J* = 2.7 Hz, 2H), 2.69–2.61 (m, 2H), 2.06 (t, *J* = 2.7 Hz, 1H), 1.28 (t, *J* = 7.2 Hz, 6H) ppm; **^{13}C NMR** (101 MHz, $CDCl_3$): δ = 169.3 (2×C), 78.2 (C), 72.0 (CH), 62.0 (2×CH_2), 56.7 (C), 35.7 (CH_2), 26.9 (CH_2), 23.3 (CH_2), 14.0 (2×CH_3) ppm; **HRMS** (EI): m/z calc'd for $C_{12}H_{17}O_4Br$ [M^+] 304.0310, found 304.0298.

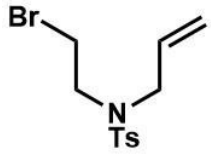

***N*-Allyl-*N*-(2-bromoethyl)-4-methylbenzenesulfonamide (2.11)**

Synthesized according to GP2 and characterized by NMR comparison.[28]

^{1}H NMR (400 MHz, $CDCl_3$): δ = 7.72 (dt, *J* = 8.2, 1.9 Hz, 2H), 7.33 (dd, *J* = 8.5, 0.7 Hz, 2H), 5.77–5.58 (m, 1H), 5.22 (dq, *J* = 6.3, 1.3 Hz, 1H), 5.19 (t, *J* = 1.3 Hz, 1H), 3.82 (dt, *J* = 6.5, 1.2 Hz, 2H), 3.53–3.37 (m, 4H), 2.45 (s, 3H) ppm; **^{13}C NMR** (101 MHz, $CDCl_3$): δ = 143.7 (C), 136.3 (C), 132.9 (CH), 129.9 (2×CH), 127.2 (2×CH), 119.7 (CH_2), 52.0 (CH_2), 48.9 (CH_2), 29.2 (CH_2), 21.5 (CH_3) ppm.

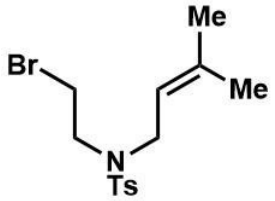

***N*-(3-methyl-but-2-en-1-yl)-*N*-(2-bromoethyl)-4-methylbenzenesulfonamide (2.12)**

Synthesized according to GP2.

IR (neat, cm^{-1}): 2913(s),1597(s), 1447(m), 1339(s), 1153(s); **^{1}H NMR** (400 MHz, $CDCl_3$): δ = 7.75–7.66 (m, 2H), 7.36–7.28 (m, 2H), 5.03 (tquin, *J* = 7.3, 1.5 Hz, 1H), 3.81 (d, *J* = 7.2 Hz, 2H), 3.49–3.36 (m, 4H), 2.44 (s, 3H), 1.70 (d, *J* = 0.9 Hz, 3H), 1.64 (s, 3 H) ppm; **^{13}C NMR** (101 MHz, $CDCl_3$): δ = 143.5 (C), 138.1 (C), 136.5 (C), 129.7 (2×CH), 127.2 (2×CH), 118.6 (CH), 48.9 (CH_2), 46.7 (CH_2), 29.6 (CH_2), 25.8 (CH_3), 21.5 (CH_3), 17.8 (CH_3) ppm; **HRMS** (EI): m/z calc'd for $C_{12}H_{17}O_4Br$ [M^+] 345.0398, found 345.0419.

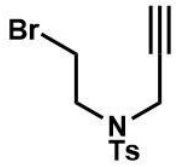

***N*-(2-bromoethyl)-4-methyl-*N*-(prop-2-yn-1-yl)benzenesulfonamide (2.13)**

Synthesized according to GP2 and characterized by NMR comparison.[28]

^{1}H NMR (400 MHz, $CDCl_3$): δ = 7.74 (dt, *J* = 8.3, 1.9 Hz, 2H), 7.32 (dd, *J* = 8.5, 0.6 Hz, 2H), 4.18 (d, *J* = 2.4 Hz, 2H), 3.62–3.49 (m, 4H), 2.44 (s, 3H), 2.12 (t, *J* = 2.5 Hz, 1H) ppm; **^{13}C NMR** (101 MHz, $CDCl_3$): δ = 144.0 (C), 135.4 (C), 129.7 (2×CH), 127.6 (2×CH), 76.6 (C), 74.2 (CH), 48.3 (CH_2), 37.9 (CH_2), 29.0 (CH_2), 21.5 (CH_3) ppm.

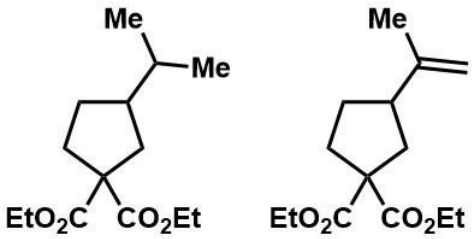

3-isopropyl-cyclopentane-1,1-dicarboxylic acid diethyl ester (2.14a)/3-isopropenyl-cyclopentane-1,1-dicarboxylic acid diethyl ester (2.14b) (65:35)

Synthesized according to GP3.

IR (neat, cm^{-1}): 2959(m), 2870(m), 1724(s), 1462(m), 1447(m), 1366(s), 1250(s);

2.14a: **^{1}H NMR** (400 MHz, $CDCl_3$): δ = 4.18 (qd, *J* = 7.0, 2.6 Hz, 4H), 2.46–2.39 (m, 1H), 2.28 (ddd, *J* = 13.5, 8.7, 3.3 Hz, 1H), 2.18–2.08 (m, 1H), 1.91–1.80 (m, 1H), 1.79–1.71 (m, 1H), 1.69–1.65 (m, 1H), 1.47–1.37 (m, 1H), 1.36–1.28 (m, 1H), 1.25 (td, *J* = 6.9, 0.9 Hz, 6H), 0.90 (dd, *J* = 7.9, 6.9 Hz, 6H) ppm; **^{13}C NMR** (101 MHz, $CDCl_3$): δ = 172.8 (C), 172.8 (C), 61.2 (2×CH_2), 60.0 (C), 47.3 (CH), 39.1 (CH_2), 33.9 (CH_2), 33.2 (CH), 30.3 (CH_2), 21.5 (CH_3), 21.4 (CH_3), 14.0 (2×CH_3) ppm; **HRMS** (EI): m/z calc'd for $C_{14}H_{24}O_4$ [M^+] 256.1675, found 256.1704;

2.14b: **^{1}H NMR** (400 MHz, $CDCl_3$): δ = 4.73 (dd, *J* = 6.9, 0.7 Hz, 2H), 4.19 (qd, *J* = 7.3, 2.9 Hz, 4H), 2.61–2.52 (m, 1H), 2.48 (ddd, *J* = 13.0, 7.0, 1.5 Hz, 1H), 2.36 (ddd, *J* = 13.6, 8.7, 3.2 Hz, 1H), 2.23–2.14 (m, 1H), 1.99 (dd, *J* = 13.1, 11.0 Hz, 1H), 1.94–1.85 (m, 1H), 1.74 (s, 3H), 1.57–1.52 (m, 1H), 1.25 (td, *J* = 7.1, 2.1 Hz, 6H) ppm; **^{13}C NMR** (101 MHz, $CDCl_3$): δ = 172.7 (C), 172.6 (C), 146.7 (C), 109.3 (CH_2), 61.3 (2×CH_2), 59.7 (C), 46.4 (CH), 38.9 (CH_2), 33.6 (CH_2), 30.7 (CH_2), 21.1 (CH_3), 14.0 (2×CH_3) ppm; **HRMS** (EI): m/z calc'd for $C_{14}H_{22}O_4$ [M^+] 254.1518, found 254.1495.

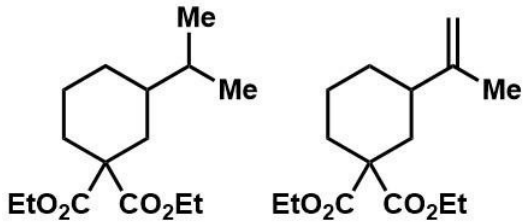

3-isopropyl-cyclohexane-1,1-dicarboxylic acid diethyl ester (2.15a)/3-isopropenyl-cyclohexane-1,1-dicarboxylic acid diethyl ester (2.15b) (84:16)

Synthesized according to GP3.

IR (neat, cm^{-1}): 2932(m), 2839(m), 1724(s), 1462(m), 1447(m), 1366(s), 1242(s);

2.15a: **^{1}H NMR** (400 MHz, $CDCl_3$): δ = 4.16 (q, *J* = 7.3 Hz, 3H), 2.37–2.30 (m, 2H), 1.78–1.59 (m, 4H), 1.56–1.50 (m, 1H), 1.49–1.30 (m, 4H), 1.24 (t, *J* = 7.1 Hz, 6H), 0.88 (dd, *J* = 6.6, 3.2 Hz, 6H) ppm; **^{13}C NMR** (101 MHz, $CDCl_3$): δ = 172.9 (C), 171.3 (C), 61.2 (CH_2), 60.9 (CH_2), 55.5 (C), 40.0 (CH), 34.5 (CH_2), 32.7 (CH), 31.3 (CH_2), 28.6 (CH_2), 22.9 (CH_2), 19.5 (CH_3), 19.4 (CH_3), 14.1 (CH_3), 14.0 (CH_3) ppm; **HRMS** (EI): m/z calc'd for $C_{15}H_{26}O_4$ [M^+] 270.1831, found 270.1835;

2.15b: **^{1}H NMR** (400 MHz, $CDCl_3$): δ = 4.74–4.69 (m, 2H), 4.16 (q, *J* = 7.3 Hz, 4H), 2.68–2.58 (m, 1H), 2.44–2.37 (m, 2H), 2.08–1.97 (m, 2H), 1.82–1.76 (m, 2H), 1.73 (s, 3H), 1.47–1.40 (m, 2H), 1.24 (t, *J* = 7.0 Hz, 6H) ppm; **^{13}C NMR** (101 MHz, $CDCl_3$): δ = 172.9 (C), 171.3 (C), 149.4 (C), 108.9 (CH_2), 61.3 (CH_2), 61.0 (CH_2), 55.4 (C), 41.1 (CH), 36.2 (CH_2), 31.6 (CH_2), 31.0 (CH_2), 30.5 (CH_2), 20.9 (CH_3), 14.1 (CH_3), 14.0 (CH_3) ppm; **HRMS** (EI): m/z calc'd for $C_{15}H_{24}O_4$ [M^+] 268.1675, found 268.1679.

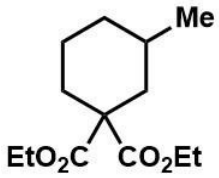

3-methyl-cyclohexane-1,1-dicarboxylic acid diethyl ester (2.16)

Synthesized according to GP3.

IR (neat, cm^{-1}): 2928(m), 1724(s), 1454(m), 1366(s), 1246(s); **^{1}H NMR** (400 MHz, $CDCl_3$): δ = 4.25–4.11 (m, 4H), 2.39–2.05 (m, 2H), 1.74–1.61 (m, 2H), 1.57–1.33 (m, 3H), 1.32–1.17 (m, 8H), 0.91 (d, *J* = 6.6 Hz, 3H) ppm; **^{13}C NMR** (101 MHz, $CDCl_3$): δ = 172.7 (C), 171.3 (C), 61.2 (CH_2), 60.9 (CH_2), 55.4 (C), 39.4 (CH_2), 34.0 (CH_2), 30.9 (CH_2), 28.9 (CH_3), 22.7 (CH_2), 22.5 (CH_3), 14.1 (CH_3), 14.0 (CH_3) ppm; **HRMS** (EI): m/z calc'd for $C_{13}H_{22}O_4$ [M^+] 242.1518, found 242.1519.

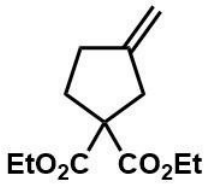

3-methenyl-cyclopentane-1,1-dicarboxylic acid diethyl ester (2.17)

Synthesized according to GP3.

IR (neat, cm^{-1}): 2964(m), 2357(m), 1724(s), 1435(m), 1366(s), 1265(s); **^{1}H NMR** (400 MHz, $CDCl_3$): δ = 4.90 (dt, *J* = 13.2, 1.8 Hz, 2H), 4.19 (q, *J* = 7.1 Hz, 4H), 2.94–2.90 (m, 2H), 2.43 (td, *J* = 7.5, 1.4 Hz, 2H), 2.27 (t, *J* = 7.4 Hz, 2H), 1.25 (t, *J* = 7.2 Hz, 6H) ppm; **^{13}C NMR** (101 MHz, $CDCl_3$): δ = 171.7 (2×C), 148.5 (C), 106.8 (CH_2), 61.4 (2×CH_2), 60.2 (C), 40.6 (CH_2), 33.7 (CH_2), 31.2 (CH_2), 14.0 (2×CH_3) ppm; **HRMS** (EI): m/z calc'd for $C_{12}H_{18}O_4$ [M^+] 226.1205, found 226.1182.

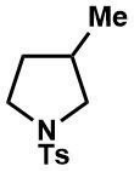

3-methyl-1-tosylpyrrolidine (2.18)

Synthesized according to GP3 and characterized by NMR comparison.[28]

^{1}H NMR (400 MHz, $CDCl_3$): δ = 7.72 (dt, *J* = 8.3, 1.7 Hz, 2H), 7.33 (dd, *J* = 8.5, 0.6 Hz, 2H), 3.43 (dd, *J* = 9.7, 7.2 Hz, 1H), 3.39–3.32 (m, 1H), 3.23 (ddd, *J* = 9.8, 8.2, 7.3 Hz, 1H), 2.76 (dd, *J* = 9.7, 7.8 Hz, 1H), 2.44 (s, 3H), 2.18–2.05 (m, 1H), 1.97–1.85 (m, 1H), 1.36 (dd, *J* = 12.3, 8.4 Hz, 1H), 0.93 (d, *J* = 6.7 Hz, 3H) ppm; **^{13}C NMR** (101 MHz, $CDCl_3$): δ = 143.2 (C), 134.0 (C), 129.6 (2×CH), 127.5 (2×CH), 54.7 (CH_2), 47.6 (CH_2), 33.3 (CH), 33.2 (CH_2), 21.5 (CH_3), 17.6 (CH_3) ppm; **HRMS** (EI): m/z calc'd for $C_{12}H_{16}DNO_2S$ [M^+] 240.1043, found 240.0995; **For D Labelling: HRMS** (EI): m/z calc'd for $C_{12}H_{17}NO_2S$ [M^+] 239.0980, found 239.0954.

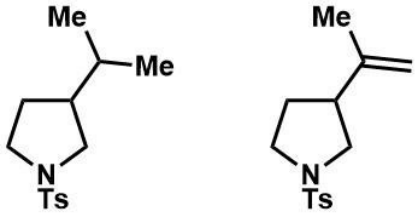

3-isopropyl-1-tosylpyrrolidine (2.19a)/3-isopropenyl-1-tosylpyrrolidine (2.19b) (50:50)

Synthesized according to GP3.

IR (neat, cm^{-1}): 2960(m), 2860(m), 1345(m), 1160(m), 1070(m), 1020(m), 810(s), 720(s); **2.19a**: **^{1}H NMR** (400 MHz, $CDCl_3$): δ = 7.72 (d, *J* = 8.2 Hz, 2H), 7.33 (d, *J* = 8.4 Hz, 2H), 3.54–3.34 (m, 2H), 3.16 (td, *J* = 9.9, 6.8 Hz, 1H), 2.79 (t, *J* = 9.7 Hz, 1H), 2.44 (s, 3H), 2.00–1.86 (m, 1H), 1.65–1.54 (m, 1H), 1.47–1.30 (m, 2H), 0.85 (d, *J* = 6.7 Hz, 6H) ppm; **^{13}C NMR** (101 MHz, $CDCl_3$): δ = 143.2 (C), 134.0 (C), 129.6 (2×CH), 127.5 (2×CH), 52.1 (CH_2), 48.1 (CH_2), 46.4 (CH), 31.8 (CH), 30.0 (CH_2), 21.5 (CH_3), 21.3 (CH_3), 20.9 (CH_3) ppm; **HRMS** (EI): m/z calc'd for $C_{14}H_{21}NO_2S$ [M^+] 267.1293, found 267.1292;

2.19b: **^{1}H NMR** (400 MHz, $CDCl_3$): δ = 7.73 (d, *J* = 8.2 Hz, 2H), 7.34 (d, *J* = 8.0 Hz, 2H), 4.74 (d, *J* = 1.0 Hz, 1H), 4.64 (d, *J* = 1.0 Hz, 1H), 3.50 (dd, *J* = 9.7, 7.6 Hz, 1H), 3.47–3.35 (m, 1H), 3.25 (td, *J* = 9.5, 6.8 Hz, 1H), 3.02 (t, *J* = 9.5 Hz, 1H), 2.62 (quin, *J* = 8.6 Hz, 1H), 2.45 (s, 3H), 2.00–1.87 (m, 1H), 1.67 (s, 3H), 1.75–1.60 (m, 1H) ppm; **^{13}C NMR** (101 MHz, $CDCl_3$): δ = 143.7 (C), 143.3 (C), 134.0 (C), 129.6 (2×CH), 127.5 (2×CH), 110.8 (CH_2), 51.5 (CH_2), 47.7 (CH_2), 45.1 (CH), 30.0 (CH_2), 21.5 (CH_3), 21.0 (CH_3) ppm; **HRMS** (EI): m/z calc'd for $C_{14}H_{19}NO_2S$ [M^+] 265.1136, found 265.1140.

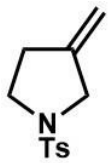

3-methenyl-1-tosylpyrrolidine (2.20)

Synthesized according to GP3 and characterized by NMR comparison.[28]

^{1}H NMR (400 MHz, $CDCl_3$): δ = 7.77–7.68 (m, 2H), 7.41–7.30 (m, *J* = 7.9 Hz, 2H), 4.97–4.85 (m, 2H), 3.84–3.74 (m, 2H), 3.29 (t, *J* = 7.1 Hz, 2H), 2.53–2.46 (m, 2H), 2.44 (s, 3H) ppm; **^{13}C NMR** (101 MHz, $CDCl_3$): δ = 144.1 (C), 143.6 (C), 132.7 (C), 129.7 (2×CH), 127.8 (2×CH), 107.4 (CH_2), 51.9 (CH_2), 48.1 (CH_2), 31.7 (CH_2), 21.5 (CH_3) ppm.

1-(allyloxy)-2-bromobenzene (2.21)

Synthesized according to GP2 and characterized by NMR comparison.[29]

^{1}H NMR (400 MHz, $CDCl_3$): δ = 7.56 (dd, *J* = 7.9, 1.6 Hz, 1H), 7.26 (ddd, *J* = 8.3, 7.4, 1.6 Hz, 1H), 6.97–6.72 (m, 2H), 6.08 (ddt, *J* = 17.3, 10.6, 5.0 Hz, 1H), 5.50 (dq, *J* = 17.3, 1.7 Hz, 1H), 5.32 (dq, *J* = 10.6, 1.5 Hz, 1H), 4.63 (dt, *J* = 5.0, 1.7 Hz, 2H); **^{13}C NMR** (101 MHz, $CDCl_3$): δ = 154.9 (C), 133.4 (CH), 132.6 (CH), 128.3(CH), 122.0 (CH), 117.7 (CH_2), 113.6 (CH), 112.3 (C), 69.6 (CH_2) ppm.

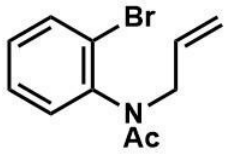

***N*-allyl-*N*-(2-bromophenyl)acetamide (2.22a)**

To a mixture of 2-bromoaniline (3.20 mmol, 1.00 equiv) and DMAP (0.16 mmol, 0.05 equiv) solvated in DCM (25 mL), was added Acetic Anhydride (3.2 mmol, 1.00 equiv). Reaction allowed to stir for 2 hr, when judged by TLC as complete, was quenched using Ammonium chloride. Mixture washed with DCM, organic fractions combined, and concentrated *in vacuo*. Crude product was then isolated by column chromatography (30% EtOAc:Hex). The resulting *N*-Acetyl-2-bromo-aniline was collected from fractions, solvent evaporated, and isolated as an off-yellow solid, quantitative yield. The resulting material was then submitted to Hassner's conditions[26] to yield the corresponding *N*-Acetyl-*N*-allylbromoaniline as yellow oil (87%). Characterized according to NMR comparison.[12]

^{1}H NMR (400 MHz, $CDCl_3$): δ =7.70 (dd, *J* = 8.0, 1.3 Hz, 1H), 7.37 (td, *J* = 7.5, 1.5 Hz, 1H), 7.27–7.19 (m, 2H), 5.94–5.84 (m, 1H), 5.10 (dq, *J* = 10.1, 1.2 Hz, 1H), 5.06 (dq, *J* = 17.0, 1.4 Hz, 1H), 4.78 (ddt, *J* = 14.7, 5.6, 1.3 Hz, 1H), 3.73 (dd, *J* = 14.7, 7.6 Hz, 1H), 1.82 (s, 3H) ppm; **^{13}C NMR** (101 MHz, $CDCl_3$): δ = 170.1 (C), 141.4 (C), 133.8 (CH), 132.8 (CH), 131.1 (CH), 129.7 (CH), 128.5 (CH), 123.9 (C), 118.5 (CH_2), 50.9 (CH_2), 22.4 (CH_3) ppm.

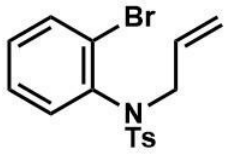

***N*-allyl-*N*-(2-bromophenyl)-4-methylbenzenesulfonamide (2.22b)**

Synthesized according to GP2 and characterized by NMR comparison.[30]

^{1}H NMR (400 MHz, $CDCl_3$): δ = 7.70–7.64 (m, 2H), 7.61 (dd, *J* = 7.9, 1.5 Hz, 1H), 7.32–7.27 (m, 2H), 7.25 (dd, *J* = 7.7, 1.6 Hz, 1H), 7.22–7.16 (m, 1H), 7.09 (dd, *J* = 7.8, 1.7 Hz, 1H), 5.84 (ddt, *J* = 16.9, 10.1, 6.7 Hz, 1H), 5.10–4.95 (m, 2H), 4.19 (dd, *J* = 11.4, 6.8 Hz, 2H), 2.45 (s, 3H) ppm; **^{13}C NMR** (101 MHz, $CDCl_3$): δ = 143.6 (C), 137.7 (C), 136.8 (C), 133.9 (CH), 132.6 (CH), 132.4 (CH), 129.8 (CH), 129.5 (2×CH), 127.9 (2×CH), 127.8 (CH), 125.8 (C), 119.3 (CH_2), 53.9 (CH_2), 21.6 (CH_3) ppm.

***N*-(2-bromophenyl)acetamide (2.23)**

Synthesized as described in **2.22a**, characterized by NMR comparison.[30]

^{1}H NMR (400 MHz, $CDCl_3$): δ = 8.35 (d, *J* = 8.2 Hz, 1H), 7.61 (br. s, 1H), 7.54 (dd, *J* = 8.1, 1.5 Hz, 1H), 7.32 (ddd, *J* = 8.4, 7.5, 1.5 Hz, 1H), 7.05–6.93 (m, 1H), 2.25 (s, 3H) ppm; **^{13}C NMR** (101 MHz, $CDCl_3$): δ = 168.2 (C), 135.7 (C), 132.2 (CH), 128.4 (CH), 125.1 (CH), 121.9 (CH), 113.1 (C), 24.9 (CH_3) ppm.

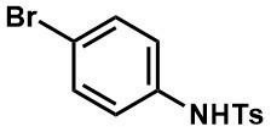

***N*-(4-bromophenyl)-4-methylbenzenesulfonamide (2.24)**

Synthesized according to GP2 and characterized by NMR comparison.[31]

^{1}H NMR (400 MHz, $CDCl_3$): δ = 7.71–7.64 (m, 2H), 7.37–7.32 (m, 2H), 7.27–7.22 (m, 2H), 7.03–6.94 (m, 2H), 2.39 (s, 3H) ppm; **^{13}C NMR** (101 MHz, $CDCl_3$): δ = 144.2 (C), 135.7 (C), 135.6 (C), 132.3 (2×CH), 129.8 (2×CH), 127.2 (2×CH), 123.0 (2×CH), 118.4 (C), 21.6 (CH_3) ppm.

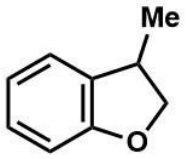

3-methyl-2,3-dihydrobenzofuran (2.25)

Synthesized according to GP3 and characterized by NMR comparison.[32]

^{1}H NMR (400 MHz, $CDCl_3$): δ = 7.17 (dt, *J* = 7.3, 1.3 Hz, 1H), 7.12 (dt, *J* = 7.8, 1.0 Hz, 1H), 6.90–6.86 (m, 1H), 6.80 (d, *J* = 8.0 Hz, 1H), 4.69 (t, *J* = 8.8 Hz, 1H), 4.08 (dd, *J* = 8.6, 7.5 Hz, 1H), 3.62–3.51 (m, 1H), 1.34 (d, *J* = 6.9 Hz, 3H) ppm; **^{13}C NMR** (101 MHz, $CDCl_3$): δ = 159.7 (C), 132.2 (C), 128.0 (CH), 123.8 (CH), 120.4 (CH), 109.4 (CH), 78.4 (CH_2), 36.5, 19.3 (CH_3) ppm.

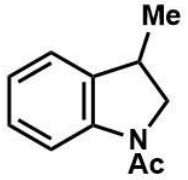

3-methyl-1-acetylindoline (2.26)

Synthesized according to GP3 and characterized by NMR comparison.[12]

^{1}H NMR (400 MHz, $CDCl_3$): δ = 8.20 (d, *J* = 8.0 Hz, 1H), 7.24–7.19 (m, 1H), 7.17 (d, *J* = 7.4 Hz, 1H), 7.05 (td, *J* = 7.4, 1.1 Hz, 1H), 4.22 (t, *J* = 9.6 Hz, 1H), 3.58 (dd, *J* = 9.9, 6.7 Hz, 1H), 3.50 (dq, *J* = 14.3, 6.8 Hz, 1H), 2.23 (s, 3H), 1.37 (d, *J* = 6.8 Hz, 3H) ppm; **^{13}C NMR** (101 MHz, $CDCl_3$): δ =^{13}C NMR (101 MHz, Chloroform-*d*) δ 168.6 (C), 142.4 (C), 136.3 (C), 127.7 (CH), 123.7 (CH), 123.3 (CH), 116.9 (CH), 56.9 (CH_2), 34.7 (CH), 24.2 (CH_3), 20.3 (CH_3) ppm.

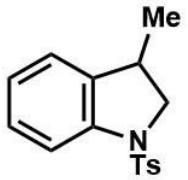

3-methyl-1-tosylindoline (2.27)

Synthesized according to GP3 and characterized by NMR comparison.[28]

^{1}H NMR (400 MHz, $CDCl_3$): δ = 7.72–7.67 (m, 2H), 7.67–7.61 (m, 1H), 7.26–7.18 (m, 3H), 7.09–6.97 (m, 2H), 4.09 (dd, *J* = 10.4, 9.0 Hz, 1H), 3.43 (dd, *J* = 10.4, 7.2 Hz, 1H), 3.20 (dt, *J* = 8.9, 7.0 Hz, 1H), 2.38 (s, 3H), 1.12 (d, *J* = 6.9 Hz, 3H) ppm; **^{13}C NMR** (101 MHz, $CDCl_3$): δ = 144.0 (C), 141.5 (C), 136.8 (C), 134.0 (C), 129.6 (2×CH), 127.8 (CH), 127.3 (2×CH), 123.9 (CH), 123.7 (CH), 114.9 (CH), 57.5 (CH_2), 34.7 (CH), 21.5 (CH_3), 19.5 (CH_3) ppm.

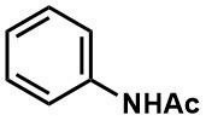

***N*-phenylacetamide (2.28)**

Synthesized according to GP3 and characterized by NMR comparison.[28]

^{1}H NMR (400 MHz, $CDCl_3$): δ = 7.55–7.47 (m, 2H), 7.33 (t, *J* = 7.9 Hz, 2H), 7.25 (br. s, 1H), 7.12 (t, *J* = 7.4 Hz, 1H), 2.19 (s, 3H) ppm; **^{13}C NMR** (101 MHz, $CDCl_3$): δ = 168.2 (C), 137.8 (C), 129.0 (2×CH), 124.3 (CH), 119.8 (2×CH), 24.6 (CH_3) ppm.

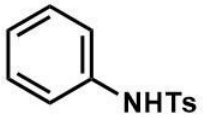

4-methyl-*N*-phenylbenzenesulfonamide (2.29)

Synthesized according to GP3 and characterized by NMR comparison.[28]

^{1}H NMR (400 MHz, $CDCl_3$): δ = 7.71–7.63 (m, 2H), 7.27–7.20 (m, 4H), 7.15–7.05 (m, 3H), 6.81 (s, 1H), 2.38 (s, 3H) ppm; **^{13}C NMR** (101 MHz, $CDCl_3$): δ = 143.8 (C), 136.5 (C), 136.0 (C), 129.6 (2×CH), 129.3 (2×CH), 127.3 (2×CH), 125.3 (CH), 121.6 (2×CH), 21.5 (CH_3) ppm.

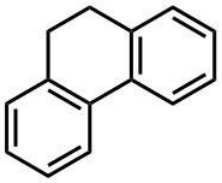

9,10-dihydrophenanthrene (2.31)

Synthesized according to GP3 and characterized by NMR comparison.[33]

^{1}H NMR (400 MHz, $CDCl_3$): δ = 7.77 (d, *J* = 7.6 Hz, 2H), 7.29–7.26 (m, 6H), 2.89 (s, 4H) ppm; **^{13}C NMR** (101 MHz, $CDCl_3$): δ = 137.4 (2×C), 134.5 (2×C), 128.1 (2×CH), 127.4 (2×CH), 126.9 (2×CH), 123.7 (2×CH), 29.0 (2×CH_2) ppm.

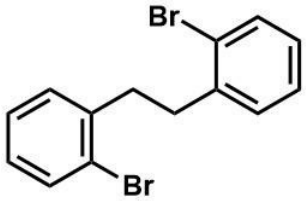

1,2-bis(2-bromophenyl)ethane (2.32)

Synthesized as described above and characterized by NMR comparison.[34]

^{1}H NMR (400 MHz, $CDCl_3$): δ = 7.56 (dd, *J* = 7.9, 1.2 Hz, 2H), 7.26–7.18 (m, 4H), 7.09 (ddd, *J* = 7.9, 6.7, 2.3 Hz, 2H), 3.05 (s, 4H) ppm; **^{13}C NMR** (101 MHz, $CDCl_3$): δ = ^{13}C NMR (101 MHz, Chloroform-*d*) δ 140.8 (2×C), 132.8 (2×CH),130.6 (2×CH), 127.8 (2×CH), 127.4 (2×CH), 124.5 (2×C), 36.4 (2×CH_2) ppm.

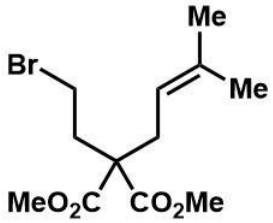

Dimethyl (2-bromoethyl)(2-prenyl)malonate (2.7')

Synthesized according to GP2 and characterized by NMR comparison.[35]

^{1}H NMR (400 MHz, $CDCl_3$): δ = 4.93 (tqt, *J* = 7.5, 1.5 Hz, 1H), 3.74 (s, 6H), 3.39–3.29 (m, 2H), 2.67–2.60 (m, 2H), 2.49–2.38 (m, 2H), 1.71 (s, 3H), 1.63 (s, 3H) ppm; **^{13}C NMR** (101 MHz, $CDCl_3$): δ = 171.0 (2×C), 136.5 (C), 116.9 (CH), 57.8 (C), 52.6 (2×CH_3), 36.3 (CH_2), 32.1 (CH_2), 27.3 (CH_2), 26.0 (CH_3), 17.9 (CH_3) ppm.

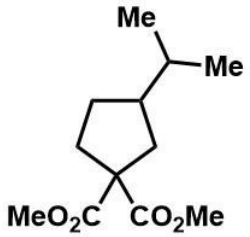

3-isopropyl-cyclopentane-1,1-dicarboxylic acid dimethyl ester (2.14')

Synthesized according to GP3 and characterized by NMR comparison.[35]

^{1}H NMR (400 MHz, $CDCl_3$): δ = 3.72 (d, *J* = 2.5 Hz, 6H), 2.49–2.40 (m, 1H), 2.29 (ddd, *J* = 13.5, 8.7, 3.4 Hz, 1H), 2.14 (ddd, *J* = 13.5, 9.7, 7.5 Hz, 1H), 1.91–1.81 (m, 1H), 1.75 (dd, *J* = 13.0, 10.8 Hz, 1H), 1.67 (ddd, *J* = 10.3, 8.3, 6.8 Hz, 1H), 1.41 (dqt, *J* = 8.4, 6.7 Hz, 1H), 1.36–1.27 (m, 1H), 0.91–0.88 (m, 6H) ppm; **^{13}C NMR** (101 MHz, CDCl3): δ = 173.2 (2×C), 60.0 (C), 52.6 (CH_3), 52.6 (CH_3), 47.2 (CH), 39.2 (CH_2), 34.0 (CH_2), 33.2 (CH), 30.2 (CH_2), 21.4 (CH_3), 21.4 (CH_3) ppm.

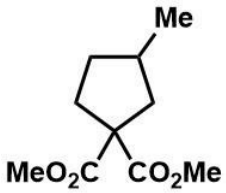

3-methyl-cyclopentane-1,1-dicarboxylic acid dimethyl ester (2.3')

Synthesized according to GP4 with addition of cyclohexadiene (3.0 equiv) and characterized according to NMR comparison.[35]

^{1}H NMR (400 MHz, $CDCl_3$): δ = 3.72 (d, *J* = 0.7 Hz, 6H), 2.51–2.41 (m, 1H), 2.34 (ddd, *J* = 13.4, 8.5, 3.9 Hz, 1H), 2.21–1.98 (m, 2H), 1.91–1.80 (m, 1H), 1.68 (dd, *J* = 13.3, 10.1 Hz, 1H), 1.02 (d, *J* = 6.6 Hz, 3H) ppm; **^{13}C NMR** (101 MHz, $CDCl_3$): δ = 173.3 (2×C), 60.2 (2×C), 52.6 (2×CH_3), 42.7 (CH_2), 34.4 (CH), 34.2 (CH_2), 34.1 (CH_2), 19.6 (CH_3) ppm.

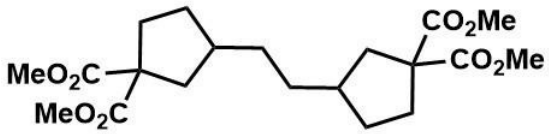

tetramethyl 3,3'-(ethane-1,2-diyl)bis(cyclopentane-1,1-dicarboxylate) (2.3a')

Synthesized according to GP4.

IR (neat, cm^{-1}): 2953(m), 2853(m), 1729(vs), 1435(s), 1251(s), 1157(s); **^{1}H NMR** (400 MHz, $CDCl_3$): δ = 3.72 (d, *J* = 1.1 Hz, 12H), 2.45 (dd, *J* = 13.1, 7.1 Hz, 2H), 2.30 (dddd, *J* = 13.5, 8.4, 3.6, 1.5 Hz, 2H), 2.14 (dddd, *J* = 13.6, 9.2, 7.2, 1.3 Hz, 2H), 1.96–1.80 (m, 4H), 1.68 (ddd, *J* = 13.3, 9.8, 1.5 Hz, 2H), 1.36–1.19 (m, 6H) ppm; **^{13}C NMR** (101 MHz, $CDCl_3$): δ = 173.2 (4×C), 59.9 (2×C), 52.6 (4×CH_3), 40.8 (2×CH_2), 39.9 (2×CH), 34.1 (2×CH_2), 33.9 (2×CH_2), 32.1 (2×CH_2) ppm; **HRMS** (EI): m/z calc'd for $C_{16}H_{18}O_4$ [M^+–$C_4H_{12}O_4$] 274.1205, found 274.1240.

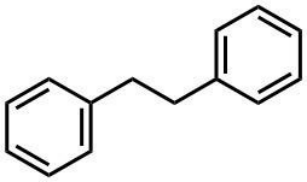

bibenzyl (2.33)

Synthesized according to GP4 and characterized by NMR comparison.[36]

^{1}H NMR (400 MHz, $CDCl_3$): δ = 7.35–7.28 (m, 4H), 7.23 (ddd, *J* = 7.7, 5.9, 1.7 Hz, 6H), 2.96 (s, 4H) ppm; **^{13}C NMR** (101 MHz, $CDCl_3$): δ = 141.8 (2×C), 128.4 (4×CH), 128.3 (4×CH), 125.9 (2×CH), 37.9 (2×CH_2) ppm.

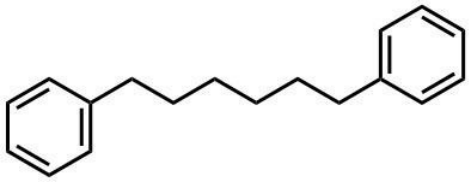

1,6-diphenylhexane (2.38)

Synthesized according to GP4 and characterized by NMR comparison.[37]

^{1}H NMR (400 MHz, $CDCl_3$): δ = 7.32–7.27 (m, 4H), 7.22–7.16 (m, 6H), 2.67–2.58 (m, 4H), 1.68–1.59 (m, 4H), 1.39 (ddd, *J* = 7.3, 4.5, 3.2 Hz, 4H) ppm; **^{13}C NMR** (101 MHz, $CDCl_3$): δ = 142.8 (2×C), 128.4 (4×CH), 128.2 (4×CH), 125.6 (2×CH), 35.9 (2×CH_2), 31.4 (2×CH_2), 29.1 (2×CH_2) ppm.

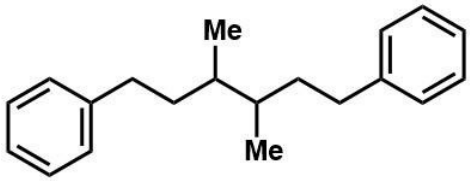

(3,4-dimethylhexane-1,6-diyl)dibenzene (2.39)

Synthesized according to GP4 and characterized by NMR comparison.[38]

^{1}H NMR (400 MHz, $CDCl_3$): δ = 7.32–7.27 (m, 4H), 7.22–7.15 (m, 6H), 2.66 (dddd, *J* = 12.9, 10.1, 7.6, 5.2 Hz, 2H), 2.59–2.44 (m, 2H), 1.71–1.59 (m, 2H), 1.54–1.33 (m, 4H), 0.93 (d, *J* = 6.5 Hz, 3H), 0.87 (d, *J* = 6.3 Hz, 3H) ppm; **^{13}C NMR** (101 MHz, $CDCl_3$): δ = 143.1 (2×C), 128.4 (4×CH), 128.3 (4×CH), 125.6 (2×CH), 37.1 (2×CH), 36.9 (2×CH_2), 36.3 (2×CH), 35.0 (2×CH_2), 34.1 (2×CH_2), 34.0 (2×CH_2), 16.3 (2×CH_3), 14.3 (2×CH_3) ppm.

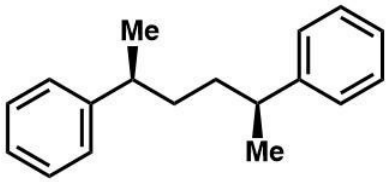

((2S,5S)-hexane-2,5-diyl)dibenzene (2.40)

Starting material (*R*)-(1-bromopropan-2-yl)benzene **2.36** was synthesized according to previously reported method[22] where **2.40** was synthesized according to GP4 and characterized by NMR comparison.[39]

^{1}H NMR (400 MHz, $CDCl_3$): δ = 7.31–7.26 (m, 4H), 7.22–7.11 (m, 6H), 2.66 (q, *J* = 7.0 Hz, 2H), 1.57–1.46 (m, 4H), 1.21 (d, *J* = 7.0 Hz, 6H) ppm; **^{13}C NMR** (101 MHz, $CDCl_3$): δ = 147.6 (2×C), 128.2 (4×CH), 127.0 (4×CH), 125.8 (2×CH), 40.0 (2×CH), 36.1 (2×CH_2), 22.5 (2×CH_3) ppm; **$[\alpha]_D^{23}$** = +13.0° (c 1.0, $CHCl_3$).

Corresponding racemic analog provided a statistical mixture of diastereomers under these conditions in similar yield.

^{1}H NMR (400 MHz, $CDCl_3$): δ = 7.32–7.24 (m, 4H), 7.21–7.09 (m, 6H), 2.70–2.57 (m, 2H), 1.61–1.39 (m, 4H), 1.20 (d, *J* = 7.0 Hz, 6H) ppm; **^{13}C NMR** (101 MHz, $CDCl_3$): δ = 147.7 (2×C), 147.6 (2×C), 128.3 (4×CH), 128.2 (4×CH), 127.0 (4×CH), 127.0 (4×CH), 125.8 (2×CH, both diastereomers), 40.1 (2×CH), 40.0 (2×CH), 36.5 (2×CH_2), 36.1 (2×CH_2), 22.5 (2×CH_3), 22.3 (2×CH_3) ppm.

2.9 References

[1] Ciamician, G. *Science* **1912**, *36*, 385–394.

[2] Albini, A.; Fagnoni, M. *Green Chem*. **2004**, *6*, 1–6.

[3] Fagnoni, M.; Dondi, D.; Ravelli, D.; Albini, A. *Chem. Rev*. **2007**, *107*, 2725–2756.

[4] Kalyanasundaram, K. *Coord. Chem. Rev*. **1982**, *46*, 159–244.

[5] Juris, A.; Balzani, V.; Barigelletti, F.; Campagna, S.; Belser, P.; von Zelewsky, A. *Coord. Chem. Rev*. **1988**, *84*, 85–277.

[6] *For recent reviews, see:* a) Yoon, T. P.; Ischay, M. A.; Du, J. *Nat. Chem*. **2010**, *2*, 527–532; b) Narayanam, J. M. R.; Stephenson, C. R. J. *Chem. Soc. Rev*. **2011**, *40*, 102–113; c) Teplý, F. *Collect. Czech. Chem. Commun*. **2011**, *76*, 859–917; d) Shi, L.; Xia, W. *Chem. Soc. Rev*. **2012**, *41*, 7687–7697; e) Xuan, J.; Xiao, W.-J. *Angew. Chem. Int. Ed*. **2012**, *51*, 6828–6838; f) Prier, C. K.; Rankic, D. A.; MacMillan, D. W. C. *Chem. Rev*. **2013**, *113*, 5322–5363.

[7] a) Curran, D. P. in *Comprehensive Organic Synthesis*; Trost, B. M.; Fleming, I.; Semmelhack, M. F., Eds.; Pergamon, Oxford, 1991; Vol. 4, 715–779; b) *Radicals in Organic Synthesis*; Renaud, P., Sibi, M. P., Eds.; Wiley-VCH: Weinheim, 2001; c) *Topics in Current Chemistry, Radicals in Synthesis I and II*; Gansuer, A., Ed.; Springer: Berlin, 2006; Vols. 263 and 264; d) *Encyclopedia of Radicals in Chemistry, Biology and Materials*; Chatgilialoglu, C., Studer, A., Eds.; Wiley: Chichester, 2012; Vols. 1 and 2.

[8] *For examples of alternatives to tin hydride mediators, see:* a) Chatgilialoglu, C. *Acc. Chem. Res*. **1992**, *25*, 188–194; b) Baguley, P. A.; Walton, J. C. *Angew. Chem. Int. Ed*. **1998**, *37*, 3072–3082; c) Ollivier, C.; Renaud, P. *Chem. Rev*. **2001**, *101*, 3415–3434; d) Studer, A.; Amrein, S. *Synthesis* **2002**, 835–849; e) Gilbert, B. C.; Parsons, A. F. *J. Chem. Soc., Perkin Trans. 2* **2002**, 367–387; f) Murphy, J. A.; Khan, T. A.; Zhou, S. Z.; Thomson,

D. W.; Mahesh, M. *Angew. Chem. Int. Ed*. **2005**, *44*, 1356–1360; g) Quiclet-Sire, B.; Zard, S. Z. *Pure Appl. Chem*. **2011**, *83*, 519–551; h) Weiss, M. E.; Kreis, L. M.; Lauber, A.; Carreira, E. M. *Angew. Chem. Int. Ed*. **2011**, *50*, 11125–11128; i) Ekomié, A.; Lefèvre, G.; Fensterbank, L.; Lacôte, E.; Malacria, M.; Ollivier, C.; Jutand, A. *Angew. Chem. Int. Ed*. **2012**, *51*, 6942–6946.

[9] Nicewicz, D. A.; MacMillan, D. W. C. *Science* **2008**, *322*, 77–80.

[10] Shih, H. W.; Vander Wal, M. N.; Grange, R. L.; MacMillan, D. W. C. *J. Am. Chem. Soc*. **2010**, *132*, 13600–13603.

[11] Nguyen, J. D.; D'Amato, E. M.; Narayanam, J. M. R.; Stephenson, C. R. J. *Nat. Chem*. **2012**, *4*, 854–859.

[12] Kim, H.; Lee, C. *Angew. Chem. Int. Ed*. **2012**, *51*, 12303–12306.

[13] a) Fry, A. J.; Krieger, R. L. *J. Org. Chem*. **1976**, *41*, 54–57; b) Rondinini, S.; Mussini, P. R.; Muttini, P.; Sello, G. *Electrochim. Acta* **2001**, *46*, 3245–3258.

[14] Kwong, H.-L.; Yam, V. W.-W.; Li, D. D.; Che, C.-M. *J. Chem. Soc., Dalton Trans*. **1992**, 3325–3329.

[15] Che, C.-M, Kwong, H.-L, Yam, V. W.-W, Choc, K. C. *J. Chem. Soc., Chem. Commun*. **1989**, 885–886.

[16] King, C.; Wang, J.-C.; Khan, M. N. I.; Fackler, Jr., J. P. *Inorg. Chem*. **1989**, *28*, 2145–2149.

[17] Narayanam, M. R. J.; Tucker, J. W.; Stephenson, C. R. J. *J. Am. Chem. Soc*. **2009**, *131*, 8756–8757.

[18] 10% deuterium incorporation was observed when the reaction was performed in d_3-MeCN.

[19] No significant differences in the isopropyl/isopropenyl ratio were observed for entries 1–4 and 10 in **Table 2.2** when procedure B (with formic acid) was used instead of procedure A. Poor conversion was observed when Hantzsch ester and NADH (the reduced form of nicotinamide adenine dinucleotide) were used as hydrogen donors.

[20] a) Hironaka, K.; Fukuzumi, S.; Tanaka, T. *J. Chem. Soc., Perkin Trans. 2* **1984**, 1705–1709; b) Kern, J.-M.; Sauvage, J.-P. *J. Chem. Soc., Chem. Commun*. **1987**, 546–548; c) Devery III, J. J.; Nguyen, J. D.; Dai, C.; Stephenson, C. R. J. *ACS Catal*. **2016**, *6*, 5962−5967.

[21] Ma, C.; Chan, C. T.-L.; To, W.-P.; Kwok, W.-M.; Che, C.-M. *Chem. Eur. J.* **2015**, *21*, 13888–13893.

[22] McTiernan, C. D.; Morin, M.; McCallum, T.; Scaiano, J. C.; Barriault, L. *Catal. Sci. Technol*. **2016**, *6*, 201–207.

[23] Schmidbaur, H.; Wohlleben, A.; Schubert, U.; Frank, A.; Huttner, G. *Chem. Ber*. **1977**, *110*, 2751–2757.

[24] Leung, K. H.; Phillips, D. L.; Mao, Z.; Che, C.-M.; Miskowski, V. M.; Chan, C.-K. *Inorg. Chem*. **2002**, *41*, 2054–2059.

[25] a) Che, C.-M.; Yip, H.-K.; Yam, V. W.-W.; Cheung, P.-Y.; Lai, T.-F.; Shieh, S.-J.; Peng, S.-M. *J. Chem. Soc., Dalton Trans*. **1992**, 427–433; b) Barnard, P. J.; Baker, M. V.; Berners-Price, S. J.; Skelton, B. W.; White, A. H. *Dalton Trans*. **2004**, 1038–1047; c)Tong, G. S. M.; Kui, S. C. F.; Chao, H.-Y.; Zhu, N.; Che, C.-M. *Chem. Eur. J*. **2009**, *15*, 10777–10789.

[26] Lokanatha, R. K. M.; Hassner, A. *Heterocycles* **1990**, *30*, 817–830.

[27] Pandey, G.; Rao, K. S. S. P.; Palit, D. K.; Mittal, J. P. *J. Org. Chem*. **1998**, *63*, 3968–3978.

[28] Dai, C.; Narayanam, J. M. R.; Stephenson, C. R. J. *Nature Chem*. **2011**, *3*, 140–145.

[29] Senboku, H.; Michinishi, J.-Y.; Hara, S. *Synlett*, **2011**, *22*, 1567–1572.

[30] Yang, C.; Mehmood, F.; Lam, T. L.; Chan, S. L.-F.; Wu, Y.; Yeung, C.-S.; Guan, X.; Li, K.; Chung, C. Y.-S.; Zhou, C.-Y.; Zou, T.; Che, C.-M. *Chem. Sci*. **2016**, *7*, 3123–3136.

[31] Teo, Y.-C.; Yong, F.-F. *Synlett*, **2011**, *22*, 837–843.

[32] Pan, X.; Lacôte, E.; Lavelée, J.; Curran, D. P.; *J. Am. Chem. Soc*. **2012**, *134*, 5669–5674.

[33] Wang, Y.; Yepremyan, A.; Ghorai, S.; Todd, R.; Aue, D. H.; Zhang, L. *Angew. Chem. Int. Ed*. **2013**, *125*, 7949–7953.

[34] Su, X.; Fox, D. J.; Blackwell, D. T.; Tanaka, K.; Spring, D. R. *Chem. Commun*. **2006**, *37*, 3883–3885.

[35] Millán, A.; Álvarez de Cienfuegos, L.; Miguel, D.; Campaña, A. G.; Cuerva, J. M. *Org. Lett*. **2012**, *14*, 5984–5987.

[36] Zhu, J.; Pérez, M.; Caputo, C. B.; Stephan, D. W. *Angew. Chem. Int. Ed*. **2016**, *55*, 1417–1421.

[37] Horino, Y.; Takahashi, Y.; Koketsu, K.; Abe, H.; Tsuge, K. *Org. Lett*. **2014**, *16*, 3184–3187.

[38] Ozaki, S.; Matsushita, H.; Ohmori, H. *J. Chem. Soc., Perkin Trans. 1*. **1993**, 649–651.

[39] a) Bywater, S.; Lachance, P.; Worsfold, D. J. *J. Phys. Chem*. **1975**, *79*, 2148–2153; b) Dulog, L.; David, K.-H. *Makromol. Chem*. **1976**, *177*, 1717–1724.

3. Photo-mediated Formal Deoxygenation of 1° Alcohols

McCallum, T.; Slavko, E.; Morin, M.; Barriault, L. Light-Mediated Deoxygenation of Alcohols with a Dimeric Gold Catalyst. *Eur. J. Org. Chem.* **2015**, 81–85.

3.1 Abstract

The transformation of alcohols to bromoalkanes is an important tool for the conversion of readily available starting materials into useful reagents for organic synthesis. The Appel reaction, a well known and regularly used reaction for the transformation of alcohols to bromoalkanes, employs triphenylphosphine and CBr_4 (or Br_2) to effect this transformation. Triphenylphosphine oxide is the major by-product of this transformation and is often difficult to remove during purification, warranting the need for the development of new methodologies in this reaction. The photoredox mediated transformation of alcohols to bromoalkanes has been achieved using Ru-based bypyridine complexes with CBr_4 in DMF. The mild and efficient reaction utilizes photoexcited $[Ru(bpy)_3]^{2+}$ to generate a highly reactive Vilsmeier-Haack reagent through activation of CBr_4. Herein, a UVA light-enabled activation of CBr_4 is described for the generation of Vilsmeier-Haack reagents capable of transforming primary alcohols to bromoalkanes. Further, a new protocol for the formal reductive deoxygenation of primary alcohols was explored. The photo-mediated approach combines the bromination of alcohols with the powerful reducing capability of $[Au_2(\mu\text{-dppm})_2]Cl_2$ as a photoredox catalyst. The highly efficient one-pot process is marked by UVA LEDs, which have significantly reduced reaction times and lowered setup cost.

3.2 Introduction

Radical reductive deoxygenation of alcohols has been a topic of interest in organic chemistry since the pioneering work of Barton and McCombie.[1] Since then, many functional groups have been utilized in radical deoxygenation reactions including xanthates, phosphites, and benzoyl esters (**Scheme 3.1**). However, the removal of these groups requires the use of hazardous radical initiators such as AIBN, peroxides or trialkylboranes, hydrogen-atom donors like organostannanes, and air unstable reducing agents as SmI_2.[2] In search of milder conditions, catalytic variations have been developed but still contain potentially toxic reagents or involve multiple steps.[3] Seldom are these alcohol protection and radical reduction reactions compatible with one-pot procedures.[4] Increasing efforts have been put forward in the development of robust waste-minimizing protocols that abate the need for stoichiometric toxic and hazardous reagents. Moreover, the protecting groups mentioned in **Scheme 3.1** are restrictive by limiting substrate precursors to secondary and tertiary alcohols.[5] Competitive fragmentation pathways between the desired reduction product and radical intermediates led to varying ratios of the desired product and by-products unless specific xanthates are used (**Scheme 3.1**).[6] For this reason, most deoxygenation protocols are limited to alcoholic precursors that result in more stable radical intermediates, which underscore the need for deoxygenation protocols of primary alcohols. Merging photo-mediated bromination with photoredox catalysis in the reduction of the resulting bromoalkane eliminates competitive pathways (**Scheme 3.2**, Eq. (1)). Herein, we report a photo-mediated one-pot reductive deoxygenation protocol that combines photochemical bromination of primary alcohols with hydrodebromination of nonactivated bromoalkanes via photoredox catalysis **(Scheme 3.2**, Eq. (2)).

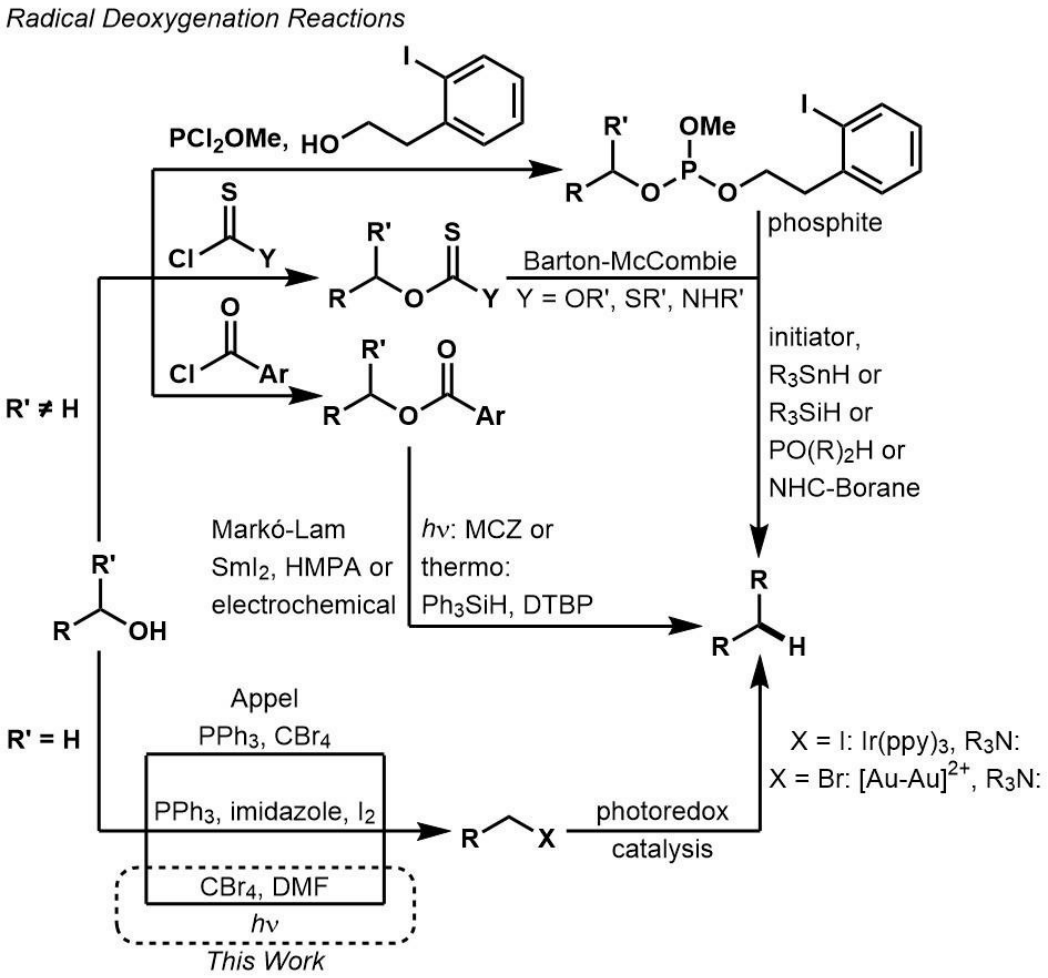

Scheme 3.1 Previous work in radical mediated deoxygenation reactions.

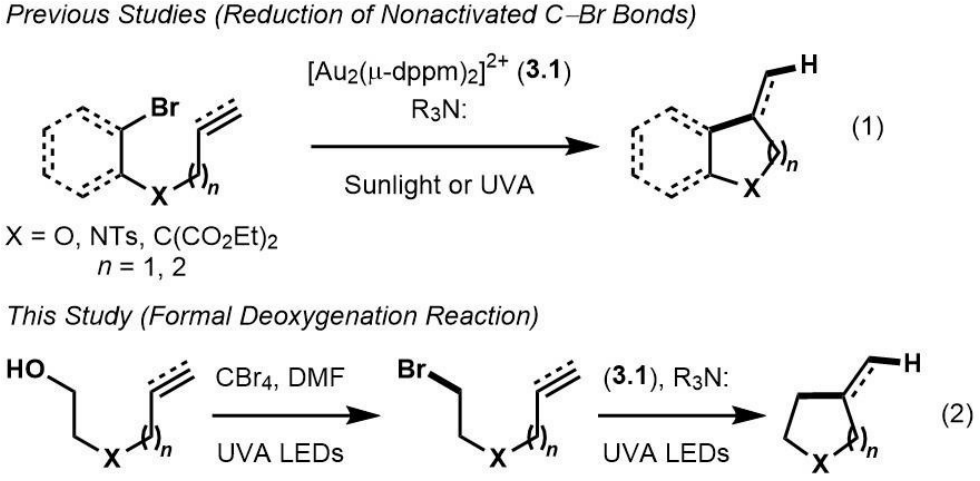

Scheme 3.2 Photo-mediated bromination/hydrodebromination of alcohols.

3.3 Results and Discussion

Although most organic compounds do not absorb visible light, chemists have developed photosensitizers that mimic the bio-inorganic capabilities of photosystem II that induce chemical reactions.[7] Even with a multitude of photosensitizers, there are a limited number of examples that utilize photochemical sensitization in reductive deoxygenation reactions.[8] Seminal contributions have demonstrated the effectiveness of Ru- and Ir-based photocatalysts in the efficient formation of C–C, C–N, and C–O bonds.[9]

The conversion of alcohols into the corresponding halides is a process commonly utilized in organic synthesis. Although there exist several halogenation methods, the Appel reaction (CX_4 and PPh_3) is among the most efficient and reliable.[10] However, stoichiometric amounts of triphenylphosphine oxide are generated as a by-product, which might render this transformation incompatible with metal-catalyzed photoredox processes. Recently, Stephenson and co-workers reported a visible light mediated halogenation reaction of alcohols by using $[Ru(bpy)_3]Cl_2$ and polyhalomethanes in DMF.[11] The proposed mechanism involves the formation of a Vilsmeier–Haack reagent through the addition of electron deficient $\cdot CBr_3$ to DMF, which activates the alcohol for a nucleophilic displacement with a halide. In 2013, the reduction of nonactivated bromoalkanes and arenes using $[Au_2(\mu\text{-dppm})_2]Cl_2$ (**3.1)** as a photocatalyst was reported.[12] While exploring orthogonal reactivity of this catalyst, we imagined that a light-mediated deoxygenation of alcohols could be achieved through a one-pot radical halogenation/reduction process.

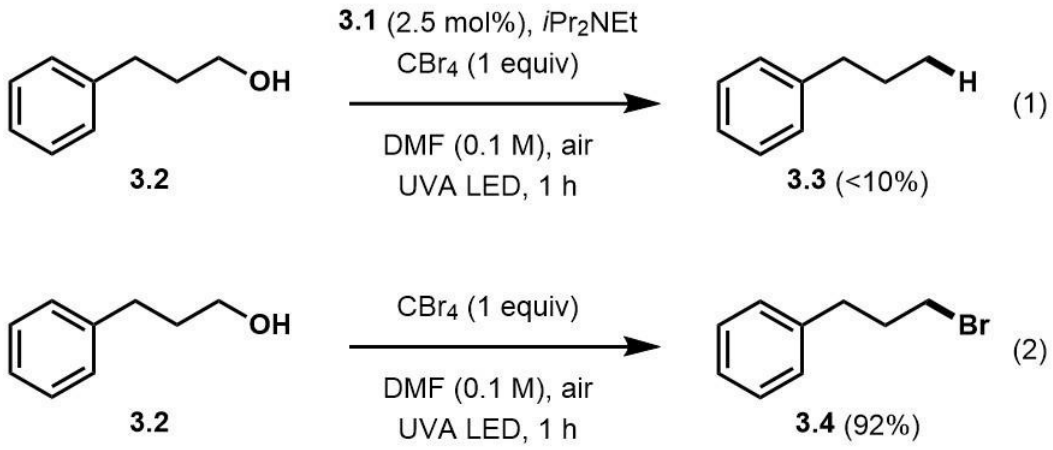

Scheme 3.3 Initial studies towards the one-pot deoxygenation of alcohols.

Initial attempts to convert phenylpropanol (**3.2**) directly into propylbenzene (**3.3**) by using $[Au_2(\mu\text{-dppm})_2]Cl_2$ (**3.1**, 5 mol%), *i*Pr_2NEt, and CBr_4 with a UVA LED in DMF were fruitless (**Scheme 3.3**, Eq. (1)). Dismal yields were observed as side reactions seemed to be taking place possibly from radical interactions with the amine base.[13] However, in a control experiment, irradiation of 3-phenylpropanol in the absence of the gold catalyst and DIPEA gave the corresponding bromoalkane in 92% yield (**Scheme 3.3**, Eq. (2)). The result indicated that a Vilsmeier–Haack reagent could be generated without the use of a photocatalyst. It prompted us to investigate a light-mediated halogenation reaction of general applicability that could be combined with photoredox processes. It should also be noted that this transformation showed no conversion when using 410 nm LED irradiation, demonstrating the need of UVA LED irradiation for reaction to occur. Furthermore, no reaction was observed in the absence of light while heating to 80°C. CCl_4 under the optimal conditions did not convert any of the starting material to the corresponding chloroalkane. Notably, multi-gram scale reaction of **3.2** (2.0 g, 14.68 mmol) at 0.2 M irradiated with 3 UVA LEDs for 2 h led to product **3.4** in 92% yield (2.7 g).

Attempts at using DMF stoichiometrically or catalytically in acetonitrile showed sluggish reactivity. DMA was also shown to be inactive as a solvent. Upon identification of the optimized conditions (CBr_4 (1 equiv), DMF (0.1 M), air, UVA LED for 1 h), a wide range of primary alcohols **3.5a**–**q** were surveyed (**Table 3.1**). Aliphatic primary bromides **3.6a** and **3.6b** were obtained in excellent yields. As expected, a wide variety of functionalities were tolerated, including alkenes (**3.6c**–**f**), alkynes (**3.6g**), and the protecting groups *O*-Bn (**3.6h**–**j**) and *N*-Cbz (**3.6k**). To achieve bromination with acid-sensitive functional groups such as *N*-Boc and *O*-TBS, the photo-mediated process was performed in the presence of 2,6-lutidine. Corresponding bromides **3.6l** and **3.6m** were produced in yields of 76% and 50%, respectively. Diols were also compatible with this method by adding 2 equivalents of CBr_4 (**3.6n** and **3.6o**). Interestingly, alkyl alcohol **3.5q** containing a pyridine was compatible with the reaction conditions to produce **3.6q**, albeit with a much longer irradiation time and the addition of NaBr (3 equiv). Reactions with secondary alcohols were not efficient; they most often led to the formation of formyl ester by-products in varying ratios.

Encouraged by these results, we examined the one-pot deoxygenation reaction. Initial experiments revealed that the subsequent addition of the binuclear gold catalyst to the reaction mixture containing the bromoalkane gave the corresponding reduced product in low and variable yield. After extensive solvent screening, we found that the addition of *i*PrOH as a co-solvent and a possible hydrogen donor after the bromination step, was necessary to obtain high conversions. With the optimal reaction conditions in hand, we explored the scope of the reaction by using primary alcohols.

Table 3.1 Scope of the photo-mediated bromination reaction.

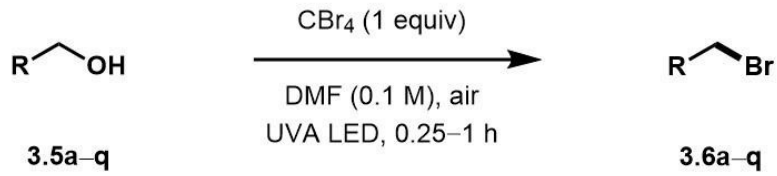

3.5a–q → **3.6a–q**

Entry	Product	Yield [%]	Entry	Product	Yield [%]
1	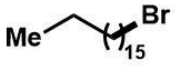 **3.6a**	98	8	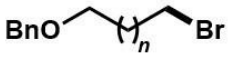 **3.6h** n = 1	99[a]
			9		80
			10	**3.6i** n = 2 **3.6j** n = 3	87
2	 **3.6b**	95[a]	11	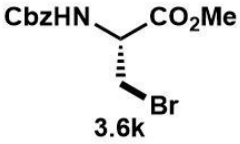 **3.6k**	97
3	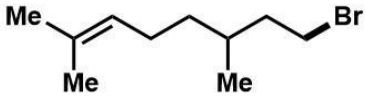 **3.6c**	80	12	 **3.6l** X = NHBoc	76[b,c]
			13	**3.6m** X = OTBS	50[b,c]
4	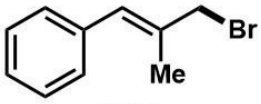 **3.6d**	70	14	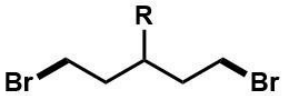 **3.6n** R = H	96[a,c]
			15	**3.6o** R = Me	87[a,c]
5	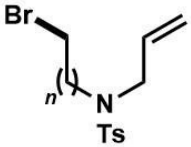 **3.6e** n = 1	91[b]	16	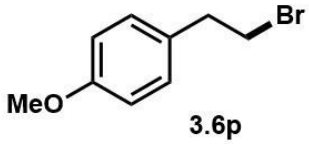 **3.6p**	95
6	**3.6f** n = 2	98			
7	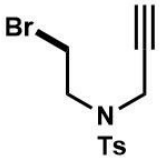 **3.6g**	95[b]	17	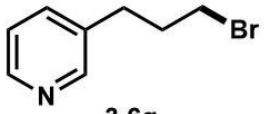 **3.6q**	75[d]

[a]Yield was determined by ^{1}H NMR spectroscopy using mesitylene as an internal standard. [b]NaBr (2 to 3 equiv) was added after irradiation and the mixture was stirred overnight in the absence of irradiation. [c]2,6-Lutidine (3 equiv) was added and the mixtured was irradiated for 6 h. [d]Irradiated overnight with NaBr (3 equiv).

1-Heptadecanol (**3.5a**) was reduced to heptadecane (**3.7a**) in excellent yield (**Table 3.2**, entry 1). Alcohols **3.5j** and **3.5r** also showed that *O*-Bn and *N*-Cbz protecting groups were well tolerated in this system (entries 2 and 3). Homoserine derivative **3.5s** was readily converted into **3.7s** in 85% yield (entry 4). The deoxygenation of alcohols such as **3.5t** containing an acid-sensitive group was achieved in the presence of 2,6-lutidine (3 equiv) to produce **3.7t** in 50% yield (entry 5). Tetra-*O*-Ac glucose **3.5u** was also compatible and desired product **3.5u** was obtained in 70% yield (entry 6). Aryl compounds **3.5v** and **3.5w** were transformed into corresponding alkanes **3.7v** and **3.7w** in yields of 70 and 84%, respectively (entries 7 and 8). Interestingly, compound **3.7w** led to a 3:1 mixture of an *E*/*Z* olefin. The described method was extended to cyclizations of alcohols **3.5e**–**g** containing allyl and propargyl groups afforded the corresponding cyclized *N*-Ts-protected pyrrolidine and piperidines **3.8e**–**g** ranging from 76–84% yield (entries 9–11).

As in Nishina's study,[14] irradiation of CBr_4 promotes the homolytic cleavage of a C–Br bond to produce an electrophilic radical, $\cdot CBr_3$. As proposed by Stephenson,[11] the electrophilic radical can add to DMF to generate intermediate **3.9**, which may be oxidized with CBr_4 or O_2 to afford Vilsmeier–Haack intermediate **3.10** (**Scheme 3.4**). The latter in the presence of primary alcohol **3.5** produces intermediate **3.11**, which undergoes nucleophilic displacement with a bromide anion to deliver corresponding bromoalkane **3.6**. At this point, photoexcited binuclear gold complex **3.1*** likely undergoes reductive quenching by SET with trialkylamine base, generating $[Au_2(\mu\text{-dppm})_2]^{1+}$, a potent

Table 3.2 Scope of the one-pot formal deoxygenation reaction.

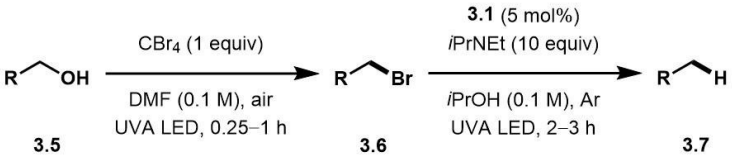

Entry	Substrate	Product	Entry	Substrate	Product
1	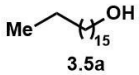 **3.5a**	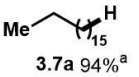 **3.7a** 94%[a]	6	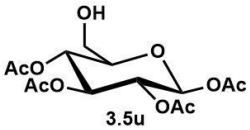 **3.5u**	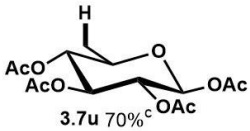 **3.7u** 70%[c]
2	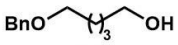 **3.5j**	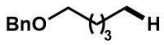 **3.7j** 90%	7	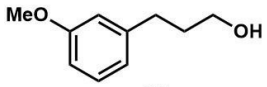 **3.5v**	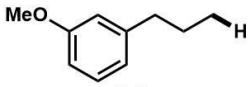 **3.7v** 70%
3	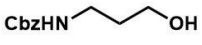 **3.5r**	 **3.7r** 80%	8	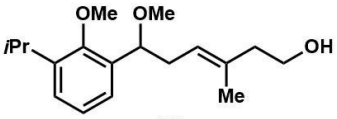 **3.5w**	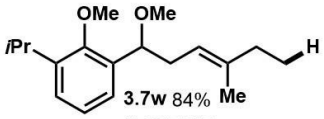 **3.7w** 84% 77:23 *E/Z*
4	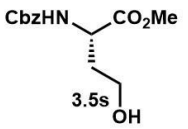 **3.5s**	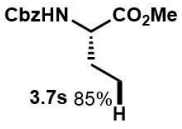 **3.7s** 85%	9 10	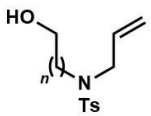 **3.5e** *n* = 1 **3.5f** *n* = 2	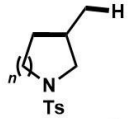 **3.7e** *n* = 1, 77%[b] **3.7f** *n* = 2, 76%[b]
5	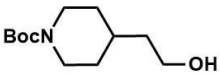 **3.5t**	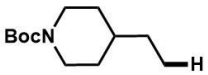 **3.7t** 50%[b]	11	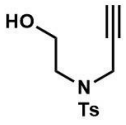 **3.5g**	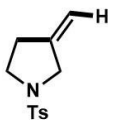 **3.7g** 84%[b]

[a]Yield was determined by ^{1}H NMR spectroscopy using mesitylene as an internal standard. [b]2,6-Lutidine (3 equiv) and/or NaBr (2 to 3 equiv) was added after irradiation and the mixture was stirred overnight in the absence of irradiation. [c]First step irradiatied overnight.

reductant that undergoes SET with bromoalkane **3.6**, generating an alkyl radical and regenerating the photoredox catalyst. In the presence of H donors such as *i*PrOH, trialkylamines, or the solvent, primary alkyl radical is converted into reduced product **3.7**. A control experiment in which trialkylamine was removed for the second irradiation showed no formation of hydrodehalogenated product; this demonstrated that the *i*PrOH/DMF solvent mixture did not participate solely in background reactions.

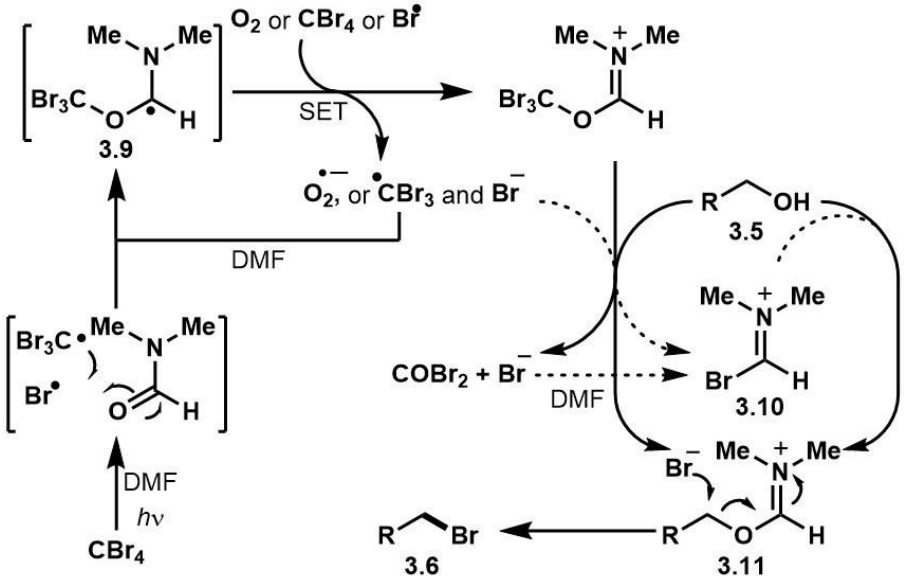

Scheme 3.4 Plausible mechanism for the photo-mediated bromination reaction.

3.4 Conclusions

In conclusion, we developed a photo-mediated reductive deoxygenation reaction of nonactivated primary alcohols. As shown, this procedure for the bromination and deoxygenation of primary alcohols is simple and functional-group tolerant. The method was enabled by the unexpected discovery of a bromination protocol for primary alcohols by using only light, CBr_4, and DMF. It was demonstrated that CBr_4 as a source of bromine was mild and compatible with photoredox processes involving the powerful reducing ability of $[Au_2(\mu\text{-dppm})_2]^{2+}$. The high synthetic value of this transformation was shown through the genesis of alkyl radicals that yield reduction and cyclization products from alcohol precursors. The bromination of alcohols seems to operate through initial photolysis of a C–Br bond in CBr_4 and proceeds through S_N-type displacement of an activated intermediate.

3.5 Experimental Procedures

General Procedure 1 (GP1) – *Bromination of Alcohols*

To an 8 mL Pyrex screw-top reaction vessel was added alcohol substrate (0.3 mmol, 1.0 equiv), DMF (3 mL, 0.1 M), and tetrabromomethane (0.3 mmol, 1.0 equiv). The reaction mixture was capped and irradiated with a UVA LED at a distance of 1 cm for 15–60 min (as judged complete by TLC). If formyl ester forming spot (hydrolysis of reaction intermediates during TLC that had not reacted with bromide) remained after 1 hr of stirring, NaBr (2.0–3.0 equiv) was added and allowed to stir for 1 h (or overnight if needed) at 23–35°C, as judged by TLC to completion. The resulting mixture was poured into a separatory funnel containing a 1:1 mixture of diethyl ether and hexanes (ethyl acetate was added for compounds that needed further solubility) and was washed with saturated sodium bicarbonate and water, where the combined aqueous fractions were re-extracted with 1:1 diethyl ether and hexanes. The combined organic portions were washed with saturated sodium thiosulfate, brine, and dried over magnesium sulfate. The solution was concentrated *in vacuo* and crude products were further purified by column chromatography, where relevant fractions were combined, concentrated, and characterized by proton and carbon NMR (400 and 101 MHz, respectively), IR, and HRMS. *In many cases products were added an internal standard (mesitylene) to confirm that yields were not overestimated in case of residual CBr_4 remaining. The methodology is also compatible with adding 3 equivalents of 2,6-lutidine for compounds with acid sensitive functional groups to attenuate the formation of HBr.

General Procedure 2 (GP2) – *Deoxygenation of Alcohols*

To an 8 mL Pyrex screw-top reaction vessel was added alcohol substrate (0.1–0.3 mmol, 1.0 equiv), DMF (1.0–3.0 mL, 0.1 M), and tetrabromomethane (0.1–0.3 mmol, 1.0 equiv). The reaction mixture was capped and irradiated with a UVA LED at a distance of 1 cm for 1 h (as judged complete by TLC). If formyl ester forming spot (hydrolysis of reaction intermediates during TLC that had not reacted with bromide) remained after 1 hr of stirring, NaBr (2.0–3.0 equiv) was added and allowed to stir for 1 h (or overnight if needed) at 23–35°C, as judged by TLC to completion. The resulting mixture was added an equal amount *i*PrOH as compared to DMF, *N*,*N*-diisopropylethylamine (1.0–3.0 mmol, 10.0 equiv) and allowed to stir for 10 minutes, then $[Au_2(\mu\text{-dppm})_2]Cl_2$ (0.005–0.015 mmol, 0.05 equiv) was added and degassed by argon sparging. The reaction mixture was then irradiated with a UVA LED at a distance of 1 cm for 2–3 h. The resulting mixture was poured into a separatory funnel containing 25 mL of a 1:1 mixture of diethyl ether and hexanes (ethyl acetate added for compounds which needed further solubility) and was washed with saturated sodium bicarbonate, water, where the combined aqueous fractions were re-extracted with 25 mL of 1:1 diethyl ether and hexanes. The combined organic portions were washed with saturated sodium thiosulfate, brine, and dried over magnesium sulfate. The solution was concentrated *in vacuo* and crude products were further purified by column chromatography, where relevant fractions were combined, concentrated, and characterized by proton and carbon NMR (400 and 101 MHz, respectively), IR, and HRMS.

3.6 Characterization Data

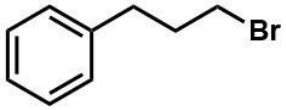

(3-bromopropyl)benzene (3.4)

Synthesized according to GP1 and characterized by NMR comparison.[15]

^{1}H NMR (400 MHz, $CDCl_3$): δ = 7.36–7.29 (m, 2H), 7.27–7.19 (m, 3H), 3.42 (td, *J* = 6.6, 1.3 Hz, 2H), 2.81 (td, *J* = 7.4, 1.6 Hz, 2H), 2.26–2.14 (m, 2H) ppm; **^{13}C NMR** (101 MHz, $CDCl_3$): δ = 140.5 (C), 128.5 (2×CH), 128.4 (2×CH), 126.1 (CH), 34.2 (CH_2), 34.0 (CH_2), 33.1 (CH_2) ppm.

heptadecane (3.7a)

Synthesized according to GP2 and characterized by NMR comparison.[16]

^{1}H NMR (400 MHz, $CDCl_3$): δ = 1.27 (s, 30H), 0.89 (t, *J* = 6.7 Hz, 6H) ppm; **^{13}C NMR** (101 MHz, $CDCl_3$): δ = 32.0 (2×CH_2), 29.7 (7×CH_2), 29.7 (2×CH_2), 29.4 (2×CH_2), 22.7 (2×CH_2), 14.1 (2×CH_3) ppm.

((pentyloxy)methyl)benzene (3.7j)

Synthesized according to GP2 and characterized by NMR comparison.[17]

^{1}H NMR (400 MHz, $CDCl_3$): δ = 7.36 (m, 5H), 4.52 (s, 2H), 3.48 (t, *J* = 6.7 Hz, 2H), 1.67–1.61 (m, 2H), 1.41–1.32 (m, 4H), 0.94–0.90 (m, 3H) ppm; **^{13}C NMR** (101 MHz, $CDCl_3$): δ = 138.7 (C), 128.3 (2×CH), 127.6 (2×CH), 127.4 (CH), 72.8 (CH_2), 70.5 (CH_2), 29.5 (CH_2), 28.4 (CH_2), 22.5 (CH_2), 14.0 (CH_3) ppm.

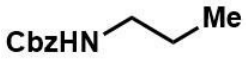

benzyl propylcarbamate (3.7r)

Synthesized according to GP2 and characterized by NMR comparison.[4b]

^{1}H NMR (400 MHz, $CDCl_3$): δ = 7.40–7.29 (m, 5H), 5.11 (s, 2H), 4.79 (br. s, 1H), 3.17 (q, *J* = 6.7 Hz, 2H), 1.52 (quin, *J* = 7.2 Hz, 2H), 0.93 (t, *J* = 7.4 Hz, 3H) ppm; **^{13}C NMR** (101 MHz, $CDCl_3$): δ = 156.4 (C), 136.6 (C), 128.5 (2×CH), 128.1 (2×CH), 128.0 (CH), 66.5 (CH_2), 42.8 (CH_2), 23.2 (CH_2), 11.2 (CH_3) ppm.

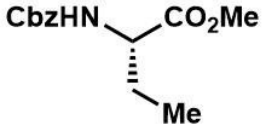

methyl (S)-2-(((benzyloxy)carbonyl)amino)butanoate (3.7s)

Synthesized according to GP2.

IR (neat, cm^{-1}): 3341(br), 2955(m), 1720(vs), 1693(s), 1523(s), 1208(vs); **^{1}H NMR** (400 MHz, $CDCl_3$): δ = 7.45–7.29 (m, 5H), 5.30 (d, *J* = 6.9 Hz, 1H), 5.12 (s, 2H), 4.41–4.31 (m, 1H), 3.76 (s, 3H), 1.90–1.65 (m, 2H), 0.93 (t, *J* = 7.5 Hz, 3H) ppm; **^{13}C NMR** (101 MHz, $CDCl_3$): δ = 172.8 (C), 155.8 (C), 136.2 (C), 128.5 (2×CH), 128.2 (CH), 128.1 (2×CH), 67.0 (CH_2), 54.9 (CH), 52.3 (CH_3), 25.8 (CH_2), 9.4 (CH_3) ppm; **HRMS** (EI): m/z calc'd for $C_{13}H_{17}NO_4$ [M^+] 251.1158, found 251.1139; **$[\alpha]_D^{23}$** = –2.8° (c 0.5, DMF).

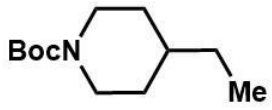

***tert*-butyl 4-ethylpiperidine-1-carboxylate (3.7t)**

Synthesized according to GP2.

IR (neat, cm^{-1}): 2965(m), 2924(m), 2852(m), 1690v(s), 1418(s), 1149(s); **^{1}H NMR** (400 MHz, $CDCl_3$): δ = 4.08 (m, 2H), 2.80–2.57 (m, 2H), 1.65 (d, *J* = 13.2 Hz, 2H), 1.42 (s, 9H), 1.33–1.20 (m, 3H), 1.12–0.99 (m, 2H), 0.88 (d, *J* = 7.4 Hz, 3H) ppm; **^{13}C NMR** (101 MHz, $CDCl_3$): δ = 154.9 (C), 79.1 (C), 44.0 (2×CH_2), 37.7 (CH), 31.8 (2×CH_2), 29.2 (CH_2), 28.5 (3×CH_3), 11.2 (CH_3) ppm; **HRMS** (EI): m/z calc'd for $C_{12}H_{23}NO_2$ [M^+] 213.1729, found 213.1710.

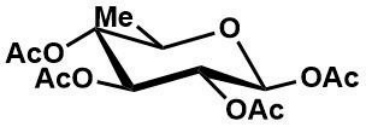

1,2,3,4-tetra-*O*-acetyl-6-deoxy-β-D-glucopyranose (3.7u)

Synthesized according to GP2 and characterized by NMR comparison.[18]

^{1}H NMR (400 MHz, $CDCl_3$): δ = 5.67 (d, *J* = 8.2 Hz, 1H), 5.18 (t, *J* = 9.5 Hz, 1H), 5.08 (dd, *J* = 9.7, 8.3 Hz, 1H), 4.83 (t, *J* = 9.6 Hz, 1H), 3.69 (dd, *J* = 9.8, 6.2 Hz, 1H), 2.08 (s, 3H), 2.02 (s, 3H), 2.00 (s, 3H), 1.98 (s, 3H), 1.22 (d, *J* = 6.2 Hz, 3H) ppm; **^{13}C NMR** (101 MHz, $CDCl_3$): δ = 170.1 (C), 169.6 (C), 169.2 (C), 169.0 (C), 91.6 (CH), 72.9 (CH), 72.7 (CH), 70.9 (CH), 70.6 (CH), 20.7 (CH_3), 20.6 (CH_3), 20.5 (2×CH_3), 17.2 (CH_3) ppm.

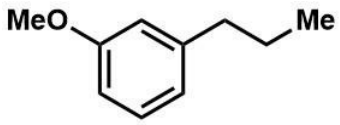

3-*n*-propylanisole (3.7v)

Synthesized according to GP2 and characterized by NMR comparison.[19]

*Methodology resulted in 25% bromoalkane remaining.

^{1}H NMR (400 MHz, $CDCl_3$): δ = 7.26–7.17 (m, 1H), 6.85–6.69 (m, 3H), 3.82 (d, *J* = 1.4 Hz, 3H), 2.65–2.53 (m, 2H), 1.78–1.59 (m, 2H), 0.96 (t, *J* = 7.3 Hz, 3H) ppm; **^{13}C NMR** (101 MHz, $CDCl_3$): δ = 159.5 (C), 144.3 (C), 129.1 (CH), 120.9 (CH), 114.2 (CH), 110.8 (CH), 55.1 (CH_3), 38.1 (CH_2), 24.5 (CH_2), 13.8 (CH_3) ppm.

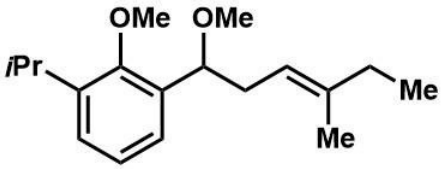

1-isopropyl-2-methoxy-3-(1-methoxy-4-methylhex-3-en-1-yl)benzene (3.7w, 77:23 *E*/*Z*)

Starting from **3.5w**[20], **3.7w** was synthesized according to GP2.

IR (neat, cm^{-1}): 2963(m), 2929(m), 2875(m), 1459(s), 1100 (s), 1051(s), 1012(s); **^{1}H NMR** (400 MHz, $CDCl_3$): δ = 7.25 (dd, *J* = 7.4, 1.9 Hz, 1H), 7.20 (dd, *J* = 7.7, 1.9 Hz, 1H), 7.13 (t, *J* = 7.6 Hz, 1H), 5.21 (dddd, *J* = 7.0, 5.5, 2.7, 1.4 Hz, 1H), 4.55 (ddd, *J* = 9.1, 7.6, 5.4 Hz, 1H), 3.75 (s, 3H), 3.37–3.29 (m, 1H), 3.25 (d, *J* = 3.3 Hz, 3H), 2.55–2.36 (m, 2H), 2.03–1.93 (m, 2H), 1.68–1.50 (m, 3H, *E/Z*), 1.29–1.21 (m, 6H), 0.98–0.86 (t, *J* = 7.5 Hz, 3H, *E/Z*) ppm; **^{13}C NMR** (101 MHz, $CDCl_3$): δ = 155.5 (C), 141.6 (C), 138.8 (C), 135.0 (C), 125.7 (CH), 124.7 (CH), 124.6 (CH), 119.1 (CH) (*Z* = 120.3 (CH)), 77.9 (CH), 62.2 (CH_3), 56.7 (CH_3), 36.1 (CH_2) (*Z* = 35.9 (CH_2)), 32.4 (CH_2) (*Z* = 24.9 (CH_2)), 26.2 (CH), 24.2 (CH_3), 23.8 (CH_3), 16.0 (CH_3) (*Z* = 22.9 (CH_3)), 12.6 (CH_3) ppm; **HRMS** (EI): m/z calc'd for $C_{12}H_{17}O_2$ [M^+–C_6H_{11}] 193.1229, found 193.1227.

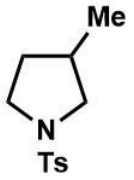

3-methyl-1-tosylpyrrolidine (3.7e)

Synthesized according to GP2 and characterized by NMR comparison.[12]

^{1}H NMR (400 MHz, $CDCl_3$): δ = 7.71 (dd, *J* = 6.8, 4.9 Hz, 2H), 7.32 (d, *J* = 7.9 Hz, 2H), 3.42 (dd, *J* = 9.6, 7.1 Hz, 1H), 3.34 (ddd, *J* = 9.7, 8.4, 4.4 Hz, 1H), 3.22 (dt, *J* = 9.7, 7.8 Hz, 1H), 2.75 (dd, *J* = 9.7, 7.8 Hz, 1H), 2.44 (s, 3H), 2.11 (dq, *J* = 14.5, 6.9 Hz, 1H), 1.90 (dtd, *J* = 11.4, 6.9, 4.1 Hz, 1H), 1.39–1.32 (m, 1H), 0.92 (d, *J* = 6.7 Hz, 3H) ppm; **^{13}C NMR** (101 MHz, $CDCl_3$): δ = 143.2 (C), 134.0 (C), 129.5 (2×CH), 127.5 (2×CH), 54.7 (CH_2), 47.6 (CH_2), 33.3 (CH), 33.2 (CH_2), 21.5 (CH_3), 17.6 (CH_3) ppm.

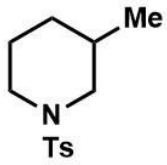

3-methyl-1-tosylpiperidine (3.7f)

Synthesized according to GP2 and characterized by NMR comparison.[21]

^{1}H NMR (400 MHz, $CDCl_3$): δ = 7.66–7.62 (m, 2H), 7.35–7.29 (m, 2H), 3.67–3.59 (m, 2H), 2.43 (s, 3H), 2.21 (td, *J* = 11.3, 2.8 Hz, 1H), 1.88 (t, *J* = 10.7 Hz, 1H), 1.73–1.66 (m, 3H), 1.64–1.59 (m, 1H), 0.87 (d, *J* = 6.5 Hz, 3H), 0.85–0.75 (m, 1H) ppm; **^{13}C NMR** (101 MHz, $CDCl_3$): δ = 143.2 (C), 133.3 (C), 129.5 (2×CH), 127.6 (2×CH), 53.2 (CH_2), 46.4 (CH_2), 32.0 (CH_2), 30.7 (CH), 24.7 (CH_2), 21.5 (CH_3), 19.0 (CH_3) ppm.

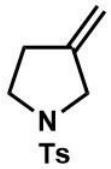

3-methenyl-1-tosylpyrrolidine (3.7g)

Synthesized according to GP2 and characterized by NMR comparison.[12]

^{1}H NMR (400 MHz, $CDCl_3$): δ = 7.74–7.70 (m, 2H), 7.36–7.32 (m, 2H), 4.92 (dquin, *J* = 6.7, 2.2 Hz, 2H), 3.78 (tt, *J* = 2.4, 1.4 Hz, 2H), 3.29 (t, *J* = 7.1 Hz, 2H), 2.48 (ttd, *J* = 7.0, 2.2, 1.1 Hz, 2H), 2.44 (s, 3H) ppm; **^{13}C NMR** (101 MHz, $CDCl_3$): δ = 144.1 (C), 143.6 (C), 132.8 (C), 129.7 (2×CH), 127.8 (2×CH), 107.4 (CH_2), 51.9 (CH_2), 48.1 (CH_2), 31.7 (CH_2), 21.5 (CH_3) ppm.

3.7 References

[1] Barton, D. H. R.; McCombie, S. W. *J. Chem. Soc. Perkin Trans. 1* **1975**, 1574–1585.

[2] a) Girard, P.; Namy, J. L.; Kagan, H. B. *J. Am. Chem. Soc.* **1980**, *102*, 2693–2698; b) Dolan, S. C.; MacMillan, J. *J. Chem. Soc., Chem. Commun.* **1985**, 1588–1589; c) Sano, H.; Ogata, M.; Migita, T. *Chem. Lett.* **1986**, *15*, 77–80; d) Barton, D. H. R.; Blundell, P.; Dorchak, J.; Jang, D. O.; Jaszberenyi, J. C. *Tetrahedron* **1991**, *47*, 8969–8984; e) Barton, D. H. R.; Jang, D. O.; Jaszberenyi, J. C. *Tetrahedron Lett.* **1992**, *33*, 2311–2314; f) Barton, D. H. R.; Jang, D. O.; Jaszberenyi, J. C. *Tetrahedron Lett.* **1992**, *33*, 5709–5712; g) Barton, D. H. R.; Jang, D. O.; Jaszberenyi, J. C. *J. Org. Chem.* **1993**, *58*, 6838–6842; h) Nishiyama, K.; Oba, M.; Oshimi, M.; Sugawara, T.; Ueno, R. *Tetrahedron Lett.* **1993**, *34*, 3745–3748; i) Oba, M.; Nishiyama, K. *Synthesis* **1994**, 624–628; j) Zhang, L.; Koreeda, M. *J. Am. Chem. Soc.* **2004**, *126*, 13190–13191; k) Lam, K.; Markó, I. E. *Org. Lett.* **2008**, *10*, 2773–2776; l) Lam, K.; Markó, I. E. *Chem. Commun.* **2009**, 95–97; m) Ueng, S.; Fensterbank, L.; Lacôte, E.; Malacria, M.; Curran, D. P. *Org. Lett.* **2010**, *12*, 3002–3005.

[3] Lopez, R.; Hays, D.; Fu, G. *J. Am. Chem. Soc.* **1997**, *119*, 6949–6950.

[4] a) Myers, A.; Movassaghi, M.; Zheng, B. *J. Am. Chem. Soc.* **1997**, *119*, 8572–8573; b) Nguyen, J. D.; Reiß, B.; Dai, C.; Stephenson, C. R. J. *Chem. Commun.* **2013**, *49*, 4352–4354.

[5] McCombie, S. W.; Motherwell, W. B.; Tozer, M. J. In *Organic Reactions;* Denmark, S. E., Ed.; Wiley: Hoboken, 2012; Vol. 77, 161–432.

[6] Barton, D. H. R.; Motherwell, W. B.; Stange, A. *Synthesis* **1981**, 743–745.

[7] Balzani, V.; Credi, A.; Venturi, M. *ChemSusChem* **2008**, *1*, 26–58.

[8] a) Saito, I.; Ikehira, H.; Kasatani, R.; Watanabe, M.; Matsuura, T. *J. Am. Chem. Soc.* **1986**, *108*, 3115–3117; b) Prudhomme, D. R.; Wang, Z.; Rizzo, C. J. *J. Org. Chem.* **1997**,

62, 8257–8260; c) Bordoni, A.; de Lederkremer, R. M.; Marino, C. *Carbohydr. Res.* **2006**, *341*, 1788–1795.

[9] *For reviews on photoredox catalysis in organic synthesis, see:* a) Narayanam, J. M. R.; Stephenson, C. R. J. *Chem. Soc. Rev.* **2011**, *40*, 102–113; b) Prier, C. K.; Rankic, D. A.; MacMillan, D. W. C. *Chem. Rev.* **2013**, *113*, 5322–5363; c) Schultz, D. M.; Yoon, T. P. *Science* **2014**, *343*, 985–1239176–8*; for dehalogenation of activated bromoalkanes, see:* d) Narayanam, J. M. R.; Tucker, J. W.; Stephenson, C. R. J. *J. Am. Chem. Soc.* **2009**, *131*, 8756–8757; *for recent examples of selected topics in photoredox catalysis, see:* e) Andrews, R. S.; Becker, J. J.; Gagné, M. R. *Angew. Chem. Int. Ed.* **2012**, *51*, 4140–4143; f) Arceo, E.; Jurberg, I. D.; Álvarez-Fernández, A.; Melchiorre, P. *Nat. Chem.* **2013**, *5*, 750–756; g) Sahoo, B.; Hopkinson, M. N.; Glorius, F. *J. Am. Chem. Soc.* **2013**, *135*, 5505–5508; h) Rono, L. J.; Yayla, H. G.; Wang, D. Y.; Armstrong, M. F.; Knowles, R. R. *J. Am. Chem. Soc.* **2013**, *135*, 17735–17738; i) Nakajima, M.; Lefebvre, Q.; Rueping, M. *Chem. Commun.* **2014**, *50*, 3619–3622; j) Pitre, S. P.; McTiernan, C. D.; Ismaili, H.; Scaiano, J. C. *ACS Catal.* **2014**, *4*, 2530–2535; k) Wilger, D. J.; Grandjean, J. M.; Lammert, T. R.; Nicewicz, D. A. *Nat. Chem.* **2014**, *6*, 720–726; l) Bergonzini, G.; Schindler, C. S.; Wallentin, C.; Jacobsen, E. N.; Stephenson, C. R. J. *Chem. Sci.* **2014**, *5*, 112–116; m) Du, J.; Skubi, K. L.; Schultz, D. M.; Yoon, T. P. *Science* **2014**, *344*, 392–396; n) Cassani, C.; Bergonzini, G.; Wallentin, C. *Org. Lett.* **2014**, *16*, 4228–4231; o) Tellis, J. C.; Primer, D. N.; Molander, G. A. *Science* **2014**, *345*, 433–436; p) Zuo, Z.; Ahneman, D. T.; Chu, L.; Terrett, J. A.; Doyle, A. G.; MacMillan, D. W. C. *Science* **2014**, *345*, 437–440; q) Beatty, J. W.; Stephenson, C. R. J. *J. Am. Chem. Soc.* **2014**, *136*, 10270–10273.

[10] Appel, R. *Angew. Chem. Int. Ed. Engl.* **1975**, *14*, 801–811.

[11] Dai, C.; Narayanam, J. M. R.; Stephenson, C. R. J. *Nat. Chem.* **2011**, *3*, 140–145.

[12] Revol, G.; McCallum, T.; Morin, M.; Gagosz, F.; Barriault, L. *Angew. Chem. Int. Ed.* **2013**, *52*, 13342–13345.

[13] Scaiano, J. C.; Barra, M.; Sinta, R. *Chem. Mater.* **1996**, *8*, 161–166.

[14] Nishina, Y.; Ohtani, B.; Kikushima, K. *Beilstein J. Org. Chem.* **2013**, *9*, 1663–1667.

[15] Liu, Y.; Xu, Y.; Jung, S. H.; Chae, J. *Synlett*. **2012**, *23*, 2692–2698.

[16] Zhao, F.; Rutherford, M.; Grisham, S. Y.; Peng, X. *J. Am. Chem. Soc*. **2009**, *131*, 5350–5358.

[17] Kleinke, A. S.; Jamison, T. F. *Org. Lett*. **2013**, *15*, 710–713.

[18] Ueng, S.; Fensterbank, L.; Lacôte, E.; Malacria, M.; Curran, D. P. *Org. Biomol. Chem*. **2011**, *9*, 3415–3420.

[19] Tietze, L. F.; Vock, C. A.; Krimmelbein, I. K.; Nacke, L. *Synthesis* **2009**, *12*, 2040–2060.

[20] Cannillo, A.; Schwantje, T. R.; Bégin, M.; Barabé, F.; Barriault, L. *Org. Lett*. **2016**, *18*, 2592–2595.

[21] Verendel, J. J.; Zhou, T.; Li, J.; Paptchikhine, A.; Lebedev, O.; Andersson, P. G. *J. Am. Chem. Soc*. **2010**, *132*, 8880–8881.

4. Photo-mediated Formation of Anhydrides and Amides

McCallum, T.; Barriault, L. Light-Enabled Synthesis of Anhydrides and Amides. *J. Org. Chem.* **2015**, *80*, 2874–2878.

4.1 Abstract

Recently, the photogeneration of Vilsmeier−Haack reagents has been possible using DMF and CBr_4 in the bromination of alcohols. It has been described that the photoredox mediated generation of Vilsmeier-Haack reagents using $[Ru(bpy)_3]Cl_2$ and CBr_4 in DMF with carboxylic acids led to the formation of symmetric anhydrides. Extending our studies of the photogeneration of Vilsmeier-Haack reagents using CBr_4 in DMF under UVA irradiation, carboxylic acids were also transformed to symmetric anhydrides. Anhydrides are difficult to isolate through purification and are unstable to extended storage under ambient conditions. To bypass anhydride decomposition, the developments made to carboxylic acid substrates were evaluated with addition of alkyl and aryl amines, which were conveniently converted to amide derivatives in a one-pot process. Carboxylic acids and amines derived from amino acids were also well tolerated in this transformation, where final products retained their initial stereochemistry and demonstrated the process's resilience to epimerization. The photo-mediated transformation led to the facile isolation of functionalized amides, an alternative to the usual amide coupling strategies employed with carboxylic acids and amines. The protocols discussed herein are marked by UVA LEDs (365 nm), which have reduced the reaction times and come with a low setup cost.

4.2 Introduction

The activation of carboxylic acids has been paramount to the synthesis of peptides in coupling reactions with amines.[1] A variety of methods make carboxylic acids more electrophilic either by transforming the carboxylic acid into the corresponding acyl halide or through the addition of coupling agents.[2] Symmetric anhydrides have also seen great use in peptide chemistry because they provide electrophilic activation of the carboxylic moiety without forming typical coupling reagent by-products, as both electrophilic sites are identical. However, these anhydrides are often formed through the same procedures that apply to amide couplings (acyl halide formation and then addition of carboxylates).[3] New protocols offering the formation of anhydrides directly from the corresponding carboxylic acids along with the direct formation of amides in a one-pot process are of high interest for research and development.[4]

Photoredox catalysis has emerged as a powerful tool in the development of new organic transformations, especially in forming C−C, C−N, and C−O bonds.[5] Vilsmeier−Haack reagents for useful organic transformations can be generated with photoredox catalysis,[6, 7] however, studies among our group found that generation of the Vilsmeier−Haack reagents without use of a photocatalyst are possible from the irradiation of CBr_4 with UVA light (365 nm LED) in DMF under air atmosphere.[8] Notably, visible light under these conditions was unable to achieve this transformation. The methodology was used as a synthetically facile route to bromoalkanes from alcohols, which was applicable to a one-pot deoxygenation protocol.[8b, 9] We sought to apply the photogeneration of Vilsmeier−Haack reagents from UVA and CBr_4 in a one-pot protocol for the synthesis of amides from readily available carboxylic acids and amines (**Scheme 4.1**).

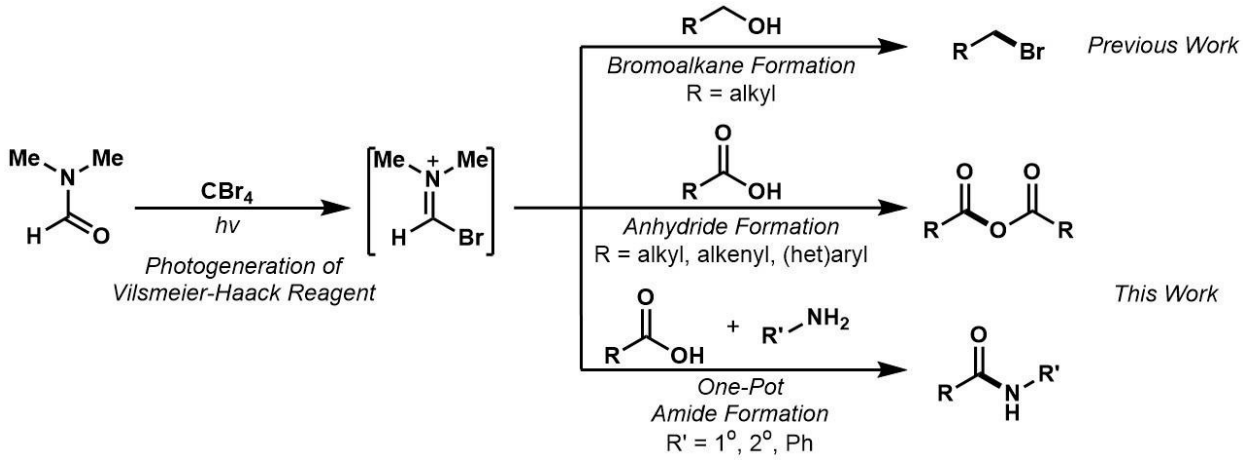

Scheme 4.1 Transformations of photo-mediated Vilsmeier-Haack reagents.

4.3 Results and Discussion

The formation of symmetric anhydrides was first optimized to minimize the reagents used in the proposed transformation (**Table 4.1**). Treating *p*-anisic acid **4.1a** with CBr_4 (1 equiv) and 2,4,6-trimethylpyridine (collidine, 2 equiv) in DMF were the conditions that gave anhydride product **4.2a** in the most reagent-minimizing protocol and the best yields (entries 1−3). The reaction was found to occur quickly, within 30 min, as indicated by the precipitation of a collidine hydrobromide salt. Removal of collidine resulted in little product formation (entry 4). Control experiments were performed that demonstrated that no reaction occurred upon heating at 80°C without light irradiation in the presence of CBr_4 (entry 5) or UVA irradiation in the absence of CBr_4 (entry 7). Notably, the transformation does not react under visible light irradiation (410 nm LED, entry 6).

Table 4.1 Optimization of the photo-mediated symmetric anhydride reaction.

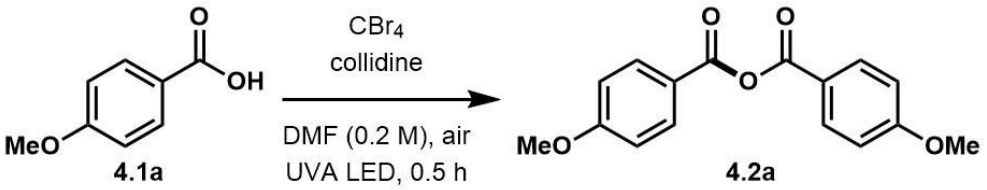

Entry	CBr_4 [equiv]	collidine [equiv]	Yield [%][a]
1	1.0	5.0	95
2	0.5	5.0	78
3	1.0	2.0	91
4	0.5	---	9
5[b]	1.0	2.0	---
6[c]	1.0	2.0	---
7	---	2.0	---

[a] ^{1}H NMR yield with mesitylene as internal standard. [b] In absence of irradiation, 80°C for overnight. [c] Using visible light.

Having these conditions in hand, we established the scope of the transformation using a wide array of carboxylic acids (**Table 4.2**). Non-aromatic carboxylic acids **4.1b–d** and **h** including long chains, primary, secondary, and tertiary α-centers were converted in nearly quantitative yields, forming stable anhydrides **4.2b−d** and **4.2h** (entries 1−3 and 7). The reaction proved to be tolerant to alkenes and alkynes **4.1e**–**g**; the corresponding anhydrides **2e**–**g** were obtained in 75 to 98% yields (entries 4−6). Various aromatic carboxylic acids were screened **4.1i**–**m**; a wide variety of functionality is tolerated in good yields, including alkyl, OMe, and naphthyl (**4.2i**–**m**, entries 8−12). Phthalic acid **4.1n** also converted quantitatively to phthalic anhydride **4.2n** (entry 13), in an intramolecular version of this transformation. Interestingly, *N*-Boc and *N*-Cbz protected L-alanine showed only degradation; however, *N*-Cbz protected L-proline **4.1o** was fully converted to the corresponding anhydride **4.2o** (entry 14).[10]

Table 4.2 Scope of photo-mediated symmetric anhydride formation.

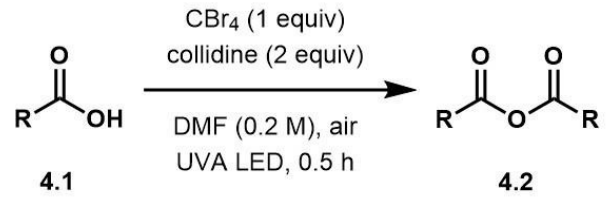

4.1 4.2

Entry	Substrate	Yield [%][a]	Entry	Substrate	Yield [%][a]
1	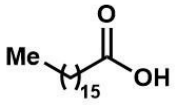 4.1b	99	8	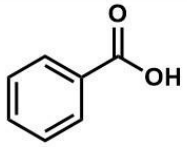 4.1i	88, 68[b]
2	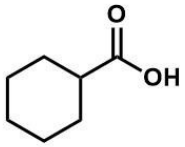 4.1c	99	9	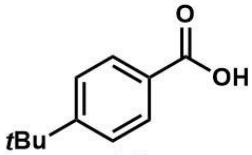 4.1j	70
3	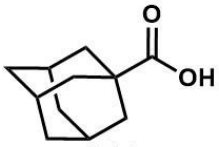 4.1d	99	10	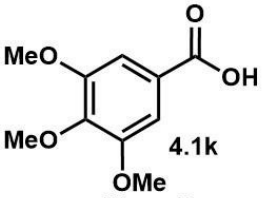 4.1k	65
4	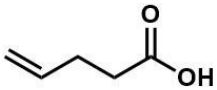 4.1e	75	11	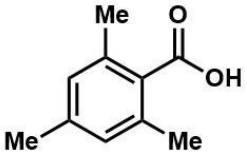 4.1l	45
5	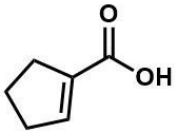 4.1f	98	12	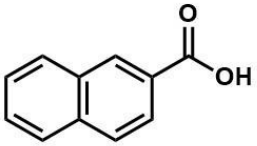 4.1m	63
6	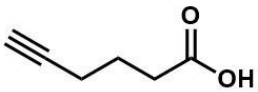 4.1g	78	13	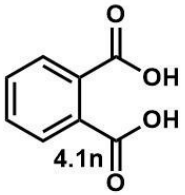 4.1n	99
7	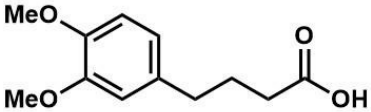 4.1h	80	14	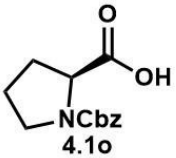 4.1o	99

[a]Yield was determined by ^{1}H NMR spectroscopy using mesitylene as an internal standard.
[b]1.0 g scale of benzoic acid.

Table 4.3 Optimization of the photo-mediated amide coupling.

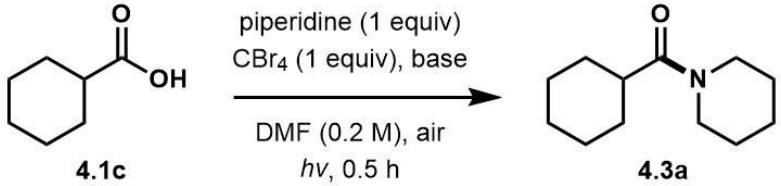

4.1c **4.3a**

Entry	base [equiv]	photocatalyst [mol%]	Light source	Yield [%][a]
1	collidine, 3	---	UVA LED	22
2	DMAP, 3	---	UVA LED	22
3	DABCO, 3	---	UVA LED	16
4	imidazole, 3	---	UVA LED	6
5	pyridine, 3	---	UVA LED	10
6	DBU, 3	---	UVA LED	5
7	DIPEA, 3	---	UVA LED	11
8	collidine, 3, DMAP, 1	---	UVA LED	27
9	collidine, 5, DMAP, 1	---	UVA LED	61[b], 38[b,c]
10	lutidine	$[Ru(bpy)_3](PF_6)_2$, 5.0, Ar	CFL, 97 h	9
11	lutidine	---, Ar	CFL, 97 h	7
12	lutidine	$[Ru(bpy)_3](PF_6)_2$, 5.0, Ar	410 nm LED	12
13	lutidine	---, Ar	410 nm LED	8

[a] ^{1}H NMR yield with mesitylene as internal standard. [b] 3 equiv of **4.1c**, 1.5 equiv CBr_4. [c] 1g scale of piperidine.

The method showed a robust general applicability, however, isolation of many aromatic anhydrides resulted in some degradation or loss of product. These compounds are often used in amide couplings as the coupling partner for an amine. It was reasoned that a one-pot procedure for the coupling of these anhydrides to an amine should be developed to avoid degradation of the anhydride through purification steps. An optimization of the organic bases added to the reaction (**Table 4.3**, entries 1–9) showed that carboxylic acid (3 equiv), collidine (5 equiv), and DMAP (1 equiv) furnished the best yield of amide formation (**4.3**) in the coupling of carboxylic acid **4.1c** and piperidine using CBr_4 (1.5 equiv) with UVA LED irradiation in DMF (entry 9). The analogous method using $[Ru(bpy)_3](PF_6)_2$ (5 mol%) with visible light (CFLs) gave little formation of either anhydride or amide product, 9% (entry 11). Moreover, the same reaction conditions without

$[Ru(bpy)_3](PF_6)_2$ gave a similar yield, 7% (entry 12) and may be due to the intensity of the lights being relatively weak compared to high-powered LED systems. A high-powered 410 nm LED was used, giving 12% yield with $[Ru(bpy)_3](PF_6)_2$ and 8% without the photocatalyst (entries 13 and 14). One aspect of using more powerful lighting sources is that background activation (reaction with light source in the absence of photocatalyst, as shown in this study) may occur, which circumvents the need for photoredox catalysts. Also, excited-state $[Ru(bpy)_3](PF_6)_2$ may be quenched by the amine in solution, which does not result in product forming pathways. For these reasons, a photo-mediated method for the combination of carboxylic acids with amines without a photocatalyst gave the best conditions for amide synthesis.

An extension of the amide protocol also showed promising results (**Table 4.4**). Carboxylic acids functionalized with cyclohexane **4.1c**, phenyl **4.1i**, and *p*-CF_3-phenyl **4.1p** groups were chosen to represent alkyl, aryl, and electron-withdrawing functionalities. These were coupled with *n*$BuNH_2$, piperidine, and aniline to represent primary, secondary, and aromatic amines. Couplings of these compounds all proceeded in yields ranging from 34−98% (**4.3b**–**l**, entries 1–8). Interestingly, the examples using *p*-CF_3-benzoic acid for amide couplings obtained much higher yields of the amide products **4g**−**i** (entries 6−8) as compared to isolation of the unstable corresponding anhydride **4.2p**. Benzoic acid was coupled with L-ala-OMe, which showed that amino acid derivative **4.3j** retained its configuration throughout the reaction with 99:1 e.r. (entry 9), where epimerization plagues many protocols.[11] Using *N*-Cbz-L-ala **4.1q** as carboxylic acid coupled with *n*$BuNH_2$ gave **4.3k**, conservation of enantiopurity was also observed with e.r. = 99:1, in 92% yield (entry 10).

Table 4.4 Scope of photo-mediated amide coupling.

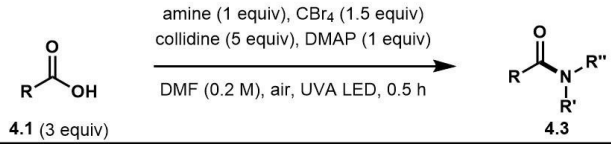

4.1 (3 equiv) → **4.3**

Entry	carboxylic acid	amine	Product	Yield [%]
1	**4.1c**	Me, NH_2	**4.3b**	98
2	**4.1c**	NH_2	**4.3c**	63
3	**4.1i**	NH	**4.3d**	80
4	**4.1i**	Me, NH_2	**4.3e**	86
5	**4.1i**	NH_2	**4.3f**	75
6	**4.1p**	NH	**4.3g**	90
7	**4.1p**	Me, NH_2	**4.3h**	98
8	**4.1p**	NH_2	**4.3i**	94
9	**4.1i**	MeO, NH_2, Me	**4.3j**	34 e.r. 99:1
10	**4.1q**	Me, NH_2	**4.3k**	92 e.r. 99:1
11	**4.1q**	MeO, NH_2, Me	**4.3l**	94 d.r. >20:1

Coupling of L-ala-OMe and *N*-Cbz-L-ala as carboxylic acid demonstrated that the chirality of both centers is retained in **4.3l**, with d.r. > 20:1 and in 94% yield (entry 11).

Mechanistic consideration of this transformation is described in **Scheme 4.2**. Irradiation of CBr_4 produces an electrophilic radical, $\bullet CBr_3$, which upon addition to DMF, generates the radical intermediate **4.4**. Under these reaction conditions, **4.4** is readily oxidized to produce the Vilsmeier−Haack reagents **4.5** or **4.6**.[6–8] In the presence of carboxylic acid, the latter is converted to intermediate **4.7**. At this point, intermediate **4.7** can be converted to corresponding anhydride **4.2** or amide **4.3**. The formation of amide **4.3** through a transient anhydride intermediate **4.2** could be also considered.

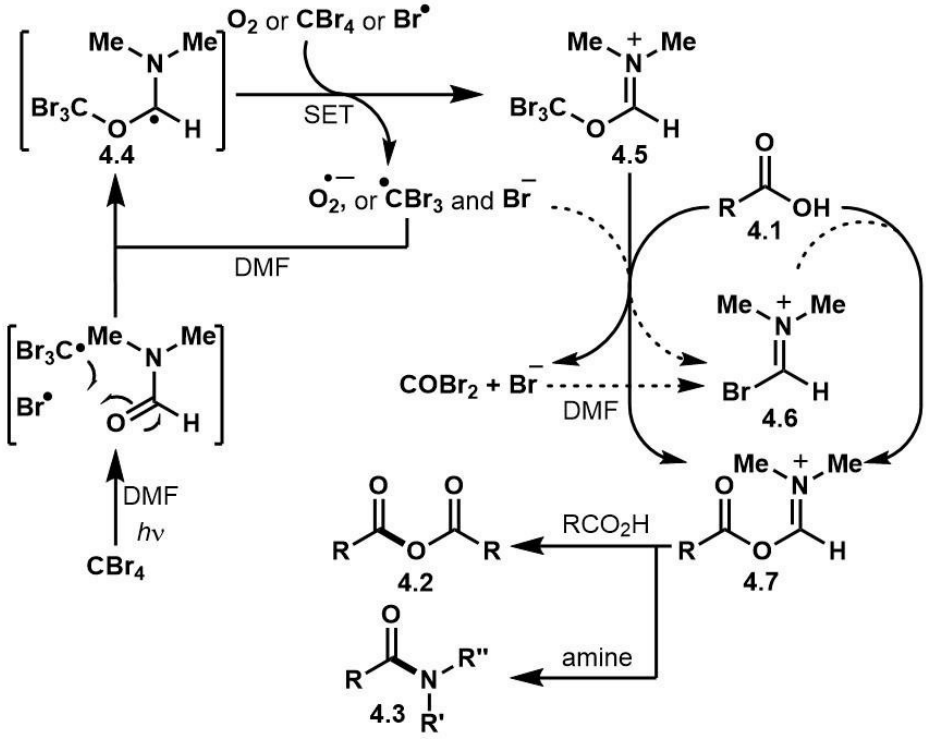

Scheme 4.2 Proposed mechanism for anhydride and amide formation.

4.4 Conclusions

In summary, the photogeneration of Vilsmeier−Haack reagents from irradiation of CBr_4 with UVA LEDs in DMF has been shown to be a useful method for the generation

of symmetric anhydrides. The process is conveniently applicable to a one-pot synthesis of amides from readily available carboxylic acids and amines, without need of a photoredox catalyst. These studies exhibit the importance of photochemical transformations in the synthesis of amide bonds in developing fast, efficient, and reagent-minimizing methods in organic synthesis.

4.5 Experimental Procedures

General Procedure 1 (GP1) – *Synthesis of Symmetric Anhydrides*

To an 8 mL Pyrex screw-top reaction vessel were added substrate (0.3 mmol, 1.0 equiv), DMF (1.5 mL, 0.2 M), collidine (0.6 mmol, 2.0 equiv) and tetrabromomethane (0.3 mmol, 1.0 equiv). The reaction mixture was capped and irradiated with a UVA LED at a distance of 1 cm for 30 min. The resulting mixture was poured into a separatory funnel containing 25 mL of a 3:1 mixture of diethyl ether and hexanes (ethyl acetate was added for compounds that needed further solubility) and was washed with water, where the combined aqueous fractions were re-extracted with 25 mL of diethyl ether. The combined organic portions were washed with saturated sodium bicarbonate, brine and dried over sodium sulfate. The solution was concentrated *in vacuo*, where products were weighed for crude yields and then added an internal standard (mesitylene) to determine yields with proton NMR by comparison to literature precedence.

General Procedure 2 (GP2) – *Synthesis of Amides*

To an 8 mL Pyrex screw-top reaction vessel were added carboxylic acid (0.6 mmol, 3.0 equiv), amine (0.2 mmol, 1.0 equiv), DMF (1.0 mL, 0.2 M), collidine (1.0 mmol, 5.0 equiv), DMAP (0.2 mmol, 1.0 equiv), and tetrabromomethane (0.3 mmol, 1.5 equiv). The reaction mixture was capped and irradiated with a UVA (365 nm) LED at a distance of 1 cm for 30

min. The resulting mixture was poured into a separatory funnel containing 25 mL of ethyl acetate and was washed with 1 M HCl, where the combined aqueous fractions were reextracted with 25 mL of ethyl acetate. The combined organic portions were washed with saturated sodium bicarbonate and brine and dried over sodium sulfate. Products were further purified by column chromatography (0−100% EtOAc/Hex), where relevant fractions were combined, concentrated, and characterized by NMR by comparison to literature precedence. Optical rotations were recorded at 589 nm with 0.1 dm/2 mL sample cell. Retention of configuration was determined by running an analogous reaction with racemic mixtures of either amine or acid with respect to the amide couplings, with work-up in the usual way. Samples were diluted with 5% *i*PrOH in hexane and run on a HPLC equipped with a chiral stationary phase (column: AD-H, 5% *i*PrOH/hexanes, 1.0 mL/min, over 60 min).

4.6 Characterization Data

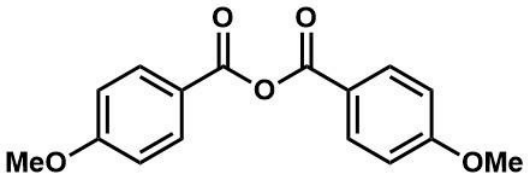

4-methoxybenzoic anhydride (4.2a)

Synthesized according to GP1 and characterized by NMR comparison.[12]

^{1}H NMR (400 MHz, $CDCl_3$): δ = 8.14–8.07 (m, 4H), 7.02–6.96 (m, 4H), 3.90 (s, 6H) ppm;

^{13}C NMR (101 MHz, $CDCl_3$): δ = 164.5 (2×C), 162.2 (2×C), 132.7 (4×CH), 121.2 (2×C), 114.1 (4×CH), 55.5 (2×CH_3) ppm.

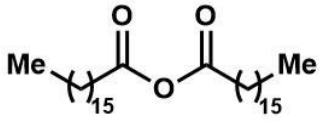

heptanoic anhydride (4.2b)

Synthesized according to GP1 and characterized by NMR comparison.[4d]

^{1}H NMR (400 MHz, $CDCl_3$): δ = 2.45 (t, *J* = 7.4 Hz, 4H), 1.67 (quin, *J* = 7.3 Hz, 4H), 1.27 (m, 52H), 0.89 (t, *J* = 6.6 Hz, 6H) ppm; **^{13}C NMR** (101 MHz, $CDCl_3$): δ = 169.5 (2×C), 35.2 (2×CH_2), 31.9 (2×CH_2), 29.7 (6×CH_2), 29.6 (6×CH_2), 29.5 (2×CH_2), 29.4 (2×CH_2), 29.3 (2×CH_2), 29.2 (2×CH_2), 28.8 (2×CH_2), 24.2 (2×CH_2), 22.7 (2×CH_2), 14.1 (2×CH_3) ppm.

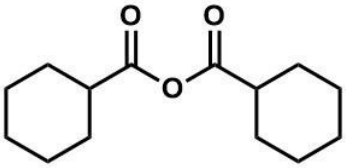

cyclohexanecarboxylic anhydride (4.2c)

Synthesized according to GP1 and characterized by NMR comparison.[13]

^{1}H NMR (300 MHz, $CDCl_3$): δ = 2.42 (tt, *J* = 11.0, 3.7 Hz, 2H), 2.03–1.91 (m, 4H), 1.85–1.74 (m, 4H), 1.70–1.61 (m, 2H), 1.58–1.44 (m, 4H), 1.33–1.21 (m, 6H) ppm; **^{13}C NMR** (75 MHz, $CDCl_3$): δ = 171.8 (2×C), 43.9 (2×CH), 28.4 (4×CH_2), 25.5 (2×CH_2), 25.1 (4×CH_2) ppm.

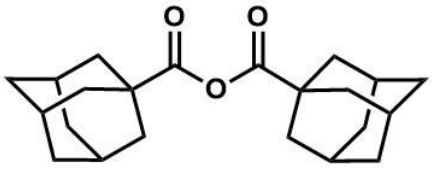

adamantane-1-carboxylic anhydride (4.2d)

Synthesized according to GP1 and characterized by NMR comparison.[3b]

^{1}H NMR (400 MHz, $CDCl_3$): δ = 2.06 (quin, *J* = 3.1 Hz, 6H), 1.95 (d, *J* = 3.0 Hz, 12H), 1.80–1.68 (m, 12H) ppm; **^{13}C NMR** (101 MHz, $CDCl_3$): δ = 173.3 (2×C), 42.2 (2×C), 38.2 (6×CH_2), 36.3 (6×CH_2), 27.6 (6×CH) ppm.

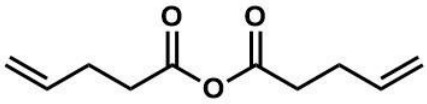

pent-4-enoic anhydride (4.2e)

Synthesized according to GP1 and characterized by NMR comparison.[14]

^{1}H NMR (400 MHz, $CDCl_3$): δ = 5.84 (ddt, *J* = 16.7, 10.2, 6.4 Hz, 2H), 5.15–5.00 (m, 4H), 2.63–2.55 (m, 4H), 2.46–2.41 (m, 4H) ppm; **^{13}C NMR** (101 MHz, $CDCl_3$): δ = 168.6 (2×C), 135.6 (2×CH), 116.1 (2×CH_2), 34.5 (2×CH_2), 28.0 (2×CH_2) ppm.

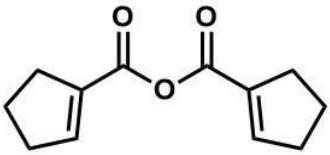

cyclopent-1-ene-1-carboxylic anhydride (4.2f)

Synthesized according to GP1 and characterized by NMR comparison.[15]

^{1}H NMR (400 MHz, $CDCl_3$): δ = 6.97 (quin, *J* = 2.4 Hz, 2H), 2.68–2.55 (m, 8H), 2.02 (quin, *J* = 7.7 Hz, 4H) ppm; **^{13}C NMR** (101 MHz, $CDCl_3$): δ = 160.6 (2×C), 148.5 (2×CH), 136.0 (2×C), 33.7 (2×CH_2), 30.9 (2×CH_2), 23.0 (2×CH_2) ppm.

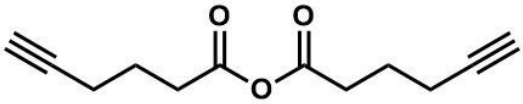

hex-5-ynoic anhydride (4.2g)

Synthesized according to GP1 and characterized by NMR comparison.[16]

^{1}H NMR (400 MHz, $CDCl_3$): δ = 2.63 (t, *J* = 7.3 Hz, 4H), 2.32 (td, *J* = 6.8, 2.6 Hz, 4H), 2.01 (t, *J* = 2.7 Hz, 2H), 1.89 (quin, *J* = 7.2 Hz, 4H) ppm; **^{13}C NMR** (101 MHz, $CDCl_3$): δ = 168.7 (2×C), 82.7 (2×C), 69.6 (2×CH), 33.7 (2×CH_2), 22.8 (2×CH_2), 17.5 (2×CH_2) ppm.

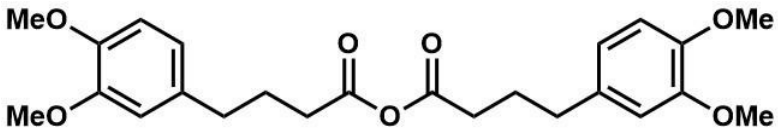

4-(3,4-dimethoxyphenyl)butanoic anhydride (4.2h)

Synthesized according to GP1.

IR (neat, cm^{-1}): 2933(m), 2836(w), 1813(s), 1745(s), 1648(m), 1591(s), 1514(vs), 1450(s), 1416(s); **^{1}H NMR** (300 MHz, $CDCl_3$): δ = 6.79 (d, *J* = 8.7 Hz, 2H), 6.71 (dd, *J* = 6.3, 2.1 Hz, 4H), 3.87–3.85 (m, 12H), 2.63 (t, *J* = 7.5 Hz, 4H), 2.44 (t, *J* = 7.3 Hz, 4H), 1.97 (quin, *J* = 7.4 Hz, 4H) ppm; **^{13}C NMR** (75 MHz, $CDCl_3$): δ = 169.2 (2×C), 148.8 (2×C), 147.3 (2×C), 133.4 (2×C), 120.2 (2×CH), 111.6 (2×CH), 111.2 (2×CH), 55.9 (2×CH_3), 55.8 (2×CH_3), 34.3 (2×CH_2), 34.2 (2×CH_2), 25.8 (2×CH_2) ppm; **HRMS** (EI): m/z calc'd for $C_{24}H_{30}O_7$ [M^+] 430.1992, found 430.1993.

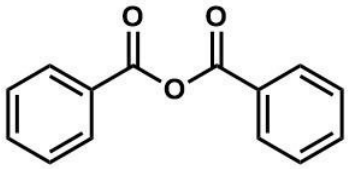

benzoic anhydride (4.2i)

Synthesized according to GP1 and characterized by NMR comparison.[4d]

^{1}H NMR (400 MHz, $CDCl_3$): δ = 8.18 (dt, *J* = 8.2, 1.0 Hz, 4H), 7.74–7.66 (m, 2H), 7.55 (t, *J* = 7.7 Hz, 4H) ppm; **^{13}C NMR** (101 MHz, $CDCl_3$): δ = 162.3 (2×C), 134.5 (2×CH), 130.5 (4×CH), 128.8 (4×CH), 128.8 (2×C) ppm.

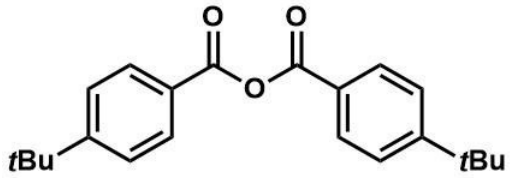

4-(*tert*-butyl)benzoic anhydride (4.2j)

Synthesized according to GP1 and characterized by NMR comparison.[12]

^{1}H NMR (300 MHz, $CDCl_3$): δ = 8.14–8.05 (m, 4H), 7.58–7.50 (m, 4H), 1.38 (s, 18H) ppm; **^{13}C NMR** (75 MHz, $CDCl_3$): δ = 162.5 (2×C), 158.4 (2×C), 130.5 (4×CH), 126.1 (2×C), 125.8 (4×CH), 35.3 (2×C), 31.0 (4×CH_3) ppm.

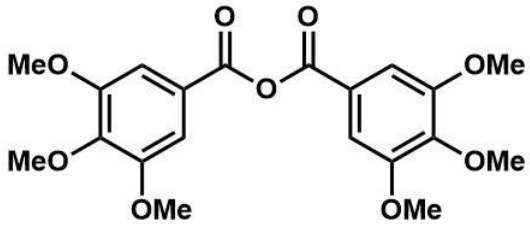

3,4,5-trimethoxybenzoic anhydride (4.2k)

Synthesized according to GP1 and characterized by NMR comparison.[17]

^{1}H NMR (400 MHz, $CDCl_3$): δ = 7.39 (s, 4H), 3.97 (s, 6H), 3.93 (s, 12H) ppm; **^{13}C NMR** (101 MHz, $CDCl_3$): δ = 162.2 (2×C), 153.2 (4×C), 143.8 (2×C), 123.5 (2×C), 107.8 (4×CH), 61.0 (2×CH_3), 56.3 (4×CH_3) ppm.

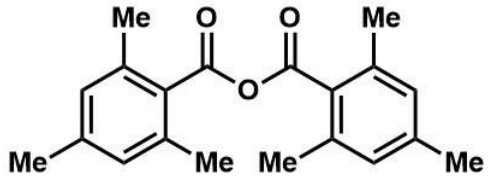

2,4,6-trimethylbenzoic anhydride (4.2l)

Synthesized according to GP1 and characterized by NMR comparison.[12]

^{1}H NMR (400 MHz, $CDCl_3$): δ = 6.89 (s, 4H), 2.42 (s, 12H), 2.31 (s, 6H) ppm; **^{13}C NMR** (101 MHz, $CDCl_3$): δ = 165.3 (2×C), 150.1 (2×C), 140.7 (2×C), 136.3 (4×C), 128.8 (4×CH), 21.2 (2×CH_3), 20.0 (4×CH_3) ppm.

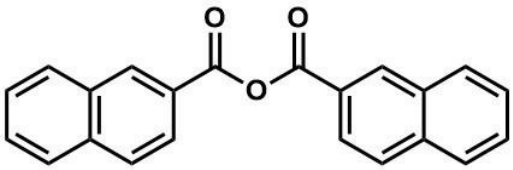

2-naphthoic anhydride (4.2m)

Synthesized according to GP1 and characterized by NMR comparison.[18]

^{1}H NMR (400 MHz, $CDCl_3$): δ = ^{1}H NMR (300 MHz, Chloroform-*d*) δ 8.80 (d, *J* = 1.7 Hz, 2H), 8.21 (dt, *J* = 8.6, 1.5 Hz, 2H), 8.07–7.94 (m, 6H), 7.73–7.59 (m, 4H) ppm; **^{13}C NMR** (101 MHz, $CDCl_3$): δ = 162.7 (2×C), 136.2 (2×C), 132.8 (2×CH), 129.6 (2×CH), 129.2 (2×CH), 128.8 (2×CH), 127.9 (2×CH), 127.1 (2×CH), 125.3 (2×CH) ppm.

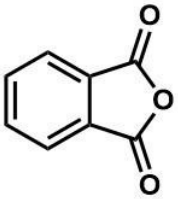

phthalic anhydride (4.2n)

Synthesized according to GP1 and characterized by NMR comparison.[7a]

^{1}H NMR (400 MHz, $CDCl_3$): δ = 8.03 (tt, *J* = 5.0, 2.4 Hz, 2H), 7.97–7.90 (m, 2H) ppm; **^{13}C NMR** (101 MHz, $CDCl_3$): δ = 162.7 (2×C), 136.0 (2×CH), 131.2 (2×C), 125.6 (2×CH) ppm.

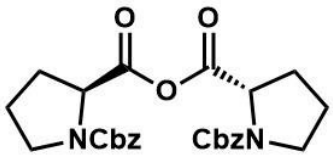

(*S*)-1-((benzyloxy)carbonyl)pyrrolidine-2-carboxylic anhydride (4.2o)

Synthesized according to GP1 (rotamers).

IR (neat, cm^{-1}): 2995(m), 2882(w), 1827(s), 1745(s), 1697(vs), 1411(s), 1352(vs); **^{1}H NMR** (400 MHz, $CDCl_3$): δ = 7.40–7.21 (m, 10H), 5.14 (tt, *J* = 17.1, 5.0 Hz, 4H), 4.53–4.19 (m, 2H), 3.71–3.41 (m, 4H), 2.22–1.82 (m, 8H) ppm; **^{13}C NMR** (101 MHz, $CDCl_3$): δ = 167.7 & 167.5 (2×C), 155.9 & 154.78 (2×C), 136.4 & 136.2 (2×C), 128.4 & 128.3 (4×CH), 128.0 & 127.9 (4×CH), 127.8 & 127.7 (2×CH), 67.3 & 67.1 (2×CH_2), 59.7 & 59.3 (2×CH), 46.9 & 46.3 (2×CH_2), 30.2 & 29.0 (2×CH_2), 24.2 & 23.3 (2×CH_2) ppm. **HRMS** (EI): m/z calc'd for $C_{26}H_{28}N_2O_7$ [M^+] 480.1897, product was unstable; **$[\alpha]_D^{20}$** = –32.1° (c 1.0, EtOH).

4.2o was hydrolyzed in EtOH with 0.5 mL of water and a KOH pellet. After overnight stirring, the solution was acidified using 1 M HCl and extracted with 3×40 mL of DCM, dried over sodium sulfate, concentrated *in vacuo*, giving *N*-Cbz-proline (**4.2o'**, *Z*-L-pro). Crude material was further purified by flash chromatography, where relevant fractions were combined, concentrated, and characterized by NMR comparison (rotamers).[19a] This was performed to assess retention of configuration during anhydride formation.

^{1}H NMR (400 MHz, $CDCl_3$): δ = 8.17 (br. s, 1H), 7.37–7.29 (m, 5H), 5.25–5.06 (m, 2H), 4.40 (dt, *J* = 9.2, 5.7 Hz, 1H), 3.71–3.40 (m, 2H), 2.32–2.06 (m, 2H), 2.02–1.87 (m, 2H) ppm; **^{13}C NMR** (101 MHz, $CDCl_3$): δ = 177.7 & 176.2 (C), 155.8 & 154.4 (C), 136.5 & 136.3 (C), 128.5 & 128.4 (2×CH), 128.1 & 127.9 (2×CH), 127.8 & 127.6 (CH), 67.4 & 67.1 (CH_2), 59.4 (CH), 46.9 & 46.6 (CH_2), 29.7 & 29.4 (CH_2), 24.37 & 23.4 (CH_2) ppm; **$[\alpha]_D^{20}$** = –37.2° (c 1.0, EtOH); lit. –40.4°(c 1.0, EtOH).[19b] A HPLC equipped with a chiral

stationary phase was taken of a mixture of 2:1 mixture of *Z*-L-pro:*Z*-D-pro *vs* the reaction described above yielding *Z*-L-pro for comparison.

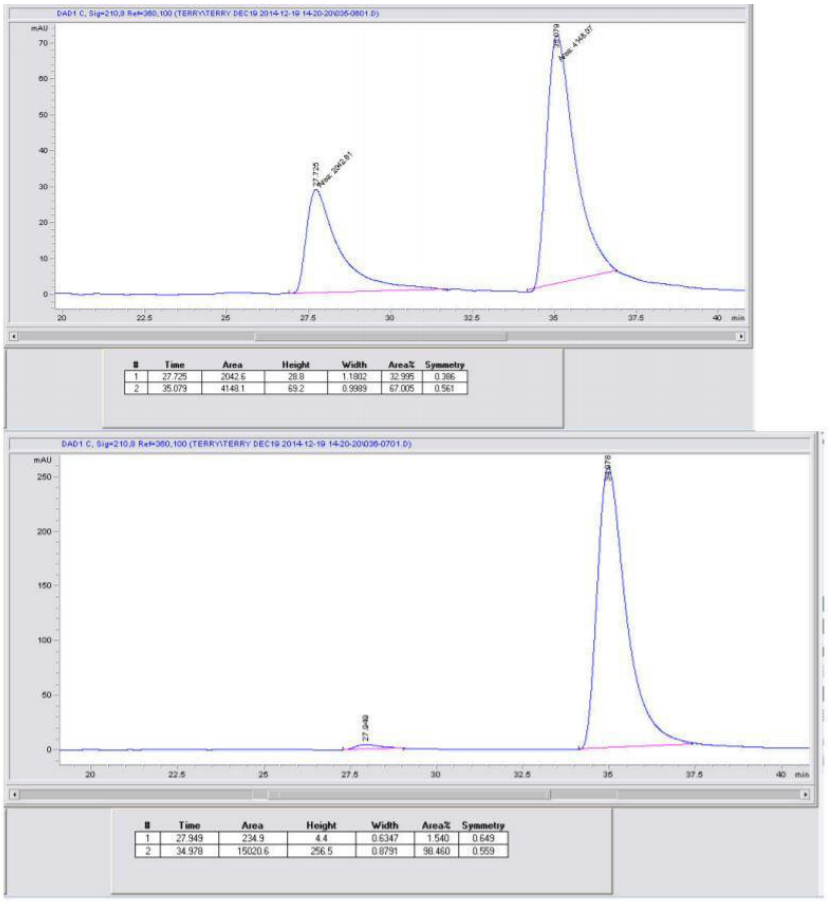

Figure 4.1 Chiral HPLC data for **4.2o**.

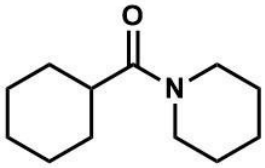

cyclohexyl(piperidin-1-yl)methanone (4.3a)

Synthesized according to GP1 and characterized by NMR comparison.[20]

^{1}H NMR (400 MHz, $CDCl_3$): δ = 3.49 (d, *J* = 6.4 Hz, 4H), 2.47 (tt, *J* = 11.6, 3.4 Hz, 1H), 1.81 (ddt, *J* = 10.2, 7.3, 4.1 Hz, 2H), 1.76–1.60 (m, 5H), 1.60–1.46 (m, 6H), 1.31–1.22 (m, 3H) ppm; **^{13}C NMR** (101 MHz, $CDCl_3$): δ = 174.4 (C), 40.5 (CH), 29.5 (2×CH_2), 26.4 (4×CH_2), 26.0 (2×CH_2), 25.9 (CH_2), 24.7 (CH_2) ppm.

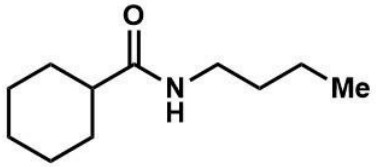

***N*-butylcyclohexanecarboxamide (4.3b)**

Synthesized according to GP1 and characterized by NMR comparison.[21]

^{1}H NMR (400 MHz, $CDCl_3$): δ = 5.42 (br. s, 1H), 3.24 (td, *J* = 7.1, 5.7 Hz, 2H), 2.05 (tt, *J* = 11.7, 3.5 Hz, 1H), 1.89–1.82 (m, 2H), 1.82–1.76 (m, 2H), 1.51–1.40 (m, 4H), 1.35–1.20 (m, 6H), 0.92 (t, *J* = 7.3 Hz, 3H) ppm; **^{13}C NMR** (101 MHz, $CDCl_3$): δ = 176.0 (C), 45.7 (CH), 39.0 (CH_2), 31.8 (CH_2), 29.8 (2×CH_2), 25.8 (3×CH_2), 20.0 (CH_2), 13.8 (CH_3) ppm.

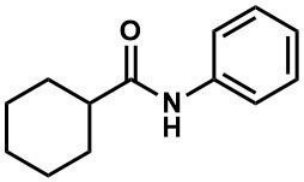

***N*-phenylcyclohexanecarboxamide (4.3c)**

Synthesized according to GP1 and characterized by NMR comparison.[22]

^{1}H NMR (400 MHz, $CDCl_3$): δ = 7.59–7.48 (m, 2H), 7.37–7.29 (m, 2H), 7.15 (br. s, 1H), 7.13–7.06 (m, 1H), 2.24 (tt, *J* = 11.7, 3.6 Hz, 1H), 1.97 (dd, *J* = 12.8, 3.7 Hz, 2H), 1.90–1.81 (m, 2H), 1.72 (d, *J* = 7.0 Hz, 1H), 1.58 (dd, *J* = 17.5, 6.9 Hz, 2H), 1.40–1.23 (m, 4H) ppm; **^{13}C NMR** (101 MHz, $CDCl_3$): δ = 174.3 (C), 138.0 (C), 129.0 (2×CH), 124.1 (CH), 119.7 (2×CH), 46.6 (CH), 29.7 (2×CH_2), 25.7 (3×CH_2) ppm.

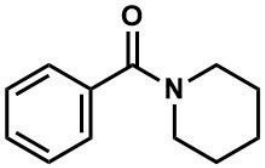

phenyl(piperidin-1-yl)methanone (4.3d)

Synthesized according to GP1 and characterized by NMR comparison.[23]

^{1}H NMR (400 MHz, $CDCl_3$): δ = 7.39 (s, 5H), 3.72 (s, 2H), 3.34 (s, 2H), 1.69 (d, *J* = 6.0 Hz, 4H), 1.55–1.48 (m, 2H) ppm; **^{13}C NMR** (101 MHz, $CDCl_3$): δ = 170.3 (C), 136.5 (C), 129.3 (CH), 128.4 (2×CH), 126.8 (2×CH), 47.9 (2×CH_2), 25.8 (2×CH_2), 24.6 (CH_2) ppm.

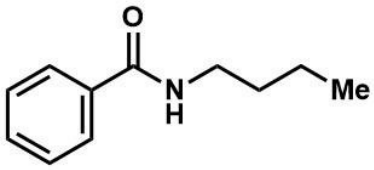

***N*-butylbenzamide (4.3e)**

Synthesized according to GP1 and characterized by NMR comparison.[21]

^{1}H NMR (400 MHz, $CDCl_3$): δ = 7.81–7.73 (m, 2H), 7.52–7.45 (m, 1H), 7.45–7.39 (m, 2H), 6.17 (br. s, 1H), 3.46 (td, *J* = 7.2, 5.7 Hz, 2H), 1.66–1.56 (m, 2H), 1.48–1.36 (m, 2H), 0.97 (t, *J* = 7.3 Hz, 3H) ppm; **^{13}C NMR** (101 MHz, $CDCl_3$): δ = 167.5 (C), 134.9 (C), 131.3 (CH), 128.5 (2×CH), 126.8 (2×CH), 39.8 (CH_2), 31.7 (CH_2), 20.1 (CH_2), 13.8 (CH_3) ppm.

***N*-phenylbenzamide (4.3f)**

Synthesized according to GP1 and characterized by NMR comparison.[24]

^{1}H NMR (400 MHz, $CDCl_3$): δ = 7.92–7.86 (m, 2H), 7.84 (br. s, 1H), 7.69–7.63 (m, 2H), 7.59–7.54 (m, 1H), 7.54–7.46 (m, 2H), 7.43–7.35 (m, 2H), 7.17 (ddt, *J* = 8.6, 7.3, 1.2 Hz, 1H) ppm; **^{13}C NMR** (101 MHz, $CDCl_3$): δ = 165.7 (C), 137.9 (C), 135.0 (C), 131.9 (CH), 129.1 (2×CH), 128.8 (2×CH), 127.0 (2×CH), 124.6 (CH), 120.2 (2×CH) ppm.

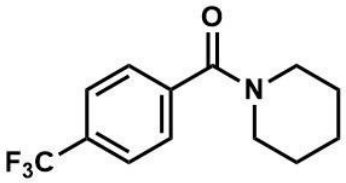

piperidin-1-yl(4-(trifluoromethyl)phenyl)methanone (4.3g)

Synthesized according to GP1 and characterized by NMR comparison.[25]

^{1}H NMR (400 MHz, $CDCl_3$): δ = 7.67 (d, *J* = 8.0 Hz, 2H), 7.50 (d, *J* = 8.0 Hz, 2H), 3.72 (s, 2H), 3.39–3.22 (m, 2H), 1.69 (d, *J* = 4.4 Hz, 4H), 1.53 (s, 2H) ppm; **^{13}C NMR** (101 MHz, $CDCl_3$): δ = 168.8 (C), 140.0 (C), 131.3 (q, *J* = 32.6 Hz, C), 127.1 (2×CH), 125.5 (q, *J* = 3.8 Hz, 2×CH), 123.7 (q, *J* = 274.4 Hz, CF_3), 48.6 (CH_2), 43.1 (CH_2), 26.5 (CH_2), 25.5 (CH_2), 24.5 (CH_2) ppm.

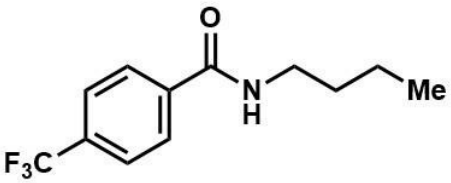

***N*-butyl-4-(trifluoromethyl)benzamide (4.3h)**

Synthesized according to GP1 and characterized by NMR comparison.[26]

^{1}H NMR (400 MHz, $CDCl_3$): δ = 7.93–7.81 (m, 2H), 7.74–7.62 (m, 2H), 6.26 (br. s, 1H), 3.47 (td, *J* = 7.2, 5.7 Hz, 2H), 1.67–1.57 (m, 2H), 1.49–1.36 (m, 2H), 0.97 (t, *J* = 7.3 Hz, 3H) ppm; **^{13}C NMR** (101 MHz, $CDCl_3$): δ = 166.2 (C), 138.1 (C), 133.0 (q, *J* = 32.7 Hz, C), 127.3 (2×CH), 125.6 (q, *J* = 3.8 Hz, 2×CH), 123.7 (q, *J* = 272.6 Hz, CF_3), 40.0 (CH_2), 31.6 (CH_2), 20.1 (CH_2), 13.7 (CH_3) ppm.

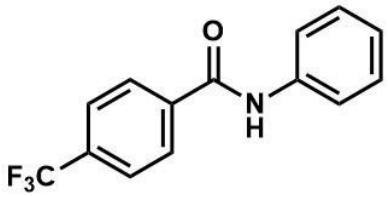

***N*-phenyl-4-(trifluoromethyl)benzamide (4.3i)**

Synthesized according to GP1 and characterized by NMR comparison.[27]

^{1}H NMR (400 MHz, $CDCl_3$): δ = 7.99 (d, *J* = 7.9 Hz, 2H), 7.83 (br. s, 1H), 7.77 (d, *J* = 8.1 Hz, 2H), 7.69–7.61 (m, 2H), 7.45–7.36 (m, 2H), 7.22–7.18 (m, 1H) ppm; **^{13}C NMR** (101 MHz, $CDCl_3$): δ = 164.4 (C), 137.4 (C), 134.0 (q, *J* = 32.7 Hz, C), 132.2 (C), 129.2 (2×CH), 127.5 (2×CH), 125.9 (q, *J* = 4.0 Hz, 2×CH), 125.1 (CH), 123.3 (q, *J* = 273.3 Hz, CF_3), 120.3 (2×CH) ppm.

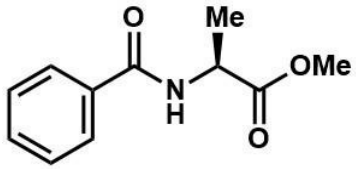

methyl benzoyl-L-alaninate (4.3j)

Synthesized according to GP1 and characterized by NMR comparison.[28]

^{1}H NMR (400 MHz, $CDCl_3$): δ = 7.89–7.77 (m, 2H), 7.56–7.49 (m, 1H), 7.45 (dd, *J* = 8.3, 6.6 Hz, 2H), 6.74 (br. s, 1H), 4.82 (quin, *J* = 7.2 Hz, 1H), 3.81 (s, 3H), 1.54 (d, *J* = 7.2 Hz, 3H) ppm; **^{13}C NMR** (101 MHz, $CDCl_3$): δ = 173.7 (C), 166.7 (C), 133.9 (C), 131.7 (CH), 128.6 (2×CH), 127.0 (2×CH), 52.6 (CH_3), 48.5 (CH), 18.7 (CH_3) ppm; **$[\alpha]_D^{20}$** = +30.2° (c 1.0, $CHCl_3$). A similar reaction using racemic alanine derivative provided racemic **4.3j** in similar yield after isolation. A HPLC equipped with a chiral stationary phase was taken of each sample to assess retention of configuration in the described amide coupling.

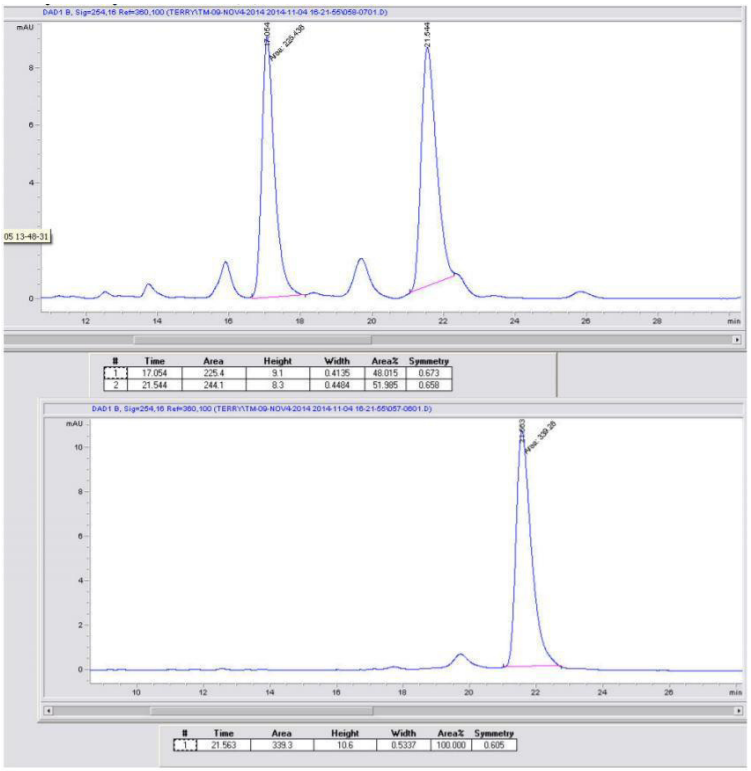

Figure 4.2 Chiral HPLC data for **4.3j**.

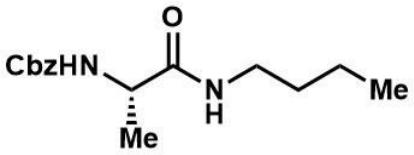

benzyl (*S*)-(1-(butylamino)-1-oxopropan-2-yl)carbamate (4.3k)

Synthesized according to GP1 and characterized by NMR comparison.[29]

^{1}H NMR (400 MHz, $CDCl_3$): δ = 7.41–7.29 (m, 5H), 6.11 (br. s, 1H), 5.40 (br. s, 1H), 5.11 (s, 2H), 4.21 (dt, *J* = 13.6, 7.0 Hz, 1H), 3.24 (q, *J* = 6.7 Hz, 2H), 1.47 (quin, *J* = 7.6 Hz, 2H), 1.38 (d, *J* = 7.0 Hz, 3H), 1.32 (q, *J* = 7.5 Hz, 2H), 0.91 (t, *J* = 7.3 Hz, 3H) ppm; **^{13}C NMR** (101 MHz, $CDCl_3$): δ = 172.0 (C), 156.0 (C), 136.1 (C), 128.5 (2×CH), 128.2 (CH), 128.0 (2×CH), 67.0 (CH_2), 50.6 (CH), 39.3 (CH_2), 31.5 (CH_2), 20.0 (CH_2), 18.7 (CH_3), 13.7 (CH_3) ppm; **$[\alpha]_D^{20}$** = –6.8° (c 1.0, EtOH). A similar reaction using racemic alanine derivative provided racemic **4.3k** in similar yield after isolation. A HPLC equipped with a chiral stationary phase was taken of each sample to assess retention of configuration in the described amide coupling.

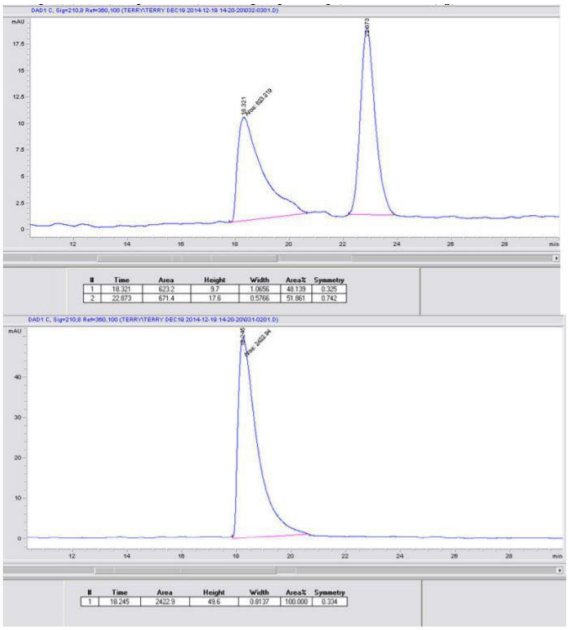

Figure 4.3 Chiral HPLC data for **4.3k**.

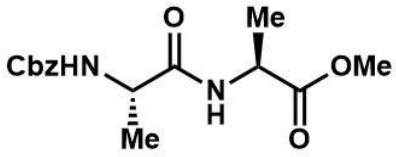

methyl ((benzyloxy)carbonyl)-L-alanyl-L-alaninate (4.3l)

Synthesized according to GP1 and characterized by NMR comparison.[30]

^{1}H NMR (400 MHz, $CDCl_3$): δ = 7.38–7.30 (m, 5H), 6.78–6.65 (br. s, 1H), 5.50 (br. s, *J* = 7.8 Hz, 1H), 5.18–5.05 (m, 2H), 4.56 (quin, *J* = 7.3 Hz, 1H), 4.30 (t, *J* = 7.7 Hz, 1H), 3.74 (s, 3H), 1.39 (d, *J* = 7.4 Hz, 6H) ppm; **^{13}C NMR** (101 MHz, $CDCl_3$): δ = 173.1 (C), 171.8 (C), 155.9 (C), 136.2 (C), 128.5 (2×CH), 128.1 (CH), 128. (2×CH), 67.0 (CH_2), 52.4 (CH_3), 50.4 (CH), 48.0 (CH), 18.7 (CH_3), 18.2 (CH_3) ppm; **$[\alpha]_D^{20}$** = –49.0° (c 1.0, MeOH). A similar reaction using racemic amino acid derivatives provided racemic **4.3l** in similar yield after isolation. A HPLC equipped with a chiral stationary phase was taken of each sample to assess retention of configuration in the described amide coupling.

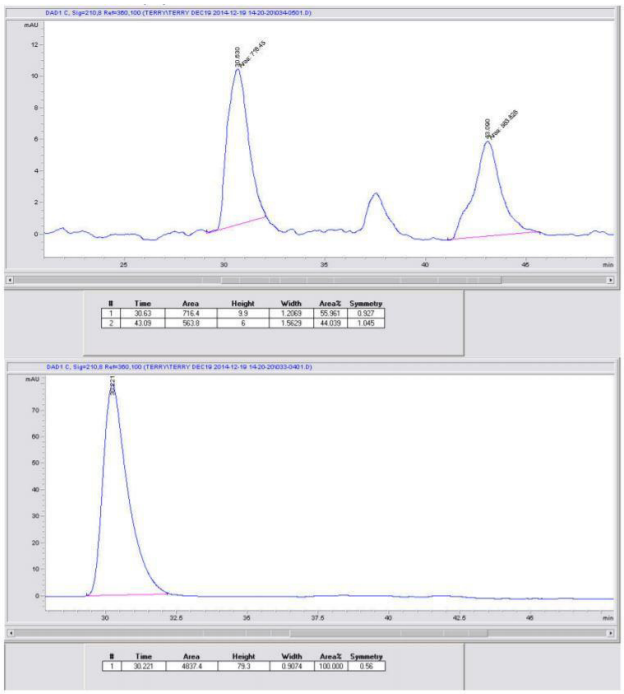

Figure 4.4 Chiral HPLC data for **4.3l**.

4.7 References

[1] a) El-Faham, A.; Albericio, F. *Chem. Rev*. **2011**, *111*, 6557−6602; b) Pattabiraman, V. R.; Bode, J. W. *Nature* **2011**, *480*, 471−479.

[2] a) Schotten, C. *Ber. Dtsch. Chem. Ges*. **1884**, *17*, 2544−2547; b) Baumann, E. *Ber. Dtsch. Chem. Ges*. **1886**, *19*, 3218−3222; c) Fischer, E. *Ber. Dtsch. Chem. Ges*. **1903**, *36*, 2982−2992; d) Zuffanti, S. *J. Chem. Educ*. **1948**, *25*, 481; e) Valeur, E.; Bradley, M. *Chem. Soc. Rev*. **2009**, *38*, 606−631; f) Joullie, M. M.; Lassen, K. M. *Arkivoc* **2010**, *VIII*, 189−250.

[3] a) Rambacher, P.; Make, S. *Angew. Chem. Int. Ed. Engl*. **1968**, *80*, 465; b) Plusquellec, D.; Roulleau, F.; Lefeuvre, M.; Brown, E. *Tetrahedron* **1988**, *44*, 2471−2476.

[4] a) Ferris, A. F.; Emmons, W. D. *J. Am. Chem. Soc*. **1953**, *75*, 232−233; b) Hata, T.; Tajima, K.; Mukaiyama, T. *Bull. Chem. Soc. Jpn*. **1968**, *41*, 2746−2747; c) Lee, J. C.; Cho, Y. H.; Lee, H. K.; Cho, S. H. *Synth. Commun*. **1995**, *25*, 2877−2881; d) Kaminski, Z. J.; Kolesinka, B.; Malgorzata, M. *Synth. Commun*. **2004**, *34*, 3349−3358; e) Liu, J.; West, K. R.; Bondy, C. R.; Sanders, J. K. M. *Org. Biomol. Chem*. **2007**, *5*, 778−786; f) Bartoli, G.; Bosco, M.; Carlone, A.; Dalpozzo, R.; Marcantoni, E.; Melchiorre, P.; Sambri, L. S*ynthesis* **2007**, *22*, 3489−3496; g) Strukil, V.; Bartolec, B.; Portada, T.; Dilovic, I.; Halasz, I.; Bargetic, D. *Chem. Commun*. **2012**, *48*, 12100−12102; h) Bai, J.; Zambron, B.; Vogel, P. *Org. Lett*. **2014**, *16*, 604−607 and references cited therein.

[5] *For reviews:* a) Prier, C. K.; Rankic, D. A.; MacMillan, D. W. C. *Chem. Rev*. **2013**, *113*, 5322−5363; b) Schultz, D. M.; Yoon, T. P. *Science* **2014**, *343*, 985–1239176–8.

[6] Dai, C.; Narayanam, J. M. R.; Stephenson, C. R. J. *Nat. Chem*. **2011**, *3*, 140−145.

[7] a) Konieczynska, M. D.; Dai, C.; Stephenson, C. R. J. *Org. Biomol. Chem*. **2012**, *10*, 4509−4511; b) Srivastava, V. P.; Yadav, A. K.; Yadav, L. D. S. *Synlett* **2014**, *25*, 665−670; c) Yadav, A. K.; Srivastava, V. P.; Yadav, L. D. S. *RSC Adv*. **2014**, *4*, 4181−4186.

[8] a) Nishina, Y.; Ohtani, B.; Kikushima, K. *Beilstein J. Org. Chem*. **2013**, *9*, 1663−1667; b) McCallum, T.; Slavko, E.; Morin, M.; Barriault, L. *Eur. J. Org. Chem*. **2015**, 1, 81−85.

[9] *For reduction of nonactivated bromoalkanes, see:* Revol, G.; McCallum, T.; Morin, M.; Gagosz, F.; Barriault, L. *Angew. Chem. Int. Ed*. **2013**, *52*, 13342−13345.

[10] Anhydride arising from *N*-Cbz protected L-proline was hydrolyzed, where the resulting acid was analyzed by HPLC equipped with a chiral stationary phase, showing retention of L-configuration in 98.5:1.5 e.r. (L/D) (section **4.6**).

[11] Bodansky, M. in *Principles of Peptide Synthesis*; Springer−Verlag: New York, 1984.

[12] Li, Y.; Xue, D.; Wang, C.; Liu, Z.; Xiao, J. *Chem. Commun*. **2012**, *48*, 1320−1322.

[13] Tsang, W.-Y.; Ahmed, N.; Hemming, K.; Page, M. *Org. Biomol. Chem*. **2007**, *5*, 3993−4000.

[14] Ellervik, U.; Magnusson, G. *Acta Chem. Scand*. **1993**, *47*, 826−828.

[15] Trost, B. M.; Whitman, P. J. *J. Am. Chem. Soc*. **1974**, *96*, 7421−7429.

[16] Moody, C.; Shah, P. *J. Chem. Soc., Perkin Trans. 1* **1988**, 3249−54.

[17] Daskiewicz, J.; Depeint, F.; Viornery, L.; Bayet, C.; Comte-Sarrazin, G.; Comte, G.; Gee, J. M.; Johnson, I. T.; Ndjoko, K.; Hostettmann, K.; Barron, D. *J. Med. Chem*. **2005**, *48*, 2790−2804.

[18] Cirriez, V.; Rasson, C.; Riant, O. *Adv. Synth. Catal*. **2013**, *355*, 3137−3140.

[19] a) Gould, E.; Lebl, T.; Slawin, A. M. Z.; Reid, M.; Davies, T.; Smith, A. D. *Org. Biomol. Chem*. **2013**, *11*, 7877−7892; b) De Luca, L; Giacomelli, G.; Masala, S.; Porcheddu, A. *J. Org. Chem*. **2003**, *68*, 4999−5001.

[20] Wannberg, J.; Larhed, M. *J. Org. Chem*. **2003**, *68*, 5750−5753.

[21] Hans, J. J.; Driver, R. W.; Burke, S. D. *J. Org. Chem*. **2000**, *65*, 2114−2121.

[22] Liu, H.; Yan, N.; Dyson, P. J. *Chem. Commun*. **2014**, *50*, 7848−7851.

[23] Toledo, H.; Pisarevsky, E.; Abramovich, A.; Szpilman, A. M. *Chem. Commun*. **2013**, *49*, 4367−4369.

[24] Murthy, S. N.; Madhav, B.; Reddy, V. P.; Nageswar, Y. V. D. *Adv. Synth. Catal*. **2010**, *352*, 3241−3245.

[25] Khan, B. A.; Buba, A. E.; Gooßen, L. J. *Chem. Eur. J*. **2012**, *18*, 1577−1581.

[26] Kaiser, N.-F. K.; Hallberg, A.; Larhed, M. *J. Comb. Chem*. **2002**, *4*, 109−111.

[27] Perry, R. J.; Wilson, B. D. *J. Org. Chem*. **1996**, *61*, 7482−7485.

[28] Reddy, K. R.; Maheswari, C. U.; Venkateshwar, M.; Kantam, M. L. *Eur. J. Org. Chem*. **2008**, 3619−3622.

[29] Kolesinska, B.; Kaminski, Z. J. *Org. Lett*. **2009**, *11*, 765−768.

[30] Brown, D. W.; Campbell, M. M.; Walker, C. V. *Tetrahedron* **1983**, *39*, 1075−1083.

5. Redox-Neutral Minisci Reactions Via Photoredox Catalysis

McCallum, T.; Barriault, L. Direct alkylation of heteroarenes with unactivated bromoalkanes using photoredox gold catalysis. *Chem. Sci.* **2016**, *7*, 4754–4758.

5.1 Abstract

The addition of alkyl radicals to protonated heteroarenes, known as the Minisci reaction, is one of the most important functionalization strategies for the synthesis of drug-like heteroaromatic scaffolds. Originating in the 1960's and 70's, carboxylic acids in the presence of silver catalysts and persulfates led to the formation of nucleophilic alkyl radicals which could functionalize electrophilic protonated heteroarenes. The methodology suffers from by-product forming pathways as well as relatively harsh reaction conditions. Although visible light photoredox catalysis has emerged as a powerful tool for the construction of C–C bonds, common catalysts and/or their photoexcited states suffer from low redox potentials, limiting their applicability to alkyl radical generation from substrates with activated carbon–halogen bonds. Radicals derived from these activated compounds, being highly electrophilic or stabilized, do not undergo efficient addition to heteroarenes. Described herein is the photocatalytic generation of relatively nucleophilic alkyl radicals from nonactivated bromoalkanes as part of a universal and efficient cross-coupling strategy for the direct alkylation of heteroarenes using a binuclear Au(I) bisphosphine complex as photoredox catalyst, $[Au_2(\mu\text{-dppm})_2]Cl_2$. The method proves to be efficient for alkylation of heteroarenes under mild conditions in the absence of directing groups. The process also demonstrates the importance of the electronic characteristics of alkyl radicals when considering addition to electrophilic heteroarenes, as demonstrated through the development of polarity reversal radical addition reactions.

5.2 Introduction

Over the past few decades, we have seen a dramatic increase in photochemical research, leading to great progress in the fields of energy storage, water splitting, photovoltaic devices, and more recently, transformations of organic molecules in the synthesis of high-value products and therapeutics.[1–5] For over a century, chemists have found inspiration in the sophistication of light-harvesting bio-molecules, owing the development of photo-excited complexes to furthering our knowledge of the well-kept "secrets of the plants".[6, 7] A fresh take on classical radical chemistry through the eyes of photoredox catalysis has produced unconventional reactivity in organic synthesis, unlocking mild and environmentally sound methodology for the construction of C–C bonds.[2–5] Photoredox catalysis methods are advantageous to classical methods of alkyl and aryl radical generation from which the use of hazardous radical initiators and/or harsh conditions are often employed.[8]

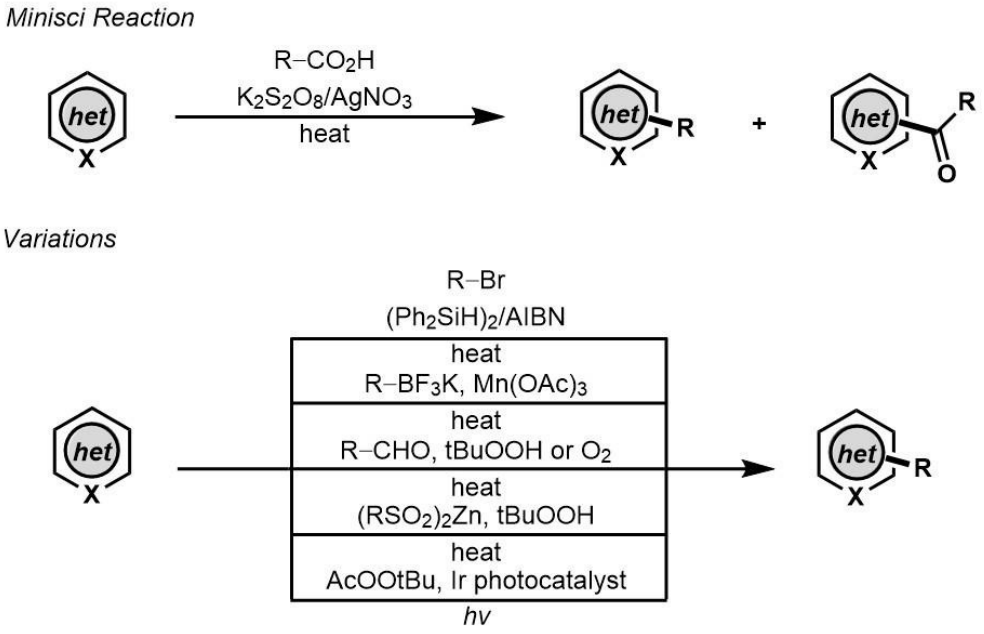

Scheme 5.1 Previous work in the Minisci reaction.

The synthesis and diversification of heteroaromatic compounds via C–H functionalization has had a great impact in organic materials and drug discovery.[9, 10] Although important advances have been made, C–H functionalization of heteroarenes without directing groups remains a standing challenge in organic synthesis.[11] The addition of carbon–centered radicals derived from carboxylic acids to heteroarenes, known as the Minisci reaction, has been instrumental in the functionalization of heteroaromatics.[12] This seminal work describes an expedient synthesis of alkyl functionalized heteroarenes but suffers from harsh conditions that often led to by-product formation. Contemporary C–H alkylation protocols have been developed from a variety of functional groups but necessitate the use of stoichiometric oxidants/reagents and are often accompanied by multi-step syntheses of the starting materials (**Scheme 5.1**).[13–21] In combination, these drawbacks limit functional group tolerance and the scope of the parent radicals. Keeping this in mind, we wondered if a practical Csp^3–Csp^2 coupling strategy for direct C–H alkylation of heteroarenes of broader applicability could be conceived using photoredox catalysis and simple bromoalkanes. Remaining a challenge in organic synthesis, few photocatalytic Minisci-type methodologies have been described involving carbon–centered radicals from simple bromoalkanes. To this effect, excited-state binuclear Au(I) complex, $[Au_2(\mu\text{-dppm})_2]Cl_2$, has been shown to undergo reduction chemistry of both nonactivated bromoalkanes and arenes (and other functional groups),[22] while recently luminescent platinum complexes[23] and organic dyes[24] have been reported to reduce nonactivated bromoalkanes and arenes.

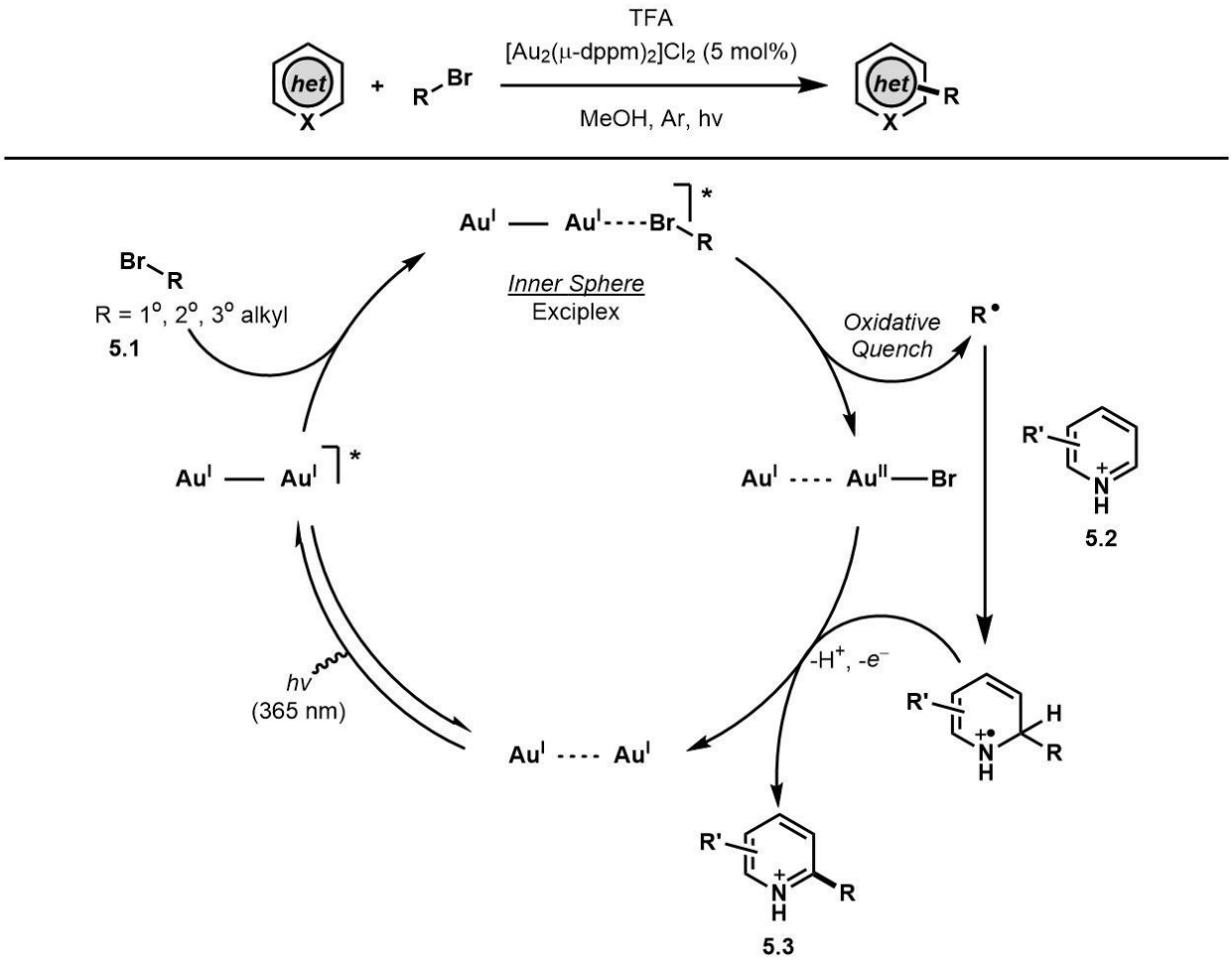

Figure 5.1 Proposed mechanism for the gold photoredox Minisci reaction.

We hypothesized that a redox-neutral C–H functionalization protocol employing a photoredox catalyst as both the reductant and the oxidant would mitigate the need for stoichiometric additives. Based on previous studies in our laboratory, we envisioned the genesis of alkyl radicals derived from broadly available bromoalkanes (**5.1**, ca. –2.0 V *vs* SCE)[25] through an oxidative quenching mechanism with photoexcited $[Au_2(\mu\text{-dppm})_2]Cl_2$ (–1.63 V *vs* SCE; **Figure 5.1**).[26] These nucleophilic alkyl radicals would then be uniquely reactive towards heteroaromatics (**5.2**) prone to addition at electron deficient locations. The resulting aminyl radical cation intermediate would be subsequently oxidized by $[Au_2(\mu\text{-dppm})_2]^{3+}$, thus completing the catalytic cycle while providing the directly alkylated

heteroarene products (**5.3**). It is conceivable that the aminyl radical cation intermediate could undergo chain propagating electron transfer with **5.1**, but this is likely to be a minor pathway considering the reduction potential of bromoalkanes. Ru- and Ir-based polypyridyl complexes operate through an outer sphere mechanism of MLCT for activation of carbon–halogen bonds. Complexes like $[Ru(bpy)_3]Cl_2$ and $Ir(ppy)_3$ have excited-state reduction potentials of –0.81 V and –1.73 V *vs* SCE, respectively. Substrate engagement is, therefore, limited to compounds with reduction potentials lower than the excited states of the Ru- and Ir-based polypyridyl complexes. These complexes are unable to undergo efficient excited-state quenching with nonactivated bromoalkanes.

Recently, it has been shown that binuclear Au(I) phosphine complexes such as $[Au_2(\mu\text{-dppm})_2]Cl_2$ bear little aurophilic interaction at ground state, but upon excitation, an Au–Au interaction is formed.[27] This interaction provides an open coordination site where association of haloalkanes may occur, leading to inner sphere PET upon generation of an exciplex between the photocatalyst and bromoalkane.[25] This phenomena allows the photocatalyst to activate bromoalkanes that have a larger reduction potential than the binuclear Au(I) complex, *vide supra*.

5.3 Results and Discussion

Initial screening of the reaction conditions was carried out with $[Au_2(\mu\text{-dppm})_2]Cl_2$ (2 mol%) as photocatalyst with a lepidine–TFA salt **5.2** along with bromocyclohexane **5.1g** in an array of solvents. To our delight, methanol was the optimal solvent, which upon concentrating to 0.5 M, allowed for quantitative conversion to the alkyl functionalized heteroarene product **5.3g** with irradiation from a UVA LED (365 nm). Further optimization increased the amount of catalyst to 5 mol% which allowed shorter irradiation times to

reach reaction completion and showed promise for generality towards other substrates (See section **5.5**). Blank and control experiments show the reaction does not proceed in the absence of catalyst when irradiated or in the absence of light when catalyst is present. $Ir(ppy)_3$ was evaluated as an alternative photocatalyst for this transformation under similar conditions using the lepidine–TFA salt and 2-iodopropane (See section **5.5**). Upon application of this photocatalyst, limited success was observed as an $*Ir^{III}/Ir^{IV}$ pathway may not have a sufficient redox potential to undergo quenching with iodoalkanes. Tertiary amines may be used to access an Ir^{II}/Ir^{III} pathway with a larger redox potential but are not compatible under the described conditions (by-product formation and reduction of alkyl radical intermediates).[28] With use of the binuclear gold(I) photocatalyst, 2-iodopropane was converted to **5.3j** quantitatively (See section **5.5**) and demonstrates that $[Au_2(\mu\text{-dppm})_2]Cl_2$ was the superior choice for the activation of nonactivated haloalkanes in the direct alkylation of heteroarenes.

After the establishment of optimized conditions, a variety of bromoalkanes were screened (**Table 5.1**). Direct alkylation of lepidine–TFA salt **5.2** with 1° bromoalkanes **5.1a**–**e** gave the target compounds **5.3a**–**e** in 32–77% yields. Using 2° and 3° bromoalkanes, the substituted lepidine compounds **5.3f**–**o** were obtained in good to excellent yields. Remarkably, the addition of 1-bromoadamantane **5.1m** proceeded in 98% yield of **5.3m**. The robustness of the direct alkylation reaction was further demonstrated in the gram scale preparation of **5.3g** in 90% yield.

Table 5.1 Bromoalkane scope for the direct alkylation of lepidine.

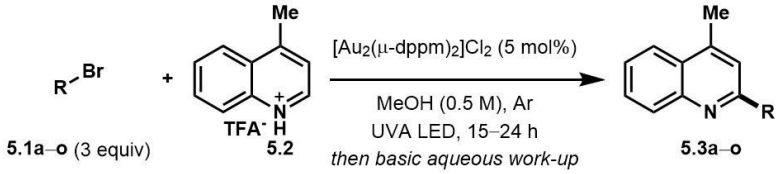

Entry	Substrate	Yield [%]	Entry	Substrate	Yield [%]	Entry	Substrate	Yield [%]
1	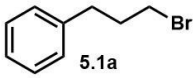 5.1a	77	6	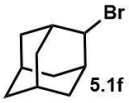 5.1f	90	11	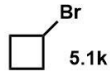 5.1k	41
2	 5.1b	73	7	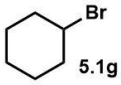 5.1g	93, 90[a]	12	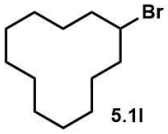 5.1l	25
3	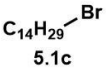 5.1c	32	8	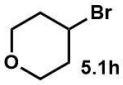 5.1h	97	13	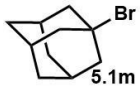 5.1m	98
4	 5.1d	45	9	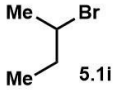 5.1i	93	14	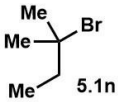 5.1n	33
5	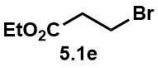 5.1e	56	10	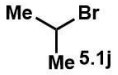 5.1j	64	15	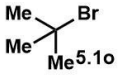 5.1o	40

[a] 1 gram scale of lepidine–TFA salt, 4 equiv. CyBr, 4 UVA LEDs, 48 h.

We then focused our efforts upon investigating ring opening and ring forming reactions characteristic of radicals (**Table 5.2**). As expected of a free radical addition, the (bromomethyl)cyclopropane **5.1p** proceeded with a radical ring opening before heteroarene addition, giving **5.3p** in 64% yield. (Bromomethyl)cyclobutane **5.1q** remained mostly unopened (87:13, 74%). 4-Bromopentene **5.1s** remained completely uncyclized while bromoalkenes **5.1r** and **5.1t** produced primary alkyl radicals that underwent *5-exo-trig* cyclization before heteroarene addition. As the chain length grew to 6- and 7-carbon spacing, **5.1u** and **5.1v**, the ratio of cyclized to uncyclized product diminished, 20:80 and 0:100 respectively. Each of these additions proceeded in 54–71% yields. Bromoalkanes thus proved to have broad generality in the C–H alkylation of lepidine.

Table 5.2 Ring-opening and cyclization reactions in the alkylation of lepidine.

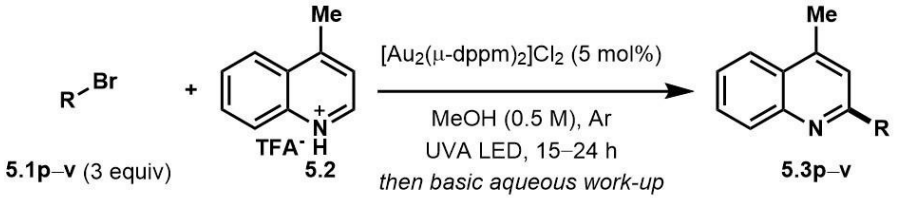

5.1p–v (3 equiv) **5.2** **5.3p–v**

Entry	Substrate	Product	Yield [%]
1	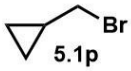 **5.1p**	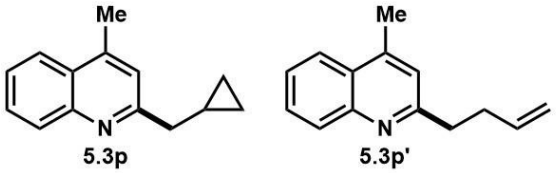 **5.3p** **5.3p'**	64 **5.3p:5.3p'** 0:100
2	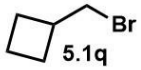 **5.1q**	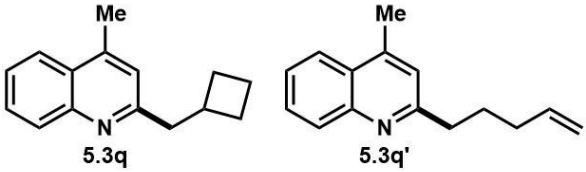 **5.3q** **5.3q'**	74 **5.3q:5.3q'** 87:13
3	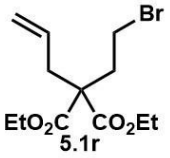 **5.1r**	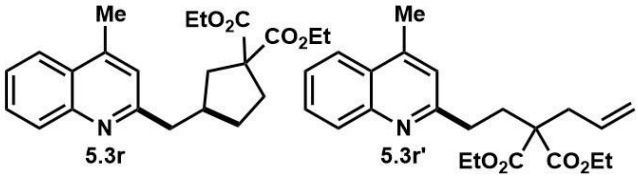 **5.3r** **5.3r'**	71 **5.3r:5.3r'** 93:7
4	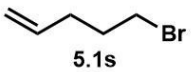 **5.1s**	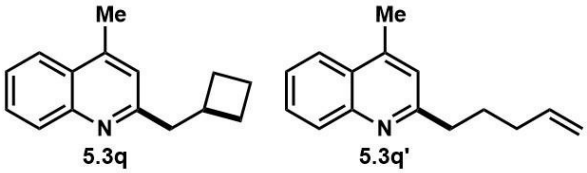 **5.3q** **5.3q'**	54 **5.3q:5.3q'** 0:100
5	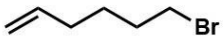 **5.1t**	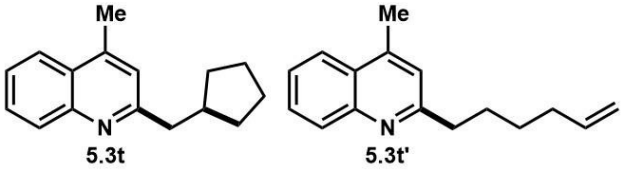 **5.3t** **5.3t'**	58 **5.3t:5.3t'** 90:10
6	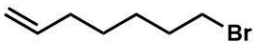 **5.1u**	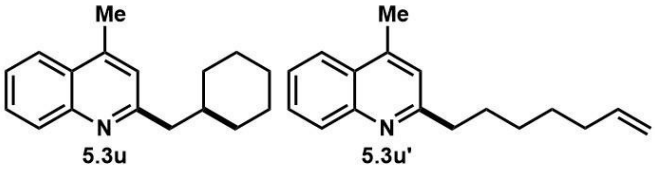 **5.3u** **5.3u'**	62 **5.3u:5.3u'** 20:80
7	 **5.1v**	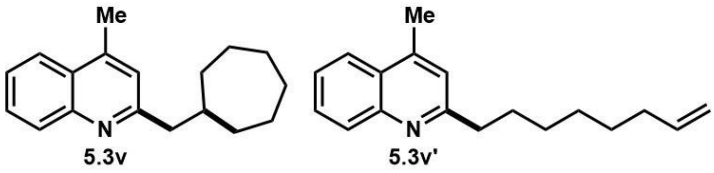 **5.3v** **5.3v'**	56 **5.3u:5.3u'** 0:100

The product distribution obtained from the addition of bromoalkane **5.1q** to lepidine was utilized to determine the absolute rate constant of 1° radical addition to lepidine (**5.2**;

Figure 5.2). In this experiment, the ratios between C–H functionalization products that remained unopened *vs* those that ring opened were measured under increasing concentrations of lepidine. The results show that the absolute rate constant of addition of primary alkyl radicals to lepidine is 8.0 ± 1.3×10^4 $M^{-1}s^{-1}$ and is indicative of a free radical addition process comparable in rate to other known clocking studies used in heteroarene functionalization.[29] This method could offer an alternative to photochemical radical clocking experiments using the pyridine-2-thione-*N*-oxycarbonyl (PTOC)–thiol method. The present method represents a significant improvement, since fewer synthetic steps are needed for substrate construction than PTOC esters. Furthermore, this new method produces clean results, whereas PTOC esters form many by-products.[30]

As outlined in **Table 5.3**, we evaluated the generality of the heterocyclic coupling partners **5a**–**l** under the optimized reaction conditions. Alkylation of quinaldine with bromocyclohexane **5.1g** and 1-bromo-3-phenylpropane **5.1a** afforded the corresponding products in a high level of efficiency; **5.5a** and **b** in 86% and 84% yields, respectively. The scope of the reaction was further extended to 7-chloroquinaldine (**5.5c**, 99%), isoquinoline (**5.5d**, 66%), 2,4-lutidine (**5.5e**, 60%), 2,6-lutidine (**5.5f**, 66%), and 2,6-diphenylpyridine (**5.5g**, 98%). 3-Methylbenzoxazole underwent smooth addition (**5.5h**, 98%) with bromocyclohexane under basic condition (K_2HPO_4). These conditions were extended to methyl indole-3-carboxylate (**5.5i**, 76%), benzoxazole (**5.5l**, 55%), and benzothiazole (**5.5m**, 90%). Under standard conditions, bromocyclohexane also coupled well with *N*-methylbenzimidazole (**5.5j**, 80%) and benzimidazole (**5.5k**, 75%). Alkylation of caffeine

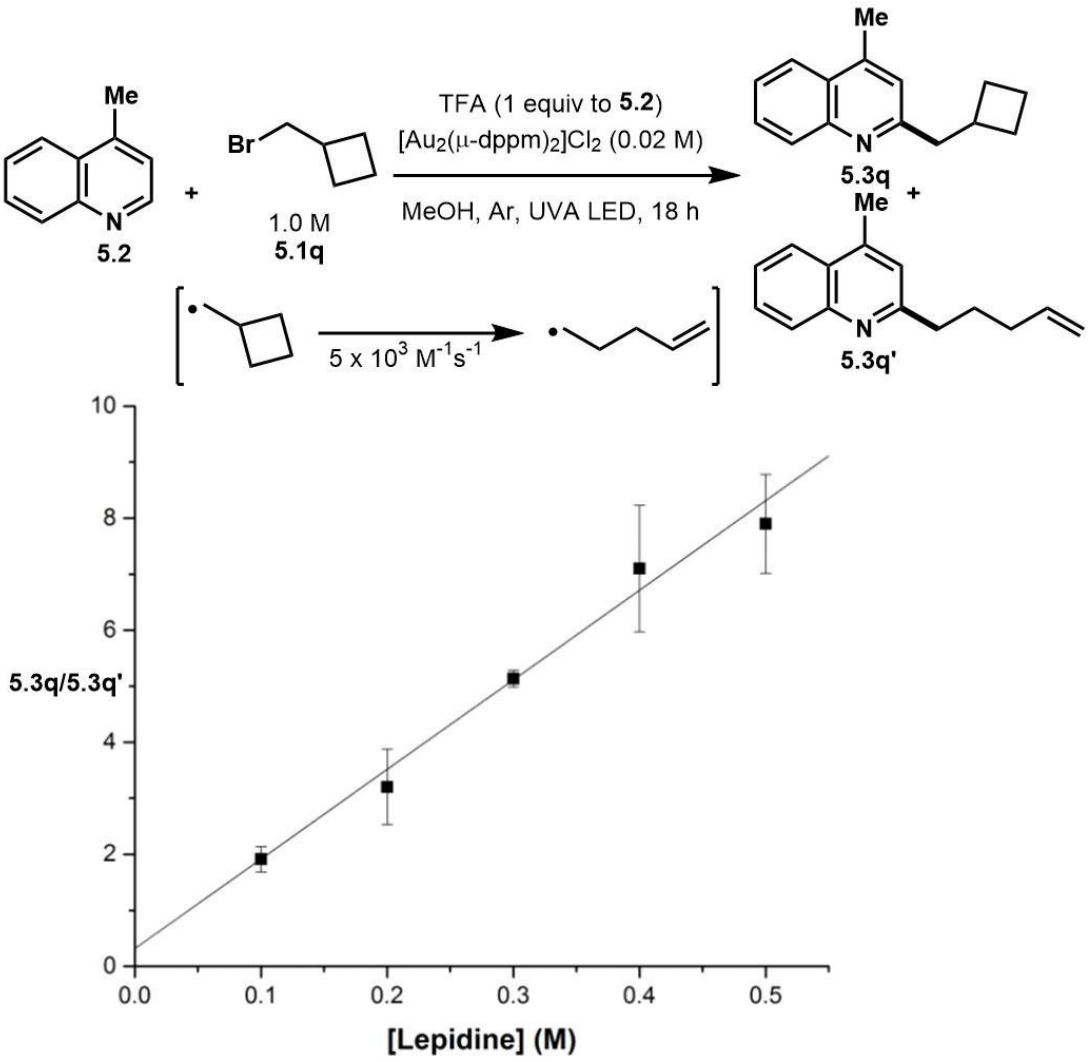

Figure 5.2 Kinetic study of the absolute rate of alkyl radical addition to lepidine, ratio of unopened to opened methylcyclobutane addition *vs* [lepidine] (M).

with 1-bromoadamantane **5.1m** and bromocyclohexane **5.1g** gave C–H functionalized products in excellent yields, **5.5n** and **o** in 95% and 92% yield, respectively. Thus, a wide variety of heterocycles were shown to undergo high yielding C–H functionalization reactions with bromoalkanes, demonstrating the potential for late-stage functionalization of scaffolds found in nature and drug design.

Table 5.3 Heteroarene scope in the alkylation reaction using bromoalkanes.

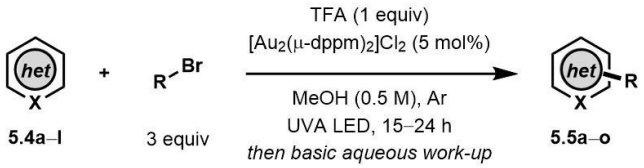

5.4a–l **5.5a–o**

Entry	Product	Yield [%]	Entry	Product	Yield [%]	Entry	Product	Yield [%]
1 2	**5.5a** R = Cy **5.5b** R = $Ph(CH_2)_3$	86 84	6	**5.5f**	66	10 11	**5.5j** R = Me **5.5k** R = H	80 75
3	**5.5c**	99	7	**5.5g**	98	12	**5.5l**	55[a]
4	**5.5d**	66	8	**5.5h**	98[a]	13	**5.5m**	90[a,b]
5	**5.5e**	60	9	**5.5i**	76[a]	14 15	**5.5n** R = Ad **5.5o** R = Cy	95 92

[a]1.2 equiv. K_2HPO_4 instead of TFA. [b]0.6 mmol scale.

Next, we turned our attention to the generation of electrophilic radicals from activated α-bromoesters and their application to complex motif construction (**Table 5.4**). Harnessing the electrophilicity of radicals generated from α-bromoester **5.1w**, it was reasoned that a polarity reversal radical addition strategy as introduced by Minisci would allow this idea to be realized.[31] Addition of an electrophilic radical to electron deficient heteroarenes is not feasible on an electronic basis and was verified experimentally. Upon addition of an acceptor alkene, the electrophilic radical becomes relatively nucleophilic; gaining access to the C–H functionalization chemistry developed thus far (**Figure 5.3**). Controlling the chemoselectivity of 3-component reactions is notoriously difficult, especially when considering radical transformations. Using only ethyl bromoacetate with

Table 5.4 Polarity reversal radical addition of electrophilic bromoalkanes and alkenes to heteroarenes.

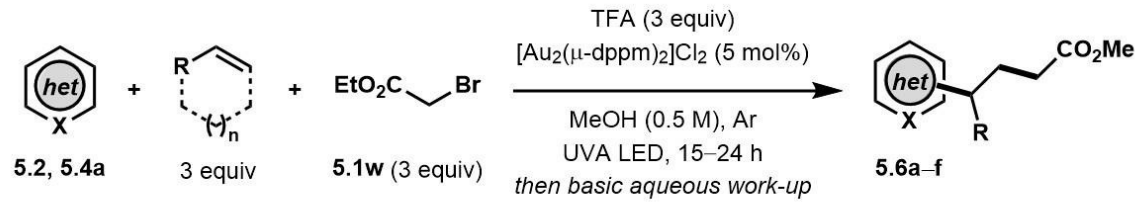

Entry	Heteroarene	Alkene	Product	Yield [%]
1	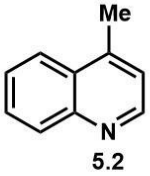 5.2	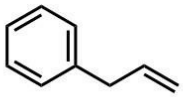	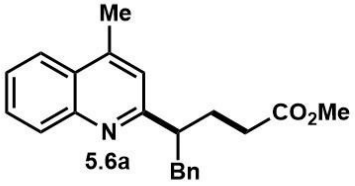 5.6a	93
2	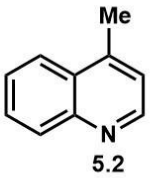 5.2	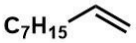	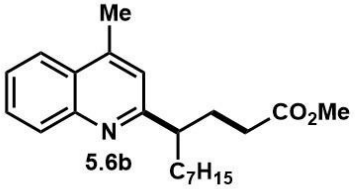 5.6b	75
3	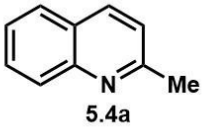 5.4a	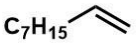	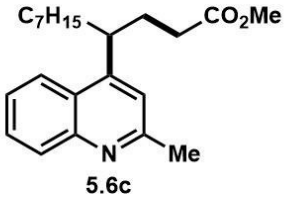 5.6c	97
4	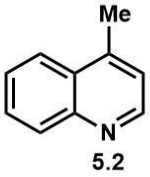 5.2		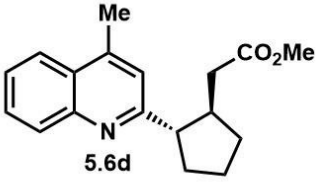 5.6d	86[a]
5	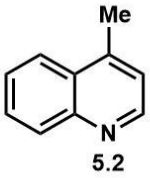 5.2		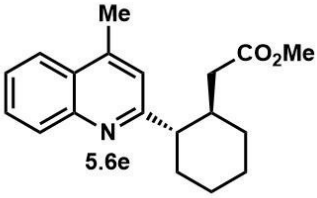 5.6e	62[a]
6	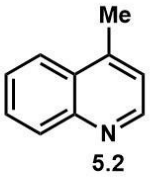 5.2		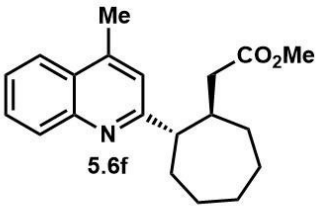 5.6f	70[a]

[a]d.r. > 20:1

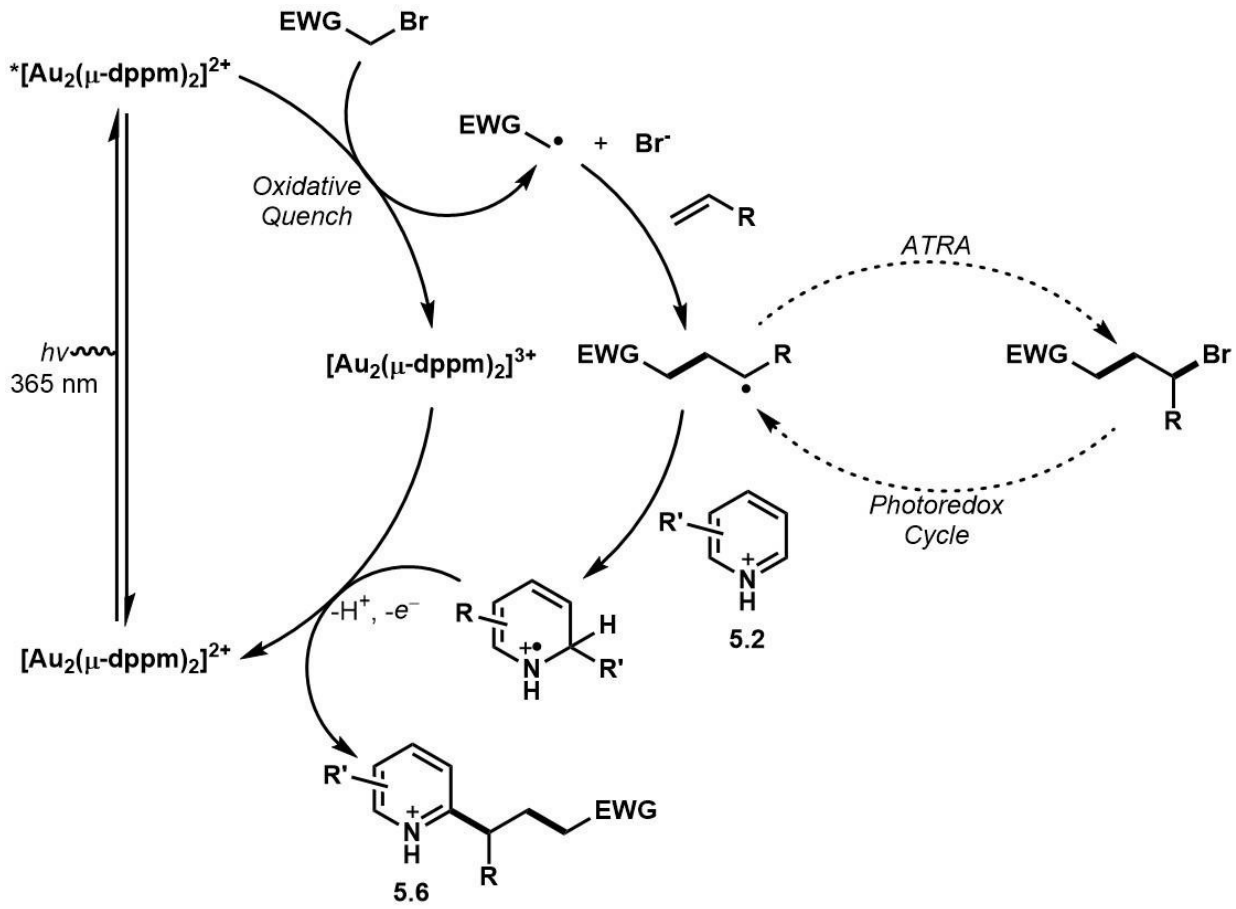

Figure 5.3 Proposed mechanism for the polarity reversal radical addition of electrophilic radicals to alkenes and heteroarenes.

lepidine or quinaldine furnished no functionalized products. With added alkenes, lepidine underwent smooth C–H alkylation. Allylbenzene, 1-nonene, cyclopentene, cyclohexene, and cycloheptene gave addition products in 62–93% yields (**5.6a**, **b**, and **d**–**f**). Addition of 1-nonene with quinaldine provided the three-component adduct **5.6c** in 97% yield. ATRA are known to be efficient chain processes with activated C–Br bonds.[32] UVA irradiation in the absence of the binuclear Au(I) photocatalyst did not produce the desired product. A small amount of product resulting from an ATRA pathway was observed (<10%).

Finally, an intramolecular example of a modified bromonucleoside **5.7** was amenable to addition under the described conditions, forming a surrogate version of a DNA lesion (**5.8**, 33% or 47% brsm.; **Scheme 5.2**). One can imagine the application of

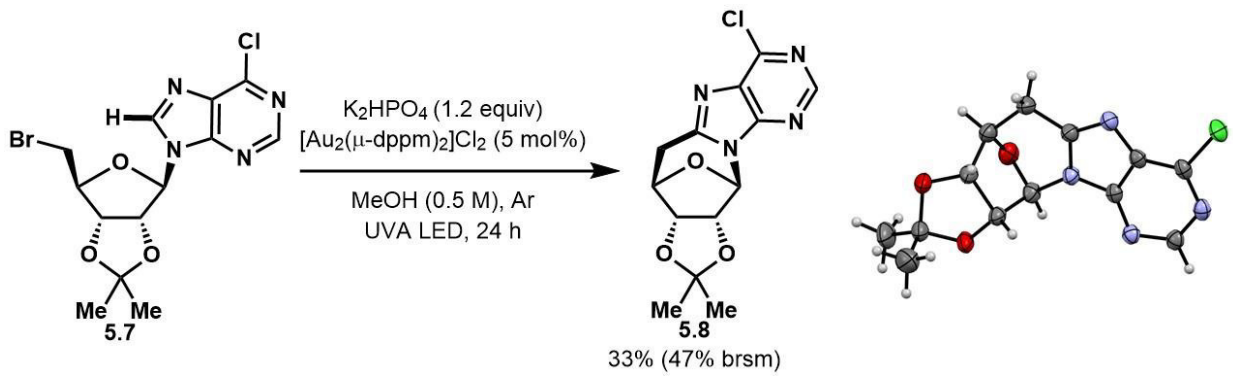

Scheme 5.2 Synthesis of a modified DNA lesion.

such a compound in the evaluation of its pharmacological properties in future studies. The successful cyclization of this sensitive and richly functionalized precursor is a testament to the mildness of these newly developed reaction conditions.

5.4 Conclusions

In summary, a protocol for direct C–H alkylation of heteroarenes was achieved using photoredox catalysis as a strategy for activation of nonactivated bromoalkanes. Binuclear Au(I) complex, $[Au_2(\mu\text{-dppm})_2]Cl_2$, served as an efficient photocatalyst for this transformation. The reaction showed robust generality in relation to the bromoalkanes and heteroarenes that were coupled in this operationally facile process. Since the publication of this work, many other studies have appeared to this topic, several of which that are also redox-neutral transformations.[33] Alkyl radical polarity was also shown to play a vital role in coupling to electron deficient heteroaromatics, exemplified by polarity reversal radical addition reactions. Further studies for the development of this process in the late-stage functionalization of medicinally important molecules are underway.

5.5 Further Information

Table 5.5 Optimization of the alkylation of heteroarenes from bromoalkanes.

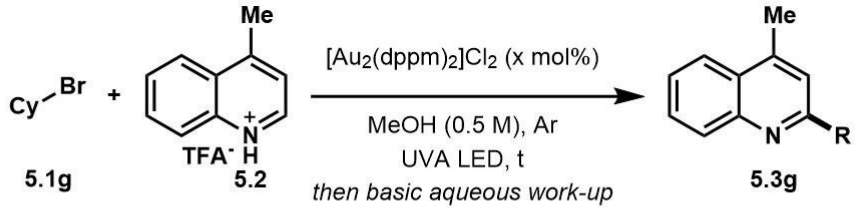

Entry	Photocatalyst [mol%]	RX [equiv]	t [h]	Yield [%][a]
1	2	3	13	79
2	2	3	26	99
3	2	1	48	60
4	5	3	13	64
5	1	3	13	99(93)
6	---	3	13	<5
7	5	3	13	0[b]
8	5	3	6.5	71
9	5	3	18	99[c]
10	5	3	18	21[d]
11	5	2	18	78
12	5	1	18	46
13	5	3	24	99[e]
14	5	4	48	99(90)[f]

[a]Optimization conducted on 0.2 mmol scale of heteroaromatic salt following GP1. NMR conversion (isolated yield). [b]Not irradiated with light and heated to 80°C. [c]Lepidine used instead of TFA salt. [d]Lepidine with 1.2 equiv K_2HPO_4. [e]1.0 mmol scale. [f]1.0 g scale of **5.2**, 4 X UVA LEDs.

Table 5.6 Comparison of photoredox catalysts and haloalkanes.

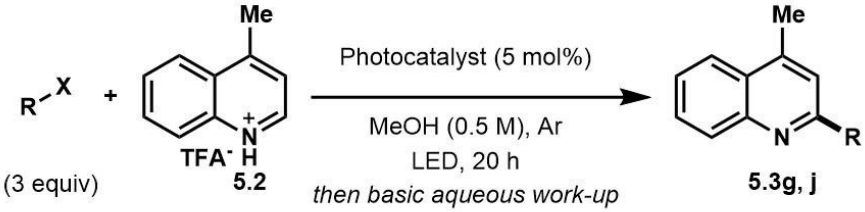

Entry	Photocatalyst	RX	K_2HPO_4 [equiv]	LED [nm]	Yield [%][a]
1	$[Au_2(dppm)_2]Cl_2$	CyBr	---	365	99(93)
2	$Ir(ppy)_3$	CyBr	2.0	410	---
3	$Ir(ppy)_3$	*i*PrI	---	410	---
4	$[Ir(ppy)_2(dtbbpy)]PF_6$	*i*PrI	2.0	410	---
5	$[Au_2(dppm)_2]Cl_2$	*i*PrI	---	365	99
6	---	*i*PrI	2.0	410	---
7	---	*i*PrI	---	365	---

[a]Experiments conducted on 0.2 mmol scale of **5.2** following GP1. For reactions containing K_2HPO_4, lepidine was used instead of the TFA salt. NMR conversion (isolated yield).

5.6 Experimental Procedures

General Procedure 1 (GP1) – *Alkylation of Heteroarenes*

To an 8 mL Pyrex screw-top reaction vessel was added the TFA salt of heterocycle (0.2–0.3 mmol, 1.0 equiv, isolated by adding 1.0 equiv of TFA to heterocycle in DCM and concentrating), then bromoalkane (0.6–0.9 mmol, 3.0 equiv), $[Au_2(\mu\text{-dppm})_2]Cl_2$ (0.010–0.015 mmol, 0.05 equiv) and MeOH (0.4–0.6 mL, 0.5 M). If heterocycle was added without being a TFA salt, TFA was added last (0.2–0.3 mmol, 1.0 equiv). *In certain cases, reaction was run under basic condition by adding K_2HPO_4 (0.24–0.36 mmol, 1.2 equiv) instead of TFA. The reaction mixture was degassed with argon by sparging and irradiated with a UVA LED at a distance of 1 cm for 15–24 h. The resulting mixture was concentrated, dissolved in DCM and poured into a separatory funnel under basic aqueous work-up (saturated sodium bicarbonate or 1 M sodium hydroxide), extracted 3 times with DCM, where the organic fractions were combined, dried over sodium sulfate, and concentrated *in vacuo*. Crude product was further purified by flash chromatography, where relevant fractions were combined, concentrated and characterized by proton and carbon NMR (400 and 101 MHz, respectively), HRMS, and IR.

General Procedure 2 (GP2) – *Polarity Reversal Radical Addition*

To an 8 mL Pyrex screw-top reaction vessel was added the heterocycle (0.2–0.3 mmol, 1.0 equiv), MeOH (0.4–0.6 mL, 0.5 M), TFA (0.6–0.9 mmol, 3.0 equiv), $[Au_2(\mu\text{-dppm})_2]Cl_2$ (0.010–0.015 mmol, 0.05 equiv), then alkene (0.6–0.9 mmol, 3.0 equiv) and ethyl bromoacetate (0.6–0.9 mmol, 3.0 equiv). The reaction mixture was degassed with argon by sparging and irradiated with a UVA LED at a distance of 1 cm for 15–24 h. *Alkenes with low boiling points (e.g. cyclohexene) were added after sparging the mixture. The

resulting mixture was concentrated, dissolved in DCM and poured into a separatory funnel under basic aqueous work-up (saturated sodium bicarbonate), extracted 3 times with DCM, where the organic fractions were combined, dried over sodium sulfate, and concentrated. Crude product was further purified by flash chromatography, where relevant fractions were combined, concentrated and characterized by proton and carbon NMR (400 and 101 MHz, respectively), HRMS, and IR.

General Procedure 3 (GP3) – *Kinetic Study*

Reactions were prepared from stock solutions of lepidine (1.0 M), TFA (2.0 M), $[Au_2(\mu\text{-dppm})_2]Cl_2$ (0.2 M) in MeOH and (bromomethyl)cyclobutane (neat). In a given run, 5 samples were prepared using the stock solutions of lepidine (100–500 µL, 0.1–0.5 M), TFA (50–250 µL, 0.1–0.5 M), $[Au_2(\mu\text{-dppm})_2]Cl_2$ (100 µL, 0.02 M each), and reactions were degassed lightly with argon for 5 minutes. (Bromomethyl)cyclobutane (113 µL, 1.0 M each) was then added and each solution was added the remaining MeOH to make a 1 mL total volume (637µL, 487 µL, 337 µL, 187 µL, 37 µL, respectively). The reactions were then irradiated for 18 h with a UVA LED. The resulting mixtures were then subjected to the work-up portion of GP1 because the crude products remained protonated after irradiation, however, the ^{1}H NMR after irradiation showed the same ratio of products as the ^{1}H NMR of material that had been worked up (also having the same ratio after flash chromatography). The worked-up products could then be analyzed by ^{1}H NMR reliably for product ratios (GC studies were not reliable for this experiment at present). Reactions ranged from 40% to complete conversion.

5.7 Characterization Data

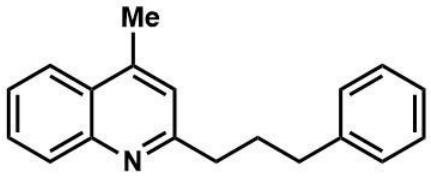

4-methyl-2-(3-phenylpropyl)quinoline (5.3a)

Synthesized according to GP1.

IR (neat, cm^{-1}): 2925(m), 2857(m), 1603(s), 1449(s), 758(vs), 700(s); **^{1}H NMR** (400 MHz, $CDCl_3$): δ = 8.07 (d, *J* = 8.3 Hz, 1H), 7.96 (d, *J* = 8.3 Hz, 1H), 7.69 (ddd, *J* = 8.2, 6.7, 1.2 Hz, 1H), 7.52 (ddd, *J* = 8.0, 6.7, 1.0 Hz, 1H), 7.33–7.27 (m, 2H), 7.26–7.17 (m, 3H), 7.14 (s, 1H), 2.99 (t, *J* = 7.7 Hz, 2H), 2.76 (t, *J* = 7.7 Hz, 2H), 2.68 (s, 3H), 2.17 (quin, *J* = 7.9 Hz, 2H) ppm; **^{13}C NMR** (101 MHz, $CDCl_3$): δ = 162.1 (C), 147.7 (C), 144.2 (C), 142.1 (C), 129.3 (CH), 129.0 (CH), 128.5 (2×CH), 128.3 (2×CH), 126.8 (C), 125.7 (CH), 125.4 (CH), 123.6 (CH), 122.0 (CH), 38.7 (CH_2), 35.7 (CH_2), 31.6 (CH_2), 18.6 (CH_3) ppm; **HRMS** (EI): m/z calc'd for $C_{19}H_{19}N$ [M^+] 261.1517, found 261.1515.

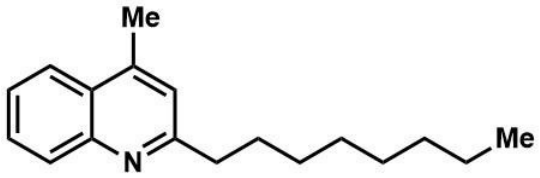

4-methyl-2-octylquinoline (5.3b)

Synthesized according to GP1.

IR (neat, cm^{-1}): 2922(vs), 2853(m), 1603(s), 1449(m), 756(vs); **^{1}H NMR** (400 MHz, $CDCl_3$): δ = 8.05 (d, *J* = 8.4 Hz, 1H), 7.95 (dd, *J* = 8.2, 0.8 Hz, 1H), 7.67 (ddd, *J* = 8.4, 6.9, 1.3 Hz, 1H), 7.50 (ddd, *J* = 8.2, 7.0, 1.2 Hz, 1H), 7.14 (s, 1H), 2.94–2.90 (m, 2H), 2.68 (d, *J* = 0.6 Hz, 3H), 1.80 (quin, *J* = 7.7 Hz, 2H), 1.42 (quin, *J* = 7.7 Hz, 2H), 1.38–1.25 (m, 8H), 0.88 (t, *J* = 7.0 Hz, 3H) ppm; **^{13}C NMR** (101 MHz, $CDCl_3$): δ = 162.8 (C), 147.7 (C), 144.1 (C), 129.3 (CH), 128.9 (CH), 126.7 (C), 125.3 (CH), 123.5 (CH), 122.0 (CH), 39.3 (CH_2), 31.8 (CH_2), 30.1 (CH_2), 29.6 (CH_2), 29.5 (CH_2), 29.2 (CH_2), 22.6 (CH_2), 18.6 (CH_3), 14.1 (CH_3) ppm; **HRMS** (EI): m/z calc'd for $C_{18}H_{25}N$ [M^+] 255.1987, found 255.1966.

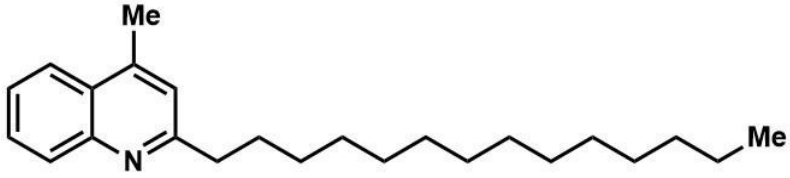

4-methyl-2-tetradecylquinoline (5.3c)

Synthesized according to GP1.

IR (neat, cm^{-1}): 2922(s), 2852(s) 1604(m), 1449(m), 756(s); **^{1}H NMR** (400 MHz, $CDCl_3$): δ = 8.06 (d, *J* = 8.2 Hz, 1H), 7.96 (dd, *J* = 8.2, 0.9 Hz, 1H), 7.68 (ddd, *J* = 8.4, 6.9, 1.4 Hz, 1H), 7.51 (ddd, *J* = 8.2, 7.0, 1.2 Hz, 1H), 7.15 (s, 1H), 2.93 (t, *J* = 7.9 Hz, 2H), 2.69 (d, *J* = 0.8 Hz, 3H), 1.80 (quin, *J* = 7.7 Hz, 2H), 1.42 (quin, *J* = 7.7 Hz, 2H), 1.34–1.20 (m, 20H), 0.89 (t, *J* = 6.7 Hz, 3H) ppm; **^{13}C NMR** (101 MHz, $CDCl_3$): δ = 162.8 (C), 147.7 (C), 144.1 (C), 129.3 (CH), 129.0 (CH), 126.8 (C), 125.4 (CH), 123.6 (CH), 122.1 (CH), 39.3 (CH_2), 31.9 (CH_2), 30.1 (CH_2), 29.7 (2×CH_2), 29.6 (4×CH_2), 29.5 (2×CH_2), 29.3 (CH_2), 22.7 (CH_2), 18.7 (CH_3), 14.1 (CH_3) ppm; **HRMS** (EI): m/z calc'd for $C_{24}H_{37}N$ [M^+] 339.2926, found 339.2931.

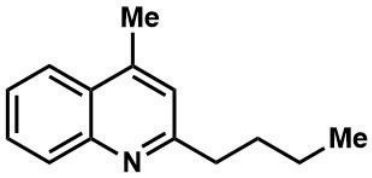

2-butyl-4-methylquinoline (5.3d)

Synthesized according to GP1 and characterized according to NMR comparison.[34]

^{1}H NMR (400 MHz, $CDCl_3$): δ = 8.06 (d, *J* = 8.3 Hz, 1H), 7.96 (dd, *J* = 8.3, 1.1 Hz, 1H), 7.68 (ddd, *J* = 8.4, 6.9, 1.4 Hz, 1H), 7.51 (ddd, *J* = 8.2, 7.0, 1.2 Hz, 1H), 7.16 (s, 1H), 2.98–2.89 (m, 2H), 2.69 (d, *J* = 0.7 Hz, 3H), 1.85–1.75 (m, 2H), 1.46 (sxt, *J* = 7.4 Hz, 2H), 0.97 (t, *J* = 7.3 Hz, 3H) ppm; **^{13}C NMR** (101 MHz, $CDCl_3$): δ = 162.7 (C), 147.6 (C), 144.1 (C), 129.2 (CH), 129.1 (CH), 126.8 (C), 125.4 (CH), 123.6 (CH), 122.1 (CH), 38.9 (CH_2), 32.2 (CH_2), 22.7 (CH_2), 18.7 (CH_3), 14.0 (CH_3) ppm.

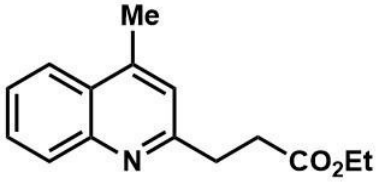

ethyl 3-(4-methylquinolin-2-yl)propanoate (5.3e)

Synthesized according to GP1 and characterized according to NMR comparison.[14]

^{1}H NMR (400 MHz, $CDCl_3$): δ = 8.02 (d, *J* = 8.4 Hz, 1H), 7.96 (dd, *J* = 8.3, 1.0 Hz, 1H), 7.68 (ddd, *J* = 8.4, 6.9, 1.4 Hz, 1H), 7.51 (ddd, *J* = 8.3, 7.0, 1.2 Hz, 1H), 7.18 (s, 1H), 4.15 (q, *J* = 7.2 Hz, 2H), 3.26 (t, *J* = 7.5 Hz, 2H), 2.91 (t, *J* = 7.5 Hz, 2H), 2.68 (d, *J* = 0.9 Hz, 3H), 1.25 (t, *J* = 7.1 Hz, 3H) ppm; **^{13}C NMR** (101 MHz, $CDCl_3$): δ = 173.2 (C), 160.2 (C), 147.6 (C), 144.4 (C), 129.4 (CH), 129.1 (CH), 126.9 (C), 125.6 (CH), 123.6 (CH), 122.2 (CH), 60.4 (CH_2), 33.4 (CH_2), 33.3 (CH_2), 18.6 (CH_3), 14.2 (CH_3) ppm.

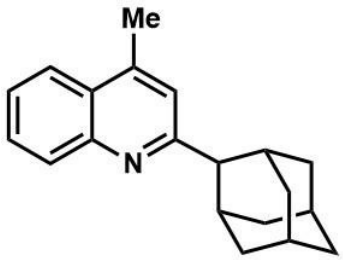

2-((1R,3S,5r,7r)-adamantan-2-yl)-4-methylquinoline (5.3f)

Synthesized according to GP1.

IR (neat, cm^{-1}): 2902(s), 2848(m), 1602(m), 1449(m), 755(m); **^{1}H NMR** (400 MHz, $CDCl_3$): δ = 8.07 (d, *J* = 8.4 Hz, 1H), 7.96 (d, *J* = 8.1 Hz, 1H), 7.67 (t, *J* = 7.4 Hz, 1H), 7.50 (t, *J* = 7.5 Hz, 1H), 7.29 (s, 1H), 3.25–3.16 (m, 1H), 2.83–2.75 (m, 2H), 2.74–2.65 (m, 3H), 2.10–1.93 (m, 7H), 1.82 (s, 3H), 1.63 (d, *J* = 12.2 Hz, 2H) ppm; **^{13}C NMR** (101 MHz, $CDCl_3$): δ = 164.1 (C), 147.7 (C), 143.3 (C), 129.8 (CH), 128.6 (CH), 126.4 (C), 125.3 (CH), 123.4 (CH), 120.5 (CH), 50.4 (CH), 39.1 (2×CH_2), 37.9 (CH_2), 32.6 (2×CH_2), 30.9 (2×CH), 28.0 (CH), 27.9 (CH), 18.9 (CH_3) ppm; **HRMS** (EI): m/z calc'd for $C_{20}H_{23}N$ [M^+] 277.1830, found 277.1841.

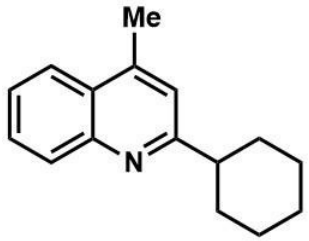

2-cyclohexyl-4-methylquinoline (5.3g)

Synthesized according to GP1 and characterized according to NMR comparison.[16]

^{1}H NMR (400 MHz, $CDCl_3$): δ = 8.05 (d, *J* = 8.3 Hz, 1H), 7.95 (dd, *J* = 8.3, 1.0 Hz, 1H), 7.67 (ddd, *J* = 8.4, 6.9, 1.4 Hz, 1H), 7.50 (ddd, *J* = 8.3, 6.9, 1.2 Hz, 1H), 7.18 (s, 1H), 2.88 (tt, *J* = 12.0, 3.3 Hz, 1H), 2.69 (d, *J* = 0.8 Hz, 3H), 2.05–1.99 (m, 2H), 1.90 (dt, *J* = 12.9, 3.1 Hz, 2H), 1.83–1.77 (m, 1H), 1.63 (qd, *J* = 12.5, 2.9 Hz, 2H), 1.48 (qt, *J* = 12.7, 3.1 Hz, 2H), 1.36 (tt, *J* = 12.5, 3.2 Hz, 1H) ppm; **^{13}C NMR** (101 MHz, $CDCl_3$): δ = 166.5 (C), 147.6 (C), 144.3 (C), 129.4 (CH), 129.0 (CH), 127.0 (C), 125.4 (CH), 123.5 (CH), 120.2 (CH), 47.6 (CH), 32.8 (2×CH_2), 26.6 (2×CH_2), 26.1 (CH_2), 18.8 (CH_3) ppm.

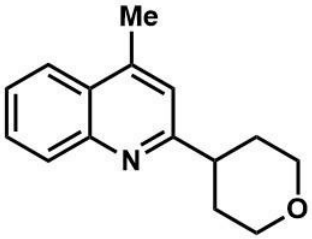

4-methyl-2-(tetrahydro-2H-pyran-4-yl)quinoline (5.3h)

Synthesized according to GP1 and characterized according to NMR comparison.[16]

^{1}H NMR (400 MHz, $CDCl_3$): δ = 8.05 (d, *J* = 8.3 Hz, 1H), 7.96 (dd, *J* = 8.4, 0.8 Hz, 1H), 7.69 (ddd, *J* = 8.3, 7.0, 1.3 Hz, 1H), 7.52 (ddd, *J* = 8.2, 7.6, 1.1 Hz, 1H), 7.18 (s, 1H), 4.14 (dd, *J* = 11.2, 4.3 Hz, 2H), 3.60 (td, *J* = 11.7, 2.2 Hz, 2H), 3.13 (tt, *J* = 11.8, 4.0 Hz, 1H), 2.70 (s, 3H), 2.03 (qd, *J* = 12.7, 4.5 Hz, 2H), 1.95–1.89 (m, 2H) ppm; **^{13}C NMR** (101 MHz, $CDCl_3$): δ = 164.2 (C), 147.6 (C), 144.6 (C), 129.5 (CH), 129.1 (CH), 127.1 (C), 125.6 (CH), 123.6 (CH), 119.9 (CH), 68.1 (2×CH_2), 44.4 (CH), 32.3 (2×CH_2), 18.8 (CH_3) ppm.

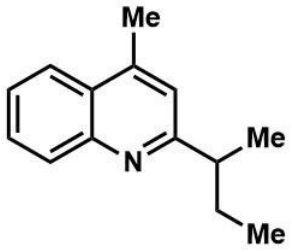

2-(sec-butyl)-4-methylquinoline (5.3i)

Synthesized according to GP1 and characterized according to NMR comparison.[16]

^{1}H NMR (400 MHz, $CDCl_3$): δ = 8.07 (d, *J* = 8.4 Hz, 1H), 7.95 (dd, *J* = 8.2, 0.9 Hz, 1H), 7.67 (ddd, *J* = 8.4, 7.0, 1.3 Hz, 1H), 7.50 (ddd, *J* = 8.2, 7.0, 1.2 Hz, 1H), 7.14 (s, 1H), 2.97 (sxt, *J* = 7.1 Hz, 1H), 2.69 (d, *J* = 0.7 Hz, 3H), 1.86 (dquin, *J* = 13.9, 7.2 Hz, 1H), 1.72 (dquin, *J* = 13.9, 7.2 Hz, 1H), 1.37 (d, *J* = 7.0 Hz, 3H), 0.91 (t, *J* = 7.4 Hz, 3H) ppm; **^{13}C NMR** (101 MHz, $CDCl_3$): δ = 166.7 (C), 147.6 (C), 144.1 (C), 129.5 (CH), 128.8 (CH), 127.0 (C), 125.3 (CH), 123.5 (CH), 120.1 (CH), 44.5 (CH), 29.9 (CH_2), 20.4 (CH_3), 18.8 (CH_3), 12.2 (CH_3) ppm.

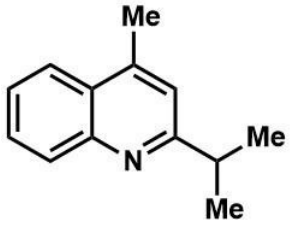

2-isopropyl-4-methylquinoline (5.3j)

Synthesized according to GP1 and characterized according to NMR comparison.[16]

^{1}H NMR (400 MHz, $CDCl_3$): δ = 8.06 (dd, *J* = 8.5, 0.7 Hz, 1H), 7.95 (dd, *J* = 8.3, 0.9 Hz, 1H), 7.67 (ddd, *J* = 8.4, 6.9, 1.4 Hz, 1H), 7.50 (ddd, *J* = 8.3, 6.9, 1.3 Hz, 1H), 7.18 (d, *J* = 0.8 Hz, 1H), 3.23 (spt, *J* = 7.0 Hz, 1H), 2.69 (d, *J* = 0.9 Hz, 3H), 1.40 (d, *J* = 7.0 Hz, 6H) ppm; **^{13}C NMR** (101 MHz, $CDCl_3$): δ = 167.3 (C), 147.5 (C), 144.3 (C), 129.5 (CH), 128.9 (CH), 127.0 (C), 125.4 (CH), 123.5 (CH), 119.7 (CH), 37.2 (CH), 22.5 (2×CH_3), 18.8 (CH_3) ppm.

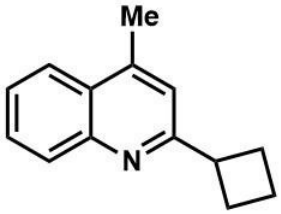

2-cyclobutyl-4-methylquinoline (5.3k)

Synthesized according to GP1 and characterized according to NMR comparison.[16]

^{1}H NMR (400 MHz, $CDCl_3$): δ = 8.07 (d, *J* = 8.4 Hz, 1H), 7.95 (dd, *J* = 8.2, 0.7 Hz, 1H), 7.68 (ddd, *J* = 8.2, 6.9, 1.3 Hz, 1H), 7.50 (ddd, *J* = 8.1, 7.0, 1.1 Hz, 1H), 7.21 (s, 1H), 3.84 (quin, *J* = 8.7 Hz, 1H), 2.70 (s, 3H), 2.50–2.42 (m, 4H), 2.19–2.07 (m, 1H), 2.00–1.91 (m, 1H) ppm; **^{13}C NMR** (101 MHz, $CDCl_3$): δ = 164.7 (C), 147.5 (C), 144.1 (C), 129.5 (CH), 128.9 (CH), 126.9 (C), 125.4 (CH), 123.5 (CH), 120.2 (CH), 42.6 (CH), 28.2 (2×CH_2), 18.8 (CH_3), 18.3 (CH_2) ppm.

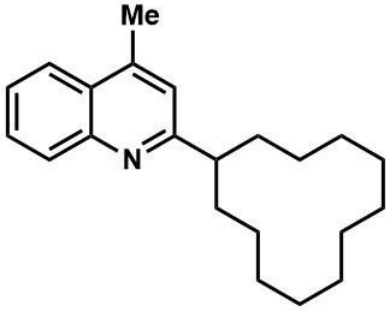

2-cyclododecyl-4-methylquinoline (5.3l)

Synthesized according to GP1.

IR (neat, cm^{-1}): 2929(vs), 2861(m), 1603(m), 1445(m), 757(s); **^{1}H NMR** (400 MHz, $CDCl_3$): δ = 8.23 (m, 1H), 7.97 (d, *J* = 8.2 Hz, 1H), 7.71 (t, *J* = 7.6 Hz, 1H), 7.54 (t, *J* = 7.3 Hz, 1H), 7.19 (s, 1H), 3.23 (s, 1H), 2.72 (s, 3H), 2.01–1.88 (m, 2H), 1.74 (td, *J* = 12.8, 5.7 Hz, 2H), 1.65–1.32 (m, 18H) ppm; **^{13}C NMR** (101 MHz, $CDCl_3$): δ = 166.4 (C), 148.0 (C), 143.2 (C), 129.5 (CH), 128.8 (CH), 126.9 (C), 125.8 (CH), 123.6 (CH), 121.3 (CH), 42.6 (CH), 30.1 (2×CH_2), 23.9 (2×CH_2), 23.8 (2×CH_2), 23.7 (2×CH_2), 23.4 (CH_2), 22.8 (2×CH_2), 19.0 (CH_3) ppm; **HRMS** (EI): m/z calc'd for $C_{22}H_{31}N$ [M^+] 309.2457, found 309.2444.

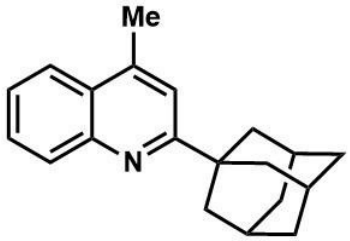

2-((1s,3s)-adamantan-1-yl)-4-methylquinoline (5.3m)

Synthesized according to GP1 and characterized according to NMR comparison.[20d]

^{1}H NMR (400 MHz, $CDCl_3$): δ = 8.07 (d, *J* = 8.4 Hz, 1H), 7.95 (dd, *J* = 8.3, 1.0 Hz, 1H), 7.66 (ddd, *J* = 8.4, 6.9, 1.4 Hz, 1H), 7.49 (ddd, *J* = 8.2, 6.9, 1.2 Hz, 1H), 7.34 (s, 1H), 2.70 (d, *J* = 0.8 Hz, 3H), 2.16 (s, 3H), 2.13 (d, *J* = 2.3 Hz, 6H), 1.84 (t, *J* = 2.8 Hz, 6H) ppm; **^{13}C NMR** (101 MHz, $CDCl_3$): δ = 168.7 (C), 147.5 (C), 143.5 (C), 130.0 (CH), 128.6 (CH), 126.7 (C), 125.3 (CH), 123.4 (CH), 118.5 (CH), 41.8 (3×CH_2), 39.5 (C), 36.9 (3×CH_2), 28.8 (3×CH), 19.0 (CH_3) ppm.

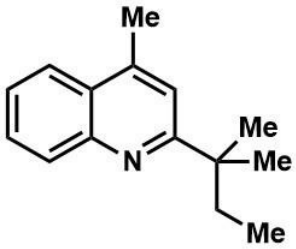

4-methyl-2-(tert-pentyl)quinoline (5.3n)

Synthesized according to GP1.

IR (neat, cm^{-1}): 2964(s), 2924(m), 1602(m), 1448(m), 757(vs); **^{1}H NMR** (400 MHz, $CDCl_3$): δ = 8.07 (d, *J* = 8.3 Hz, 1H), 7.95 (dd, *J* = 8.2, 1.0 Hz, 1H), 7.67 (ddd, *J* = 7.6, 1.3 Hz, 1H), 7.53–7.47 (m, 1H), 7.31 (s, 1H), 2.70 (d, *J* = 0.6 Hz, 3H), 1.86 (q, *J* = 7.4 Hz, 2H), 1.44 (s, 6H), 0.75 (t, *J* = 7.4 Hz, 3H) ppm; **^{13}C NMR** (101 MHz, $CDCl_3$): δ = 168.0 (C), 147.4 (C), 143.3 (C), 130.0 (CH), 128.6 (CH), 126.5 (C), 125.3 (CH), 123.4 (CH), 119.4 (CH), 41.2 (C), 35.8 (CH_2), 27.3 (2×CH_3), 19.0 (CH_3), 9.2 (CH_3) ppm; **HRMS** (EI): m/z calc'd for $C_{15}H_{19}N$ [M^+] 213.1517, found 213.1520.

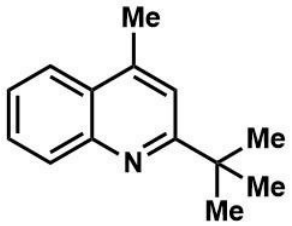

2-(tert-butyl)-4-methylquinoline (5.3o)

Synthesized according to GP1 and characterized according to NMR comparison.[34]

^{1}H NMR (400 MHz, $CDCl_3$): δ = 8.06 (d, *J* = 8.3 Hz, 1H), 7.95 (dd, *J* = 8.2, 0.8 Hz, 1H), 7.66 (ddd, *J* = 8.3, 7.0, 1.3 Hz, 1H), 7.50 (ddd, *J* = 8.2, 6.9, 1.2 Hz, 1H), 7.36 (s, 1H), 2.70 (d, *J* = 0.7 Hz, 3H), 1.47 (s, 9H) ppm; **^{13}C NMR** (101 MHz, $CDCl_3$): δ = 168.9 (C), 147.3 (C), 143.6 (C), 130.0 (CH), 128.7 (CH), 126.5 (C), 125.4 (CH), 123.4 (CH), 118.9 (CH), 37.9 (C), 30.1 (3×CH_3), 18.9 (CH_3) ppm.

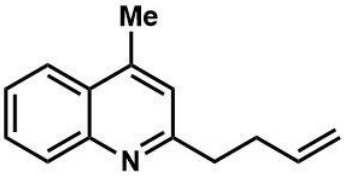

2-(but-3-en-1-yl)-4-methylquinoline (5.3p')

Synthesized according to GP1.

IR (neat, cm^{-1}): 3068(m), 2923(m), 2854(m), 1641(m), 1604(s), 1448(m), 997(m), 913(m), 758(vs); **^{1}H NMR** (400 MHz, $CDCl_3$): δ = 8.05 (d, *J* = 8.4 Hz, 1H), 7.96 (dd, *J* = 8.3, 0.9 Hz, 1H), 7.68 (ddd, *J* = 8.4, 7.0, 1.3 Hz, 1H), 7.51 (ddd, *J* = 8.2, 7.0, 1.1 Hz, 1H), 7.15 (s, 1H), 5.94 (ddt, *J* = 17.0, 10.3, 6.6 Hz, 1H), 5.10 (dq, *J* = 17.0, 1.6 Hz, 1H), 5.00 (dq, *J* = 10.2, 1.6 Hz, 1H), 3.03 (dd, *J* = 9.3, 7.6 Hz, 2H), 2.68 (d, *J* = 0.6 Hz, 3H), 2.63–2.55 (m, 2H) ppm; **^{13}C NMR** (101 MHz, $CDCl_3$): δ = 161.7 (C), 147.7 (C), 144.2 (C), 137.8 (CH), 129.3 (CH), 129.0 (CH), 126.8 (C), 125.5 (CH), 123.6 (CH), 122.1 (CH), 115.1 (CH_2), 38.4 (CH_2), 33.8 (CH_2), 18.7 (CH_3) ppm; **HRMS** (EI): m/z calc'd for $C_{14}H_{15}N$ [M^+] 197.1204, found 197.1190.

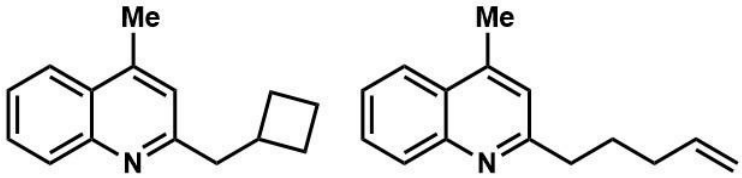

2-(cyclobutylmethyl)-4-methylquinoline (5.3q)/4-methyl-2-(pent-4-en-1-yl)quinoline (5.3q') (87:13)

Synthesized according to GP1.

IR (neat, cm^{-1}): 2933(m), 2857(m), 1603(s), 1447(m), 757(vs);

5.3q: ^{1}H NMR (400 MHz, $CDCl_3$): δ = 8.05 (d, *J* = 8.3 Hz, 1H), 7.95 (d, *J* = 8.3 Hz, 1H), 7.67 (ddd, *J* = 8.3, 7.0, 1.3 Hz, 1H), 7.50 (ddd, *J* = 8.1, 6.9, 1.1 Hz, 1H), 7.09 (s, 1H), 3.03 (d, *J* = 7.6 Hz, 2H), 2.82 (spt, *J* = 7.9 Hz, 1H), 2.67 (s, 3H), 2.13–2.01 (m, 2H), 1.97–1.79 (m, 4H) ppm; **^{13}C NMR** (101 MHz, $CDCl_3$): δ = 161.3 (C), 147.7 (C), 144.0 (C), 129.4 (CH), 128.9 (CH), 126.8 (C), 125.3 (CH), 123.5 (CH), 122.1 (CH), 46.0 (CH_2), 36.2 (CH), 28.3 (2×CH_2), 18.7 (CH_3), 18.5 (CH_2) ppm;

5.3q': ^{1}H NMR (400 MHz, $CDCl_3$): δ = 8.05 (d, *J* = 8.3 Hz, 1H), 7.95 (d, *J* = 8.3 Hz, 1H), 7.67 (ddd, *J* = 8.3, 7.0, 1.3 Hz, 1H), 7.50 (ddd, *J* = 8.1, 6.9, 1.1 Hz, 1H), 7.15 (s, 1H), 5.88 (ddt, *J* = 17.0, 10.3, 6.7 Hz, 1H), 5.13–4.93 (m, 2H), 2.94 (dd, *J* = 7.8, 7.1 Hz, 2H), 2.68 (s, 3H), 2.19 (q, *J* = 7.3 Hz, 2H), 1.97–1.79 (m, 2H) ppm; **^{13}C NMR** (101 MHz, $CDCl_3$): δ = 162.3 (C), 147.7 (C), 144.0 (C), 138.4 (CH), 129.4 (CH), 129.0 (CH), 126.8 (C), 125.4 (CH), 123.5 (CH), 122.1 (CH), 114.8 (CH_2), 38.6 (CH_2), 33.6 (CH_2), 29.2 (CH_2), 18.7 (CH_3) ppm;

HRMS (EI): m/z calc'd for $C_{15}H_{17}N$ [M^+] 211.1361, found 211.1354.

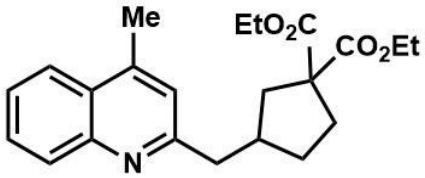

diethyl 3-((4-methylquinolin-2-yl)methyl)cyclopentane-1,1-dicarboxylate (5.3r)

Synthesized according to GP1.

IR (neat, cm^{-1}): 2978(m), 2939(m), 1725(s), 1251(s), 1176(m), 1158(m), 761(m); **^{1}H NMR** (400 MHz, $CDCl_3$): δ = 8.05 (d, *J* = 8.6 Hz, 1H), 7.96 (dd, *J* = 8.3, 0.8 Hz, 1H), 7.69 (t, *J* = 7.3 Hz, 1H), 7.52 (t, *J* = 7.2 Hz, 1H), 7.14 (s, 1H), 4.17 (dq, *J* = 14.0, 7.1 Hz, 4H), 3.00 (d, *J* = 7.2 Hz, 2H), 2.69 (s, 3H), 2.62–2.52 (m, 1H), 2.46 (dd, *J* = 12.9, 6.6 Hz, 1H), 2.35 (ddd, *J* = 13.4, 8.4, 3.8 Hz, 1H), 2.17 (ddd, *J* = 13.6, 9.4, 7.5 Hz, 1H), 1.95 (dd, *J* = 13.4, 9.9 Hz, 1H), 1.90–1.82 (m, 1H), 1.49 (dq, *J* = 12.5, 9.2 Hz, 1H), 1.23 (dt, *J* = 11.3, 7.1 Hz, 6H) ppm; **^{13}C NMR** (101 MHz, $CDCl_3$): δ = 172.6 (C), 172.5 (C), 161.0 (C), 147.4 (C), 144.3 (C), 129.2 (2×CH), 126.8 (C), 125.6 (CH), 123.6 (CH), 122.3 (CH), 61.3 (CH_2), 61.3 (CH_2), 60.0 (C), 44.0 (CH_2), 40.4 (CH_2), 40.2 (CH), 33.7 (CH_2), 32.0 (CH_2), 18.7 (CH_3), 14.0 (CH_3), 14.0 (CH_3) ppm; **HRMS** (EI): m/z calc'd for $C_{22}H_{27}NO_4$ [M^+] 369.1940, found 369.1942.

***5.3r'** too little to fully characterized but ratio could be estimated by allyl peaks and a C–H aryl peak by proton NMR.

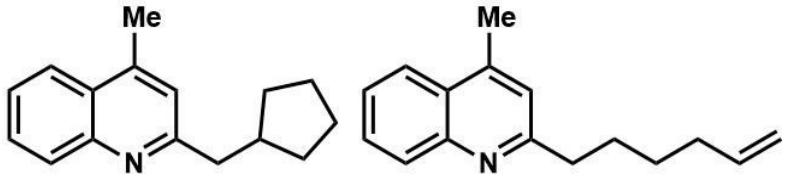

2-(cyclopentylmethyl)-4-methylquinoline (5.t)/2-(hex-5-en-1-yl)-4-methylquinoline (5.3t') (90:10)

Synthesized according to GP1 and characterized according to NMR comparison.[29]

5.3t: ^{1}H NMR (400 MHz, $CDCl_3$): δ = 8.08 (d, *J* = 8.2 Hz, 1H), 7.96 (dd, *J* = 8.3, 0.8 Hz, 1H), 7.68 (ddd, *J* = 8.4, 7.0, 1.4 Hz, 1H), 7.51 (ddd, *J* = 8.3, 7.0, 1.2 Hz, 1H), 7.15 (d, *J* = 0.7 Hz, 1H), 2.95 (d, *J* = 7.5 Hz, 2H), 2.69 (d, *J* = 0.9 Hz, 3H), 2.37 (quin, *J* = 7.8 Hz, 1H), 1.89–1.61 (m, 4H), 1.61–1.47 (m, 2H), 1.36–1.25 (m, 2H) ppm; **^{13}C NMR** (101 MHz, $CDCl_3$): δ = 162.2 (C), 147.4 (C), 144.2 (C), 129.2 (CH), 129.1 (CH), 126.8 (C), 125.4 (CH), 123.6 (CH), 122.4 (CH), 44.9 (CH_2), 40.7 (CH), 32.5 (2×CH_2), 25.0 (2×CH_2), 18.7 (CH_3) ppm.

5.3t': ^{1}H NMR (400 MHz, $CDCl_3$): δ = 8.08 (d, *J* = 8.2 Hz, 1H), 7.96 (dd, *J* = 8.3, 0.8 Hz, 1H), 7.68 (ddd, *J* = 8.4, 7.0, 1.4 Hz, 1H), 7.51 (ddd, *J* = 8.3, 7.0, 1.2 Hz, 1H), 7.10 (s, 1H), 5.82 (ddt, *J* = 17.0, 10.3, 6.7 Hz, 1H), 5.10–4.87 (m, 2H), 2.95 (m, 2H), 2.70 (d, *J* = 0.9 Hz, 3H), 2.18–2.07 (m, 2H), 1.89–1.25 (m, 4H) ppm; **^{13}C NMR** (101 MHz, $CDCl_3$): δ = 162.4 (C), 147.4 (C), 144.2 (C), 138.8 (CH), 129.2 (CH), 129.1 (CH), 126.8 (C), 125.4 (CH), 123.6 (CH), 122.0 (CH), 114.4 (CH_2), 39.0 (CH_2), 33.6 (CH_2), 29.5 (CH_2), 28.8 (CH_2), 18.7 (CH_3) ppm.

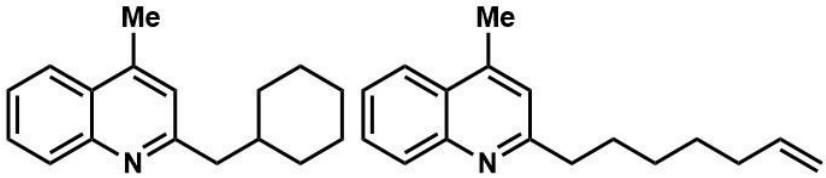

2-(cyclohexylmethyl)-4-methylquinoline (5.3u)/2-(hept-6-en-1-yl)-4-methylquinoline (5.3u') (20:80)

Synthesized according to GP1.

IR (neat, cm^{-1}): 3065(m), 2924(s), 2853(m), 1641(m), 1603(s), 1448(m), 994(m), 910(m), 758(vs);

5.3u: ^{1}H NMR (400 MHz, $CDCl_3$): δ = 8.09 (d, *J* = 8.3 Hz, 1H), 7.96 (d, *J* = 8.3 Hz, 1H), 7.69 (ddd, *J* = 8.3, 7.4, 1.3 Hz, 1H), 7.57–7.48 (m, 1H), 7.13 (s, 1H), 2.84 (d, *J* = 7.3, 2H), 2.70 (s, 3H), 1.76–1.62 (m, 1H), 1.62–1.00 (m, 10H) ppm; **^{13}C NMR** (101 MHz, $CDCl_3$): δ = 161.5 (C), 147.3 (C), 144.6 (C), 129.2 (CH), 129.0 (CH), 126.8 (C), 125.5 (CH), 123.6 (CH), 122.9 (CH), 46.6 (CH_2), 38.9 (CH), 33.3 (2×CH_2), 26.4 (CH_2), 26.2 (2×CH_2), 18.8 (CH_3) ppm;

5.3u': ^{1}H NMR (400 MHz, $CDCl_3$): δ = 8.09 (d, *J* = 8.3 Hz, 1H), 7.96 (d, *J* = 8.3 Hz, 1H), 7.69 (ddd, *J* = 8.3, 7.4, 1.3 Hz, 1H), 7.57–7.48 (m, 1H), 7.16 (s, 1H), 5.82 (ddt, *J* = 17.0, 10.3, 6.7 Hz, 1H), 5.08–4.86 (m, 2H), 2.99–2.88 (m, 2H), 2.70 (s, 3H), 2.12–2.02 (m, 2H), 1.90–1.77 (m, 2H), 1.52–1.38 (m, 4H) ppm; **^{13}C NMR** (101 MHz, $CDCl_3$): δ = 162.5 (C), 147.3 (C), 144.6 (C), 139.0 (CH), 129.2 (CH), 129.0 (CH), 126.8 (C), 125.5 (CH), 123.6 (CH), 122.0 (CH), 114.2 (CH_2), 38.9 (CH_2), 33.6 (CH_2), 29.9 (CH_2), 29.0 (CH_2), 28.8 (CH_2), 18.7 (CH_3) ppm;

HRMS (EI): m/z calc'd for $C_{17}H_{21}N$ [M^+] 239.1674, found 239.1676.

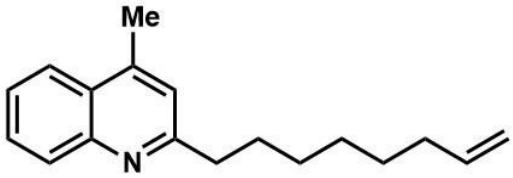

4-methyl-2-(oct-7-en-1-yl)quinoline (5.3v')

Synthesized according to GP1.

IR (neat, cm^{-1}): 3065(m), 2924(s), 2853(m), 1640(m), 1603(s), 1448(m), 994(m), 908(m), 756(vs); **^{1}H NMR** (400 MHz, $CDCl_3$): δ = 8.08 (d, *J* = 8.4 Hz, 1H), 7.96 (d, *J* = 8.3 Hz, 1H), 7.73–7.61 (m, 1H), 7.58–7.45 (m, 1H), 7.15 (s, 1H), 5.81 (ddt, *J* = 17.0, 10.2, 6.7 Hz, 1H), 5.11–4.87 (m, 2H), 3.02–2.86 (m, 2H), 2.69 (s, 3H), 2.05 (q, *J* = 6.7 Hz, 2H), 1.81 (quin, *J* = 7.5 Hz, 2H), 1.40 (m, 6H) ppm; **^{13}C NMR** (101 MHz, $CDCl_3$): δ = 162.6 (C), 147.4 (C), 144.4 (C), 139.1 (CH), 129.1 (2×CH), 126.7 (C), 125.5 (CH), 123.6 (CH), 122.0 (CH), 114.2 (CH_2), 39.1 (CH_2), 33.7 (CH_2), 30.0 (CH_2), 29.4 (CH_2), 29.0 (CH_2), 28.8 (CH_2), 18.7 (CH_3) ppm; **HRMS** (EI): m/z calc'd for $C_{18}H_{23}N$ [M^+] 253.1830, found 253.1797.

4-cyclohexyl-2-methylquinoline (5.5a)

Synthesized according to GP1 and characterized according to NMR comparison.[17a]

^{1}H NMR (400 MHz, $CDCl_3$): δ = 8.05 (t, *J* = 7.7 Hz, 2H), 7.73–7.58 (m, 1H), 7.56–7.42 (m, 1H), 7.18 (s, 1H), 3.33–3.27 (m, 1H), 2.73 (s, 3H), 2.08–1.80 (m, 5H), 1.62–1.44 (m, 4H), 1.37–1.32 (m, 1H) ppm; **^{13}C NMR** (101 MHz, $CDCl_3$): δ = 158.7 (C), 153.5 (C), 147.9 (C), 129.3 (CH), 128.8 (CH), 125.3 (CH), 125.1 (C), 122.8 (CH), 118.3 (CH), 38.8 (CH), 33.5 (2×CH_2), 26.9 (2×CH_2), 26.3 (CH_2), 25.4 (CH_3) ppm.

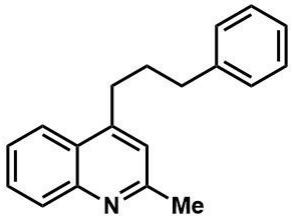

2-methyl-4-(3-phenylpropyl)quinoline (5.5b)

Synthesized according to GP1.

IR (neat, cm^{-1}): 2936(m), 2860(m), 1602(vs), 1454(m), 763(s), 700(s); **^{1}H NMR** (400 MHz, $CDCl_3$): δ = 8.05 (d, *J* = 8.3 Hz, 1H), 7.90 (d, *J* = 8.3 Hz, 1H), 7.66 (t, *J* = 7.6 Hz, 1H), 7.50–7.45 (m, 1H), 7.34–7.31 (m, 2H), 7.24–7.22 (m, 3H), 7.13 (s, 1H), 3.13–2.99 (m, 2H), 2.77 (t, *J* = 7.6 Hz, 2H), 2.72 (s, 3H), 2.10 (quin, *J* = 7.7 Hz, 2H) ppm; **^{13}C NMR** (101 MHz, $CDCl_3$): δ = 158.5 (C), 148.0 (C), 148.0 (C), 141.5 (C), 129.3 (CH), 128.9 (CH), 128.4 (2×CH), 128.4 (2×CH), 125.9 (CH), 125.7 (C), 125.3 (CH), 123.2 (CH), 121.5 (CH), 35.7 (CH_2), 31.4 (2×CH_2), 25.2 (CH_3) ppm; **HRMS** (EI): m/z calc'd for $C_{16}H_{18}ClN$ [M^+] 261.1517, found 261.1551.

7-chloro-4-cyclohexyl-2-methylquinoline (5.5c)

Synthesized according to GP1.

IR (neat, cm^{-1}): 2924(s), 2851(m), 1599(vs), 1447(m), 820 (vs), 769(s); **^{1}H NMR** (400 MHz, $CDCl_3$): δ = 8.02 (d, *J* = 2.3 Hz, 1H), 7.96 (d, *J* = 9.0 Hz, 1H), 7.44 (dd, *J* = 9.0, 2.2 Hz, 1H), 7.16 (s, 1H), 3.32–3.09 (m, 1H), 2.71 (s, 3H), 2.01–1.84 (m, 5H), 1.60–1.48 (m, 4H), 1.41–1.31 (m, 1H) ppm; **^{13}C NMR** (101 MHz, $CDCl_3$): δ = 160.1 (C), 153.3 (C), 148.7 (C), 134.6 (C), 128.5 (CH), 126.1 (CH), 124.3 (CH), 123.6 (C), 118.5 (CH), 38.9 (CH), 33.5 (2×CH_2), 26.9 (2×CH_2), 26.2 (CH_2), 25.5 (CH_3) ppm; **HRMS** (EI): m/z calc'd for $C_{16}H_{18}ClN$ [M^+] 259.1128, found 259.1101.

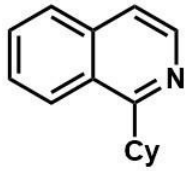

1-cyclohexylisoquinoline (5.5d)

Synthesized according to GP1 and characterized according to NMR comparison.[17a]

^{1}H NMR (400 MHz, $CDCl_3$): δ = 8.49 (d, *J* = 5.7 Hz, 1H), 8.23 (d, *J* = 8.4 Hz, 1H), 7.81 (d, *J* = 8.0 Hz, 1H), 7.65 (ddd, *J* = 8.0, 6.9, 1.2 Hz, 1H), 7.59 (ddd, *J* = 8.3, 7.0, 1.5 Hz, 1H), 7.48 (d, *J* = 5.7 Hz, 1H), 3.57 (tt, *J* = 11.6, 3.2 Hz, 1H), 2.05–1.91 (m, 4H), 1.88–1.76 (m, 3H), 1.55 (qt, *J* = 12.7, 3.1 Hz, 2H), 1.42 (tt, *J* = 12.6, 3.3 Hz, 1H) ppm; **^{13}C NMR** (101 MHz, $CDCl_3$): δ = 165.7 (C), 141.9 (CH), 136.4 (C), 129.5 (CH), 127.5 (CH), 126.8 (CH), 126.3 (C), 124.7 (CH), 118.8 (CH), 41.5 (CH), 32.6 (2×CH_2), 26.9 (2×CH_2), 26.2 (CH_2) ppm.

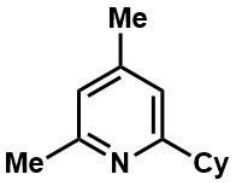

2-cyclohexyl-4,6-dimethylpyridine (5.5e)

Synthesized according to GP1.

IR (neat, cm^{-1}): 2923(vs), 2851(s), 1607(s), 1571(m), 1449(m), 843(s); **^{1}H NMR** (400 MHz, $CDCl_3$): δ = 6.79 (d, *J* = 3.4 Hz, 2H), 2.65 (tt, *J* = 11.6, 3.3 Hz, 1H), 2.49 (s, 3H), 2.28 (s, 3H), 2.00–1.92 (m, 2H), 1.88–1.81 (m, 2H), 1.78–1.72 (m, 1H), 1.48–1.38 (m, 4H), 1.33–1.28 (m, 1H) ppm; **^{13}C NMR** (101 MHz, $CDCl_3$): δ = 165.9 (C), 157.1 (C), 147.4 (C), 121.6 (CH), 118.3 (CH), 46.6 (CH), 33.2 (2×CH_2), 26.6 (2×CH_2), 26.1 (CH_2), 24.4 (CH_3), 21.0 (CH_3) ppm; **HRMS** (EI): m/z calc'd for $C_{13}H_{19}N$ [M^+] 189.1517, found 189.1523.

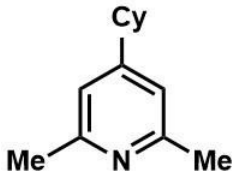

4-cyclohexyl-2,6-dimethylpyridine (5.5f)

Synthesized according to GP1.

IR (neat, cm^{-1}): 2924(vs), 2852(s), 1605(vs), 1565(s), 1448(m), 850(s); **^{1}H NMR** (400 MHz, $CDCl_3$): δ = 6.80 (s, 2H), 2.50 (s, 6H), 2.46–2.36 (m, 1H), 1.85–1.74 (m, 5H), 1.42–1.24 (m, 5H) ppm; **^{13}C NMR** (101 MHz, $CDCl_3$): δ = 157.4 (2×C), 157.2 (C), 118.9 (2×CH), 43.8 (CH), 33.5 (2×CH_2), 26.6 (2×CH_2), 26.0 (CH_2), 24.4 (2×CH_3) ppm; **HRMS** (EI): m/z calc'd for $C_{13}H_{19}N$ [M^+] 189.1517, found 189.1534.

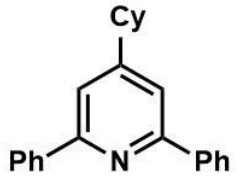

4-cyclohexyl-2,6-diphenylpyridine (5.5g)

Synthesized according to GP1 and characterized according to NMR comparison.[35]

^{1}H NMR (400 MHz, $CDCl_3$): δ = 8.22–8.12 (m, 4H), 7.55 (s, 2H), 7.53–7.47 (m, 4H), 7.46–7.40 (m, 2H), 2.66 (tt, *J* = 11.7, 3.3 Hz, 1H), 2.04–1.88 (m, 4H), 1.85–1.79 (m, 1H), 1.62–1.26 (m, 5H and grease) ppm; **^{13}C NMR** (101 MHz, $CDCl_3$): δ = 158.0 (C), 156.9 (C), 139.9 (C), 128.7 (CH), 128.6 (2×CH), 127.0 (2×CH), 117.6 (CH), 44.4 (CH), 33.7 (2×CH_2), 26.6 (2×CH_2), 26.0 (CH_2) ppm.

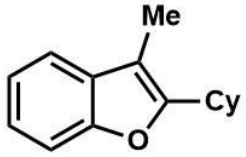

2-cyclohexyl-3-methylbenzofuran (5.5h)

Synthesized according to GP1.

IR (neat, cm^{-1}): 2925(s), 2853(m), 1453(s), 743(vs); **^{1}H NMR** (400 MHz, $CDCl_3$): δ = 7.46–7.41 (m, 1H), 7.41–7.36 (m, 1H), 7.24–7.16 (m, 2H), 2.82 (tt, *J* = 11.8, 3.5 Hz, 1H), 2.19 (s, 3H), 1.91–1.82 (m, 4H), 1.80–1.69 (m, 3H), 1.48–1.33 (m, 3H) ppm; **^{13}C NMR** (101 MHz, $CDCl_3$): δ = 158.1 (C), 153.6 (C), 130.6 (C), 122.8 (CH), 121.8 (CH), 118.6 (CH), 110.5 (CH), 107.7 (C), 36.3 (CH), 31.3 (2×CH_2), 26.5 (2×CH_2), 25.9 (CH_2), 7.8 (CH_3) ppm; **HRMS** (EI): m/z calc'd for $C_{15}H_{18}O$ [M^+] 214.1358, found 214.1346.

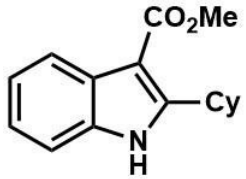

methyl 2-cyclohexyl-1H-indole-3-carboxylate (5.5i)

Synthesized according to GP1.

IR (neat, cm^{-1}): 3311 (br), 2925(s), 2851(m), 1664 (vs), 1449(vs), 1196(vs), 1081(s), 793 (m), 744(s); **^{1}H NMR** (400 MHz, $CDCl_3$): δ = 8.58 (br. s., 1H), 8.16–8.07 (m, 1H), 7.39–7.32 (m, 1H), 7.26–7.18 (m, 2H), 3.95 (s, 3H), 3.81 (tt, *J* = 11.8, 3.1 Hz, 1H), 2.14–2.04 (m, 2H), 1.93–1.77 (m, 3H), 1.58–1.39 (m, 4H), 1.33–1.22 (m, 1H) ppm; **^{13}C NMR** (101 MHz, $CDCl_3$): δ = 166.4 (C), 153.0 (C), 134.4 (C), 127.0 (C), 122.3 (CH), 121.7 (CH), 121.5 (CH), 110.7 (CH), 102.8 (C), 50.7 (CH_3), 36.3 (CH), 32.4 (2×CH_2), 26.4 (2×CH_2), 26.1 (CH_2) ppm; **HRMS** (EI): m/z calc'd for $C_{16}H_{19}NO_2$ [M^+] 257.1416, found 257.1650.

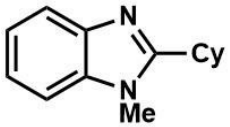

2-cyclohexyl-1-methyl-1H-benzo[d]imidazole (5.5j)

Synthesized according to GP1 and characterized according to NMR comparison.[17c]

^{1}H NMR (400 MHz, $CDCl_3$): δ = 7.81–7.69 (m, 1H), 7.33–7.28 (m, 1H), 7.25–7.19 (m, 2H), 3.75 (s, 3H), 2.86 (tt, *J* = 11.7, 3.3 Hz, 1H), 2.05–1.89 (m, 4H), 1.88–1.75 (m, 3H), 1.50–1.34 (m, 3H) ppm; **^{13}C NMR** (101 MHz, $CDCl_3$): δ = 159.0 (C), 142.5 (C), 135.6 (C), 121.9 (CH), 121.7 (CH), 119.3 (CH), 108.8 (CH), 36.3 (CH), 31.4 (2×CH_2), 29.5 (CH_3), 26.3 (2×CH_2), 25.8 (CH_2) ppm.

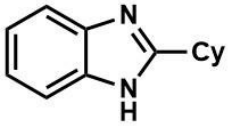

2-cyclohexyl-1H-benzo[d]imidazole (5.5k)

Synthesized according to GP1 and characterized according to NMR comparison.[36]

^{1}H NMR (400 MHz, DMSO-d_6): δ = 12.09 (s, 1H), 7.50–7.40 (m, 2H), 7.10 (s, 2H), 2.83 (t, *J* = 11.3 Hz, 1H), 2.01 (d, *J* = 12.3 Hz, 2H), 1.81–1.56 (m, 5H), 1.46–1.21 (m, 3H) ppm; **^{13}C NMR** (101 MHz, DMSO-d_6): δ = 158.9 (C), 143.1 (C), 134.2 (C), 121.3 (CH), 120.7 (CH), 118.2 (CH), 110.7 (CH), 37.7 (CH), 31.2 (2×CH_2), 25.6 (CH_2), 25.5 (2×CH_2) ppm.

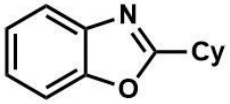

2-cyclohexylbenzo[d]oxazole (5.5l)

Synthesized according to GP1 and characterized according to NMR comparison.[20g]

^{1}H NMR (400 MHz, $CDCl_3$): δ = 7.74–7.66 (m, 1H), 7.52–7.45 (m, 1H), 7.34–7.28 (m, 2H), 2.97 (tt, *J* = 11.4, 3.7 Hz, 1H), 2.22–2.15 (m, 2H), 1.88 (dt, *J* = 12.9, 3.3 Hz, 2H and grease), 1.80–1.66 (m, 2H and grease), 1.51–1.36 (m, 4H) ppm; **^{13}C NMR** (101 MHz, $CDCl_3$): δ = 170.4 (C), 150.6 (C), 141.3 (C), 124.3 (CH), 124.0 (CH), 119.6 (CH), 110.3 (CH), 37.9 (CH), 30.5 (2×CH_2), 25.8 (CH_2), 25.6 (2×CH_2) ppm.

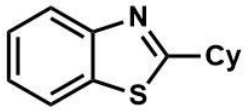

2-cyclohexylbenzo[d]thiazole (5.5m)

Synthesized according to GP1 and characterized according to NMR comparison.[37]

^{1}H NMR (400 MHz, $CDCl_3$): δ = 8.01–7.95 (m, 1H), 7.88–7.83 (m, 1H), 7.48–7.42 (m, 1H), 7.37–7.31 (m, 1H), 3.12 (tt, *J* = 11.7, 3.6 Hz, 1H), 2.25–2.19 (m, 2H), 1.90 (dt, *J* = 13.1, 3.3 Hz, 2H), 1.81–1.75 (m, 1H), 1.71–1.60 (m, 2H), 1.46 (qt, *J* = 12.6, 3.2 Hz, 2H), 1.35 (tt, *J* = 12.3, 3.2 Hz, 1 H) ppm; **^{13}C NMR** (101 MHz, $CDCl_3$): δ = 177.6 (C), 153.1 (C), 134.5 (C), 125.8 (CH), 124.5 (CH), 122.5 (CH), 121.5 (CH), 43.4 (CH), 33.4 (2×CH_2), 26.1 (2×CH_2), 25.8 (CH_2) ppm.

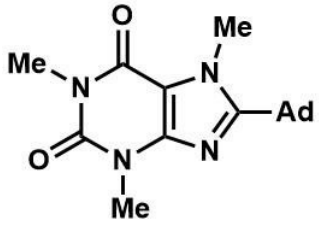

8-((3r,5r,7r)-adamantan-1-yl)-1,3,7-trimethyl-3,7-dihydro-1H-purine-2,6-dione (5.5n)

Synthesized according to GP1 and characterized according to NMR comparison.[20g]

^{1}H NMR (400 MHz, $CDCl_3$): δ = 4.17 (s, 3H), 3.57 (s, 3H), 3.40 (s, 3H), 2.20–2.09 (m, 9H), 1.88–1.75 (m, 6H) ppm; **^{13}C NMR** (101 MHz, $CDCl_3$): δ = 159.5 (C), 155.7 (C), 151.8 (C), 147.1 (C), 108.1 (C), 39.8 (3×CH_2), 36.8 (C), 36.4 (3×CH_2), 34.4 (CH_3), 29.6 (CH_3), 28.2 (3×CH), 27.9 (CH_3) ppm.

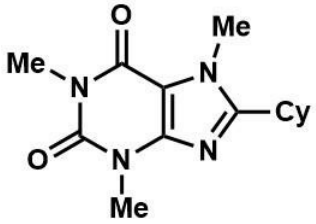

8-cyclohexyl-1,3,7-trimethyl-3,7-dihydro-1H-purine-2,6-dione (5.5o)

Synthesized according to GP1 and characterized according to NMR comparison.[20g]

^{1}H NMR (400 MHz, $CDCl_3$): δ = 3.93 (s, 3H), 3.57 (s, 3H), 3.40 (s, 3H), 2.71 (tt, *J* = 11.7, 3.4 Hz, 1H), 1.93–1.83 (m, 4H), 1.79–1.63 (m, 3H), 1.45–1.31 (m, 3H) ppm; **^{13}C NMR** (101 MHz, $CDCl_3$): δ = 158.0 (C), 155.5 (C), 151.8 (C), 148.1 (C), 107.0 (C), 35.8 (CH), 31.4 (CH_3), 30.9 (2×CH_2), 29.7 (CH_3), 27.8 (CH_3), 26.0 (2×CH_2), 25.5 (CH_2) ppm.

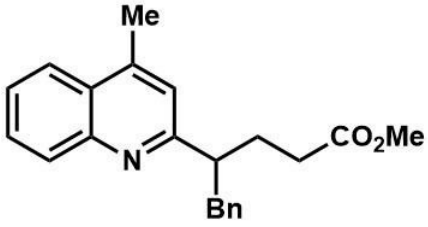

methyl 4-(4-methylquinolin-2-yl)-5-phenylpentanoate (5.6a)

Synthesized according to GP2.

IR (neat, cm^{-1}): 2982(s), 2953(m), 1737(vs), 1602(m), 1451(m), 1159(s), 759(m), 702(m); **^{1}H NMR** (400 MHz, $CDCl_3$): δ **=** 8.08 (d, *J* = 8.4 Hz, 1H), 7.95 (dd, *J* = 8.3, 0.9 Hz, 1H), 7.69 (ddd, *J* = 8.4, 6.9, 1.4 Hz, 1H), 7.52 (ddd, *J* = 8.2, 7.0, 1.3 Hz, 1H), 7.24–7.19 (m, 2H), 7.17–7.11 (m, 3H), 7.02 (s, 1H), 3.56 (s, 3H), 3.28–3.17 (m, 2H), 3.05–2.95 (m, 1H), 2.65 (d, *J* = 0.7 Hz, 3H), 2.26–2.08 (m, 4H) ppm; **^{13}C NMR** (101 MHz, $CDCl_3$): δ = 173.9 (C), 163.4 (C), 147.8 (C), 144.2 (C), 140.1 (C), 129.7 (CH), 129.2 (2×CH), 128.9 (CH), 128.2 (2×CH), 127.1 (C), 125.9 (CH), 125.6 (CH), 123.6 (CH), 121.7 (CH), 51.4 (CH_3), 49.5 (CH), 41.8 (CH_2), 32.1 (CH_2), 29.4 (CH_2), 18.7 (CH_3) ppm; **HRMS** (EI): m/z calc'd for $C_{22}H_{23}NO_2$ [M^+] 333.1729, found 333.1769.

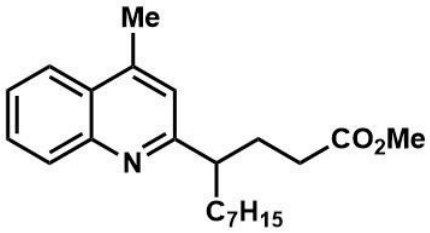

methyl 4-(4-methylquinolin-2-yl)undecanoate (5.6b)

Synthesized according to GP2.

IR (neat, cm^{-1}): 2926(s), 2855(m), 1736(vs), 1603(m), 1450(m), 1163(m), 760(m); **^{1}H NMR** (400 MHz, $CDCl_3$): δ = 8.06 (d, *J* = 8.4 Hz, 1H), 7.95 (d, *J* = 8.3 Hz, 1H), 7.67 (td, *J* = 7.6, 1.2 Hz, 1H), 7.55–7.47 (m, 1H), 7.11 (s, 1H), 3.59 (s, 3H), 2.97–2.83 (m, 1H), 2.69 (s, 3H), 2.33–2.21 (m, 1H), 2.20–2.07 (m, 3H), 1.86–1.67 (m, 2H), 1.30–1.16 (m, 10H), 0.84 (t, *J* = 6.9 Hz, 3H) ppm; **^{13}C NMR** (101 MHz, $CDCl_3$): δ = 174.1 (C), 164.5 (C), 147.6 (C), 144.3 (C), 129.6 (CH), 128.9 (CH), 127.1 (C), 125.5 (CH), 123.5 (CH), 120.8 (CH), 51.4 (CH_3), 48.0 (CH), 35.6 (CH_2), 32.2 (CH_2), 31.7 (CH_2), 30.4 (CH_2), 29.6 (CH_2), 29.1 (CH_2), 27.5 (CH_2), 22.6 (CH_2), 18.8 (CH_3), 14.0 (CH_3) ppm; **HRMS** (EI): m/z calc'd for $C_{22}H_{31}NO_2$ [M^+] 341.2355, found 341.2392.

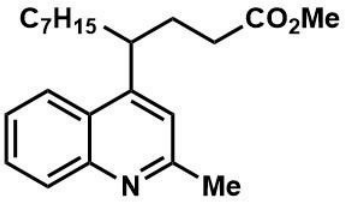

methyl 4-(2-methylquinolin-4-yl)undecanoate (5.6c)

Synthesized according to GP2.

IR (neat, cm^{-1}): 2927(s), 2855(m), 1736(vs), 1598(m), 1169(m), 763(m); **^{1}H NMR** (400 MHz, $CDCl_3$): δ = 8.05–8.01 (m, 2H), 7.66 (t, *J* = 7.4 Hz, 1H), 7.48 (t, *J* = 7.4 Hz, 1H), 7.15 (s, 1H), 3.57 (s, 3H), 3.51–3.50 (m, 1H), 2.73 (s, 3H), 2.23–2.10 (m, 3H), 2.08–1.97 (m, 1H), 1.81–1.68 (m, 2H), 1.26–1.14 (m, 10H), 0.83 (t, *J* = 6.9 Hz, 3H) ppm; **^{13}C NMR** (101 MHz, $CDCl_3$): δ = 173.7 (C), 158.5 (C), 151.4 (C), 148.1 (C), 129.5 (CH), 129.0 (CH), 126.2 (C), 125.4 (CH), 122.7 (CH), 118.8 (CH), 51.4 (CH_3), 37.8 (CH), 36.1 (CH_2), 31.7 (CH_2), 31.7 (CH_2), 30.9 (CH_2), 29.6 (CH_2), 29.0 (CH_2), 27.3 (CH_2), 25.4 (CH_3), 22.5 (CH_2), 14.0 (CH_3) ppm; **HRMS** (EI): m/z calc'd for $C_{22}H_{31}NO_2$ [M^+] 341.2355, found 341.2364.

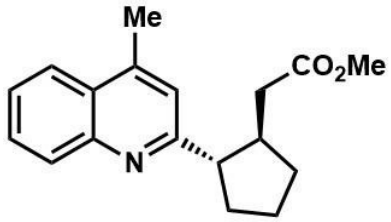

methyl 2-(2-(4-methylquinolin-2-yl)cyclopentyl)acetate (5.6d)

Synthesized according to GP2.

IR (neat, cm^{-1}): 2949(s), 2870(m), 1735(vs), 1602(s), 1438(m), 1165(m), 760(s); **^{1}H NMR** (400 MHz, $CDCl_3$): δ = 8.04 (d, *J* = 8.3 Hz, 1H), 7.95 (dd, *J* = 8.3, 0.6 Hz, 1H), 7.67 (ddd, *J* = 8.3, 6.9, 1.2 Hz, 1H), 7.50 (ddd, *J* = 8.2, 7.0, 1.1 Hz, 1H), 7.18 (s, 1H), 3.50 (s, 3H), 2.96 (td, *J* = 9.4, 9.2 Hz, 1H), 2.71–2.63 (m, 4H (CH_3 + CH), 2.49 (dd, *J* = 15.2, 4.8 Hz, 1H), 2.31 (dd, *J* = 15.2, 9.5 Hz, 1H), 2.33–2.15 (m, 2H), 1.96–1.88 (m, 2H), 1.86–1.80 (m, 1H), 1.49–1.42 (m, 1H) ppm; **^{13}C NMR** (101 MHz, $CDCl_3$): δ = 173.5 (C), 163.9 (C), 147.6 (C), 144.3 (C), 129.5 (CH), 128.9 (CH), 127.1 (C), 125.5 (CH), 123.5 (CH), 120.7 (CH), 54.8 (CH), 51.3 (CH_3), 43.4 (CH), 38.7 (CH_2), 33.7 (CH_2), 32.6 (CH_2), 24.2 (CH_2), 18.8 (CH_3) ppm; **HRMS** (EI): m/z calc'd for $C_{18}H_{21}NO_2$ [M^+] 283.1572, found 283.1570.

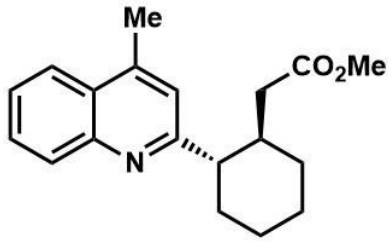

methyl 2-(2-(4-methylquinolin-2-yl)cyclohexyl)acetate (5.6e)

Synthesized according to GP2.

IR (neat, cm^{-1}): 2925(s), 2853(m), 1735(vs), 1603(s), 1447(m), 1158(m), 759(s**); ^{1}H NMR** (400 MHz, $CDCl_3$): δ = 8.04 (d, *J* = 8.4 Hz, 1H), 7.96 (dd, *J* = 8.3, 1.0 Hz, 1H), 7.68 (ddd, *J* = 8.4, 6.9, 1.4 Hz, 1H), 7.51 (ddd, *J* = 8.2, 6.9, 1.2 Hz, 1H), 7.19 (s, 1H), 3.50 (s, 3H), 2.70 (d, *J* = 0.7 Hz, 3H), 2.65 (dd, *J* = 11.4, 3.6 Hz, 1H), 2.40–2.30 (m, 1H), 2.14 (dd, *J* = 15.3, 3.9 Hz, 1H), 2.05 (dd, *J* = 9.7, 6.1 Hz, 1H), 2.02–1.93 (m, 2H), 1.90–1.81 (m, 2H), 1.66 (qd, *J* = 12.5, 3.4 Hz, 2H), 1.46 (qt, *J* = 13.0, 3.3 Hz, 2H), 1.22 (td, *J* = 12.1, 2.6 Hz, 1H) ppm; **^{13}C NMR** (101 MHz, $CDCl_3$): δ = 173.5 (C), 164.7 (C), 147.6 (C), 144.6 (C), 129.6 (CH), 129.0 (CH), 127.1 (C), 125.6 (CH), 123.6 (CH), 120.5 (CH), 52.9 (CH), 51.2 (CH_3), 39.5 (CH_2), 38.6 (CH), 33.9 (CH_2), 32.6 (CH_2), 26.3 (CH_2), 26.0 (CH_2), 18.9 (CH_3) ppm; **HRMS** (EI): m/z calc'd for $C_{19}H_{23}NO_2$ [M^+] 297.1729, found 297.1701.

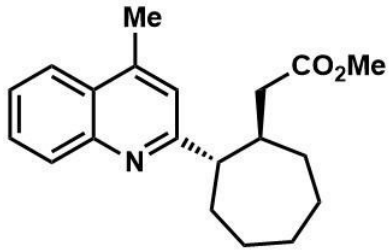

methyl 2-(2-(4-methylquinolin-2-yl)cycloheptyl)acetate (5.6f)

Synthesized according to GP2.

IR (neat, cm^{-1}): 2922(s), 2855(m), 1734(vs), 1602(s), 1443(m), 1147(m), 759(s); **^{1}H NMR** (400 MHz, $CDCl_3$): δ = 8.04 (d, *J* = 8.4 Hz, 1H), 7.94 (d, *J* = 8.1 Hz, 1H), 7.67 (ddd, *J* = 8.1, 7.0, 1.1 Hz, 1H), 7.51 (ddd, *J* = 7.9, 6.8, 0.8 Hz, 1H), 7.17 (s, 1H), 3.50 (s, 3H), 2.82–2.74 (m, 1H), 2.69 (s, 3H), 2.61–2.51 (m, 1H), 2.21–2.15 (m, 2H), 1.93–1.83 (m, 4H), 1.79–1.68 (m, 3H), 1.64–1.56 (m, 3H) ppm; **^{13}C NMR** (101 MHz, $CDCl_3$): δ = 173.7 (C), 166.5 (C), 147.3 (C), 144.7 (C), 129.6 (CH), 129.0 (CH), 127.0 (C), 125.5 (CH), 123.5 (CH), 120.6 (CH), 54.9 (CH), 51.2 (CH_3), 40.9 (CH), 39.9 (CH_2), 33.8 (CH_2), 32.5 (CH_2), 28.8 (CH_2), 27.3 (CH_2), 24.9 (CH_2), 18.8 (CH_3) ppm; **HRMS** (EI): m/z calc'd for $C_{20}H_{25}NO_2$ [M^+] 311.1885, found 311.1915.

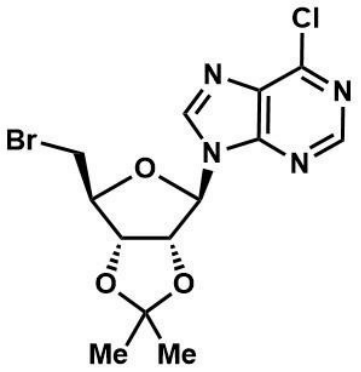

9-((3aR,4R,6S,6aS)-6-(bromomethyl)-2,2-dimethyltetrahydrofuro[3,4-d][1,3]dioxol-4-yl)-6-chloro-9H-purine (5.7)

To a flame dried 25 mL round bottomed flask under argon atmosphere was added triphenylphosphine (1.84 mmol, 1.2 equiv) and 15 mL of DCM. Upon cooling to 0°C, the reaction mixture was slowly added tetrabromomethane (1.84 mmol, 1.2 equiv) and allowed to stir for 30 minutes, reaching room temperature. 6-Chloro-9-β-D-(2,3-isopropylidene)ribofuranosylpurine (1.53 mmol, 1.0 equiv) was then added and the mixture was heated to reflux for overnight. Upon completion as judged by TLC analysis, the mixture was added silica, concentrated under reduced pressure, and dry packed directly onto a flash chromatography column and eluted (0–50% EtOAc:Hex). Relevant fractions were combined affording the brominated product in 30% yield.

IR (neat, cm^{-1}): 2970(m), 2938(w), 1592 (w), 1560(vs), 1204(s), 1085(s), 952(m), 864 (m); **^{1}H NMR** (400 MHz, $CDCl_3$): δ = 8.79 (s, 1H), 8.32 (s, 1H), 6.21 (d, *J* = 2.5 Hz, 1H), 5.42 (dd, *J* = 6.4, 2.5 Hz, 1H), 5.11 (dd, *J* = 6.4, 3.0 Hz, 1H), 4.56 (ddd, *J* = 6.9, 4.8, 3.1 Hz, 1H), 3.64 (dd, *J* = 10.7, 6.9 Hz, 1H), 3.51 (dd, *J* = 10.7, 4.9 Hz, 1H), 1.65 (s, 3H), 1.41 (s, 3H) ppm; **^{13}C NMR** (101 MHz, $CDCl_3$): δ = 152.2 (CH), 151.7 (C), 150.8 (C), 144.3 (CH), 132.4 (C), 115.1 (C), 91.2 (CH), 86.0 (CH), 84.1 (CH), 83.2 (CH), 31.7 (CH_2), 27.1 (CH_3), 25.3 (CH_3) ppm; **HRMS** (EI): m/z calc'd for $C_{13}H_{14}BrClN_4O_3$ [M^+] 387.9938, found [M^+-$CH_3^{\cdot}$] 372.9750.

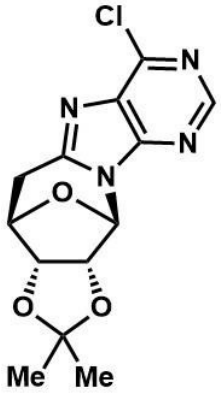

(3aR,4R,12R,12aR)-9-chloro-2,2-dimethyl-3a,11,12,12a-tetrahydro-4H-4,12-epoxy[1,3]dioxolo[4',5':5,6]azepino[1,2-e]purine (5.8)

Synthesized according to GP1.

IR (neat, cm^{-1}): 2980(m), 2936(m), 1600(s), 1560(s), 1441(m), 1376(m), 1094(s), 845(s), 734(s); **^{1}H NMR** (400 MHz, $CDCl_3$): δ = 8.70 (s, 1H), 6.40 (s, 1H), 4.91 (d, *J* = 6.5 Hz, 1H), 4.75–4.67 (dd, *J* = 18.5, 5.5 Hz, 2H), 3.63 (dd, *J* = 18.5, 6.6 Hz, 1H), 3.13 (d, *J* = 18.4 Hz, 1H), 1.57 (s, 3H), 1.31 (s, 3H) ppm; **^{13}C NMR** (101 MHz, $CDCl_3$): δ = 151.7 (CH), 150.0 (C), 149.7 (C), 149.4 (C), 131.1 (C), 114.1 (C), 86.4 (CH), 85.5 (CH), 83.0 (CH), 79.8 (CH), 29.4 (CH_2), 26.0 (CH_3), 24.9 (CH_3) ppm; **HRMS** (EI): m/z calc'd for $C_{13}H_{13}ClN_4O_3$ [M^+] 308.0676, found 308.0668; **[m.p.]** 208–212 °C.

5.8 References

[1] Juris, A.; Balzani, V.; Barigelletti, F.; Campagna, S.; Belser, P.; von Zelewsky, A. *Coord. Chem. Rev*. **1988**, *84*, 85–277.

[2] Narayanam, J. M. R.; Stephenson, C. R. J. *Chem. Soc. Rev*. **2011**, *40*, 102–113.

[3] Prier, C. K.; Rankic, D. A.; MacMillan, D. W. C. *Chem. Rev*. **2013**, *113*, 5322−5363.

[4] Schultz, D. M.; Yoon, T. P. *Science* **2014**, *343*, 985–1239176–8.

[5] Nicewicz, D. A.; Nguyen, T. M. *ACS Catal*. **2014**, *4*, 355–360.

[6] Ciamician, G. *Science* **1912**, *36*, 385–394.

[7] Balzani, V.; Credi, A.; Venturi, M. *ChemSusChem* **2008**, *1*, 26–58.

[8] *Radicals in Organic Synthesis*; Renaud, P., Sibi, M. P., Eds.; Wiley-VCH: Weinheim, 2001.

[9] Wencel-Delord, J.; Glorius, F. *Nat. Chem*. **2013**, *5*, 369–375.

[10] Godula, K.; Sames, D. *Science* **2006**, *312*, 67–72.

[11] Stuart, D. R.; Fagnou, K. *Science* **2007**, *316*, 1172–1175.

[12] Minisci, F.; Bernardi, R.; Bertini, F.; Galli, R.; Perchinummo, M. *Tetrahedron* **1971**, *27*, 3575–3579.

[13] *For reviews on the Minisci reaction, see:* a) Minisci, F. *Synthesis* **1973**, 1–24; b) Minisci, F.; Citterio, A.; Giordano, C. *Acc. Chem. Res*. **1983**, *16*, 27–32; c) Minisci, F.; Fontana, F.; Vismara, E. *J. Heterocycl. Chem*. **1990**, *27*, 79–96; d) Punta, C.; Minisci, F. *Trends Heterocycl. Chem*. **2008**, *13*, 1–68; e) Duncton, M. A. J. *Med. Chem. Commun*. **2011**, *2*, 1135–1161.

[14] Minisci, F.; Vismara, E.; Fontana, F.; Morini, G.; Serravalle, M.; Giordano, C. *J. Org. Chem.* **1986**, *51*, 4411–4416.

[15] Yamazaki, O.; Togo, H.; Matsubayashi, S.; Yokoyama, M. *Tetrahedron Lett*. **1988**, *39*, 1921–1924.

[16] a) Seiple, I. B.; Su, S.; Rodriguez, R. A.; Gianatassio, R.; Fujiwara, Y.; Sobel, A. L.; Baran, P. S. *J. Am. Chem. Soc*. **2010**, *132*, 13194–13196; b) Molander, G.; Colombel, V.; Braz, V. *Org. Lett*. **2011**, *13*, 1852–1855.

[17] a) Antonchick, A. P.; Burgmann, L. *Angew. Chem. Int. Ed*. **2013**, *125*, 3267–3271; b) Fang, L.; Chen, L.; Yu, J.; Wang, L. *Eur. J. Org. Chem*. **2015**, 1910–1914; c) Tang, R.-J.; Kang, L.; Yang, L. *Adv. Synth. Catal*. **2015**, *357*, 2055–2060; d) Paul, S.; Guin, J. *Chem. Eur. J*. **2015**, *21*, 17618–17622.

[18] Xiao, B.; Liu, Z.-J.; Liu, L.; Fu, Y. *J. Am. Chem. Soc*. **2013**, *135*, 616–619.

[19] a) DiRocco, D. A.; Dykstra, D.; Krska, S.; Vachal, P.; Conway, D. V.; Tudge, M. *Angew. Chem. Int. Ed*. **2014**, *53*, 4802–4806; b) Jin, J.; MacMillan, D. W. C. *Nature* **2015**, 525, 87–90.

[20] *For methodology involving haloalkanes:* a) Murphy, J. A.; Sherburn, M. S. *Tetrahedron Lett*. **1990**, *31*, 1625–1628; b) Murphy, J. A.; Sherburn, M. S.; *Tetrahedron* **1991**, *47*, 4077–4088; c) Artis, D. R.; Cho, I.-S.; Jaime-Figueroa, S.; Muchowski, J. M. *J. Org. Chem*. **1994**, *59*, 2456–2466; d) Togo, H.; Taguchi, R.; Yamaguchi, K.; Yokoyama, M. *J. Chem. Soc., Perkin Trans. 1* **1995**, 2135–2139; e) Duncton, M. A. J.; Estiarte, M. A..; Johnson, R. J.; Cox, M.; O'Mahony, D. J. R.; Edwards, W. T.; Kelly, M. G. *J. Org. Chem*. **2009**, *74*, 6354–6357; f) Wu, X.; See, J. W. T.; Xu, K.; Hirao, H.; Roger, J.; Hierso, J.-C.; Zhou, J. *Angew. Chem. Int. Ed*. **2014**, *53*, 13573–13577; g) He, L.; Natte, K.; Rabeah, J.; Taeschler, C.; Neumann, H.; Brückner, A.; Beller, M. *Angew. Chem. Int. Ed*. **2015**, *54*, 4320–4324.

[21] a) Ji, Y.; Brueckl, T.; Baxter, R. D.; Fujiwara, Y.; Seiple, I. B.; Su, S., Blackmond, D. G.; Baran, P. S. *Proc. Natl. Acad. Sci. USA* **2011**, *108*, 14411–14415; b) Fujiwara, Y.; Dixon, J. A.; Rodriguez, R. A.; Baxter, R. D.; Dixon, D. D.; Collins, M. R.; Blackmond, D. G.; Baran, P. S. *J. Am. Chem. Soc*. **2012**, *134*, 1494–1497; c) Fujiwara, Y.; Dixon, J. A.; O'Hara, F.; Funder, E. D.; Dixon, D. D.; Rodriguez, R. A.; Baxter, R. D.; Herlé, B.; Sach, N.; Collins, M. R.; Ishihara, Y.; Baran, P. S. *Nature* **2012**, *492*, 95–99; d) Zhou, Q.: Ruffoni, A.; Gianatassio, R.; Fujiwara, Y.; Sella, E.; Shabat, D.; Baran, P. S. *Angew. Chem. Int. Ed*. **2013**, *52*, 3949–3952; e) Gianatassio, R.; Kawamura, S.; Eprile, C.; L.; Foo, K.; Ge, J.; Burns, A. C.; Collins, M. R.; Baran, P. S. *Angew. Chem. Int. Ed*. **2014**, *53*, 9851–9855.

[22] a) Revol, G.; McCallum, T.; Morin, M.; Gagosz, F.; Barriault, L. *Angew. Chem. Int. Ed.* **2013**, *52*, 13342–13345; b) McCallum, T.; Slavko, E.; Morin, M.; Barriault, L. *Eur. J. Org. Chem*. **2015**, 81–85; c) Kaldas, S. J.; Cannillo, A.; McCallum, T.; Barriault, L. *Org. Lett*. **2015**, *17*, 2864–2866; d) Xie, J.; Shi, S.; Zhang, T.; Mehrkens, N.; Rudolph, M.; Hashmi, A. S. K. *Angew. Chem. Int. Ed*. **2015**, *54*, 6046–6050; e) Nzulu, F.; Telitel, S.; Stoffelbach, F.; Graff, B.; Marlet-Savary, F.; Lalevée, J.; Fensterbank, L.; Goddard, J.-P.; Ollivier, C. *Polym. Chem*. **2015**, *6*, 4605–4611; f) Xie, J.; Zhang, T.; Chen, F.; Mehrkens, N.; Rominger, F.; Rudolf, M.; Hashmi, A. S. K. *Angew. Chem. Int. Ed*. **2016**, *128*, 2934–2938.

[23] Chow, P.K.; Cheng, G.; Tong, G. S. M.; To, W.-P.; Kwong, W.-L.; Low, K.-H.; Kwok, C-C.; Ma, C.; Che, C.-M. *Angew. Chem. Int. Ed*. **2015**, *54*, 2084–2089.

[24] a) Ghosh, I.; Ghosh, T.; Bardagi, J. I.; Konig, B. *Science* **2014**, *346*, 725–728; b) Discekici, E. H.; Treat, N. J.; Poelma, S. O.; Mattson, K. M.; Hudson, Z. M.; Luo, Y.; Hawker, C. J.; Read de Alaniz, J. *Chem. Commun*. **2015**, *51*, 11705–11708.

[25] Fry, A. J.; Krieger, R. L. *J. Org. Chem*. **1976**, *41*, 54–57.

[26] McTiernan, C. D.; Morin, M.; McCallum, T.; Scaiano, J. C.; Barriault, L. *Catal. Sci. Technol*. **2016**, *6*, 201–207.

[27] a) Che, C.-M.; Kwong, H.-L.; Yam, V. W.-W.; Cho, K.-C. *J. Chem. Soc., Chem. Commun*. **1989**, 885–886; b) Kwong, H.-L.; Yam, V. W.-W.; Li, D. D.; Che, C.-M. *J. Chem. Soc., Dalton Trans*. **1992**, 3325–3329; c) Ma, C.; Chan, C. T.-L.; To, W.-P.; Kwok, W.-M.; Che, C.-M. *Chem. Eur. J*. **2015**, *21*, 13888–13893.

[28] a) Nguyen, J. D.; D'Amato, E. M.; Narayanam, J. M. R.; Stephenson, C. R. J. *Nat. Chem*. **2012**, *4*, 854–859; b) Kim, H.; Lee, C. *Angew. Chem. Int. Ed*. **2012**, *51*, 12303–12306.

[29] Citterio, A.; Minisci, F.; Porta, O.; Sesana, G. *J. Am. Chem. Soc*. **1977**, *99*, 7960–7966.

[30] *For information on classical radical clocking experiments and determination of absolute rate constants, see:* Newcomb, M. *Tetrahedron* **1993**, *49*, 1151–1176.

[31] Antonietti, F.; Mele, A.; Minisci, F.; Punta, C.; Recupero, F.; Fontana, F. *J. Fluorine Chem*. **2004**, *125*, 205–211.

[32] Kharasch, M. S.; Skell, P. S.; Fisher, P. *J. Am. Chem. Soc*. **1948**, *70*, 1055–1059.

[33] a) Li, G.-X. Morales-Rivera, C. A.; Wang, Y.; Guo, F.; He, G.; Liu, P.; Chen, G. *Chem. Sci*. **2016**, *7*, 6407–6412; b) Jin, Y.; Jiang, M.; Wang, H.; Fu, H. *Sci. Rep*. **2016**, *6*, 20068; c) Cheng, W.-M.; Shang, R.; Fu, Y. *ACS Catal*. **2017**, *7*, 907; d) Cheng, W.-M.; Shang, R.; Fu, M.-C.; Fu, Y. *Chem. Eur. J*. **2017**, *23*, 2537–2541; e) Matsui, J. K.; Molander, G. A. *Org. Lett*. **2017**, *19*, 950−953; f) Matsui, J. K.; Primer, D. N.; Molander, G. A. *Chem. Sci*. **2017**, *8*, 3512–3522; g) Quattrini, M. C.; Fujii, S.; Yamada, K.; Fukuyama, T.; Ravelli, D.; Fagnoni, M.; Ryu, I. *Chem. Commun*. **2017**, *53*, 2335–2338; h) Garza-Sanchez, R.

A.; Tlahuext-Aca, A.; Tavakoli, G.; Glorius, F. *ACS Catal*. **2017**, *7*, 4057−4061; i) Klauck, F. J. R.; James, M. J.; Glorius, F. *Angew. Chem. Int. Ed*. **2017**, *56*, 12336−12339; j) Nuhant, P.; Oderinde, M. S.; Genovino, J.; Juneau, A.; Gagne, Y.;´ Allais, C.; Chinigo, G. M.; Choi, C.; Sach, N. W.; Bernier, L.; Fobian, Y. M.; Bundesmann, M. W.; Khunte, B.; Frenette, M.; Fadeyi, O. O. *Angew. Chem. Int. Ed*. **2017**, *56*, 15309−15313; k) Sherwood, T. C.; Li, N.; Yazdani, A. N.; Dhar, T. G. M. *J. Org. Chem*. **2018**, *83*, 3000−3012; l) Zhou, W.; Miura, T.; Murakami, M. *Angew. Chem. Int. Ed*. **2018**, *57*, 5139−5142.

[34] Gabriele, B.; Mancuso, R.; Salerno, G.; Ruffolo, G.; Plastina, P. *J. Org. Chem*. **2007**, *72*, 6873–6877.

[35] Wenkert, E.; Hanna Jr., J. M.; Leftin, M. H.; Michelotti, E. L.; Potts, K. T.; Usifer, D. *J. Org. Chem*. **1985**, *50*, 1125–1126.

[36] Park, S.; Jung, J.; Cho, E. J. *Eur. J. Org. Chem*. **2014**, 4148–4154.

[37] Yao, Y.; Hirano, K.; Satoh, T.; Miura, M. *Angew. Chem. Int. Ed*. **2012**, *51*, 775–779.

6. Light-Enabled Alkylation and Reduction of Heteroarenes

McCallum, T.; Pitre, S. P.; Morin, M.; Scaiano, J. C.; Barriault, L. The photochemical alkylation and reduction of heteroarenes. *Chem. Sci.* **2017**, *8*, 7412–7418.

6.1 Abstract

The functionalization of heteroarenes has been integral to the structural diversification of medicinally active molecules such as quinolines, pyridines, and phenanthridines. Electron-deficient heteroarenes are electronically compatible to react with relatively nucleophilic free radicals such as hydroxyalkyl. However, the radical functionalization of such heteroarenes has been marked with use of transition-metal catalyzed processes that require initiators and stoichiometric oxidants. The development of photoredox catalysis methodology has enabled a variety of new strategies for the generation of nucleophilic alkyl radicals and their addition to electrophilic protonated heteroarenes. From an atom economy standpoint, the activation of functional groups bearing heavy atoms such as halogens can be considered not ideal. Methodology with incorporating readily available starting materials such as alcohols is needed, where alkyl radicals derived from such substrates may only produce hydrogen or water as their formal by-products. Described herein is the photochemical alkylation of quinolines, pyridines and phenanthridines, where through direct excitation of the protonated heterocycle, alcohols and ethers, such as methanol and THF, can serve as alkylating agents. Also reported is the discovery of a photochemical reduction of these heteroarenes using only *i*PrOH and HCl. Mechanistic studies to elucidate the underlying mechanism of these transformations, and preliminary results on catalytic methylations are also reported.

6.2 Introduction

Over the past decade, the rapidly increasing development of photochemical based organic transformations has been driven by research in photoredox catalysis. Transition-metal photocatalysts and organic dyes have granted chemists access to ever increasing alternatives to classical radical chemistry transformations as well as unconventional reactivity in the discovery of new organic transformations.[1] Implementation of photochemical processes is preferential to the classical, thermal methods of radical generation, as they often eliminate the need for radical initiators, stoichiometric additives and harsh reaction conditions.

The functionalization of heteroaromatic scaffolds is an important topic in organic chemistry for its applications in the synthesis of biologically active molecules and other medicinally relevant studies such as structure–activity relationships.[2] The Minisci reaction has been famously important in the alkyl/aryl functionalization of electron-deficient heteroaromatic scaffolds.[3] In this regard, a relatively nucleophilic radical (alkyl or aryl) is generated by an initiation process, where upon addition to an electron-deficient heteroaromatic (usually protonated), can undergo rearomatization by an oxidation event, leading to the functionalized product. In the original report,[3] the silver mediated decarboxylation of carboxylic acids in the presence of persulfates was described, however, this reaction suffers from by-product formation, low yields in some cases, and the need for relatively harsh conditions (**Figure 6.1**, Eq. (1)). With respect to the redox profile of this reaction, an oxidation event is needed to initiate the alkyl or aryl radical and an oxidation event is needed for rearomatization, warranting the need for persulfates as the oxidant. Since then, a variety of mild methodological advancements have been made using many functional groups.[4] One such functionalization that has been particularly

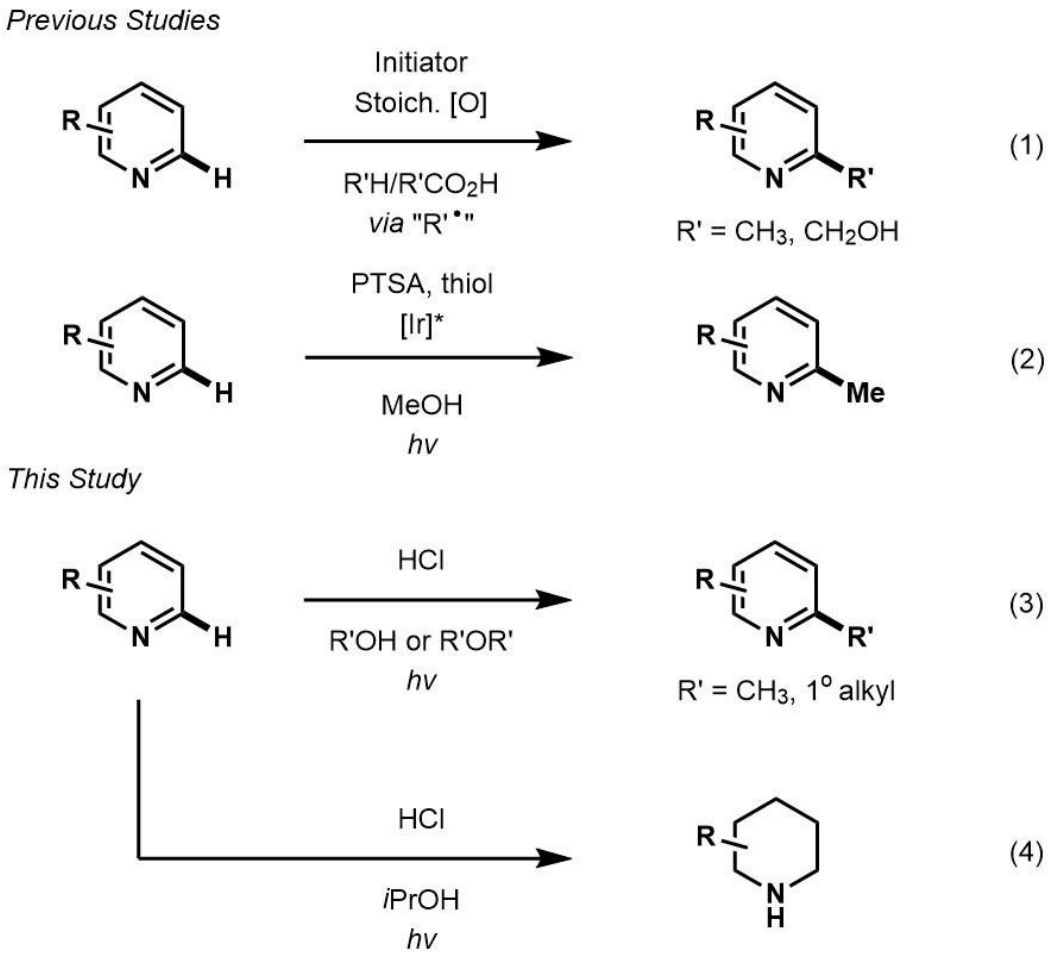

Figure 6.1 Previous and present work in direct heteroarene alkylation.

challenging to organic chemists is the methylation of heteroaromatic scaffolds. Only a few striking protocols exist for this ambitious disconnection, demonstrating the need for further methodological development (Eq. (2)).[5] The use of methanol as a precursor for methyl functionality also presents a significant challenge in organic synthesis as few methodologies have been developed (mostly with transition-metals and require additives or oxidants) for this difficult disconnection.[6] In light of these reports, a mild and waste-limiting, redox-neutral organic-based protocol employing MeOH would provide ideal methylation conditions.[7] Herein, we report the photochemical activation of protonated heteroarenes for their methylation in methanol (Eq. (3)) as well as studies with a variety

of other alcohols and ethers. The use of catalytic quantities of 2,4-diphenylquinoline for the methylation of heteroarenes that do not absorb in the UVA region or that degrade upon direct excitation is also disclosed. Additionally, we also report the discovery of an *i*PrOH mediated reduction of heteroarenes (Eq. (4)), which to the best of our knowledge is the first organic mediated photochemical protocol for the reduction of heteroarenes. Finally, mechanistic studies were performed to aid in the elucidation of the overall reaction mechanism is also disclosed.

6.3 Results and Discussion

Over the course of our previous study on the photo-mediated alkylative functionalization of heteroarenes such as lepidine (**6.1a**) using haloalkanes in methanol,[4i] methanesulfonyl chloride was found to afford 2,4-dimethylquinoline (**6.2a**) without use of a photoredox catalyst. Furthermore, the use of butyl- or tosyl-functionalized sulfonyl chlorides also gave rise to the methylated product rather than the corresponding sulfonyl alkyl/aryl functionalities that may have derived from the addition or fragmentation of sulfonyl radicals. Subsequently, it was found that the methylation proceeded to give **6.2a** (76% yield) in the presence of concentrated hydrochloric acid (c = 2.0 M) under UVA LED irradiation (**Table 6.1**, entry 1). On one hand, a screening of various co-solvents was performed to test the viability of extending this methodology to a variety of alcohols. It was found that MeCN can be a good co-solvent, yielding **6.2a** in 77% (entry 5). On the other hand, the optimization of HCl equivalents and reaction concentration gave **6.2a** in 80% yield using HCl (5 equiv.) in MeOH (0.5 M) (entry 11). Interestingly, the by-product **6.4a** was isolated in 40% yield after 60 h of UVA irradiation (entry 12). Starting from **6.1a** or **6.2a** gave the same product distribution over the 60 h experiment, indicating that the

Table 6.1 Optimization of the reaction conditions.

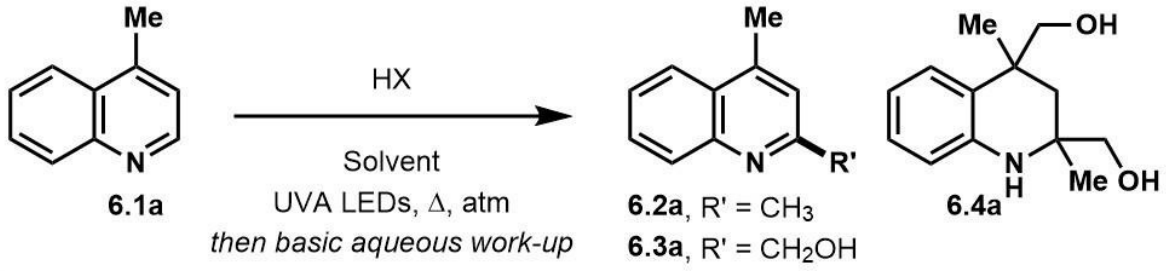

Entry	HX	HX [equiv]	Solvent	M	atm	t [h]	Conv. SM [%]	6.2a [%]	6.3a [%]	6.4a [%]
1	HCl	5	MeOH	0.5	Ar	16	100	76	--	20
2	HCl	5	MeOH:H_2O (1:1)	0.5	Ar	16	39	27	--	--
3	HCl	5	MeOH:DMSO (1:1)	0.5	Ar	16	33	16	--	--
4	HCl	5	MeOH:DMF (1:1)	0.5	Ar	16	58	29	--	--
5	HCl	5	MeOH:MeCN (1:1)	0.5	Ar	16	90	77	--	5
6	HCl	5	MeOH	1.0	Ar	16	76	69	--	5
7	HCl	5	MeOH	0.3	Ar	16	100	51	--	30
8	HCl	5	MeOH	0.1	Ar	16	100	50	--	13
9	HCl	3	MeOH	0.5	Ar	16	97	82	--	7
10	HCl	1	MeOH	0.5	Ar	16	48	27	10	3
11	**HCl**	**5**	**MeOH**	**0.5**	**Ar**	**8**	**100**	**87(80)**	**--**	**10**
12	HCl	5	MeOH	0.5	Ar	60	100	35	--	40(40)[a]
13	HCl	5	MeOH	0.5	Ar	16	72	65[b]	--	5
14	--	-	MeOH	0.5	Ar	16	0	--	--	--
15	HCl	5	MeOH	0.5	Ar	16	0	--[c]	--	--
16	TFA	5	MeOH	0.5	Ar	8	10	5	--	--
17	PTSA	5	MeOH	0.5	Ar	8	94	28	12	--
18	H_2SO_4	5	MeOH	0.5	Ar	8	12	7	--	--
19	HOTf	5	MeOH	0.5	Ar	8	7	6	--	--
20	HCl	5	MeOH	0.5	Air	8	100	84	--	7
21	HCl	2	MeOH	0.5	O_2	4	97	38	59(56)	--

[a]Isolated as a 2:1 ratio of diastereomers (d.r. determined by ^{1}H NMR analysis). The same reaction conditions using **6.2a** as starting material resulted in the same product distribution. [b]10.0 mmol scale of **6.1a**. [c]In absence of irradiation and heating to reflux.

methylation reaction occurs at a faster rate relative to the onset of photochemical degradation of **6.2a**. The reaction was also amenable to scale up (10 mmol), producing **6.2a** in 65% yield (entry 13). Control experiments verified that the transformation required acid as well as UVA LED irradiation for product formation (entries 14 and 15). The use of

acids such as TFA, H_2SO_4, and HOTf gave little to no conversion of the starting material whereas PTSA led mostly to degradation (entries 16–19). Finally, the reaction conditions were not hampered when exposed to air atmosphere, indicating that the reaction likely proceeds via the excited singlet state (entry 20). Notably, exposing the reaction to oxygen atmosphere resulted in the hydroxymethylated product **6.3a** in 59% yield (56% isolated, entry 21). In our hands, this reaction only converted **6.1a** to **6.2a** when using 2 UVA LEDs at ~ 1 mm away from the reaction vessel, resulting in the generation of heat (~70°C). Using a temperature-controlled setup, the optimized conditions gave no conversion after 16 h at 20°C, showing the need for both light and heat for the successful transformation of **6.1a**. A survey of the literature reveals that previous photo-mediated methylation reactions were described in low yield (<10%). These examples employed intense sources of irradiation, possibly leading to the degradation of the methylated heteroarene products.[8] Given the simplicity of this transformation, we surmised an investigation of reaction scope/mechanistic studies would be beneficial to understanding our results.

In the investigation of the methylation scope under optimized conditions, a variety of heteroarenes were evaluated (**Table 6.2**). Quinaldine and 8-chloroquinaldine gave mostly the corresponding degradation products related to **6.4a**. Interestingly, 6- and 7-haloquinaldine (X = F, Cl, and Br) gave 2,4-dimethylquinoline products **6.2b**–**e** in 32–68% yields, where the main by-products were found to be **6.4d** (similar to **6.4a**, by-product for X = Cl characterized, See section **6.6**). 2,6-Diphenylpyridine, fluorinated-ppy and ppy afforded methylated products **6.2f**, **6.2g,** and **6.2h** in 82%, 61% and 59% yields, respectively. Using 410 nm LEDs for 2-phenylquinoline and phenanthridine, methylated products **6.2i** and **6.2j** were obtained in nearly quantitative yields.

Table 6.2 Scope of heteroarene methylation.

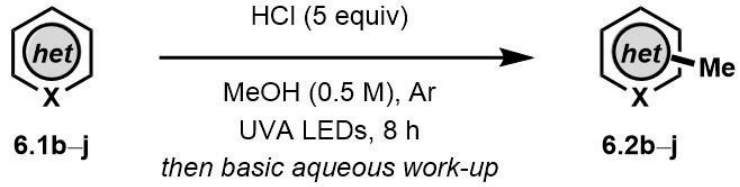

6.1b–j → 6.2b–j

Entry	Product		Yield [%]
1	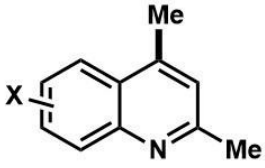	**6.2b**, X = 6-F	33[a]
2		**6.2c**, X = 6-Br	32
3		**6.2d**, X = 6-Cl	68
4		**6.2e**, X = 7-Cl	59
5	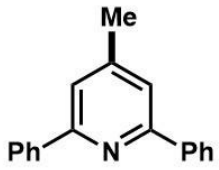 **6.2f**		82
6	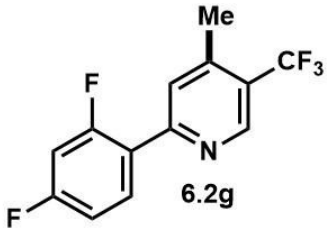 **6.2g**		61[b]
7	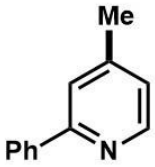 **6.2h**		59[c]
8	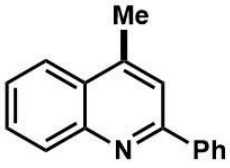 **6.2i**		99[d]
9	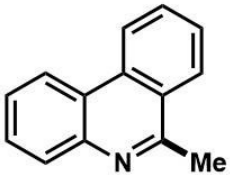 **6.2j**		91[d]

[a]16 h irradiation. [b]40 h irradiation. [c]24 h irradiation, 20% SM along with 8% 2-methyl-6-phenylpyridine and 6% 2,4-dimethyl-6-phenylpyridine observed. [d]410 nm LED was used for 16 h irradiation.

Extending this methodology to other alcohol and ether coupling partners with lepidine was also evaluated (**Table 6.3**). The reaction conditions in ethanol gave the corresponding ethylated **6.2k** in 54% yield whereas the use of diethyl ether gave only 15% of the product. Methyl *tert*-butyl ether was found to give **6.2a** in 34% yield. Interestingly, THF, known to be one of the best H-atom donors among ethers,[9] gave the corresponding addition and fragmentation product **6.2l** in 88% yield. Tetrahydrofurfuryl alcohol gave **6.2m** in 77% yield, showing regio- and chemoselectivity towards functionalization at the 5-position of the furan. 1,4-Dioxane gave **6.2n** in 28% yield, where products **6.2k** and **6.2n'** were also isolated in 26% and 20% yields.

To our surprise, when using *i*PrOH with lepidine, the tetrahydroquinoline product **6.5a** was observed in 31% yield (**Table 6.4**) and is likely a reflection of the reducing characteristics of the ketyl radical derived from *i*PrOH.[10] We then extended this light-enabled reduction to other heteroarenes such as methyl and adamantyl functionalized quinolines to produce the desired heterocycles **6.5b**–**e** in moderate to excellent yields. Notably, the bromo–functionality in **6.5c** remained intact.[11] Using 410 nm LEDs, phenanthridine and acridine also gave reduced heterocycles **6.5f** and **6.5g** in 53% and 32% (60% brsm), respectively.

Table 6.3 Scope of heteroarene functionalization using alcohols and ethers.

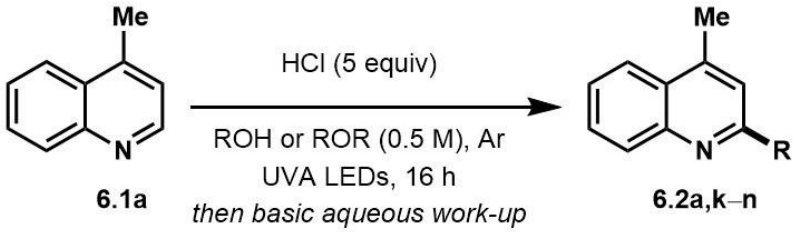

Entry	Solvent	Product	Yield [%]
1		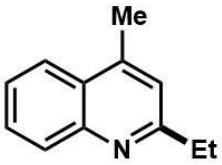 **6.2k**	54
2	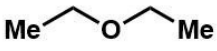	**6.2k**	15
3	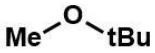	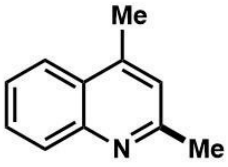 **6.2a**	34
4		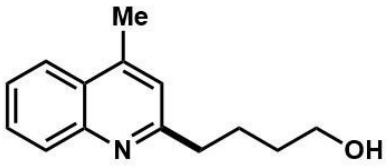 **6.2l**	88
5	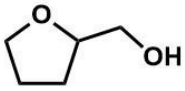	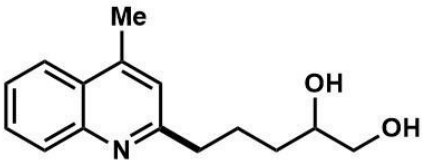 **6.2m**	77
6	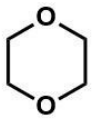	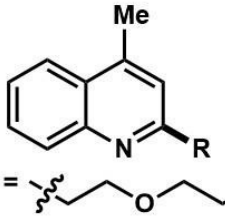 **6.2n, R =** **6.2n', R =** 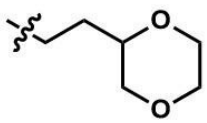	28:20:26 **6.2n**:**6.2n'**:**6.2k**

Table 6.4 Scope of heteroarene reduction using *i*PrOH.

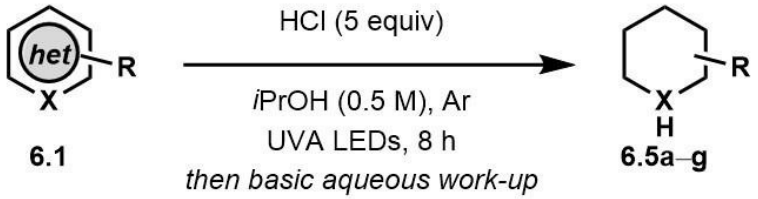

6.1 **6.5a–g**

Entry	Product	Yield [%]
1	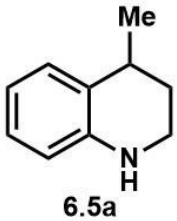 **6.5a**	31
2	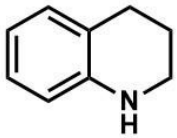 **6.5b**	28
3	 **6.5c**	56
4	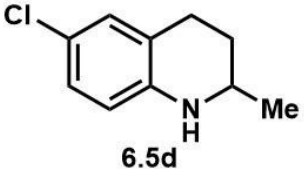 **6.5d**	64
5	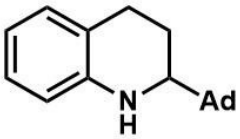 **6.5e**	87[a]
6	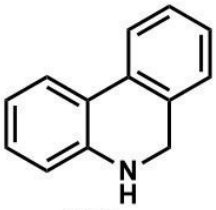 **6.5f**	53[b]
7	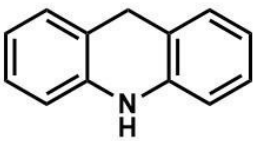 **6.5g**	32[b] (60 brsm)

[a]16 h irradiation. [b]410 nm LED was used for 16 h irradiation.

A systematic approach to deuterium labeling experiments was performed to help distinguish plausible mechanistic pathways (**Table 6.5**, **A**). As expected, under fully deuterated conditions using CD_3OD and DCl in D_2O gave **d_3-6.2a** in 73% yield (85% brsm, entry 1). When using CD_3OH with HCl in H_2O, the **d_2-6.2a** in 78% yield (entry 2). Implementation of CH_3OD and DCl in D_2O provided the **d-6.2a** in 77% yield (entry 3). Interestingly, the conditions do not generate ratios of deuterium incorporation where scrambling of benzylic protons is observed in other methodology.[12] These results likely indicate that the final product derives from an enamine intermediate that is not under equilibrium and is determined by the nature of the broadly exchanging solvent. To test if **6.3a** is a viable intermediate in the production of the final product (**6.2a**), **6.3a** was first subjected to the optimized reaction conditions, yielding **6.2a** in 30% (entry 4). Examining the product generated from **6.3a** using CD_3OH with HCl in H_2O produced **6.2a** in 54% yield (entry 5). However, **d-6.2a** was obtained in 51% using CH_3OD with DCl in D_2O (entry 6). These experiments support the hypothesis that **6.3a** is not likely to be a major intermediate in this process under optimized conditions but gives a similar distribution if it is formed as a minor intermediate. Using a mixture of CH_3OH and CD_3OH (1:1), a ratio of products **6.2a**:**d_2-6.2a** (65:35) was obtained thereby giving a KIE of 1.86 (entry 7). In addition, a mixture of **6.1a** and **d-6.1a** (51:49), was treated under optimal conditions to give a KIE of 1.77 (entry 8, see section **6.6**). To compare the corresponding data for ethers, THF and d_8-THF (1:1) were submitted to the optimal conditions, where a mixture of **6.2l** and **d_7-6.2l** were obtained in 54% yield as a 55.5:44.5 ratio, providing an observed KIE of 1.20 (entry 9).

Table 6.5 Deuterium isotope labelling experiments.

A

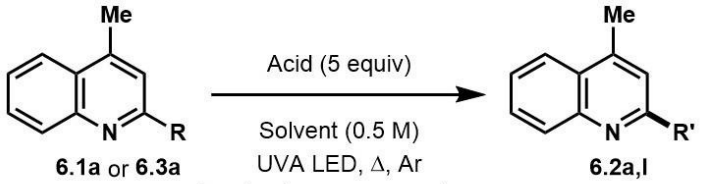

6.1a or **6.3a** — *then basic aqueous work-up* — **6.2a,l**

Entry	R	Acid	Solvent	R'	t [h]	6.2 [%]
1	**6.1a**, H	DCl in D_2O	CD_3OD	CD_3	16	**d_3-6.2a**, 73 (85 brsm)
2	**6.1a**, H	HCl in H_2O	CD_3OH	CD_2H	16	**d_2-6.2a**, 78
3	**6.1a**, H	DCl in D_2O	CH_3OD	CDH_2	16	**d-6.2a**, 77
4	**6.3a**, CH_2OH	HCl in H_2O	CH_3OH	CH_3	8	**6.2a**, 30
5	**6.3a**, CH_2OH	HCl in H_2O	CD_3OH	CH_3	20	**6.2a**, 54
6	**6.3a**, CH_2OH	DCl in D_2O	CH_3OD	CDH_2	20	**d-6.2a**, 51
7	**6.1a**, H	HCl in H_2O	CH_3OH/ CD_3OH (1:1)	CH_3/ CD_2H (65:35)	16	**6.2a**:**d_2-6.2a**, 73 (65:35) KIE = 1.86
8	**6.1a**:**d-6.1a**, H:D (51:49)	HCl in H_2O	CH_3OH	CH_3	1	**6.2a**, 70 SM H:D (37:63) KIE = 1.77
9	**6.1a**, H	HCl in H_2O	THF/ d_8-THF (1:1)	$(CH_2)_4OH$/ $CHD(CD_2)_3OH$ (57:43)	16	**6.2l**:**d_7-6.2l**, 54 (55.5:45.5) KIE = 1.20

B

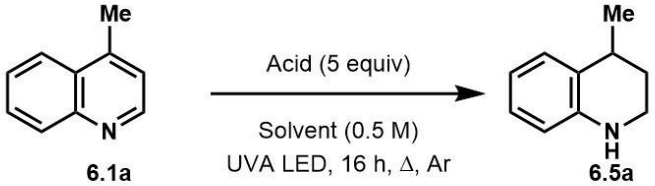

6.1a — *then basic aqeous work-up* — **6.5a**

Entry	Acid	Solvent	Product [%]
1	DCl in D_2O	$(CD_3)_2CDOD$	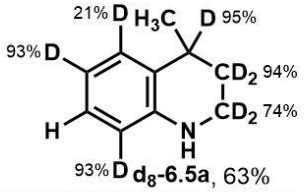 **d_8-6.5a**, 63%
2	HCl in H_2O	$(CD_3)_2CDOH$	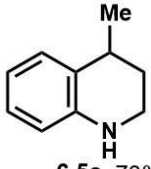 **6.5a**, 73%
3	DCl in D_2O	$(CH_3)_2CHOD$	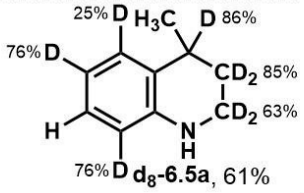 **d_8-6.5a**, 61%

A similar approach was taken for further understanding of the photochemical reduction of heteroarenes using *i*PrOH (**Table 6.5**, **B**). Using d_8-*i*PrOH with DCl in D_2O for the light mediated reduction of lepidine, **d_8-6.5a** was isolated in 63% yield (entry 1). Interestingly, when using d_7-*i*PrOH with HCl in H_2O, deuterium incorporation is not observed in **6.5a**, isolated in 73% yield (entry 2). Finally, when using *i*PrOD with DCl in D_2O (entry 3, 61% yield), **d_8-6.5a** was obtained with a similar deuterium distribution as in entry 1. These results are indicative of the excited-state protonated lepidine and the associated reactive intermediates during formation of **6.5a** do not undergo HAT reactions with *i*PrOH. However, it is possible that HAT may occur on the nitrogen atom, where erosion of deuterium incorporation by the broadly exchanging nature of the N–H bond would occur during purification.

To gain further insight into the underlying mechanism of these transformations, we performed a series of mechanistic studies. UV-vis absorption studies confirmed lepidine only absorbs at the irradiation wavelengths of our UVA LED in the presence of acid (**Figure 6.2**, **A**). To prove that the reaction is initiated by quenching of the lepidine singlet state by MeOH, Stern–Volmer quenching studies were performed. As seen in **Figure 6.2**, the emission of lepidine in 2 M HCl in MeCN was found to be quenched by the addition of MeOH, with a Stern–Volmer constant (K_{SV}) of 1.07 M^{-1}. During our quenching studies, we also observed a slight redshift in the emission maxima of lepidine, which could be due to the change in the environmental conditions upon addition of MeOH. In good agreement, we also observed quenching of lepidine by MeOH when employing H_2O as the solvent with no change in the emission maximum (See section **6.6**). Furthermore, the decreased quenching efficiency in H_2O (0.078 M^{-1}) correlates with our previous experimental observations which showed that H_2O is detrimental to the reactivity of this

system (**Table 6.1**, entry 2). However, we cannot rule out that a portion of the observed increase in quenching in MeCN is due to the change in the environmental conditions upon addition of MeOH. Clearly a change in the environmental conditions is not the sole cause of the quenched emission, as no quenching would be observed in H_2O if this were the case. Based on the results of our deuterated studies which showed a KIE of 1.86, we propose that this quenching event proceeds through a SET (PCET), forming a protonated lepidine intermediate and a hydroxymethyl radical. Considering the observed KIE of 1.86, it is proposed that this reaction proceeds via a sequential PCET, with electron-transfer occurring first, followed by proton–transfer.[13] Furthermore, it is unlikely that this quenching event results in the single–electron oxidation of MeOH to form a MeOH radical cation, as this would not be expected to produce a KIE. It is also possible that this reaction could proceed through a HAT mechanism, however this may also be unlikely as we may expect larger KIE values than those observed in this work if a HAT was involved in the rate determining step.[14]

We also examined the emission of steady–state quenching of lepidine by THF, one of the ethers employed in this work (**Table 6.3**, **6.2l**). Once again, quenching of the lepidine emission was observed upon addition of THF (See section **6.6**; K_{SV} = 1.08 M^{-1}). Due to the observation of minimal KIE in this system (1.25, **Table 6.5**, **A**, entry 9), it is proposed that this quenching event proceeds solely through electron transfer, and not through a PCET event such as the system employing MeOH.

To determine if chain propagation is present in the underlying mechanism of these transformations, we decided to perform intermittent illumination studies. It is evident that many in the field of photoredox catalysis understand that one can probe a photo-initiated chain reaction through use of intermittent illumination.[15] However, as the lifetime of most

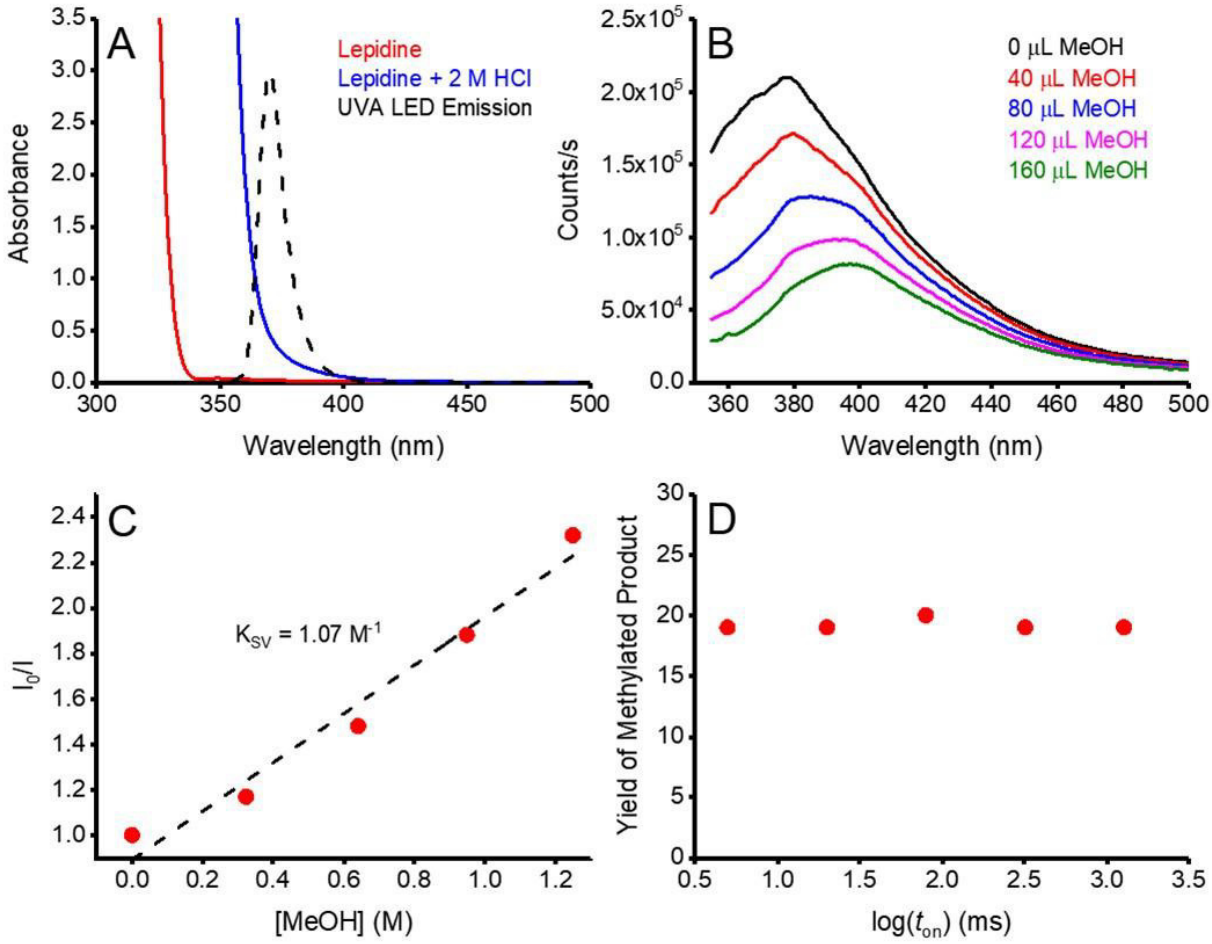

Figure 6.2 Mechanistic/quenching studies for protonated lepidine. (**A**) Absorption spectra of lepidine (0.5 M) in MeOH (red), and lepidine (0.5 M) in 2 M HCl in MeOH (blue). When comparing these spectra to the emission profile of the 365 nm LED employed, it becomes evident that lepidine can only be excited in its protonated form under our reaction conditions. (**B**) Quenching of the emission of lepidine upon increasing concentrations of MeOH in 2 M HCl in MeCN. (**C**) Corresponding Stern–Volmer plot, the slight curvature likely reflects the small special shift in panel B. (**D**) Yield of methylated lepidine *vs* the log of the light-on period (t_{on}). For a full description of the experimental procedure and set-up, See section **6.6**.

chains is in the sub-second timescale, current attempts to establish whether or not a photoredox transformation involves a chain by testing the effect of switching the light source on and off on the time scale of minutes are futile. Therefore, a more appropriate test would be the "rotating sector" method, which has been employed in the past to produce intermittent illumination on the appropriate timescale for typical chain reactions.[15] Recently, the Scaiano group presented an updated version of the "rotating sector" method, employing current LED technologies to pulse LEDs down to the nanosecond

timescale, and by using this technique were able to successfully characterize multiple chain reactions.[16] Using this technique, we were able to demonstrate that the temporal profile of irradiation does not have any effect on the yield of methylated lepidine (**Figure 6.2**, **D**) and indicates the absence of a propagating chain in the underlying mechanism, hinting that a sacrificial amount of lepidine is used as a photocatalyst to promote the photochemical methylation (*vide infra*).

With the data obtained for the methylation/alkylation of a variety of heteroarenes taken with the mechanistic data, it is proposed that upon protonation, the heteroarene (**I**) is excited to the singlet state (**I***), where it can be quenched by MeOH to give a protonated radical intermediate (**I'–H**) and a hydroxymethyl radical (**Figure 6.3**, **A**). The quenching event likely proceeds via a sequential PCET type mechanism stabilized by hydrogen–bonding between the heteroarene and methanol, based on the KIEs observed in our deuterated studies. A HAT mechanism cannot be ruled out and is shown. The relatively nucleophilic hydroxymethyl radical can then react readily with an electrophilic protonated heteroarene (**6.1**), leading to intermediate (**II**). Intermediate (**II**) may then be reduced by intermediate (**I'–H**), giving amino alcohol (**III**) and regenerating the ground state heterocycle (**I**, catalyst or as stoichiometric reactant). The process may also proceed via PCET based on the observed KIE in **Table 6.5**, entry 8. Intermediate **III** leads to intermediate **IV** by elimination of water, which after tautomerization, gives the methylated product (**6.2**). Under reducing conditions with *i*PrOH (**Figure 6.3**, **B**), it is likely that the intermediate (**I'–H**) becomes reduced by the incumbent ketyl radical derived from quenching with *i*PrOH. Intermediate **V** has several resonance forms under equilibrium,

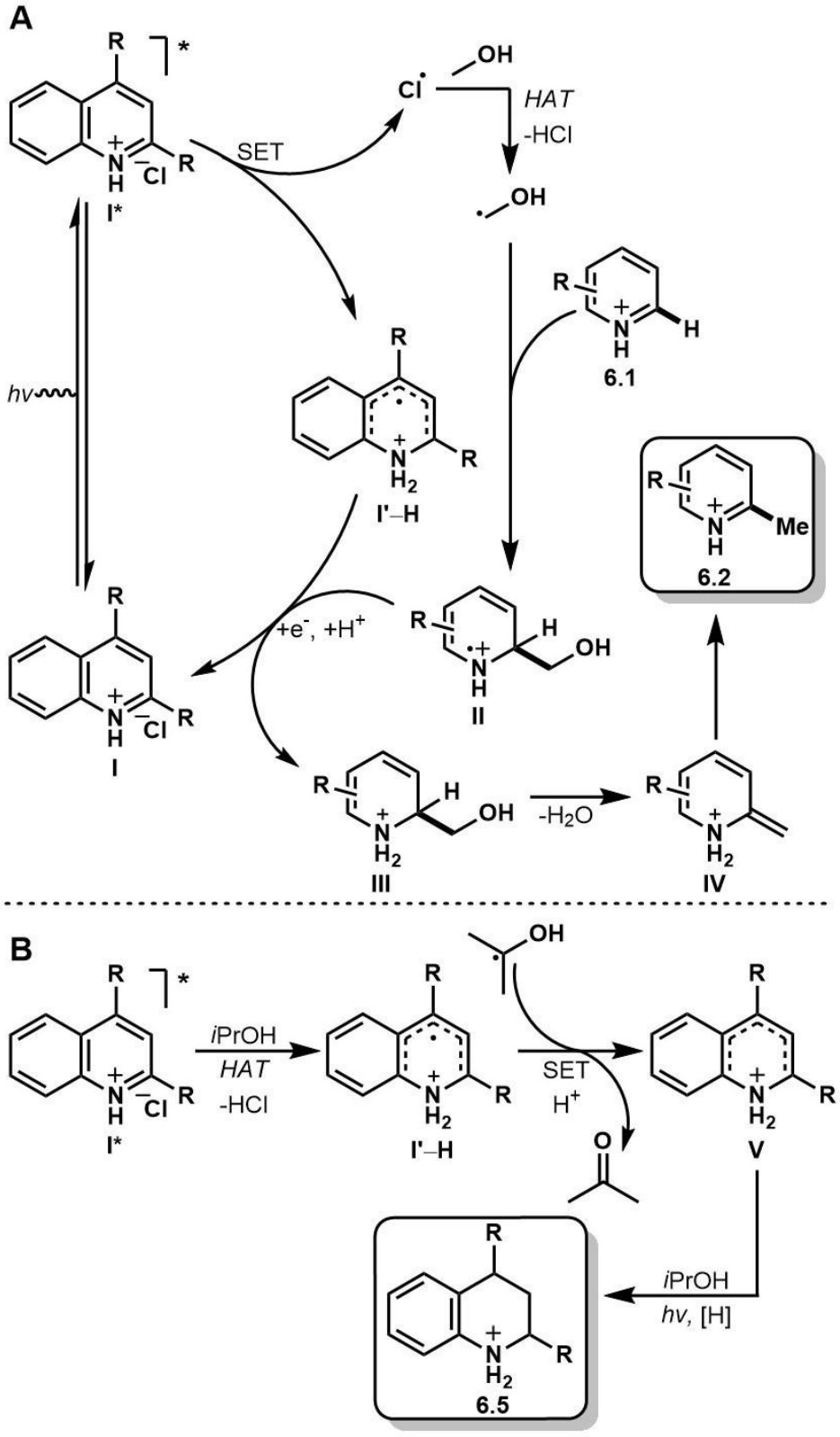

Figure 6.3 Proposed heteroarene methylation (**A**) and reduction (**B**).

which undergo exchange reactions with the broadly exchanging portion of the solvent as observed with product **d_8-5a** (**Table 6.5**, **B**, entries 1 and 3). Upon further photochemical reduction with *i*PrOH, the reduced heteroarene **6.5** is realized. The proposed mechanism is distinct from the photo-mediated reduction of halo- and selected arenes HAT mechanism in the presence of *i*PrOH.[17]

Finally, with the results and mechanistic data obtained in this study, we gathered that the methylation of heteroarenes that do not absorb in the UVA may be catalyzed by

Table 6.6 Catalytic methylation of heteroarenes.

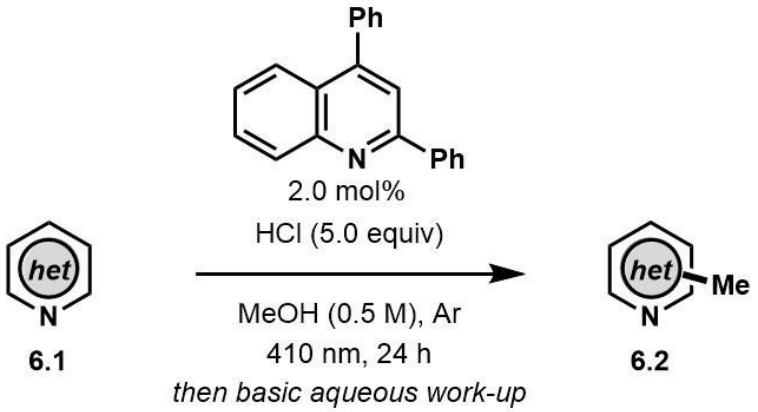

Entry	Product		Yield [%]
1	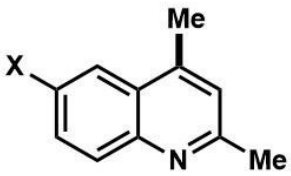	**6.2a**, X = H	57
2		**6.2b**, X = F	71
3		**6.2c**, X = Br	62
4	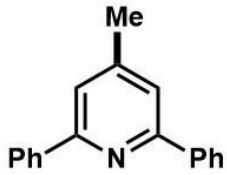 **6.2f**		90
5	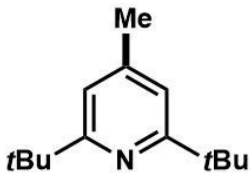 **6.2o**		71

a heteroarene such as 2,4-diphenylquinoline with 410 nm irradiation (**Table 6.6**). Gratifyingly, the transformation using 2,6-di-tertbutylpyridine was found to proceed to full conversion in 24 h using 2.0 mol% of 2,4-diphenylquinoline, yielding 71% of **6.2o**, whereas less than 10% conversion was observed in the absence of 2,4-diphenylquinoline. Other heteroarenes that were found to either undergo degradation or react poorly in the UVA mediated methodology such as quinaldines were found to be improved in this catalytic process, providing the methylated products **6.2a**–**c** in 57%, 71% and 62% yields, respectively. The improved yields highlight the advantage of employing a photocatalyst using irradiation wavelengths that avoid direct excitation of the reaction products. Finally, the photocatalytic methylation of 2,6-diphenylpyridine proceeded to give **6.2f** in 90% yield. The facile photocatalytic methylation described demonstrates the high potential for this system to have broad applicability in the alkylation of a variety of heteroarenes and will be investigated further.

6.4 Conclusions

In summary, the photochemical alkylation of quinolines, pyridines, and phenanthridine from alcohols and ethers was described. Deuterium labelling studies showed the ability to control the formation of CD_3, CD_2H, and CDH_2 products, indicating the reaction likely proceeds through an enamine intermediate. We also reported the first photochemically driven organic-mediated reduction of heteroarenes using *i*PrOH and HCl. The study also provides mechanistic insights to a complex reaction pathway and the possibility of a broadly applicable catalytic system that will be disclosed in due course.

6.5 Experimental Procedures

General Procedure 1 (GP1) – *Alkylation and Reduction of Heteroarenes*

To an 8 mL screw-topped Pyrex reaction vessel was added the heteroarene (0.4 mmol, 1.0 equiv), alcohol/ether (0.8 mL, 0.5 M) and then concentrated HCl (2.0 mmol, 5.0 equiv, 150 μL). The solution was degassed by sparging under argon for 5 minutes, sealed with parafilm, and irradiated with 2×UVA LEDs (365 nm) or 1×410 nm LEDs (depending on the absorbance profile of the protonated heterocycle) at a distance of 1 mm for 8 h. Upon completion, the solution was poured into a separatory funnel with 1 M NaOH and extracted with DCM. The combined organic extracts were dried over Na_2SO_4, filtered, and concentrated. The crude residue was further purified by flash column chromatography (0–100% EtOAc:Hex or 0–20% MeOH:DCM), where relevant fractions were combined, concentrated and characterized by proton and carbon NMR (400 and 101 MHz, respectively), HRMS, and IR.

General Procedure 2 (GP2) – *Catalytic Methylation of Heteroarenes*

To an 8 mL screw-topped Pyrex reaction vessel was added the heteroarene (0.4 mmol, 1.0 equiv), 2,4-diphenylquinoline (0.008, 2 mol%), MeOH (0.8 mL, 0.5 M) and then concentrated HCl (2.0 mmol, 5.0 equiv, 150 μL). The solution was degassed by sparging under argon for 5 minutes, sealed with parafilm, and irradiated with 1×410 nm LEDs at a distance of 1 mm for 24 h. Upon completion, the reaction mixture was purified and characterized in the same way as GP1. 2,4-diphenylquinoline was synthesized according to literature procedure.[18]

6.6 Characterization Data

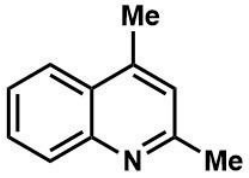

2,4-dimethylquinoline (6.2a)

Synthesized according to GP1 and characterized according to NMR comparison.[5c]

^{1}H NMR (400 MHz, $CDCl_3$): δ = 8.02 (dd, *J* = 8.4, 0.6 Hz, 1H), 7.95 (dd, *J* = 8.4, 0.6 Hz, 1H), 7.68 (ddd, *J* = 8.4, 6.9, 1.4 Hz, 1H), 7.51 (ddd, *J* = 8.2, 6.9, 1.2 Hz, 1H), 7.14 (s, 1H), 2.70 (s, 3H), 2.67 (s, 3H) ppm; **^{13}C NMR** (101 MHz, $CDCl_3$): δ = 158.7 (C), 147.7 (C), 144.1 (C), 129.2 (CH), 129.1 (CH), 126.5 (C), 125.4 (CH), 123.6 (CH), 122.7 (CH), 25.2 (CH_3), 18.6 (CH_3) ppm.

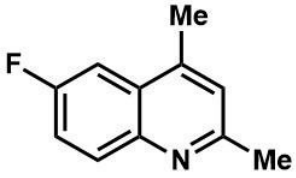

6-fluoro-2,4-dimethylquinoline (6.2b)

Synthesized according to GP1.

IR (neat, cm^{-1}): 3021(m), 2974(m), 2925(m), 1609(vs), 1509(vs), 1403(s), 1371(vs), 845(vs), 835(vs); **^{1}H NMR** (400 MHz, $CDCl_3$): δ = 8.00 (dd, *J* = 9.2, 5.5 Hz, 1H), 7.52 (dd, *J* = 9.9, 2.8 Hz, 1H), 7.43 (ddd, *J* = 9.1, 8.2, 2.8 Hz, 1H), 7.14 (s, 1H), 2.68 (s, 3H), 2.60 (s, 3H) ppm; **^{13}C NMR** (101 MHz, $CDCl_3$): δ = 159.9 (d, *J* = 246.1 Hz, CF), 157.9 (d, *J* = 2.6 Hz, C), 144.8 (C), 143.5 (d, *J* = 5.5 Hz, C), 131.4 (d, *J* = 8.8 Hz, CH), 127.2 (d, *J* = 9.2 Hz, C), 123.2 (CH), 118.9 (d, *J* = 25.7 Hz, CH), 107.2 (d, *J* = 22.4 Hz, CH), 25.0 (CH_3), 18.5 (CH_3) ppm; **HRMS** (EI): m/z calc'd for $C_{11}H_{10}FN$ [M^+] 175.0797, found 175.0797.

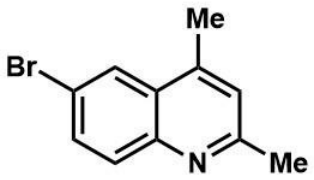

6-bromo-2,4-dimethylquinoline (6.2c)

Synthesized according to GP1 and characterized according to NMR comparison.[5c]

^{1}H NMR (400 MHz, $CDCl_3$): δ = 8.09 (d, *J* = 2.3 Hz, 1H), 7.88 (d, *J* = 8.9 Hz, 1H), 7.73 (dd, *J* = 8.9, 2.2 Hz, 1H), 7.15 (s, 1H), 2.68 (s, 3H), 2.63 (d, *J* = 0.9 Hz, 3H) ppm; **^{13}C NMR** (101 MHz, $CDCl_3$): δ = 159.2 (C), 146.3 (C), 143.3 (C), 132.4 (CH), 130.9 (CH), 127.9 (C), 126.1 (CH), 123.4 (CH), 119.3 (C), 25.2 (CH_3), 18.5 (CH_3) ppm.

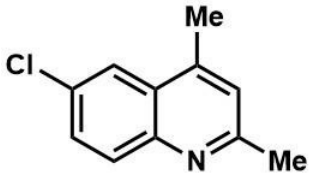

6-chloro-2,4-dimethylquinoline (6.2d)

Synthesized according to GP1.

IR (neat, cm^{-1}): 2921(m), 2853(m), 1606(vs), 1494(s), 1439(s), 1375(s), 1088(s), 872(s), 839(vs); **^{1}H NMR** (400 MHz, $CDCl_3$): δ = 7.93 (d, *J* = 8.9 Hz, 1H), 7.89 (d, *J* = 2.3 Hz, 1H), 7.59 (dd, *J* = 8.9, 2.4 Hz, 1H), 7.13 (s, 1H), 2.67 (s, 3H), 2.61 (d, *J* = 0.9 Hz, 3H) ppm; **^{13}C NMR** (101 MHz, $CDCl_3$): δ = 159.0 (C), 146.1 (C), 143.3 (C), 131.1 (C), 130.7 (CH), 129.8 (CH), 127.3 (C), 123.4 (CH), 122.7 (CH), 25.1 (CH_3), 18.5 (CH_3) ppm; **HRMS** (EI): m/z calc'd for $C_{11}H_{10}ClN$ [M^+] 191.0502, found 191.0495.

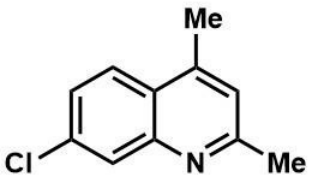

7-chloro-2,4-dimethylquinoline (6.2e)

Synthesized according to GP1.

IR (neat, cm^{-1}): 2920(m), 2855(m), 1603(vs), 1494(s), 1404(s), 898(s), 812(s); **^{1}H NMR** (400 MHz, $CDCl_3$): δ = 8.01 (d, *J* = 2.1 Hz, 1H), 7.86 (d, *J* = 8.8 Hz, 1H), 7.44 (dd, *J* = 8.9, 2.1 Hz, 1H), 7.12 (s, 1H), 2.68 (s, 3H), 2.64 (s, 3H) ppm; **^{13}C NMR** (101 MHz, $CDCl_3$): δ = 159.9 (C), 148.2 (C), 144.2 (C), 134.8 (C), 128.1 (CH), 126.3 (CH), 125.0 (C), 124.9 (CH), 122.9 (CH), 25.2 (CH_3), 18.5 (CH_3) ppm; **HRMS** (EI): m/z calc'd for $C_{11}H_{10}ClN$ [M^+] 191.0502, found 191.0513.

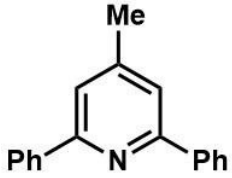

4-methyl-2,6-diphenylpyridine (6.2f)

Synthesized according to GP1 and characterized according to NMR comparison.[19]

^{1}H NMR (400 MHz, $CDCl_3$): δ = 8.18–8.14 (m, 4H), 7.54 (d, *J* = 0.8 Hz, 2H), 7.53–7.48 (m, 4H), 7.46–7.41 (m, 2H), 2.50 (s, 3H) ppm; **^{13}C NMR** (101 MHz, $CDCl_3$): δ = 156.8 (2×C), 148.3 (C), 139.6 (2×C), 128.8 (2×CH), 128.6 (4×CH), 127.0 (4×CH), 119.7 (2×CH), 21.4 (CH_3) ppm.

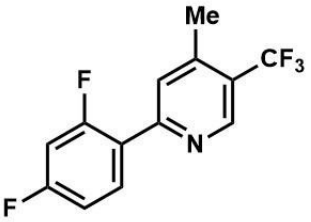

2-(2,4-difluorophenyl)-4-methyl-5-(trifluoromethyl)pyridine (6.2g)

Synthesized according to GP1.

IR (neat, cm^{-1}): 2930(m), 1600(s), 1490(m), 1323(vs), 1121(vs), 1037(s), 970(s), 849(s), 721(m); **^{1}H NMR** (400 MHz, $CDCl_3$): δ = 8.86 (s, 1H), 8.06 (td, *J* = 8.9, 6.6 Hz, 1H), 7.73–7.68 (m, 1H), 7.03 (dddd, *J* = 8.8, 7.8, 2.5, 1.0 Hz, 1H), 6.94 (ddd, *J* = 11.2, 8.6, 2.4 Hz, 1H), 2.56 (d, *J* = 1.0 Hz, 3H) ppm; **^{13}C NMR** (101 MHz, $CDCl_3$): δ = 163.8 (dd, *J* = 252.4, 12.5 Hz, CF), 160.8 (dd, *J* = 253.1, 11.7 Hz, CF), 155.5 (C), 146.7 (C), 146.6 (q, *J* = 5.9 Hz, CH), 132.4 (dd, *J* = 9.9, 4.0 Hz, CH), 126.5 (d, *J* = 10.3 Hz, CH), 124.0 (q, *J* = 273.6 Hz, CF_3), 123.9 (q, *J* = 30.1 Hz, C), 122.5 (dd, *J* = 11.7, 3.7 Hz, C), 112.1 (dd, *J* = 21.3, 3.7 Hz, CH), 104.5 (dd, *J* = 27.1, 25.7 Hz, CH), 19.2 (dd, *J* = 3.7, 1.5 Hz, CH_3) ppm; **HRMS** (EI): m/z calc'd for $C_{13}H_8F_5N$ [M^+] 273.0577, found 273.0578.

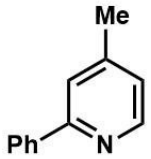

4-methyl-2-phenylquinoline (6.2h)

Synthesized according to GP1 and characterized according to NMR comparison (containing 20% SM not separable by column chromatography).[5c]

^{1}H NMR (400 MHz, $CDCl_3$): δ = 8.53 (d, *J* = 5.0 Hz, 1H), 8.00–7.93 (m, 2H), 7.53 (dt, *J* = 1.5, 0.7 Hz, 1H), 7.48–7.41 (m, 2H), 7.41–7.35 (m, 1H), 7.04 (ddd, *J* = 5.0, 1.6, 0.7 Hz, 1H), 2.40 (s, 3H) ppm; **^{13}C NMR** (101 MHz, $CDCl_3$): δ = 157.4 (C), 149.4 (CH), 147.7 (C), 139.5 (C), 128.8 (CH), 128.6 (2×CH), 126.9 (2×CH), 123.1 (CH), 121.5 (CH), 21.2 (CH_3) ppm.

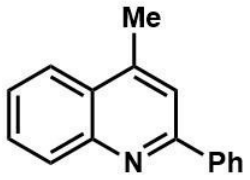

4-methyl-2-phenylquinoline (6.2i)

Synthesized according to GP1 and characterized according to NMR comparison.[5c]

^{1}H NMR (400 MHz, $CDCl_3$): δ = 8.21–8.14 (m, 3H), 8.02 (dd, *J* = 8.4, 1.0 Hz, 1H), 7.76–7.71 (m, 2H), 7.59–7.51 (m, 3H), 7.50–7.44 (m, 1H), 2.79 (d, *J* = 0.8 Hz, 3H) ppm; **^{13}C NMR** (101 MHz, $CDCl_3$): δ = 157.1 (C), 148.2 (C), 144.8 (C), 139.9 (C), 130.3 (CH), 129.3 (CH), 129.2 (CH), 128.8 (2×CH), 127.5 (2×CH), 127.3 (C), 126.0 (CH), 123.6 (CH), 119.8 (CH), 19.0 (CH_3) ppm.

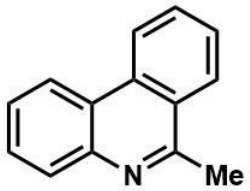

6-methylphenanthridine (6.2j)

Synthesized according to GP1 and characterized according to NMR comparison.[5c]

^{1}H NMR (400 MHz, $CDCl_3$): δ = 8.62–8.56 (m, 1H), 8.51 (dd, *J* = 8.2, 1.4 Hz, 1H), 8.18 (dd, *J* = 8.2, 1.4 Hz, 1H), 8.11 (dd, *J* = 8.0, 1.0 Hz, 1H), 7.81 (ddd, *J* = 8.3, 7.1, 1.3 Hz, 1H), 7.71 (ddd, *J* = 8.2, 7.0, 1.5 Hz, 1H), 7.67 (ddd, *J* = 8.1, 7.0, 1.2 Hz, 1H), 7.61 (ddd, *J* = 8.2, 7.1, 1.4 Hz, 1H), 3.03 (s, 3H) ppm; **^{13}C NMR** (101 MHz, $CDCl_3$): δ = 158.8 (C), 143.7 (C), 132.5 (C), 130.4 (CH), 129.3 (CH), 128.5 (CH), 127.2 (CH), 126.4 (CH), 126.2 (CH), 125.8 (C), 123.7 (C), 122.2 (CH), 121.9 (CH), 23.3 (CH_3) ppm.

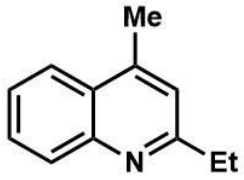

2-ethyl-4-methylquinoline (6.2k)

Synthesized according to GP1 and characterized according to NMR comparison.[20]

^{1}H NMR (400 MHz, $CDCl_3$): δ = 8.09–8.02 (m, 1H), 7.96 (dd, *J* = 8.3, 1.1 Hz, 1H), 7.68 (ddd, *J* = 8.4, 6.9, 1.4 Hz, 1H), 7.51 (ddd, *J* = 8.3, 6.9, 1.3 Hz, 1H), 7.19–7.15 (m, 1H), 2.97 (q, *J* = 7.6 Hz, 2H), 2.69 (d, *J* = 1.0 Hz, 3H), 1.40 (t, *J* = 7.7 Hz, 3H) ppm; **^{13}C NMR** (101 MHz, $CDCl_3$): δ = 163.7 (C), 147.7 (C), 144.3 (C), 129.4 (CH), 129.0 (CH), 126.8 (C), 125.4 (CH), 123.6 (CH), 121.5 (CH), 32.2 (CH_2), 18.7 (CH_3), 14.0 (CH_3) ppm.

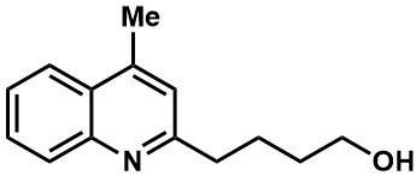

4-(4-methylquinolin-2-yl)butan-1-ol (6.2l)

Synthesized according to GP1.

IR (neat, cm^{-1}): 3286(br), 2932(m), 2862(m), 1604(s), 1062(m), 780(s); **^{1}H NMR** (400 MHz, $CDCl_3$): δ = 8.03 (d, *J* = 8.4 Hz, 1H), 7.95 (d, *J* = 8.2 Hz, 1H), 7.67 (td, *J* = 7.1, 1.2 Hz, 1H), 7.51 (td, *J* = 7.3, 1.2 Hz, 1H), 7.14 (s, 1H), 3.71 (t, *J* = 6.3 Hz, 2H), 3.14 (br. s., 1H), 2.98 (t, *J* = 7.4 Hz, 2H), 2.67 (s, 3H), 1.94 (quin, *J* = 7.1 Hz, 2H), 1.70 (quin, *J* = 7.1 Hz, 2H) ppm; **^{13}C NMR** (101 MHz, $CDCl_3$): δ = 162.2 (C), 147.4 (C), 144.5 (C), 129.2 (CH), 129.1 (CH), 126.8 (C), 125.5 (CH), 123.6 (CH), 122.2 (CH), 62.1 (CH_2), 38.1 (CH_2), 32.2 (CH_2), 25.4 (CH_2), 18.7 (CH_3) ppm; **HRMS** (EI): m/z calc'd for $C_{14}H_{17}NO$ [M^+] 215.1310, found 215.1301.

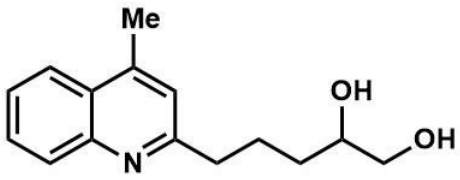

5-(4-methylquinolin-2-yl)pentane-1,2-diol (6.2m)

Synthesized according to GP1.

IR (neat, cm^{-1}): 3390(br), 2926(m), 2863(m), 1604(s), 1449(m), 1056(s), 760(vs); **^{1}H NMR** (400 MHz, $CDCl_3$): δ = 8.03 (dd, *J* = 8.4, 0.6 Hz, 1H), 7.96 (dd, *J* = 8.3, 0.9 Hz, 1H), 7.68 (ddd, *J* = 8.4, 6.9, 1.4 Hz, 1H), 7.52 (ddd, *J* = 8.3, 7.0, 1.2 Hz, 1H), 7.14 (d, *J* = 0.6 Hz, 1H), 3.78 (m, 1H), 3.69–3.61 (m, 1H), 3.53–3.47 (m, 1H), 3.01 (t, *J* = 7.1 Hz, 2H), 2.68 (d, *J* = 0.9 Hz, 3H), 1.99 (quin, *J* = 7.2 Hz, 2H), 1.60–1.53 (m, 2H) ppm; **^{13}C NMR** (101 MHz, $CDCl_3$): δ = 161.8 (C), 147.1 (C), 144.9 (C), 129.3 (CH), 128.8 (CH), 126.8 (C), 125.7 (CH), 123.6 (CH), 122.3 (CH), 71.4 (CH), 66.9 (CH_2), 37.7 (CH_2), 32.4 (CH_2), 24.6 (CH_2), 18.7 (CH_3) ppm; **HRMS** (EI): m/z calc'd for $C_{15}H_{19}NO_2$ [M^+] 245.1416, found 245.1408.

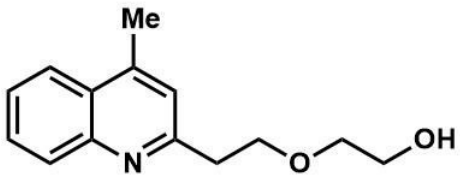

2-(2-(4-methylquinolin-2-yl)ethoxy)ethan-1-ol (6.2n)

Synthesized according to GP1.

IR (neat, cm^{-1}): 3352(br), 2918(m), 2861(m), 1604(m), 1120(vs), 1060(m), 761(s); **^{1}H NMR** (400 MHz, $CDCl_3$): δ = 8.09 (d, *J* = 8.4 Hz, 1H), 7.96 (d, *J* = 8.2 Hz, 1H), 7.68 (ddd, *J* = 8.1, 7.0, 1.2 Hz, 1H), 7.52 (ddd, *J* = 8.2, 7.0, 1.2 Hz, 1H), 7.17 (s, 1H), 4.28 (br. s., 1H), 4.03 (t, *J* = 6.1 Hz, 2H), 3.77–3.73 (m, 2H), 3.69–3.65 (m, 2H), 3.22 (t, *J* = 6.1 Hz, 2H), 2.68 (s, 3H) ppm; **^{13}C NMR** (101 MHz, $CDCl_3$): δ = 159.3 (C), 147.5 (C), 144.7 (C), 129.3 (CH), 129.1 (CH), 126.9 (C), 125.7 (CH), 123.6 (CH), 122.6 (CH), 72.0 (CH_2), 69.3 (CH_2), 61.8 (CH_2), 38.5 (CH_2), 18.6 (CH_3) ppm; **HRMS** (EI): m/z calc'd for $C_{14}H_{17}NO_2$ [M^+-C_2H_5O] 186.0919, found 186.0923.

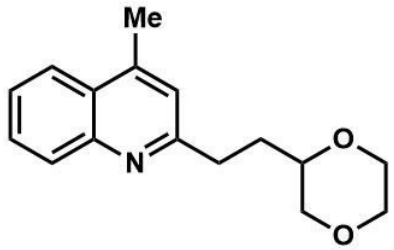

2-(2-(1,4-dioxan-2-yl)ethyl)-4-methylquinoline (6.2n')

Synthesized according to GP1.

IR (neat, cm^{-1}): 2957(m), 2916(m), 2850(m), 1603(s), 1122(vs), 760(m); **^{1}H NMR** (400 MHz, $CDCl_3$): δ = 8.00 (d, *J* = 7.8 Hz, 1H), 7.93 (dd, *J* = 8.4, 0.8 Hz, 1H), 7.65 (ddd, *J* = 8.4, 6.9, 1.4 Hz, 1H), 7.49 (ddd, *J* = 8.2, 6.9, 1.2 Hz, 1H), 7.13 (s, 1H), 3.81–3.66 (m, 4H), 3.64–3.55 (m, 2H), 3.32 (dd, *J* = 11.3, 10.0 Hz, 1H), 3.12–3.01 (m, 1H), 2.99–2.89 (m, 1H), 2.65 (d, *J* = 0.8 Hz, 3H), 1.93–1.84 (m, 2H) ppm; **^{13}C NMR** (101 MHz, $CDCl_3$): δ = 161.5 (C), 147.8 (C), 144.4 (C), 129.4 (CH), 129.1 (CH), 126.8 (C), 125.5 (CH), 123.6 (CH), 122.1 (CH), 74.8 (CH), 71.3 (CH_2), 66.8 (CH_2), 66.5 (CH_2), 34.3 (CH_2), 31.4 (CH_2), 18.7 (CH_3) ppm; **HRMS** (EI): m/z calc'd for $C_{16}H_{19}NO_2$ [M^+] 257.1416, found 257.1419.

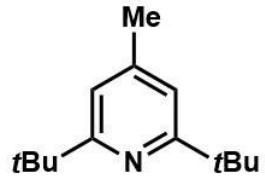

2,6-di-tert-butyl-4-methylpyridine (6.2o)

Synthesized according to GP1 and characterized according to NMR comparison.[21]

^{1}H NMR (400 MHz, $CDCl_3$): δ = 6.92 (d, *J* = 0.6 Hz, 2H), 2.33–2.30 (m, 3H), 1.34 (s, 18H) ppm; **^{13}C NMR** (101 MHz, $CDCl_3$): δ = 167.4 (2×C), 146.4 (C), 116.2 (2×CH), 37.4 (2×C), 30.1 (6×CH_3), 21.5 (CH_3) ppm.

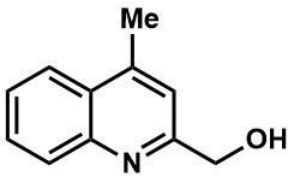

(4-methylquinolin-2-yl)methanol (6.3a)

Synthesized according to GP1 and characterized according to NMR comparison.[22]

^{1}H NMR (400 MHz, $CDCl_3$): δ = 8.08 (d, *J* = 8.4 Hz, 1H), 7.99 (dd, *J* = 8.3, 1.0 Hz, 1H), 7.72 (ddd, *J* = 8.4, 6.9, 1.4 Hz, 1H), 7.61–7.54 (m, 1H), 7.13 (s, 1H), 4.88 (s, 2H), 4.50 (br. s., 1H), 2.71 (d, *J* = 0.8 Hz, 3H) ppm; **^{13}C NMR** (101 MHz, $CDCl_3$): δ = 158.5 (C), 146.5 (C), 145.0 (C), 129.4 (CH), 129.2 (CH), 127.6 (C), 126.1 (CH), 123.8 (CH), 118.9 (CH), 64.0 (CH_2), 18.8 (CH_3) ppm.

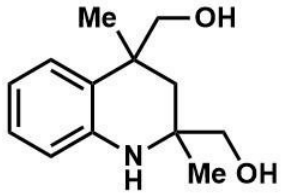

(2,4-dimethyl-1,2,3,4-tetrahydroquinoline-2,4-diyl)dimethanol (6.4a, *d.r.* 2:1)

Synthesized according to GP1.

IR (neat, cm^{-1}): 3355(br), 2960(m), 2929(m), 2860(m), 1604(m), 1482(s), 1312(m), 1030(vs), 752(vs);

Major: ^{1}H NMR (400 MHz, $CDCl_3$): δ = 7.19–7.13 (m, 1H), 7.06–6.99 (m, 1H), 6.77–6.72 (m, 1H), 6.58–6.54 (m, 1H), 3.65–3.36 (m, 4H), 2.02 (d, *J* = 14.1 Hz, 1H), 1.60 (d, *J* = 14.1 Hz, 1H), 1.31 (s, 3H), 1.27 (s, 3H) ppm; **^{13}C NMR** (101 MHz, $CDCl_3$): δ = 144.1 (C), 127.4 (CH), 126.5 (C), 126.4 (CH), 118.4 (CH), 115.6 (CH), 71.4 (CH_2), 68.9 (CH_2), 53.0 (C), 40.6 (CH_2), 37.5 (C), 26.5 (CH_3), 26.1 (CH_3) ppm;

Minor: ^{1}H NMR (400 MHz, $CDCl_3$): δ = 7.19–7.13 (m, 1H), 7.06–6.99 (m, 1H), 6.77–6.72 (m, 1H), 6.58–6.54 (m, 1H), 3.65–3.36 (m, 4H), 2.30 (d, *J* = 14.1 Hz, 1H), 1.41 (d, *J* = 14.1 Hz, 1H), 1.35 (s, 3H), 1.23 (s, 3H) ppm; **^{13}C NMR** (101 MHz, $CDCl_3$): δ = 143.9 (C), 127.3 (CH), 126.4 (C), 126.3 (CH), 118.4 (CH), 115.7 (CH), 71.6 (CH_2), 70.9 (CH_2), 53.2 (C), 39.1 (CH_2), 37.4 (C), 27.0 (CH_3), 26.1 (CH_3) ppm;

HRMS (EI): m/z calc'd for $C_{13}H_{19}NO_2$ [M^+] 221.1416, found 221.1432.

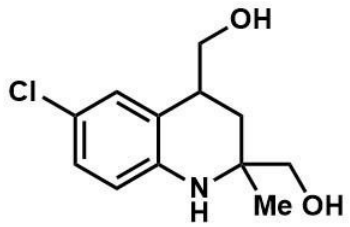

(6-chloro-2-methyl-1,2,3,4-tetrahydroquinoline-2,4-diyl)dimethanol (6.4d, *d.r.* 85:15)

Synthesized according to GP1.

IR (neat, cm^{-1}): 3339(br), 2967(m), 2927(m), 2874(m), 1602(m), 1487v(s), 1301(m), 1034(s), 812(s); **^{1}H NMR** (400 MHz, $CDCl_3$): δ = 7.21 (dd, *J* = 2.4, 1.0 Hz, 1H, minor), 7.18 (dd, *J* = 2.4, 1.0 Hz, 1H, major), 7.03–6.93 (m, 1H), 6.51–6.45 (m, 1H), 4.03–3.89 (m, 2H), 3.87 (br. s., 1H), 3.52–3.42 (m, 2H), 3.06 (sxt, *J* = 5.6 Hz, 1H, minor), 2.95 (sxt, *J* = 5.7 Hz, 1H, major), 2.02 (dd, *J* = 13.5, 6.1 Hz, 1H), 1.77 (br. s., 1H), 1.68 (dd, *J* = 13.5, 11.5 Hz, 1H), 1.58 (br. s., 1H), 1.28 (s, 3H) ppm; **^{13}C NMR** (101 MHz, $CDCl_3$): δ = 142.9 (C), 127.3 (CH), 126.6 (CH), 122.5 (C), 122.1 (C), 116.1 (CH), 68.0 (CH_2), 65.5 (CH_2), 52.5 (C), 35.3 (CH), 33.9 (CH_2), 26.0 (CH_3) ppm; **HRMS** (EI): m/z calc'd for $C_{12}H_{16}ClNO_2$ [M^+] 241.0870, found 241.0853.

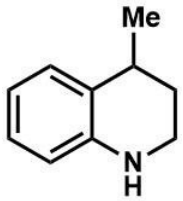

4-methyl-1,2,3,4-tetrahydroquinoline (6.5a)

Synthesized according to GP1 and characterized according to NMR comparison (containing ~10% of impurities not separable by column chromatography).[23]

^{1}H NMR (400 MHz, $CDCl_3$): δ = 7.07 (d, *J* = 7.6 Hz, 1H), 7.00–6.94 (m, 1H), 6.64 (td, *J* = 7.4, 1.2 Hz, 1H), 6.49 (dd, *J* = 8.0, 1.0 Hz, 1H), 3.87 (br. s., 1H), 3.39–3.20 (m, 2H), 2.93 (sxt, *J* = 6.4 Hz, 1H), 2.05–1.95 (m, 1H), 1.75–1.65 (m, 1H), 1.30 (d, *J* = 7.1 Hz, 3H) ppm; **^{13}C NMR** (101 MHz, $CDCl_3$): δ = 144.2 (C), 128.4 (CH), 126.7 (CH), 126.6 (C), 116.9 (CH), 114.1 (CH), 39.0 (CH_2), 30.2 (CH), 29.9 (CH_2), 22.6 (CH_3) ppm.

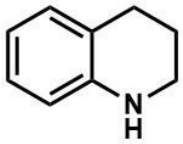

1,2,3,4-tetrahydroquinoline (6.5b)

Synthesized according to GP1 and characterized according to NMR comparison.[23]

^{1}H NMR (400 MHz, $CDCl_3$): δ = 7.03–6.92 (m, 2H), 6.61 (td, *J* = 7.4, 1.1 Hz, 1H), 6.53–6.44 (m, 1H), 3.83 (br. s., 1H), 3.38–3.25 (m, 2H), 2.78 (t, *J* = 6.5 Hz, 2H), 2.01–1.91 (m, 2H) ppm; **^{13}C NMR** (101 MHz, $CDCl_3$): δ = 144.7 (C), 129.5 (CH), 126.7 (CH), 121.4 (C), 116.9 (CH), 114.2 (CH), 42.0 (CH_2), 26.9 (CH_2), 22.2 (CH_2) ppm.

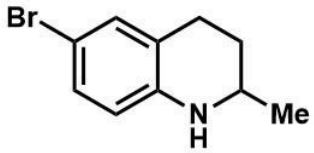

6-bromo-2-methyl-1,2,3,4-tetrahydroquinoline (6.5c)

Synthesized according to GP1 and characterized according to NMR comparison.[24]

^{1}H NMR (400 MHz, $CDCl_3$): δ = 7.10–7.00 (m, 2H), 6.35 (d, *J* = 8.4 Hz, 1H), 3.72 (br. s., 1H), 3.39 (dtq, *J* = 9.7, 6.4, 3.3 Hz, 1H), 2.81 (ddd, *J* = 16.7, 11.3, 5.6 Hz, 1H), 2.75–2.65 (m, 1H), 1.98–1.85 (m, 1H), 1.55 (dddd, *J* = 12.9, 11.4, 9.9, 5.3 Hz, 1H), 1.21 (d, *J* = 6.3 Hz, 3H) ppm; **^{13}C NMR** (101 MHz, $CDCl_3$): δ = 143.7 (C), 131.6 (CH), 129.3 (CH), 123.1 (C), 115.3 (CH), 108.3 (C), 47.1 (CH), 29.6 (CH_2), 26.4 (CH_2), 22.4 (CH_3) ppm.

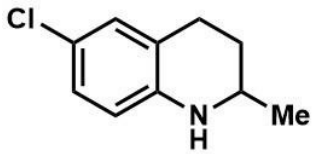

6-chloro-2-methyl-1,2,3,4-tetrahydroquinoline (6.5d)

Synthesized according to GP1 and characterized according to NMR comparison.[25]

^{1}H NMR (400 MHz, $CDCl_3$): δ = 6.98–6.86 (m, 2H), 6.39 (d, *J* = 8.4 Hz, 1H), 3.71 (br. s., 1H), 3.39 (dqd, *J* = 9.6, 6.4, 2.8 Hz, 1H), 2.88–2.64 (m, 2H), 1.98–1.88 (m, 1H), 1.56 (dddd, *J* = 12.9, 11.4, 10.0, 5.3 Hz, 1H), 1.22 (d, *J* = 6.4 Hz, 3H) ppm; **^{13}C NMR** (101 MHz, $CDCl_3$): δ = 143.3 (C), 128.8 (CH), 126.4 (CH), 122.6 (C), 121.2 (C), 114.9 (CH), 47.1 (CH), 29.7 (CH_2), 26.4 (CH_2), 22.4 (CH_3) ppm.

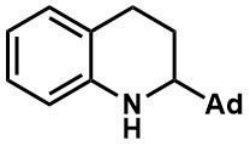

2-((1s,3s)-adamantan-1-yl)-1,2,3,4-tetrahydroquinoline (6.5e)

Synthesized according to GP1.

IR (neat, cm^{-1}): 3426(br), 2903(vs), 2847(m), 1482(m), 744(m); **^{1}H NMR** (400 MHz, $CDCl_3$): δ = 6.97–6.87 (m, 2H), 6.55 (td, *J* = 7.3, 1.0 Hz, 1H), 6.47 (d, *J* = 7.9 Hz, 1H), 3.83 (br. s., 1H), 2.83–2.66 (m, 3H), 2.01 (m, 3H), 1.97–1.92 (m, 1H), 1.76–1.54 (m, 13H) ppm; **^{13}C NMR** (101 MHz, $CDCl_3$): δ = 145.5 (C), 128.9 (CH), 126.7 (CH), 121.6 (C), 116.6 (CH), 114.0 (CH), 61.1 (CH), 38.3 (3×CH_2), 37.3 (3×CH_2), 35.2 (C), 28.5 (3×CH), 27.4 (CH_2), 21.7 (CH_2) ppm; **HRMS** (EI): m/z calc'd for $C_{19}H_{25}N$ [M^+] 267.1987, found 267.2019.

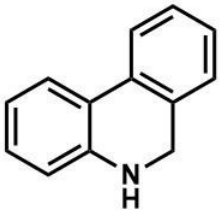

5,6-dihydrophenanthridine (6.5f)

Synthesized according to GP1 and characterized according to NMR comparison.[23]

^{1}H NMR (400 MHz, $CDCl_3$): δ = 7.75–7.64 (m, 2H), 7.32 (td, *J* = 7.6, 1.4 Hz, 1H), 7.22 (td, *J* = 7.4, 1.3 Hz, 1H), 7.16–7.06 (m, 2H), 6.85 (td, *J* = 7.5, 1.2 Hz, 1H), 6.68 (dd, *J* = 7.9, 1.0 Hz, 1H), 4.41 (s, 2H), 3.99 (br. s., 1H) ppm; **^{13}C NMR** (101 MHz, $CDCl_3$): δ = 145.7 (C), 132.7 (C), 132.1 (C), 128.8 (CH), 127.6 (CH), 127.1 (CH), 126.0 (CH), 123.6 (CH), 122.4 (CH), 122.1 (C), 119.3 (CH), 115.1 (CH), 46.4 (CH_2) ppm.

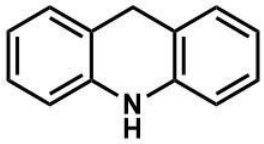

9,10-dihydroacridine (6.5g)

Synthesized according to GP1 and characterized according to NMR comparison.[23]

^{1}H NMR (400 MHz, $CDCl_3$): δ = 7.15–7.06 (m, 4H), 6.88 (td, *J* = 7.4, 1.1 Hz, 2H), 6.68 (dd, *J* = 7.9, 0.8 Hz, 2H), 5.96 (br. s., 1H), 4.08 (s, 2H) ppm; **^{13}C NMR** (101 MHz, $CDCl_3$): δ = 140.1 (2×C), 128.6 (2×CH), 127.0 (2×CH), 120.6 (2×CH), 120.0 (2×C), 113.4 (2×CH), 31.4 (CH_2) ppm.

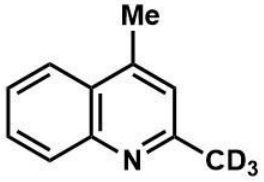

2-[$^{2}H_3$]-methyl-4-methylquinoline (d_3-6.2a)

Synthesized according to GP1.

IR (neat, cm^{-1}): 3061(m), 2923(m), 1603(s), 1561(m), 756(vs); **^{1}H NMR** (600 MHz, $CDCl_3$): δ = 8.02 (dd, *J* = 8.4, 0.6 Hz, 1H), 7.94 (dd, *J* = 8.3, 1.1 Hz, 1H), 7.67 (ddd, *J* = 8.3, 6.9, 1.5 Hz, 1H), 7.50 (ddd, *J* = 8.3, 6.9, 1.2 Hz, 1H), 7.13 (d, *J* = 0.9 Hz, 1H), 2.66 (d, *J* = 0.9 Hz, 3H) ppm; **^{13}C NMR** (151 MHz, $CDCl_3$): δ = 158.6 (C), 147.7 (C), 144.1 (C), 129.1 (CH), 129.1 (CH), 126.5 (C), 125.4 (CH), 123.5 (CH), 122.7 (CH), 24.4 (spt, *J* = 19.6 Hz, CD_3), 18.5 (CH_3) ppm (CD_3 observed in spectrum when using 30° pulse and 30 second interpulse delay); **HRMS** (EI): m/z calc'd for $C_{11}H_9D_2N$ [M^+] 160.1080, found 160.1087.

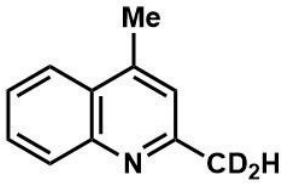

2-[$^2H_2$]-methyl-4-methylquinoline (d_2-6.2a)

Synthesized according to GP1.

IR (neat, cm^{-1}): 3062(m), 2924(m), 1603(s), 1561(m), 756(vs); **^{1}H NMR** (400 MHz, $CDCl_3$): δ = 8.02 (dd, *J* = 8.4, 0.6 Hz, 1H), 7.94 (d, *J* = 8.4 Hz, 1H), 7.67 (ddd, *J* = 8.2, 7.1, 1.2 Hz, 1H), 7.50 (ddd, *J* = 8.2, 7.1, 1.2 Hz, 1H), 7.13 (s, 1H), 2.66 (s, 4H) ppm; **^{13}C NMR** (101 MHz, $CDCl_3$): δ = 158.6 (C), 147.7 (C), 144.1 (C), 129.1 (CH), 129.0 (CH), 126.5 (C), 125.4 (CH), 123.5 (CH), 122.7 (CH), 24.7 (quin, *J* = 19.5 Hz, CD_2H), 18.5 (CH_3) ppm; **HRMS** (EI): m/z calc'd for $C_{11}H_9D_2N$ [M^+] 159.1017, found 159.1024.

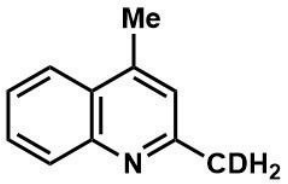

2-[^{2}H]-methyl-4-methylquinoline (d-6.2a)

Synthesized according to GP1.

IR (neat, cm^{-1}): 3060(m), 2923(m), 1602(s), 1561(m), 756(vs); **^{1}H NMR** (400 MHz, $CDCl_3$): δ = 8.03 (dd, *J* = 8.4, 0.6 Hz, 1H), 7.94 (d, *J* = 8.4 Hz, 1H), 7.67 (ddd, *J* = 8.3, 7.0, 1.2 Hz, 1H), 7.50 (ddd, *J* = 8.2, 7.1, 1.0 Hz, 1H), 7.13 (s, 1H), 2.69–2.67 (m, 2H), 2.66 (s, 3H) ppm; **^{13}C NMR** (101 MHz, $CDCl_3$): δ = 158.6 (C), 147.7 (C), 144.1 (C), 129.1 (CH), 129.0 (CH), 126.5 (C), 125.4 (CH), 123.5 (CH), 122.7 (CH), 24.9 (t, *J* = 19.5 Hz, CDH_2), 18.5 (CH_3) ppm; **HRMS** (EI): m/z calc'd for $C_{11}H_{10}DN$ [M^+] 158.0954, found 158.0984.

Kinetic Isotope Effect Experiments

For kinetic isotope effect experiments (KIE) varying the solvent, the reaction was setup in the same way using a 1:1 mixture of CH_3OH:CD_3OH, where the reaction produced a 65:35 mixture of **6.2a**:**d$_2$-6.2a**, indicating a KIE of 1.86 (see spectrum on page 76). For the KIE study conducted using **6.1a** and **d-6.1a**, the synthesis of **d-6.1a** was as follows:

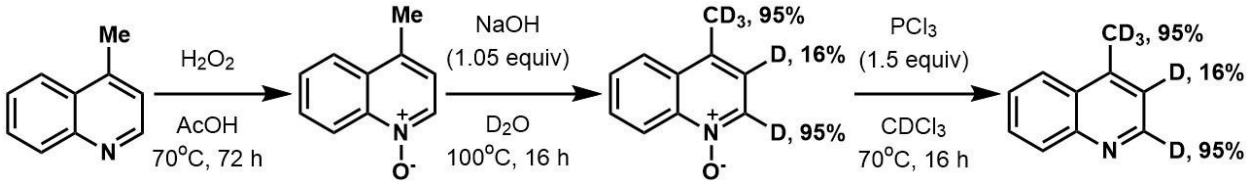

Scheme 6.1 Synthesis of a deuterated lepidine analog.

The corresponding lepidine *N*-oxide was formed using literature procedure.[26] The resulting compound was treated under basic conditions (NaOH, 1.05 equiv) in D_2O following literature procedure.[27] The resulting product was then reduced using PCl_3 following literature procedures,[28] affording the corresponding deuterated lepidine **d-6.1a** (95% D at C2, 16% D at C3, 95% CD_3 at Me, shown in top spectrum of **Figure 6.4**). The compound was partitioned (51:49, **6.1a**:**d-6.1a**, middle spectrum of **Figure 6.4**) and the optimized reaction conditions were applied. When the reaction was not complete (~70% conversion) the reaction was stopped and the ratio of starting materials remaining were analyzed. It was found that the starting material remaining was a 37:63 mixture of **6.1a**:**d-6.1a**, indicating that **6.1a** reacted faster than its deuterated counterpart, and can be calculated by comparison of ratio of starting materials converted to product followed by accounting for initial ratio, giving a KIE of 1.77 (bottom spectrum of **Figure 6.4**, (63/37)×(51/49)).

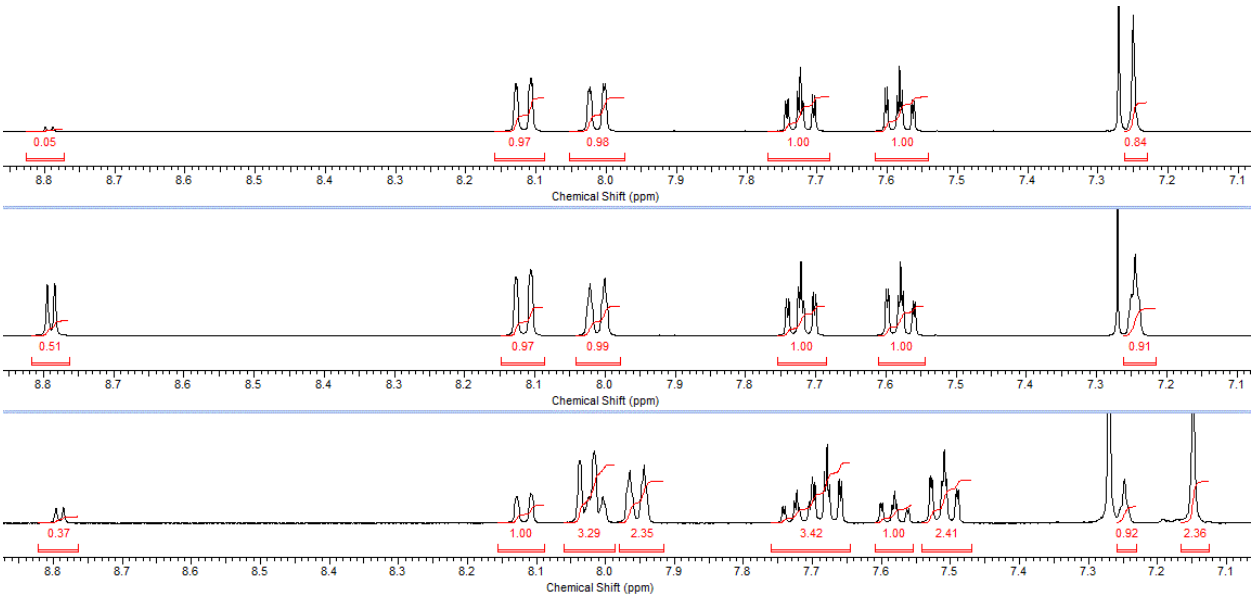

Figure 6.4 KIE study between **6.1a**:**d-6.1a** under optimized conditions.

Steady-State Fluorescence Quenching of Lepidine

The fluorescence emission measurements required for the lepidine singlet quenching experiments were carried out in a Photon Technology International (PTI) spectrofluorimeter at room temperature using 1 × 1 cm^2 quartz cuvettes. Samples of lepidine were prepared with a final absorbance of 0.3 at 340 nm, the wavelength employed for excitation, in 2 M HCl in MeCN. The MeOH solution used in the quenching studies were also prepared with HCl (2 M) and with lepidine with an absorbance of 0.3 at 340 nm to ensure that any observed quenching was not due to the dilution of lepidine.

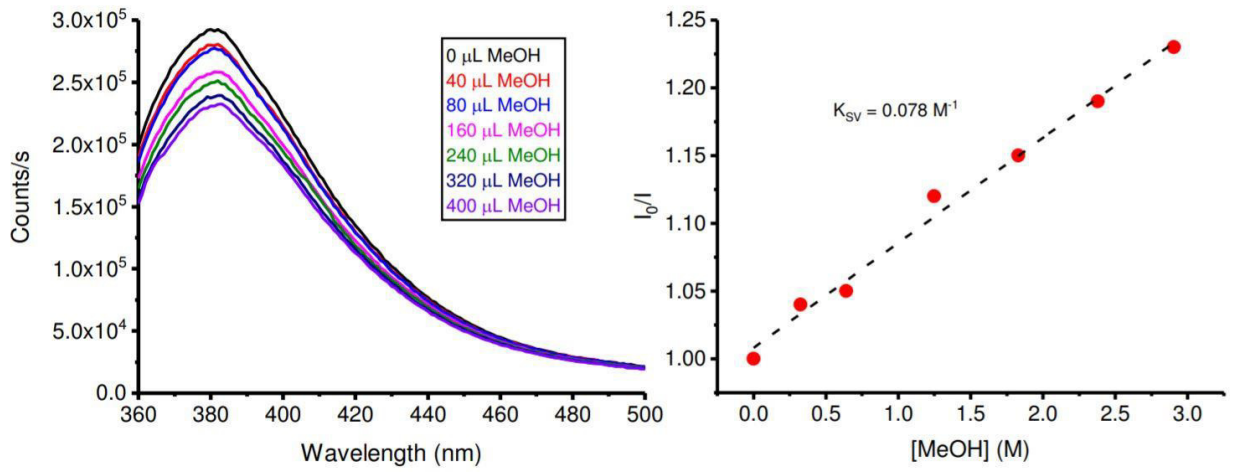

Figure 6.5 Data for the steady-state quenching experiments of lepidine by MeOH in 2 M HCl in H_2O. Quenching of the emission of lepidine upon increasing concentrations of MeOH (Left). Corresponding Stern-Volmer plot (Right).

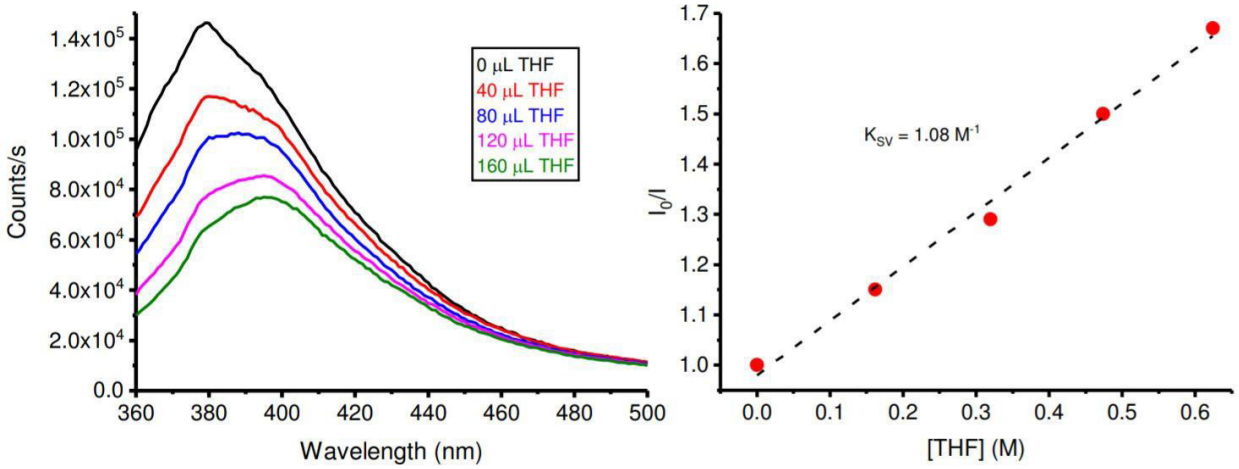

Figure 6.6 Data for the steady-state quenching experiments of lepidine by THF in 2 M HCl in MeCN. Quenching of the emission of lepidine upon increasing concentrations of THF (Left). Corresponding Stern-Volmer plot (Right).

Intermittent Illumination Experimental

Typically, lepidine (0.4 mmol, 1.0 equiv), MeOH (0.8 mL) and then concentrated HCl (2.0 mmol, 5.0 equiv) was added to a 3 mL quartz cuvette fitted with a septum. The reaction mixture was then degassed with argon for 15 minutes before it was intermittently irradiated at 70°C for 30 minutes (total light on time) using a pulsed 365 nm LED, which was powered by a constant current driver (designed and built in house) and controlled by a digital delay/pulse generator (Stanford Research System Inc.- MODEL DG535). In all

cases the system was interfaced with an oscilloscope (Tektronix–MODEL TDS3052), which monitored the delivered voltage and resulting current of the system. The system was also interfaced with a photodiode, which allowed the shape and duration of the light pulse emitted from the LED to be monitored along with real time monitoring of the light pulse to ensure that the appropriate light on:light off ratio was being employed. A light on:light off ratio of 1:2 was used in all trials, and the length of the on and off times were increased proportionally with each successive trial. After irradiation, the solution was poured into a separatory funnel with 1 M NaOH and extracted with DCM. The combined organic extracts were dried over Na_2SO_4, filtered, and concentrated. Yield were determined by ^1H NMR using mesitylene as standard.

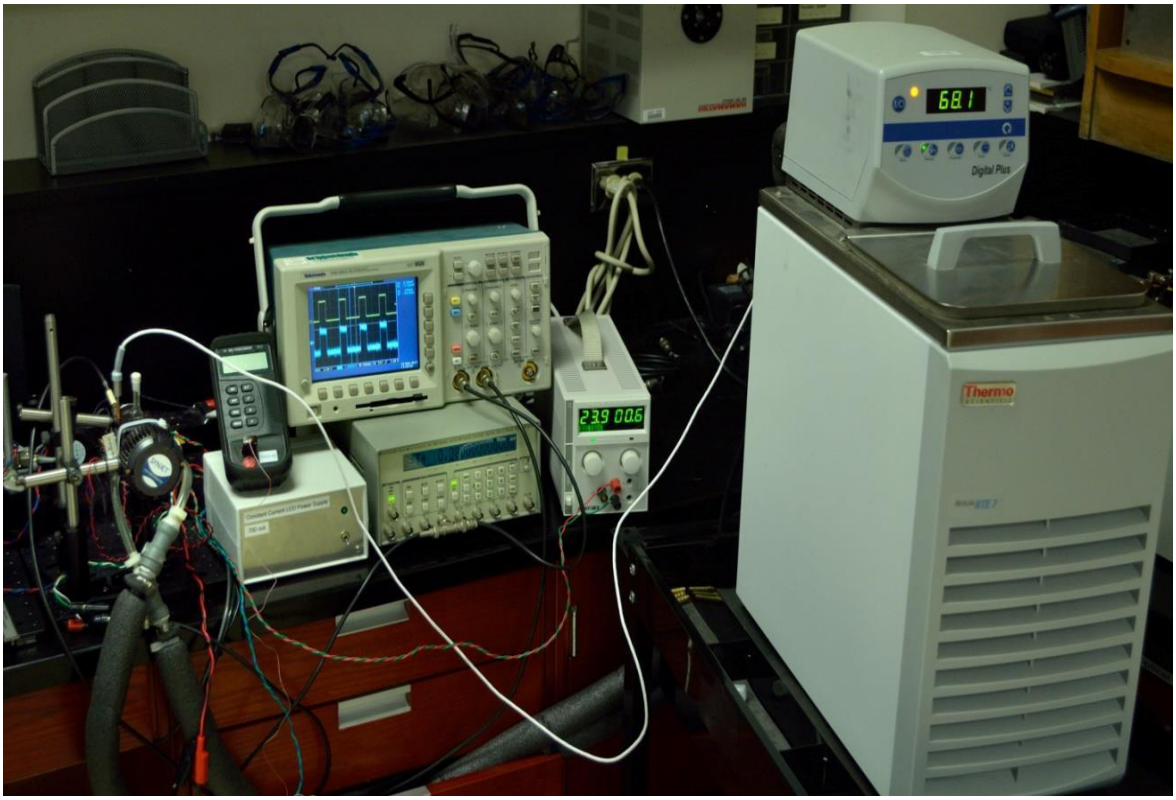

Figure 6.7 The experimental set-up for intermittent illumination experiments.

6.7 References

[1] a) *Radicals in Organic Synthesis*; Renaud, P., Sibi, M. P., Eds.; Wiley-VCH: Weinheim, 2001; b) *Encyclopedia of Radicals in Chemistry, Biology and Materials*; Chatgilialoglu, C., Studer, A., Eds.; Wiley: Chichester, 2012; Vols. 1 and 2; c) Prier, C. K.; Rankic, D. A.; MacMillan, D. W. C. *Chem. Rev*. **2013**, *113*, 5322–5363; d) Schultz, D. M.; Yoon, T. P. *Science* **2014**, *343*, 985–1239176–8; e) Ravelli D.; Protti, S.; Fagnoni, M. *Chem. Rev*. **2016**, *116*, 9850–9913; f) Romero, N. A.; Nicewicz, D. A. *Chem. Rev*. **2016**, *116*, 10075–10166; g) Boubertakh, O.; Goddard, J.-P. *Eur. J. Org. Chem*. **2017**, 2072–2084.

[2] Duncton, M. A. J. *Med. Chem. Commun*. **2011**, *2*, 1135–1161.

[3] Minisci, F.; Bernardi, R.; Bertini, F.; Galli, R.; Perchinummo, M. *Tetrahedron* **1971**, *27*, 3575–3579.

[4] a) Buratti, W.; Gardini, G. P.; Minisci, F.; Bertini, F.; Galli, R.; Perchinunno, M. *Tetrahedron* **1971**, *27*, 3655–3668; b) Seiple, I. B.; Su, S.; Rodriguez, R. A.; Gianatassio, R.; Fujiwara, Y.; Sobel, A. L.; Baran, P. S. *J. Am. Chem. Soc*. **2010**, *132*, 13194–13196; c) Molander, G.; Colombel, V.; Braz, V. *Org. Lett*. **2011**, *13*, 1852–1855; d) Antonchick, A. P.; Burgmann, L. *Angew. Chem. Int. Ed*. **2013**, *125*, 3267–3271; e) Wu, X.; See, J. W. T.; Xu, K.; Hirao, H.; Roger, J.; Hierso, J.-C.; Zhou, J. *Angew. Chem. Int. Ed*. **2014**, *53*, 13573–13577; f) Fang, L.; Chen, L.; Yu, J.; Wang, L. *Eur. J. Org. Chem*. **2015**, 1910–1914; g) Tang, R.-J.; Kang, L.; Yang, L. *Adv. Synth. Catal*. **2015**, *357*, 2055–2060; h) Paul, S.; Guin, J. *Chem. Eur. J*. **2015**, *21*, 17618–17622; i) McCallum, T.; Barriault, L. *Chem. Sci.* **2016**, *7*, 4754–4758; j) Huff, C. A.; Cohen, R. D.; Dykstra, K. D.; Streckfuss, E.; DiRocco D. A.; Krska, S. W. *J. Org. Chem*. **2016**, *81*, 6980–6987; k) Li, G.-X.; Morales-Rivera, C. A.; Wang, Y.; Gao, F.; He, G.; Liu, P.; Chen, G.; *Chem. Sci*. **2016**, *7*, 6407–6412; l) Garza-Sanchez, R. A.; Tlahuext-Aca, A.; Tavakoli, G.; Glorius, F. *ACS Catal*.

2017, *7*, 4057–4061; m) Cheng, W.-M.; Shang, R.; Fu, M.-C.; Fu, Y. *Chem. Eur. J*. **2017**, *23*, 2537–2541; n) Quattrini, M. C.; Fujii, S.; Yamada, K.; Fukuyama, T.; Ravelli, D.; Fagnoni, M.; Ryu, I. *Chem. Commun*. **2017**, *53*, 2335–2338; o) Matsui, J. K.; Primer, D. N.; Molander, G. A. *Chem. Sci*. **2017**, *8*, 3512–3522.

[5] a) DiRocco, D. A.; Dykstra, D.; Krska, S.; Vachal, P.; Conway, D. V.; Tudge, M. *Angew. Chem. Int. Ed*. **2014**, *53*, 4802–4806; b) Gui, J.; Zhou, Q.; Pan, C.-M.; Yabe, Y.; Burns, A. C.; Collins, M. R.; Ornelas, M. A.; Ishihara, Y; Baran, P. S. *J. Am. Chem. Soc*. **2014**, *136*, 4853–4856; c) Jin, J.; MacMillan, D. W. C. *Nature* **2015**, 525, 87–90; d) Jo, W.; Kim, J.; Choi, S.; Cho, S. H. *Angew. Chem. Int. Ed*. **2016**, *55*, 9690–9694.

[6] Natte, K.; Neumann, H.; Beller, M.; Jagadeesh, R. V. *Angew. Chem. Int. Ed*. **2017**, *56*, 6384–6394.

[7] Kim, J.; Cho, S. H. *Synlett* **2016**, *27*, 2525–2529.

[8] a) Ochiai, M.; Morita, K. *Tetrahedron Lett*. **1967**, *8*, 2349–2351; b) Stermitz, F. R.; Wei, C. C.; Huang, W. H. *Chem. Commun. (London)* **1968**, 482–483; c) Stermitz, F. R.; Seiber, R. P.; Nicodem, D. E. *J. Org. Chem*. **1968**, *33*, 1136–1140; d) Taylor, E. C.; Maki, Y.; Evans, B. E. *J. Am. Chem. Soc*. **1969**, *91*, 5181–5182; e) Travecedo, E. F.; Stenberg, V. I. *J. Chem. Soc. D* **1970**, 609–610; f) Stermitz, F. R.; Wei, C. C.; O'Donnell, C. M. *J. Am. Chem. Soc*. **1970**, *92*, 2745–2752; g) Padwa, A. *Chem. Rev*. **1977**, *77*, 37–68; h) Mariano, P. S. *Tetrahedron*, **1983**, *39*, 3845–3879; i) Sugimori, A.; Yamada, T.; Ishida, H.; Nose, M.; Terashima, K.; Oohata, N. *Bull. Chem. Soc. Jpn*. **1986**, *59*, 3905–3909; *during the preparation of this manuscript, a photochemical methylation protocol was described:* j) Liu, W.; Yang, X.; Zhou, Z.-Z.; Li, C.-J. *Chem* **2017**, *2*, 688–702.

[9] Malatesta, V.; Scaiano, J. C. *J. Org. Chem*. **1982**, *47*, 1455–1459.

[10] Scaiano, J. C.; Barra, M.; Krzywinski, M.; Hancock, T.; Calabrese, G.; Sinta, R. *Chem. Mater*. **1995**, *7*, 936–944.

[11] Ueno, R.; Shimizu, T.; Shirakawa, E. *Synlett* **2016**, *27*, 741–744.

[12] Liu, M.; Chen, X.; Chen, T.; Yin, S.-F. *Org. Biomol. Chem*. **2017**, *15*, 2507–2511.

[13] a) Concepcion, J. J.; Brennaman, M. K.; Deyton, J. R.; Lebedeva, N. V.; Forbes, M. D. E.; Papanikolas, J. M.; Meyer, T. J. *J. Am. Chem. Soc*. **2007**, *129*, 6968–6969; b) Ravensbergen, J.; Brown, C. L.; Moore, G. F.; Frese, R. N.; van Grondelle, R.; Gust, D.; Moore, T. A.; Moore, A. L.; Kennis, J. T. M. *Photochem. Photobiol. Sci*. **2015**, *14*, 2147–2150.

[14] a) Huynh, M. H. V.; Meyer, J. M. *Chem. Rev*. **2007**, *107*, 5004–5064; b) Meyer, J. M. *Acc. Chem. Res*. **2011**, *44*, 36–46.

[15] a) Burnett, G. M.; Melville, H. W. *Proc. R. Soc. London, Ser. A* **1947**, *189*, 456–480; b) Ingold, K. U. *Pure Appl. Chem*. **1997**, *69*, 241–244.

[16] a) Pitre, S. P.; McTiernan, C. D.; Vine, W.; DiPucchio, R.; Grenier, M.; Scaiano, J. C. *Sci. Rep*. **2015**, *5*, 16397 (1–10); b) McTiernan, C. D.; Pitre, S. P; Scaiano, J. C. *ACS Catal*. **2014**, *4*, 4034–4039.

[17] a) Yoshimi, Y.; Ishise, A.; Oda, H.; Moriguchi, Y.; Kanezaki, H.; Nakaya, Y.; Katsuno, K.; Itou, T.; Inagaki, S.; Morita, T.; Hatanaka, M. *Tetrahedron Lett*. **2008**, *49*, 3400–3404; b) Yoshimi, Y.; Kanai, H.; Nishikawa, K.; Ohta, Y.; Okita, Y.; Maeda, K.; Morita, T. *Tetrahedron Lett*. **2013**, *54*, 2419–2422.

[18] Naidoo, S.; Jeena, V. *Heterocycles* **2016**, *92*, 1655–1664.

[19] Wang, Y.-F.; Toh, K.-K.; Ng, E. P. J.; Chiba, S. *J. Am. Chem. Soc.* **2011**, *133*, 6411–6421.

[20] Bellan, A. B.; Kuzmina, O. M.; Vetsova, V. A.; Knochel, P. *Synthesis* **2017**, *49*, 188–194.

[21] Balaban, T.-S.; Uncuta, C.; Gheorghiu, M. D.; Balaban, A. T. *Tetrahedron Lett.* **1985**, *26*, 4669–4672.

[22] Zhang, J.; Canary, J. W. *Org. Lett*. **2006**, *8*, 3907–3910.

[23] Chen, F.; Surkus, A.-E.; He, L.; Pohl, M.-M.; Radnik, J.; Topf, C.; Junge, K.; Beller, M. *J. Am. Chem. Soc*. **2015**, *137*, 11718–11724.

[24] Xia, Y.-T.; Sun, X.-T.; Zhang, L.; Luo, K.; Wu, L. *Chem. Eur. J.* **2016**, *22*, 17151–17155.

[25] Kojima, M.; Kanai, M. *Angew. Chem. Int. Ed*. **2016**, *55*, 12224–12227.

[26] Zhu, C.; Yi, M.; Wei, D.; Chen, X.; Wu, Y.; Cui, X. *Org. Lett*. **2014**, *16*, 1840–1843.

[27] Jo, W.; Kim, J.; Choi, S.; Cho, S. H. *Angew. Chem. Int. Ed*. **2016**, *55*, 9690–9694.

[28] Sylvester, K. T.; Wu, K.; Doyle, A. G. *J. Am. Chem. Soc*. **2012**, *134*, 16967–16970.

7. Summary and Future Directions

7.1 Summary

The work described herein has focused on the investigation of photochemically enabled organic transformations. With the development of mild and facile methodology in mind, highly reactive radical intermediates were utilized in broadly applicable and synthetically useful processes. These strategies entailed the evolution of catalytic systems employing binuclear Au(I) complexes for the genesis of alkyl radicals from nonactivated bromoalkanes while developing waste-minimizing protocols discovered over the course of control reactions. In our hands, many of the projects were born from the novelty of utilizing photochemical processes within our group, where the more interesting findings came from asking, “what if?”, and “can we construct an experiment?”. In many cases, methodology rivaling the gold-standards in synthesis were developed.

In a fast-growing field under the pressure to carve-out unique catalytic systems, new reactivity, and library-scale scopes, many breakthroughs have been made at the expense of in depth understanding. In this sense, we have benefitted from collaboration amongst the faculty with extraordinary expertise and knowledge in radical chemistry and photochemistry. We are grateful for the opportunity to further our understanding of radical and photochemical principles along with the skills gained that our laboratory did not possess previously.

In chapter 2, the powerful reducing ability of photoexcited binuclear Au(I) bisphosphine complexes was demonstrated through the reductive hydrodebromination of nonactivated bromoalkanes and arenes as exhibited by their use in radical cyclization reactions. The identification that reductive quenching of the excited-state gold complex by tertiary amines was in most cases faster than oxidative quenching with bromoalkanes

allowed for the ability to better understand and plan further organic transformations. Serendipitously, a dimerization reaction was discovered that provided experimental evidence that Au(I)/Au(III) redox systems may be possible triggered our interest in concept of combining photoredox and gold Lewis acid catalysis using one complex.

Inspired by work in the Stephenson group, chapter 3 outlined our initial attempts at developing a photo-mediated one-pot process for the formal deoxygenation of primary alcohols. As it happened, the tetrabromomethane mediated bromination of alcohols occurred readily under UVA LED irradiation in DMF in the absence of gold photoredox catalyst. The finding was elaborated in a broad scope of alcohol substrates and the corresponding bromoalkanes were subjected to similar methodology as described in chapter 2. A photo-mediated one-pot deoxygenation reaction utilizing a photogenerated Vilsmeier-Haack intermediate was found.

Further investigation of the Vilsmeier-Haack intermediate generated by UVA irradiation of tetrabromomethane in DMF was performed using different nucleophiles in chapter 4. Synonymous to Stephenson's findings, carboxylic acids in this system led to the formation of symmetric anhydrides. With the ultimate goal of developing an alternative amide coupling methodology using carboxylic acids and amines, conditions for the mild synthesis of a variety of amides were identified. Amongst alkyl and aryl carboxylic acids, primary and secondary amines as well as aniline were successfully coupled. Notably, amino acids were compatible under these conditions without loss of stereochemical information.

In chapter 5, the removal of trialkylamine from reactions using binuclear Au(I) complexes to activate bromoalkanes was explored. The redox-neutral Minisci-type alkylation of heteroarenes was discovered through employing the oxidative quenching

pathway of excited-state gold complexes with bromoalkanes. Upon addition of alkyl radicals to heteroarenes, the resulting heteroaryl aminyl radical intermediates were then oxidized by interaction with an [Au^{I}–Au^{II}] intermediate that furnished final product and regenerated the ground-state photoredox catalyst. The reaction represents a significant advancement in Minisci-type alkylation methodology with high yields, broad scope, without need of additives/oxidants. The chemistry also hinted that significantly oxidizing intermediates could be generated in gold mediated photoredox processes in addition to their powerful reducing capabilities. The principles of polarity reversal radical additions were also explored in this research through three component coupling reactions. In this respect, an electrophilic radical was generated from α-bromoester that was not capable of addition to quinoline based heterocycles, where upon addition of an alkene, the incumbent nucleophilic radical was then capable of addition to heteroarenes; a notoriously difficult challenge in radical coupling methodology. The reactivity described in these paragraphs is summarized in **Figure 7.1**. The Minisci-type alkylative coupling protocol is currently being applied to the addition of isocyanide substrates that led to the formation of substituted phenanthridines.

Lastly, chapter 6 details the development of a redox-neutral Minisci-type alkylation strategy using methanol and ethers involving the direct excitation of heteroarenes was described. Initially found through attempts to couple sulfonyl chlorides to heteroarenes under conditions developed in chapter 5, the *in situ* generation of HCl enabled the methylation of lepidine using methanol as solvent. Surprised by this, a screen of acids showed that only HCl effected the photochemical reaction of lepidine and methanol to give 2,4-dimethylquinoline. The direct excitation of lepidine and other heteroarenes in the presence of HCl with a variety of alcoholic and ether solvents was shown to give alkylated

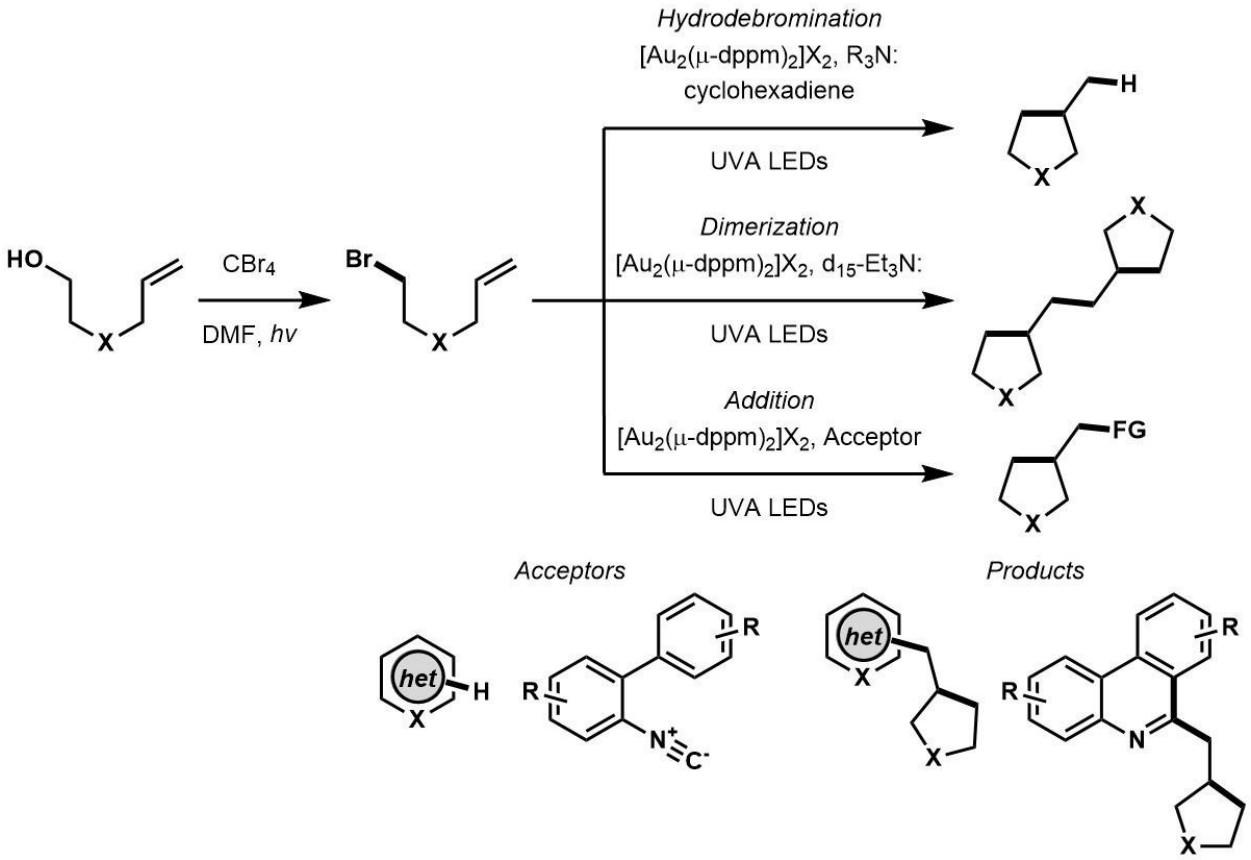

Figure 7.1 Summary of binuclear Au(I) photoredox transformations.

heteroarene products. Mechanistic studies demonstrated the ability for the excited-state heteroarenes to undergo reductive quenching with alcohols and ethers, however, the requirement for chloride indicated that it may be essential to the formation of chlorine atoms that later undergo HAT reactions with the solvent. Kinetic isotope studies could not definitively disprove either pathway, but deuterium labeling experiments highlighted the nature of the elimination of water or ROH required for rearomatization of the heteroarenes. The described reaction represents an ideal methylation protocol of heteroarenes.

7.2 Future Directions

While the work presented herein has demonstrated the usefulness of binuclear Au(I) complexes as photoredox catalysts in organic transformations, there are many interesting questions yet to be answered. Mentioned briefly in Chapter 2, the ability of these complexes to undergo Au(I)/Au(III) redox chemistry to ultimately produce functionalized products from relatively simple starting materials under redox-neutral conditions is highly desirable. Seminal publication of gold and photoredox dual catalytic systems by Glorius and Toste have demonstrated the ability of diazonium salts and photocatalysts to generate highly active aryl-functionalized Au(III) complexes that participate in well known Lewis acid catalyzed reactions, however, reductive elimination regenerates the Au(I) complex rather than a protodeauration event (**Figure 7.2**).[1, 2] Under these mild conditions, readily available Au- and Ru-based complexes are utilized to catalyze alkene oxy- and aminoarylation reactions as well as arylative semipinacol rearrangements. To this end, recent work in our group has focused on the development of a gold dual photoredox system that utilized one complex, $[Au_2(\mu\text{-dppm})_2]Cl_2$, to play two roles in the alkylative semipinacol rearrangement using nonactivated bromoalkanes (**Figure 7.3**). In this transformation, excited-state gold complex undergoes oxidative quenching with a bromoalkane, generating an alkyl radical along with an $[Au^{I}–Au^{II}]$ complex. Proposed is a recombination of the alkyl radical to the gold complex, generating an alkyl-functionalized $[Au^{I}–Au^{III}]$ complex that may act as a Lewis acid catalyst towards the alkylative semipinacol rearrangement of silyl-protected styryl-functionalized cyclobutanols upon reductive elimination. Although these substrates are prone to radical addition, mechanistic studies did not support a free radical mechanism. For these

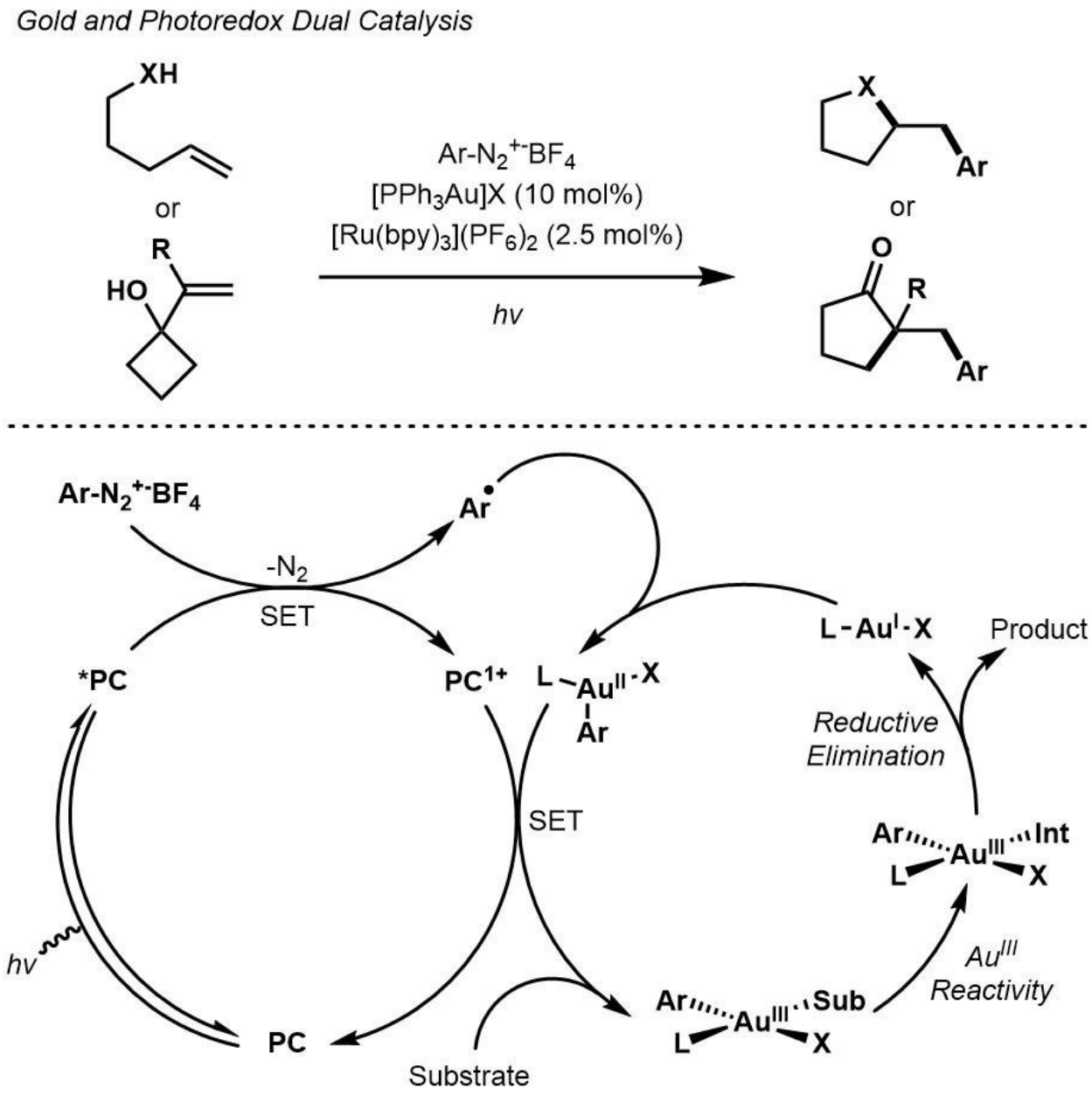

Figure 7.2 Organic transformations of gold and photoredox dual catalysis.

reasons, we are interested in applying this proposed strategy towards nonactivated alkenes/alkynes in intra- and intermolecular coupling reactions to further understand the synthetic potential of this approach.

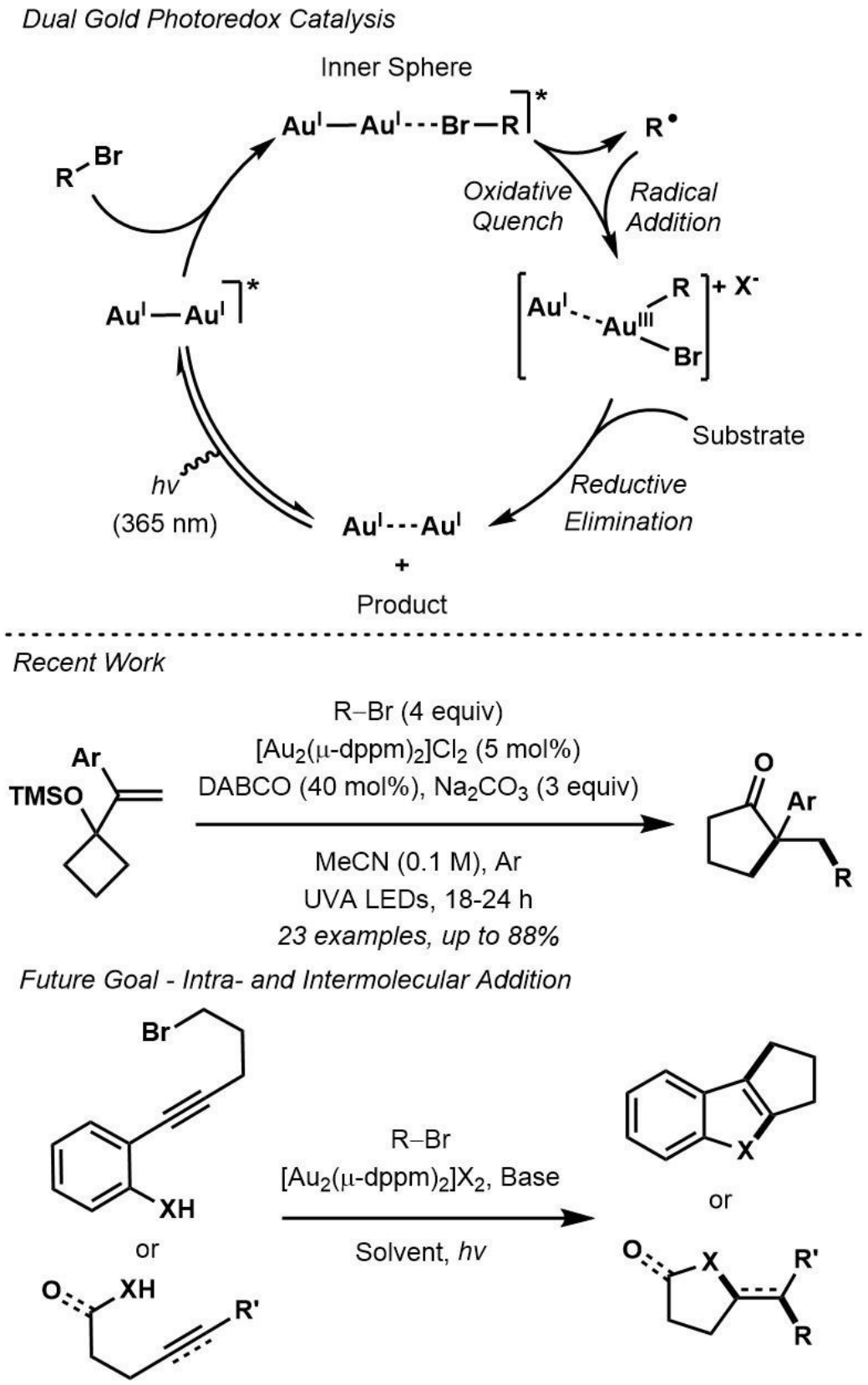

Figure 7.3 Binuclear Au(I)/Au(III) dual gold photoredox catalysis.

Another intriguing by-product was realized upon performing cyclization reactions of bromoalkane-functionalized allyl malonates in the absence of trialkylamine bases/additives. The formal Kharasch-type bromine-ATRA reaction was observed upon isolation of the corresponding bromoalkane that underwent *5-exo-trig* cyclization (**Figure 7.4**). As nonactivated bromoalkanes are not known to be effective bromo-transfer reagents, a mechanistically unique pathway is proposed. After excitation of a binuclear Au(I) complex and oxidative quenching of a nonactivated bromoalkane via an inner sphere exciplex, $[Au^{I}–Au^{II}]$–Br complex and a free alkyl radical are formed, as eluded by the ability to undergo radical *5-exo-trig* cyclization. The incumbent radical may then react in two ways; path a) the alkyl radical may undergo bromo atom transfer with the activated $[Au^{I}–Au^{II}]$–Br complex, forming product and regenerating the ground-state photocatalyst, or path b) where upon alkyl radical addition to a gold centre in the $[Au^{I}–Au^{II}]$–Br complex (shown as $[Au^{I}–Au^{III}]$, however a $[Au^{II}–Au^{II}]$ complex cannot be ruled out) would lead to reductive elimination of the desired product and regeneration of the ground-state catalyst. Future goals in this project would be elaboration of the intramolecular substrate scope to probe compound functionality tolerance and reactivity trends in the bromo-transfer step for primary, secondary, and tertiary alkyl radical intermediates. Also, cascade radical additions would be an interesting extension, where relatively nucleophilic alkyl radicals may participate in addition reactions to electrophilic alkene acceptors, where the intermediate relatively electrophilic radical may add to a pendant alkene and finish by undergoing the novel bromo-transfer step.

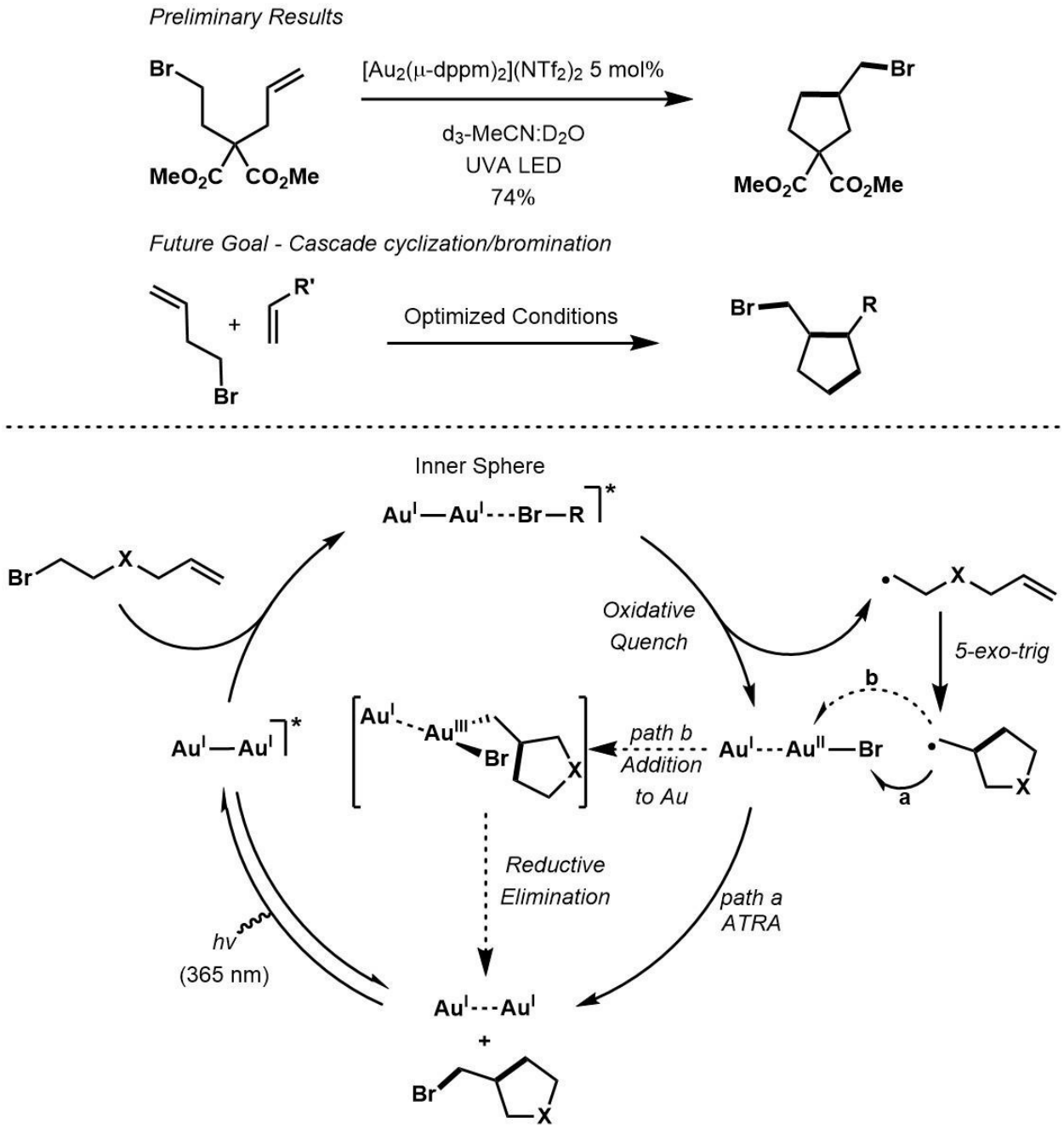

Figure 7.4 The formal bromine ATRA reaction of nonactivated bromoalkanes.

Next, the Minisci-type alkylation of heteroarenes using alcohols and eithers could benefit from further reaction optimization. Notably, many heterocycles underwent photochemical degradation as the starting materials required direct photoexcitation. Adding to this obstacle, the alcohol/ether coupling partner was limited in scope as well as

requiring its use of super-stoichiometric amounts as solvent. Also, the mechanistic data was somewhat ambiguous with respect to the nature of the excited-state quenching of the heteroarene. Preliminary results have shown that Ir-based polypyridyl complexes, such as $[Ir(dF(CF_3)ppy)_2(dtbbpy)]PF_6$, are capable of reaction under similar conditions (**Figure 7.5**). Blue light is required for excitation of such Ir complexes and photochemical degradation of the protonated heterocycle is mitigated by its lack of absorbance at these wavelengths. Furthermore, the equivalents of the alcohol/ether coupling partners scope may be expanded in functionality and reduced to stoichiometric amounts as determined by exploring an applicable solvent screen. Lastly, the nature of the excited-state

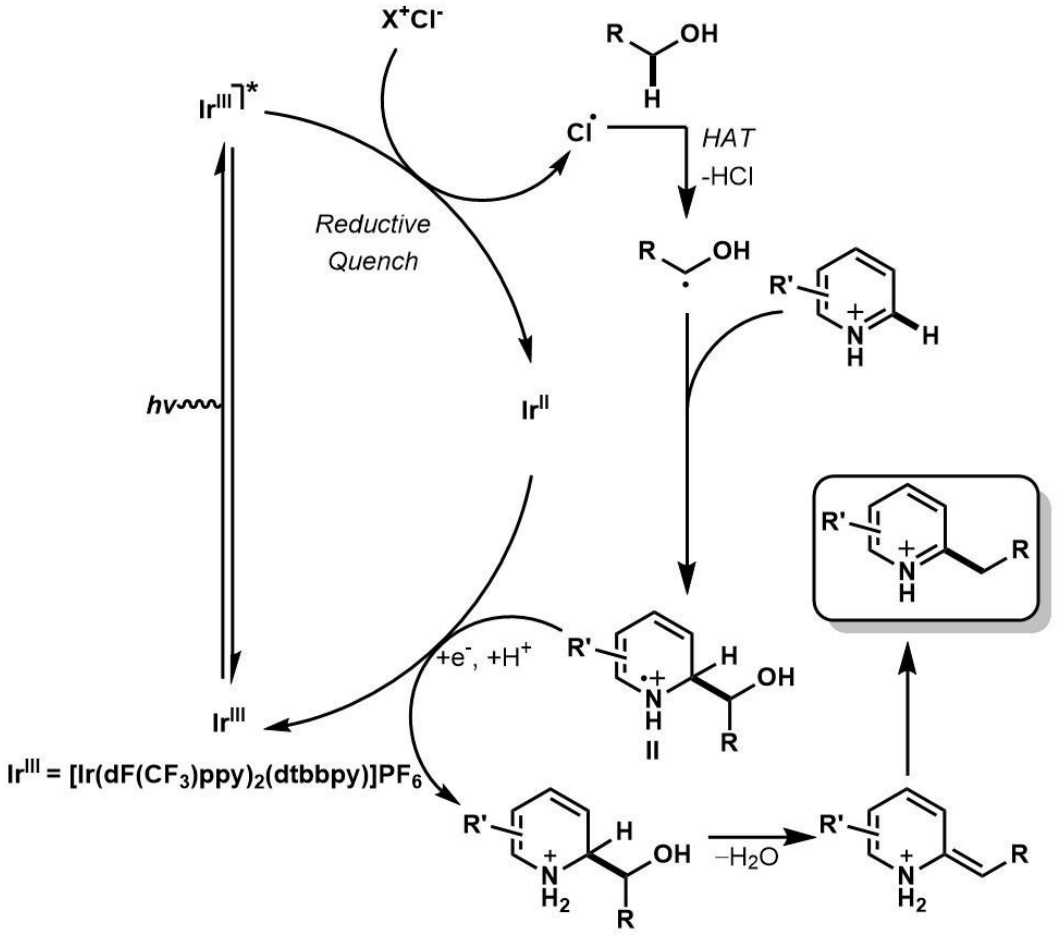

Figure 7.5 Photo-mediated Minisci-type alkylation of heteroarenes.

quenching process may be closely studied to understand the role of chloride and possible androgynous reactive pathways to the previously established conditions.

Finally, the ability of chloride to undergo reductive quenching with Ir-based polypyridyl reactions would serve a greater purpose with respect to its further implications to organic transformations (**Figure 7.6**). When considering this prospect, the mild generation of chlorine atoms is of great interest to the organic synthesis community. The ability of chlorine atoms (HCl BDE = 103 kcal/mol) to undergo HAT reactions with substrates bearing C–H bonds with BDE values lower than 103 kcal/mol. Polarity reversal catalysis principles may demonstrate that an electrophilic chlorine atom may have increased selectivity towards more nucleophilic or "hydridic" C–H bonds in complex substrates (i.e. alkyl, α-alkoxyl, aldehydic, trialkylsilane/germane/stannane).[3] To demonstrate such reactivity, $[Ir(dF(CF_3)ppy)_2(dtbbpy)]Cl$ may be used to facilitate interaction between the Ir complex and chloride, with possible applications to Giese-type addition, heteroarylation, and allylation reactions. Mechanistically, excited-state $\mathbf{Ir^{III}}$ may be thermodynamically unfavourable to undergo reductive quenching with chloride ($E_{1/2}^{(M^*/M^-)}$ = 1.21 V *vs* SCE compared to $E_{1/2}^{ox}$ = 2.03 V *vs* SCE for chloride) and supported by having relatively slow kinetic quenching rates ($k_q = 5.3\times10^4$ $M^{-1}s^{-1}$).[4] This process may be facilitated by the heat generated by the light source (as seen in the Minisci-type alkylation of heteroarenes described above). Upon generation of the electrophilic chlorine atom, HAT with a substrate generates a relatively nucleophilic radical, capable of adding to an electrophilic acceptor (i.e. an acrylate is depicted below). While similar electrophilic intermediates have been proposed to regenerate the ground-state catalyst through reduction by the $\mathbf{Ir^{II}}$ intermediate, it is likely that this process may undergo chain-propagating HAT reactions. Support is given by the relatively electrophilic radical

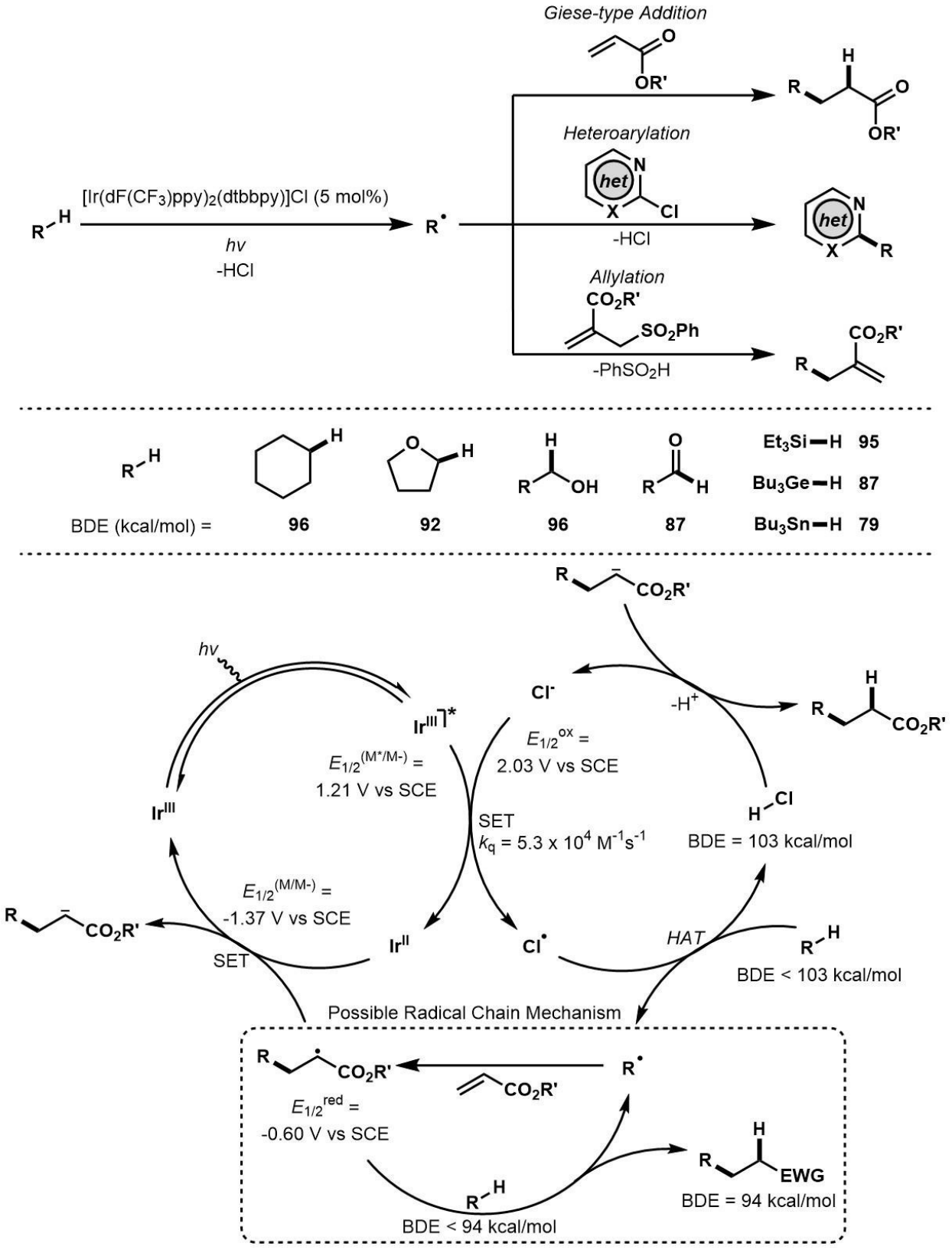

Figure 7.6 Transformations mediated by photoredox generation of chlorine.

intermediate having a reasonably similar BDE than the coupling partner and electronically favourable by principles of polarity reversal catalysis. In the case of the heteroarylation and allylation reactions, each acceptor contains a group that may undergo fragmentation and/or undergo chain-propagating HAT reactions in addition to the closed catalytic cycles typically proposed for these reactions. Preliminary results show great promise of generality in these potential organic transformations requiring further mechanistic investigation, however, these details may be the topics of discussion on another day in another thesis.

At the onset, this expedition was set with the ambitious goals of discovery and exploration of the fundamental underlying principles concerned with shining light on gold complexes and the organic transformations that they may produce. With the initial finding that these complexes were capable of powerful reactions upon illumination with sunlight, careful observation of the resulting products in an assortment of substrates has blossomed many projects into fruition. To that end, stopping to smell the flowers has led to new discoveries in this field and each of our undertakings were connected in some small way – usually by a side product observed in a proton NMR spectrum. Although the total understanding of these luminous structures has not been realized, a variety of insights to the nature of their reactivity have been cultivated, perhaps more appropriately likened to planting seeds in a garden than summiting a mountain. To boot, collaborative propagation of these ideas in the same garden sometimes leads to hybrid projects that often form into something special.

7.3 References

[1] Sahoo, B.; Hopkinson, M. N.; Glorius, F. *J. Am. Chem. Soc.* **2013**, *135*, 5505–5508.

[2] Shu, X.-Z.; Zhang, M.; He, Y.; Frei, H.; Toste, F. D. *J. Am. Chem. Soc*. **2014**, *136*, 5844–5847.

[3] a) Baguley, P. A.; Walton, J. C. *Angew. Chem. Int. Ed*. **1998**, *37*, 3072–3082; b) Chatgilialoglu, C.; Newcomb, M. *Adv. Organomet. Chem*. **1999**, *44*, 67–112; c) Blanksby, S. J.; Ellison, G. B. *Acc. Chem. Res*. **2003**, *36*, 255–263.

[4] Shields, B. J.; Doyle, A. G. *J. Am. Chem. Soc*. **2016**, *138*, 12719–12722.

7.4 Claims to Original Research

- Development of a photo-mediated reductive hydrodebromination/cyclization of nonactivated bromoalkanes using binuclear Au(I) bisphosphine complexes.
- Light-mediated bromination of primary alcohols through formation of a Vilsmeier-Haack intermediate using tetrabromomethane and dimethylformamide.
- Formation of anhydrides and amides from carboxylic acids and amines employing the light-mediated formation of a Vilsmeier-Haack intermediate.
- Discovery of a photo-mediated redox-neutral Minisci-type alkylation of heteroarenes using nonactivated bromoalkanes and binuclear Au(I) complexes.
- Development of a photo-mediated redox-neutral Minisci-type alkylation of heteroarenes using nonactivated alcohols and ethers.

7.5 Publications

Publications Resulting from Work Presented in this Thesis

1) Revol, G.; McCallum, T.; Morin, M.; Gagosz, F.; Barriault, L. Photoredox Transformations with Dimeric Gold Complexes. *Angew. Chem. Int. Ed*. **2013**, *52*, 13342–13345.

2) McCallum, T.; Slavko, E.; Morin, M.; Barriault, L. Light-Mediated Deoxygenation of Alcohols with a Dimeric Gold Catalyst. *Eur. J. Org. Chem.* **2015**, 81–85.

3) McCallum, T.; Barriault, L. Light-Enabled Synthesis of Anhydrides and Amides. *J. Org. Chem.* **2015**, *80*, 2874–2878.

4) McCallum, T.; Barriault, L. Direct alkylation of heteroarenes with unactivated bromoalkanes using photoredox gold catalysis. *Chem. Sci.* **2016**, *7*, 4754–4758.

5) McCallum, T.; Pitre, S. P.; Morin, M.; Scaiano, J. C.; Barriault, L. The photochemical alkylation and reduction of heteroarenes. *Chem. Sci.* **2017**, *8*, 7412–7418.

Publications Arising from Further Information Provided in Chapter 2

1) McTiernan, C. D.; Morin, M.; McCallum, T.; Scaiano, J. C.; Barriault, L. Polynuclear gold(I) complexes in photoredox catalysis: understanding their reactivity through characterization and kinetic analysis. *Catal. Sci. Technol*. **2016**, *6*, 201–207.

2) Tran, H.; McCallum, T.; Morin, M.; Barriault, L. Homocoupling of Iodoarenes and Bromoalkanes Using Photoredox Gold Catalysis: A Light Enabled Au(III) Reductive Elimination. *Org. Lett*. **2016**, *18*, 4308–4311.

Publications Resulting from Work Not Presented in this Thesis

1) Kaldas, S. J.; Cannillo, A.; McCallum, T.; Barriault, L. Indole Functionalization via Photoredox Gold Catalysis. *Org. Lett.* **2015**, *17*, 2864–2866.

2) McCallum, T.; Jouanno, L.-A.; Cannillo, A.; Barriault, L. Persulfate-Enabled Direct C–H Alkylation of Heteroarenes with Unactivated Ethers. *Synlett* **2016**, *27*, 1282–1286.

3) McCallum, T.; Rohe, S.; Barriault, L. Thieme Chemistry Journals Awardees – Where Are They Now? What's Golden: Recent Advances in Organic Transformations Using Photoredox Gold Catalysis. *Synlett*, **2017**, *28*, 289–305.

4) Zidan, M.; McCallum, T.; Thai-Savard, L.; Barriault, L. Photoredox meets gold Lewis acid catalysis in the alkylative semipinacol rearrangement: a photocatalyst with a dark side. *Org. Chem. Front*. **2017**, *4*, 2092–2096.

5) Rohe, S.; McCallum, T.; Morris, A. O.; Barriault, L. Transformations of Isonitriles with Bromoalkanes Using Photoredox Gold Catalysis. *J. Org. Chem*. **2018**, *In Press*.

Collective Spectral Data: Radical Adventures in Photochemistry

Terry M^{c}Callum

Supporting information for the thesis submitted to the

Faculty of Graduate and Postdoctoral Studies

In partial fulfillment of the requirements for the

PhD degree in Chemistry

Department of Chemistry and Biomolecular Sciences

Faculty of Science

University of Ottawa

1. Table of Contents

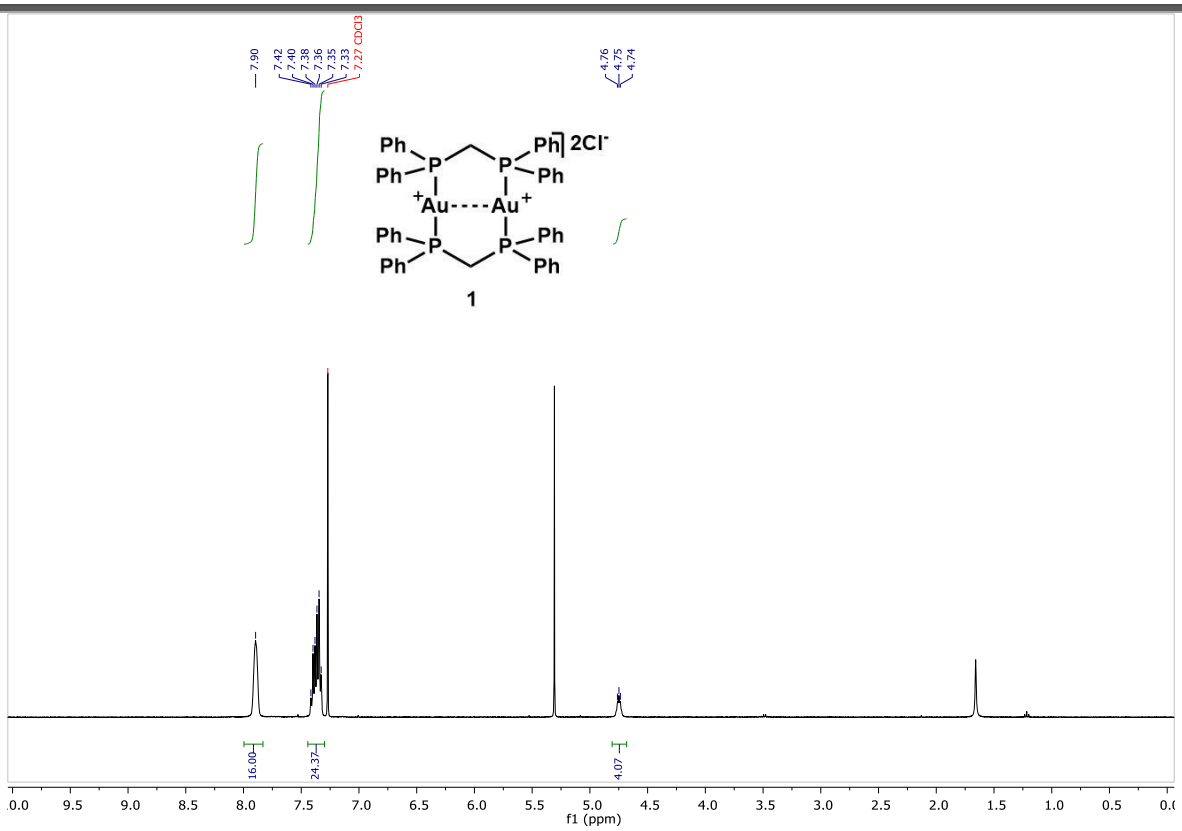
7.90
7.42
7.40
7.38
7.36
7.35
7.33
7.27 CDCl3
4.76
4.75
4.74
Ph
Ph
P
P
Ph
Ph
2Cl-
+Au----Au+
Ph
Ph
P
P
Ph
Ph
1
16.00
24.37
4.07
f1 (ppm)

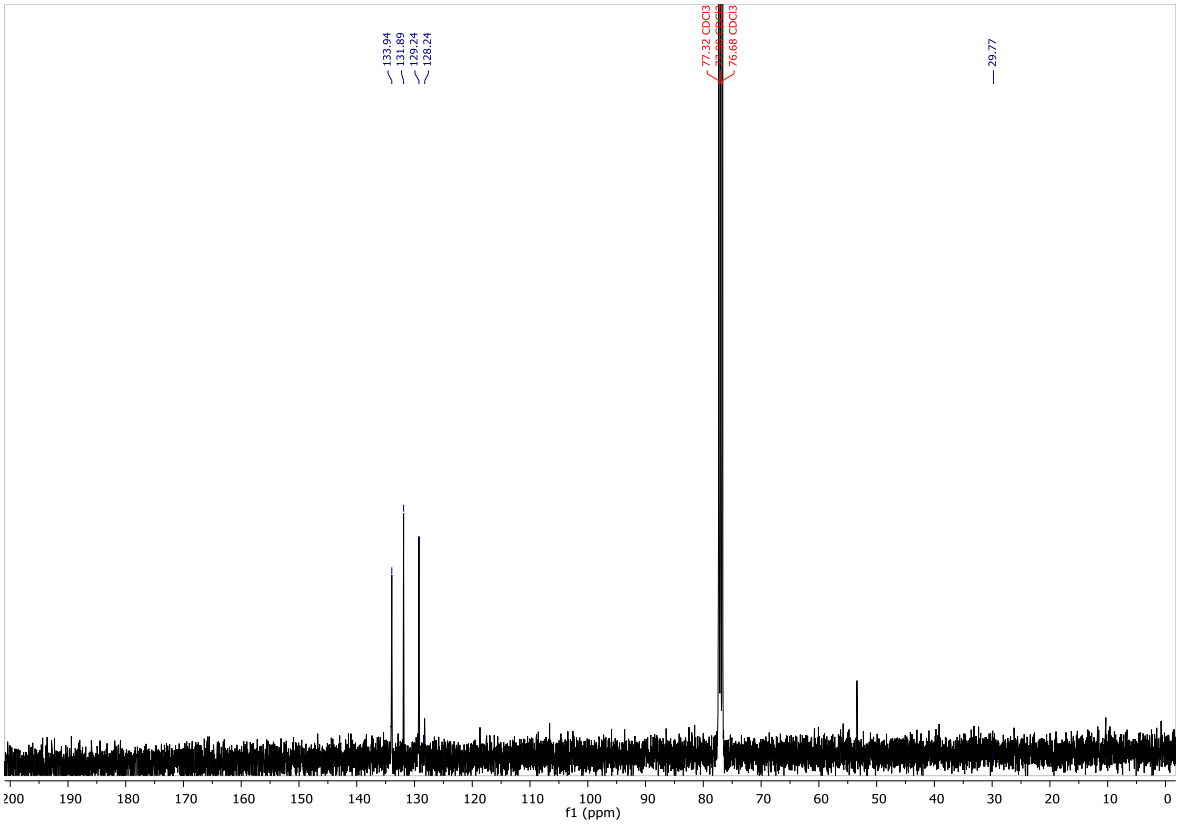
133.94
131.89
129.24
128.24
77.32 CDCl3
76.68 CDCl3
29.77
f1 (ppm)

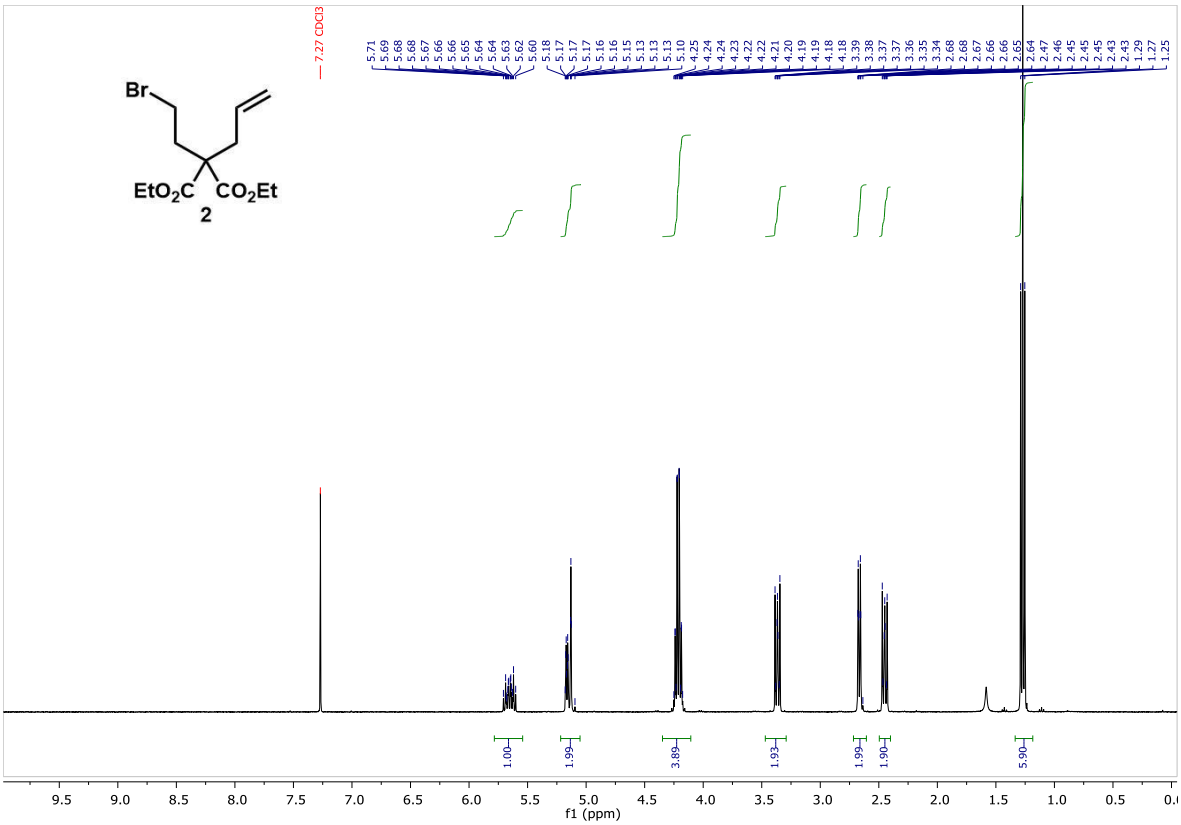
Br
EtO2C CO2Et
2
7.27 CDCl3
f1 (ppm)

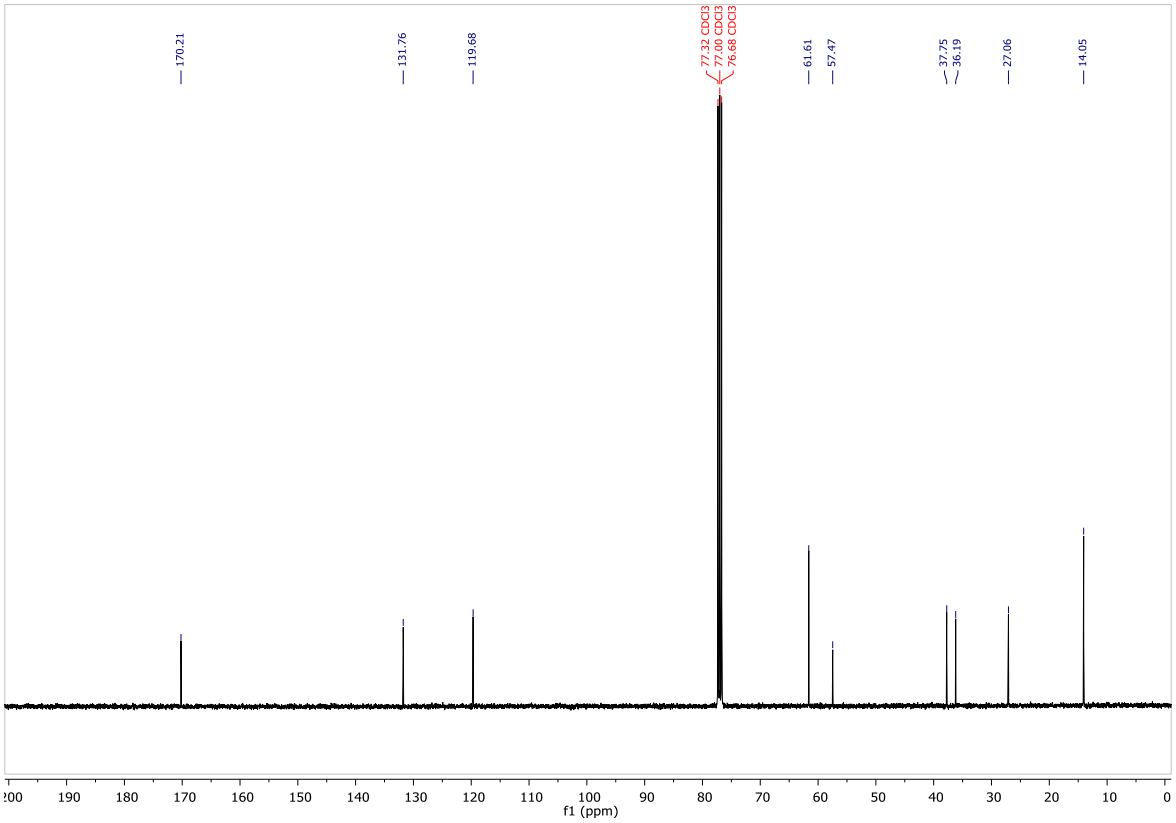
170.21
131.76
119.68
77.32 CDCl3
77.00 CDCl3
76.68 CDCl3
61.61
57.47
37.75
36.19
27.06
14.05
f1 (ppm)

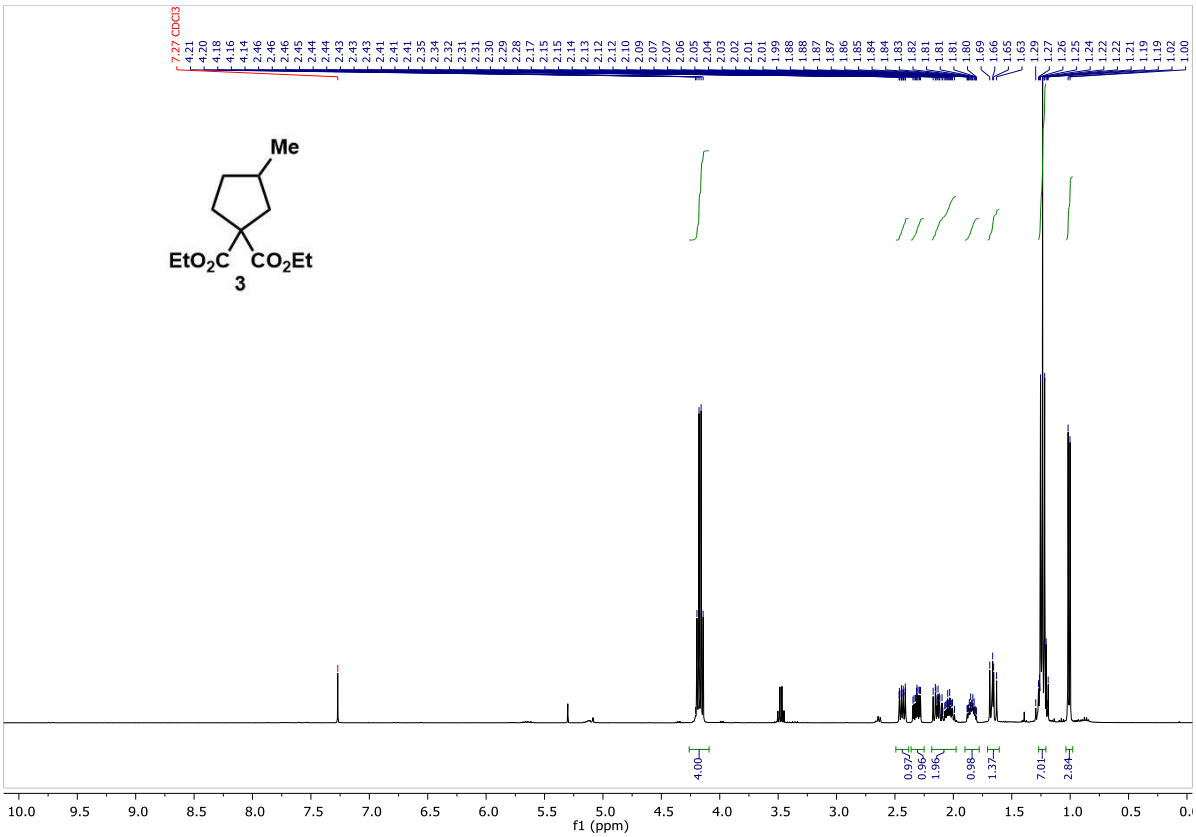
Me
EtO2C CO2Et
3
f1 (ppm)

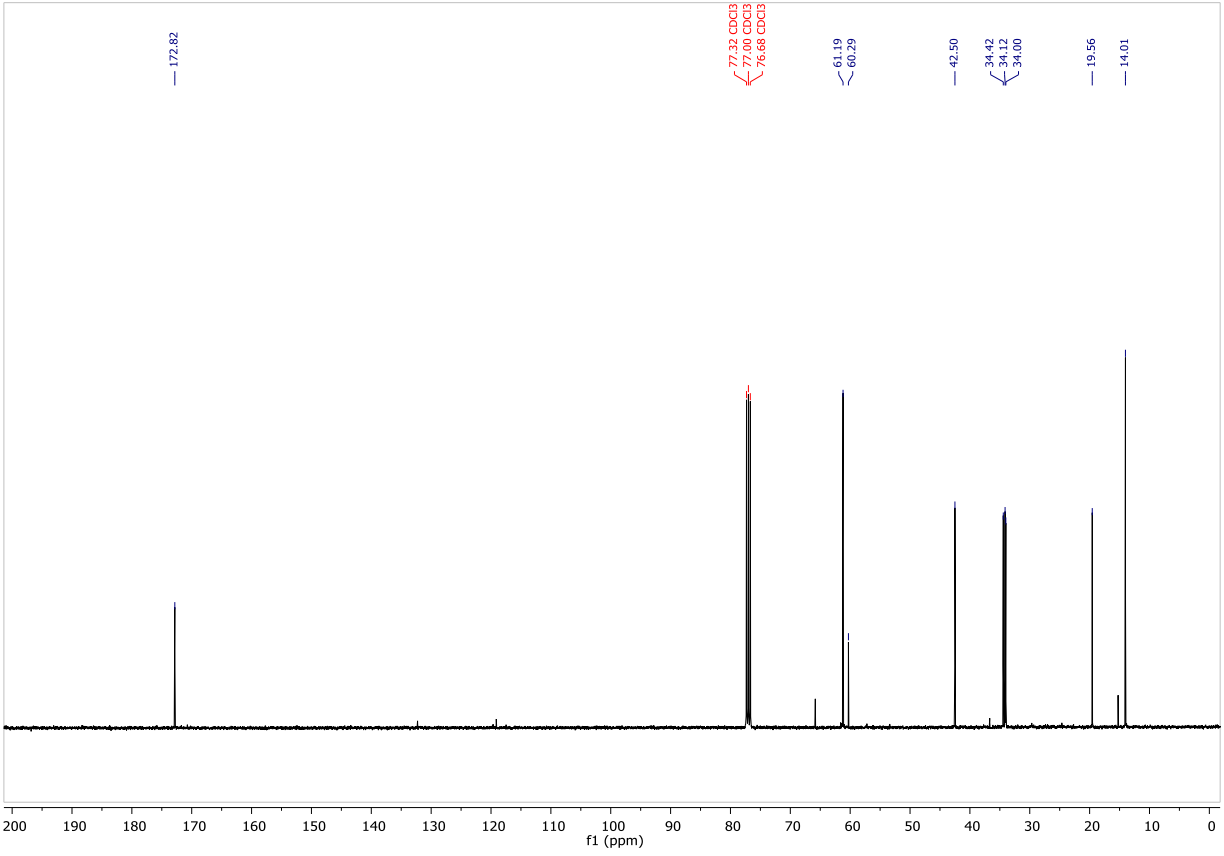
172.82
77.32 CDCl3
77.00 CDCl3
76.68 CDCl3
61.19
60.29
42.50
34.42
34.12
34.00
19.56
14.01
f1 (ppm)

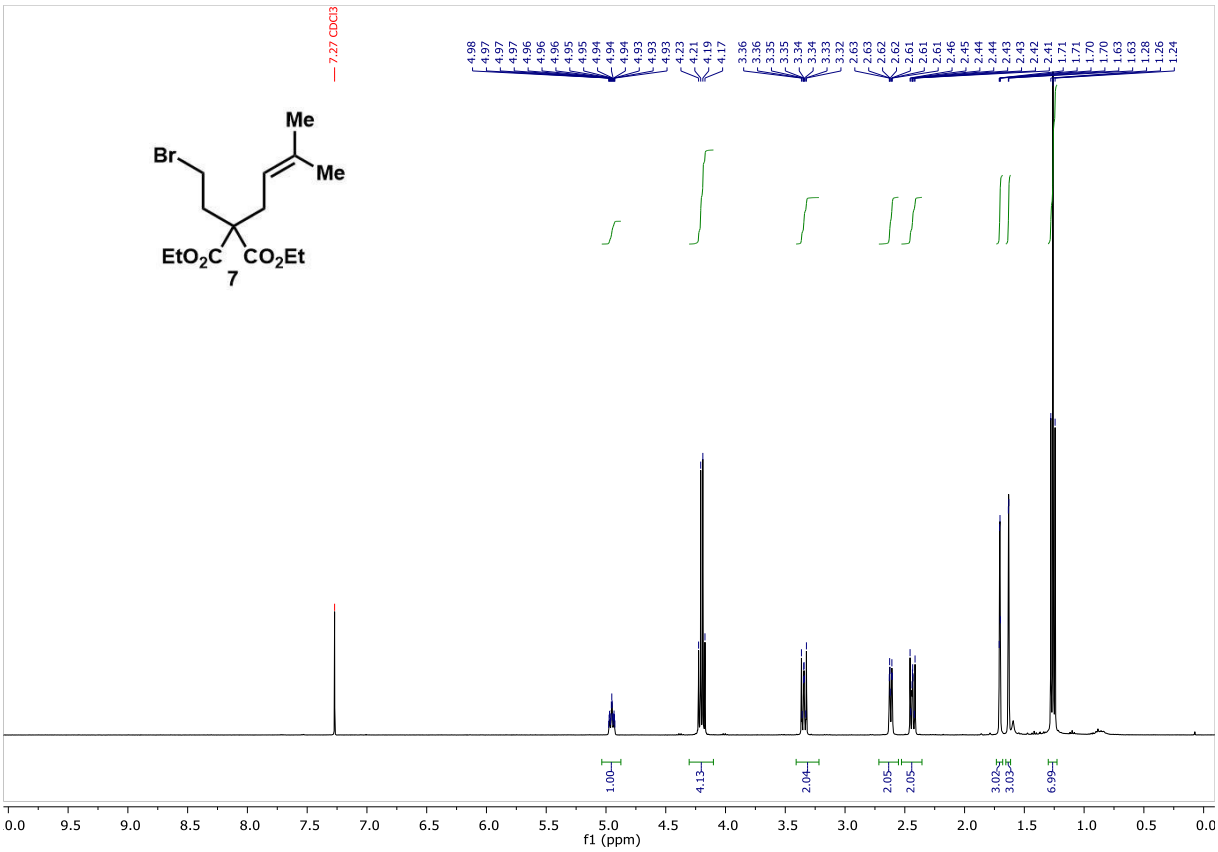
7.27 CDCl3
Me
Br
Me
EtO2C
CO2Et
7
f1 (ppm)

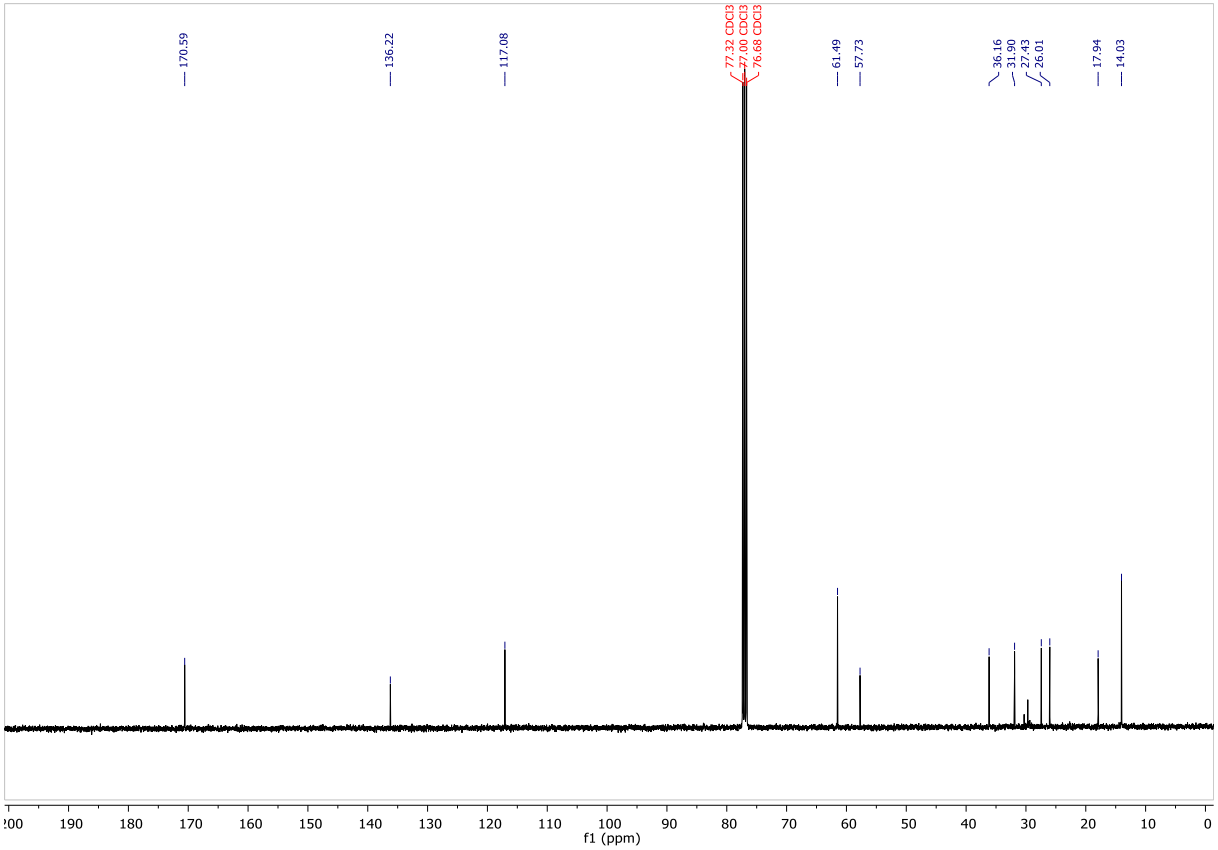
170.59
136.22
117.08
77.32 CDCl3
77.00 CDCl3
76.68 CDCl3
61.49
57.73
36.16
31.90
27.43
26.01
17.94
14.03
f1 (ppm)

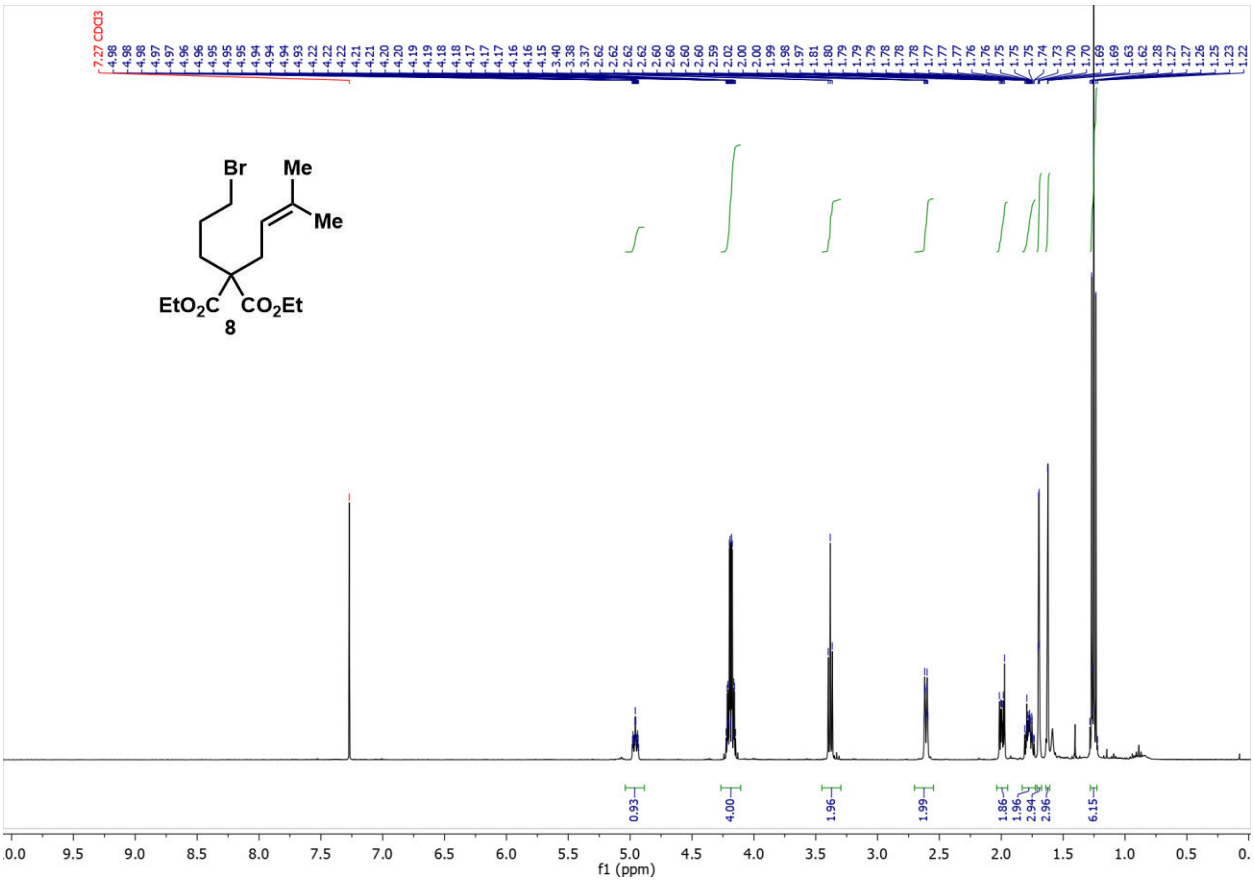
Br
Me
Me
EtO2C
CO2Et
8
f1 (ppm)

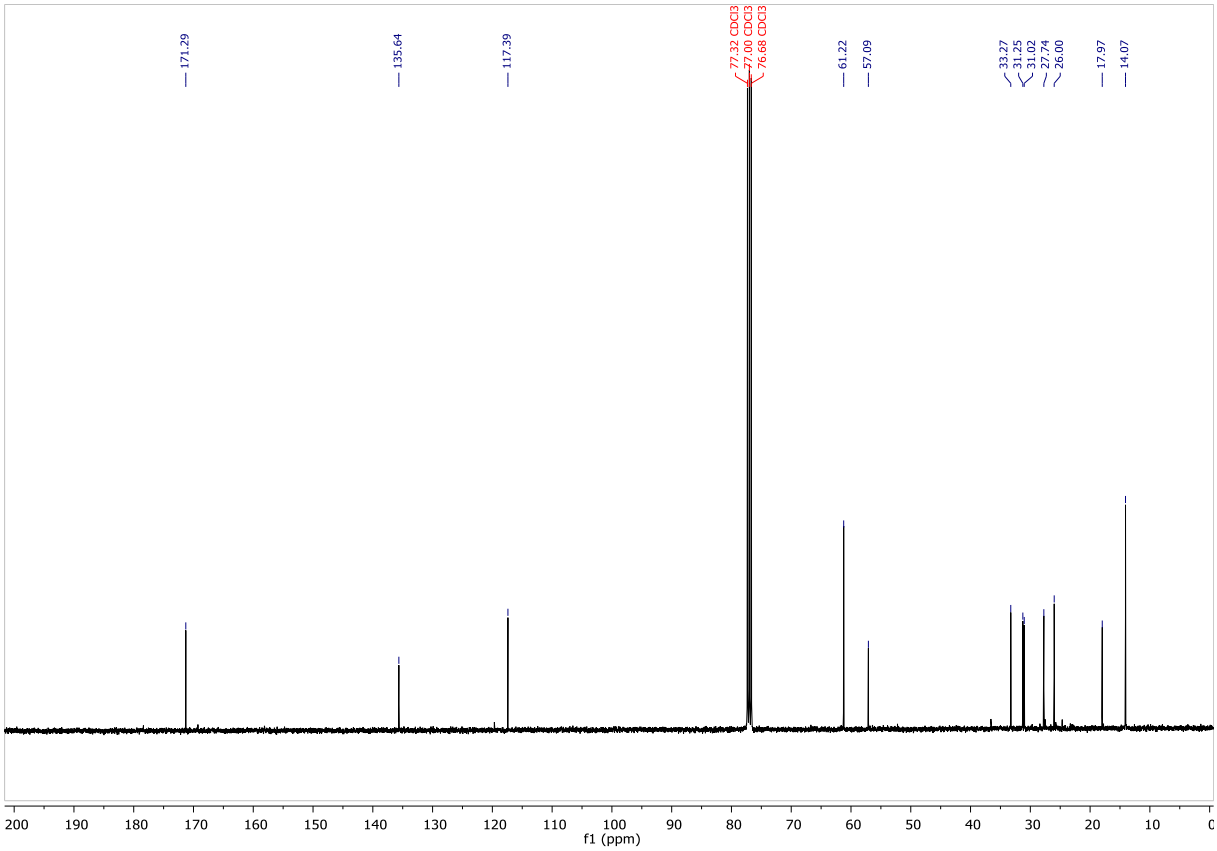
171.29
135.64
117.39
77.32 CDCl3
77.00 CDCl3
76.68 CDCl3
61.22
57.09
33.27
31.25
31.02
27.74
26.00
17.97
14.07
f1 (ppm)

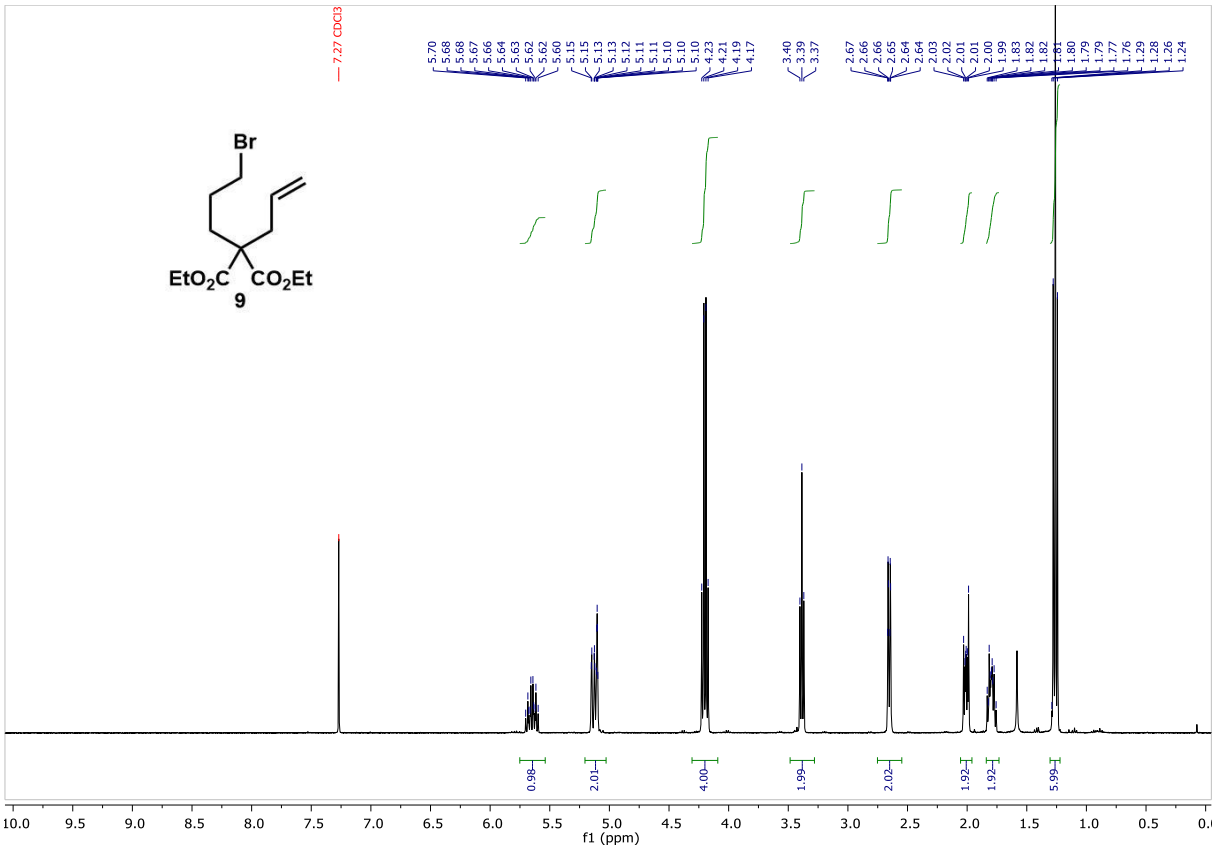
7.27 CDCl3
Br
EtO2C CO2Et
9
f1 (ppm)

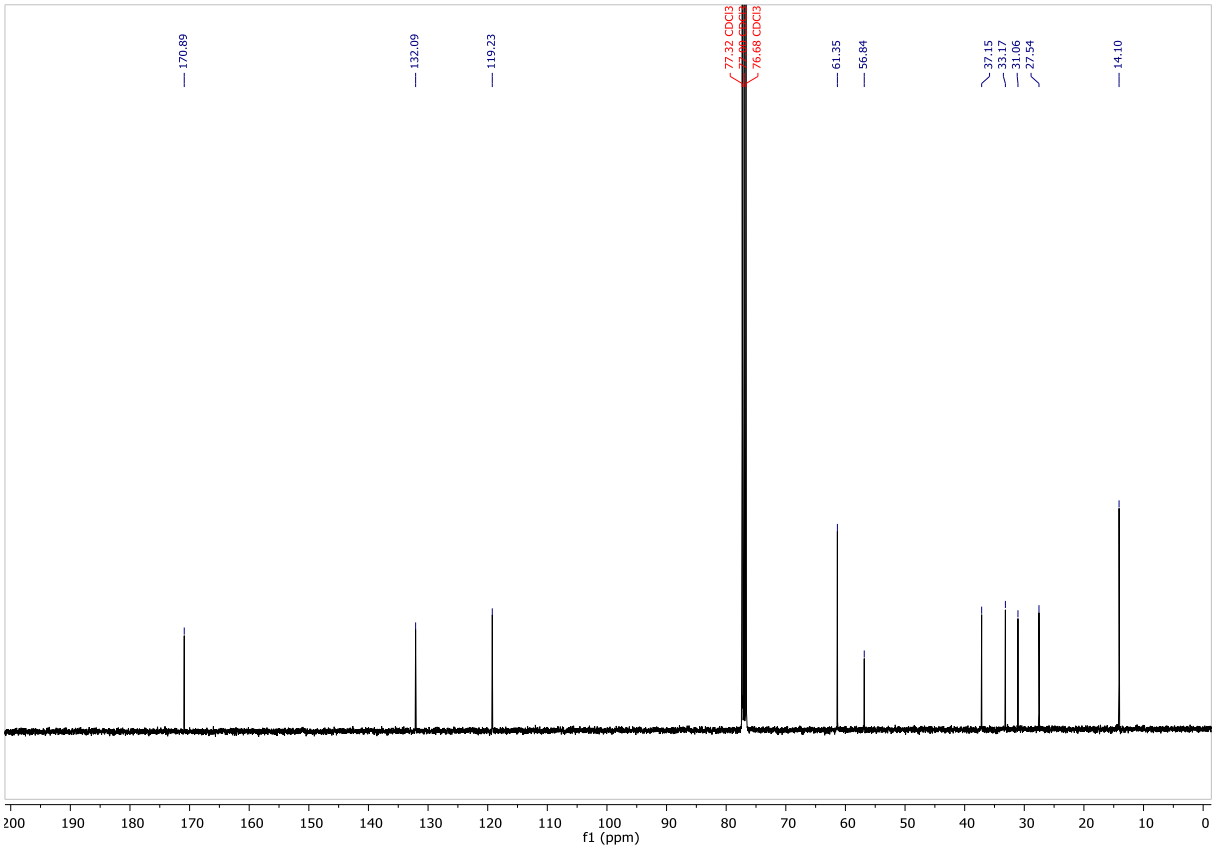
170.89
132.09
119.23
77.32 CDCl3
76.68 CDCl3
61.35
56.84
37.15
33.17
31.06
27.54
14.10
f1 (ppm)

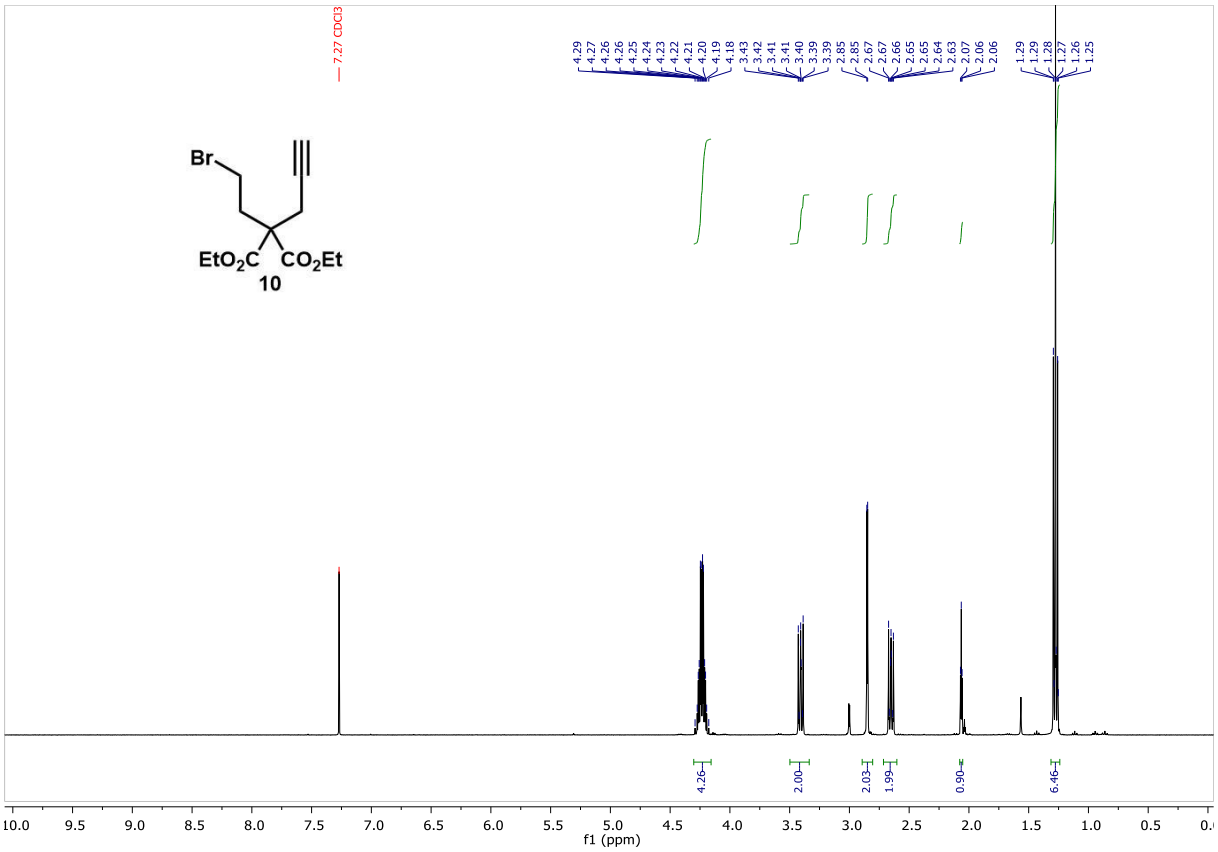
7.27 CDCl3
Br
EtO2C CO2Et
10
4.29
4.27
4.26
4.26
4.26
4.25
4.24
4.23
4.22
4.21
4.20
4.19
4.18
3.43
3.42
3.41
3.41
3.40
3.39
2.85
2.85
2.67
2.67
2.66
2.65
2.65
2.64
2.63
2.07
2.06
2.06
1.29
1.29
1.28
1.27
1.26
1.25
4.26
2.00
2.03
1.99
0.90
6.46
f1 (ppm)

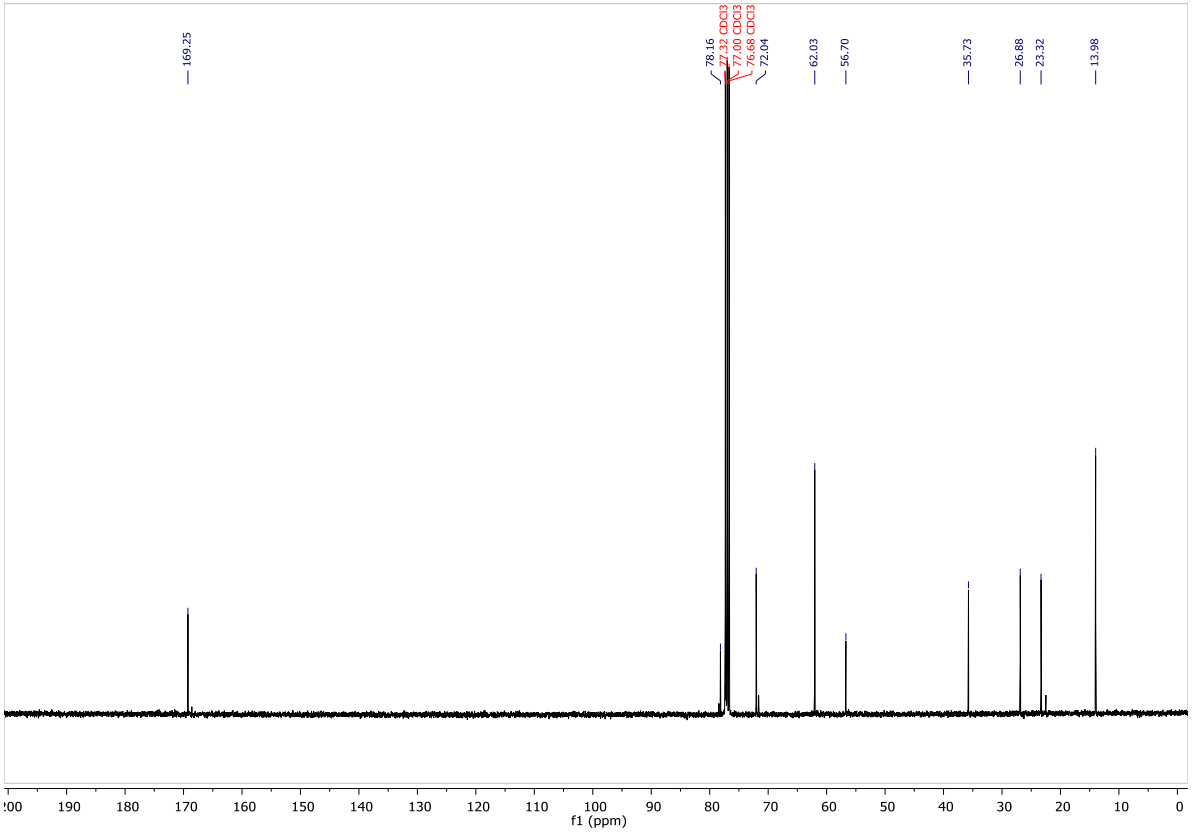
169.25
78.16
77.32 CDCl3
77.00 CDCl3
76.68 CDCl3
72.04
62.03
56.70
35.73
26.88
23.32
13.98
f1 (ppm)

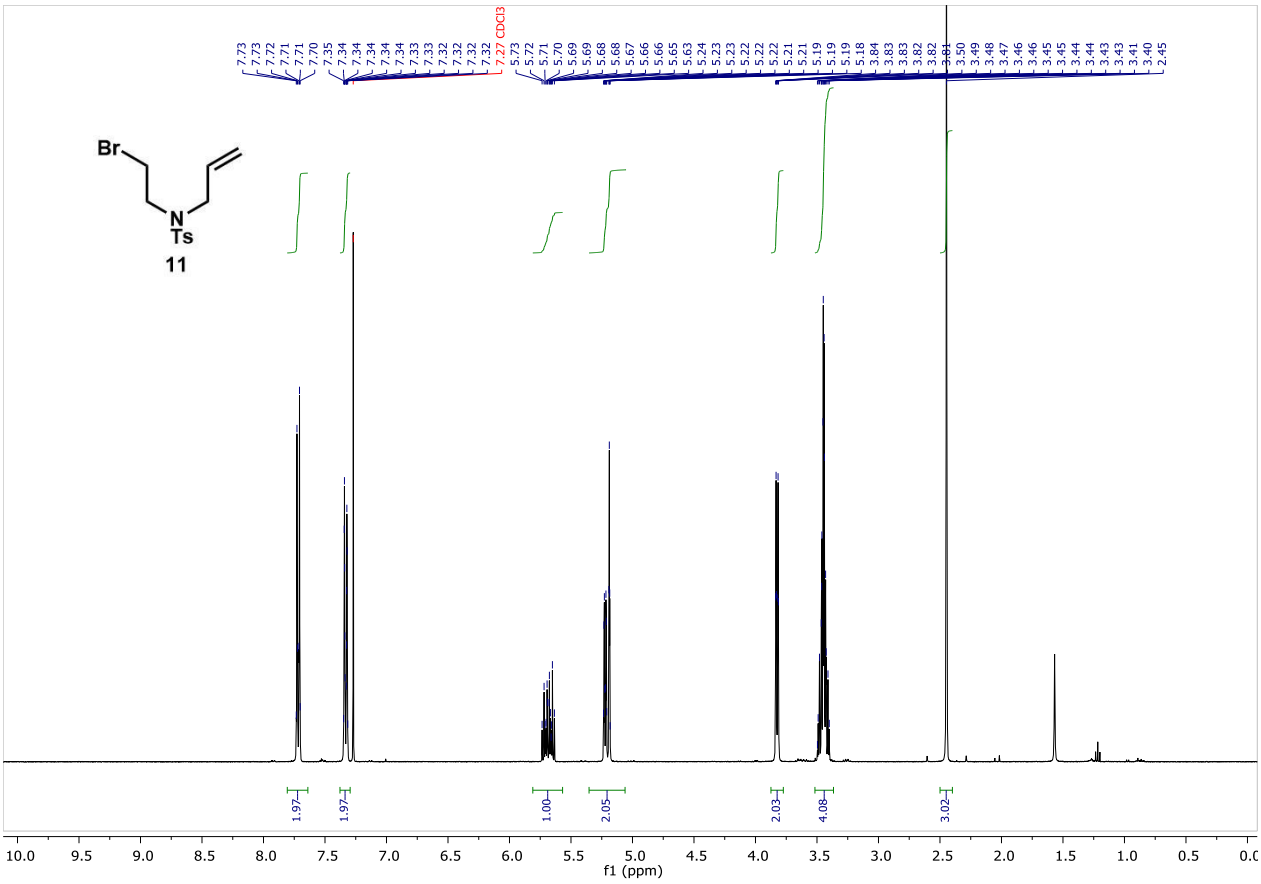
Br
N
Ts
11
7.27 CDCl3
1.97
1.97
1.00
2.05
2.03
4.08
3.02
f1 (ppm)

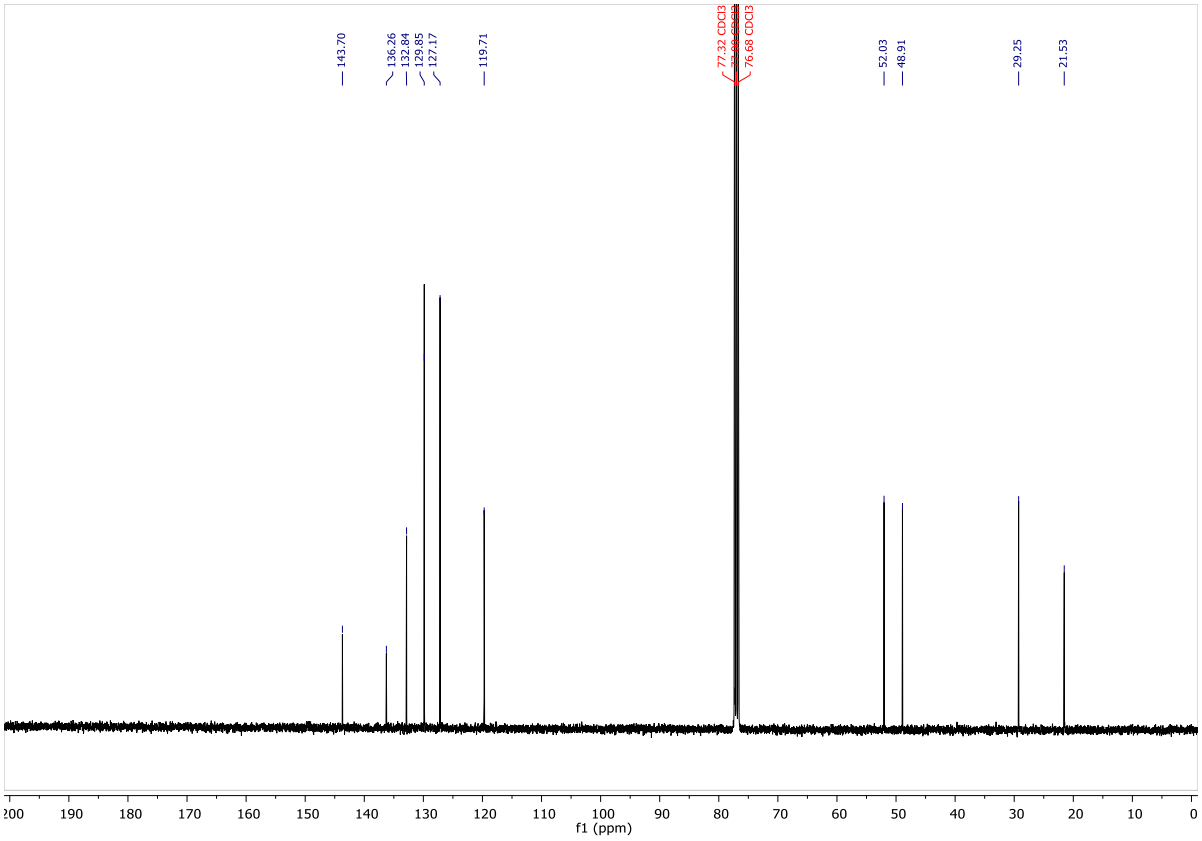
143.70
136.26
132.84
129.85
127.17
119.71
77.32 CDCl3
76.68 CDCl3
52.03
48.91
29.25
21.53
f1 (ppm)

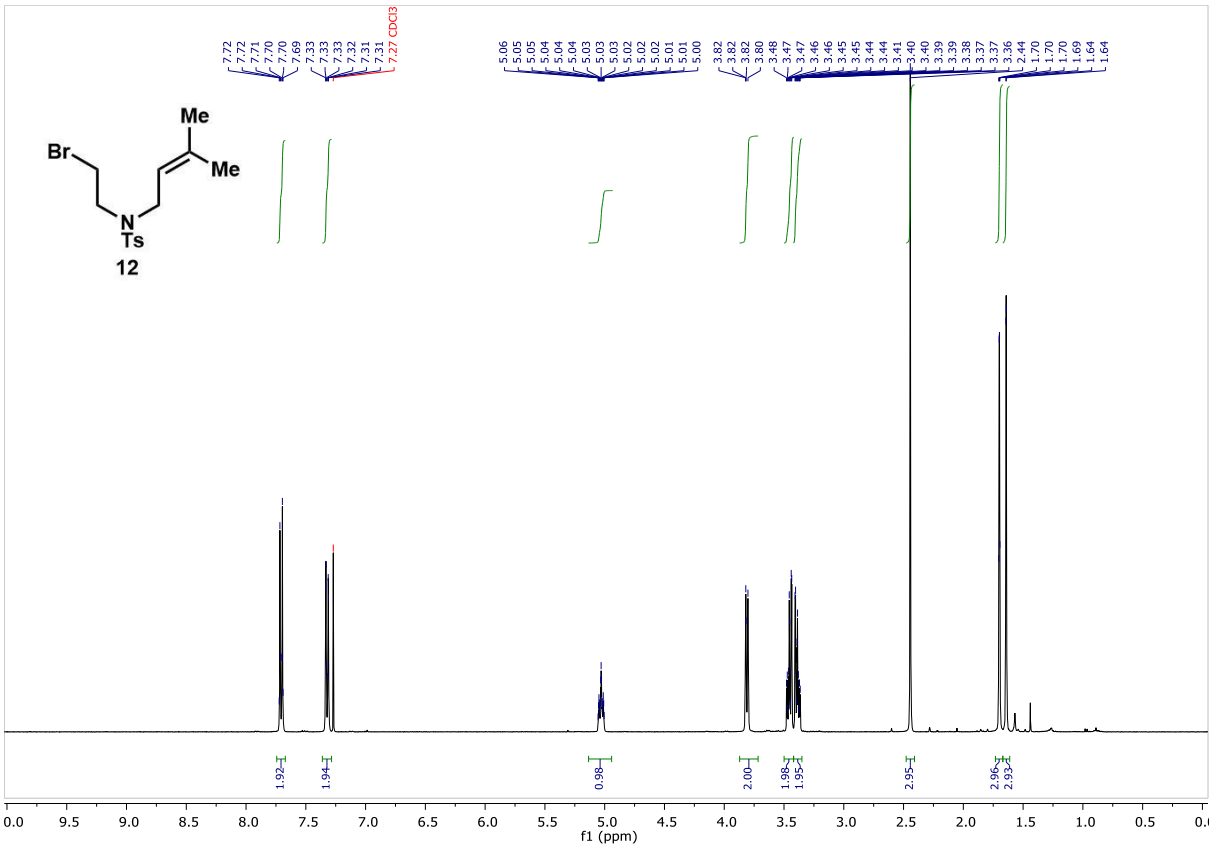
Br
Me
Me
N
Ts
12
f1 (ppm)

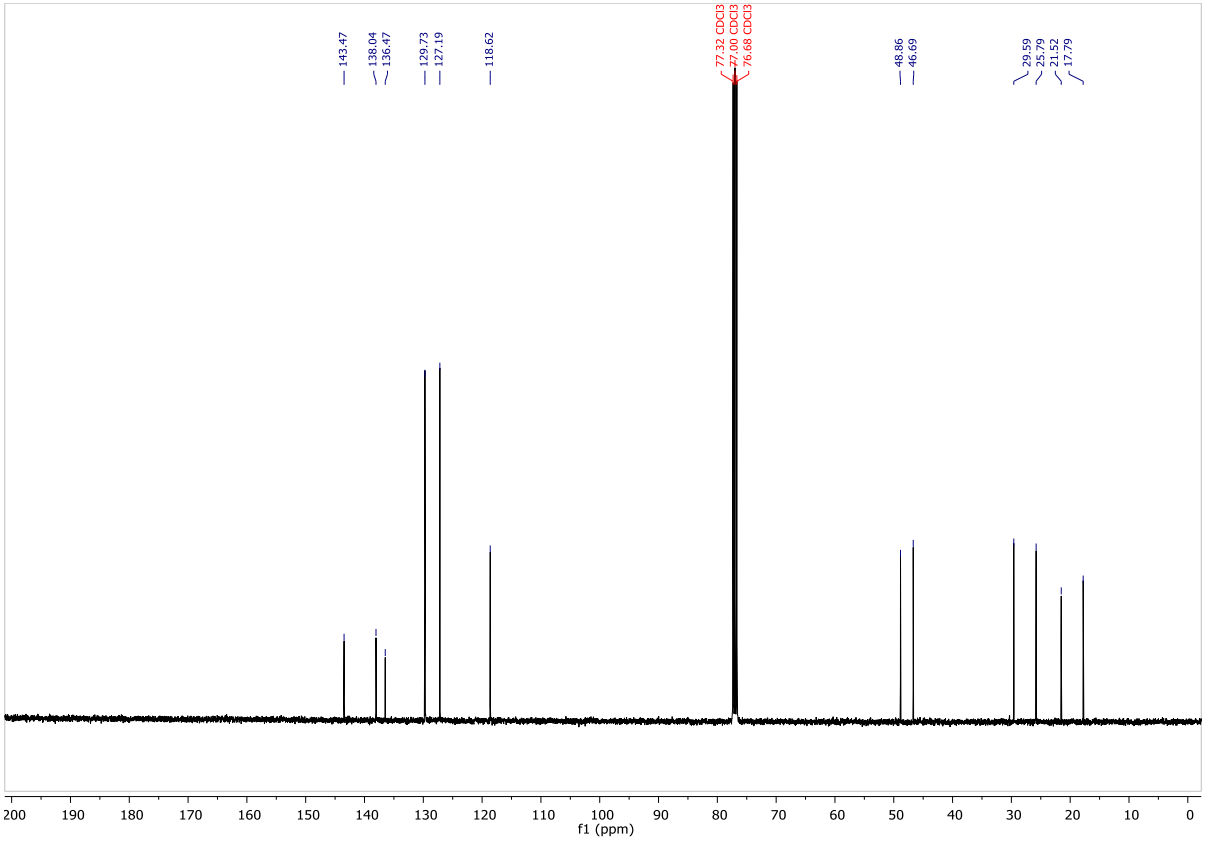
f1 (ppm)

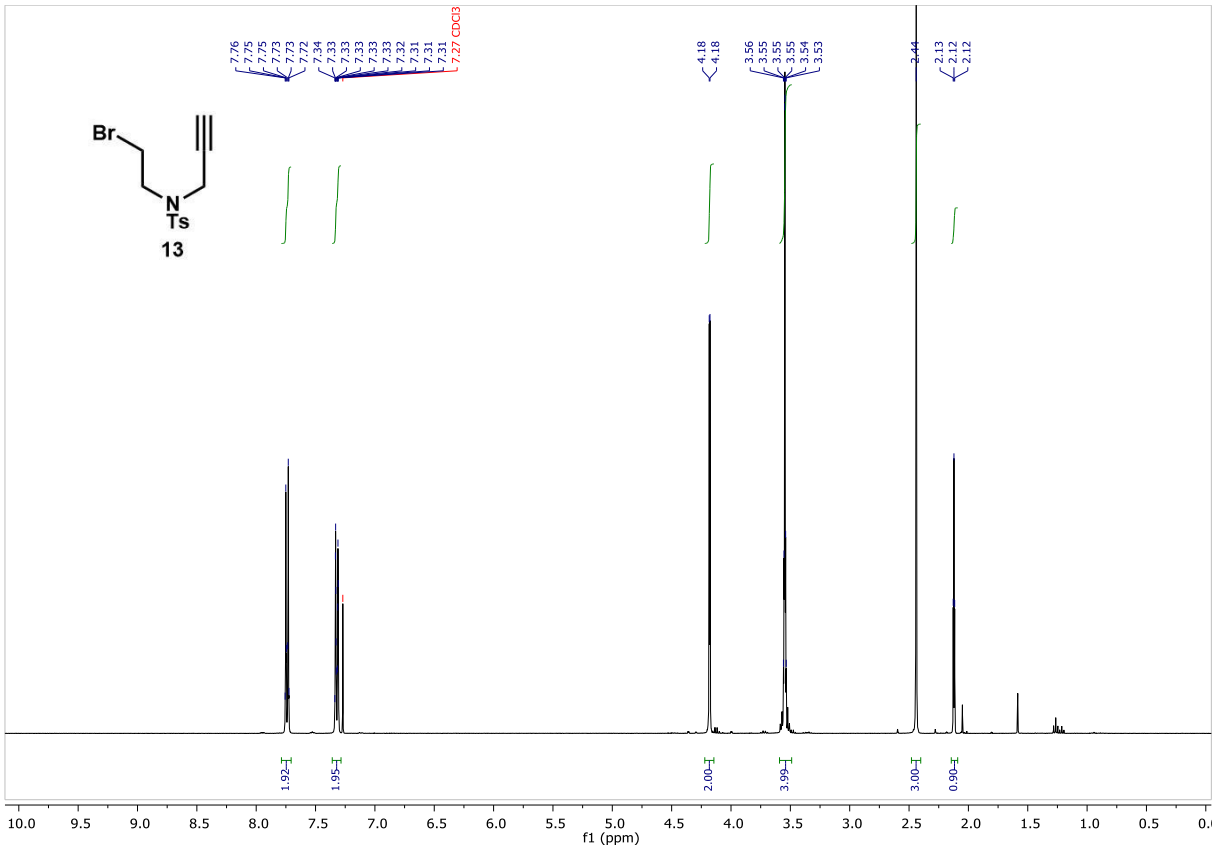
Br
N
Ts
13
7.76
7.75
7.75
7.73
7.73
7.72
7.34
7.33
7.33
7.33
7.33
7.32
7.31
7.31
7.31
7.27 CDCl3
4.18
4.18
3.56
3.55
3.55
3.55
3.55
3.54
3.53
2.44
2.13
2.12
2.12
1.92
1.95
2.00
3.99
3.00
0.90
f1 (ppm)

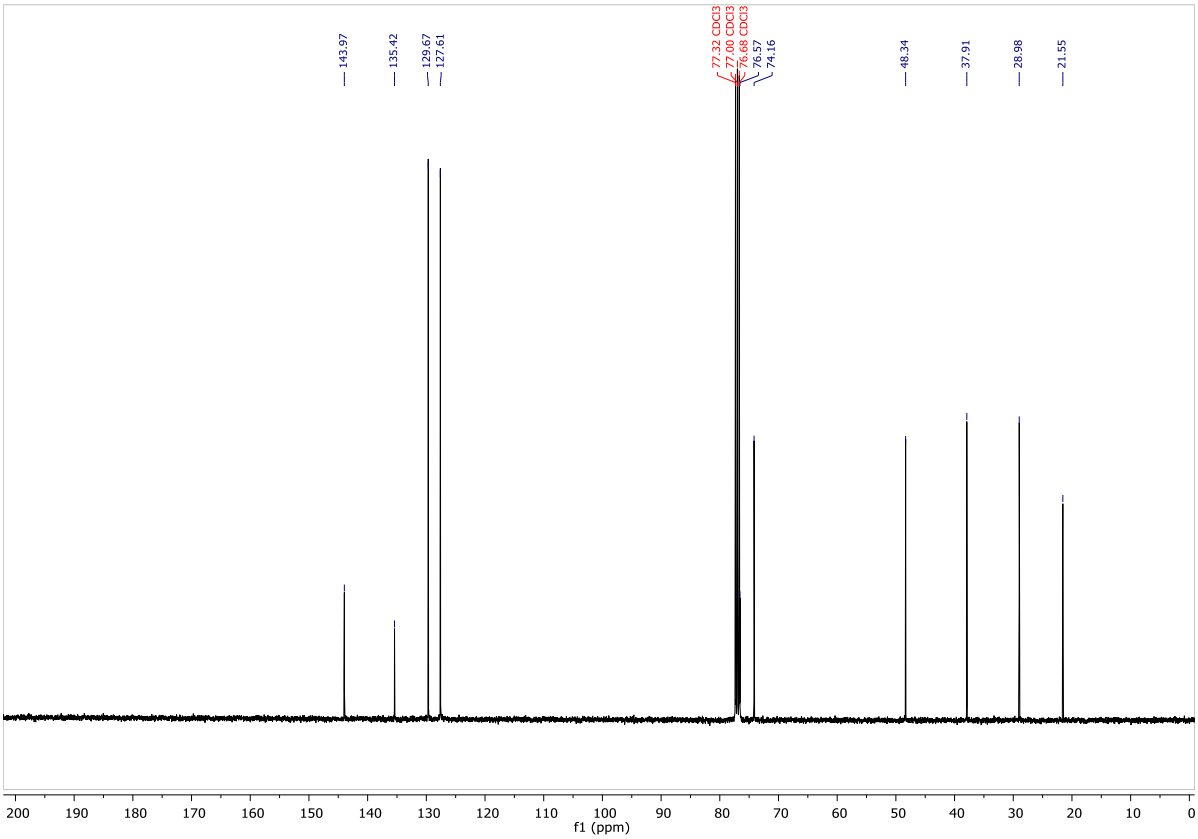
143.97
135.42
129.67
127.61
77.32 CDCl3
77.00 CDCl3
76.68 CDCl3
76.57
74.16
48.34
37.91
28.98
21.55
f1 (ppm)

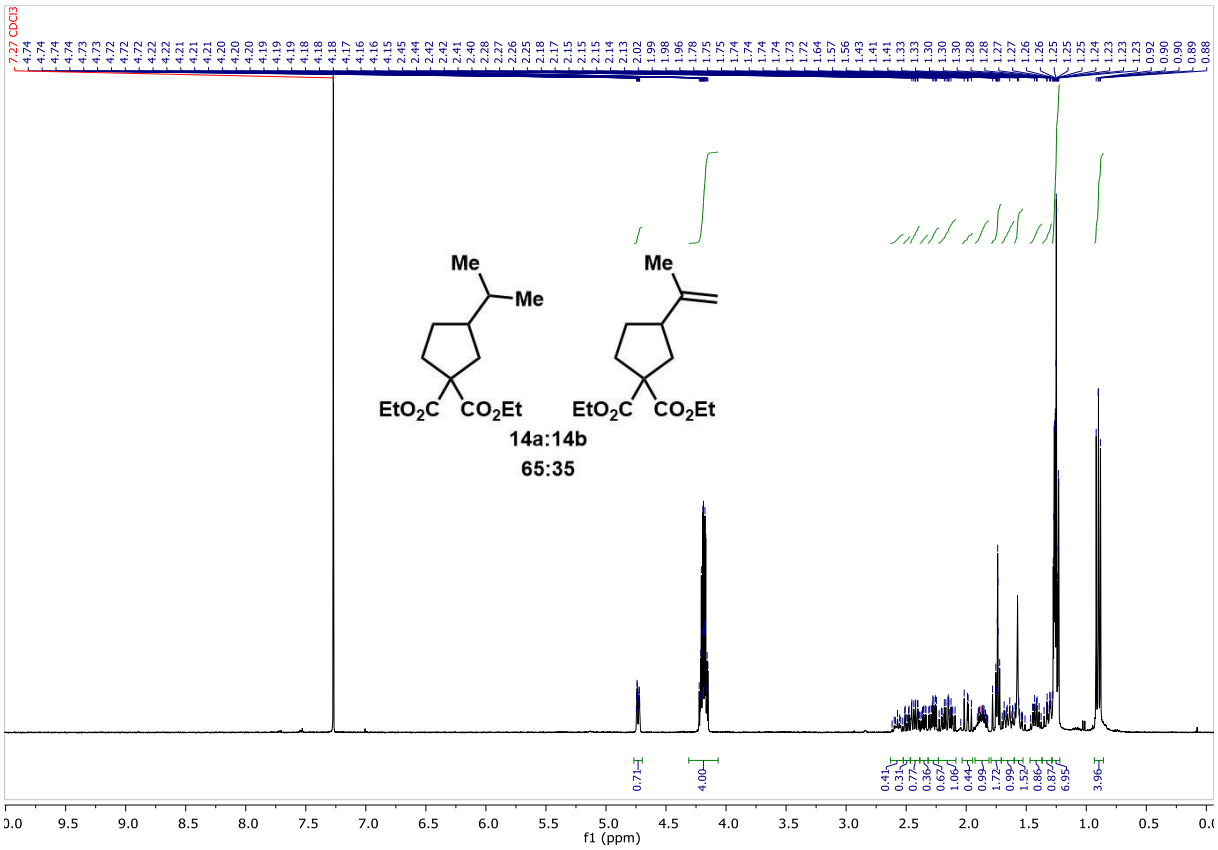
Me
Me
EtO2C
CO2Et
Me
EtO2C
CO2Et
14a:14b
65:35
f1 (ppm)

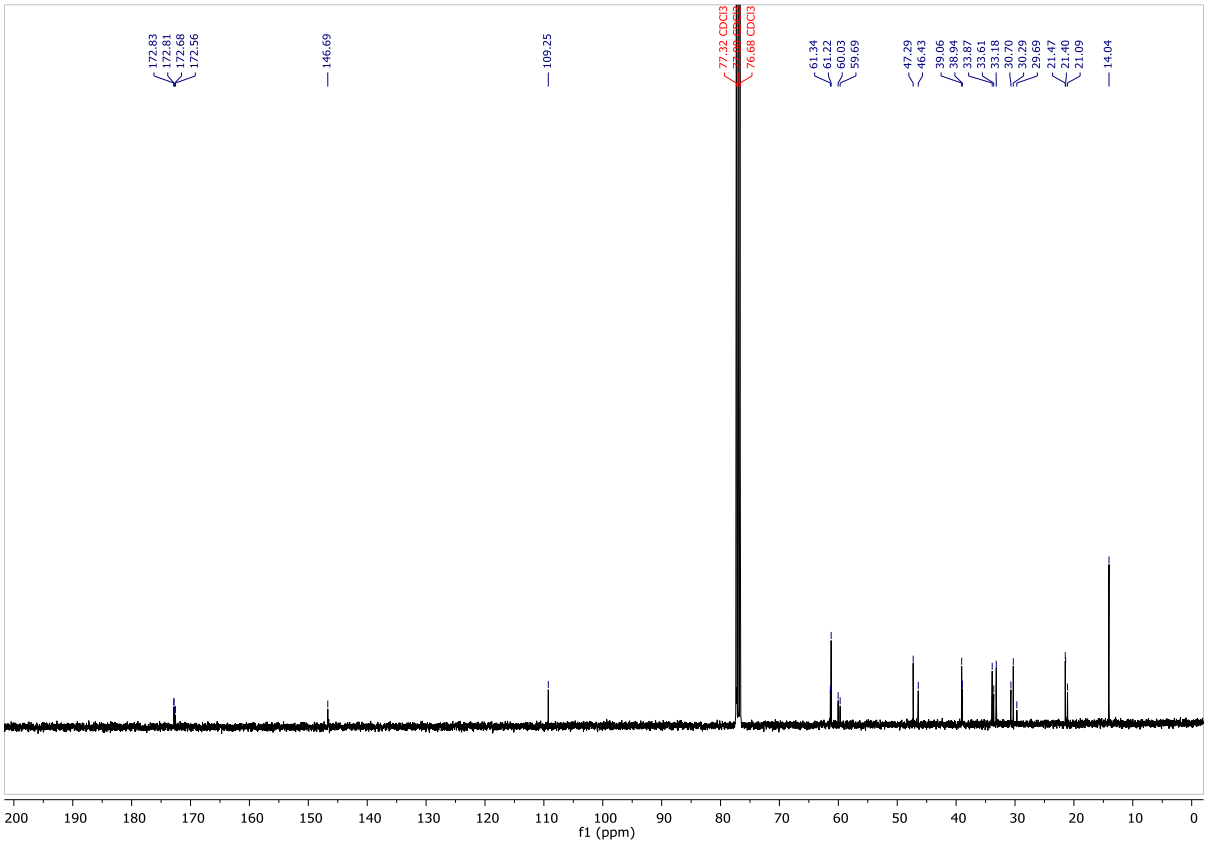
f1 (ppm)

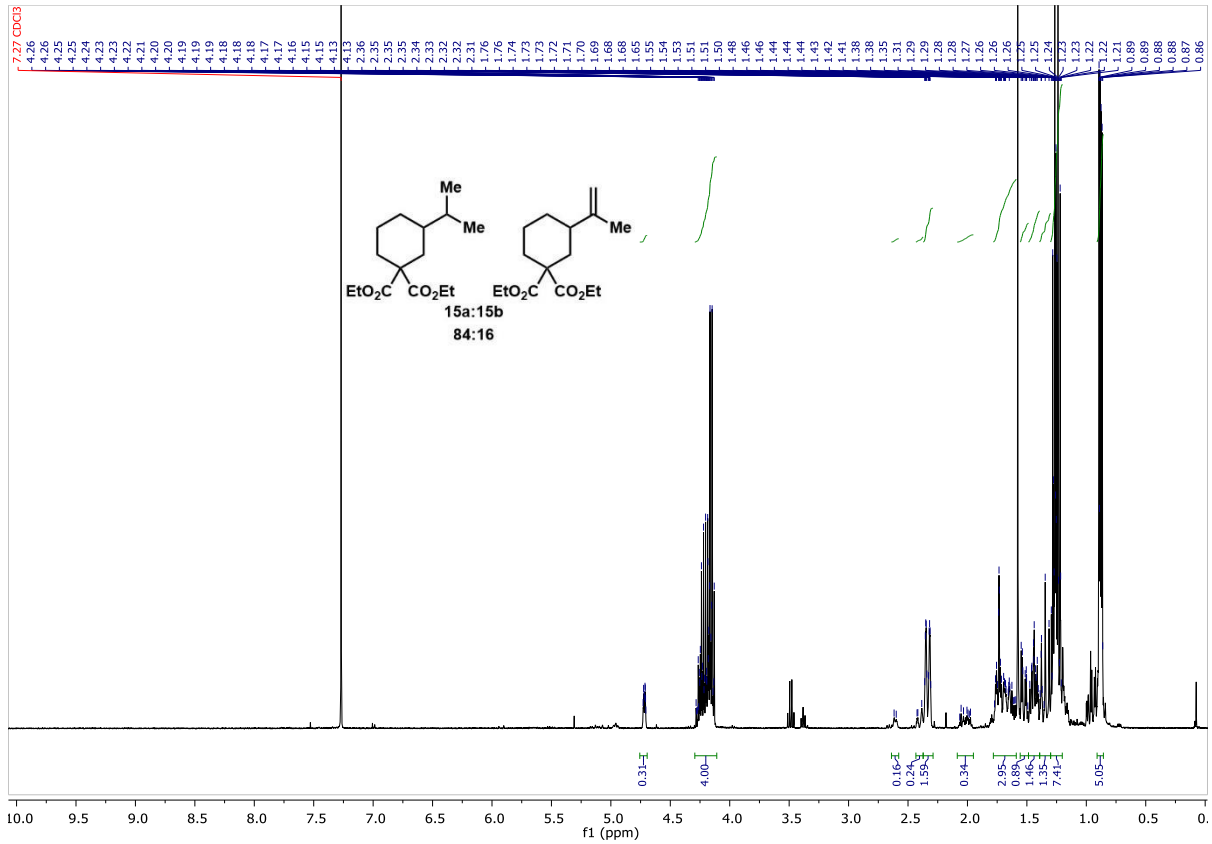
Me
Me
EtO2C CO2Et
15a:15b
84:16
Me
EtO2C CO2Et
f1 (ppm)

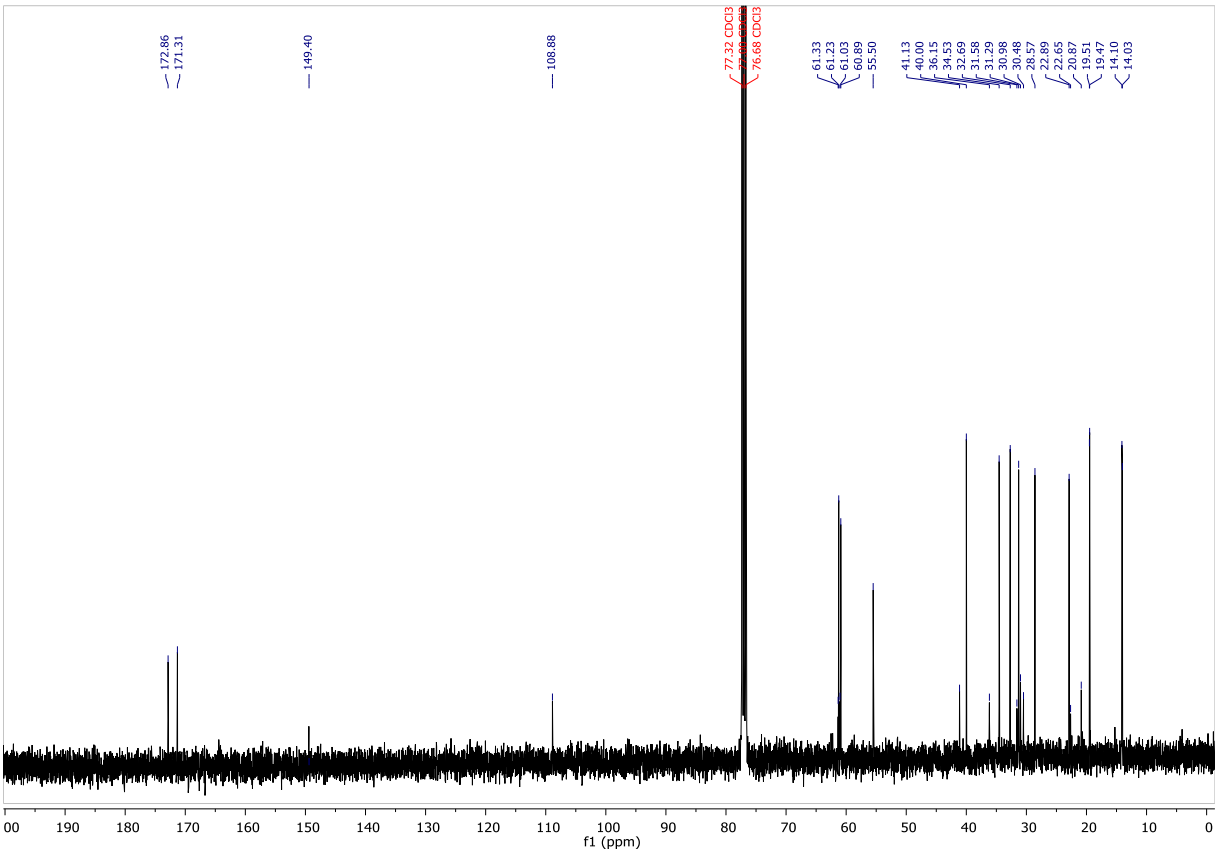
f1 (ppm)

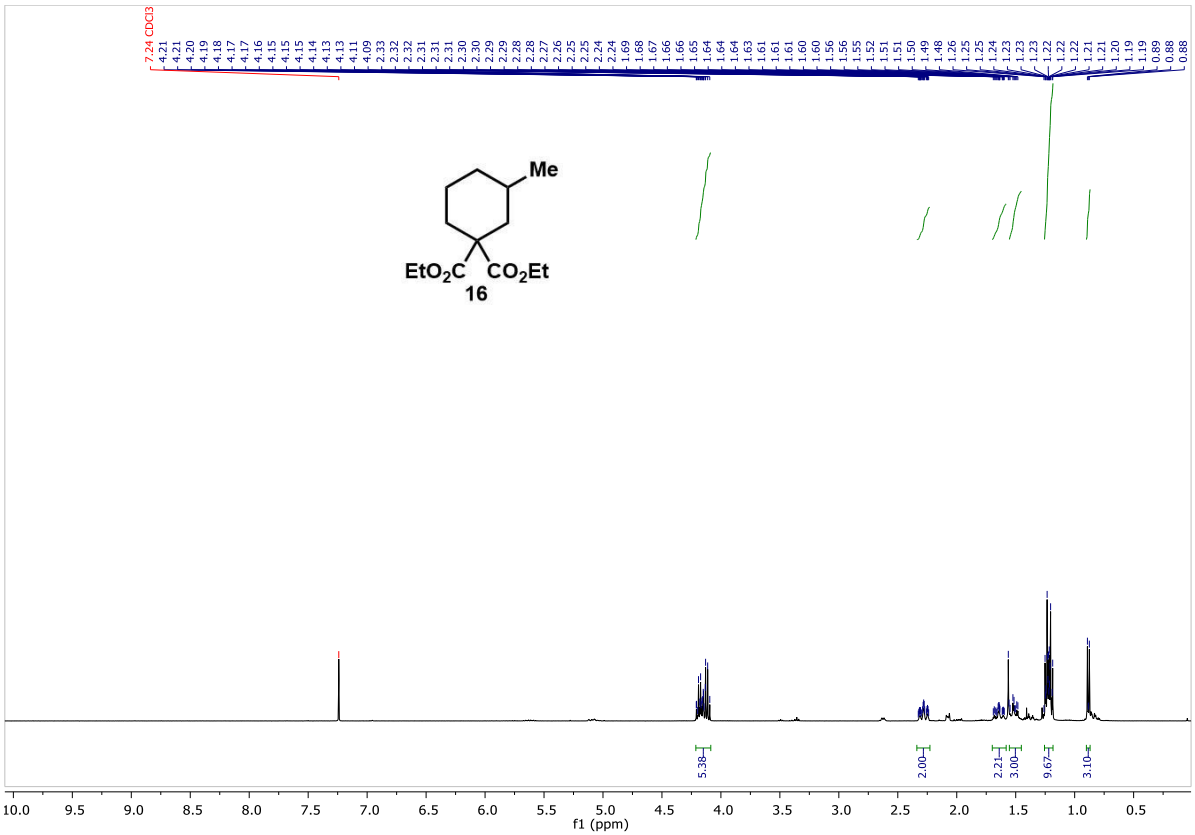
Me
EtO2C CO2Et
16
f1 (ppm)

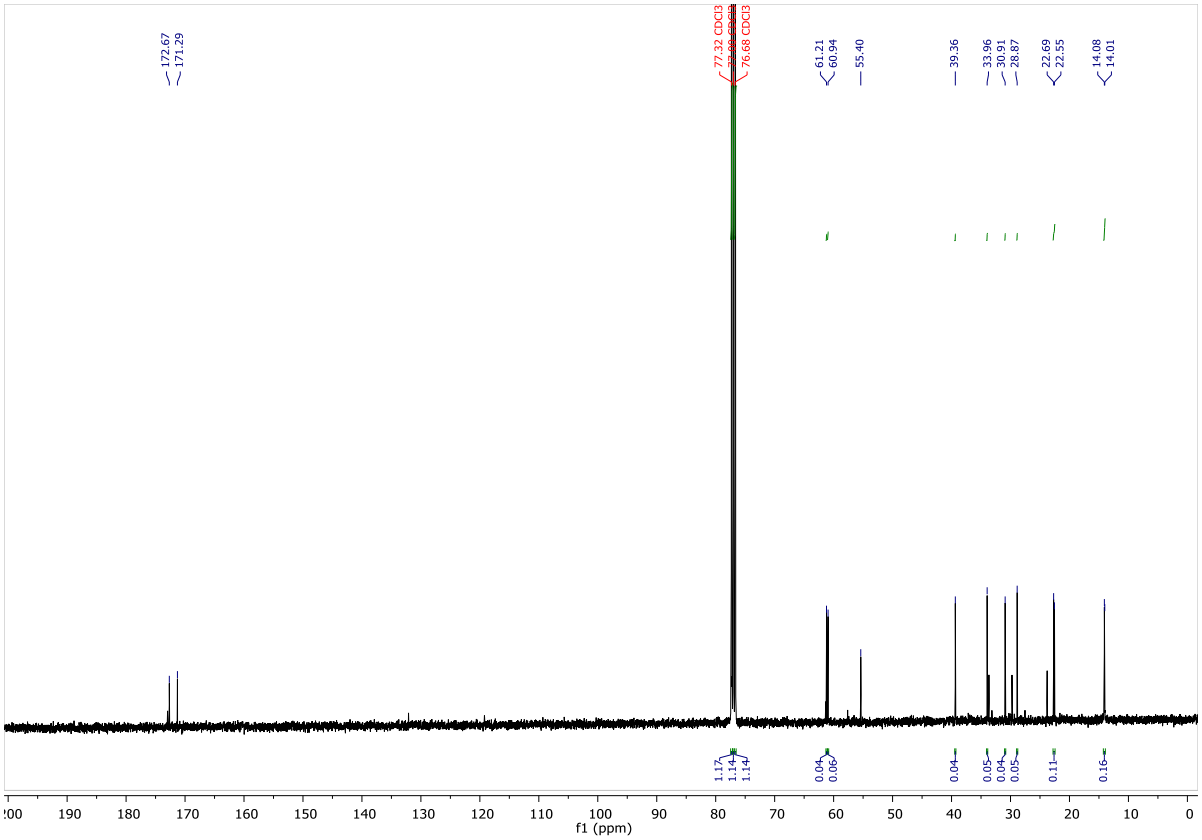
f1 (ppm)

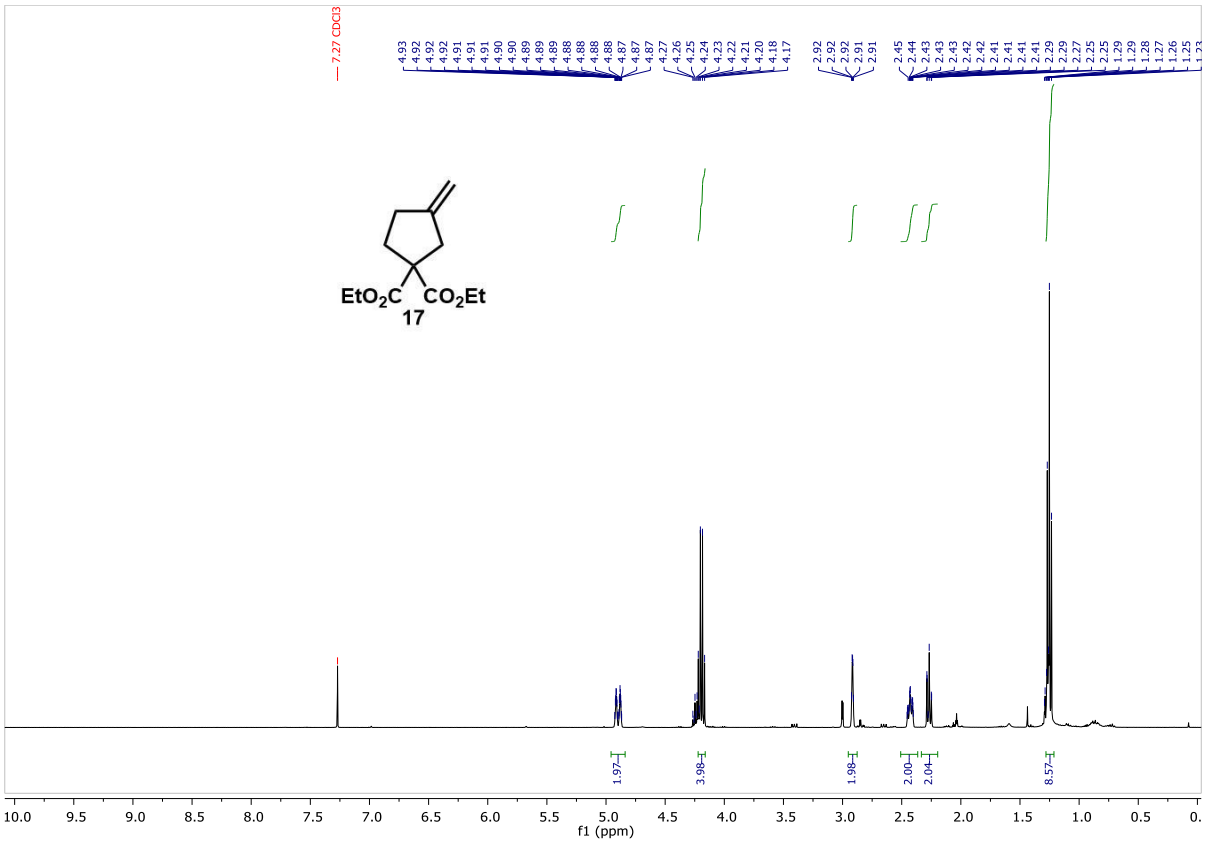
7.27 CDCl3
4.93 4.92 4.92 4.92 4.91 4.91 4.91 4.90 4.90 4.89 4.89 4.88 4.88 4.88 4.88 4.87 4.87 4.87
4.27 4.26 4.25 4.24 4.23 4.22 4.21 4.20 4.18 4.17
2.92 2.92 2.92 2.91 2.91
2.45 2.44 2.43 2.43 2.43 2.42 2.42 2.41 2.41 2.41 2.41 2.29 2.29 2.27 2.25 2.25 1.29 1.29 1.28 1.27 1.26 1.25 1.23
EtO2C CO2Et
17
1.97
3.98
1.98
2.00
2.04
8.57
10.0 9.5 9.0 8.5 8.0 7.5 7.0 6.5 6.0 5.5 5.0 4.5 4.0 3.5 3.0 2.5 2.0 1.5 1.0 0.5 0.
f1 (ppm)

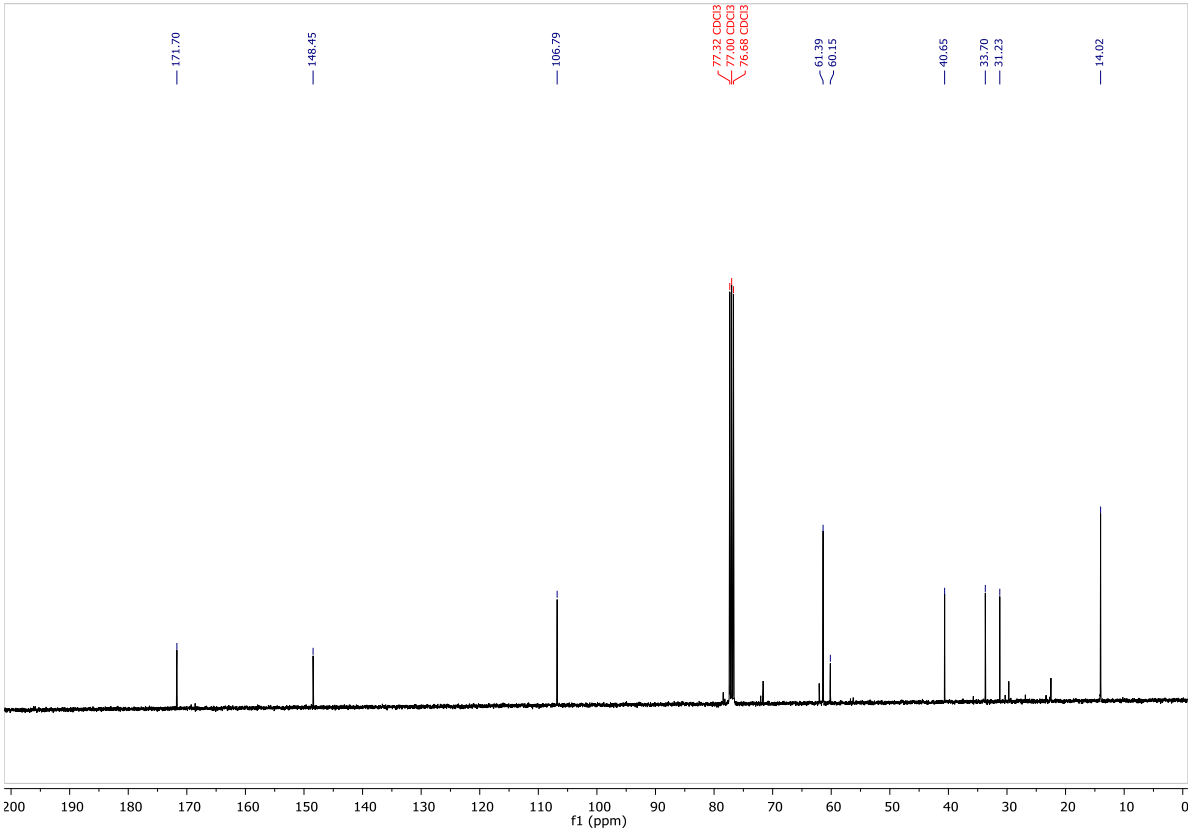
171.70
148.45
106.79
77.32 CDCl3
77.00 CDCl3
76.68 CDCl3
61.39
60.15
40.65
33.70
31.23
14.02
200 190 180 170 160 150 140 130 120 110 100 90 80 70 60 50 40 30 20 10 0
f1 (ppm)

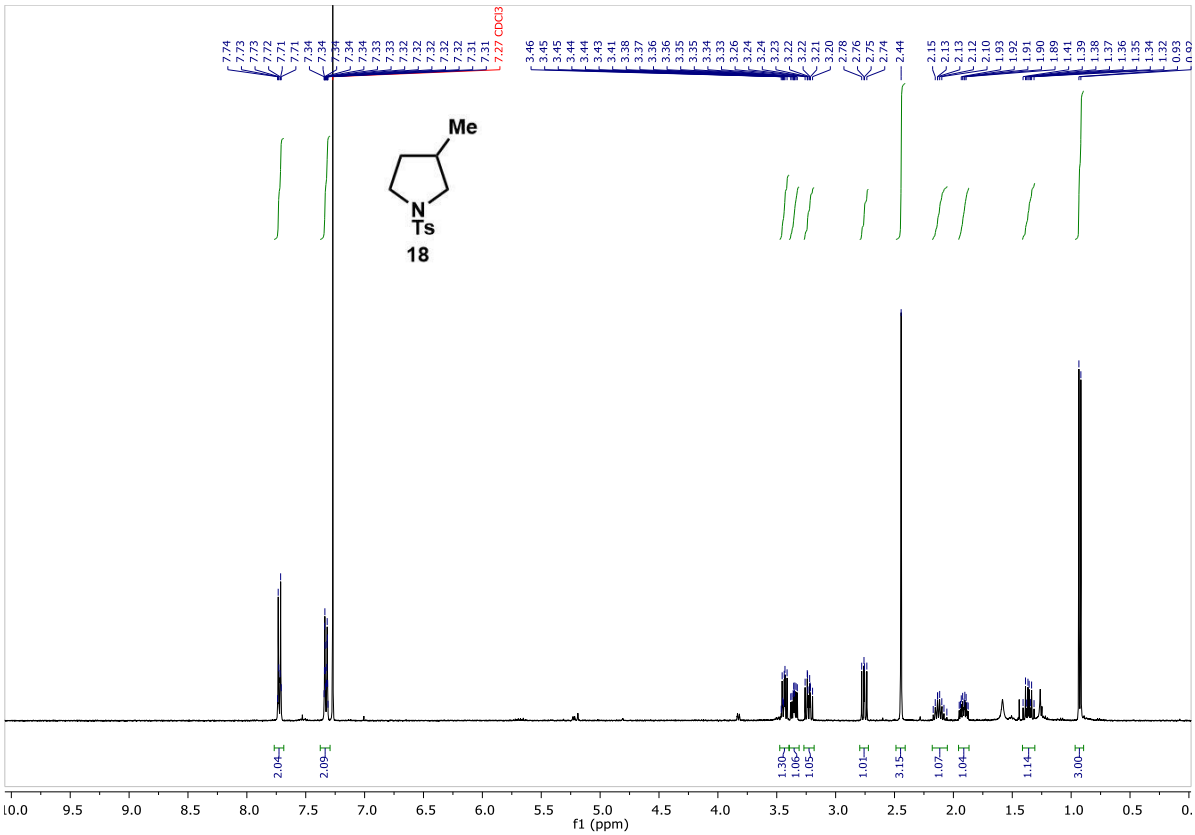
Me
N
Ts
18
f1 (ppm)

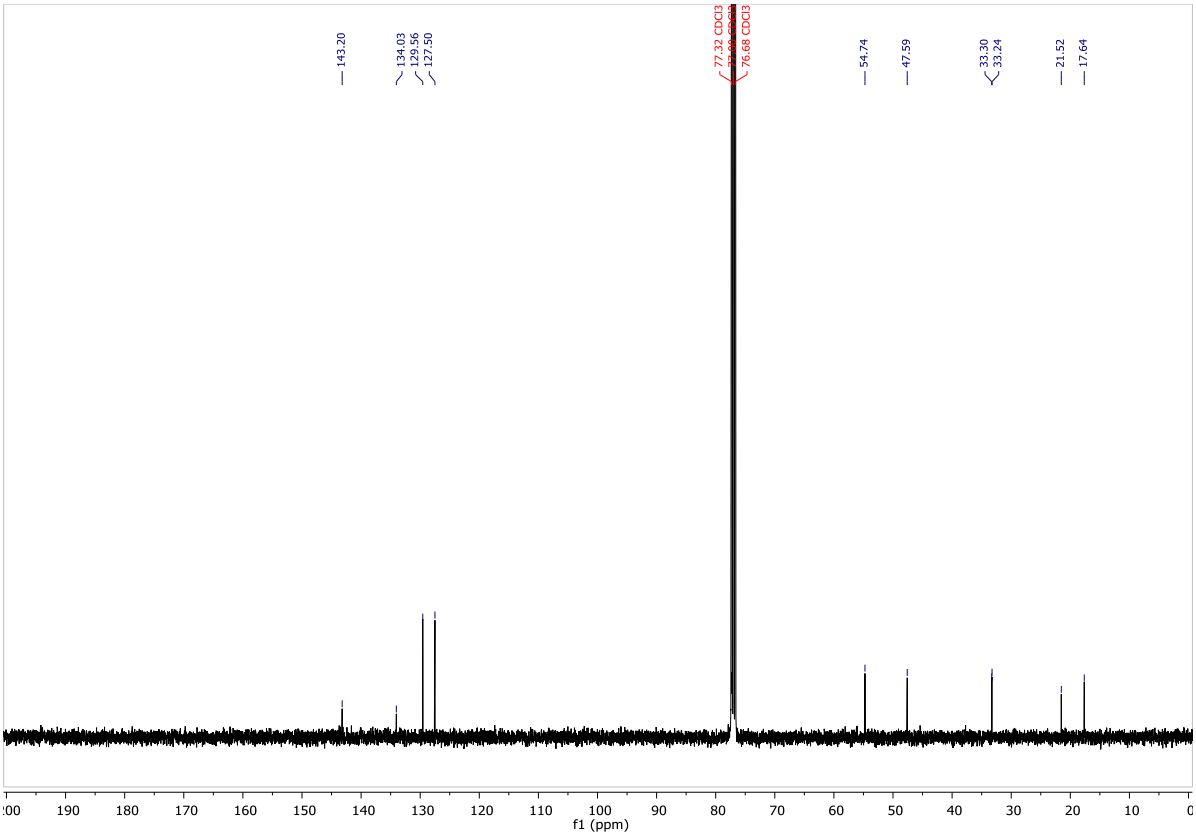
143.20
134.03
129.56
127.50
77.32 CDCl3
76.68 CDCl3
54.74
47.59
33.30
33.24
21.52
17.64
f1 (ppm)

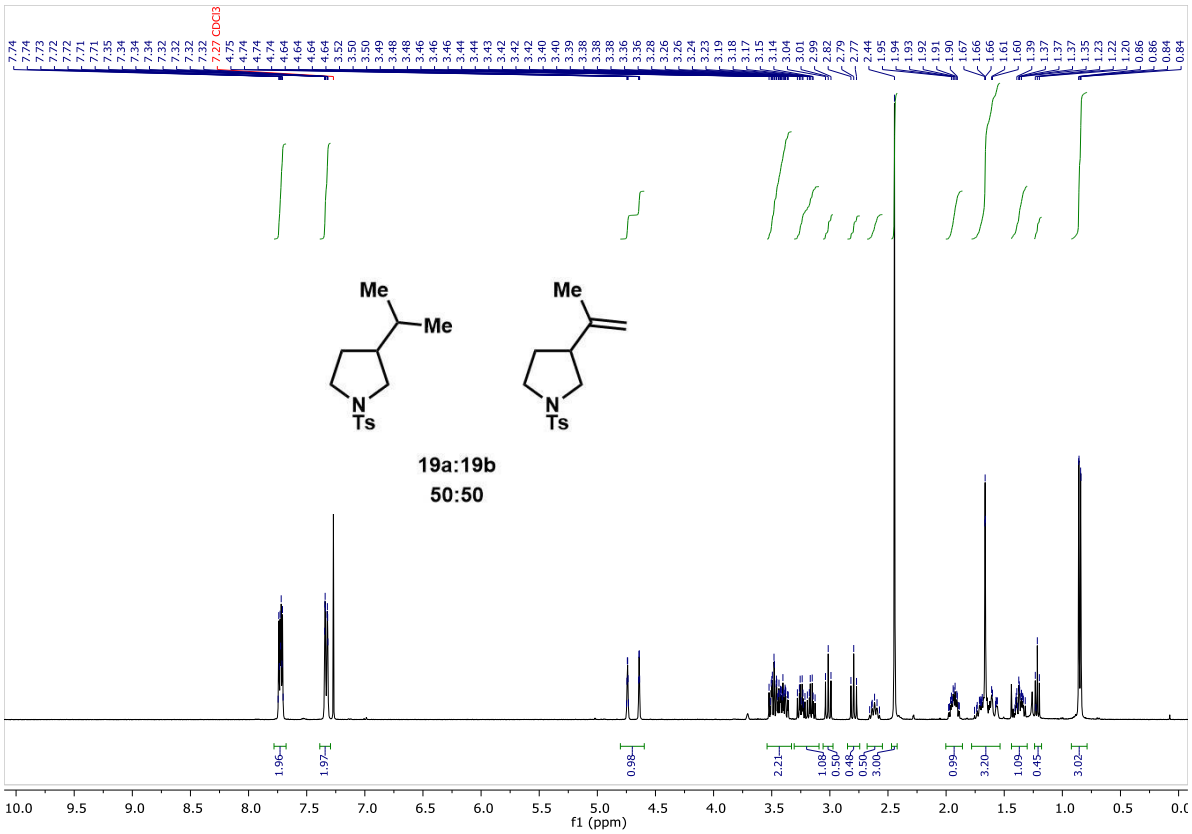
Me
Me
N
Ts
Me
N
Ts
19a:19b
50:50
f1 (ppm)

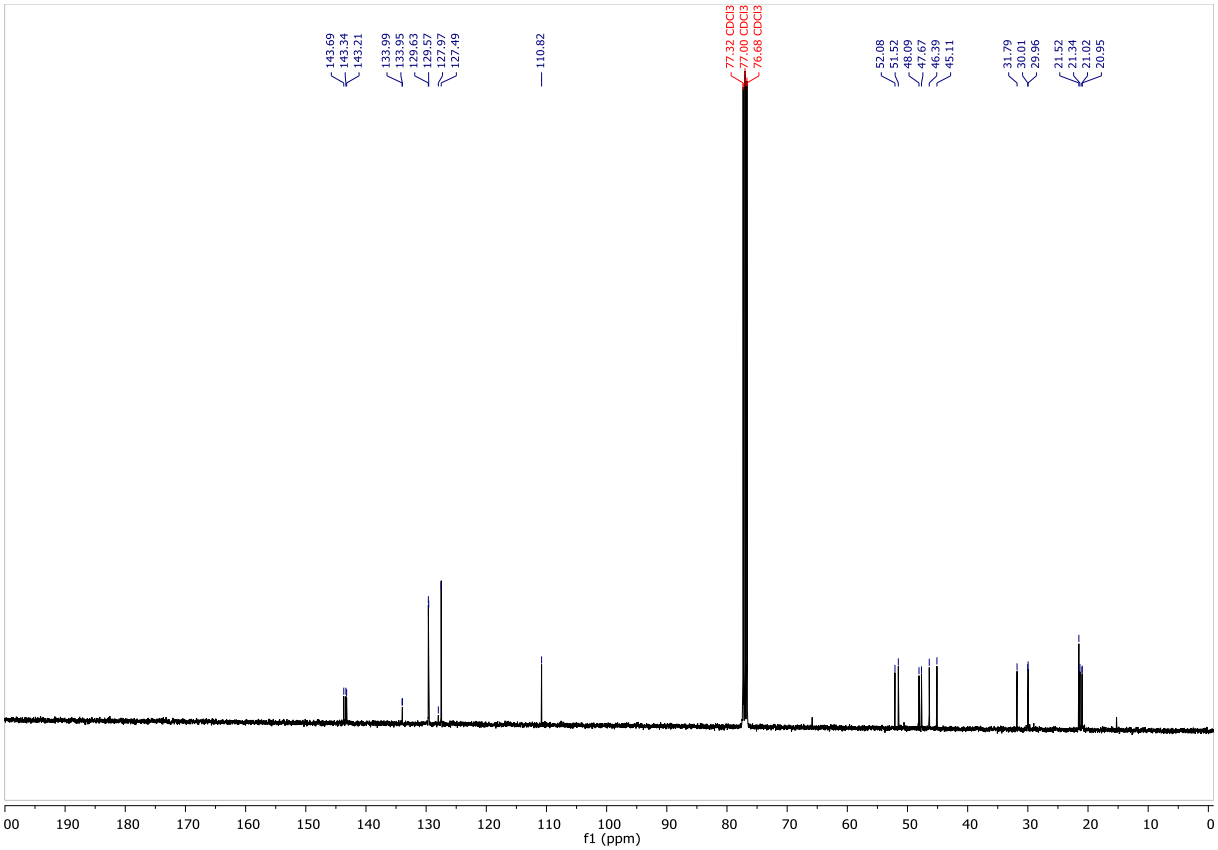
f1 (ppm)

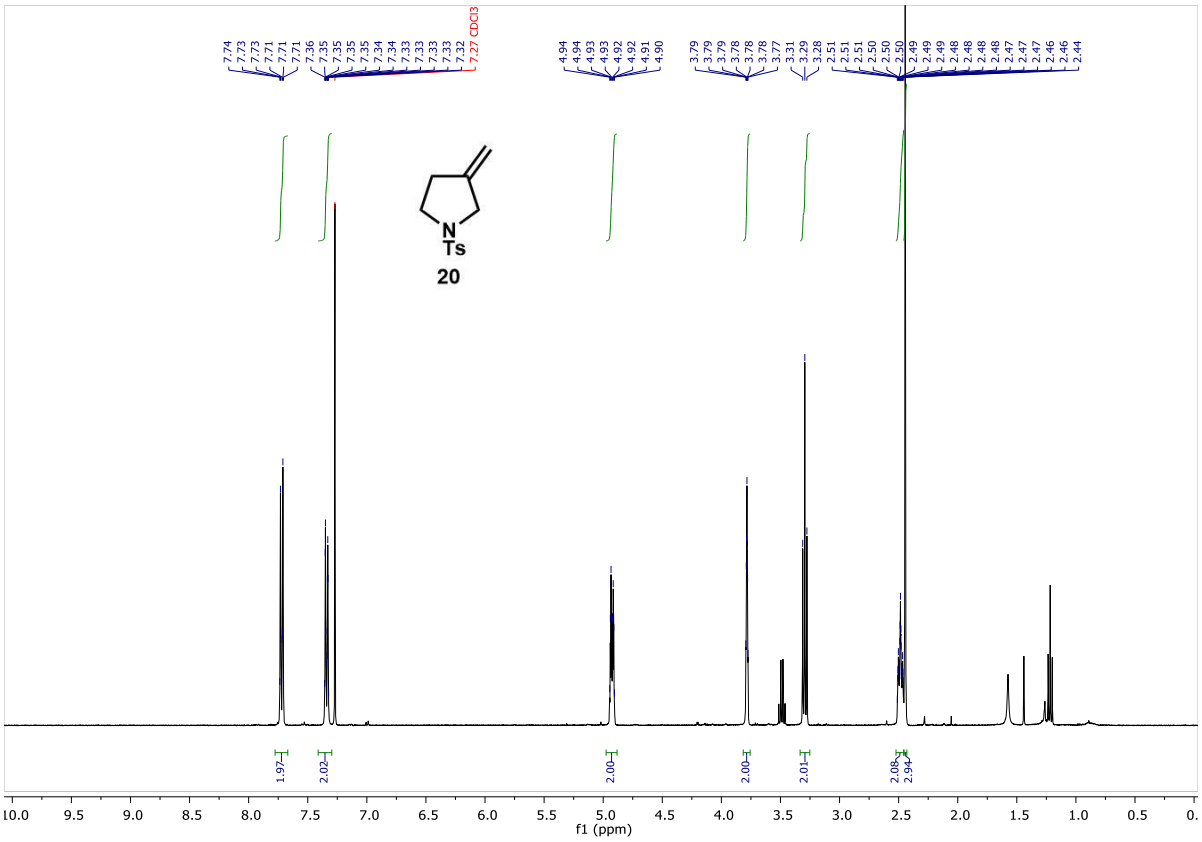
7.74 7.73 7.73 7.71 7.71 7.71 7.36 7.35 7.35 7.35 7.35 7.34 7.34 7.33 7.33 7.33 7.33 7.32 7.27 CDCl3
4.94 4.94 4.93 4.93 4.92 4.92 4.91 4.90
3.79 3.79 3.79 3.78 3.78 3.78 3.77 3.31 3.29 3.28
2.51 2.51 2.51 2.50 2.50 2.50 2.49 2.49 2.49 2.48 2.48 2.48 2.48 2.47 2.47 2.47 2.46 2.46 2.46 2.44
N
Ts
20
1.97
2.02
2.00
2.00
2.01
2.08
2.94
10.0 9.5 9.0 8.5 8.0 7.5 7.0 6.5 6.0 5.5 5.0 4.5 4.0 3.5 3.0 2.5 2.0 1.5 1.0 0.5 0.
f1 (ppm)

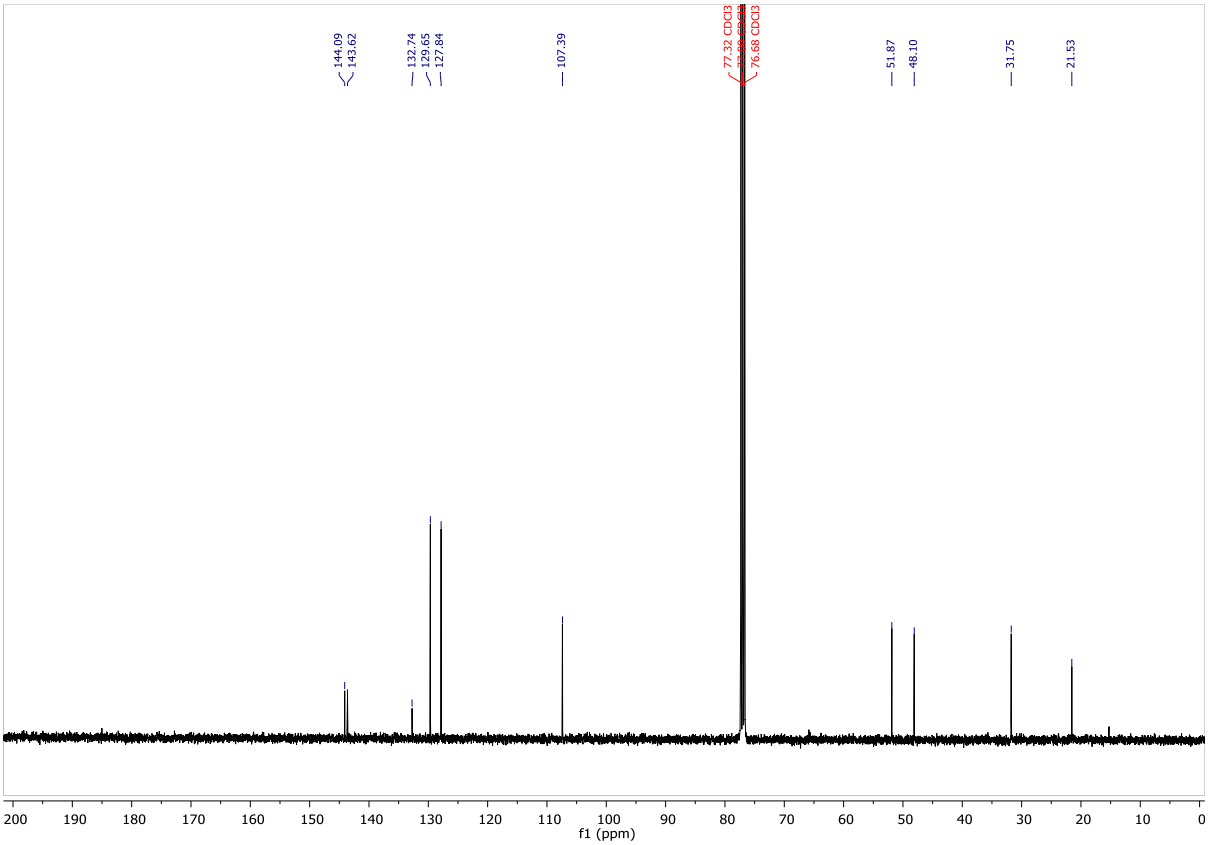
144.09
143.62
132.74
129.65
127.84
107.39
77.32 CDCl3
76.68 CDCl3
51.87
48.10
31.75
21.53
200 190 180 170 160 150 140 130 120 110 100 90 80 70 60 50 40 30 20 10 0
f1 (ppm)

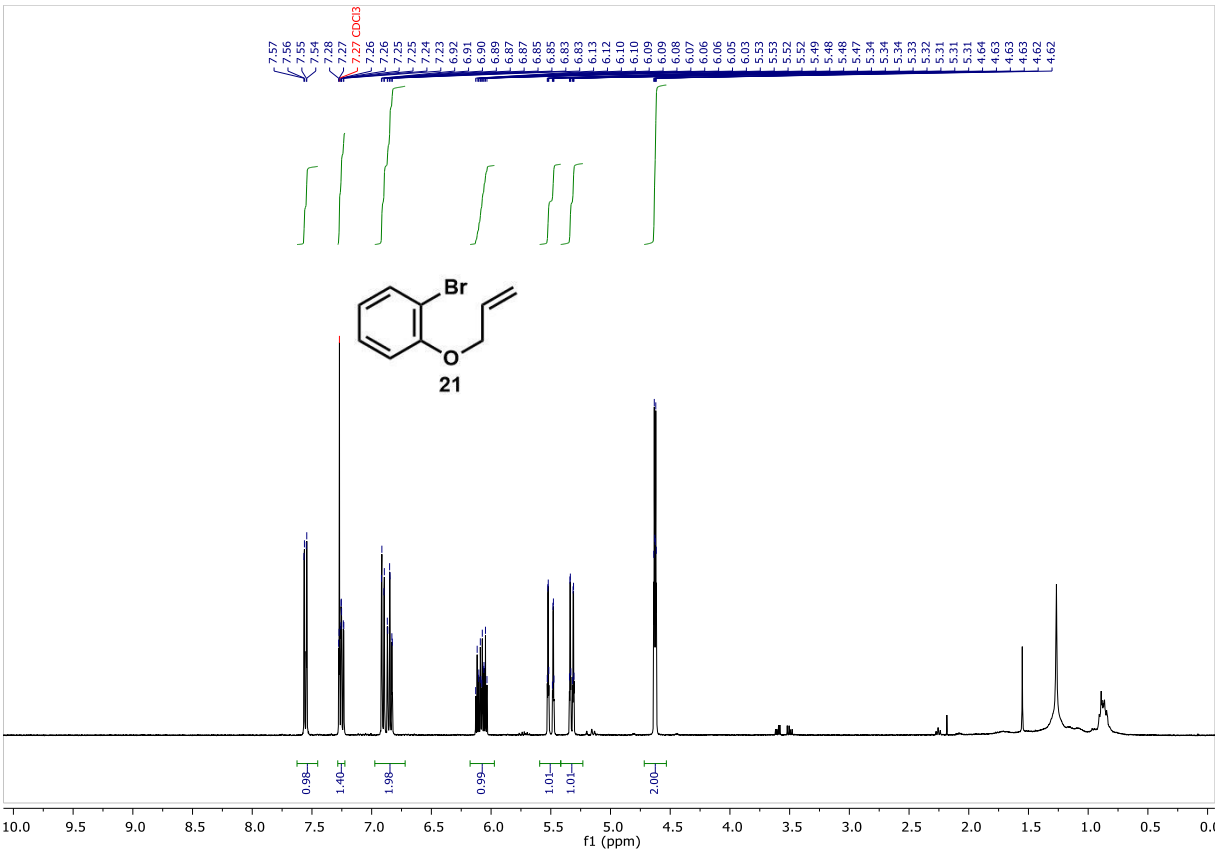
7.57
7.56
7.55
7.54
7.28
7.27
7.27 CDCl3
7.26
7.26
7.25
7.25
7.24
7.23
6.92
6.91
6.90
6.89
6.87
6.87
6.85
6.85
6.83
6.83
6.13
6.12
6.10
6.10
6.09
6.09
6.08
6.07
6.06
6.06
6.06
6.05
6.03
5.53
5.53
5.52
5.52
5.49
5.48
5.48
5.47
5.34
5.34
5.34
5.33
5.32
5.31
5.31
5.31
4.64
4.63
4.63
4.63
4.62
4.62
Br
O
21
0.98
1.40
1.98
0.99
1.01
1.01
2.00
10.0
9.5
9.0
8.5
8.0
7.5
7.0
6.5
6.0
5.5
5.0
4.5
4.0
3.5
3.0
2.5
2.0
1.5
1.0
0.5
f1 (ppm)

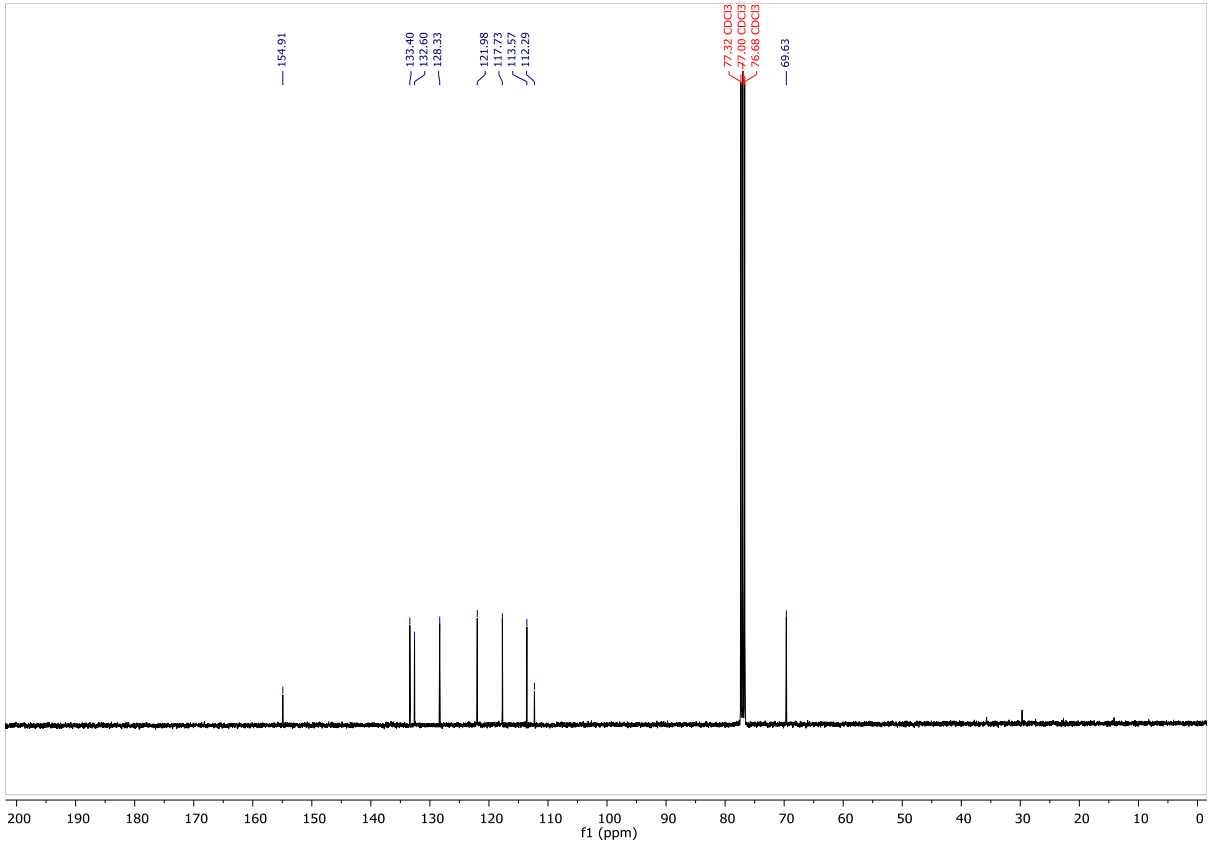
154.91
133.40
132.60
128.33
121.98
117.73
113.57
112.29
77.32 CDCl3
77.00 CDCl3
76.68 CDCl3
69.63
200
190
180
170
160
150
140
130
120
110
100
90
80
70
60
50
40
30
20
10
0
f1 (ppm)

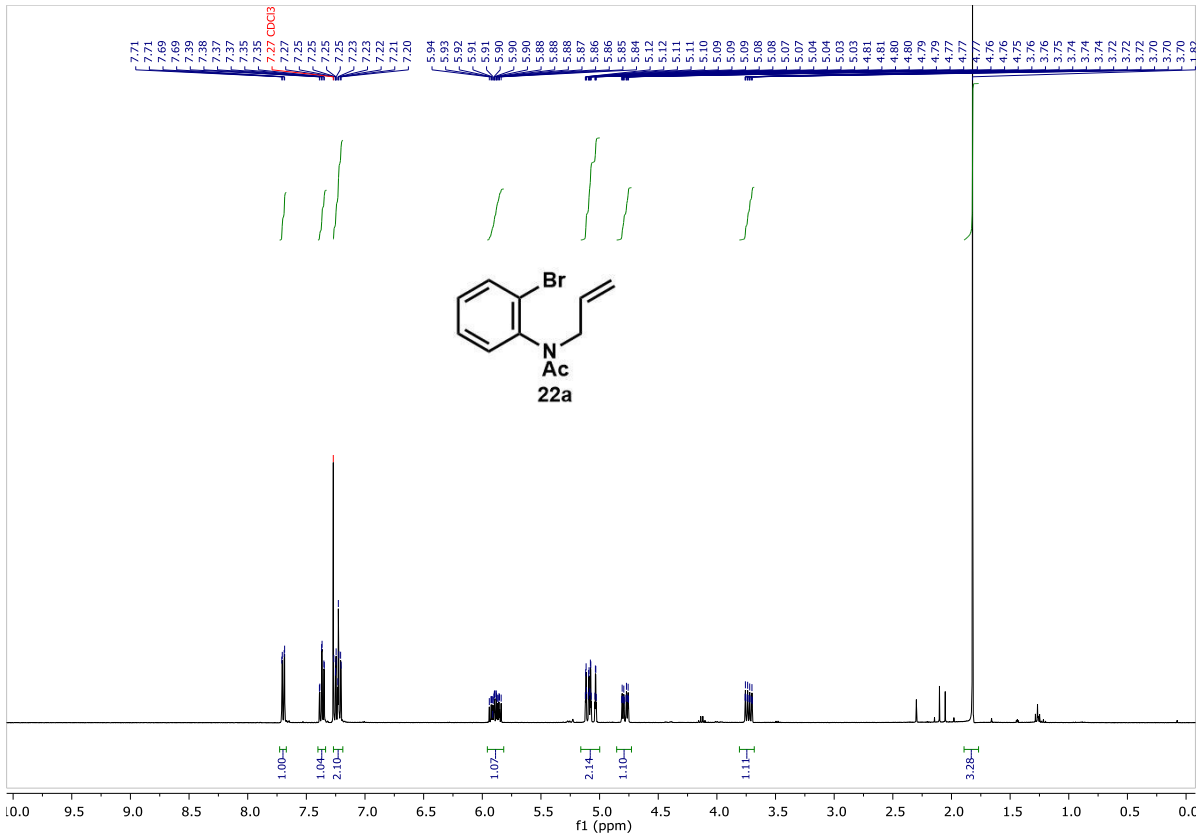
Br
N
Ac
22a
f1 (ppm)

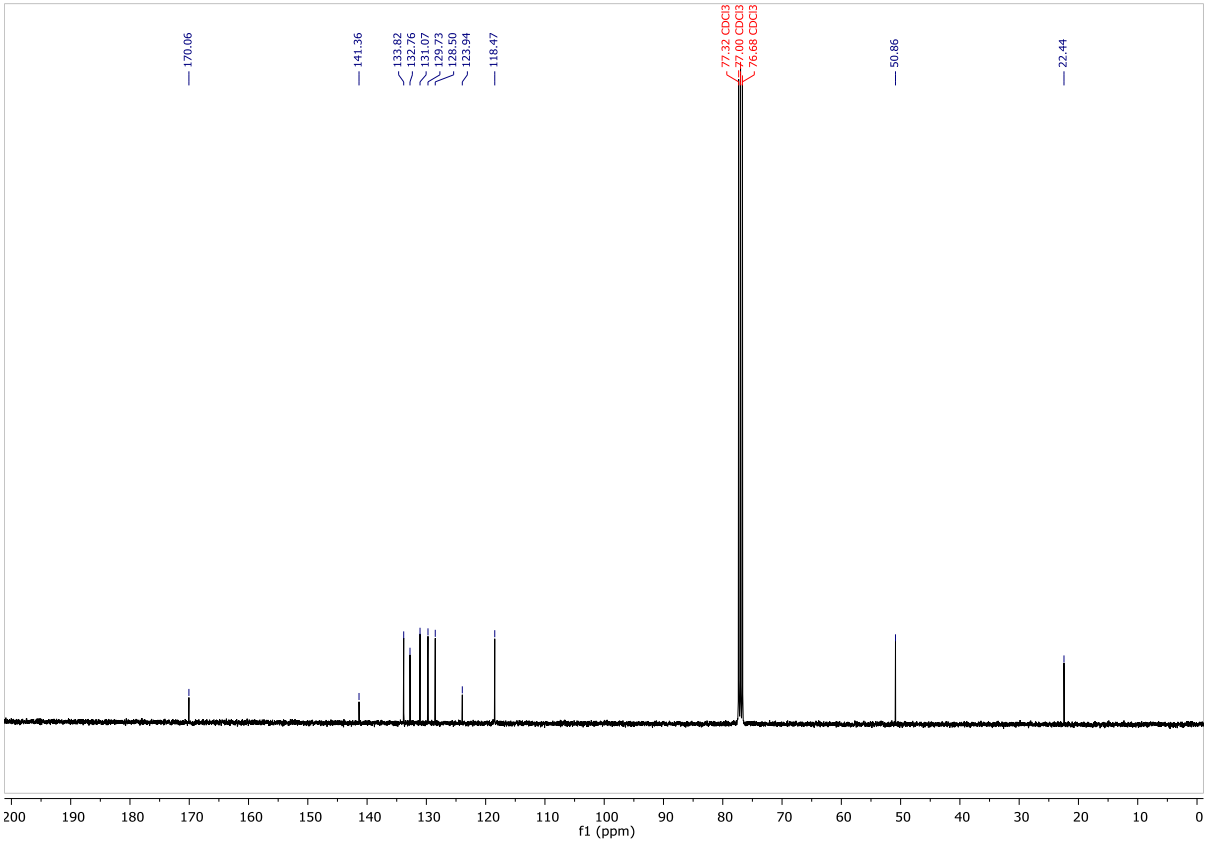
170.06
141.36
133.82
132.76
131.07
129.73
128.50
123.94
118.47
77.32 CDCl3
77.00 CDCl3
76.68 CDCl3
50.86
22.44
f1 (ppm)

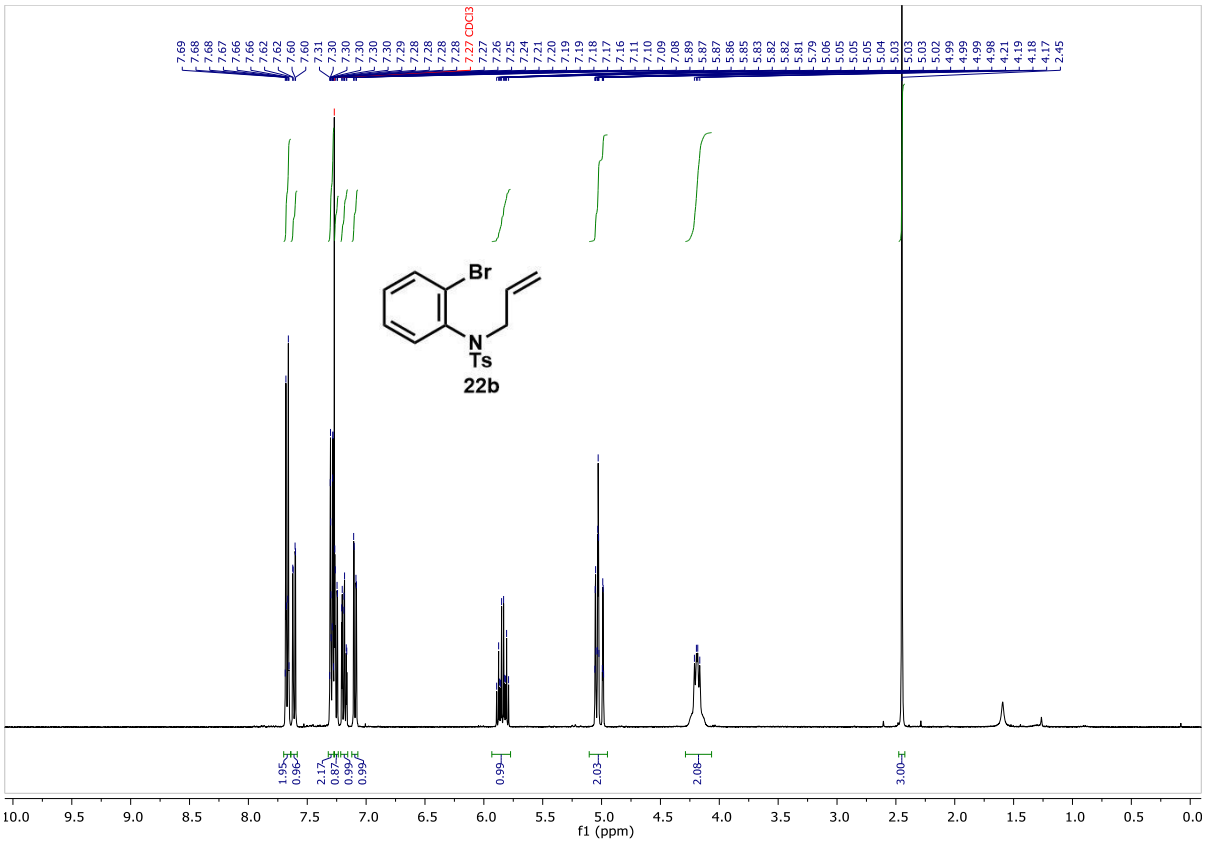
Br
N
Ts
22b
f1 (ppm)

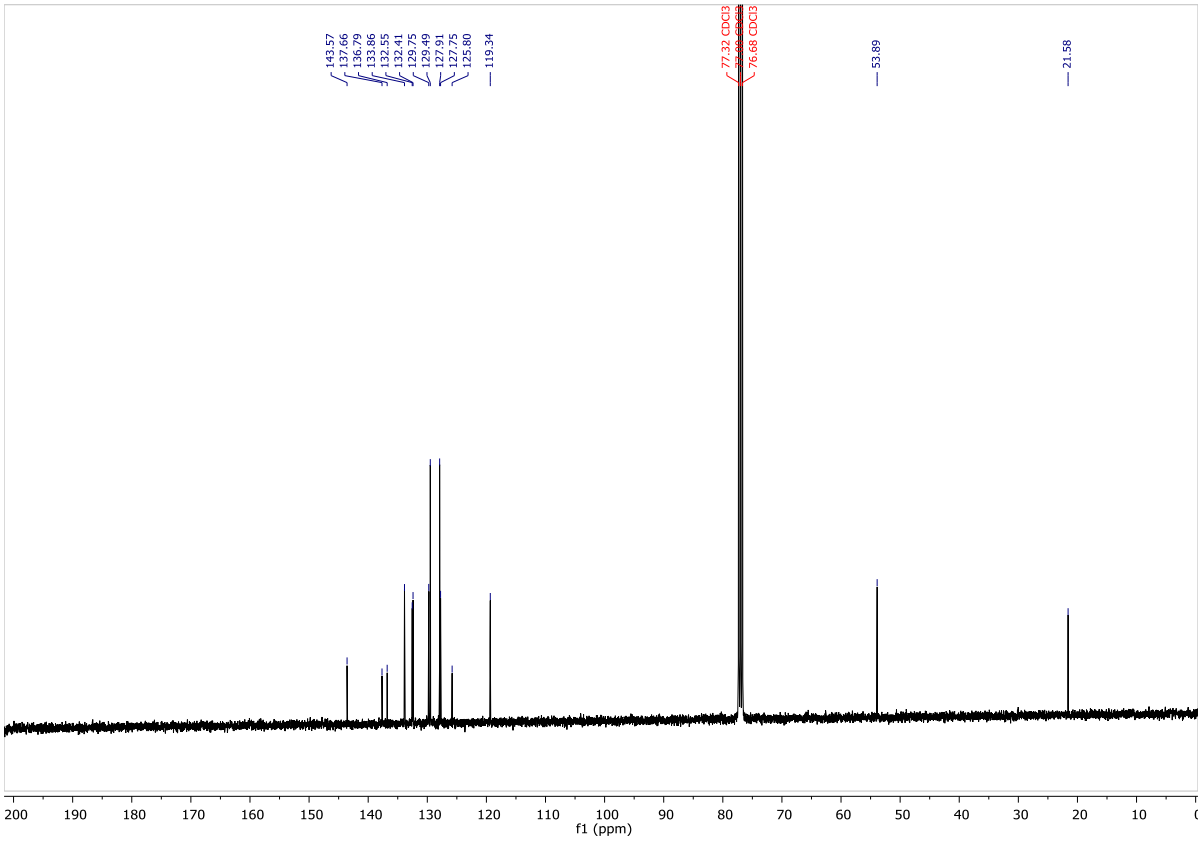
143.57
137.66
136.79
133.86
132.55
132.41
129.75
129.49
127.91
127.75
125.80
119.34
77.32 CDCl3
76.68 CDCl3
53.89
21.58
f1 (ppm)

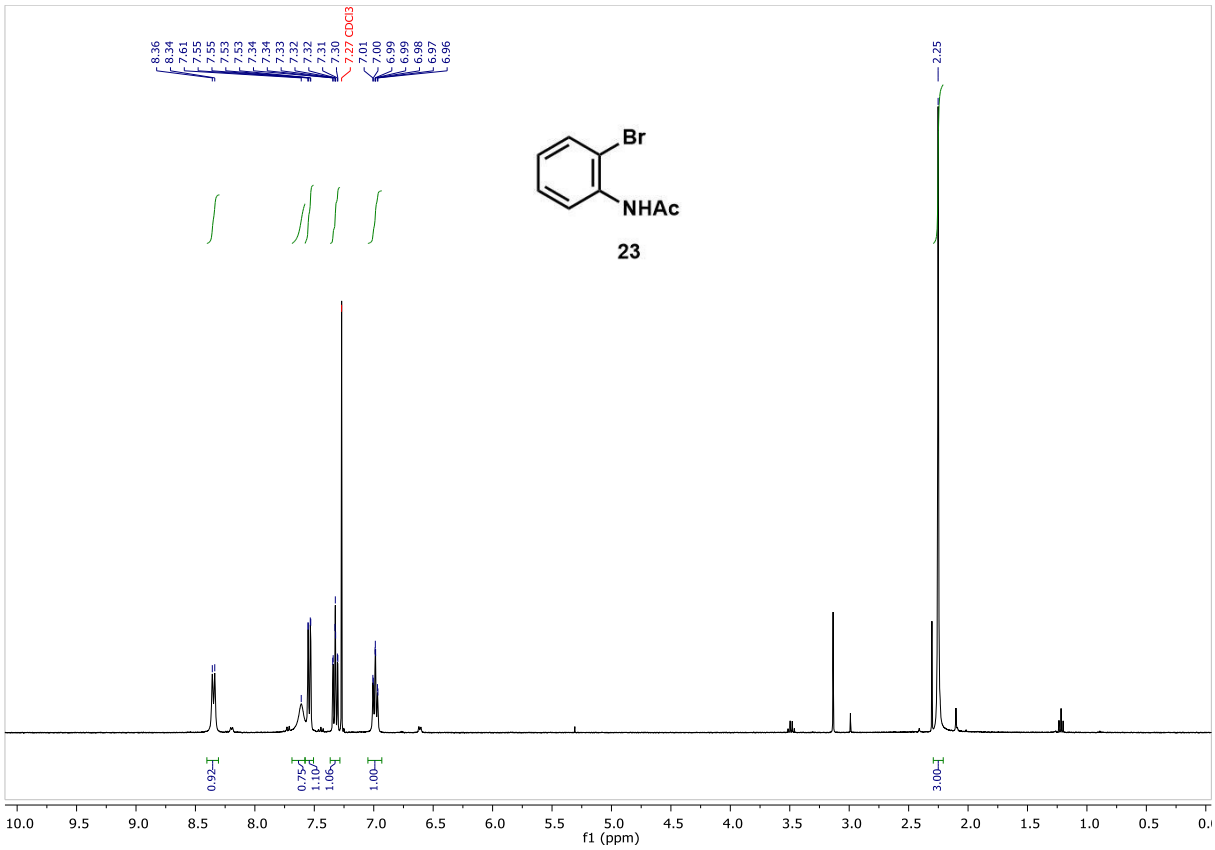
8.36
8.34
7.61
7.55
7.55
7.53
7.53
7.34
7.34
7.33
7.32
7.32
7.31
7.30
7.27 CDCl3
7.01
7.00
6.99
6.99
6.98
6.97
6.96
2.25
Br
NHAc
23
0.92
0.75
1.10
1.06
1.00
3.00
f1 (ppm)

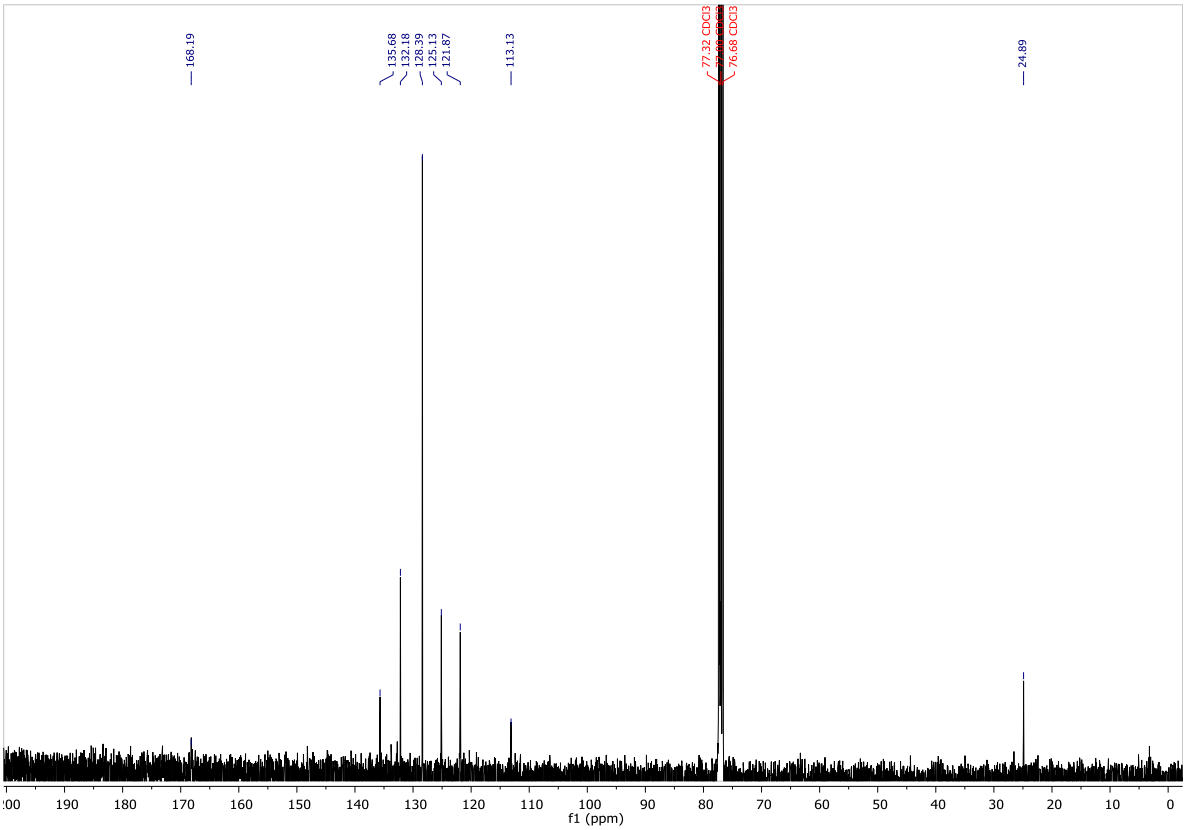
168.19
135.68
132.18
128.39
125.13
121.87
113.13
77.32 CDCl3
76.68 CDCl3
24.89
f1 (ppm)

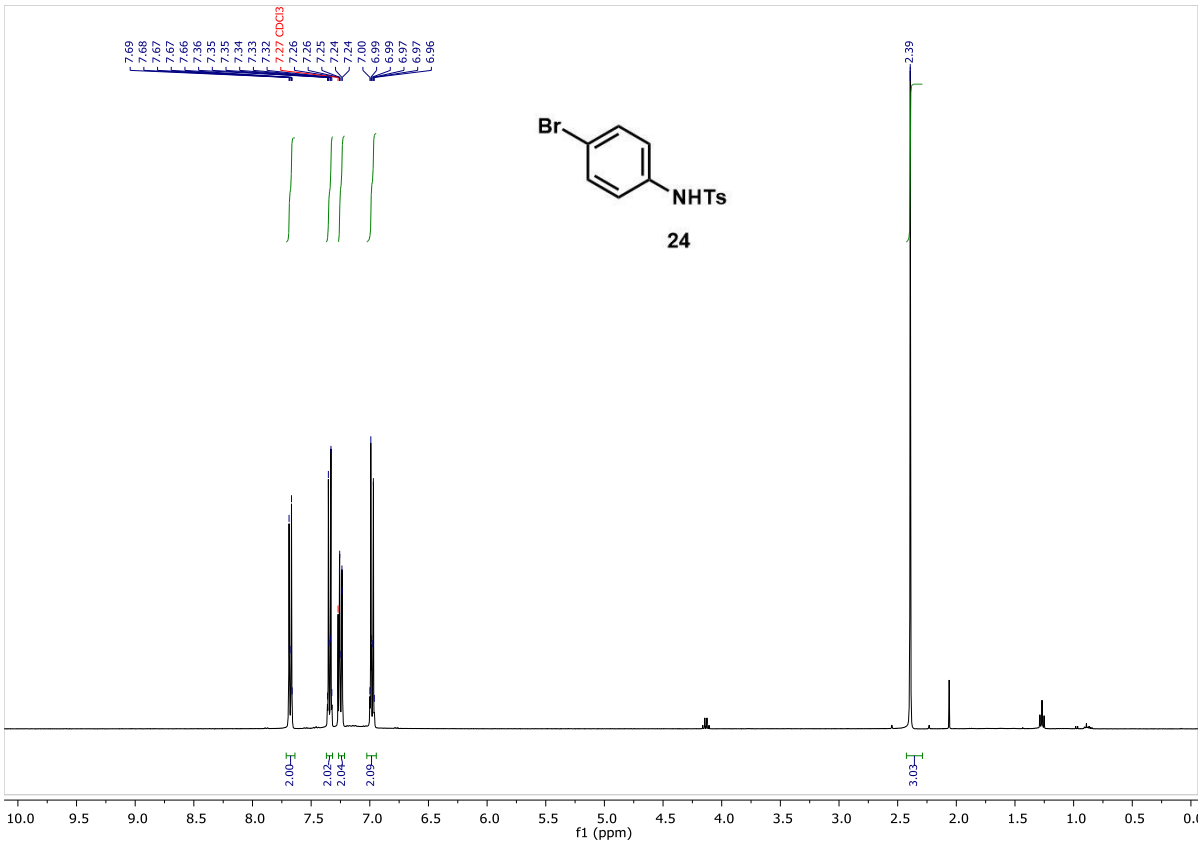
7.69
7.68
7.67
7.67
7.67
7.66
7.36
7.35
7.35
7.34
7.33
7.32
7.27 CDCl3
7.26
7.26
7.25
7.24
7.24
7.00
6.99
6.99
6.97
6.97
6.96
2.39
Br
NHTs
24
2.00
2.02
2.04
2.09
3.03
f1 (ppm)

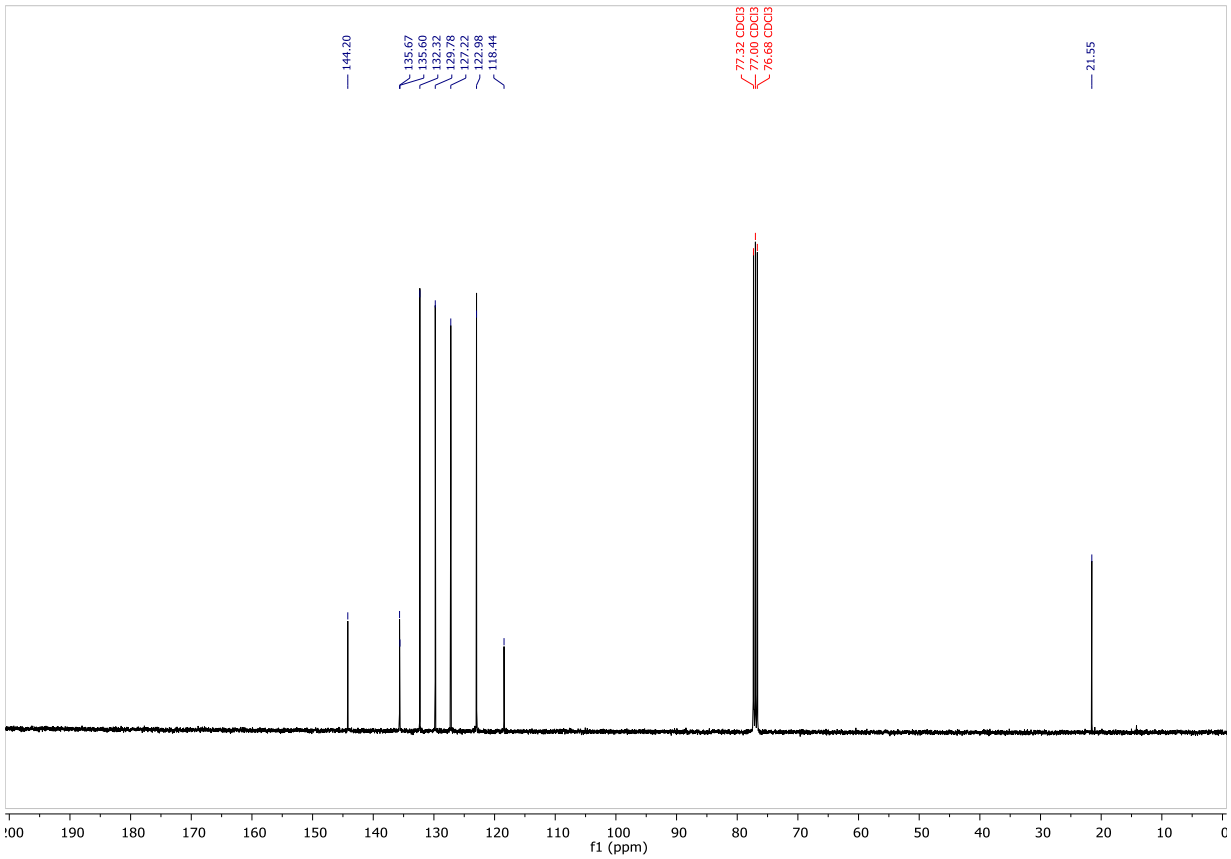
144.20
135.67
135.60
132.32
129.78
127.22
122.98
118.44
77.32 CDCl3
77.00 CDCl3
76.68 CDCl3
21.55
f1 (ppm)

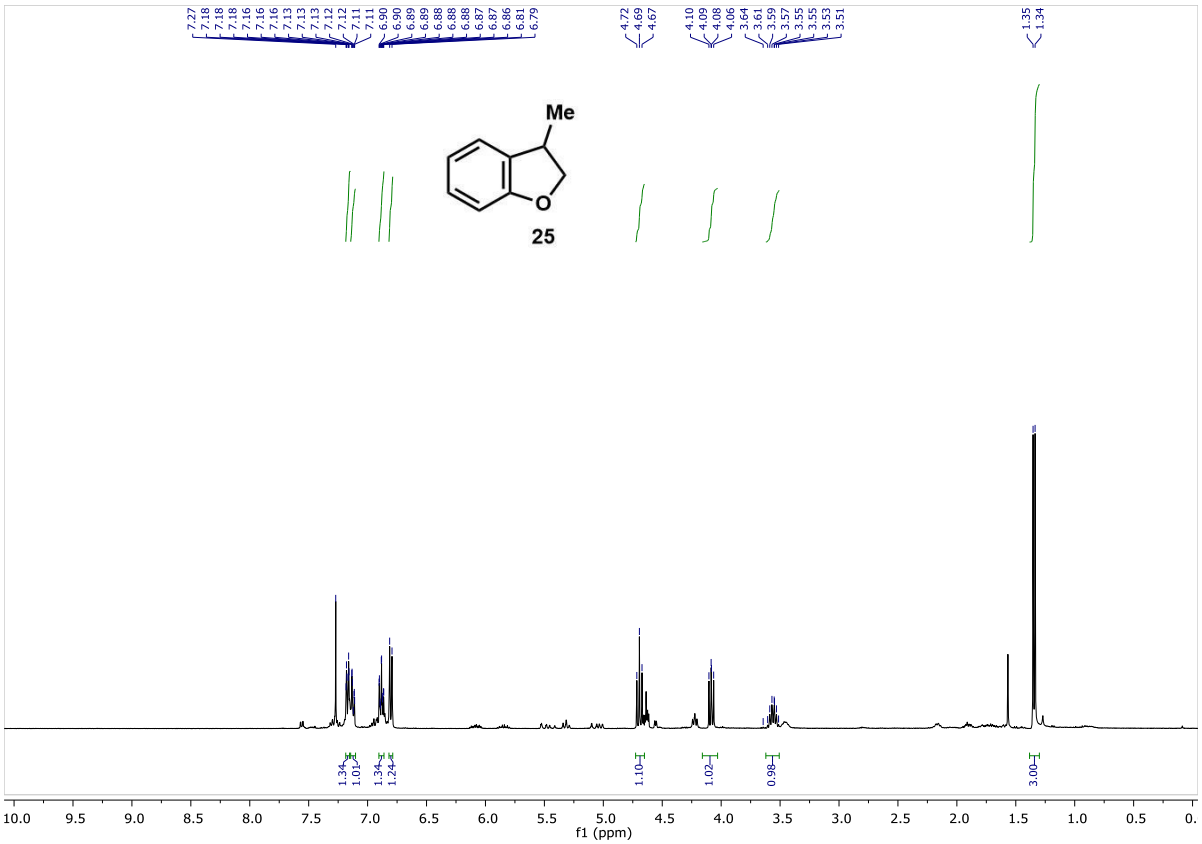
7.27
7.18
7.18
7.18
7.16
7.16
7.16
7.13
7.13
7.13
7.12
7.12
7.11
7.11
6.90
6.90
6.89
6.89
6.88
6.88
6.88
6.87
6.87
6.86
6.81
6.79
4.72
4.69
4.67
4.10
4.09
4.08
4.06
3.64
3.61
3.59
3.57
3.55
3.55
3.53
3.51
1.35
1.34
Me
O
25
1.34
1.01
1.34
1.24
1.10
1.02
0.98
3.00
10.0
9.5
9.0
8.5
8.0
7.5
7.0
6.5
6.0
5.5
5.0
4.5
4.0
3.5
3.0
2.5
2.0
1.5
1.0
0.5
f1 (ppm)

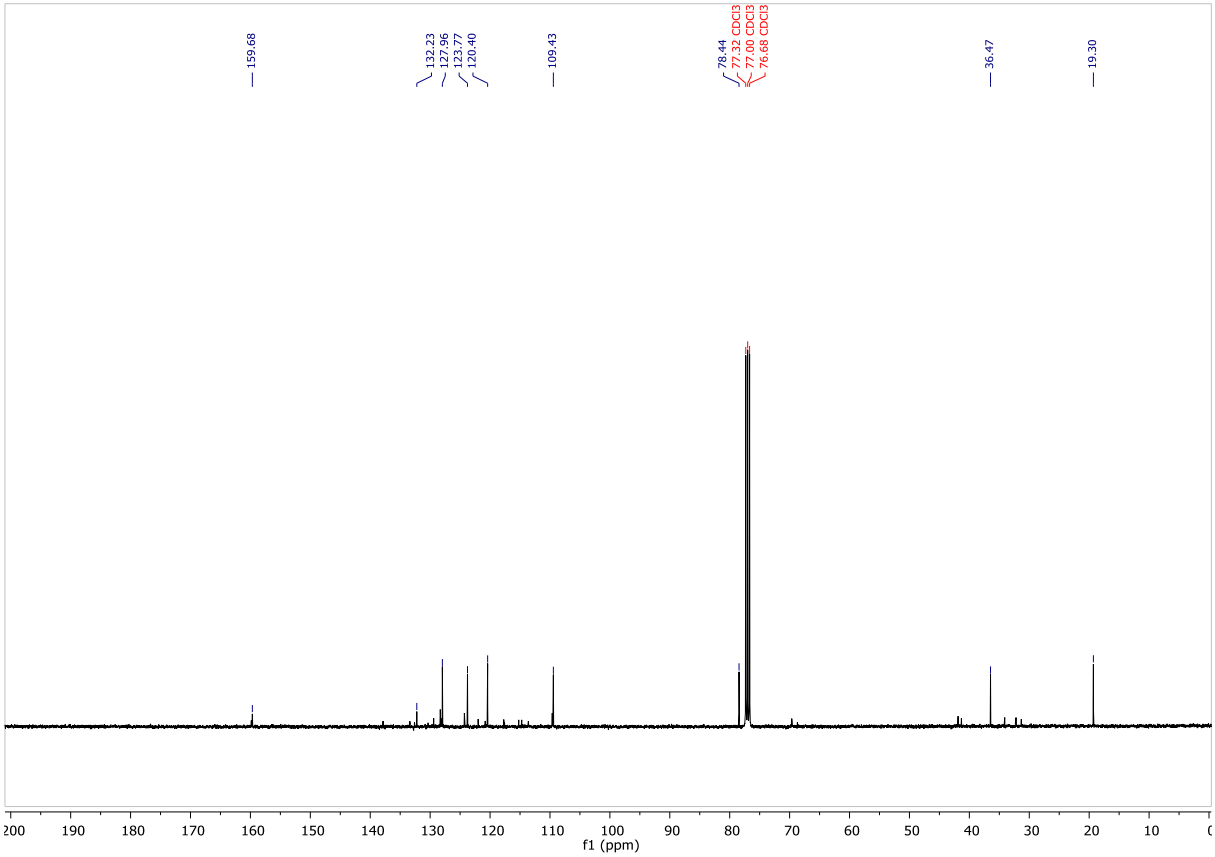
159.68
132.23
127.96
123.77
120.40
109.43
78.44
77.32 CDCl3
77.00 CDCl3
76.68 CDCl3
36.47
19.30
200
190
180
170
160
150
140
130
120
110
100
90
80
70
60
50
40
30
20
10
f1 (ppm)

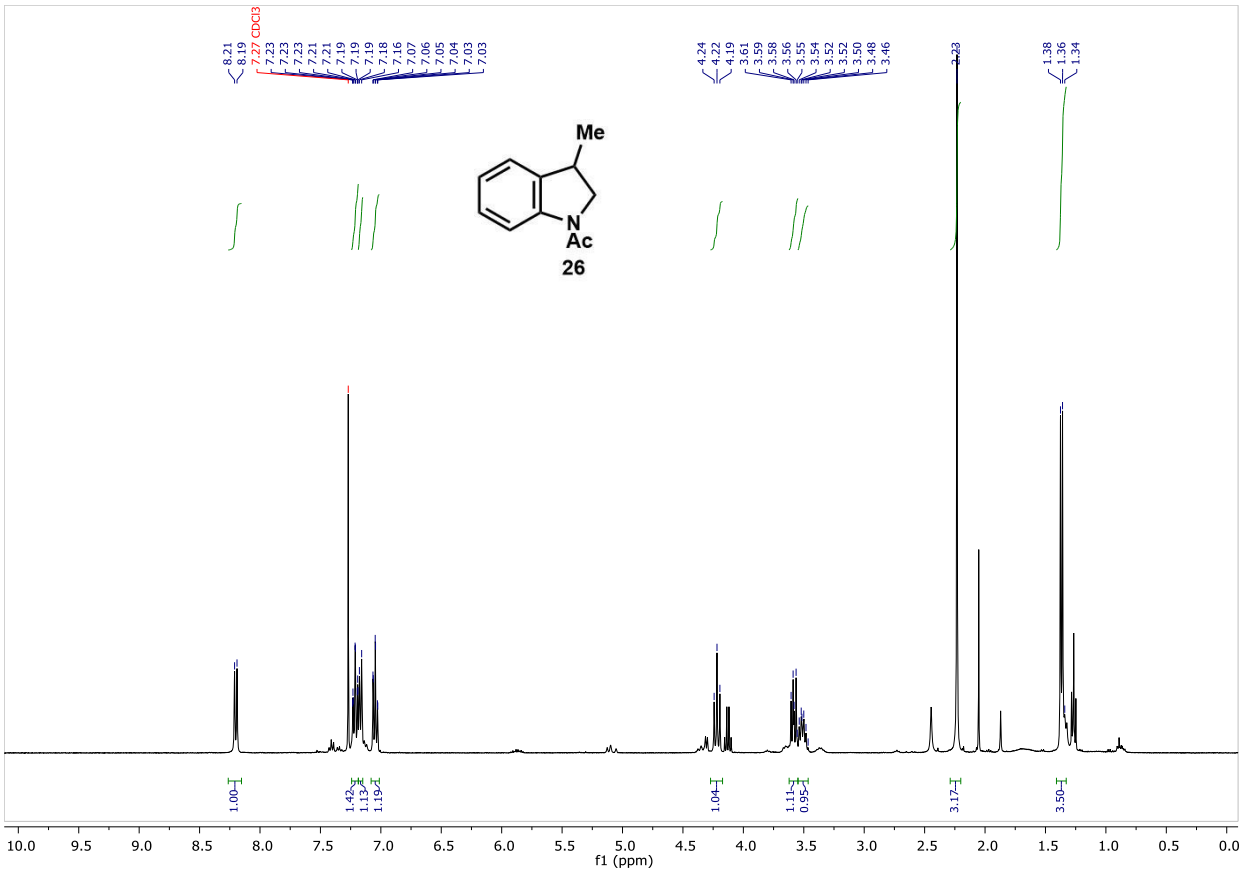
Me
N
Ac
26
f1 (ppm)

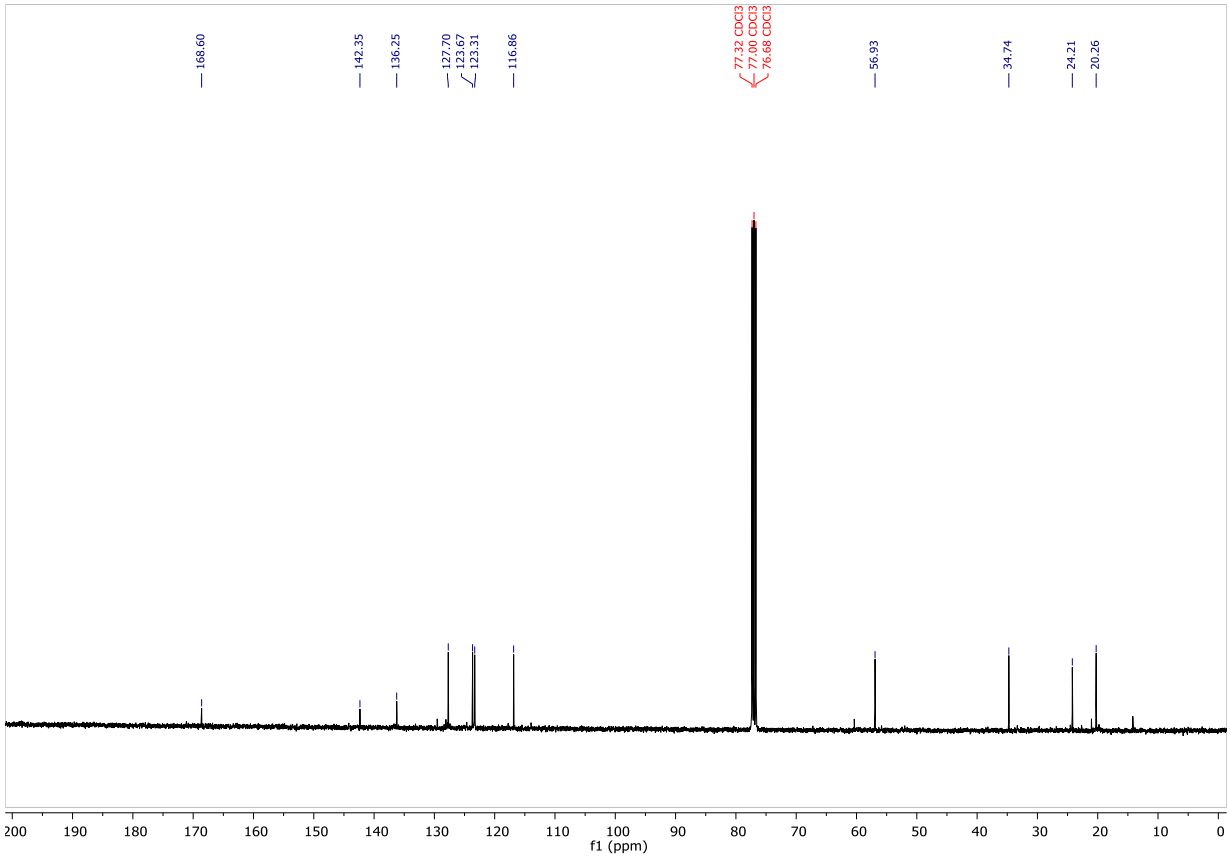
f1 (ppm)

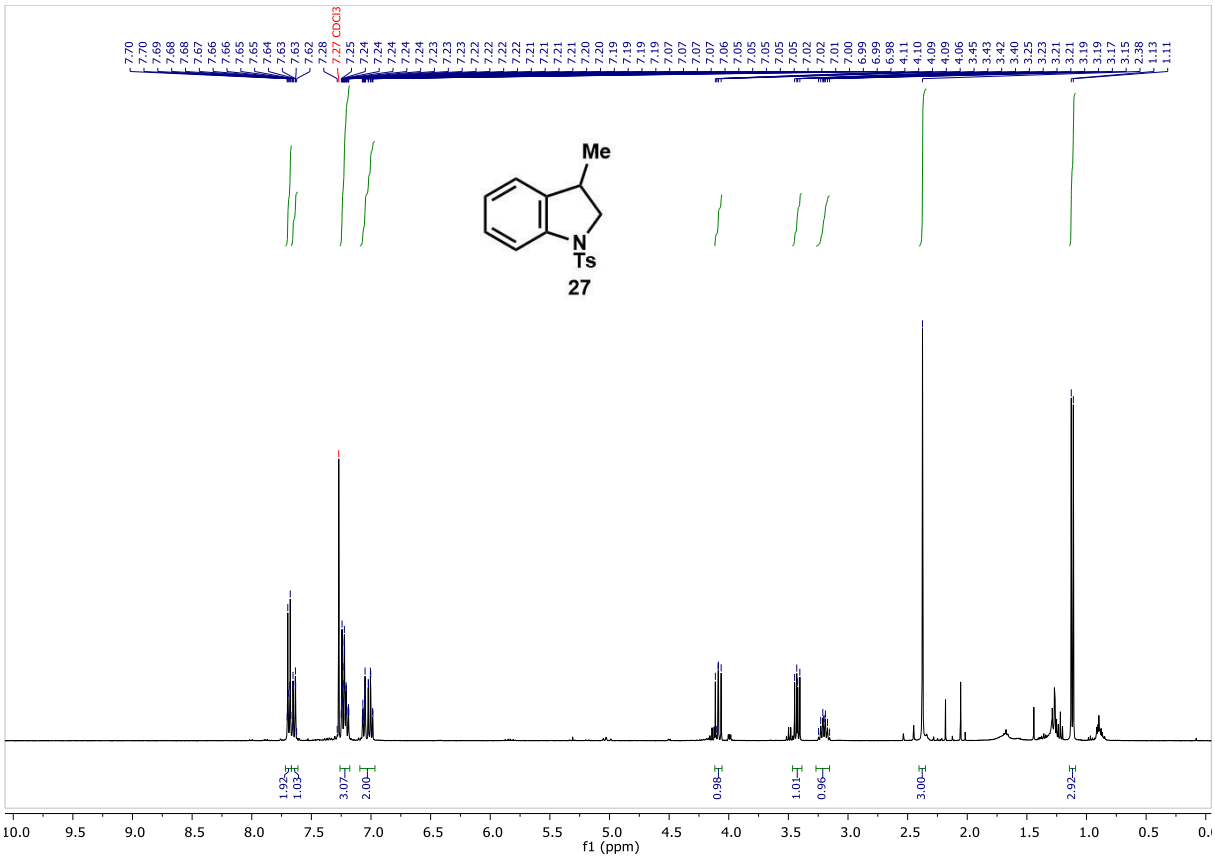
Me
N
Ts
27
f1 (ppm)

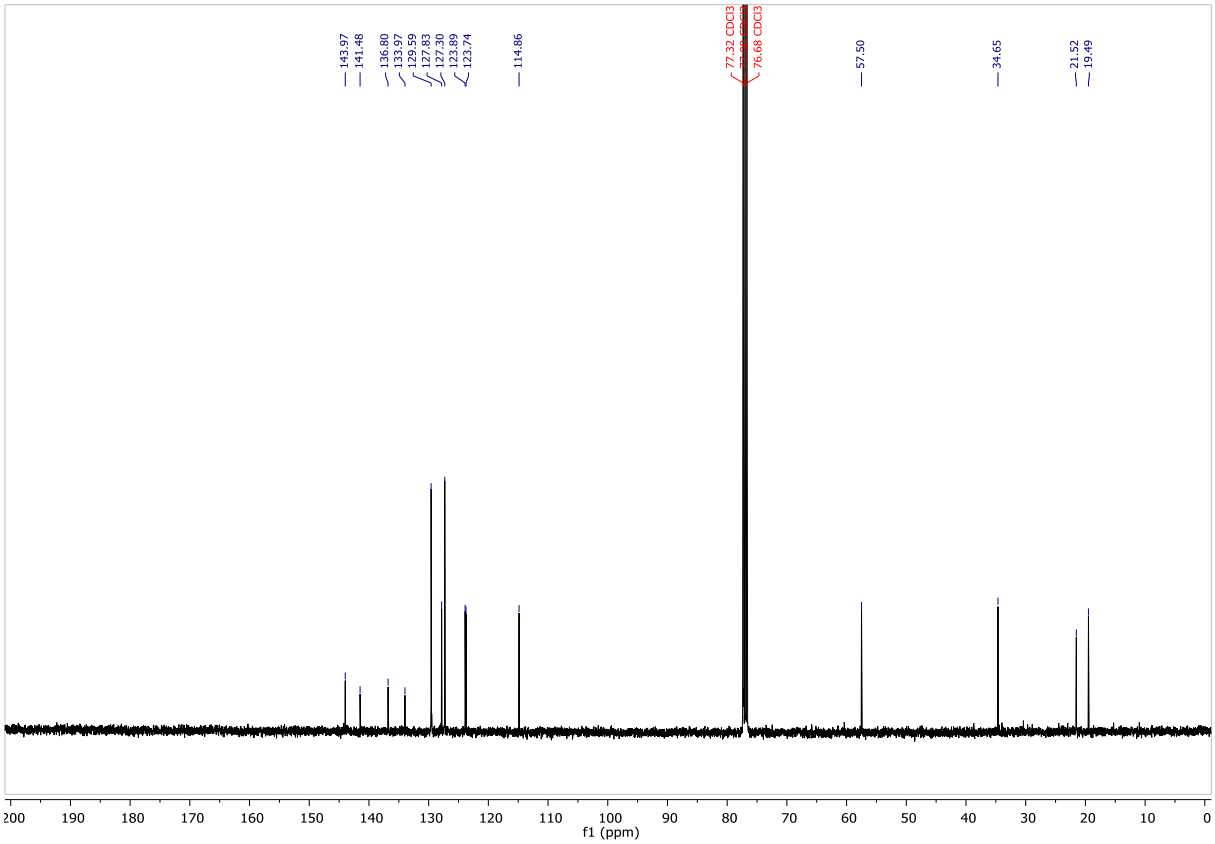
f1 (ppm)

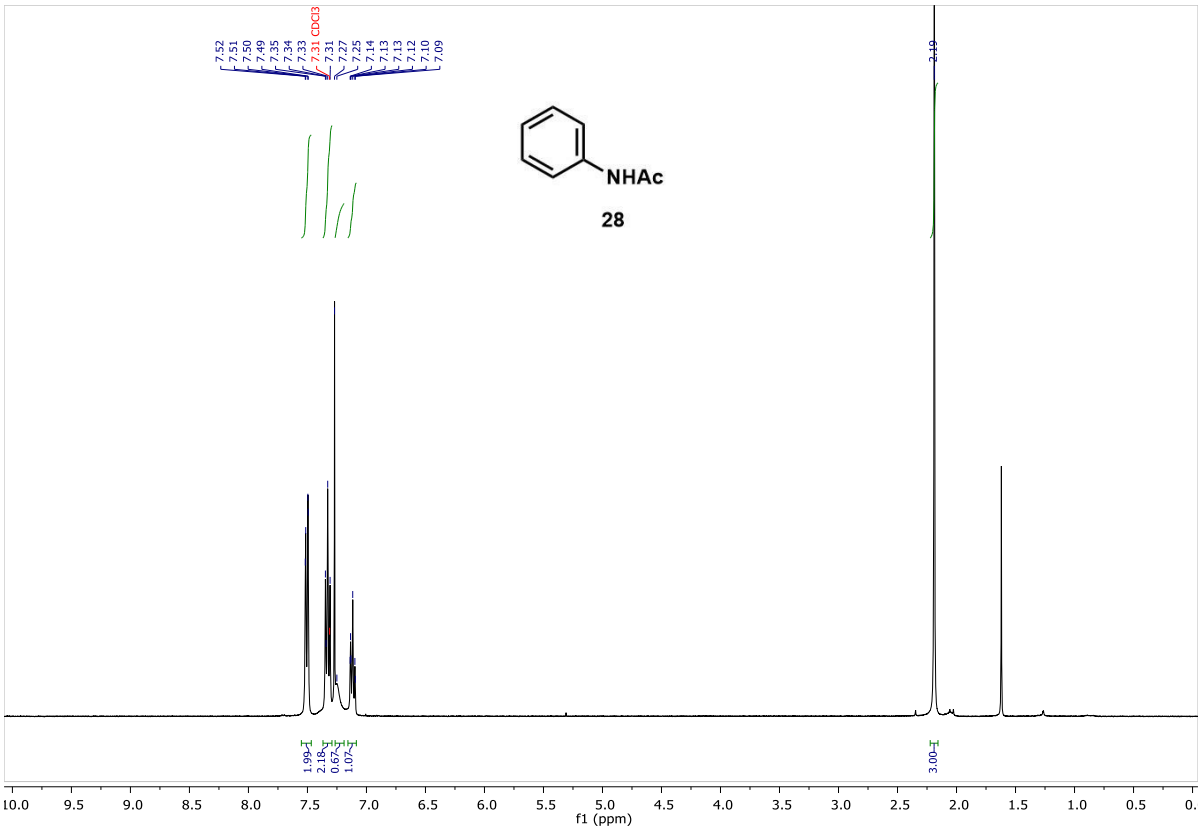
7.52
7.51
7.50
7.49
7.35
7.34
7.33
7.31 CDCl3
7.31
7.27
7.25
7.14
7.13
7.13
7.12
7.10
7.09
2.19
NHAc
28
1.99
2.18
0.67
1.07
3.00
f1 (ppm)

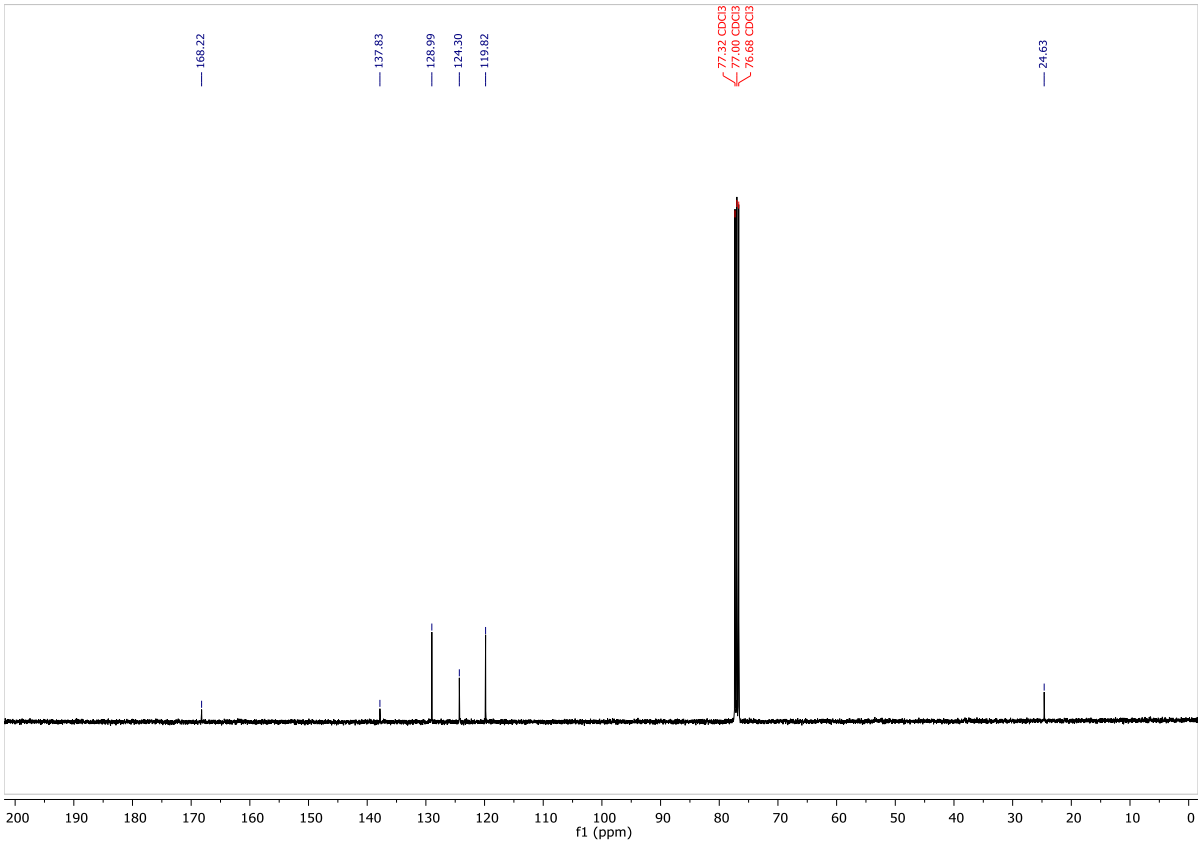
168.22
137.83
128.99
124.30
119.82
77.32 CDCl3
77.00 CDCl3
76.68 CDCl3
24.63
f1 (ppm)

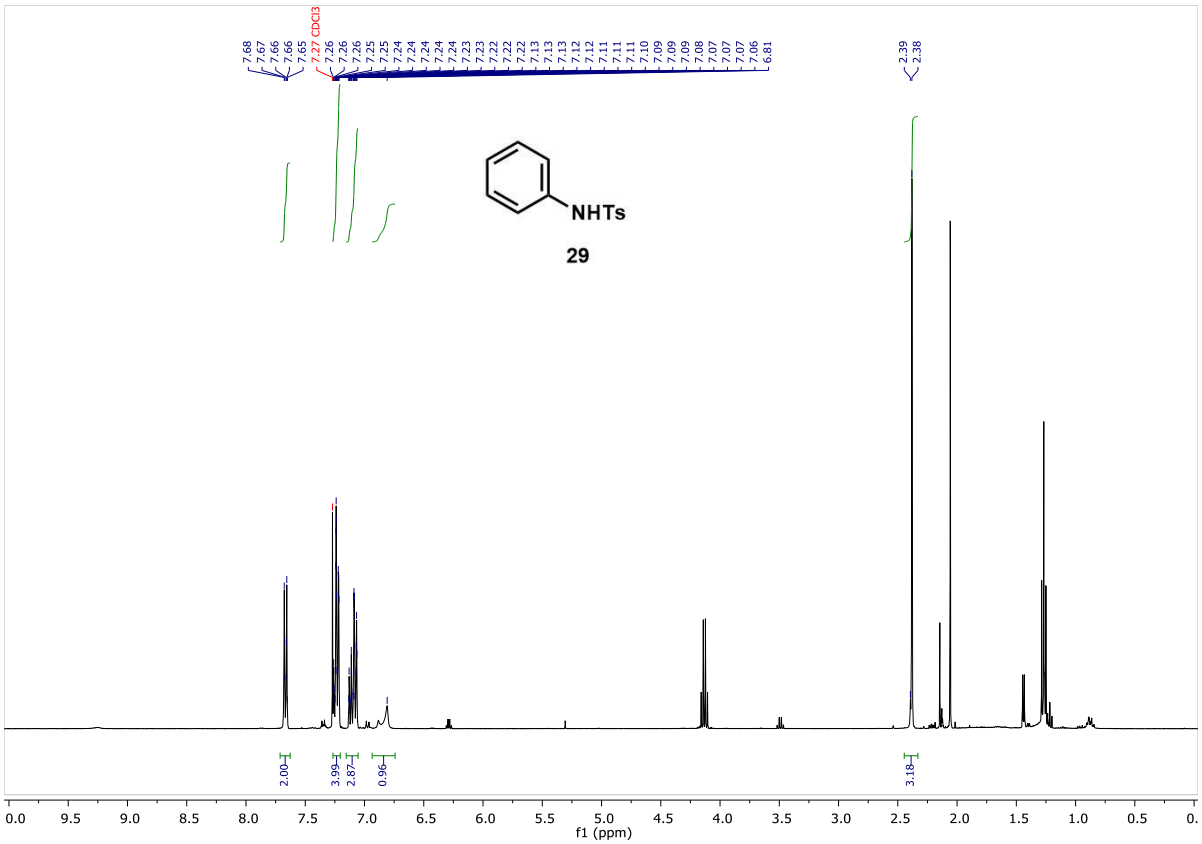
7.68
7.67
7.66
7.66
7.65
7.27 CDCl3
7.26
7.26
7.26
7.25
7.25
7.24
7.24
7.24
7.24
7.24
7.23
7.23
7.22
7.22
7.22
7.13
7.13
7.13
7.12
7.12
7.11
7.11
7.11
7.10
7.09
7.09
7.09
7.08
7.07
7.07
7.07
7.06
6.81
2.39
2.38
NHTs
29
2.00
3.99
2.87
0.96
3.18
0.0 9.5 9.0 8.5 8.0 7.5 7.0 6.5 6.0 5.5 5.0 4.5 4.0 3.5 3.0 2.5 2.0 1.5 1.0 0.5 0.
f1 (ppm)

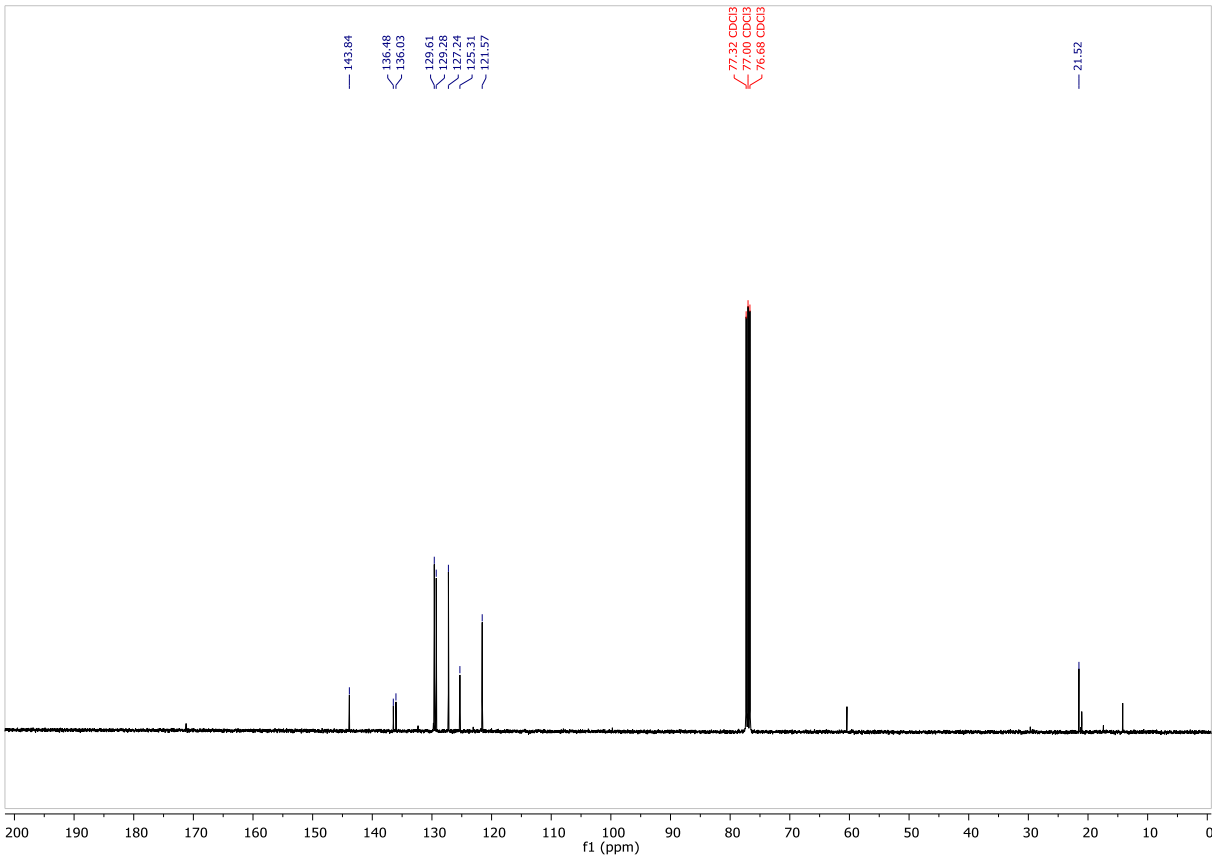
143.84
136.48
136.03
129.61
129.28
127.24
125.31
121.57
77.32 CDCl3
77.00 CDCl3
76.68 CDCl3
21.52
200 190 180 170 160 150 140 130 120 110 100 90 80 70 60 50 40 30 20 10 0
f1 (ppm)

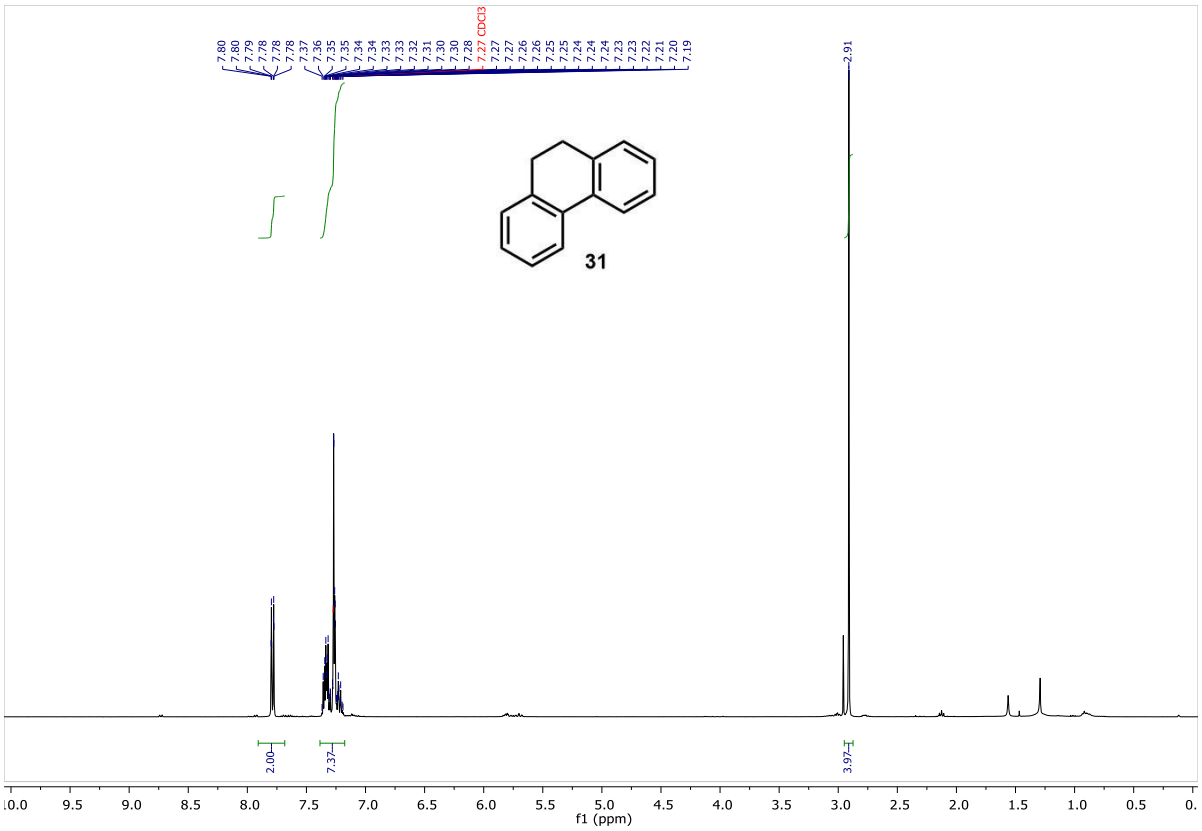
7.80
7.80
7.79
7.78
7.78
7.78
7.78
7.37
7.36
7.35
7.35
7.34
7.34
7.33
7.33
7.32
7.31
7.30
7.30
7.28
CDCl3
7.27
7.27
7.27
7.26
7.26
7.25
7.25
7.24
7.24
7.24
7.23
7.23
7.22
7.21
7.20
7.19
2.91
31
2.00
7.37
3.97
f1 (ppm)

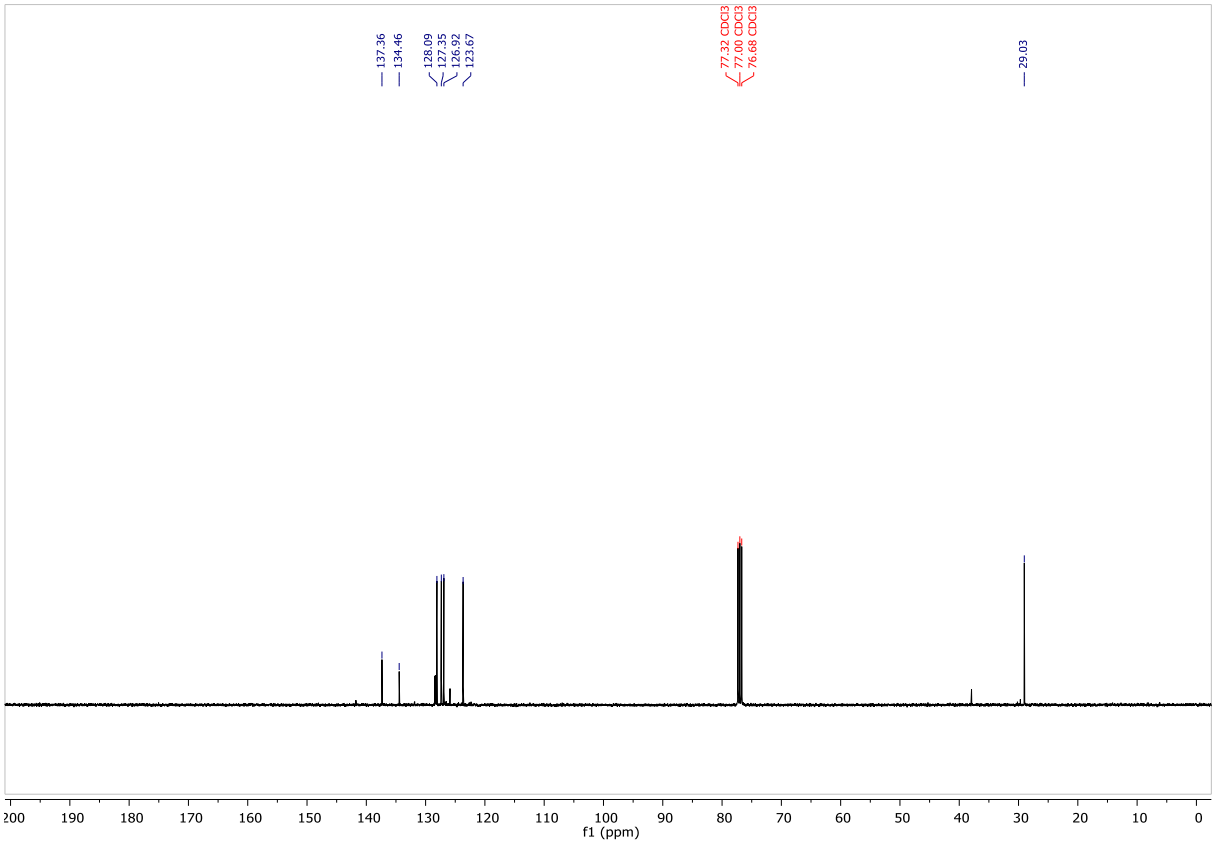
137.36
134.46
128.09
127.35
126.92
123.67
77.32 CDCl3
77.00 CDCl3
76.68 CDCl3
29.03
f1 (ppm)

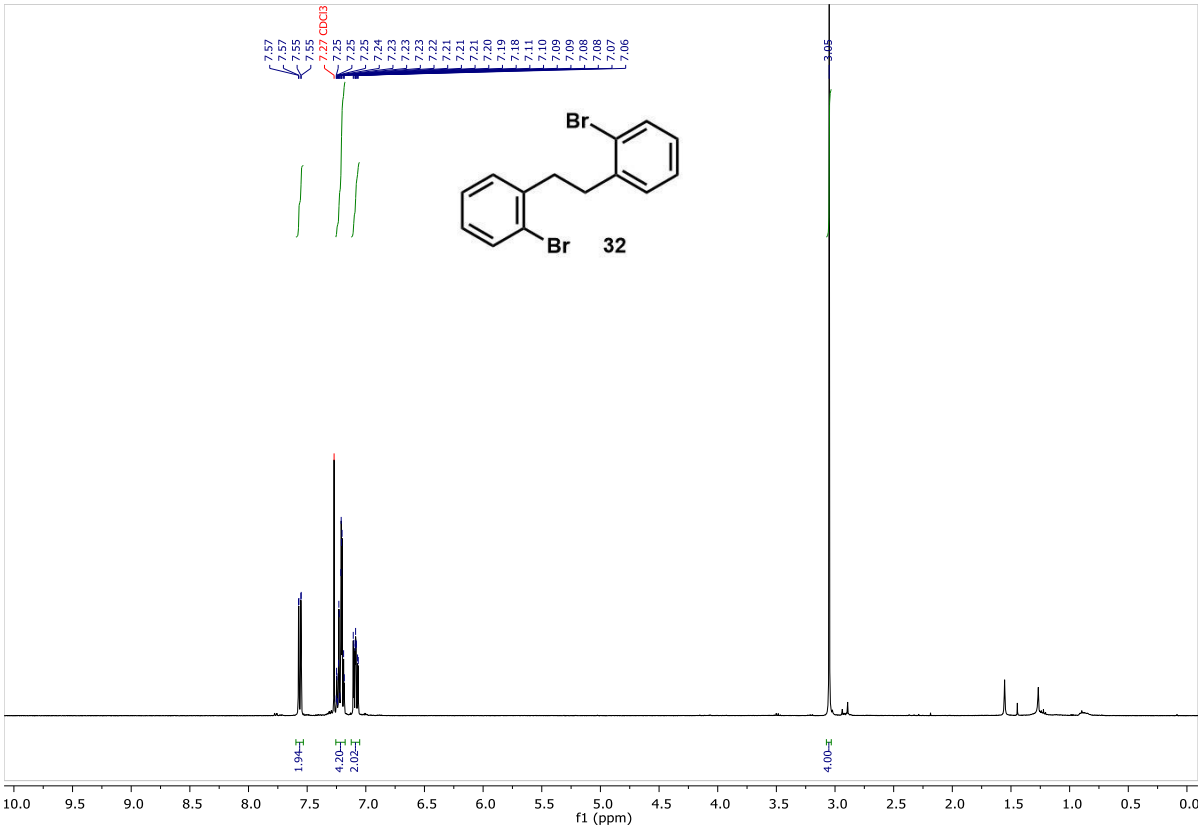
7.57
7.57
7.55
7.55
7.27 CDCl3
7.25
7.25
7.25
7.24
7.23
7.23
7.23
7.22
7.21
7.21
7.21
7.20
7.19
7.18
7.11
7.10
7.09
7.09
7.08
7.08
7.07
7.06
3.05
Br
Br
32
1.94
4.20
2.02
4.00
10.0
9.5
9.0
8.5
8.0
7.5
7.0
6.5
6.0
5.5
5.0
4.5
4.0
3.5
3.0
2.5
2.0
1.5
1.0
0.5
f1 (ppm)

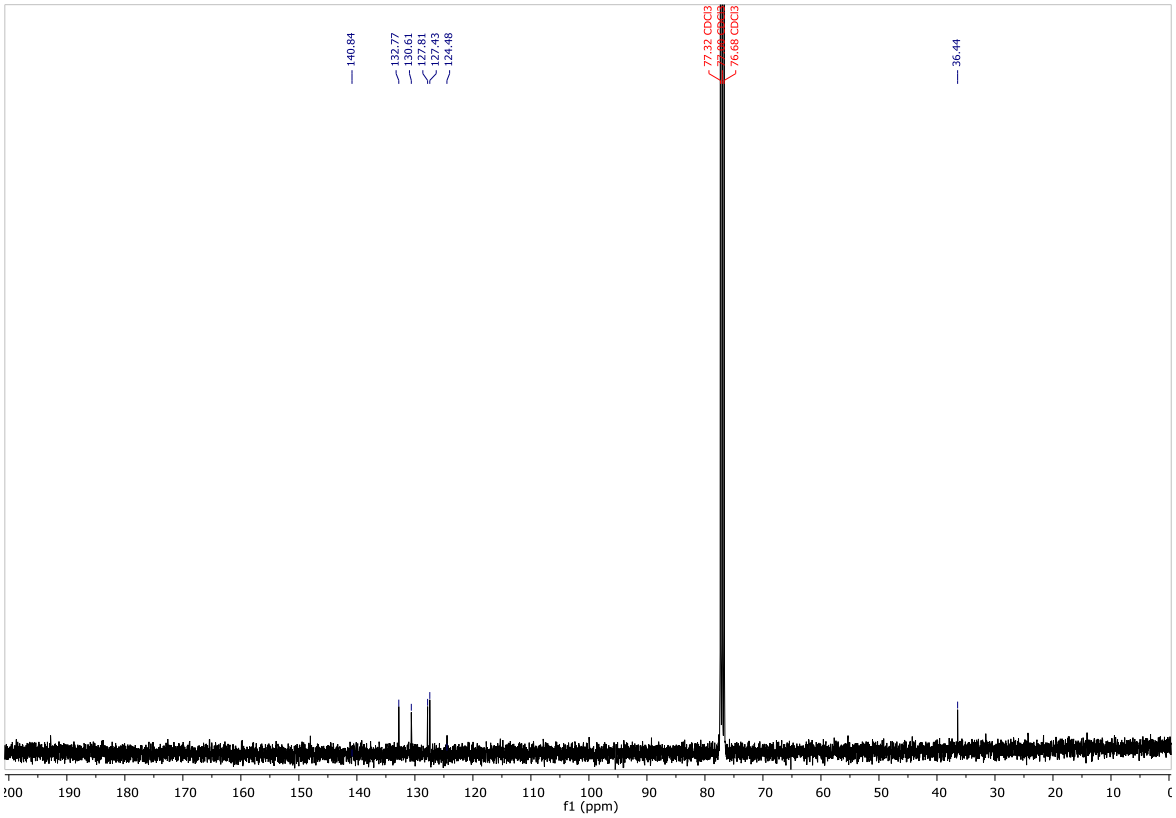
140.84
132.77
130.61
127.81
127.43
124.48
77.32 CDCl3
76.68 CDCl3
36.44
200
190
180
170
160
150
140
130
120
110
100
90
80
70
60
50
40
30
20
10
f1 (ppm)

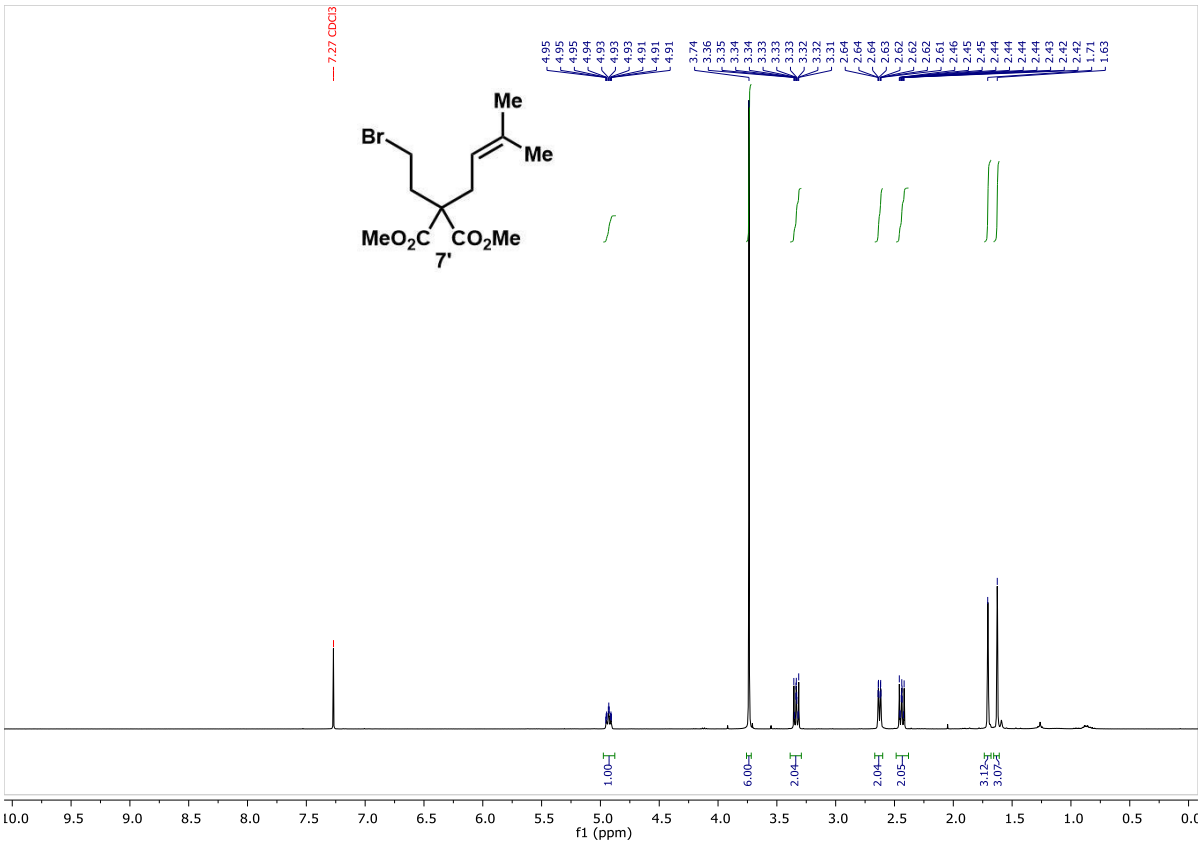
7.27 CDCl3
Me
Br
Me
MeO2C
CO2Me
7'
f1 (ppm)

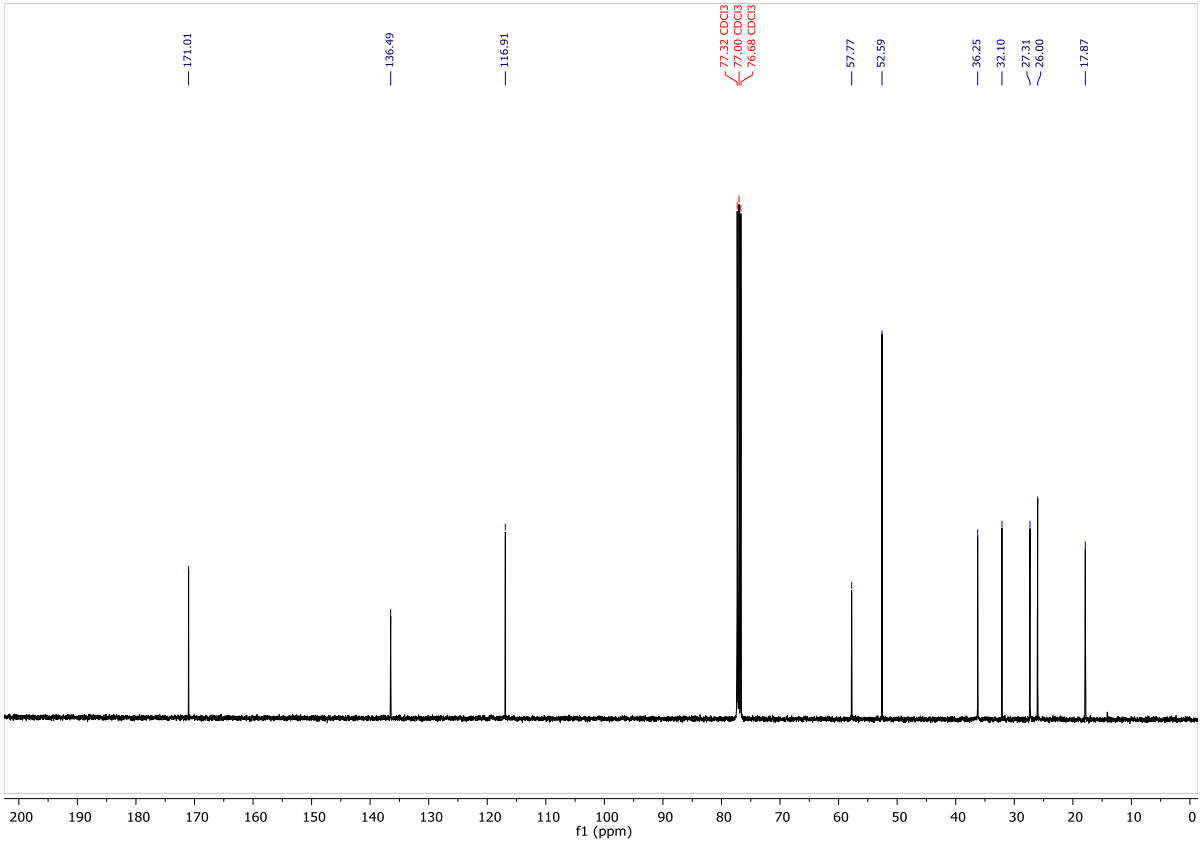
171.01
136.49
116.91
77.32 CDCl3
77.00 CDCl3
76.68 CDCl3
57.77
52.59
36.25
32.10
27.31
26.00
17.87
f1 (ppm)

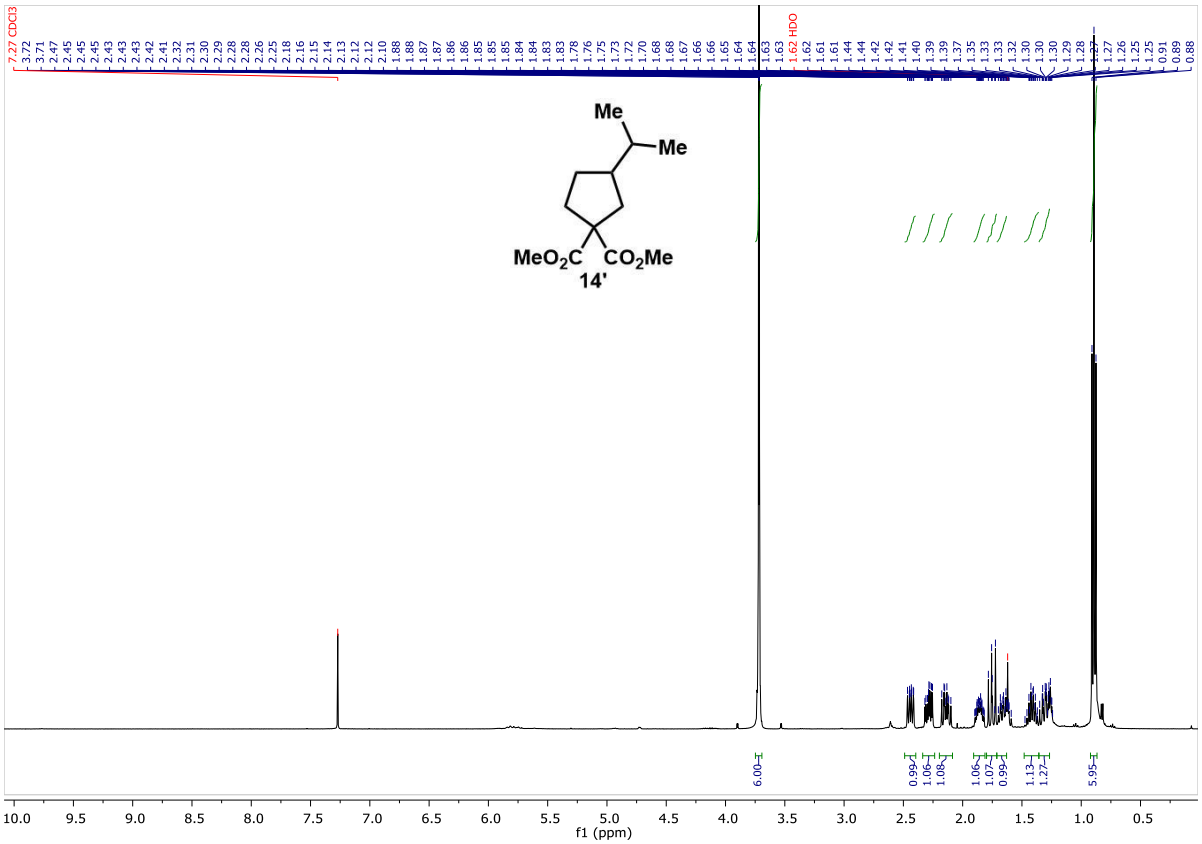
Me
Me
MeO2C
CO2Me
14'
f1 (ppm)

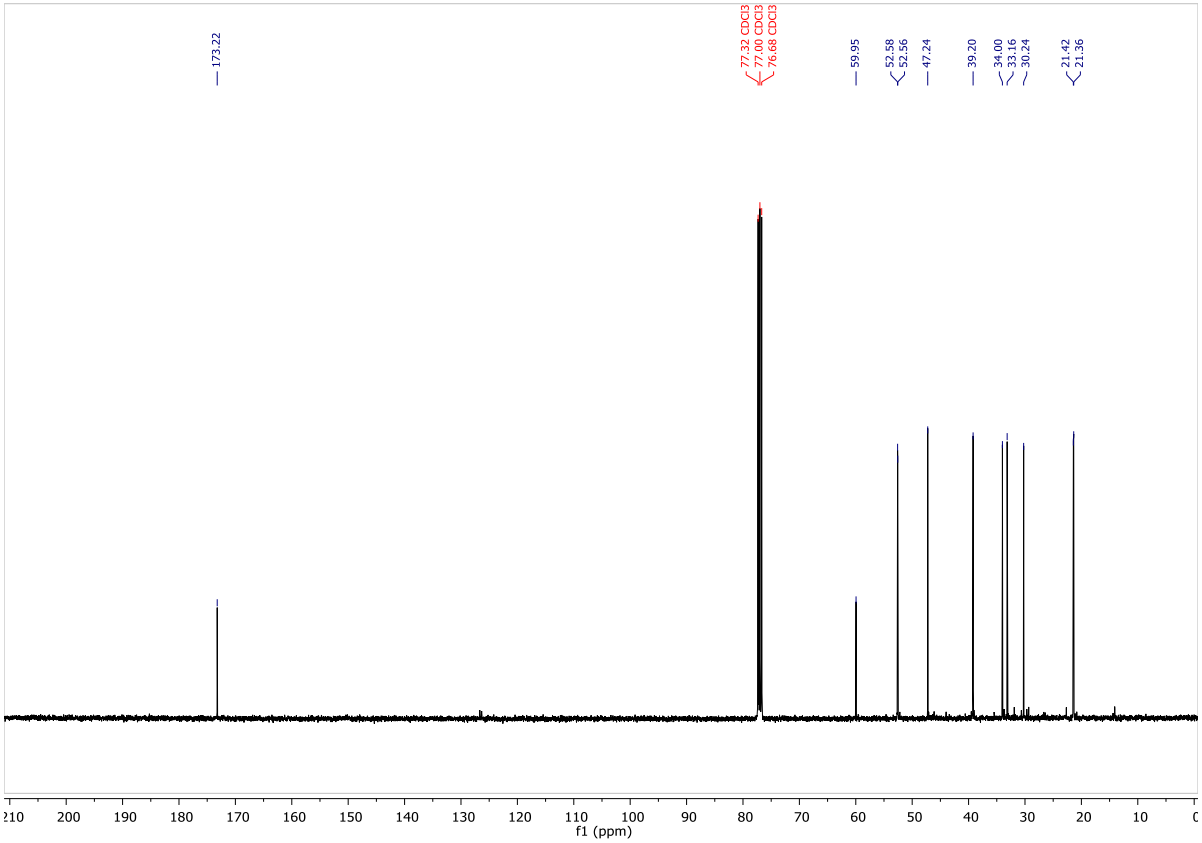
f1 (ppm)

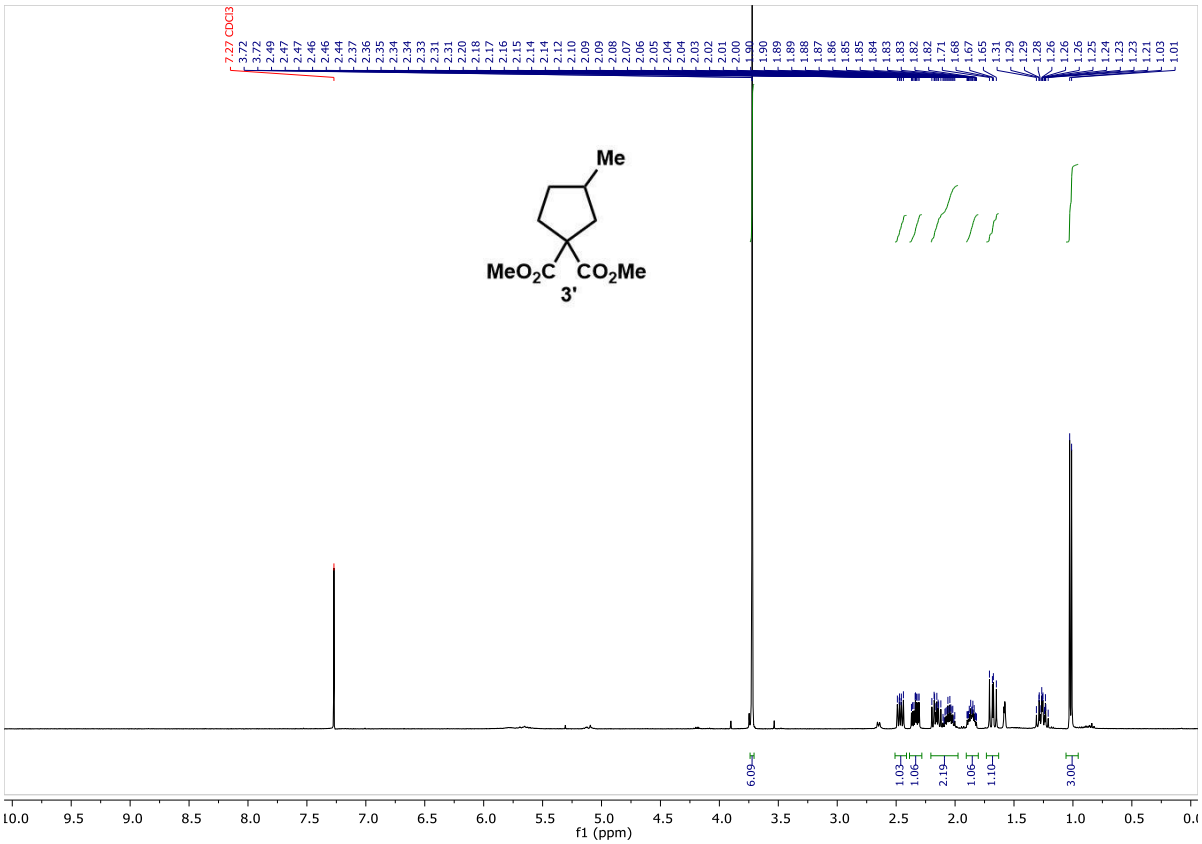
Me
MeO2C
CO2Me
3'
f1 (ppm)

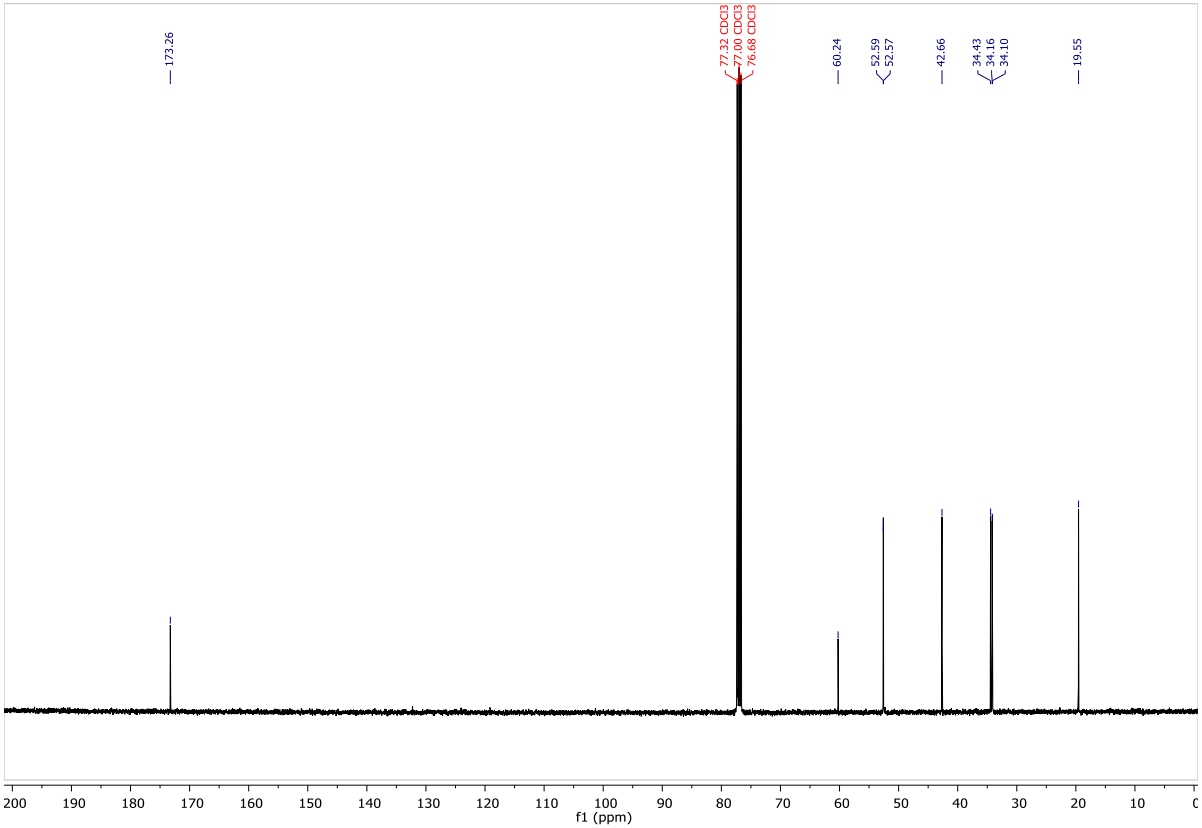
173.26
77.32 CDCl3
77.00 CDCl3
76.68 CDCl3
60.24
52.59
52.57
42.66
34.43
34.16
34.10
19.55
f1 (ppm)

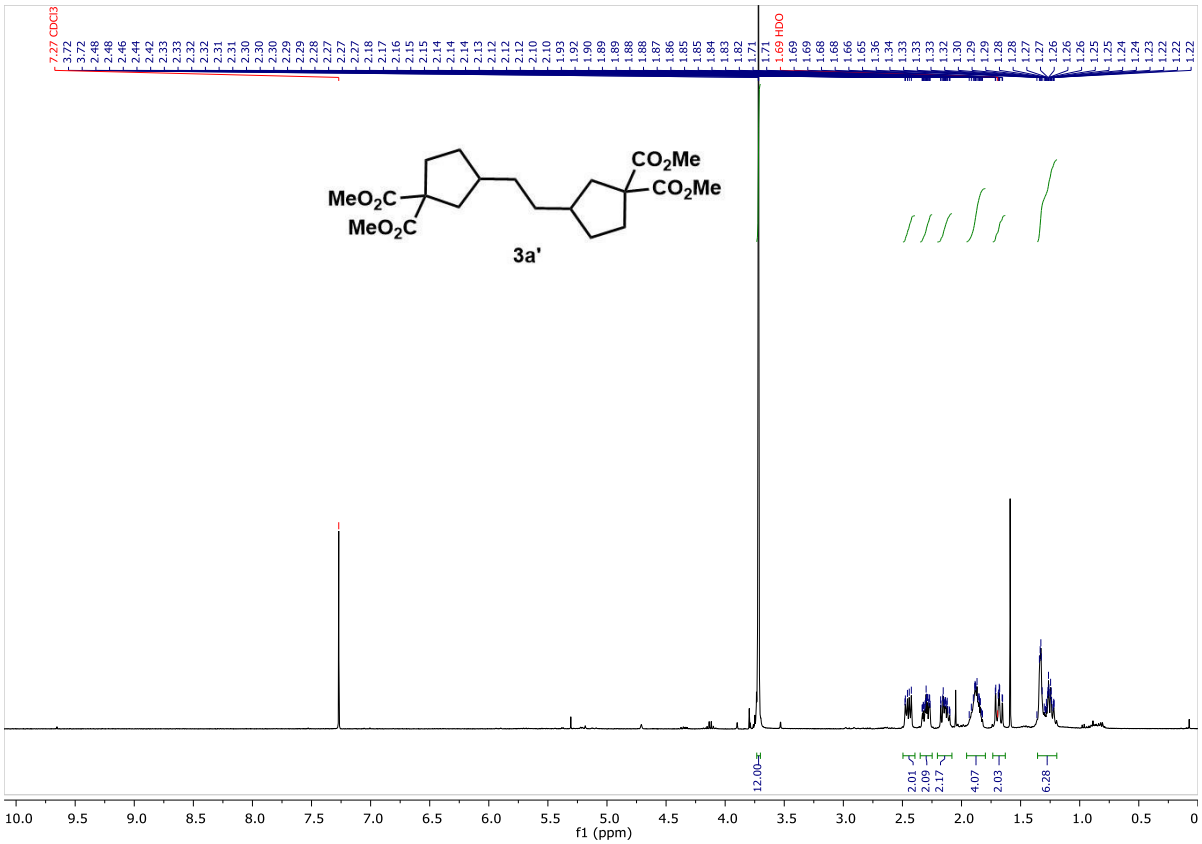
7.27 CDCl3
1.69 HDO
CO2Me
CO2Me
MeO2C
MeO2C
3a'
12.00
2.01
2.09
2.17
4.07
2.03
6.28
f1 (ppm)

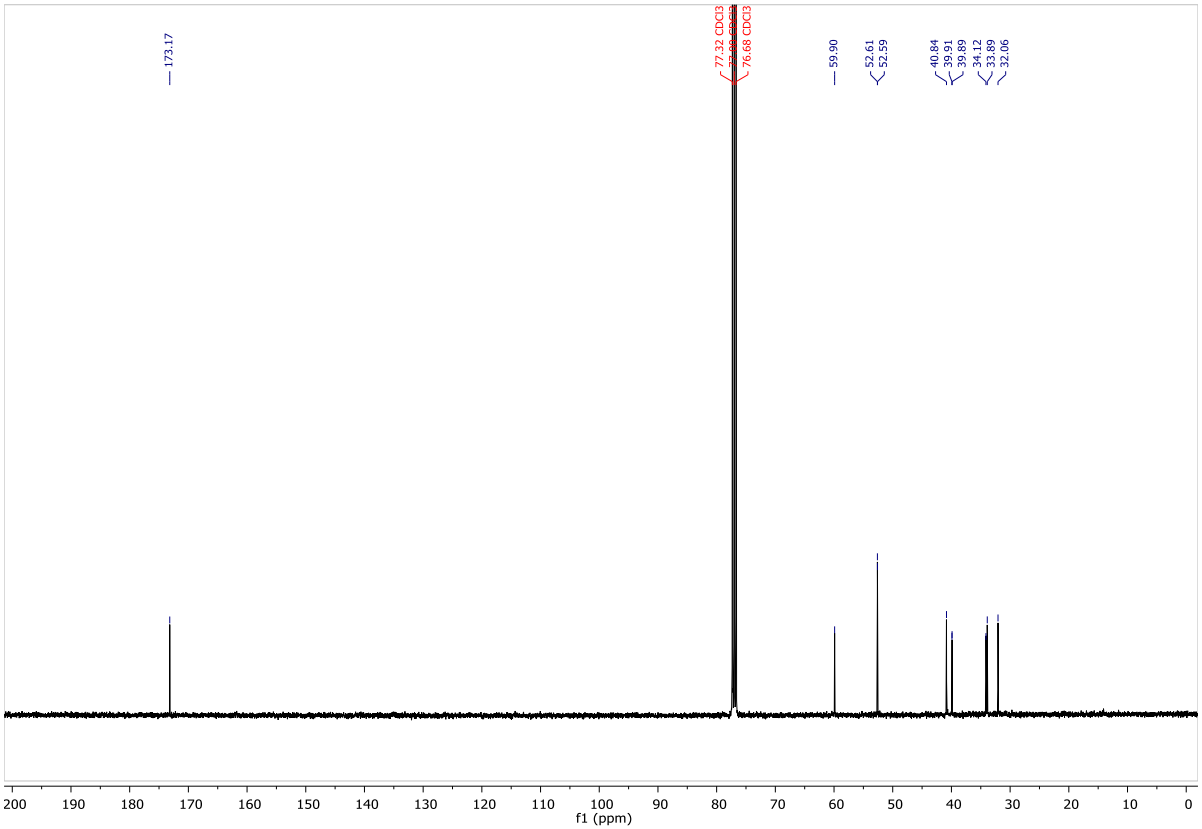
173.17
77.32 CDCl3
76.68 CDCl3
59.90
52.61
52.59
40.84
39.91
39.89
34.12
33.89
32.06
f1 (ppm)

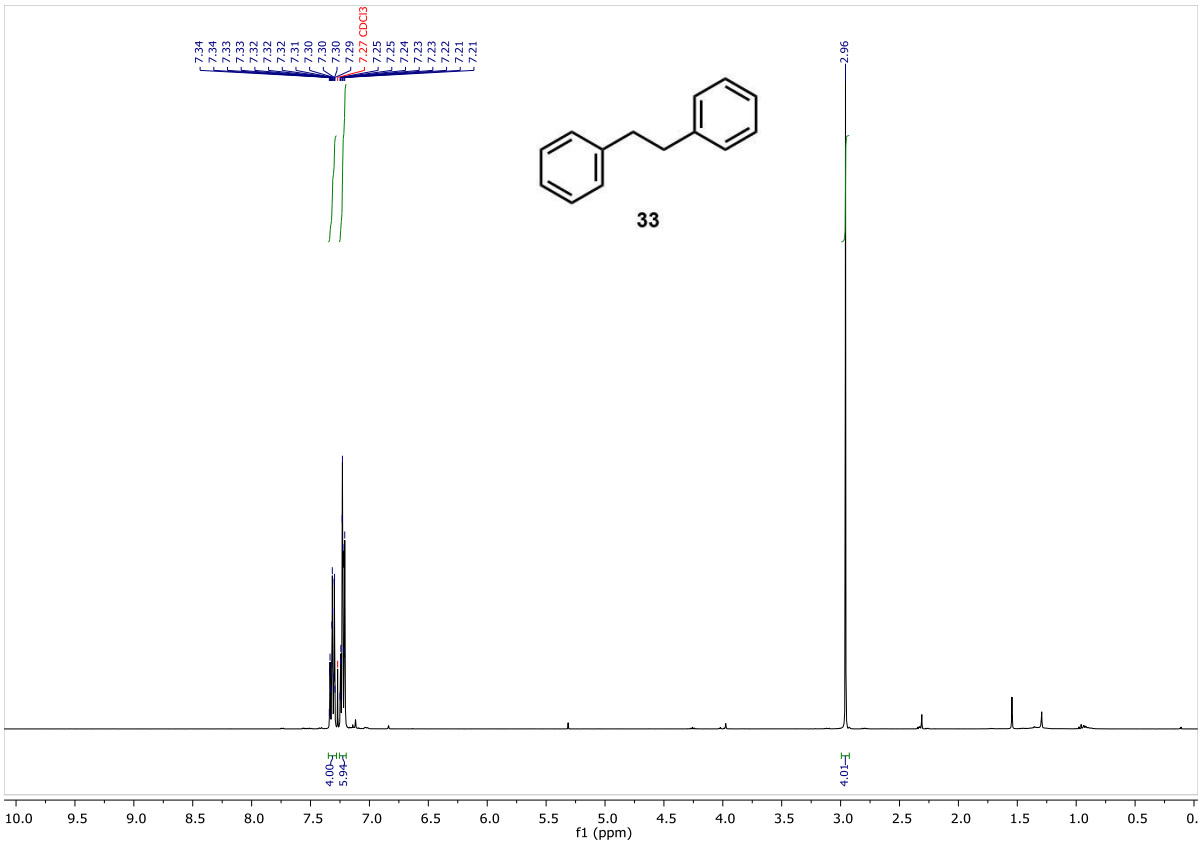
7.34
7.34
7.33
7.33
7.32
7.32
7.32
7.31
7.30
7.30
7.30
7.29
7.27 CDCl3
7.25
7.25
7.24
7.23
7.23
7.22
7.21
7.21
2.96
33
4.00
5.94
4.01
10.0
9.5
9.0
8.5
8.0
7.5
7.0
6.5
6.0
5.5
5.0
4.5
4.0
3.5
3.0
2.5
2.0
1.5
1.0
0.5
f1 (ppm)

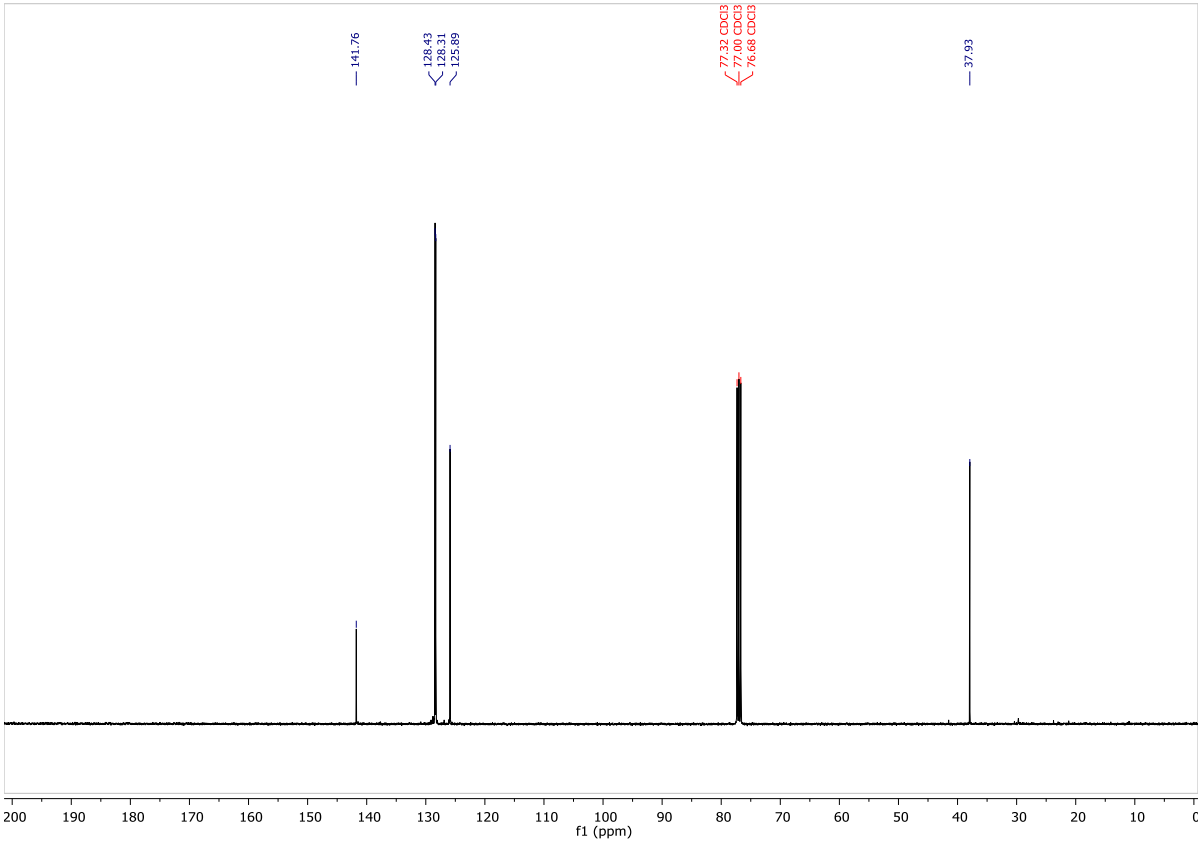
141.76
128.43
128.31
125.89
77.32 CDCl3
77.00 CDCl3
76.68 CDCl3
37.93
200
190
180
170
160
150
140
130
120
110
100
90
80
70
60
50
40
30
20
10
f1 (ppm)

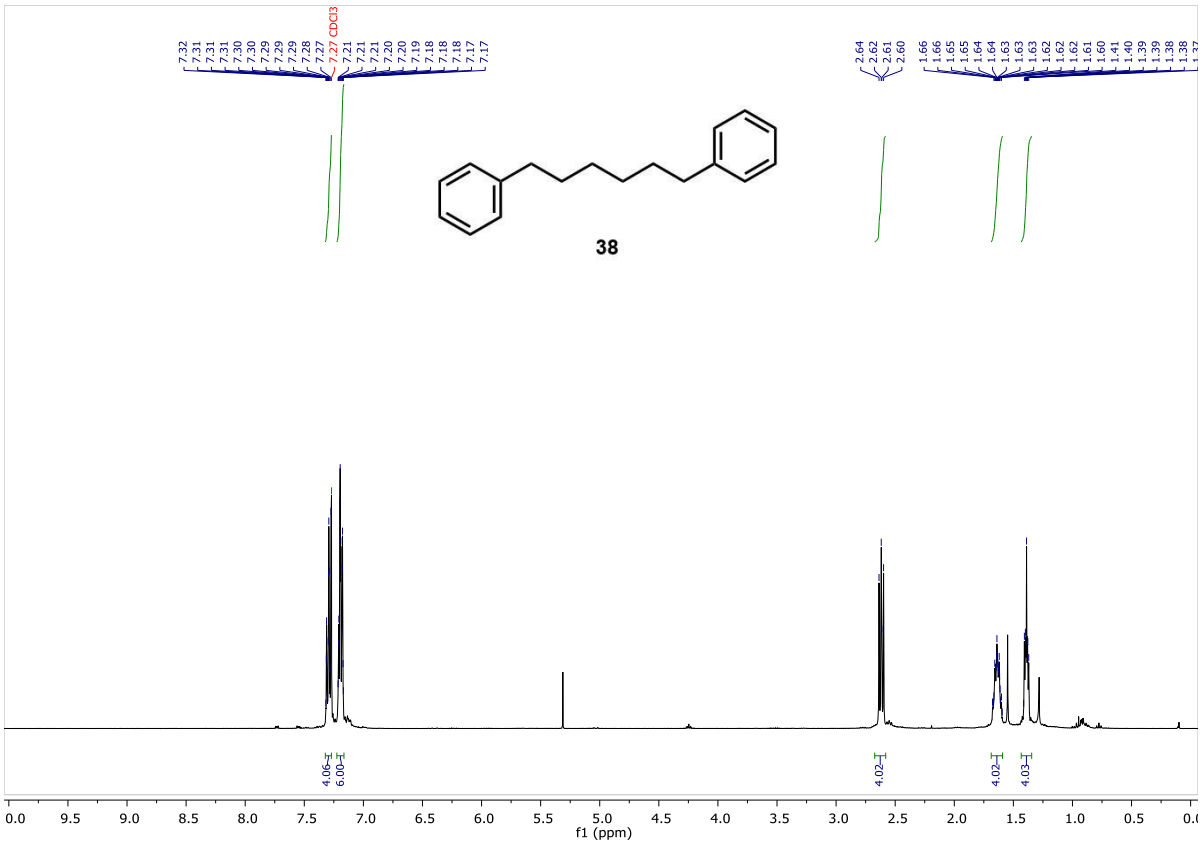
7.32
7.31
7.31
7.31
7.30
7.30
7.29
7.29
7.29
7.28
7.27
7.27 CDCl3
7.21
7.21
7.21
7.20
7.20
7.19
7.18
7.18
7.18
7.17
7.17
2.64
2.62
2.61
2.60
1.66
1.66
1.65
1.65
1.64
1.64
1.63
1.63
1.63
1.62
1.62
1.62
1.61
1.60
1.44
1.40
1.39
1.39
1.38
1.38
38
4.06
6.00
4.02
4.02
4.03
f1 (ppm)

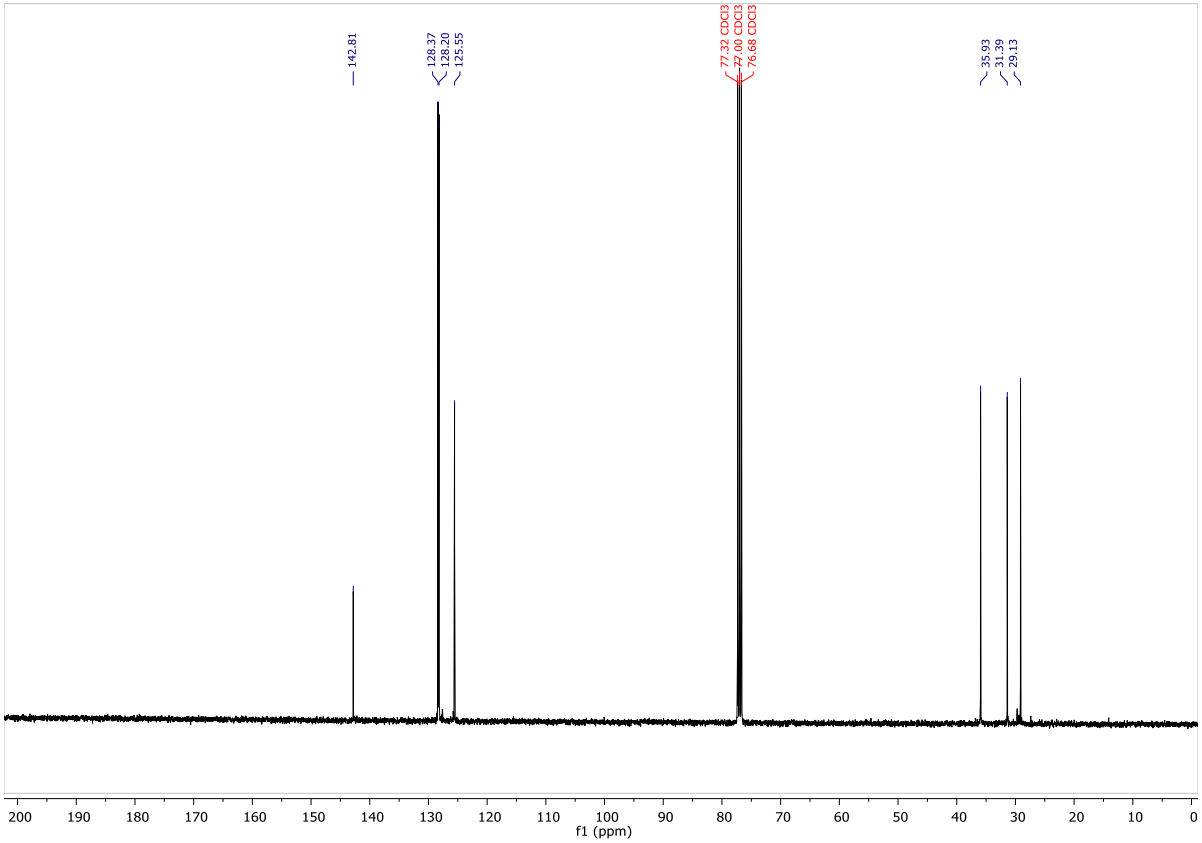
142.81
128.37
128.20
125.55
77.32 CDCl3
77.00 CDCl3
76.68 CDCl3
35.93
31.39
29.13
f1 (ppm)

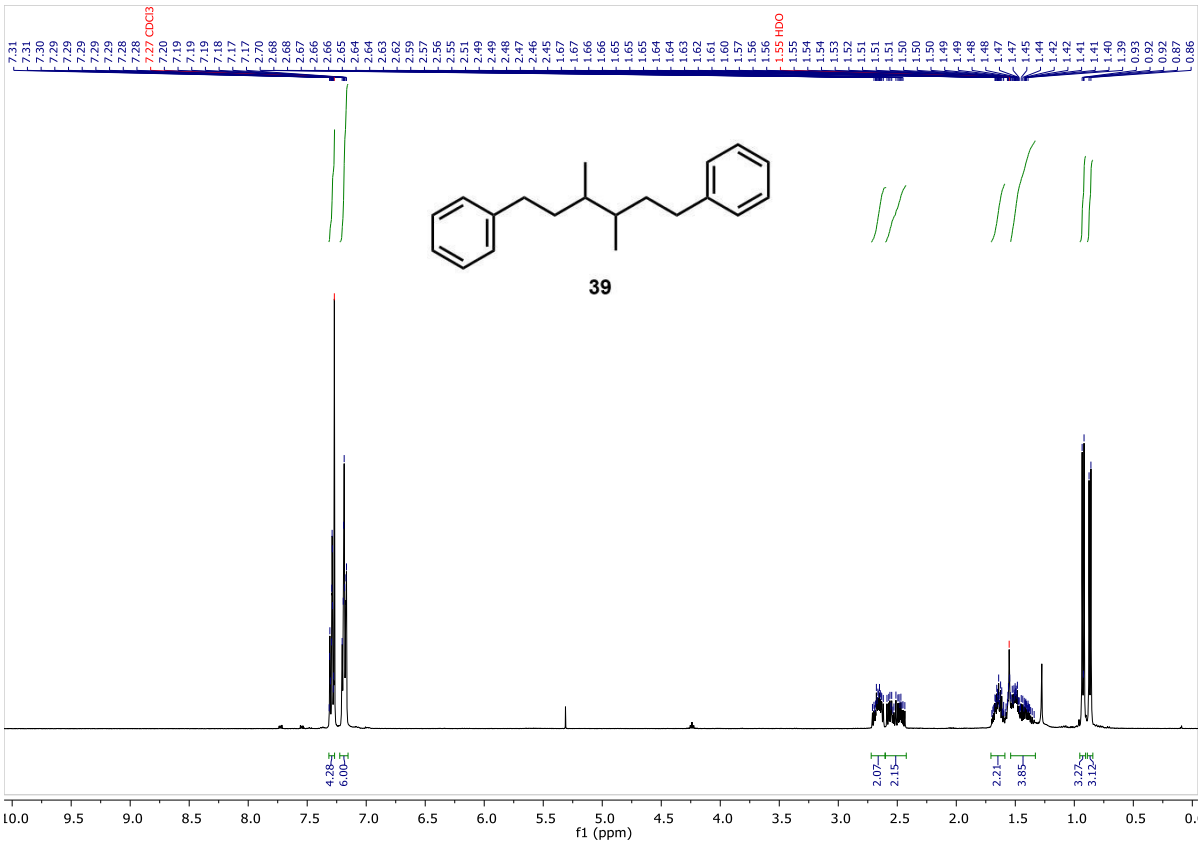
39
f1 (ppm)

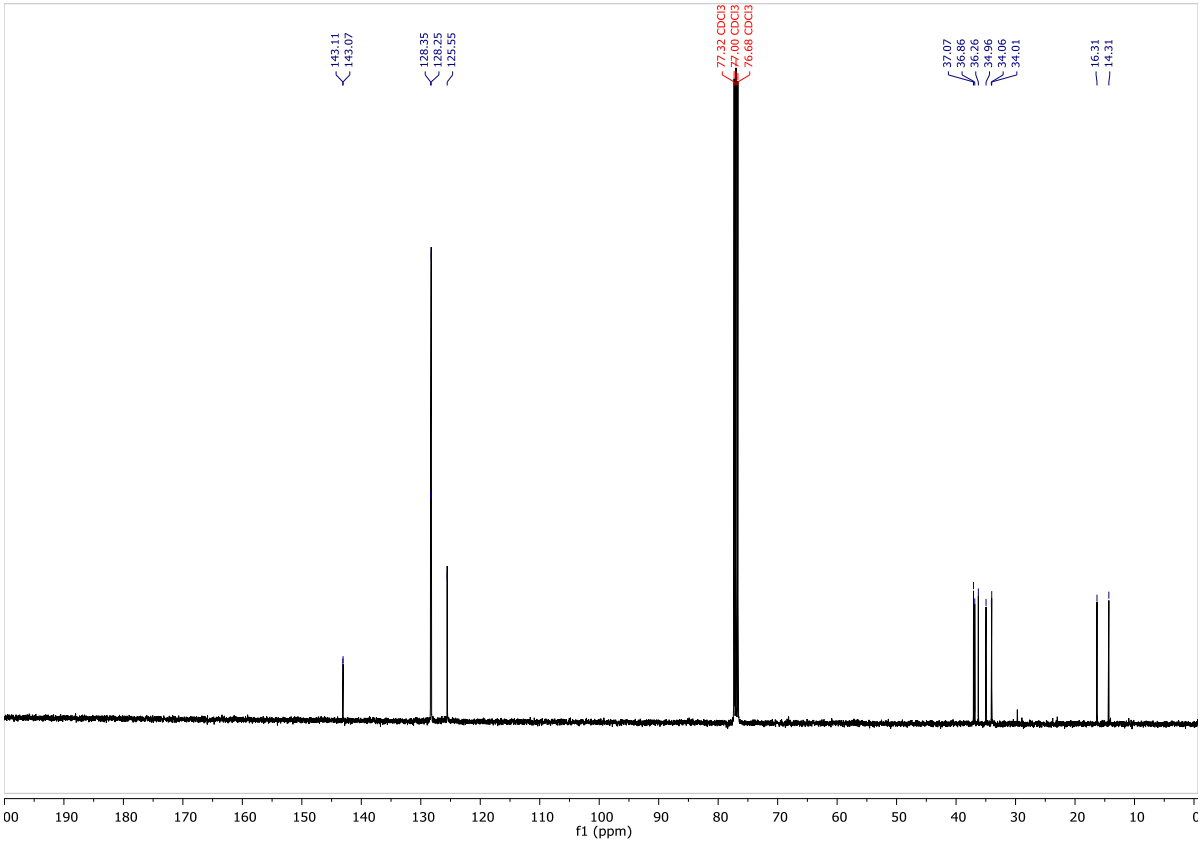
f1 (ppm)

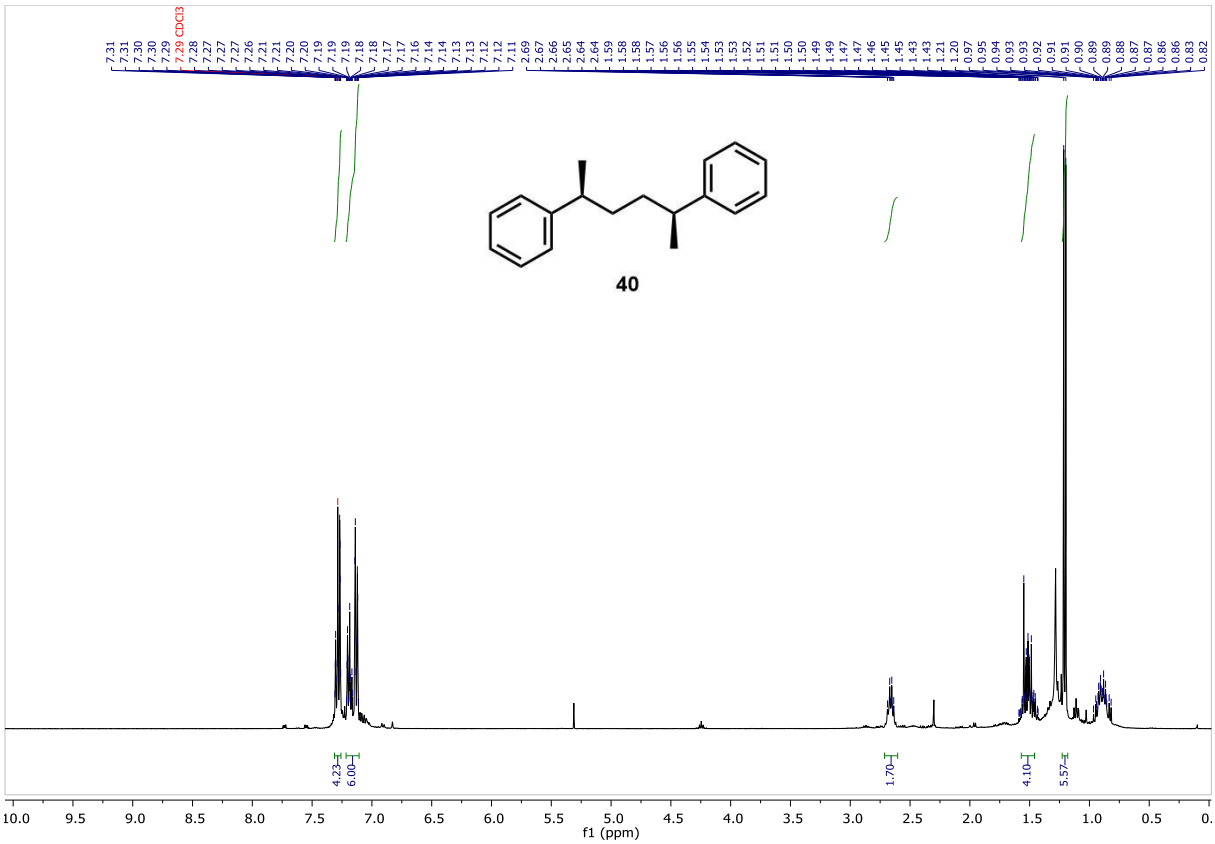
7.31 7.31 7.30 7.30 7.29 7.29 CDCl3 7.28 7.27 7.27 7.27 7.26 7.21 7.20 7.20 7.19 7.19 7.19 7.18 7.18 7.17 7.17 7.16 7.14 7.14 7.13 7.13 7.12 7.12 7.11
2.69 2.67 2.66 2.65 2.64 2.64 1.59 1.58 1.58 1.57 1.56 1.56 1.55 1.54 1.53 1.53 1.52 1.51 1.51 1.50 1.50 1.49 1.49 1.47 1.47 1.46 1.45 1.45 1.43 1.43 1.21 1.20 0.97 0.95 0.94 0.93 0.92 0.91 0.91 0.90 0.89 0.89 0.88 0.87 0.87 0.86 0.86 0.83 0.82
40
4.23
6.00
1.70
4.10
5.57
10.0 9.5 9.0 8.5 8.0 7.5 7.0 6.5 6.0 5.5 5.0 4.5 4.0 3.5 3.0 2.5 2.0 1.5 1.0 0.5 0.
f1 (ppm)

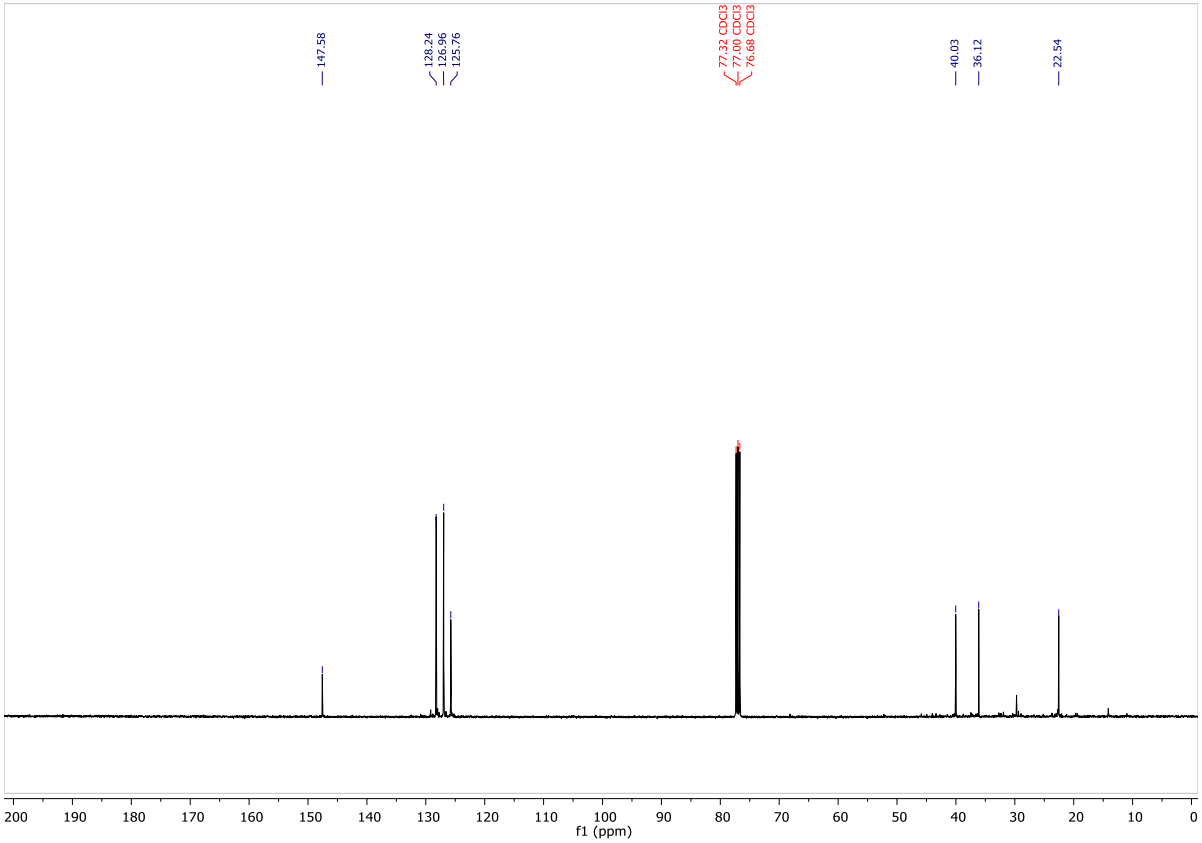
147.58
128.24
126.96
125.76
77.32 CDCl3
77.00 CDCl3
76.68 CDCl3
40.03
36.12
22.54
200 190 180 170 160 150 140 130 120 110 100 90 80 70 60 50 40 30 20 10 0
f1 (ppm)

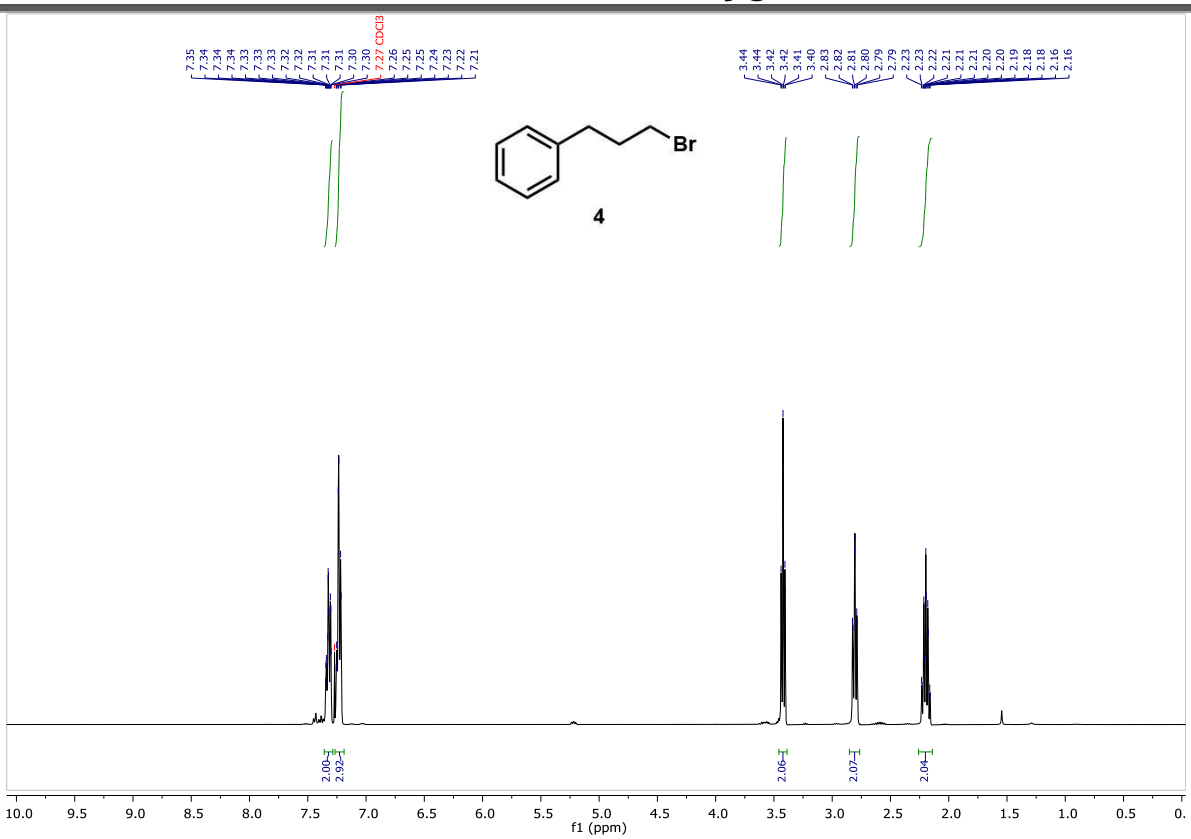
7.35
7.34
7.34
7.34
7.33
7.33
7.32
7.32
7.31
7.31
7.31
7.30
7.27 CDCl3
7.26
7.25
7.25
7.24
7.23
7.22
7.21
3.44
3.44
3.42
3.42
3.41
3.40
2.83
2.82
2.81
2.80
2.79
2.79
2.23
2.23
2.22
2.21
2.21
2.21
2.20
2.20
2.19
2.18
2.18
2.16
2.16
Br
4
2.00
2.92
2.06
2.07
2.04
10.0
9.5
9.0
8.5
8.0
7.5
7.0
6.5
6.0
5.5
5.0
4.5
4.0
3.5
3.0
2.5
2.0
1.5
1.0
0.5
f1 (ppm)

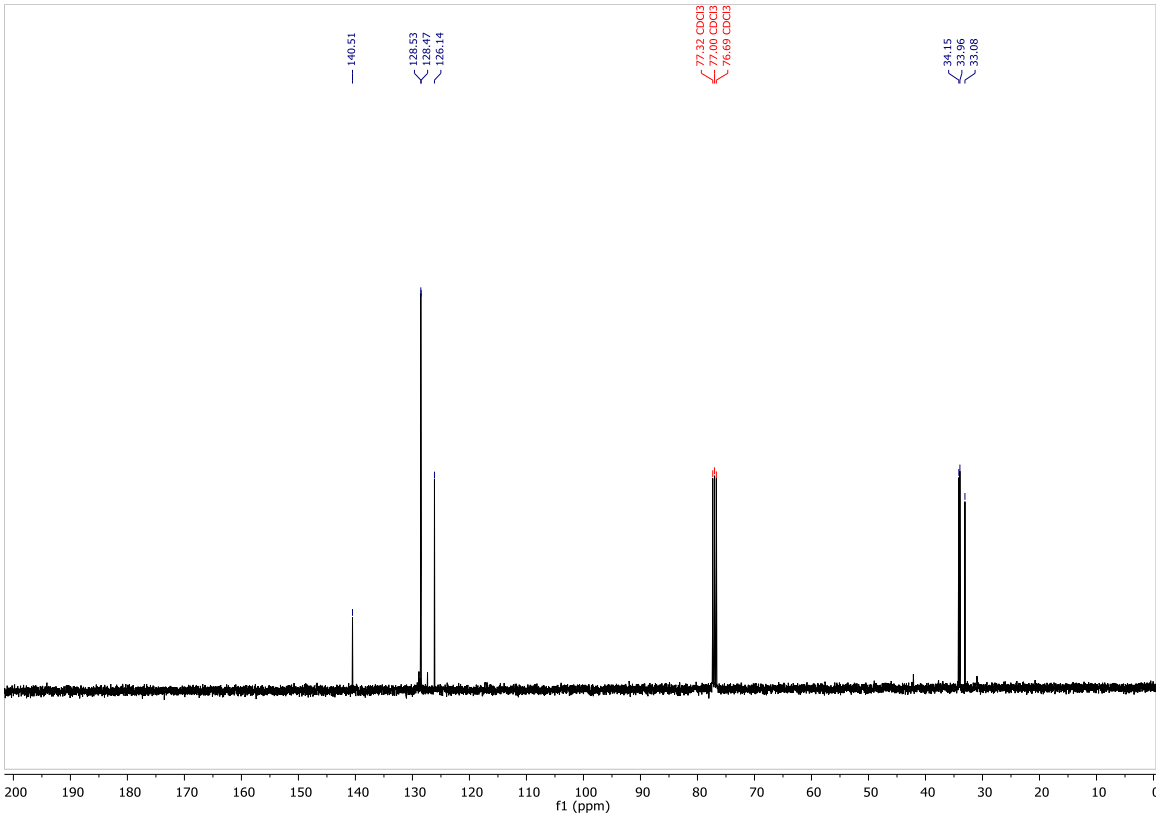
140.51
128.53
128.47
126.14
77.32 CDCl3
77.00 CDCl3
76.69 CDCl3
34.15
33.96
33.08
200
190
180
170
160
150
140
130
120
110
100
90
80
70
60
50
40
30
20
10
f1 (ppm)

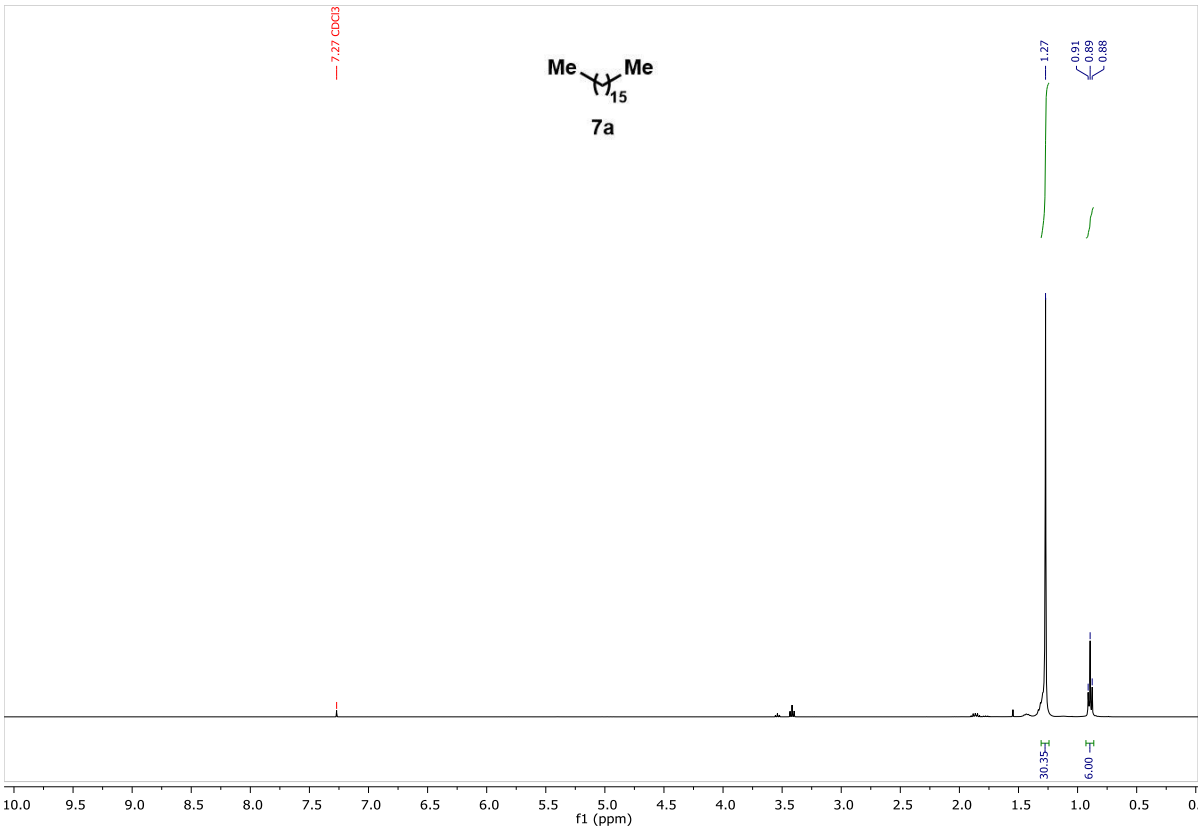
7.27 CDCl3
Me
Me
15
7a
1.27
0.91
0.89
0.88
30.35
6.00
f1 (ppm)

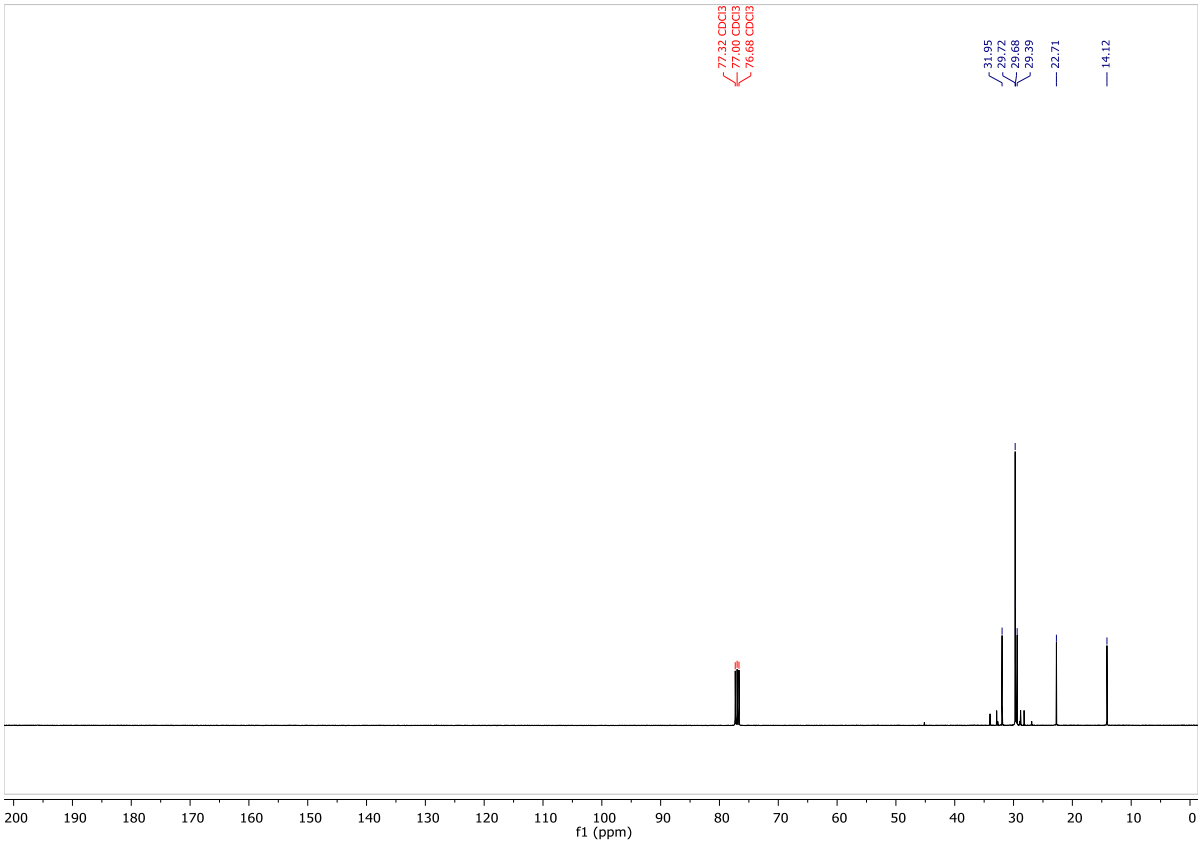
77.32 CDCl3
77.00 CDCl3
76.68 CDCl3
31.95
29.72
29.68
29.39
22.71
14.12
f1 (ppm)

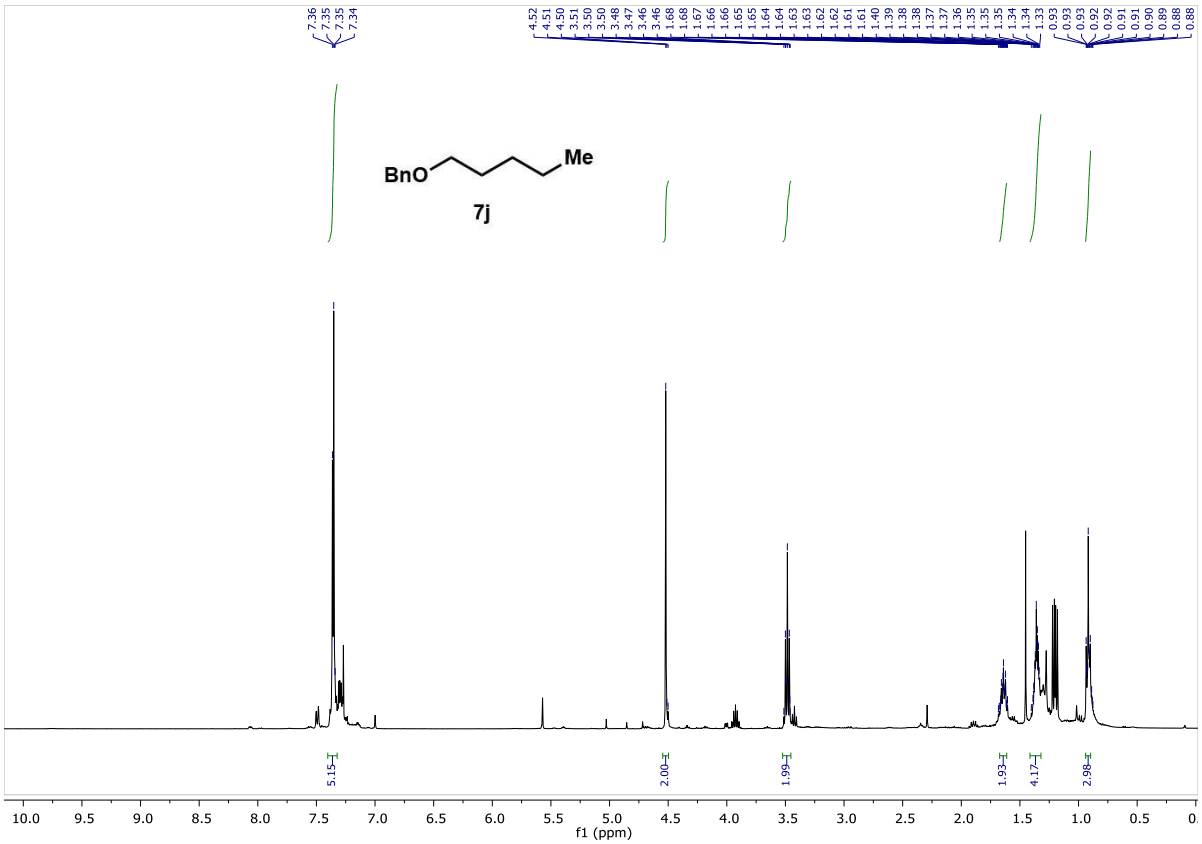
BnO
Me
7j
f1 (ppm)

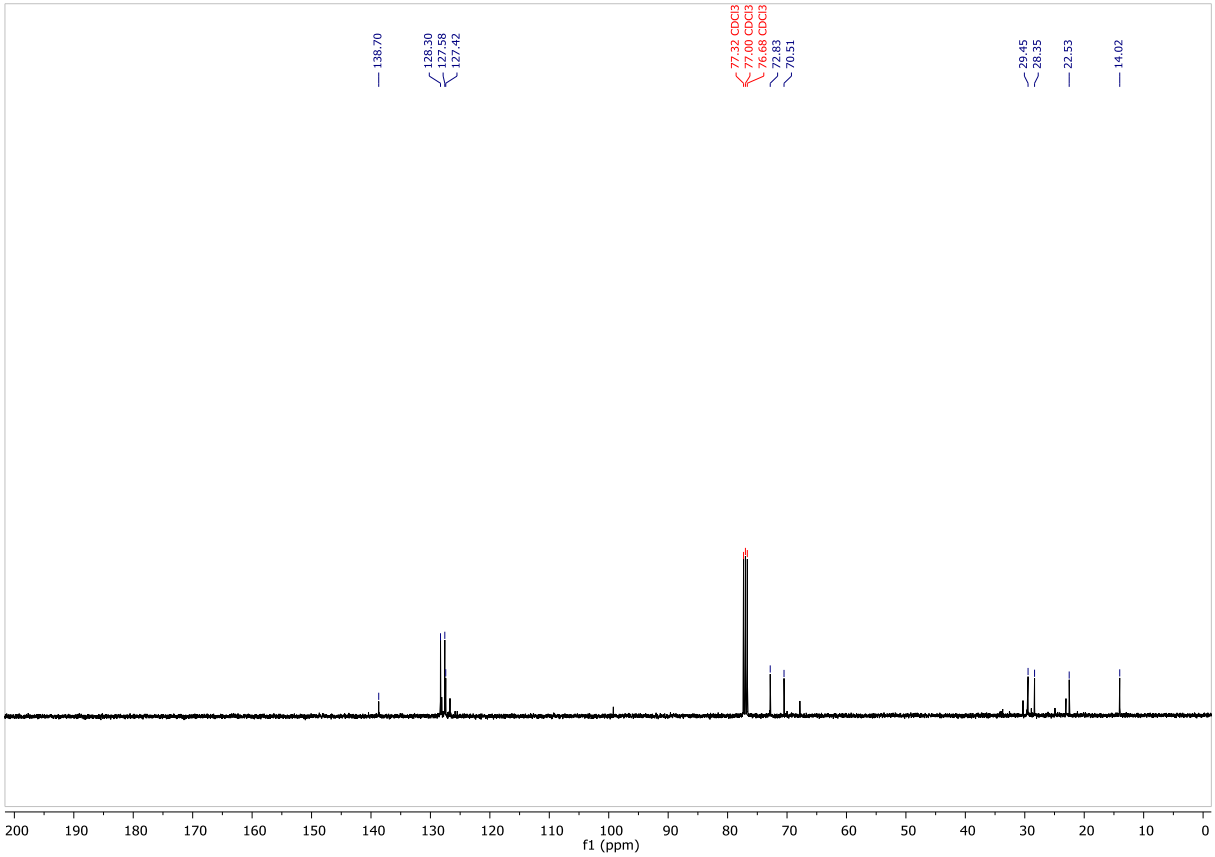
f1 (ppm)

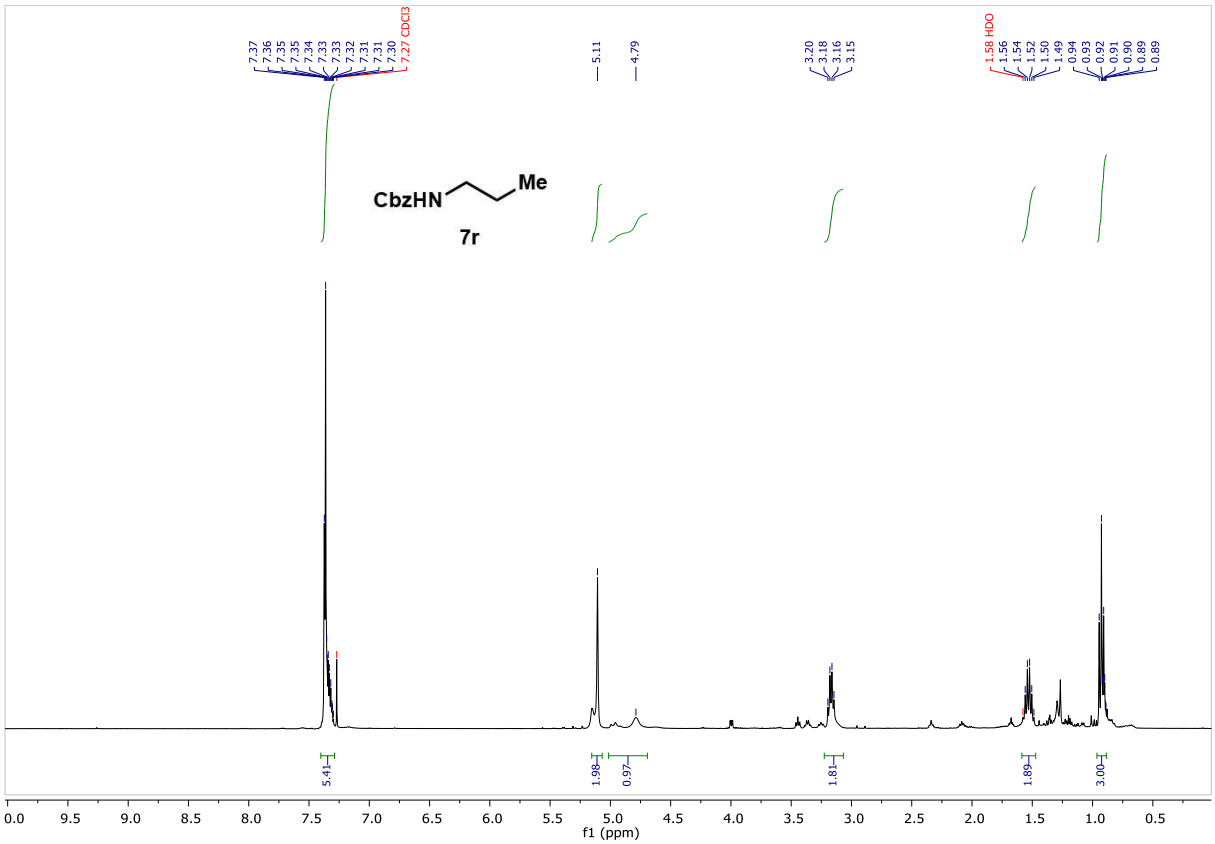
7.37
7.36
7.35
7.35
7.34
7.33
7.33
7.32
7.31
7.31
7.30
7.27 CDCl3
5.11
4.79
3.20
3.18
3.16
3.15
1.58 HDO
1.56
1.54
1.52
1.50
1.49
0.94
0.93
0.92
0.91
0.90
0.89
0.89
CbzHN
Me
7r
5.41
1.98
0.97
1.81
1.89
3.00
f1 (ppm)

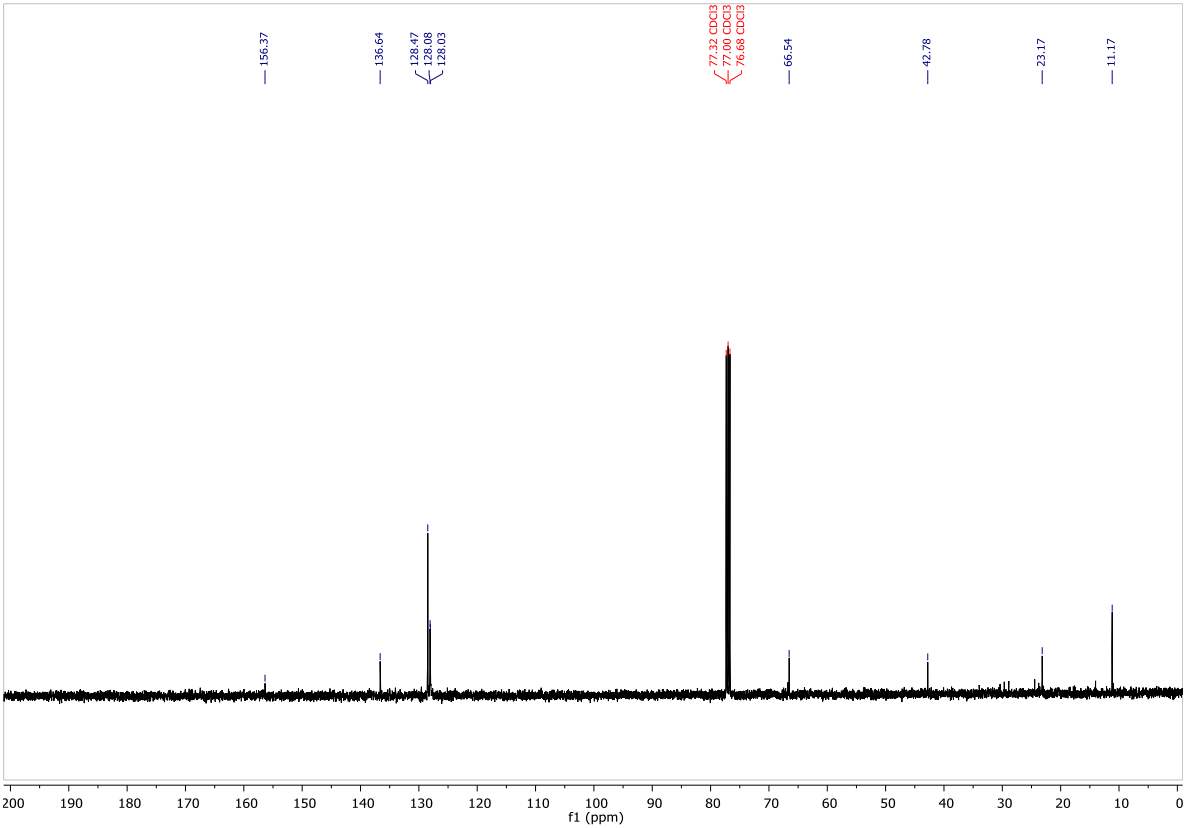
156.37
136.64
128.47
128.08
128.03
77.32 CDCl3
77.00 CDCl3
76.68 CDCl3
66.54
42.78
23.17
11.17
f1 (ppm)

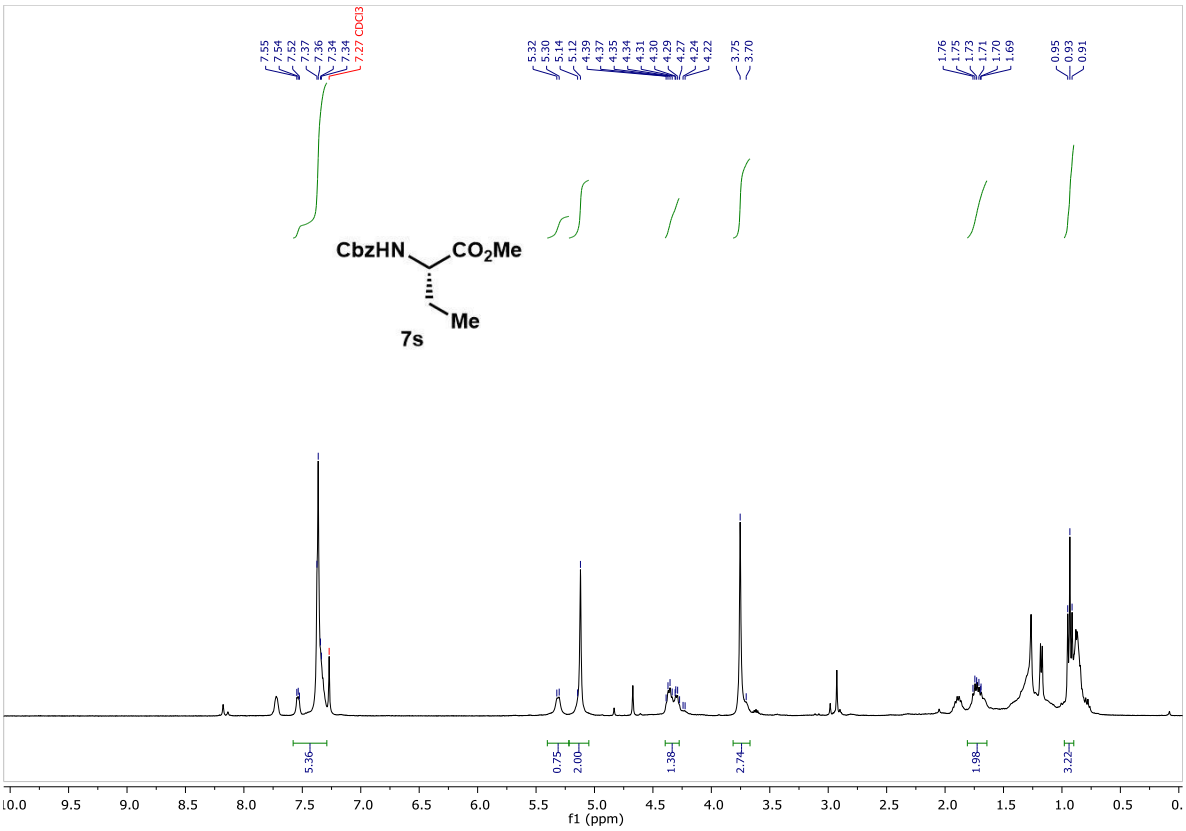
7.55
7.54
7.52
7.37
7.36
7.34
7.34
7.27 CDCl3
5.32
5.30
5.14
5.12
4.39
4.37
4.35
4.34
4.31
4.30
4.29
4.27
4.24
4.22
3.75
3.70
1.76
1.75
1.73
1.71
1.70
1.69
0.95
0.93
0.91
CbzHN
CO2Me
Me
7s
5.36
0.75
2.00
1.38
2.74
1.98
3.22
f1 (ppm)

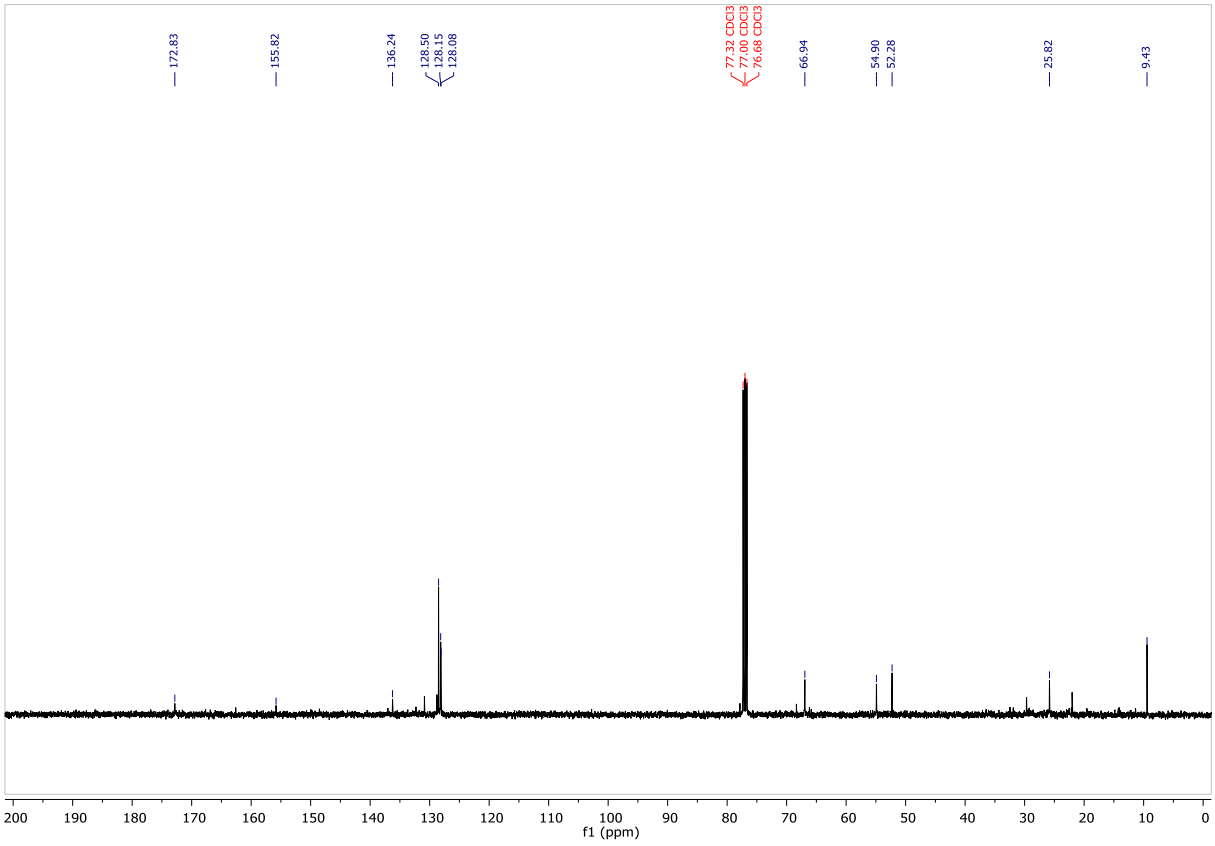
172.83
155.82
136.24
128.50
128.15
128.08
77.33 CDCl3
77.00 CDCl3
76.68 CDCl3
66.94
54.90
52.28
25.82
9.43
f1 (ppm)

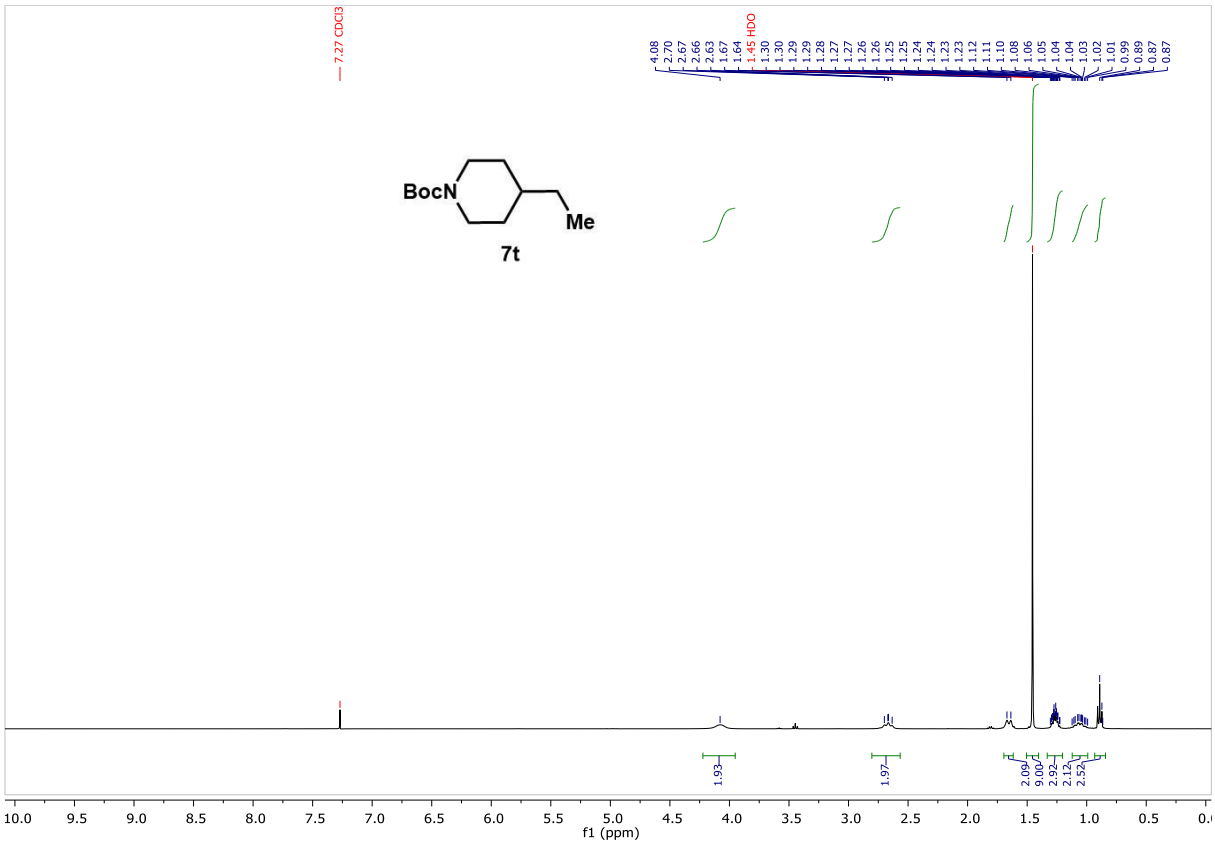
7.27 CDCl3
1.45 H2O
BocN
Me
7t
f1 (ppm)

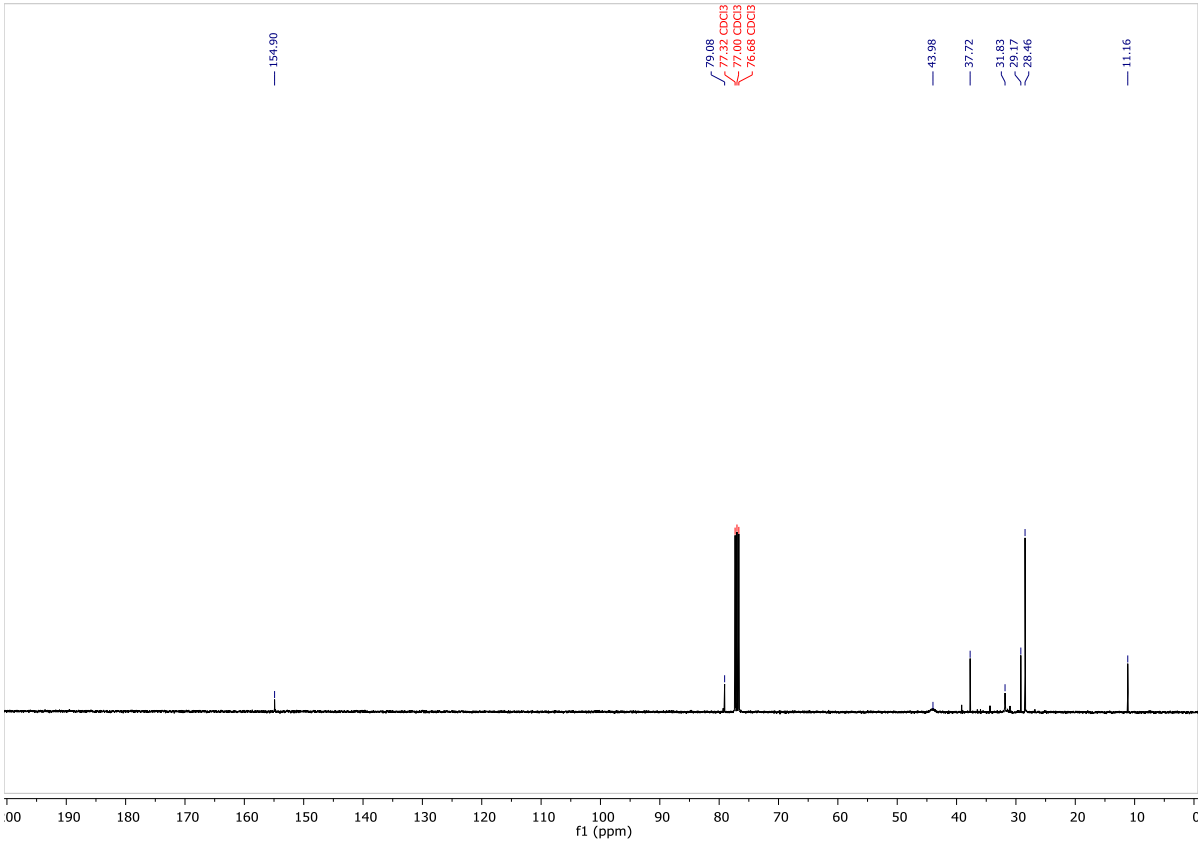
154.90
79.08
77.32 CDCl3
77.00 CDCl3
76.68 CDCl3
43.98
37.72
31.83
29.17
28.46
11.16
f1 (ppm)

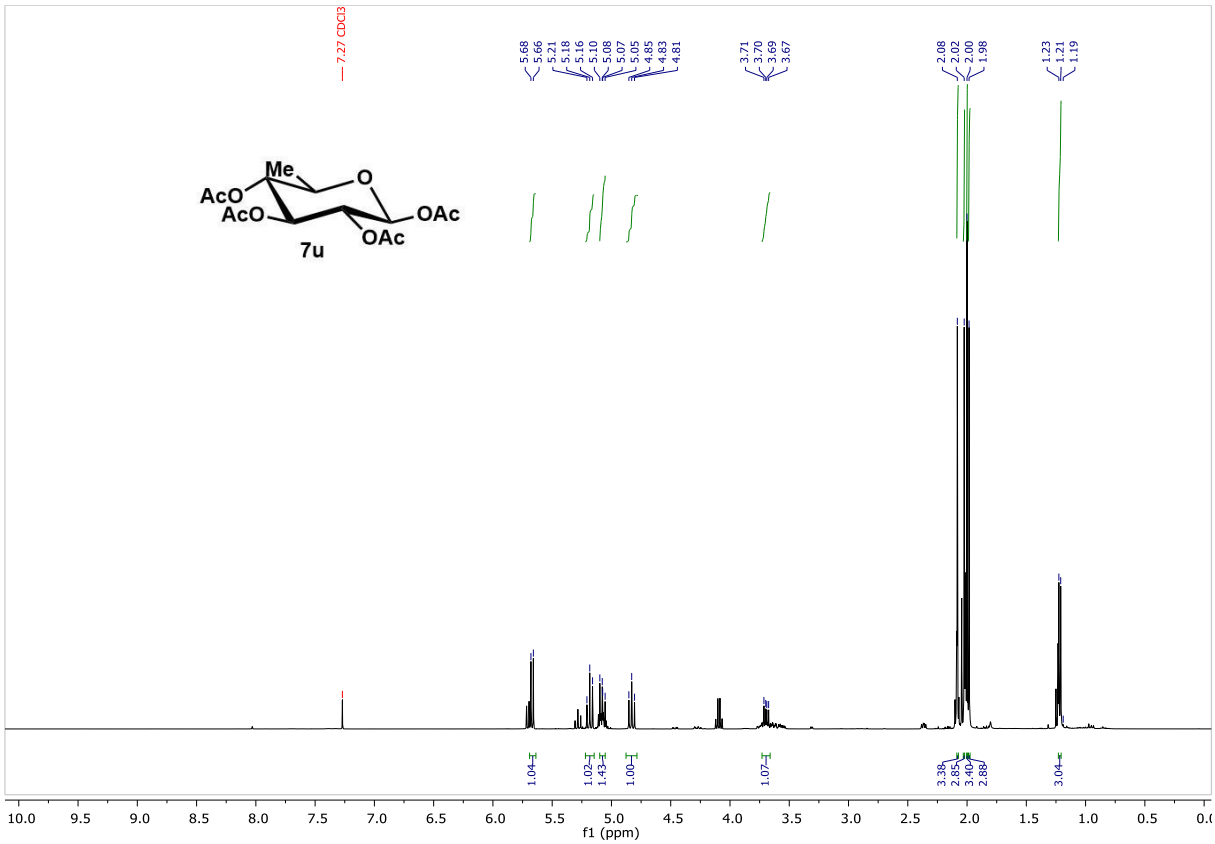
7.27 CDCl3
5.68
5.66
5.21
5.18
5.16
5.10
5.08
5.07
5.05
4.85
4.83
4.81
3.71
3.70
3.69
3.67
2.08
2.02
2.00
1.98
1.23
1.21
1.19
Me
O
AcO
AcO
OAc
OAc
7u
1.04
1.02
1.43
1.00
1.07
3.38
2.85
3.40
2.88
3.04
f1 (ppm)

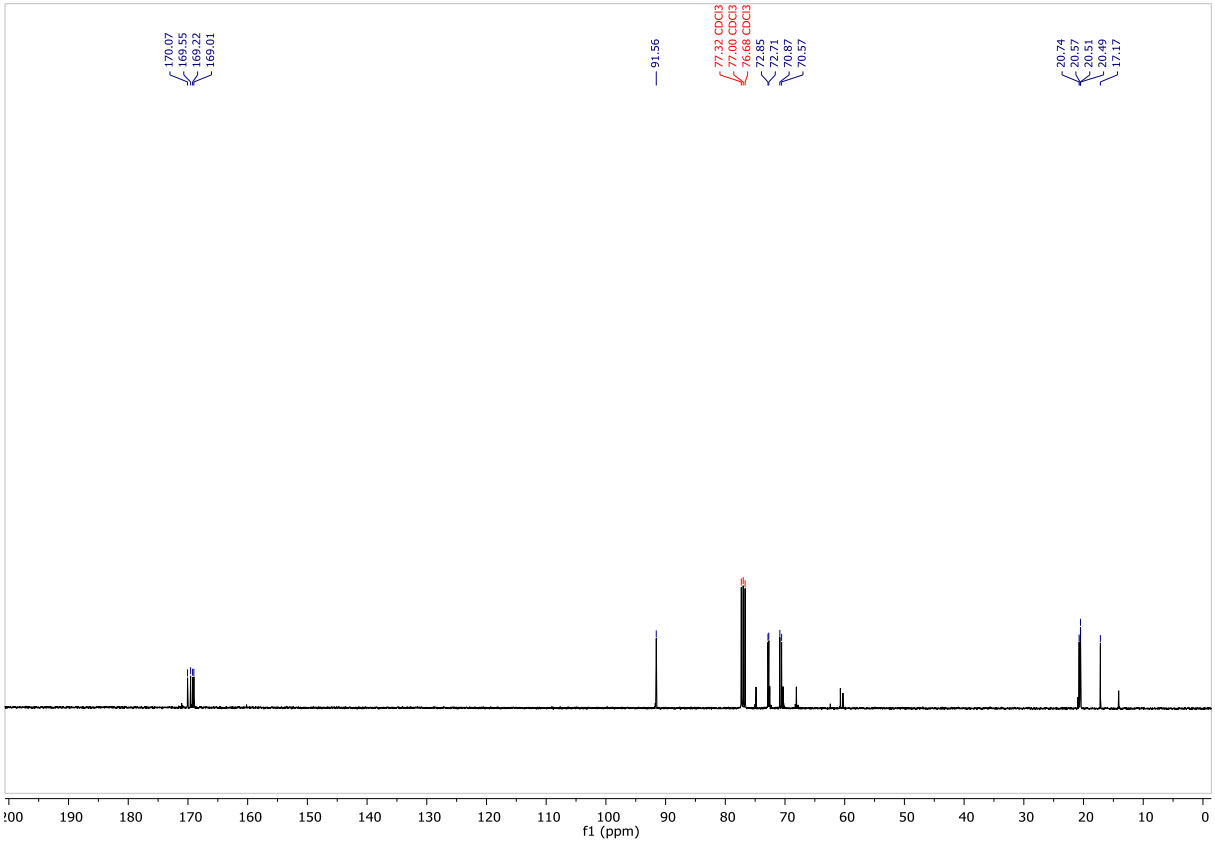
170.07
169.55
169.22
169.01
91.56
77.32 CDCl3
77.00 CDCl3
76.68 CDCl3
72.85
72.71
70.87
70.57
20.74
20.57
20.51
20.49
17.17
f1 (ppm)

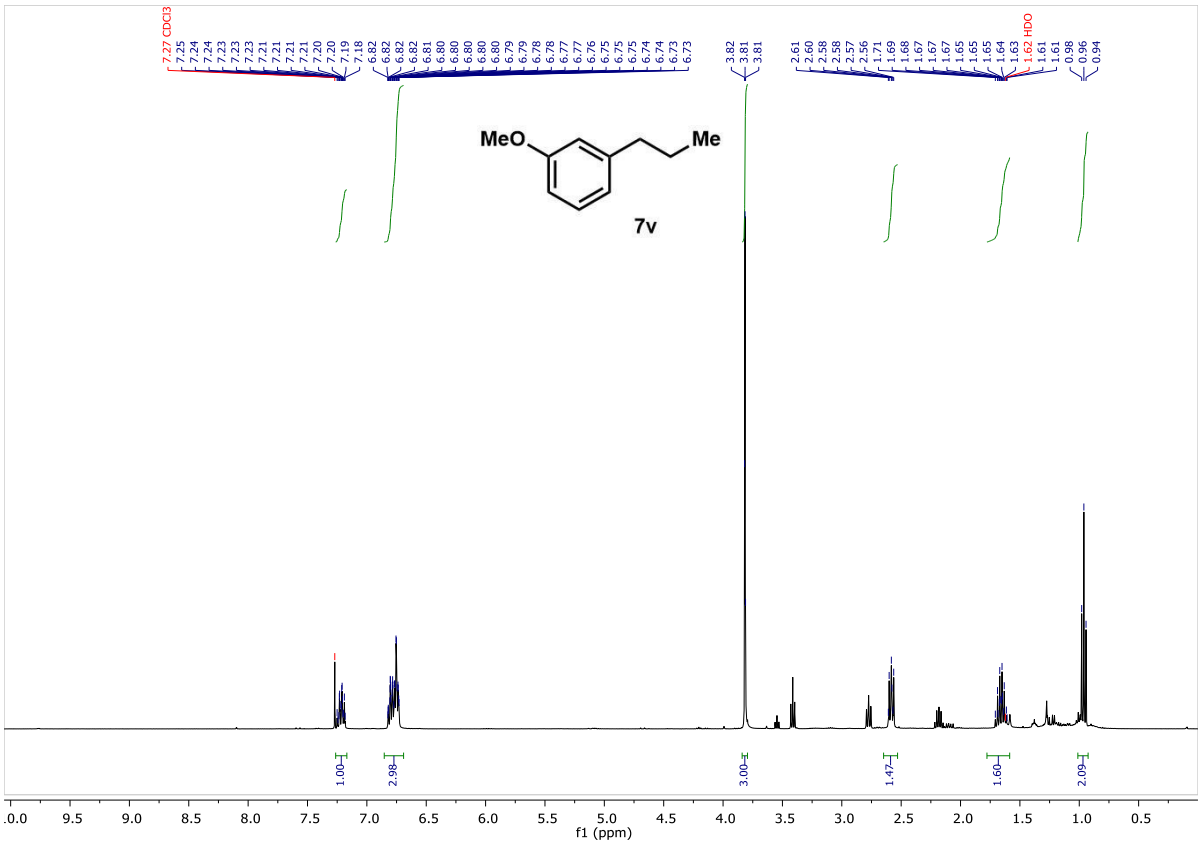
MeO
Me
7v
f1 (ppm)

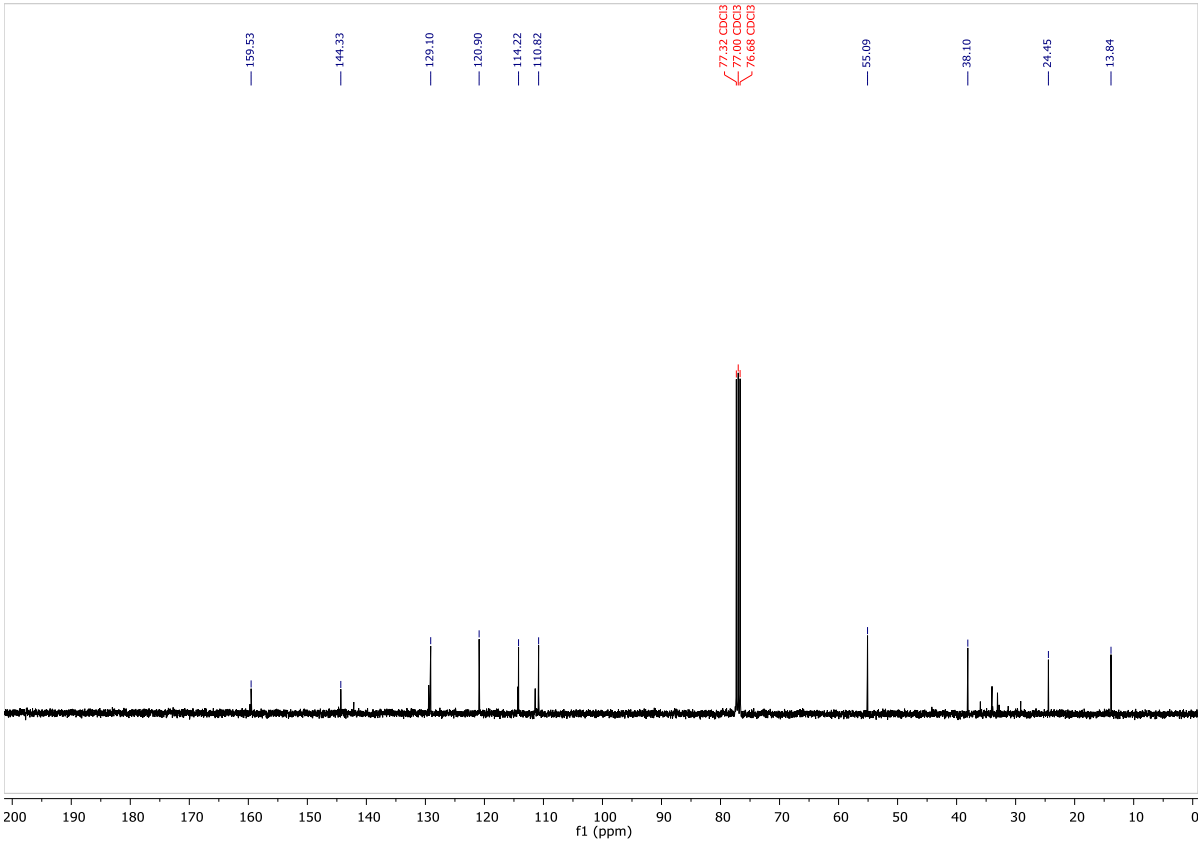
f1 (ppm)

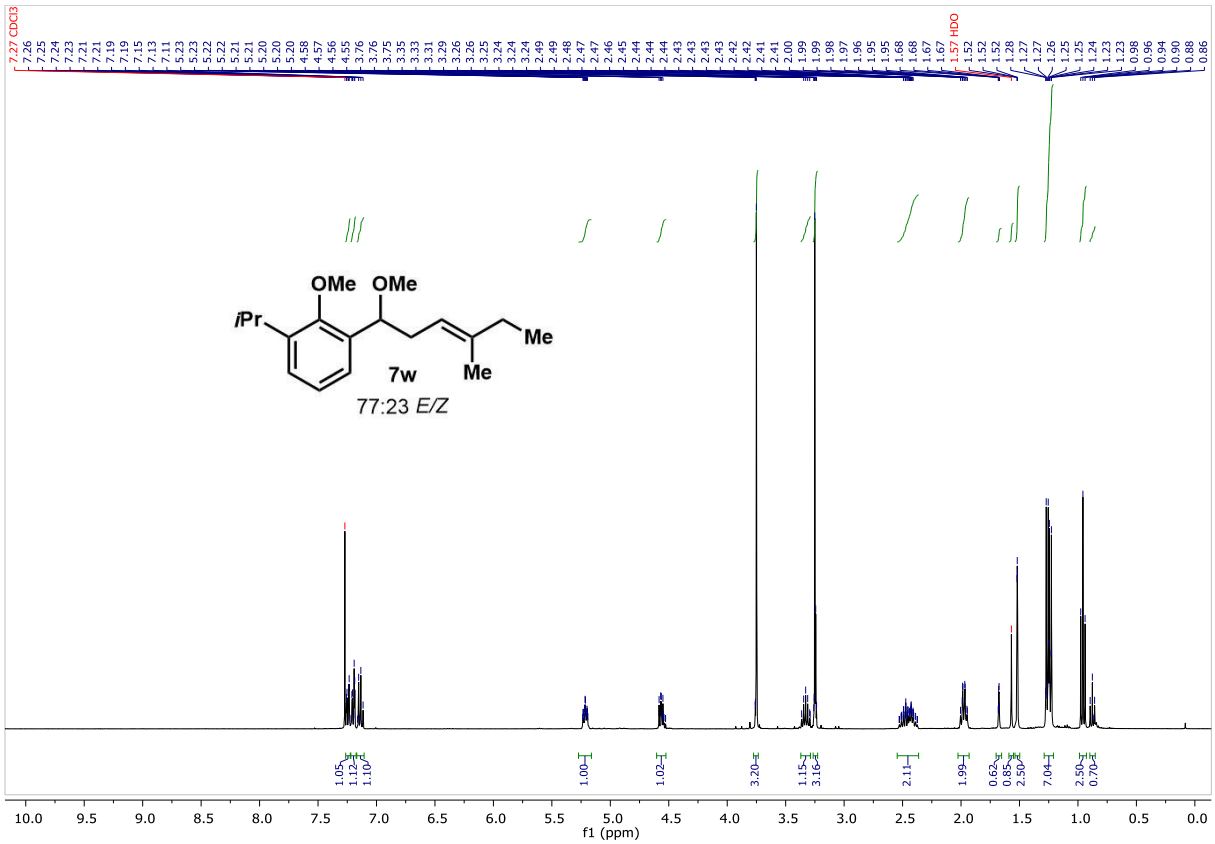
OMe
OMe
iPr
Me
Me
7w
77:23 E/Z
f1 (ppm)

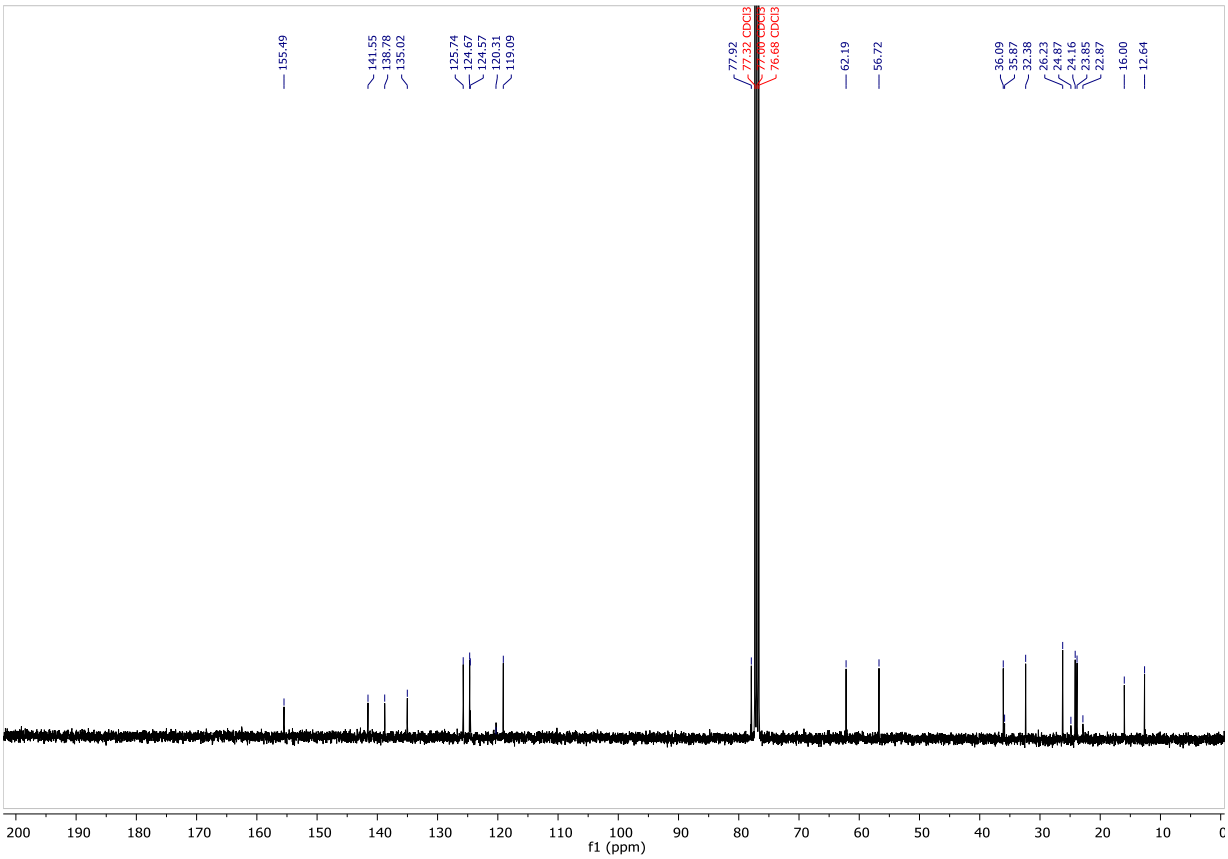
f1 (ppm)

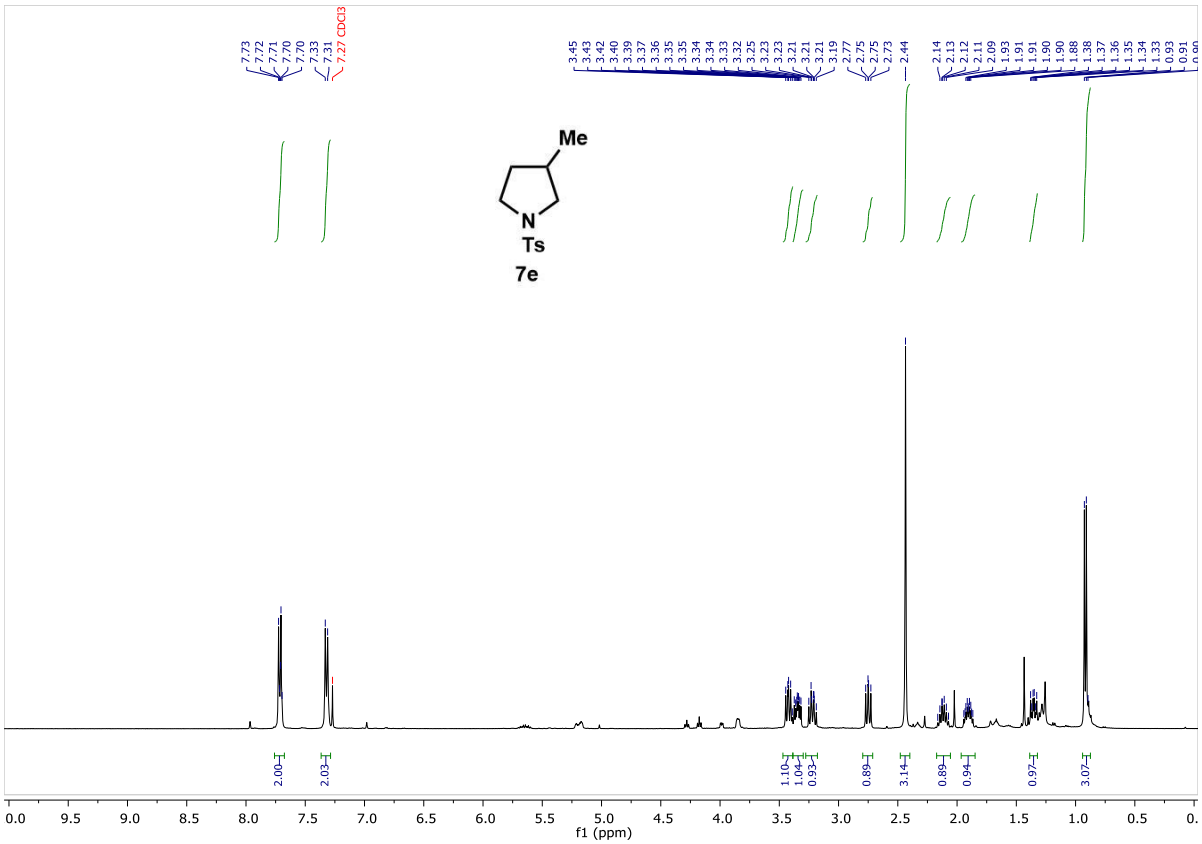
Me
N
Ts
7e
f1 (ppm)

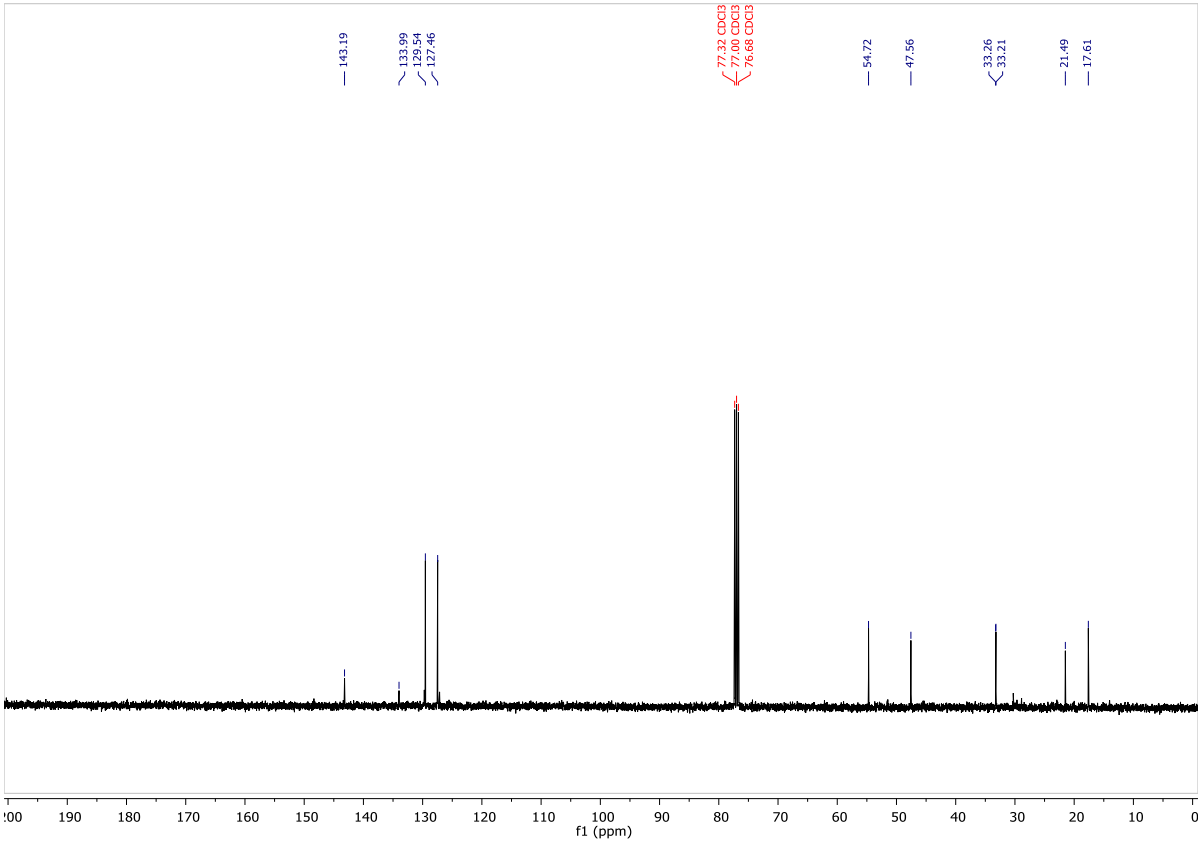
f1 (ppm)

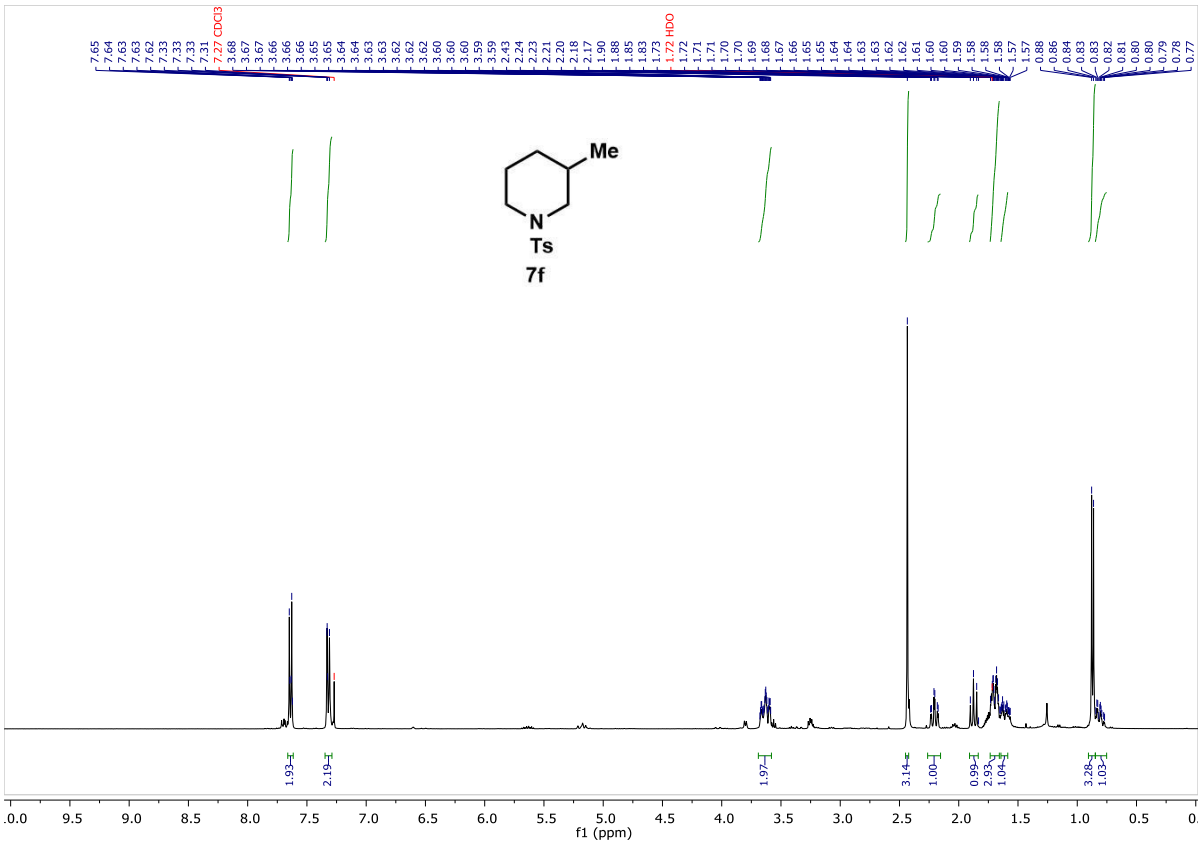
Me
N
Ts
7f
f1 (ppm)

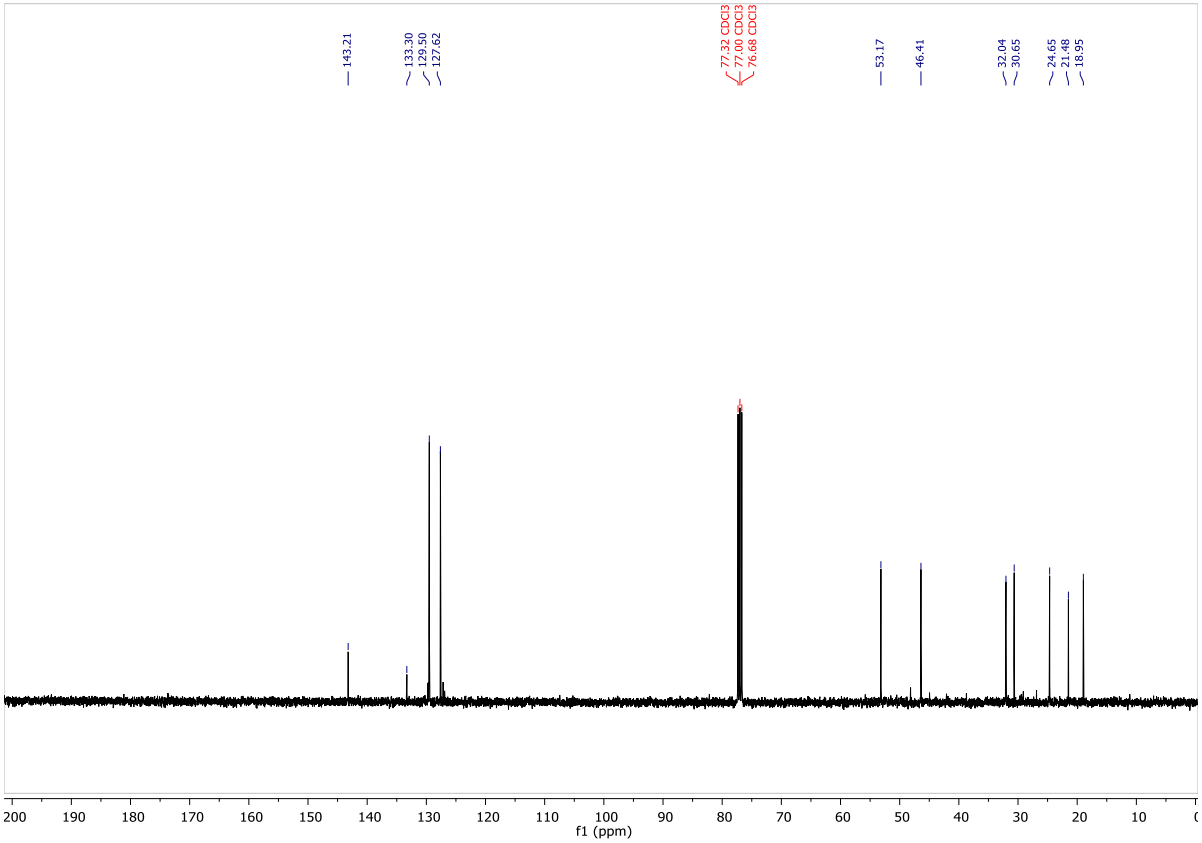
143.21
133.30
129.50
127.62
77.32 CDCl3
77.00 CDCl3
76.68 CDCl3
53.17
46.41
32.04
30.65
24.65
21.48
18.95
f1 (ppm)

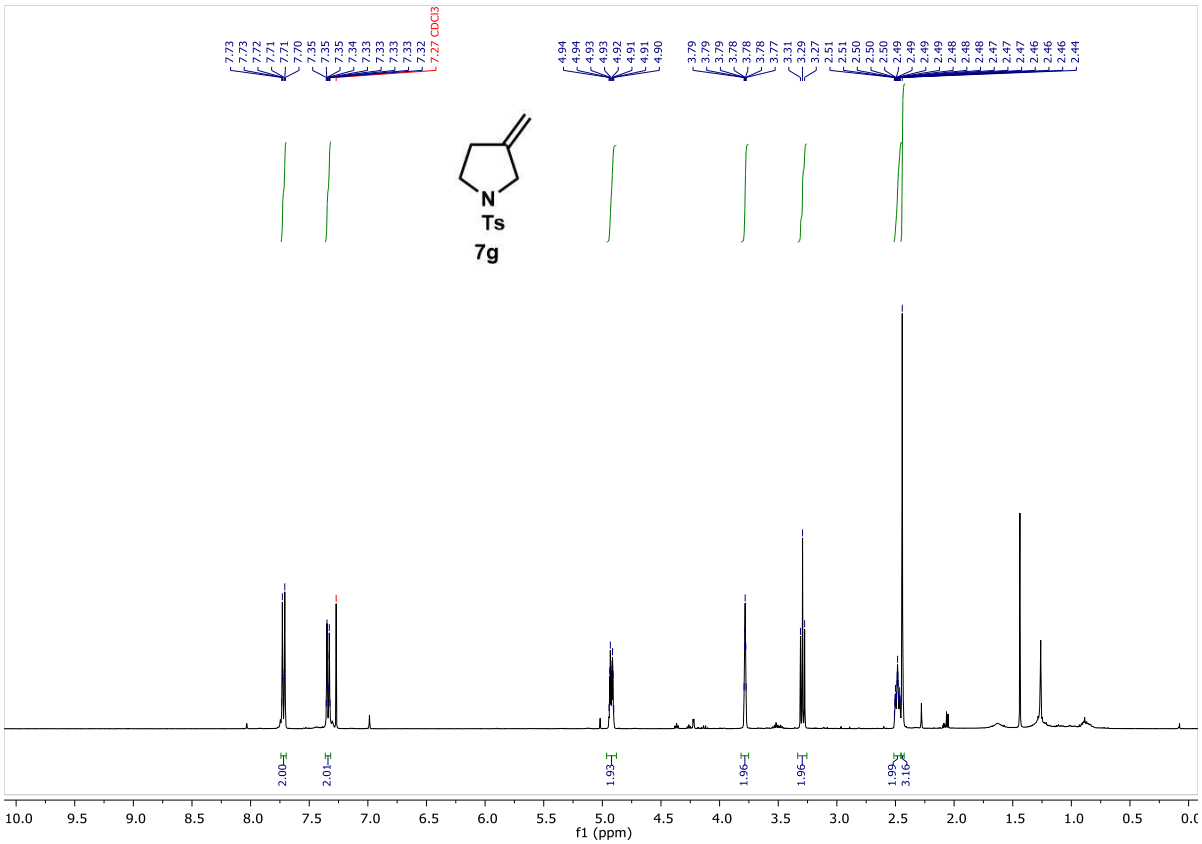
7.73 7.73 7.72 7.71 7.71 7.70 7.35 7.35 7.35 7.34 7.33 7.33 7.33 7.33 7.32 7.27 CDCl3
4.94 4.94 4.93 4.93 4.92 4.91 4.91 4.90
3.79 3.79 3.79 3.78 3.78 3.78 3.77 3.31 3.29 3.27
2.51 2.51 2.50 2.50 2.50 2.49 2.49 2.49 2.49 2.48 2.48 2.48 2.47 2.47 2.47 2.46 2.46 2.46 2.46 2.44
N
Ts
7g
2.00 2.01 1.93 1.96 1.96 1.99 3.16
10.0 9.5 9.0 8.5 8.0 7.5 7.0 6.5 6.0 5.5 5.0 4.5 4.0 3.5 3.0 2.5 2.0 1.5 1.0 0.5 0.0
f1 (ppm)

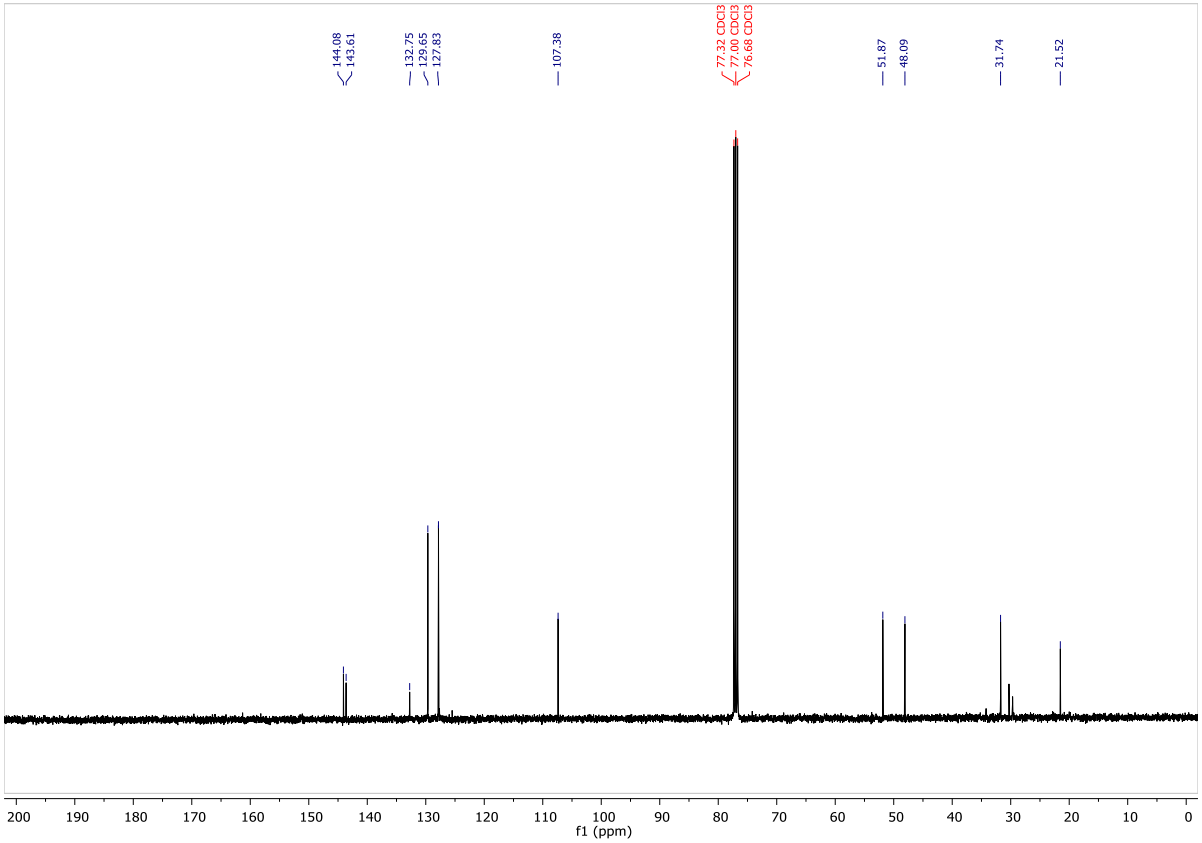
144.08 143.61 132.75 129.65 127.83 107.38 77.32 CDCl3 77.00 CDCl3 76.68 CDCl3 51.87 48.09 31.74 21.52
200 190 180 170 160 150 140 130 120 110 100 90 80 70 60 50 40 30 20 10 0
f1 (ppm)

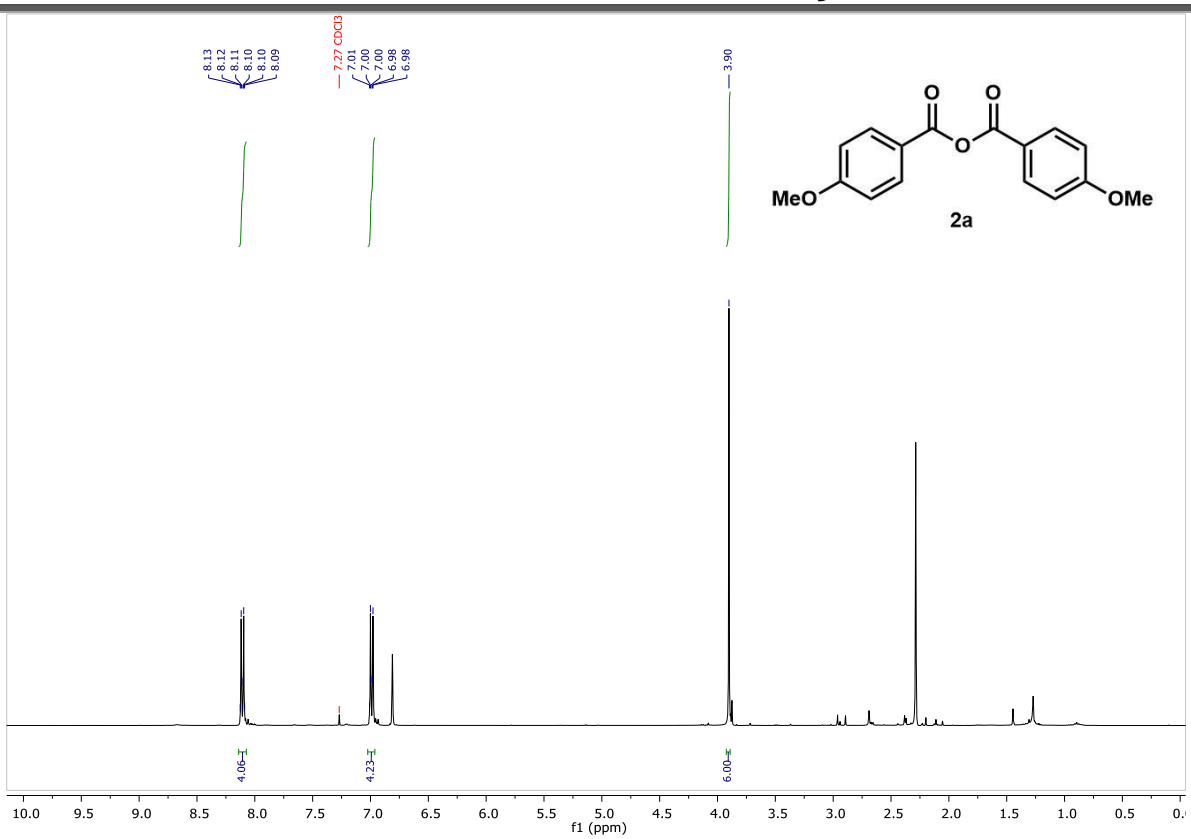
8.13
8.12
8.11
8.10
8.10
8.09
7.27 CDCl3
7.01
7.00
7.00
6.98
6.98
3.90
MeO
OMe
2a
4.06
4.23
6.00
f1 (ppm)

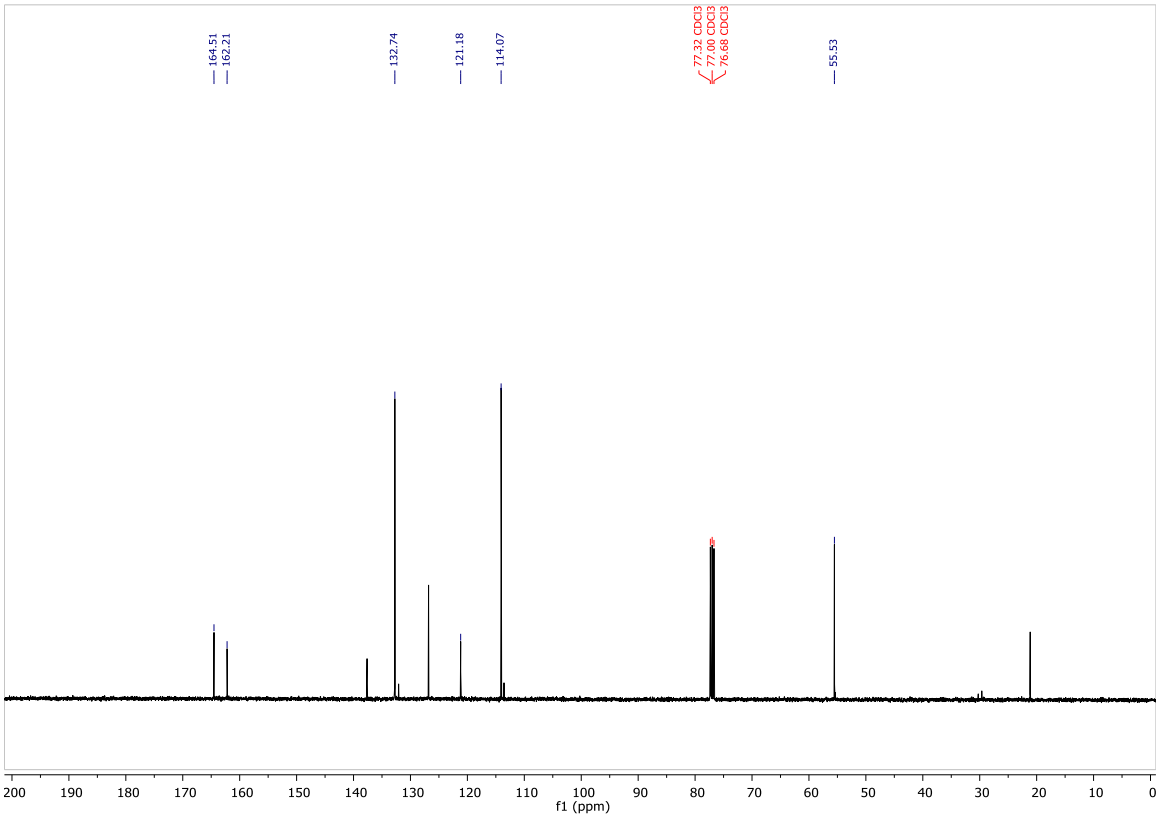
164.51
162.21
132.74
121.18
114.07
77.32 CDCl3
77.00 CDCl3
76.68 CDCl3
55.53
f1 (ppm)

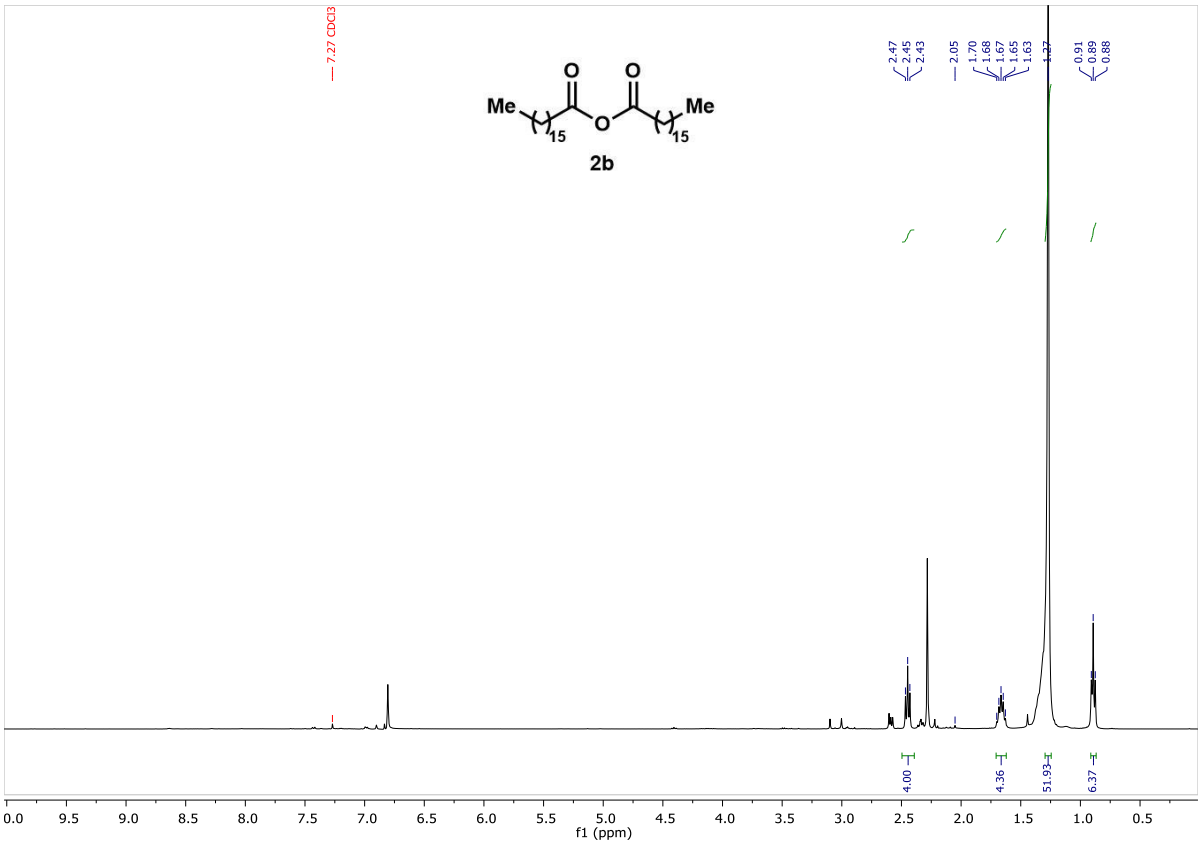
7.27 CDCl3
2.47
2.45
2.43
2.05
1.70
1.68
1.67
1.65
1.63
1.37
0.91
0.89
0.88
Me
15
O
O
O
Me
15
2b
4.00
4.36
51.93
6.37
f1 (ppm)

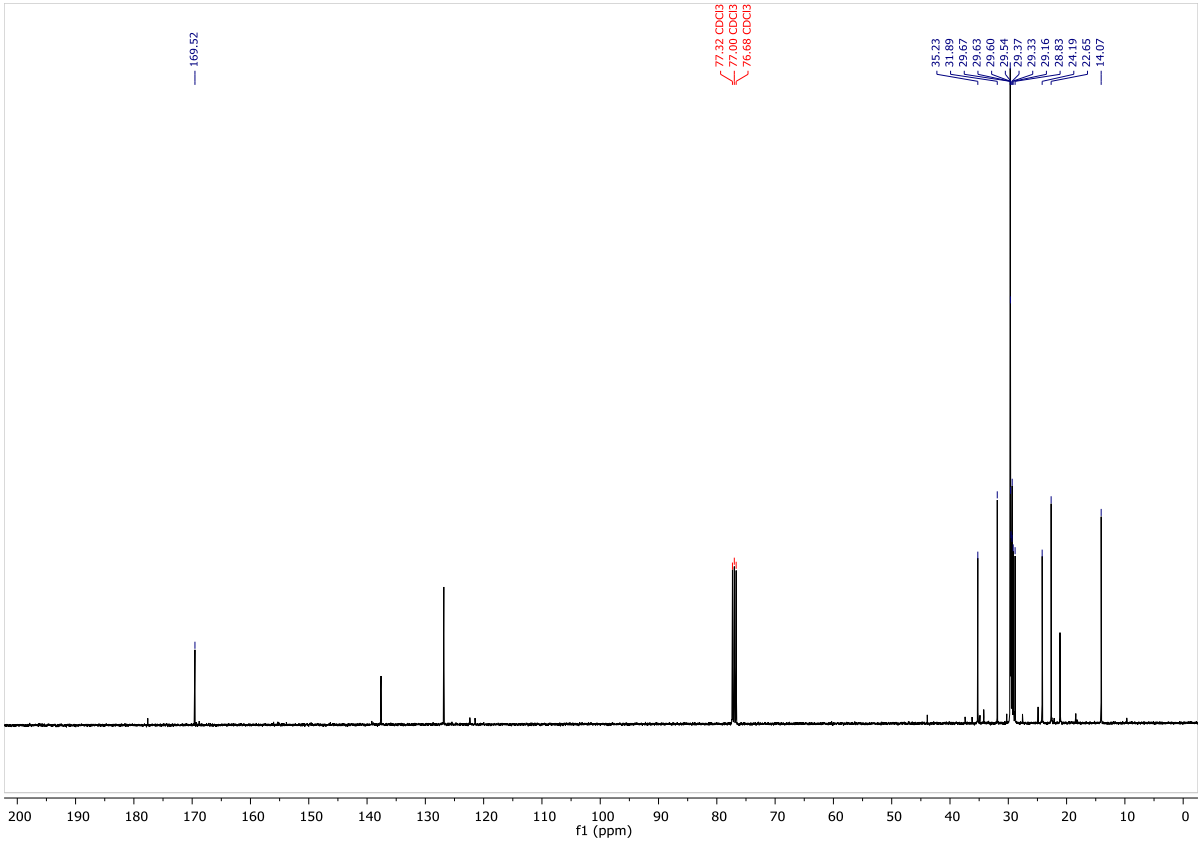
169.52
77.32 CDCl3
77.00 CDCl3
76.68 CDCl3
35.23
31.89
29.67
29.63
29.60
29.54
29.37
29.33
29.16
28.83
22.69
22.65
14.07
f1 (ppm)

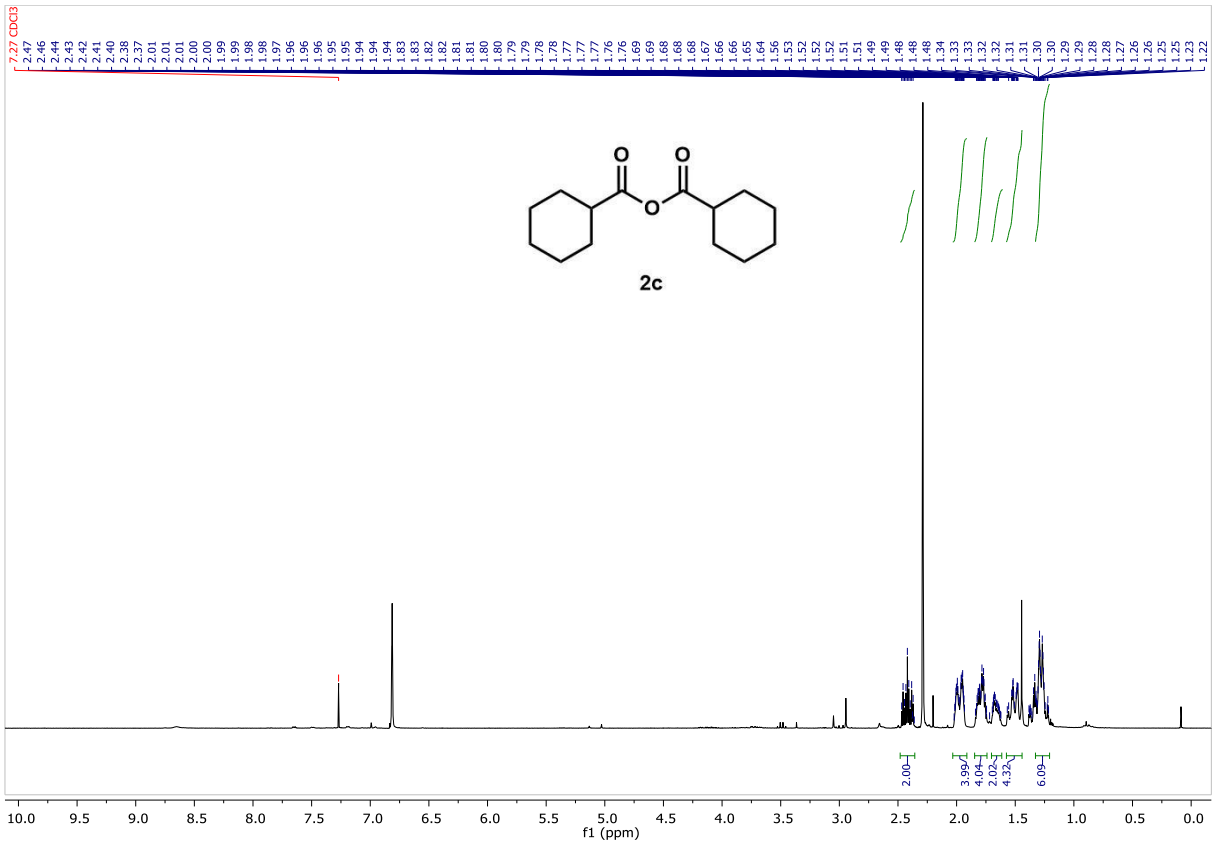
7.27 CDCl3
2c
2.00
3.99
4.04
2.02
4.32
6.09
f1 (ppm)

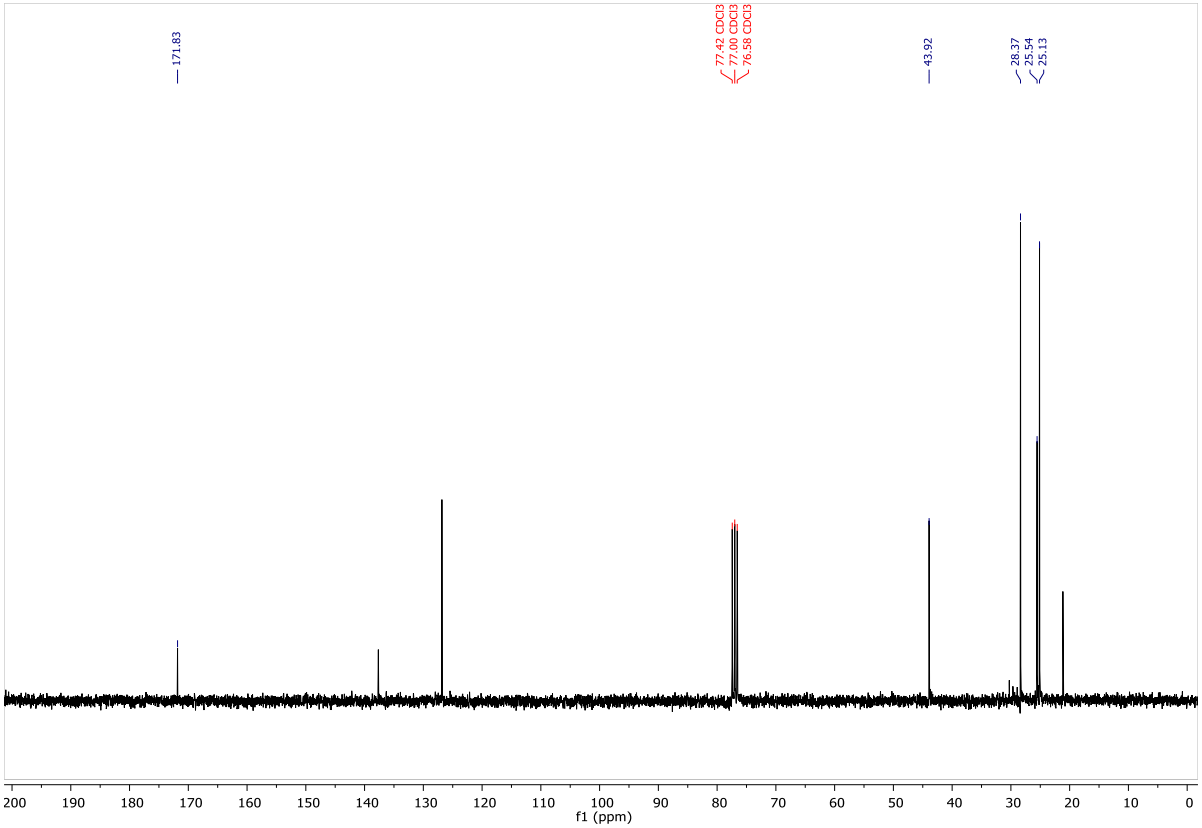
171.83
77.42 CDCl3
77.00 CDCl3
76.58 CDCl3
43.92
28.37
25.54
25.13
f1 (ppm)

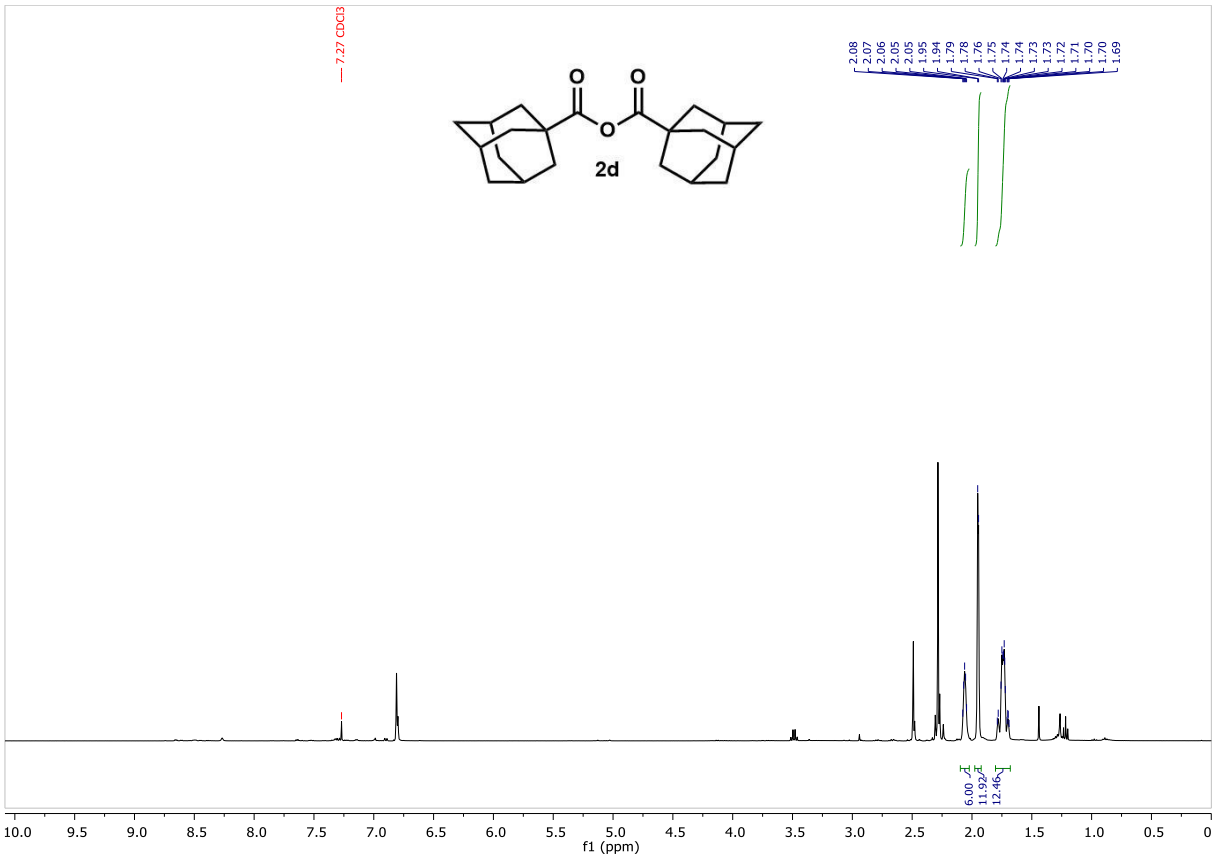
7.27 CDCl3
2d
2.08
2.07
2.06
2.05
2.05
1.95
1.94
1.79
1.78
1.76
1.75
1.74
1.74
1.73
1.73
1.72
1.71
1.70
1.70
1.69
6.00
11.92
12.46
f1 (ppm)

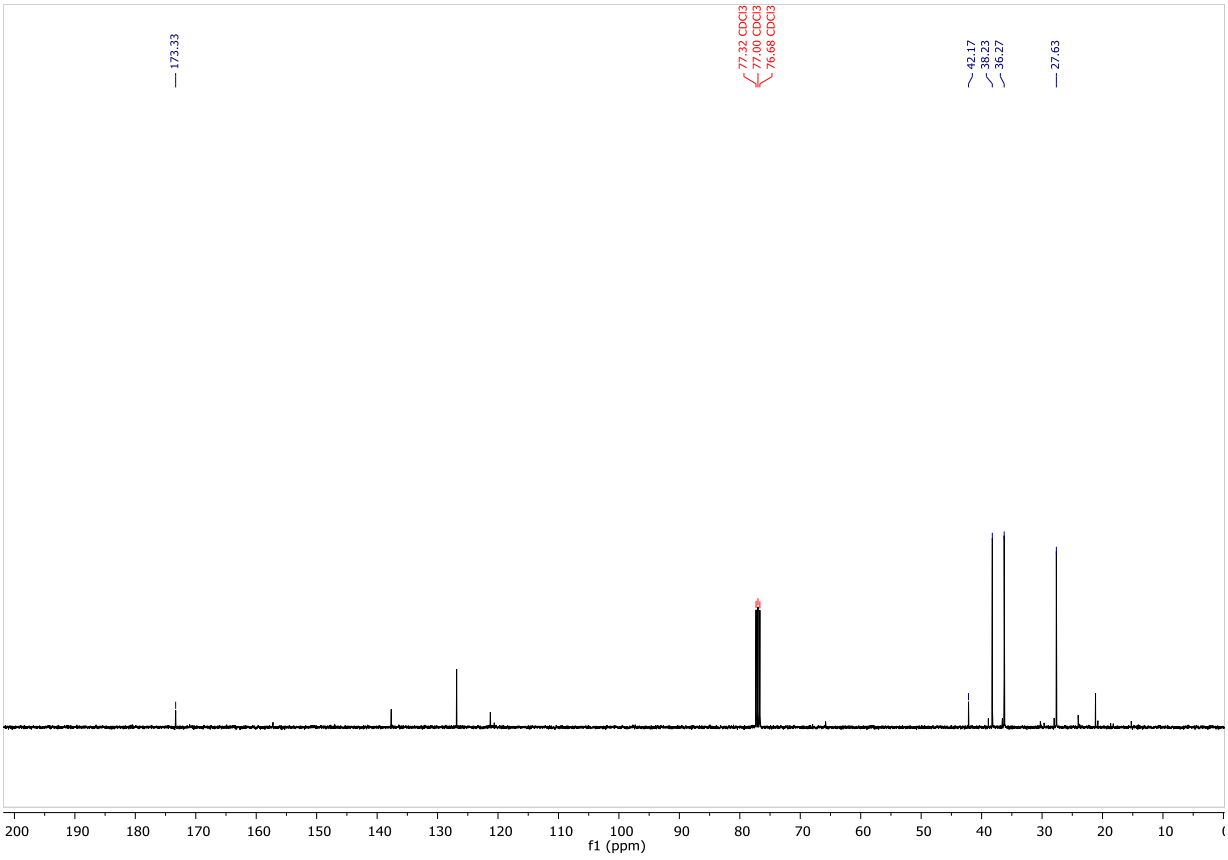
173.33
77.32 CDCl3
77.00 CDCl3
76.68 CDCl3
42.17
38.23
36.27
27.63
f1 (ppm)

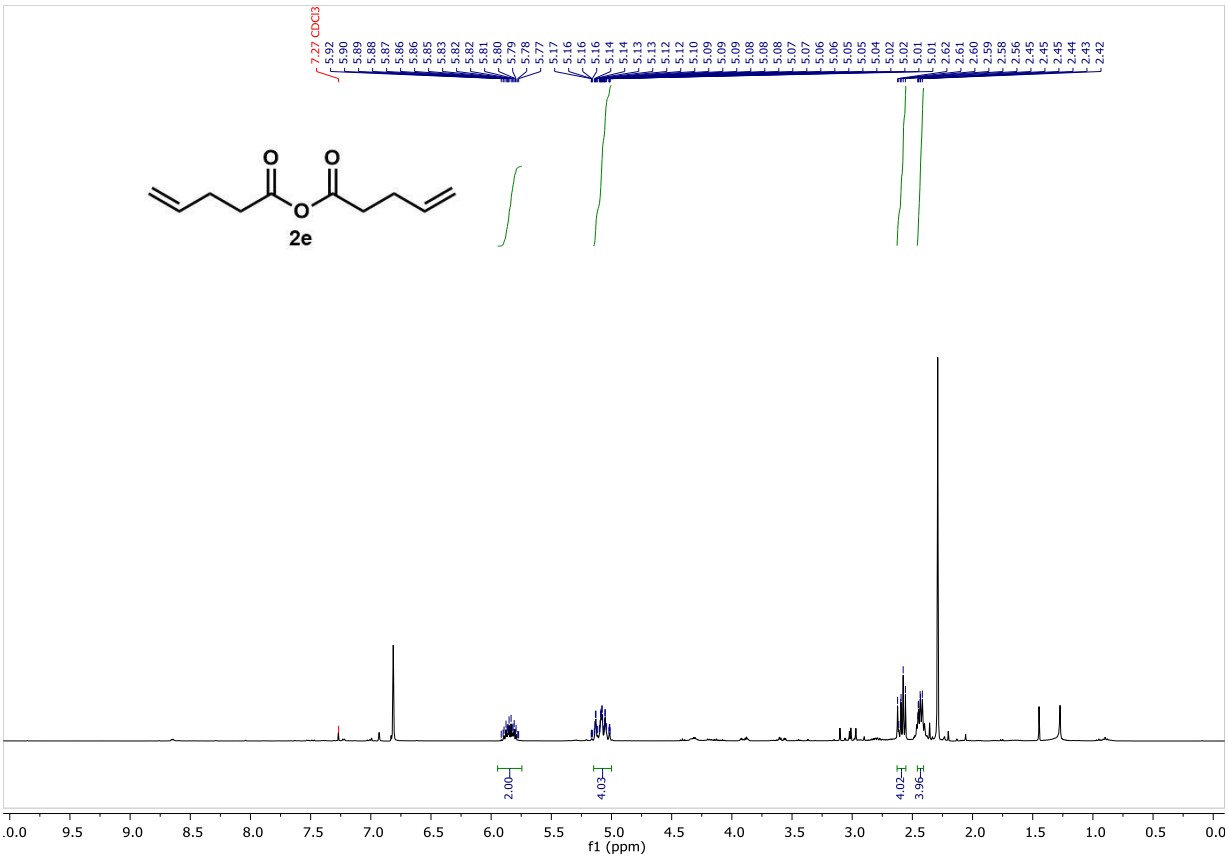
7.27 CDCl3
2e
2.00
4.03
4.02
3.96
f1 (ppm)

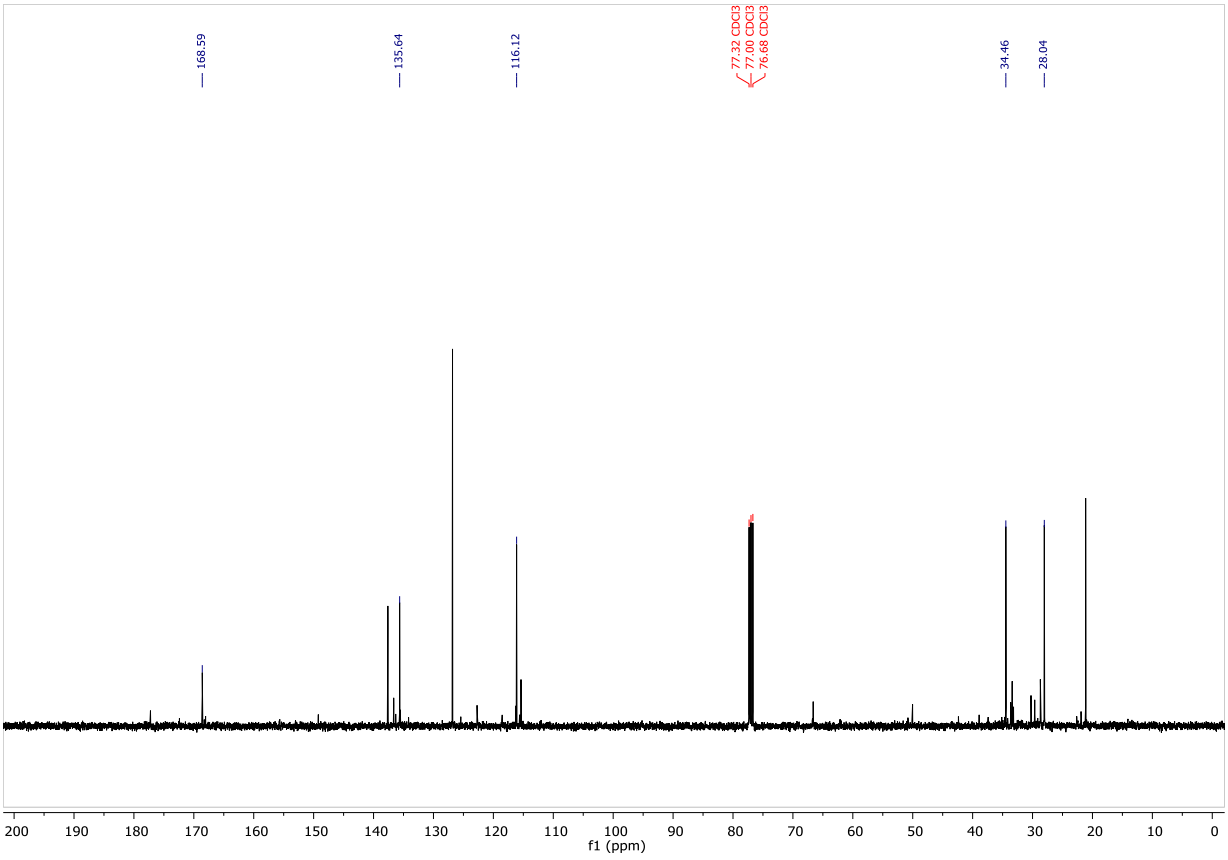
168.59
135.64
116.12
77.32 CDCl3
77.00 CDCl3
76.68 CDCl3
34.46
28.04
f1 (ppm)

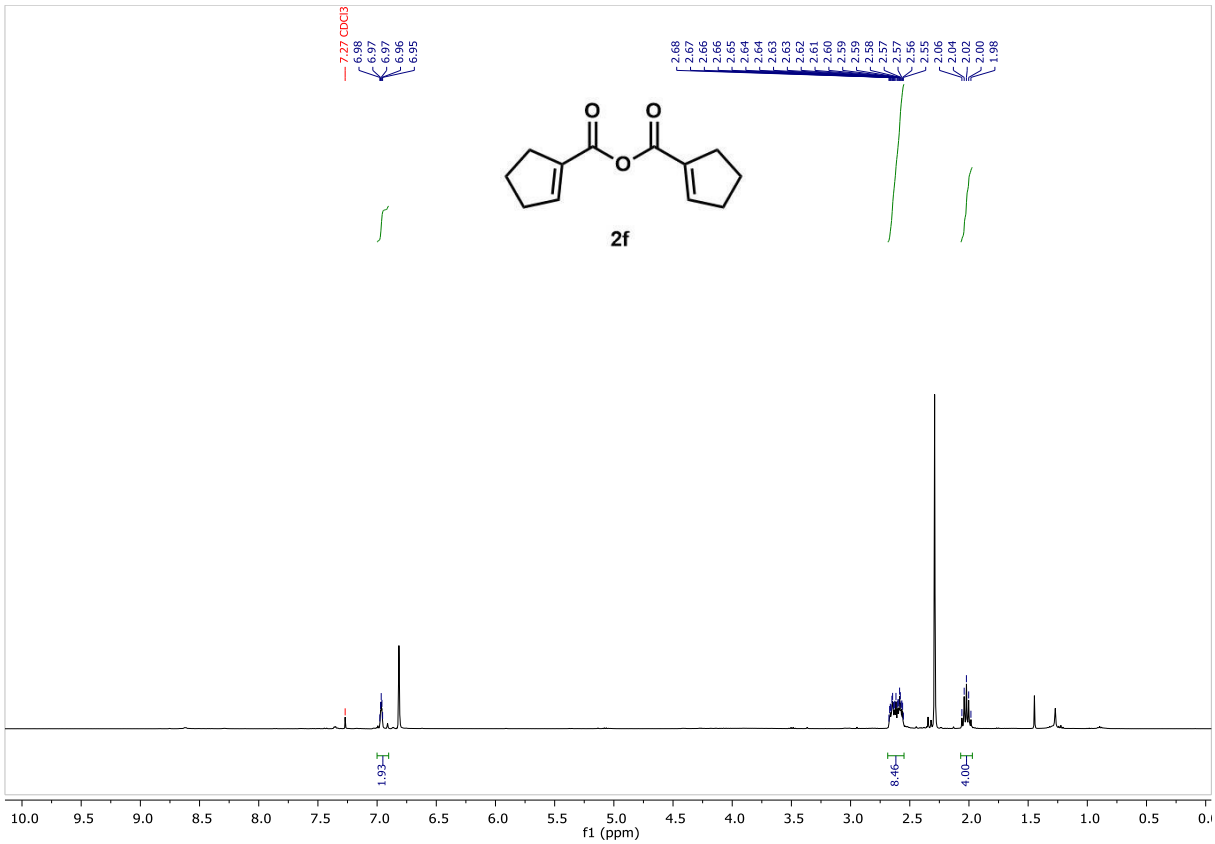
7.27 CDCl3
6.98
6.97
6.97
6.96
6.95
2.68
2.67
2.66
2.66
2.65
2.64
2.64
2.63
2.63
2.62
2.61
2.60
2.59
2.58
2.57
2.57
2.56
2.55
2.06
2.04
2.02
2.00
1.98
O
O
O
2f
1.93
8.46
4.00
10.0
9.5
9.0
8.5
8.0
7.5
7.0
6.5
6.0
5.5
5.0
4.5
4.0
3.5
3.0
2.5
2.0
1.5
1.0
0.5
f1 (ppm)

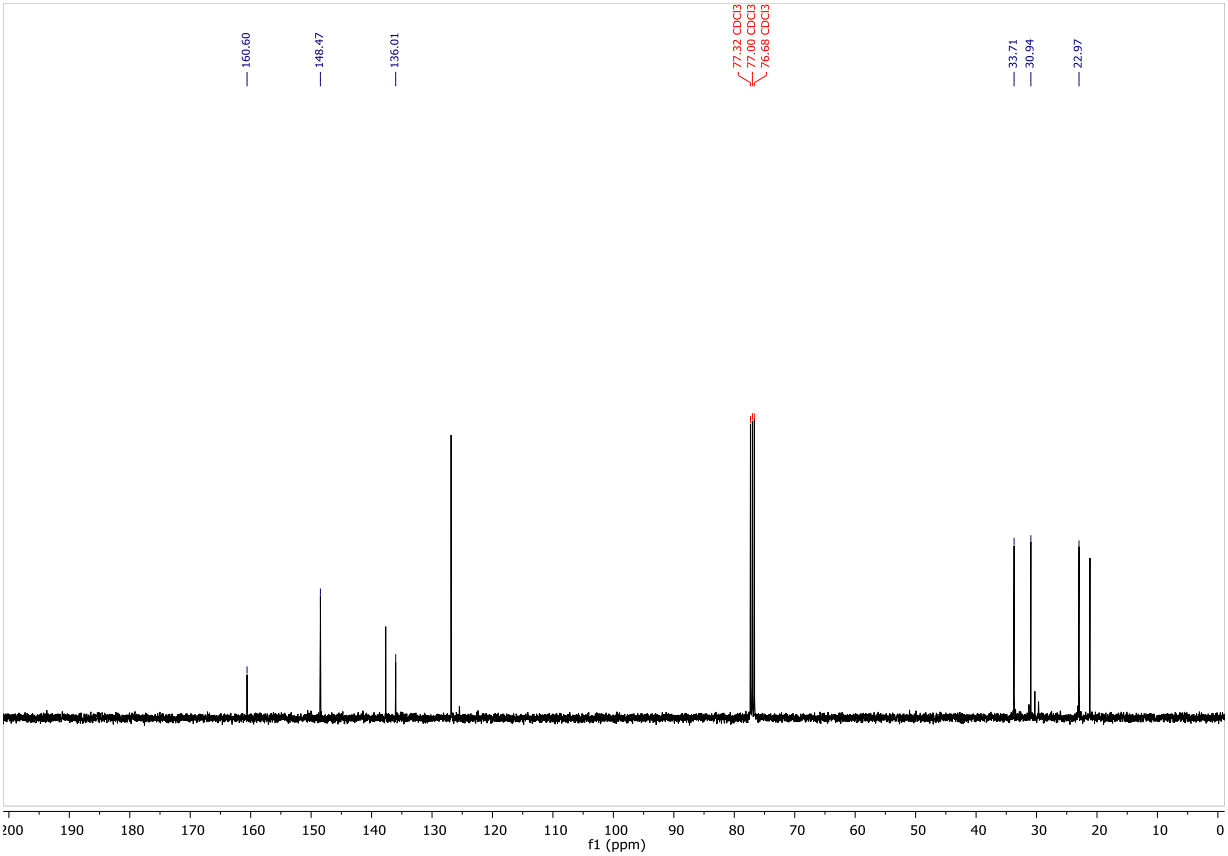
160.60
148.47
136.01
77.32 CDCl3
77.00 CDCl3
76.68 CDCl3
33.71
30.94
22.97
200
190
180
170
160
150
140
130
120
110
100
90
80
70
60
50
40
30
20
10
0
f1 (ppm)

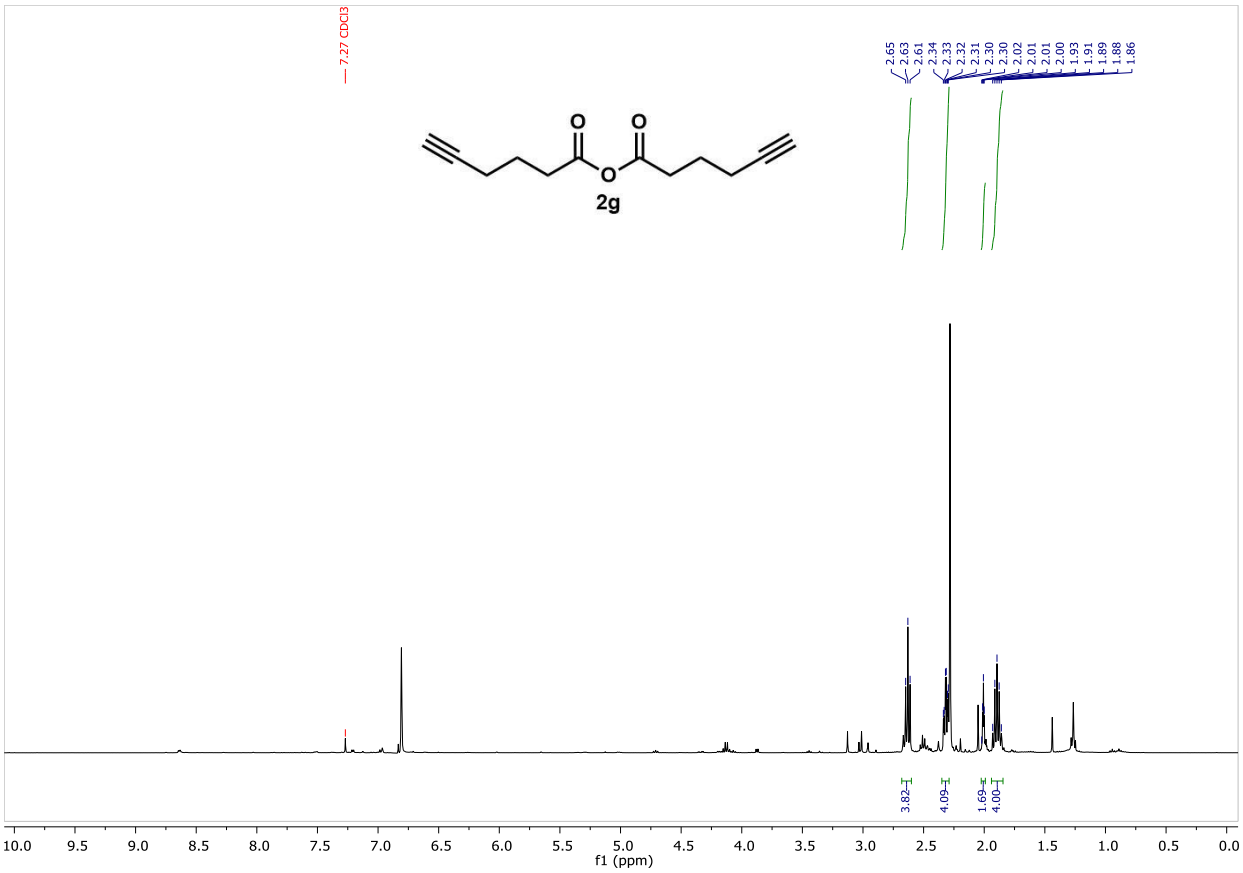
7.27 CDCl3
2.65
2.63
2.61
2.34
2.33
2.32
2.31
2.30
2.30
2.02
2.01
2.01
2.00
1.93
1.91
1.89
1.88
1.86
O
O
O
2g
3.82
4.09
1.69
4.00
10.0 9.5 9.0 8.5 8.0 7.5 7.0 6.5 6.0 5.5 5.0 4.5 4.0 3.5 3.0 2.5 2.0 1.5 1.0 0.5 0.0
f1 (ppm)

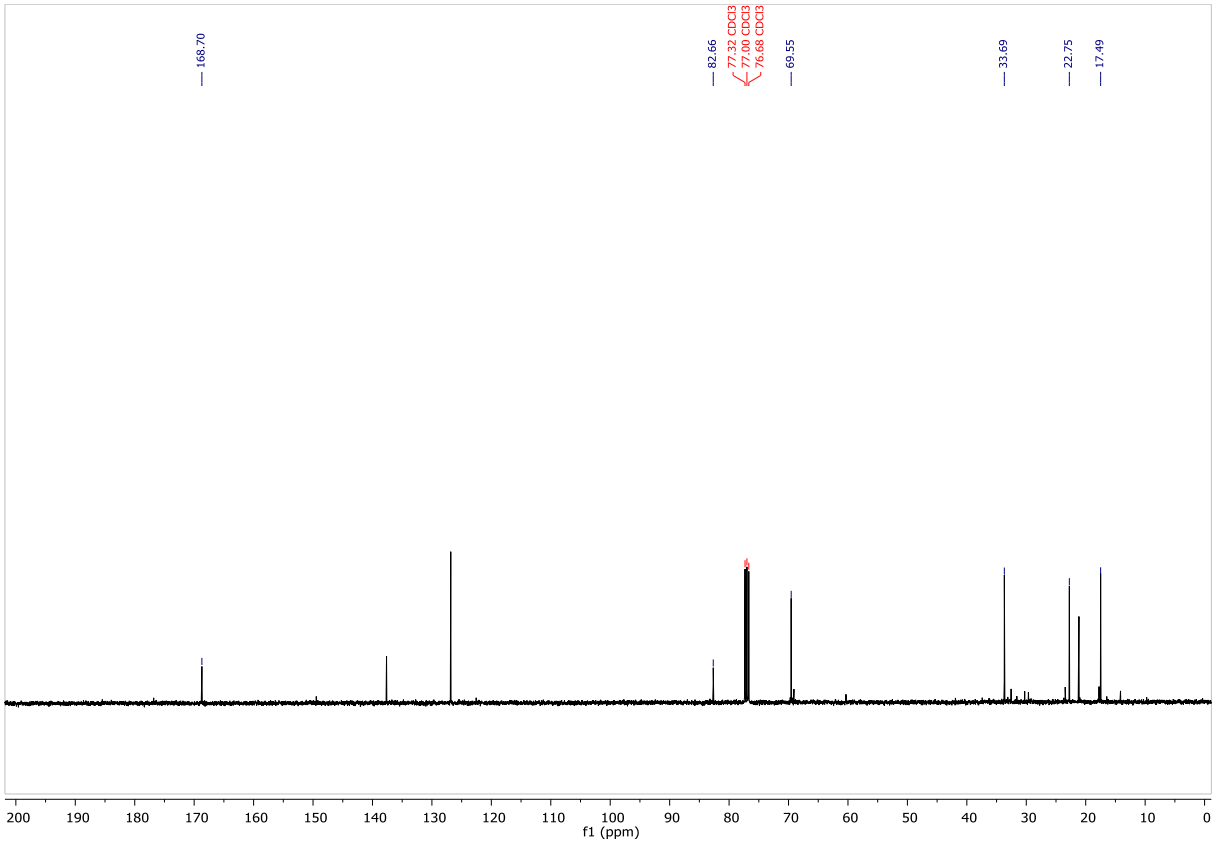
168.70
82.66
77.32 CDCl3
77.00 CDCl3
76.68 CDCl3
69.55
33.69
22.75
17.49
200 190 180 170 160 150 140 130 120 110 100 90 80 70 60 50 40 30 20 10 0
f1 (ppm)

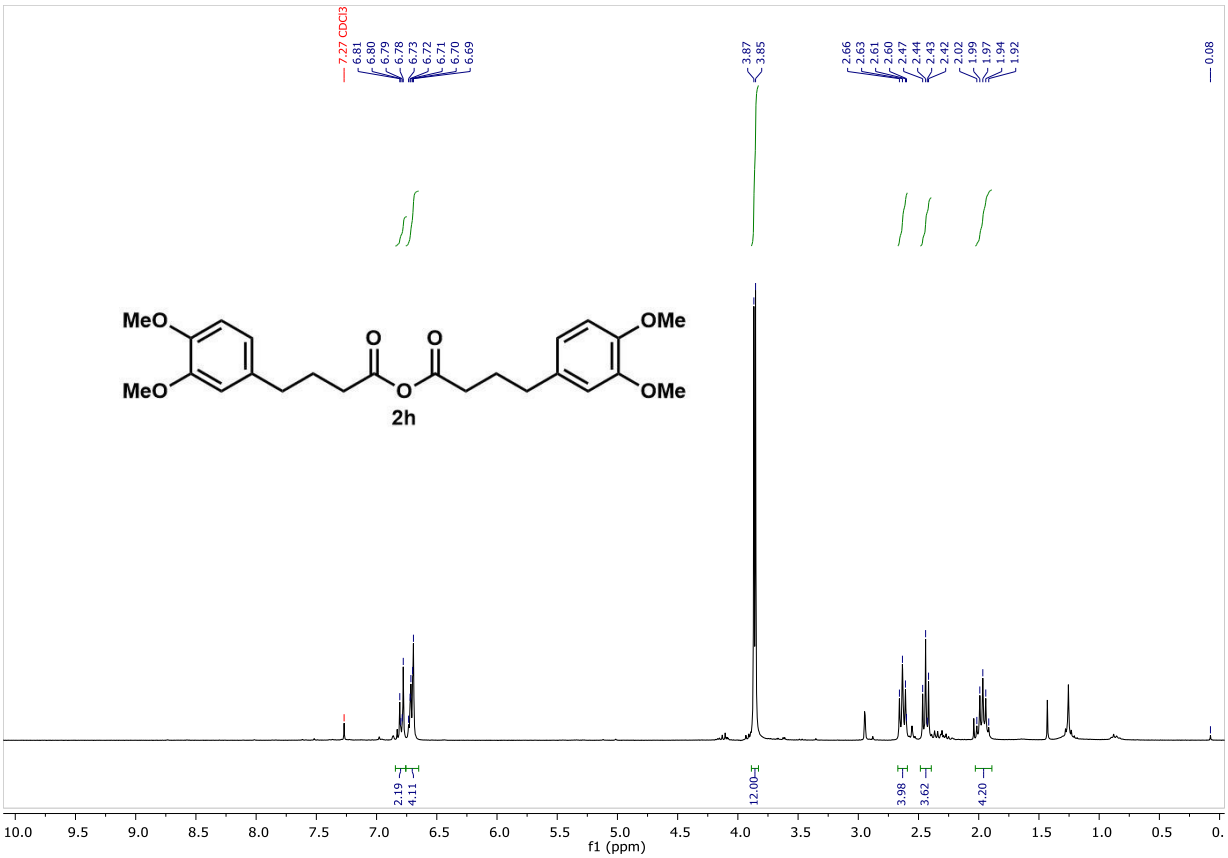
7.27 CDCl3
6.81
6.80
6.79
6.78
6.73
6.72
6.71
6.70
6.69
3.87
3.85
2.66
2.63
2.61
2.60
2.47
2.44
2.43
2.42
2.02
1.99
1.97
1.94
1.92
0.08
MeO
MeO
OMe
OMe
O
O
O
2h
2.19
4.11
12.00
3.98
3.62
4.20
f1 (ppm)

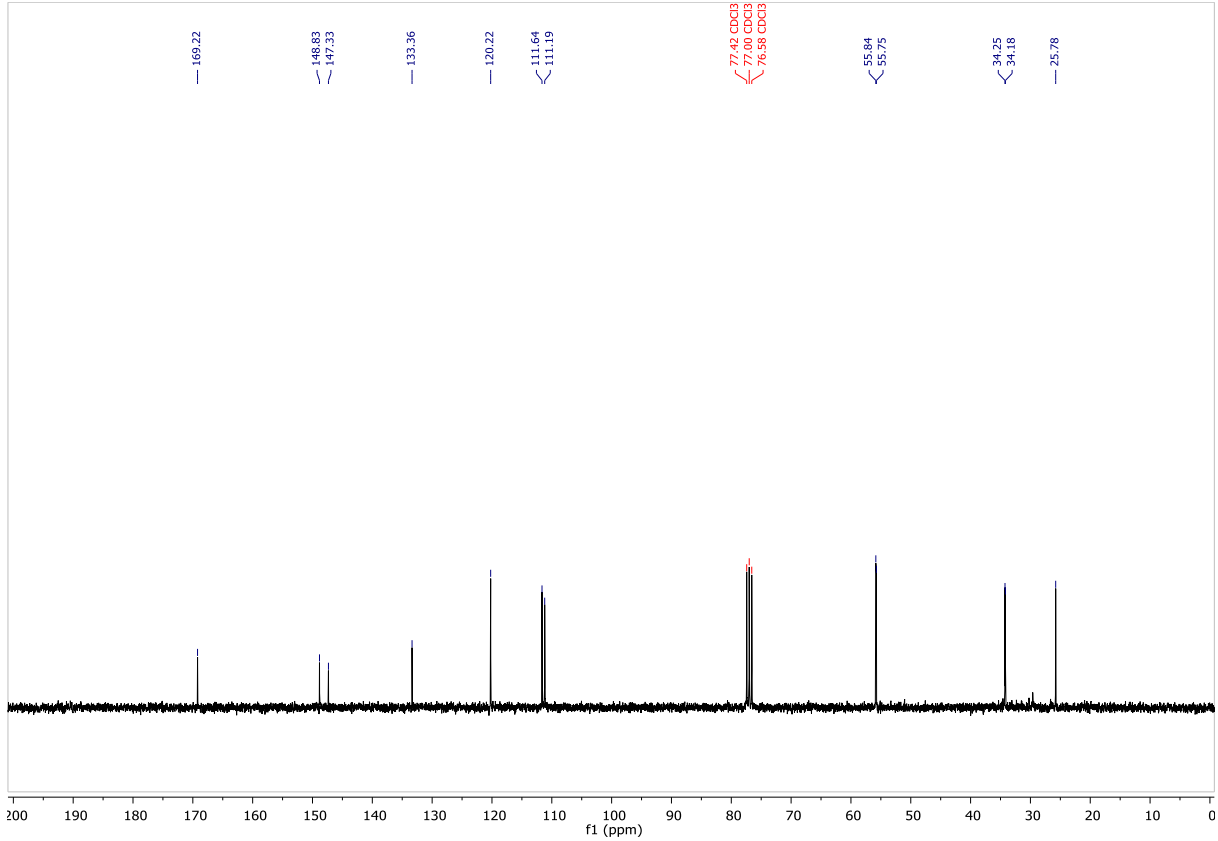
169.22
148.83
147.33
133.36
120.22
111.64
111.19
77.42 CDCl3
77.00 CDCl3
76.58 CDCl3
55.84
55.75
34.25
34.18
25.78
f1 (ppm)

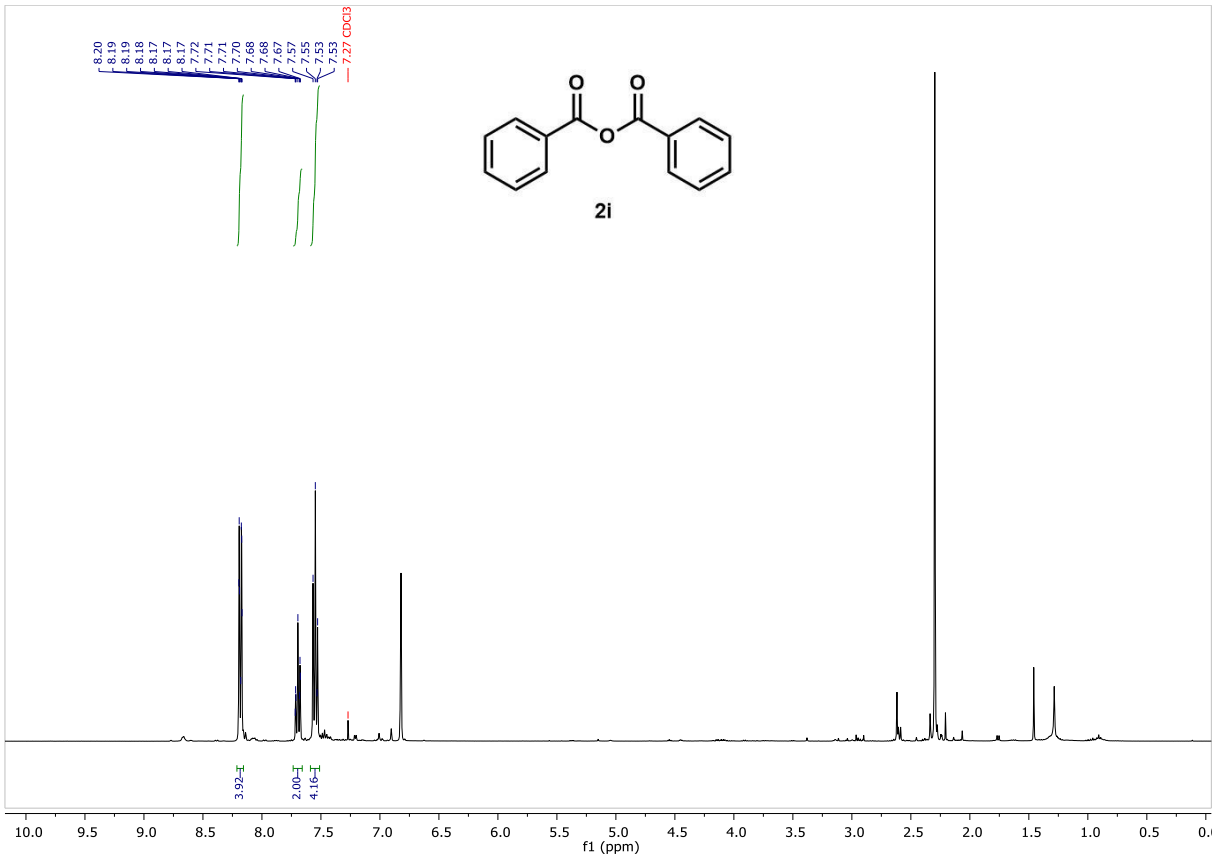
8.20
8.19
8.19
8.18
8.17
8.17
8.17
7.72
7.71
7.71
7.70
7.68
7.68
7.67
7.57
7.55
7.53
7.53
7.27 CDCl3
O
O
O
2i
3.92
2.00
4.16
f1 (ppm)

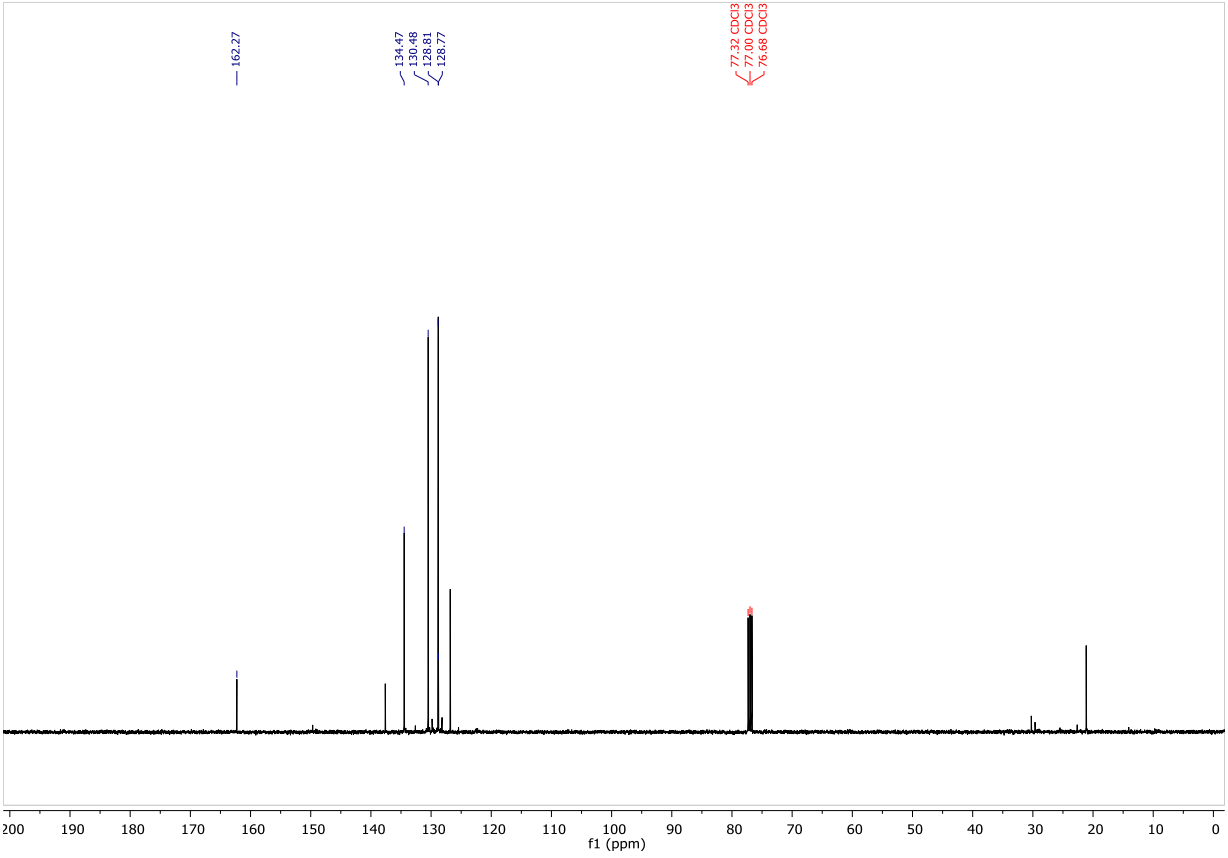
162.27
134.47
130.48
128.81
128.77
77.32 CDCl3
77.00 CDCl3
76.68 CDCl3
f1 (ppm)

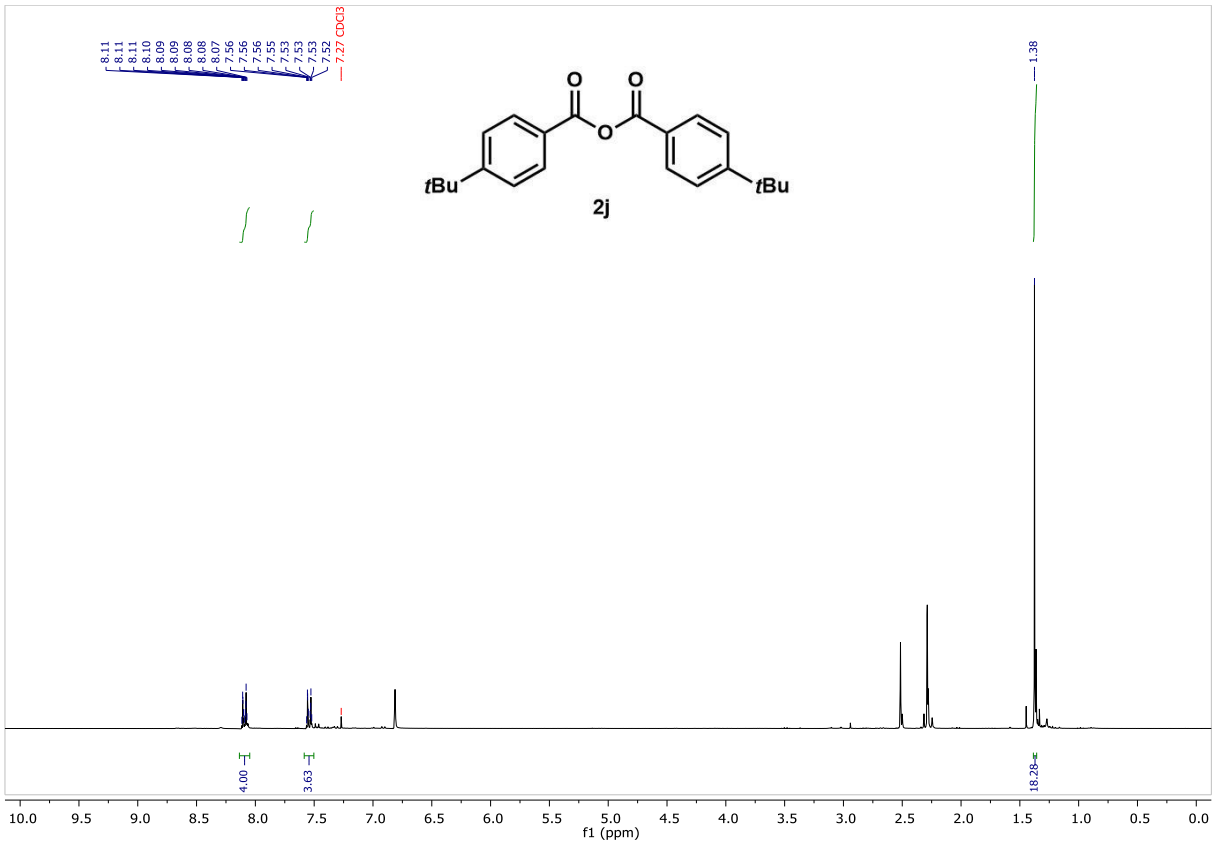
8.11
8.11
8.11
8.10
8.09
8.09
8.08
8.08
8.07
7.56
7.56
7.56
7.55
7.53
7.53
7.53
7.52
7.27 CDCl3
1.38
tBu
tBu
2j
4.00
3.63
18.28
10.0
9.5
9.0
8.5
8.0
7.5
7.0
6.5
6.0
5.5
5.0
4.5
4.0
3.5
3.0
2.5
2.0
1.5
1.0
0.5
0.0
f1 (ppm)

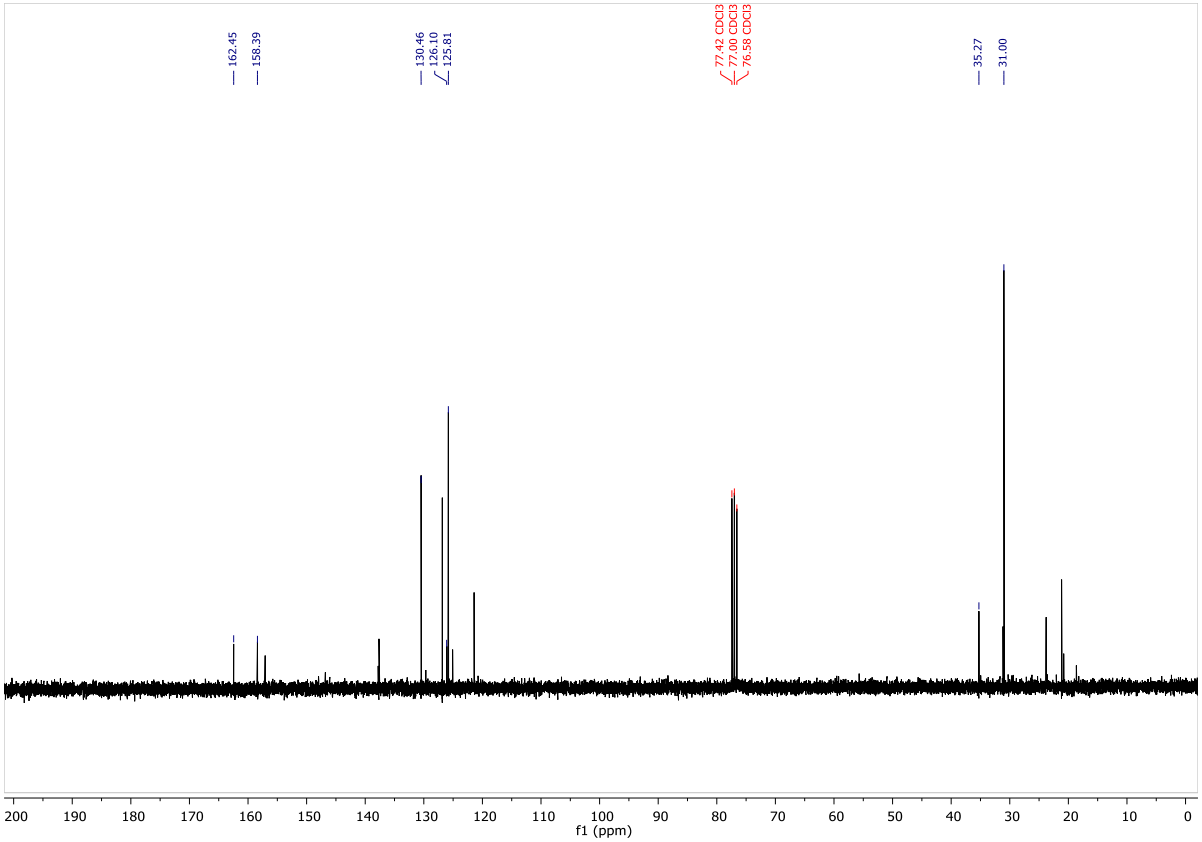
162.45
158.39
130.46
126.10
125.81
77.42 CDCl3
77.00 CDCl3
76.58 CDCl3
35.27
31.00
200
190
180
170
160
150
140
130
120
110
100
90
80
70
60
50
40
30
20
10
0
f1 (ppm)

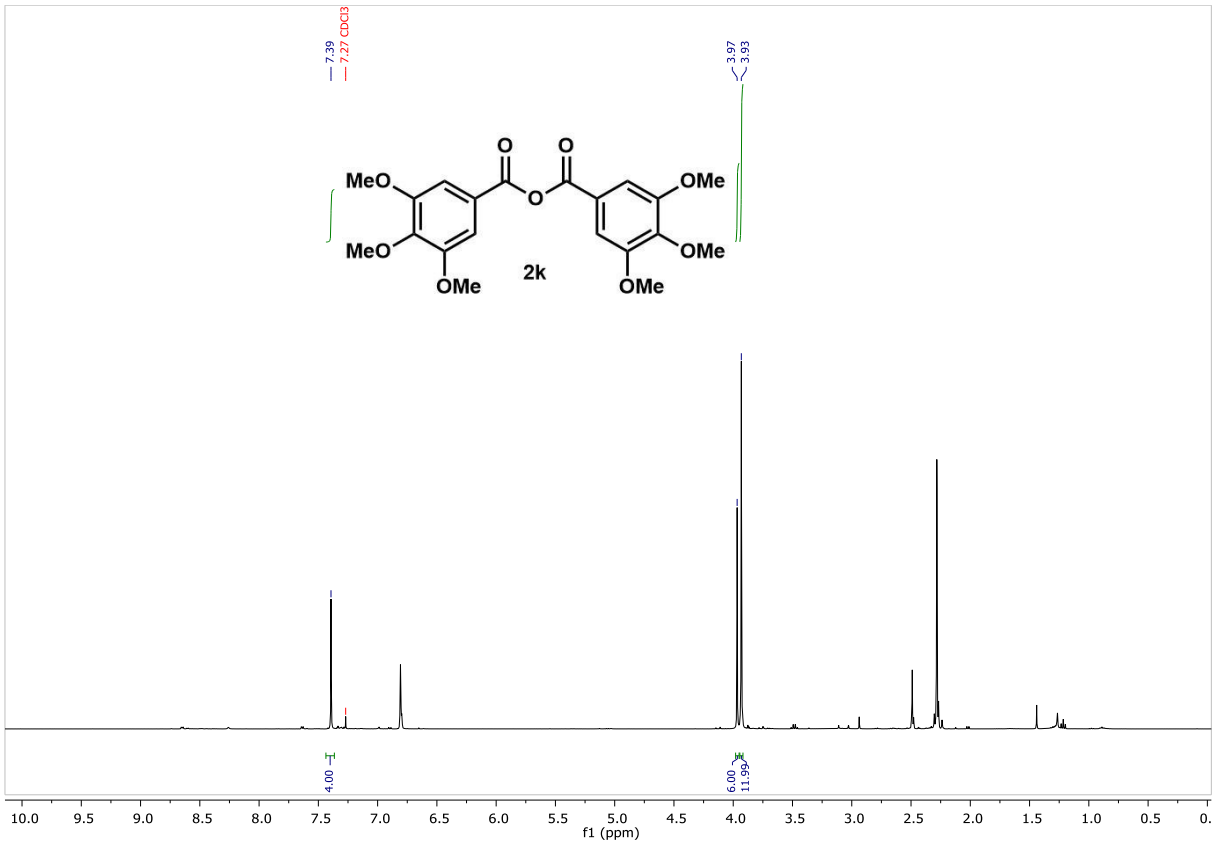
7.39
7.27 CDCl3
3.97
3.93
MeO
MeO
OMe
OMe
OMe
OMe
2k
4.00
6.00
11.99
f1 (ppm)

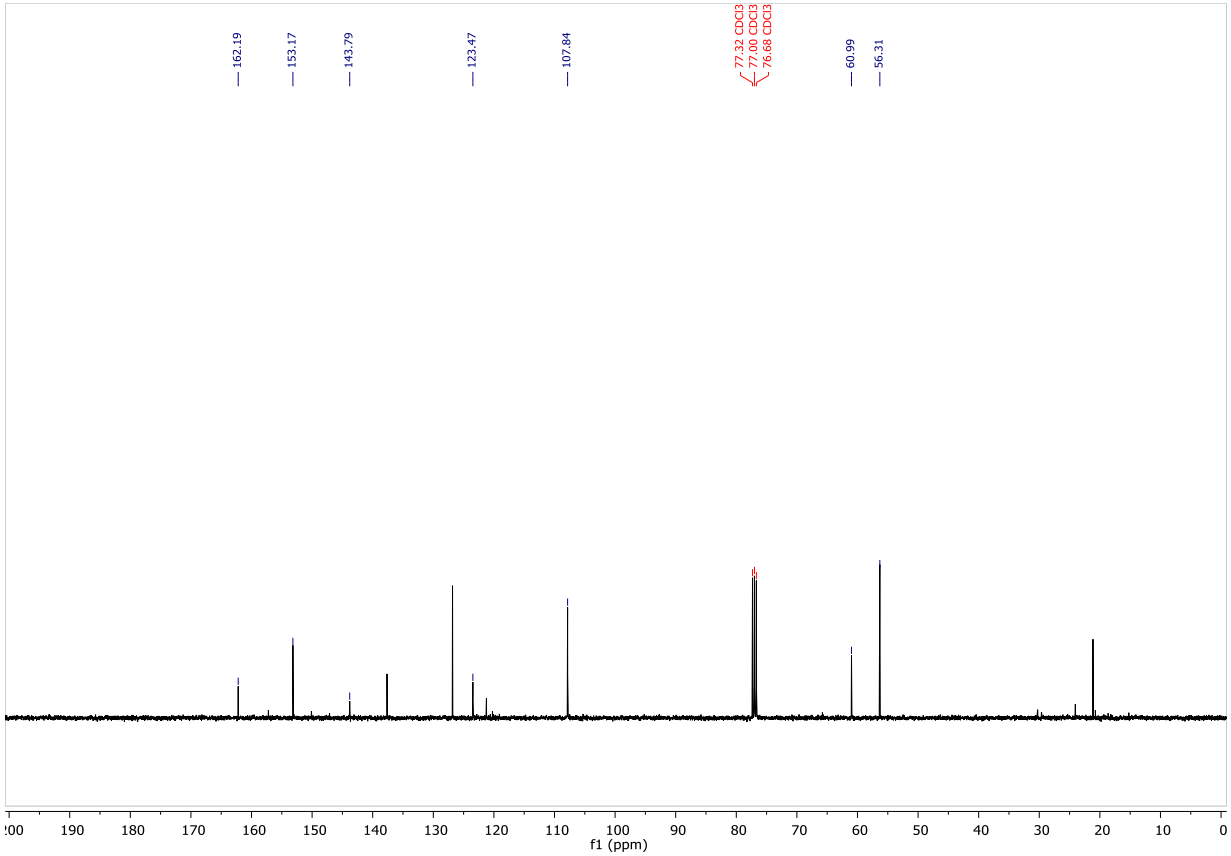
162.19
153.17
143.79
123.47
107.84
77.32 CDCl3
77.00 CDCl3
76.68 CDCl3
60.99
56.31
f1 (ppm)

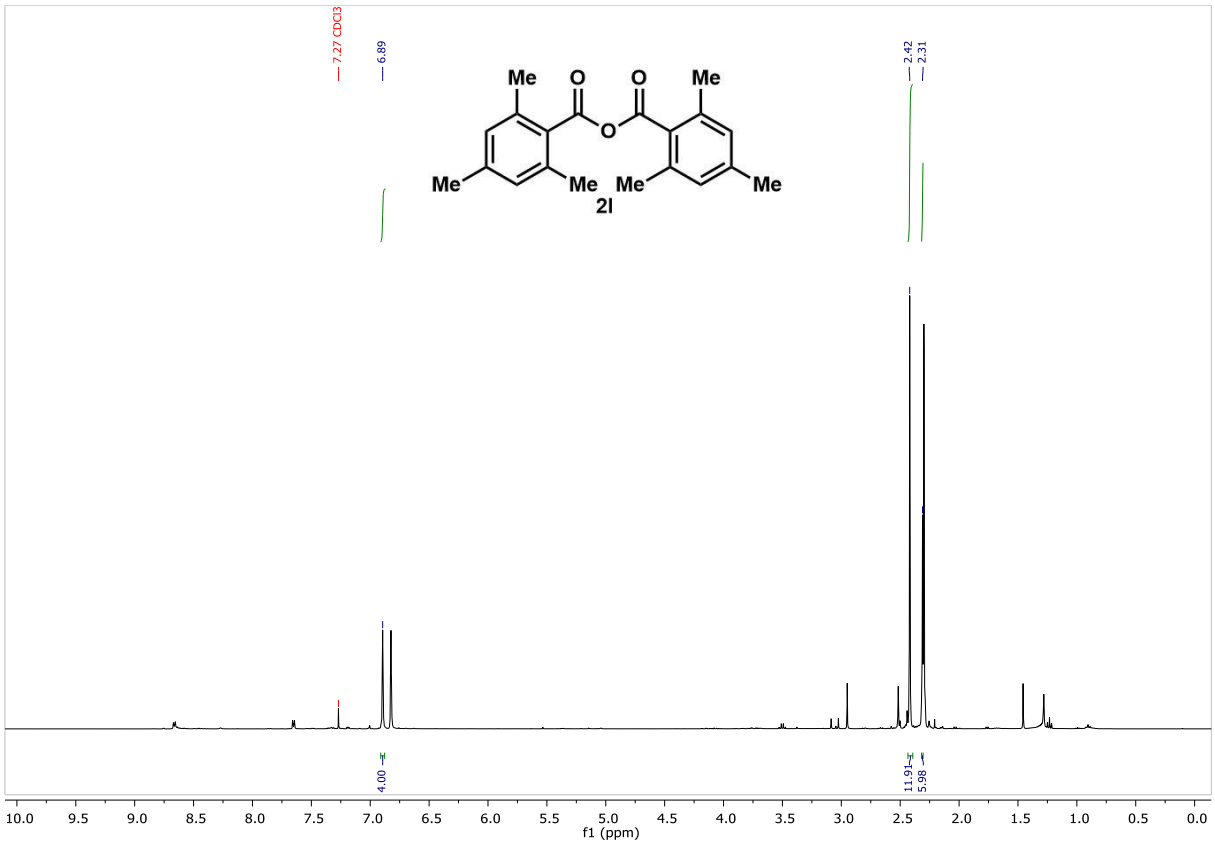
7.27 CDCl3
6.89
2.42
2.31
Me
O
O
Me
Me
Me
Me
Me
2l
4.00
11.91
5.98
10.0 9.5 9.0 8.5 8.0 7.5 7.0 6.5 6.0 5.5 5.0 4.5 4.0 3.5 3.0 2.5 2.0 1.5 1.0 0.5 0.0
f1 (ppm)

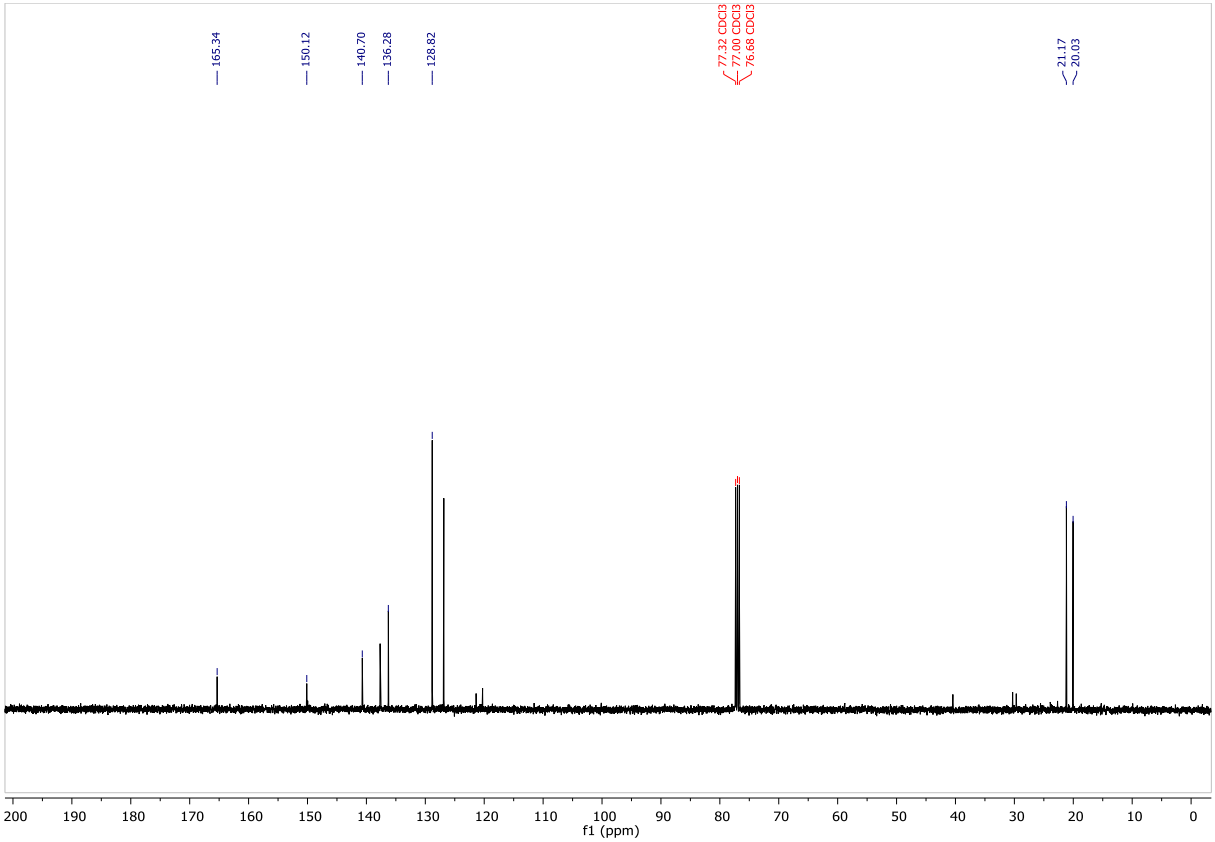
165.34
150.12
140.70
136.28
128.82
77.32 CDCl3
77.00 CDCl3
76.68 CDCl3
21.17
20.03
200 190 180 170 160 150 140 130 120 110 100 90 80 70 60 50 40 30 20 10 0
f1 (ppm)

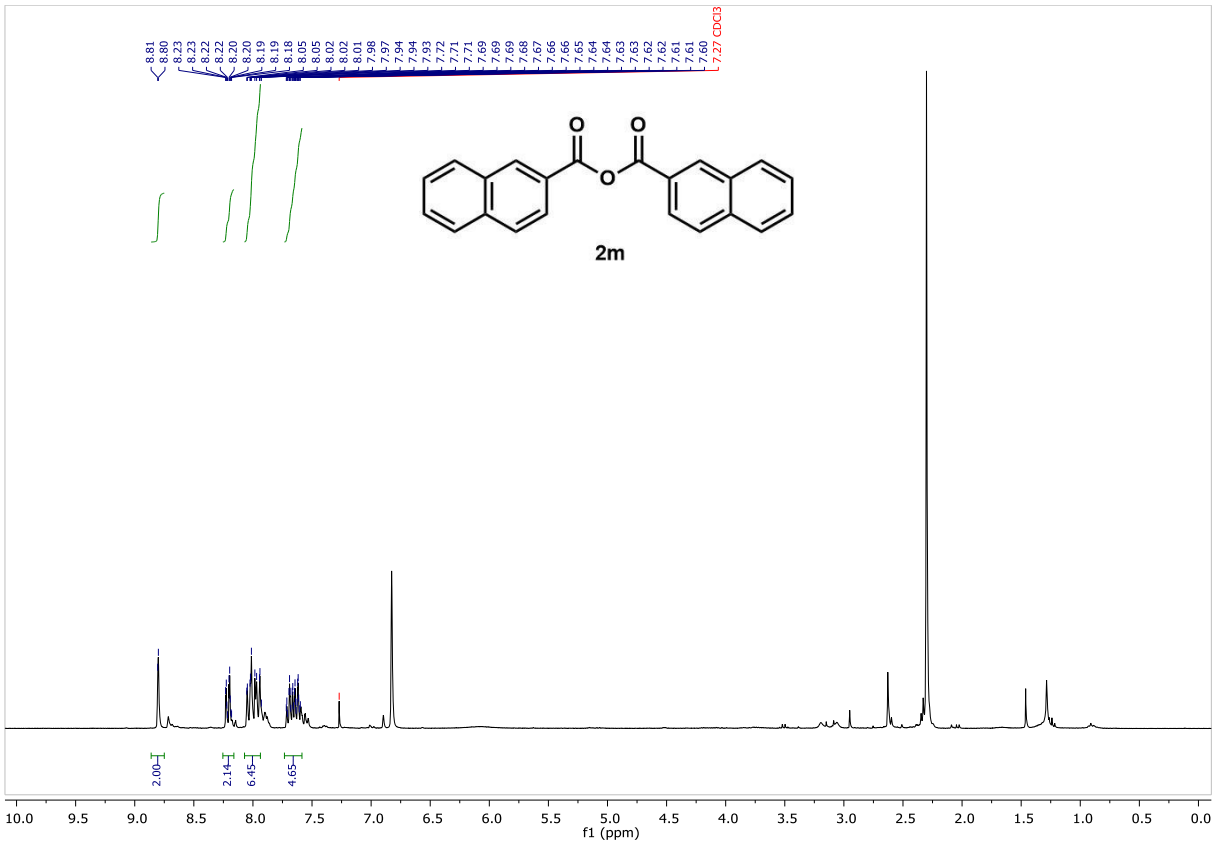
8.81
8.80
8.23
8.23
8.22
8.22
8.20
8.20
8.19
8.19
8.18
8.05
8.05
8.02
8.02
8.01
7.98
7.97
7.94
7.94
7.93
7.72
7.71
7.71
7.69
7.69
7.69
7.68
7.67
7.66
7.66
7.65
7.64
7.64
7.63
7.63
7.62
7.62
7.61
7.61
7.60
7.27 CDCl3
O
O
O
2m
2.00
2.14
6.45
4.65
10.0
9.5
9.0
8.5
8.0
7.5
7.0
6.5
6.0
5.5
5.0
4.5
4.0
3.5
3.0
2.5
2.0
1.5
1.0
0.5
0.0
f1 (ppm)

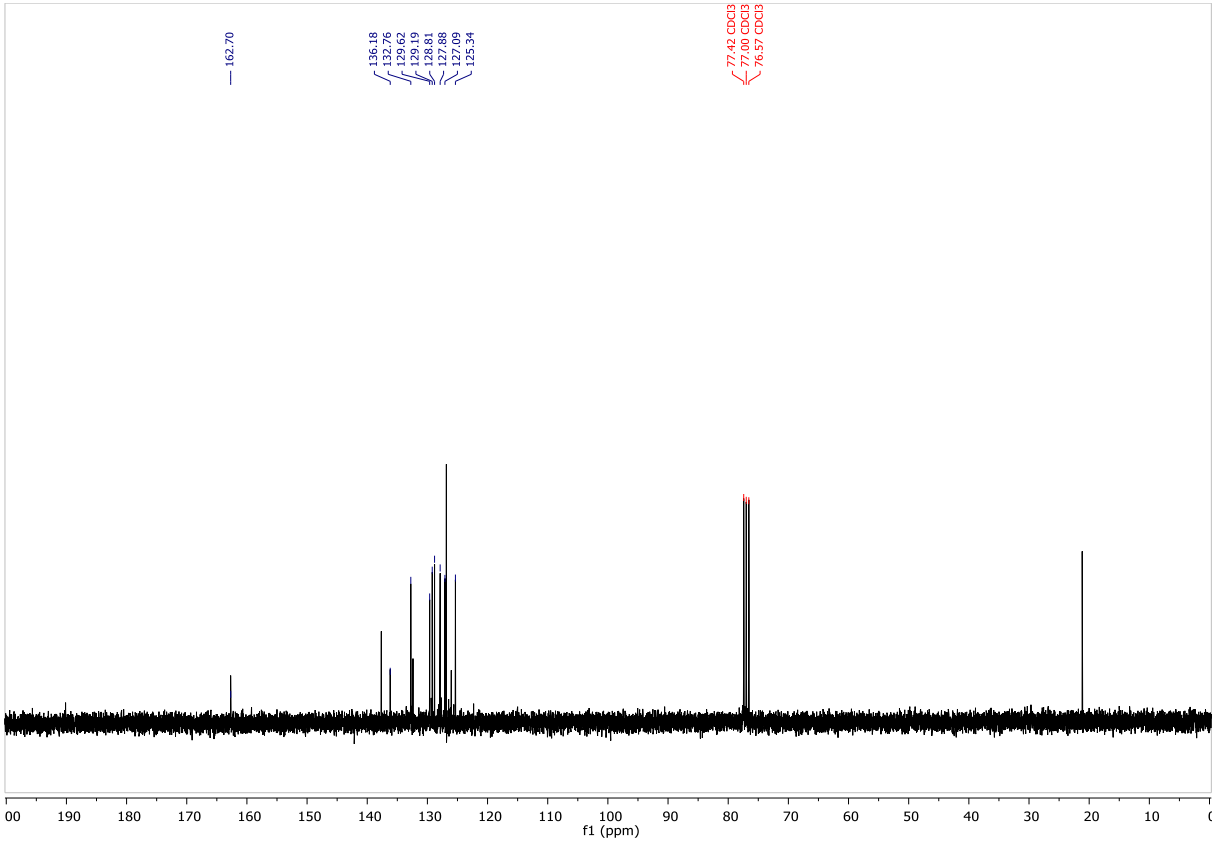
162.70
136.18
132.76
129.62
129.19
128.81
127.88
127.09
125.34
77.42 CDCl3
77.00 CDCl3
76.57 CDCl3
190
180
170
160
150
140
130
120
110
100
90
80
70
60
50
40
30
20
10
f1 (ppm)

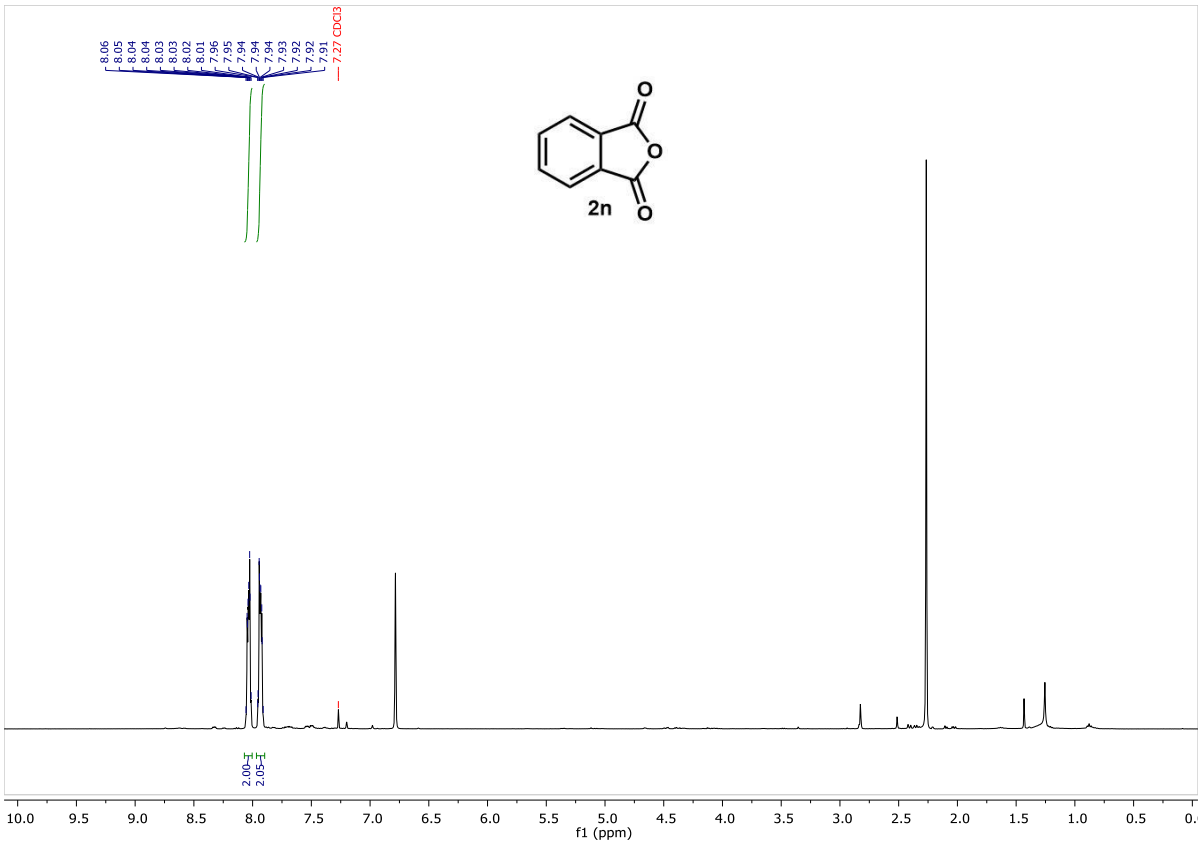
8.06
8.05
8.04
8.04
8.04
8.03
8.03
8.02
8.01
7.96
7.95
7.94
7.94
7.93
7.92
7.92
7.91
7.27 CDCl3
2n
O
O
O
2.00
2.05
10.0
9.5
9.0
8.5
8.0
7.5
7.0
6.5
6.0
5.5
5.0
4.5
4.0
3.5
3.0
2.5
2.0
1.5
1.0
0.5
f1 (ppm)

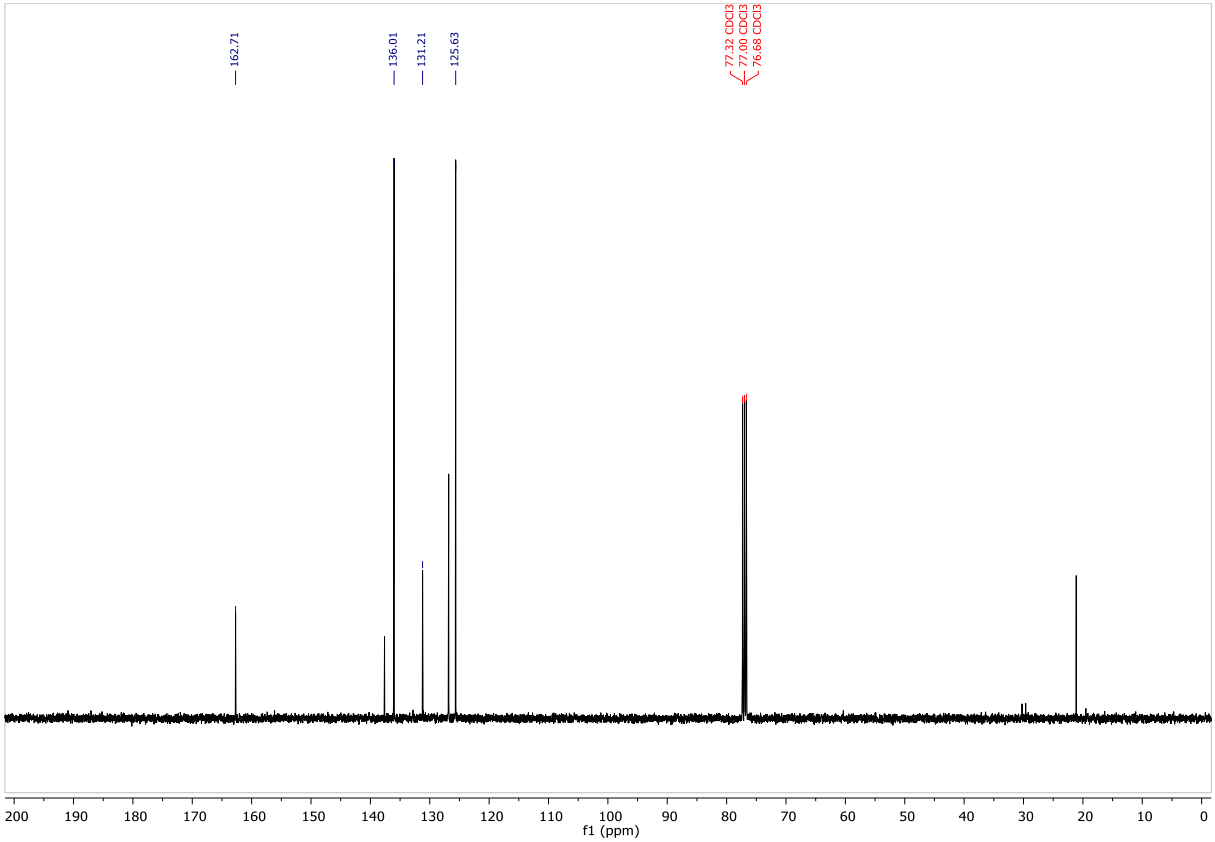
162.71
136.01
131.21
125.63
77.32 CDCl3
77.00 CDCl3
76.68 CDCl3
200
190
180
170
160
150
140
130
120
110
100
90
80
70
60
50
40
30
20
10
0
f1 (ppm)

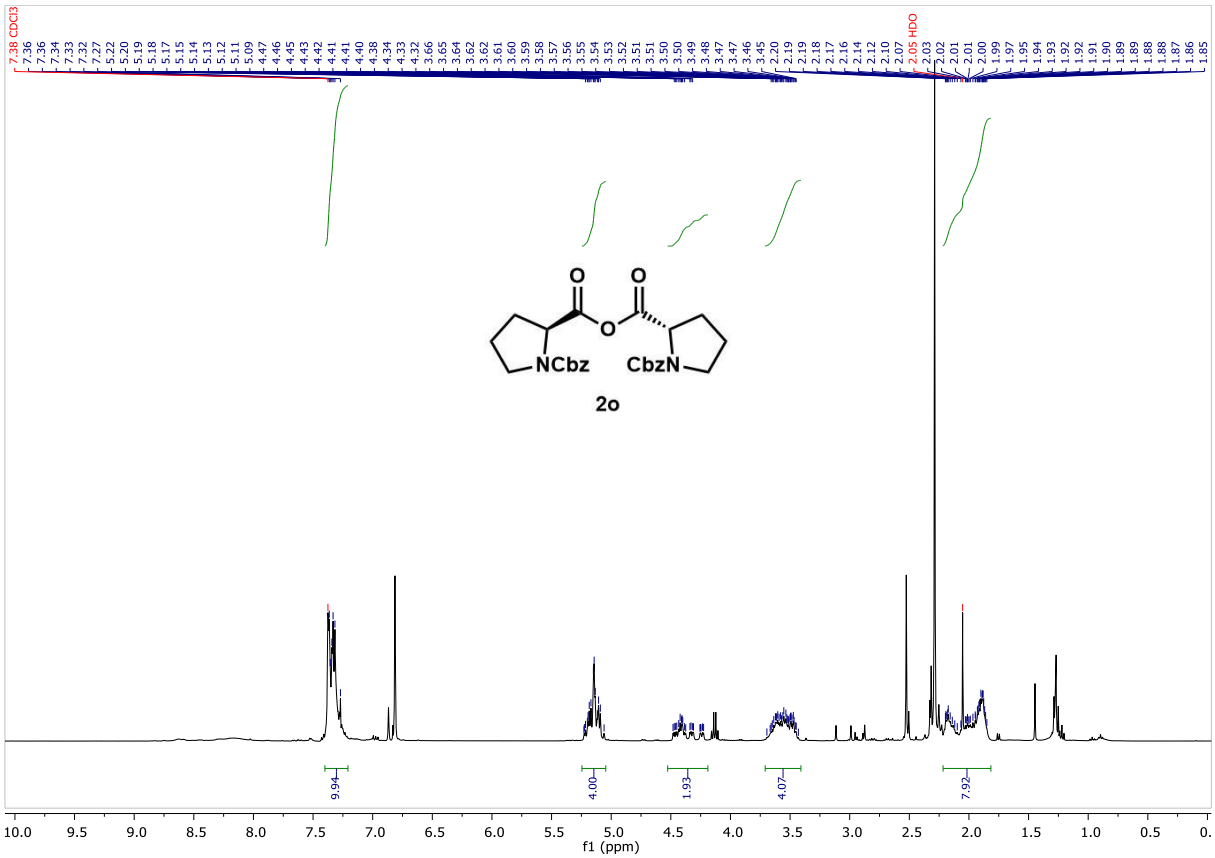
7.38 CDCl3
2.05 HDO
O
O
O
NCbz
CbzN
2o
9.94
4.00
1.93
4.07
7.92
f1 (ppm)

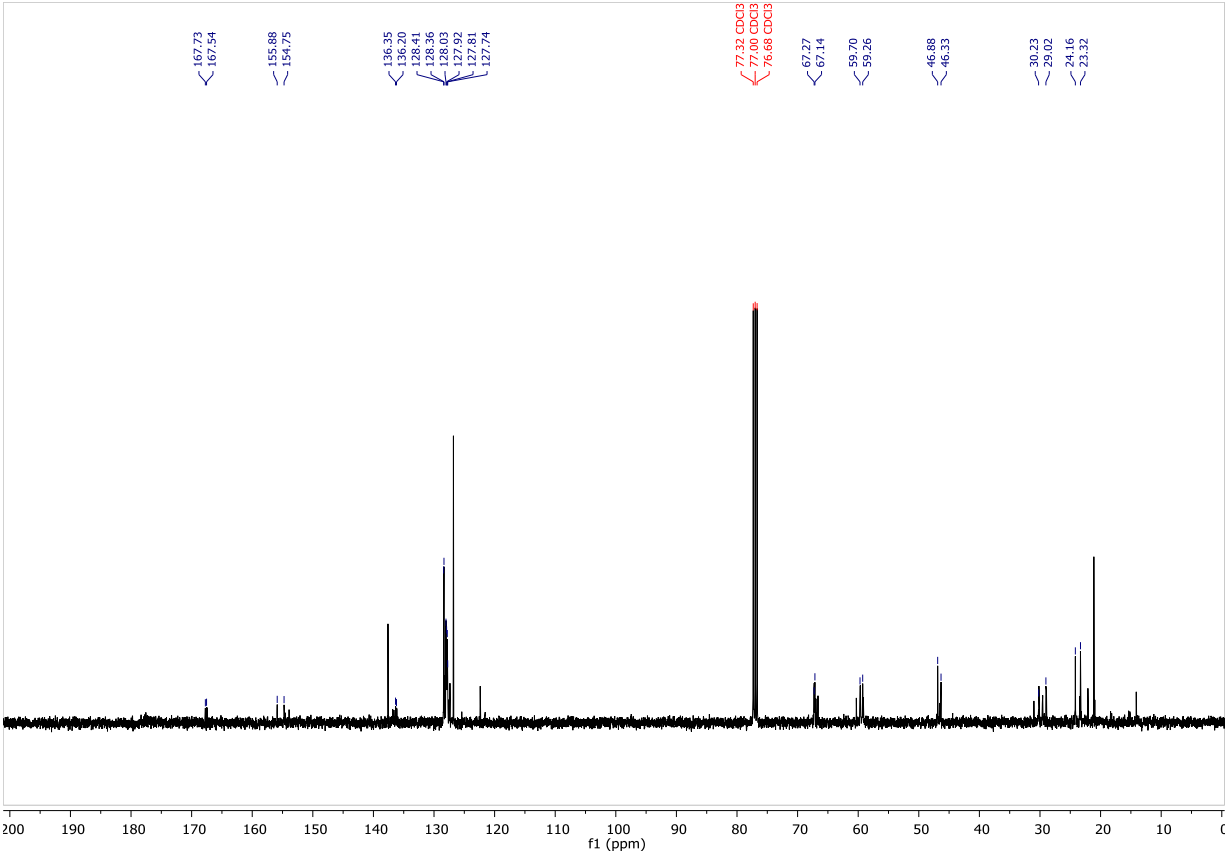
167.73
167.54
155.88
154.75
136.35
136.20
128.41
128.36
128.03
127.92
127.81
127.74
77.32 CDCl3
77.00 CDCl3
76.68 CDCl3
67.27
67.14
59.70
59.26
46.88
46.33
30.23
29.02
24.16
23.32
f1 (ppm)

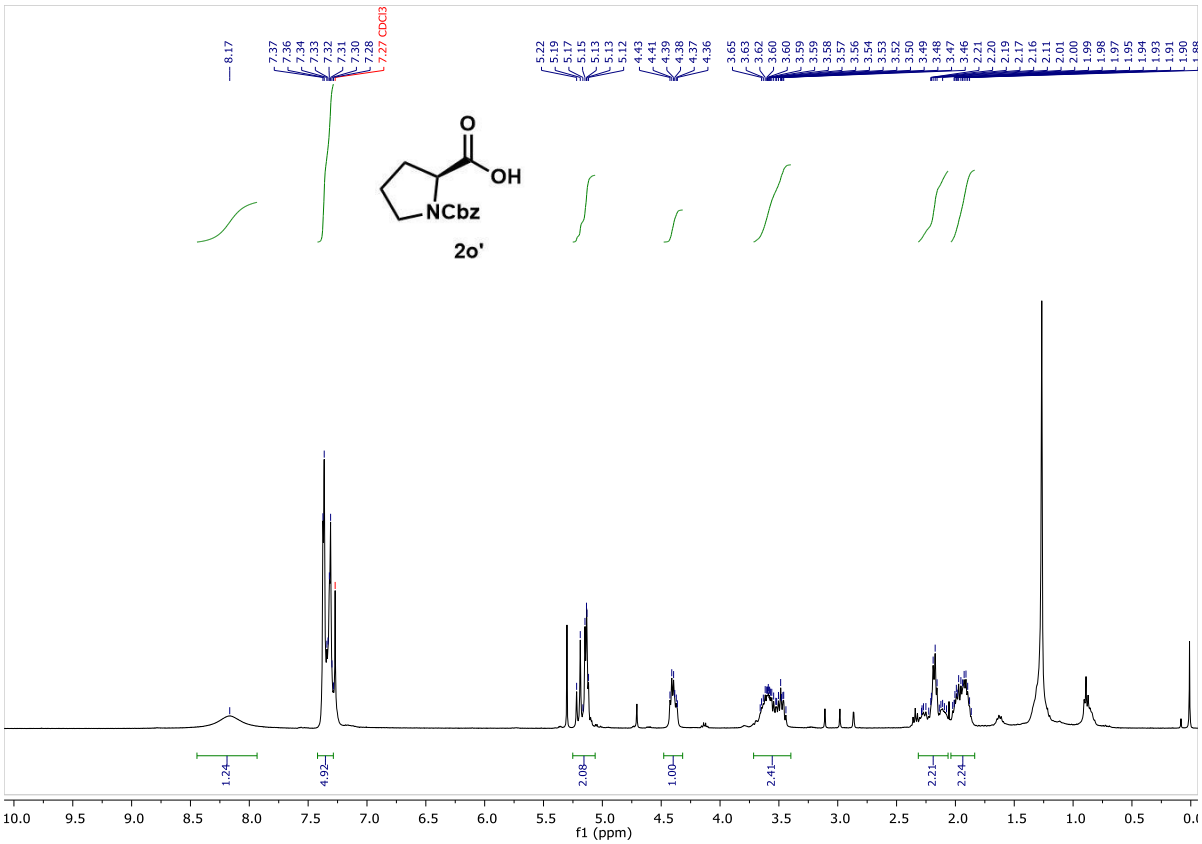
8.17
7.37
7.36
7.34
7.33
7.32
7.31
7.30
7.28
7.27 CDCl3
5.22
5.19
5.17
5.15
5.13
5.12
4.43
4.41
4.39
4.38
4.37
4.36
3.65
3.63
3.62
3.60
3.59
3.58
3.57
3.56
3.54
3.53
3.52
3.50
3.49
3.48
3.47
3.46
2.21
2.20
2.19
2.17
2.16
2.11
2.01
2.00
1.99
1.98
1.97
1.95
1.94
1.93
1.91
1.90
O
OH
NCbz
2o'
1.24
4.92
2.08
1.00
2.41
2.21
2.24
f1 (ppm)

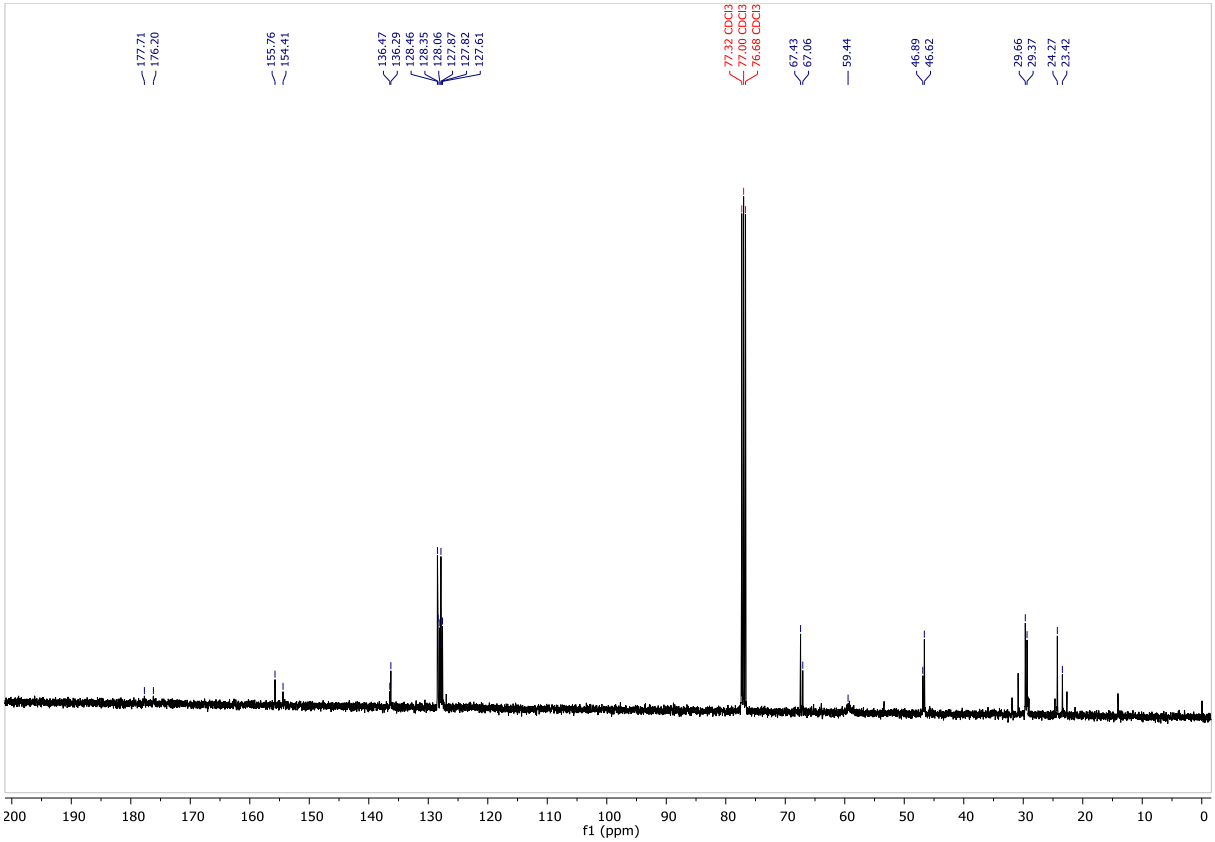
177.71
176.20
155.76
154.41
136.47
136.29
128.46
128.35
128.06
127.87
127.82
127.61
77.32 CDCl3
77.00 CDCl3
76.68 CDCl3
67.43
67.06
59.44
46.89
46.62
29.66
29.37
24.27
23.42
f1 (ppm)

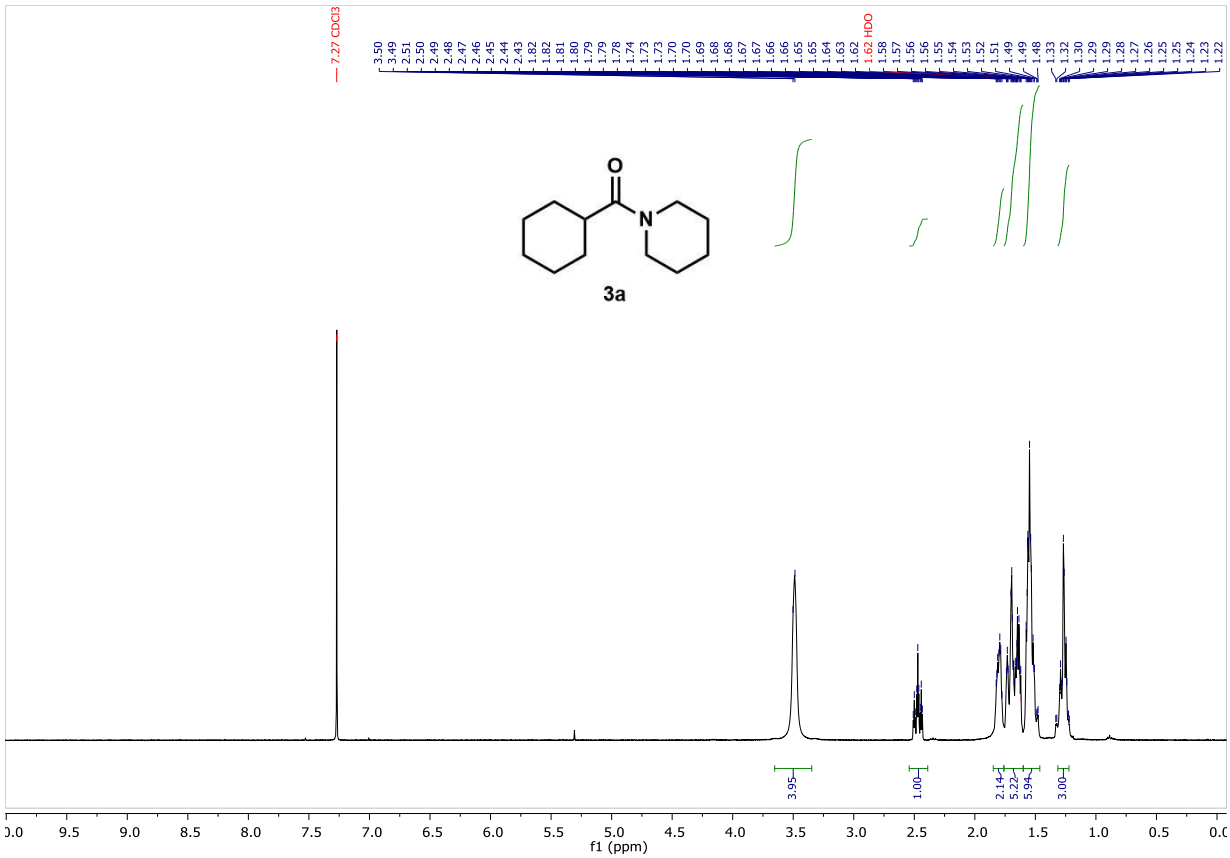
7.27 CDCl3
1.62 HDO
3a
3.95
1.00
2.14
5.22
5.94
3.00
f1 (ppm)

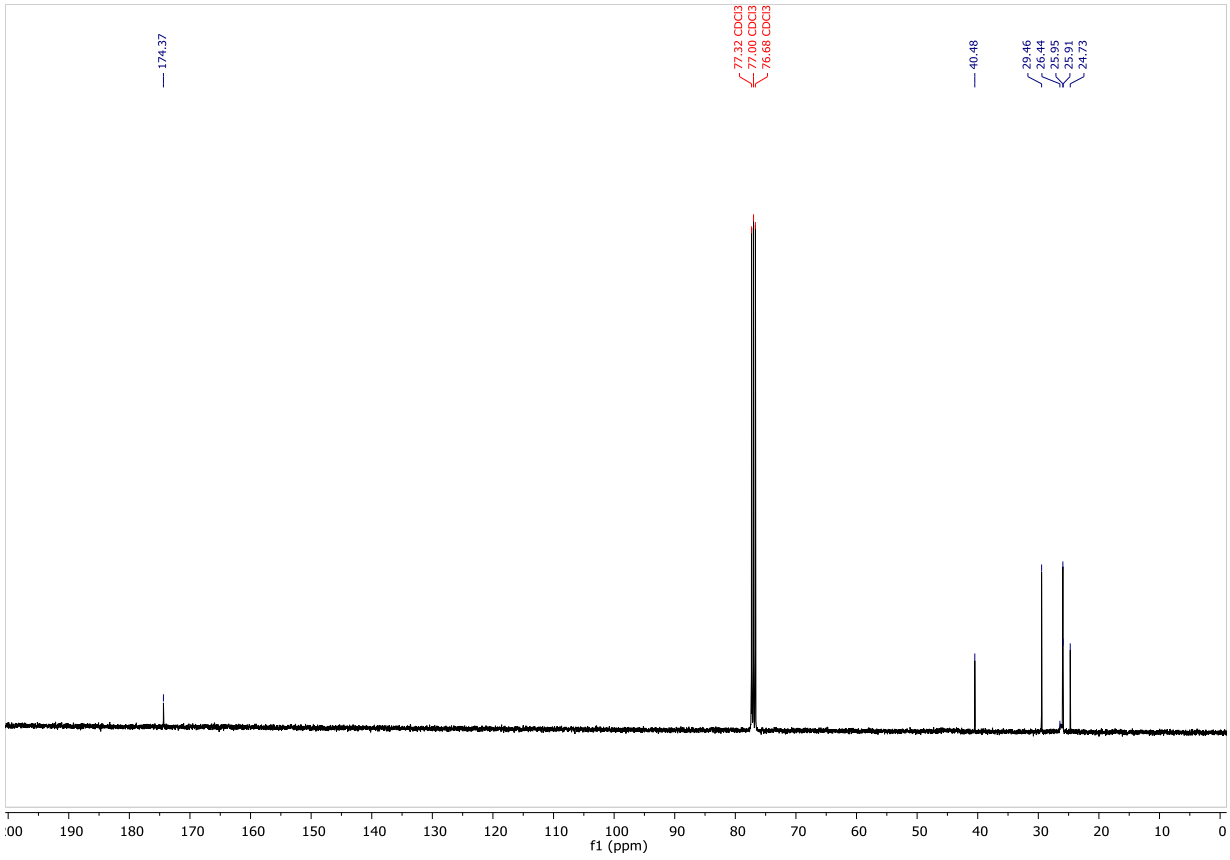
174.37
77.33 CDCl3
77.00 CDCl3
76.68 CDCl3
40.48
29.46
26.44
25.95
25.91
24.73
f1 (ppm)

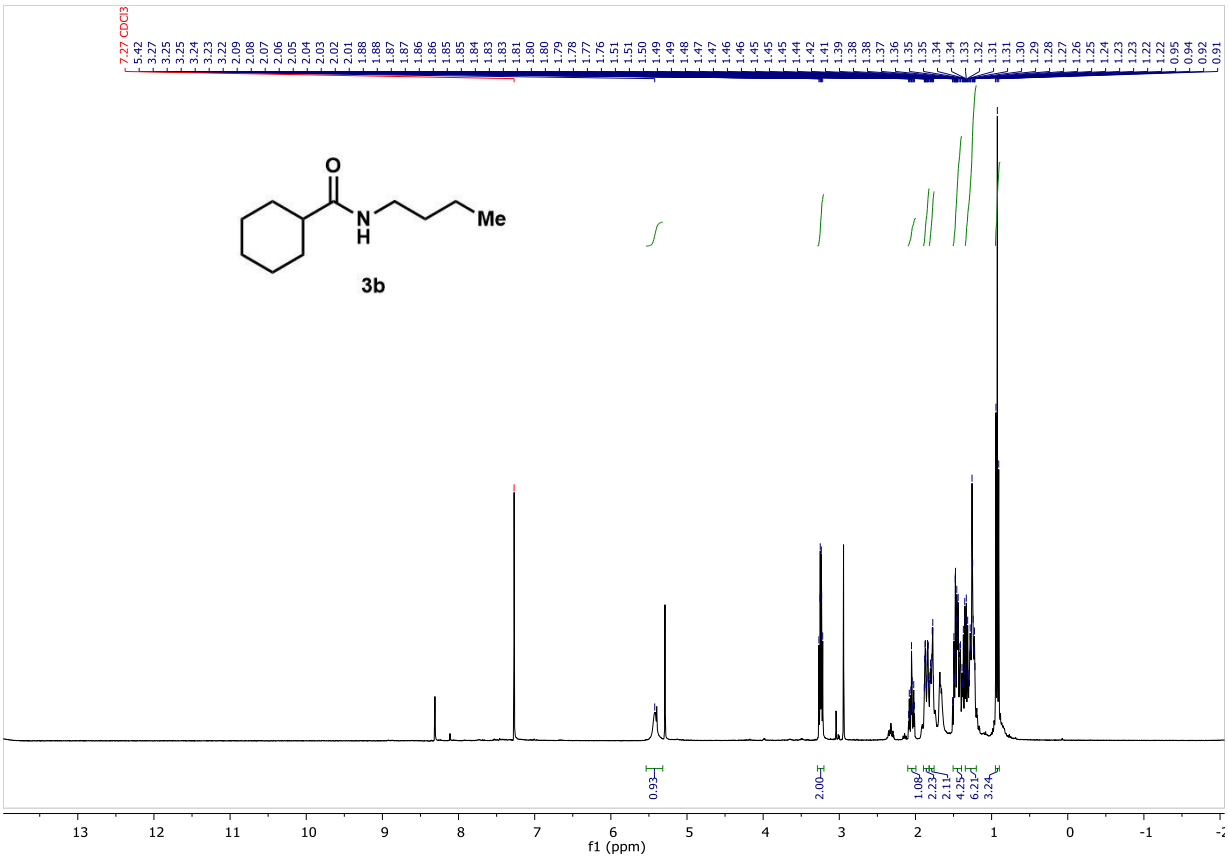
7.27 CDCl3
O
N
H
Me
3b
0.93
2.00
1.08
2.23
2.11
4.25
6.22
3.24
f1 (ppm)

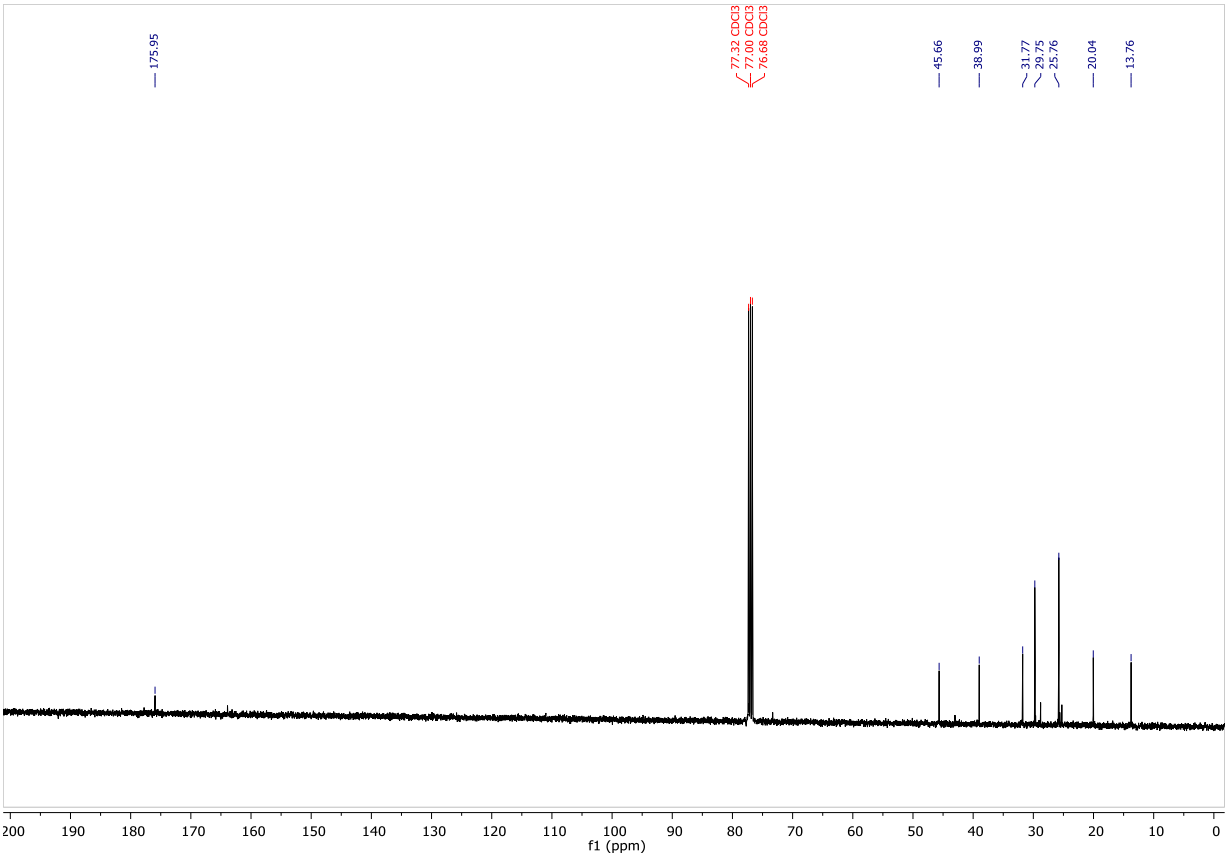
175.95
77.32 CDCl3
77.00 CDCl3
76.68 CDCl3
45.66
38.99
31.77
29.75
25.76
20.04
13.76
f1 (ppm)

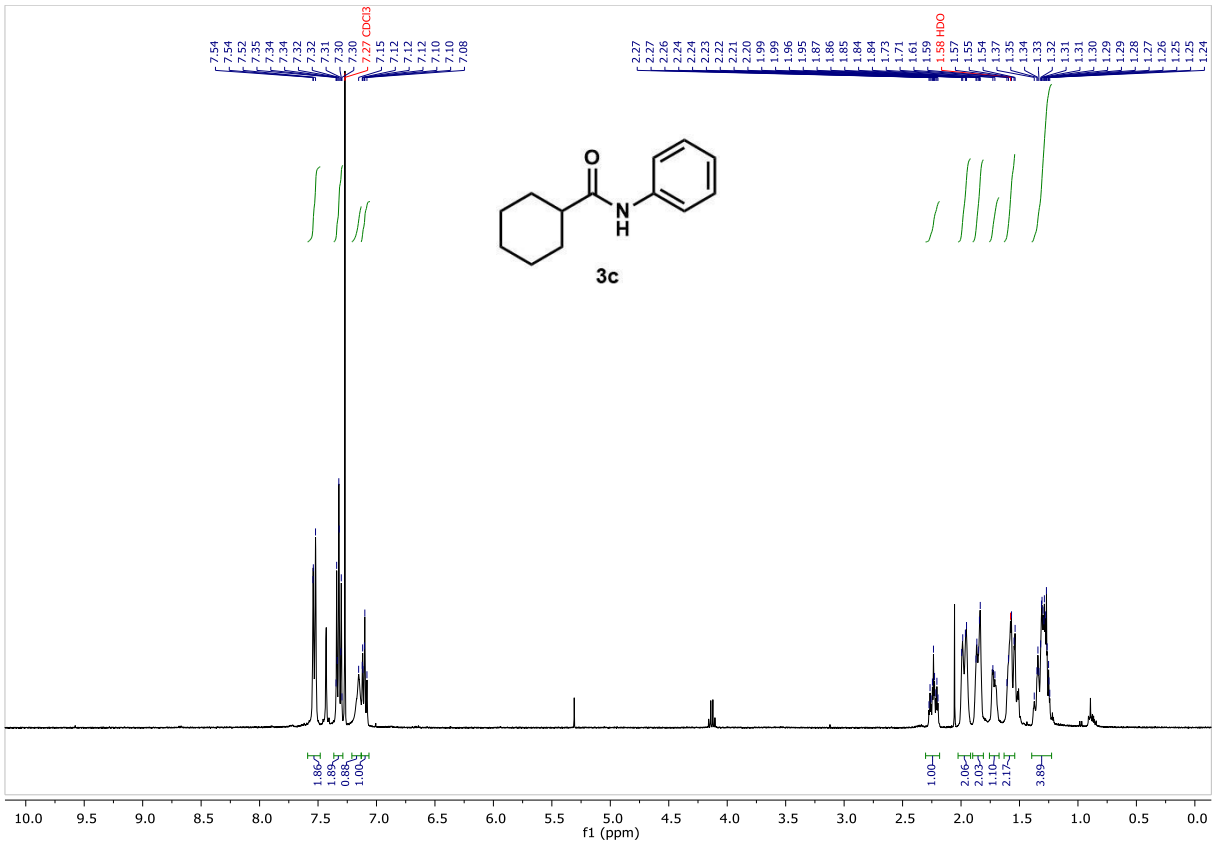
7.54
7.54
7.52
7.35
7.34
7.34
7.32
7.32
7.31
7.30
7.30
CDCl3
7.27
7.15
7.12
7.12
7.12
7.10
7.10
7.08
2.27
2.27
2.26
2.24
2.24
2.23
2.22
2.21
2.20
1.99
1.99
1.96
1.95
1.87
1.86
1.85
1.84
1.84
1.73
1.71
1.61
1.59
1.58 HDO
1.57
1.55
1.54
1.37
1.35
1.34
1.33
1.32
1.31
1.31
1.30
1.29
1.28
1.27
1.26
1.25
1.25
1.24
O
N
H
3c
1.86
1.89
0.88
1.00
1.00
2.06
2.03
1.10
2.17
3.89
10.0
9.5
9.0
8.5
8.0
7.5
7.0
6.5
6.0
5.5
5.0
4.5
4.0
3.5
3.0
2.5
2.0
1.5
1.0
0.5
0.0
f1 (ppm)

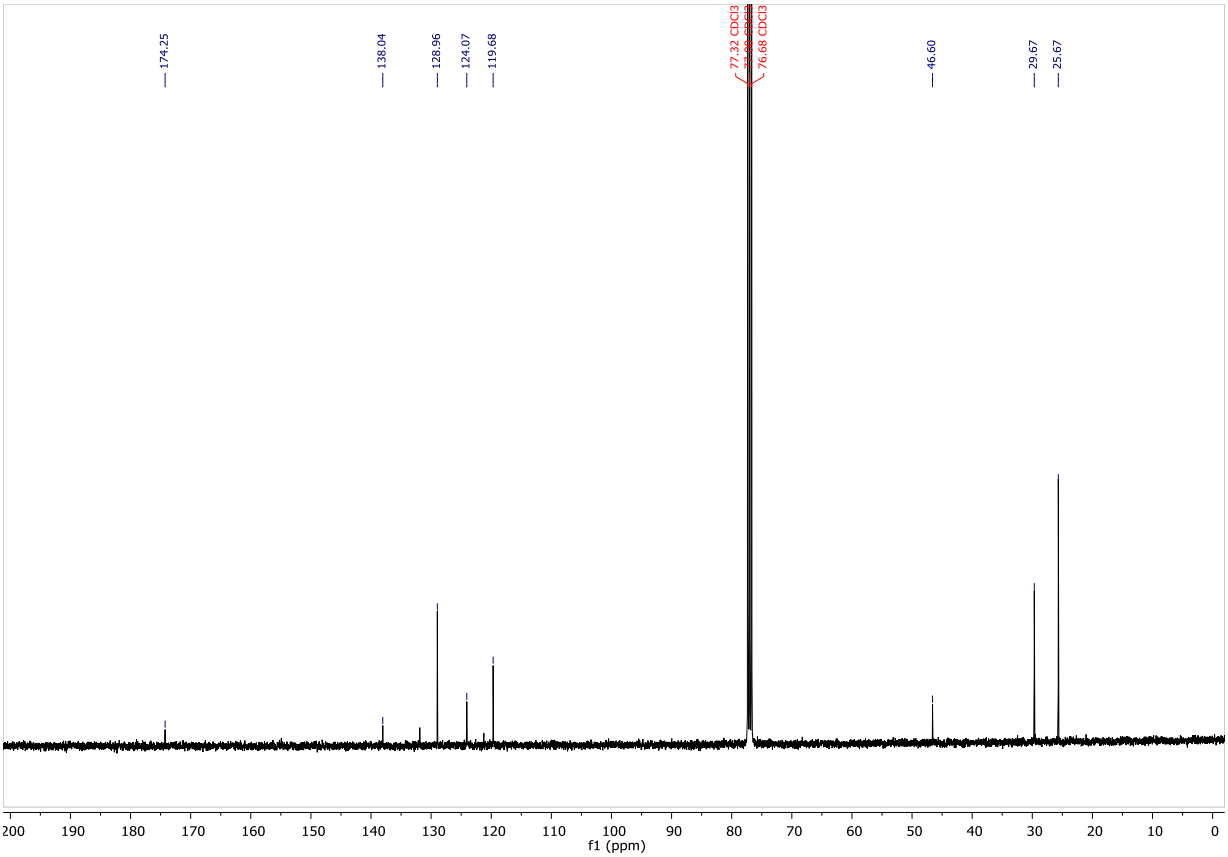
174.25
138.04
128.96
124.07
119.68
77.32 CDCl3
76.68 CDCl3
46.60
29.67
25.67
200
190
180
170
160
150
140
130
120
110
100
90
80
70
60
50
40
30
20
10
0
f1 (ppm)

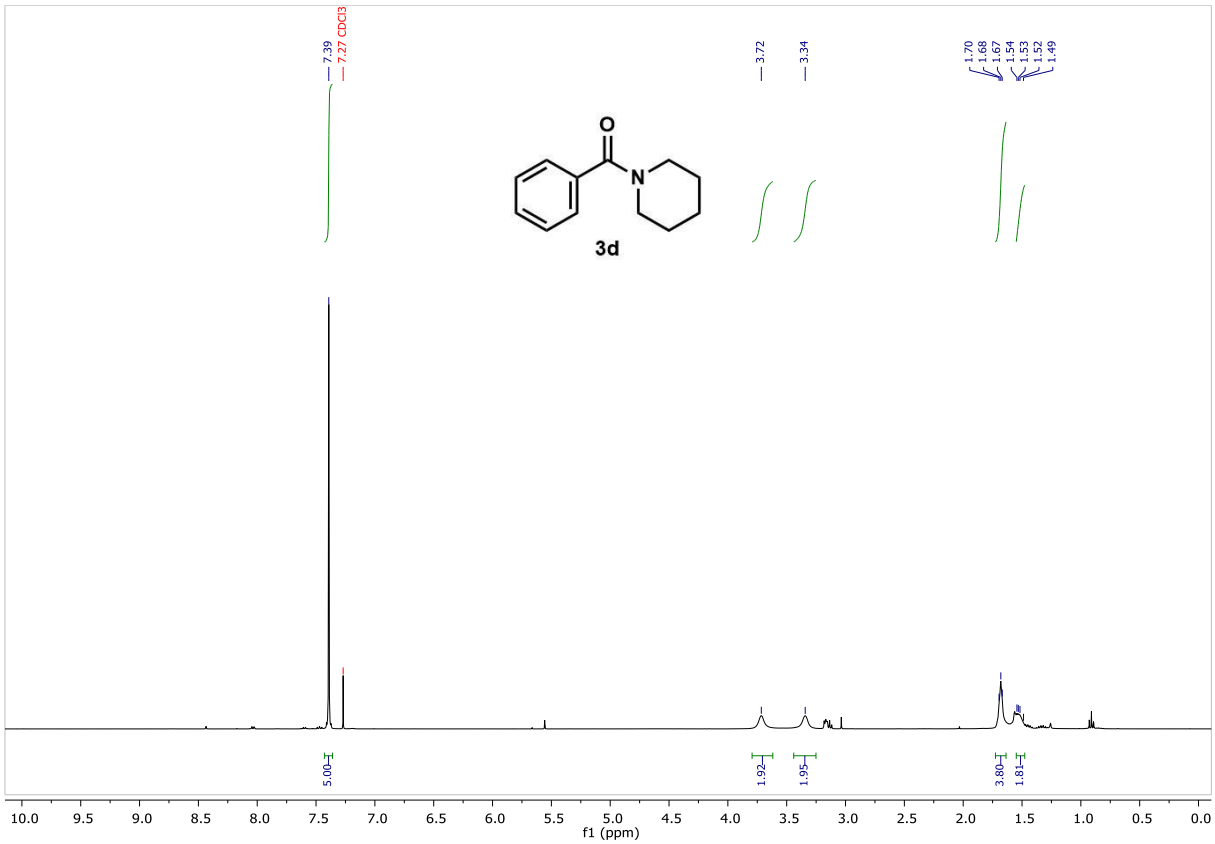
7.39
7.27 CDCl3
3.72
3.34
1.70
1.68
1.67
1.54
1.53
1.32
1.49
O
N
3d
5.00
1.92
1.95
3.80
1.81
f1 (ppm)

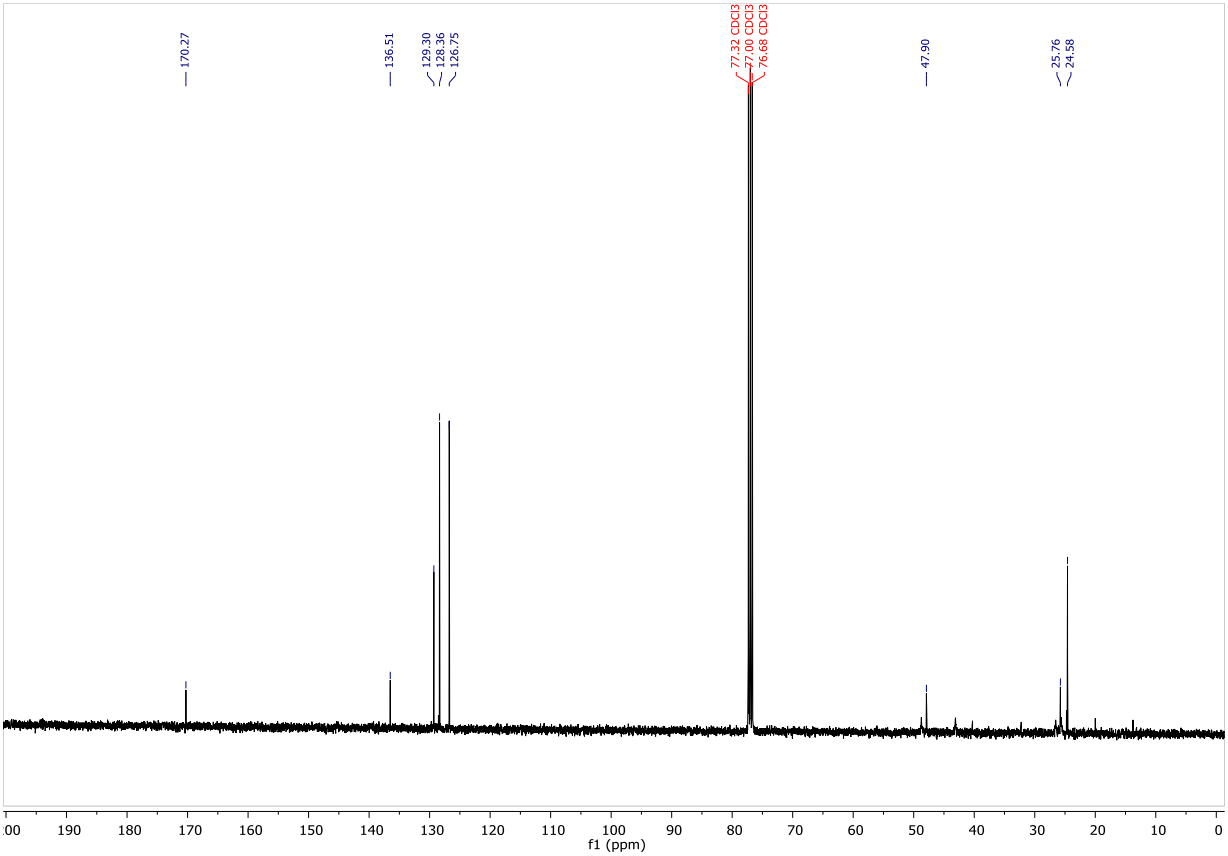
170.27
136.51
129.30
128.36
126.75
77.32 CDCl3
77.00 CDCl3
76.68 CDCl3
47.90
25.76
24.58
f1 (ppm)

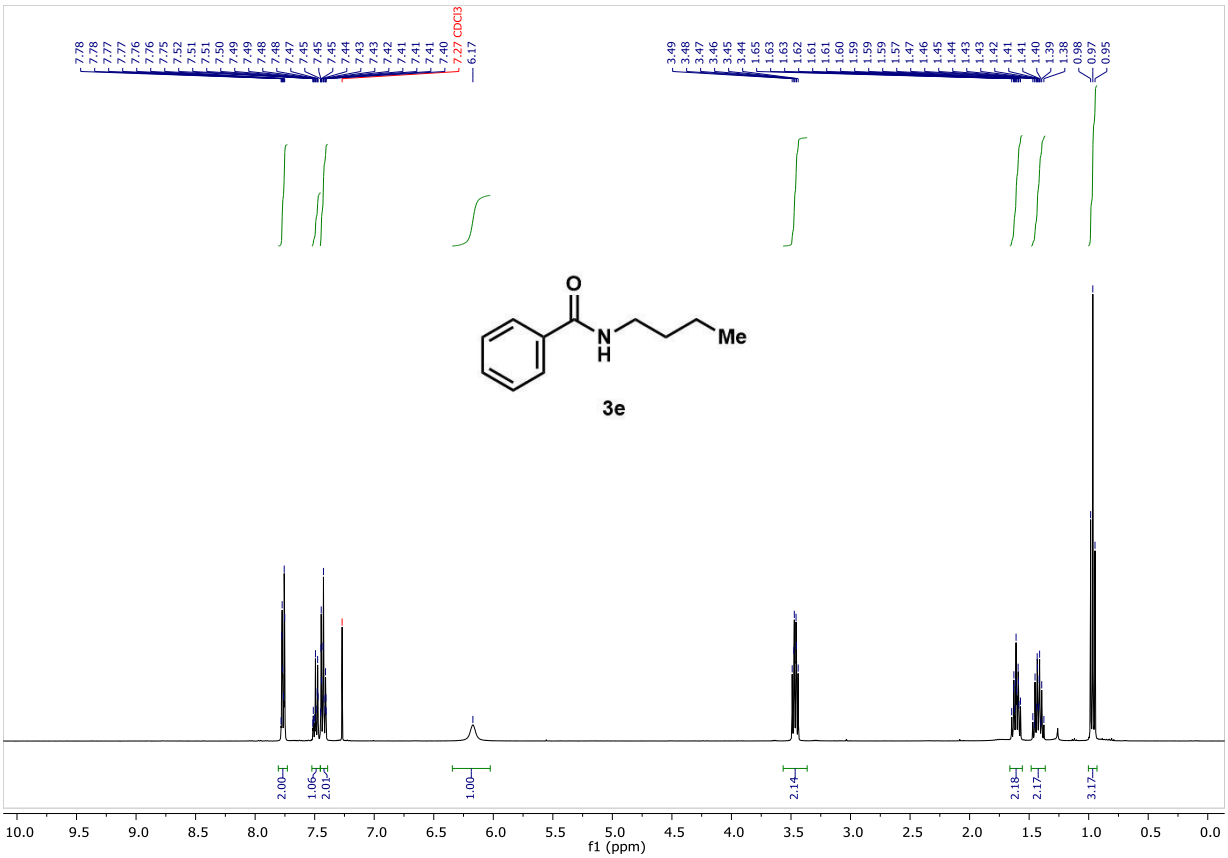
7.78
7.78
7.77
7.77
7.77
7.76
7.76
7.75
7.52
7.51
7.51
7.50
7.49
7.49
7.48
7.48
7.47
7.45
7.45
7.45
7.44
7.43
7.43
7.42
7.41
7.41
7.41
7.40
7.27 CDCl3
6.17
3.49
3.48
3.47
3.46
3.45
3.44
3.65
1.63
1.63
1.62
1.61
1.61
1.60
1.59
1.59
1.59
1.57
1.47
1.46
1.45
1.44
1.43
1.43
1.42
1.41
1.41
1.40
1.39
1.38
0.98
0.97
0.95
O
N
H
Me
3e
2.00
1.06
2.01
1.00
2.14
2.18
2.17
3.17
10.0
9.5
9.0
8.5
8.0
7.5
7.0
6.5
6.0
5.5
5.0
4.5
4.0
3.5
3.0
2.5
2.0
1.5
1.0
0.5
0.0
f1 (ppm)

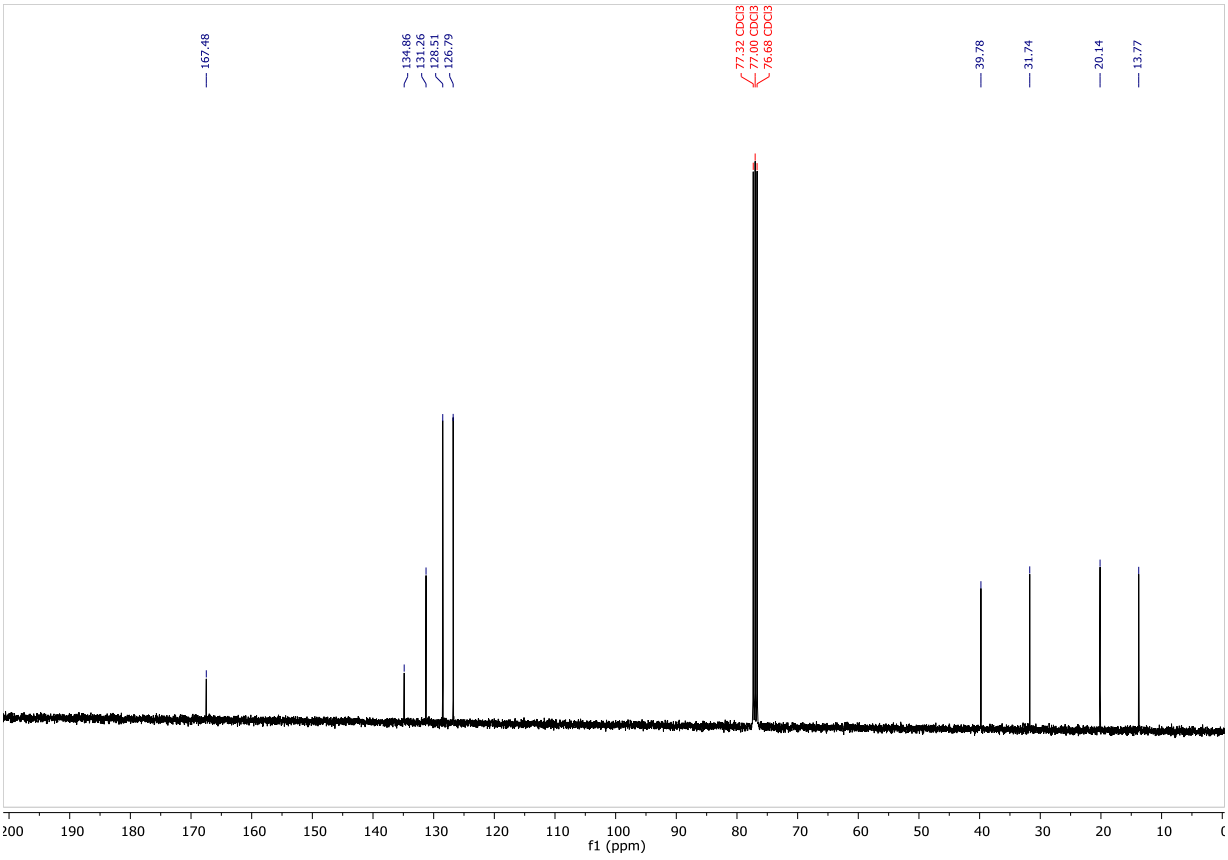
167.48
134.86
131.26
128.51
126.79
77.32 CDCl3
77.00 CDCl3
76.68 CDCl3
39.78
31.74
20.14
13.77
200
190
180
170
160
150
140
130
120
110
100
90
80
70
60
50
40
30
20
10
f1 (ppm)

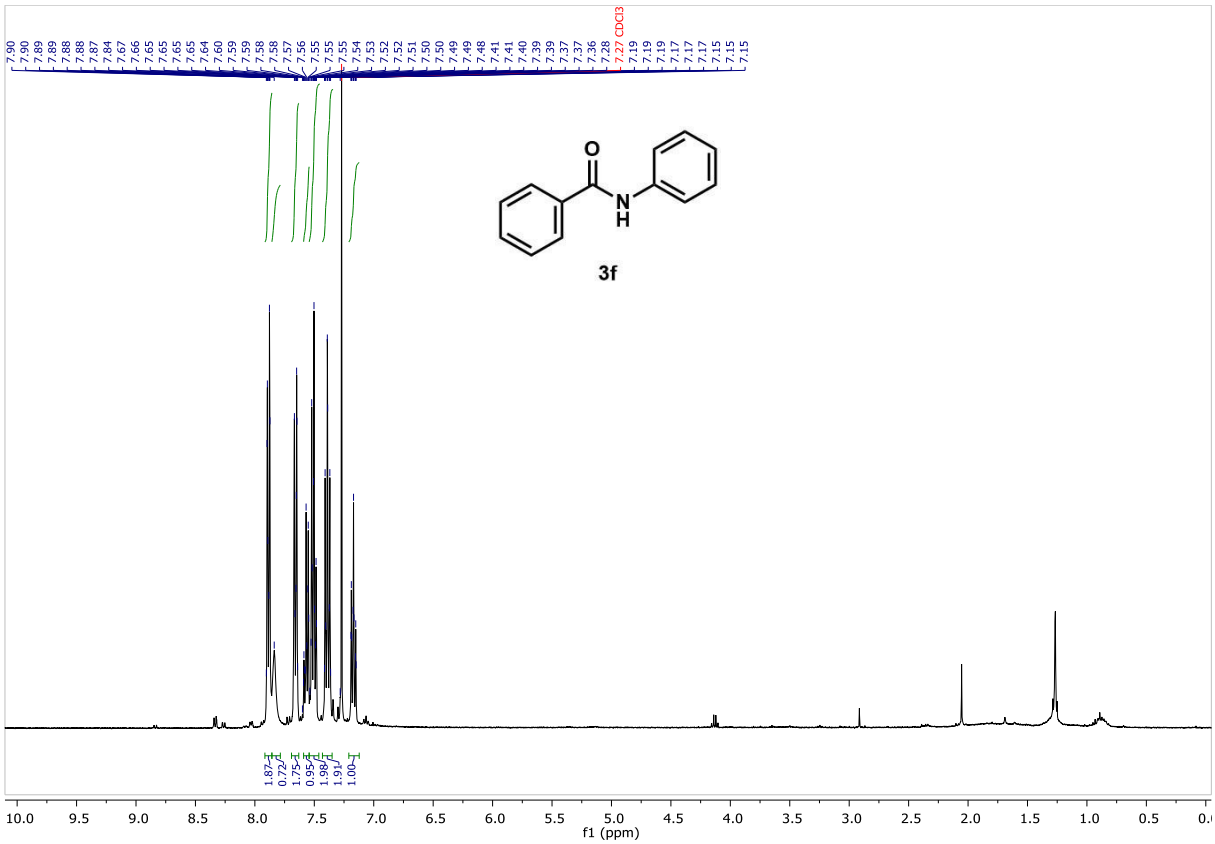
7.90 7.90 7.89 7.89 7.88 7.88 7.87 7.84 7.67 7.66 7.65 7.65 7.65 7.65 7.64 7.60 7.59 7.59 7.58 7.58 7.57 7.56 7.55 7.55 7.55 7.54 7.53 7.52 7.52 7.51 7.50 7.50 7.49 7.49 7.48 7.41 7.41 7.40 7.39 7.39 7.37 7.37 7.36 7.28 7.27 CDCl3 7.19 7.19 7.19 7.17 7.17 7.17 7.15 7.15 7.15
O
N
H
3f
1.87 0.72 1.05 0.99 1.94 1.00 1.00
10.0 9.5 9.0 8.5 8.0 7.5 7.0 6.5 6.0 5.5 5.0 4.5 4.0 3.5 3.0 2.5 2.0 1.5 1.0 0.5
f1 (ppm)

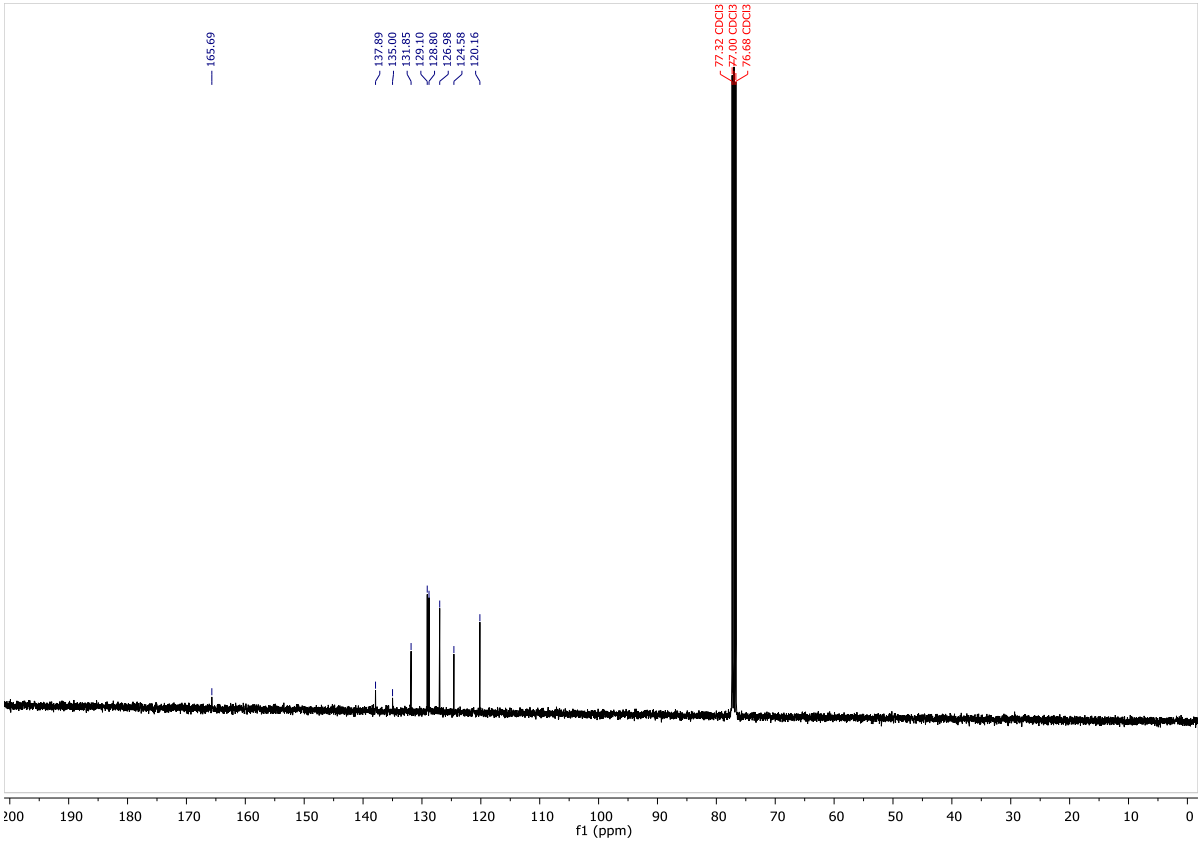
165.69
137.89 135.00 131.85 129.10 128.80 126.98 124.58 120.16
77.32 CDCl3 77.00 CDCl3 76.68 CDCl3
200 190 180 170 160 150 140 130 120 110 100 90 80 70 60 50 40 30 20 10 0
f1 (ppm)

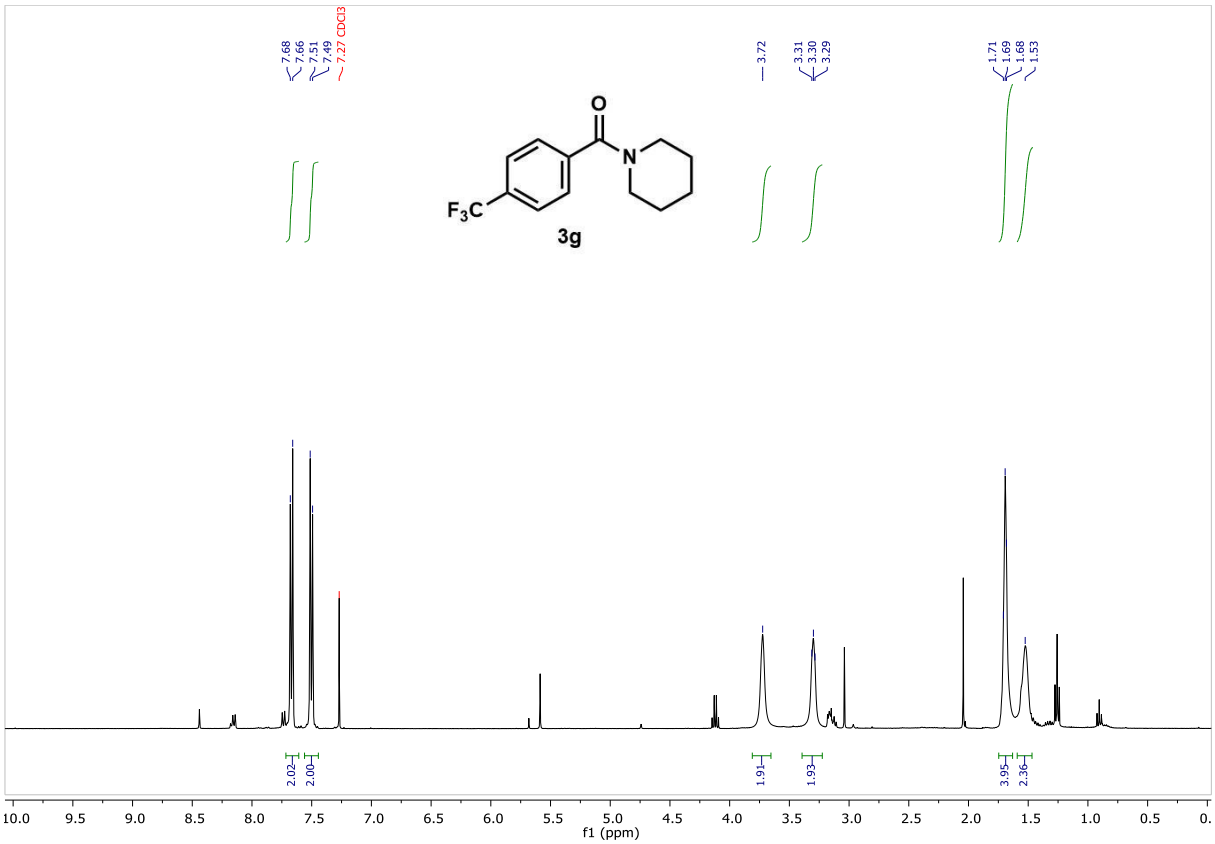
7.68
7.66
7.51
7.49
7.27 CDCl3
3.72
3.31
3.30
3.29
1.71
1.69
1.68
1.53
O
N
F3C
3g
2.02
2.00
1.91
1.93
3.95
2.36
f1 (ppm)

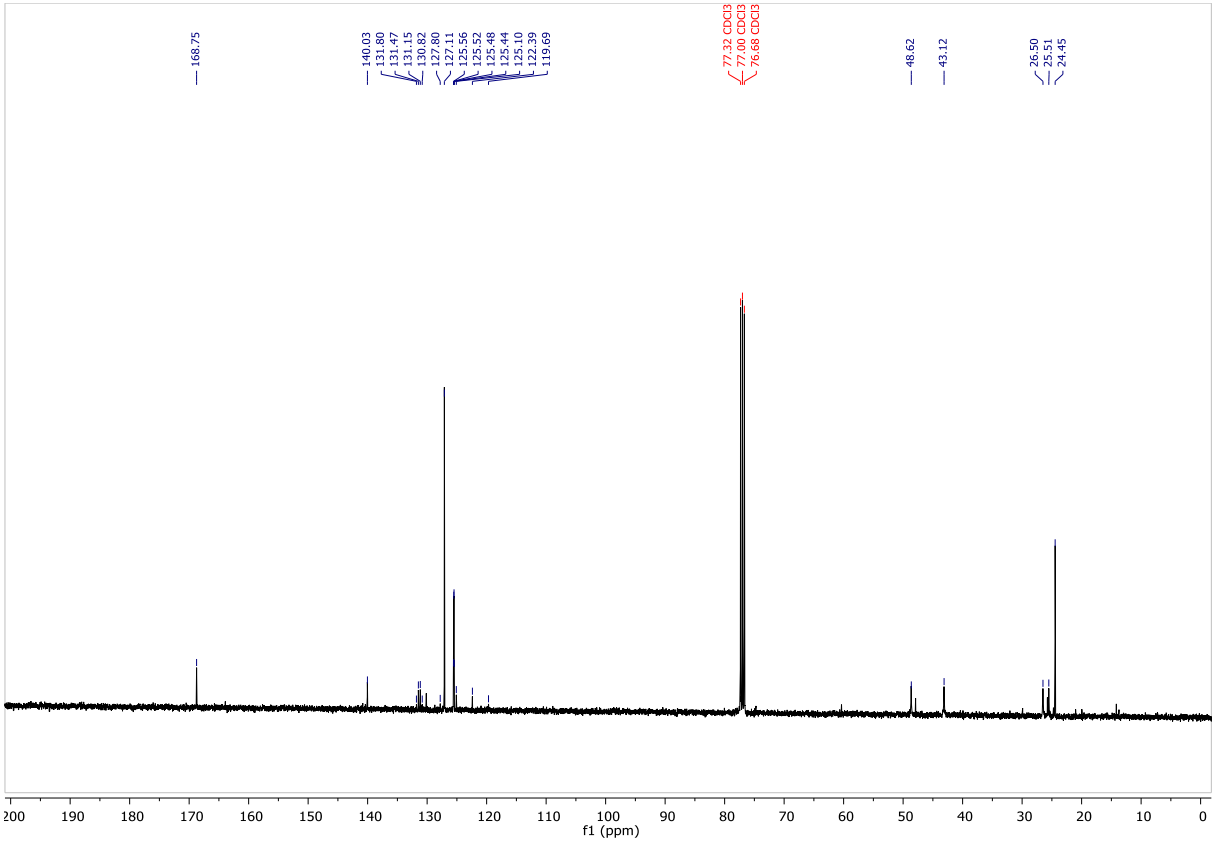
168.75
140.03
131.80
131.47
131.15
130.82
127.80
127.11
125.56
125.52
125.48
125.44
125.10
122.39
119.69
77.32 CDCl3
77.00 CDCl3
76.68 CDCl3
48.62
43.12
26.50
25.51
24.45
f1 (ppm)

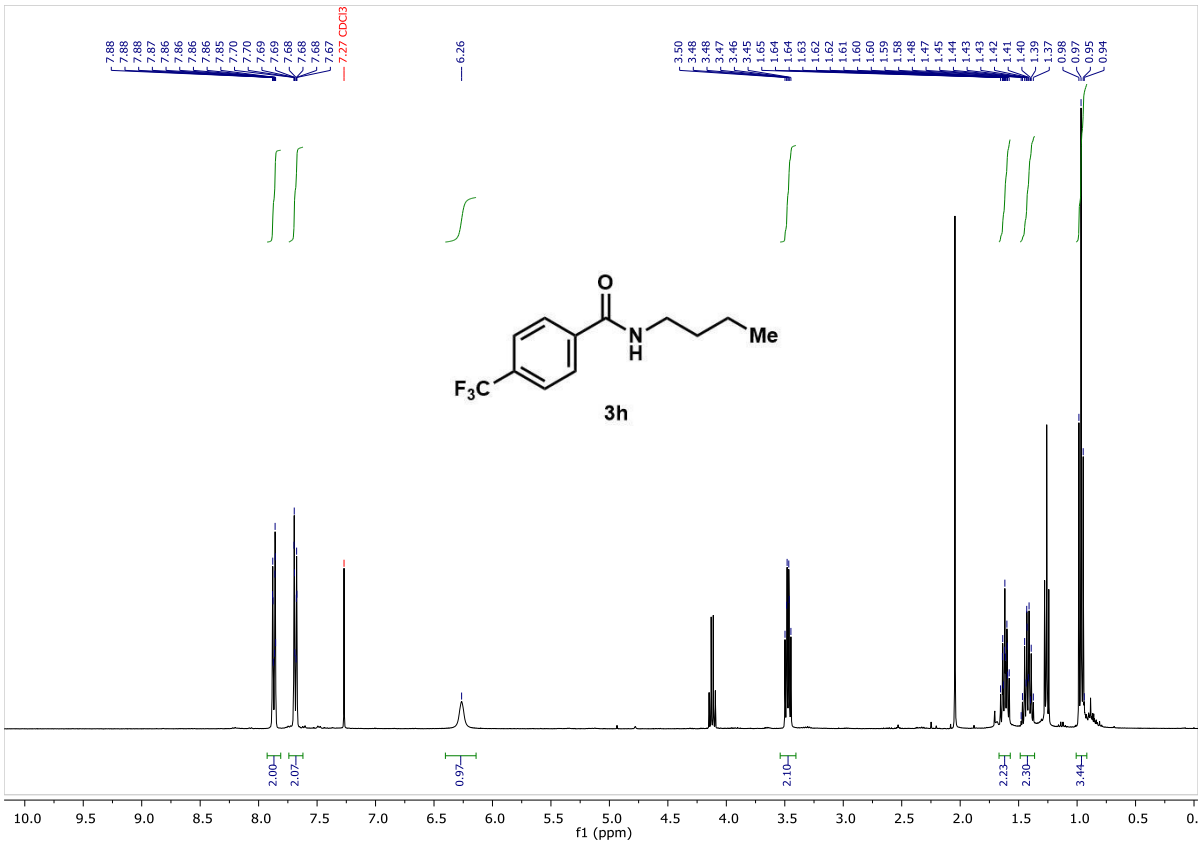
7.88
7.88
7.88
7.87
7.86
7.86
7.86
7.86
7.85
7.70
7.69
7.69
7.68
7.68
7.68
7.67
7.27 CDCl3
6.26
3.50
3.48
3.48
3.47
3.46
3.45
1.65
1.64
1.64
1.63
1.62
1.62
1.61
1.60
1.60
1.59
1.58
1.48
1.47
1.45
1.44
1.43
1.43
1.42
1.41
1.40
1.39
1.37
0.98
0.97
0.95
0.94
O
N
H
Me
F3C
3h
2.00
2.07
0.97
2.10
2.23
2.30
3.44
f1 (ppm)

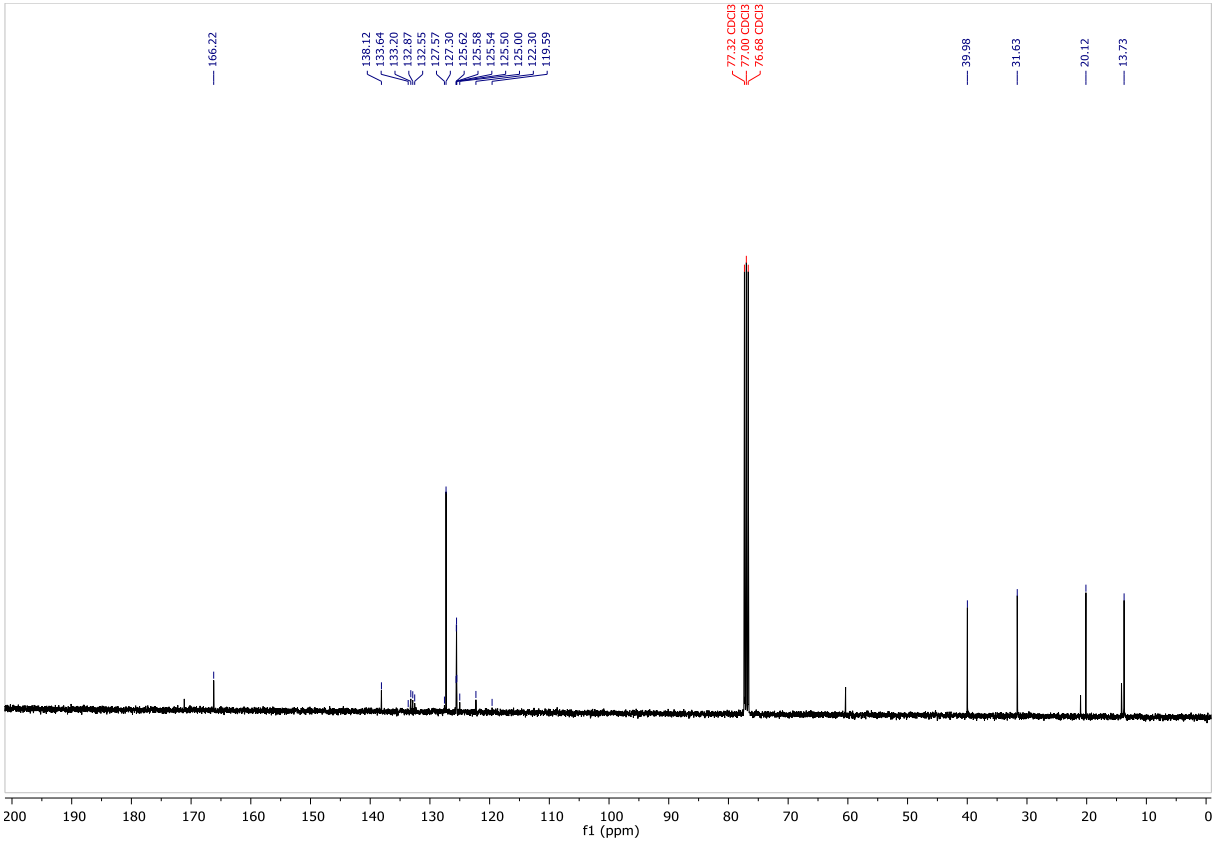
166.22
138.12
133.64
133.20
132.87
132.55
127.57
127.30
125.62
125.58
125.54
125.50
125.00
122.30
119.59
77.32 CDCl3
77.00 CDCl3
76.68 CDCl3
39.98
31.63
20.12
13.73
f1 (ppm)

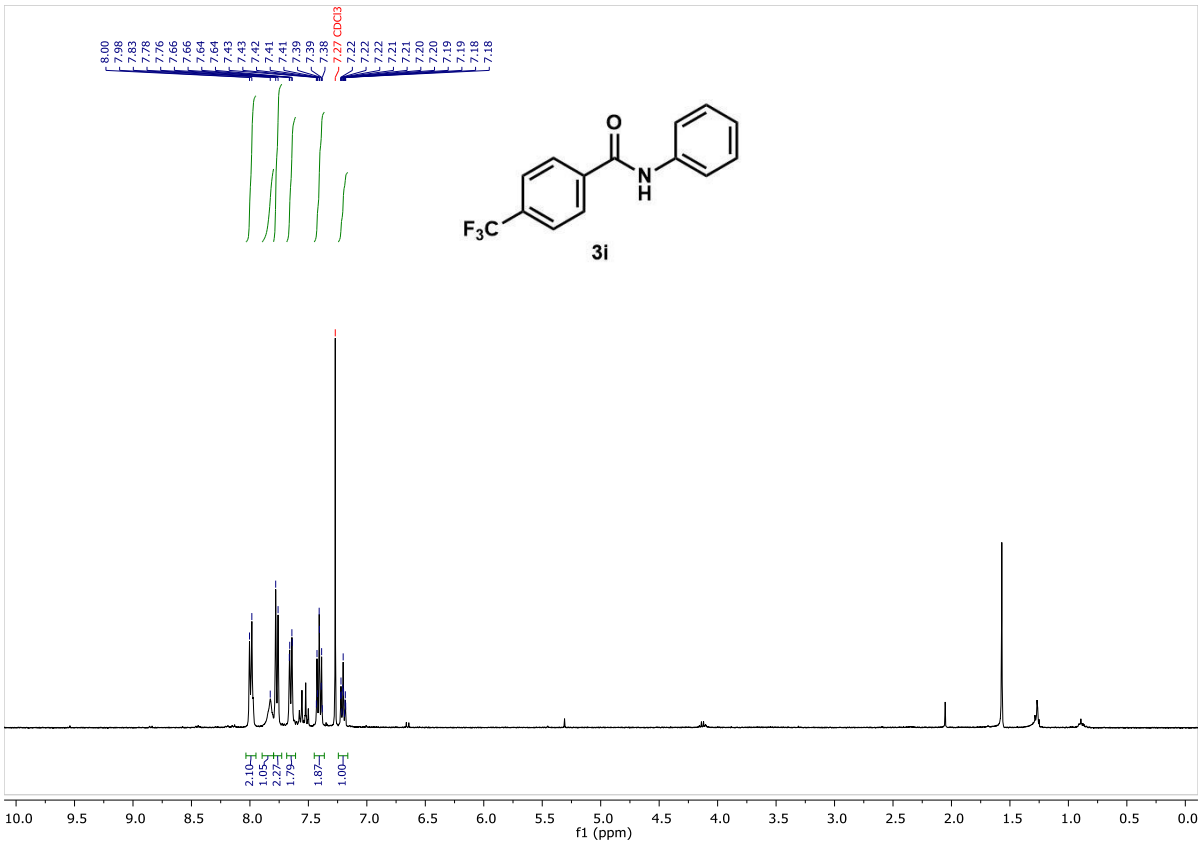
8.00
7.98
7.83
7.78
7.76
7.66
7.66
7.64
7.64
7.43
7.43
7.42
7.41
7.41
7.39
7.39
7.38
7.27 CDCl3
7.22
7.22
7.22
7.21
7.21
7.20
7.20
7.19
7.19
7.18
7.18
O
N
H
F3C
3i
2.10
1.05
2.27
1.79
1.87
1.00
10.0
9.5
9.0
8.5
8.0
7.5
7.0
6.5
6.0
5.5
5.0
4.5
4.0
3.5
3.0
2.5
2.0
1.5
1.0
0.5
0.0
f1 (ppm)

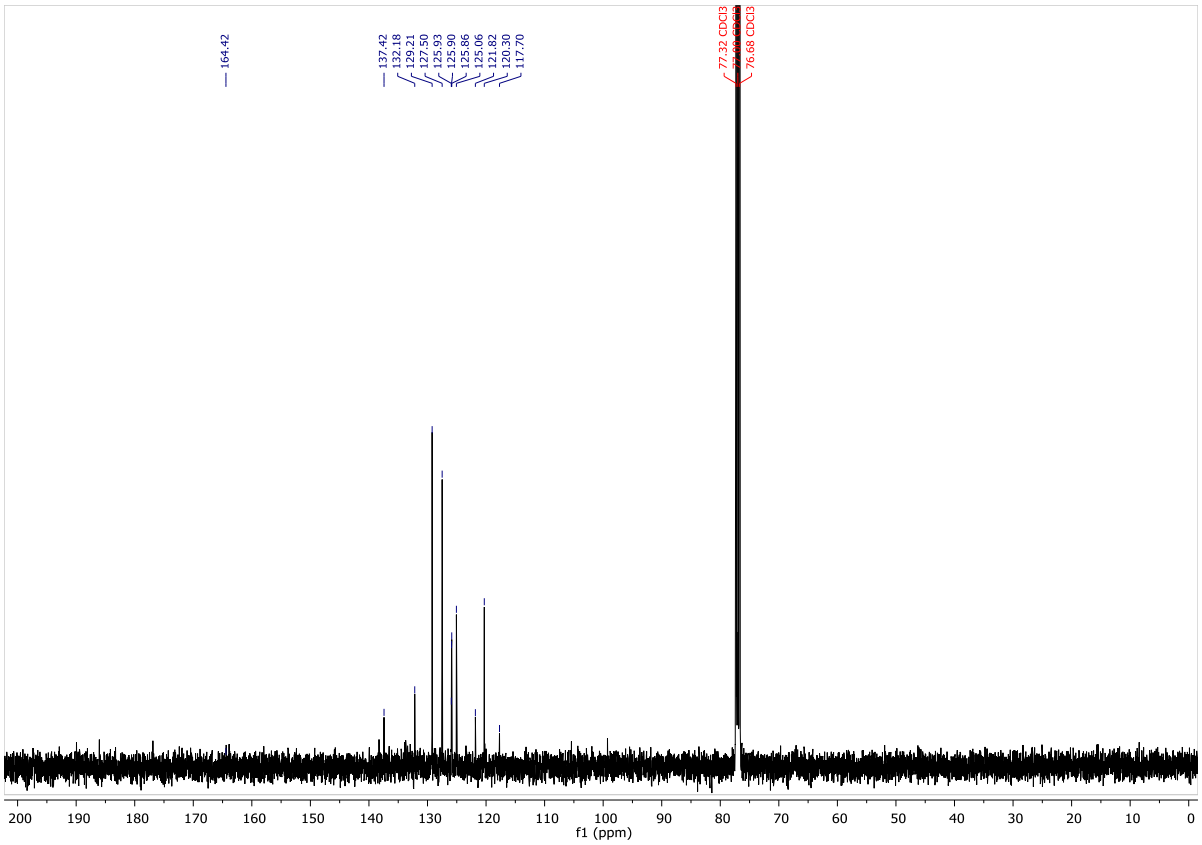
164.42
137.42
132.18
129.21
127.50
125.93
125.90
125.86
125.06
121.82
120.30
117.70
77.32 CDCl3
76.68 CDCl3
200
190
180
170
160
150
140
130
120
110
100
90
80
70
60
50
40
30
20
10
0
f1 (ppm)

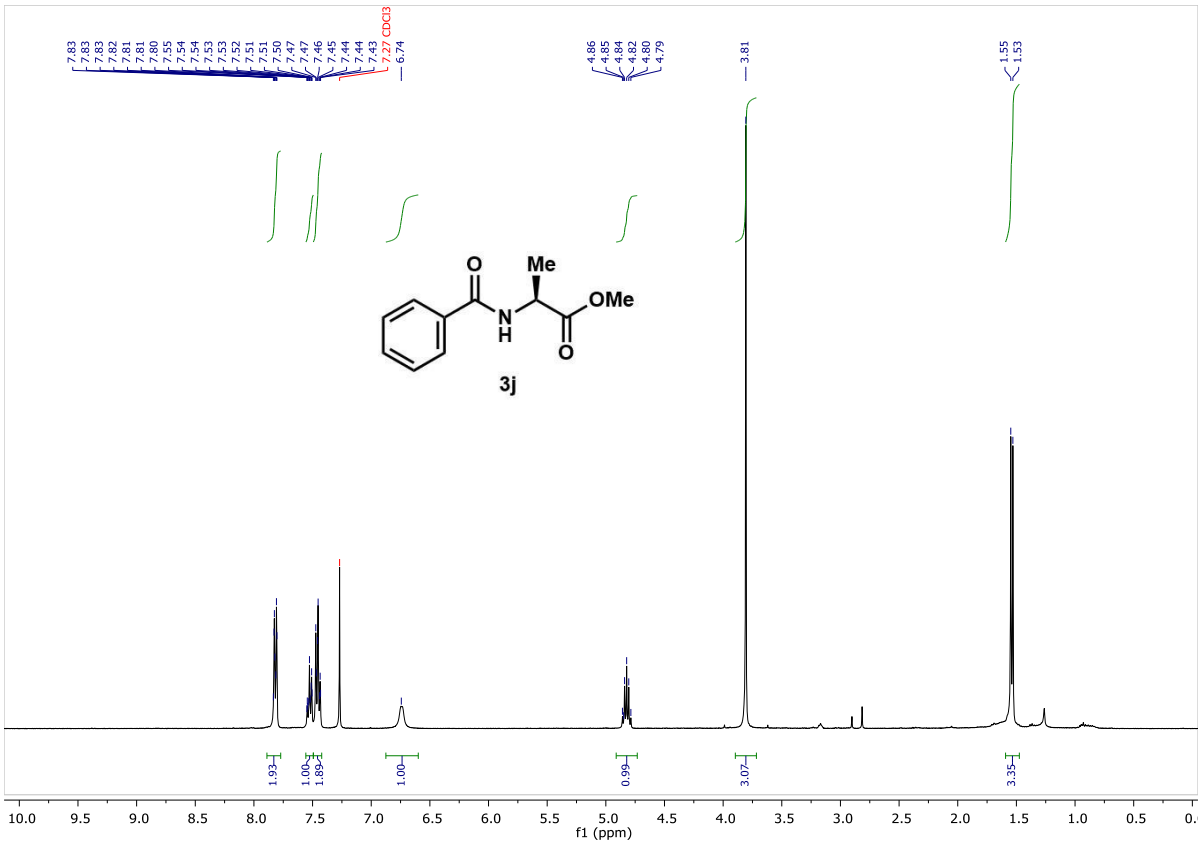
7.83
7.83
7.83
7.82
7.81
7.81
7.80
7.55
7.54
7.54
7.53
7.53
7.52
7.51
7.51
7.50
7.47
7.47
7.46
7.45
7.44
7.44
7.43
7.27 CDCl3
6.74
4.86
4.85
4.84
4.82
4.80
4.79
3.81
1.55
1.53
O
Me
N
H
OMe
O
3j
1.93
1.00
1.89
1.00
0.99
3.07
3.35
10.0
9.5
9.0
8.5
8.0
7.5
7.0
6.5
6.0
5.5
5.0
4.5
4.0
3.5
3.0
2.5
2.0
1.5
1.0
0.5
f1 (ppm)

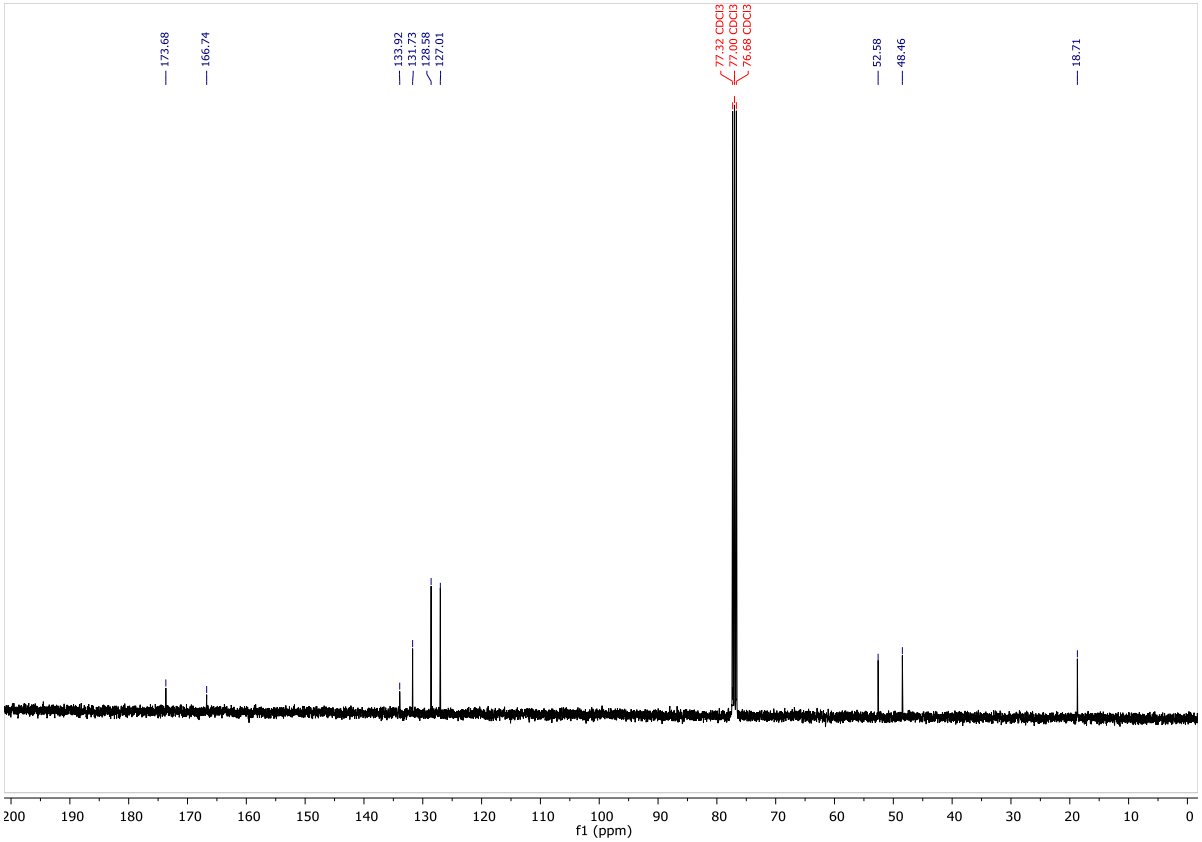
173.68
166.74
133.92
131.73
128.58
127.01
77.32 CDCl3
77.00 CDCl3
76.68 CDCl3
52.58
48.46
18.71
200
190
180
170
160
150
140
130
120
110
100
90
80
70
60
50
40
30
20
10
0
f1 (ppm)

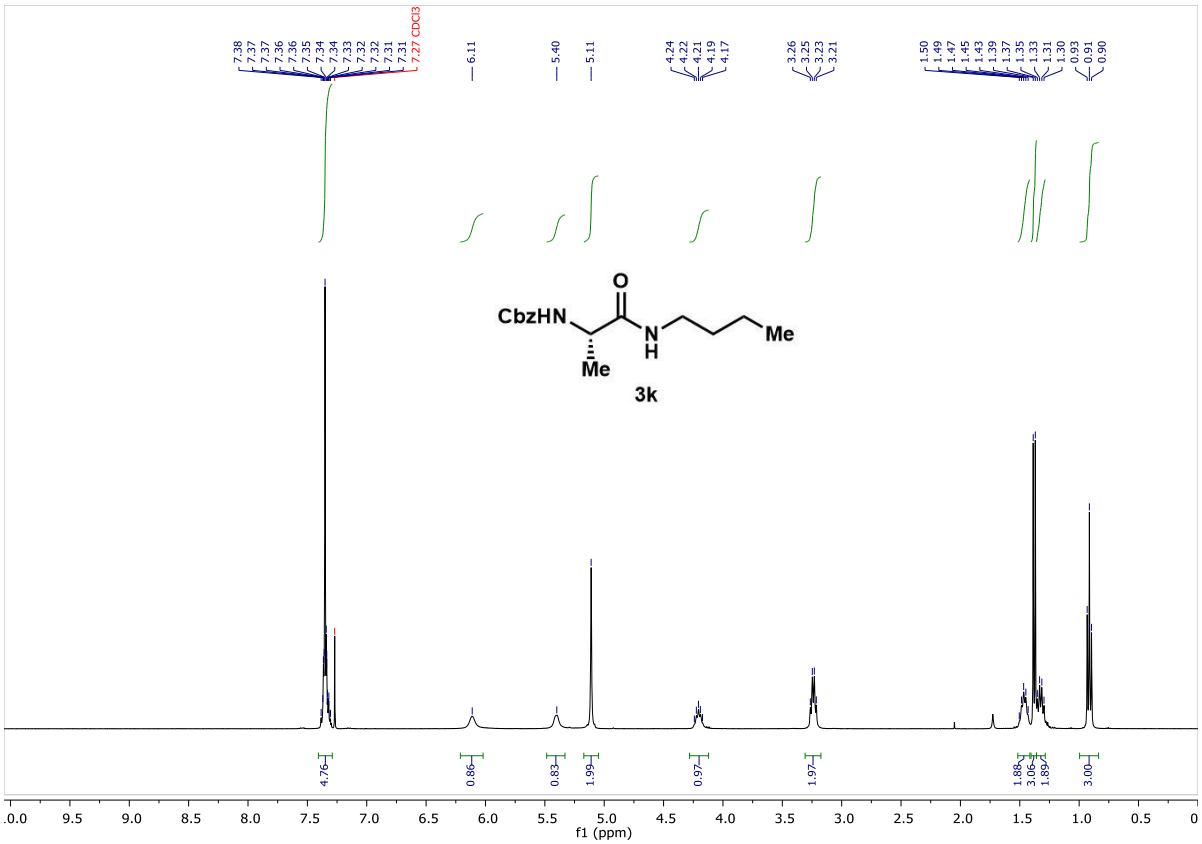
7.38
7.37
7.37
7.36
7.36
7.35
7.34
7.34
7.33
7.32
7.32
7.31
7.31
7.27 CDCl3
6.11
5.40
5.11
4.24
4.22
4.21
4.19
4.17
3.26
3.25
3.23
3.21
1.50
1.49
1.47
1.45
1.43
1.39
1.37
1.35
1.33
1.31
1.30
0.93
0.91
0.90
CbzHN
O
N
H
Me
Me
3k
4.76
0.86
0.83
1.99
0.97
1.97
1.88
3.06
1.89
3.00
f1 (ppm)

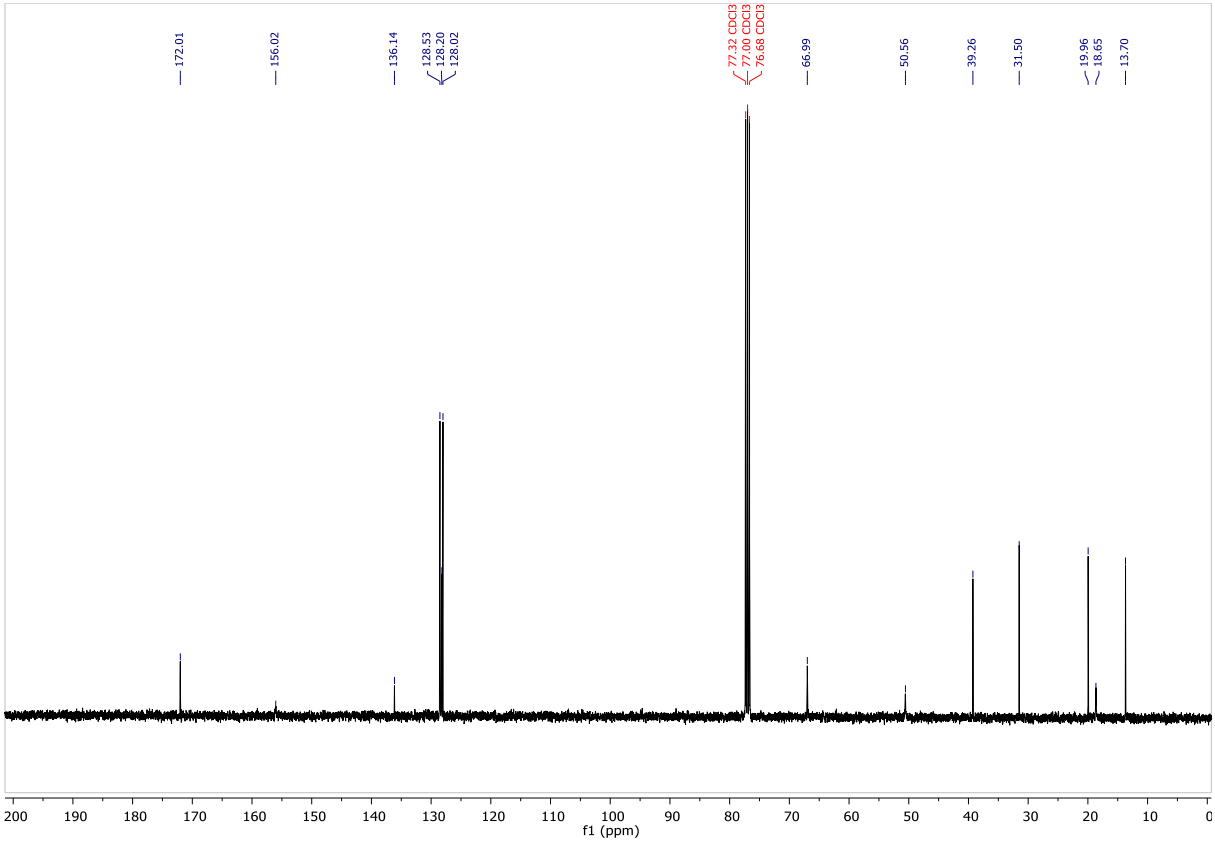
172.01
156.02
136.14
128.53
128.20
128.02
77.32 CDCl3
77.00 CDCl3
76.68 CDCl3
66.99
50.56
39.26
31.50
19.96
18.65
13.70
f1 (ppm)

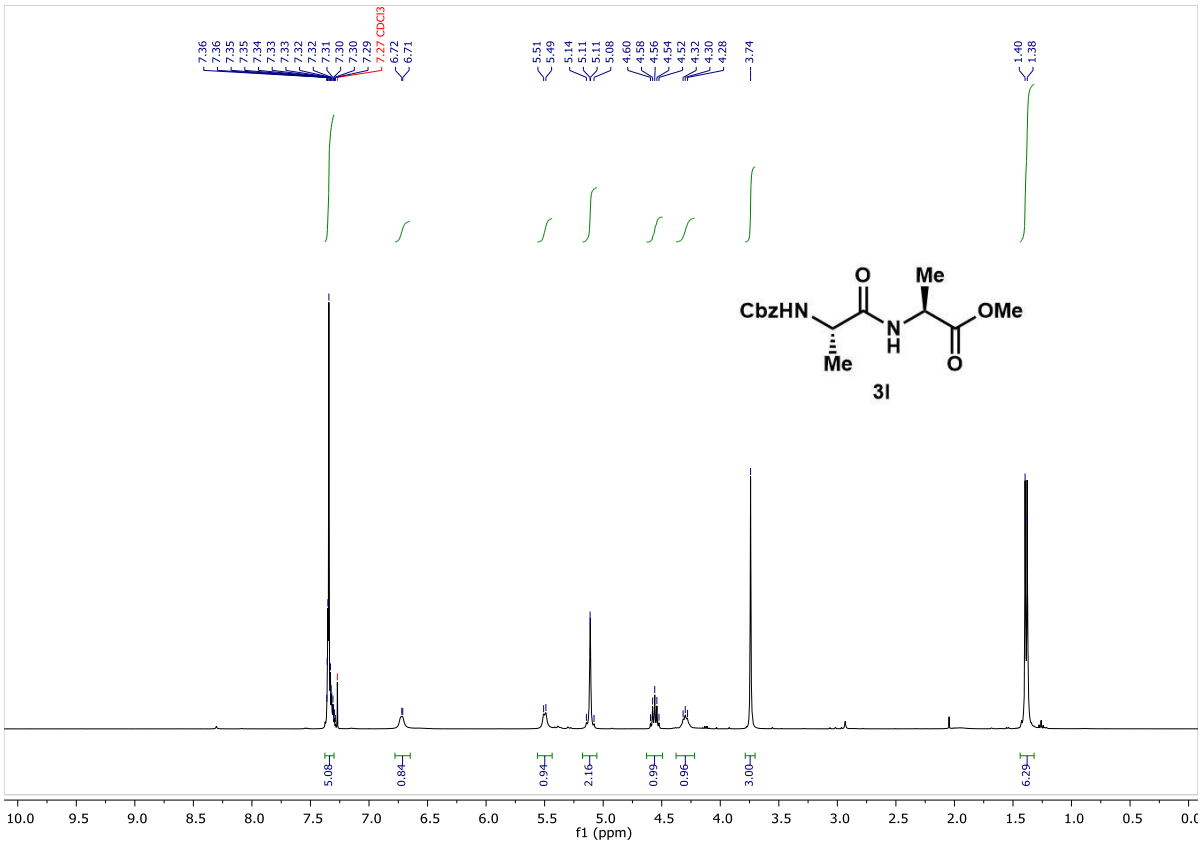
7.36
7.36
7.35
7.35
7.34
7.33
7.33
7.32
7.32
7.31
7.30
7.30
7.29
7.27 CDCl3
6.72
6.71
5.51
5.49
5.14
5.11
5.11
5.08
4.60
4.58
4.56
4.54
4.52
4.32
4.30
4.28
3.74
1.40
1.38
CbzHN
O
Me
N
H
OMe
Me
O
3l
5.08
0.84
0.94
2.16
0.99
0.96
3.00
6.29
f1 (ppm)

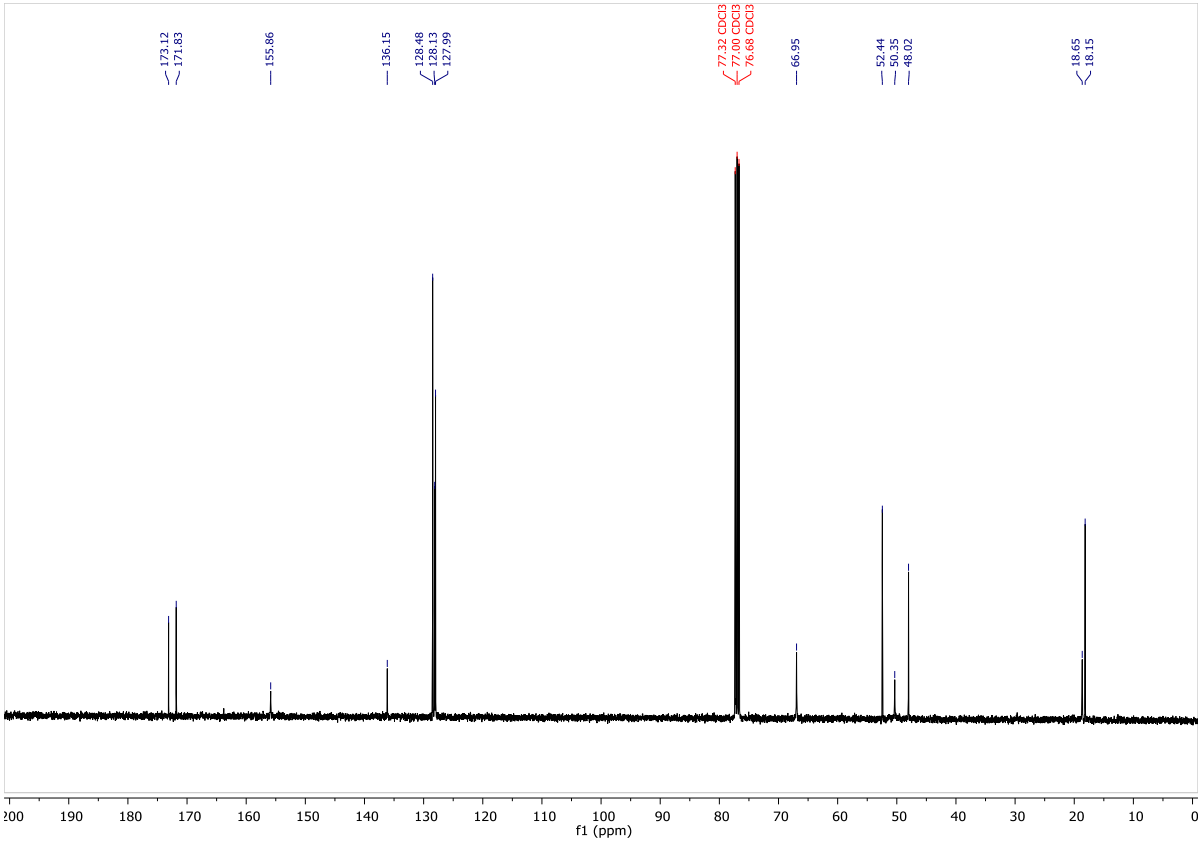
173.12
171.83
155.86
136.15
128.48
128.13
127.99
77.32 CDCl3
77.00 CDCl3
76.68 CDCl3
66.95
52.44
50.35
48.02
18.65
18.15
f1 (ppm)

5. Redox-Neutral Minisci Reactions Via Photoredox Catalysis

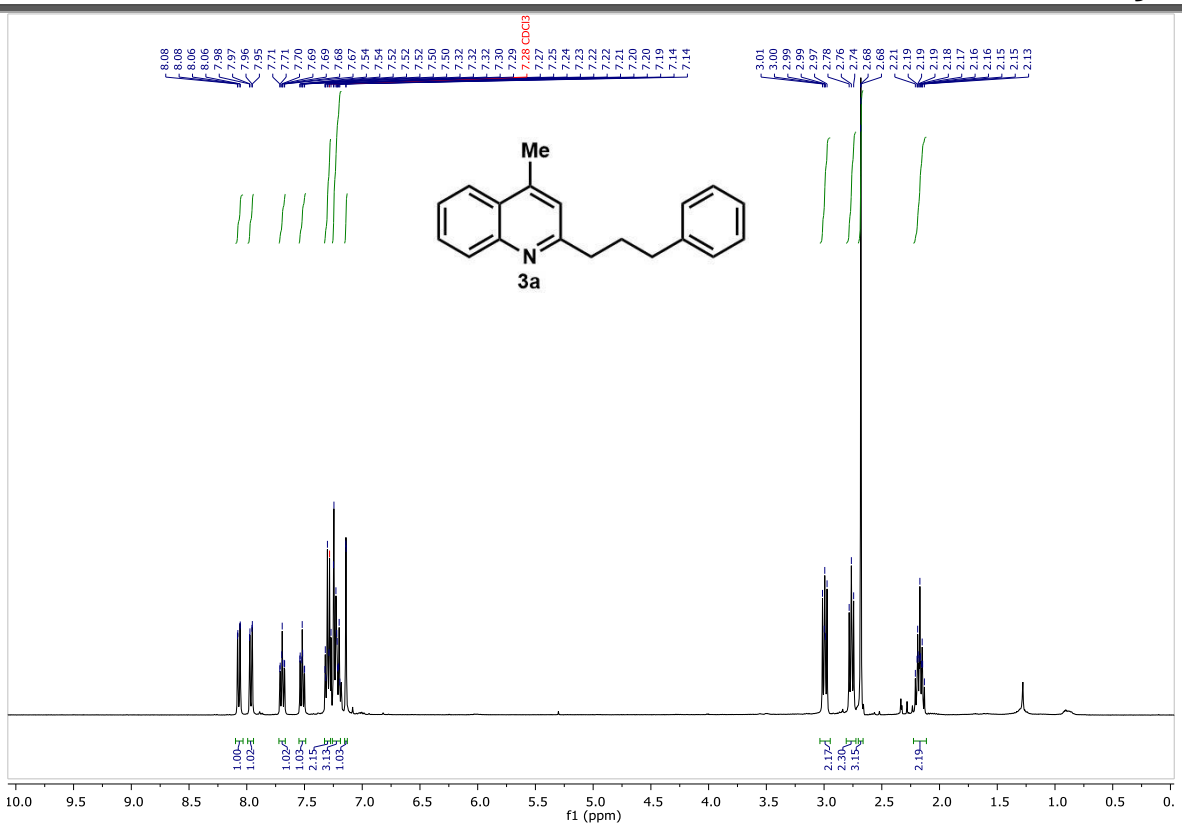

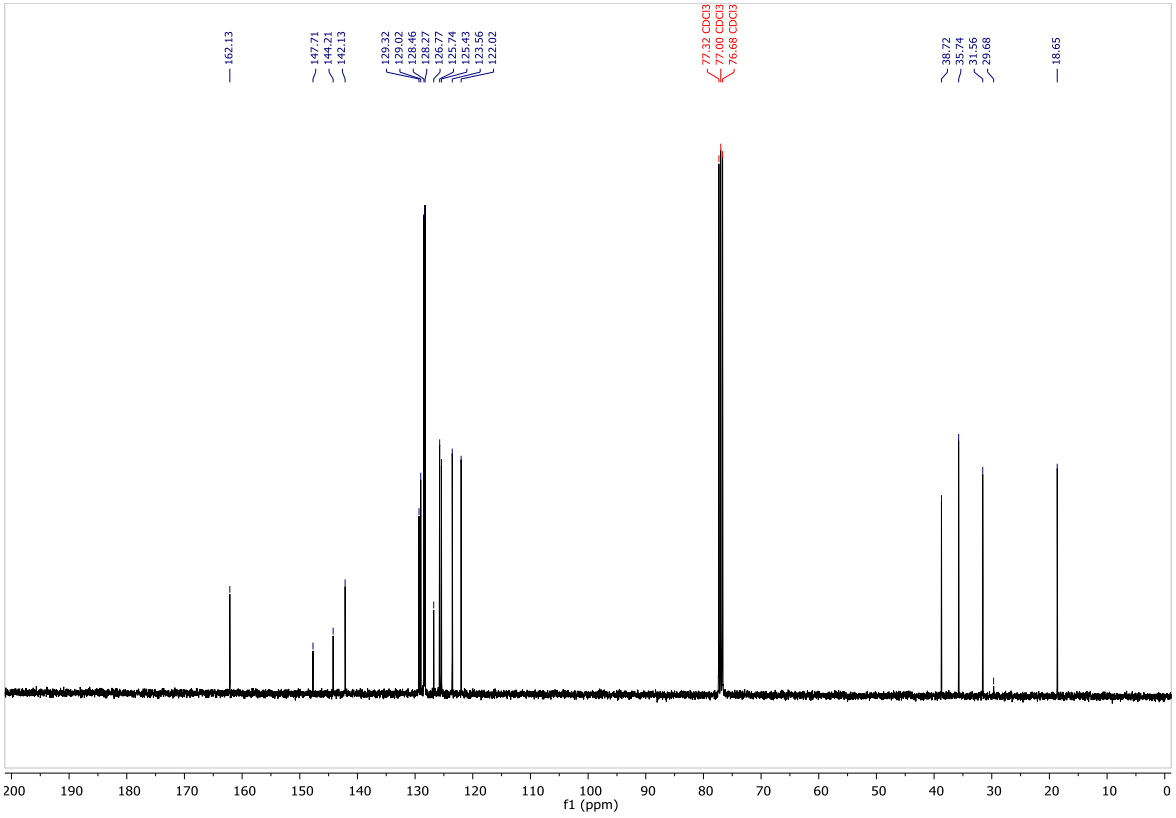

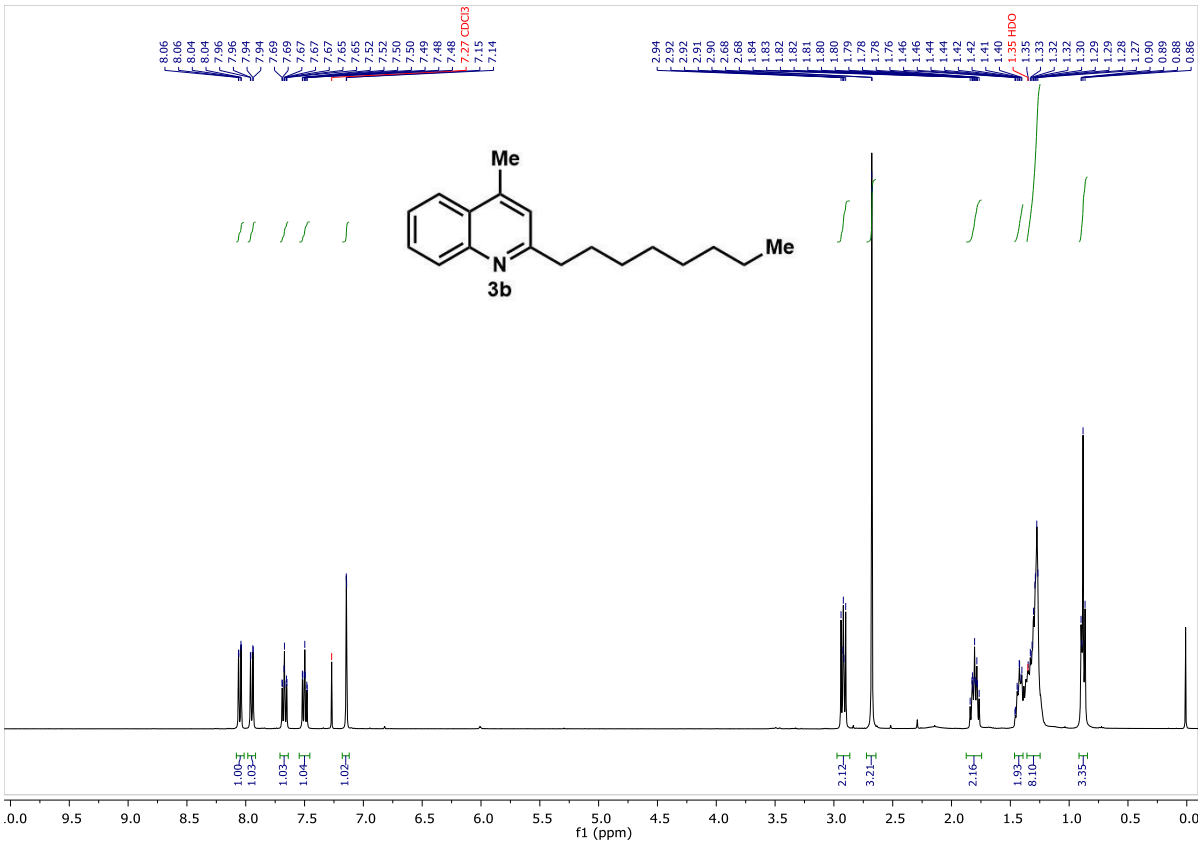
Me
N
Me
3b
f1 (ppm)

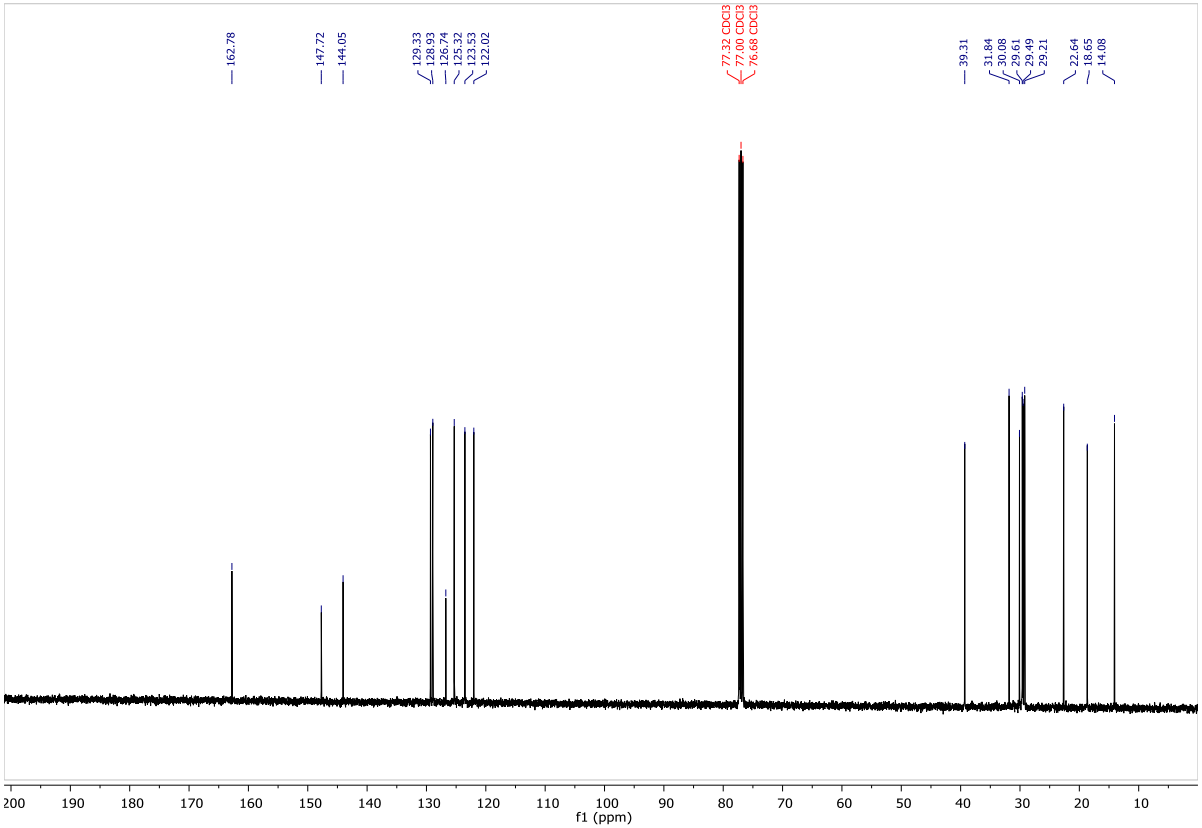
f1 (ppm)

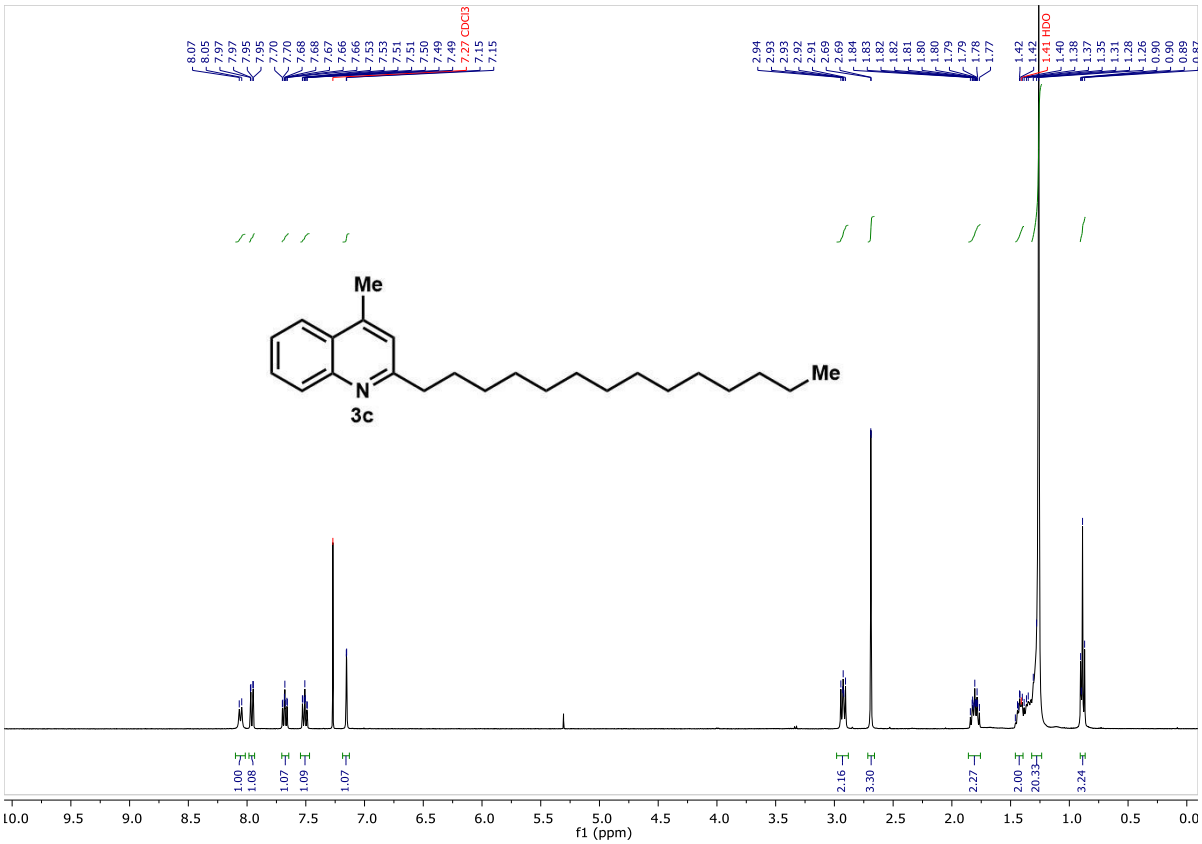
Me
N
Me
3c
f1 (ppm)

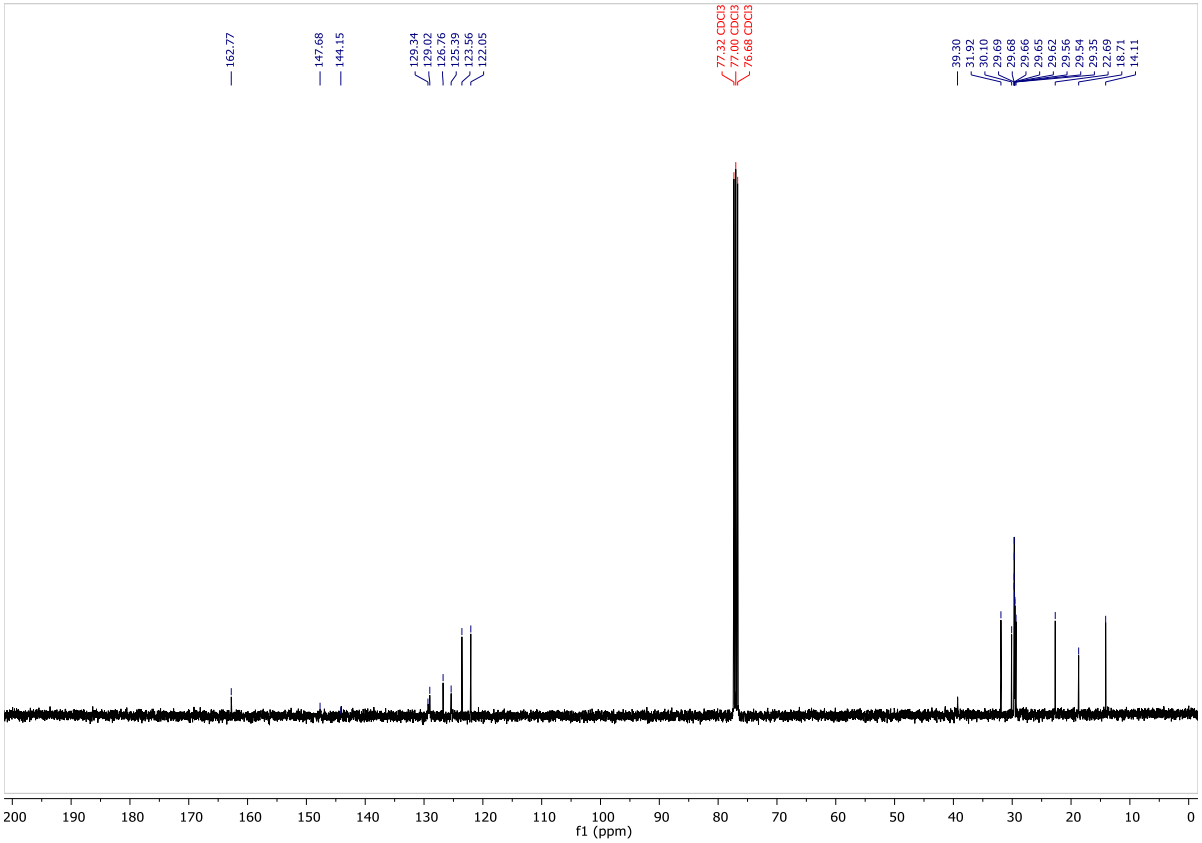
f1 (ppm)

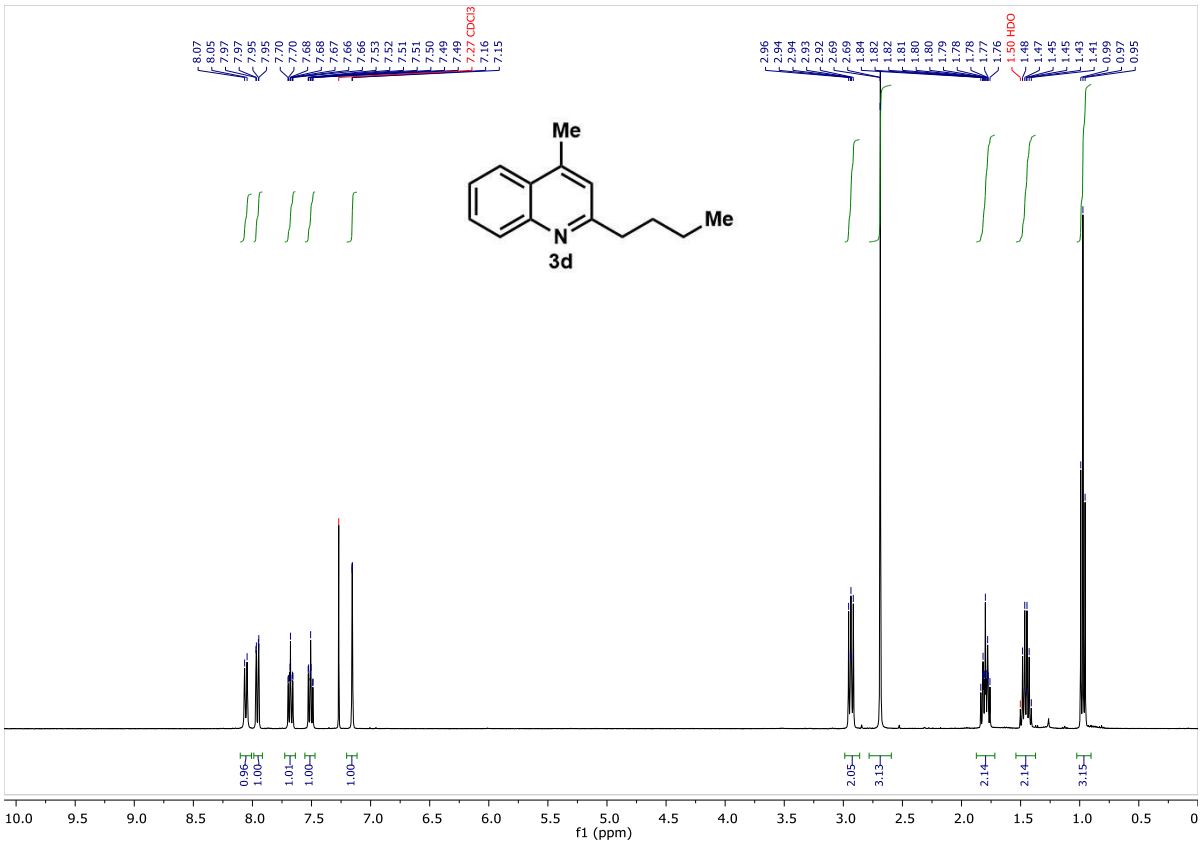
8.07
8.05
7.97
7.97
7.95
7.95
7.70
7.70
7.68
7.68
7.67
7.66
7.66
7.53
7.52
7.51
7.51
7.50
7.49
7.27 CDCl3
7.16
7.15
2.96
2.94
2.94
2.93
2.92
2.69
2.69
1.84
1.82
1.82
1.81
1.80
1.80
1.79
1.78
1.78
1.77
1.76
1.50 HDO
1.48
1.47
1.45
1.45
1.43
1.41
0.99
0.97
0.95
Me
Me
N
3d
0.96
1.00
1.01
1.00
1.00
2.05
3.13
2.14
2.14
3.15
10.0
9.5
9.0
8.5
8.0
7.5
7.0
6.5
6.0
5.5
5.0
4.5
4.0
3.5
3.0
2.5
2.0
1.5
1.0
0.5
0
f1 (ppm)

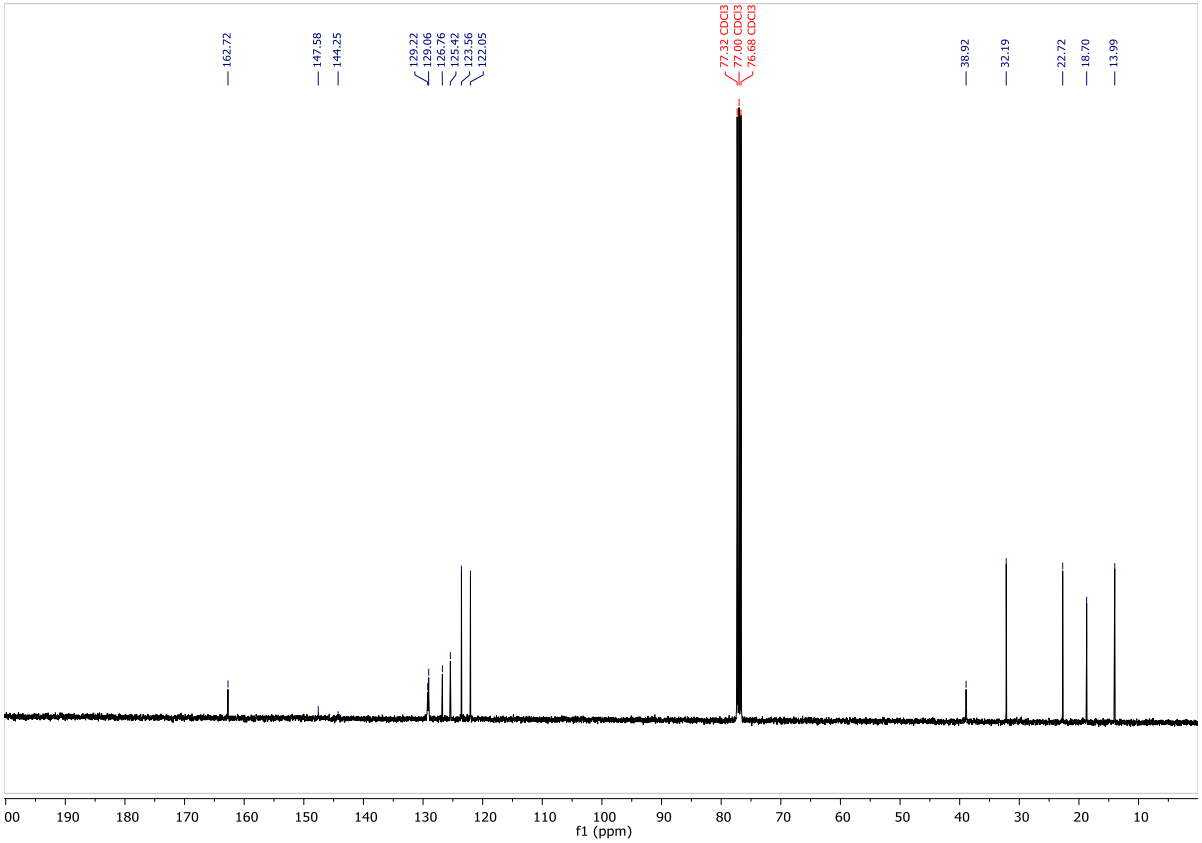
162.72
147.58
144.25
129.22
129.06
126.76
125.42
123.56
122.05
77.32 CDCl3
77.00 CDCl3
76.68 CDCl3
38.92
32.19
22.72
18.70
13.99
00
190
180
170
160
150
140
130
120
110
100
90
80
70
60
50
40
30
20
10
f1 (ppm)

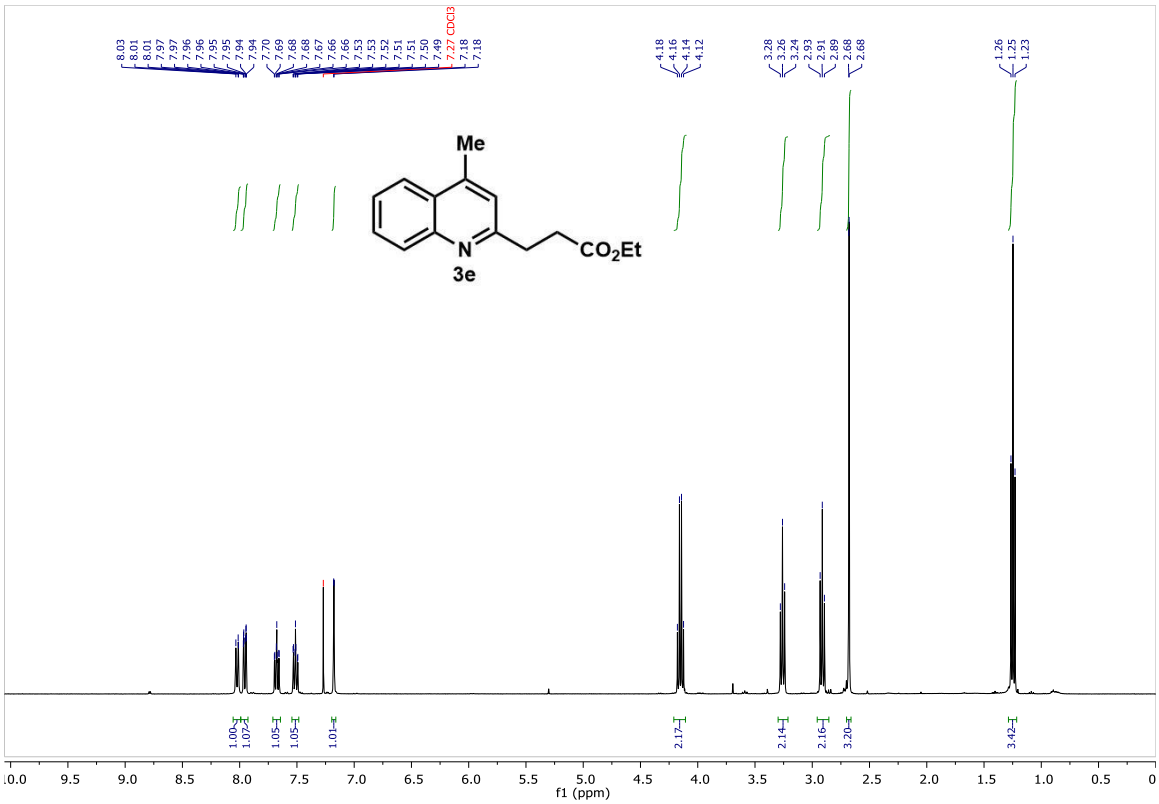
Me
N
CO2Et
3e
f1 (ppm)

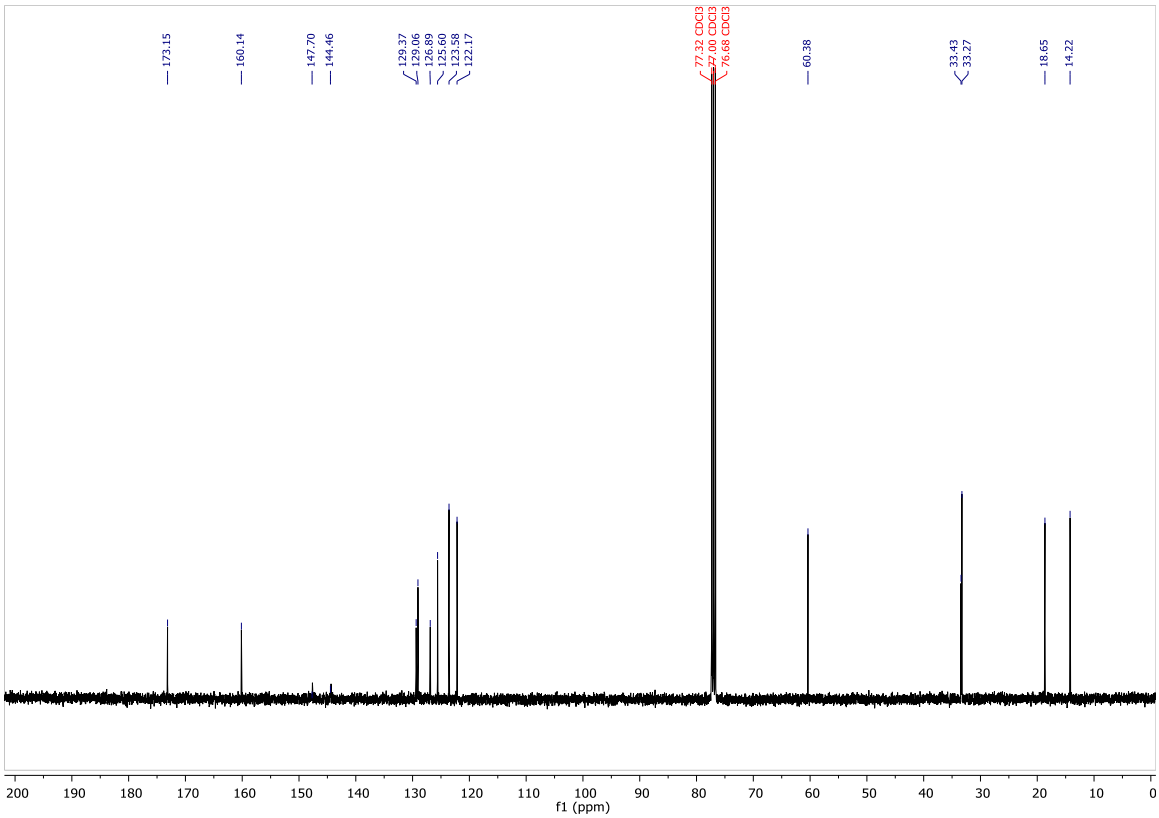
f1 (ppm)

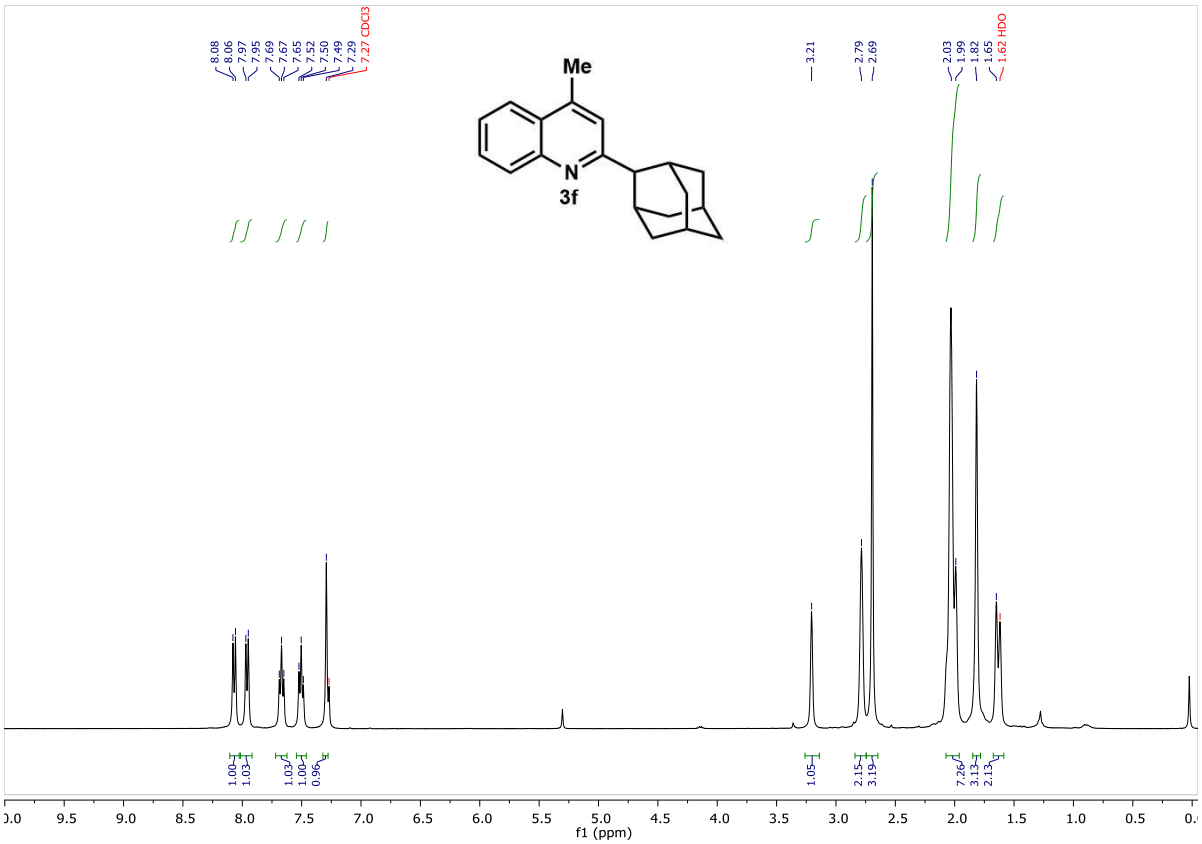
8.08
8.06
7.97
7.95
7.69
7.67
7.65
7.52
7.50
7.49
7.29
7.27 CDCl3
3.21
2.79
2.69
2.03
1.99
1.89
1.65
1.62 HDO
Me
N
3f
1.00
1.03
1.03
1.00
0.96
1.05
2.15
3.19
7.26
3.13
2.13
f1 (ppm)

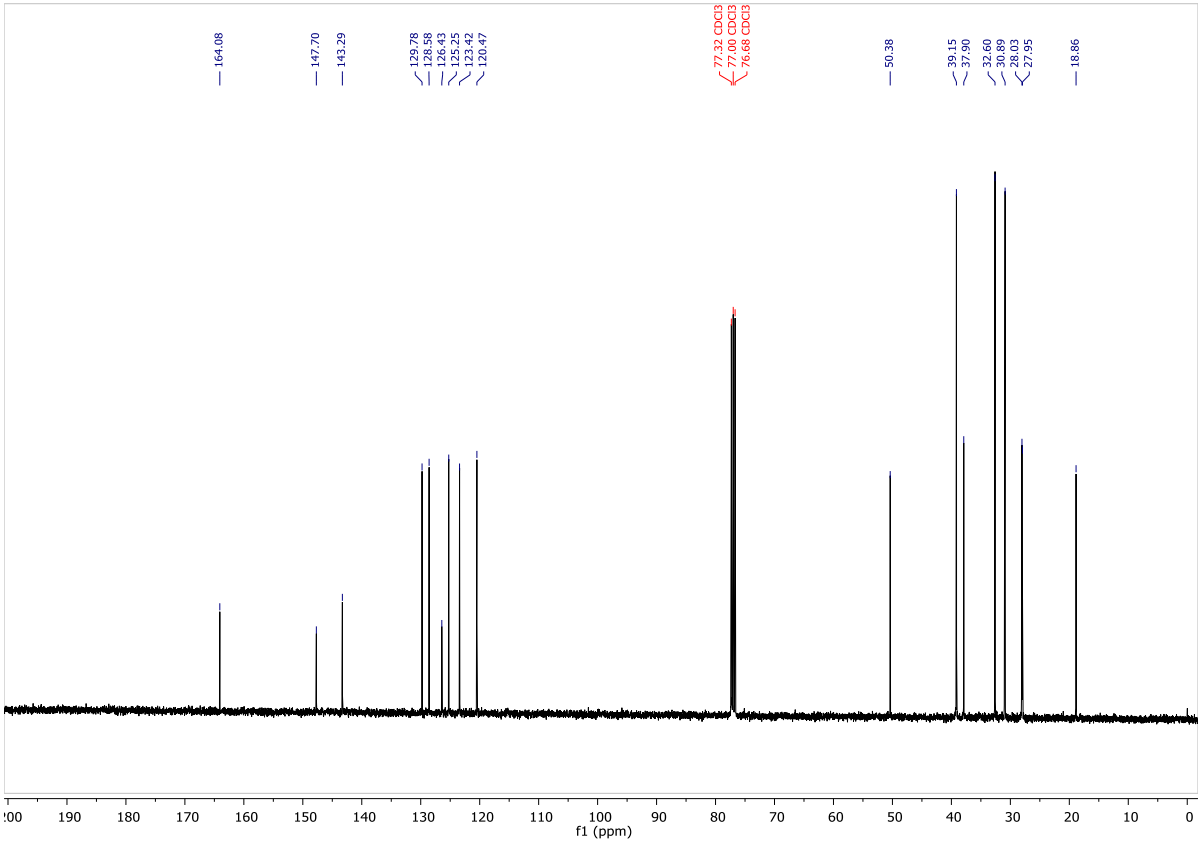
164.08
147.70
143.29
129.78
128.58
126.43
125.25
123.42
120.47
77.32 CDCl3
77.00 CDCl3
76.68 CDCl3
50.38
39.15
37.90
32.60
30.89
28.03
27.95
18.86
f1 (ppm)

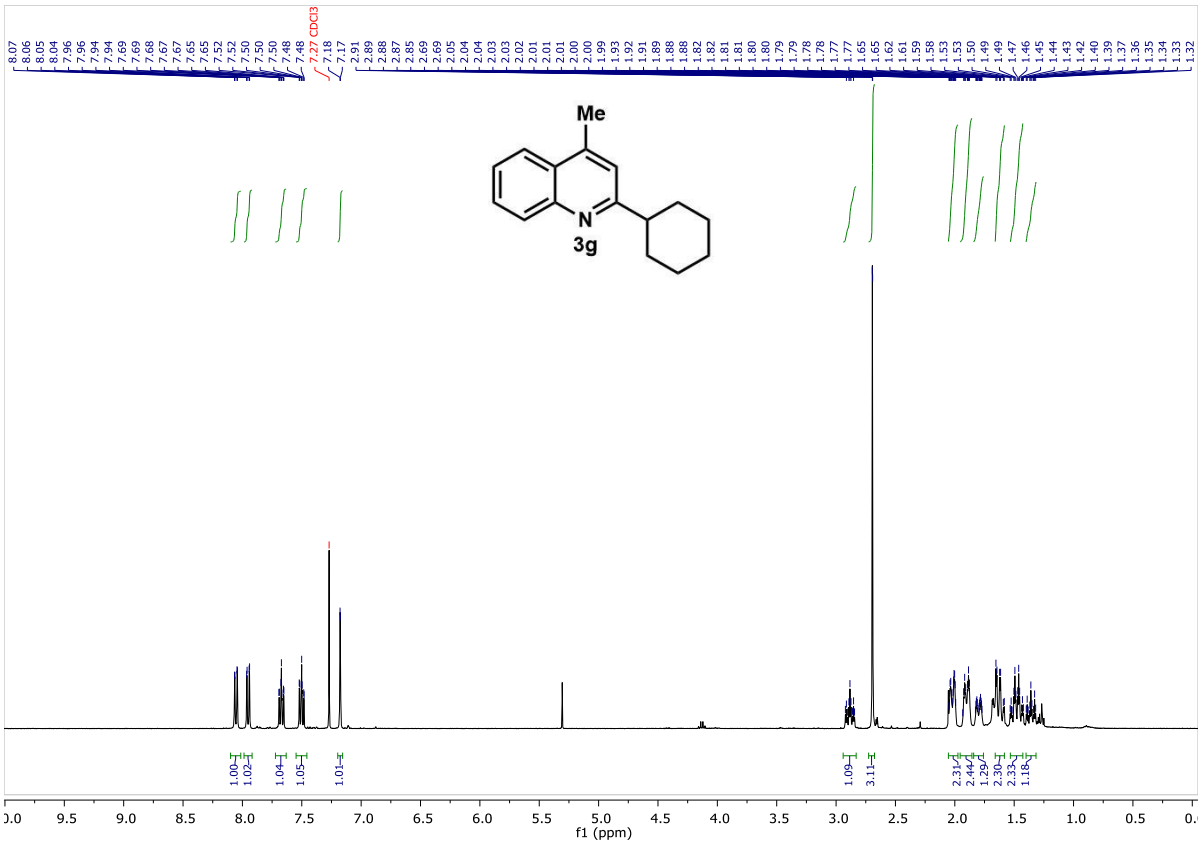
Me
N
3g
f1 (ppm)

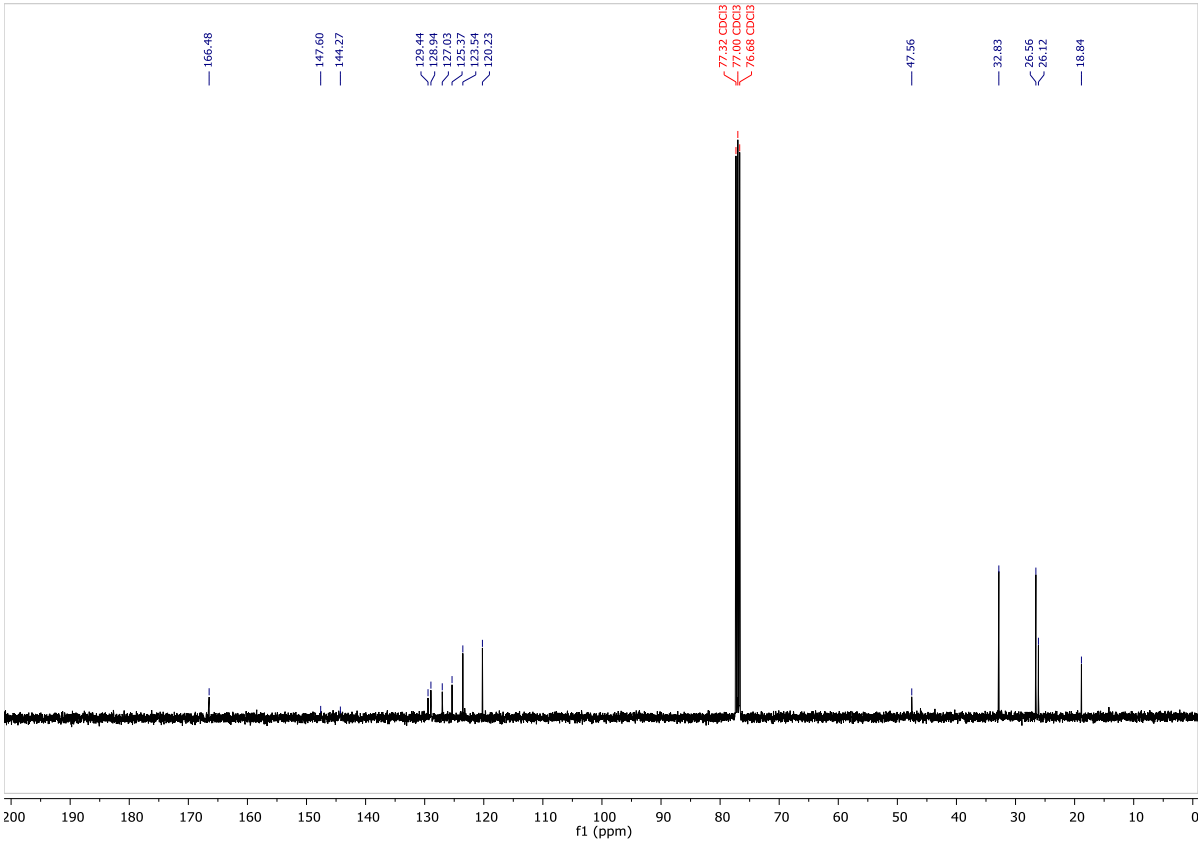
166.48
147.60
144.27
129.44
128.94
127.03
125.37
123.54
120.23
77.32 CDCl3
77.00 CDCl3
76.68 CDCl3
47.56
32.83
26.56
26.12
18.84
f1 (ppm)

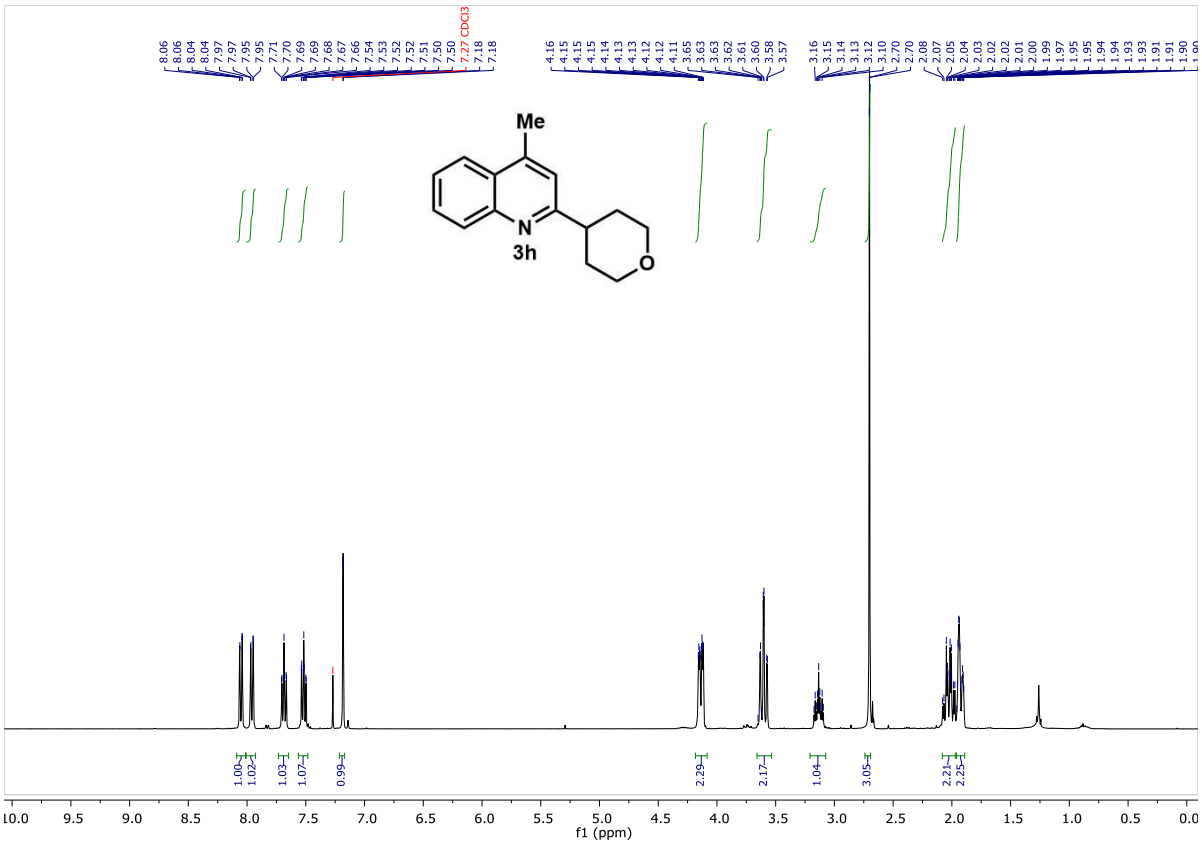
Me
N
3h
O
f1 (ppm)

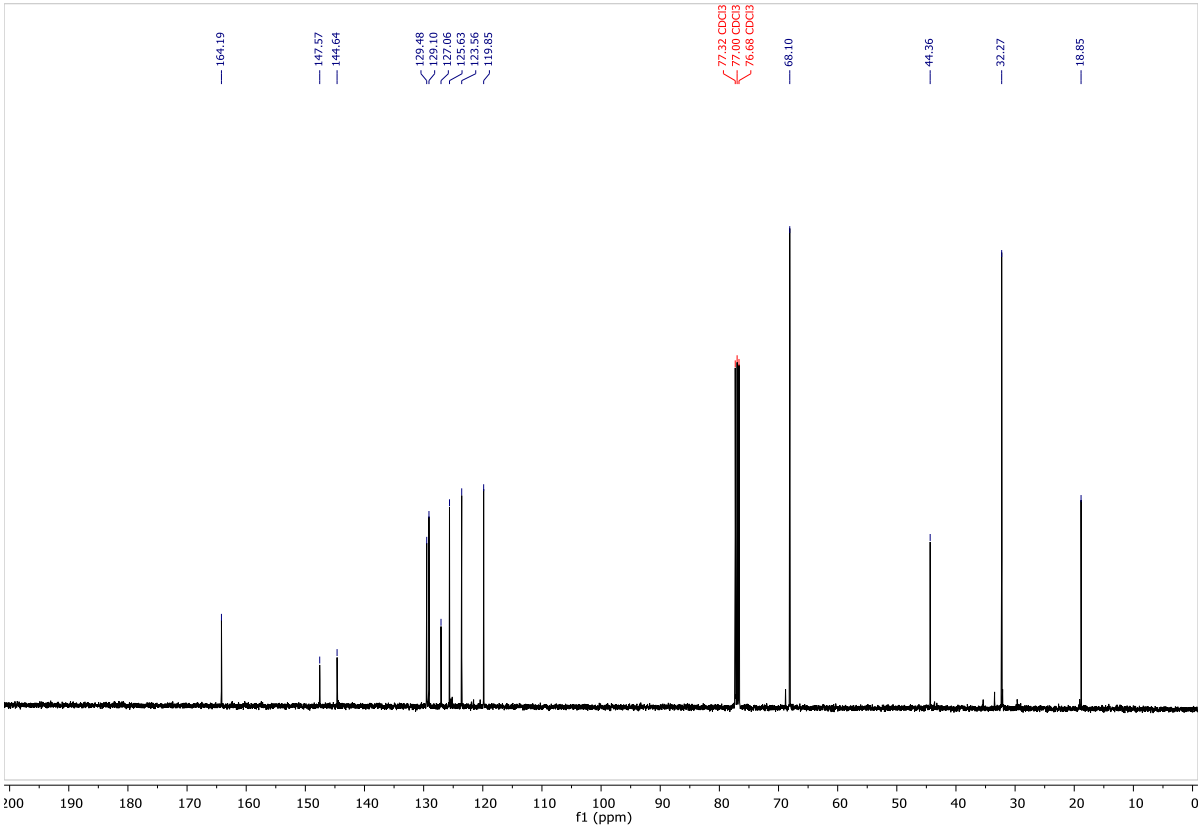
164.19
147.57
144.64
129.48
129.10
127.06
125.63
123.56
119.85
77.32 CDCl3
77.00 CDCl3
76.68 CDCl3
68.10
44.36
32.27
18.85
f1 (ppm)

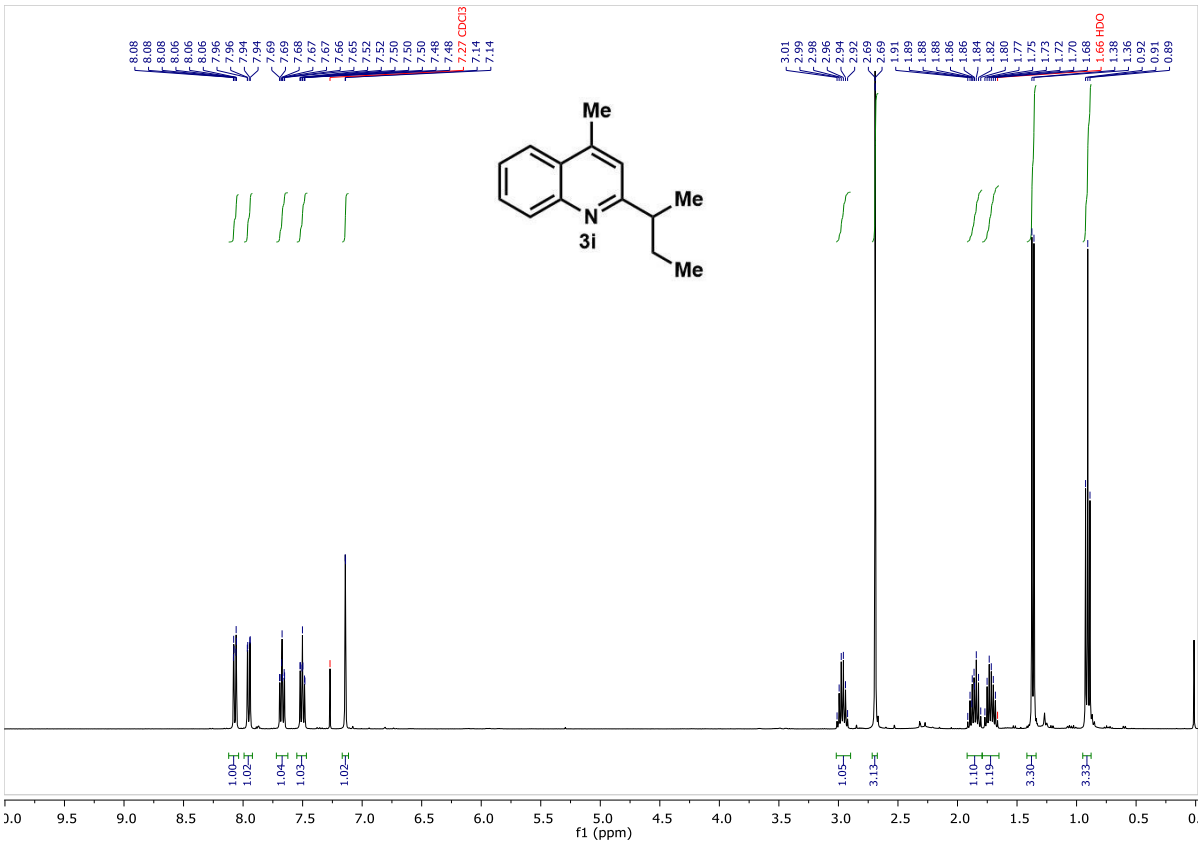
Me
Me
N
Me
3i
f1 (ppm)

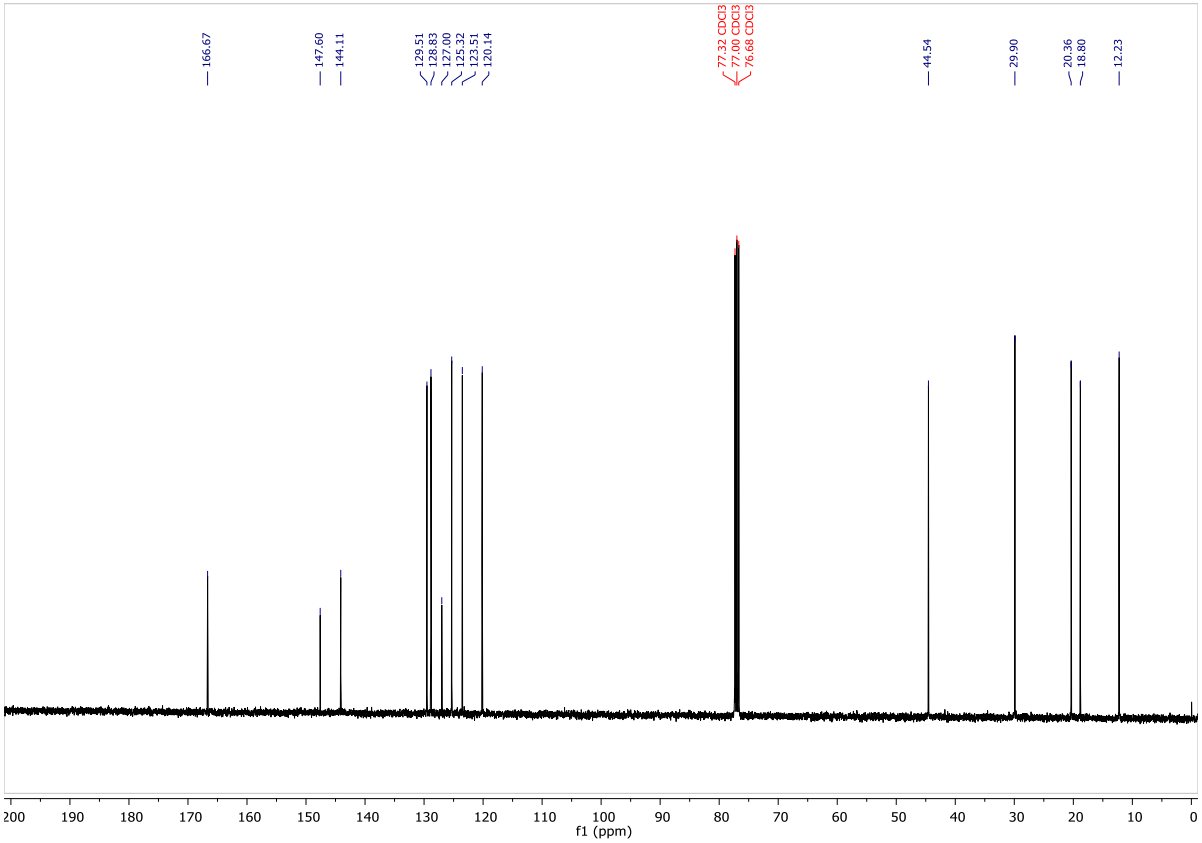
f1 (ppm)

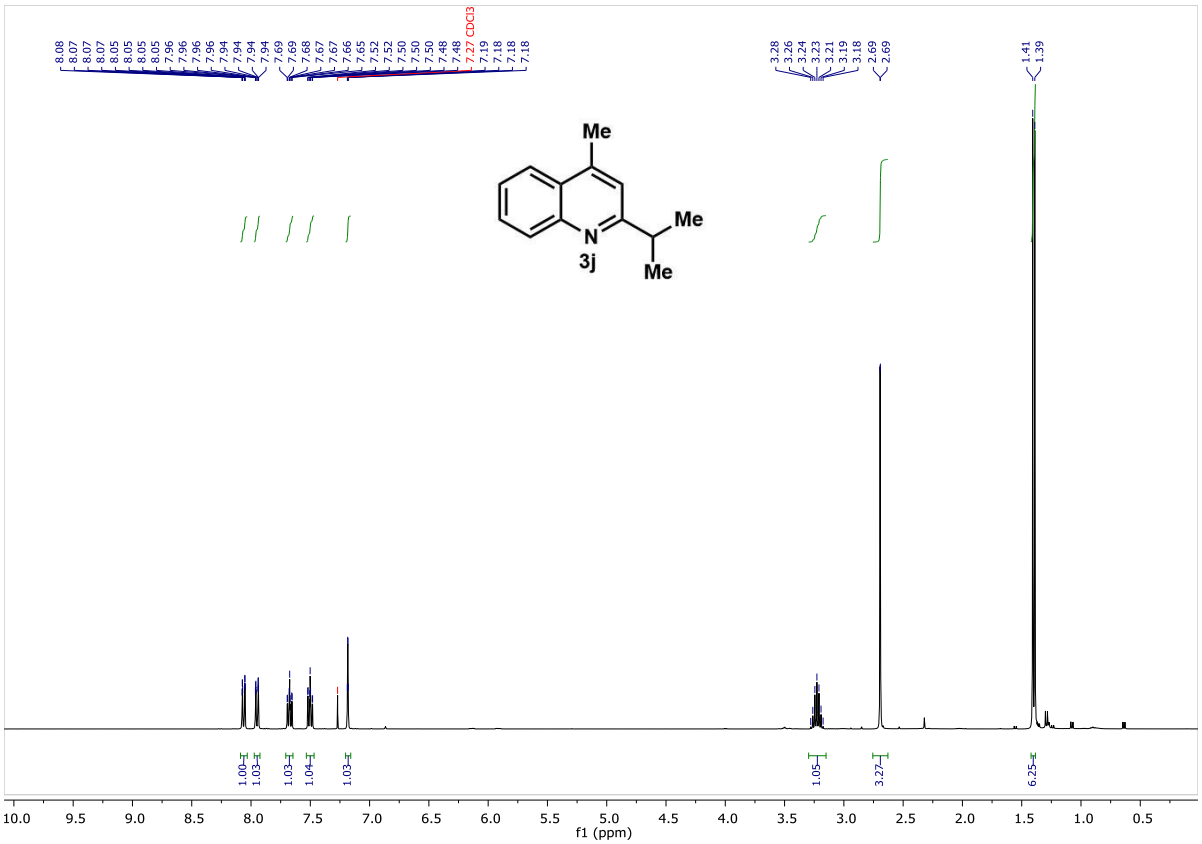
Me
Me
N
Me
3j
f1 (ppm)

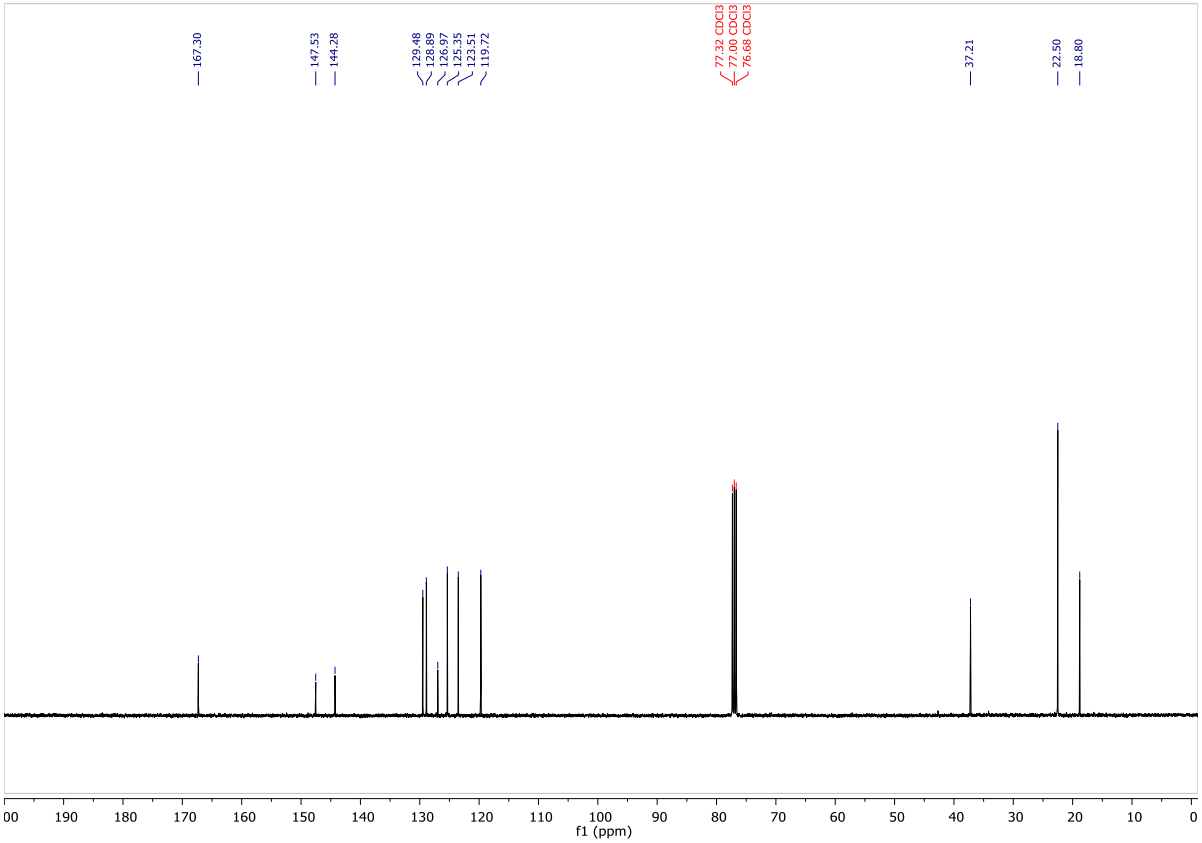
f1 (ppm)

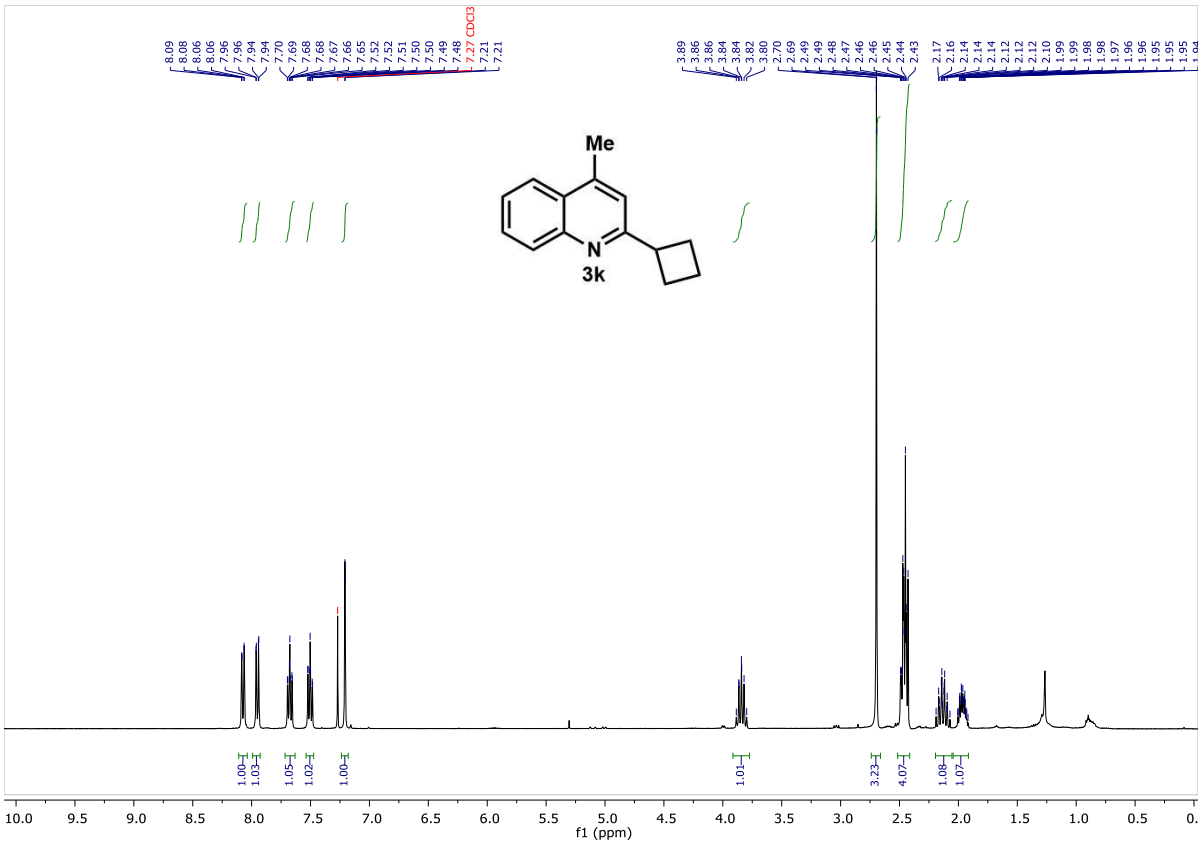
Me
N
3k
CDCl3
f1 (ppm)

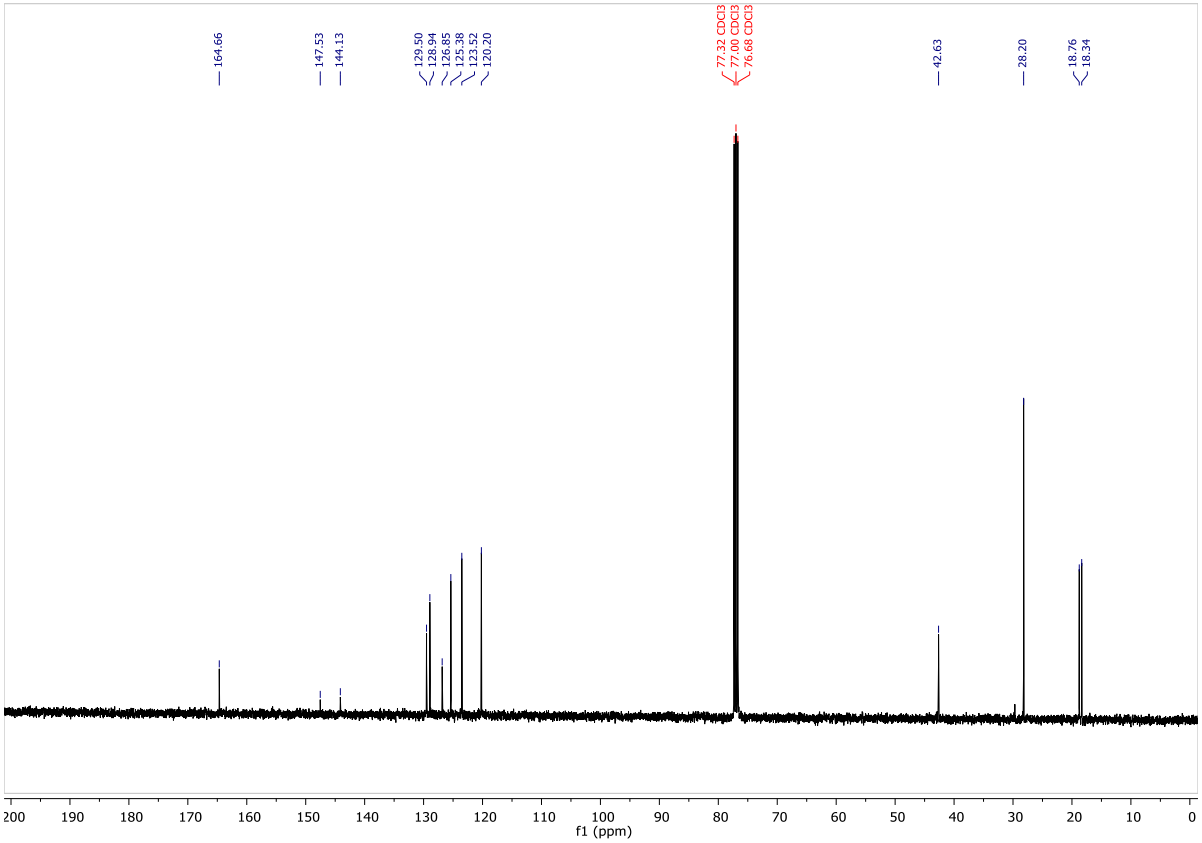
164.66
147.53
144.13
129.50
128.94
126.85
125.38
123.52
120.20
77.32 CDCl3
77.00 CDCl3
76.68 CDCl3
42.63
28.20
18.76
18.34
f1 (ppm)

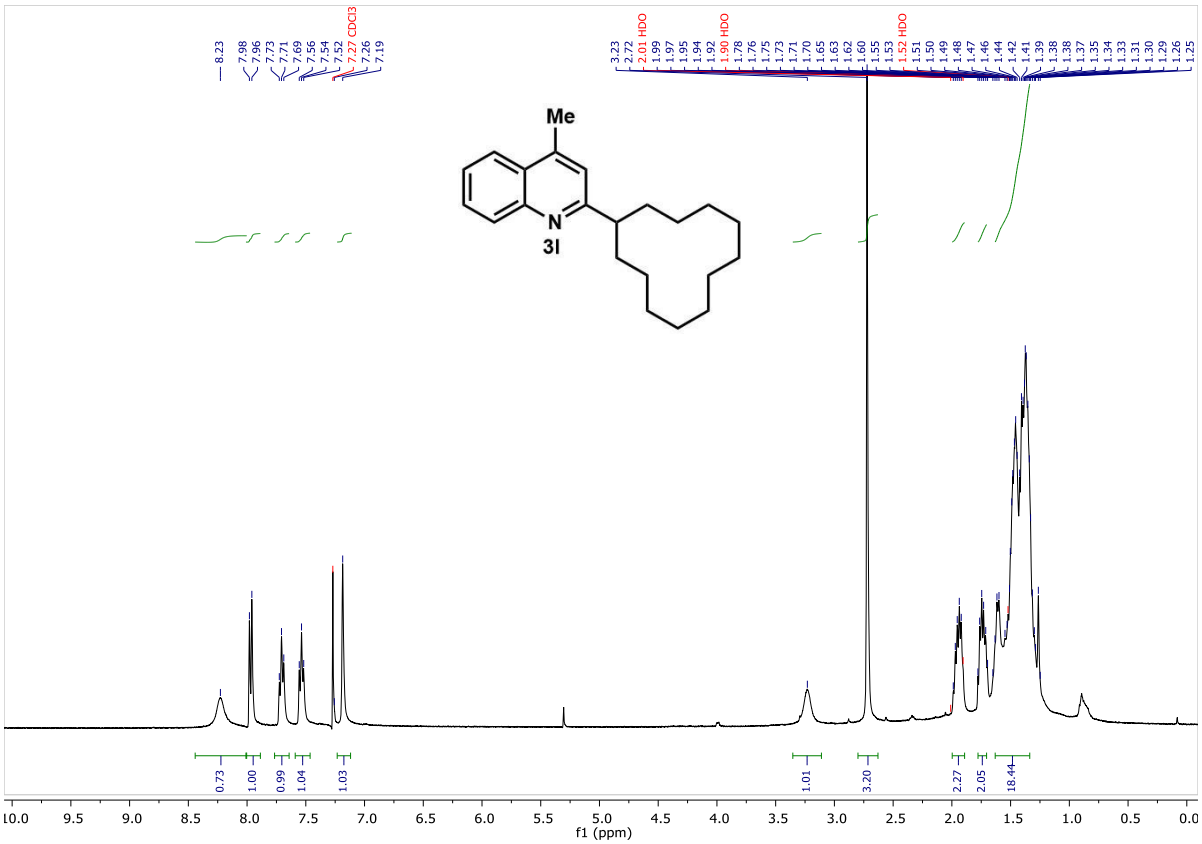
Me
N
3l
f1 (ppm)

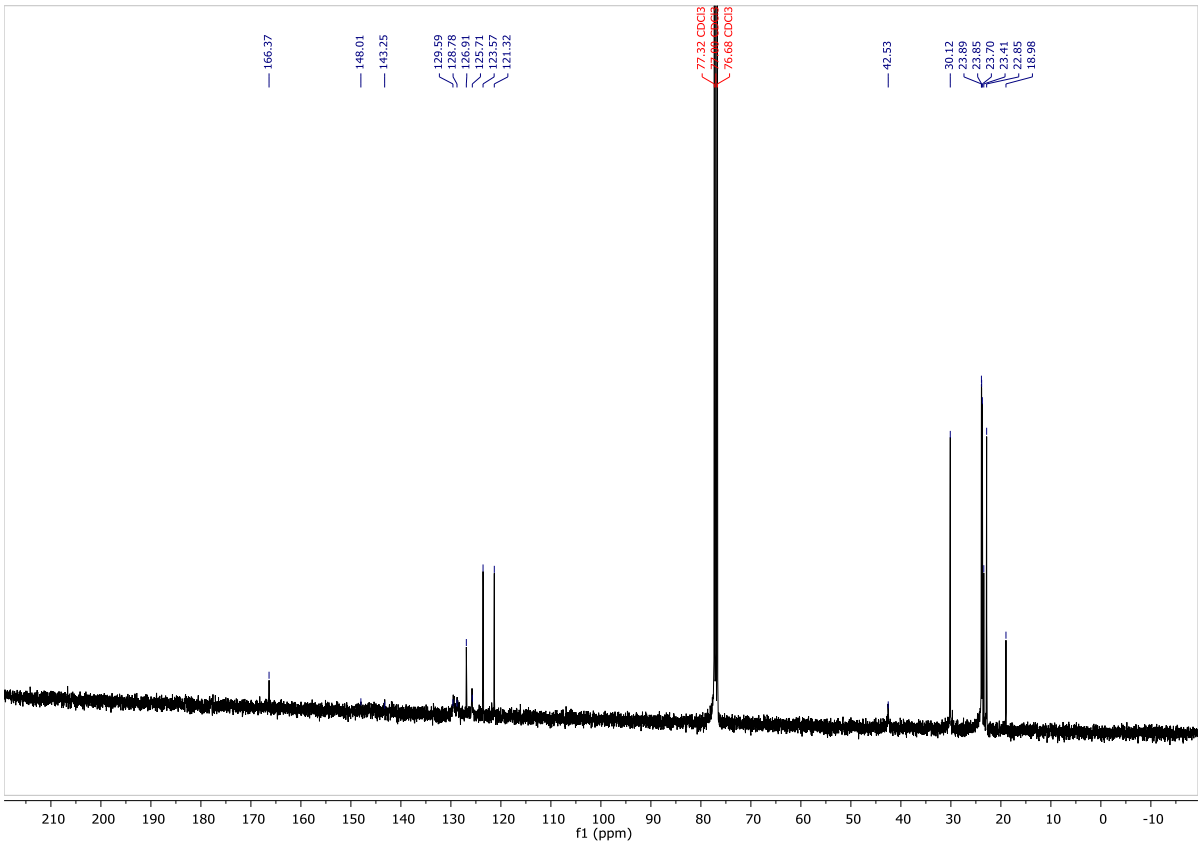
f1 (ppm)

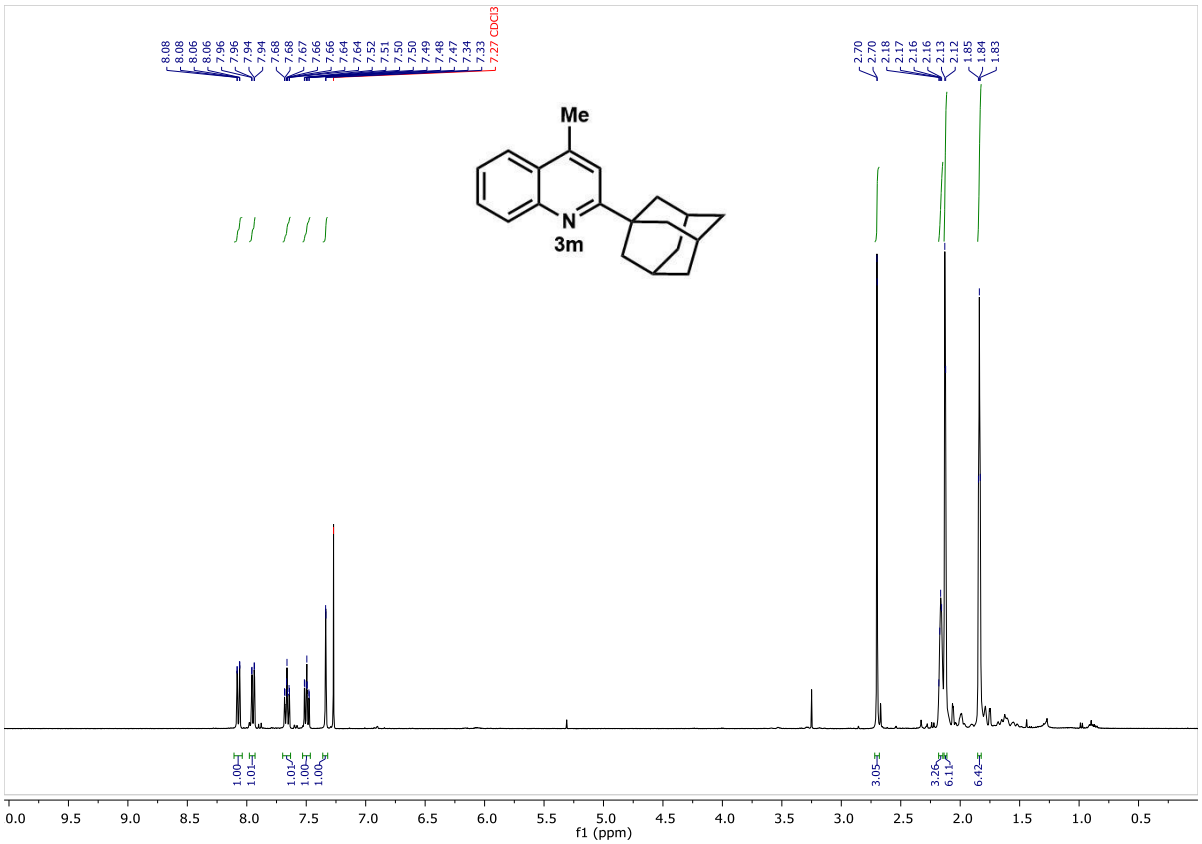
8.08
8.08
8.06
8.06
8.06
7.96
7.96
7.94
7.94
7.68
7.68
7.67
7.66
7.66
7.64
7.64
7.52
7.51
7.50
7.50
7.49
7.48
7.47
7.34
7.33
7.27 CDCl3
2.70
2.70
2.18
2.17
2.16
2.16
2.13
2.12
1.85
1.84
1.83
Me
N
3m
1.00
1.01
1.01
1.00
1.00
3.05
3.26
6.11
6.42
f1 (ppm)

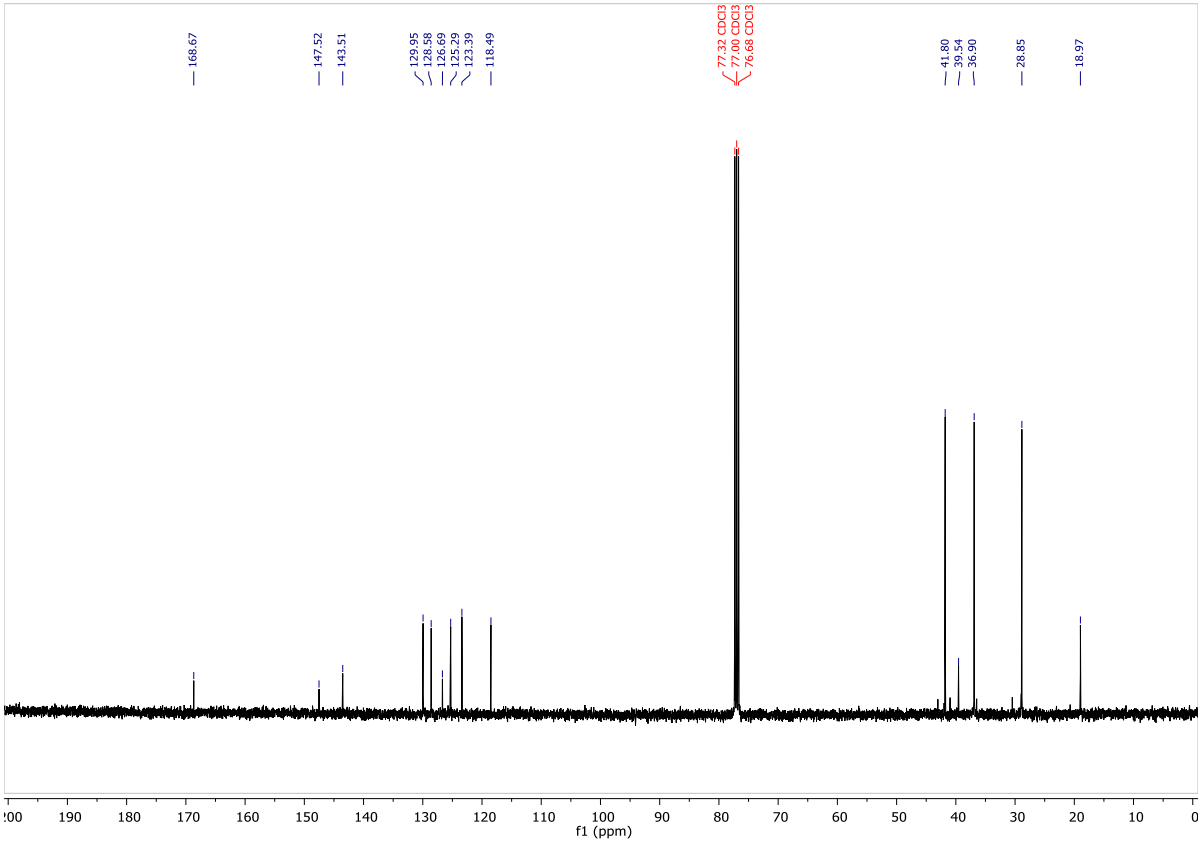
168.67
147.52
143.51
129.95
128.58
126.69
125.29
123.39
118.49
77.32 CDCl3
77.00 CDCl3
76.68 CDCl3
41.80
39.54
36.90
28.85
18.97
f1 (ppm)

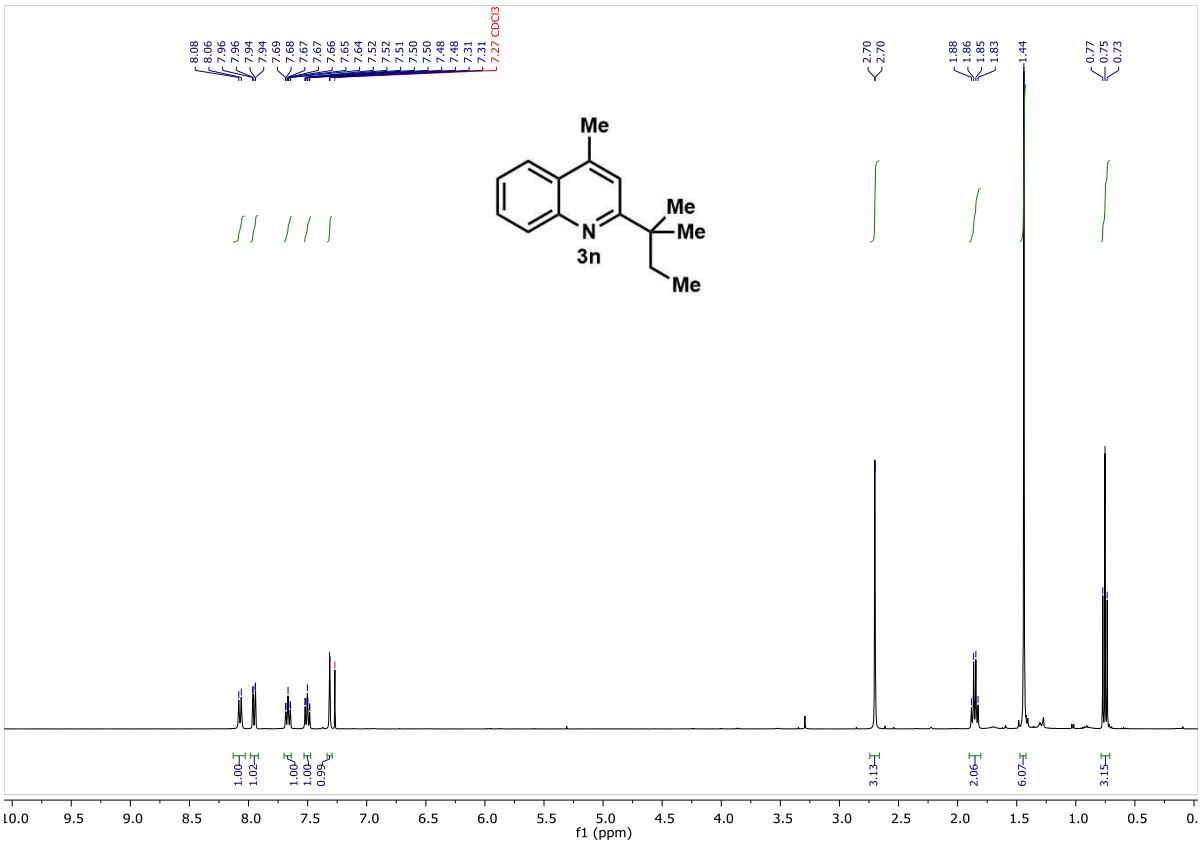
8.08
8.06
7.96
7.96
7.94
7.94
7.69
7.68
7.67
7.67
7.66
7.65
7.64
7.52
7.51
7.50
7.50
7.48
7.48
7.31
7.31
7.27 CDCl3
2.70
2.70
1.88
1.86
1.85
1.83
1.44
0.77
0.75
0.73
Me
Me
Me
N
3n
Me
1.00
1.02
1.00
1.00
0.99
3.13
2.06
6.07
3.15
f1 (ppm)

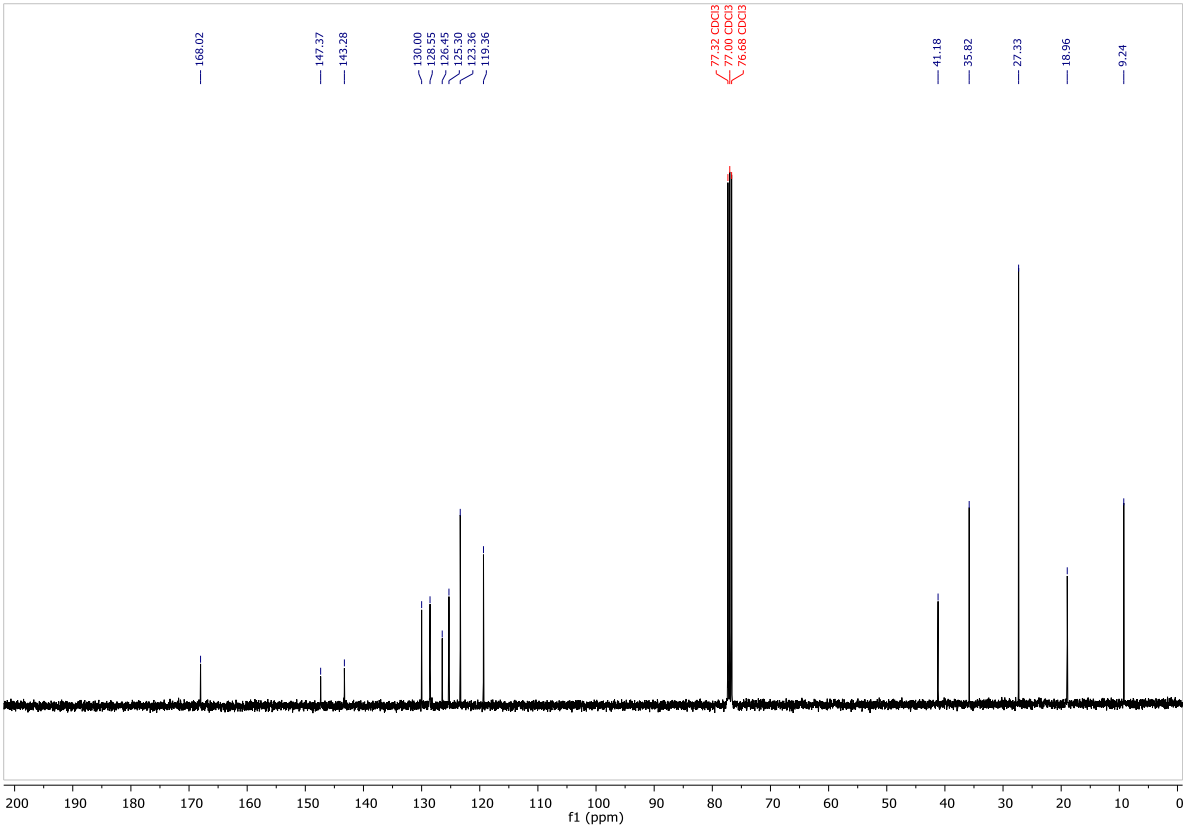
168.02
147.37
143.28
130.00
128.55
126.45
125.30
123.36
119.36
77.33 CDCl3
77.00 CDCl3
76.68 CDCl3
41.18
35.82
27.33
18.96
9.24
f1 (ppm)

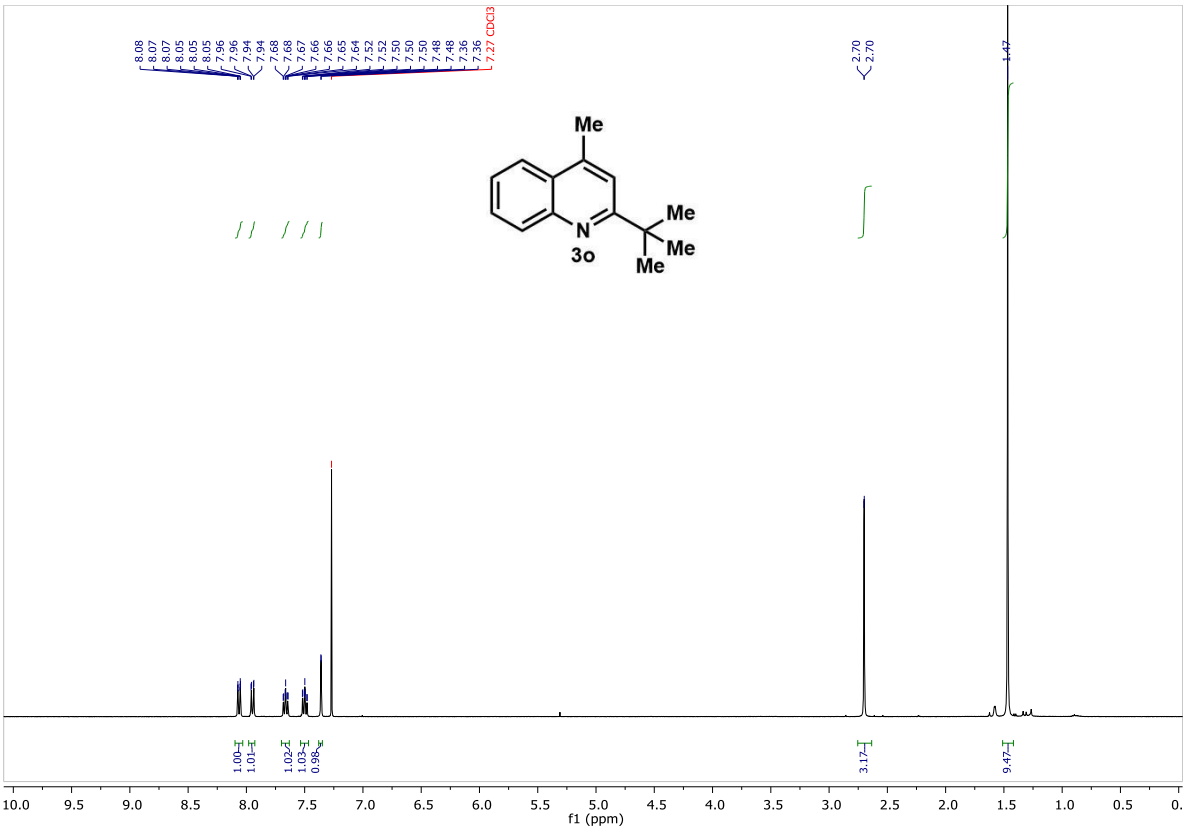
8.08
8.07
8.07
8.05
8.05
8.05
7.96
7.96
7.94
7.94
7.68
7.68
7.67
7.66
7.66
7.65
7.64
7.52
7.50
7.50
7.50
7.48
7.36
7.36
7.27 CDCl3
2.70
2.70
1.47
Me
N
Me
Me
Me
3o
1.00
1.01
1.02
1.03
0.98
3.17
9.47
f1 (ppm)

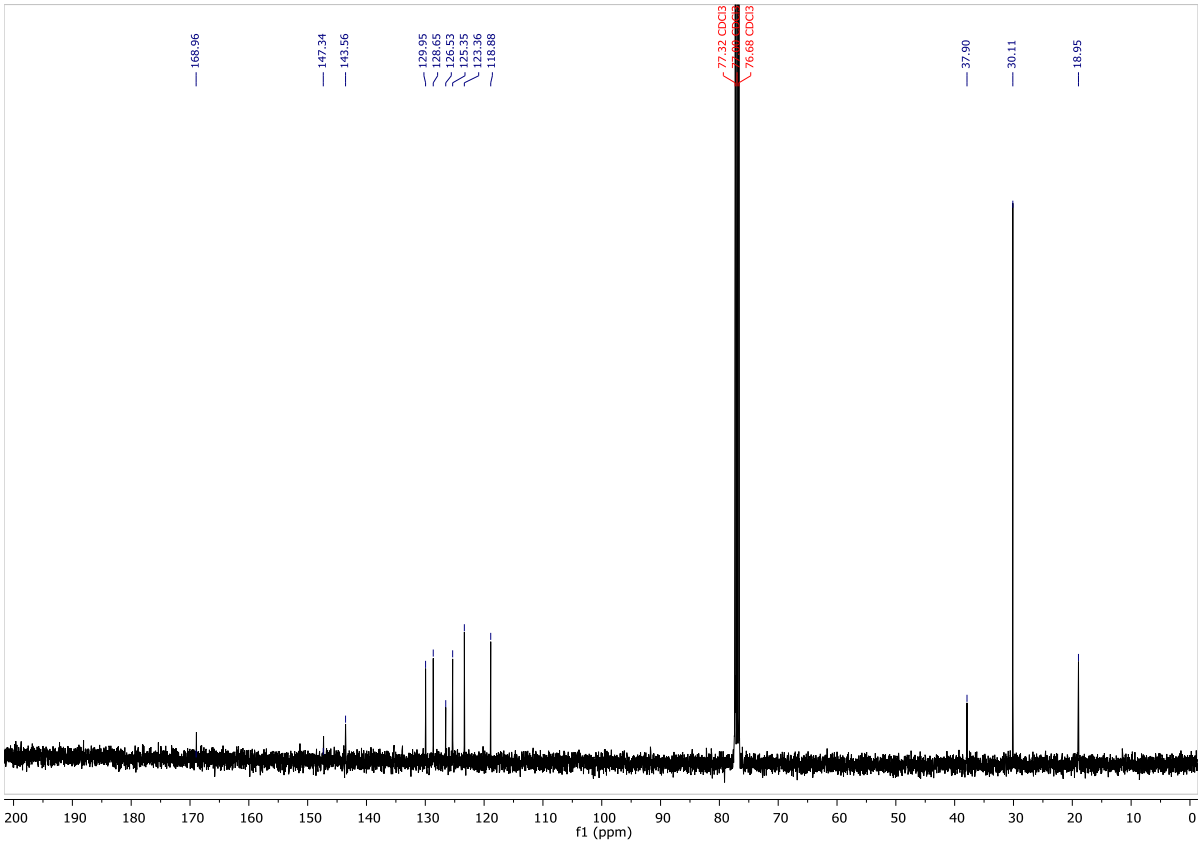
168.96
147.34
143.56
129.95
128.65
126.53
125.35
123.36
118.88
77.32 CDCl3
76.68 CDCl3
37.90
30.11
18.95
f1 (ppm)

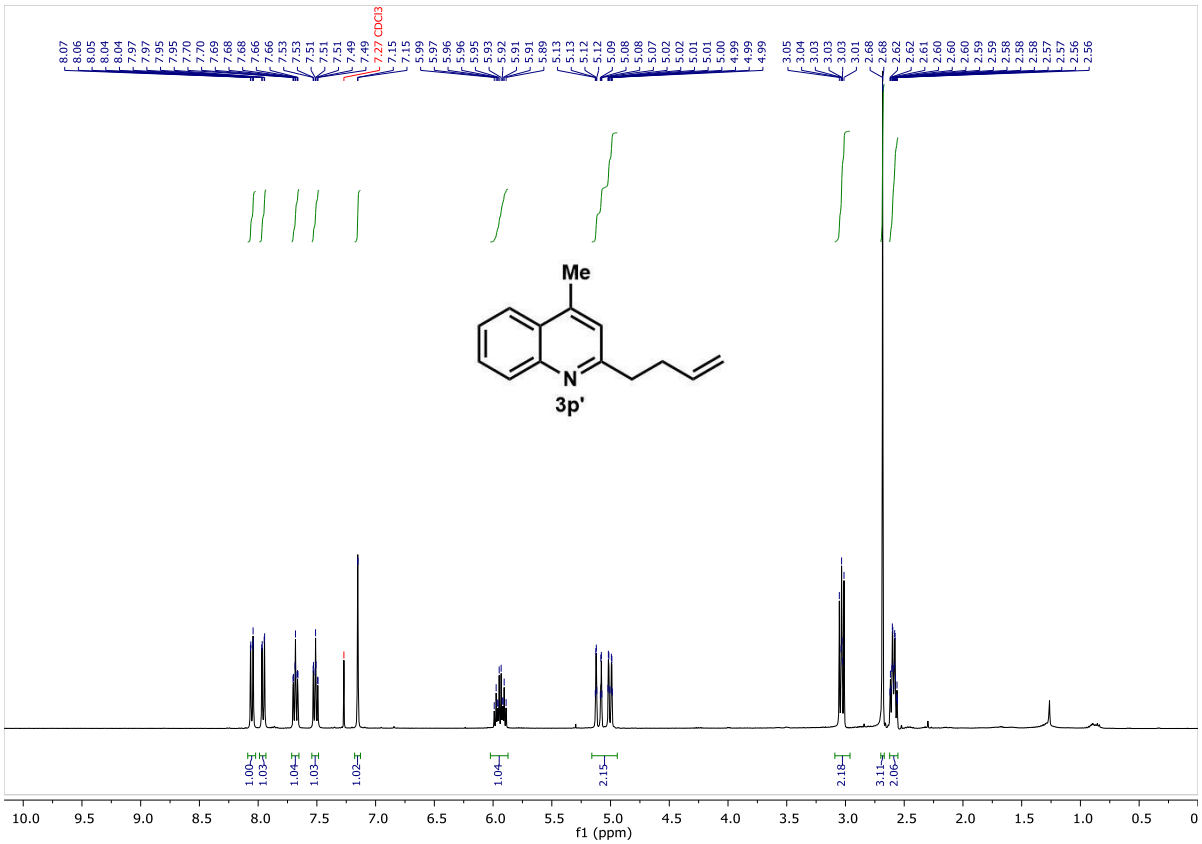
Me
N
3p'
f1 (ppm)

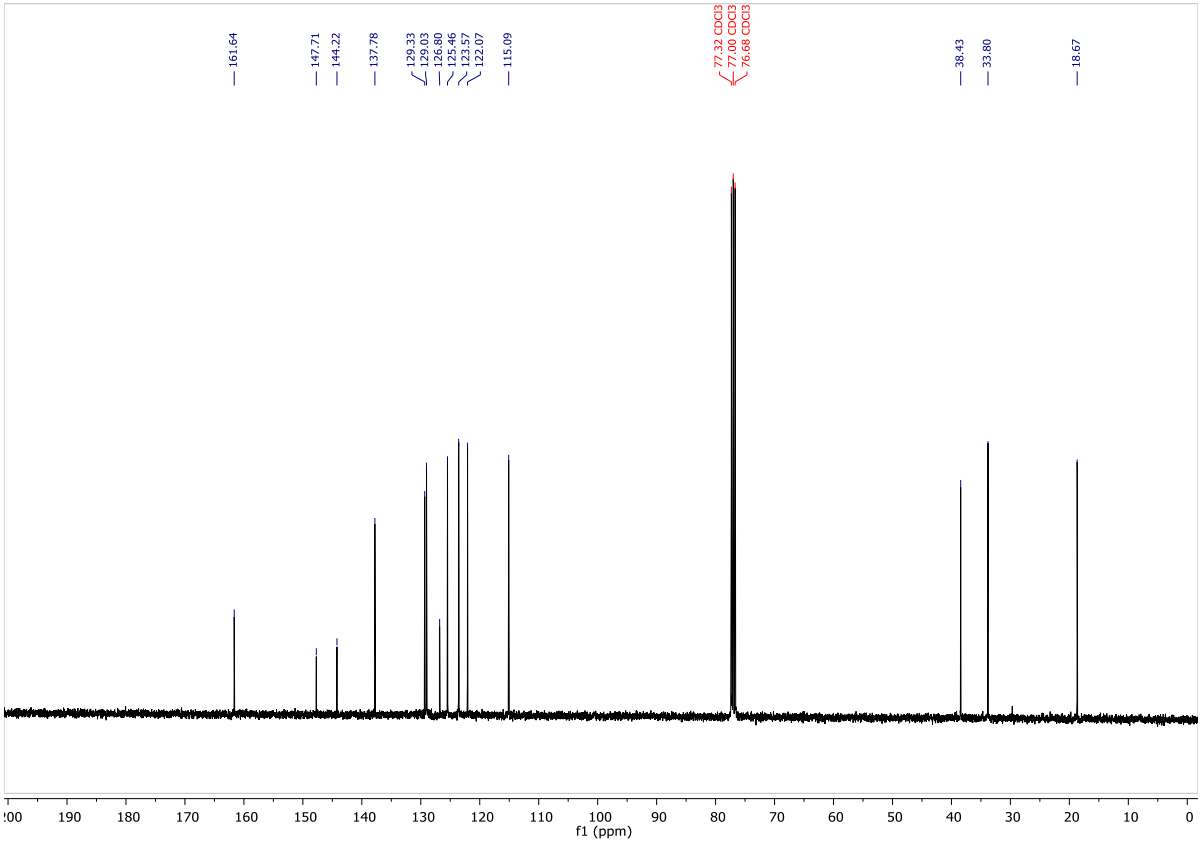
161.64
147.71
144.22
137.78
129.33
129.03
126.80
125.46
123.57
122.07
115.09
77.32 CDCl3
77.00 CDCl3
76.68 CDCl3
38.43
33.80
18.67
f1 (ppm)

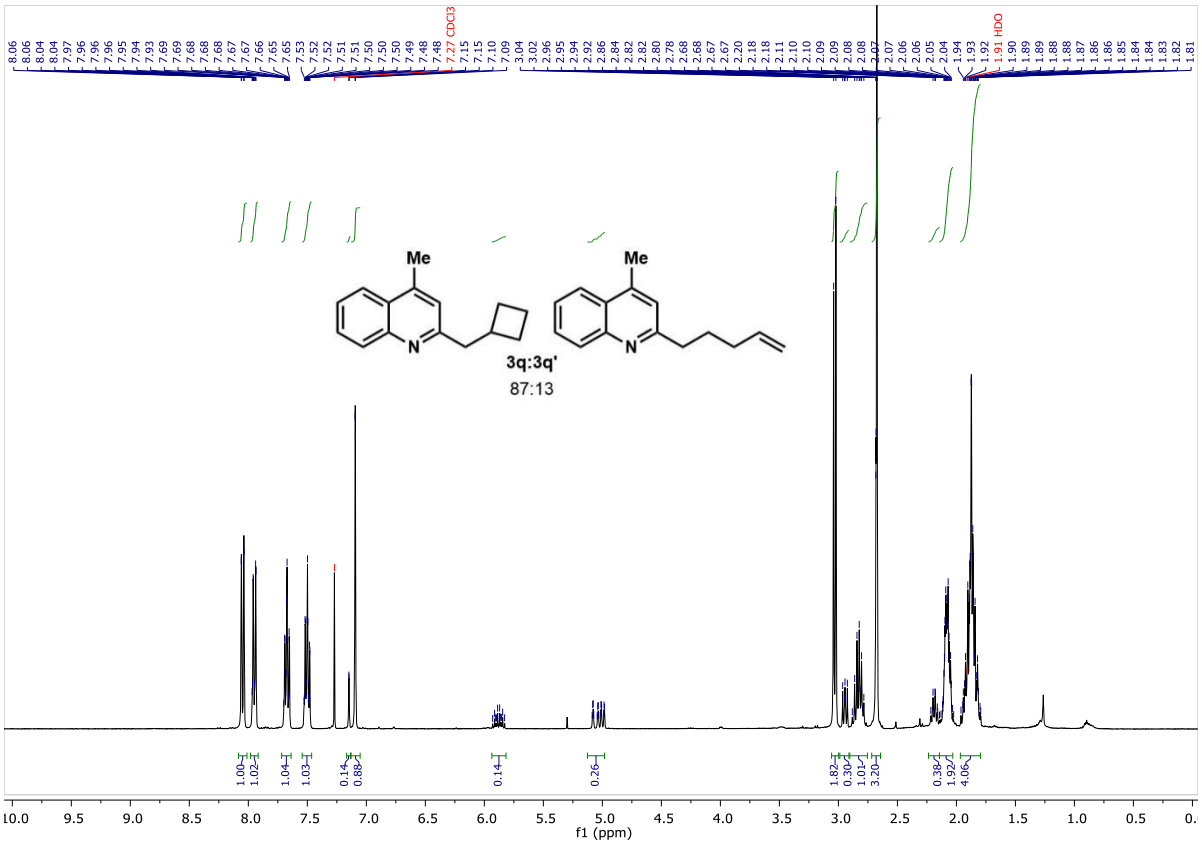
Me
N
Me
N
3q:3q'
87:13
f1 (ppm)

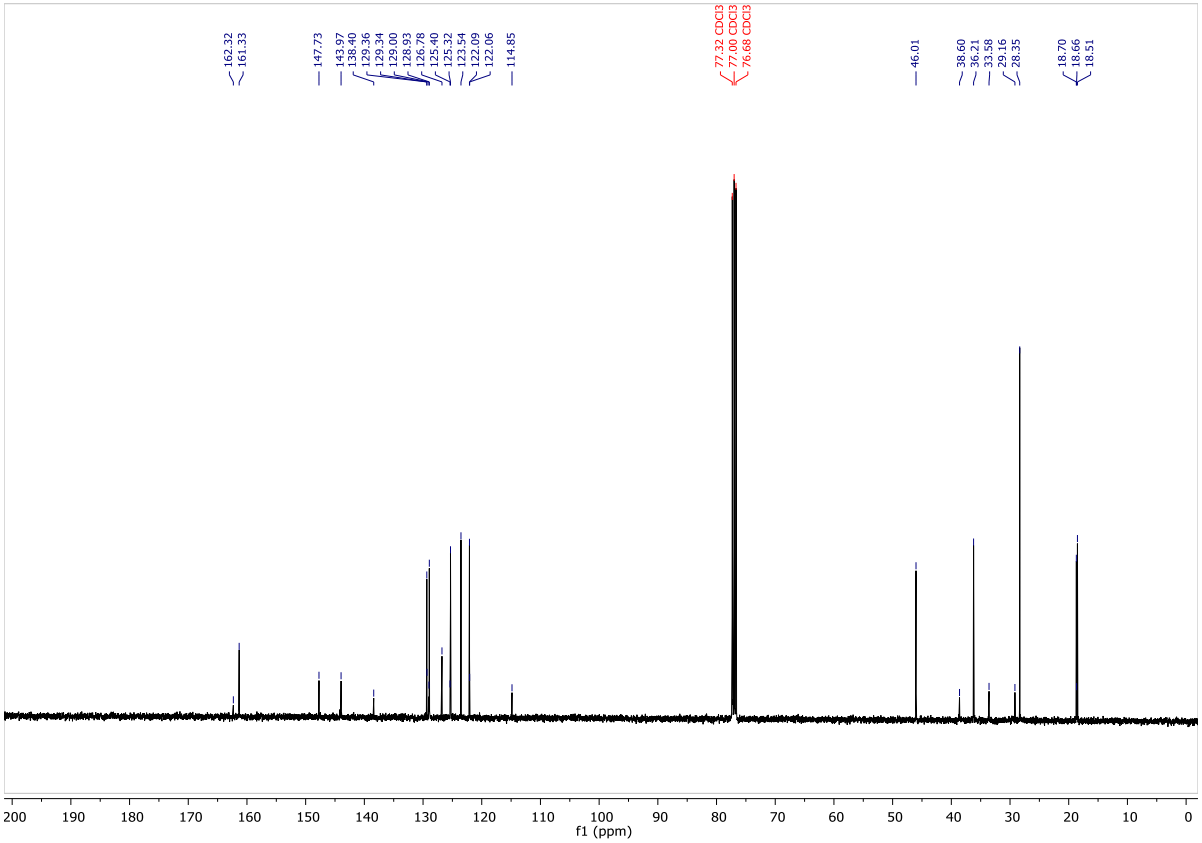
f1 (ppm)

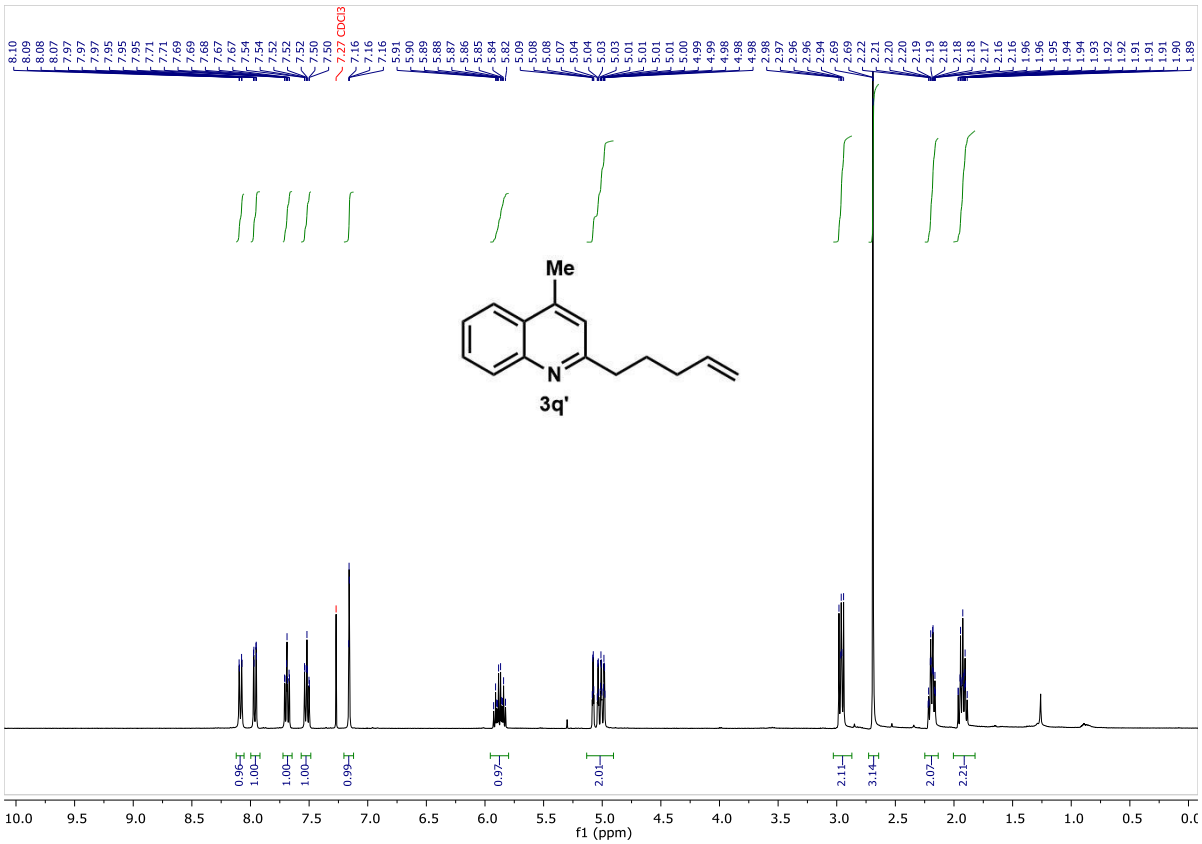
Me
N
3q'
f1 (ppm)

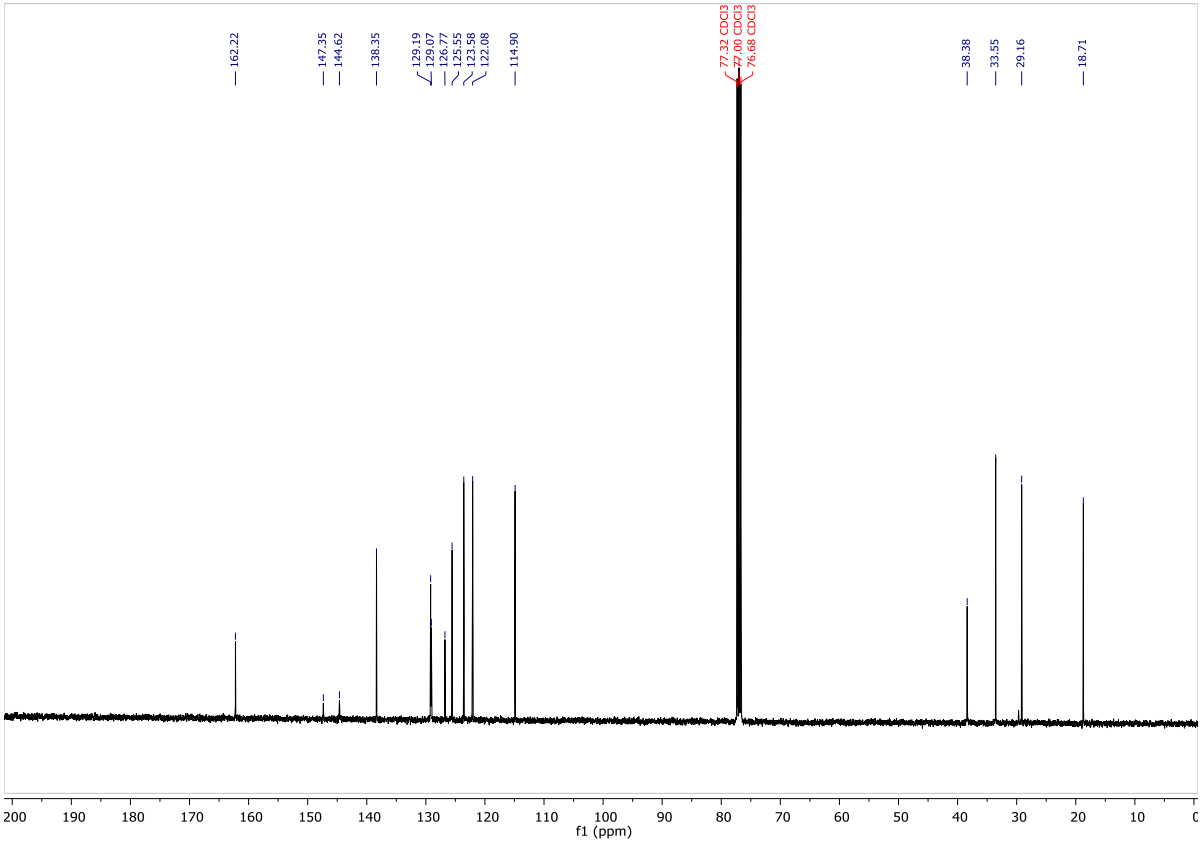
f1 (ppm)

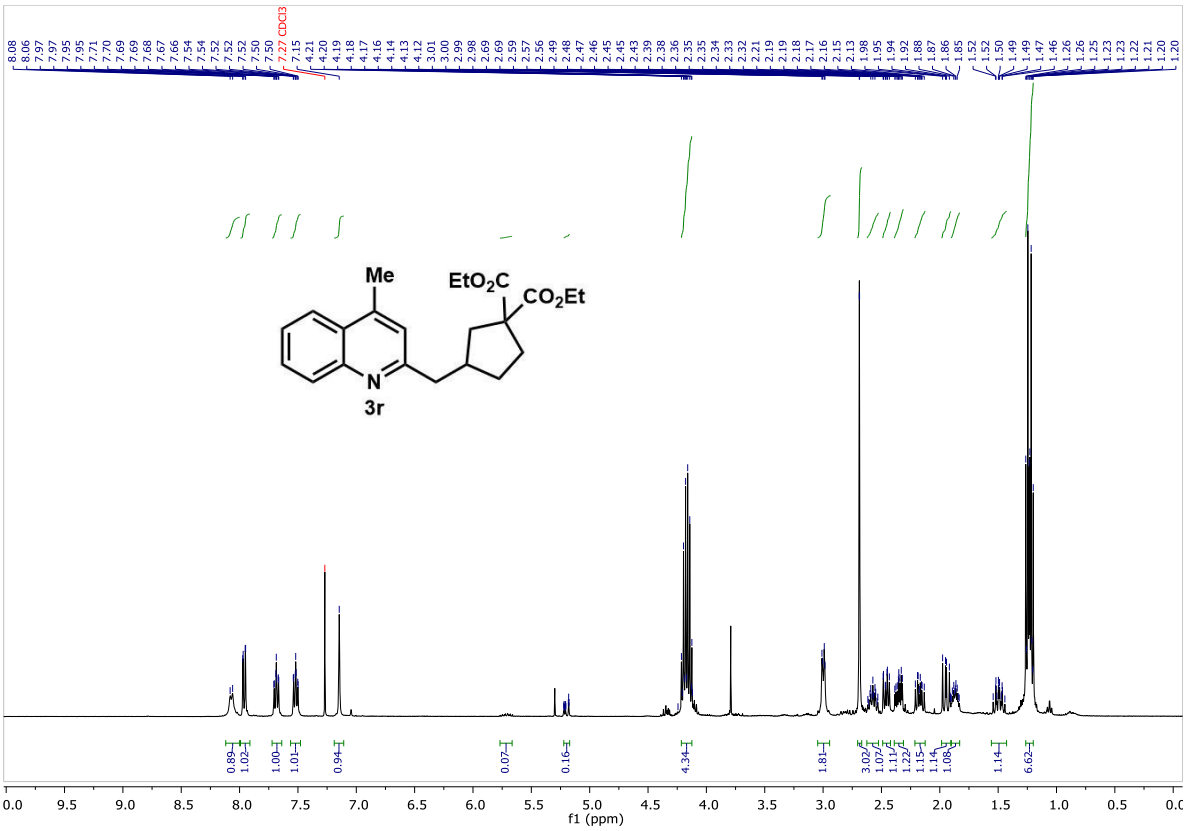
Me
EtO2C
CO2Et
N
3r
f1 (ppm)

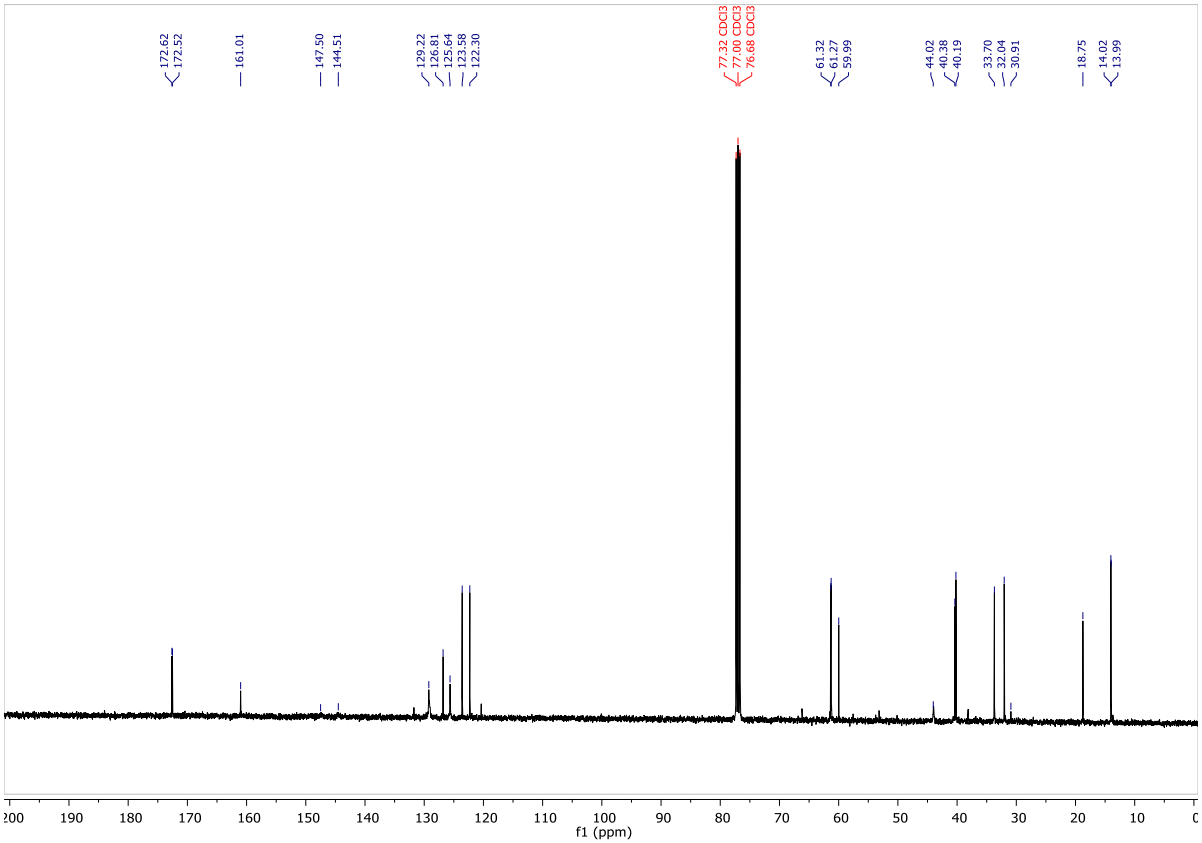
f1 (ppm)

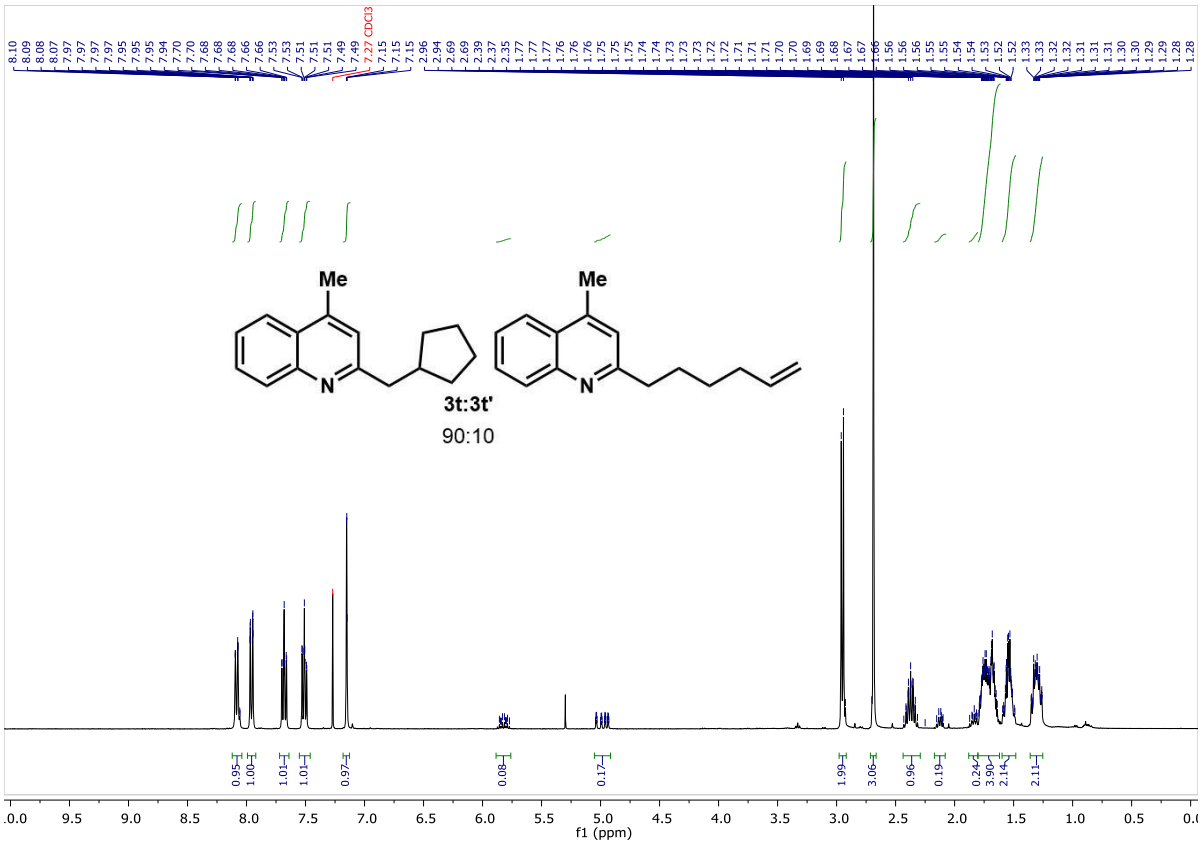
Me
N
Me
N
3t:3t'
90:10
f1 (ppm)

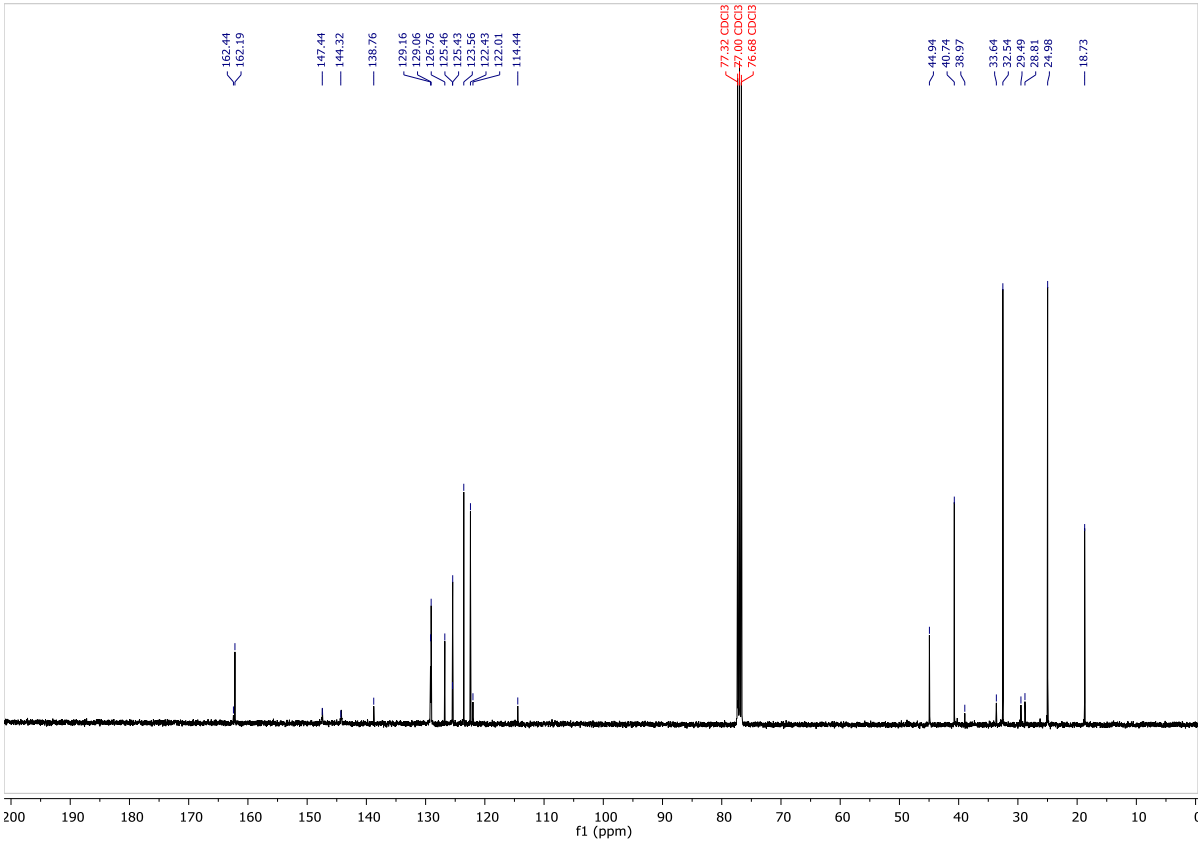
f1 (ppm)

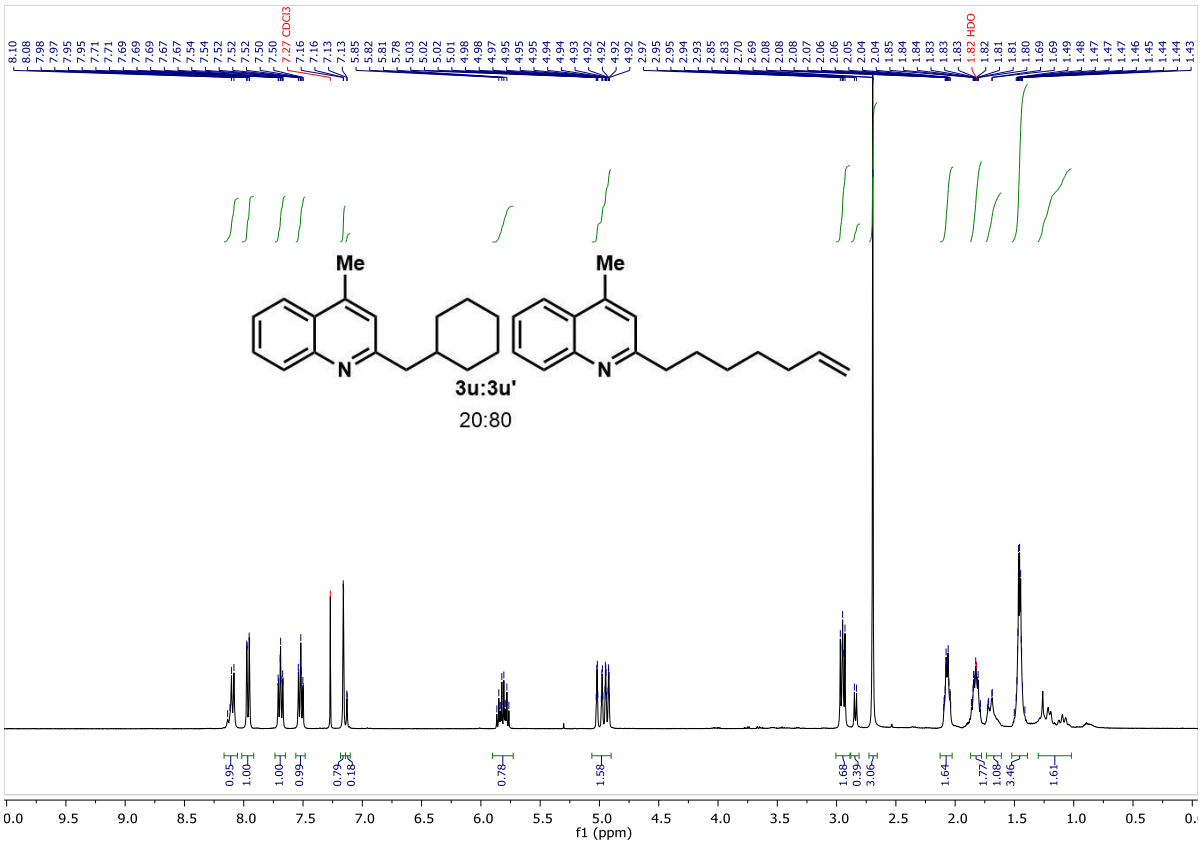
Me
Me
N
N
3u:3u'
20:80
f1 (ppm)

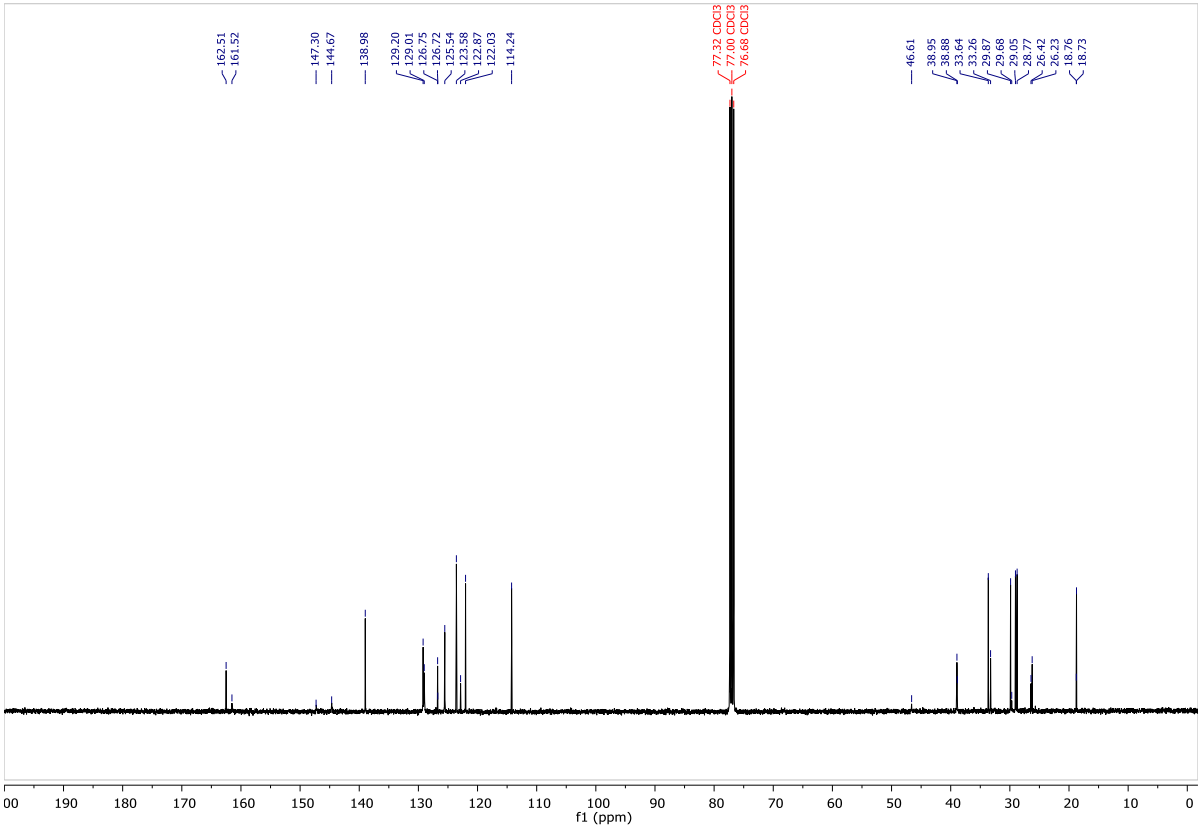
f1 (ppm)

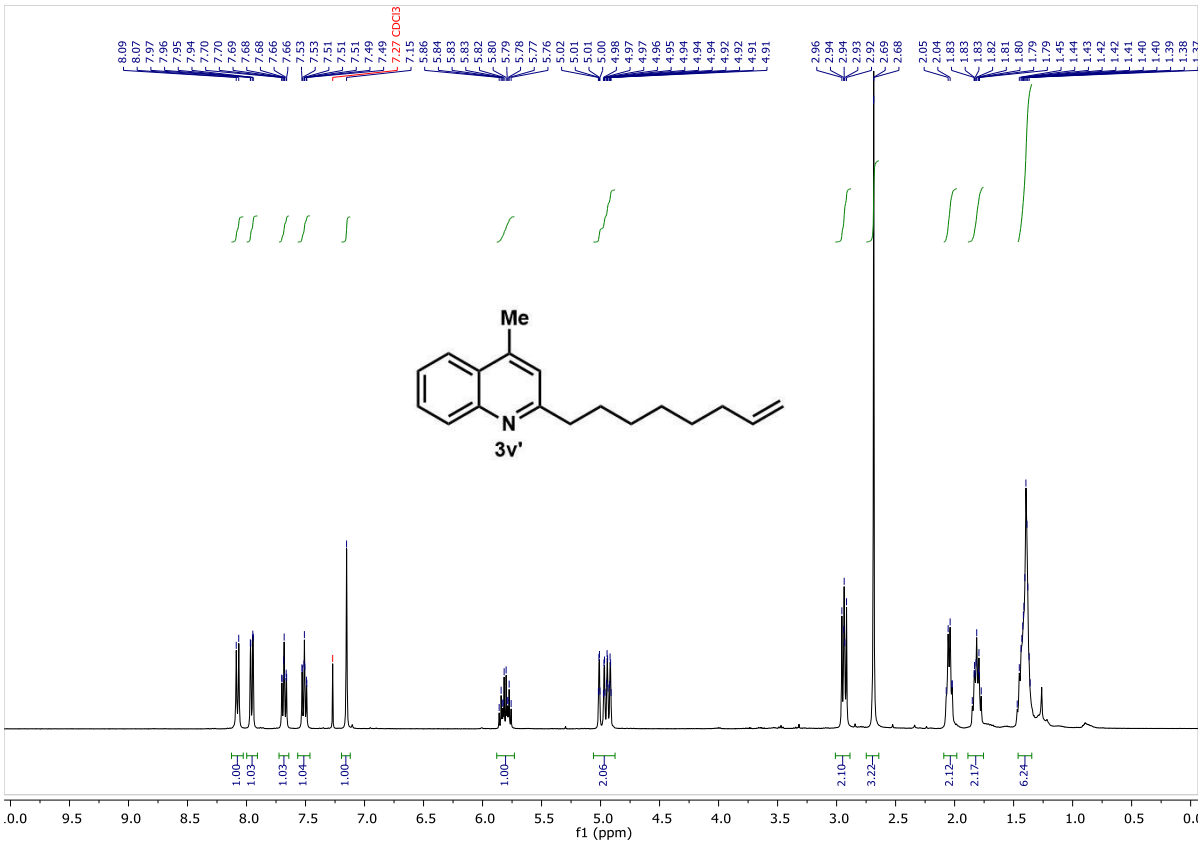
Me
N
3v'
f1 (ppm)

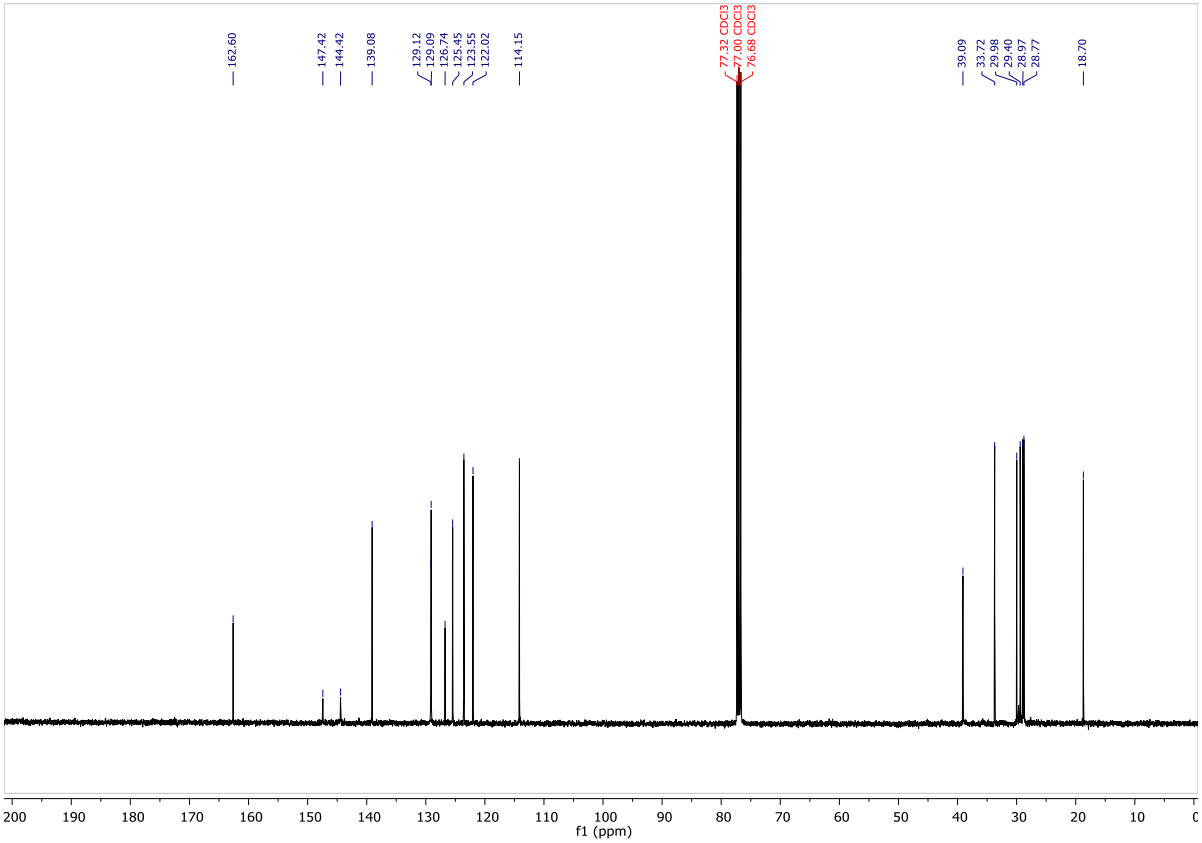
f1 (ppm)

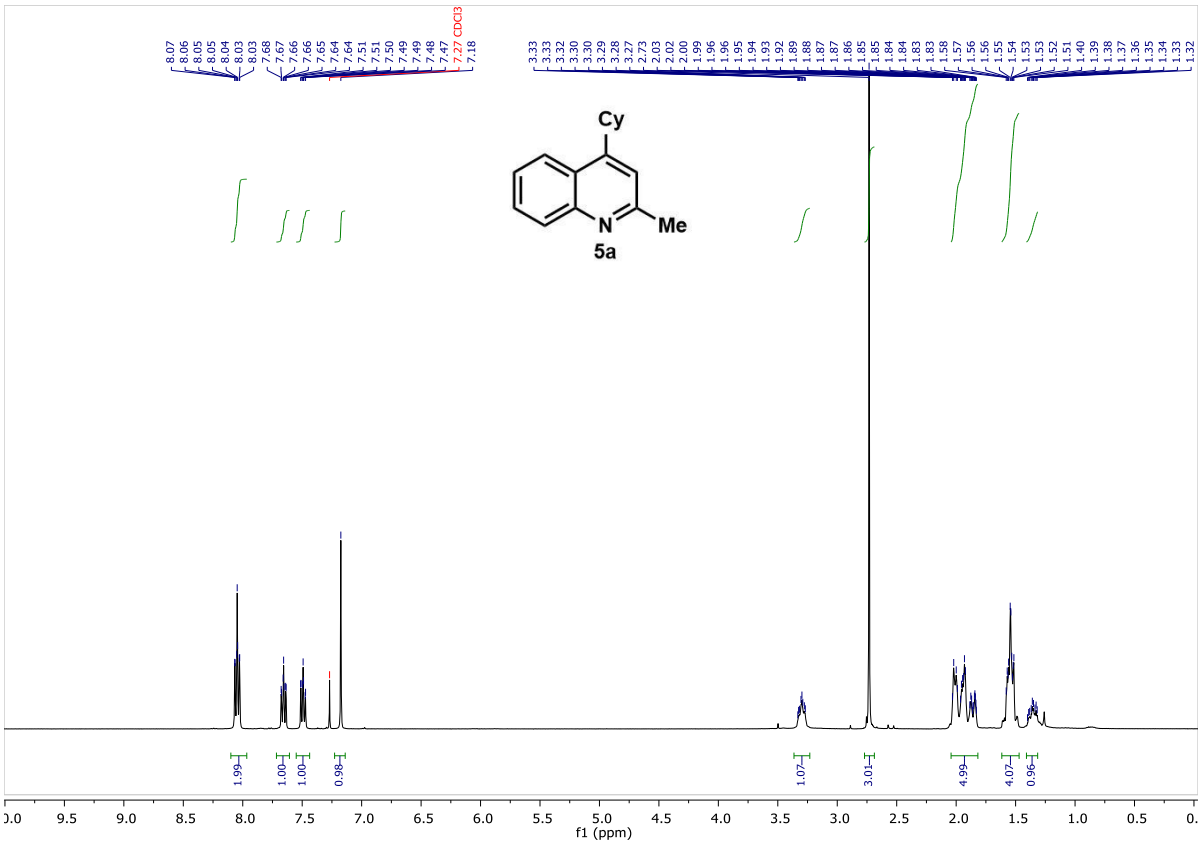
Cy
N
Me
5a
f1 (ppm)

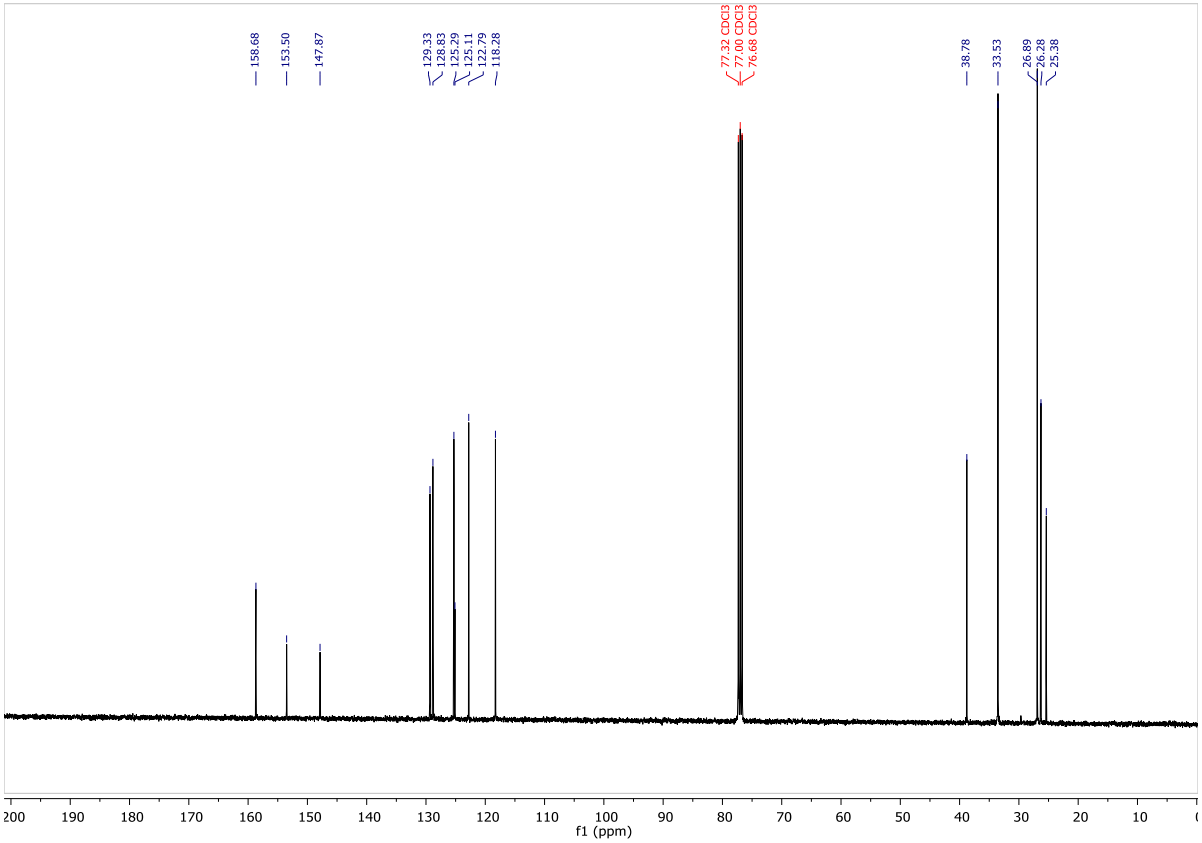
158.68
153.50
147.87
129.33
128.83
125.29
125.11
122.79
118.28
77.32 CDCl3
77.00 CDCl3
76.68 CDCl3
38.78
33.53
26.89
26.28
25.38
f1 (ppm)

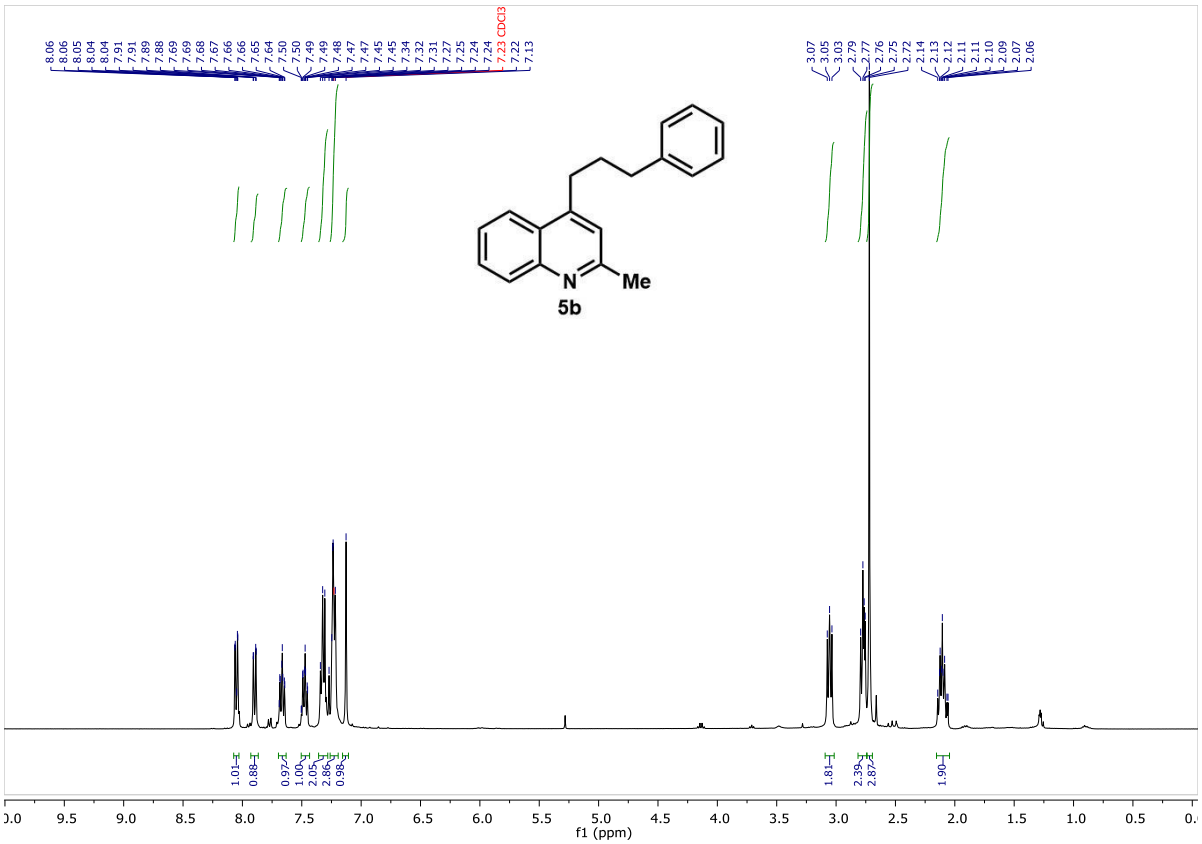
8.06
8.06
8.05
8.05
8.04
8.04
7.91
7.91
7.89
7.88
7.69
7.69
7.68
7.67
7.66
7.66
7.65
7.64
7.50
7.50
7.49
7.49
7.48
7.47
7.47
7.45
7.45
7.34
7.32
7.31
7.27
7.25
7.24
7.24
7.23 CDCl3
7.22
7.13
3.07
3.05
3.03
2.79
2.77
2.76
2.75
2.72
2.14
2.13
2.12
2.11
2.11
2.10
2.09
2.07
2.06
N
Me
5b
1.01
0.88
0.97
1.00
2.05
2.86
0.98
1.81
2.39
2.87
1.90
f1 (ppm)

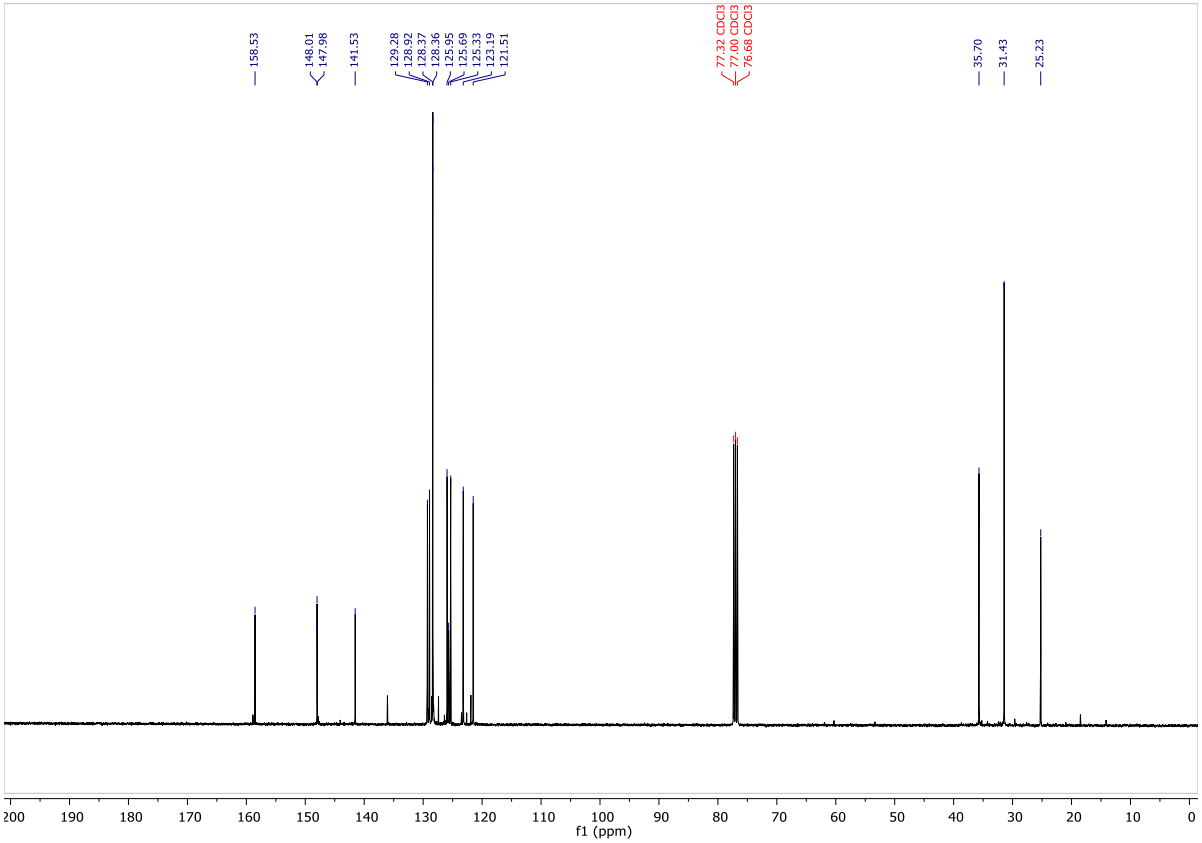
158.53
148.01
147.98
141.53
129.28
128.92
128.37
128.36
125.95
125.69
125.33
123.19
121.51
77.32 CDCl3
77.00 CDCl3
76.68 CDCl3
35.70
31.43
25.23
f1 (ppm)

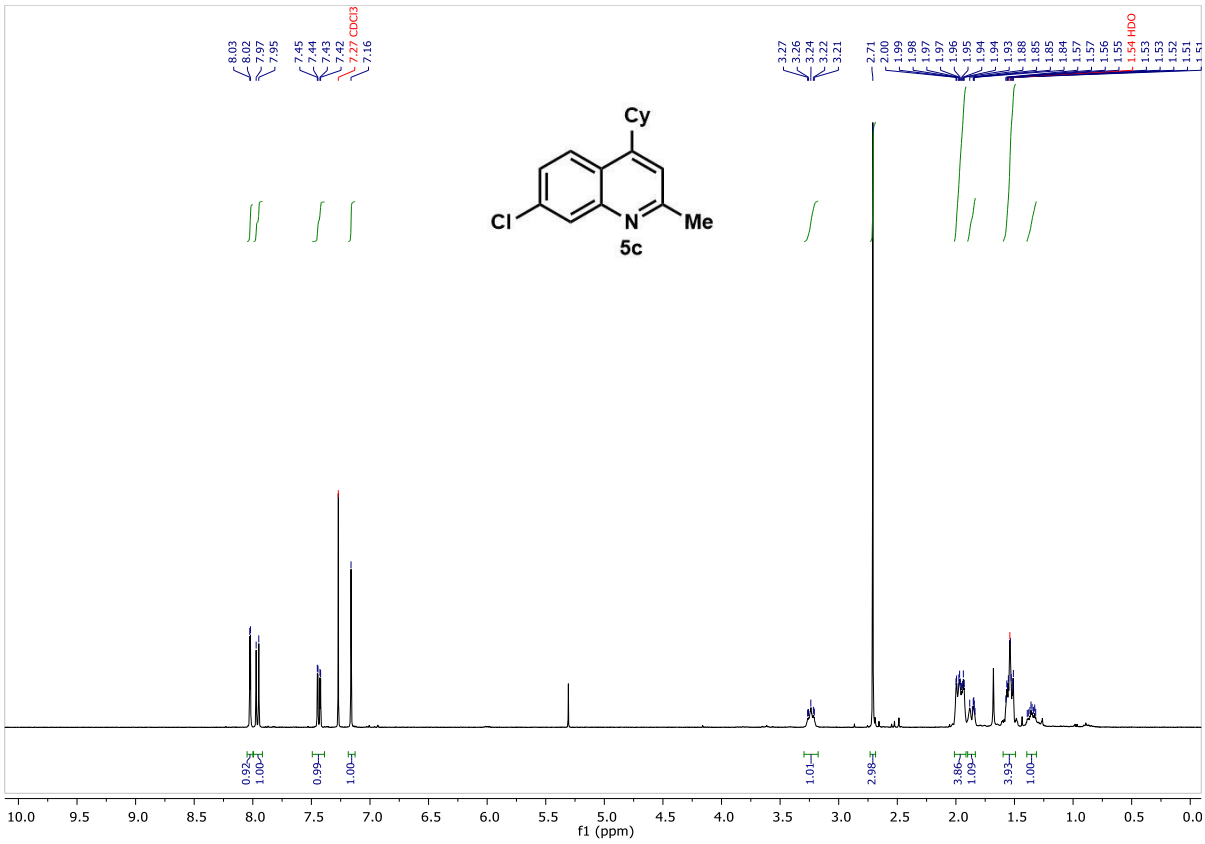
8.03
8.02
7.97
7.95
7.45
7.44
7.43
7.42
7.27 CDCl3
7.16
3.27
3.26
3.24
3.22
3.21
2.71
2.00
1.99
1.98
1.97
1.97
1.96
1.95
1.94
1.94
1.93
1.88
1.85
1.85
1.84
1.57
1.57
1.56
1.55
1.54 HDO
1.53
1.53
1.52
1.52
1.51
Cy
Cl
N
Me
5c
0.92
1.00
0.99
1.00
1.01
2.98
3.86
1.09
3.93
1.00
f1 (ppm)

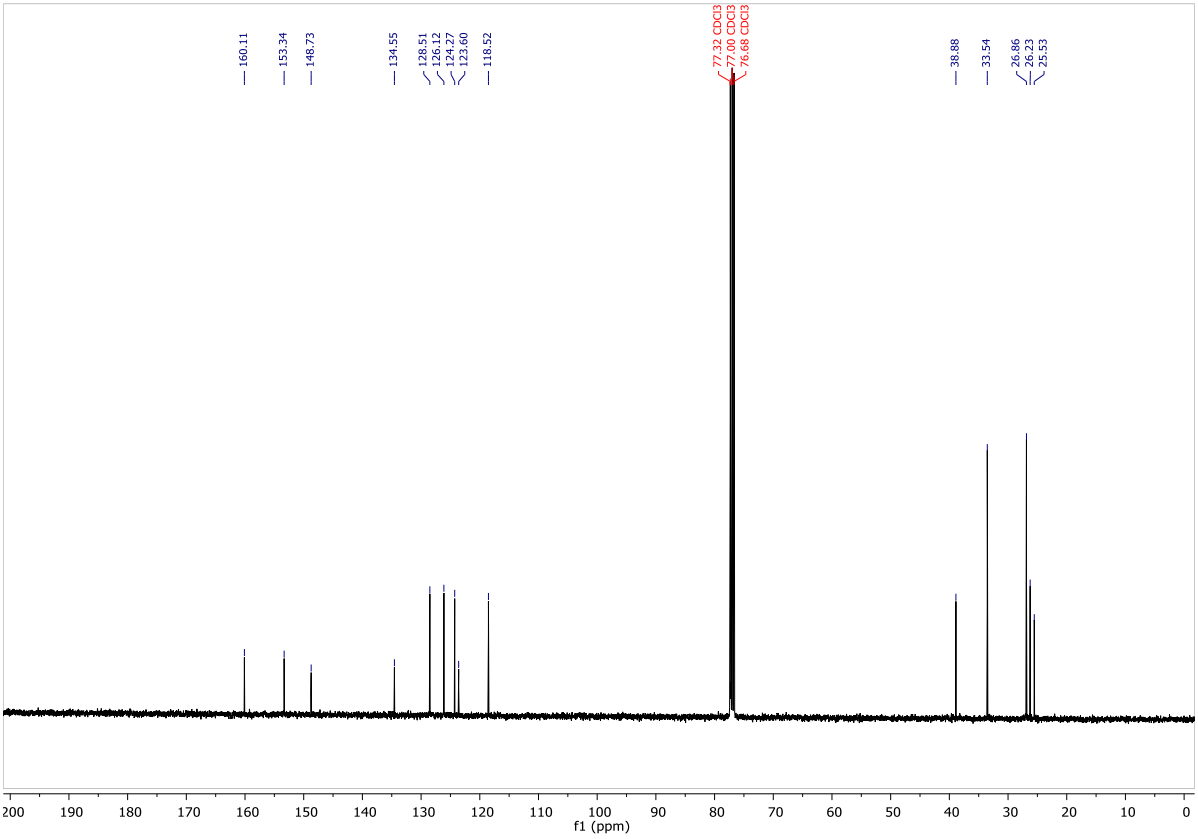
160.11
153.34
148.73
134.55
128.51
126.12
124.27
123.60
118.52
77.32 CDCl3
77.00 CDCl3
76.68 CDCl3
38.88
33.54
26.86
26.23
25.53
f1 (ppm)

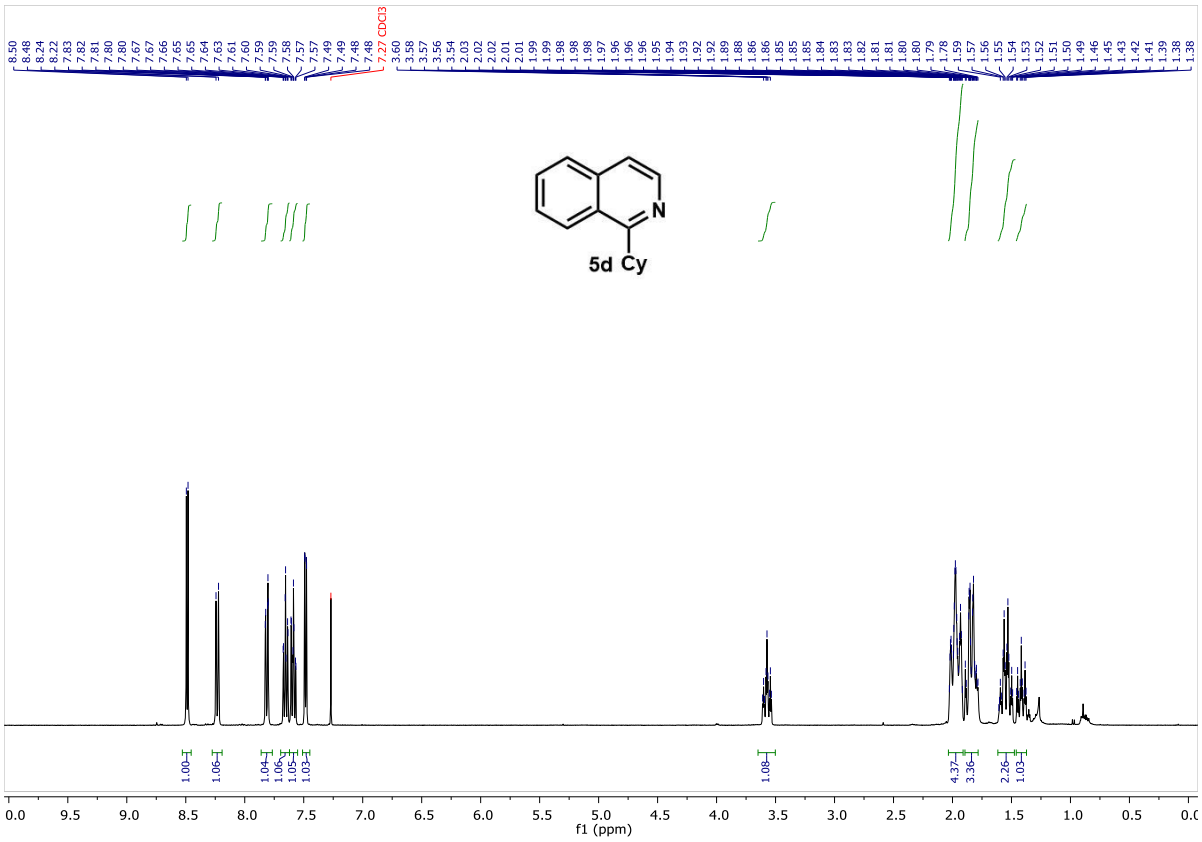
5d Cy
f1 (ppm)

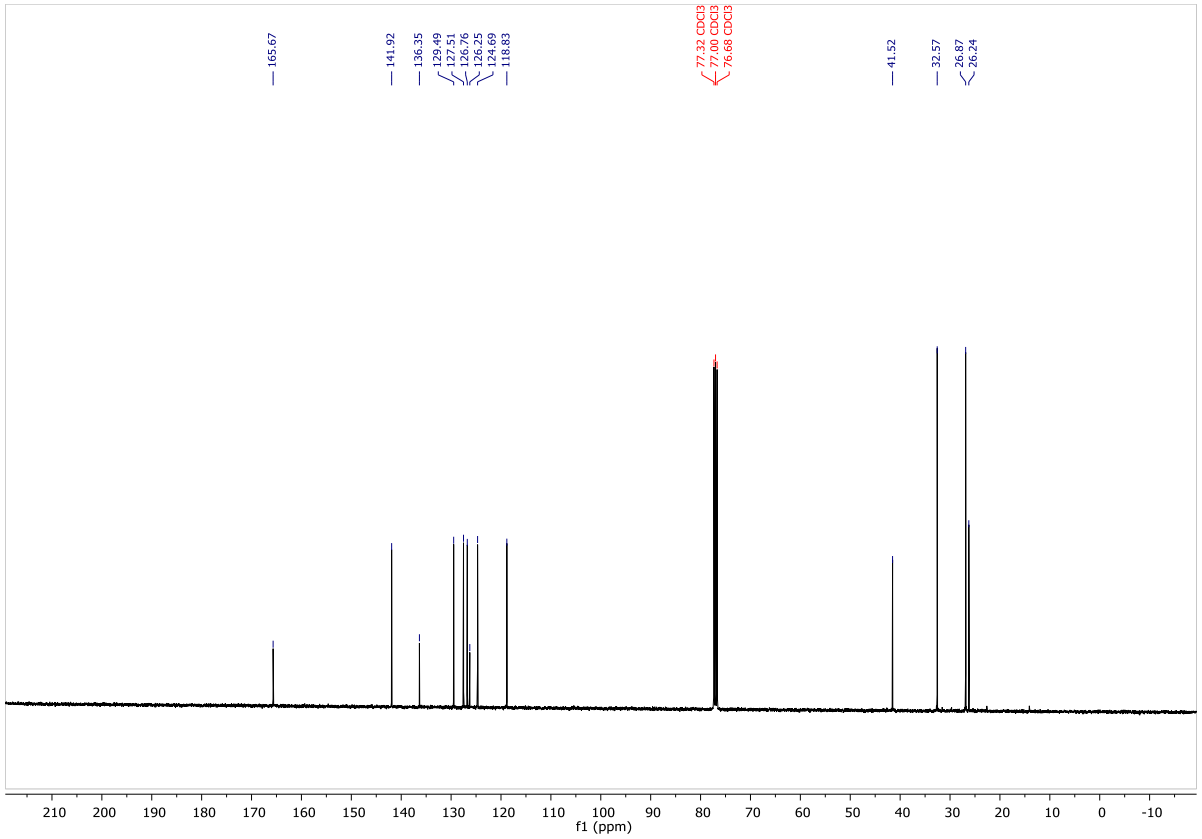
f1 (ppm)

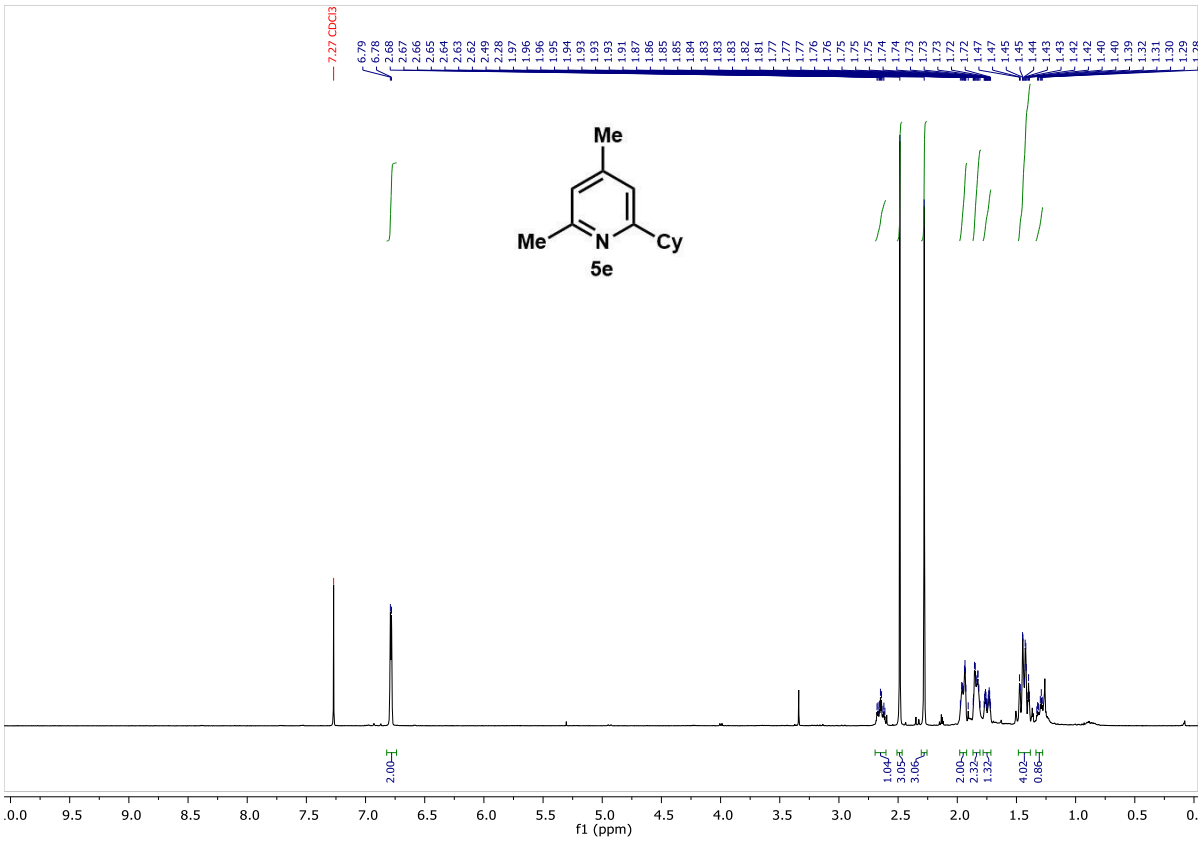
7.27 CDCl3
Me
Me
N
Cy
5e
f1 (ppm)

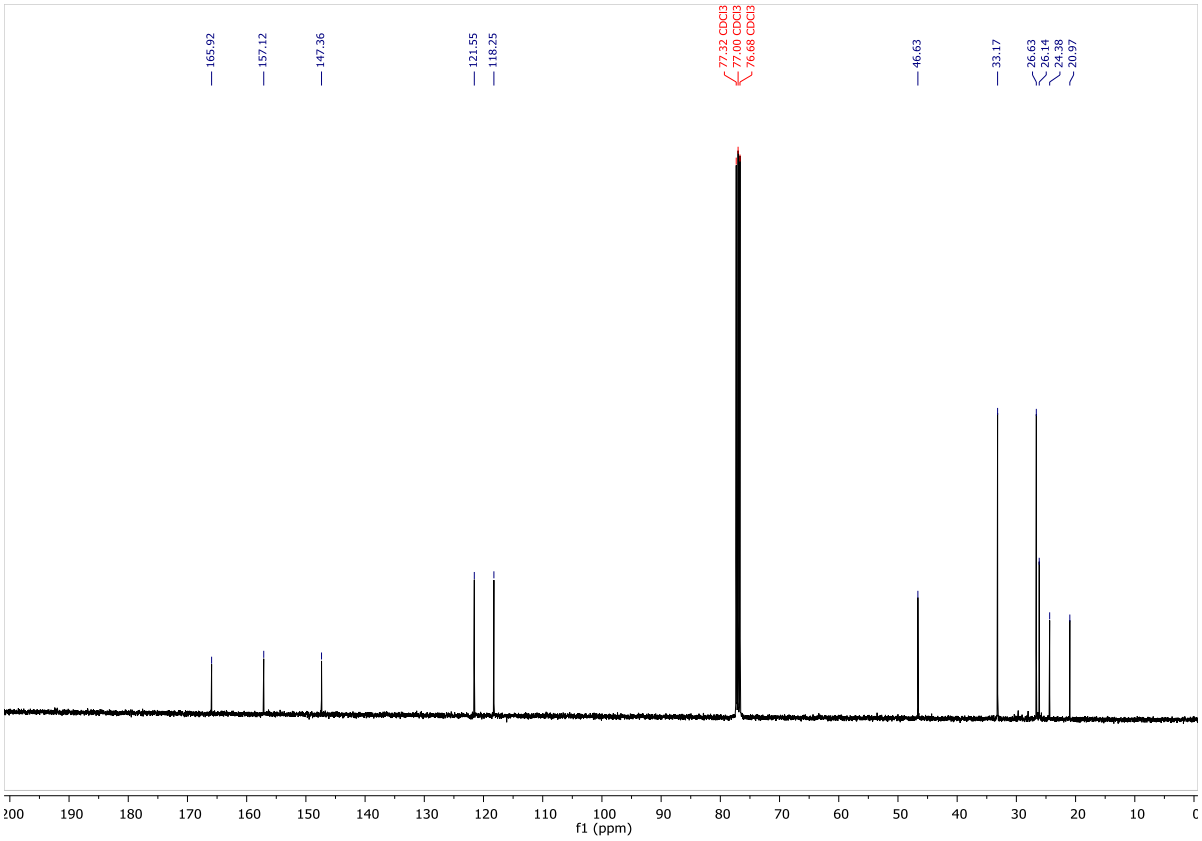
165.92
157.12
147.36
121.55
118.25
77.32 CDCl3
77.00 CDCl3
76.68 CDCl3
46.63
33.17
26.63
26.14
25.38
20.97
f1 (ppm)

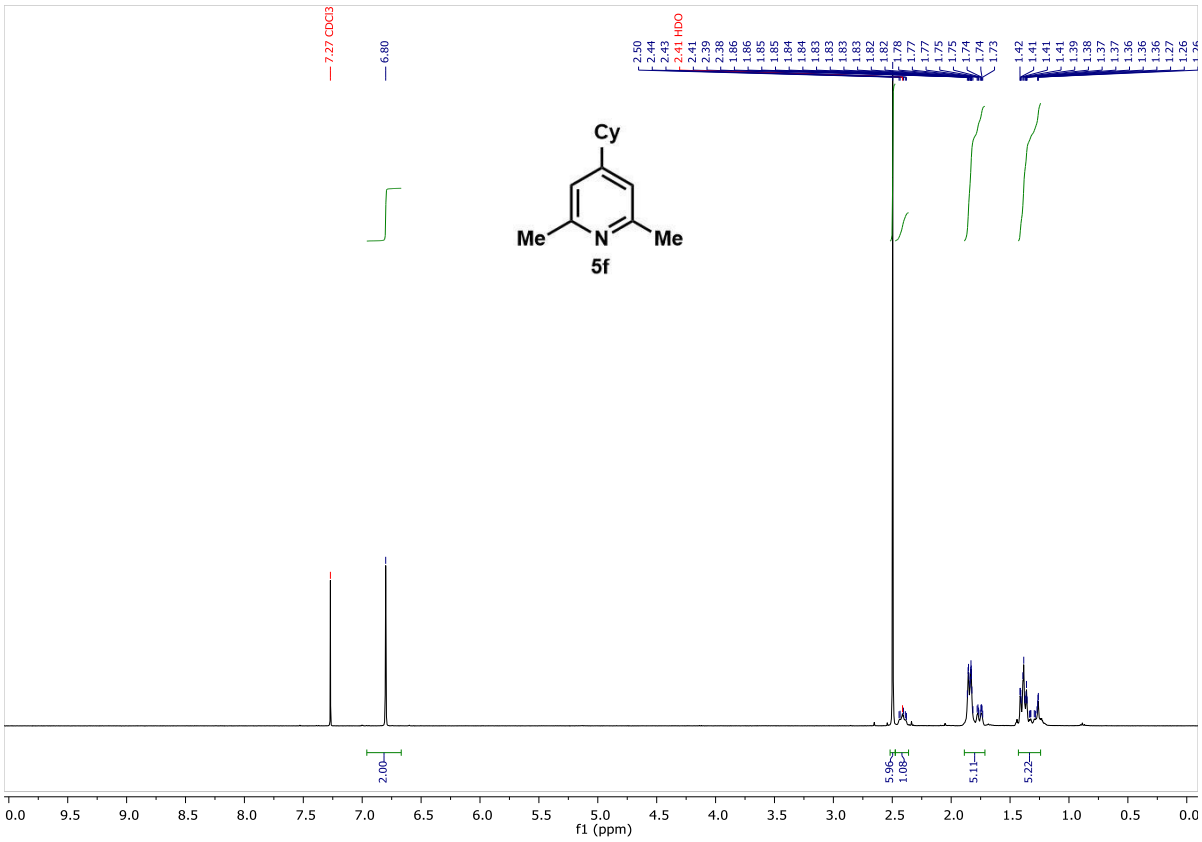
7.27 CDCl3
6.80
2.50
2.44
2.43
2.41 HDO
2.41
2.39
2.38
1.86
1.86
1.85
1.85
1.84
1.84
1.83
1.83
1.83
1.83
1.82
1.82
1.78
1.77
1.77
1.75
1.75
1.74
1.74
1.73
1.42
1.41
1.41
1.41
1.39
1.38
1.37
1.37
1.36
1.36
1.36
1.27
1.26
Cy
Me
N
Me
5f
2.00
5.96
1.08
5.11
5.22
f1 (ppm)

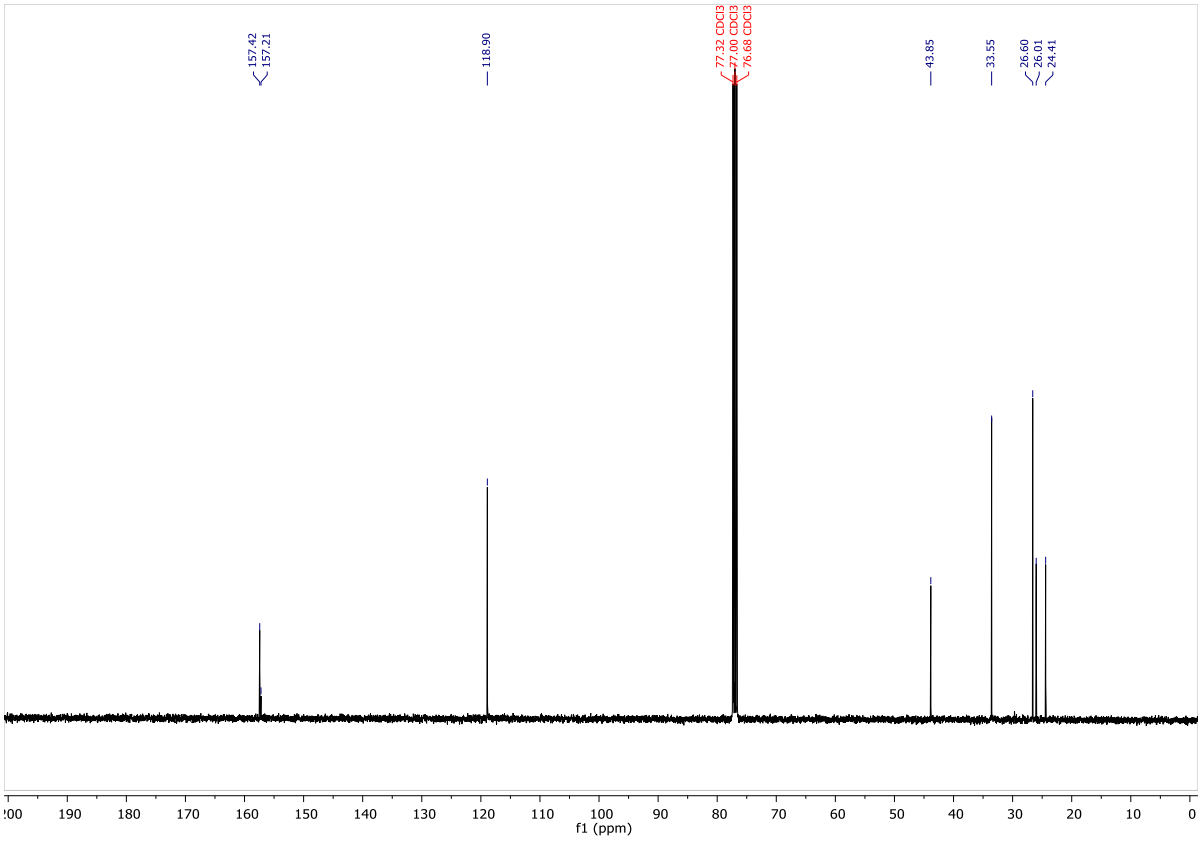
157.42
157.21
118.90
77.32 CDCl3
77.00 CDCl3
76.68 CDCl3
43.85
33.55
26.60
26.01
24.41
f1 (ppm)

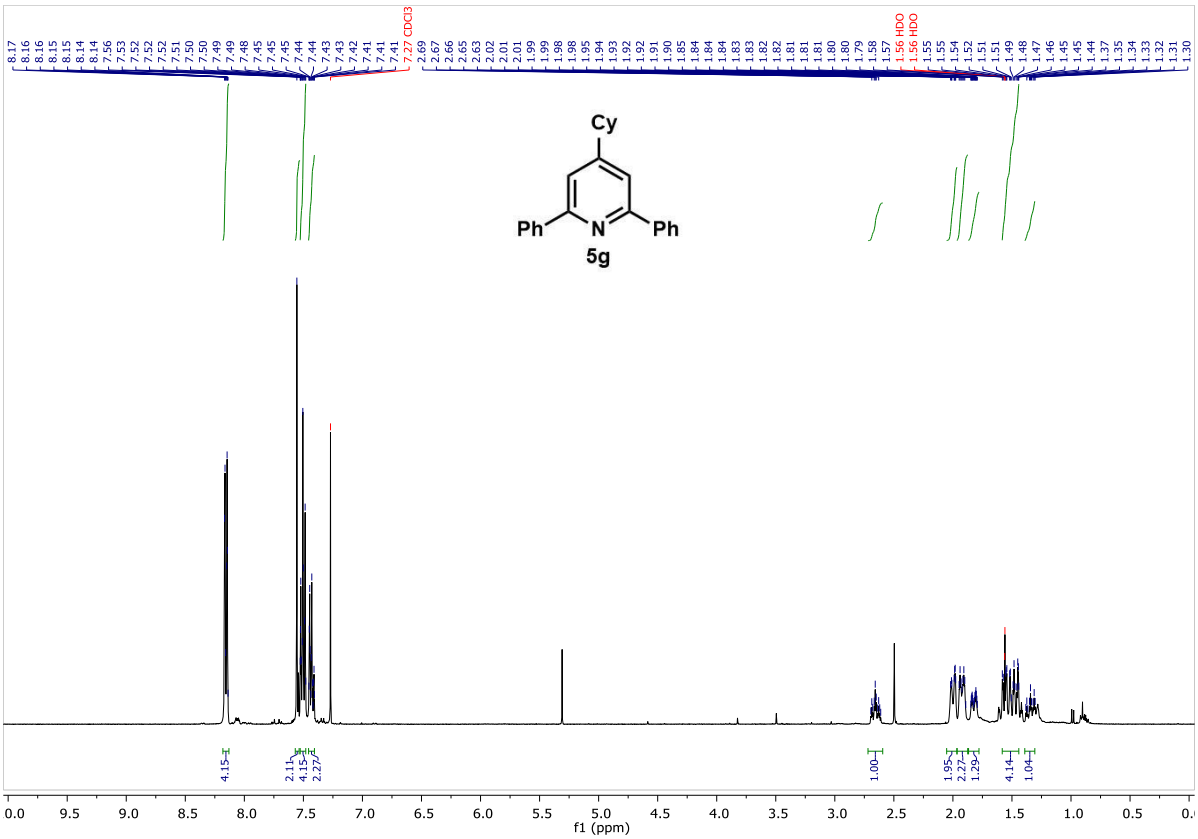
Cy
Ph
N
Ph
5g
f1 (ppm)

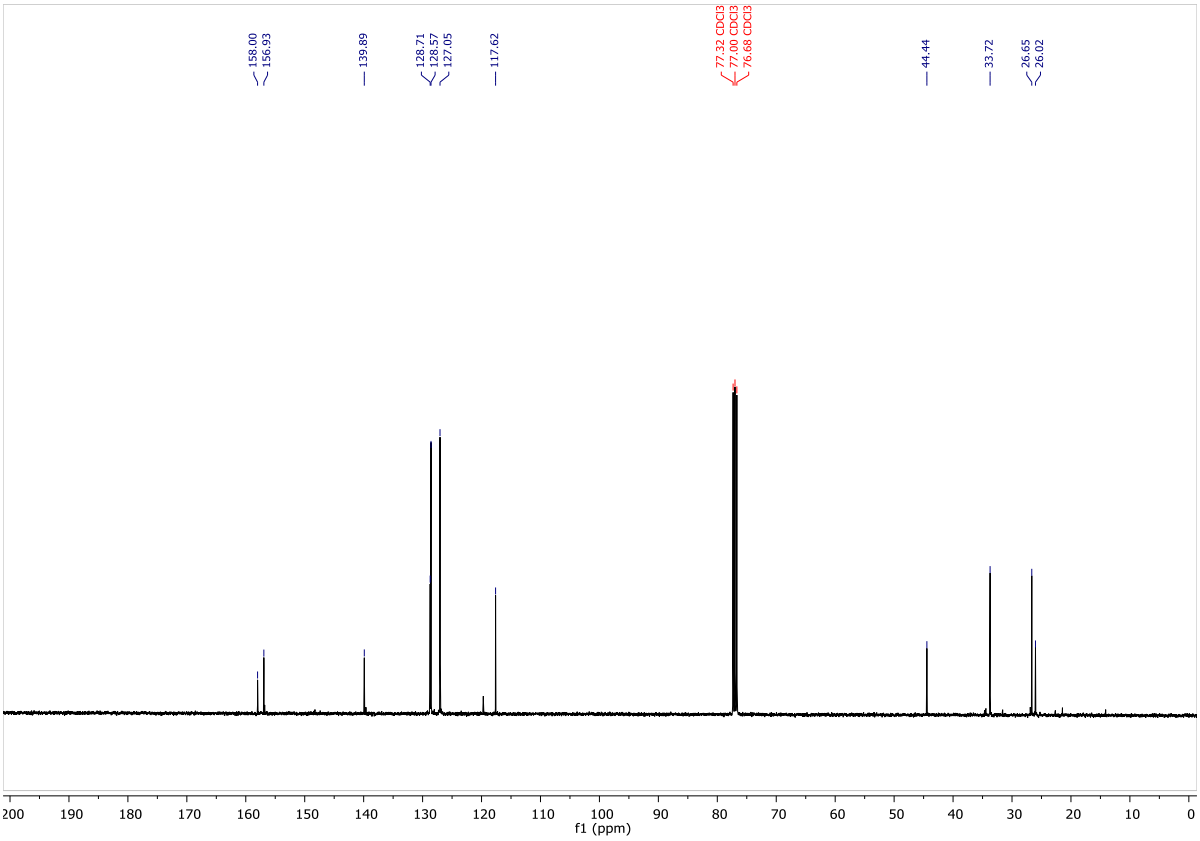
158.00
156.93
139.89
128.71
128.57
127.05
117.62
77.32 CDCl3
77.00 CDCl3
76.68 CDCl3
44.44
33.72
26.65
26.02
f1 (ppm)

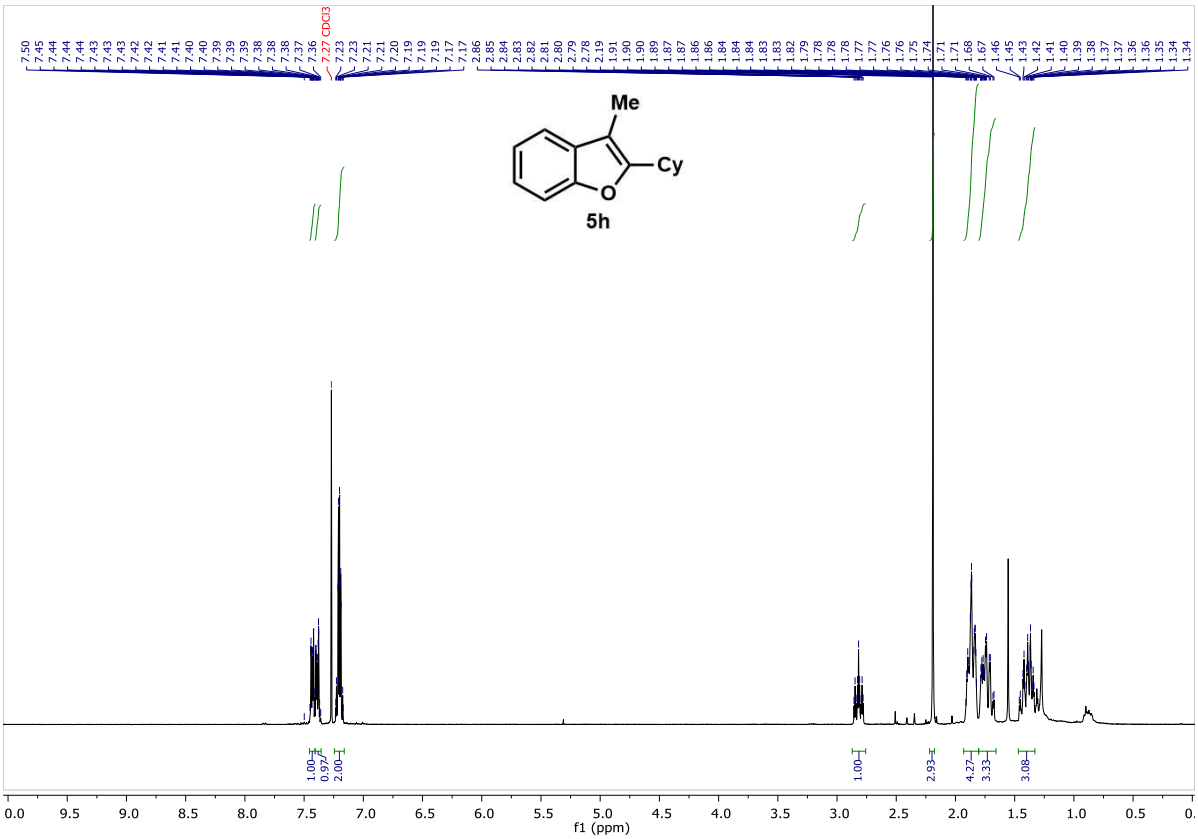
Me
Cy
O
5h
f1 (ppm)

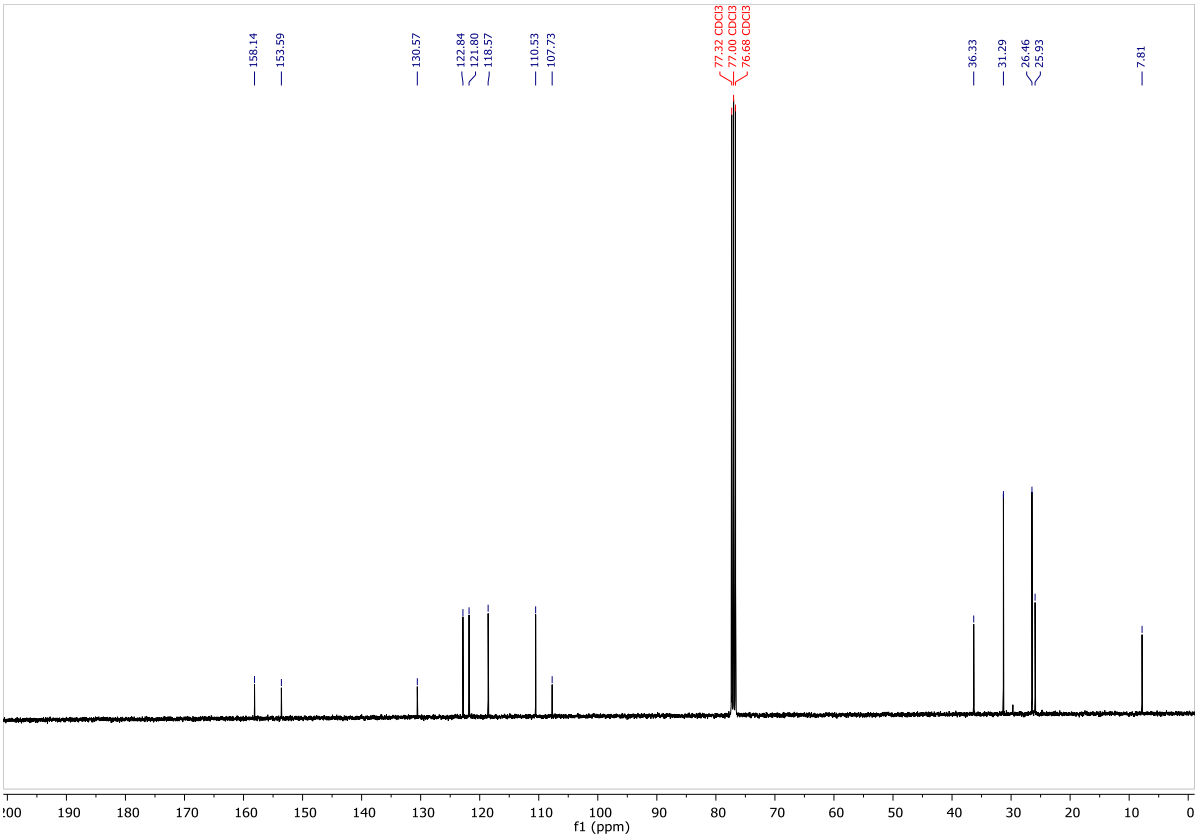
158.14
153.59
130.57
122.84
121.80
118.57
110.53
107.73
77.32 CDCl3
77.00 CDCl3
76.68 CDCl3
36.33
31.29
26.46
25.93
7.81
f1 (ppm)

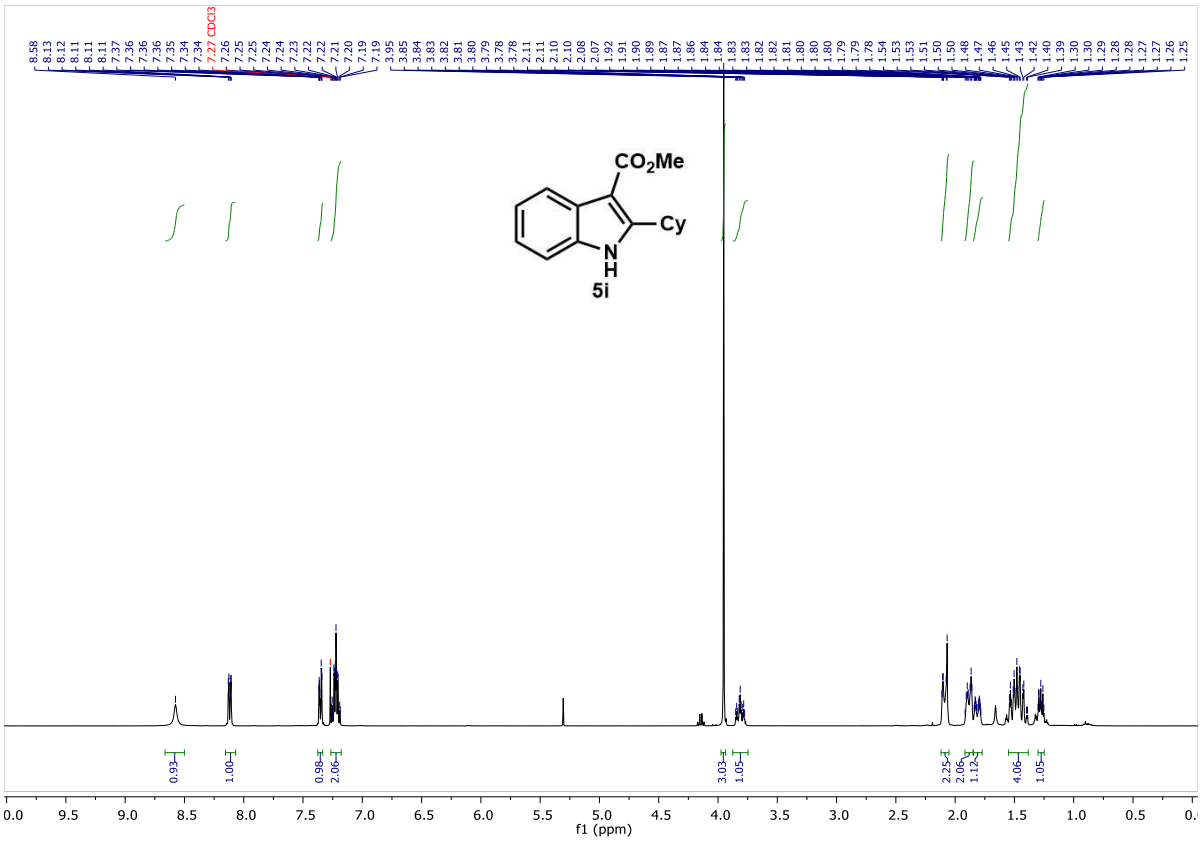
CO2Me
Cy
N
H
5i
f1 (ppm)

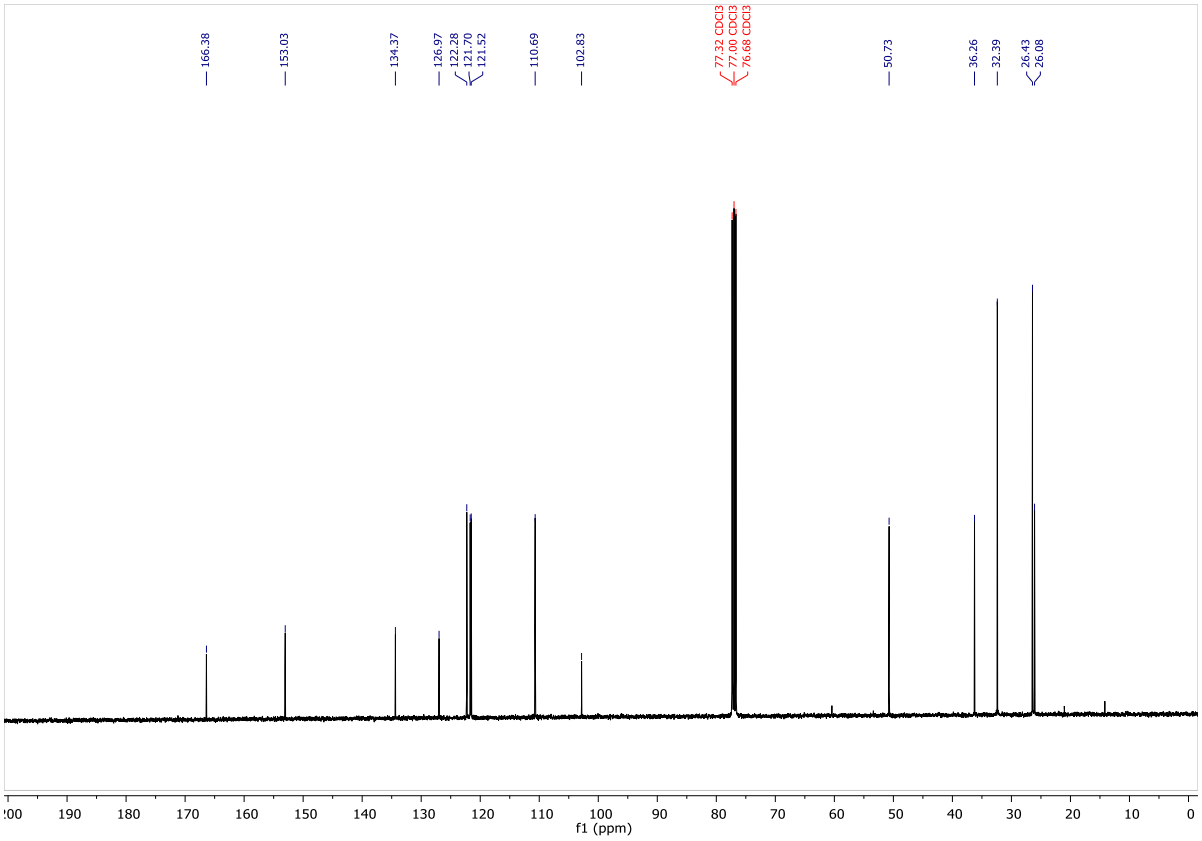
f1 (ppm)

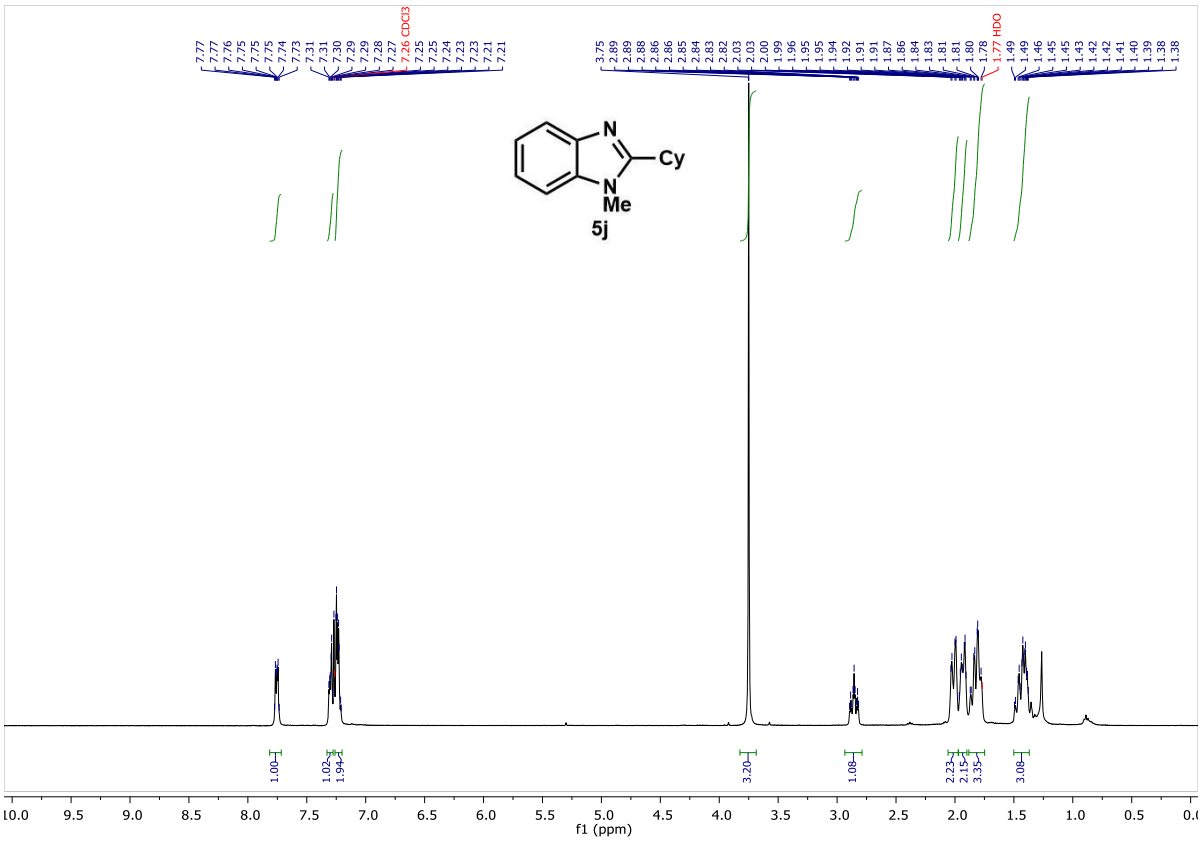
N
Cy
N
Me
5j
f1 (ppm)

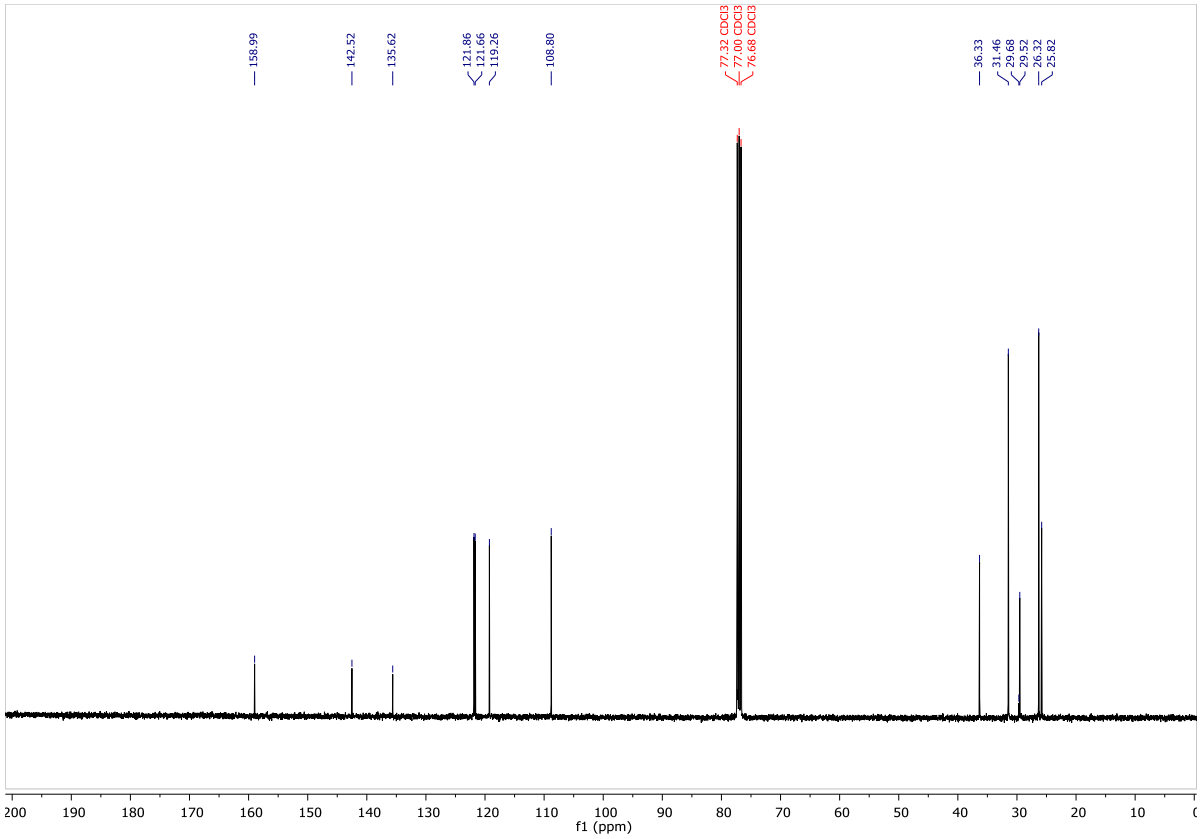
f1 (ppm)

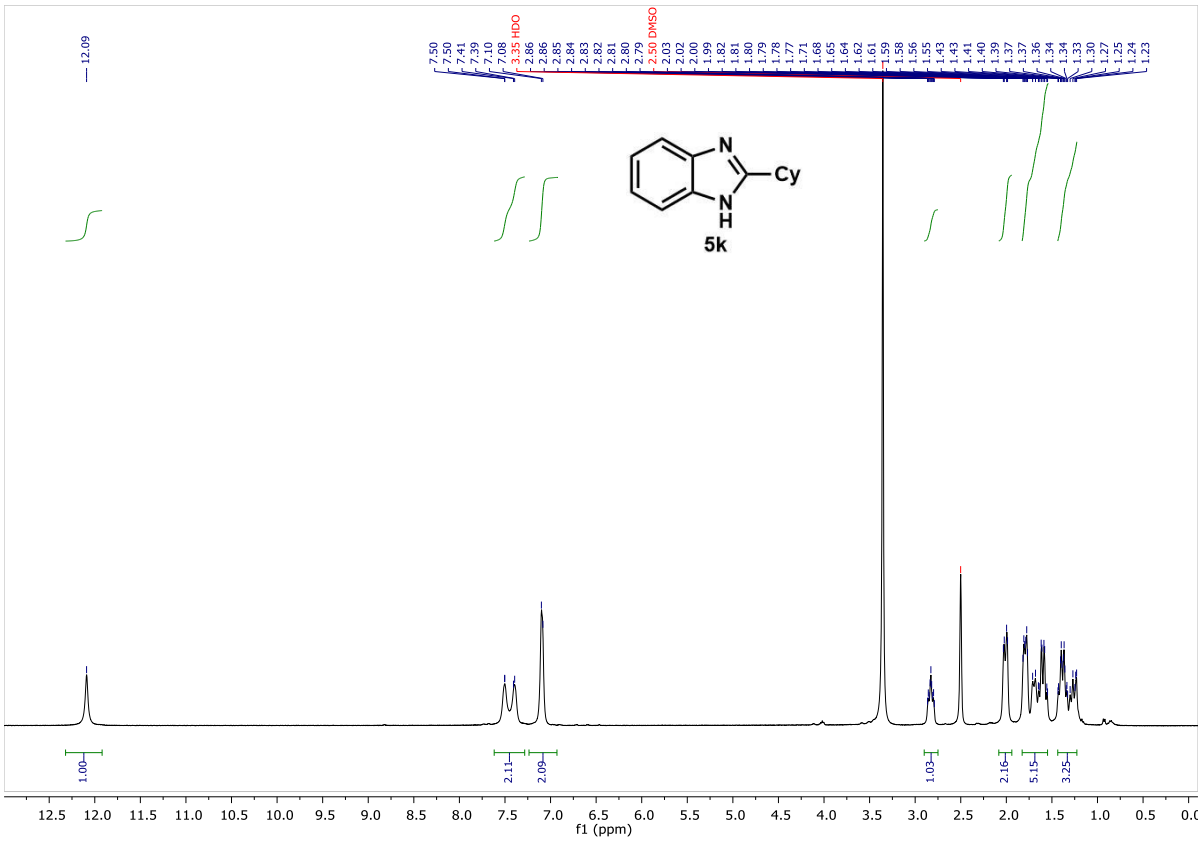
12.09
7.50
7.50
7.41
7.39
7.10
7.08
3.35 HDO
2.86
2.86
2.85
2.84
2.83
2.82
2.81
2.80
2.79 DMSO
2.03
2.02
2.00
1.99
1.82
1.81
1.80
1.79
1.78
1.77
1.71
1.68
1.65
1.64
1.62
1.61
1.59
1.58
1.56
1.55
1.43
1.43
1.41
1.40
1.39
1.37
1.37
1.36
1.34
1.34
1.33
1.30
1.27
1.25
1.24
1.23
N
Cy
N
H
5k
1.00
2.11
2.09
1.03
2.16
5.15
3.25
f1 (ppm)

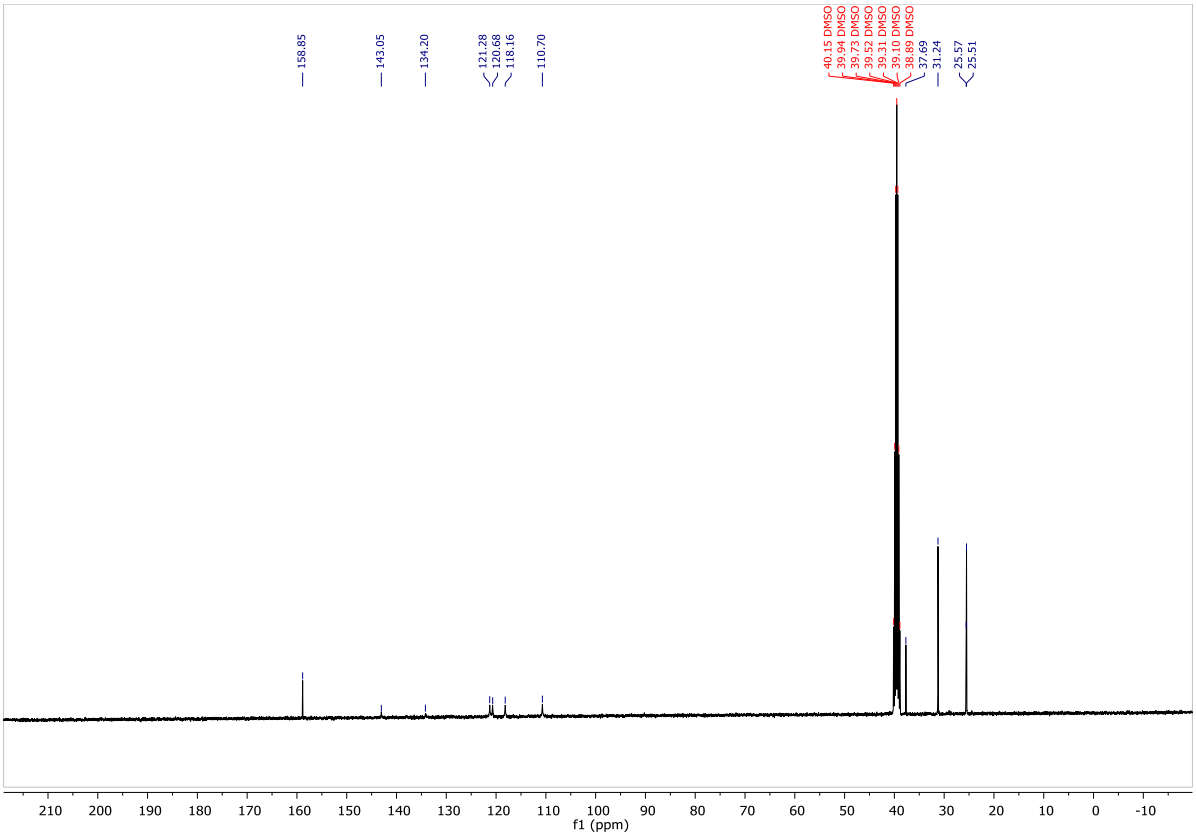
158.85
143.05
134.20
121.28
120.68
118.16
110.70
40.15 DMSO
39.94 DMSO
39.73 DMSO
39.52 DMSO
39.31 DMSO
39.10 DMSO
38.89 DMSO
37.69
31.24
25.57
25.51
f1 (ppm)

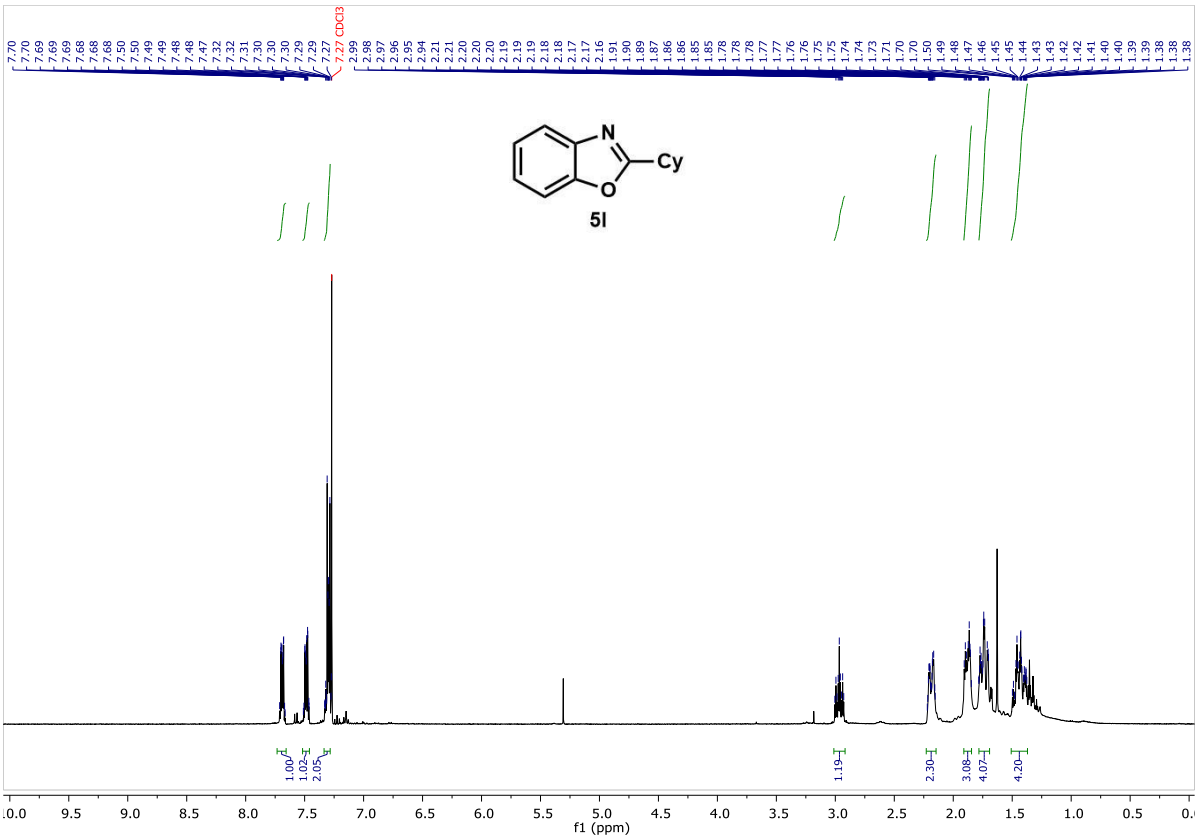
7.27 CDCl3
N
Cy
O
5l
1.00
1.02
2.05
1.19
2.30
3.08
4.07
4.20
f1 (ppm)

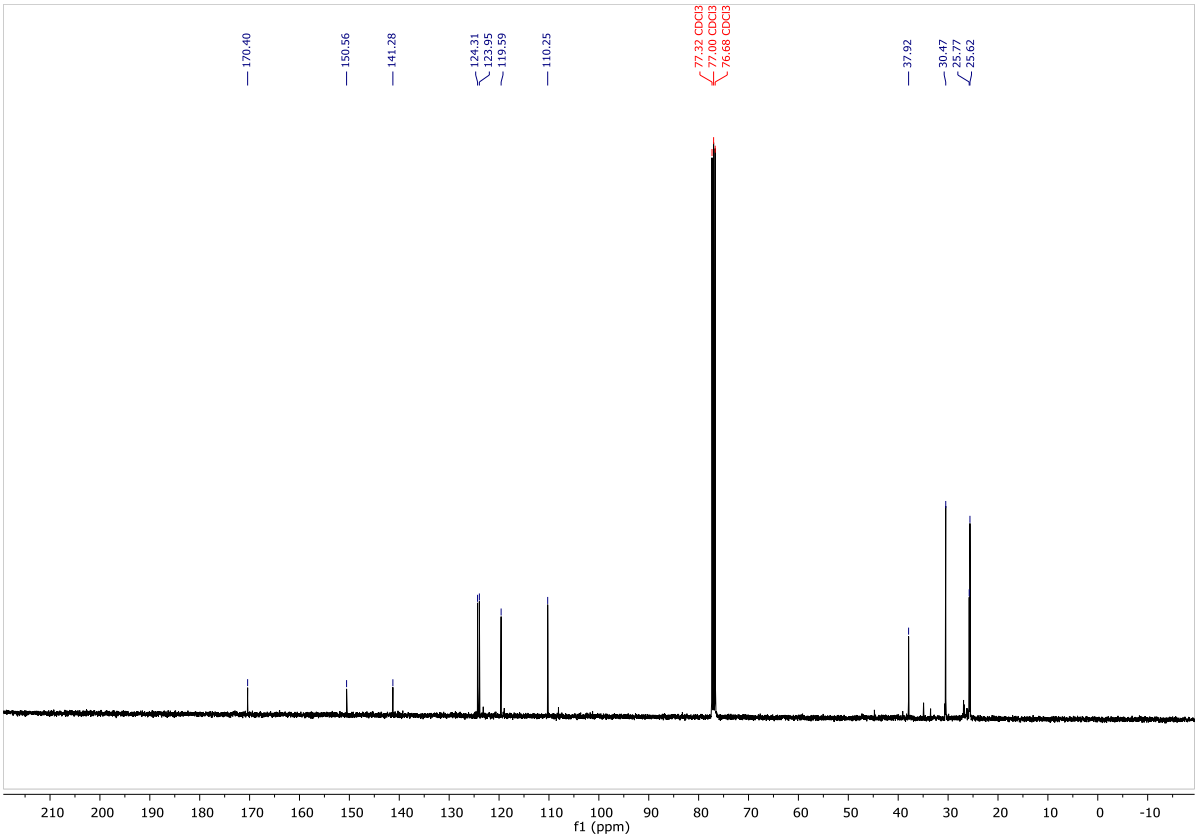
170.40
150.56
141.28
124.31
123.95
119.59
110.25
77.32 CDCl3
77.00 CDCl3
76.68 CDCl3
37.92
30.47
25.77
25.62
f1 (ppm)

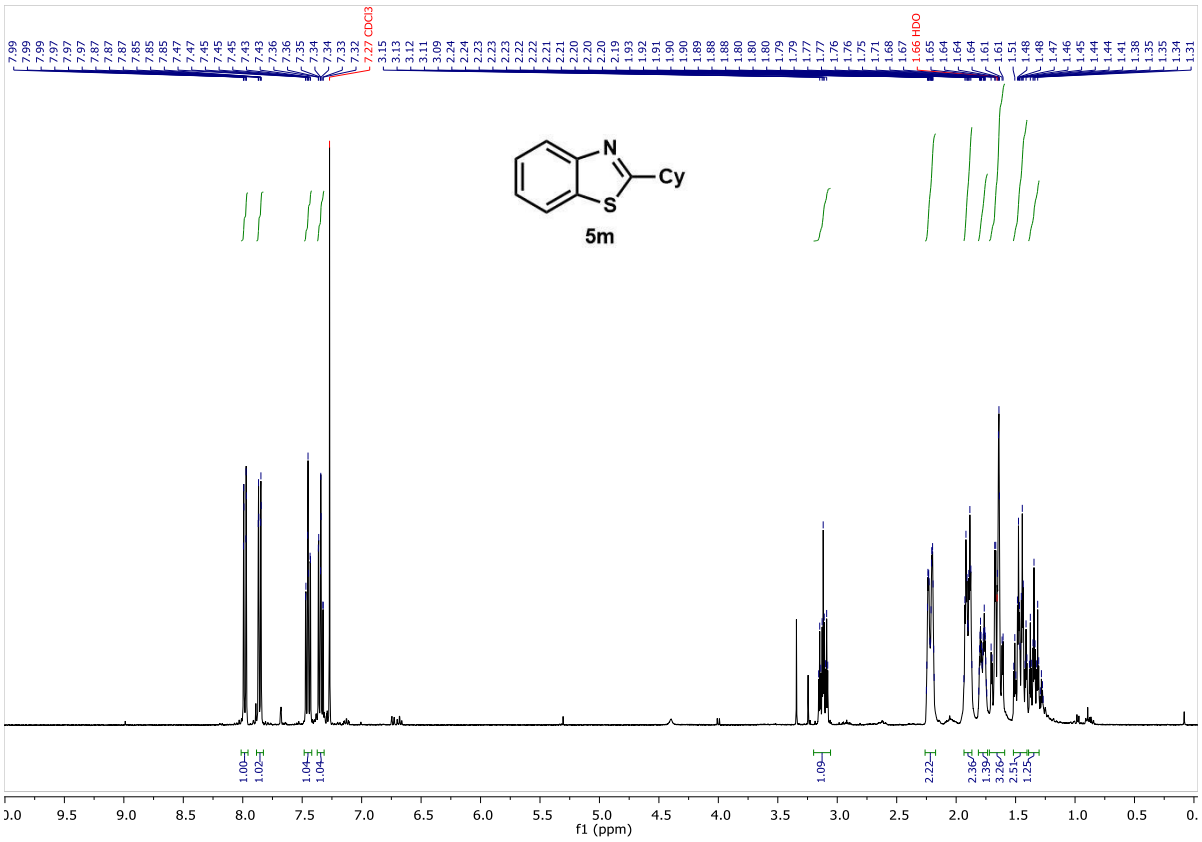
N
Cy
S
5m
f1 (ppm)

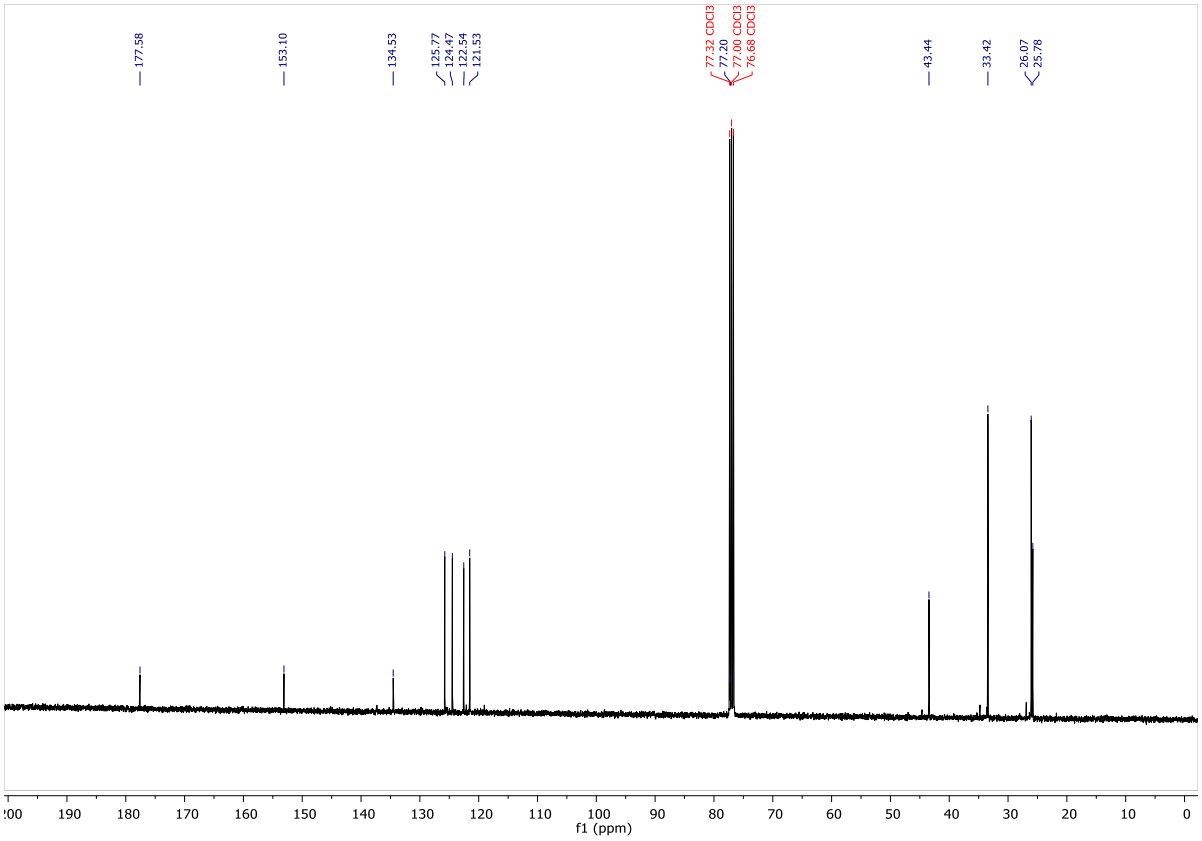
177.58
153.10
134.53
125.77
124.47
122.54
121.53
77.32 CDCl3
77.20
77.00 CDCl3
76.68 CDCl3
43.44
33.42
26.07
25.78
f1 (ppm)

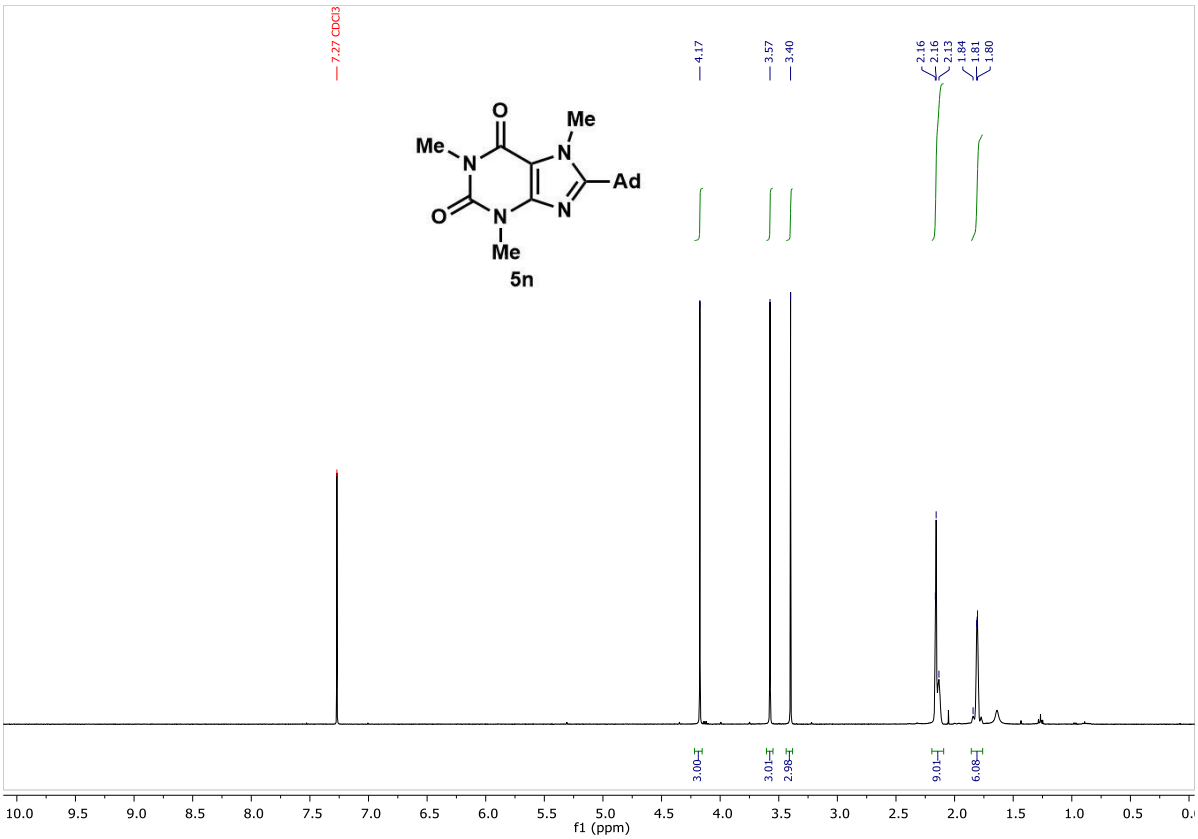
7.27 CDCl3
4.17
3.57
3.40
2.16
2.16
2.13
1.84
1.81
1.80
Me
Me
Ad
Me
5n
3.00
3.01
2.98
9.01
6.08
f1 (ppm)

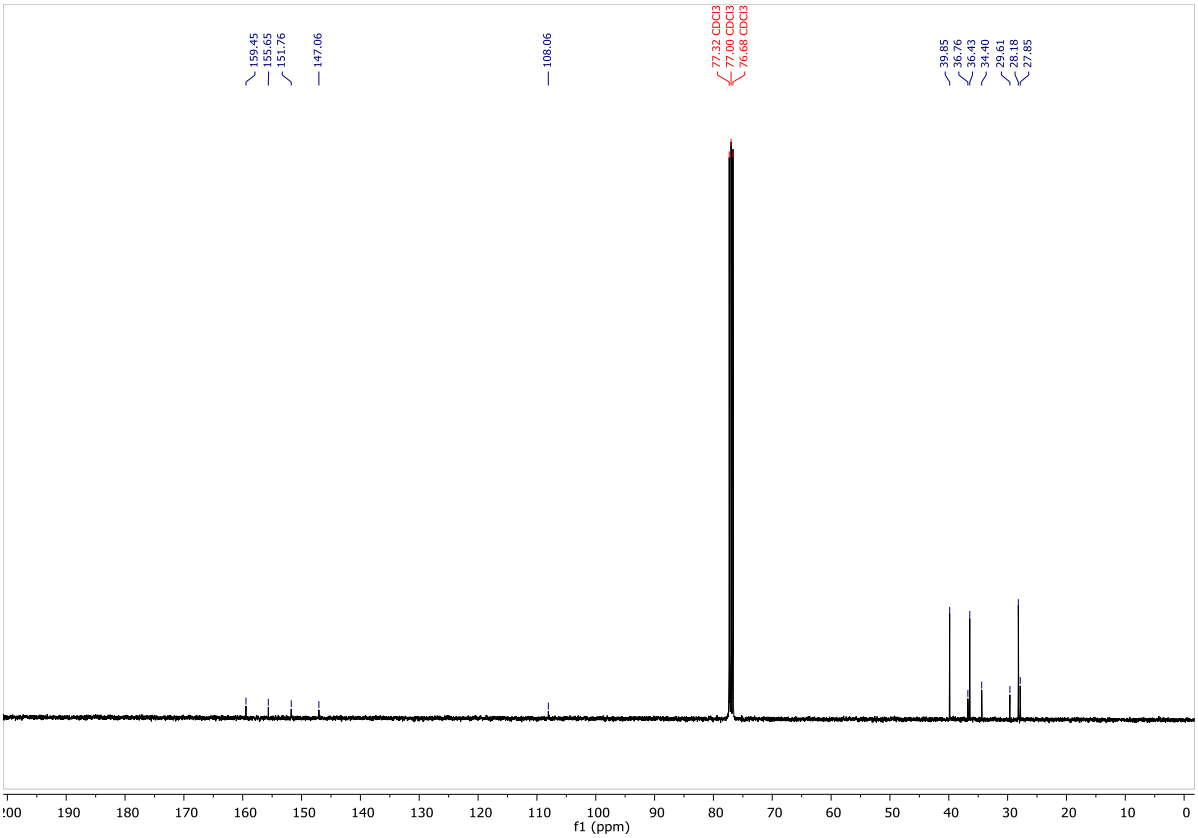
159.45
155.65
151.76
147.06
108.06
77.32 CDCl3
77.00 CDCl3
76.68 CDCl3
39.85
36.76
36.43
34.40
29.61
28.18
27.85
f1 (ppm)

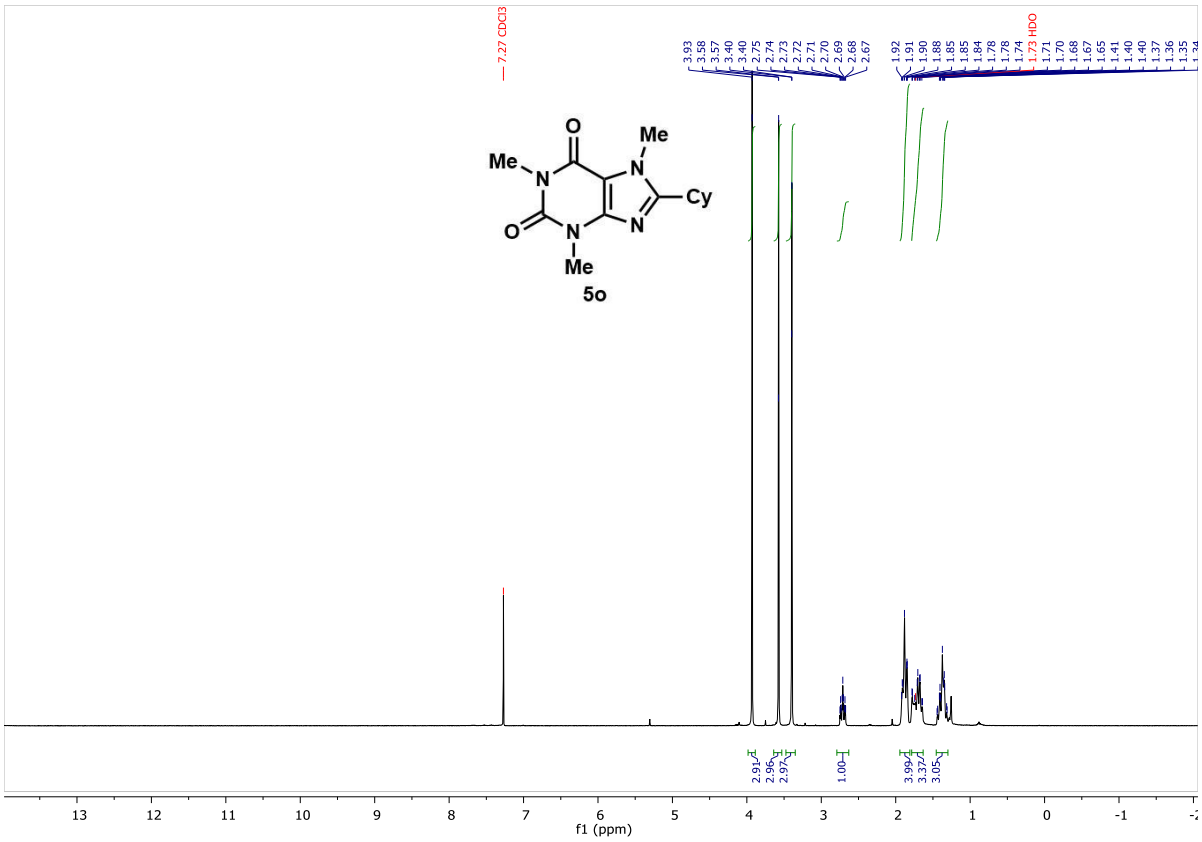
7.27 CDCl3
1.73 HDO
Me
Me
Me
Cy
5o
f1 (ppm)

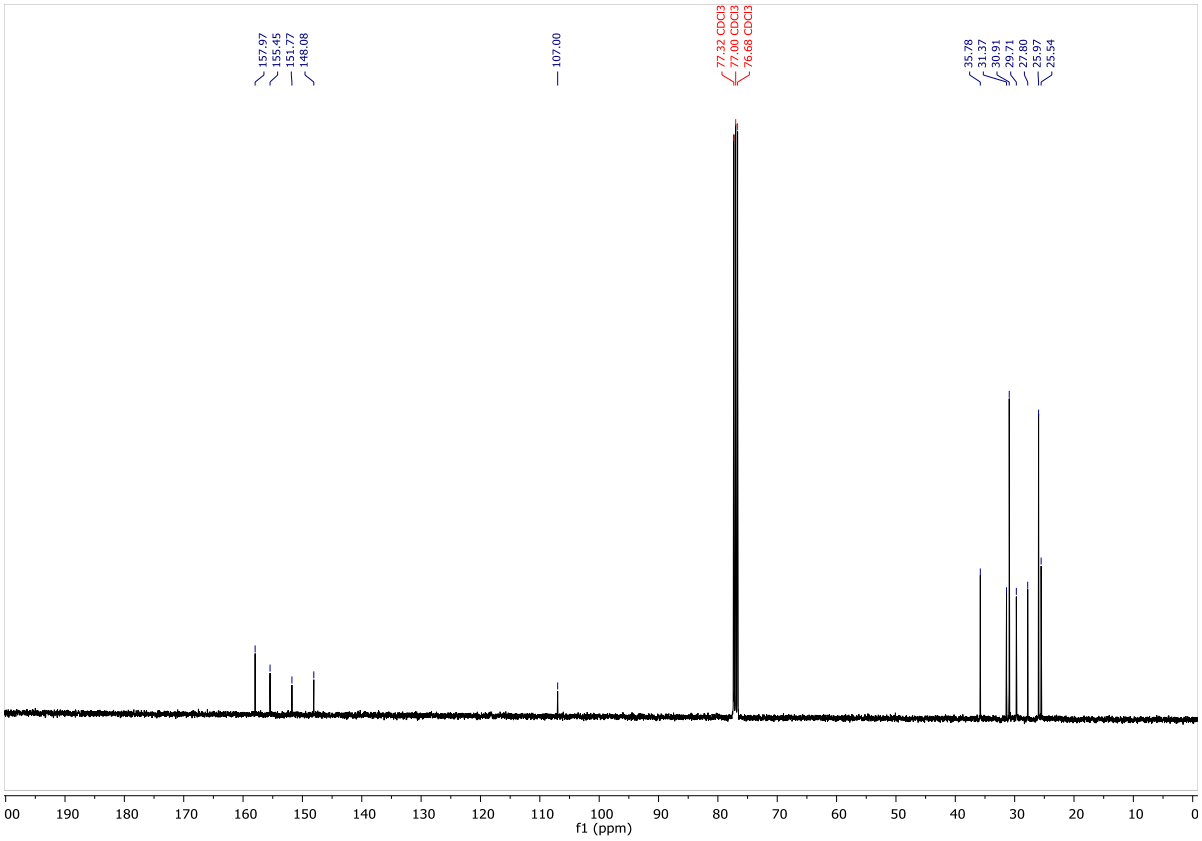
157.97
155.45
151.77
148.08
107.00
77.32 CDCl3
77.00 CDCl3
76.68 CDCl3
35.78
31.37
30.91
29.71
27.80
25.97
25.54
f1 (ppm)

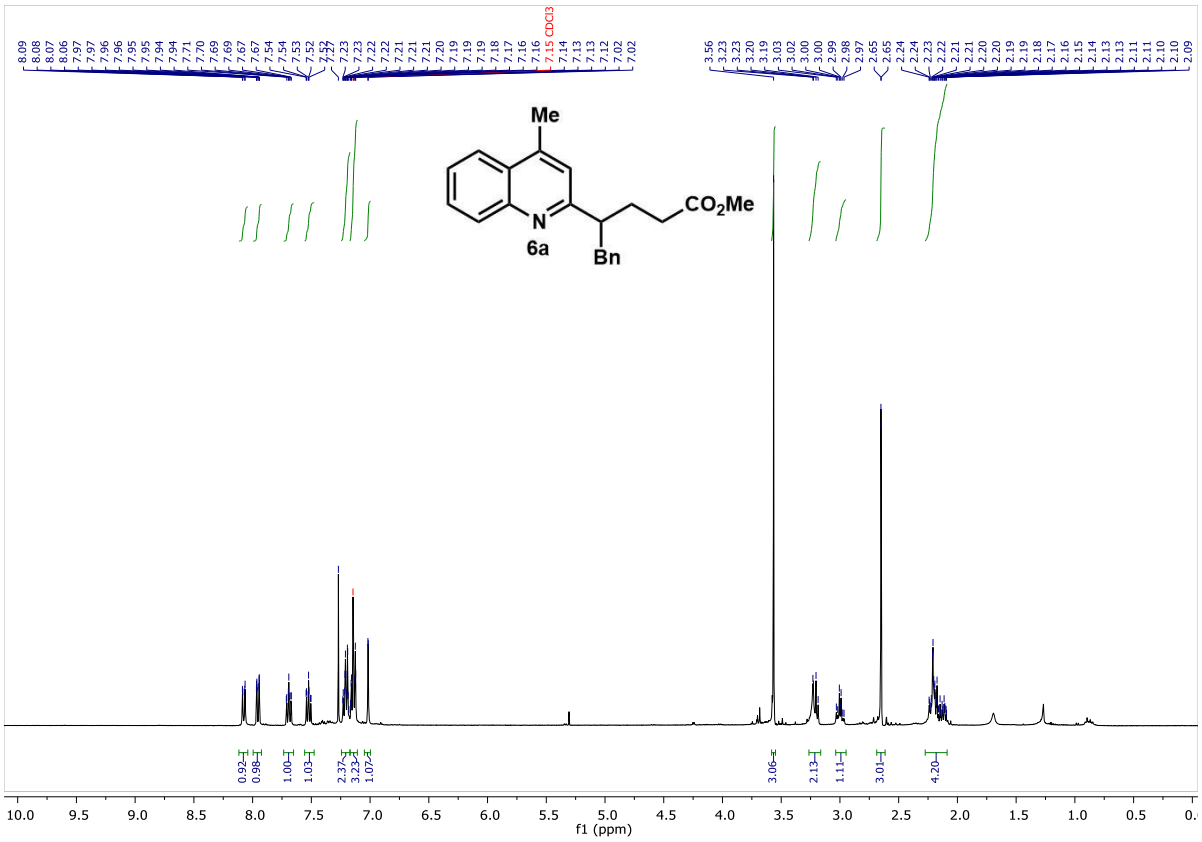
Me
N
6a
Bn
CO2Me
f1 (ppm)

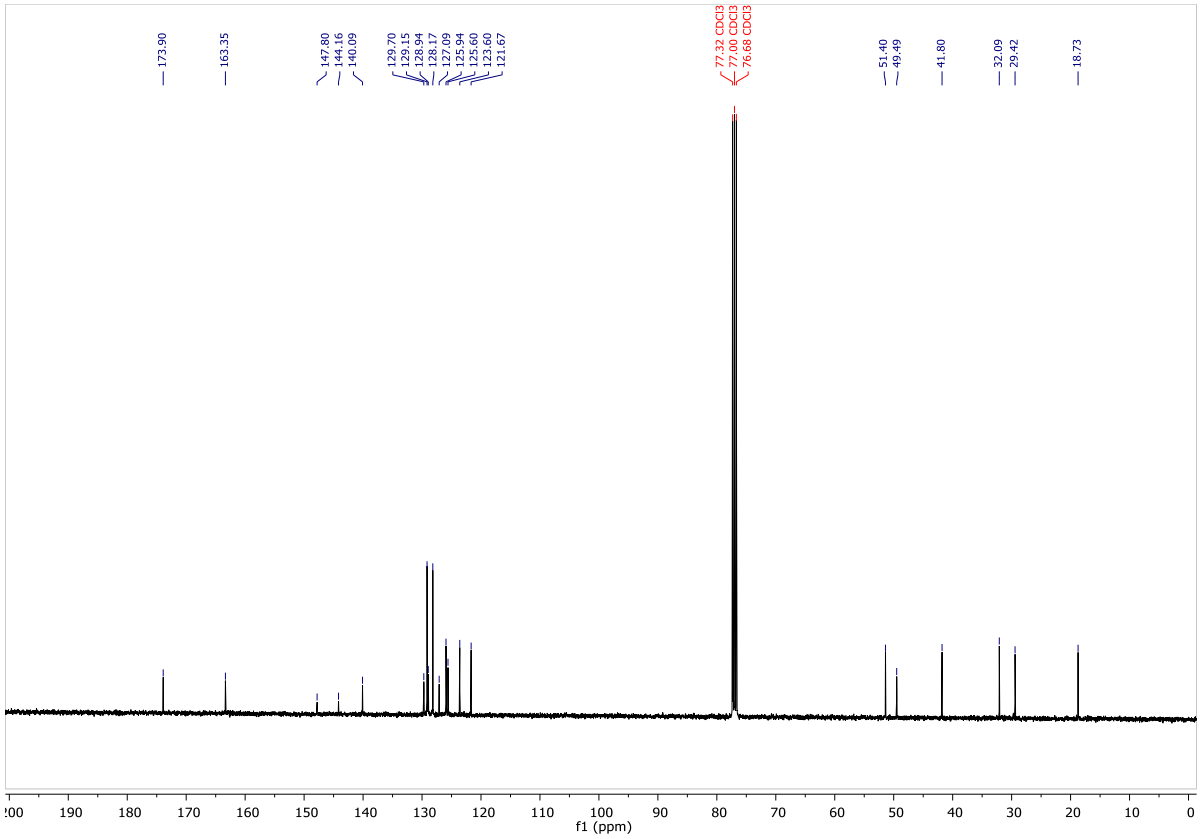
f1 (ppm)

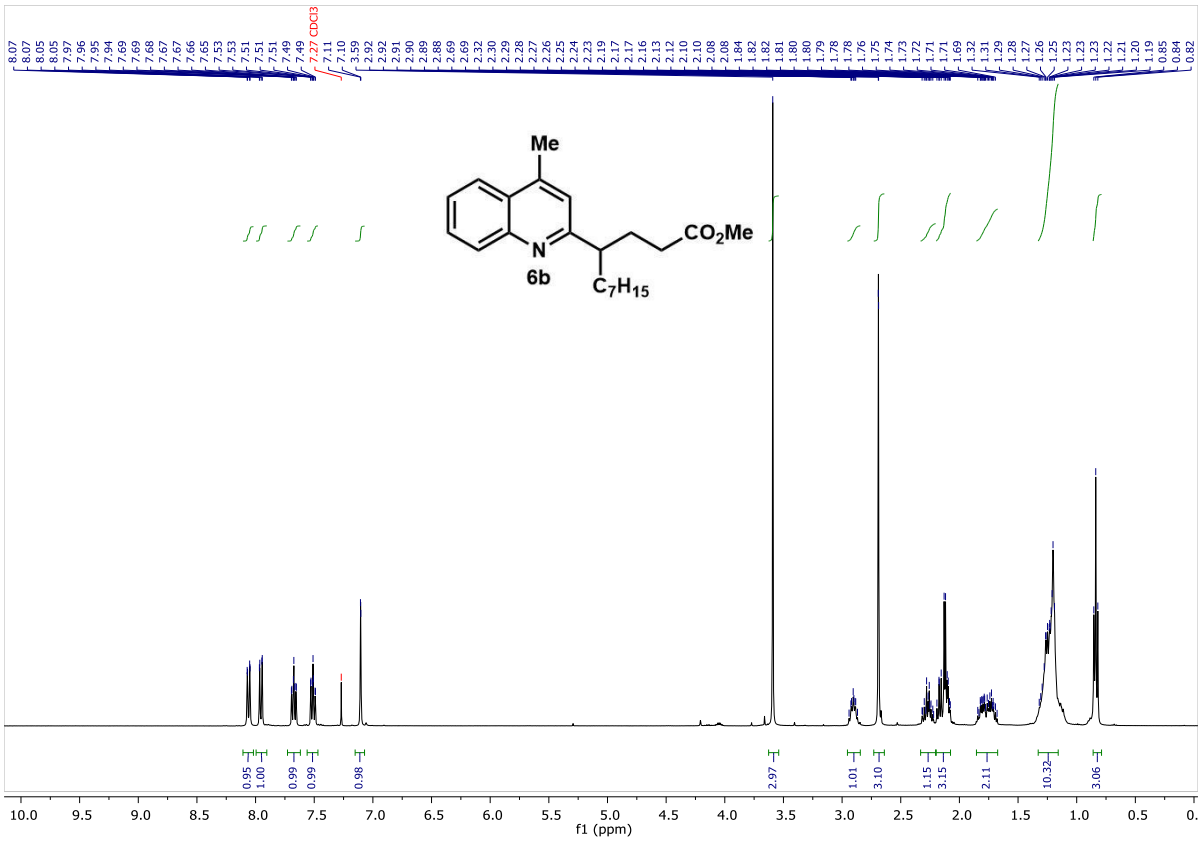
Me
N
6b
C_7H_{15}
CO_2Me
f1 (ppm)

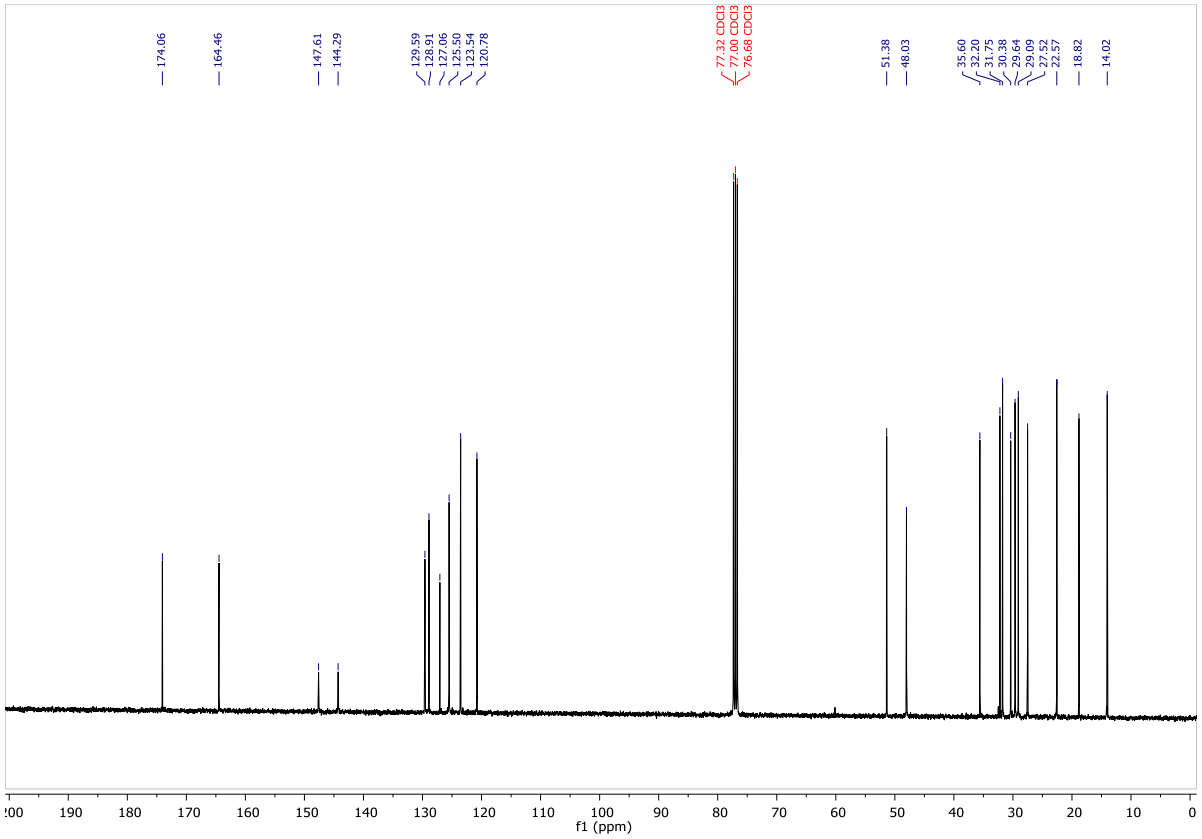
f1 (ppm)

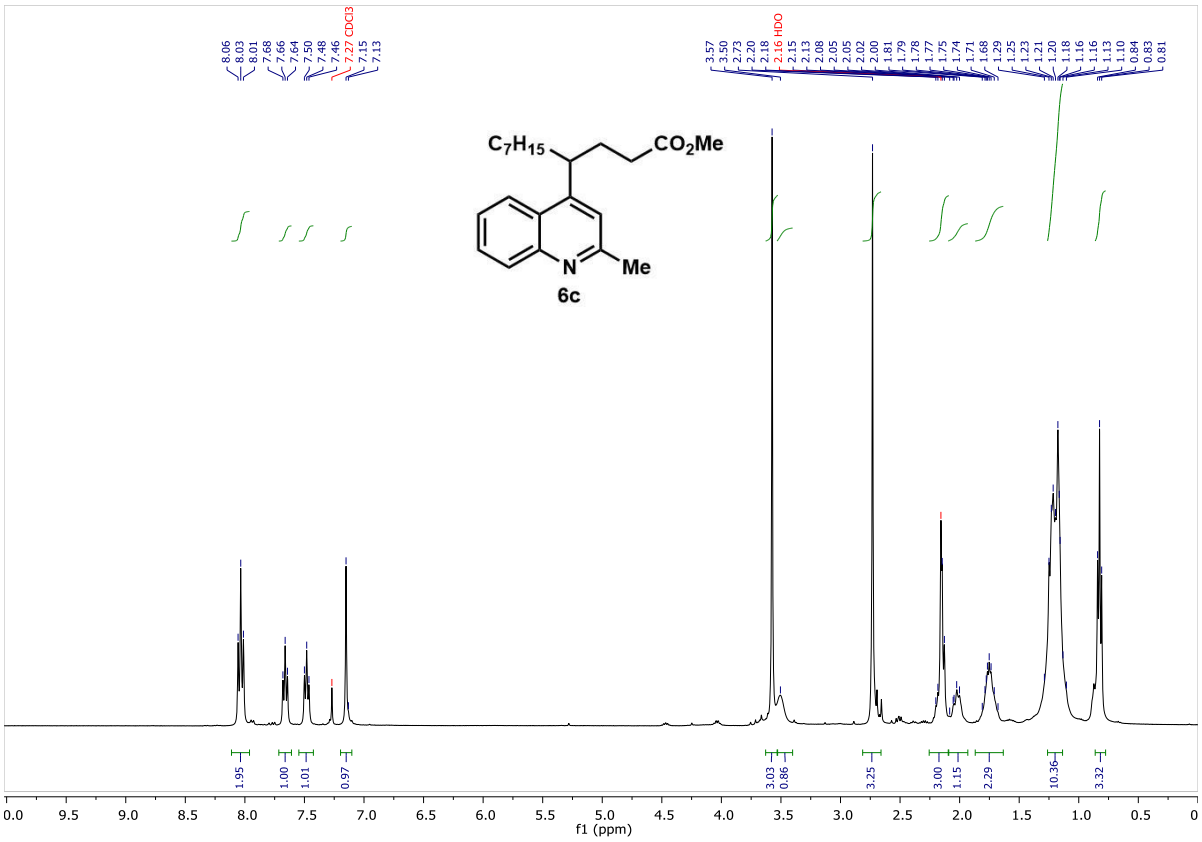
8.06
8.03
8.01
7.68
7.66
7.64
7.50
7.48
7.46
7.27 CDCl3
7.15
7.13
3.57
3.50
3.23
2.20
2.18
2.16 HDO
2.15
2.13
2.08
2.05
2.05
2.02
2.00
1.81
1.79
1.78
1.77
1.75
1.74
1.71
1.68
1.29
1.25
1.23
1.21
1.20
1.18
1.16
1.16
1.13
1.10
0.84
0.83
0.81
C7H15
CO2Me
N
Me
6c
1.95
1.00
1.01
0.97
3.03
0.86
3.25
3.00
1.15
2.29
10.36
3.32
f1 (ppm)

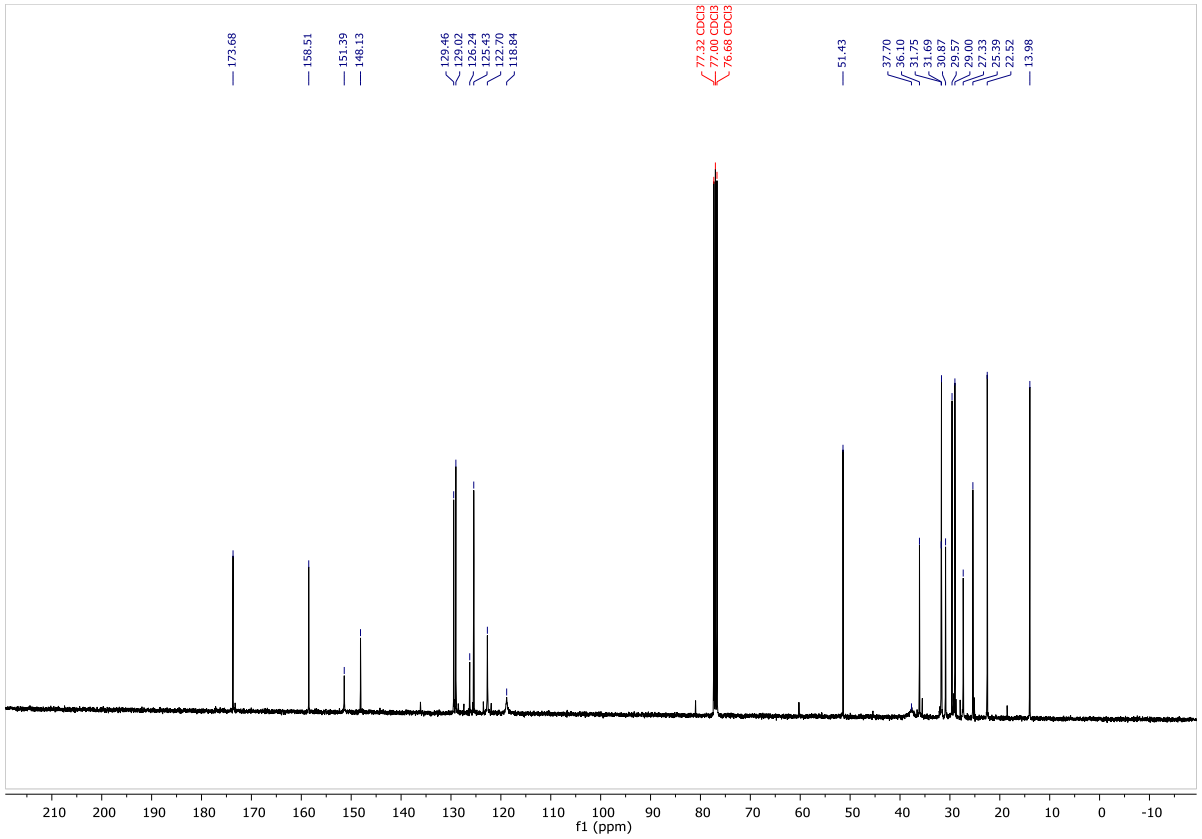
173.68
158.51
151.39
148.13
129.46
129.02
126.24
125.43
122.70
118.84
77.32 CDCl3
77.00 CDCl3
76.68 CDCl3
51.43
37.70
36.10
31.75
31.69
30.87
29.57
29.00
27.33
25.39
22.52
13.98
f1 (ppm)

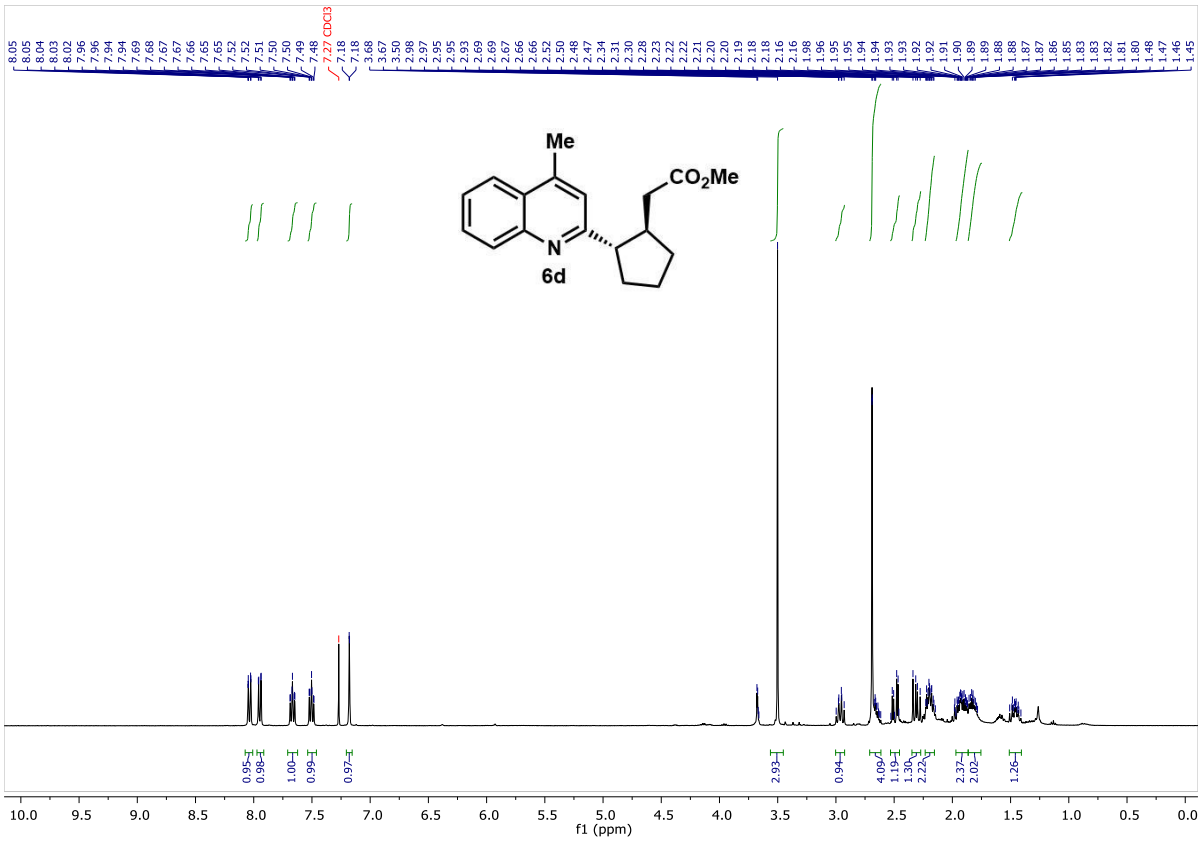
Me
CO2Me
N
6d
f1 (ppm)

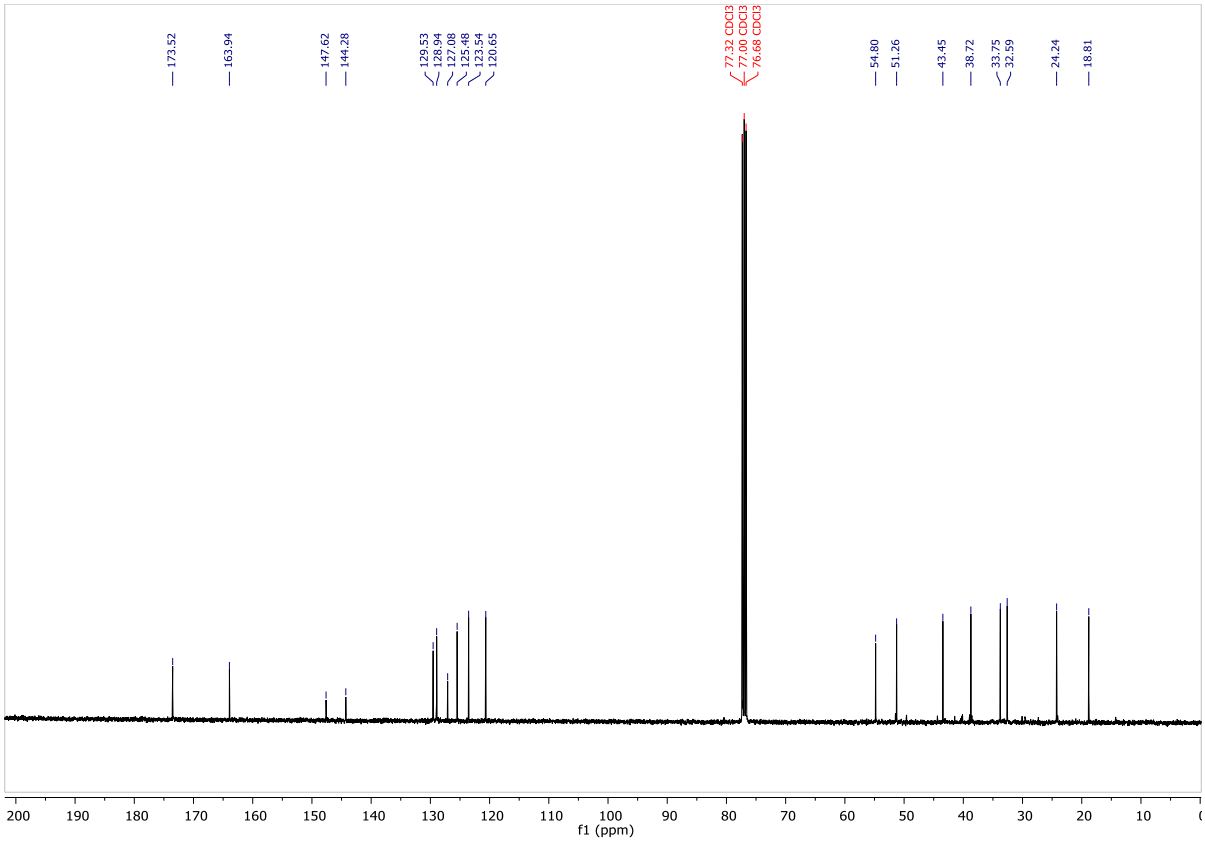
f1 (ppm)

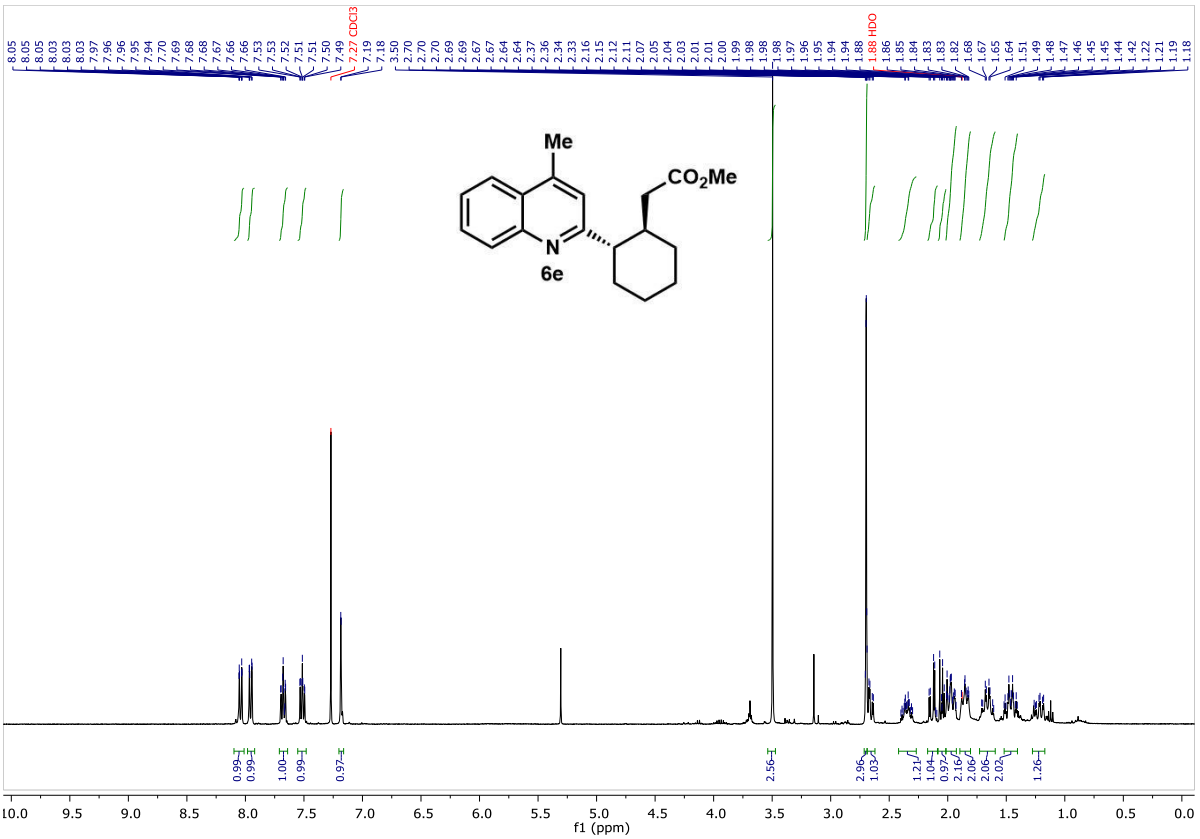
Me
CO2Me
N
6e
f1 (ppm)

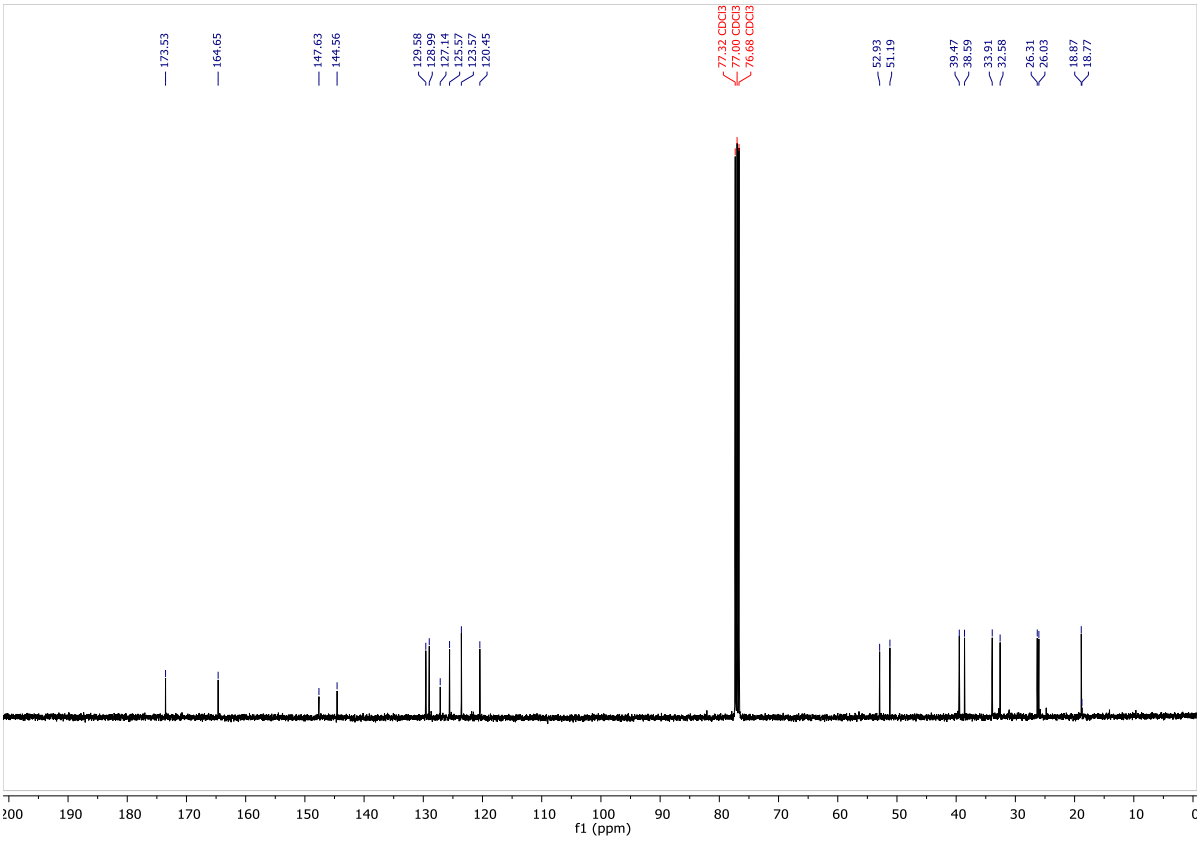
f1 (ppm)

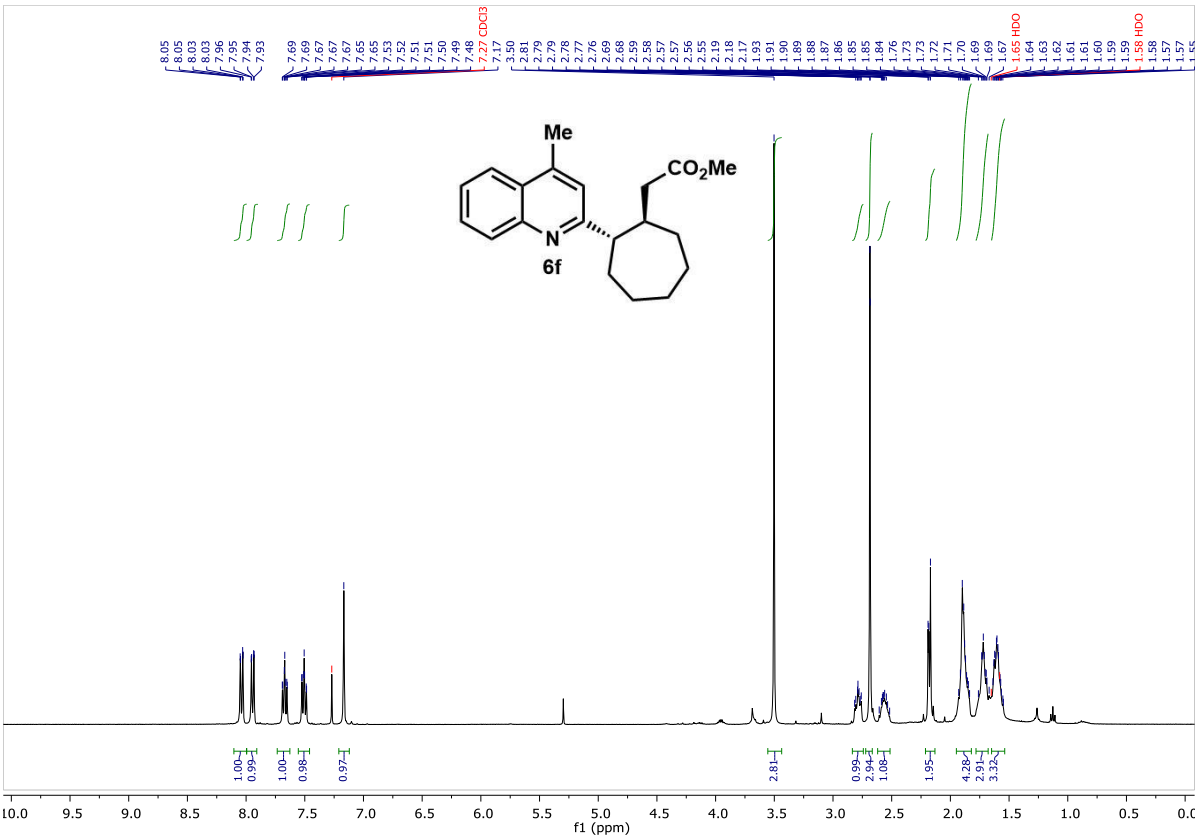
Me
CO2Me
N
6f
f1 (ppm)

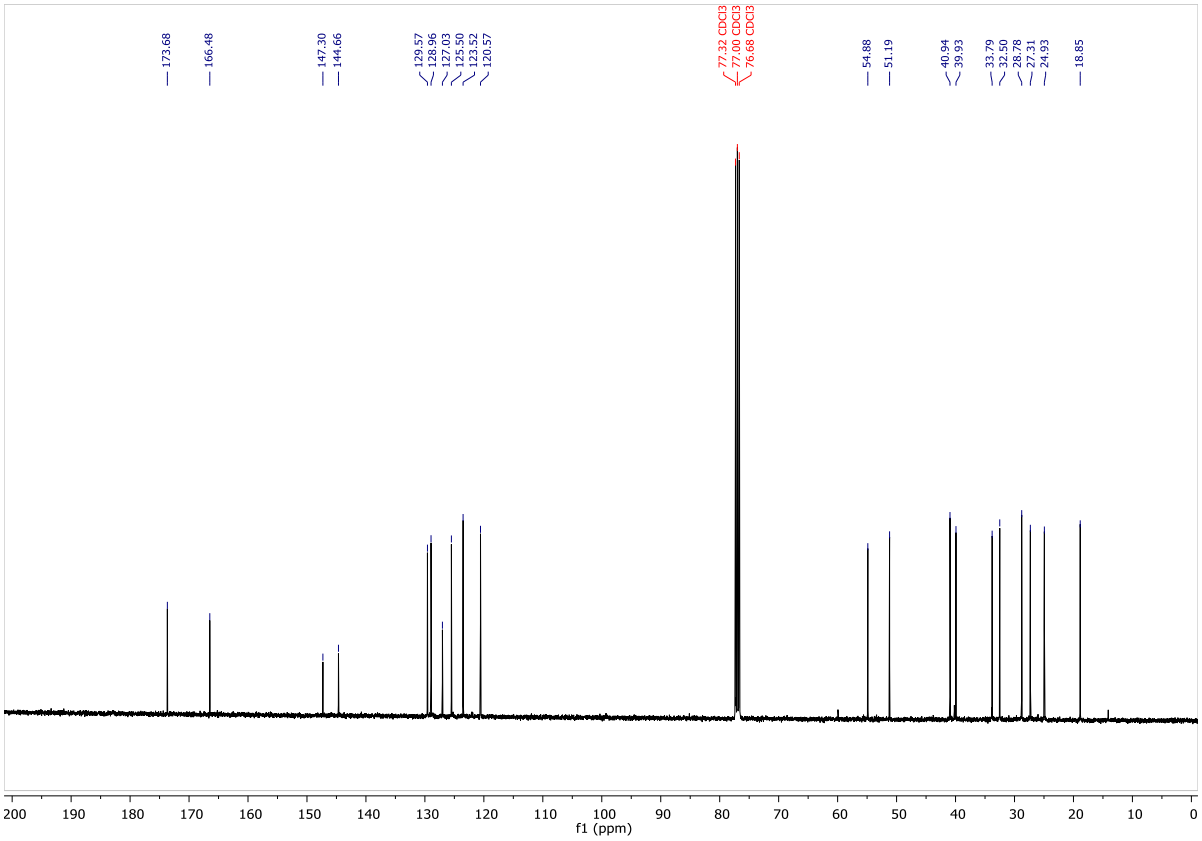
f1 (ppm)

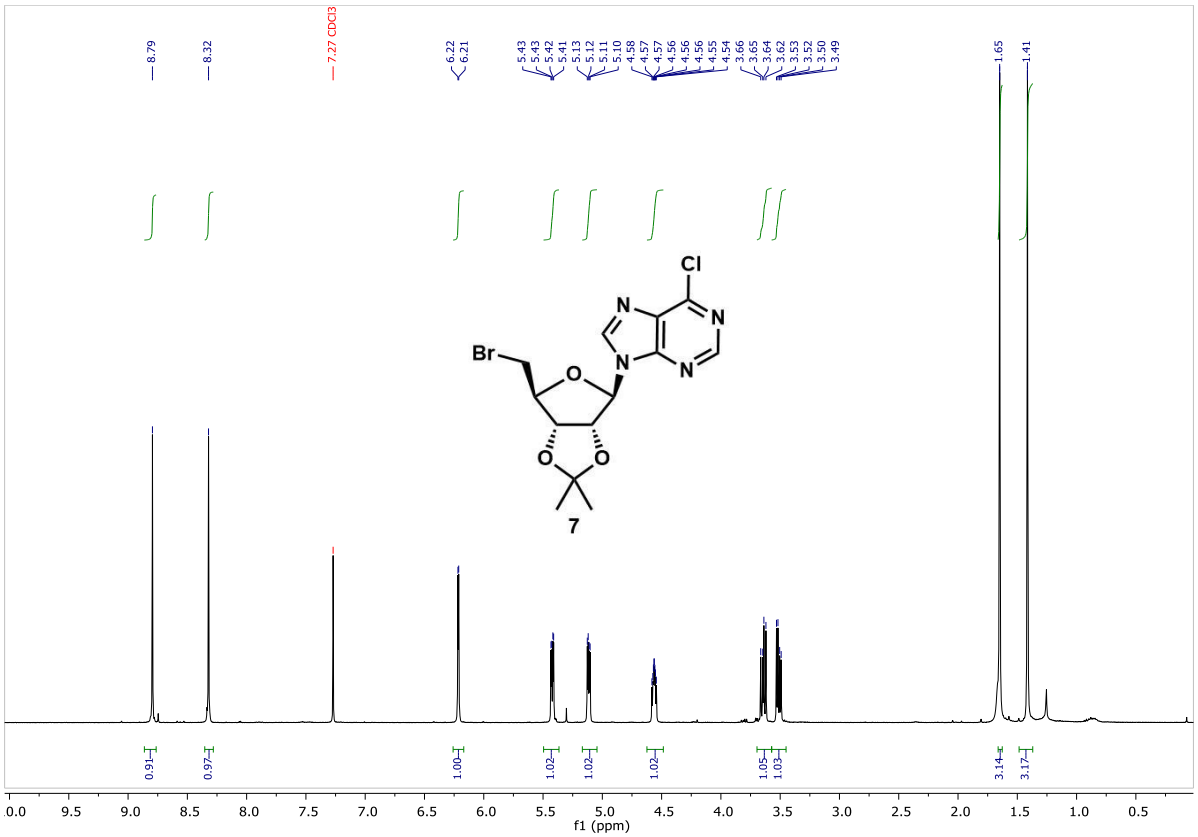
8.79
8.32
7.27 CDCl3
6.22
6.21
5.43
5.43
5.42
5.41
5.13
5.12
5.11
5.10
4.58
4.57
4.57
4.56
4.56
4.56
4.55
4.54
3.66
3.65
3.64
3.62
3.53
3.52
3.50
3.49
1.65
1.41
Cl
N
N
N
N
Br
O
O
O
7
0.91
0.97
1.00
1.02
1.02
1.02
1.05
1.03
3.14
3.17
f1 (ppm)

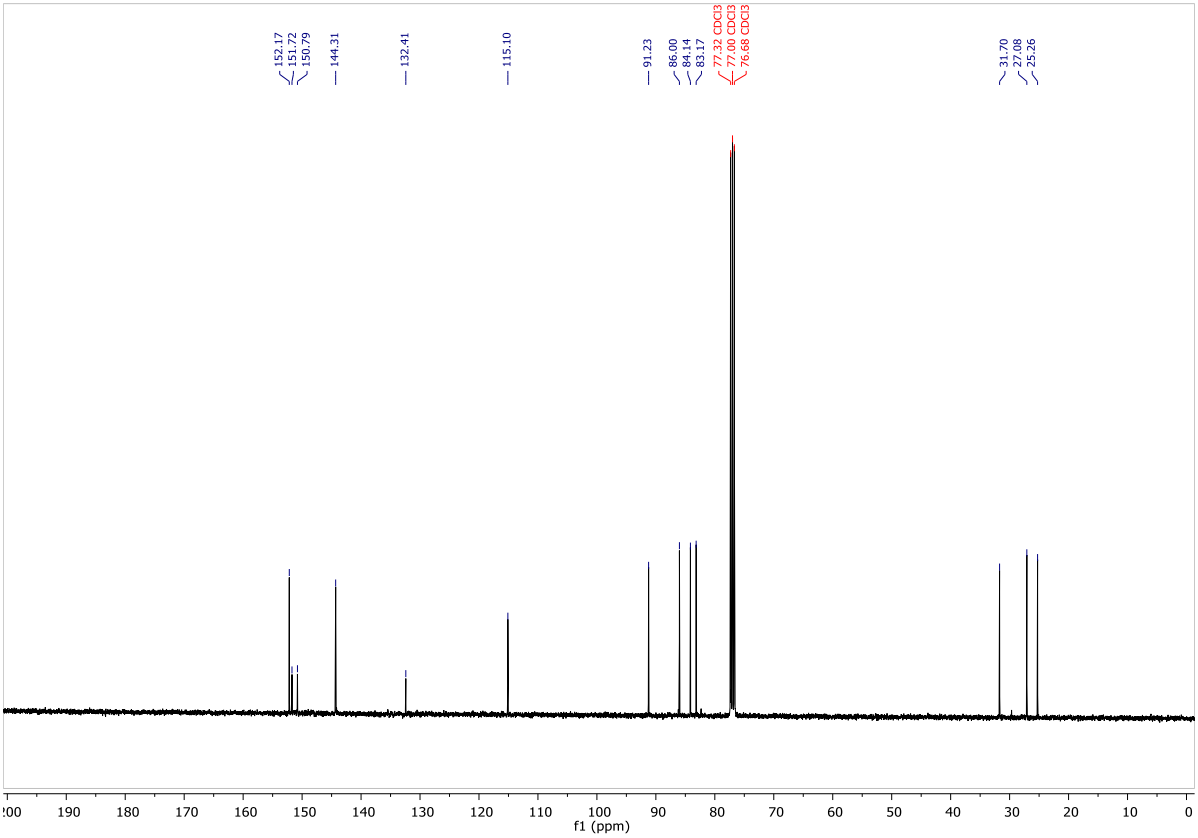
152.17
151.72
150.79
144.31
132.41
115.10
91.23
86.00
84.14
83.17
77.32 CDCl3
77.00 CDCl3
76.68 CDCl3
31.70
27.08
25.26
f1 (ppm)

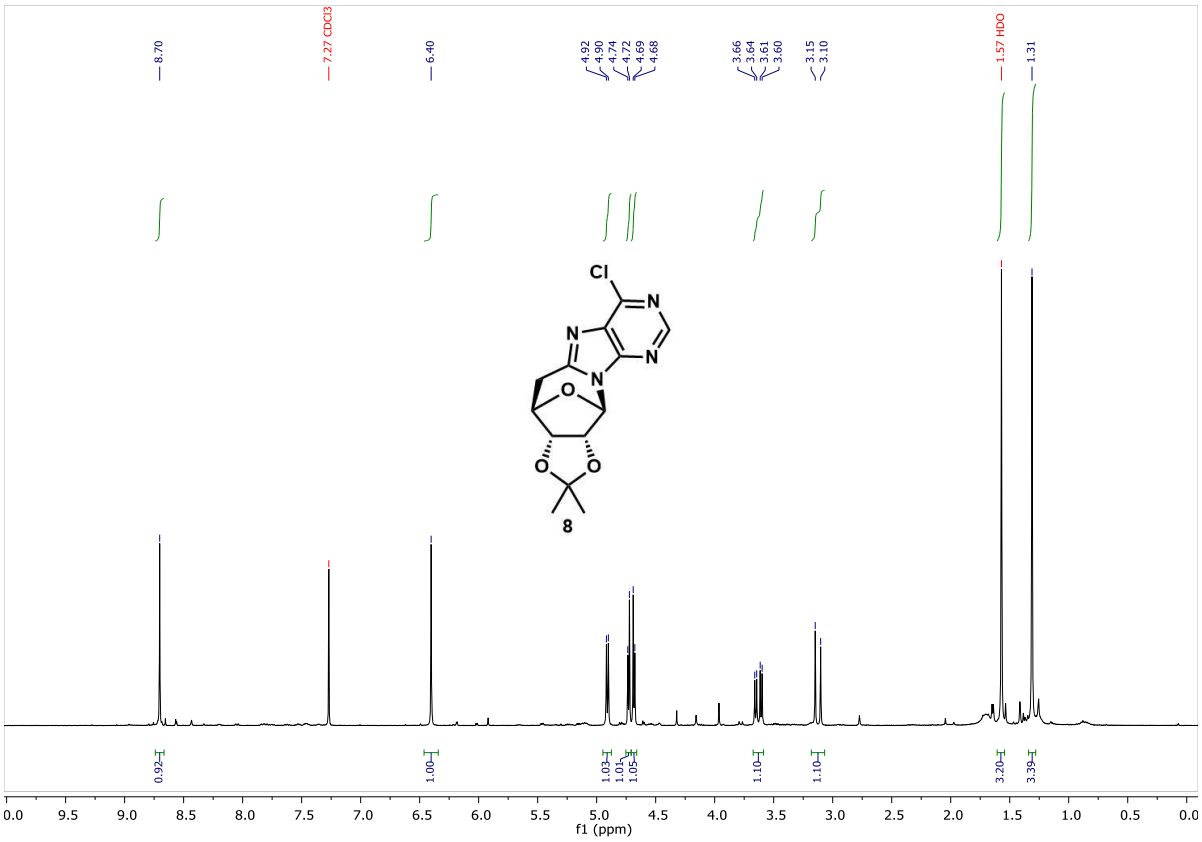
8.70
7.27 CDCl3
6.40
4.92
4.90
4.74
4.72
4.69
4.68
3.66
3.64
3.61
3.60
3.15
3.10
1.57 HDO
1.31
Cl
N
N
N
N
O
O
O
8
0.92
1.00
1.03
1.01
1.05
1.10
1.10
3.20
3.39
f1 (ppm)

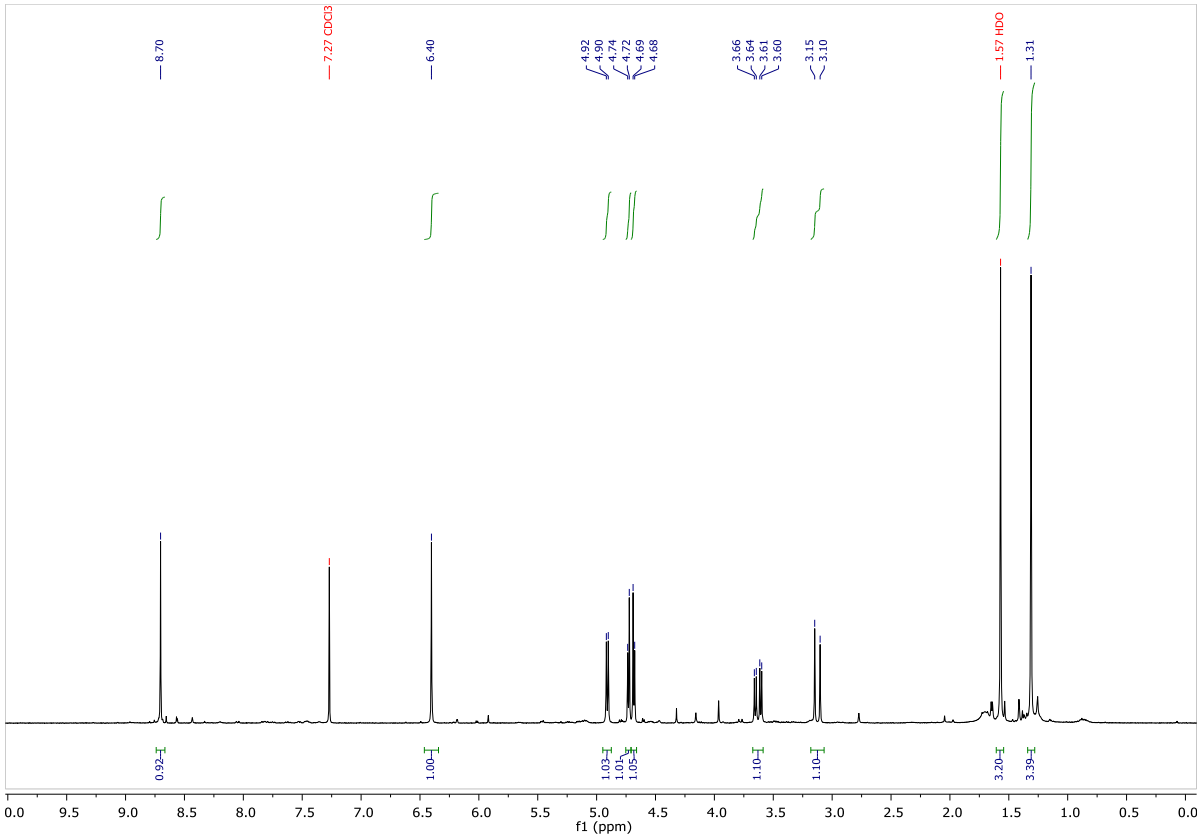
8.70
7.27 CDCl3
6.40
4.92
4.90
4.74
4.72
4.69
4.68
3.66
3.64
3.61
3.60
3.15
3.10
1.57 HDO
1.31
0.92
1.00
1.03
1.01
1.05
1.10
1.10
3.20
3.39
f1 (ppm)

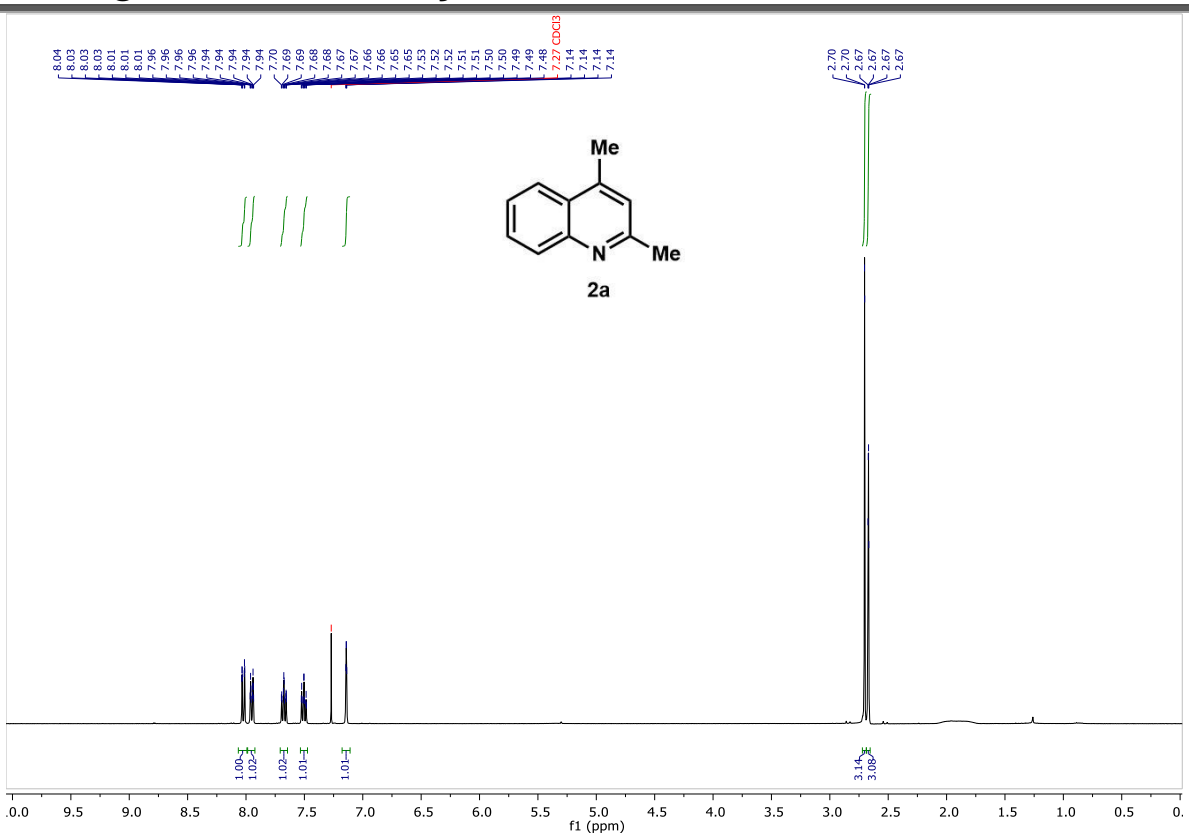
Me
N
Me
2a
f1 (ppm)

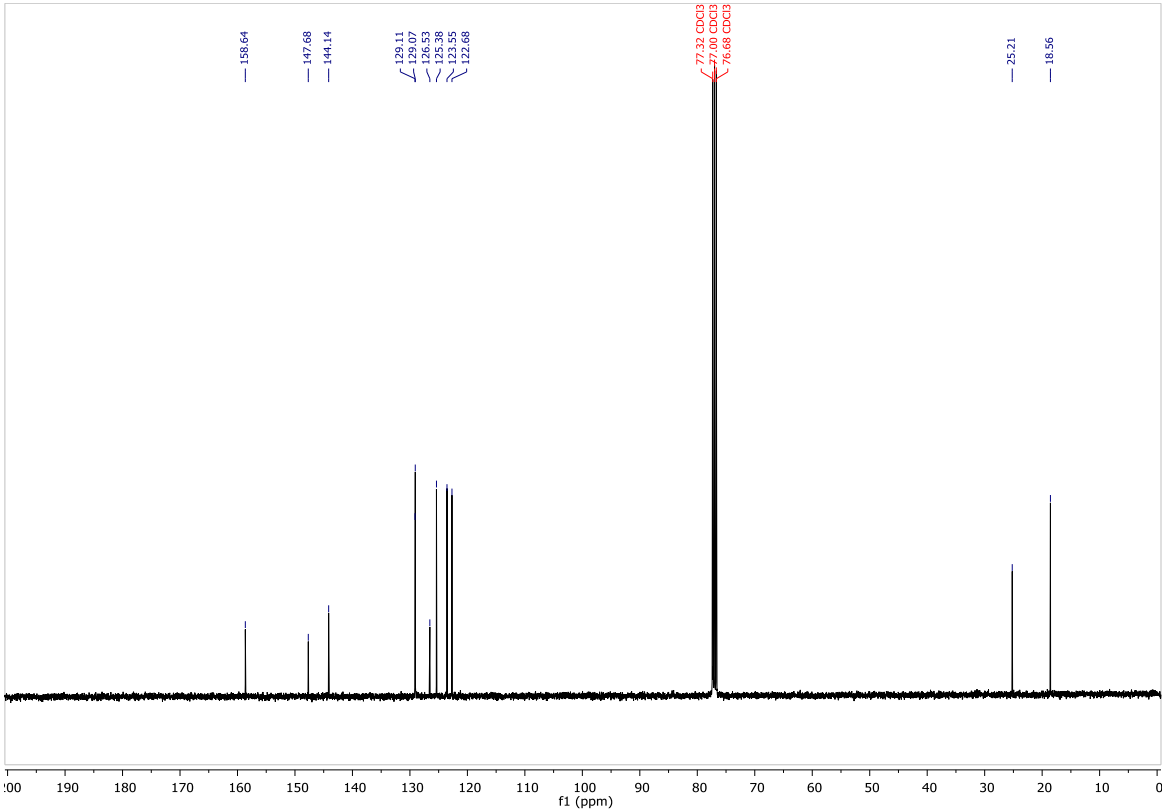
158.64
147.68
144.14
129.11
129.07
126.53
123.58
123.55
122.68
77.32 CDCl3
77.00 CDCl3
76.68 CDCl3
25.21
18.56
f1 (ppm)

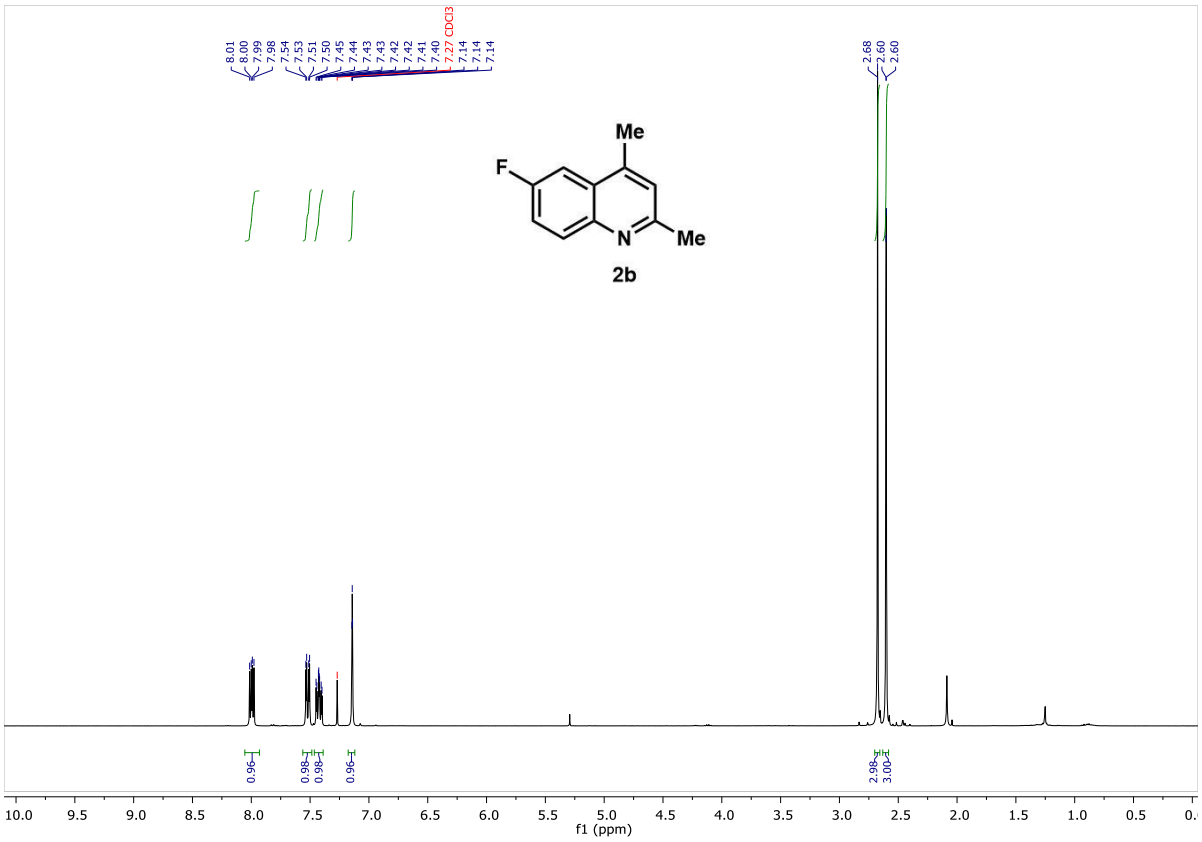
8.01
8.00
7.99
7.98
7.54
7.53
7.51
7.50
7.45
7.44
7.43
7.43
7.42
7.42
7.41
7.40
7.27 CDCl3
7.14
7.14
7.14
2.68
2.60
2.60
2.60
Me
F
N
Me
2b
0.96
0.98
0.98
0.96
2.98
3.00
f1 (ppm)

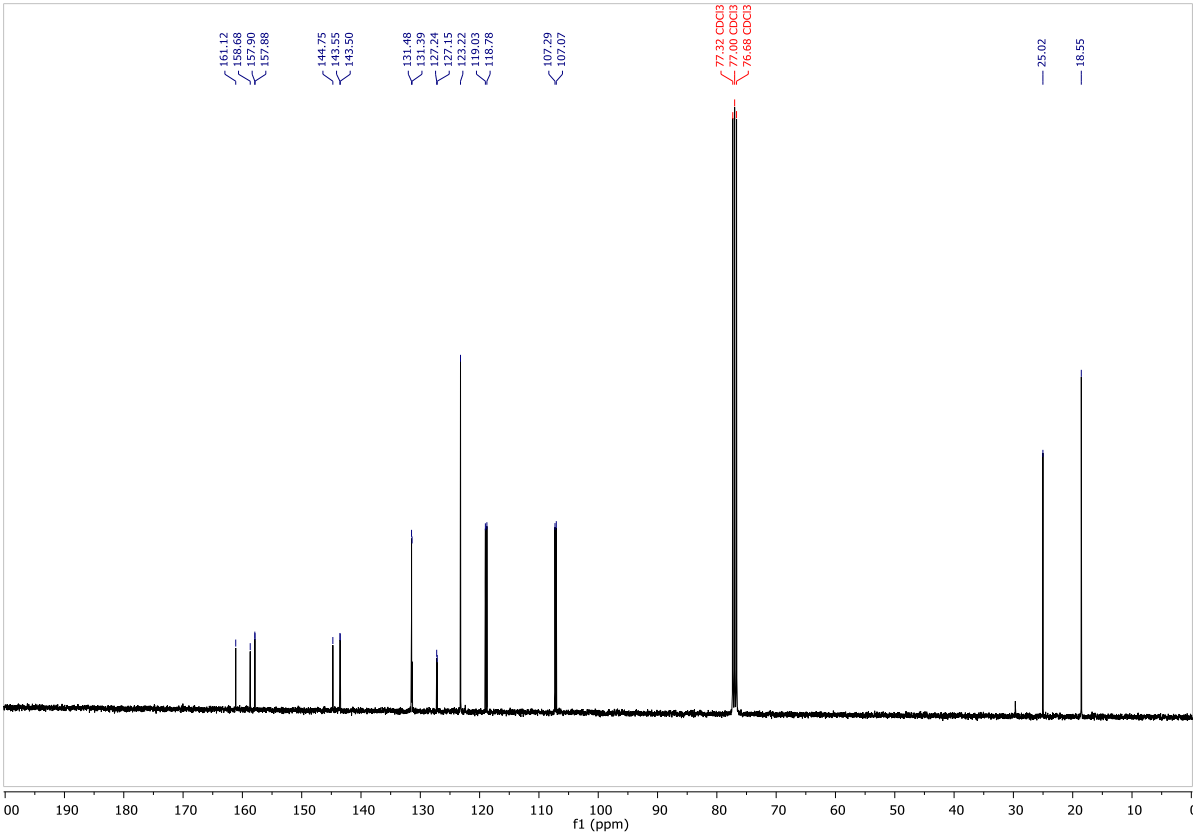
161.12
158.68
157.90
157.88
144.75
143.55
143.50
131.48
131.39
127.24
127.15
123.22
119.03
118.78
107.29
107.07
77.32 CDCl3
77.00 CDCl3
76.68 CDCl3
25.02
18.55
f1 (ppm)

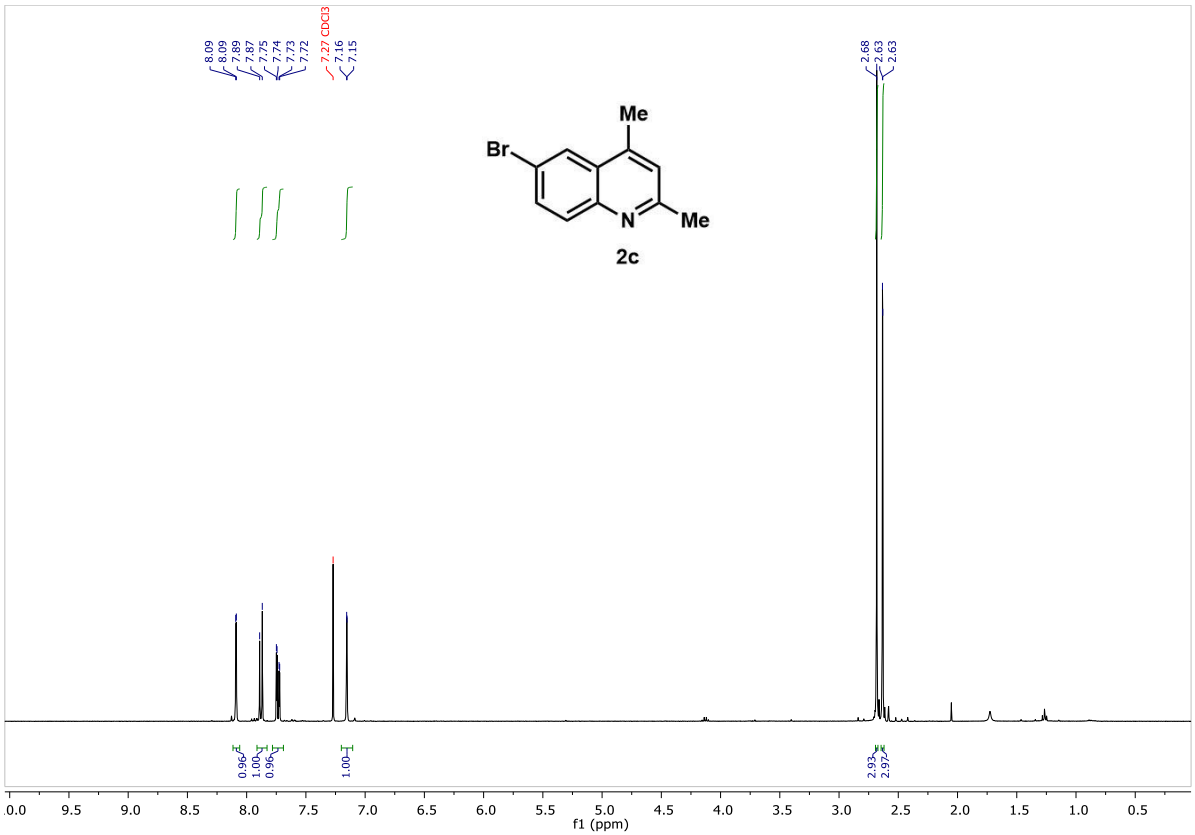
8.09
8.09
7.89
7.87
7.75
7.74
7.73
7.72
7.27 CDCl3
7.16
7.15
2.68
2.63
2.63
Me
Br
N
Me
2c
0.96
1.00
0.96
1.00
2.93
2.97
f1 (ppm)

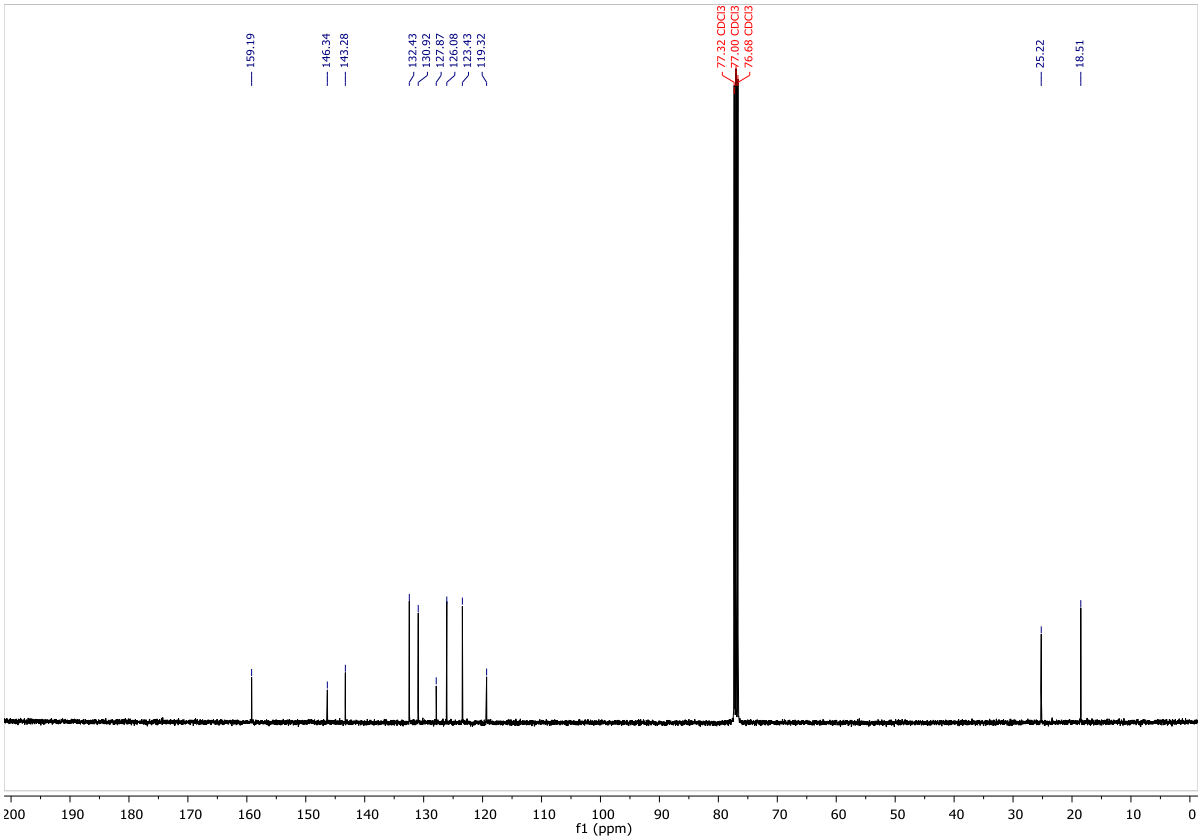
159.19
146.34
143.28
132.43
130.92
127.87
126.08
123.43
119.32
77.32 CDCl3
77.00 CDCl3
76.68 CDCl3
25.22
18.51
f1 (ppm)

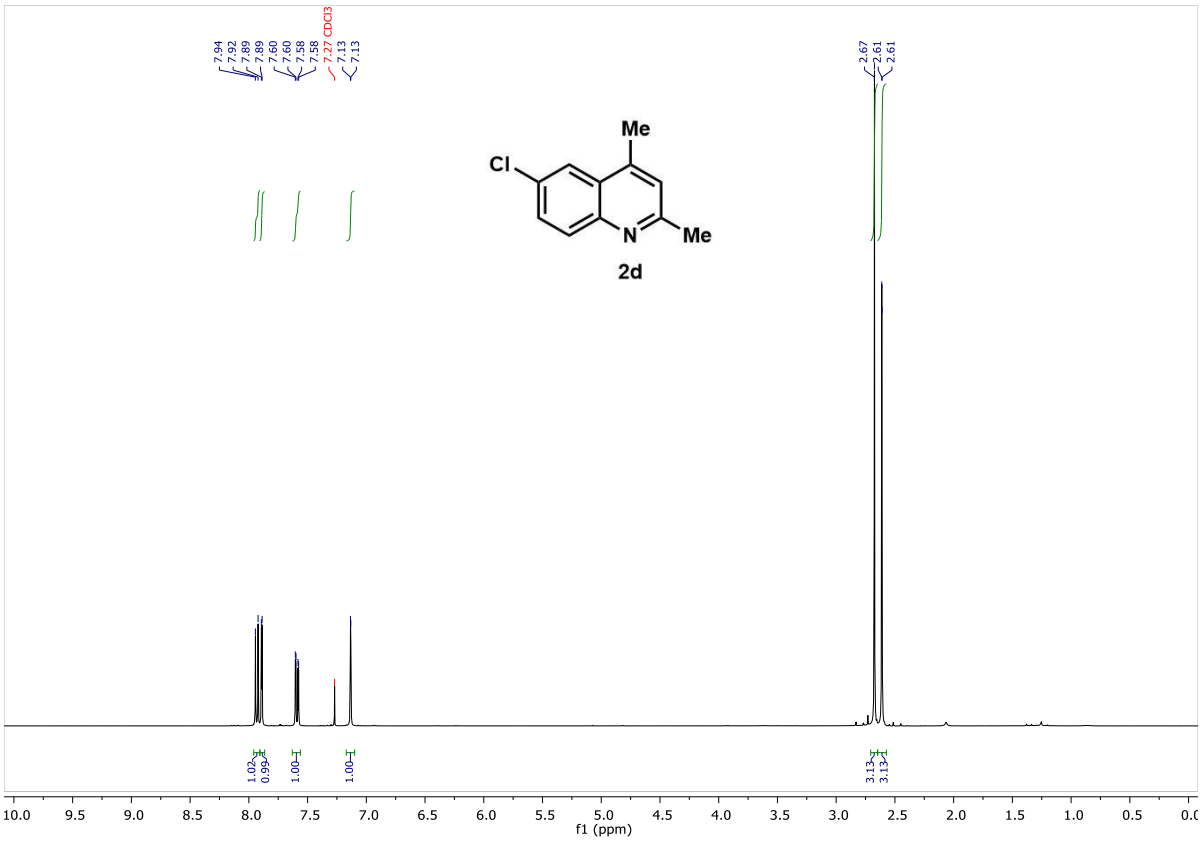
7.94
7.92
7.89
7.89
7.60
7.60
7.58
7.58
7.27 CDCl3
7.13
7.13
2.67
2.61
2.61
Me
Cl
N
Me
2d
1.02
0.99
1.00
1.00
3.13
3.13
f1 (ppm)

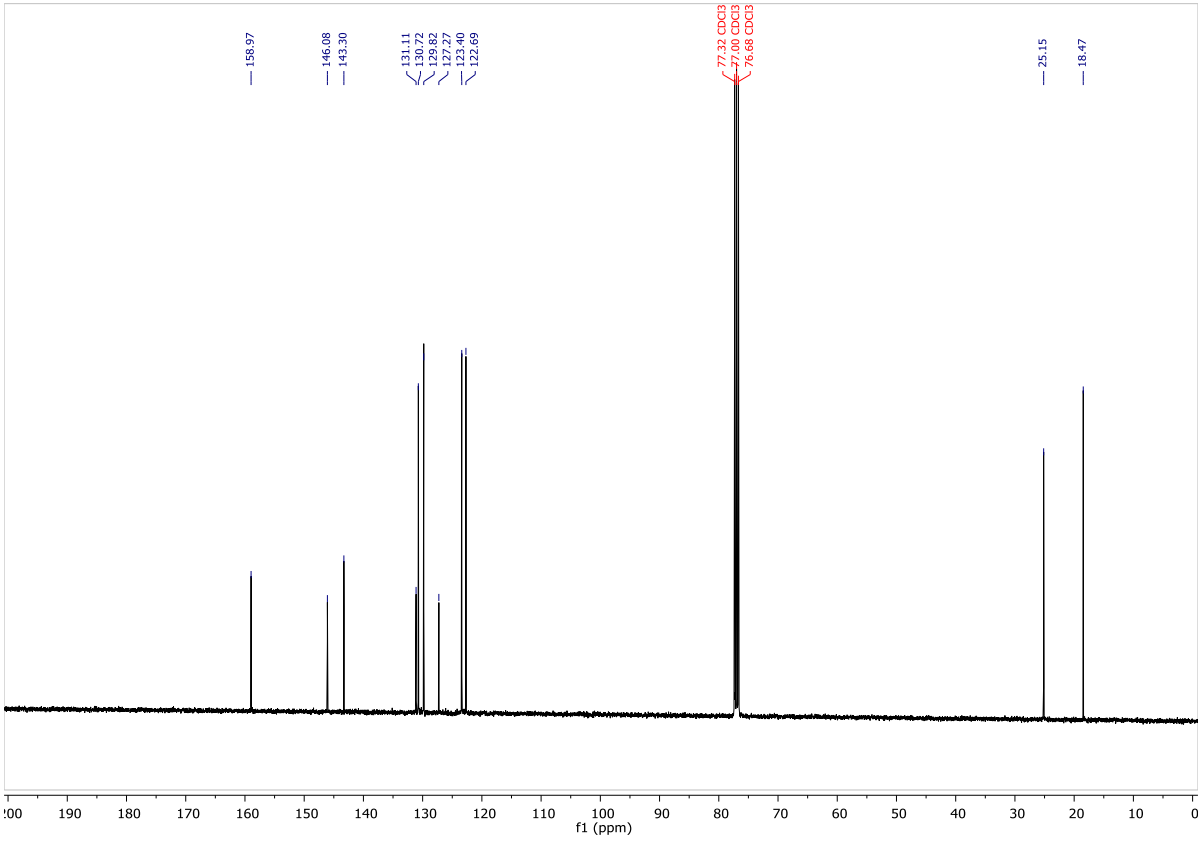
158.97
146.08
143.30
131.11
130.72
129.82
127.27
123.40
122.69
77.32 CDCl3
77.00 CDCl3
76.68 CDCl3
25.15
18.47
f1 (ppm)

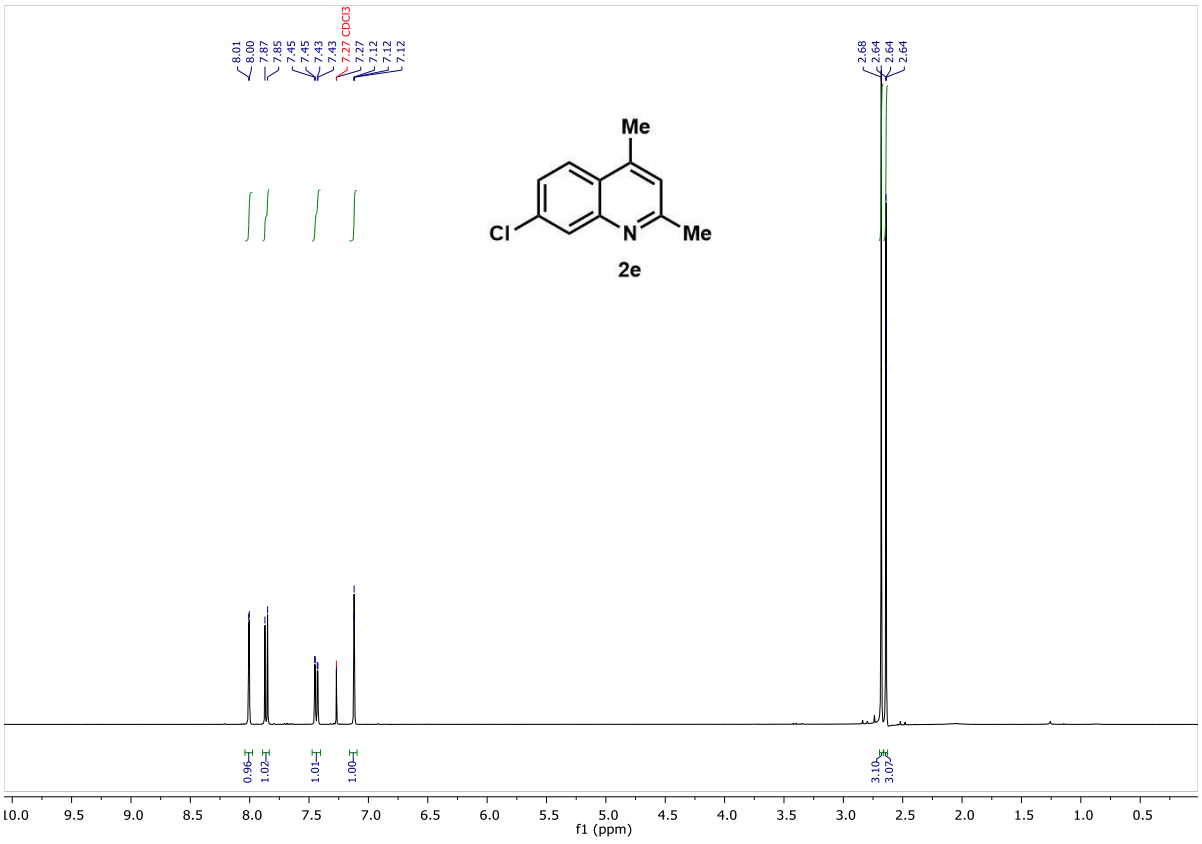
8.01
8.00
7.87
7.85
7.45
7.45
7.43
7.43
7.27 CDCl3
7.27
7.12
7.12
7.12
2.68
2.64
2.64
2.64
Me
Cl
N
Me
2e
0.96
1.02
1.01
1.00
3.10
3.07
f1 (ppm)

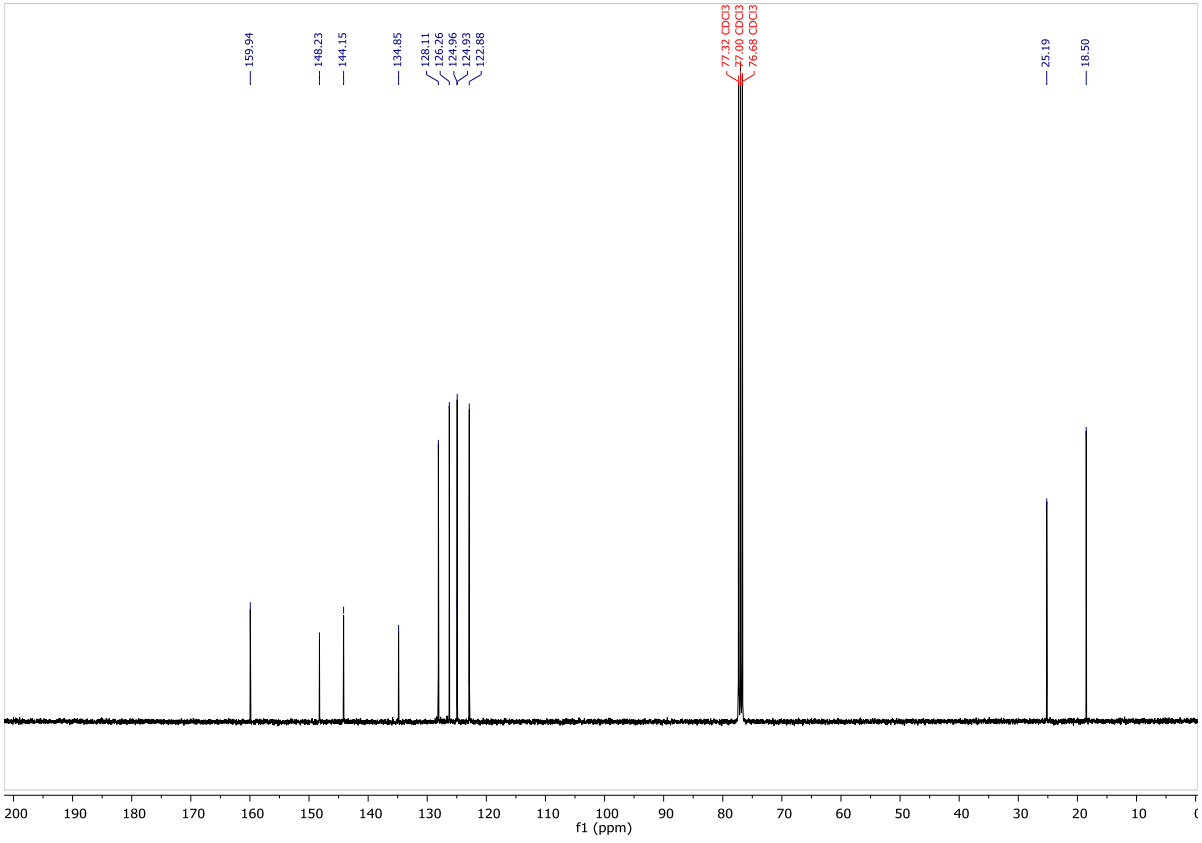
159.94
148.23
144.15
134.85
128.11
126.26
124.96
124.93
122.88
77.32 CDCl3
77.00 CDCl3
76.68 CDCl3
25.19
18.50
f1 (ppm)

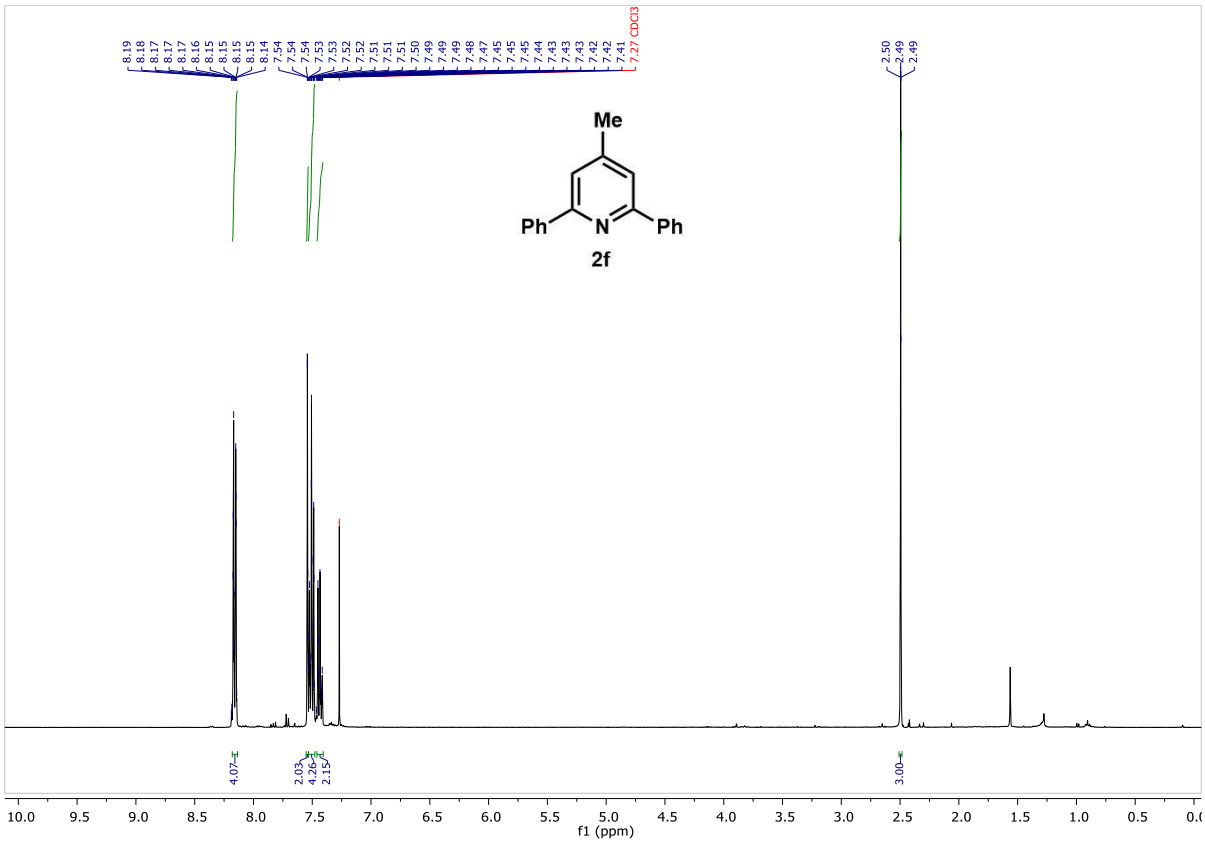
Me
Ph
N
Ph
2f
f1 (ppm)

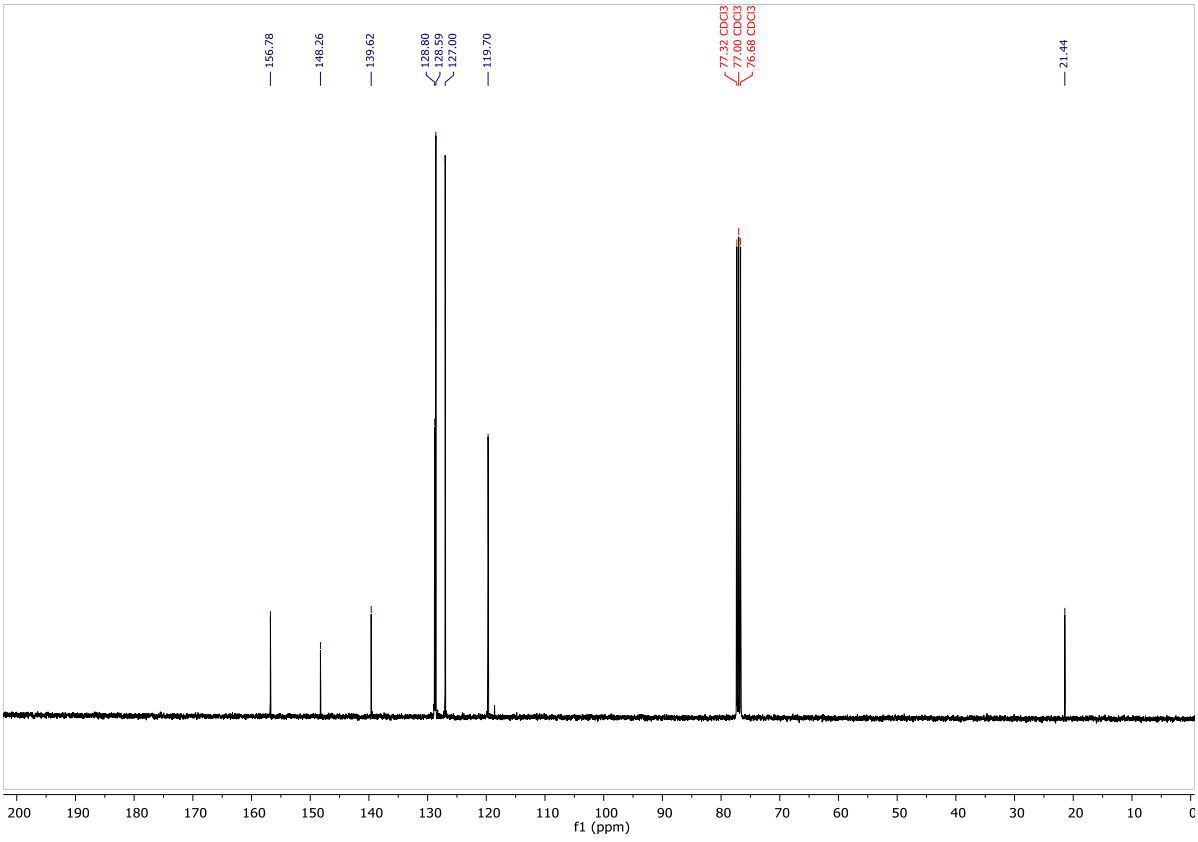
156.78
148.26
139.62
128.80
128.59
127.00
119.70
77.32 CDCl3
77.00 CDCl3
76.68 CDCl3
21.44
f1 (ppm)

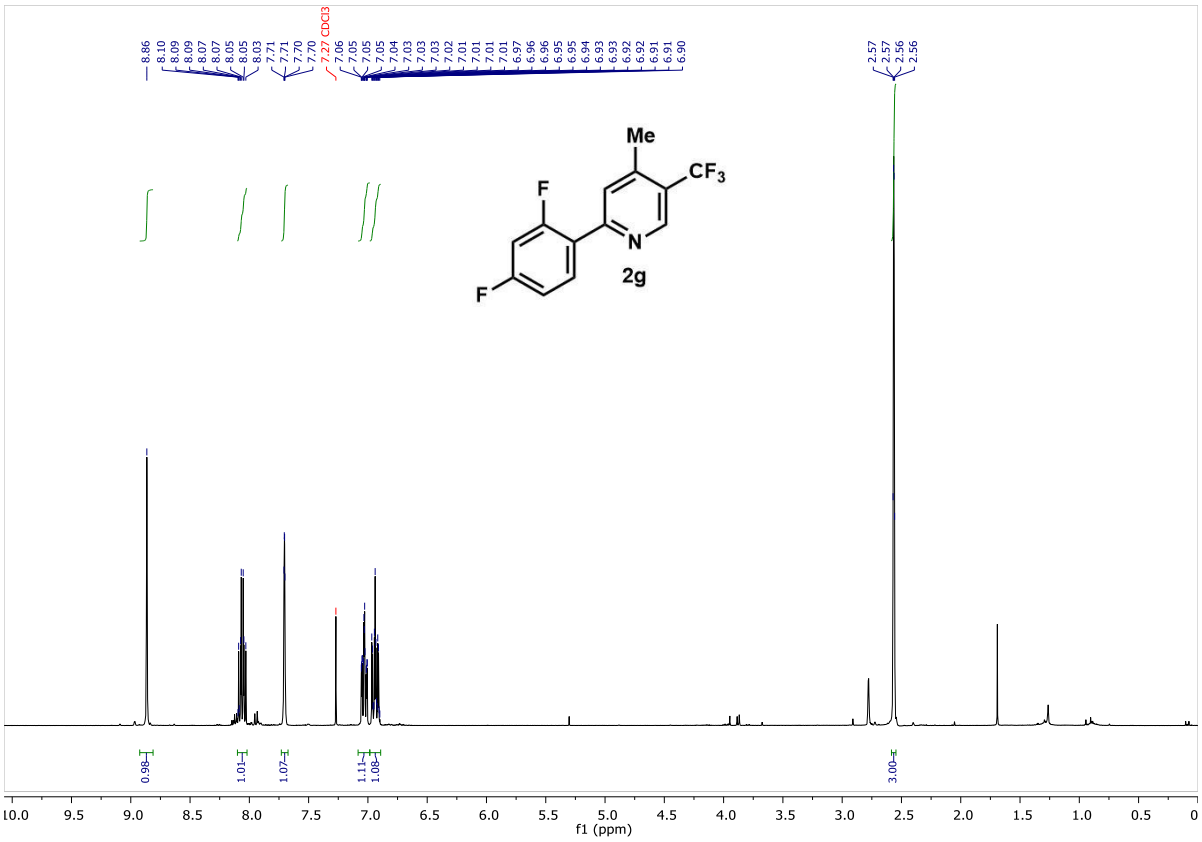
Me
CF3
F
N
F
2g
f1 (ppm)

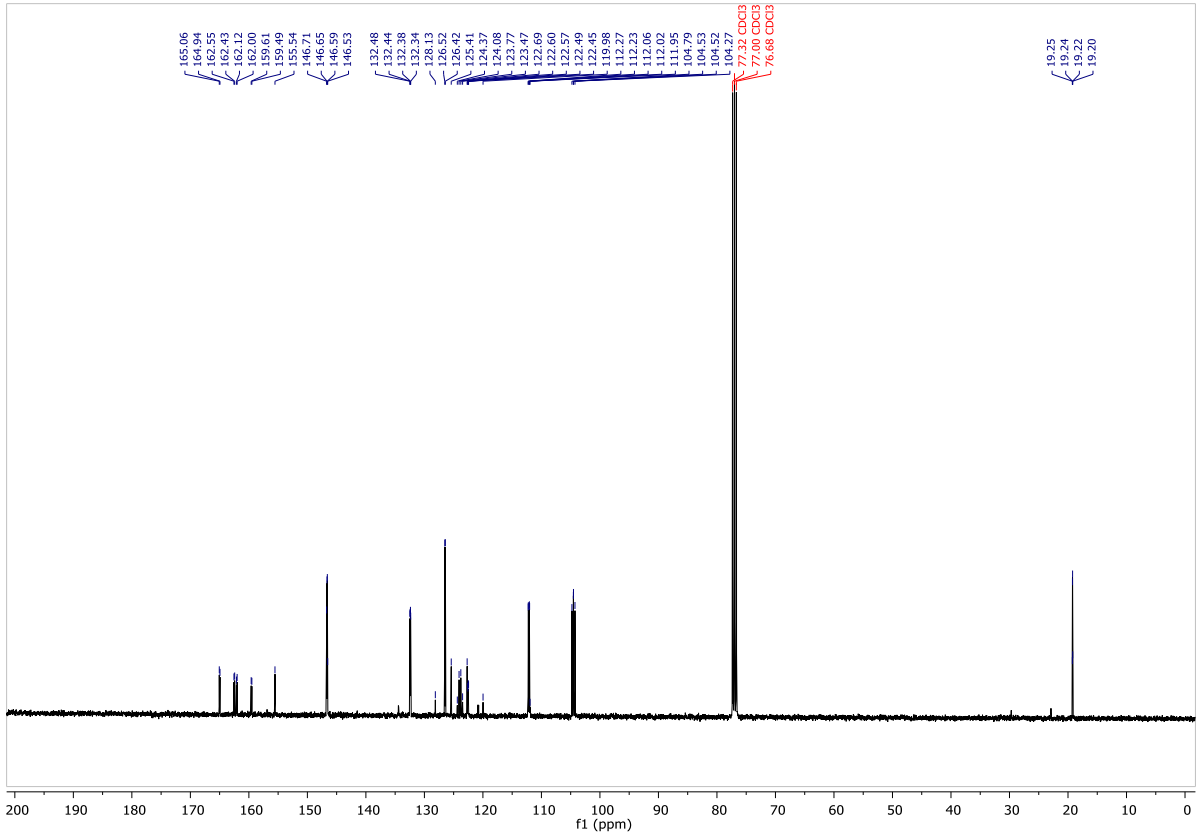
f1 (ppm)

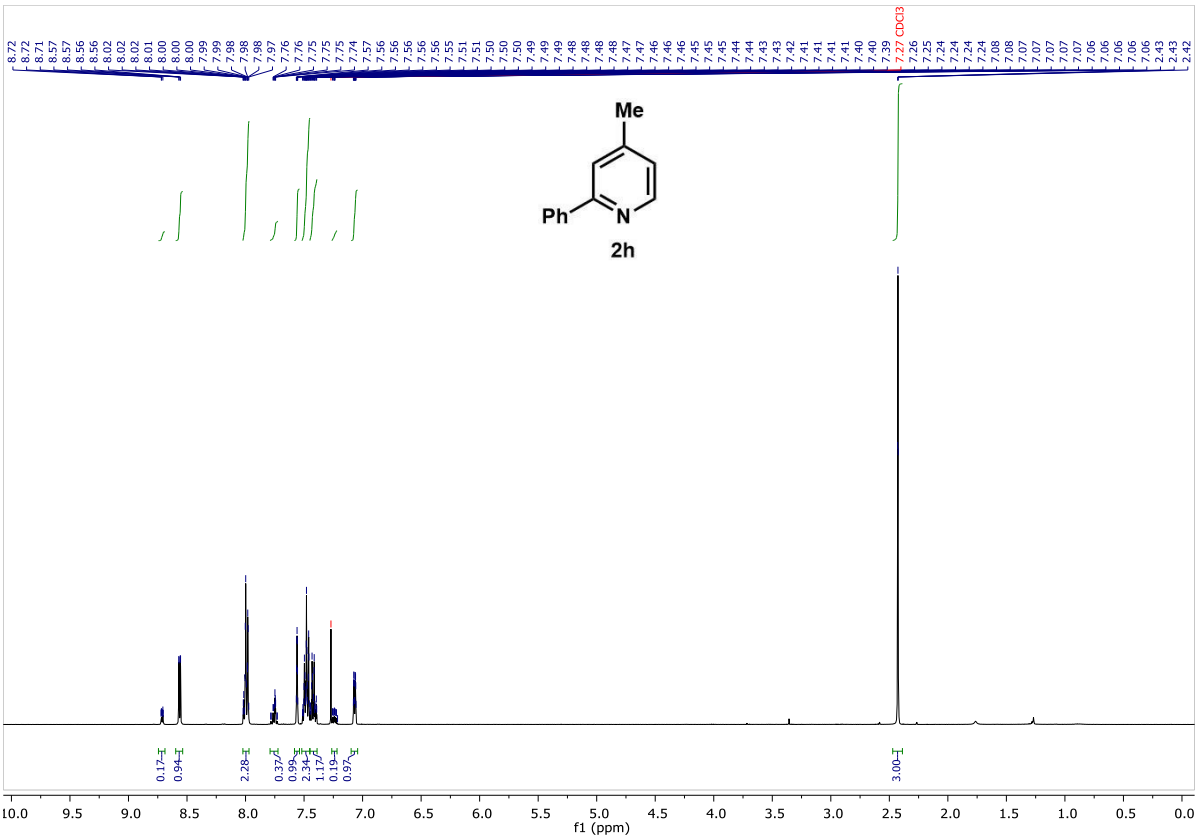
Me
Ph
N
2h
CDCl3
f1 (ppm)

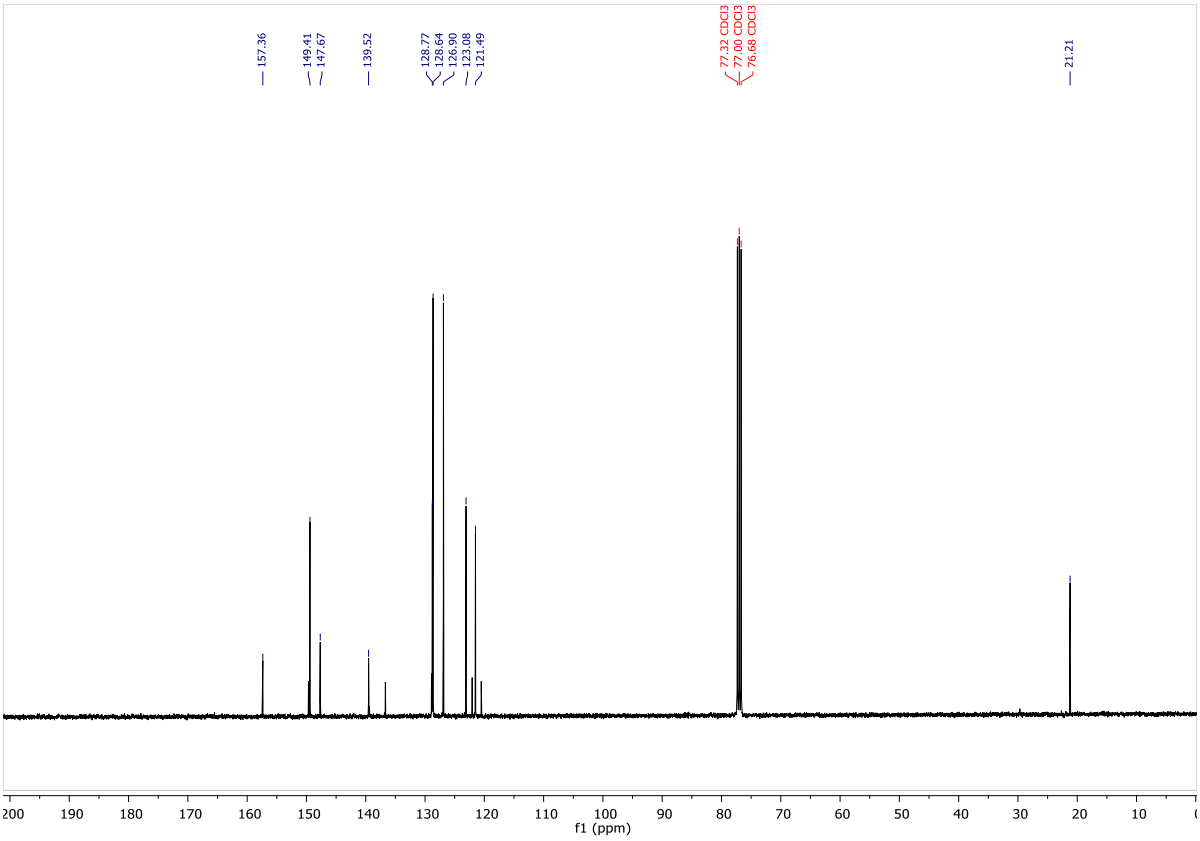
157.36
149.41
147.67
139.52
128.77
128.64
126.90
123.08
121.49
77.32 CDCl3
77.00 CDCl3
76.68 CDCl3
21.21
f1 (ppm)

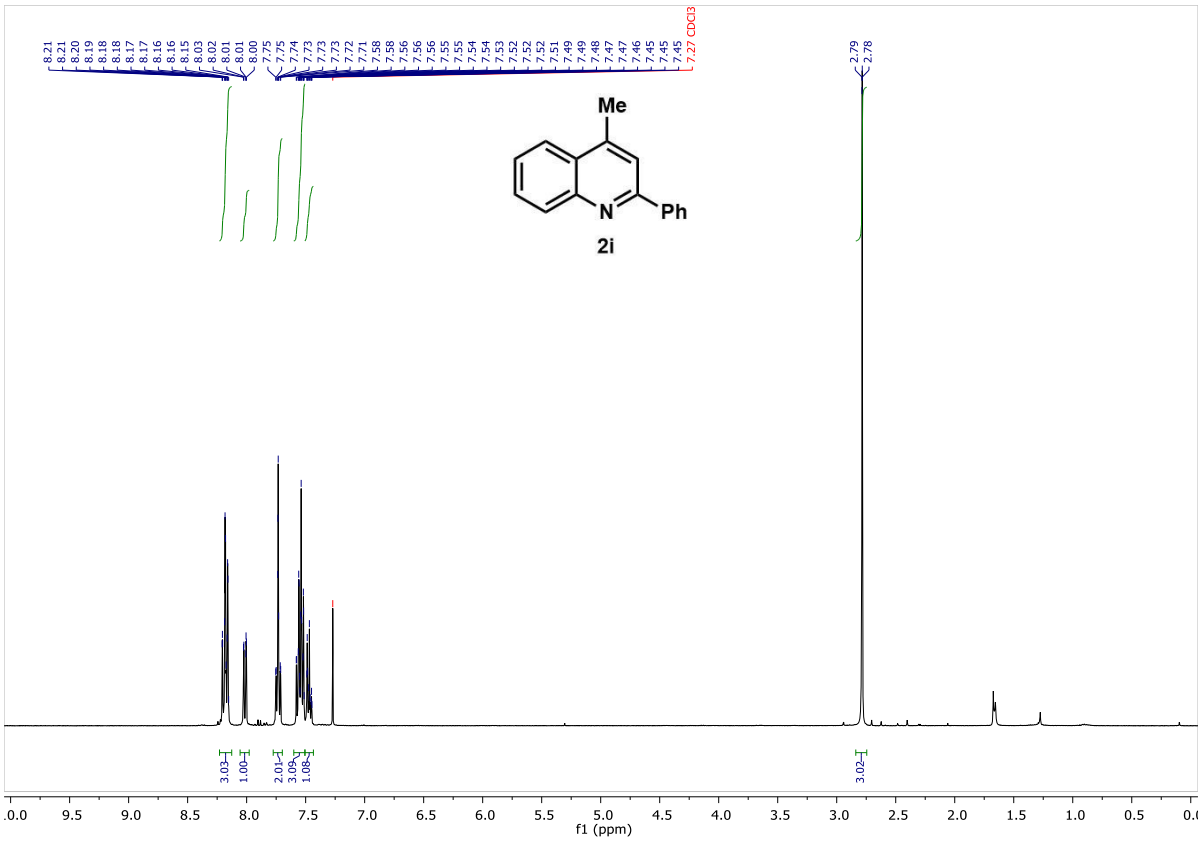
Me
N
Ph
2i
f1 (ppm)

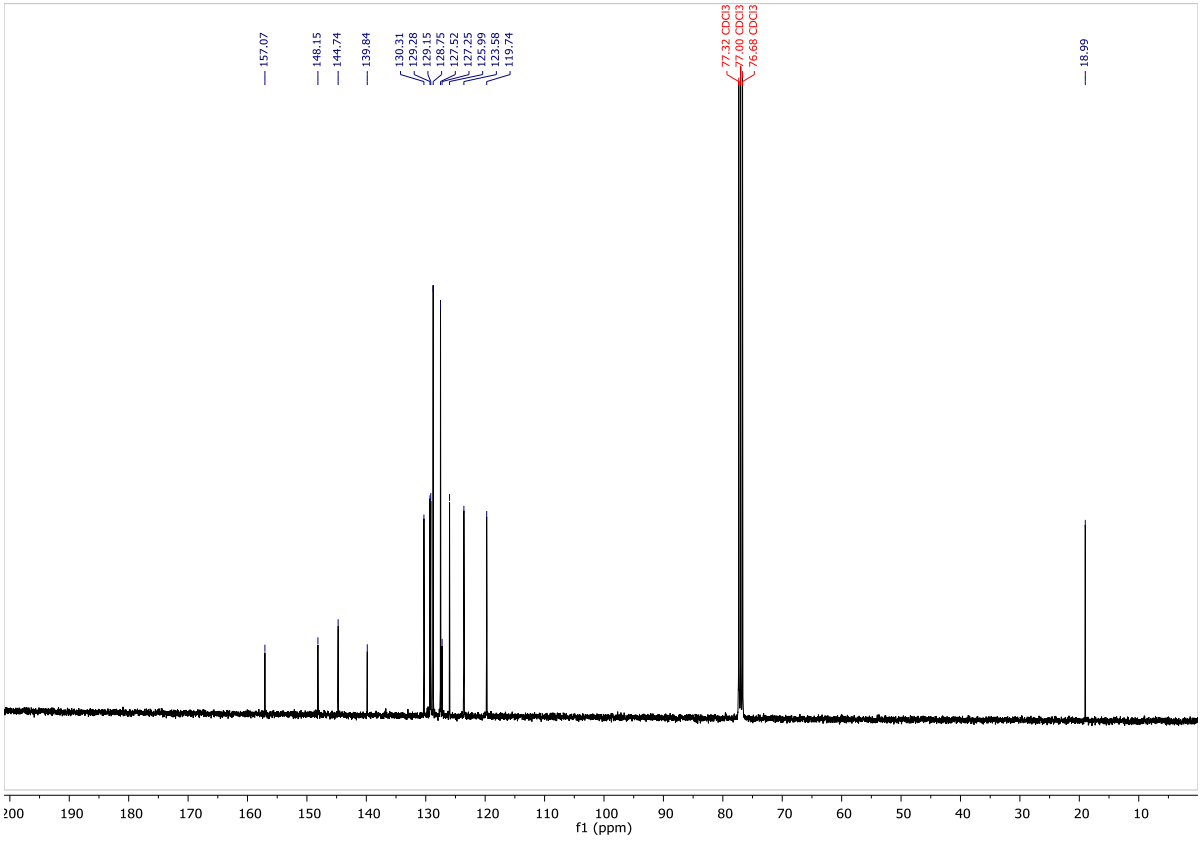
f1 (ppm)

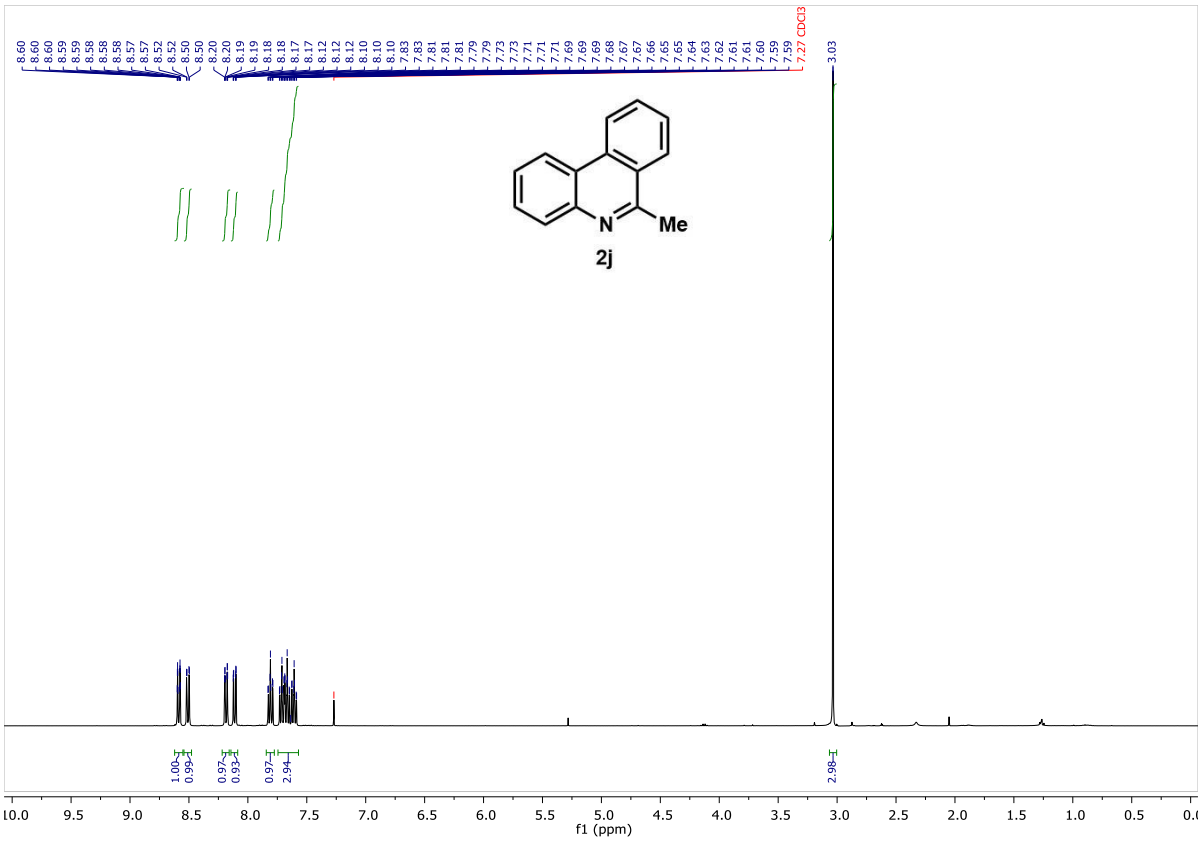
8.60
8.60
8.60
8.59
8.59
8.58
8.58
8.58
8.58
8.57
8.57
8.52
8.52
8.50
8.50
8.20
8.20
8.19
8.19
8.18
8.18
8.17
8.17
8.12
8.12
8.12
8.10
8.10
8.10
7.83
7.81
7.81
7.81
7.79
7.79
7.73
7.73
7.71
7.71
7.71
7.69
7.69
7.68
7.67
7.67
7.66
7.65
7.65
7.64
7.63
7.62
7.61
7.61
7.60
7.59
7.59
7.59
7.27 CDCl3
3.03
N
Me
2j
1.00
0.99
0.97
0.93
0.97
2.94
2.98
10.0
9.5
9.0
8.5
8.0
7.5
7.0
6.5
6.0
5.5
5.0
4.5
4.0
3.5
3.0
2.5
2.0
1.5
1.0
0.5
f1 (ppm)

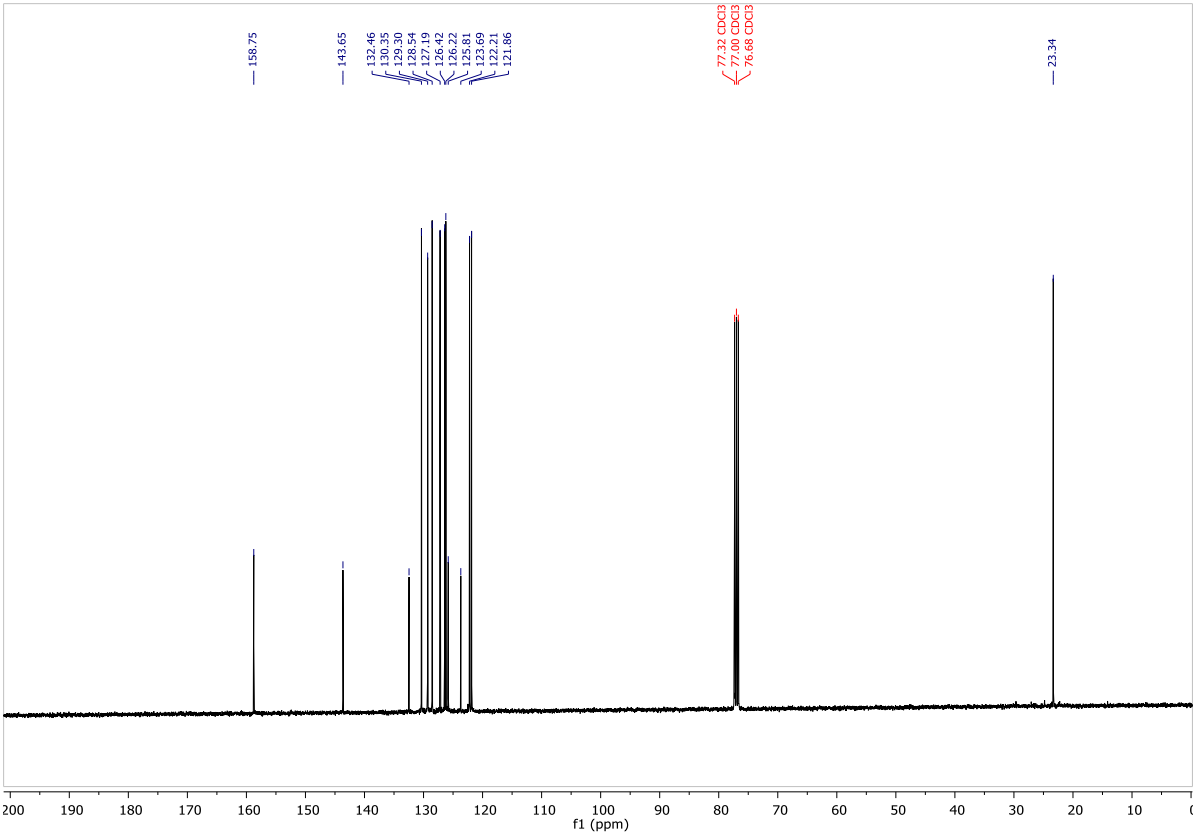
158.75
143.65
132.46
130.35
129.30
128.54
127.19
126.42
126.22
125.81
123.69
122.21
121.86
77.32 CDCl3
77.00 CDCl3
76.68 CDCl3
23.34
200
190
180
170
160
150
140
130
120
110
100
90
80
70
60
50
40
30
20
10
f1 (ppm)

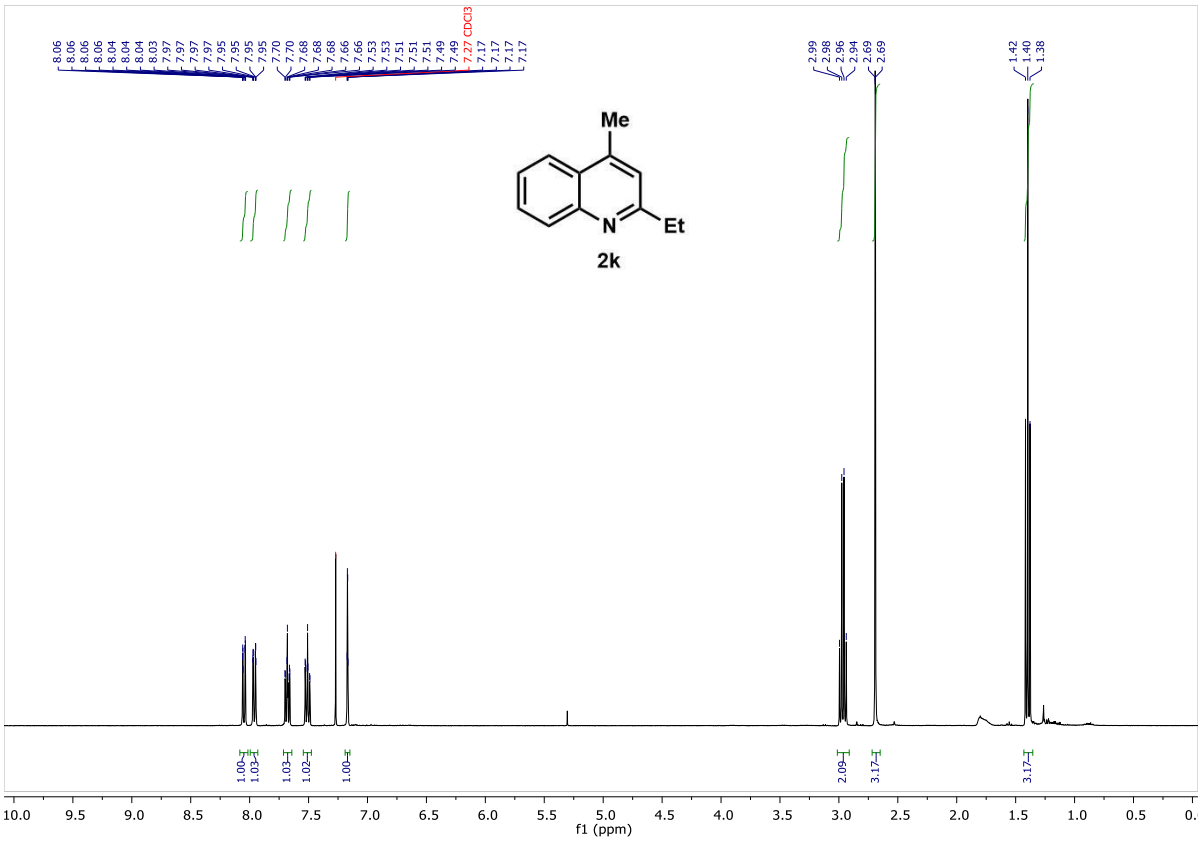
Me
N
Et
2k
f1 (ppm)

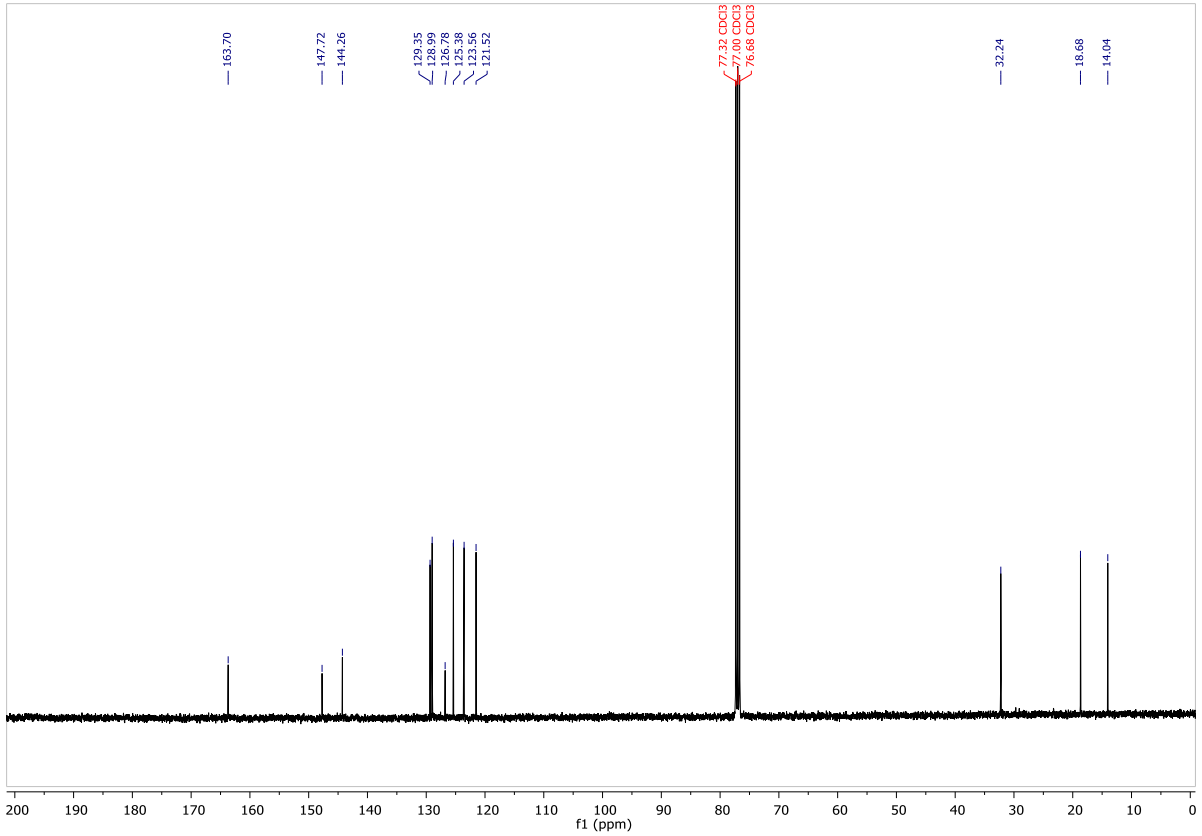
f1 (ppm)

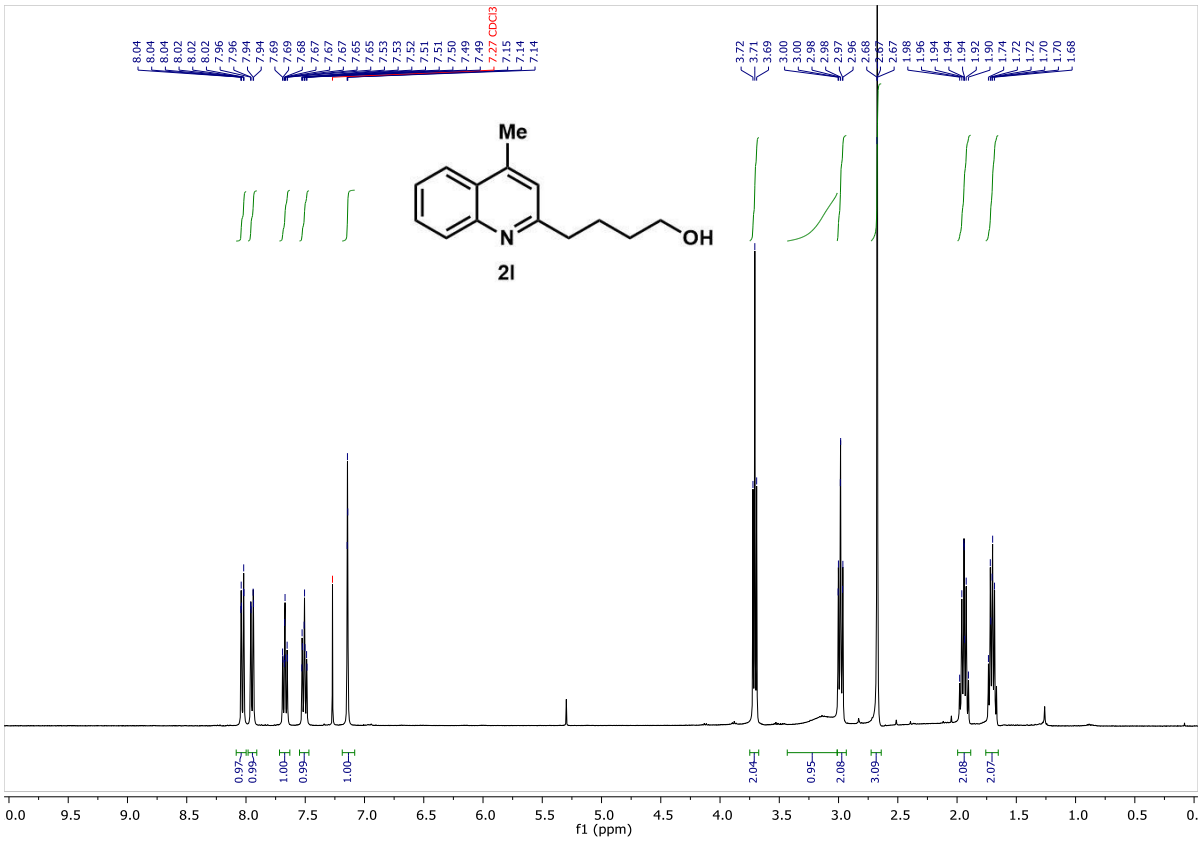
Me
N
OH
2l
f1 (ppm)

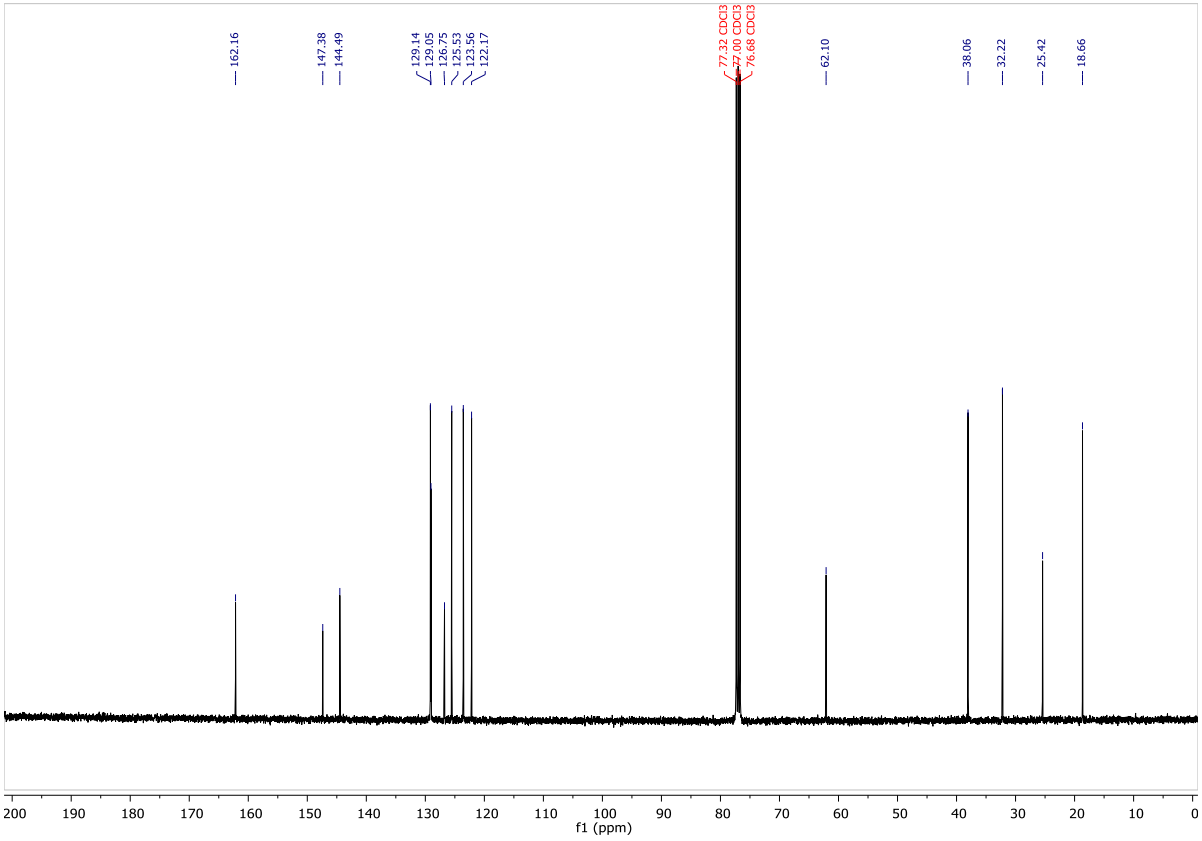
f1 (ppm)

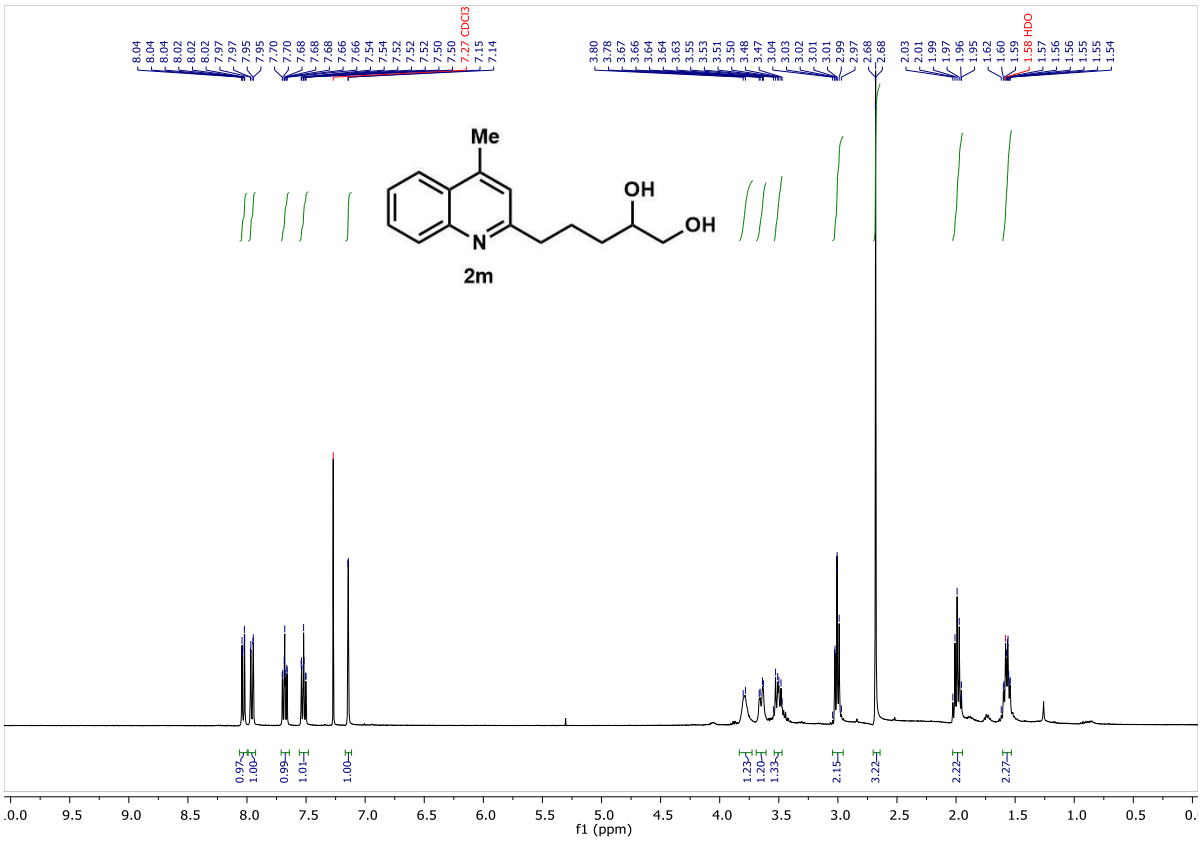
Me
OH
OH
N
2m
f1 (ppm)

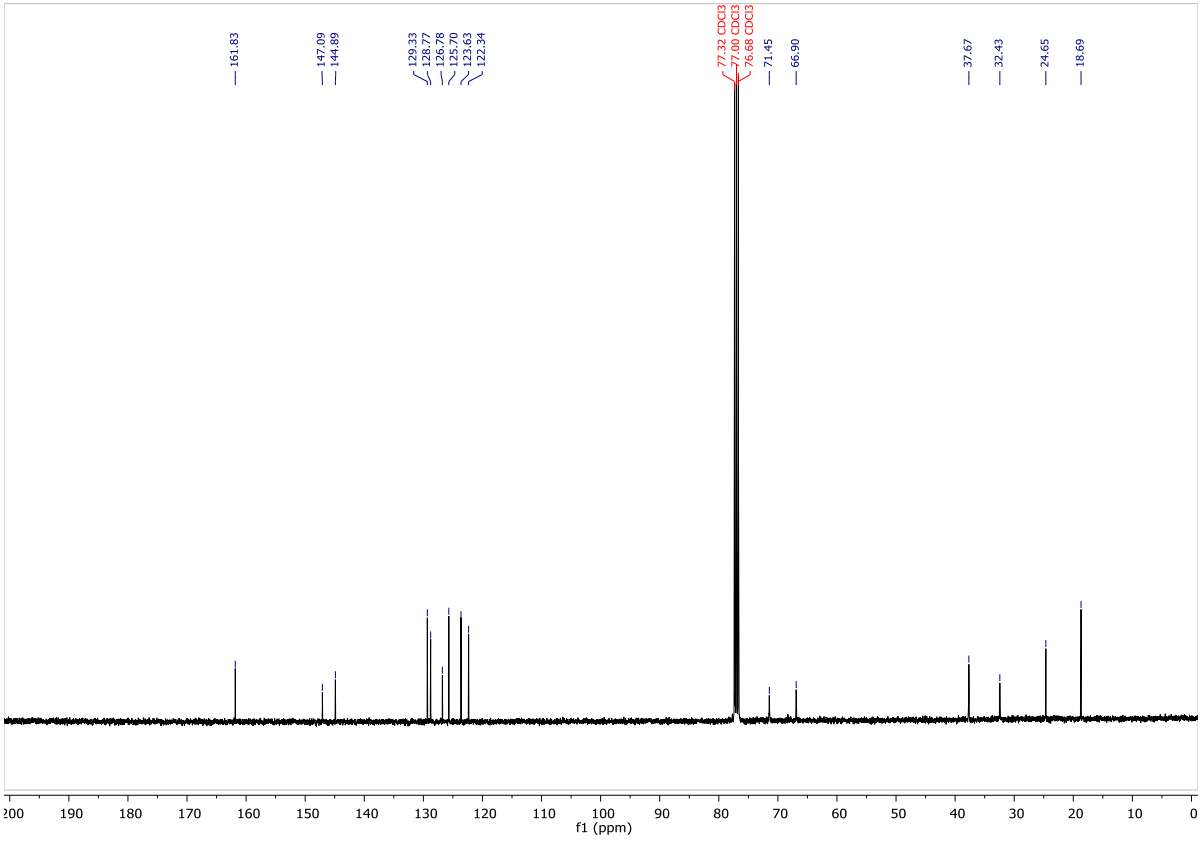
161.83
147.09
144.89
129.33
128.77
126.78
125.70
123.63
122.34
77.32 CDCl3
77.00 CDCl3
76.68 CDCl3
71.45
66.90
37.67
32.43
24.65
18.69
f1 (ppm)

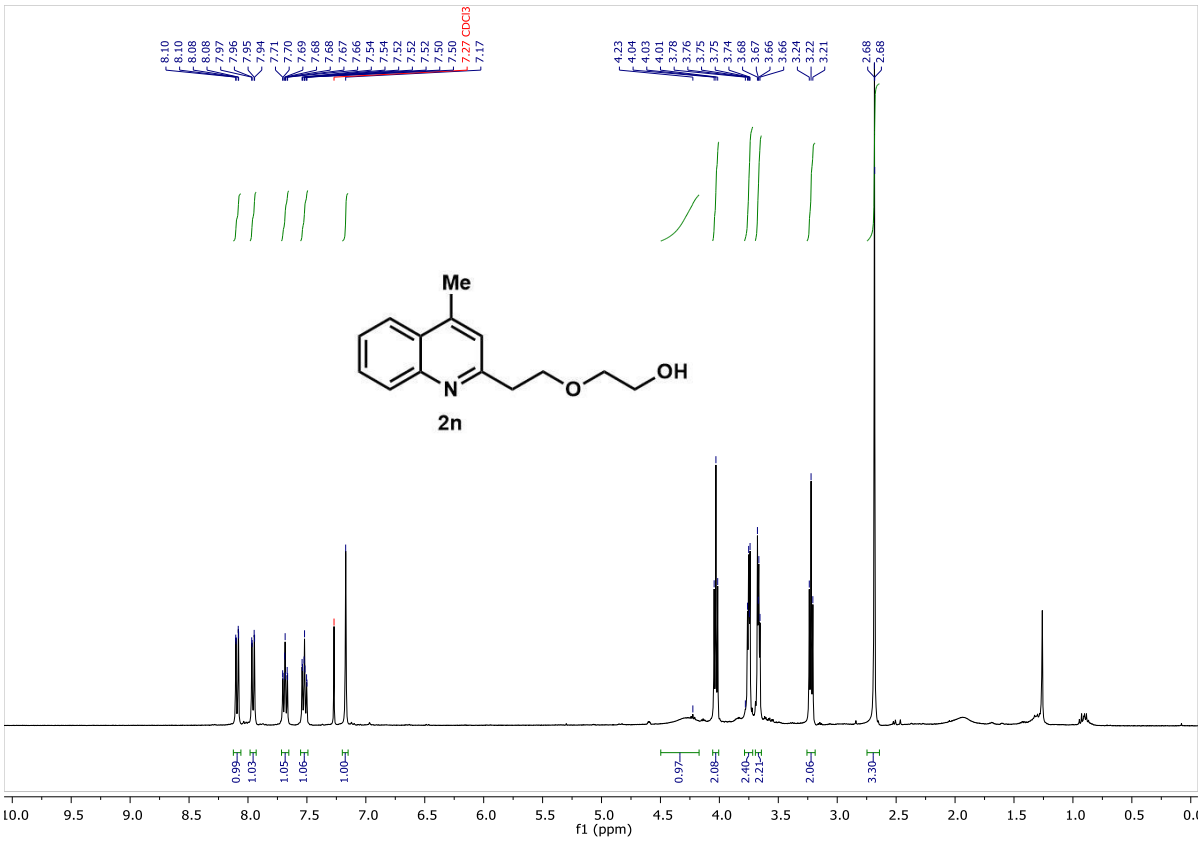
Me
N
O
OH
2n
f1 (ppm)

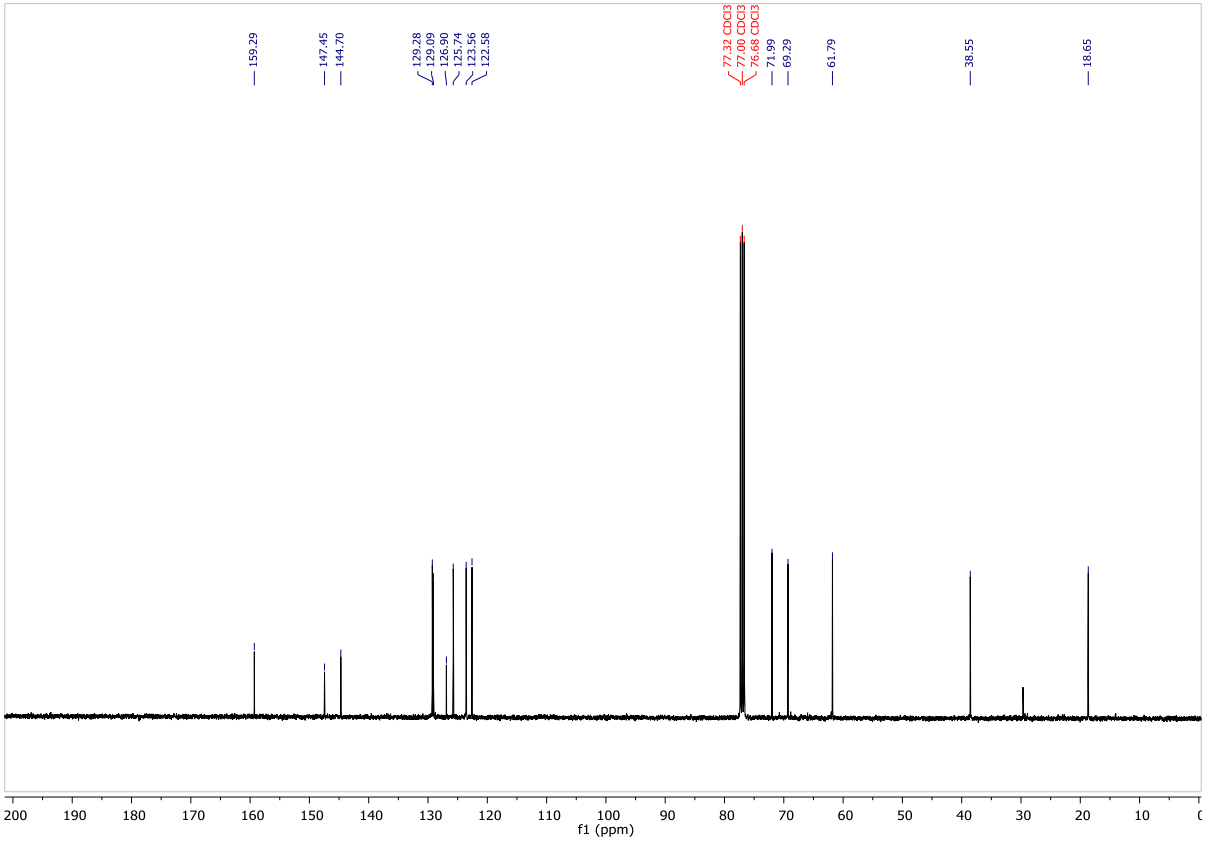
159.29
147.45
144.70
129.28
129.09
126.90
125.74
123.56
122.58
77.32 CDCl3
77.00 CDCl3
76.68 CDCl3
71.99
69.29
61.79
38.55
18.65
f1 (ppm)

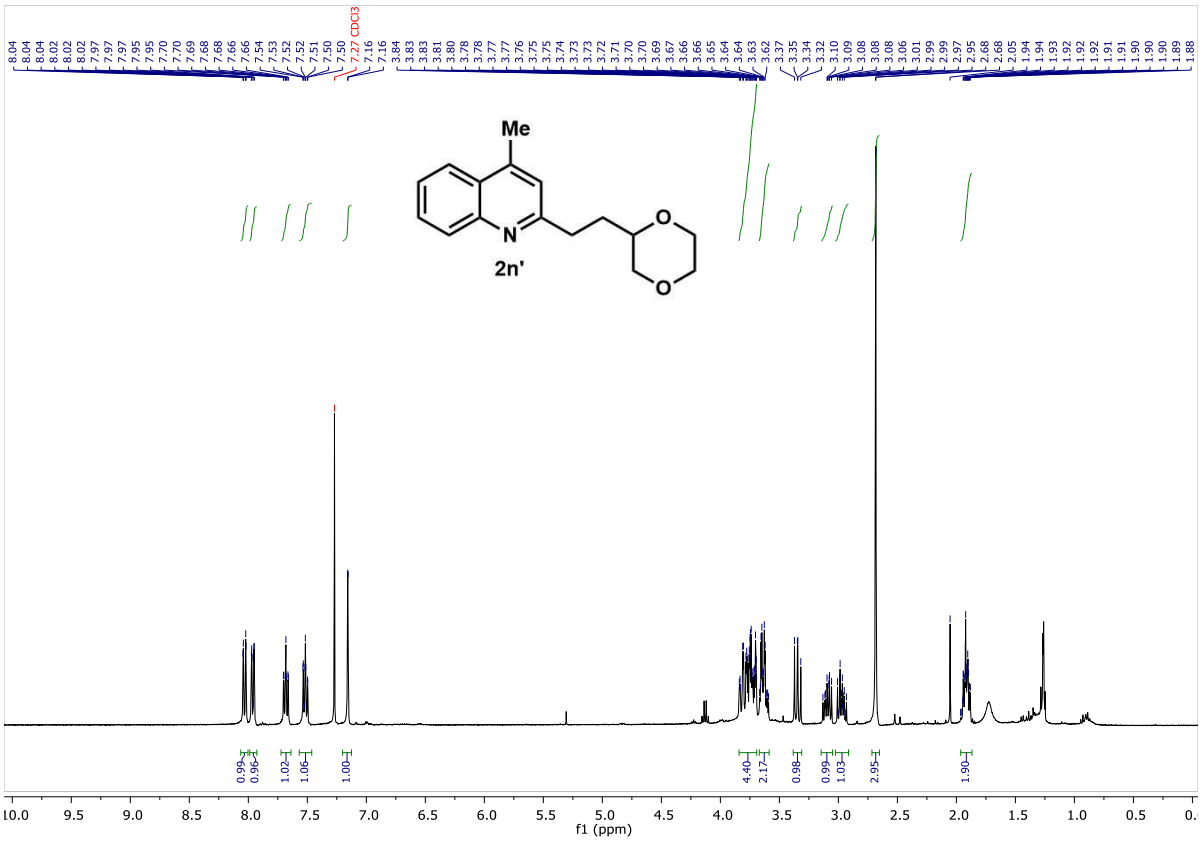
Me
N
O
O
2n'
f1 (ppm)

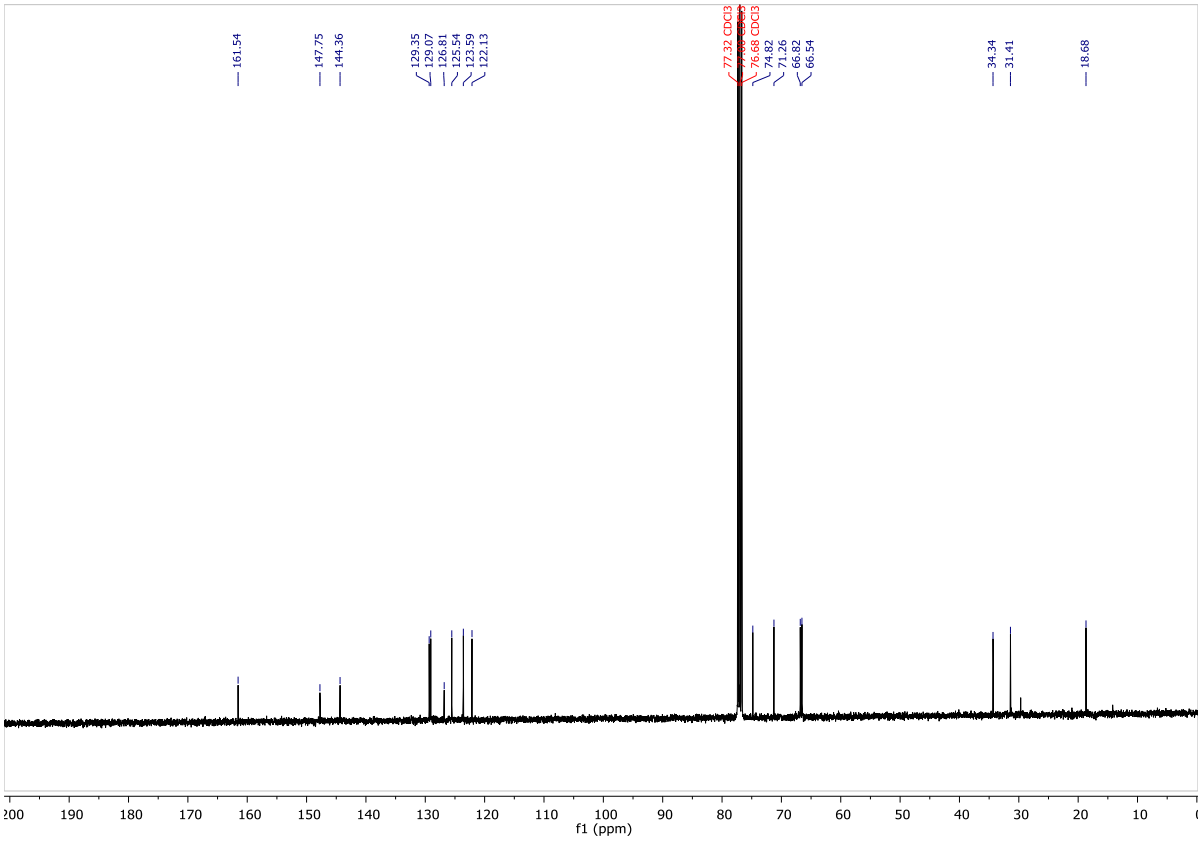
161.54
147.75
144.36
129.35
129.07
126.81
125.54
123.59
122.13
77.32 CDCl3
76.68 CDCl3
74.82
71.26
66.82
66.54
34.34
31.41
18.68
f1 (ppm)

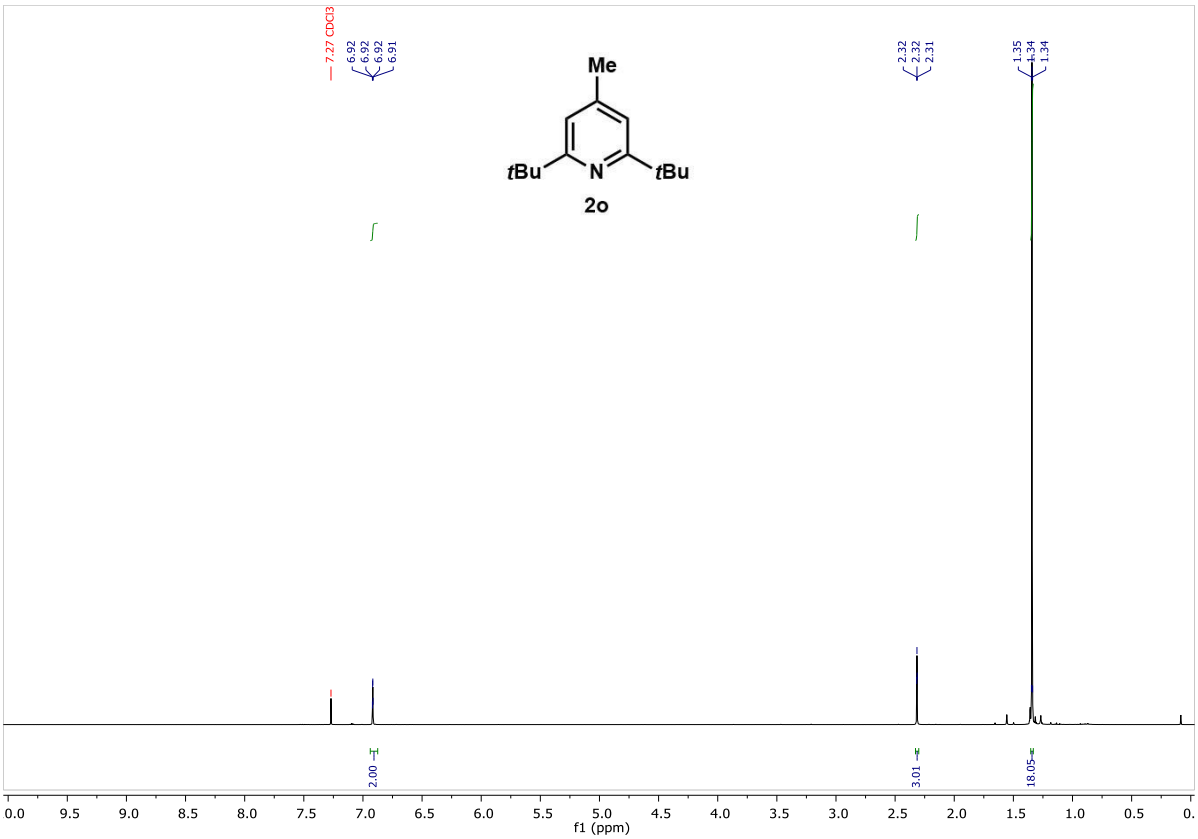
7.27 CDCl3
6.92
6.92
6.92
6.91
2.32
2.32
2.31
1.35
1.34
1.34
Me
tBu
N
tBu
2o
2.00
3.01
18.05
f1 (ppm)

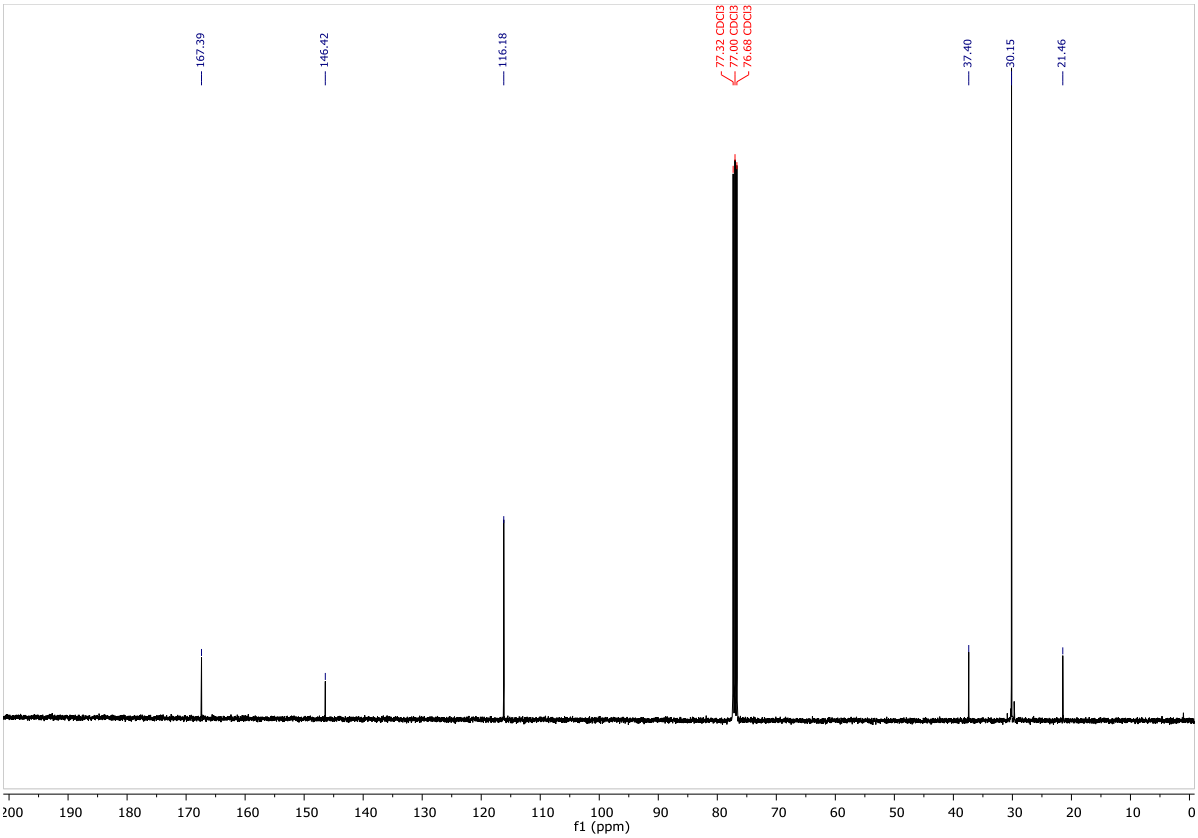
167.39
146.42
116.18
77.32 CDCl3
77.00 CDCl3
76.68 CDCl3
37.40
30.15
21.46
f1 (ppm)

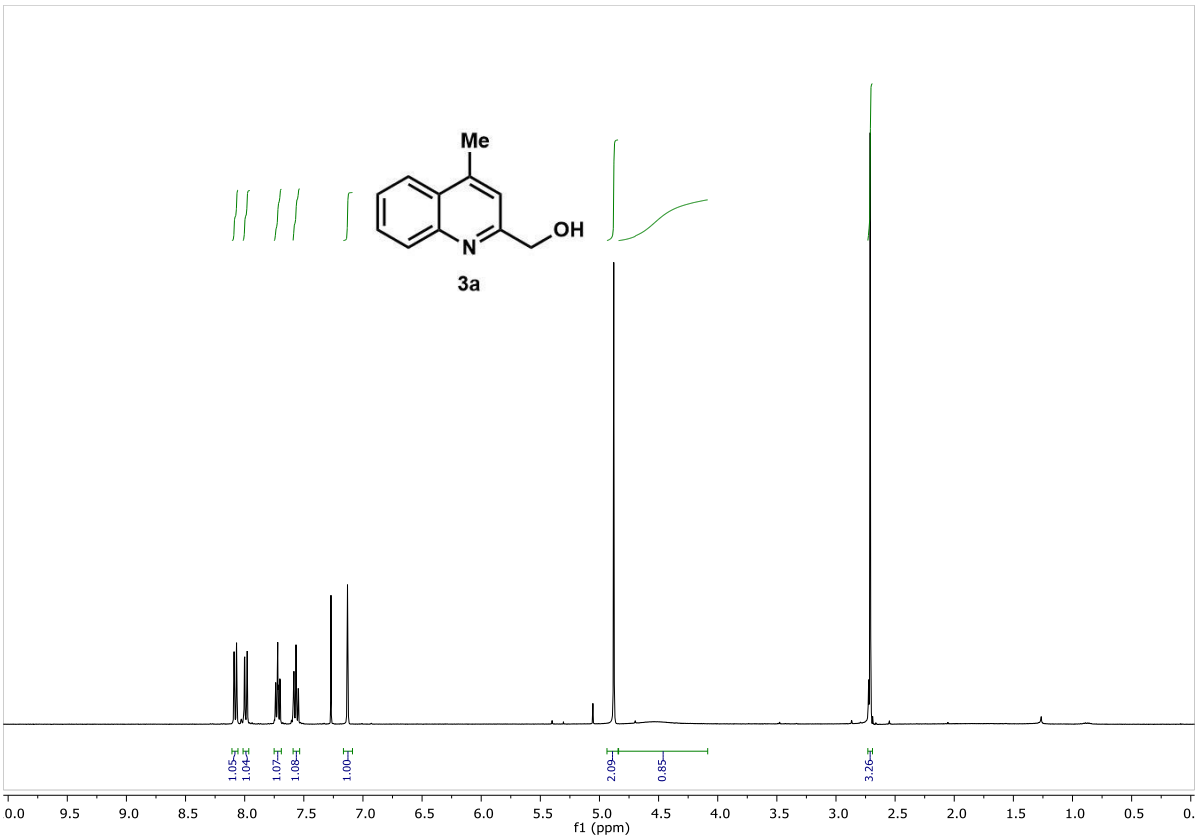
Me
OH
N
3a
1.05
1.04
1.07
1.08
1.00
2.09
0.85
3.26
f1 (ppm)

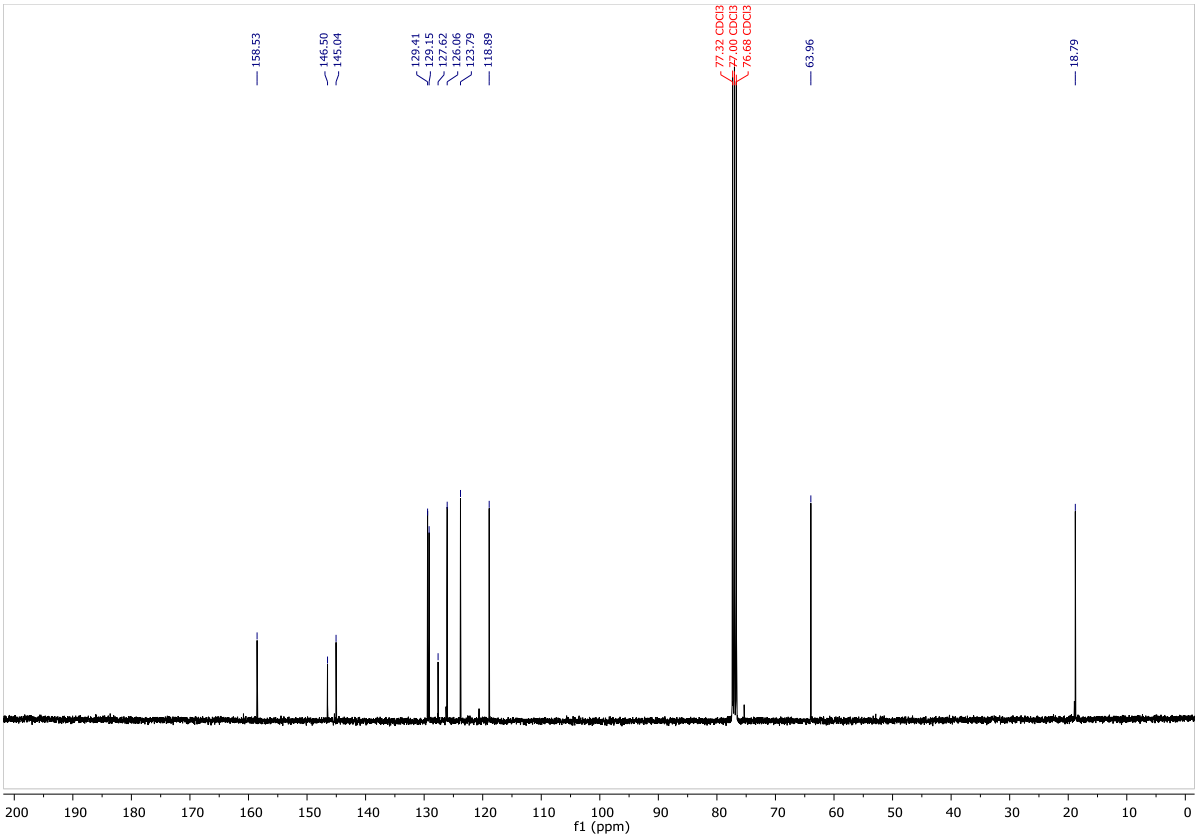
158.53
146.50
145.04
129.41
129.15
127.62
126.06
123.79
118.89
77.32 CDCl3
77.00 CDCl3
76.68 CDCl3
63.96
18.79
f1 (ppm)

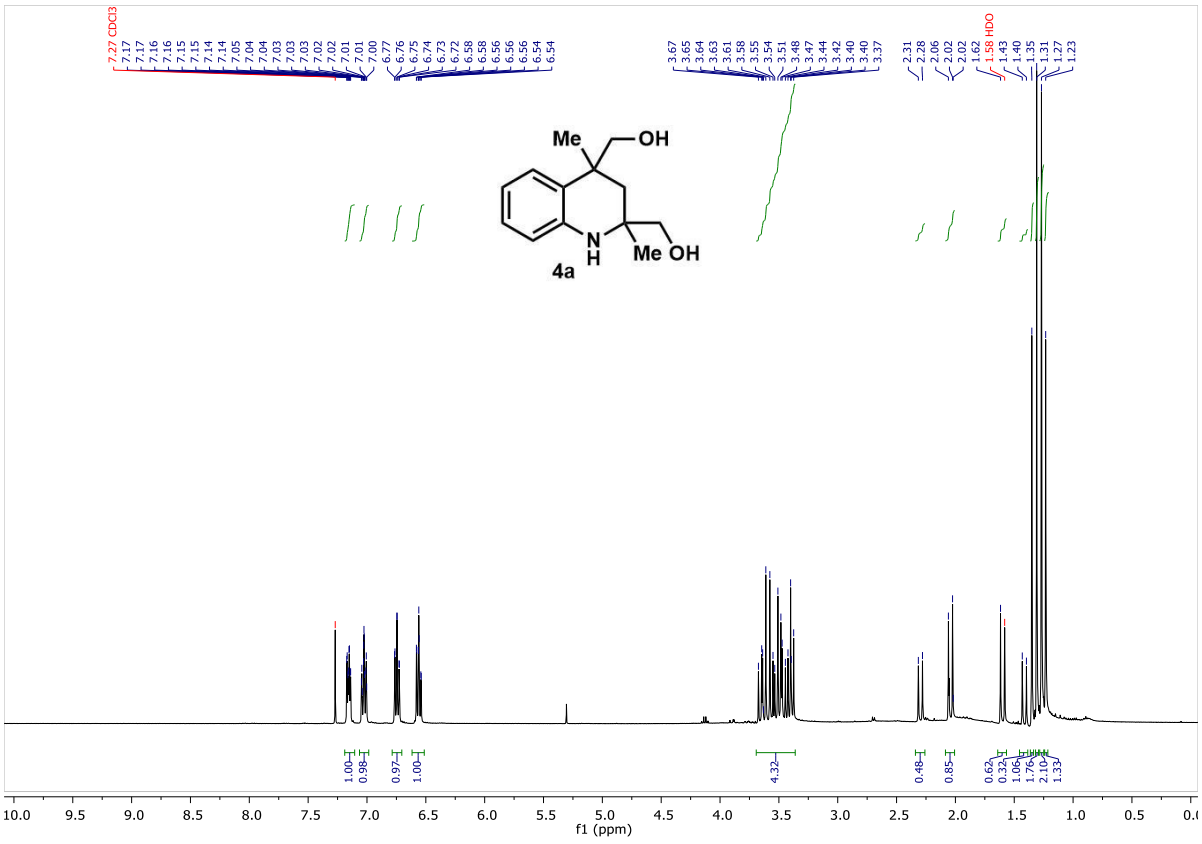
7.27 CDCl3
7.17
7.16
7.15
7.14
7.05
7.04
7.03
7.02
7.01
7.00
6.77
6.76
6.75
6.74
6.73
6.72
6.58
6.56
6.54
3.67
3.65
3.64
3.63
3.61
3.58
3.55
3.54
3.51
3.48
3.47
3.44
3.42
3.40
3.37
2.31
2.28
2.06
2.02
2.02
1.62
1.58 HDO
1.43
1.40
1.35
1.31
1.27
1.23
Me
OH
N
H
Me OH
4a
1.00
0.98
0.97
1.00
4.32
0.48
0.85
0.63
0.32
1.06
1.76
2.10
1.33
10.0
9.5
9.0
8.5
8.0
7.5
7.0
6.5
6.0
5.5
5.0
4.5
4.0
3.5
3.0
2.5
2.0
1.5
1.0
0.5
f1 (ppm)

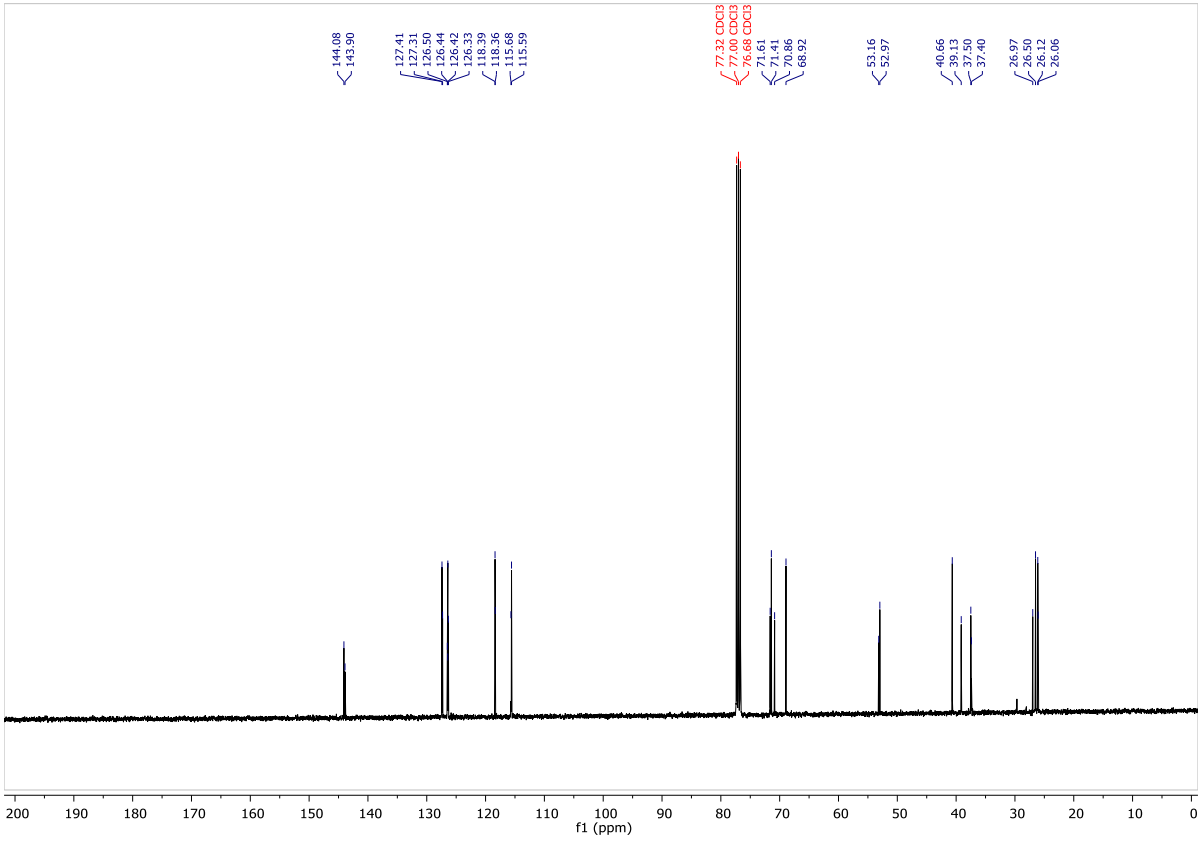
144.08
143.90
127.41
127.31
126.50
126.44
126.42
126.33
118.39
118.36
115.68
115.59
77.32 CDCl3
77.00 CDCl3
76.68 CDCl3
71.61
71.41
70.86
68.92
53.16
52.97
40.66
39.13
37.50
37.40
26.97
26.50
26.12
26.06
200
190
180
170
160
150
140
130
120
110
100
90
80
70
60
50
40
30
20
10
0
f1 (ppm)

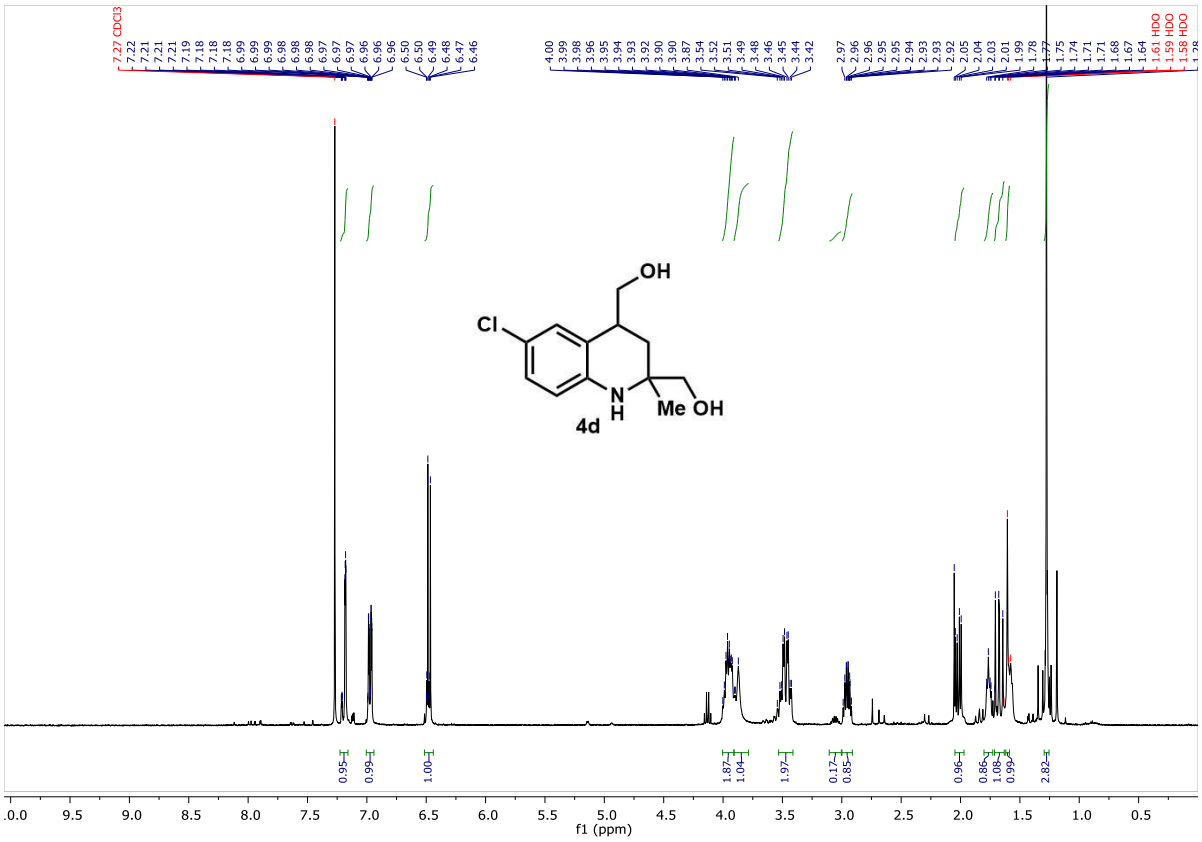
OH
Cl
N
H
Me OH
4d
f1 (ppm)

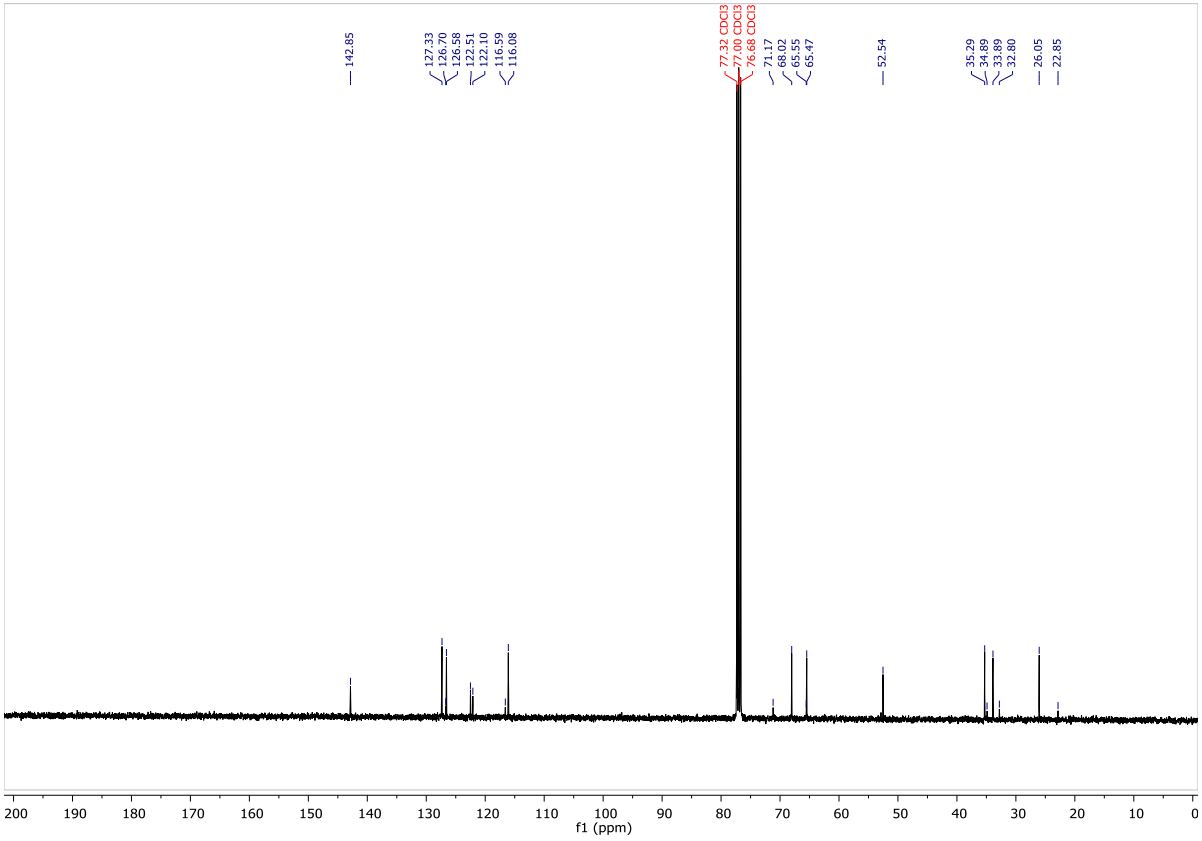
f1 (ppm)

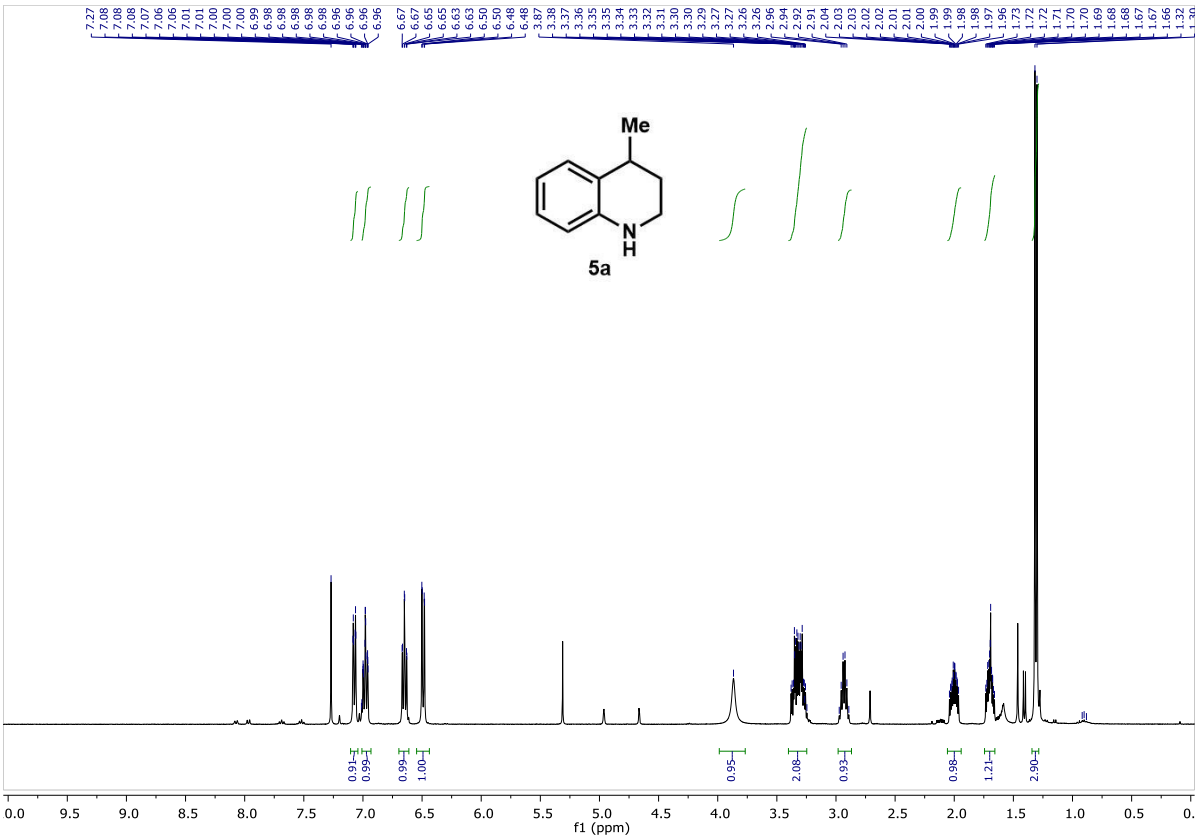
Me
N
H
5a
f1 (ppm)

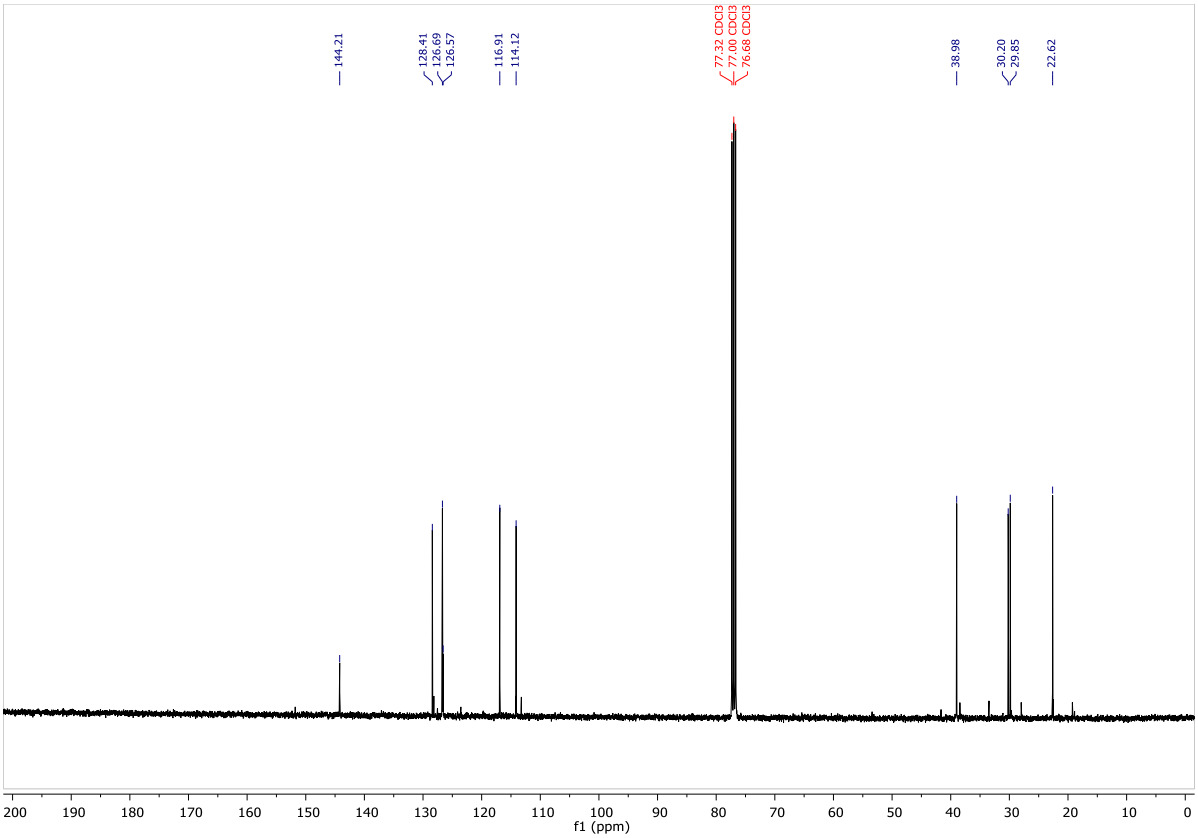
144.21
128.41
126.69
126.57
116.91
114.12
77.32 CDCl3
77.00 CDCl3
76.68 CDCl3
38.98
30.20
29.65
22.62
f1 (ppm)

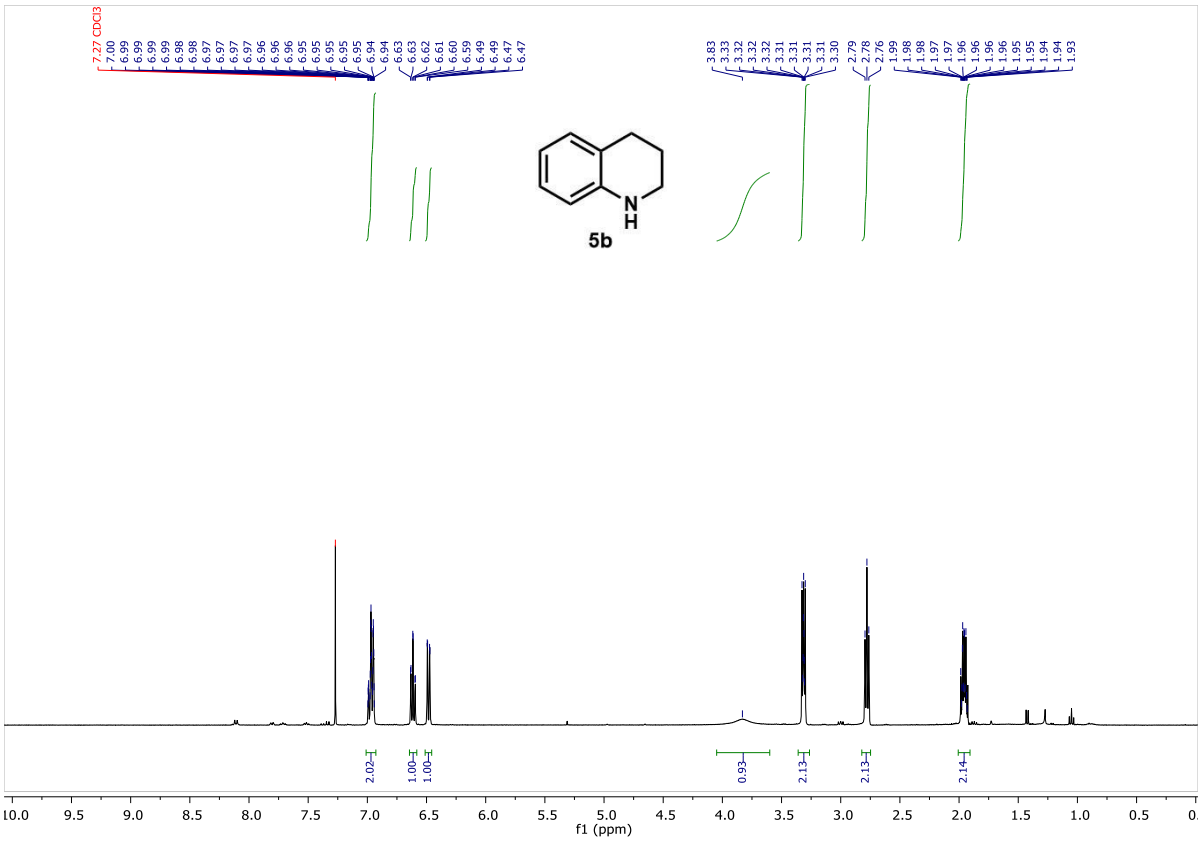
7.27 CDCl3
3.83
3.33
3.32
3.32
3.32
3.31
3.31
3.31
3.31
3.30
2.79
2.78
2.76
1.99
1.98
1.98
1.97
1.97
1.96
1.96
1.96
1.96
1.96
1.95
1.95
1.94
1.94
1.93
6.99
6.99
6.99
6.99
6.99
6.98
6.98
6.97
6.97
6.97
6.97
6.96
6.96
6.96
6.96
6.95
6.95
6.95
6.95
6.95
6.94
6.94
6.63
6.63
6.62
6.61
6.60
6.59
6.49
6.49
6.47
6.47
N
H
5b
2.02
1.00
1.00
0.93
2.13
2.13
2.14
10.0
9.5
9.0
8.5
8.0
7.5
7.0
6.5
6.0
5.5
5.0
4.5
4.0
3.5
3.0
2.5
2.0
1.5
1.0
0.5
f1 (ppm)

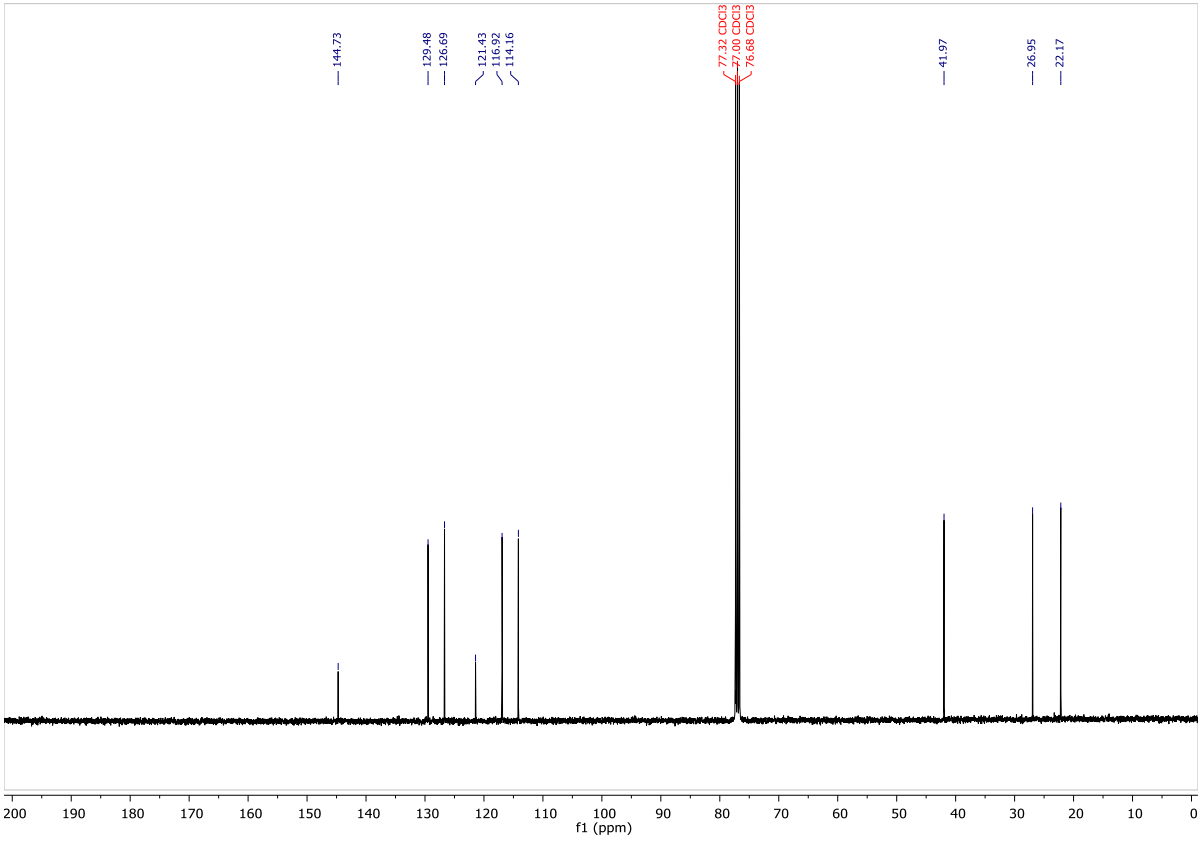
144.73
129.48
126.69
121.43
116.92
114.16
77.32 CDCl3
77.00 CDCl3
76.68 CDCl3
41.97
26.95
22.17
200
190
180
170
160
150
140
130
120
110
100
90
80
70
60
50
40
30
20
10
0
f1 (ppm)

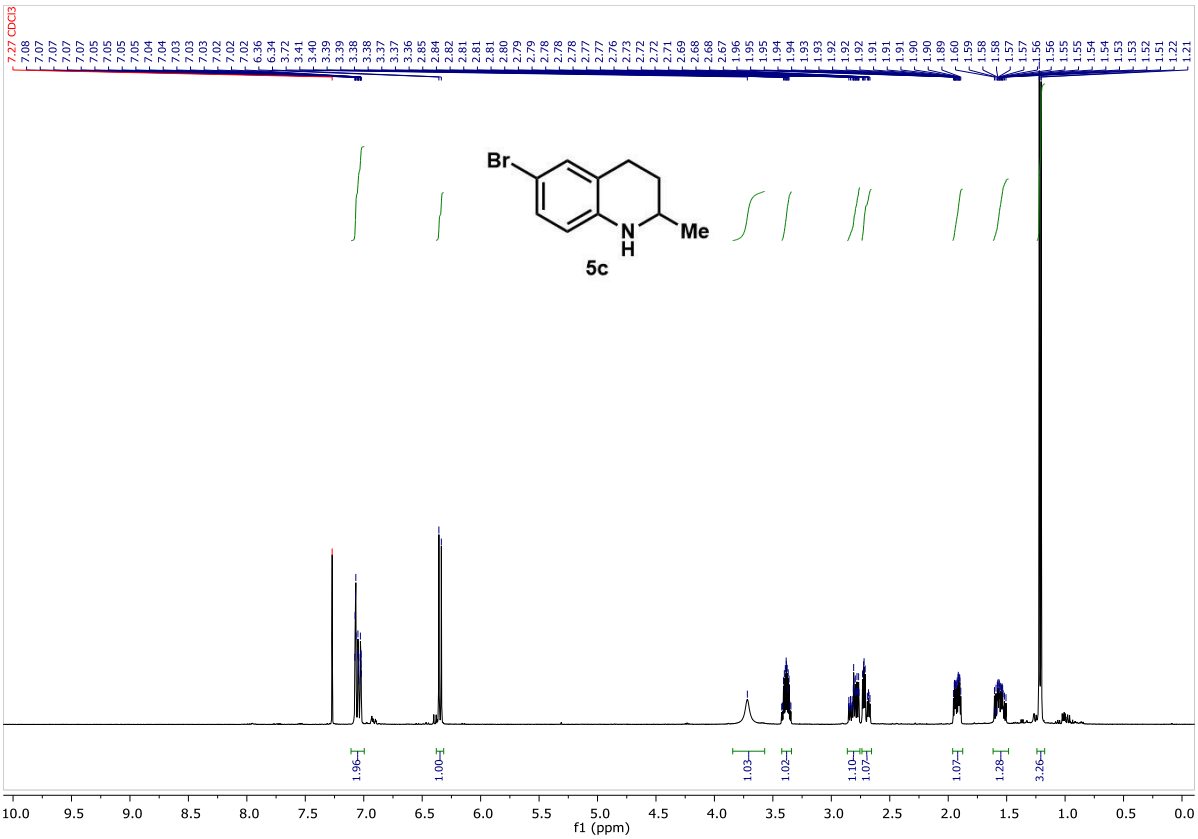
Br
N
H
Me
5c
1.96
1.00
1.03
1.02
1.10
1.07
1.07
1.28
3.26
f1 (ppm)

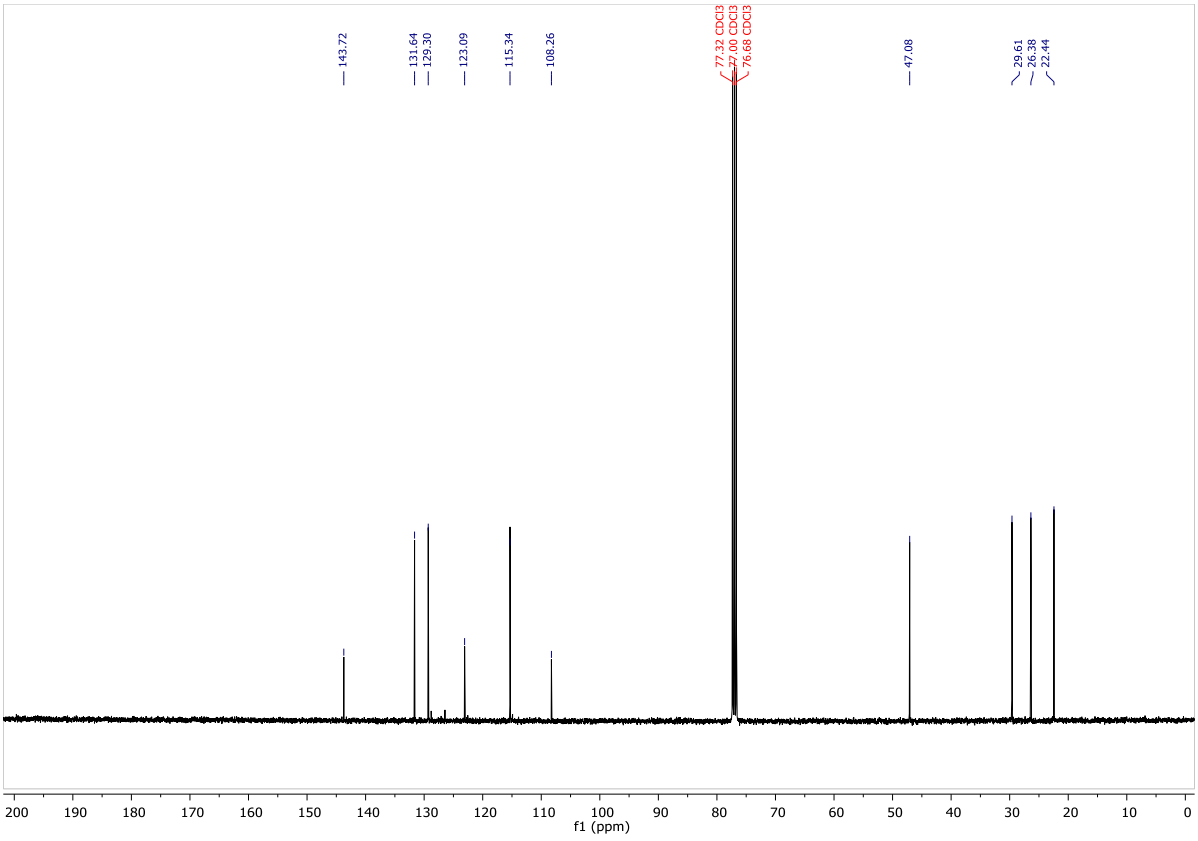
143.72
131.64
129.30
123.09
115.34
108.26
77.32 CDCl3
77.00 CDCl3
76.68 CDCl3
47.08
29.61
26.38
22.44
f1 (ppm)

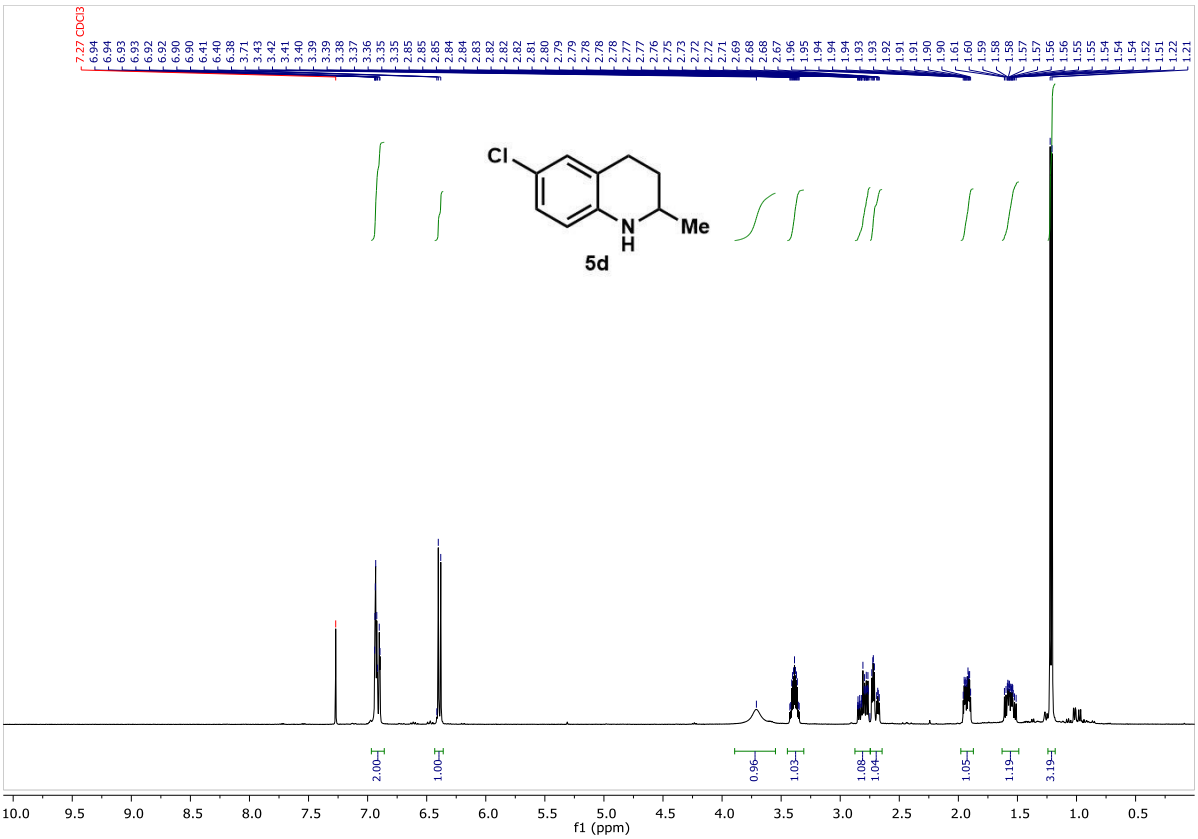
Cl
N
H
Me
5d
f1 (ppm)

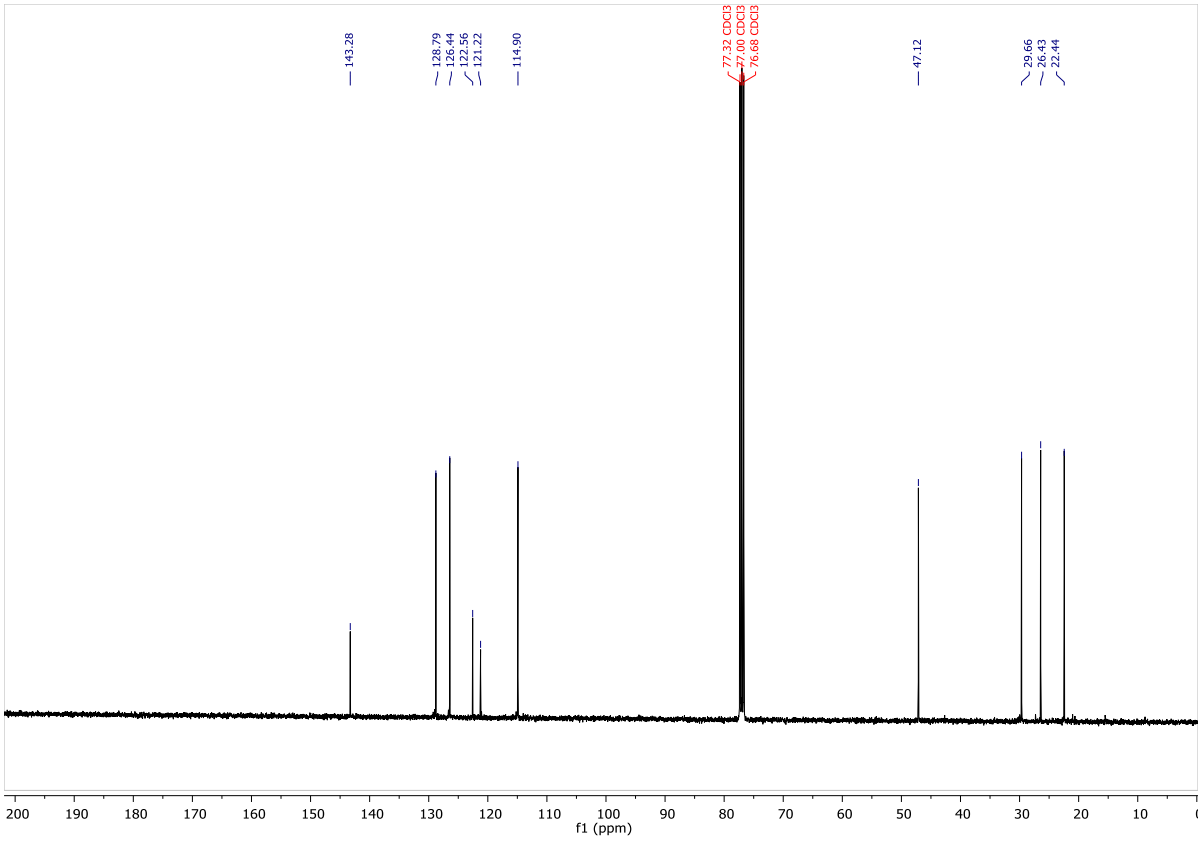
143.28
128.79
126.44
122.56
121.22
114.90
77.32 CDCl3
77.00 CDCl3
76.68 CDCl3
47.12
29.66
26.43
22.44
f1 (ppm)

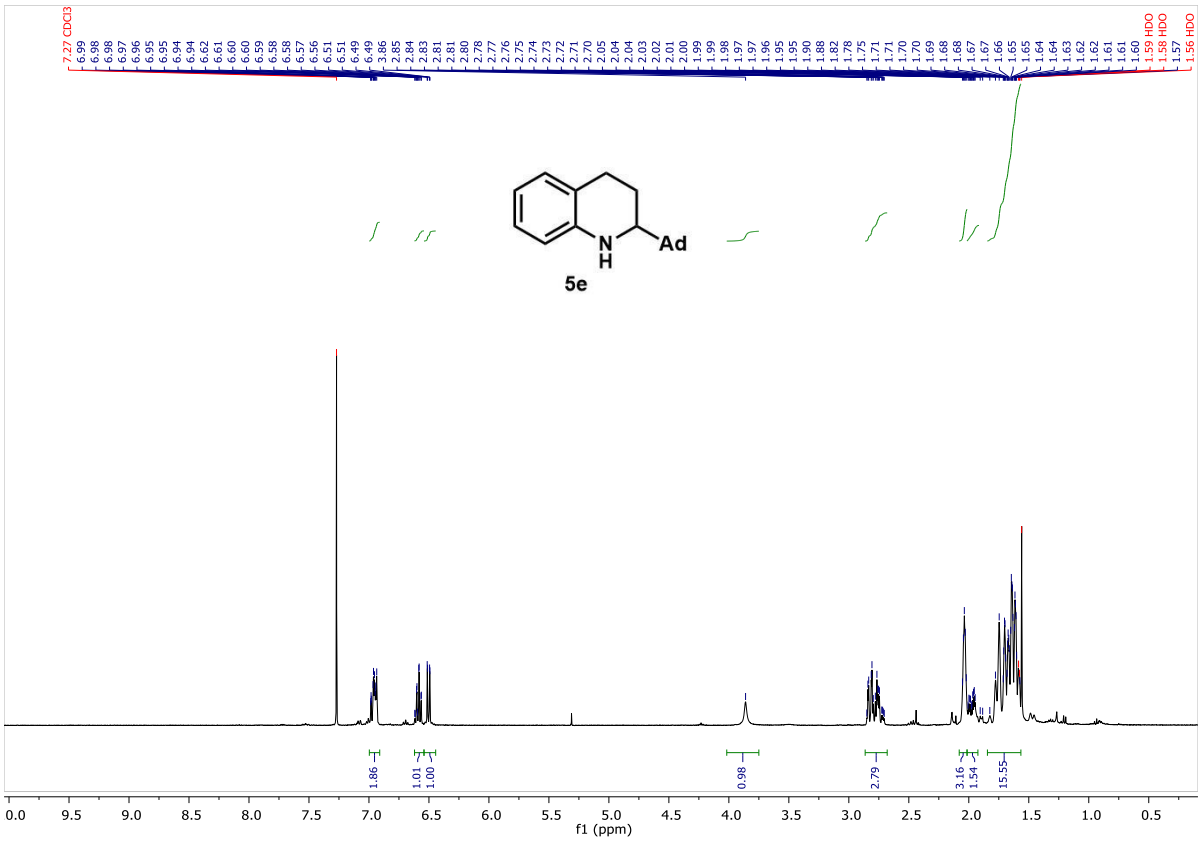
7.27 CDCl3
1.59 HDO
1.58 HDO
1.56 HDO
Ad
N
H
5e
1.86
1.01
1.00
0.98
2.79
3.16
1.54
15.55
f1 (ppm)

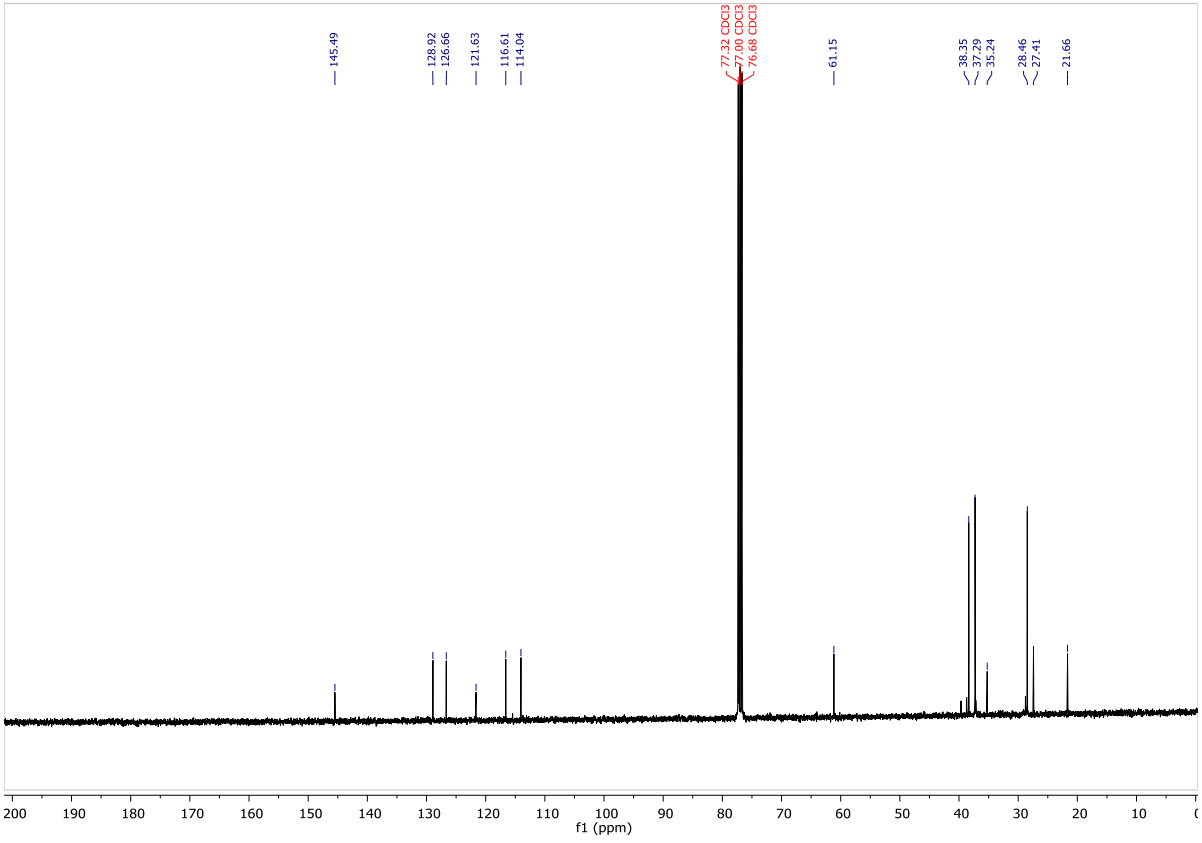
145.49
128.92
126.66
121.63
116.61
114.04
77.32 CDCl3
77.00 CDCl3
76.68 CDCl3
61.15
38.35
37.29
35.24
28.46
27.41
21.66
f1 (ppm)

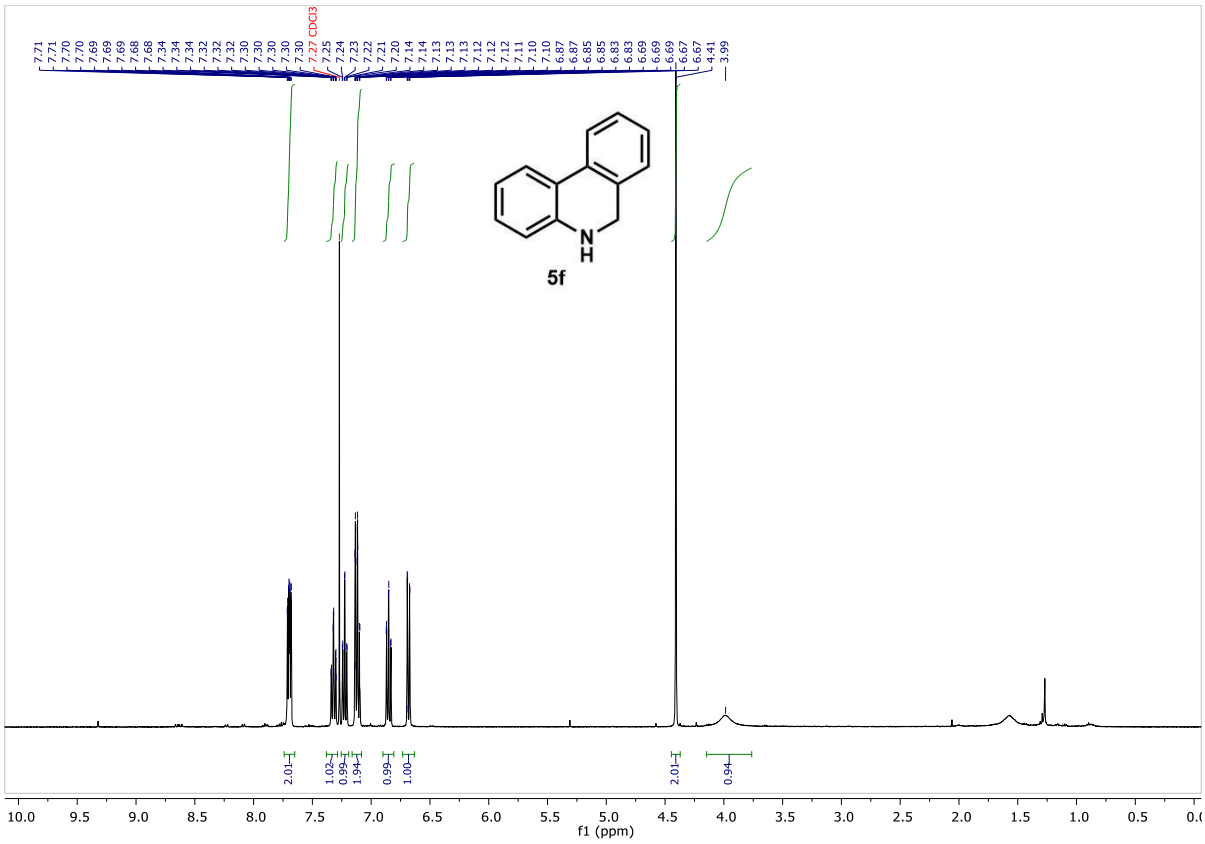
7.71
7.71
7.70
7.70
7.69
7.69
7.69
7.68
7.68
7.34
7.34
7.32
7.32
7.32
7.30
7.30
7.30
7.30
7.30
7.27 CDCl3
7.25
7.24
7.23
7.22
7.21
7.20
7.14
7.14
7.13
7.13
7.13
7.12
7.12
7.12
7.12
7.11
7.10
6.87
6.87
6.85
6.85
6.83
6.83
6.69
6.69
6.69
6.69
6.67
6.67
4.41
3.99
N
H
5f
2.01
1.02
0.99
1.94
0.99
1.00
2.01
0.94
10.0
9.5
9.0
8.5
8.0
7.5
7.0
6.5
6.0
5.5
5.0
4.5
4.0
3.5
3.0
2.5
2.0
1.5
1.0
0.5
f1 (ppm)

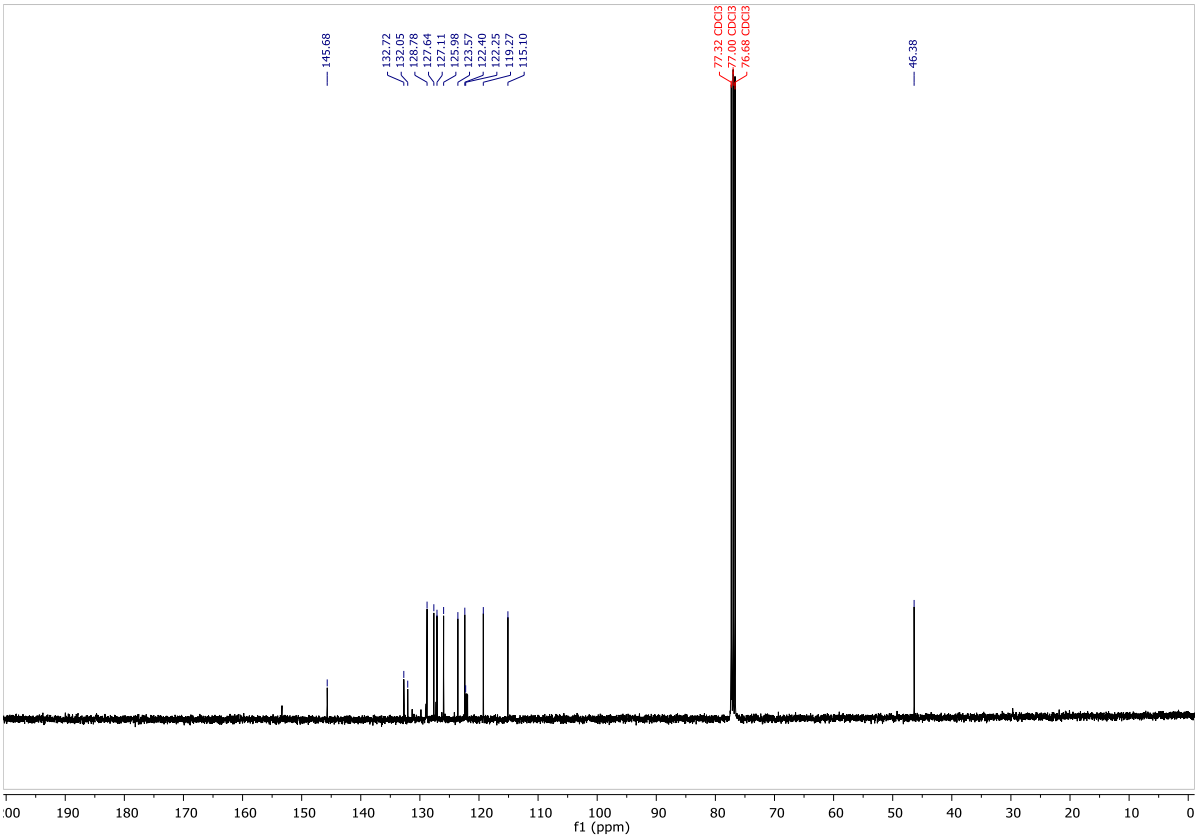
145.68
132.72
132.05
128.78
127.64
127.41
125.98
125.57
122.40
122.25
119.27
115.10
77.32 CDCl3
77.00 CDCl3
76.68 CDCl3
46.38
190
180
170
160
150
140
130
120
110
100
90
80
70
60
50
40
30
20
10
0
f1 (ppm)

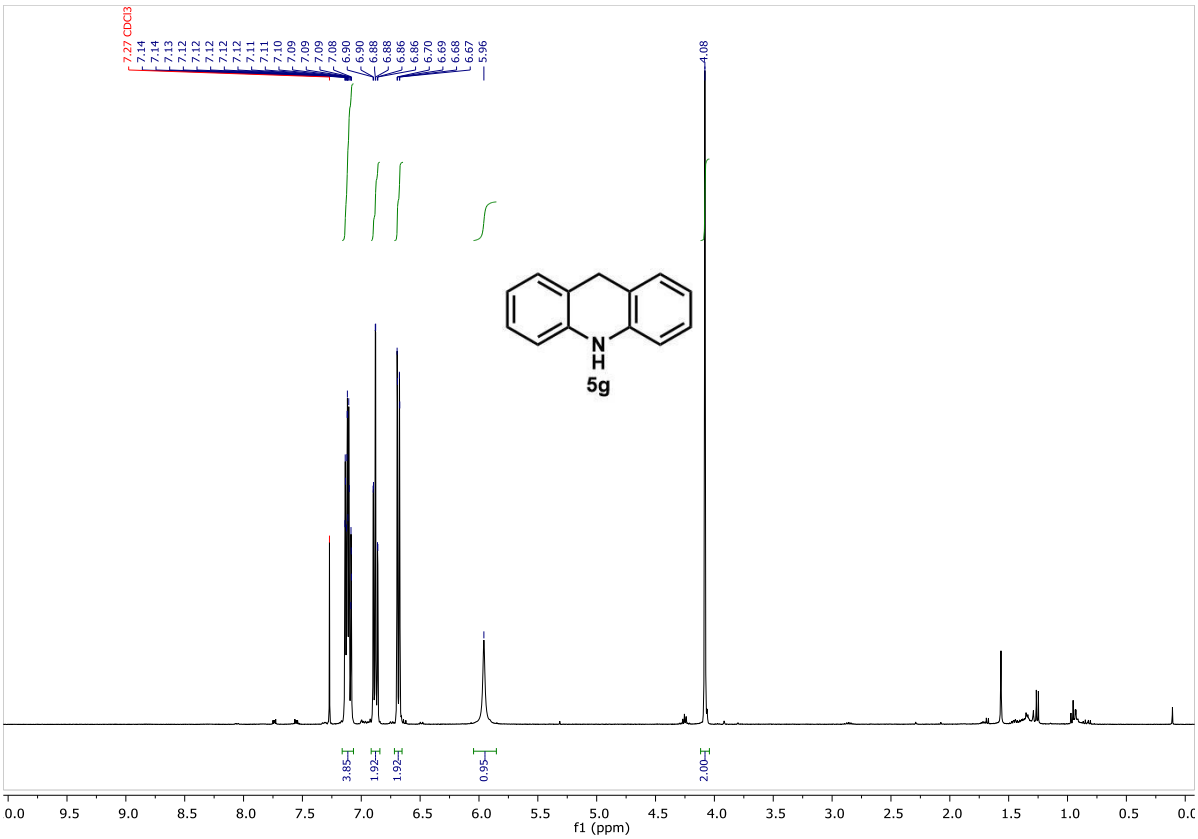
7.27 CDCl3
7.14
7.14
7.13
7.12
7.12
7.12
7.12
7.12
7.11
7.11
7.10
7.09
7.09
7.09
7.09
7.08
6.90
6.90
6.88
6.88
6.86
6.86
6.70
6.69
6.68
6.67
5.96
4.08
N
H
5g
3.85
1.92
1.92
0.95
2.00
f1 (ppm)

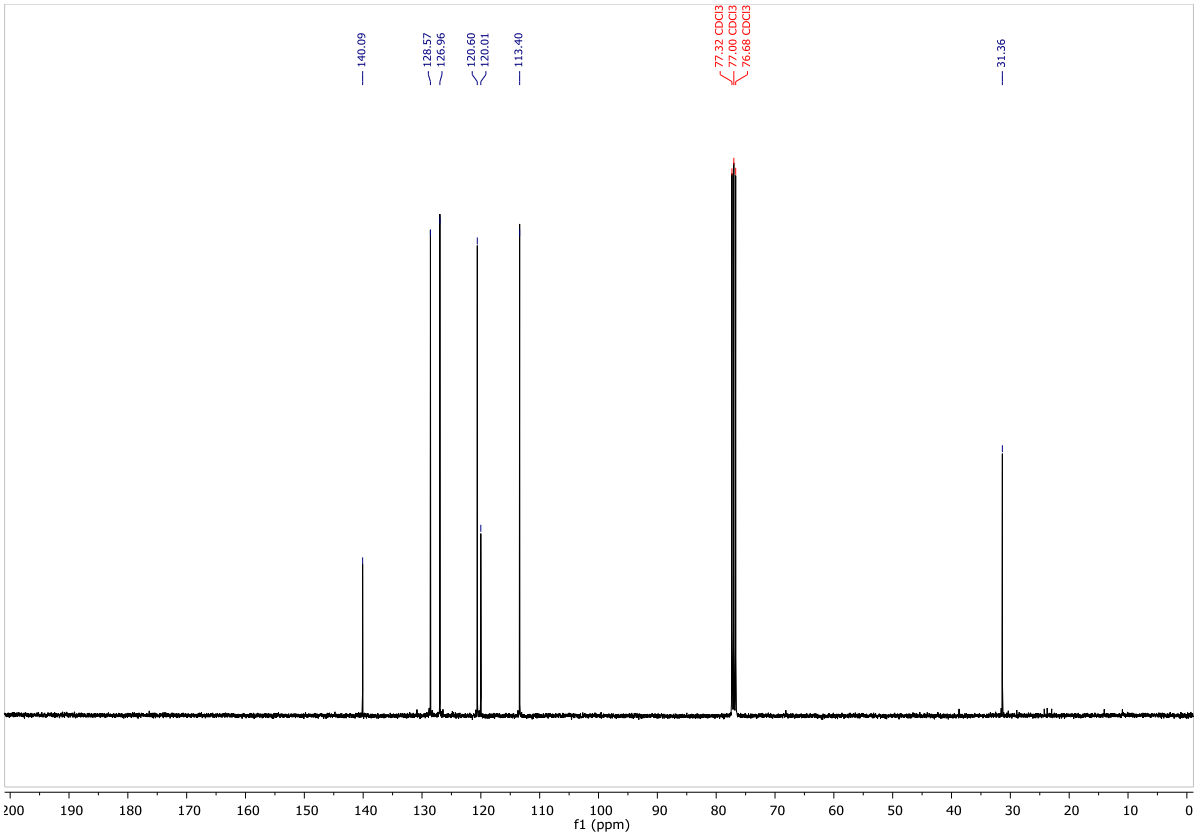
140.09
128.57
126.96
120.60
120.01
113.40
77.32 CDCl3
77.00 CDCl3
76.68 CDCl3
31.36
f1 (ppm)

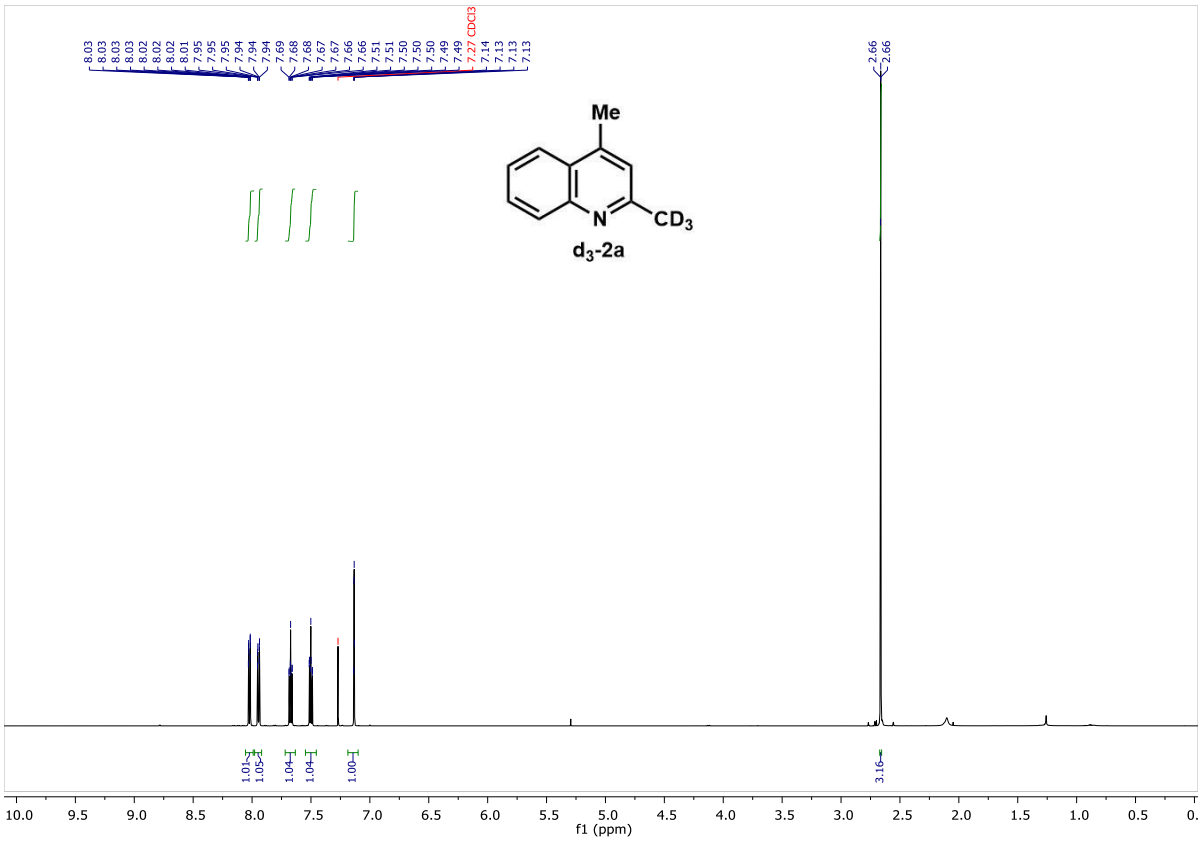
Me
N
CD3
d3-2a
f1 (ppm)

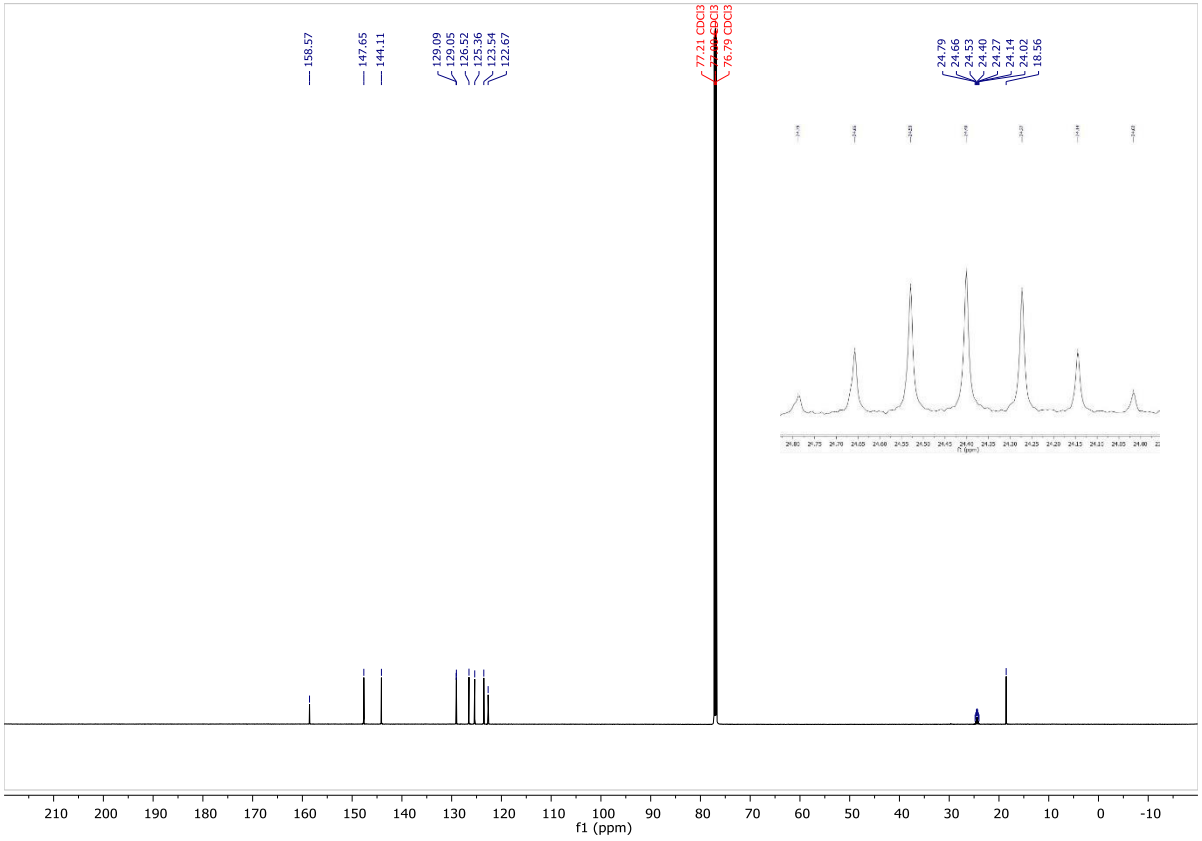
158.57
147.65
144.11
129.09
129.05
126.52
125.36
123.54
122.67
77.21 CDCl3
76.79 CDCl3
24.79
24.66
24.53
24.40
24.27
24.14
24.02
18.56
f1 (ppm)

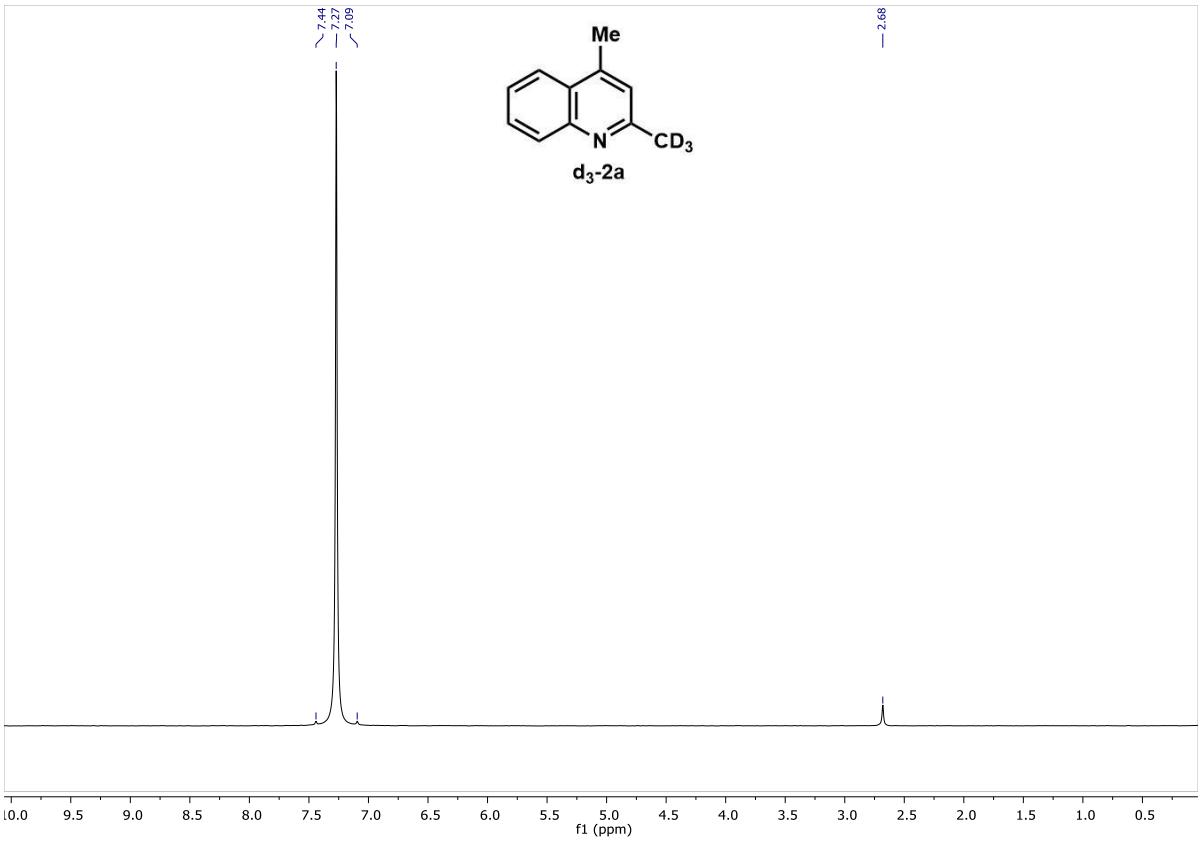
7.44
7.27
7.09
2.68
Me
N
CD3
d3-2a
f1 (ppm)

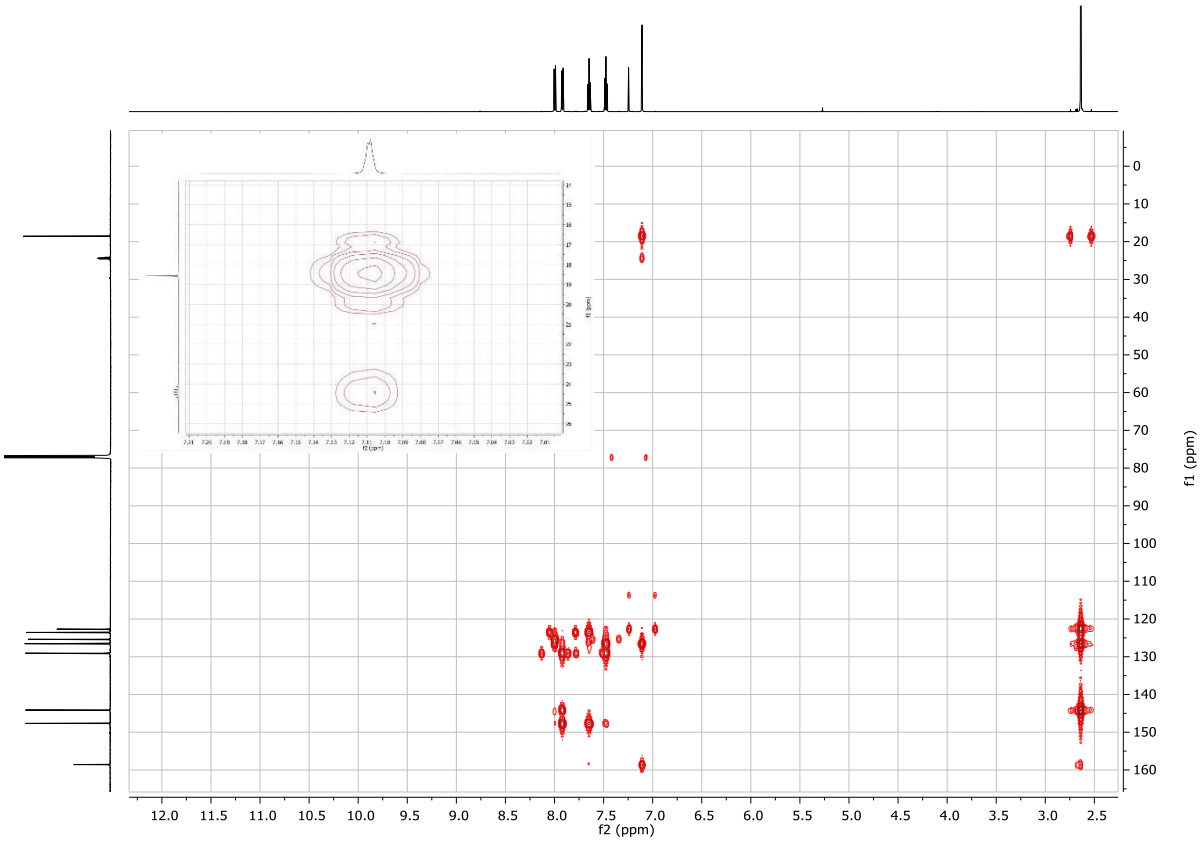
f2 (ppm)
f1 (ppm)

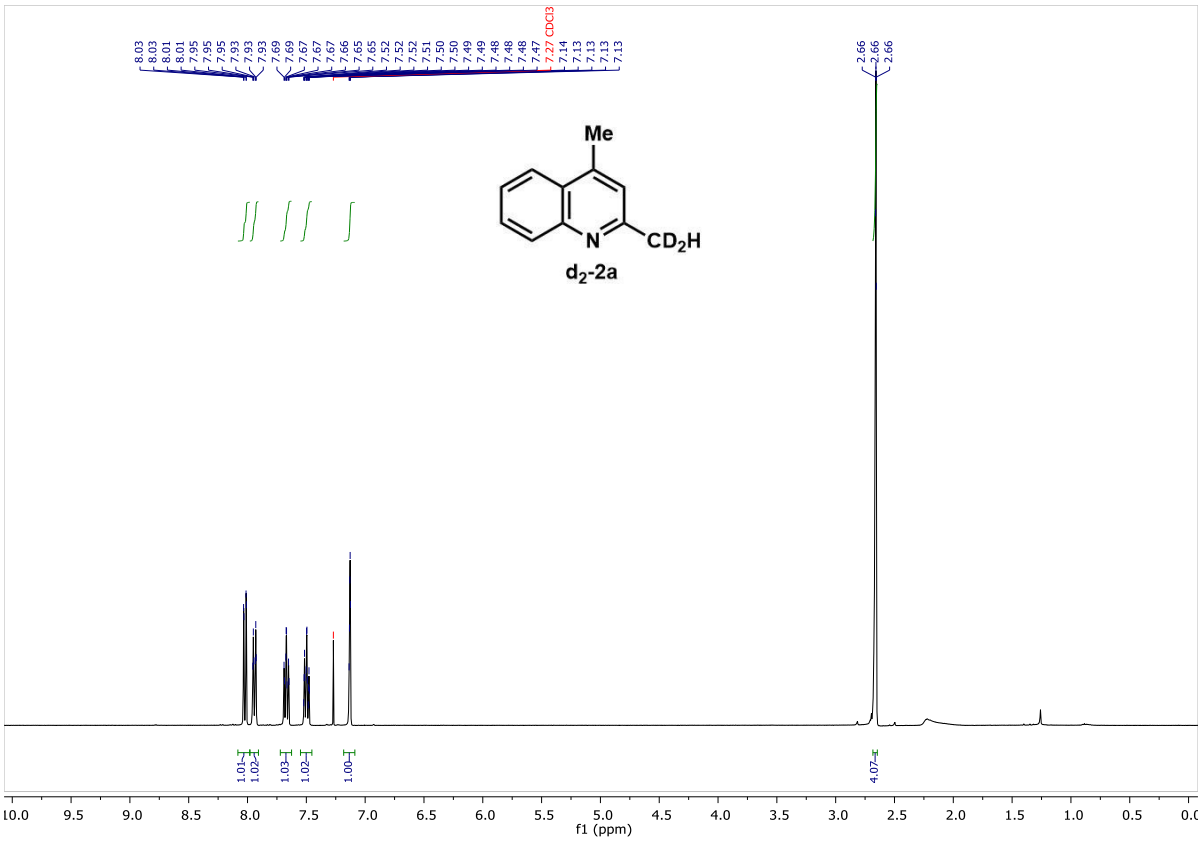
Me
N
CD2H
d2-2a
f1 (ppm)

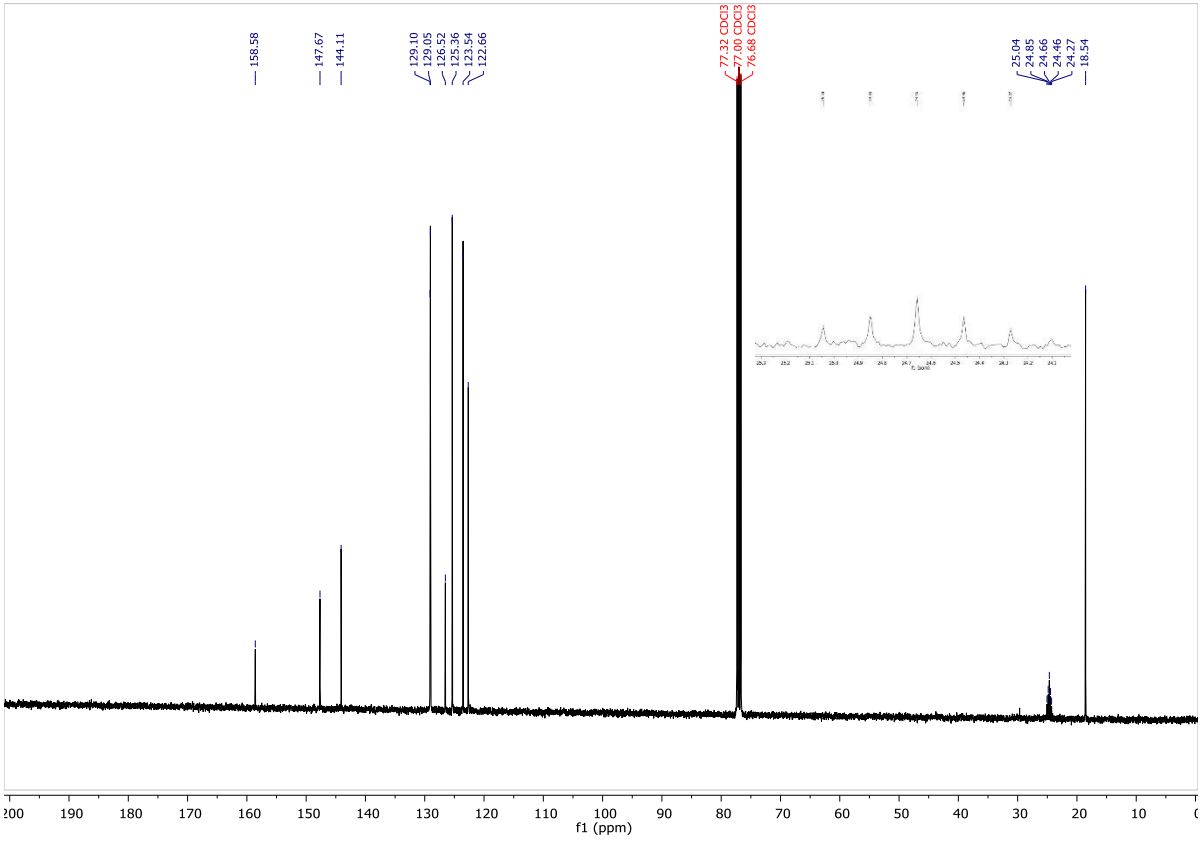
158.58
147.67
144.11
129.10
129.05
126.52
125.36
123.54
122.66
77.32 CDCl3
77.00 CDCl3
76.68 CDCl3
25.04
24.85
24.66
24.46
24.27
18.54
f1 (ppm)

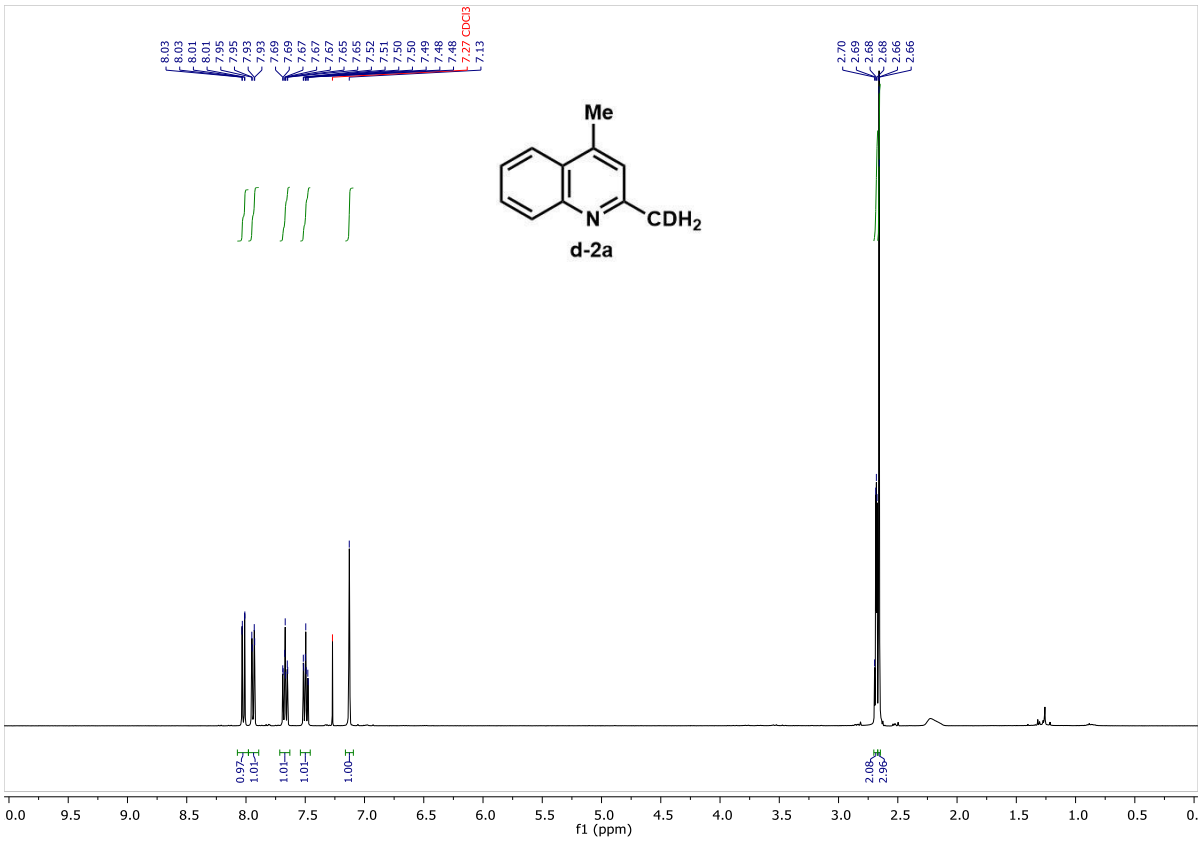
8.03
8.03
8.01
8.01
7.95
7.95
7.93
7.93
7.69
7.69
7.67
7.67
7.67
7.65
7.65
7.52
7.51
7.50
7.50
7.49
7.48
7.48
7.27 CDCl3
7.13
2.70
2.69
2.68
2.68
2.66
2.66
Me
N
CDH2
d-2a
0.97
1.01
1.01
1.01
1.00
2.08
2.96
f1 (ppm)

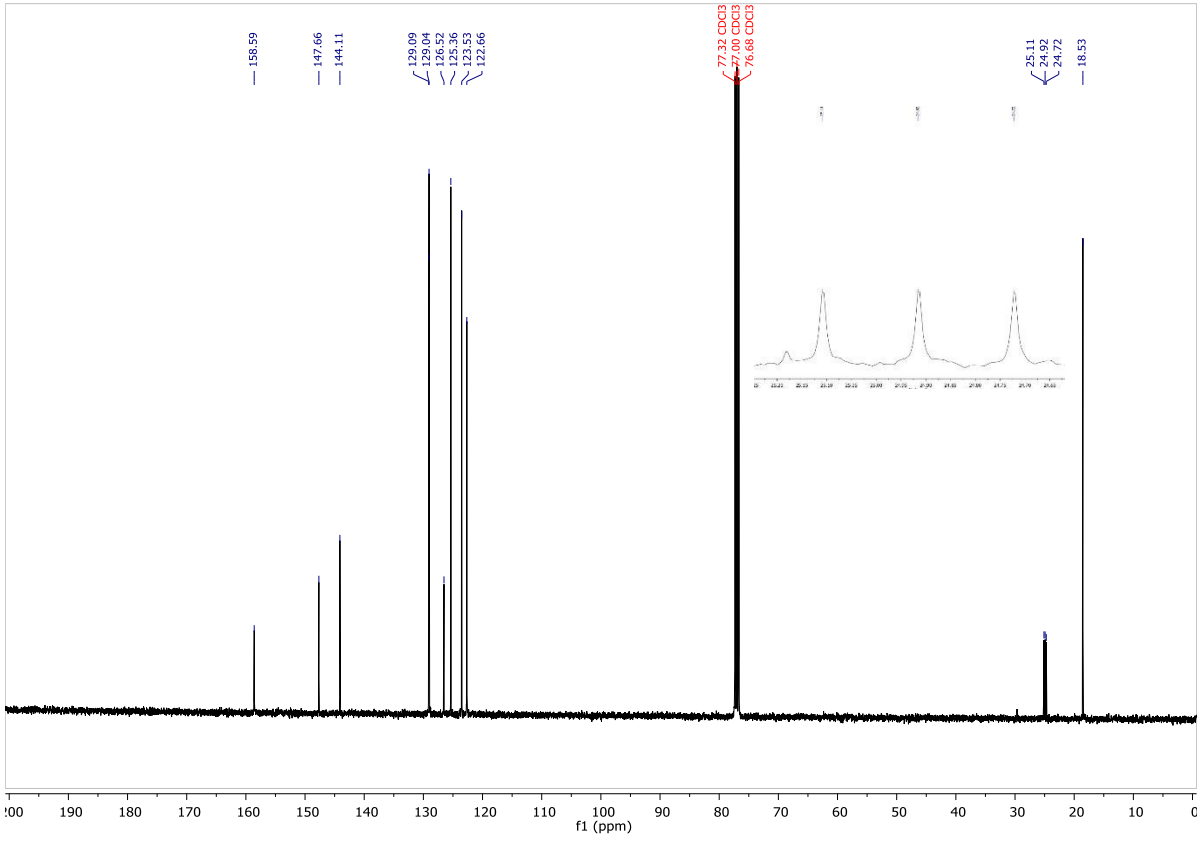
158.59
147.66
144.11
129.09
129.04
126.52
125.36
123.53
122.66
77.32 CDCl3
77.00 CDCl3
76.68 CDCl3
25.11
24.92
24.72
18.53
f1 (ppm)

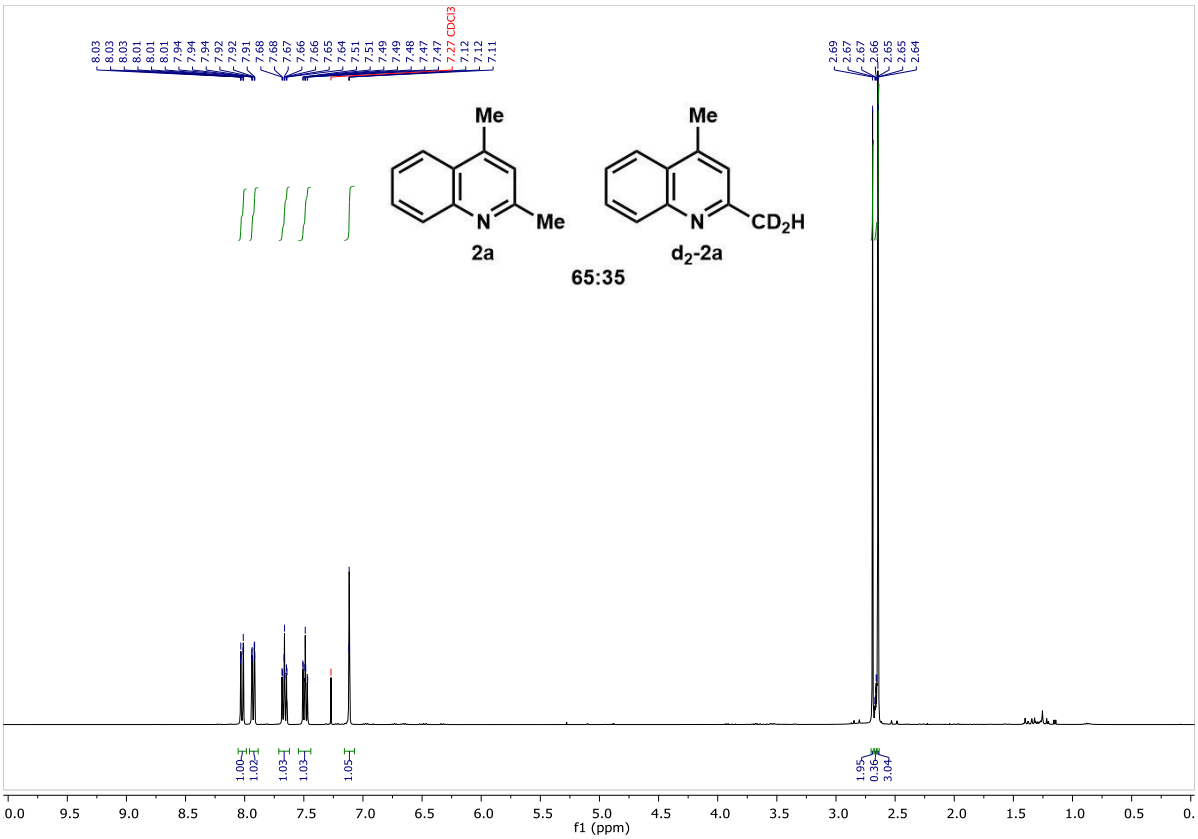
Me
N
Me
2a
Me
N
CD2H
d2-2a
65:35
f1 (ppm)

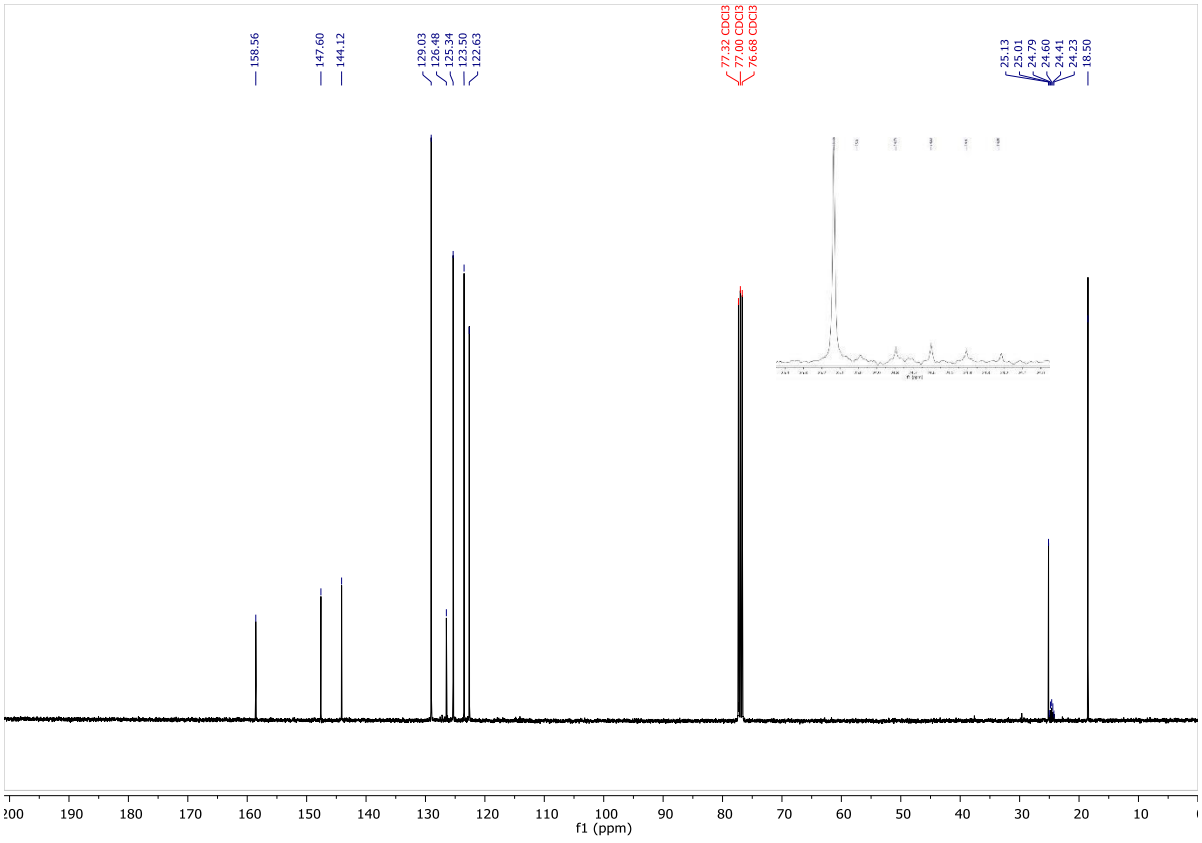
158.56
147.60
144.12
129.03
126.48
125.34
123.50
122.63
77.32 CDCl3
77.00 CDCl3
76.68 CDCl3
25.13
25.01
24.79
24.60
24.41
24.23
18.50
f1 (ppm)

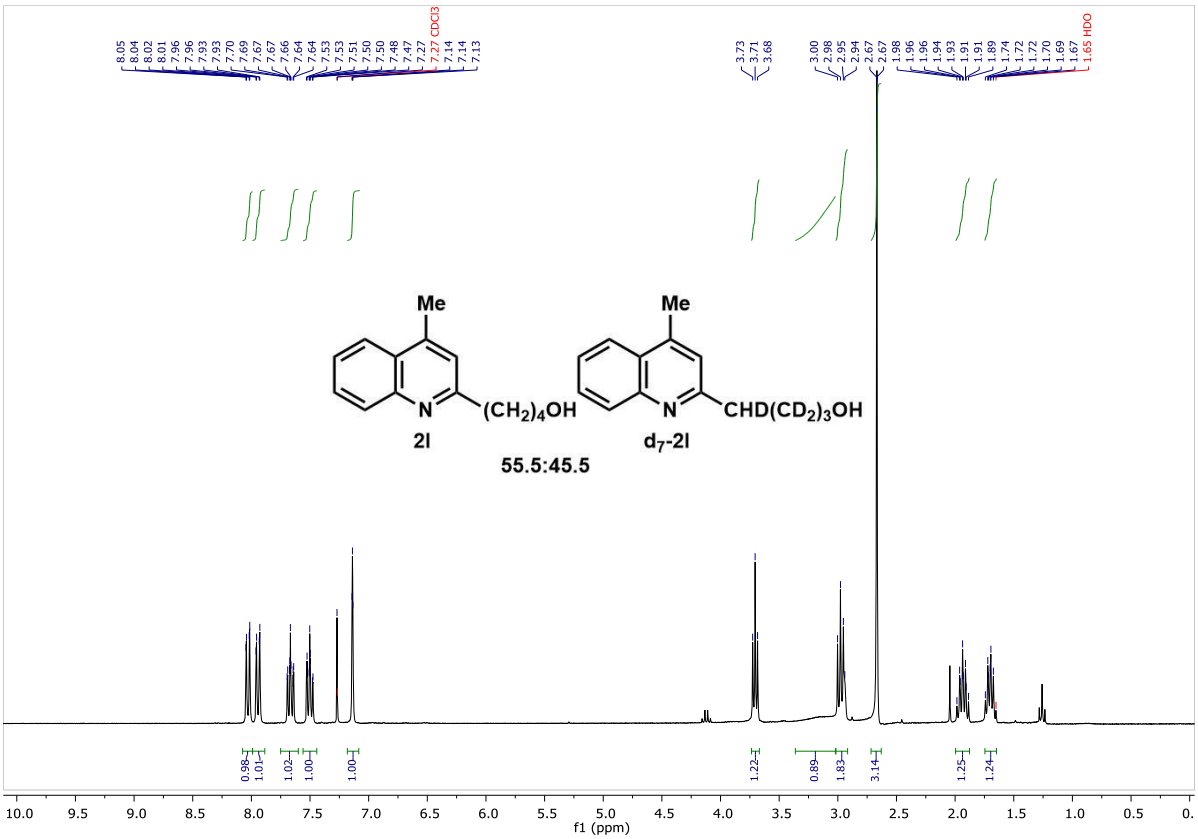
Me
N
(CH2)4OH
2l
Me
N
CHD(CD2)3OH
d7-2l
55.5:45.5
f1 (ppm)

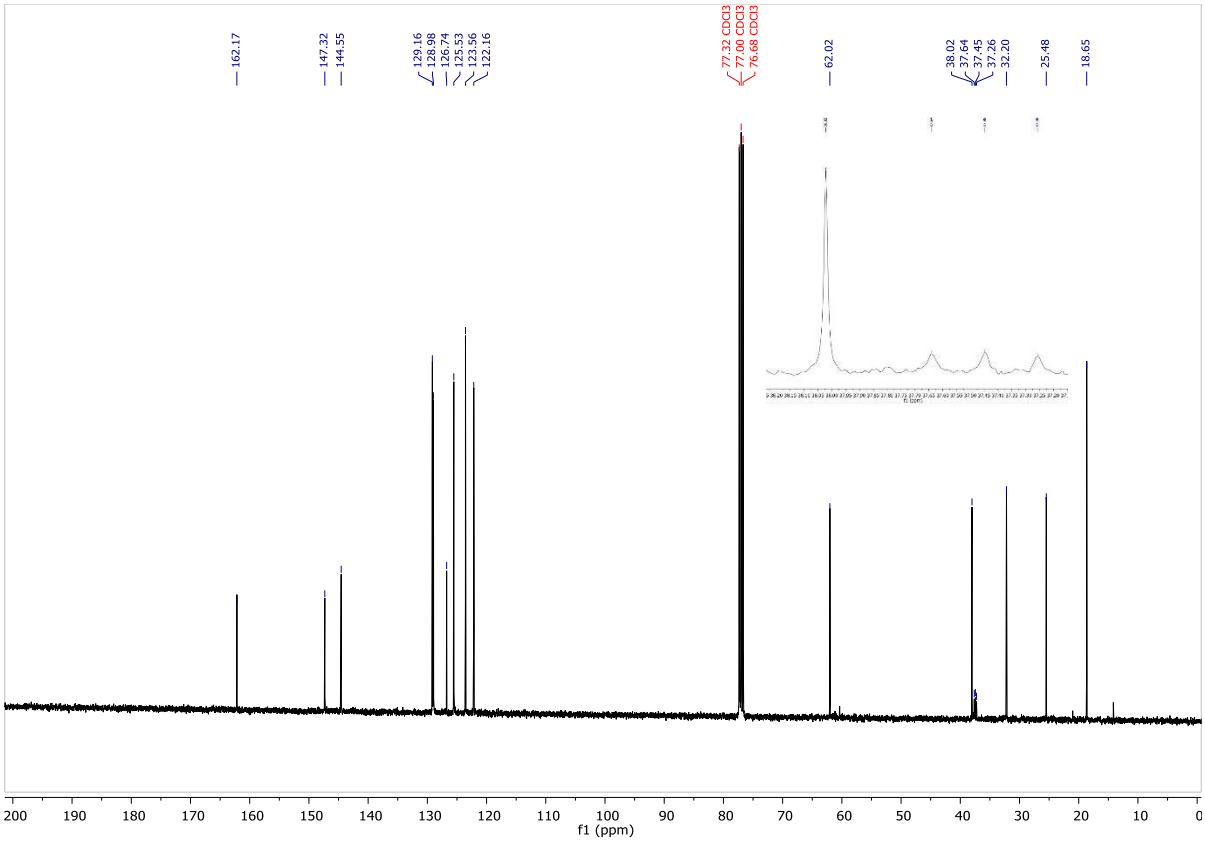
162.17
147.32
144.55
129.16
128.98
126.74
125.53
123.56
122.16
77.32 CDCl3
77.00 CDCl3
76.68 CDCl3
62.02
38.02
37.64
37.45
37.26
32.20
25.48
18.65
f1 (ppm)

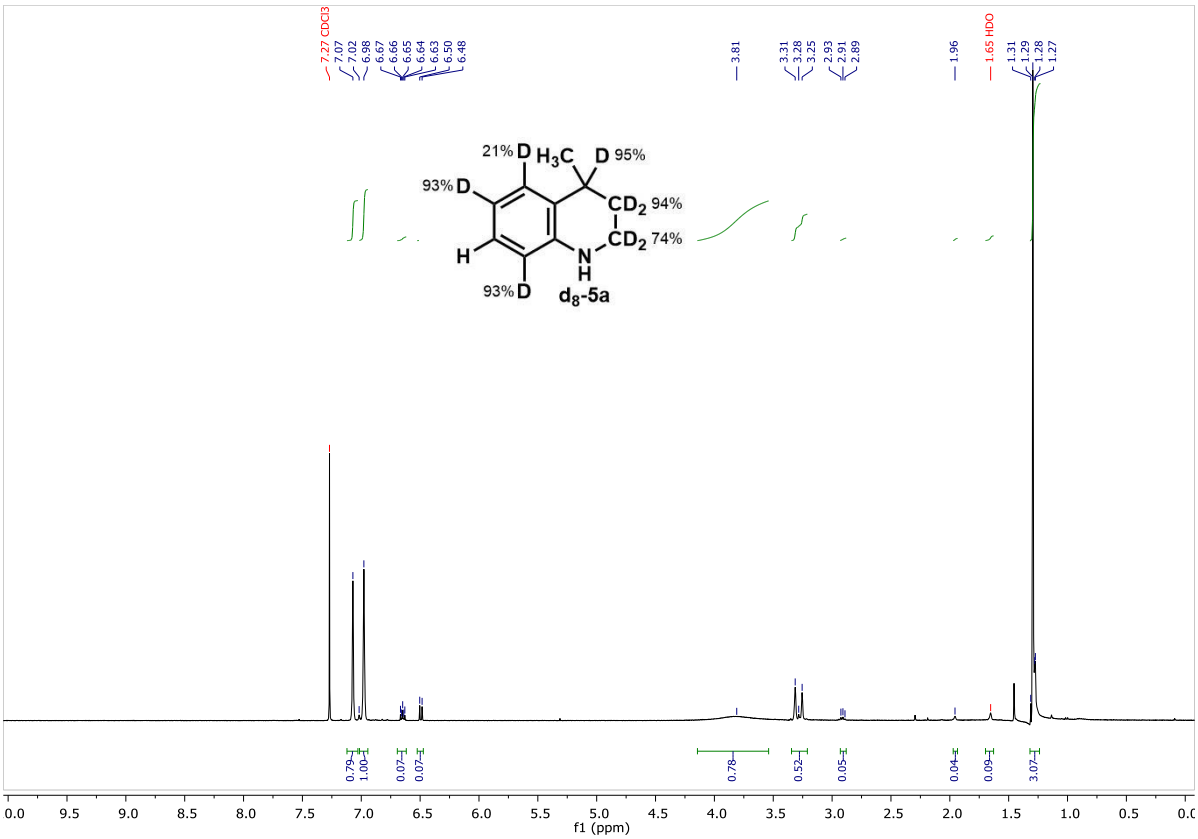
7.27 CDCl3
7.07
7.02
6.98
6.67
6.66
6.65
6.64
6.63
6.50
6.48
3.81
3.31
3.28
3.25
2.93
2.91
2.89
1.96
1.65 HDO
1.31
1.29
1.28
1.27
21% D
H3C
D 95%
93% D
CD2 94%
CD2 74%
H
N
H
93% D
d8-5a
0.79
1.00
0.07
0.07
0.78
0.52
0.05
0.04
0.09
3.07
f1 (ppm)

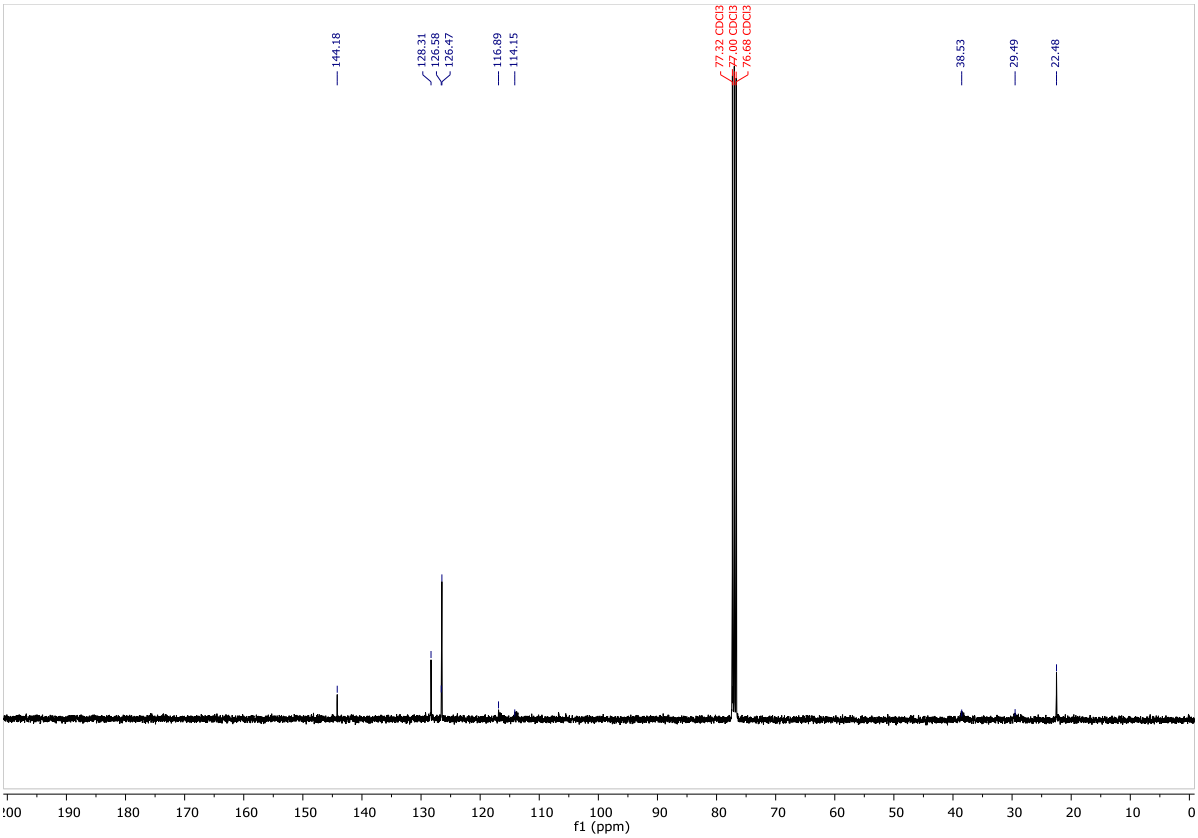
144.18
128.31
126.58
126.47
116.89
114.15
77.32 CDCl3
77.00 CDCl3
76.68 CDCl3
38.53
29.49
22.48
f1 (ppm)

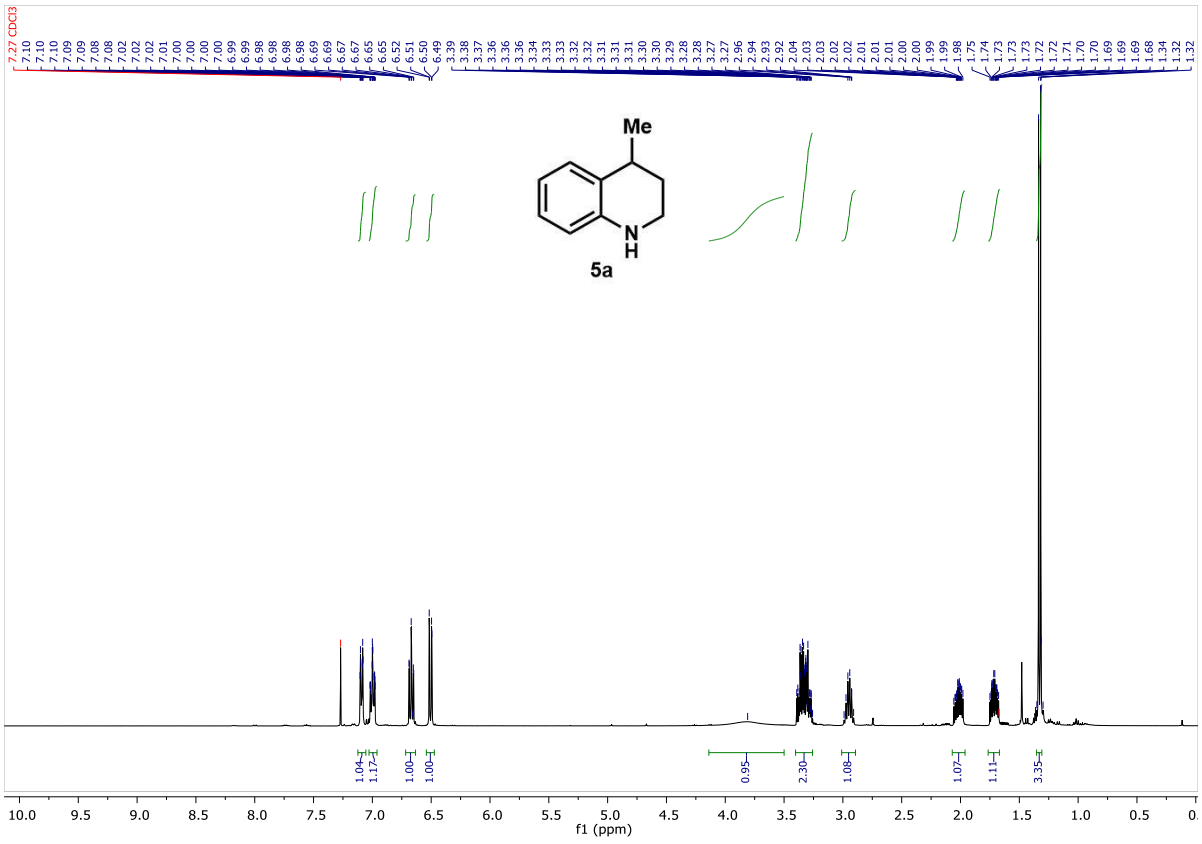
Me
N
H
5a
f1 (ppm)

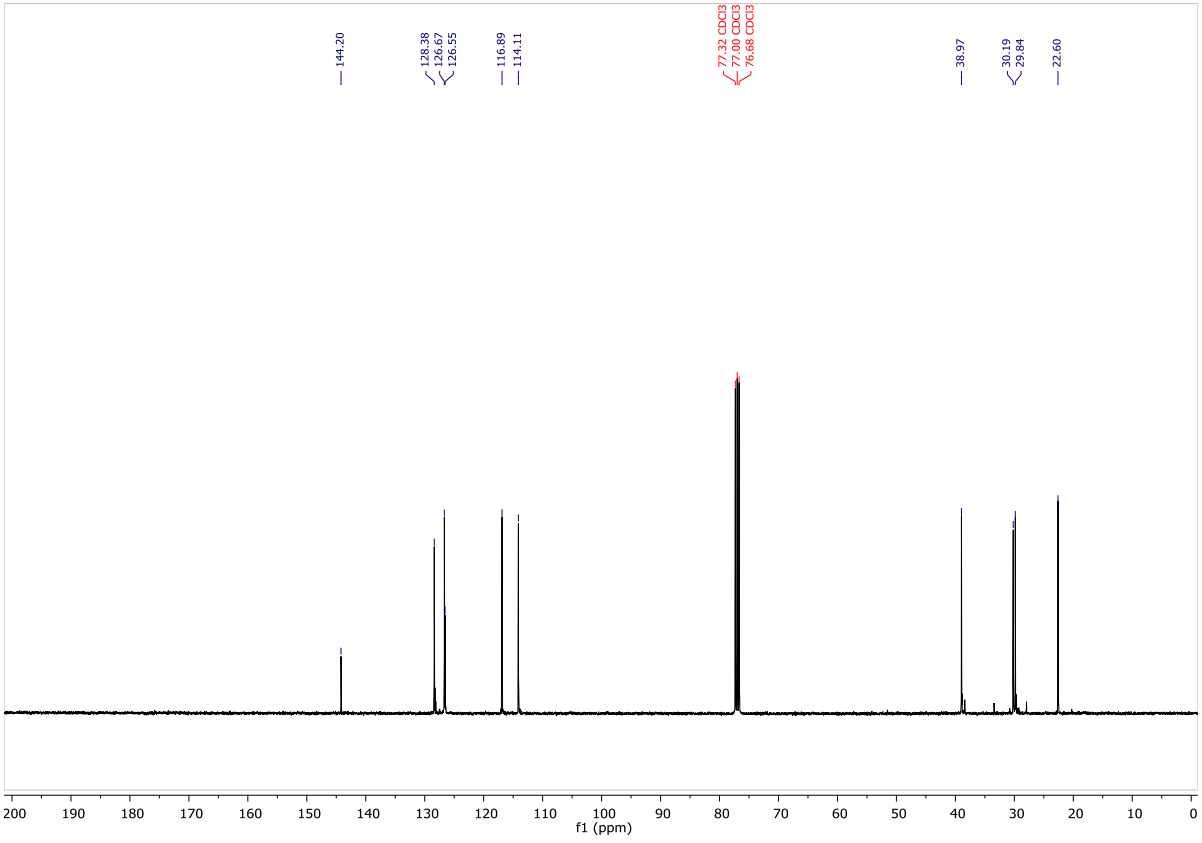
144.20
128.38
126.67
126.55
116.89
114.11
77.32 CDCl3
77.00 CDCl3
76.68 CDCl3
38.97
30.19
29.84
22.60
f1 (ppm)

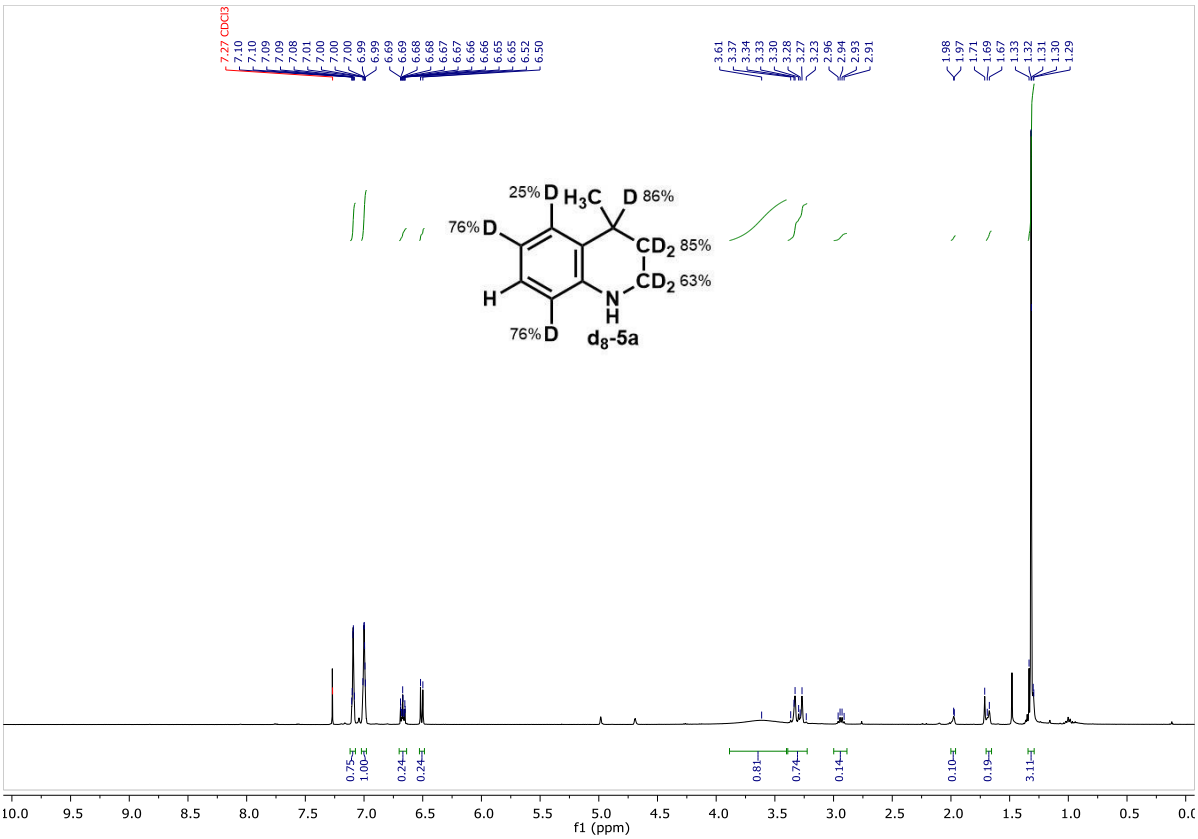
7.27 CDCl3
25% D
H3C
D 86%
76% D
CD2 85%
CD2 63%
H
N
H
76% D
d8-5a
f1 (ppm)

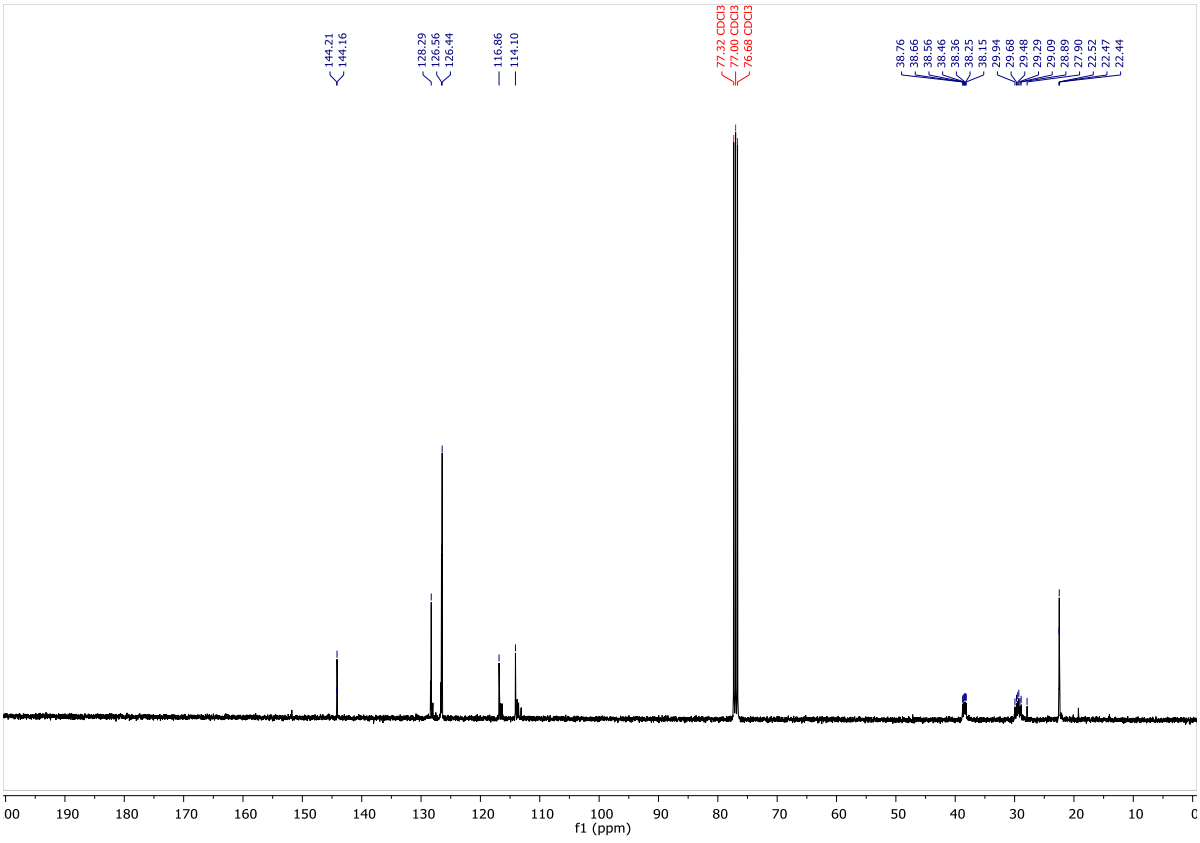
144.21
144.16
128.29
126.56
126.44
116.86
114.10
77.32 CDCl3
77.00 CDCl3
76.68 CDCl3
38.76
38.66
38.56
38.46
38.36
38.25
38.15
29.94
29.68
29.48
29.29
29.09
28.89
27.90
22.52
22.47
22.44
f1 (ppm)